

Innovations in Landscape Research



Elmira Saljnikov
Lothar Mueller
Anton Lavrishchev
Frank Eulenstein *Editors*

Advances in Understanding Soil Degradation

 Springer

Innovations in Landscape Research

Series Editor

Lothar Mueller, Leibniz Centre for Agricultural Landscape Research
(ZALF), Müncheberg, Brandenburg, Germany

Aims & Scope

The Springer series “Innovations in Landscape Research” presents novel methodologies and technologies to understand, monitor and manage landscapes of the Anthropocene. The aim is to achieve landscape sustainability at high productivity. This includes halting degradation of landscapes and their compartments, developing cultural landscapes, and preserving semi-natural landscapes. Clean water and air, fertile and healthy soils for food and other ecosystem services, and a green and bio-diverse environment are attributes of landscapes for the survival and well-being of humans who inhabit them.

How do landscapes function? How do future landscapes look like? How can we sustainably develop intensively used and stressed kinds of landscapes? Scientific innovations and decision tools are key to answer and solve those challenging questions. The series will inform about advanced methods and results of disciplinary, interdisciplinary and transdisciplinary work in landscape research. It presents a broad array of methods to measure, assess, forecast, utilize and control landscapes and their compartments. These include field and laboratory measurement methods, methods of resource evaluation, functional mapping and risk assessment, and sensing methods for landscape monitoring, advanced methods for data analysis and ecosystem modeling, methods and technologies for optimizing the use of multi-functional landscapes, for the bioremediation of soil and water, and basics and procedures of landscape planning. The series provides a new view on landscapes with some focus on scientific and technological innovations, on soils and problems of optimizing agricultural landscapes under conditions of progressive urbanization. Landscape research in a globalized world of the Anthropocene is based on gathering big data and scenario modeling. International long-term experiments and agri-environmental monitoring systems will deliver data for ecosystem models and decision support systems.

Edited volumes of this series will address the following topics at high priority: Status and Trends of Landscape Research; Understanding Key Landscape Processes; Landscape Services, Functions and Biodiversity; Assessing Soil Resources and Quality; Water Resource and Quality Monitoring; Landscape Monitoring Concepts and Studies; Landscape Sensor and Monitoring Technologies; Landscape Modeling and Decision Support; Agricultural Soil and Plant Management; Basics and Tools for Landscape Planning; Tools for Water and Wetland Management; Forest Management and Agroforestry; Rehabilitation of Degraded Landscapes.

The books of this series are a source of information for researchers, teachers, students, and stakeholders interested in the topics of landscape science and related disciplines. They present status analyses, methodical chapters and case studies showing the practical relevance and feasibility of novel decision tools and technologies. Thus, the books of this series will be a particular valuable information basis for managers and decision makers at various levels, from local up to international decision bodies.

An author/editor questionnaire, instructions for authors and a book proposal form can be obtained by contacting the Publisher.


More information about this series at <https://link.springer.com/bookseries/16118>

Elmira Saljnikov • Lothar Mueller •
Anton Lavrishchev •
Frank Eulenstein
Editors

Advances in Understanding Soil Degradation

 Springer

Editors

Elmira Saljnikov 
Department of Pedology
Institute of Soil Science
Belgrade, Serbia

Lothar Mueller
Leibniz Center Agricultural
Landscape Research
Müncheberg, Brandenburg, Germany

Anton Lavrishchev 
Department of Soil Science
and Agrochemistry
Saint-Petersburg State
Agrarian University
St. Petersburg, Russia

Frank Eulenstein
Leibniz Centre for Agricultural
Landscape Research
Müncheberg, Brandenburg, Germany

ISSN 2524-5155 ISSN 2524-5163 (electronic)
Innovations in Landscape Research
ISBN 978-3-030-85681-6 ISBN 978-3-030-85682-3 (eBook)
<https://doi.org/10.1007/978-3-030-85682-3>

© The Editor(s) (if applicable) and The Author(s), under exclusive license to Springer Nature Switzerland AG 2022

This work is subject to copyright. All rights are solely and exclusively licensed by the Publisher, whether the whole or part of the material is concerned, specifically the rights of translation, reprinting, reuse of illustrations, recitation, broadcasting, reproduction on microfilms or in any other physical way, and transmission or information storage and retrieval, electronic adaptation, computer software, or by similar or dissimilar methodology now known or hereafter developed. The use of general descriptive names, registered names, trademarks, service marks, etc. in this publication does not imply, even in the absence of a specific statement, that such names are exempt from the relevant protective laws and regulations and therefore free for general use.

The publisher, the authors and the editors are safe to assume that the advice and information in this book are believed to be true and accurate at the date of publication. Neither the publisher nor the authors or the editors give a warranty, expressed or implied, with respect to the material contained herein or for any errors or omissions that may have been made. The publisher remains neutral with regard to jurisdictional claims in published maps and institutional affiliations.

This Springer imprint is published by the registered company Springer Nature Switzerland AG
The registered company address is: Gewerbestrasse 11, 6330 Cham, Switzerland

Contents

1	Understanding Soils: Their Functions, Use and Degradation	1
	Elmira Saljnikov, Frank Eulenstein, Anton Lavrishchev, Wilfried Mirschel, Winfried E. H. Blum, Blair M. McKenzie, Linda Lilburne, Jörg Römbke, Berndt-Michael Wilke, Uwe Schindler, and Lothar Mueller	
2	Types of Physical Soil Degradation and Implications for Their Prevention and Monitoring	43
	Elmira Saljnikov, Wilfried Mirschel, Volker Prasuhn, Thomas Keller, Winfried E. H. Blum, Alexander S. Chumbaev, Jianhui Zhang, Jilili Abuduwaili, Frank Eulenstein, Anton Lavrishchev, Uwe Schindler, and Lothar Mueller	
3	Understanding and Monitoring Chemical and Biological Soil Degradation	75
	Elmira Saljnikov, Anton Lavrishchev, Jörg Römbke, Jörg Rinklebe, Christoph Scherber, Berndt-Michael Wilke, Tibor Tóth, Winfried E. H. Blum, Undine Behrendt, Frank Eulenstein, Wilfried Mirschel, Burghard C. Meyer, Uwe Schindler, Kairat Urazaliev, and Lothar Mueller	
4	Classification and Causes of Soil Degradation by Irrigation in Russian Steppe Agrolandscapes	125
	Vladimir G. Mamontov	
5	Desertification in Western Siberia: Identification, Assessment and Driving Forces in Temporal Scale	141
	V. Schreiner and Burghard C. Meyer	
6	Environmental and Economic Assessment of Land Degradation in Different Regions of the Russian Plain	161
	Oleg Makarov, Anton Stokov, Evgeny Tsvetnov, Dina Abdulkhanova, Vladislav Kudelin, and Nina Marakhova	
7	Measurement and Assessment of Snowmelt Erosion in Western Siberia	181
	Alexander S. Chumbaev and Anatoly A. Tanasienko	

8	The Potential Impact of Climate Change and Land Use on Future Soil Erosion, Based on the Example of Southeast Serbia	207
	Veljko Perović, Dragan Čakmak, Miroslava Mitrović, and Pavle Pavlović	
9	Ground-Based Dust Deposition Monitoring in the Aral Sea Basin	229
	Michael Groll, Christian Opp, Oleg Semenov, Gulnura Issanova, and Alexander Shapov	
10	How Does Tillage Accelerate Soil Production and Enhance Soil Organic Carbon Stocks in Mudstone and Shale Outcrop Regions?	245
	Jianhui Zhang, Yong Wang, Jiadong Dai, and Haichao Xu	
11	Risks and Permissible Rates of Soil Erosion in the Agrolandscapes of the Crimea	257
	Elena I. Ergina and Vladimir O. Zhuk	
12	Effect of Deer Browsing and Clear-Cutting of Trees on Soil Erosion in a Forest Ecosystem in Japan	271
	Nanami Murashita, Atsushi Nakao, Keiko Nagashima, and Junta Yanai	
13	Soil Compaction Due to Agricultural Field Traffic: An Overview of Current Knowledge and Techniques for Compaction Quantification and Mapping	287
	Thomas Keller, Mathieu Lamandé, Mojtaba Naderi-Boldaji, and Renato Paiva de Lima	
14	Modeling of Field Traffic Intensity and Soil Compaction Risks in Agricultural Landscapes	313
	Rainer Duttmann, Katja Augustin, Joachim Brunotte, and Michael Kuhwald	
15	Ecotoxicological Assessment of Brownfield Soil by Bioassay	333
	Tamara V. Bardina, Marina V. Chugunova, Valery V. Kulibaba, and Victoria I. Bardina	
16	Methodology for the Preparation and Study of Multicomponent Certified Reference Materials for Soils Contaminated with Heavy Metals	351
	Galina A. Stupakova, Elena E. Ignateva, Tatyana I. Shchiplitsova, and Dmitrii K. Mitrofanov	
17	Bioaugmentation and Biostimulation: Comparison of Their Long-Term Effects on Ecotoxicity and Biological Activity of Oil-Contaminated Soil	361
	Yulia Polyak, Lyudmila Bakina, Marina V. Chugunova, Natalya Mayachkina, Alexander Gerasimov, and Vladimir M. Bure	

18 Environmental Pollution in the Vicinity of an Aluminium Smelter in Siberia	379
Irina A. Belozertseva, Marija Milić, Sonja Tošić, and Elmira Saljnikov	
19 Technogenic Fluorine in the Siberian Steppe Soils Due to a Metallurgical Plant Operation	403
Nina D. Davydova	
20 Contamination of the Agroecosystem with Stable Strontium Due to Liming: An Overview and Experimental Data	423
Anton Lavrishchev, Andrey V. Litvinovich, Olga Yu Pavlova, Vladimir M. Bure, Uwe Schindler, and Elmira Saljnikov	
21 Concentration, Background Values and Limits of Potential Toxic Elements in Soils of Central Serbia	451
Vesna V. Mrvić, Elmira Saljnikov, Biljana Sikirić, and Darko Jaramaz	
22 Impact of Weathering and Revegetation on Pedological Characteristics and Pollutant Dispersion Control at Coal Fly Ash Disposal Sites	473
Olga Kostić, Miroslava Mitrović, and Pavle Pavlović	
23 Impact of Flood Disaster on Agricultural Land and Crop Contamination at the Confluence of the Bosna River	507
Tihomir Predić, Petra Nikić Nauth, Bojana Tanasić, Tatjana Docić-Kojadinović, Tatjana Cvijanović, and Duška Bjelobrč	
24 Poorly Soluble and Mobile Forms of Heavy Metals in the Soils of the Volga Steppes	529
Victor V. Pronko, Dmitry Yu. Zhuravlev, Tatyana M. Yaroshenko, Nadezhda F. Klimova, and Sonja Tošić	
25 Impact of Tailing Outflow on Soil Quality Around the Former Stolica Mine (Serbia)	553
Snežana Belanović Simić, Dušica Delić, Predrag Miljković, Jelena Beloica, Sara Lukić, Olivera Stajković-Srbiljinović, Milan Knežević, and Ratko Kadović	
26 Hazards and Usability of Coal Fly Ash	571
Dušica Delić, Olivera Stajković-Srbiljinović, and Aneta Buntić	
27 Crop Yield Limitation by Soil Organic Matter Decline: A Case Study from the US Pacific Northwest	609
Rajan Ghimire, Prakriti Bista, and Stephen Machado	

- 28 Changes in the Composition and Dynamics of Soil Humus and Physical Properties in Dark Chestnut Soils of Trans-Volga Dry Steppes After 75 and 35 years of Irrigation Agriculture** 623
Nina A. Pronko, Viktor V. Korsak, Lubov G. Romanova, and Alexandr S. Falkovich
- 29 Fertility Decline in Arable Chernozem and Chestnut Soils in Volga Steppes Versus Their Virgin Analogues** 649
Victor V. Pronko, Dmitry Yu. Zhuravlev, Tatyana M. Yaroshenko, and Nadezhda F. Klimova
- 30 Labile Soil Carbon as an Indicator of Soil Organic Matter Quality in the Province of Vojvodina, Serbia** 667
Srđan Šeremešić and Vladimir Ćirić
- 31 Changes in Key Physical Soil Properties of Post-pyrogenic Forest Ecosystems: a Case Study of Catastrophic Fires in Russian Sub-boreal Forest** 687
Ekaterina Chebykina and Evgeny Abakumov
- 32 Remote Sensing Sensors and Recent Techniques in Desertification and Land Degradation Mapping—A Review** 701
Subramanian Dharumarajan, S. Veeramani, Amar Suputhra, Manish Parmar, B. Kalaiselvi, Manickam Lalitha, R. Vasundhara, Rajendra Hegde, and A. S. Rajawat
- 33 Mapping the Caspian Sea’s North Coast Soils: Transformation and Degradation** 717
Konstantin Pachikin, Olga Erohina, Gabit Adamin, Azamat Yershibulov, and Yersultan Songulov
- 34 Soil Acidification Patterns Due to Long-Term Sulphur and Nitrogen Deposition and How They Affect Changes in Vegetation Composition in Eastern Serbia** 737
Jelena Beloica, Snežana Belanović Simić, Dragana Čavlović, Ratko Kadović, Milan Knežević, Dragica Obratov-Petković, Predrag Miljković, and Nenad Marić
- 35 Urban Soils in the Historic Centre of Saint Petersburg (Russia)** 755
Natalia N. Matinian, Ksenia A. Bakhmatova, and Anastasia A. Sheshukova
- 36 Agrosols in the City of St. Petersburg: Anthropogenic Evolution and Current State** 775
Vyacheslav Polyakov, Evgeny Abakumov, George Shamilishvily, Ekaterina Chebykina, and Anton Lavrishchev



Understanding Soils: Their Functions, Use and Degradation

1

Elmira Saljnikov, Frank Eulenstein,
Anton Lavrishchev, Wilfried Mirschel,
Winfried E. H. Blum, Blair M. McKenzie,
Linda Lilburne, Jörg Römbke, Berndt-Michael Wilke,
Uwe Schindler, and Lothar Mueller

Abstract

Soils, the thin skin of the earth, a living body, are the basis of all highly developed life and have ensured human existence and culture since millennia. Their functions and ecosystem services are crucial for the survival of humanity. Increasing pressure on soils through overuse and mismanagement has exceeded their capacity to perform, which is considered as soil degradation. To meet the mission of the Sustainable Development Goals of the United Nations, soil degradation

must be stopped and reversed. We reviewed framework conditions of soil degradation, scientific concepts of research and status and trends of their operationalization. Soil performance and degradation processes must be understood, monitored, mitigated and combated in the context of different categories and scales such as ecosystems, land and landscapes. Approaches to the assessment and monitoring of soil dynamics, degradation and desertification show inconsistencies and knowledge gaps at several levels. Concepts of soil health and ecosystem services of soil

E. Saljnikov (✉)
Institute of Soil Science, Teodora Drajzera 7, 11000
Belgrade, Serbia
e-mail: elmira.saljnikov@soilinst.rs

E. Saljnikov · F. Eulenstein · U. Schindler
Mitscherlich Academy for Soil Fertility (MITAK),
GmbH, Prof.-Mitscherlich-Allee 1, Paulinenaue,
14641 Brandenburg, Germany
e-mail: feulenstein@zalf.de

U. Schindler
e-mail: schindler@mitak.com

F. Eulenstein · W. Mirschel · L. Mueller
Leibniz-Centre for Agricultural Landscape Research
(ZALF), Eberswalder Str. 84, 15374 Müncheberg,
Germany

A. Lavrishchev
St. Petersburg State Agrarian University,
Peterburgskoye Ave. 2, 196601 St. Petersburg,
Pushkin, Russia

W. E. H. Blum
Institute of Soil Research, University of Natural
Resources and Life Sciences, Peter-Jordan-Str. 82,
1190 Vienna, Austria
e-mail: winfried.blum@boku.ac.at

B. M. McKenzie
Geography and Environmental Science, University
of Dundee, D1 4HN Dundee, Scotland, UK
e-mail: b.mckenzie@dundee.ac.uk

L. Lilburne
Manaaki Whenua—Landcare Research, PO
Box 69040, Lincoln, Canterbury, New Zealand
e-mail: lilburnel@landcareresearch.co.nz

J. Römbke
ECT Oekotoxikologie, GmbH, Böttgerstr. 2–14,
65439 Flörsheim, Germany
e-mail: j-roembke@ect.de

B.-M. Wilke
Department of Ecology, TU Berlin, BH 10-1,
Ernst-Reuter-Platz 1, 10587 Berlin, Germany
e-mail: bmwilke@tu-berlin.de

should be backed by “hard data” based on field and landscape indicators and measurements. Participatory approaches to mediate conflicting demands of stakeholders are crucial for a broad understanding of soil and its long-term sustainable use. This requires an advanced field diagnostic system of soil performance based on reliable on-site measurement technology in combination with expert-based knowledge and assessment methodologies. Strengthening field soil science is essential for progress in reducing and reversing soil degradation.

Keywords

Soil degradation · Soil functions · Ecosystem services · Soil quality · Indicators · Field methods

Abbreviations

AI	Aridity index
CASH	Comprehensive assessment of soil health
CICES	Common international classification of ecosystem services
DEX	Decision EXpert
DPSIR	Driving forces, pressures, states, impacts and responses
DSS	Decision support system
EC	Electrical conductivity
EEA	European environmental agency
ENVISSO	Environmental assessment of soil for monitoring
ES	Ecosystem services
ESAI	Environmentally sensitive area index
EU	European union
FAO	Food and agriculture organization of the united nations
GLASOD	Global assessment of soil degradation
LCA	Life cycle analysis
LRC	Land resource circle concept
MDS	Minimum data sets

M-SQR	Muencheberg soil quality rating
N ₂ O	Nitrous oxide
NDVI	Normalized difference vegetation index
PCA	Principal component analysis
RUSLE	Revised universal soil loss equation
SAR	Sodium absorption ratio
SDG	Sustainable development goals
SD	Soil degradation
SB	Soil biodiversity
SF	Soil fertility
SH	Soil health
SMAF	Soil management assessment framework
SoilHealthDB	Soil health DataBase
SOM	Soil organic matter (SOM)
SQ	Soil quality
SQI	Soil quality index
UAV	Unmanned aerial vehicle
UN	United Nations
UNCCD	United Nations convention to combat desertification
UNEP	United nation environmental programme
VESS	Visual examination of soil structure
VSA	Visual soil assessment method
WRB	World reference base for soil resources

1.1 Introduction

The world’s population grows at an explosive pace. Production of food, fibre and other goods must keep pace with this growth in order to prevent the rollback of humanity and the reduction of the level of well-being of the world’s population (Foley et al. 2011). To simply feed the additional billions of people in future, a

further unprecedented increase in food production through agriculture is required.

Productive soils are the basis of agriculture. Agriculture in the late Holocene and Anthropocene has required the introduction of modern agricultural technologies based on the widespread use of machinery, fertilizers and pesticides, the latest irrigation methods, etc. (Dobrovolskiy et al. 2012; Mueller et al. 2020). Also, rapid globalization and urbanization, the emergence of many large cities dramatically increased the requirements for the elementary quality of housing, minimally at the level of household and sanitary comfort and transportation. Everywhere, large-scale construction activities, such as urban development, transport and traffic facilities or the creation of reliable sources of water and energy, are needed. All these, and other factors such as climate change, put pressure on all global resources, including agricultural land.

Soils are the most important parts of the global land resource. Soils are the upper layer of the earth, their skin, a living body. They are a result of parent rock, climate, vegetation, organism activities and relief over time and of human activity (Dokuchaev 1951; Thorp 1942). Like other natural systems, soils underlie the processes of development, ageing and disturbances (Walker et al. 2010).

Soils have a capacity and resiliency to provide biomass for food, fodder and other ecosystem services to humans and to recycle their waste (Blum 2005; Mueller et al. 2010; Blum and Nortcliff 2013). If the status of soil falls irreversibly beyond these limits of capacity and resiliency, it is considered as degraded.

Understanding the functioning of soils and developing tools for wise decisions of soil management are crucial for meeting the Sustainable Development Goals (SDG) (UN 2015) of the United Nations (Keesstra et al. 2016; Tóth et al. 2018). The World Soil Charter (FAO 2015) supports the achievement of SDGs through principles of understanding and sustainable use of soils. Principle 10 of the World Soil Charter addresses the need to minimize or eliminate soil degradation.

This chapter reviews the main aspects of soil degradation, their causes, triggering factors, consequences and monitoring problems. Attention is paid to degradation caused by anthropogenic impacts through land-use change and agricultural management practices. The chapter also addresses different approaches in assessing the degree and forms of degradation, indicators and attributes of changes in soil quality and health in the context of ecosystem functioning. Processes of soil degradation require better understanding. Knowledge gaps in the reliable assessment of soil degradation and desertification will be identified.

1.2 Soils, Ecosystems and Humans

1.2.1 Pedosphere and Anthroposphere

To understand the mechanisms of soil degradation requires information about soils. Soil is a cornerstone component of pedosphere, which is an intersection of atmosphere, hydrosphere, lithosphere and biosphere. Only in the pedosphere, minerals, organic matter, air and water come into a dynamic complex interaction, thus wonderfully providing and sustaining life on earth.

Entire civilizations can rise and fall depending on the ability of the soil to supply food. The knowledge about soil and its fertility has been accumulated during the last several thousand years in different regions. An especially high level of this knowledge was achieved in the ancient riverine civilizations of Egypt (first irrigation cultivation), Mesopotamia, India and China. Broader knowledge about soil and its treatment was accumulated by farmers and compiled by what might be called the first soil scientists in the Roman empire. In those days, soil fertility was seen as a divine power of the earth and it was worshipped in numerous legends and myths. Traditionally, soil was considered as the natural environment for the growth of terrestrial plants, regardless of its physical structure (e.g. whether it has identifiable horizons or not).

However, even in the earliest agricultural societies, it was known that there is a need of providing “food” such as compost for the soil in order to keep soil fertile. People also recognized the importance of soil not only as a source of food, fibre, medicine and other necessary raw materials but also as a medium for filtering water and recycling wastes.

Between 1877 and 1880, Dokuchaev, the pioneer in soil studies, introduced a new concept of soil. It was defined as an independent natural body, consisting of a high but limited number of types, each with a unique morphology and properties, conditioned by the site-specific combined effects of climate, living organisms, geology, relief and age (Dokuchaev 1951; Trofimov et al. 2020). It was a revolutionary concept, which allowed the consideration of all soil characteristics together, as a complete, integrated natural body, where the effect of one property depends on the combined interactions of other properties in space and time. The Russian view of soils as an independent natural body with genetic horizons has led to the concept that soil is a part of the earth’s crust with properties reflecting the influence of local or regional soil-forming agents. After extended soil expeditions in the nineteenth century, Dokuchaev’s team of researchers concluded that soil fertility decline (i.e. the loss of favourable soil properties) is caused by humans, i.e. an inappropriate land use such as the destruction of the soil layers as well as deterioration of its water regime.

Soil acts as an intermediary for chemical and biogeochemical flows in and out of the whole earth system and consists of gaseous, mineral, liquid and biological components. Soil is a starter and generator of energy flowing through a chain: soils, plants and organisms (microbes and animals). Food chains are the channels of life and by death and decay this energy is returned to the soil, being available for another circle.

With accelerated industrial development, a new anthropogenic influence was added to this interaction. Given that the soil is an integrated part of the network of food, energy and water interactions, it is a functional component of environmental sustainability that is linked to

climate change, decline in biodiversity, water, energy and food security (Bouma 2014; Gupta et al 2019).

Soil is considered as a non-renewable resource, since it takes thousands of years for rocks to weather into soils, and hundreds of years for rich organic matter layers to build up. Our welfare depends, to a large extent, on our soils since soil is the end product of the combined influence of climate, topography, organisms (flora, fauna and human) on parent materials (original rocks and minerals) over time.

Since more than 99% of the world’s food is produced via soils, the importance of soil in the food, energy and water nexus is crucial (Pimentel and Burgess 2013; FAO 2019). An increase in the production of food, fibre and bioenergy by increasing soil productivity with the help of new technologies may result in an increased rate of soil degradation up to a critical point when technological progress cannot overcome the limits of degraded and depleted soil (Hatfield et al. 2017).

1.2.2 Soil Functions

The environmental importance of soil is not limited to food production as soil is a multi-functional system (Dobrovolskiy et al. 2012). Blum (2005) divided soil functions into two main domains: ecological functions (biomass production, protection of humans and the environment and gene reservoir) and non-ecological function (physical basis of human activities, source of raw materials and geogenic and cultural heritage). Independently, ecologists have developed the Ecosystem Service Concept (ESS) (Costanza et al. 1997; MEA 2005), which quickly became the main theoretical approach in environmental policies, but which has—at least in the beginning—neglected soils (Dominati et al. 2010). Soil environmental functions include every aspect of life support on the earth, such as primary production, renewable energy and raw material as well as transportation and recycling of water and nutrients. In fact, the decontamination of groundwater and the maintenance of the food

chain are among the most important soil environmental functions (Keesstra et al. 2016), which are controlled by the capacity of soil for (1) filtration of solid and liquid compounds, (2) compound buffering via adsorption and precipitation and (3) compound transformation via alteration and decomposition by soil biota (Blum 2005).

Summarizing, the soil functions can be grouped into the following domains (Larson and Pierce 1991; Arshad and Coen 1992; Snakin et al. 1996; Singer and Ewing 2000; Blum and Nortcliff 2013; Bampa et al. 2019), Fig. 1.1:

- Biomass production: medium for plant/crop growth (food, fodder and renewable energy).
- Filtering and buffering organic and inorganic components: ensures healthy food, fodder, water and fibre.
- Gene reserve and environment for the growth and development of biodiversity: plants, animals, and microorganisms contribute to maintaining and improving soil quality.
- Basis for technical, residential and industrial structures and infrastructures: ever-growing population and urbanization inevitable put an increasing pressure on soil quality and accessibility.
- Source of minerals, materials and fossil fuels: intensive mining negatively affects climate change and landscape properties.
- Natural and cultural heritage: contribute to the history of the evolution of life and environment.
- Regulation of biochemical processes:
The cycling of carbon and nutrients, water and energy through pedosphere, biosphere, atmosphere and hydrosphere by participating in the two cornerstone biochemical processes on earth: photosynthesis and decomposition.
- Regulation of geochemical processes:
Gas exchange between the pedosphere and atmosphere
Geochemical runoff into the ocean.

For the area covered by states of the European Union recognizes seven soil functions that are vulnerable to soil threats were identified (FAO and ITPS 2015):

1. biomass production, including agriculture and forestry,
2. storing, filtering and transforming nutrients, substances and water,
3. biodiversity pool, such as habitats, species and genes,
4. physical and cultural environment for humans and human activities,
5. source of raw materials,
6. acting as a carbon pool,
7. archive of geological and archaeological heritage.

Soil enables the function of terrestrial ecosystems (Doran et al. 1996). Every environmental function of soil is directly or indirectly linked with food, energy and water nexus (Adhikari and Hartemink 2016) and is associated with the physical, chemical and biological processes taking place in the soil–water–plant–organism system. Within the soil ecosystem, the microbial and zoological biodiversity is largely unexplored. This requires basic research in order to improve the understanding of soil functioning in general, since it affects all other soil functions significantly (Heintz-Buschart et al. 2020).

1.2.3 Soils for Sustainable Development of Humans in the Anthropocene

The awareness about increasing conflicts between human demands and limited global resources has inspired ideas on how to ensure livelihoods at a better level of sustainability. The Millennium Ecosystem Assessment (MEA 2005) provided a status analysis of global ecosystems based on the concept of ecosystem services (Daily et al. 1997; Costanza et al. 1997). This concept has initiated a broader view of the role of soil in global ecosystems. The Intergovernmental Technical Panel on Soils (FAO and ITPS 2015) has demonstrated this by linking the most important ecosystem services (ES) with soil functions (Table 1.1).

Table 1.1 should be considered as a first step and as an inspiration for more specific definitions

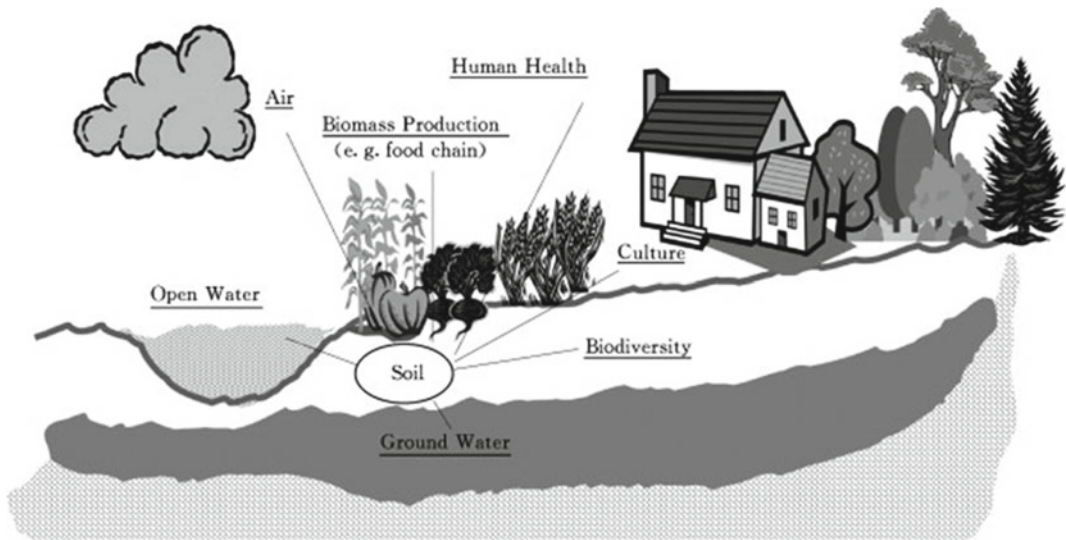


Fig. 1.1 Goods and services are provided by land and soil. 2013 Source Blum (2012)

and quantifications at different levels. A number of specific soil functions and ecosystem services (ES) were not yet mentioned here. This was done in numerous later studies (e.g. Schulte et al. 2014; Schwilch et al. 2018; Drobnik et al. 2018; Van Leeuwen et al. 2019). Soil policies of the European Union (EU) and elsewhere assess soil multifunctionality based on these concepts (Vrebos et al. 2017; Schwilch et al. 2018).

Emerging concepts of ecosystem services are based on theories that consider soils as a natural capital and public good. On the other hand, global tendencies of land concentration in the hands of fewer people, land grabbing, privatization of public land and privatization of public research in agriculture and soil science are on the rise (Mueller et al. 2020). This has led to conflicts and controversial debates in the scientific community with implications for research on how to measure and control soil quality/health and degradation (Wander et al. 2019).

McBratney et al. (2014) introduced the overarching concept of Soil Security. This concept addresses existential global environmental challenges based on soil's performance in the same

manner as food security or water security, including the idea of sufficient access to these resources by individuals or communities. They propose five dimensions of Soil Security:

- Capability that relates to maintain the soil in its place in the landscape.
- Condition that relates to the state of the soil, e.g. free from contamination.
- Capital that includes a clear economic value particularly as part of ecosystem service.
- Connectivity that brings in the social aspects of stewardship, management and tenure.
- Codification that aligns with the policy and legislation to protect and enhance soil (McBratney et al. 2014).

This concept requires assessment frames, parameterization and interlinkage with other concepts such as that of ES, but it has the potential to help meet the UN's SDGs (Bouma 2019a). SDG 15 of UN (2015): "Life on Land", explicitly addresses "Sustainably manage forests, combat desertification, halt and reverse land degradation, halt biodiversity loss" (UN 2015), that is a mandate to act.

Table 1.1 Ecosystem services provided by the soil and the soil functions that support these services

Ecosystem service	Soil functions
Supporting services: Services that are necessary for the production of all other ecosystem services; their impacts on people are often indirect or occur over a very long time	
Soil formation	Weathering of primary minerals and release of nutrients
	Transformation and accumulation of organic matter
	Creation of structures (aggregates, horizons) for gas and water flow and root growth
	Creation of charged surfaces for ion retention and exchange
Primary production	Medium for seed germination and root growth
	Supply of nutrients and water for plants
Nutrient cycling	Transformation of organic materials by soil organisms
	Retention and release of nutrients on charged surfaces
Regulating services: benefits obtained from the regulation of ecosystem processes	
Water quality regulation	Filtering and buffering of substances in soil water
	Transformation of contaminants
Water supply regulation	Regulation of water infiltration into soil and water flow within the soil
	Drainage of excess water out of soil and into groundwater and surface water
Climate regulation	Regulation of CO ₂ , N ₂ O and CH ₄ emissions
Erosion regulation	Retention of soil on the land surface
Provisioning Services: products (“goods”) obtained from ecosystems of direct benefit to people	
Food supply	Providing water, nutrients, and physical support for growth of plants for human and animal consumption
Water supply	Retention and purification of water
Fibre and fuel supply	Providing water, nutrients, and physical support for growth of plant growth for bioenergy and fibre
Raw earth material supply	Provision of topsoil, aggregates, peat, etc
Surface stability	Supporting human habitations and related infrastructure
Refugia	Providing habitat for soil animals, birds, etc
Genetic resources	Source of unique biological material and information
Cultural services: non-material benefits that people obtain from ecosystems through spiritual enrichment, aesthetic experiences, heritage preservation and recreation	
Aesthetic and spiritual	Preservation of natural and cultural landscape diversity
	Source of pigments and dyes
Heritage	Preservation of archaeological records

Source FAO and ITPS (2015)

1.2.4 Soils as Compartments of Land and Landscapes

Neighbour disciplines of soil science such as geography, landscape ecology and agriculture consider soils as a crucial compartment of their central subject of study, such as geosystem,

landscape and land, respectively (Hole 1978; Van Eetvelde and Antrop 2005; Amato et al. 2017; Nikiforova et al. 2019).

The categories “land” and “landscape” are broader than “soil”. From understanding of the Food and Agriculture Organization of the United Nations (FAO), “soil” is an essential component

of “land” and “ecosystems” where both are wider concepts encompassing vegetation, water and climate in the case of land, and in addition to those three aspects, also social and economic considerations in the case of ecosystems (FAO 2020a). From a definition of the European Environmental Agency (EEA), “Land” commonly refers to the planet’s surface not covered by seas, lakes or rivers. It includes the total land mass including continents and islands. In more daily use and legal texts, “land” often refers to a designated piece of land. “It consists of rocks, stones, soil, vegetation, animals, ponds, buildings, etc.” (EEA 2020). From understanding of the United Nations Convention to Combat Desertification (UNCCD), land is “the terrestrial bio-productive system that comprises soil, vegetation, other biota and the ecological and hydrological processes that operate within the system” (UNCCD 1994). This is very similar to the operation field of soil science.

“Landscape” is a still broader concept with focus on the interaction between nature and humans at regional and local levels. Antrop and van Eetvelde (2019) characterize the “landscape” as a holistic concept. “As a spatial unit, it characterizes the identity of the land of a community and defines a territory where custom rights apply. Both territory and scenery are manifestations of local, regional or national relationships between a community and the way it is using the environment” (Antrop and Van Eetvelde 2019). Landscape approaches are promising for understanding, monitoring and tackling problems of sustainable use of natural resources, use, degradation and conservation of soils included (Mueller et al. 2019).

To consider soils as parts of landscapes has implications for soil conservation and restoration strategies. Measures of landscape conservation are based on the ES concept and consider soil, land and landscapes as a natural capital (Costanza et al. 1997, 2017; Müller et al. 2015; Grunewald et al. 2015). The Land Resource Circle (LRC) concept, developed by Lilburne et al. (2020) (Fig. 1.2), is a framework, linking soil functions with land and landscape functions to

inform users about the suitability and value of a local land parcel.

Soil erosion is a typical example of a complex landscape-related process (Dotterweich 2013). Erosion translocates soils, mainly by wind and water (Figs. 1.3, 1.4, 1.5, 1.6). However, processes are not soil processes only. They depend on landscape attributes (Ouyang et al. 2010), have shaped landscapes over geological periods and have been impacting the survival of humans and civilizations over millennia (Montgomery 2007). Accelerated rates of man-made erosion of soil on agricultural land, about 10–40 times higher than the natural process (Dotterweich 2013), have to be considered as a soil degradation process. Combating processes of accelerated soil erosion that causes harmful off-site effects, such as degradation of drylands and pollution of water in particular, requires approaches at landscape scale (Issanova and Abuduwaili 2017; Boardman et al 2019; Smetanová et al. 2019; Prasuhn 2020).

Changes in the overall economy and socio-economic system of a country or region cause expansion or reduction in the area of cropping land and are a main factor of spatiotemporal alterations in soil degradation. A typical example is Asian Russia, where soil erosion has reduced by about 70–90% in some regions in the last decades as compared with the period of intensive cropping in the 1960–1990th (Litvin et al. 2021). On the other hand, those processes are often associated with a decline of rural regions, and shifts of environmental problems and soil degradation to industrial and urban centres. Abandoned lands can be seen as untapped agricultural potentials whose soil’s risks for new cycles of degradation must be minimized (Prishchepov et al. 2020; Frühauf et al. 2020).

1.2.5 Land Use and Stress on Soils

Multifunctional use of land and soils. Soils have experienced alterations, stress and disturbances since the Neolithic Revolution when humans began to settle, to develop agriculture on

Fig. 1.2 The Land Resource Circle (LRC) framework for describing the key soil, land and ecosystem functions of a land parcel. *Source* Lilburne et al. (2020), with kind permission of Elsevier

Land Resource Circle

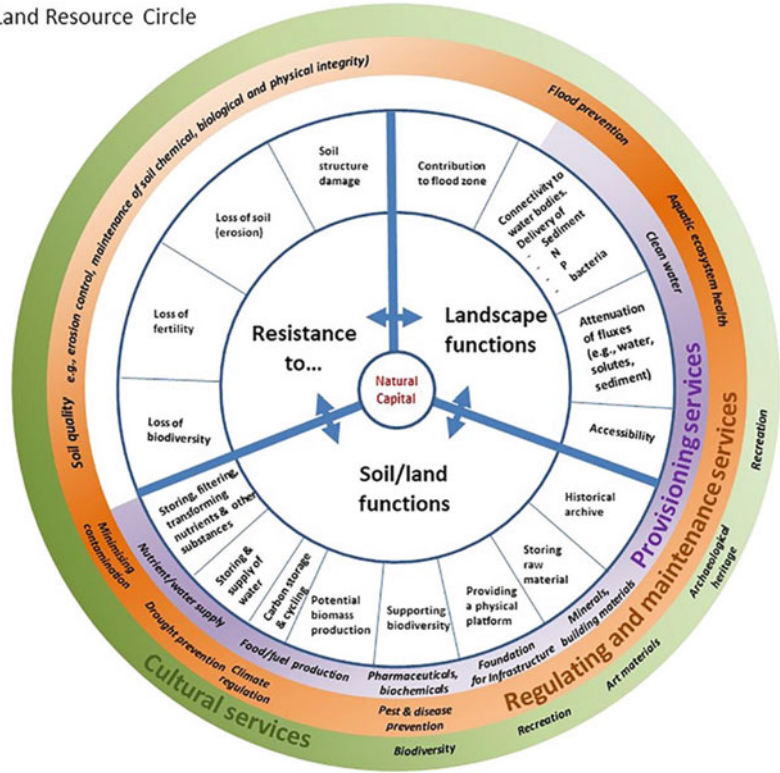


Fig. 1.3 Water erosion as a landscape forming process. Canyon of a tributary of the Charyn river in Kazakhstan (left). Zonal soils are brown desert soils. Dry valley (ovrag) near Kursk, Russia (right). Zonal soils in the

region are Chernozems on Loess parent material. Historical erosion removed the Loess down to the Tertiary basis. *Photos* L. Mueller

former grasslands and forests, to dig for minerals and other natural resources for the production of tools and weapons and to develop civilizations and cultural landscapes. These processes accelerated with the increasing size of human populations, ever-increasing division of labour and

innovations. Figure 1.7 shows the degrading impacts of human activities on soils.

Currently, in the Anthropocene, the age shaped by humans, soil, land, landscapes and all spheres of the globe are exposed to extreme pressure (Crutzen 2002; Lewis and Maslin



Fig. 1.4 Accelerated soil erosion by water on sloped cropland, considered as a soil degrading process. Canola field in Germany. Denudation field part (left) and accumulation field part (right). Zonal soils in this region

are Luvisols and Retisols (Albeluvisols) on Late Pleistocene parent material. New soil types are developing on eroded field parts. *Photos L. Mueller*

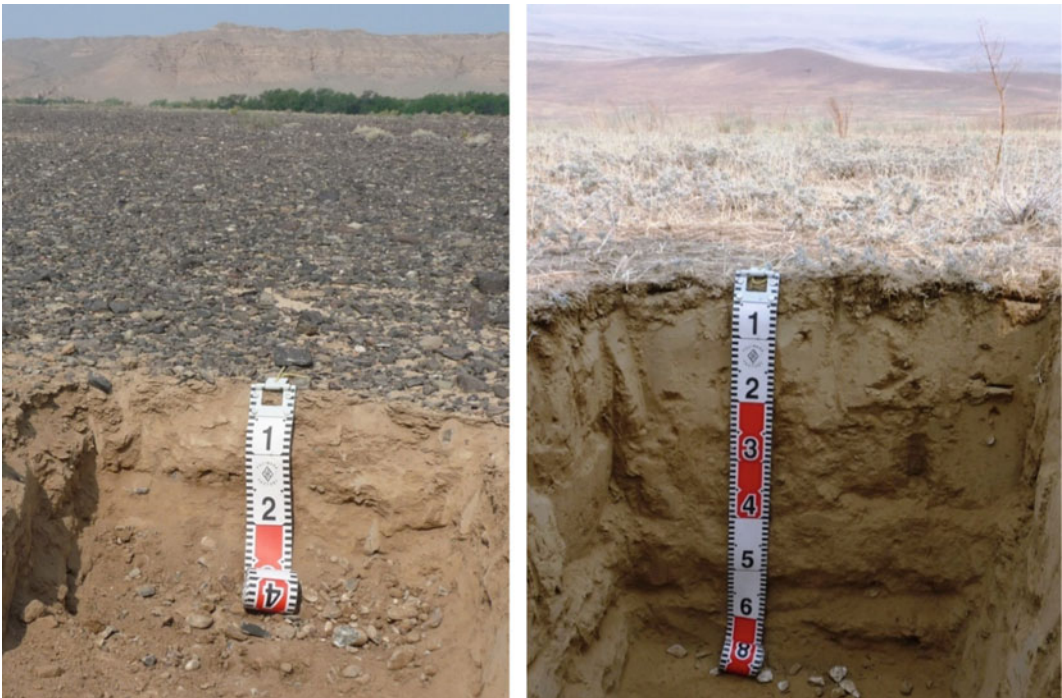


Fig. 1.5 Wind erosion as a landscape forming process. Photos show soil profiles in deserts and semi-deserts of Kazakhstan. Brown desert soil with surface gravel lag (left). Surface gravel accumulation is the result of long-term blowing off of finer soil particles. It reduces further erosion largely, maintaining its potential to re-vegetate.

Light Chestnut soil developed on fine sandy aeolian sediments. CIS Alatau region near Almaty (right). Vegetation is degraded grassland/rangeland and, thus, prone to current accelerated erosion, degrading the soil and land. *Photos L. Mueller*



Fig. 1.6 Wind erosion induced by soil tillage on Loess soils as a soil degradation process on cropland of the Columbia Plateau in the Northwestern USA (location near Pendleton, OR). Climate is semiarid. Soils are

Kastanozem. Tillage for seedbed preparation. As fine material and organic matter are blown off first, the remaining topsoil became coarser textured and humus depleted. *Photos L. Mueller*

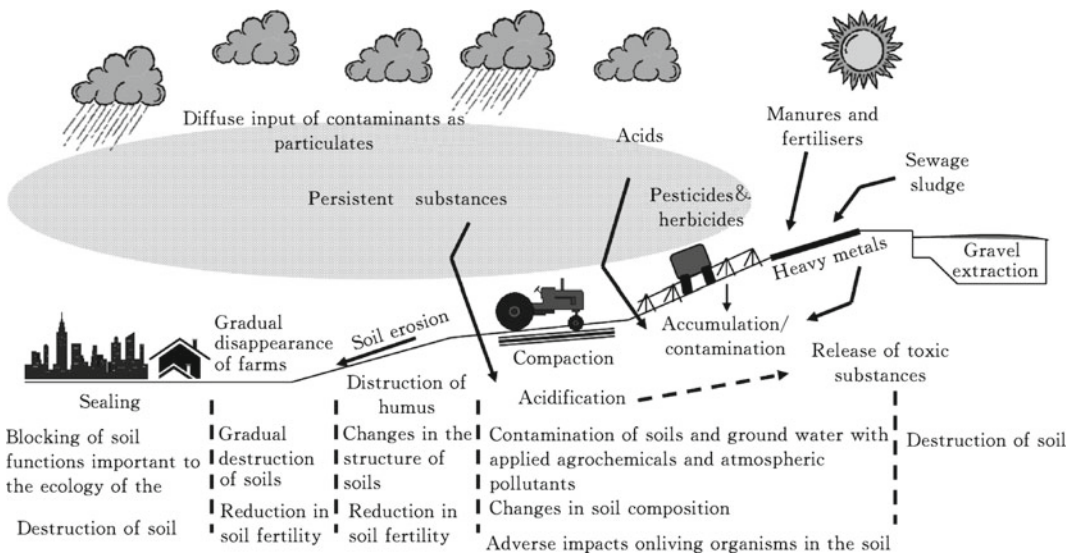


Fig. 1.7 The impact of human activities on soil (Source Blum 2008)

2015). Besides agriculture, the focus of soil functioning or destruction is more and more triggered by problems associated with localized extreme overpopulation, such as land transformed by urbanization and the construction of infrastructure, waste disposal, air pollution and others. Meanwhile, all soils and landscapes worldwide carry signs of human activity including “alien” substances (plastic particles, artificial, radioactive and chemical substances, nitrogen and phosphorus loads, etc.), impacting ecosystems in a complex manner (Tarolli et al. 2018).

Pressure on agricultural soils. Since humans started agriculture to meet their basic needs for food and fibre and to improve their livelihoods, they tried to achieve high yields from soil through its intensified management. Problems with insufficient soil performance for food production root back to antiquity. The decline in high natural soil fertility due to agriculture and the resulting drop in crop yields have been significant problems throughout history (Montgomery 2007). Soil and land degradation, erosion, in particular, in Northern Africa, the “grain chamber” of Rome contributed to the collapse of the Roman Empire (Montgomery 2007).

During the 10 thousand years of soil cultivation, agriculture developed gradually with ups and downs, discoveries and inventions. Land-use intensity increased due to increased demands for food, which could only be satisfied by scientific and technological innovations. Over the past 200 years, agricultural science and soil science have developed as acknowledged scientific disciplines (Dickson 1805; Thaer 1809; Körte 1839; Dokuchaev 1951). Since the industrial age, knowledge gains in soil science and plant nutrition speeded up. Innovations based on technological progress and sophisticated agricultural experiments improved fertilizer production and machinery, while at the same time, agricultural decision support and scheduling systems optimized plant and soil resources, thus enabling a rapid growth of agricultural production (Ascough et al. 2002; Bochtis et al. 2014; Dobrovolskiy et al. 2012; Mueller et al. 2020; Poulton and Johnston 2020; Trofimov et al. 2020).

Unfortunately, understanding of ecological problems lags behind the development of science and technology (Kazakov 2019). Despite of much progress in understanding land-use effects on soils, practical problems with decreasing soil performance have increased. Many scientists and more and more informed citizens recognize the crucial importance of soil as the basis of human life. Decision-makers and low-resource farmers, however, often neglect the importance of soil resources due to lack of awareness and/or lack of accessible information or tools and resources (Packer et al. 2019; Tamene et al. 2019).

Negative effects of soil’s overexploitation. In the pursuit to increase land productivity, soil is exposed to a permanent overexploitation of its potential (Fig. 1.7). This has led to a wide range of consequences such as accelerated soil erosion processes caused by deforestation and overgrazing, improper irrigation and tillage (Montgomery 2007; Olsson et al. 2019; Gupta et al. 2019; Gajić et al. 2020); loss of top soil layer due to deflation (Zhu et al. 2020); dissection of the terrain due to rill erosion and gully formation (Guo et al. 2019; Hassen and Bantider 2020); loss of fertility due to nutrient mining and leaching (Gupta et al. 2019; Zhang et al. 2020); contamination due to overuse of pesticides, ameliorants, airborne toxic elements, industrial and urban landfills (Khan et al 2018; Steffan et al. 2018; Huang et al. 2019; Gruszecka-Kosowska et al. 2020; Orlova et al. 2017); loss of biodiversity due to use of agrochemicals, excess tillage (Borelli et al. 2017; Guerra et al. 2020); salinization due to improper irrigation, lack of drainage systems (Abdollahpour et al. 2020; Nguyen et al. 2020), overcompaction due to heavy mechanical loads (Arvidsson and Keller 2007; Schjønning et al. 2016; Parkhomenko et al. 2019) and acidification due to misuse of fertilizer and airborne acidic depositions (Jones et al. 2020; Liu et al. 2020). Furthermore, these impacts might cause off-site effects such as sedimentation, siltation and eutrophication of water bodies or enhanced flooding, reduced watershed function, changes in natural habitats leading to loss of genetic stock and biodiversity.

Another indirect effect of the above-listed impacts is the adverse effect on climate via increased carbon dioxide (CO₂) emissions due to accelerated mineralization of soil organic matter (SOM) (Lal 2004; UNDP 2019; Franko and Witing 2020) and nitrous oxide (N₂O) as a result of land conversion (Borelli et al. 2017). Overall, about half of global land used for agriculture is moderately or severely degraded (UN 2015).

Challenges for soil governance and soil science. Within an 11-year period (from 2001 to 2012) production rate of most common crops increased by 13% (Borelli et al. 2017) due to advanced technologies in land management (Foley et al. 2011) and the increased use of fertilizers (Mueller et al. 2012a, b). Sufficient food production requires sufficient area of both arable and pastoral agricultural land, while production of safe and nutritious food requires healthy, fertile and biogenic soil (Blum and Nortcliff 2013).

The area of fertile soils has been decreasing while the area of degraded soils has been increasing as the world's population is growing, expected to reach 9 billion by 2050. Fertile soils have been irreversibly lost by sealing as part of the expansion of cities and other infrastructure. In general, a higher population density is associated with increasing areas of highly degraded soils (Nachtergaele 2000). Very probably, this will trigger social problems such as "ecological" migrations from the most affected regions to regions with low population densities (Bouma and Bajtes 2000). All these trends pose serious challenges and great responsibility for agricultural policy to reduce the human impact on soil and initiate sustainable land management. Scientific technical innovation and decision tools are demanded to support this process.

1.3 Assessment of Soil Performance

1.3.1 Concepts of Soil Fertility, Soil Quality and Soil Health

Which soil states are considered as regular and well performing, which states need to be considered as degraded and which processes lead to

degradation? Answering these questions requires evaluation of concepts of soil performance, including suitable indicators, measurement methods and data, data evaluation scales and thresholds and sustainable technologies of soil management (Blum and Eswaran 2004).

Soil fertility, quality and health are concepts to characterize the performance of soil for meeting its functions for humans. These concepts were developed and became popular in different times and regions, have a different focus in aims and contents, have some overlapping and still coexist.

Soil fertility (SF). Soil fertility is a traditional concept, referring to the ability of soil to sustain plant growth in agriculture. It has been the domain of agricultural plant nutrition and soil science, has been popular for around 100 years, especially in the second half of the twentieth century (Kundler 1989; Patzel et al. 2000). About more than 40 different definitions exist in the German literature (Term: Bodenfruchtbarkeit) of the twentieth century (Patzel et al. 2000), where the degree of human impact on soils and crop yields is the most modifying factor. As harvested crops withdraw nutrients from the soil, their site-specific replacement by fertilization is a key topic of maintaining SF. Soil fertility can also be enhanced through complex practices of fertilization, mechanization, soil water management and best cropping practices (Kundler 1989), leading not only to higher crop yields but to aggradations (e.g. the opposite of degradation) of soil.

Soil quality (SQ). This concept has been developed in the USA and became very popular in the 1990s. As a result of an extended scientific debate, it considered more soil functions than food and fibre production by agriculture. Soil quality is "the capacity of a specific kind of soil to function, within natural or managed ecosystem boundaries, to sustain plant and animal productivity, maintain or enhance water and air quality and support human health and habitation" (Karlen et al. 1997). The broad definition of soil quality includes a potentially wide array of soil functional services, such as environmental, economical, social, physical, biological and chemical. However, in practice, assessment of all soil

parameters that relate to these functions is still impossible. Also, no soil is capable of successfully performing all of these functions (Singer and Ewing 2000). Going from the plausible hypothesis that soil quality is a pillar of environmental quality, Bünemann et al. (2018) pledge for a better operationalization of this concept by specifying targeted soil threats, functions and ecosystem services, developing interactive assessment tools with target users, and consideration of biological/biochemical indicators. Sustainable agricultural soil use has also been a main target of practical approaches to quantify SQ. Soil quality and crop yield potentials depend on soil inherent properties, which change very slowly with time such as soil texture and mineral composition, and dynamic properties such as soil structure, which can, in the short term, be influenced by management (Karlen et al. 1997; Mueller et al. 2010).

Soil health (SH). The concept became popular in the wake of the soil quality discussion in the USA in the late 1990s and still dominates the current scientific debate. The soil is seen as a biological system whose health status must be maintained or restored (Sekera 1943). It is also considered as a promising path of reversing existing soil degradation, and meeting SDG (UN 2015) as long as soil biological processes are better understood (Lehman et al. 2015, 2020). The terms SQ and SH are often used interchangeably. However, SH emphasizes more on soil biological and biochemical processes and methods. Doran and Zeiss (2000) defined soil health as, “the capacity of a specific kind of soil to function, within natural or managed ecosystem boundaries, to sustain plant and animal productivity, maintain or enhance water and air quality and support human health and habitation”. Rinot et al. (2019) proposed to improve the SH methodology by combining the SH with the ecosystem services (ES) concept. Meanwhile, the European Commission has adopted the soil health terminology and will use it for achieving ambitious targets to improve soil’s performance by 2030 (Mission Board 2020). The main goal is to ensure >75% healthy soils, i.e. soils that are able to provide essential ecosystem services, in

each EU member state. Their priority objective is reducing land degradation and restoring 50% of degraded land (Mission Board 2020).

1.3.2 Methods and Indicators of Soil Performance

Characteristic of indicators. Indicators are statistics or units related to changes in the quality or the condition of an object evaluated (Dumanski and Pieri 2000; Eurostat 2019). They provide simplified information, describe the state of specific phenomena and are useful for monitoring changes, providing an opportunity to compare trends and progress over a period of time. The main problem of selecting indicators is that one has to choose those that are suitable and representative for a certain condition, but at the same time, easy to understand and easy to measure on a regular basis (LADA 2013; Xie et al 2020). Soil quality indicators are based on and derived from soil parameters and indices. A soil parameter is a unit of primary information measured directly and quantitatively (i.e. dimensional), while a soil index is a unit of derivative information obtained via empirical models or mathematical calculations (mean, ratio, etc.) and it is non-dimensional (Enne and Zucca 2000). An indicator can be a parameter or index that provides brief and clear information about the condition or process to be assessed, measured and controlled in accordance with a specific goal. An indicator should contain quantitative information on how the processes evolve over time and vary in space, while selection of an optimal set of indicators should be reliable, environmentally and socially relevant, sensitive and cost-effective. An indicator should also be able to translate the present status of soils as well as predict trends of soil loss or change (Bünemann et al. 2018). The most important soil parameters/indicators are usually a subset of the palette of landscape indicators (Mirschel et al. 2020).

Soil state assessment. State indicators give a description of the quantity and quality of physical, chemical and biological phenomena (Smeets and Weterings 1999). Their measurement was

normalized in many standards by ISO TC 190 “Soil Quality” and CEN/TC 444 “Test methods for environmental characterization of solid matrices” (CEN 2020). The use of these standards is essential for comparing soil data. Soil state assessment consisting of soil inventories in different time steps based on constant protocols is common in scientific-based monitoring of soil performance. Soil performance can be assessed by indicators comparing current soil conditions with established control points or baseline values (Snakin et al 1996; Boehn and Anderson 1997). Soil monitoring systems in many countries are based on such state assessment systems (Sychev et al. 2016; Glante et al. 2018; Gubler et al. 2018; Romanenkov et al. 2020). At local levels, participation of landowners, managers and other stakeholders in the development of monitoring systems of soil quality, including degradation aspects, has become an ethical standard over the past years (Schwilch et al. 2018) and is indispensable for achieving significant progress for keeping soil healthy (Bouma 2019b; Mission Board 2020). Indicators and assessment schemes have to be understandable at the field scale.

At a national scale, soil monitoring systems in many countries are implemented by different centres of competence, institutions and authorities and follow different concepts and methods. Yakovlev (2013) developed the principles of ecological regulation of soils, which consist in substantiating the criteria and levels of the permissible ecological state (quality) of soils and anthropogenic impact on them on the example of Russia. On the basis of these criteria and a five-level rating scale of the ecological state of the environment and the impact on the environment, he developed a system of consolidated indicators “state-impact” for soils, represented by uniform relative numerical values.

Although the data are potentially freely available, their practical availability for scientific evaluations and advice is severely restricted. Data collection, analysis, storage, administration and evaluation are usually separated in a disciplinary manner. For example, in Germany, widespread monitoring exists (Kaufmann-Boll et al. 2020) including about 800 soil long-term

monitoring plots on cropland, grassland, forests, long-term field experiments as well as scientific studies on ecosystem monitoring, erosion monitoring, soil carbon and peat monitoring and other topics. There is a German database on soil biodiversity (Edaphobase) and an extended European version is under preparation, called EUdaphobase (Russel and Krogh 2020). Modern data repositories are under construction (Grosse et al. 2020). An international soil health database (SoilHealthDB, Jian et al. 2020) provides information about the magnitude and distribution of 42 soil health indicators and 46 background indicators for cropping regions of the globe, enabling definitions of thresholds and baselines. Rules for health and degradation assessments of grasslands and rangelands were developed by Herrick et al. (2019). There are (at least) two types of activity visible within the EU in the last few years.

- Implementation of EU-wide measurement schemes in order to collect data on the properties of European soils (see also CEN/TC 444), partly by financing respective projects, partly by collecting data in national databases and making them available in JRC databases. These data are then used to either describe the state-of-the-art or to predict further developments (e.g. including publishing these activities in order to prove that there is a need in the real world, e.g. Yigini and Panagos (2016)).
- Promoting soil issues have been neglected so far, not just in Europe but actually on a global scale. One example of this kind of activity is the publication of reports (e.g. Turbé et al. 2010) and even more attractive and highly successful in the form of atlases, e.g. for Europe (Jeffrey et al. 2010).

The US systems of soil quality and soil health assessments. Doran and Parkin (1994, 1996) developed soil state indicators of soil quality/health assessment for measuring and evaluating soil functions. These indicators needed to meet the criteria of reflecting ecosystem processes, include soil physical, chemical and biological properties and are sensitive to

management and climate factors (Doran and Parkin 1996). On their basis, the Natural Resources Conservation Service of the United States Department of Agriculture developed, adopted and recommends tools and procedures for soil health and quality assessment, applicable to science and practice (USDA/NRCS 2020). Soil Quality Indicators are identified for characterising physical, chemical and biological soil properties (Table 1.2) that support potentially different functions. Practically, the productivity function is the focal aim and most common cause of application.

The Soil Management Assessment Framework (SMAF, Andrews et al. 2002) supports the selection of relevant soil functional and site-specific indicators and the computation of an overall soil quality (SQ) index based on dimensionless scoring functions from data of soil physical, chemical and biological indicator sets (Wienhold et al. 2009). SMAF was updated over recent years by including more chemical and biological parameters and was applied to other regions such as Southern Brazil or South Africa (Karlen et al. 2019; da Luz et al. 2019; Gura and Mnkeni 2019). The College of Agriculture & Life Sciences at Cornell University (New York, USA) has developed Comprehensive Assessment of Soil Health (CASH) protocols and offers analyses of CASH indicators and scientific advice in soil health assessment to farmers and other clients (Moebius-Clune et al. 2016; Soil Health Team 2020). A Soil Health Database has been developed for meta-analyses of soil health changes related to cropland conservation management (Jian et al. 2020).

Williams et al. (2020) applied the CASH methodology on 20 farms in south Sweden and found lower SH indexes of farm fields in comparison with unmanaged soil. Improved soil management through higher crop diversity, less mechanical soil disturbance and higher organic matter inputs improved soil health (Williams et al. 2020). This study confirmed the suitability of the mentioned SH state indicator methods for scientific studies.

Soil state indicator systems as shown in Table 1.2 and being part of the SMAF and

CASH approaches are step forwards to recognizing the performance and deficiencies of soils. Evaluation scales and thresholds indicating whether soil is degraded are available for a few indicators, for example, pH and EC indicating acidification and sodification and salinization, respectively. Some more work is needed to develop the scales for the majority of other methods recommended here. Just biological properties and methods are partly very specific and have still unknown variability over space and time, requiring further studies (Wander et al. 2019). Also, it needs to be mentioned that methods developed by now are country specific and rarely comparable. Stronger efforts towards international studies for developing conversion rules and algorithms and international standards would be useful (Römbke et al. 2006, 2018; Höss and Römbke 2019; Jänsch et al. 2019; Thiele-Bruhn et al. 2020; Batjes et al. 2020).

Overall, the review shows that a comprehensive assessment of soil performance using the methodologies recommended by the USDA/NRCS is the domain of specialists. As some analyses are time-consuming, they require special laboratory analyses or can last some hours in the field (for example, steady-state field infiltration) to some weeks (for example, analyses of organic matter and carbon fractions) before reliable results for representative observation points will be available to clients. Also, field inspection and sampling are often decoupled from the analysis and assessment of data.

Field methods of assessing soil performance. Some scientists take the view that a single field inspection should provide a good estimate of soil quality/soil health. This view is related to the proven family doctor principle in human health care. The “soil doctor” must have good and comprehensive education, skills and experience, some modern fast-operating diagnostic equipment, and be well interlinked with acknowledged specialists and laboratories.

Examples of those field express methods are the SOILpak methods (McKenzie 1998, 2013), Visual Soil Assessment Method (VSA, Shepherd 2000, 2009) and the Muencheberg Soil Quality Rating (M-SQR, Mueller et al. 2012a, b, 2013,

Table 1.2 State indicators of soil quality/health recommended by the USDA (USDA/NRCS 2020)

Indicators are reflecting	Indicator	Remarks on methods
Physical properties	Aggregate stability	Field/lab, test kit
	Available water capacity	Special laboratory
	Bulk density	Cylindrical core method, laboratory
	Infiltration	Steady infiltration rate, field method
	Slaking	Slake test, field kit
	Soil crusts	Field method
	Soil structure and macropores	Descriptive field method
Chemical Properties	Reactive carbon	Laboratory, potassium permanganate oxidation method, also NRCS Active carbon field test kit
	Soil electrical conductivity	Measure of salinity, EC pocket metre
	Soil nitrate	Field test strip
	Soil pH	Portable pH pocket metre
Biological properties	Earthworms	Field methods (abundance, biomass, diversity), but lack of other groups of soil invertebrates
	Particulate organic matter	Laboratory, time-consuming
	Potentially mineralizable nitrogen	Different special laboratory methods
	Soil enzymes	Different laboratory methods using biochemical assays
	Soil respiration	Different commercial field test kits available
	Total organic carbon	Special laboratory methods

2016). Indicators of visual recognizable soil structure like demonstrated in Fig. 1.8 are in the focus of these methods. Further soil structure assessment methods were developed and locally adapted (Murphy et al. 2013; Newell-Price et al. 2013; Pulido Moncada et al. 2014; Emmet-Booth et al. 2019). Development of these methods was inspired by the Visual Examination of Soil Structure (VESS) developed by Ball et al. (2007, 2017) and its preceding approaches. Methods are related to the productivity function of soil and are based on expert knowledge in terms of field manuals and simple field procedures of in situ measurement and evaluation (Mueller et al. 2014). Existing soil regular and thematic maps and data (status of nutrients, contaminants, crop

yields, smart-farming maps, climate, cadastral data, etc.) should be used as basic and supporting information. This is important because climate factors in terms of temperature, precipitation and evapotranspiration determine the soil temperature and moisture regime of soils and thus the most important biophysical processes of plant growth and decay worldwide.

While SOILpak and VSA focus on dynamic aspects of soil quality in terms of soil structure parameters, M-SQR includes indicators reflecting both dynamic, soil inherent and climate parameters, thus enabling a functional fingerprint of soil's performance for cropping and grazing. Rating tables of M-SQR hazard indicators give information about soil states being considered as

degraded. M-SQR also provides rating scores for the overall soil quality, which are correlated to crop yields both on regional and global scales (Smolentseva et al. 2014; Hennings et al. 2016; DWA 2018).

The soil testing method manual of the FAO (FAO 2020b) also orientates field methods for advising and educating farmers. Besides visual-tactile methods, vegetation analyses, simple devices of soil survey (Mueller et al. 2014) and field measurement kits (Table 1.2) serve as indicators of soil quality/health. Further field procedures for soil health assessment compatible with the SH assessment system of the USDA/NRCS (United States Department of Agriculture/Natural Resource Conservation Service) have been developed and tested (Thomsen et al. 2019). Those field methods of soil structure and/or overall soil quality are also the domain of experts. However, they enable participatory assessments of SQ/SH over some sampling points in quasi-real-time and provide ad-hoc results for all participating stakeholders.

SQ/SH assessment for more functions than soil productivity. To assess changes of soil at a complex level, e.g. as tools for decision making and considering causes of changes and consequences for the society, more comprehensive approaches for evaluating the multifunctional performance of soils are necessary. The DPSIR approach is a proven and popular indicator model for monitoring environmental processes in Europe at complex level, for example, for the Pan-European assessment and monitoring of soil erosion (Gobin et al. 2004). DPSIR is the abbreviation for **D**iving forces, **P**ressures, **S**tates, **I**mpacts and **R**esponses.

Soil functional indicators are important elements of Life Cycle Analysis (LCA) models (Roesch et al. 2019; Thoumazeau et al. 2019; Sonderegger et al. 2020). Soil databases and algorithms for a flexible mapping of purpose-targeted soil indicators have been developed (Panagos and van Liedekerke 2008; Makó et al. 2017).

Schulte et al. (2014) worked up a framework for managing soil-based ES for the sustainable intensification of agriculture which, besides

productivity function, considered the functions of water purification, carbon sequestration, habitats for biodiversity and recycling external inputs. Similar ideas have already been proposed by Gardi et al. (2009) and were afterwards checked within the EU project EcoFINDERS, focusing both on the diversity of individual organism groups as well as specific ecosystem functions (Griffiths et al. 2016; Faber et al. 2020). The comprehensive approach of Schwilch et al (2018) includes definition and quantification of several provisioning, regulating and cultural ES from the natural capital of numerous locations characterized by soil threats. ES were used then as indicators for a state assessment and a 10-year scenario at field plot level.

Drobnik et al. (2018) developed an overall soil quality index for special planning by combining soil functions with ecosystem services. Van Leeuwen et al. 2019 created a decision expert model (DEX model) to quantify the capacity of a soil to supply the function of soil biodiversity and habitat provision (SB function). They defined a biodiversity function of soil and an indicator system based on soil attributes of nutrient status, biological status, structure and hydrological status. To develop decision tools for society, approaches and methods in SQ evaluation have been constantly updated.

Despite the progress made in the quantification of soil performance, there remain great knowledge gaps in understanding complex functional processes in soils, plant–soil–biota interactions and relationships between soil biodiversity and biogeochemical function across a range of ecosystems in particular (Jänsch et al. 2019; Wander et al. 2019; Chen et al. 2020).

1.4 Soil Degradation

1.4.1 Definitions and Concepts of Assessment and Monitoring

Essence and definition. The FAO defines soil degradation “as a change in the soil health status resulting in a diminished capacity of the



Fig. 1.8 Examples of visual-tactile methods of soil structure as semi-quantitative indicators of soil quality/health in the frame of existing evaluation schemes. **a** Favourable soil aggregates in a cropping systems, **b** unfavourable aggregates on same site, **c** soil slaking and crusting with implications for water and gas exchange

between soil and atmosphere, **d** re-arrangement of aggregates after a drop-shatter test of the VSA procedure (Shepherd 2000), **e** favourable naturally crumbly structure of a Chernozem, **f** coarse columnar structure of a Solonetz. *Photos* L. Mueller

ecosystem to provide goods and services for its beneficiaries” (FAO 2020a, b). The terms “land degradation” and “soil degradation” are often used interchangeably as most authors agree that any degradation of soil is reflected in land degradation and often vice versa. Monitoring and assessing soil is, thus, a proper measure for sustainable development and achieving land degradation neutrality (Tóth et al. 2018). This is a challenging task as clear limits or thresholds identifying when soils or land are being degraded do not exist. From a local perspective, falling crop yields are seen as indicators of land degradation (Stocking and Murnaghan 2002). Soil and land degradation are the result of interactive processes of humans with nature. Multiple factors of soil, climate, land-use, economic dynamics and sociodemographic forces play a key role (Salvia et al. 2019).

Another term very closely related to soil and land degradation is desertification. Desertification is degradation of drylands (Dregne 1977), the worst case of soil degradation because it is very difficult to stop and to combat it. Desertification was defined by experts of the United Nations in 1977 as “the diminution or destruction of the biological potential of land” and can lead ultimately to desert-like conditions. It is an aspect of the widespread deterioration of ecosystems, and has diminished or destroyed the biological potential, i.e. plant and animal production, for multiple use purposes at a time when increased productivity is needed to support growing populations in quest of development” (UNEP 2020). The United Nations Convention to Combat Desertification (UNCCD 2012) defines desertification as “land degradation in arid, semi-arid and dry sub-humid areas resulting from various factors, including climatic variations and human activities”. This process is interlinked with other threats to nature and society such as biodiversity loss and poverty, all strong obstacles to meet the sustainable development goals of the UN (IPBES 2018).

Disadvantage of the term “soil degradation”. The use of the term “soil degradation” does not allow any clear interpretation. This arises from a disciplinary perspective and even

from a sub-disciplinary perspective in soil science. In soil genetics, the term “degraded” is used when a soil type develops due to changing environmental conditions and management in the direction of another soil type. Degraded chernozems (leached chernozems), which develop from chernozems under more humid conditions, are known (Nikiforoff 1937). In this case, the term “degraded” has no functional meaning. Assessments can be even more contradictory if changes in soil properties due to use lead to changes in soil functions. It is more the rule than the exception, that one soil function is enhanced but another diminished. The productivity function and the biodiversity function mostly develop in opposite directions in the course of agricultural use. Then a disciplinary assessment decides whether the soil development is described as positive (aggraded) or negative (degraded). This discourse often arises in debates about the use-related change in hydromorphic soils with wet humus accumulation after drainage. Wetland conservationists refer to this development of peat soil as degradation, though crop-yield relevant soil parameters are not diminished (Schindler et al. 2003). Agriculturists value the improved productivity function of drained peat soils.

In the literature, there are many other definitions and concepts of soil and land degradation (Eswaran et al. 2001; IPCC SRCCL 2019). Some of them seem to be timeless and universal. However, all definitions need to be interpreted according to their purpose and temporal and local scale.

Attempts to quantify soil degradation. The GLASOD (Global Assessment of Soil Degradation) methodology was developed and coordinated about 30 years ago by the International Soil Reference and Information Centre, ISRIC, the Netherlands (Oldeman 1992), leading to global maps of about 1:10 million scale. This approach was based on existing soil and topographic maps and supplemented by expert-based regional and countrywide information. The underlying working definition of soil degradation (SD) was that “Soil degradation is defined as a process which lowers the current and/or future capacity of the soils to produce goods or

services” (Oldeman 1992). Different types of degradation, the degree, the relative extent and causative factors of soil degradation were specified and delineated (Oldeman et al. 1990). Later, this methodology was refined and applied to specific regions (FAO 1994; Oldeman and van Lynden 1998). At this time, it remains the only basic and globally consistent information source on land degradation, which covers the whole area of the globe (Gibbs and Salmon 2015). GLASOD estimated 1216 million hectares worldwide while estimates of other scientists cover a huge range from about 470 to 6140 million hectares (Gibbs and Salmon 2015).

The GLASOD study and consecutive regional studies were intended as information for national action plans, including novel concepts in researching and monitoring soil changes, studying the driving forces and economic and social effects on local people and developing plans to halt degradation and desertification. Later studies utilized the great potential of enhanced and fast-developing remote-sensing methods and other geospatial technologies in combination with geographical information systems (Bai et al. 2008; Vågen et al. 2016; Dubovyk 2017; Dwivedi 2018; Panagos et al. 2020) and the open availability of high-resolution data and modelling tools (Eberle 2019; Giuliani et al. 2020).

Many regional and local experimental and modelling studies have been initiated to better understand the most relevant degradation and desertification processes at regional and local levels. Novel measurement systems were constructed, novel experimental setups generated, new data were obtained and understanding of the nature and magnitude of single degradation processes, as well as mitigation and combating strategies at farm and regional scales has increased were achieved. Examples are experimental and modelling studies of wind erosion (Funk et al. 2016; Zhu et al. 2020; Jarrah et al. 2020; Webb et al. 2020), water erosion (Chumbaev and Tanasienko 2016; Prasuhn 2020), soil compaction (Arvidsson and Keller 2007; Schjønning et al. 2016) and many others (Kosmas et al. 2014). In some EU countries, every single agricultural field has been classified

regarding its risk of water and wind erosion (Steininger and Wurbs 2016). However, soil degradation state monitoring at the field level in the framework of soil quality/health assessment for soil functions does not yet exist.

1.4.2 Soil State Indication on Degradation and Desertification

Functional soil state indication on degradation, which is compatible with the soil quality/health concept as a basis for participatory decisions at regional and local levels, would be desirable. However, such concepts only exist to some extent (Virto et al. 2015).

Attempts to create a soil threat monitoring at EU level. A soil monitoring project for countries of the EU had been developed and tested 15 years ago in the framework of the ENVASSO project (Environmental Assessment of Soil for Monitoring) (Kibblewhite et al. 2008; Huber et al. 2008). It was an attempt to create a regular soil monitoring system, which provides reliable data at intervals of several years based on key indicators and harmonized national and regional approaches to measure and characterize soil degradation. The approach was based on the DPSIR concept, but the majority of indicators are state indicators. Tables 1.3, 1.4, 1.5 show the main threats identified and top three indicators selected by the international team of experts.

ER = Water, wind and tillage erosion, OM = Decline in Soil Organic Matter, SE = Soil sealing, land consumption and brownfield redevelopment, CP = Soil compaction and structural degradation, BI = Soil biodiversity, LS = Landslide activity, DE = Desertification. Dryness index = (annual precipitation)/(annual potential evapotranspiration), NA = not yet available, site-specific, CLC = Corine land cover, Calc = Calculation: average of 5 years out of the last 20 with the smallest area burnt annually (km²), DM = Dry matter

Table 1.3 demonstrates that except for soil erosion, no clear baselines and thresholds in terms of absolute data could be quantified. For

Table 1.4 Range of background concentrations and thresholds of heavy metals for soil in different European soils/regulations or recommendations (data from Huber et al. 2008)

Heavy metal	Range of contents (mg kg ⁻¹ dry soil)	
	Background concentrations	Thresholds
Cadmium (Cd)	0.07–1.48	0.4–3
Lead (Pb)	9–88	40–300
Chromium (Cr)	5–68	30–100
Copper (Cu)	2–32	20–140
Mercury (Hg)	0.02–0.29	0.1–2
Nickel (Ni)	3–48	15–75
Zinc (Zn)	6–130	60–300

Table 1.5 Baseline and threshold values for indicators of salinization and sodification (data from Huber et al. 2008)

	Indicator	Input	Units	Baseline	Threshold
Salinization	Salt profile	Salt content (total)	%	<0.05	>0.10
		Electrical conductivity (EC)	dS m ⁻¹	<2	>4
		Depth	cm	0–150	0–30...50
Sodification	Exchange able sodium percentage	pH		5–8	>8.5
		Exchangeable sodium percentage (ESP)	%	<5	>15
		Sodium absorption ratio (SAR)		<4	>10
Potential soil salinization/sodification	Potential salt sources	Salt concentration of irrigation water	mg l ⁻¹	<500	500–2000
		EC of irrigation water	dS m ⁻¹	<0.5	0.5–5
		SAR of irrigation water		<4	
		Salt concentration of groundwater	mg l ⁻¹	<500	1000
		EC of groundwater	dS m ⁻¹	<0.5	
		SAR of groundwater		<4	>10

soil threats associated with the complex biological system, such as soil biodiversity and organic matter decline, knowledge about possible baselines and thresholds was particularly missing. Meanwhile, some progress has been made regarding biological systems (e.g. by using earthworm abundance and/or diversity both in general monitoring efforts) (see Beylich and Graefe 2009; ISO 15799:2019-11 2019; ISO 17616:2019-11 2019) as well as in the area of chemical regulation (Dinter et al. 2013). Also,

processes of soil compaction and soil structure deterioration, though already well quantified in disciplinary studies, are not yet expressed by quantitative baseline data and thresholds. As machinery loads are permanently increasing and effects on soil compaction depths and intensity are already well understood and quantified on most soils (Keller et al. 2019) the inclusion of a simple pressure indicator such as axle load or total machinery weight could be taken into consideration. The continued advances in

machinery, e.g. the introduction of four-wheel drive tractors, have meant that steeply sloping land not previously cultivated is now being used for crop production. Change in land use from pasture to cropping further exacerbates risks such as tillage erosion (Kouselou et al. 2018). In contrast, a lot of theoretical and practical knowledge has been accumulated on soil indicators that can be measured by chemical analyses, such as heavy metals (Table 1.4) and salinity/sodicity (Table 1.5). It became clear that regionally specific thresholds are useful and possible because of the large spatial variability of background concentrations, depending on soil parent material, soil texture, pH of soil and historic land use. An overview of threshold values is available (Carlon 2007).

It is also visible that three indicators per threat were not enough. When coming to monitor soil degradation over a broader range of scales, down to regional and field level, much more than three indicators (like had been desired in the ENVASSO project) are required to characterize a single soil degradation process adequately. Based on a comprehensive data set from field sites in 17 global regions of high soil degradation and desertification, Kosmas et al. (2014) derived the most important indicators by multivariate statistical methods. They found that between 6 (Tillage erosion) and 14 (Water erosion) indicators affected processes significantly (Kosmas et al. 2014).

A comprehensive analysis by Virto et al. 2015 revealed that soil degradation is on the rise in countries of the EU, while work of addressing, regular monitoring and combating these threats are stagnating. From a legislative perspective, water and air receive much more attention than soil (McBratney et al. 2014). Logically, despite all progress during the past decades, but related to other threats and issues of the Anthropocene, public awareness of soils and their research and monitoring remain still undervalued, deficitary and patchy. A field indicator system for soil degradation that is comparable and compatible with the soil health/quality approach does not yet exist (Virto et al. 2015). It would be a challenging task to initiating work of an operating monitoring

system of soil degradation, which matches with the soil quality/soil health approach.

Advances in soil functional modelling and the need for indicators and data. Soil functional modelling can be used to quantify soil degradation. There has been much progress in modelling and forecasting soil processes and agroecosystems, their productivity and other functions (Ascough et al. 2002; Mirschel et al. 2020). Ecosystem modelling is an emerging branch in knowledge generation and decision support. A crucial part of this is models describing soil–water–atmosphere interactions and crop growth (SWAT models).

Innovative ecosystem models require reliable data provided by smart sensor technologies, soil information systems at several levels and other high-resolution data including weather and vegetation data. They are often coupled with field observatories or research sites where those detailed data are available. Where data are insufficient to allow for the multiple possible permutations and it may be possible to include expert knowledge using Bayesian Belief Networks. For example, Troldborg et al. (2013) used this approach to map areas at risk of soil compaction. This approach, however, does require access to several soil scientists with experience in both threat and soils as well as the availability of good soil survey information.

Simple indicator-based GIS models are another option to create current spatial or spatiotemporal information and to forecast future states. Regionalized field data of soil functional properties based on pedotransfer functions enable a consistent modelling of soil functional processes such as groundwater formation, crop productivity potentials, the dynamics of soil organic matter and risks of soil pollution from field scale up to large regions (Hennings 2014; Hennings et al. 2016; Badenko et al., 2020; Franko and Witing 2020; Trapp et al. 2020).

Three further examples, demonstrating the usefulness of relatively simple spatial data for scale-embracing modelling of specific soil degradation risks, are given here. Panagos et al. 2020 modelled water erosion across the EU on the basis of a European version of the Revised

Table 1.3 Top three indicators for monitoring soil threats in the European Union (EU), data from the ENVASO project (Huber et al. 2008, modified)

Soil threat	Indicator	Unit	Baseline	Threshold
ER	Estimated soil loss by rill, inter-rill and sheet erosion	t ha ⁻¹ year ⁻¹	0–5 t ha ⁻¹ year ⁻¹	1–2 t ha ⁻¹ year ⁻¹
ER	Estimated soil loss by wind erosion	t ha ⁻¹ year ⁻¹	0–2 t ha ⁻¹ year ⁻¹	2 t ha ⁻¹ year ⁻¹
ER	Estimated soil loss by tillage erosion	t ha ⁻¹ year ⁻¹	0–5 t ha ⁻¹ year ⁻¹	2 t ha ⁻¹ year ⁻¹
OM	Topsoil organic carbon content (measured)	%	NA	NA
OM	Soil organic carbon stocks (measured)	t ha ⁻¹	NA	NA
OM	Peat stocks (calculated or modelled)	Mt	NA	NA
SE	Sealed area	ha and ha y ⁻¹	Area and growth rate	Policy judgement
SE	Land take (CLC)	% of initial status or ha	Reference year	Threshold < baseline
SE	New settlement area established on previously developed land	%	Area and growth rate	Thresholds > baseline
CP	Density (bulk density, packing density, total porosity)	g cm ⁻³ or t m ⁻³ ; %	NA	NA
CP	Air-filled pore volume at a specified suction	%	NA	NA
CP	Vulnerability to compaction (estimated)	Classes	NA	NA
BI	Earthworms diversity and fresh biomass	Number m ⁻² , g fresh weight m ⁻²	NA	NA
BI	Collembola diversity (Enchytraeids diversity if no earthworms)	Number m ⁻²	NA	NA
BI	Microbial respiration	g CO ₂ kg ⁻¹ soil (DM)	NA	NA
LS	Occurrence of landslide activity	ha affected	0 ha ha ⁻¹	≥ 0.1 ha ha ⁻¹
LS	Volume or mass of displaced material	m ³ of displaced material	0 m ³	≥ 0 m ³
LS	Landslide hazard assessment	Variable	No hazard	Dependent on model used
DE	Vulnerability to desertification	Area of aridity index <0.75, km ²	Desertified area (km ² or %)	Desertified area as a proportion of the potential (km ² or %) aridity index ≤ 0.5
DE	Wild fires (burnt land area)	km ² year ⁻¹	Calc	<30% above baseline
DE	Soil organic carbon content in desertified land	g kg ⁻¹	NA	% change in last 15 or 20 years

Universal Soil Loss Equation (RUSLE). A quarter of the EU lands, mainly located in the south, had higher erosion rates than the sustainable threshold (2 t/ha), and about 6% of soils had severe erosion (>11 t/ha) (Panagos et al. 2020). Results indicate enhanced efforts to reduce soil degradation through better soil conservation achievable within the framework of improved Common Agricultural Policy (CAP) regulations.

Based on a national standard (DIN 19, 706:2013–02 2013), Steininger and Wurbs (2016) elaborated a uniform methodology for assessing the wind erosion risk of all agricultural fields in Germany based on spatial soil, climate, vegetation, management and landscape structure data. Yue et al. 2019 developed a data-mining-based approach to mapping aeolian desertification based on spatially available data of climate, vegetation and soil. Inputs were mean annual precipitation, aridity index, wind speed, vegetation index and an off the grid-soil erodibility index.

Desertification monitoring. An inventory of the IPCC on the current state of knowledge of desertification in the context of climate change (Mirzabaev et al. 2019) revealed that the Aridity Index (AI) based on regionalized climate data and the Normalized Difference Vegetation Index (NDVI) calculated from remote sensing data are the most common indicators for assessing desertification status and risk at regional and global scales. Soil data do not play a pivotal role in this monitoring. Also, assessments are not underpinned with compatible indicators and data at sub-regional and local levels. Olsson et al. (2019) state there is no coherent and systematic global inventory of land degradation. They demand regionally differentiated sustainable land management strategies, which need to be implemented and adequately monitored.

In former studies, about 40–50 years ago, FAO and United Nations Environmental Programme (UNEP) had supported studies of desertification at field levels. They yielded in recommendations and thresholds (Table 1.6) to

classify desertification and developing on-farm and regional combating strategies (Stocking and Murnaghan 2002). They lost importance in theory and practice because remote-sensing and GIS technologies evolved (Verón et al. 2006).

Table 1.6 shows that these classifications are based on measured field data. Data sets are not free from contradictions between single indicators, but can serve as a reliable decision basis for functional soil maps at local and regional levels. Those indicators and data should become part of modern soil information systems and databases, supporting models for different purposes. They enable the computation of synthetic indexes (complex indicators) such as the Environmentally Sensitive Area Index (ESAI) based on indexes of soil quality, climate, vegetation and land management usable in DSS for characterising and functional mapping land degradation and desertification risks (Salvia et al. 2019) consistently over large regions (Salvati et al. 2009; Salvia et al. 2019) and are the basis for other complex indicator schemes considering soil quality, climate, vegetation and management (Sommer et al. 2011; Lee et al. 2019).

Participatory processes of governing and revitalizing rural regions such as environmental impact assessment (Cashmore 2004), landscape planning (De Montis 2014; Trovato and Ali 2019) and partial or other related procedures of them such as landscape character assessment (Bartlett and Milliken 2019), land consolidation (FAO 2003), and landscape conservation design (Campellone et al. 2019) cannot be based on downscaled regional soil data but require local data characterizing the performance of soils at landscape level by those indicators shown in Table 1.6. These participative procedures include spatiotemporal information of soil's degradation and desertification at current state and model-based future scenarios. Those indicator-based models must be interlinked with more detailed data-intensive process-based models such as agroecosystem models (Mirschel et al. 2020).

Table 1.6 Field-based criteria of vegetation, water erosion and salinization for the evaluation of desertification status (proposed by FAO/UNEP 1984, quoted by Verón et al. 2006, excerpt, modified)

Variables	Class limits			
	Slight	Moderate	Severe	Very severe
Vegetation				
Perennial plant cover (%)	>50	50–20	20–5	<5
Grassland (%)	>75	50–75	20–50	<25
Actual productivity (% potential)	85–100	65–85	25–65	<25
Water erosion				
Surface status (% area)	Gravel and stones < 10	Stones and boulders 10–25	Boulders and rocks 25–50	Boulders and rock outcrops > 50
Type of erosion	Slight to moderate in sheets and rills	Moderate to severe in sheet and rills	Severe in sheet, rill and gully	Very severe in sheets, rills, and gully
Exposed sub-soil (% area)	<10	10–25	25–50	>50
Gully area (%)	<10	10–25	25–50	>50
Soil thickness (cm)	>90	90–50	50–10	<10
Soil loss (%)				
Original soil depth < 1 m	<25	25–50	50–75	>75
Original soil depth > 1 m	<30	30–60	60–90	>90
Actual productivity (% potential)	85–100	65–85	25–65	<25
Salinization				
Morphology	No salts	Salt spots	Salt spots and filaments	Crystalline efflorescence and salt crusts
Soil electrical conductivity (dS/m)	<4	4–8	8–16	>16
Exchangeable sodium (%)	<5	5–20	20–45	>45
Crop yield (% potential)	85–100	65–85	20–65	<45
Affected areas (%)	<5	5–20	20–50	>50

1.5 Towards a Comprehensive Field Diagnostic System of Soil Performance

Challenges of keeping overview and secure data quality of complex monitoring systems.

From soil indicator data sets, it is known that indicators are intercorrelated with others, requiring minimum data sets of soil indicators (Doran and Parkin 1996; Andrews et al. 2002; Arshad and Martin 2002). Use of existing information about soil functions from soil maps and databases is possible, but as some soil attributes and qualities (dynamic soil quality) alter in the relative short-term depending on management, actual soil data are required. Soil health cluster analysis revealed that soil classes from topsoil properties were more related to land use (soil phenofoms) than soil map classifications (soil genoforms) (Seaton et al. 2020).

Multicollinearity of data, autocorrelations of spatial data, and trends in time series are a challenge for advanced multivariate statistical method of data analyses. Principal component analysis (PCA) and complex Analytic Hierarchy Processes which reveal in consistent minimum data sets (MDS), weight and scoring function for different locations, studies and management are needed (Xue et al. 2019).

The awareness about the crucial role of soils for ecosystem functioning (Adhikari and Hartemink 2016) and their multifunctionality has led to the fact that soil indicators are part of ecosystem indicator systems and are applied for ecosystem monitoring, landscape planning and other purposes (Schwilch et al. 2018; Van Leeuwen et al. 2019; Drobnik et al. 2020). As different ES can be derived from the same soil data, this problem of multicollinearity and reliability of data can be exacerbated. Over the past years, a Common International Classification of Ecosystem Services (CICES) has been worked out, which updates, describes, codes and classifies ecosystem services for all users (Haines-Young and Potschin 2018). The growing list in its hierarchical structure poses questions about

reliability and clarity of those complex indicator systems.

Is a quantification of soil-based ES in terms of economic valuation possible? Attempts have been made, e.g. Bartkowski et al. (2020). Other scientists (Baveye et al. 2018) argue that the ES concept complicates the measurement and quantitative prediction of a number of the services and does not reflect stakeholders' concerns.

Is the status of an ecosystem still in acceptable limits if single soil indicators have changed significantly and are driven beyond thresholds? Is a certain technology or control measure sustainable because a single ES derived from soil indicators has been markedly improved? Which soil indicators perform best in those complex systems? These questions are still open. Significance rules for multiple indicator/ data sets need to be elaborated.

Complex ES information can be debated in comprehensive studies but is not useful for participatory stakeholder processes on-site. On-site stakeholder's concerns are more related to soil and vegetation. "Hard" soil measurement data can disappear in the confusion of complex ES service systems and become less important than estimated data (Baveye et al. 2018). Directly measurable indicators and data are required that have a relationship to the known world of experience of the stakeholders, i.e. can be sensed, are visible, tangible and smellable and directly linked to observations of ecosystem processes such as plant growth and yield and animal prosperity.

There is some hope that field methodologies of soil measurements and evaluation methods could play a greater role again. Statistical tests for robustness, spatial and temporal variability and expected rate of change of physical SQIs regarding their capacity to deliver ecosystem goods and services (Corstanje et al. 2017) revealed a preference of the following indicators: soil packing density, soil water retention characteristics, aggregate stability, rate of soil erosion, depth of soil, soil structure (assessed by visual soil evaluation) and soil sealing (Corstanje



Fig. 1.9 Joint evaluation of the soil functional status during a meeting of soil scientists with agronomists, economists and practitioners. *Photo* L. Mueller

et al. 2017). All these are either field indicators, are measurable from simple field sampling, or in case of certain ranges of the water retention curve (soil drier than field capacity), they can be derived from field diagnostic properties using pedotransfer functions (Schindler et al. 2004).

On-site measurements and assessment of soils for learning and participatory decision processes.

Agriculture is the largest user of land and soil worldwide but public attention and funding for education and science of agriculture and rural landscapes are declining (Evans 2019; Mueller et al. 2021) Thus, the number of people who are capable to interact with the soil in the field and in the landscape at a high educational level must be stabilized and grown. Improved interaction of soil scientists with scientists of adjacent disciplines and stakeholders has growing importance for obtaining significant research results that can

be applied in the field (Bouma 2019b; Mission Board 2020). It is a kind of transdisciplinary research and debates in the field while looking at the soil profile are the best arena for this. This puts much more focus on touching the ground, and using field measurement methods and field indicators as shown in Table 1.6.

On-site soil information (Fig. 1.9) should start with an allocation of a specific soil in the landscape, explain processes of soil formation (climate, parent material, vegetation, anthropogenic impacts) and a name-giving soil classification based on genetic horizons and diagnostic material. Besides local and national and soil classification, an internationally comparable soil name based on the World Reference Base for Soil Resources (IUSS Working Group WRB 2014) needs to be given.

On land in agricultural use, the main soil function of productivity can be assessed by

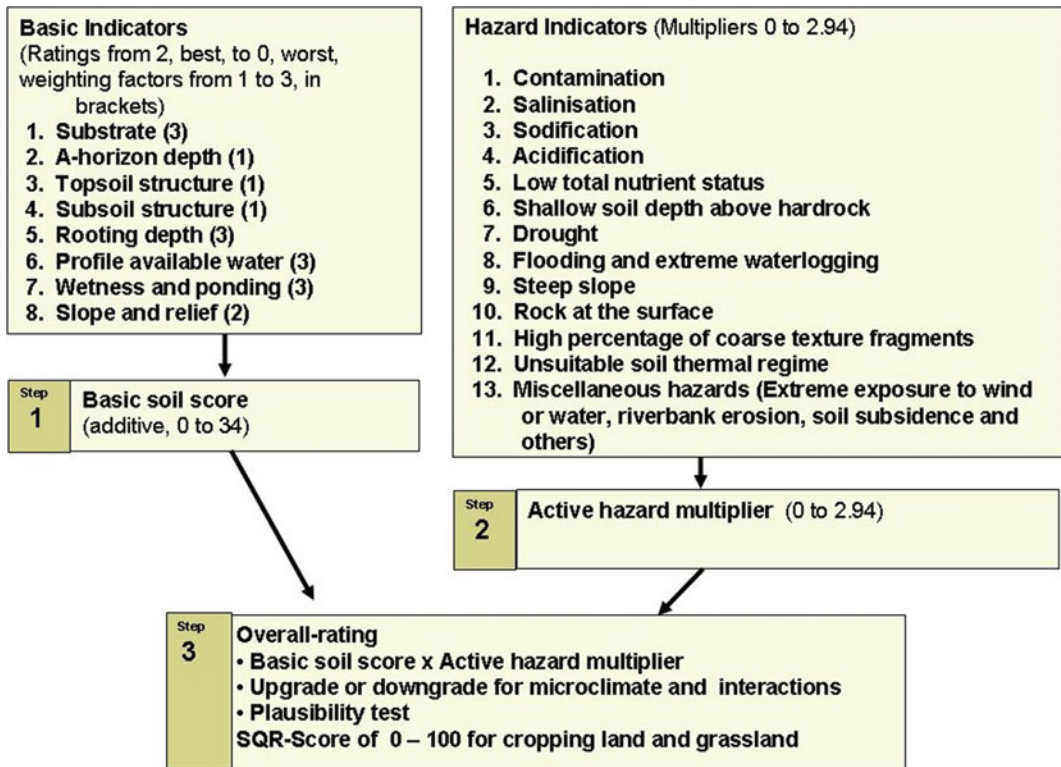


Fig. 1.10 Indicators and rating scheme of the Muencheberg Soil Quality Rating (M-SQR), a fast method for rating soil productivity potentials. Source: Mueller et al. (2016). The method is recommended by Mueller et al.

(2016) being applied in the field in combination with the World Reference Base for Soil Resources (WRB, IUSS Working Group WRB 2014)

application of national soil rating (bonitation) schemes and of the Muencheberg Soil Quality Rating procedure, based on a handbook of 2007 (M-SQR Manual 2007) and several updated rating tables shown in Mueller et al. (2016). By now, M-SQR is the only soil evaluation method, applicable to the majority of croplands and grasslands worldwide. The soil profile will be scanned by indicators shown in Fig. 1.10. Hazard indicators characterize soil degradation factors and other threats to soils that can drastically diminish the soil quality and crop yield potential.

Besides soil genetic classification (provided by WRB 2014) and productivity-functional classification (provided by M-SQR), other soil functional evaluations, field express methods characterizing these functions (Mueller et al. 2014; Wessel-Bothe and Weihermüller 2020),

field test kits and soil sampling for special analyses are advisable. New sensor technologies such as electrochemical sensing combined with ion-selective membrane-based transducers made applicable for quick in situ monitoring of soil chemical parameters (nitrate, phosphate, potassium) are in progress (Ali et al. 2020). Modern field diagnostic tools such as electronic field books, images of landscape and vegetation heterogeneity made by unmanned aerial vehicles (UAV's) (Florinsky 2016; Ivushkin et al. 2019; Olenin et al. 2020) can support the process of express on-site soil functional and threat evaluation.

Recent international studies confirm that visual field assessment methods of soil quality/health in combination with quick diagnostic measurement methods and background regional and local site data are proven tools for

assessment of management practices (Alaoui et al. 2020). They largely meet the experience-based perceptions of farmers and other local stakeholders, and they are particularly valuable for participatory studies. Installation and application of those technologies require scientific protocols, guidance and training of extension specialists, otherwise the results can be ambiguous (Andersson and Orgill 2019).

1.6 Conclusions

1. Soil degradation is a collective term for many complex phenomena diminishing the functionality of soils. In many cases, such as wind and water erosion, salinization and sodification, it is caused by the acceleration of natural processes through overuse and mismanagement of soil. In other cases, such as soil sealing through the construction of infrastructure, tillage erosion and soil compaction by agricultural machinery, it is caused solely by overuse and mismanagement of soil. Last but not least, the effects of chemicals on biological structures and functions have to be considered on different scales of biological organization and time scales.
2. Soil degradation processes must be understood, monitored, mitigated and combated in the context of soils as living dynamic systems, of ecosystems, land, landscapes and other categories and scales. Handling this extreme complexity in research and practice requires disciplinary, inter- and trans-disciplinary work.
3. Existing concepts of assessment and monitoring of degradation and desertification show knowledge gaps at several levels. The soil quality/soil health concept of soil functionality should be backed by measured data of soil degradation, both in a laboratory but most importantly at the sub-field and field scale. Especially, the last step is a particularly neglected area of research, taking into consideration the different pedological and biological properties of soils on the local and regional levels.
4. We pledge for an advanced field diagnostic system of soil performance based on reliable on-site measurement technology in combination with expert-based knowledge and assessment methodologies. It is essential for the progress of soil health care in participatory decision processes.

Acknowledgements Preparation of this chapter was supported by the Ministry of Education, Science and Technological Development of the Republic of Serbia (contract number 451-03-09/2021-14/200011).

References

- Abdollahpour M, Rahnamaie R, Lutzenkirchen J (2020) The vulnerability of calcareous soils exposed to Mg-rich irrigation water. *Land Degrad Develop*. <https://doi.org/10.1002/ldr.3605>
- Adhikari K, Hartemink AE (2016). Linking soils to ecosystem services: a global review. *Geoderma* 262:101–111. <https://doi.org/10.1016/j.geoderma.2015.08.009>
- Alaoui A, Barao L, Ferreira CSS, Schwilch G, Basch G, Garcia-Orenes F, Morugan A, Mataix-Solera J, Kosmas C, Glavan M, Szabó B, Hermann T, Vizitiu OP, Lipiec J, Fraç M, Reintam E, Xu M, Di J, Fan H, Sukkel W, Lemesle J, Geissen V, Fleskens L (2020) Visual assessment of the impact of agricultural management practices on soil quality. *Agron J*. <https://doi.org/10.1002/agj2.20216>
- Ali MA, Dong L, Dhau J, Khosla A, Kaushik A (2020) Perspective-electrochemical sensors for soil quality assessment. *J Electrochem Soc* 167(3). <https://doi.org/10.1149/1945-7111/ab69fe/meta>
- Amato F, Martellozzo F, Nolè G, Murgante B (2017) Preserving cultural heritage by supporting landscape planning with quantitative predictions of soil consumption. *J Cult Heritage* 23:44–54. <https://doi.org/10.1016/j.culher.2015.12.009>
- Andersson KO, Orgill SE (2019) Soil extension needs to be a continuum of learning; soil workshop reflections 10 years on. *Soil Use Manage* 35:117–127. <https://doi.org/10.1111/sum.12486>
- Andrews SS, Karlen DL, Mitchell JP (2002) A comparison of soil quality indexing methods for vegetable production systems in Northern California. *Agr Ecosyst Environ* 90:25–45. [https://doi.org/10.1016/S0167-8809\(01\)00174-8](https://doi.org/10.1016/S0167-8809(01)00174-8)
- Antrop M, Van Eetvelde V (2019) Territory and/or scenery: concepts and prospects of western landscape research. In: Mueller L, Eulenstein F (eds) *Current trends in landscape research*. *Innovations in landscape*

- research. Springer, Cham. https://doi.org/10.1007/978-3-030-30069-2_1
- Arshad MA, Coen GM (1992) Characterization of soil quality: physical and chemical criteria. *Am J Altern Afr* 7:25–31
- Arshad MA, Martin S (2002) Identifying critical limits for soil quality indicators in agro-ecosystems. *Agr Ecosyst Environ* 88:153–160. [https://doi.org/10.1016/S0167-8809\(01\)00252-3](https://doi.org/10.1016/S0167-8809(01)00252-3)
- Arvidsson J, Keller T (2007) Soil stress as affected by wheel load and tyre inflation pressure. *Soil Tillage Res* 96:284–291. <https://doi.org/10.1016/j.still.2007.06.012>
- Ascough JC, Rector HD, Hoag DL, McMaster GS, Vandenberg BC, Shaffer MJ, Weltz MA, Ahuja LR (2002) Multicriteria spatial decision support systems for agriculture: overview, applications, and future research directions. Environmental modeling international conference proceedings. In: Rizzoli AE, Jake-man AJ (eds) Integrated assessment and decision support proceedings of the 1st biennial meeting of the IEMSS. Lugano, Switzerland, vol 3, pp 175–180
- Badenko V, Topaj A, Medvedev S, Zakharova E, Dunaeva I (2020) Estimation of agro-landscape productivity in regional scale using dynamic crop models in a GIS-environment. In: Mirschel W, Terleev V, Wenkel KO (eds) Landscape modelling and decision support. *Innovations in Landscape Research*. Springer, Cham, pp 545–565. https://doi.org/10.1007/978-3-030-37421-1_28
- Bai ZG, Dent DL, Olsson L, Schaepman ME (2008) Proxy global assessment of land degradation. *24 (3):223–234*. <https://doi.org/10.1111/j.1475-2743.2008.00169.x>
- Ball BC, Batey T, Munkholm LJ (2007) Field assessment of soil structural quality: a development of the Peerlkamp test. *Soil Use Manage*. 23:329–337
- Ball BC, Guimarães RML, Cloy JM, Hargreaves PR, Shepherd TG, McKenzie BM (2017) Visual soil evaluation: a summary of some applications and potential developments for agriculture. *Soil Tillage Res* 173:114–124. <https://doi.org/10.1016/j.still.2016.07.006>
- Bampa F, O’Sullivan MK et al (2019) Harvesting European knowledge on soil functions and land management using multi-criteria decision analysis. *Soil Use Manag* 35(1):6–20. <https://doi.org/10.1111/sum.12506>
- Bartkowski B, Bartke S, Helming K, Paul C, Techen A-K, Hansjürgens B (2020) Potential of the economic valuation of soil-based ecosystem services to inform sustainable soil management and policy. *Peer J* 8: e8749. <https://doi.org/10.7717/peerj.8749>. eCollection 2020
- Bartlett D, Milliken S (2019) Landscape character and ecosystem services assessment: a case study from India. In: Mueller L, Eulenstein F (eds) Current trends in landscape research. *Innovations in landscape research*. Springer, Cham, pp 521–543. https://doi.org/10.1007/978-3-030-30069-2_23
- Batjes NH, Ribeiro Eloi, van Oostrum A (2020) Standardised soil profile data to support global mapping and modelling (WoSIS snapshot 2019). *Earth Syst Sci Data* 12:299–320. <https://doi.org/10.5194/essd-12-299-2020>
- Baveye PC, Chalhoub M, Choquet P, Montagne D (2018) Is the focus on “Ecosystems” a liability in the research on Nature’s services? *Front Ecol Evol*. <https://doi.org/10.3389/fevo.2018.00226>
- Beylich A, Graefe U (2009) Investigations of annelids at soil monitoring sites in northern Germany: reference ranges and time-series data. *Soil Organisms* 81:175–196
- Blum WEH (2005) Functions of soil for society and the environment. *Rev Environ Sci Biotechnol* 4(3):75–79
- Blum WEH, Nortcliff S (2013) Soils and food security, in Soils and human health. In: Brevik EC, Burgess LC (eds). CRC Press, Boca Raton, FL, USA, pp 290–321
- Blum WEH, Eswaran H (2004) Soils for sustaining global food production. *J Food Sci* 69(2):37–42. <https://doi.org/10.1111/j.1365-2621.2004.tb15490.x>
- Blum, WEH (2008) Characterization of soil degradation risk: an overview. In: Toth G, Montanarella L, Rusco E (eds) Threats to soil quality in Europe, Ispra, Italy. JRC Scientific and Technical Reports EUR 23438 EN, pp. 5–10
- Blum WEH (2012) *Boenkunde in Stichworten*. Gebr. Borntraeger, Stuttgart, Germany
- Blum WEH (2013) Soil and land resources for agricultural production: general trends and future scenarios—a worldwide perspective. *Int Soil Water Conserv Res* 1 (3):1–14. [https://doi.org/10.1016/S2095-6339\(15\)30026-5](https://doi.org/10.1016/S2095-6339(15)30026-5)
- Boardman J, Vandaele K, Evans R, Foster IDL (2019) Off-site impacts of soil erosion and runoff: why connectivity is more important than erosion rates. *Soil Use Manage* 35(2):245–256. <https://doi.org/10.1111/sum.12496>
- Bochtis DD, Sørensen CGC, Busato P (2014) Advances in agricultural machinery management: a review. *Biosys Eng* 126:69–81
- Boehn MM, Anderson DW (1997) A landscape-scale study of soil quality in three prairie farming systems. *Soil Sci Soc Am* 61:1147–1159
- Borelli P, Robinson D, Fleischer L et al (2017) An assessment of the global impact of 21st century land use change on soil erosion. *Nat Commun* 8(1):2013. <https://doi.org/10.1038/s41467-017-02142-7>
- Bouma J (2014) Soil science contributions towards sustainable development goals and their implementation: linking soil functions with ecosystem services. *J Soil Fert Soil Sci* 177:111–120. <https://doi.org/10.1002/jpln.201300646>
- Bouma J, Batjes NH (2000) Trends of world-wide soil degradation. In: Böcker R (ed) *Hohenheimer Umwelttagung 32*. Verlag Gunter Heimbach, pp 33–43
- Bouma J (2019a) Soil security in sustainable development. *Soil Syst* 3(1):5. <https://doi.org/10.3390/soilsystems3010005>

- Bouma J (2019b) How to communicate soil expertise more effectively in the information age when aiming at the UN sustainable development goals. *Soil Use Manage* 35(1):32–38. <https://doi.org/10.1111/sum.12415>
- Bünemann EK, Bongiorno G, Bai Zh, Creamer RE, De Deyn G, de Goede R, Fleskens L, Geissen V, Kuyper TW, Mäder P, Pulleman M, Sukkel W, van Groenigen JW, Brussaard L (2018) Soil quality: a critical review. *Soil Biol Biochem* 120:105–125. <https://doi.org/10.1016/j.soilbio.2018.01.030>
- Campellone RM, Chouinard KM, Fisichelli NA, Gallo JA, Lujan JR, McCormick RJ, Miewald TA, Murry BA, Pierce DJ, Shively DR (2019) The iCASS platform: nine principles for landscape conservation design. In: Mueller L, Eulenstein F (eds) *Current trends in landscape research. Innovations in landscape research*. Springer, Cham, pp 339–365. https://doi.org/10.1007/978-3-030-30069-2_14
- Carlson CE (2007) Derivation methods of soil screening values in Europe. A review and evaluation of national procedures towards harmonization. European Commission, Joint Research Centre, Ispra, Italy, 306 pp
- Cashmore M (2004) The role of science in environmental impact assessment: process and procedure versus purpose in the development of theory. *Environ Impact Assess Rev* 24(4):403–426. <https://doi.org/10.1016/j.ear.2003.12.002>
- CEN (2020) European committee for standardization, CEN/TC 444 test methods for environmental characterization of solid matrices. <https://www.cen.eu/work/ENdev/Pages/default.aspx>. Accessed on 22 Dec 2020
- Chen XD, Dunfield KE, Fraser TD, Wakelin SA, Richardson AE, Condon LM (2020) Soil biodiversity and biogeochemical function in managed ecosystems. *Soil Research* 58:1–20. <https://doi.org/10.1071/SR19067>
- Cherubin MR, Karlen DL, Franco ALC, Cerri CEP, Tormena CA, Cerri CC (2016) A soil management assessment framework (SMAF) evaluation of Brazilian sugarcane expansion on soil quality. *Soil Sci Soc Am J* 80:215–226. <https://doi.org/10.2136/sssaj2015.09.0328>
- Chumbaev AS, Tanasienko AA (2016) Measuring Snowmelt in Siberia: Causes, Process, and Consequences. In: Mueller L., Sheudshen A., Eulenstein F. (eds) *Novel Methods for Monitoring and Managing Land and Water Resources in Siberia*. Springer Water. Springer, Cham, pp. 213–231, https://doi.org/10.1007/978-3-319-24409-9_7
- Corstanje R, Mercer TG, Rickson JR, Deeks LK, Newell-Price P, Holman I, Kechavarsi C, Waine TW (2017) Physical soil quality indicators for monitoring British soils. *Solid Earth* 8:1003–1016. <https://doi.org/10.5194/se-8-1003-2017>
- Costanza R, DArge R, de Groot R, Farber S, Grasso M, Hannon B, Limburg K, Naeem S, O'Neill RV, Paruelo J, Raskin RG, Sutton P, van den Belt M (1997) The value of the world's ecosystem services and natural capital. *Nature* 387(6630):253–260
- Costanza R, de Groot R, Braat L, Kubiszewski I, Fioramonti L, Sutton P, Farber S, Grasso M (2017) Twenty years of ecosystem services: how far have we come and how far do we still need to go? *Ecosyst Serv* 28:1–16. <https://doi.org/10.1016/j.ecoser.2017.09.008>
- Crutzen PJ (2002) Geology of mankind. *Nature* 415:23. <https://doi.org/10.1038/415023a>
- Daily GC, Matson PA, Vitousek PM (1997) Ecosystem services supplied by soil. In: Daily G (ed) *Nature's services: societal dependence on natural ecosystems*. Washington, DC, Island Press, pp 113–132
- Dickson RW (1805) *Practical agriculture, or, a complete system of modern husbandry, with the methods of planting and the management of livestock*, vol 1. R. Phillips, London
- DIN 19706:2013–02 (2013) Soil quality: determination of the soil erosion risk caused by wind (In German: Bodenbeschaffenheit - Ermittlung der Erosionsgefährdung von Böden durch Wind). <https://www.beuth.de/de/norm/din-19706/169471310>. Accessed on May 23, 2020.
- Dinter A, Oberwalder C, Kabouw P, Coulson M, Ernst G, Leicher T, Miles M, Weyman G, Klein O (2013) Occurrence and distribution of earthworms in agricultural landscapes across Europe with regard to testing for responses to plant protection products. *J Soils Sediments* 13:278–293
- Dobrovolskiy GV, Kust GS, Sanaev VG (eds) (2012) *Soils in biosphere and life of human*. Monograph, Moscow, Publishing house of the Moscow State Forest University, 584 pp (In Russian: Г.В. Добровольский, Г.С. Куст, Санаев В.Г. Почвы в биосфере и жизни человека. Монография Москва. Издательство Московского государственного университета леса. 2012, 584 с)
- Dokuchaev VV (1951) *Izbranniye sochineniya*, vol VI. Moscow, 515 p
- Dominati E, Patterson M, Mackay A (2010) A framework for classifying and quantifying the natural capital and ecosystem services of soils. *Ecol Econ* 69:1858–1868
- Doran JW, Zeiss MR (2000) Soil health and sustainability: managing the biotic component of soil quality. *Appl Soil Ecol* 15(2000):3–11
- Doran JW, Sarrantonio M, Liebig MA (1996) Soil health and sustainability. *Adv Agron* 1996(56):1–54
- Doran JW, Parkin TB (1994) Defining soil quality for a sustainable environment. In: Doran JW, Coleman DC, Bezdicek DF, Stewart BA (eds) *SSSA Spec Pub* 35, Madison WI
- Doran JW, Parkin TB (1996) Quantitative indicators of soil quality: a minimum data set. In: Doran JW, Jones AJ (eds) *Methods for assessing soil quality*. SSSA, Inc., Madison, Wisconsin, USA
- Dotterweich M (2013) The history of human-induced soil erosion: geomorphic legacies, early descriptions and research, and the development of soil conservation—A global synopsis. *Geomorphology* 201:1–34. <https://doi.org/10.1016/j.geomorph.2013.07.021>

- Dregne HE (1977) Desertification of arid lands. *J Econ Geogr* 53(4): 322–331. The Human Face of Desertification
- Drobnik T, Greiner L, Keller A, Grêt-Regamey A (2018) Soil quality indicators: from soil functions to ecosystem services. *Ecol Indicators* 94:151–169. <https://doi.org/10.1016/j.ecolind.2018.06.052>
- Drobnik T, Schwaab J, Grêt-Regamey A (2020) Moving towards integrating soil into spatial planning: No net loss of soil-based ecosystem services. *J Environ Manage* 263:110406. <https://doi.org/10.1016/j.jenvman.2020.110406>
- Dubovyyk O (2017) The role of remote sensing in land degradation assessments: opportunities and challenges. *Eur J Remote Sensing* 50(1):601–613. <https://doi.org/10.1080/22797254.2017.1378926>
- Dumanski J, Pieri C (2000) Land quality indicators: research plan. *Agr Ecosyst Environ* 81(2):93–102. [https://doi.org/10.1016/S0167-8809\(00\)00183-3](https://doi.org/10.1016/S0167-8809(00)00183-3)
- DWA (2018) DWA Regelwerk Merkblatt DWA-M 920–4 Bodenfunktionsansprache- Teil 4: Ableitung des landwirtschaftlichen Ertragspotenzials nach dem Müncheberger Soil Quality Rating. Deutsche Vereinigung für Wasserversorgung, Abwasser und Abfall e.V. (DWA), 36 p. ISBN 978–3–88721–715–0 (E-book)
- Dwivedi RS (2018) Geospatial technologies for land degradation assessment and management. CRC Press Boca Raton
- Eberle J (2019) Web service-based exploration of earth observation time-series data for analyzing environmental changes. Ph.D. thesis Jena, p. 201. https://www.db-thueringen.de/receive/dbt_mods_00040272. Accessed on 23 May 2019
- EEA (2020) Land and soil: towards the sustainable use and management of these vital resources. <https://www.eea.europa.eu/signals/signals-2019-content-list/articles/land-and-soil-towards-the>. Accessed on 23 May 2020
- Emmet-Booth JP, Forristal BD, Fenton O, Bondi G, Holden NM (2019) Visual soil evaluation—spade vs. profile methods and the information conveyed for soil management. *Soil Tillage Res* 187:135–143. <https://doi.org/10.1016/j.still.2018.12.002>
- Enne G, Zucca C (2000) Desertification indicators for the European Mediterranean region: state of the art and possible methodological approaches [= Indicatori di desertificazione per il Mediterraneo europeo: stato dell'arte e proposte di metodo]. http://eprints.uniss.it/3166/1/Enne_G_Libro_2000_Desertification.pdf
- Eswaran H, Lal R, Reich PF (2001) Land degradation: an overview. In: Bridges EM, Hannam ID, Oldeman LR, Pening FW, de Vries T, Scherr SJ, Sompatpanit S (eds) Responses to land degradation. Proceedings of the 2nd international conference on land degradation and desertification, Khon Kaen, Thailand. Oxford Press, New Delhi, India. Online: https://www.nrcs.usda.gov/wps/portal/nrcs/detail/soils/use/?cid=nrcs142p2_054028. Accessed on 23 May 2020
- Eurostat (2019) <https://ec.europa.eu/eurostat/web/environment/environmental-indicator-catalogue>. Accessed on 23 May 2020
- Evans S (2019) The “Age of Agricultural Ignorance”: trends and concerns for agriculture knee-deep into the twenty-first century. *Agric Hist* 93(1):4–34. Agricultural history society. <https://doi.org/10.3098/ah.2019.093.1.004>. <https://www.jstor.org/stable/10.3098/ah.2019.093.1.004>
- Faber J, Suhadolc M, Römcke J, Schmidt O, Krogh PH, De Groot A, Keith AM, Chabbi A (2020) EcoFIN-DERS: earthworms, water infiltration and soil aggregates (in prep.)
- FAO (2020) Soil testing methods manual—soil doctors global programme: a farmer-to-farmer training programme. Rome. <https://doi.org/10.4060/ca2796en>
- FAO (1994) GLASOD methodology <http://www.fao.org/3/v4360e/v4360E04.htm>. In: World soil resources reports 1994. Food and agriculture organization of the united nations. Rome, 1994. <http://www.fao.org/3/v4360e/v4360E00.htm#Contents>. Accessed on 23 May 2020
- FAO (2003) The design of land consolidation pilot projects in central and Eastern Europe. FAO Land Tenure Studies 6, Rome, 2003. <http://www.fao.org/3/Y4954E/y4954e00.htm>. Accessed on 23 May 2020
- FAO (2015) World soil charter. <http://www.fao.org/3/a-mn442e.pdf>. Accessed on 23 May 2020
- FAO (2019) The state of the world’s biodiversity for food and agriculture. In: Belanger J, Pilling D (eds) FAO Commission on Genetic Resources for Food and Agriculture Assessment. Rome 572 pp. <http://www.fao.org/3/CA3129EN/CA3129EN.pdf>
- FAO (2020b) FAO soils portal 2020. <http://www.fao.org/soils-portal/about/all-definitions/en/>. Accessed on 23 May 2020
- FAO/ITPS (2015) Status of the world’s soil resources (SWSR)—main report. Rome, Italy, food and agriculture organization of the united nations and inter-governmental technical panel on soils, 607 pp. <http://www.fao.org/3/a-i5199e.pdf>. Accessed on 23 May 2020
- FAO/UNEP (1984) Provisional methodology for assessment and mapping of desertification. Food and Agriculture Organization of the United Nations, United Nations Environmental Programme, Rome, 73 pp
- Florinsky I (2016) Digital terrain analysis in soil science and geology, 2nd edn. Elsevier 2016, 486 pp
- Foley J, Ramankutty N, Brauman KA, Cassidy ES, Gerber JS, Johnston M, Mueller ND, O’Connell C, Ray DK, West PC, Balzer C, Bennett EM, Carpenter SR, Hill J, Monfreda C, Polasky S, Rockström R, Sheehan J, Siebert S, Tilman D, Zaks DPM (2011) Solutions for a cultivated planet. *Nature* 478: 337–342. <https://doi.org/10.1038/nature10452>
- Franko U, Witing F (2020) Dynamics of soil organic matter in agricultural landscapes. In: Mirschel W, Terleev V, Wenkel KO (eds) Landscape modelling and decision support. Innovations in landscape

- research. Springer, Cham, pp 283–298. https://doi.org/10.1007/978-3-030-37421-1_14
- Frühhauf M, Guggenberger G, Meinert T, Theesfeld I, Lentz S (eds) (2020) KULUNDA: climate smart agriculture. South Siberian agro-steppe as pioneering region for sustainable land use. *Innovations in landscape research*. Springer, Cham. <https://doi.org/10.1007/978-3-030-15927-6>
- Funk R (2016) Assessment and measurement of wind erosion. In: Mueller L, Sheudshen A, Eulenstein F (eds) *Novel methods for monitoring and managing land and water resources in Siberia*. Springer Water. Springer, Cham, pp 425–449. https://doi.org/10.1007/978-3-319-24409-9_18
- Gajić B, Kresović B, Pejić B, Tapanarova A, Dugalić G, Životić Lj, Sredojević Z, Tolimir M (2020) Some physical properties of long-term irrigated fluvisols of valley the river Beli Drim in Klina (Serbia). *Zemljiste I Biljka* 69(1):21–35. http://www.sdpz.rs/images/casopis/2020/zin_69_1_64.pdf
- Gardi C, Montanarella L, Arruays D, Bispo A, Lemanceau P, Jolivet C, Mulder C, Ranjard L, Römbke J, Rutgers M, Menta C (2009) Soil biodiversity monitoring in Europe: ongoing activities and challenges. *Eur J Soil Sci* 60:807–819
- Gibbs HK, Salmon JM (2015) Mapping the world's degraded lands. *Appl Geogr* 57:12–21. <https://doi.org/10.1016/j.apgeog.2014.11.024>
- Giuliani G, Chatenoux B, Benvenuti A, Lacroix P, Santoro M, Mazzetti P (2020) Monitoring land degradation at national level using satellite Earth Observation time-series data to support SDG15 - exploring the potential of data cube. *Big Earth Data* 4(1):3–22. <https://doi.org/10.1080/20964471.2020.1711633>
- Glante F, Marx M, Römbke J (2018) Chapter II/18: soil monitoring in Germany. In: Sychev VG, Mueller L (Eds) *Novel methods and results of landscape research in Europe, Central Asia and Siberia, vol II understanding and monitoring processes in soils and water bodies*. © FSBI “VNIИ Agrochemistry”, pp 89–93. <https://doi.org/10.25680/7493.2018.26.90.115>, <http://vniia-pr.ru/monografii/pdf/tom2-18.pdf>. Accessed on 23 May 2020
- Gobin A, Jones R, Kirkby M, Campling P, Govers G, Kosmas C, Gentile AR (2004) Indicators for pan-European assessment and monitoring of soil erosion by water. *Environ Sci Policy* 7(1):25–38. <https://doi.org/10.1016/j.envsci.2003.09.004>
- Griffiths BS, Römbke J, Schmelz R, Scheffczyk A, Faber J, Bloem J, Peres G, Cluzeau D, Chabbi A, Suhadolc M, Sousa JP, Martins da Silva P, Carvalho F, Mendes S, Morais P, Francisco R, Costa D, Pereira C, Bonkowski M, Geisen S, Bardgett RD, Bolger T, Schmidt O, Winding A, Hendriksen NB, Johansen A, Philippot L, Plassart P, Bru D, Thomson B, Griffiths RI, Rutgers M, Mulder C, Hannula E, Creamer R, Stone D (2016) Selecting cost effective and policy-relevant biological indicators for European monitoring of soil biodiversity and ecosystem function (EcoFIN-DERS). *Ecol Indicators*. 69:213–223
- Grosse M, Hoffmann C, Specka X, Svoboda N (2020) Chapter 9: managing long-term experiment data: a repository for soil and agricultural research. In: Bhullar GS, Riar A (eds) *Long-term farming systems research ensuring food security in changing scenarios 2020*, pp 167–182. <https://doi.org/10.1016/B978-0-12-818186-7.00010-2>
- Grunewald K, Bastian O, Mannsfeld K (2015) Development and fundamentals of the ES approach. In: Grunewald K, Bastian O (eds) *Ecosystem services—concept, methods and case studies*. Springer, Berlin, Heidelberg. https://doi.org/10.1007/978-3-662-44143-5_2
- Gruszecka-Kosowska A, Baran A, Wdowin M et al (2020) The contents of the potentially harmful elements in the arable soils of southern Poland, with the assessment of ecological and health risks: a case study. *Environ Geochem Health* 42:419–442. <https://doi.org/10.1007/s10653-019-00372-w>
- Gubler A, Wächter D, Schwab P, Hug A, Meuli R, Keller A (2018) Chapter II/19: long-term observation of soils within the swiss soil monitoring network NABO. In: Sychev VG, Mueller L (Eds) *Novel methods and results of landscape research in Europe, Central Asia and Siberia, vol II understanding and monitoring processes in soils and water bodies*. © FSBI “VNIИ Agrochemistry”, pp 93–99. <https://doi.org/10.25680/4039.2018.68.24.116>. <http://vniia-pr.ru/monografii/pdf/tom2-19.pdf>. Accessed on 23 May 2020
- Guerra CA, Rosa IMD, Valentini E et al (2020) Global vulnerability of soil ecosystems to erosion. *Landscape Ecol*. <https://doi.org/10.1007/s10980-020-00984-z>
- Guo M, Yang B, Wang W et al (2019) Distribution, morphology and influencing factors of rills under extreme rainfall conditions in main land on the Loess Plateau of China. *Geomorphology* 345:106847. <https://doi.org/10.1016/j.geomorph.2019.106847>
- Gupta R, Sahoo RN, Abrol I (2019) Does soil testing for fertilizer recommendation fall short of a soil health card? *J Agron Res* 1(3):15–26. <https://doi.org/10.14302/issn.2639-3166.jar-18-2496>
- Gura I, Mnkeni PNS (2019) Crop rotation and residue management effects under no till on the soil quality of a Haplic Cambisol in Alice, Eastern Cape, South Africa. *Geoderma* 337:927–934. <https://doi.org/10.1016/j.geoderma.2018.10.042>
- Haines-Young R, Potschin MB (2018) Common international classification of ecosystem services (CICES) V5.1 and guidance on the application of the revised structure. <https://cices.eu/content/uploads/sites/8/2018/01/Guidance-V51-01012018.pdf>. Accessed on 23 May 2020
- Hassen G, Bantider A (2020) Assessment of drivers and dynamics of gully erosion in case of Tabota Koromo and Koromo Danshe watersheds, South Central Ethiopia. *Geoenviro Disasters* 7, 5 (2020). <https://doi.org/10.1186/s40677-019-0138-4>

- Hatfield JL, Sauer TJ, Cruse RM (2017) Soil: the forgotten piece of the water, food, energy Nexus. *Adv Agron* 143:1–46. <https://doi.org/10.1016/bs.agron.2017.02.001>
- Heintz-Buschart A, Guerra C, Djukic I, Cesarz S, Chatzinotas A, Patoine G, Sikorski J, Buscot F, Küsel K, Wegner C-E, Eisenhauer N (2020) Microbial diversity-ecosystem function relationships across environmental gradients. *Res Ideas Outcomes* 6: e52217. <https://doi.org/10.3897/rio.6.e52217>
- Hennings V, Höper H, Mueller L (2016) Small-scale soil functional mapping of crop yield potentials in Germany. In: Mueller L, Sheudshen A, Eulenstein F (eds) *Novel methods for monitoring and managing land and water resources in Siberia*. Springer Water. Springer, Cham. https://doi.org/10.1007/978-3-319-24409-9_27
- Hennings V (2014) Use of pedotransfer functions for land evaluation: mapping groundwater recharge rates under semi-arid conditions. In: Mueller L, Saparov A, Lischeid G (eds) *Novel measurement and assessment tools for monitoring and management of land and water resources in agricultural landscapes of Central Asia*. Environmental science and engineering. Springer, Cham, pp 249–262. https://doi.org/10.1007/978-3-319-01017-5_14
- Herrick JE, Shaver P, Pyke DA, Pellant M, Toledo D, Lepak N (2019) A strategy for defining the reference for land health and degradation assessments. *Ecol Indicators* 97:225–230. <https://doi.org/10.1016/j.ecolind.2018.06.065>
- Hole FD (1978) An approach to landscape analysis with emphasis on soils. *Geoderma* 21(1):1–23. [https://doi.org/10.1016/0016-7061\(78\)90002-2](https://doi.org/10.1016/0016-7061(78)90002-2)
- Höss S, Römbke J (2019) Effects of waste materials on *Caenorhabditis elegans* (Nematoda) using the ISO standard soil toxicity test. *Environ Sci Pollut Res* 26:26304–26312. <https://doi.org/10.1007/s11356-019-05891-8>
- Huang J, Peng S, Mao X, Li F, Guo S, Shi L et al (2019) Source apportionment and spatial and quantitative ecological risk assessment of heavy metals in soils from a typical Chinese agricultural county. *Process Saf Environ Prot* 126:339–347
- Huber S, Prokop G, Arrouays D, Banko G, Bispo A, Jones RJA, Kibblewhite MG, Lexer W, Möller A, Rickson RJ, Shishkov T, Stephens M, Toth G, Van den Akker JH, Varallyay G, Verheijen FGA, Jones AR (eds) (2008) *Environmental assessment of soil for monitoring: volume I indicators & criteria*. EUR 23490 EN/1, Office for the Official Publications of the European Communities, Luxembourg, 339 pp. <https://doi.org/10.2788/93515>
- IPBES (2018) Intergovernmental science-policy platform on biodiversity and ecosystem services (IPBES) summary for policymakers of the assessment report on land degradation and restoration of the intergovernmental science-policy platform on biodiversity and ecosystem services. In: Scholes R, Montanarella L, Brainich A, Barger N, ten Brink B, Cantele M, Erasmus B, Fisher B, Gardner T, Holland TJ et al (eds) *IPBES Secretariat*. Bonn, Germany. https://www.ipbes.net/system/tdf/spm_3bi_ldr_digital.pdf?file=1&type=node&id=28335. Accessed on 23 May 2020
- ISO 15799:2019–11 (2019) *Soil quality—guidance on the ecotoxicological characterization of soils and soil materials*
- ISO 17616:201911 (2019) *Soil quality—Guidance on the choice and evaluation of bioassays for ecotoxicological characterization of soils and soil materials*
- Issanova G, Abuduwaili J (2017) Aeolian processes as dust storms in the deserts of Central Asia and Kazakhstan. Springer Nature Singapore Pte Ltd. <https://doi.org/10.1007/978-981-10-3190-8>
- IUSS Working Group WRB (2014) *World reference base for soil resources 2014*. In: Schad P, van Huyssteen C, Micheli E (eds) *World soil resources reports no. 106*. FAO, Rome, 189 p. ISBN 978–92–5–108369–7
- Ivushkin K, Bartholomeus H, Bregt AK, Pulatov A, Franceschini MHD, Kramer H, van Loo EN, Roman VJ, Finkers R (2019) UAV based soil salinity assessment of cropland. *Geoderma* 338:502–512. <https://doi.org/10.1016/j.geoderma.2018.09.046>
- Jänsch S, Kaiser F, Krogh PH, Natal-da-Luz T, Rojo V, Scheffczyk A, Schmelz RM, Sousa J-P, Vierna J, Vizcaino A, Römbke J (2019) Determination of soil invertebrate diversity using morphological and DNA-based methods at 25 sites in Germany: first experiences. In: 14th SETAC Europe special science symposium, 2019. <https://www.forskningsdatabasen.dk/en/catalog/2471459646>. Accessed on 23 May 2020
- Jarrah M, Mayel S, Tatarko J, Funk R, Kuka K (2020) A review of wind erosion models data requirements, processes, and validity. *CATENA* 187:104388. <https://doi.org/10.1016/j.catena.2019.104388>
- Jeffrey S, Gardi C, Jones A, Montanarella L, Marmo L, Miko L, Ritz K, Peres G, Römbke J, Van der Putten W (eds) (2010) *European atlas of soil biodiversity*. European Commission, Publications Office of the European Union, Luxembourg. EUR 24375 EN, 128 pp
- Jian J, Du X, Stewart RD (2020) A database for global soil health assessment. *Sci Data* 7:16. <https://doi.org/10.1038/s41597-020-0356-3>
- Jones C, Engel R, Olson-Rutz K (2020) Soil acidification in the semiarid regions of North America's Great Plains. *Crops and Soils* 52(2):28–56. <https://doi.org/10.2134/cs2019.52.0211>
- Karlen DL, Mausbach MJ, Doran JW, Cline RG, Harris RF, Schuman GE (1997) Soil quality: a concept, definition and framework for evaluation. *Soil Sci. Soc Am J* 61:4–10
- Karlen DL, Nancel CD, Dinnes DL, Meek DW (2013) SMAF: a soil health assessment tool. *Jour Iowa Acad Sci* 120(1–4):1–13
- Karlen DL, Veum KS, Sudduth KA, Obrycki JF, Nunes MR (2019). *Soil health assessment: past accomplishments, current activities, and future*

- opportunities. *Soil Tillage Res.* Elsevier B.V. <https://doi.org/10.1016/j.still.2019.104365>
- Kaufmann-Boll C, Kern M, Niederschmidt S (2020) Soil data in Germany. Overview of the most important measurement and survey activities for soils (In German; Bodendaten in Deutschland. Übersicht über die wichtigsten Mess- und Erhebungsaktivitäten für Böden. UBA-TEXTE 52/2020, 196 pp. https://www.umweltbundesamt.de/sites/default/files/medien/1410/publikationen/2020-05-04_texte_broschuere_bodendaten.pdf. Accessed on 23 May 2020
- Kazakov LK (2019) Landscape ecology culture and some principles of sustainable nature use. In: Mueller L, Eulenstein F (eds) *Current trends in landscape research. Innovations in landscape research.* Springer, Cham. https://doi.org/10.1007/978-3-030-30069-2_3
- Keesstra SD, Bouma J, Wallinga J, Tittonell P, Smith P, Cerdà A, Montanarella L, Quinton JN, Pachepsky Y, van der Putten WH, Bardgett RD, Moolenaar S, Mol G, Jansen B, Fresco LO (2016) The significance of soils and soil science towards realization of the United Nations Sustainable Development Goals. *Soil* 2:111–128. <https://doi.org/10.5194/soil-2-111-2016>
- Keller T, Sandin M, Colombi T, Horn R, Or D (2019) Historical increase in agricultural machinery weights enhanced soil stress levels and adversely affected soil functioning. *Soil Tillage Res* 194. <https://doi.org/10.1016/j.still.2019.104293>
- Khan MN, Mobin M, Abbas ZK, Alamri SA (2018) Fertilizers and their contaminants in soils, surface and groundwater. In: Dominick A, Sala D, Goldstein MI (eds) *The encyclopedia of the Anthropocene*, vol 5. Elsevier, Oxford, pp 225–240
- Kibblewhite MG, Jones RJA, Montanarella L, Baritz R, Huber S, Arrouays D, Micheli E, Stephens M (eds) (2008) *Environmental assessment of soil for monitoring volume VI, soil monitoring system for Europe; Office for Official Publications of the European Communities: Luxembourg*, 72 pp. <https://doi.org/10.2788/95007>
- Körte W (1839): *Albrecht Thaer. Sein Leben und Wirken, als Arzt und Landwirth.* 1839, Brockhaus Leipzig 442 p
- Kosmas C, Kairis O, Karavitis C, Ritsema C, Salvati L et al. (2014) Evaluation and selection of indicators for land degradation and desertification monitoring: types of degradation, causes, and implications for management. *Environ Manage* 54(5):971–982. <https://doi.org/10.1007/s00267-013-0109-6.ird-01223238>
- Kouselou M, Hashemi S, Eskandari I, McKenzie BM, Karimi E, Rezaei A, Rahmati M (2018) Quantifying soil displacement and tillage erosion rate by different tillage systems in dryland, northwest of Iran. *Soil Use Manag* 34:48–59
- Kundler P (1989) *Erhöhung der Bodenfruchtbarkeit.* VEB Deutscher Landwirtschaftsverlag Berlin, 1st edn, 452 pp
- LADA (2013) *Land degradation assessment in drylands, LADA project, methodology and results.* Food and Agriculture Organization of the United Nations. Rome, 2013, 56 pp
- Lal R (2004) Soil carbon sequestration impacts on global climate change and food security. *Science* 304:1623–1627. <https://doi.org/10.1126/science.1097396>
- Larson WE, Pierce FJ (1991) Conservation and enhancement of soil quality. In: Dumanski J et al (eds) *Evaluation for sustainable land management in the developing world*, vol 2. Technical papers, pp 175–203
- Lee EJ, Piao D, Song C, Kim J, Lim C-H, Kim E, Moon J, Kafatos M, Lamchin M, Jeon SW, Lee W-K (2019) Assessing environmentally sensitive land to desertification using MEDALUS method in Mongolia. *Forest Sci Technol* 15(4):210–220. <https://doi.org/10.1080/21580103.2019.1667880>
- Lehman RM, Cambardella CA, Stott DE, Acosta-Martinez V, Manter DK, Buyer JS, Maul JE, Smith JL, Collins HP, Halvorson JJ, Kremer RJ, Lundgren JG, Ducey TF, Jin VL, Karlen DL (2015) Understanding and enhancing soil biological health: the solution for reversing soil degradation. *Sustainability* 7(1):988–1027. <https://doi.org/10.3390/su7010988>
- Lehmann J, Bossio DA, Kögel-Knabner I, Rillig MC (2020) The concept and future prospects of soil health. *Nat Rev Earth Environ* 1:544–553. <https://doi.org/10.1038/s43017-020-0080-8>
- Lewis SL, Maslin MA (2015) Defining the anthropocene. *Nature* 519:171–180. <https://doi.org/10.1038/nature14258>
- Lilburne L, Eger A, Mudge P, Ausseil A-G, Stevenson B, Herzig A, Beare M (2020) The land resource circle: supporting land-use decision making with an ecosystem-service-based framework of soil functions. *Geoderma* 363:114134. <https://doi.org/10.1016/j.geoderma.2019.114134>
- Litvin LF, Kiryukhina ZP, Krasnov SF, Dobrovolskaya NG, Gorobets AV (2021) Geography of the dynamics of agricultural erosion of soils in Siberia and the Far East. *Soil Science* (In Russian: Литвин Л. Ф., Кирюхина З. П., Краснов С. Ф., Добровольская Н. Г., Горобец А. В. География динамики земельной эрозии почв Сибири и Дальнего Востока // Почвоведение. 2021. № 1. С. 136–148) <https://doi.org/10.31857/S0032180X2101007X>
- Liu X, Shi H, Bai Z, Liu X, Yang B, Yan D (2020) Assessing soil acidification of croplands in the Poyang lake basin of China from 2012 to 2018. *Sustainability* 12:3072. <https://doi.org/10.3390/su12083072>
- Da Luz FB, Da Silva VR, Mallmann FJK, Pires CAB, Debiasi H, Franchini JC, Cherubin MR (2019) Monitoring soil quality changes in diversified agricultural cropping systems by the soil management assessment framework (SMAF) in southern Brazil. *Agric Ecosyst Environ* 281:100–110. <https://doi.org/10.1016/j.agee.2019.05.006>
- Makó A, Kocsis M, Barna GY, Tóth G (2017) Mapping the storing and filtering capacity of European soils. *EUR* 28392. <https://doi.org/10.2788/49218>

- McKenzie DC (2013) Visual soil examination techniques as part of a soil appraisal framework for farm evaluations in Australia. *Soil Tillage Res* 127:26–33
- McKenzie DC (ed) (1998) SOILpak for cotton growers—third edition. NSW Agriculture
- MEA (2005) Millennium ecosystem assessment. Ecosystems and human well-being: synthesis. Washington, DC, Island Press, 800 pp. <https://www.millenniumassessment.org/documents/document.356.aspx.pdf>. Accessed on 23 May 2020
- Mirschel W, Berg-Mohndicke M, Wieland R, Wenkel K-O, Terleev VV, Topaj AG, Mueller L (2020) Modelling and simulation of agricultural landscapes. In: Mirschel W, Terleev VV, Wenkel K-O (eds) Landscape modelling and decision support. Innovations in landscape research. Springer, Cham, pp 3–21. https://doi.org/10.1007/978-3-030-37421-1_1
- Mirzabaev A, Wu J, Evans J, Garcia-Oliva F, Hussein IAG, Iqbal MH, Kimutai J, Knowles T, Meza F, Nedjraoui D, Tena F, Türkeş M, Vázquez RJ, Weltz M (2019) Desertification. In: Climate change and land: an IPCC special report on climate change, desertification, land degradation, sustainable land management, food security, and greenhouse gas fluxes in terrestrial ecosystems [P.R. Shukla, J. Skea, E. Calvo Buendia, V. Masson-Delmotte, H.-O. Pörtner, D.C. Roberts, P. Zhai, R. Slade, S. Connors, R. van Diemen, M. Ferrat, E. Haughey, S. Luz, S. Neogi, M. Pathak, J. Petzold, J. Portugal Pereira, P. Vyas, E. Huntley, K. Kissick, M. Belkacemi, J. Malley, (eds.)]. <https://www.ipcc.ch/srccl/chapter/chapter-3/>. Accessed on 23 May 2020
- Mission Board (2020) Mission board soil health and food (2020) Caring for soil is caring for life. Ensure 75% of soils are healthy by 2030 for healthy food, people, nature and climate. Luxembourg: Publications Office of the European Union, 2020, 52 pp. ISBN 978–92–76–19954–0. <https://doi.org/10.2777/918775>
- Moebius-Clune BN, Moebius-Clune DJ, Gugino BK, Idowu OJ, Schindelbeck RR, Ristow AJ, van Es HM, Thies JE, Shayler HA, McBride MB, Kurtz KSM, Wolfe DW, Abawi GS (2016) Comprehensive assessment of soil health—the Cornell framework. Edition 3.2, Cornell University, Geneva, NY, 123 pp
- Montgomery D (2007) Soil erosion and agricultural sustainability. In: Proceedings of the national academy of sciences of the United States of America, vol 104, 13268–13272. <https://doi.org/10.1073/pnas.0611508104>
- De Montis A (2014) Impacts of the European landscape convention on national planning systems: a comparative investigation of six case studies. *Landscape Urban Planning* 124:53–65. <https://doi.org/10.1016/j.landurbplan.2014.01.005>
- M-SQR Manual (2007) http://www.zalf.de/de/forschung_lehre/publikationen/Documents/Publication_Mueller_L/field_mueller.pdf. Accessed on 23 May 2020
- Mueller L, Schindler U, Mirschel W, Shepherd TG, Ball B, Helming K, Rogasik J, Eulenstein F, Wiggering H (2010) Assessing the productivity function of soils: a review. *Agron Sustain Dev* 30(3):601–614. <https://doi.org/10.1051/agro/2009057>
- Mueller ND, Gerber JS, Johnston M, Ray DK, Ramankutty N, Foley JA (2012a) Closing yield gaps through nutrient and water management. *Nature* 490:254–257. <https://doi.org/10.1038/nature11420>
- Mueller L, Schindler U, Shepherd TG, Ball BC, Smolentsev E, Hu C, Hennings V, Schad P, Rogasik J, Zeitz J, Schlindwein SL, Behrendt A, Helming K, Eulenstein F (2012b) A framework for assessing agricultural soil quality on a global scale. *Arch Agron Soil Sci* 58(Supplement 1):S76–S82
- Mueller L, Shepherd G, Schindler U, Ball BC, Munkholm LJ, Hennings V, Smolentseva E, Rukhovich O, Lukin S, Hu C (2013) Evaluation of soil structure in the framework of an overall soil quality rating. *Soil Tillage Res* 127:74–84
- Mueller L, Behrendt A, Shepherd TG, Schindler U, Ball BC, Khudyaev S, Kaiser T, Dannowski R, Eulenstein F (2014) Simple field methods for measurement and evaluation of grassland quality. In: Mueller L, Saparov A, Lischeid G (eds) Novel measurement and assessment tools for monitoring and management of land and water resources in agricultural landscapes of Central Asia. Springer International Publishing, Cham, pp 199–222. https://doi.org/10.1007/978-3-319-01017-5_11
- Mueller L, Schindler U, Hennings V, Smolentseva EN, Rukhovich OV, Romanenkov VA, Sychev VG, Lukin S, Sheudshen AK, Onishenko L, Saparov A, Pachikin K, Behrendt A, Mirschel W, Eulenstein F (2016) An emerging method of rating global soil quality and productivity potentials. In: Mueller L, Sheudshen AK, Eulenstein F (eds) Novel methods for monitoring and managing land and water resources in Siberia. Springer Water. Springer International Publishing, Cham, pp 573–595 http://link.springer.com/chapter/10.1007%2F978-3-319-24409-9_26
- Mueller L, Eulenstein F, Mirschel W, Antrop M, Jones M, McKenzie BM, Dronin NN, Kazakov LK, Kravchenko VV, Khoroshev A, Gerasimova M, Dannowski R, Schindler U, Rukhovich O, Sychev VG, Sheudshen AK, Couvet D, Robinson G, Blum W, Joniak T, Eisendle U, Trovato MG, Salnjikov E, Haubold-Rosar M, Knoche D, Köhl M, Bartlett D, Hoffmann J, Römbke J, Glante F, Sumina OI, Saparov A, Bukvareva E, Terleev VV, Topaj AG, Kienast F (2019) Landscapes, their exploration and utilisation: status and trends of landscape research. In: Mueller L, Eulenstein F (eds) Current trends in landscape research. Innovations in landscape research. Springer, Cham, pp 105–164. https://doi.org/10.1007/978-3-030-30069-2_5
- Mueller L, Eulenstein F, Dronin NM, Mirschel W, McKenzie BM, Antrop M, Jones M, Dannowski R, Schindler U, Behrendt A, Rukhovich OV, Sychev VG, Sheudshen AK, Romanenkov VA, Trofimov I, Robinson GM, Schreg R, Blum WEH, Salnjikov E, Saparov A, Pachikin K, Römbke J, Manton M, Angelstam P, Hennings V, Poulton P (2021)

- Agricultural landscapes: history, status and challenges. In: Mueller L, Sychev VG, Dronin NM, Eulenstein F (eds) Exploring and optimizing agricultural landscapes. Springer Cham, in print ISBN 978–3–030–67448–9
- Müller F, Fohrer N, Chicharo L (2015) The basic ideas of the ecosystem service concept. In: Chicharo L, Müller F, Fohrer N (eds) Ecosystem services and river basin ecohydrology. Springer, Dordrecht. https://doi.org/10.1007/978-94-017-9846-4_2
- Murphy BW, Crawford MH, Duncan DA, McKenzie DC, Koen TB (2013) The use of visual soil assessment schemes to evaluate surface structure in a soil monitoring program. *Soil Tillage Res* 127:3–12
- Nachtergaele FON (2000) Soil vulnerability evaluation and location fragility assessment. In: Sequi P (ed) Proceedings international congress on soil vulnerability and sensitivity (Florence, 18–21 October 1999). European Soil Bureau and Italian Society of Soil Science, Florence
- Newell-Price JP, Whittingham MJ, Chambers BJ, Peel S (2013) Visual soil evaluation in relation to measured soil physical properties in a survey of grassland soil compaction in England and Wales. *Soil Tillage Res* 127:65–73
- Nguyen KA, Liou YA, Tran HP, Hoang PP, Nguyen TH (2020) Soil salinity assessment by using near-infrared channel and vegetation soil salinity index derived from landsat 8 OLI data: a case study in the Tra Vinh Province, Mekong Delta, Vietnam. *Prog Earth Planet Sci* 7, 1. <https://doi.org/10.1186/s40645-019-0311-0>
- Nikiforoff CC (1937) Some general aspects of the chernozem formation. *Soil Sci Soc Am J* 1(C):333–342
- Nikiforova AA, Bastian O, Fleis ME, Nyrtsov MV, Khropov AG (2019) Theoretical development of a natural soil-landscape classification system: an interdisciplinary approach. *CATENA* 177:238–245. <https://doi.org/10.1016/j.catena.2019.02.026>
- Oldeman LR, Van Lynden GWJ (1998) Revisiting the GLASOD methodology. In: Lal R, Blum WH, Valentine C, Steward BR (eds) Methods for assessment of soil degradation. CRC press, pp 423–440, 555 pp
- Oldeman LR, Hakkeling RTA, Sombroek WG (1990). World map of the status of human-induced soil degradation: an explanatory note. Wageningen, International Soil Reference and Information Centre ISRIC, Wageningen and UNEP; Nairobi, 27 pp + 3 maps
- Oldeman LR (1992) Global extent of soil degradation. ISRIC Bi-Annual Report 1991–1992, pp 19–36. <https://library.wur.nl/WebQuery/wurpubs/fulltext/299739>. Accessed on 23 May 2020
- Olenin O, Zudilin S, Osorgin Yu, Shevchenko S, Chernov A (2020) Digital monitoring of agro-ecosystems indicators on the basis of space and unmanned technologies BIO Web Conf. Volume 17, 2020. <https://doi.org/10.1051/bioconf/20201700113>
- Olsson L, Barbosa H, Bhadwal S, Cowie A, Delusca K., Flores-Renteria D, Hermans K, Jobbagy E, Kurz W, Li D, Sonwa DJ, Stringer L, (2019) Land degradation. In: Shukla PR, Skea J, Calvo Buendia E, Masson-Delmotte V, Pörtner H-O, Roberts DC, Zhai P, Slade R, Connors S, van Diemen R, Ferrat M, Haughey E, Luz S, Neogi S, Pathak M, Petzold J, Portugal Pereira J, Vyas P, Huntley E, Kissick K, Belkacemi M, Malley J (eds) Climate change and land: an IPCC special report on climate change, desertification, land degradation, sustainable land management, food security, and greenhouse gas fluxes in terrestrial ecosystems. <https://www.ipcc.ch/srccl/chapter/chapter-4/>. Accessed on 23 May 2020
- Orlova T, Melnichuk A, Klimenko K, Vitivitskaya V, Popovych V, Dunaieva I, Terleev V, Nikonorov A, Togo, I, Volkova Y, Mirschel W, Garmanov V (2017) Reclamation of landfills and dumps of municipal solid waste in a waste management system: methodology and practice. In: IOP conference series: earth and environmental science, vol 90, Article No.: 012110, 13 p. <https://doi.org/10.1088/1755-1315/90/1/012110>
- Ouyang W, Skidmore AK, Hao F, Wang T (2010) Soil erosion dynamics response to landscape pattern. *Sci Total Environ* 408(6):1358–1366. <https://doi.org/10.1016/j.scitotenv.2009.10.062>
- Packer IJ, Chapman GA, Lawrie JW (2019) On-Ground extension of soil information to improve land management. *Soil Use Manag* 35(1):75–84. <https://doi.org/10.1111/sum.12494>
- Panagos P, Van Liedekerke M (2008) Multi-scale European soil information system (Meusis): novel ways to derive soil indicators through upscaling. In: Toth G, Montanarella L, Rusco E (eds) Threats to soil quality in Europe, Ispra, Italy, pp 5–10, pp 139–150. JRC Scientific and Technical Reports EUR 23438 EN
- Panagos P, Ballabio C, Poesen J, Lugato E, Scarpa S, Montanarella L, Borrelli PA (2020) Soil erosion indicator for supporting agricultural, environmental and climate policies in the European Union. *Remote Sens* 12:1365. <https://doi.org/10.3390/rs12091365>
- Parkhomenko GG, Voinash SA, Sokolova VA, Krivonogova AS, Rzhavtsev AA (2019) Reducing the negative impact of undercarriage systems and agricultural machinery parts on soils. *IOP Conf Series Earth Environ Sci* 316: 012049. <https://doi.org/10.1088/1755-1315/316/1/012049>
- Patzel N, Sticher H, Karlen DL (2000) Soil fertility—phenomenon and concept. *J Plant Nutr Soil Sci* 163 (2): 129–142. [https://doi.org/10.1002/\(SICI\)1522-2624\(200004\)163:2<129::AID-JPLN129>3.0.CO;2-D](https://doi.org/10.1002/(SICI)1522-2624(200004)163:2<129::AID-JPLN129>3.0.CO;2-D)
- Pimentel D, Burgess M (2013) soil erosion threatens food production. *Agriculture* 3(3):443–463. <https://doi.org/10.3390/agriculture3030443>
- Poulton PT, Johnston AE (2020) Can long-term experiments help us understand, and manage, the wider landscape—examples from Rothamsted, England. In: Exploring and optimizing agricultural landscapes. Springer 2020, in print ISBN 978–3–030–67448–9
- Prasuhn V (2020) Twenty years of soil erosion on-farm measurement: annual variation, spatial distribution and the impact of conservation programmes for soil loss

- rates in Switzerland. Earth surface processes and landforms. <https://doi.org/10.1002/esp.4829>
- Prishchepov AV, Schierhorn F, Dronin N, Ponkina EV, Müller D (2020) 800 years of agricultural land-use change in Asian (Eastern) Russia. In: Frühauf M, Guggenberger G, Meinel T, Theesfeld I, Lentz S (eds) KULUNDA: climate smart agriculture. Innovations in landscape research. Springer, Cham. https://doi.org/10.1007/978-3-030-15927-6_6
- Pulido Moncada M, Gabriels D, Lobo D, Rey JC, Cornelis WM (2014) Visual field assessment of soil structural quality in tropical soils. *Soil Tillage Res* 139:8–18
- Qu L, Dong G, De Boeck H, et al (2020) Joint forcing by heat and mowing poses a threat to grassland ecosystem: evidence from a manipulative experiment. *Land Degrad Develop* 785–800. <https://doi.org/10.1002/ldr.3483>
- Rinot O, Levy GJ, Steinberger Y, Svoray T, Eshel G (2019) Soil health assessment: a critical review of current methodologies and a proposed new approach. *Sci Total Environ* 648:1484–1491. <https://doi.org/10.1016/j.scitotenv.2018.08.259>
- Roesch A, Weisskopf P, Oberholzer, Valsangiacomo A, Nemecek T (2019) An approach for describing the effects of grazing on soil quality in life-cycle assessment. *Sustainability* 11:4870
- Romanenkov VA, Shevtsova LK, Rukhovich OV, Belichenko MV (2020) Chapter 8: geographical network: legacy of the Soviet era long-term field experiments in Russian agriculture. In: Bhullar GS, Riar A (eds) Long-term farming systems research. *Ensuring Food Security in Changing Scenarios*, pp 147–165. <https://doi.org/10.1016/B978-0-12-818186-7.00009-6>
- Römbke J, Bernard J, Martin-Laurent F (2018) Standard methods for the assessment of structural and functional diversity of soil organisms: a review. *Integr Environ Assess Manage (IEAM)* 14:463–479
- Römbke J, Sousa J-P, Schouten T, Riepert F (2006) Monitoring of soil organisms: a set of standardized field methods proposed by ISO. *Eur J Soil Biol* 42: S61–S64. <https://doi.org/10.1016/j.ejsobi.2006.07.016>
- Russell DJ, Krogh PH (2020) EUDaphnbase—European soil-biology data warehouse for soil protection global symposium on soil biodiversity. FAO HQ, Rome, Italy. https://pure.au.dk/portal/files/177775095/GSOBI20_Abstract_RUSSELL.pdf. Accessed on 2 Sept 2020
- Salvati L, Zitti M, Ceccarelli T, Perini L (2009) Developing a synthetic index of land vulnerability to drought and desertification. *Geogr Res* 473:280–291
- Salvia R, Egidi G, Vinci S, Salvati L (2019) Desertification risk and rural development in Southern Europe: permanent assessment and implications for sustainable land management and mitigation policies. *Land* 8:191
- Schindler U, Mueller L, Behrendt A (2003) Field investigations of soil hydrological properties of fen soils in North-East Germany. *J Plant Nutr Soil Sci* 166 (3):364–369. <https://doi.org/10.1002/jpln.200390056>
- Schindler U, Thiere J, Steidl J, Mueller L (2004) Bodenhydrologische Kennwerte heterogener Flächeneinheiten: Methodik der Ableitung und Anwendungsbeispiel für Nordostdeutschland. Landesumweltamt Brandenburg, Potsdam, 56 pp. http://www.lfu.brandenburg.de/cms/media.php/lbm1.a.3310.de/luas_bd87.pdf. Accessed on 23 May 2020
- Schjønning P, Akker J, Keller T, Greve M, Lamandé M, Simojoki A, Stettler M, Arvidsson J, Breuning-Madsen H (2016) Soil compaction. Chapter 6. In: Stolte J et al (eds) *Soil threats in Europe*; EUR 27607 EN. <https://doi.org/10.2788/488054> (print). <https://doi.org/10.2788/828742> (online). <https://doi.org/10.2788/828742>
- Schulte RPO, Creamer RE, Donnellan T, Farrelly N, Fealy R, O'Donoghue C, O'Huallachain D (2014) Functional land management: a framework for managing soil-based ecosystem services for the sustainable intensification of agriculture. *Environ Sci Policy* 38:45–58. <https://doi.org/10.1016/j.envsci.2013.10.002>
- Schwilch G, Lemann T, Berglund Ö, Camarotto C, Cerdà A; Daliakopoulos I, Kohnová S, Krzeminska D, Marañón T, Rietra R, Siebielec G, Thorsson J, Tibbett M, Valente S, van Delden H, van den Akker Jan, Verzandvoort S, Vrinceanu NO, Zoumides C, Hessel R (2018) Assessing impacts of soil management measures on ecosystem services. *Sustainability* 10(12):4416. <https://www.mdpi.com/2071-1050/10/12/4416>
- Seaton FM, Barrett G, Burden A, Creer S, Fitos E, Garbutt A, Griffiths RI, Henrys P, Jones DL, Keenan P, Keith A, Lebron I, Maskell L, Pereira MG, Reinsch S, Smart SM, Williams B, Emmett BA, Robinson DA (2020) Soil health cluster analysis based on national monitoring of soil indicators. *Eur J Soil Sci*. <https://doi.org/10.1111/ejss.12958>
- Sekera F (1943) *Gesunder und kranker Boden. Ein praktischer Wegweiser zur Gesunderhaltung des Ackers*, Wien, p 1943
- Shepherd TG (2000) *Visual soil assessment, vol 1, Field guide for cropping and pastoral grazing on flat to rolling country*, Horizons.mw/Landcare Research, Palmerston North, 84 p
- Shepherd TG (2009) *Visual soil assessment, vol 1. Field guide for pastoral grazing and cropping on flat to rolling country*, 2nd ed., Horizons Regional Council, Palmerston North, New Zealand, 118 p
- Singer MJ, Ewing S (2000) Soil quality. Chapter 11. In: Sumner ME (ed) *Handbook of soil science*. CRC Press Boca Raton, FL, pp 271–298
- Smeets E, Weterings R (1999) Environmental indicators: typology and overview. *Eur Environ Agency* 19
- Smetanová A, Follain S, David M, Ciampalini R, Raclot D, Crabit A, Le Bissonnais Y (2019) Landscaping compromises for land degradation neutrality: the case of soil erosion in a Mediterranean agricultural landscape. *J Environ Manage* 235:282–292. <https://doi.org/10.1016/j.jenvman.2019.01.063>

- Smolentseva E, Smolentsev B, Pachkin K, Mueller L (2014) Assessing the soil quality and crop yield potentials of some soils of Eurasia. In: Mueller L, Saparov A, Lischeid G (eds) Novel measurement and assessment tools for monitoring and management of land and water resources in agricultural landscapes of Central Asia. Springer International Publishing, pp 505–517. https://doi.org/10.1007/978-3-319-01017-5_31
- Snakin VV, Krchetov PP, Kuzovnikova TA, Alyabina IO, Gurov AF, Stepichev AV (1996) The system of assessment of soil degradation. *Soil Tech* 8:331–343
- Soil Health Team (2020) Cornell university. Comprehensive assessment of soil health <https://soilhealth.cals.cornell.edu/testing-services/>. Accessed on 23 May 2020
- Sommer S, Zucca, C, Grainger A, Cherlet M, Zougmore R, Sokona Y, Hill J (2011) Application of indicator systems for monitoring and assessment of desertification from national to global scales. *Land Degrad Develop* 22:184–197. <https://doi.org/10.1002/ldr.1084>
- Sonderegger T, Pfister S, Hellweg S (2020) Assessing impacts on the natural resource soil in life cycle assessment: methods for compaction and water Erosion. *Environ Sci Technol*. <https://doi.org/10.1021/acs.est.0c01553>
- IPCC SRCCL (2019) Chapter 4: land degradation, 186 pp. https://www.ipcc.ch/site/assets/uploads/2019/08/2e.-Chapter-4_FINAL.pdf. accessed on 23 May 2020
- Steffan JJ, Brevik EC, Burgess LC, Cerdà A. The effect of soil on human health: an overview. *Eur J Soil Sci* 69 (1):159–171. <https://doi.org/10.1111/ejss.12451>
- Steininger M, Wurbs D (2016) Bundesweite Gefährdung der Böden durch Winderosion und Bewertung der Veränderung infolge des Wandels klimatischer Steuergrößen als Grundlage zur Weiterentwicklung der Vorsorge und Gefahrenabwehr im Bodenschutzrecht. https://www.umweltbundesamt.de/sites/default/files/medien/1410/publikationen/2017-11-30_texte_13-2017_winderosion-ackerflaechen.pdf. Accessed on 23 May 2020
- Stocking MA, Murnaghan N (2002) A Handbook for the field assessment of land degradation. Routledge London, 169 pp. <https://doi.org/10.4324/9781849776219>
- Sychev VG, Yefremov EN, Romanenkov VA (2016) Monitoring of soil fertility (agroecological monitoring). In: Mueller L, Sheudshen A, Eulenstein F (eds) Novel methods for monitoring and managing land and water resources in Siberia. Springer Water. Springer, Cham. https://doi.org/10.1007/978-3-319-24409-9_24
- Tamene L, Sileshi GW, Ngengu G, Mponela P, Kihara J, Sila TJ (2019) Soil structural degradation and nutrient limitations across land use categories and climatic zones in Southern Africa. *Land Degrad Develop* 30(11):1288–1299. <https://doi.org/10.1002/ldr.3302>
- Tarolli P, Sofia G, Wenfang CAO (2018) The geomorphology of the human age. In: Dellasala DA, Goldstein MI (eds) *Encyclopedia of the anthropocene*. Elsevier Inc, pp 35–43. <https://doi.org/10.1016/B978-0-12-809665-9.10501-4>
- Thaer A (1809) Grundsätze der rationellen Landwirtschaft. Erster Band. Berlin 1809. Grundsätze der rationellen Landwirtschaft, 4 Bde. Realschulbuchhandlung, Berlin 1809–1812
- Thiele-Bruhn S, Schloter M, Wilke B-M, Beaudette LA, Martin-Laurent F, Cheviron N, Mougin C, Römcke J (2020) Identification of new microbial functional standards for soil quality assessment. *SOIL* 6:17–34. <https://doi.org/10.5194/soil-6-17-2020>
- Thomsen EO, Reeve JR, Culumber CM, Alston DG, Newhall R, Cardon G (2019) Simple soil tests for on-site evaluation of soil health in orchards. *Sustainability* 11:6009. <https://www.mdpi.com/2071-1050/11/21/6009>
- Thorp J (1942) The influence of environment on soil formation. *Soil Sci Soc Am J* 6(C):39–46
- Thoumazeau A, Bustany C, Rodrigues J, Bessou C (2019) Using the LANCA® model to account for soil quality within LCA: First application and approach comparison in two contrasted tropical case studies. *Indonesian J Life Cycle Assess Sustain* 3(1):13. <https://ijolcas.ilcan.or.id/index.php/IJoLCAS/article/view/42>
- Tóth G, Hermann T, Da Silva MR, Montanarella L (2016) Heavy metals in agricultural soils of the European Union with implications for food safety. *Environ Internat* 88:299–309
- Tóth G, Hermann T, Szatmári G, Pásztor L (2016) Maps of heavy metals in the soils of the European Union and proposed priority areas for detailed assessment. *Sci Total Environ* 565:1054–1062
- Tóth G, Hermann T, da Silva MR, Montanarella L (2018) Monitoring soil for sustainable development and land degradation neutrality. *Environ Monit Assess* 190:57. <https://doi.org/10.1007/s10661-017-6415-3>
- Trapp M, Deubert M, Streib L, Scholz-Starke B, Roß-Nickoll M, Toschki A (2020) Simulating the effects of agrochemicals and other risk-bearing management measures on the terrestrial agrobiodiversity: the RISKMIN approach. In: Mirschel W, Terleev V, Wenkel KO (eds) *Landscape modelling and decision support. Innovations in landscape research*. Springer, Cham, pp 443–459. https://doi.org/10.1007/978-3-030-37421-1_23
- Trofimov IA, Trofimova LS, Yakovleva EP (2020) The work of VV Dokuchaev in the Chernozem zone of Russia: a contribution towards productive and sustainable agrolandscapes, and a basis for recent research. In: Mueller L, Sychev VG, Dronin NM, Eulenstein F (eds) *Exploring and optimizing agricultural landscapes*. Springer 2020, in print ISBN 978–3–030–67448–9
- Troldborg M, Aalders I, Towers W, Hallett PD, McKenzie BM, Bengough AG, Lilly A, Ball BC, Hough RL (2013) Application of Bayesian belief networks to quantify and map areas at risk to soil threats: using soil

- compaction as an example. *Soil Tillage Res* 132:56–68
- Trovato MG, Ali D (2019) Planning tools for the protection of the natural and cultural heritage in the Eastern Mediterranean area. In: Mueller L, Eulenstein F (eds) *Current trends in landscape research. Innovations in landscape research*. Springer, Cham, pp 467–486. https://doi.org/10.1007/978-3-030-30069-2_20
- Turbé A, De Toni A, Benito P, Lavelle P, Ruiz N, Van der Putten W, Labouze E, Mudgal S (2010) Soil biodiversity: functions, threats, and tools for policy makers. BioIntelligence Service, IRD, and NIOO, Report for European Commission (DG Environment), Brussels, Belgium, 250 pp
- UN (2015) Agenda 2030: sustainable development goals. 17 Goals to transform our world. <https://www.un.org/sustainabledevelopment/>. Accessed on 23 May 2020
- UNCCD (1994) United Nations convention to combat desertification in those countries experiencing serious drought and/or desertification, particularly in Africa. Paris, France, 54 pp
- UNCCD (2012) United Nations convention to combat desertification. <https://web.archive.org/web/20160607231107/>, <http://www.unccd.int/en/about-the-convention/Pages/Text-Part-I.aspx>. Accessed on 23 May 2020
- UNDP (2019) Combatting land degradation. Securing a sustainable future. https://www.undp.org/content/dam/undp/library/planet/environment/Combatting_Land_Degradation%20%80%93Securing_A_Sustainable_Future.pdf. Accessed on 23 May 2020
- UNEP (2020) United Nations environment programme. <https://na.unep.net/siouxfalls/des/unccdpl.php>. Accessed on 23 May 2020
- USDA/NRCS (2020) Soil quality indicator sheets. <https://www.nrcs.usda.gov/wps/portal/nrcs/detail/soils/health/assessment/>. Accessed on 23 May 2020
- Vågen T-G, Winowiecki LA, Tondoh JE, Desta LT, Gumbrecht T (2016) Mapping of soil properties and land degradation risk in Africa using MODIS reflectance. *Geoderma* 263:216–225. <https://doi.org/10.1016/j.geoderma.2015.06.023>
- Van Eetvelde V, Antrop M (2005) The significance of landscape relic zones in relation to soil conditions, settlement pattern and territories in Flanders. *Landscape Urban Planning* 70(1–2):127–141. <https://doi.org/10.1016/j.landurbplan.2003.10.009>
- Van Leeuwen JP, Creamer RE, Cluzeau D, Debeljak M, Gatti F, Henriksen C, Kuzmanovski V, Menta C, Peres G, Picaud C, Saby N, Trajanova T-G, Visioli G, Rutgers M (2019) Modeling of soil functions for assessing soil quality: soil biodiversity and habitat provisioning. *Front Environ Sci* 7:113. <https://doi.org/10.3389/fenvs.2019.00113>
- Verón SR, Paruelo JM, Oesterheld M (2006) Assessing desertification. *J Arid Environ* 66:751–763. <https://doi.org/10.1016/j.jaridenv.2006.01.021>
- Virto I, Imaz MJ, Fernández-Ugalde O, Gartzia-Bengoetxea N, Enrique A, Bescansa P (2015) Soil degradation and soil quality in Western Europe: current situation and future perspectives. *Sustainability* 7:313–365. <https://doi.org/10.3390/su7010313>
- Vrebos D, Bampa F, Creamer RE, Gardi C, Ghaley BB, Jones A, Rutgers M, Sandén T, Staes J, Meire P (2017) The impact of policy instruments on soil multifunctionality in the European Union. *Sustainability* 9(3):407. <https://doi.org/10.3390/su9030407>
- Walker LR, Wardle DA, Bardgett RD, Clarkson BD (2010) The use of chronosequences in studies of ecological succession and soil development. *J Ecol* 98(4):725–736. <https://doi.org/10.1111/j.1365-2745.2010.01664.x>
- Wander MM, Cihacek LJ, Coyne M, Drijber RA, Grossman JM, Gutknecht JLM, Horwath WR, Jagadamma S, Olk DC, Ruark M, Snapp SS, Tiemann LK, Weil R, Turco RF (2019) Developments in agricultural soil quality and health: reflections by the research committee on soil organic matter management. *Front Environ Sci*. <https://doi.org/10.3389/fenvs.2019.00109>
- Webb NP, Kachergis E, Miller SW, McCord SE, Bestelmeyer BT, Brown JR, Chappell A, Edwards BL, Herrick JKE, Karl JW, Leys JF, Metz LJ, Smarik S, Tatarko J, Van Zee JW, Zwicke G (2020) Indicators and benchmarks for wind erosion monitoring, assessment and management. *Ecol Indicators* 110:10588. <https://doi.org/10.1016/j.ecolind.2019.105881>
- Wessel-Bothe S, Weihermüller L (2020) *Field measurement methods in soil science*. Borntraeger Science Publishers, 210 pp
- Wienhold B, Karlen D, Andrews SS, Stott DE (2009) Protocol for indicator scoring in the soil management assessment framework (SMAF). *Renew Agric Food Syst* 24(4):260–266. <https://doi.org/10.1017/S1742170509990093>
- Williams H, Colombi T, Keller T (2020) The influence of soil management on soil health: an on-farm study in southern Sweden. *Geoderma* 360:114010. <https://doi.org/10.1016/j.geoderma.2019.114010>
- Xie H, Zhang Y, Wu Zh, Lv T (2020) A bibliometric analysis on land degradation: current status, development, and future direction. *Land* 9(1):28. <https://doi.org/10.3390/land9010028>
- Xue R, Wang C, Liu M, Zhang D, Li K, Li N (2019) A new method for soil health assessment based on Analytic Hierarchy Process and meta-analysis. *Sci Total Environ* 650:2771–2777. <https://doi.org/10.1016/j.scitotenv.2018.10.049>
- Yakovlev AS (2013) Permissible ecological state of soils and anthropogenic influence as the basis of their ecological standard and quality management. In: Shoba SA, Yakovlev AS, Rybalsky NG (eds) *Standardization and regulation of environmental and soils quality and land management*. NIA Priroda, Moscow, p 373. (Допустимое экологическое состояние почв и антропогенное воздействие как основа их экологического нормирования и управления качеством)

- Yigini Y, Panagos P (2016) Assessment of soil organic carbon stocks under future climate and land cover changes in Europe. *Sci Total Environ* 557–558:838–850
- Yue Y, Li M, Wang L, Zhu A-X (2019) A data-mining-based approach for aeolian desertification susceptibility assessment: a case-study from Northern China. *Land Degrad Develop* 30(16):1968–1983. <https://doi.org/10.1002/ldr.3393>
- Zhang X, Davidson EA, Zou T, Lassaletta L, Quan Z, Li T, Zhang W (2020) Quantifying nutrient budgets for sustainable nutrient management. *Glob Biogeochem Cycles* 34(3):e2018GB006060. <https://doi.org/10.1029/2018GB006060>
- Zhu Ch, Fan X, Bai Zh (2020) Spatiotemporal pattern of wind erosion on unprotected topsoil replacement sites in mainland China. *Sustainability* 12(8):3237. <https://doi.org/10.3390/su12083237>



Types of Physical Soil Degradation and Implications for Their Prevention and Monitoring

2

Elmira Saljnikov, Wilfried Mirschel,
Volker Prasuhn, Thomas Keller, Winfried
E. H. Blum, Alexander S. Chumbaev,
Jianhui Zhang, Jilili Abuduwaili,
Frank Eulenstein, Anton Lavrishchev,
Uwe Schindler, and Lothar Mueller

Abstract

Physical soil degradation is a deterioration of the soil's structure diminishing its functions and ecosystem services. It is mainly initiated

and manifested by physical forces and processes, such as energy impacts of water, wind and mechanical pressure on soils, and it is accelerated by various kinds of anthropogenic

E. Saljnikov (✉)
Institute of Soil Science, Teodora Drajzera 7, 11000
Belgrade, Serbia

E. Saljnikov · F. Eulenstein · U. Schindler
Mitscherlich Academy for Soil Fertility (MITAK)
GmbH, Prof.-Mitscherlich-Allee 1, Paulinenaue,
14641 Brandenburg, Germany
e-mail: feulenstein@zalf.de

U. Schindler
e-mail: schindler@mitak.com

W. Mirschel · F. Eulenstein · L. Mueller
Leibniz-Centre for Agricultural Landscape Research
(ZALF), Eberswalder Str. 84, 15374 Müncheberg,
Germany

V. Prasuhn · T. Keller
Department of Agroecology & Environment,
Reckenholzstrasse 191, 8046 AgroscopeZürich,
Switzerland
e-mail: volker.prasuhn@agroscope.admin.ch

T. Keller
e-mail: thomas.keller@slu.se

T. Keller
Department of Soil & Environment, Swedish
University of Agricultural Sciences, Box 7014,
75007 Uppsala, Sweden

T. Keller
Centre for Sustainable Agricultural Systems,
University of Southern Queensland, Toowoomba,
Qld 4350, Australia

J. Zhang
Institute of Mountain Hazards and Environment
(IMHE), Chinese Academy of Sciences and Ministry
of Water Conservancy, No. 9, Block 4, South
Renmin Road, Chengdu 610041, China
e-mail: zjh@imde.ac.cn

W. E. H. Blum
Institute of Soil Research, University of Natural
Resources and Life Sciences, Peter-Jordan-Str. 82,
1190 Vienna, Austria
e-mail: winfried.blum@boku.ac.at

A. S. Chumbaev
Institute of Soil Science and Agrochemistry, Siberian
Branch of the Russian Academy of Science (ISSA
SB RAS), Ac. Lavrentieva av., 8, Novosibirsk
630090, Russia

J. Abuduwaili
State Key Laboratory of Desert and Oasis Ecology,
Xinjiang Institute of Ecology and Geography,
Chinese Academy of Sciences, Urumqi, China
e-mail: jilil@ms.xjb.ac.cn

A. Lavrishchev
St. Petersburg State Agrarian University,
Peterburgskoye Ave. 2, 196601 St. Petersburg,
Pushkin, Russia

pressure. This is a threat to meeting visions of the Sustainable Development Goals of the United Nations. We review the current state of some types of physical soil degradation, such as erosion by water, wind and tillage, soil compaction and soil sealing/land take. Despite some knowledge in research of degradation processes, gaps in knowledge and need for action exist at several levels. There is a need to understand the event-wise, stochastic character of erosion and compaction processes and the complex interaction of mechanical disturbances of soil structure with soil hydrological and biochemical processes. The implications of these processes for soil health and ecosystem functioning must be better quantified, yielding indicators, baseline values and thresholds. Progress is needed to develop simulation models of soil erosion and compaction towards complex modular models that can figure and forecast ecosystem processes. There is a demand to construct manageable decision support systems, which can help to plan and conduct zero-soil degradation projects at a landscape level. Cross-comparisons of models and strengthening the databases in terms of field laboratories and long-term experiments are essential to prevent and monitor soil degradation at different scales.

Keywords

Soil degradation · Soil erosion · Soil compaction · Soil sealing · Soil health · Ecosystem modelling

2.1 Introduction

Physical soil degradation is a deterioration of the natural composition and structure of the soil. It comprises very different processes and morphometric forms, mainly through the deformation of the inner soil structure due to excessive external natural and human-induced forces (Blum 2011). It is manifested in a change in the thickness of topsoil horizons such as in cases of erosion

and/or in the destruction of soil horizons and the entire profile (mechanical degradation). It can also result in a change in specific physical properties such as in cases of compaction (Snakin et al. 1996). The extreme degree of physical degradation is the complete destruction of the soil up to the state of a rock or a largely abiotic desert such as in case of land take for buildings or brownfields (Dobrovolskiy et al. 2012).

Physical degradation can be initiated by various natural factors and can develop under conditions of natural biogeocenoses as a result of changes in climatic conditions, natural processes of weathering, denudation, erosion and desertification. However, physical degradation often develops everywhere in the soil as a result of excessive mechanical, chemical, physico-chemical, water or biological loads caused by human activity (Dobrovolskiy et al. 2012; Selivanovskaya et al. 2014).

On agricultural land, one of the most important soil properties is aggregation that is greatly responsible for soil physical resistance to degradation (Karlen et al. 2008). An optimum level of aggregation is more resistant to surface sealing allowing more rapid water and air penetration. In agroecosystems, soil aggregation is primarily influenced by kinds of landuse, cropping systems, tillage intensity and residue management (Tisdall and Oades 1982; Oliveira et al. 2019; Nunes et al. 2020). In addition, soil physical degradation is manifested in the removal of fine-loamy and colloidal particles from the surface horizons of soils, which can occur both under the influence of wind (wind erosion, or deflation), and under the influence of surface runoff (water erosion) (Ivlev and Derbentseva 2003).

Mechanical destruction of soil occurs during the construction of roads, construction of gas and oil pipelines, mining and agriculture, especially by grazing and tillage (Snakin et al. 1992). Dobrovolskiy et al. (2012) classified main processes accompanying physical soil degradation: (1) surface crusting and compaction due to the impact of water drops from rain and sprinkler irrigation, animal trampling and agronomic activities, (2) loss of topsoil due to excessive tillage and loss of soil organic matter (SOM) and

(3) subsoil compaction due to machinery loads or wrong depth and frequency of ploughing. These processes may lead to (1) deteriorated soil water and air regimes, (2) increased surface runoff resulting in soil erosion and (3) limitation in spatial growth and development of plant roots.

Soil erosion is a popular type of physical soil degradation. It is one of the ten major soil threats identified in the 2015 Status of the World's Soil Resources report (FAO and ITPS 2015) and subsequently addressed in the FAO's Voluntary Guidelines for Sustainable Soil Management (VGSSM) (FAO 2017). Soil erosion could also have the potential being a net carbon sink (Berhe et al. 2007). About 75 billion tonnes of soil are eroded every year from arable lands worldwide (GSP 2016). About 60% of these soil losses are due to human activity (Yang et al. 2003; Naipal et al. 2015). Changes in land use, agricultural mismanagement and climate change (Walther et al. 2002; Borrelli et al. 2020) will lead to accelerated soil erosion. Soil erosion was responsible for the decline of ancient civilizations (Montgomery 2007) and is a threat to the livelihood and survival of mankind. In 2015, the UN formulated 17 global Sustainable Development Goals (SDG) (UN 2015). They address soil functions and degradation issues indirectly in most clauses such as eradication of hunger.

In drylands, erosion and other types of degradation lead to desertification, the worst case of soil and land degradation. Since 1994, the United Nations (UN) Convention to Combat Desertification exists (UNCCD, UNCCD 1994). Other organizations such as the Food and Agriculture Organization of the United Nations (FAO) and the Intergovernmental Technical Panel on Soils (ITPS) (FAO and ITPS 2015), the UN Development Programme (UNDP) support the UNCCD 2018–2030 Strategic Framework of combating land degradation (UNDP 2019).

Actions of panels at different levels require sophisticated and innovative knowledge and databases. Despite some recent progress in diagnosis, prevention and therapy of soil degradation processes, this basis must become broader (Bouma 2019). Decision-makers, stakeholders and informed citizens want to have better

knowledge and data about soil processes for their assessment and sustainable action to prevent and combat degradation, to optimize soil functions and ecosystem services. Soil degradation needs to be better understood, forecasted and evaluated in the soil health and landscape context (Mission Board 2020). To detect knowledge gaps in monitoring and modelling of specific soil physical degradation processes, we reviewed the current state of knowledge. Most widespread and severe types of degradation considered in this chapter are erosion by water, wind and tillage, soil compaction and soil sealing.

2.2 Types of Physical Soil Degradation

2.2.1 Soil Erosion by Water

Essence and causes. Water erosion is a process driven by intense rainfall, runoff, melting snow or ice, incorrect irrigation, topography, low soil organic matter content, low percentage of crop cover and non-optimal type of vegetation. It is intensified and accelerated by human activities, such as inappropriate land management, periods of bare soil through deforestation, tillage of steep slopes, cultivation techniques and cropping practices, deforestation and land marginalization or abandonment (e.g., Chumbaev and Tana-sienko 2016).

Detachment of soil particles occurs by force of raindrops on bare soil (Tarolli et al. 2018). The intensity and dispersion of raindrops have an initial and dominant effect on the soil (Shainberg and Levy 1996; Huo et al. 2020). When the drop hits the soil surface, it compresses the soil and removes particles and aggregates entrained by a crown of lateral droplets that are ejected laterally and upward (Torri and Borselli 2000). Then the mechanism of transportation of soil particles occurs due to gravity or by overland flow (flooding, furrow irrigation, etc.). The extent of water erosion generally increases with rising flow energy, decreasing soil structure stability and high rainfall energies. These parameters are determined by the following factors: rainfall

distribution (intensity, drop sizes and volume), electrolyte content and composition of rainwater, slope steepness, slope length and slope shape, soil texture, cohesion of the soil (putty substances, soil moisture), infiltration capacity, land cover (living plants, crop residues, stones) and root penetration (Wischmeier and Mannering 1969; Blanco-Canqui and Lal 2010; Wu et al. 2020).

These processes are further subdivided based on other criteria into (1) diffuse surface erosion (splash and interrill erosion, sheet erosion), (2) linear erosion (rill and gully), (3) subsurface erosion (piping) and (4) shallow mass movements. The rainfall intensity increases the overall rate of detachment and destruction of soil aggregates into smaller soil particles, which are redeposit and form soil crusts. These crusts seal the soil surface and limit infiltration, filling the macropores between the aggregates thus preventing water percolation into the soils and increasing runoff from storm rainfall (Zuazo and Pleguezuelo 2009; Blanco-Canqui and Lal 2010). Surface runoff is the most important direct factor in severe soil erosion.

A major reason for causing soil erosion is the cultivation of agricultural land, in particularly arable land. According to model calculations by Borrelli et al. (2020), 54% of the total soil loss worldwide results from the main agricultural land (annual crops, permanent crops, managed pasture). Especially, ploughing and fine seedbed preparation leaves the soil prone to erosion. But even after harvesting or in the intercropping period, when no cover crop is sown and the soil is bare, the soil is unprotected and susceptible to erosion. Soil compaction by heavy machinery is another trigger for runoff and erosion on arable fields. In most cases, soil erosion occurs in pathways, either shaped topographically (thalwegs, slope depressions) or human-made flow pathways (wheel tracks, headlands, furrows) (Prasuhn 2020).

Another cause of water erosion can be animal activity such as trampling and burrowing. Grazing animals can destroy vegetation leaving a bare soil surface exposing to water erosion. In addition, uncontrolled amount of grazing cattle may

compact the topsoil by hooves thus being a driver of runoff and erosion. Obviously, bare soil surfaces increase the erosion since vegetation has a direct effect (canopy reduces the total kinetic energy of the rainfall that is dissipated on the soil surface) and an indirect effect (reduces shallow mass movements; roots resistance to the soil passing through the sliding surface and fixing the potentially sliding portion to the underneath layers).

Another important type of water erosion is snow-melt erosion, which recently is paid more attention to, particularly in the West Siberian slopes, where the amount of solid precipitation, snow depth and their water equivalents are basic factors of snowmelt erosion in spring (Chumbaev and Tanasienko 2016). Snowmelt erosion is the most dangerous type of soil degradation on the territories with a long period of snow cover (more than 4 months), seasonally freezing soils and active agricultural human activity. Under certain conditions, during the period of snow melting (5–7 days), up to 30 t/ha of solid soil material can be removed from the fields by water flows.

Extent, features and implications of water erosion.

In a recent study, Borrelli et al. (2020) predict global potential soil erosion rates of 43 Gt year⁻¹, while FAO and ITPS (2015) estimate that the global soil erosion by water is 20–30 Gt year⁻¹. However, Montgomery (2007) mentions an average of 3.939 mm year⁻¹ (~47 t ha⁻¹ year⁻¹) soil loss rates for fields with conventional agriculture compiled from 448 studies worldwide. But it is not easy to correlate these global estimates with accurate national, regional or local soil erosion rates, as soil erosion is highly variable both in time and space. Measured or modelled erosion rates around the world vary over >4 orders of magnitude (Montgomery 2007). However, these estimates differ in part because of the method used to generate the soil loss rates (FAO 2019). Exemplary average modelled water erosion rates range between 4.6 t ha⁻¹ year⁻¹ for cropland for Australia (Lu et al. 2003), 6.70 t ha⁻¹ year⁻¹ for cultivated cropland in the United States (Nearing et al. 2017), 7.65–49.38 t ha⁻¹

year⁻¹ on farmland under conventional tillage of five water erosion regions in China (Guo et al. 2015) and 2.45 t ha⁻¹ year⁻¹ for all land uses as well as 2.65 t ha⁻¹ year⁻¹ for arable land in 28 European countries (Panagos et al. 2020), with the highest erosion rates for Malta (9.49 t ha⁻¹ year⁻¹), Italy (8.59 t ha⁻¹ year⁻¹) and Spain (4.0 t ha⁻¹ year⁻¹) and the lowest erosion rates for Finland (0.46 t ha⁻¹ year⁻¹), Netherlands (0.52 t ha⁻¹ year⁻¹) and Denmark (0.57 t ha⁻¹ year⁻¹).

Some forms of erosion on cropland are shown in Fig. 2.1. The direct effects of water erosion are losses of organic matter, degradation of soil structure, soil surface compaction, reduced water infiltration, changes in hydrological conditions (lack of groundwater recharge), surface soil loss, nutrient removal, rill and gully formation, plant uprooting and reduced soil productivity. The main mechanisms of water erosion are the detachment, transport and deposition of soil particles. The indirect and often far-reaching effects of water erosion are water and soil pollution, water eutrophication, floods, infrastructure burial, destruction of drainage network, silting of waterways and ports (Louwagie et al. 2009). Accelerated erosion occurs when the plant cover is depleted, the spaces between plants become larger, and soil structure is degraded by excessive disturbance or reduced inputs of organic matter (Tarolli et al. 2018).

In addition, the loss and redistribution of the topsoil layer can result inter alia, in an unfavourable vegetation succession, since the fertile soil layer is removed/reduced and destroyed, and the root depth is shallower. The shifted vegetation cover ultimately leads to changes in soil biological characteristics, such as altered composition and diversity of soil microflora (Domichin et al. 2019). Soil compaction increases runoff and the risk of accelerated erosion. Another example is a poorly designed infrastructural network that can also cause accelerated erosion on adjacent slopes and in roadways (Tarolli et al. 2018).

Furthermore, the transportation and deposition of soil particles lead to sedimentation, water pollution and siltation of watercourses, which have wider environmental implications (Pimentel

2006). Therefore, the processes that directly or indirectly lead or trigger the runoff are important variables in the estimation of soil erosion intensity, since they play a major role in developing the site-specific countermeasures. Runoff is a portion of rainfall or irrigation water that does not percolate the soil but is discharged from the area into streams. Surface runoff, which is lost without getting into the soil, is the most important direct factor in severe soil erosion. One of the most important factors in controlling runoff is the degree of the soil surface crust. A minor but still important microrelief of the soil surface and the subsurface structure of the soil, in particular the presence or absence of macropores, are in the form of cracks and/or voids between the soil aggregates.

On cultivated lands, water erosion means a severe threat to soil resources as the rates of soil loss on arable lands are mostly equal to the rates of soil loss of Alpine terrains (the rate of erosion in traditional agricultural fields is one to two times higher than the rate of soil production) (Montgomery 2007). This hypothesis has been confirmed by many studies (e.g., Panagos and Katsoyiannis 2019), which report that the rate of erosion in agriculture is one of the highest among all types of land use. FAO and ITPS (2015) quote a median value for soil formation of approximately 0.15 t ha⁻¹ year⁻¹. Verheijen et al. (2009) provide a range of 0.3–1.4 t ha⁻¹ year⁻¹ for soil formation rates by both weathering and dust in most European situations. However, Alewell et al. (2015) could show that soil formation in the Swiss Alps can be very high on geological young (>1,000–10,000 years) and very young soils (<1,000 years) with 1.2–2.5 t ha⁻¹ year⁻¹ and 4.2–8.8 t ha⁻¹ year⁻¹, respectively.

In agricultural areas, water erosion can be controlled by crop residue management, contouring, strip cropping, conservation tillage, terraces and buffer strips on an irrigated area (Morgan and Rickson 1995; Xiong et al. 2018). No-till farming effectively mitigates all forms of soil erosion caused by machinery use and water. Seitz et al. (2020) stated that the further acceptance of no-till practices by farmers is one of the most important measures to successfully tackle

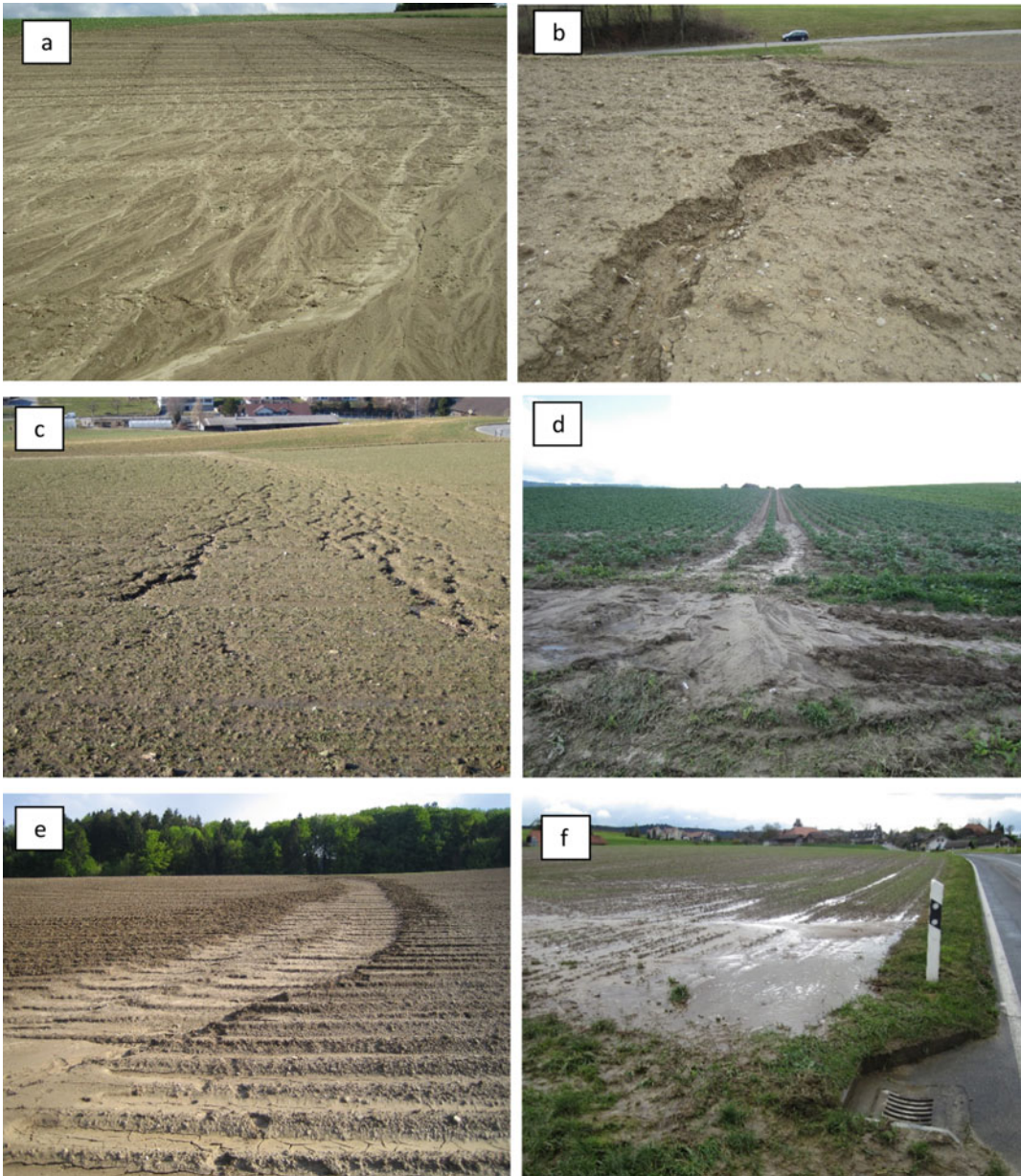


Fig. 2.1 Forms of erosion by water in agricultural landscapes and damage to soils and waters. Examples from Switzerland. **a** Sheet erosion, **b** rill erosion, **c** sheet-to-linear erosion, **d** erosion in wheel tracks, **e** ephemeral gully erosion due to breakthrough of ridges in a potato

field in a slope depression, **f** off-site damage through siltation and contamination of brooks and other open waters via inlet shaft and pipe drainage. *Photos V. Prasuhn*

the threat of soil erosion globally. Soane et al. (2012) presented the state of no-till in Europe and advantages and disadvantages of no-till.

They noted that less erosion and run-off can be widely observed after the introduction of no-tillage.

In addition to the technical feasibility and documented effects of an erosion control measure, the acceptance and motivation of farmers is an important driver of change in land management practices (Boardman and Evans 2019). The triggers can be multi-layered (environmental, economic, social). Climatic changes, technical innovations, political incentive strategies, mitigation measures, market development, farmers' rising awareness, etc. can influence the extent and spread of soil loss rates and may change over time. It is obvious that farmers' decisions on cultivated crop and management practices are markedly determined by socio-economic factors such as financial returns, land-use policies, introduced technology, food security pressure, consumer demands and poverty (Govers et al. 2017).

Water erosion monitoring and modelling.

Erosion measurements form the basis of all erosion models and are essential for the calibration and validation of the models. There are numerous options for measuring and monitoring water erosion:

- bounded test plots: defined experimental areas of various sizes, limited on all sides (a few square centimetres (splash cups), standard USLE plots (22 m long, 4 m wide) for interrill and rill erosion, often linked to sprinkler systems; entire slope for rill erosion)
- unbounded test areas: Sediment trap boxes in the field ("Gerlach through") or sediment collecting channels at the edge of the field with sampling divider ("Coshocton wheel")
- Measurement using erosion nails, pins, etc.
- Mapping and volumetric measurement of visible erosion features in the field
- Use of remote sensing, aerial photography, drones and 3D laser scanning to identify and quantify forms of erosion
- Use of tracers such as caesium, beryllium, etc.
- Analysis of soil profiles ("truncated profiles")
- Measurement of the sediment delivery from a catchment area

The soil profile truncation method is a proven field method (Golosov et al. 2021), applicable in

soil survey and in stakeholder meetings on field days. Several authors (Alewell et al. 2019; Batista et al. 2019; Evans 2017; Parsons 2019) have recently evaluated these methods to assess soil erosion. Most measurement methods are expensive and time-consuming. However, long-term measurements are necessary since soil erosion often depends on randomly occurring major events (Prasuhn 2011; Evans 2017). Only long-term studies reduce the bias resulting from low-frequency high-magnitude effects. However, erosion measurements are the basis of all erosion models and are essential for the calibration and validation of the models.

The potential rate and degree of soil erosion can be estimated by certain soil and terrain properties (Tarolli et al. 2018) and attributes such as (i) *inherent soil properties*: clay and sand content (water retention and drainage), bulk density (compaction), SOM content (water retention, aggregation); (ii) *terrain characteristics*: slope (steepness and length), topography (concave or convex slope); (iii) *climate*: intensity and frequency of rainfall and (iv) *vegetation* type and density (root depth, degree of crop covering, canopy gaps, etc.).

The prediction and assessment of erosion are challenging for researchers since the 1930s (Lal 2001). Of great scientific interest are assessments of land erosion risk based on mathematical modelling of erosion processes because they allow predicting the possibility of development of erosion upon combined action of certain factors. Soil losses due to water erosion can be characterized by three types of modelling: empirical, semi-empirical and physical. Nowadays, there are many different erosion models available (Pandey et al. 2016), nevertheless, the USLE is the most common model worldwide. Borrelli et al. (2018) estimate that more than 90% of soil erosion assessment worldwide is performed with USLE-based models. The most used empirical and semi-empirical models are based on the Wischmeier equation USLE (Universal Soil Loss Equation) developed for predicting soil losses due to water erosion on arable lands and slopes (Wischmeier and Smith 1978) and on the Revised Universal Soil Loss Equation (RUSLE),

an updated version of USLE with an improved accuracy of soil loss prediction (Renard et al. 2001; Alewell et al. 2019; Gianinetto et al. 2019). The PESERA model for a Europe-wide estimation of water erosion (Kirkby et al. 2008) is a physically based and spatially distributed model with integrated input data of topography, climate and soil to predict run-off and soil erosion. The WaTEM-SEDEM long-term erosion model is used to simulate the runoff and soil erosion (Panagos and Katsoyiannis 2019; Konečná et al. 2020). KINEROS (USDA 2019), a kinematic erosion simulation model is an event-oriented, physically based model describing the processes of interception, infiltration, surface runoff and erosion from small agricultural and urban watersheds. The WEPP (water erosion prediction) (Flanagan et al. 2001) and GeoWEPP models are probably the most complex and sophisticated simulation models that simulate many of the physical processes important in soil erosion, including infiltration, runoff, raindrop and flow detachment, sediment transport, deposition, plant growth and residue decomposition (Srivastava et al. 2020; Haas et al. 2020). It involves high-frequency input data such as daily rates of hydrologic, plant growth and even litter-decay processes.

All these erosion modelling tools are successfully used for many catchments and regions such as the catchment area of the River Quillow with about 170 km², North-East Germany (Mirschel et al. 2006). Models describing the erosion risk are also used within decision support systems for assessing landscape indicators. An example is the EROSION model within the decision support system LandCaRe-DSS (Wenkel et al. 2013; Mirschel et al. 2020), an interactive model-based decision support system for assessing the impact of climate change on agriculture and agricultural landscapes. The EROSION model calculates the potential erosion risk dependent on site, farm management and climate using the modified Revised Universal Soil Loss Equation (RUSLE) (DIN19708 2005; Wieland 2010). EROSION 3D (Schmidt et al. 1999; Hänsel et al. 2019) is sophisticated, broadly applied physically based simulation

model to estimate sediment yields on a catchment scale.

Evans (2013, 2017) casts doubt on the reliability of the predictions of soil losses due to erosion obtained by different empirical models, due to lack of validation of the model results, which limits extrapolation of the plot data over a catchment or wider area. This might be due to the present total eroded area, which is poorly related to current, site-scale levels of environmental stress (Streeter and Cutler 2020). If using those models, regional and local adaption of input factors and data based on experiments are necessary (Bircher et al. 2019a).

Probably, further development and upgrading of existing empirical and physical based simulation models should be focused on deeper integration with field studies and validated to produce realistic outputs and prediction of soil losses due to water erosion on all landscape and spatial levels. Numerous studies proved that an integrated approach of the combination of empirical modelling with GIS and Remote Sensing capabilities gives a wide range of possibilities (e.g., Kheir et al. 2006; Wu and Wang 2007; Wenkel et al. 2013; Mirschel et al. 2020).

Area-wide mapping erosion risk is based on algorithms combining different data sources, such as topographic maps, soil maps and recent airborne data of land use, on GIS platforms. Those maps are meanwhile available nationwide in many countries, having high resolution down to single fields and hotspots of erosion within them (Bircher et al. 2019b). Borelli et al. (2017) developed a high resolution (250 × 250 m) global potential soil erosion model, using a combination of remote sensing, GIS modelling and census data. Based on a RUSLE approach, Guerra et al. (2020) modelled the vulnerability of soil conditions to erosion and its implications for soil macrofauna and soil fungi with high resolution on a global scale.

2.2.2 Soil Erosion by Wind

Essence and causes. Like water erosion, wind erosion has three phases: detachment

(entrainment), movement and deposition (Zobeck and Van Pelt 2014). The detachment of soil particles is initiated by forces of blowing wind, when soil particles are dislodged and transported along the soil surface in different ways, such as *creep*, *saltation* and *suspension* (Zobeck and Van Pelt 2014). During the process of wind erosion, a kind of chain reaction takes place: larger aggregates that pass shorter distances hit smaller aggregates thus breaking them into finer particles (e.g., dust) and suspending them into the air, and naturally smaller particles are transported in longer distances (Zobeck and Van Pelt 2014).

As to climatic factors, wind erosion is closely related to rainfall and temperature. With increasing aridity of the climate and decreasing humidity, soil deflation increases. Unlike water erosion, wind erosion is observed both on the slopes and in perfectly levelled areas. Wind carries erosion products into different directions and even up a slope. However, convex surface areas and wind-impact slopes are primarily affected by wind erosion. Vegetation is the most powerful factor counteracting wind erosion. On soils covered with virgin vegetation, wind erosion is practically absent. The environmental impact of windstorms is related to the speed of the wind flow and the size of soil particles, where up to 30–40% of particles are transported in suspension. In this case, dry and windy weather, poorly aggregated and coarse soil, bare and smooth relief are the factors that contribute most to wind erosion (Zobeck and Van Pelt 2014). Furthermore, rainfall intensity and duration, freezing and thawing cycle also pose a manifest impact on soil vulnerability to wind erosion (Lyles and Tatarko 1988) since the soil aggregation is disturbed by water actions. The method and intensity of tillage also contribute to the effect of wind on the soil.

The granulometric composition of the soil and its aggregation has a significant impact on the occurrence and development of wind erosion. Wind erosion starts when the velocity of the wind at the soil surface exceeds the threshold velocity required to move the least stable soil particle (static threshold). Commonly, the light-

textured soils (sands and sandy loam as well as peat soil) are easily blown, while heavy soils are blown out only after loosening by ploughing or other soil tillage methods.

Soil erodibility by wind is related to the percentage of dry non-erodible surface soil aggregates larger than 0.84 mm and is classified into Wind Erodibility Groups (WEG). Lyles and Tatarko (1988) identify eight groups of soil wind erodibility based on the percent of the >0.84 mm sized aggregates, including soil characteristics such as particle size distribution, texture, bulk density, percentage of exchangeable calcium, content of organic matter and soil water.

Soil properties and the attributes related to soil vegetation topography, such as soil roughness, erodibility, wetness and crop residue, quantify an orientation. These parameters mostly determine the vulnerability of soils to wind erosion. If the erodible soil surface is covered with vegetation or residues from a previous crop, the force of the wind is transferred to the non-erodible cover and erosion is controlled. Webb et al. (2020) identified the following indicators describing wind erosion risk or air quality: fractional group cover by type, canopy gap size distribution, canopy height, dust emission flux and dust concentration.

Extent, features and implications. Wind erosion is often a largely hidden and a still underestimated threat to soil resources, productivity and ecosystem services (e.g., Funk 2016; IPCC SRCCL 2019; Webb et al. 2020). Its acceleration through human-induced actions is the main source of threat to soils across the globe. It is disabling huge areas of fertile land, which are mainly the result of ill-considered use of soils caused by uncontrolled deforestation, excessive grazing, irregular plowing on the slopes and improper farming methods. Therefore, the complex and dynamic nature of the wind erosion process presents a significant challenge to science, there is not yet an effective way to prevent severe wind erosion until now.

In Inner Mongolia on dry sandy soil with rainfed farming, Zhao et al. (2006) showed that severe wind erosion resulted in a reduction of clay by 59.6%, organic C by 71.2%, total N by 67.4%, total P by 31.4%, available N by 64.5%,

available P by 38.8% and an average soil water content by 51.8%, compared with non-eroded farmland. Ploughing of light soils, their loosening is especially dangerous in spring, when they are deprived of a protective green cover, which makes them vulnerable to deflation. A huge influence on its development is exerted by anthropogenic factors, such as destruction of vegetation, unregulated grazing, and the improper use of agricultural measures sharply activate erosion processes.

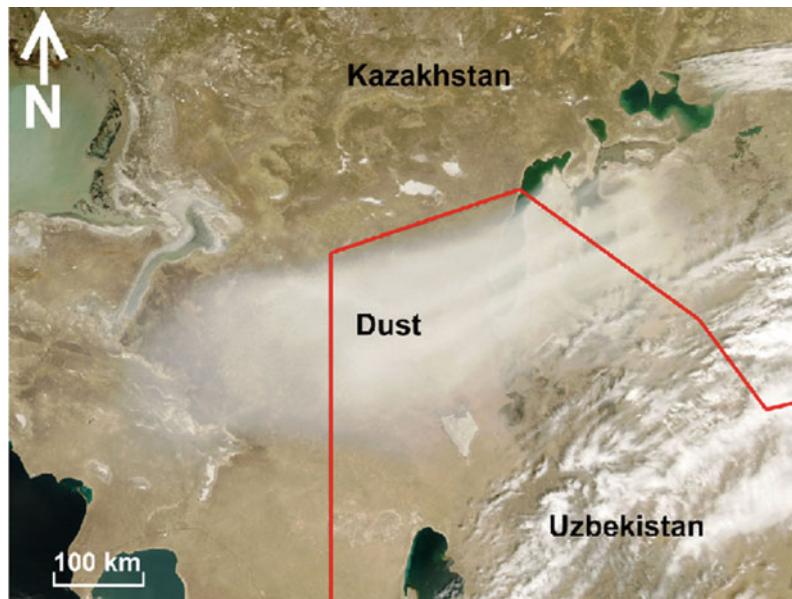
One of the manifestations of wind erosion of soils is dust storms, which are associated with three main factors: (1) prolonged exposure to wind flow on an unprotected vegetation surface of the soil, (2) the critical speed of the wind flow and (3) the nature of the disaggregation of the surface soil layer. The blowing sand may bury roads and fill in drainage ditches, necessitating expensive maintenance. The wind-borne soil particle may damage fruits and crops, as well as the surfaces of vehicles and buildings long distance downwind from eroding sites. Thus, after the devastated drying up of the world's fourth-biggest lake, the Aral Sea, the shrinking waters left behind dust, salt and pesticides that saline dust storms would carry as far as the Himalayas. Satellite images showed major salt- and dust-

cloud extending as far as 500 km downwind the shore of the Aral Sea (Issanova and Abuduwaili 2017) (Fig. 2.2).

At the same time, erosive particles have a large destructive force, moving spasmodically, they break up larger lumps and damage crops. In addition, wind erosion affects human environment through exposition to dust and reduced visibility on highways, railroads and airports, and agriculture through loss of soil fertility (Greeley and Iverson 1985). In drylands, the interaction of different disturbances including fire, livestock grazing and off-highway vehicles can increase horizontal eolian flux up to 40-fold as compared with largely undisturbed rangelands (Duniway et al. 2019). The threshold for wind erosion that demarks tolerable and hazardous soil conditions has been under discussion since long in literature. Attempts to improve existing approaches in estimation of the tolerable soil loss due to wind erosion have been regularly developed worldwide (such as the microbiological approaches to increase soil tolerance to erosive force of wind (e.g., Fattahi et al. 2020).

Dust deposits affect remote ecosystems, for example enrich them with nutrients and change the albedo of snow cover on the mountains (Duniway et al. 2019).

Fig. 2.2 Extended dust cloud in Central Asia as a result of accelerated wind erosion in the shore of the Aral Sea (Source Issanova and Abuduwaili 2017)



Monitoring and modelling wind erosion.

Wind erosion is influenced by several factors such as wind force, soil wetness, surface roughness, soil texture and aggregation, soil organic matter, agricultural activities, vegetation cover and field size (Bagnold 1943; Chepil and Woodruff 1963; Jarrah et al. 2020).

Considerable success has been achieved in measuring and monitoring wind erosion processes during the past two decades. Process parameters of soil dust particles were measured with high precision for understanding mechanisms of wind erosion, dust transport and deposition and for quantifying input parameters of models (Funk and Engel 2015; Funk 2016; Siegmund et al. 2018; Groll et al. 2018).

Major factors contributing to wind erosion can be modelled physically, empirically or theoretically. Wind modelling is an important prerequisite for wind erosion research (Zhang et al. 2011). A recent overview on existing wind erosion models is given by Jarra et al. (2020). The spread software programme WEQ (Wind Erosion Prediction Equation) for the prediction of soil loss by wind erosion, based on the wind erodibility index, which expresses stability of dry aggregates under tillage and abrasion, has been successfully used by Woodruff and Siddoway (1965). However, Zobeck and Van Pelt (2014) doubt that it has certain limitations related to the climatic input data, lack of prediction frequency, changes of soil surface attributes (aggregation, roughness), vegetation and land-use factors. To overcome these limitations, a new approach as a prediction tool for wind erosion monitoring was developed by USDA-ARS. The Wind Erosion Prediction System (WEPS) provides the user with a simple tool for inputting initial field and management conditions, calculating soil loss and displaying simple or detailed outputs for designing erosion control systems (Pi et al. 2020).

Recognizing and mapping areas prone to wind erosion are possible by remote sensing data, geographical information systems and advanced statistical tools (Baumgertel et al. 2019). Numerous studies showed that the integration of various indicators (particularly soil and

vegetation parameters and attributes) using wind erosion models (Munson et al. 2011; Pierre et al. 2018; Tatarko et al. 2019), including remote sensing (Chappel et al. 2019), are proved to be successful and provide more reliable estimate of wind erosion than using the indicators independently.

Webb et al. (2020), in reviewing the existing approaches to monitor indicators of wind erosion including *meteorological* (Aerosol Robotic Network; Interagency Monitoring of Protected Visual Environments; Campaign on Atmospheric Aerosol Research network of China; and Australian DustWatch program) (Leys et al. 2008), satellite monitoring and empirical modelling (Sand and Dust Storm Warning Advisory and Assessment System (WMO 2020; Chappel et al. 2019), noted that these methodologies need to be adapted for the use by managers, and the data need to be synchronized.

2.2.3 Soil Erosion by Tillage

Essence and causes.

Soil erosion is caused by natural and anthropogenic forces. Water, wind or gravity erosion are usually thought of as a natural process, as they are induced by natural driving factors. On the other hand, soil erosion also occurs as a result of human driving factors, mainly derived from tillage in agricultural practices, independent of those natural processes. Tillage erosion is a process of soil translocation by operations of tillage tools. It occurs mainly in sloped areas where gravity acts as an important translocation force (Winnige 2004; Li 2006; Zhang 2011). The most common tillage device, the mouldboard plough, by its construction, causes a permanent sideways mass movement of soil in the mechanized agricultural areas. In the non-mechanized agricultural areas, where the animal-drawn plow and manual hoeing tillage are used, the soil is typically turned downslope to maintain energy saving, thus leading to the downslope movement of soil. Tillage erosion is expressed in units of volume, mass or depth per unit width of tillage (Zhang 2011).

Extent, features and implications.

Studies of tillage translocation and tillage erosion have been focused on the redistribution of soil mass. Tillage erosion has been recognized and defined as a separate process, different from water and wind erosion during the past decades (Li et al. 2007; Zhang et al. 2008, 2009). Tillage erosion largely causes soil loss in shoulder slope or downslope sides of the field boundary, while water erosion usually occurs in the middle to lower back-slope positions. In the convex positions, where water erosion is weakest, tillage erosion is most severe. In the concave positions, where water erosion is most intense due to convergent water flow, soil accumulation by tillage occurs. Tillage erosion moves soil over a short distance, and the eroded soil does not transport off the field, which is different from water erosion that transports soil over a long distance and off the field. As tillage-deposited soil occurs towards the downslope boundary of the field, there is an approximate balance between soil loss and gain within the field. Among the factors influencing tillage erosion rates, the most important ones are slope gradient and slope length. With respect to slope length, its effects on tillage erosion display

a contrary role to those on water erosion. Tillage erosion rates are negatively proportional to slope length, while water erosion rates increase with increasing slope length.

Tillage erosion influences soil erodibility to water and wind erosion in the cultivated layer, as the eroded topsoil contains more SOC, and has more stable soil structure than subsoils. Tillage erosion may interact with water erosion, leading to accelerating each other. On one hand, tillage erosion transports soil into convergent areas of overland water flow, where the most severe water erosion is present, causing more severe soil loss (Lobb et al. 1995; Zhang et al. 2011; Wang et al. 2016; Dai et al. 2020). On the other hand, the impact of water erosion on soil redistribution by tillage is evident on the rilled hillslopes, as changes in the slope microtopography occur due to rill occurrence and development (Wang et al. 2020).

Tillage erosion brings in a threat to hilly landscapes (Fig. 2.3) but can be reduced by conservation tillage (Zhang et al. 2009). Contour tillage is a common technique and one of the most effective ones to control tillage erosion, reducing 51–77% soil loss compared with

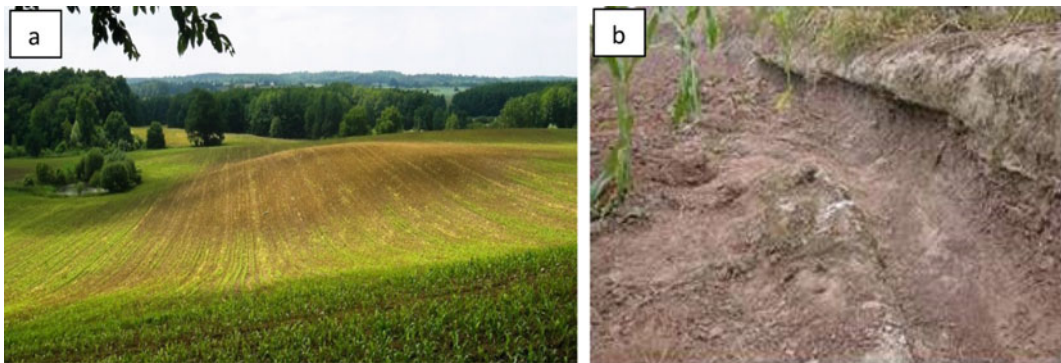


Fig. 2.3 Features of tillage erosion in different landscapes. **a** Result of tillage erosion in an undulated subhumid Late Pleistocene landscape in Germany. The brown colour of the soil surface indicates the former illuviation (Bt) horizon, which is now forming a new topsoil. The former Ap horizon had been moved downwards due to ploughing over centuries. Because this topsoil is loamy-clayey, of low humus content and prone to clumping after tillage, germination and emergence of crop seedlings are hampered. *Photo* L. Mueller. **b** Tillage

erosion in a hillslope landscape of the Sichuan Basin, southwest China. Soil at upslope has been substantially eroded due to intense tillage, and the bedrock in the vicinity of the upslope has been dug to provide for soil matrix, resulting in the appearance of a flume at the wall side. Tillage erosion subsequently leads to bedrock erosion by hoeing, as bedrock is soft and soil-eroded areas need to be offset by external material (Xu et al. 2020). *Photo* J. H. Zhang

conventional up- and downslope tillage (Poesen et al. 2000; Thapa et al. 1999; Zhang et al. 2004a). In southwest China, the non-overturning tillage has significantly diminished tillage erosion rates, with a reduction of 63% compared with those by conventional tillage (Zhang et al. 2009).

Monitoring and modelling tillage erosion.

Several techniques including physical and chemical ones are used to trace the soil translocation by tillage. Physical tracers used in measuring tillage translocation have involved metal cubes (e.g., Govers et al. 1994), rock fragments (e.g., Nyssen et al. 2000) and stone chips (e.g., Zhang et al. 2004a, b), and chemical tracer radiocaesium (e.g., Lobb et al. 1995; Li et al. 2007) and chloride (e.g., Lobb et al. 1999). The low-induction electromagnetic (EM) (De Alba et al. 2006) and magnetic tracer techniques (Zhang et al. 2009) were also used to determine soil translocation rates, which are characterized by a quick manipulation and low workload. Recently, researchers employed the unmanned aerial vehicles (UAVs) and passive radio-frequency identification transponders (RFIDs) to measure soil displacement, and thus determine tillage erosion rates (Fiener et al. 2018; Yang et al. 2020).

The diffusion model proposed by Lindstrom et al. (1990) and Govers et al. (1994) is used and developed worldwide to describe tillage translocation in different tillage systems (e.g., Quine et al. 1997; Lobb and Kachanoski, 1999a). In the diffusion models, the intensity of tillage translocation is characterized by the tillage transport coefficient. There is no information provided on the transferring of surface soil and subsoil. Later, Lobb and Kachanoski (1999b) suggested the use of an exponential function to simulate tillage translocation. Van Oost et al. (2000a) proposed the use of a convoluting procedure to simulate the translocation process. He established a model to predict soil constituent redistributions. In further studies, Van Oost et al. (2003a, c) extended the model to two dimensions, which accounts for both forward and lateral translocation. His

WaTEM model (van Oost et al. 2000b, 2003b) was developed to calculate the extent of tillage erosion in different landscapes.

The Tillage Translocation Model (TillTM) that is described in detail by Li (2006) is a two-dimensional model (horizontal and vertical dimension) and was developed and written in Visual Basic. The inputs for the TillTM are the topography data and soil constituent concentration as a function of depth at a series of data points along the tillage direction.

Van der Meij et al (2020) created the HydroLorica model, which considers the co-existence of water erosion and tillage erosion in soil–landscape evolution. Innovative measurement methodologies such as the development of optically stimulated luminescence (OSL) dating (Reimann et al. 2017; Van der Meij et al. 2019) were a precondition for the evolvement and calibration of this model.

2.2.4 Soil Compaction

Essence and causes. Soil compaction is a physical (mechanical) process that results in an increase in soil bulk density (and conversely, a decrease in soil total porosity), with adverse impacts on soil structure resulting in decreased water and gas transport capabilities, enhanced penetration resistance and reduced nutrient availability (Wolkowsky and Lowery 2008; Houšková and Montanarella 2008). Soils can be naturally dense due to their particle size distribution or caused by natural high loads from glaciers or translocated soil (Fabiola et al. 2003). Shrinkage of soil induced by freezing and drying (temporally) increases soil bulk density (Horn et al. 1994). Compaction can be caused by animal trampling (Bondi et al. 2020). Most compaction problems of agricultural lands are related to the use of agricultural vehicles and implements (Håkansson et al. 1988; Soane and van Ouwwerkerk 1994; Horn et al. 1995; Schjønning et al. 2015). Soil compaction in forests due to increased mechanization of logging operations

and associated timber transport has become a great concern during the past decades (Cambi et al. 2017; Khitrov et al. 2019). Moreover, compaction of soil (of any land use) may be caused by construction machinery (Berli et al. 2004), military manoeuvres (Webb 2002; Silveira et al. 2010) and other types of off-road traffic (Waever and Dale 1978). Thirty years ago, it was estimated that 33 Mha of arable lands were affected by compaction (Oldeman 1992). More recent studies estimate that 25–45% of arable land in Europe are degraded due to compaction (Graves et al. 2015; Schjønning et al. 2015; Brus and van den Akker 2018).

Compaction results in ecological as well as economic damage to land users and society, and this damage can be divided into on-site and off-site costs. The largest on-site costs relate to crop productivity losses, but on-site costs also include enhance nutrient losses (e.g., N) and increased fuel consumption for tillage operations (Graves et al. 2015). Major off-site costs are caused by flooding, erosion and increased greenhouse gas emissions (Graves et al. 2015). Although exact numbers of compaction costs are difficult to assess, the costs are significant. Graves et al. (2015) estimated the total annual cost of soil compaction in England and Wales to 470 M£ per year.

Most studies that have quantified compaction impacts on soil functions have focussed on crop yields. For example, compaction has been shown to cause yield reductions of 25–50% on cropland in some regions of Europe and North America (Håkansson et al. 1988), and between 40 and 90% in West African countries (Kayombo and Lal 1994). Wolkowsky and Lowery (2008) reported that compacted soil reduces crop yield as much as 50% (yield reduction in Ohio for maize is 25%, for soybean is 20% and for oat is 30%).

Soil compaction can induce or accelerate other soil degradation processes, such as flooding, erosion or landslides due to a reduced infiltration rate and increased run-off (Roger et al. 2017). Also, the upper soil layer is more prone to water saturation due to (subsoil) compaction and thus imposes a higher risk of sliding. On plain

areas, compaction can cause waterlogging, resulting in the destruction of aggregates, and causing crust formation (Ayuso et al. 2019).

The vulnerability of soil to compaction is a combination of the inherent soil susceptibility to compaction (soil texture, packing density; Jones et al. 2003), soil moisture at the time of a certain field operation, land use and soil management (e.g., crops grown, which affect the timing of critical field operations) and machinery (size and weight) used (Keller and Arvidsson 2006). Low levels of organic matter result in weakly structured soils that are prone to compaction. Loosely packed coarse and medium-fine textured soils are inherently more susceptible to compaction (Jones et al. 2003), but soil moisture has generally a much stronger control on compaction susceptibility. Soil strength generally decreases as soils become wetter (although completely saturated soil is incompressible). Moreover, the impact (mechanical stress the soil is exposed to, caused by the machinery driving on the soil) largely determines whether or not a soil compacts.

Soil compaction is by definition an increase in bulk density and decreases in total porosity, but compaction effects are better evaluated by its impact on soil structure properties such as water holding capacity, hydraulic conductivity, gas transport properties, soil mechanical resistance, and directly detectable in the field by visual soil assessment (Bondi et al. 2020).

Extent, features and implications. Soil compaction is a particular threat to intensively used soils in mechanized agriculture. The weight of agricultural machinery has permanently increased during recent decades, and this trend is continuing (Keller et al. 2019, Figs. 2.4, 2.5).

Many soil functions are directly or indirectly influenced by soil structure, i.e., the geometrical arrangement of voids and solids. The soil pore architecture and soil aggregates play a key role in water, gas and nutrient movement and storage within soil. Large, inter-connected soil pore spaces enhance water infiltration into soil, water percolation into the root zone and subsoil, and gas exchange with the atmosphere. Reduced pore size and number will affect soil biological and chemical processes, such as the reduced cycling

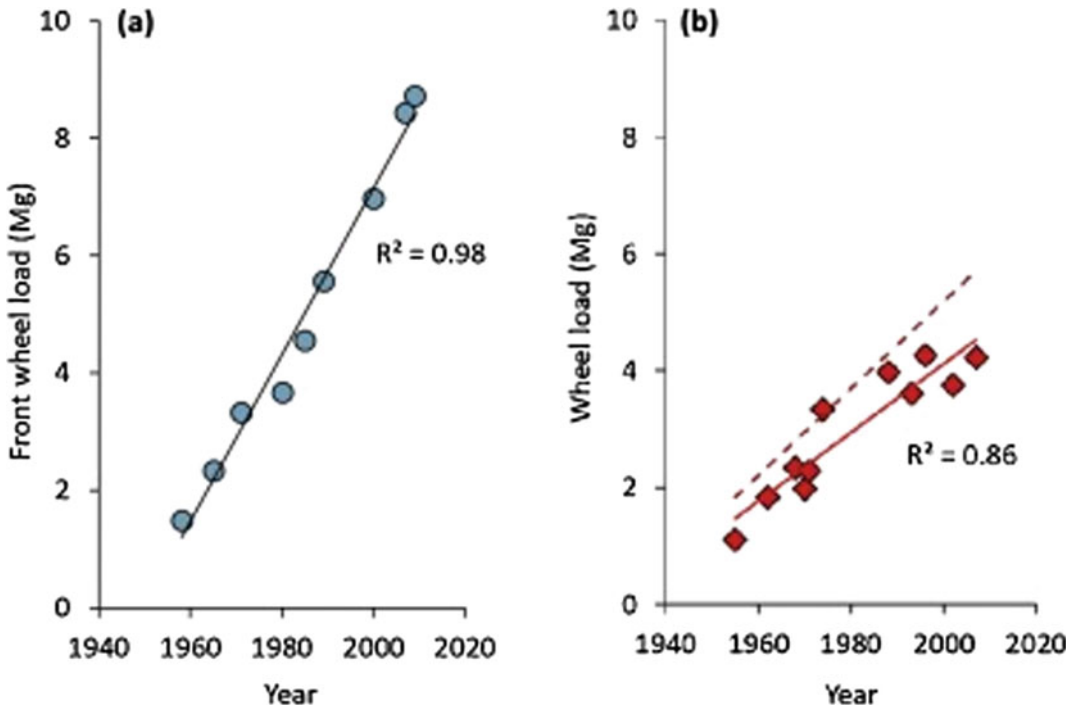


Fig. 2.4 Historical evolution of **a** front wheel loads of combine harvesters, **b** rear wheel loads of tractors. *Source* Keller et al. (2019), kind permission of Elsevier



Fig. 2.5 Self-propelled Trac for transport and application/injection of liquid manure and digestate from biogas plants. Though rules for the prevention of soil compaction exist (e.g., Weyer and Boeddinghaus 2016),

high weights of machinery and spatio-temporally variable soil moisture conditions can create compaction damage. *Photo* L. Mueller

and release of plant-available nutrients and affect carbon dioxide concentration (De Neve and Hofman 2000). Soil structure affects mechanical

resistance to root growth and bioturbation by soil fauna and governs the habitat for soil organisms. Compaction has adverse impacts on soil

structure, with negative effects on most soil properties and functions (Horn et al. 1995). All mentioned on-site and off-site effects of soil compaction result in a physical limitation for plant roots growth (Unger and Kaspar 1994). Schneider and Don (2019) revealed that potential rooting was restricted by compaction in the half of cropland and one-third of grassland in Germany. On about a quarter of cropland, soil compaction by agricultural management was the cause of restricted rooting (Schneider and Don 2019). In forest ecosystems, detrimental effects of compaction on soil structure, emergence of seedlings, soil biodiversity and overall soil quality and health are significant (e.g., Cambi et al. 2017; Lewandowski et al. 2019), requiring certification of forest machinery and forest technologies (Khitrov et al. 2019).

Besides direct impacts from vehicles, soil tillage can induce soil compaction. First, conventional in-furrow ploughing results in high subsoil stress because one side of the tractor drives in the furrow, i.e., on the subsoil (Keller et al. 2002). In addition, soil tillage may cause compaction of tillage-produced fragments and disruption of aggregates in the topsoil that may lead to soil surface crusting.

Recovery of soil structure following compaction is a very slow process, particularly in the subsoil (Peng and Horn 2008; Berisso et al. 2012; Keller et al. 2017). Therefore, the prevention of soil compaction is the best strategy. Prevention of compaction is basically simple by ensuring applied stresses are smaller than soil strength at the time of any field operations. The risk of soil compaction for a given field operation can be estimated by decision support tools, e.g., Terranimo[®]; (Stettler et al. 2014). Situations with a high compaction risk can be avoided by site-adapted soil and crop management and the choice of machinery (e.g., size and weight), which influences the time (i.e., soil moisture) of field operations and involved machinery as well as shapes soil structure and soil strength in the long run.

Monitoring and modelling soil compaction.

Monitoring of soil compaction at large scales is difficult, mainly because there is no “soil

compaction state sensor” that could simply be installed in-situ, and because quantification using remote sensing techniques is not trivial either (compaction may be “hidden” in the subsoil, and compaction may result in subtle changes to soil structure that are difficult to quantify, etc.). Hence, we have little knowledge of the extent and severity of soil compaction at regional, country or continent scales (despite a few studies that present estimates of compaction-affected areas, see above). There are also only very few field studies that monitor compaction impacts and the evolution of soil structure and function after a compaction event (Keller et al. 2017).

The prediction of soil compaction processes in terms of soil stresses and deformation can be done with models of different complexity and requirements for input data, including empirical, analytical and numerical (finite element and discrete element modelling) approaches (for an overview, see Défossez and Richards 2002; Nawaz et al. 2013; Keller et al. 2013). Models based on the analytical solution for stress propagation in elastic media (Boussinesq 1885) are widely used for the assessment of soil compaction risks due to agricultural vehicles (for an overview, see Keller and Lamandé 2010). Such models either compare simulated stress with an estimate of precompression stress or include calculation of soil deformation based on a parameterized stress–strain relationship. These models seem to yield realistic and reliable predictions, despite some of the model assumptions (e.g., the Boussinesq analytical solution is for elastic material) not being accurate for soil. Moreover, it remains unclear how soil structure and soil moisture affect stress propagation, and whether and to what extent stress concentration (similar to force chains known from granular material) develop in soil, and these questions may be better evaluated with distinct element models (e.g., Keller et al. 2013).

Soil structure quality evaluation in the field is possible by site-specific sets of measuring and expert-based estimation soil physical and hydrological properties over large scales (Muel-ler et al. 2009a, b; Bondi et al. 2020). However, soil structure is depending on a multitude of

current and past forces on soil (for example: energetic status of water, upload of former glaciers, root elongation, soil tillage, etc.) and is variable in space and time. Thus, identifying a particular soil structure as compacted and degraded is only possible by developing regional, soil-group specific or site-specific thresholds of bulk density, shear strength, hydraulic conductivity and others.

2.2.5 Soil Sealing

Essence and causes. “Soil sealing means covering of the soil by a completely or partly impermeable artificial material (asphalt, concrete, etc.), causing an irreversible loss of soil and its biological functions and loss of biodiversity, either directly or indirectly, due to fragmentation of the landscape” (Prokop et al. 2011, page 15).

“Land take” is another term for characterizing this process. It is the conversion of open areas into built-up areas (Figs. 2.6 and 2.7). Factually, it is a physical destruction and sealing of soil. Sealing by urban infrastructure includes pavements and buildings (grey infrastructure) and can also include non-sealed areas such as parks and gardens (green infrastructure) (Artmann 2014).

The latter has great importance for livelihoods, biodiversity and bioeconomy (Schneider et al. 2020), mitigating the soil degradation effects of land take. Soil sealing and land take are largely associated with urbanization and industrialization.

Extent, features and implications. Urban land cover is correlated with population growth, land take rates are expanding at twice population growth rates (Angel et al. 2011). While it is expected to permanently expanding in developing countries by 2050, trends in Europe show a slowdown of land take, and zero net rates could be achieved in Europe (Gardi 2015; Penn-Bressel 2018).

Land take for infrastructure and soil sealing cause the irretrievable loss of soil ecosystems and of landscapes of a higher degree of naturalness. Sealing has important hydrological consequences, exacerbating surface runoff, soil erosion and flood risks (Assouline and Mualem 2000; Chen et al. 2013; Luti et al. 2020).

Overall, it affects ecosystem services, including agriculture and food security, biodiversity, hydrology and climate of soils and landscapes, therefore it has become an important issue of environment and sustainability policies (Gardi 2017; Penn-Bressel 2018). Improvement of



Fig. 2.6 Land take for buildings, highways and other urban infrastructure is an extreme case of soil sealing. Soil sealing affects just most fertile soils as cities have developed historically in those places. *Photo* L. Mueller



Fig. 2.7 Pipeline and cable laying for gas, power and communication lines causes physical disturbances of soil with long-term detrimental effects for soil health and plant rooting in many cases. *Photo L. Mueller*

microclimate regulation and reduction of floods are important arguments to minimize sealing and to protect urban green (Artmann 2014).

Monitoring and modelling soil sealing.

Monitoring of land use changes is largely provided by standard methods based on remote sensing data, such as CORINE LAND COVER data, which provide information on landuse changes (Penn-Bressel 2018). In Europe, it is conducted by the European Environmental Agency (EEA). Another multi-sensor and orthorectified satellite imagery has been used to derive soil sealing data (Maucha et al. 2011; Gardi 2017).

In Germany, the Leibniz Institute of Ecological Urban and Regional Development (IÖR) has developed a Monitor of Settlement and Open Space Development (IÖR Monitor) since 2010. It is a complex soil sealing information system, which combines different data sources in model-based simulation and decision support systems for the monitoring of land use structures and developments in Germany (Behnisch et al. 2016).

For projections of future urban expansion and assessing their implications, Gardi (2017) derived ecosystem services from airborne

monitored data. As soil sealing has impacts on other threats to soils such as landslides, digital soil sealing maps have been combined with landslide risk (Shu et al. 2019; Luti et al. 2020). For better understanding, the soil sealing process on common land, a physically based model of soil sealing in dependence of rainfall characteristics, flow conditions and soil properties was developed by Assouline and Mualem (2000).

2.2.6 Other Types of Soil Physical Degradation

Terrain deformation is an irregular displacement of soil material causing clearly visible scars in the terrain. It may be caused by water (as with gully or rill erosion) or mass movements of land, or by wind action (causing deflation hollows, hummocks and dunes) (Oldeman and van Lynden 1997). Landslides and solifluction after permafrost melting affect large regions in the permafrost zone of Siberia with implications for the decay of existing linear infrastructure (roads, railways and pipelines) and biophysical processes such as methane release (Stanilovskaya 2019).



Fig. 2.8 Waterlogging on high-value cropland in Northern Germany. Main wetness features are visible in the course of a levelled former field drain. Tillage of

overwetted clayey soils leads to clumpy and blocky aggregates hampering the emergence of crop seeds. *Photos L. Mueller*

Subsidence is a lowering of the soil surface with implications for hydrological and biochemical processes in soils. It is a common phenomenon after drainage of peats and organic clays. At the first stage, subsidence is caused by a higher upload on soil due to missing hydrostatic buoyancy (Mulqueen 1986; Donaldson et al. 1995). Shrinking of the soil matrix and oxidation of organic matter enhances the effect.

Another kind of land and soil subsidence is a consequence in mining areas. It brings soil in a deeper terrain position and can aggravate soil erosion and soil nutrient distributions in croplands (Jing et al. 2018).

Waterlogging is a natural process in humid regions, on soils in lowlands and depression and on other soils having stagnant properties. It also occurs due to the effects of human-induced hydromorphism through soil compaction. Other causes are a rising water table (for example, due to construction of reservoirs or irrigation) or increased flooding caused by higher peak flows of rivers, and missing maintenance of land drainage systems. The waterlogging results in an oxygen deficit and in conversion of some soil oxides into toxic for crops compounds (e.g., protoxides of iron, copper, nitrogen, etc.). Semi-natural and natural vegetation of grasslands and forests are largely adapted to waterlogging. In semi-arid and arid regions, waterlogging causes

salinization. Waterlogging is a threat to cropland productivity in temperate and boreal landscape zones as anaerobic soil layers impede crop rooting (Vlotman et al. 2020). Waterlogging leads to delay and low-quality soil and plant management operations (Figs. 2.8, 2.9).

Soil crusting is a clogging of soil pores with fine soil material and the development of a thin impervious layer at the soil surface that obstructs the infiltration of rainwater. It is a common phenomenon on cultivated soils occurring often in silty and clayey sodic soils and in other soils of high silt content, low organic matter and high dispersibility of microaggregates (Sumner and Miller 1992; Bajracharya and Lal 1999). The main causes include poor vegetation cover that exposes the soil surface to the action of raindrops; the destruction of soil structure (mechanical crushing or breaking of larger soil aggregates). Considerable degradation and destruction of soil aggregates as a result of which soil particles are suspended in water fused together and then dry in a hard surface soil crust. The crusted soil can limit water infiltration into soil and limit the sprouting of crops. Crusted soils are easily detected visually by examining the soil surface for the presence of lamellar horizontal layered structure. If the crust has formed after sowing, then the seedlings cannot break through the crust and such fields can be easily diagnosed



Fig. 2.9 Ditches for land drainage and other land reclamation constructions are primarily physical impacts in to soils of wetlands. They initiate physical and biological soil reclamation processes. Their positive effect

on crop yields and livelihoods in rural landscapes is evident. On the other hand, if water tables are not properly managed excessive soil subsidence and loss of biodiversity are consequential effects. *Photo L. Mueller*

for crust formation. Surface soil crusting is the result of leaving bare soil exposed to the effects of rainfall and/or irrigation water.

Soil hardsetting is a natural physical change in the soil structure that leads to the formation of a layer impermeable to roots or water flow (Franzmeier et al. 1996; Tebebu et al. 2020), which contributes to increased runoff and soil erosion. Often it occurs in soils of low structural stability prone to crusting as well. Hardsetting is a phenomenon of soils in arid regions as soil drying causes high tensile strengths leading to natural compaction (Mullins et al. 1990). Climate, soil chemistry and soil management play an important role, leading to different types of hardsetting. Examples are lateraization, fragipan formations

and clay-pan formations. The process can be enhanced through tillage-induced remoulding and compaction in soils of a higher silt and clay content. In this case, a “hardpan,” or “plow pan” is formed in the layer of soil just below the depth of tillage (Lal et al. 1989). It occurs when soils are cultivated repeatedly at the same depth, and the weight of the field machinery causes compression and smearing at the base of the contact between the soil and instrument implemented. The presence of hardpan can be detected by removing the arable soil layer to the till depth and checking the direction of the roots’ growth. If hardpan is present, then the crop roots grow horizontally along the surface of the hardpan experiencing difficulty in penetrating the hardpan.

2.3 Gaps of Knowledge and Tasks in Exploring Physical Soil Degradation

As functions and ecosystem services of soils are crucial items to meeting the UN's SDG for a better world (Keesstra et al. 2016; Mission Board 2020), further important gaps of knowledge in understanding, preventing and combating soil degradation need to be closed.

In the area of *experimental basic and applied research*, the complexity of soil physical processes with the following processes is largely still unexplored. The interplay of physical initial effects with soil hydrological, biochemical and biological processes needs to be better understood. Application of mitigation and protective measures against degradation must be explored in the landscape context (Naylor et al. 2020; Daldabayeva et al. 2020). This includes unravelling complex effects of changes in soil structure due to degradation processes on environmental processes such as material flows from soils into groundwater, surface water, atmosphere and vice-versa, effects of those processes on biodiversity such as survival of waterborne insects and food webs in soil and water (Vereecken et al. 2019; Melsbach et al. 2020). Also, qualitative composition of dust (chemical compounds, microbes) in wind erosion (Soleimani et al. 2020), biological regeneration effects of soil compaction (Lewandowski et al. 2019), exact carbon balances of erosion in different landscapes (de Nijs and Cammeraat 2019; Lal 2020) are important and promising areas of experimental research. Based on international cooperation, development of erosion processes and mass flows of soils in permafrost areas and impact on soil functions and ecosystem services should be evolved as a focal research topic (Chumbaev and Tanasienko 2016; Lafrenière and Lamoureux 2019).

In the area of *monitoring physical soil degradation processes*, preservation and improvement of existing long-term experiments and landscape experiments and observatories are important. To maintain and continue reliable

time-series data, measurement and data processing methods need to be updated and harmonized with traditional ones. Development of precise analysis systems for the detection of changes in the status of soils and land through the combination of methods of remote sensing and photogrammetry with field methods and laboratory methods is needed (Li et al. 2019; Chave et al. 2019).

On this basis, regionally specific, robust limit values for indicators of soil quality and soil health can be derived. Integration of indicators and data in soil health concepts and soil information systems is to improve. Data flows require automatization that enables quasi real-time analyses. Monitoring is to be embedded into transdisciplinary ecosystem research networks to develop algorithms, models and decision support systems (Musche et al. 2019; Mueller et al. 2019).

In the area of *modelling and forecasting degradation processes* existing models for calculating the effects of physical soil degradation are very different in architecture, suitability for specific cases and handling. It is important to use and improve existing “degradation models” to understand implications of physical soil degradation for ecosystem performance and to inform for altered soil, air, and water health (Jarrah et al. 2020), and to develop ability of models to direct land management decisions such as wind erosion impacts on ecosystem services (Jarrah et al. 2020). Future models should be adaptable for plot to regional scales.

Soil “degradation models” should become a part of ecosystem models. In case of the broad area of process-based ecosystem modelling, e.g., dynamic modelling of the soil–water–atmosphere–plant system, soil states and data are often a starting point only. Implementation of erosion, compaction and other models of physical degradation processes into ecosystem models allows understanding and forecasting both changes in the soil physical state, consequent changes of the soil and responses of the overall ecosystem, basically in terms of plant growth (Bonfante et al. 2019) or carbon dynamics

(Bouchoms et al. 2019). In the area of ecosystem modelling, usually the soil values are taken into account as constant parameters. In improved ecosystem models, these values have to be considered as dynamic soil parameter functions, which depend on time. Models need to be implemented with advanced tools and data from freshest insights into biological cycles and feedback processes coming from theories, field observatories, experiments and other sources. Existing approaches require to improve the accuracy of the models, professionalization of the models in terms of data flows and manageability and fast calculations. Cross-comparison model tests will enable choices for region- and landscape-specific optimal models.

In case of the broad area of indicator- and GIS-based spatio-temporal models, complexity, accuracy and speed will increase as well. Development of more complex models for scenario calculations, adaptation of the models to new real-world situations regarding input data for weather, land use, economy, policies, etc., are expected. In this regard, USLE-RUSLE models have great potentials for further implementation into decision support systems for practical application in landscape planning and for assessing the impacts of climate and land-use changes on soil characteristics.

2.4 Conclusions

1. Soils are highly dynamic and multifunctional systems of crucial importance for life on earth and survival of humankind. Soil degradation threatens soil's performance to meet these functions and ecosystem services.
2. We addressed the main specific kinds of physical soil degradation such as erosion, compaction and sealing and show their partly not yet understood implications for ecosystems.
3. Advances in monitoring and modelling soil degradation processes in the frame of soil quality/soil health and ecosystem modelling are key to understanding and monitoring soil physical degradation.

References

- Alewell C, Egli M, Meusburger K (2015) An attempt to estimate tolerable soil erosion rates by matching soil formation with denudation in Alpine grasslands. *J Soils Sediments* 15(6):1383–1399
- Alewell C, Borelli P, Meusburger K, Panagos P (2019) Using the USLE: chances, challenges and limitations of soil erosion modelling. *Int Soil Water Cons Res* 7:203–225
- Angel S, Parent J, Civco DL, Blei A, Potere D (2011) The dimensions of global urban expansion: Estimates and projections for all countries, 2000–2050. *Progress Planning* 75(2):53–107. <https://doi.org/10.1016/j.progress.2011.04.001>
- Artmann M (2014) Assessment of soil sealing management responses, strategies, and targets toward ecologically sustainable urban land use management. *AMBIO* 43:530–541. <https://doi.org/10.1007/s13280-014-0511-1>
- Assouline S, Mualem Y (2000) Modeling the dynamics of soil seal formation: analysis of the effect of soil and rainfall properties. *Water Resour Res* 36(8):2341–2349. <https://doi.org/10.1029/2000WR900069>
- Ayuso SV, Onatibia GR, Maestre FT, Yahdjian L (2019) Grazing pressure interacts with aridity to determine the development and diversity of biological soil crusts in Patagonian rangelands. *Land Degrad Develop* 31(4):488–499
- Bagnold RA (1943) *The physics of blown sand and desert dunes*. Methuen London, 265 pp
- Bajracharya RM, Lal R (1999) Land use effects on soil crusting and hydraulic response of surface crusts on a tropical Alfisol. *Hydrol Process* 13(1):59–72
- Batista PV, Davies J, Silva M, Quinton JN (2019) On the evaluation of soil erosion models: are we doing enough? *Earth-Sci Rev* 197
- Baumgartel A, Lukić S, Belanović Simić S, Kadović R (2019) Identifying areas sensitive to wind erosion—a case study of the AP Vojvodina (Serbia). *Appl Sci* 9(23):5106. <https://doi.org/10.3390/app9235106>
- Behnisch M, Poglitsch H, Krüger T (2016) Soil sealing and the complex bundle of influential factors: Germany as a case study. *ISPRS Int J Geo-Inf* 5:132. <https://doi.org/10.3390/ijgi5080132>
- Berhe AA, Harte J, Harden J W, Torn MS (2007) The significance of the erosion-induced terrestrial carbon sink. *Bioscience* 57:337–346. <https://doi.org/10.1641/B570408>
- Berisso FE, Schjønning P, Keller T, Lamandé M, Etana A, de Jonge LW, Iversen BV, Arvidsson J, Forkman J (2012) Persistent effects of subsoil compaction on pore size distribution and gas transport in a loamy soil. *Soil Tillage Res* 122:42–51. <https://doi.org/10.1016/j.still.2012.02.005>
- Berli M, Kulli B, Attinger W, Keller M, Leuenberger J, Flüher H, Springman SM, Schulin R (2004) Compaction of agricultural and forest subsoils by tracked

- heavy construction machinery. *Soil Tillage Res* 75 (1):37–52. [https://doi.org/10.1016/S0167-1987\(03\)00160-0](https://doi.org/10.1016/S0167-1987(03)00160-0)
- Bircher P, Liniger HP, Prasuhn V (2019) Comparing different multiple flow algorithms to calculate RUSLE factors of slope length (L) and slope steepness (S) in Switzerland. *Geomorphology* 346(106850):1–19
- Bircher P, Liniger HP, Prasuhn V (2019b) Aktualisierung und Optimierung der Erosionsrisikokarte (ERK2). Die neue ERK2 (2019) für das Ackerland der Schweiz.: Schlussbericht 2019. Hrsg. Agroscope, Bern. August, 2019, 61 S
- Blanco-Canqui H, Lal R (2010) Water erosion. In: *Principles of soil conservation and management*. Springer, Dordrecht. https://doi.org/10.1007/978-1-4020-8709-7_2
- Blum WEH (2011) Physical degradation of soils, risks and threats. In: Gliński J, Horabik J, Lipiec J (eds) *Encyclopedia of agrophysics*. Encyclopedia of earth sciences series. Springer, Dordrecht. https://doi.org/10.1007/978-90-481-3585-1_111
- Boardman J, Evans R (2019) The measurement, estimation and monitoring of soil erosion by runoff at the field scale: challenges and possibilities with particular reference to Britain. *Progress in physical geography: earth and environment*
- Bondi G, O’Sullivan L, Fenton O, Creamer R, Marongiu I, Wall DP (2020) Trafficking intensity index for soil compaction management in grasslands. *Soil Use Manag.* <https://doi.org/10.1111/sum.12586>
- Bonfante A, Terribile F, Bouma J (2019) Refining physical aspects of soil quality and soil health when exploring the effects of soil degradation and climate change on biomass production: an Italian case study. *SOIL* 5:1–14. <https://doi.org/10.5194/soil-5-1-2019>
- Borelli P, Robinson DA, Fleischer LR, Lugato E, Ballabio C, Alewell C, Meusburger K, Modugno S, Schütt B, Ferro V, Bagarello V, Van Oost K, Montanarella L, Panagos P (2017) An assessment of the global impact of 21st century land use change on soil erosion. *Nat Commun* 8(1). <https://doi.org/10.1038/s41467-017-02142-7>
- Borrelli P, Meusburger K, Ballabio C, Panagos P, Alewell C (2018) Object-oriented soil erosion modelling: a possible paradigm shift from potential to actual risk assessments in agricultural environments. *Land Degrad Dev* 29(4):1270–1281
- Borrelli P, Robinson DA, Panagos P, Lugato E, Yang JE, Alewell C, Ballabio C (2020) Land use and climate change impacts on global soil erosion by water (2015–2070). *Proceedings of the National Academy of Sciences*
- Bouchoms S, Wang Z, Vanacker V, Van Oost K (2019) Evaluating the effects of soil erosion and productivity decline on soil carbon dynamics using a model-based approach. *SOIL* 5:367–382. <https://doi.org/10.5194/soil-5-367-2019>
- Bouma J (2019) How to communicate soil expertise more effectively in the information age when aiming at the UN Sustainable Development Goals. *Soil Use Manag* 35(1):32–38. <https://doi.org/10.1111/sum.12415>
- Boussinesq J (1885) Application des potentiels à l’étude de l’équilibre et du mouvement des solides élastiques, principalement au calcul des déformations et des pressions que produisent, dans ces solides, des efforts quelconques exercés sur une petite partie de leur surface ou de leur intérieur; mémoire suivi de notes étendues sur divers points de physique mathématique et d’analyse. Gauthier-Villars, Paris, p 722
- Brus DJ, van den Akker JHH (2018) How serious a problem is subsoil compaction in the Netherlands? A survey based on probability sampling. *SOIL* 4:37–45. <https://doi.org/10.5194/soil-4-37-2018>
- Cambi M, Hoshika Y, Mariotti B, Paoletti E, Picchio R, Venanzi R, Marchi E (2017) Compaction by a forest machine affects soil quality and *Quercus robur* L. seedling performance in an experimental field. *Forest Ecol Manage* 384:406–414. <https://doi.org/10.1016/j.foreco.2016.10.045>
- Chappel A, Webb NP, Leys JF, Waters CM, Orgill S, Eyres MJ (2019) Minimizing soil organic carbon erosion by wind is critical for land degradation neutrality. *Environ Sci Policy* 93:43–52. <https://doi.org/10.1016/j.envsci.2018.12.020>
- Chave J, Davies SJ, Phillips OL, Lewis SL, Sist P, Schepaschenko D, Armston J, Baker TR, Coomes D, Disney M, Duncanson L, Héroult B, Labrière N, Meyer V, Réjou-Méchain M, Scipal K, Saatchi S (2019) Ground data are essential for biomass remote sensing missions. *Surv Geophys* 40:863–880. <https://doi.org/10.1007/s10712-019-09528-w>
- Chen L, Sela S, Svoray T, Assouline S (2013) The role of soil-surface sealing, microtopography, and vegetation patches in rainfall-runoff processes in semiarid areas. *Water Resour Res* 49:5585–5599
- Chepil WS, Woodruff NP (1963) The physics of wind erosion and its control. *Adv Agron* 15(1963):211–302. [https://doi.org/10.1016/S0065-2113\(08\)60400-9](https://doi.org/10.1016/S0065-2113(08)60400-9)
- Chumbaev AS, Tanasienko AA (2016) Measuring snowmelt in Siberia: causes, process, and consequences. In: Mueller L, Sheudshen A, Eulenstein F (eds) *Novel methods for monitoring and managing land and water resources in Siberia*. Springer Water. Springer, Cham, pp 213–231. https://doi.org/10.1007/978-3-319-24409-9_7
- Dai JD, Zhang JH, Zhang ZH, Jia LZ, Xu HC, Wang Y (2020) Effects of water discharge rate and slope gradient on runoff and sediment yield related to tillage erosion. *Arch Agron Soil Sci* 66. <https://doi.org/10.1080/03650340.2020.1766676>
- Daldabayeva G, Nurymova R, Baizhanova B, Akhanov S (2020) Socio-economic evaluation of the reclaimed dry bottom during the development of the Kazakhstan part of the Aral Sea. *Zemljiste i Biljka* 69(1):36–45. http://www.sdpz.rs/images/casopis/2020/zin_69_1_65.pdf
- De Neve S, Hofman G (2000) Influence of soil compaction on carbon and nitrogen mineralization of soil

- organic matter and crop residues. *Biol Fert Soils* 30:544–549
- De Alba S, Borselli L, Torri D, Pellegrini S, Bazzoffi P (2006) Assessment of tillage erosion by mouldboard plough in Tuscany (Italy). *Soil Tillage Res* 85:123–142
- De Nijs EA, Cammeraat ELH (2019) The stability and fate of soil organic carbon during the transport phase of soil erosion. *Earth Sci Rev* 201:103067. <https://doi.org/10.1016/j.earscirev.2019.103067>
- Défosses P, Richard G, Keller K, Adamiade V, Govind A, Mary B (2014) Modelling the impact of declining soil organic carbon on soil compaction: application to a cultivated Eutric Cambisol with massive straw exportation for energy production in northern France. *Soil Tillage Res* 141:44–54. <https://doi.org/10.1016/j.still.2014.03.003>
- Défosses P, Richard G (2002) Models of soil compaction due to traffic and their evaluation. *Soil Tillage Res* 67 (1):41–64. [https://doi.org/10.1016/S0167-1987\(02\)00030-2](https://doi.org/10.1016/S0167-1987(02)00030-2)
- DIN19708 (2005) Bodenbeschaffenheit – Ermittlung der Erosionsgefährdung von Böden durch Wasser mit Hilfe der ABAG (Soil quality – Predicting soil erosion by water by means of ABAG). DIN 19708:2005–02, Normenausschuss Wasserwesen (NAW) im DIN, pp 25
- Dobrovolskiy GV, Kust GS, Sanaev VG (eds) (2012) Soils in biosphere and life of human. Monograph, Moscow, Publishing house of the Moscow State Forest University, 584 pp (In Russian: Г.В. Добровольский, Г.С. Куст, Санаев В.Г. Почвы в биосфере и жизни человека. Монография Москва. Издательство Московского государственного университета леса. 2012, 584 с)
- Dominchin MF, Verdenelli RA, Aoki A, Meriles JM (2019) Soil microbiological and biochemical changes as a consequence of land management and water erosion in a semiarid environment. *Arch Agron Soil Sci* 66(6):763–777. <https://doi.org/10.1080/03650340.2019.1638915>
- Donaldson EC, Chilingarian GV, Yen TF (eds) (1995) Subsidence due to fluid withdrawal. Elsevier Science, 488 pp
- Duniway MC, Pfennigwerth AA, Fick SE, Nauman TW, Belnap J, Barger NN (2019) Wind erosion and dust from US drylands: a review of causes, consequences, and solutions in a changing world. *Ecosphere* 19(3): e02650. <https://doi.org/10.1002/ecs2.2650>
- Evans R (2013) Assessment and monitoring of accelerated water erosion of cultivated land—when will reality be acknowledged? *Soil Use Manage* 704, 29 (1): 105–118
- Evans R (2017) Factors controlling soil erosion and runoff and their impacts in the upper Wissey catchment, Norfolk, England: a ten year monitoring programme: monitoring soil erosion and its impacts, Norfolk, England. *Earth Surf Process Landforms* 42(14). <https://doi.org/10.1002/esp.4182>
- Fabiola N, Giarola B, da Silva A, Imhoff S, Dexter A (2003) Contribution of natural soil compaction on hardsetting behavior. *Geoderma* 113:95–108
- FAO and ITPS (2015) Status of the World’s soil resources (SWSR)—main report. Rome, Italy, Food and Agriculture Organization of the United Nations and Intergovernmental Technical Panel on Soils, 607 pp. <http://www.fao.org/3/a-i5199e.pdf>. Accessed on 23 May 2020
- FAO (2017). Voluntary guidelines for sustainable soil management. In: 155th session of the FAO Council (5th December 2016), Rome, Italy, 26 p. <http://www.fao.org/3/a-bl813e.pdf>. Accessed on 5 Oct 23, 2020
- FAO (2019) Soil erosion: the greatest challenge to sustainable soil management. Rome, 100 pp. Licence: CC BY-NC-SA 3.0 IGO
- Fattahi SM, Soroush A, Huang N (2020) Wind erosion control using of Aeolian sand with cyanobacteria. *Land Degrad Develop.* <https://doi.org/10.1002/ldr.3590>
- Fiener P, Wilken F, Aldana-Jague E, Deumlich D, Gómez JA, Guzmán G, Hardy RA, Quinton JN, Sommer M, Van Oost K, Wexler R (2018) Uncertainties in assessing tillage erosion—How appropriate are our measuring techniques? *Geomorphology* 304: 214–225
- Flanagan DC, Ascough JC, Nearing MA, Lafen JM (2001) The water erosion prediction project (WEPP) model. In: Harmon RS, Doe WW (eds) Landscape erosion and evolution modeling. Springer, Boston, MA. https://doi.org/10.1007/978-1-4615-0575-4_7
- Franzmeier DP, Chartres CJ, Wood JT (1996) Hardsetting soils in Southeast Australia: landscape and profile processes. *Soil Sci Soc Am J* 60(4):1178–1187
- Funk R, Engel W (2015) Investigations with a field wind tunnel to estimate the wind erosion risk of row crops. *Soil Tillage Res* 145:224–232
- Funk R (2016) Assessment and measurement of wind erosion. In: Mueller L, Sheudshen A, Eulenstein F (eds) Novel methods for monitoring and managing land and water resources in Siberia. Springer Water. Springer, Cham, pp 425–449. https://doi.org/10.1007/978-3-319-24409-9_18
- Gardi C (2015) Toward zero net land take by 2050: an EU perspective. In: Fregolent L, Tonin S (eds) Growing compact. FrancoAngeli Milano, pp 177–190
- Gardi C (ed) (2017) Urban expansion, land cover and soil ecosystem services, 1st edn, published April 6, 2017 by Routledge, 302 pp. ISBN 9781138885097
- Gianinetto M, Aiello M, Polinelli F, Frassy F, Rulli MC, Ravazzani G, Bocchiola D, Chiarelli DD, Soncini A, Vezzoli R (2019) D-RUSLE: a dynamic model to estimate potential soil erosion with satellite time series in the Italian Alps. *Eur J Remote Sens* 52(sup4):34–53. <https://doi.org/10.1080/22797254.2019.1669491>
- Golosov VN, Collins AL, Dobrovolskaya NG, Bazhenova OI, Ryzhov YV, Sidorchuk AY (2021) Soil loss on the arable lands of the forest-steppe and steppe zones of European Russia and Siberia during the period of intensive agriculture. *Geoderma*

- 381:114678. <https://doi.org/10.1016/j.geoderma.2020.114678>
- Govers G, Vandaele K, Desmet PJJ, Poesen J, Bunte K (1994) The role of tillage in soil redistribution on hillslopes. *Eur J Soil Sci* 45:469–478
- Govers G, Merckx R, Wesemael BV, Oost KV (2017) Soil conservation in the 21st century: why we need smart agricultural intensification. *Soil* 3(1):45–59
- Graves AR, Morris J, Deeks LK, Rickson J, Kibblewhite MG, Harris JA, Farewell TS, Truckle I (2015) The total costs of soil degradation in England and Wales. *Ecol Econ* 119:399–413. <https://doi.org/10.1016/j.ecolecon.2015.07.026>
- Greeley R, Iverson JD (1985) Wind as a geological process on Earth, Mars, venus, and Titan. Cambridge Univ. Press, New York, NY
- Groll M, Opp C, Semenov O; Shapov A (2018) Chapter II/57: ground-based measurement of aeolian dust deposition in the aral sea region. In: Sychev VG, Mueller L (eds) Novel methods and results of landscape research in Europe, Central Asia and Siberia, vol II understanding and monitoring processes in soils and water bodies. © FSBI “VNII Agrochemistry”, pp. 265–269. <https://doi.org/10.25680/5865.2018.94.78.154>, <http://vniia-pr.ru/monografii/pdf/tom2-57.pdf>. Accessed on 8 Oct 2019
- GSP (2016) Global soil partnership endorses guidelines on sustainable soil management. <http://www.fao.org/global-soil-partnership/resources/highlights/detail/en/c/416516/>
- Guerra CA, Rosa IMD, Valentini E, Wolf F, Filipponi F, Karger DN, Nguyen Xuan A, Mathieu J, Lavelle P, Eisenhauer N (2020) Global vulnerability of soil ecosystems to erosion. *Landscape Ecol*. <https://doi.org/10.1007/s10980-020-00984-z>
- Guo Q, Hao Y, Liu B (2015) Rates of soil erosion in China: a study based on runoff plot data. *CATENA* 124:68–76. <https://doi.org/10.1016/j.catena.2014.08.013>
- Haas J, Schack-Kirchner H, Lang F (2020) Modeling soil erosion after mechanized logging operations on steep terrain in the Northern Black Forest. *Eur J Forest Res*, Germany. <https://doi.org/10.1007/s10342-020-01269-5>
- Håkansson I, Voorhees WB, Riley H (1988) Vehicle and wheel factors influencing soil compaction and crop response in different traffic regimes. *Soil Tillage Res* 11(3–4):239–282. [https://doi.org/10.1016/0167-1987\(88\)90003-7](https://doi.org/10.1016/0167-1987(88)90003-7)
- Hänsel P, Langel S, Schindewolf M, Kaiser A, Buchholz A, Böttcher F, Schmidt J (2019) Prediction of muddy floods using high-resolution radar precipitation forecasts and physically-based erosion modeling in agricultural landscapes. *Geosciences* 9(9):401. <https://doi.org/10.3390/geosciences9090401>
- Horn R, Taubner H, Wuttke M, Baumgartl T (1994) Soil physical properties related to soil structure. *Soil Tillage Res* 30(2–4):187–216. [https://doi.org/10.1016/0167-1987\(94\)90005-1](https://doi.org/10.1016/0167-1987(94)90005-1)
- Horn R, Domžal H, Słowińska-Jurkiewicz A, van Ouwerkerk C (1995) Soil compaction processes and their effects on the structure of arable soils and the environment. *Soil Tillage Res* 35(1–2):23–36. [https://doi.org/10.1016/0167-1987\(95\)00479-C](https://doi.org/10.1016/0167-1987(95)00479-C)
- Houšková B, Montanarella L (2008) The natural susceptibility of European soils to compaction. In: Tóth G, Montanarella L, Rusco E (eds) Threats to soil quality in Europe. Office for Official Publications of the European Communities, Luxembourg, pp 23–35
- Huo J, Yu X, Liu CH, Chen L, Zheng W, Yang Y, Tang ZH (2020) Effects of soil and water conservation management and rainfall types on runoff and soil loss for a sloping area in North China. *Land Degrad Develop*. <https://doi.org/10.1002/ldr.3584>
- IPCC SRCCL (2019) Chapter 4: land degradation https://www.ipcc.ch/site/assets/uploads/2019/08/2e.-Chapter-4_FINAL.pdf, 186 pp. Accessed on 23 May 2020
- Issanova G, Abuduwaili J (2017) Aeolian processes as dust storms in the deserts of Central Asia and Kazakhstan. Springer Nature Singapore Pte Ltd. <https://doi.org/10.1007/978-981-10-3190-8>
- Ivlev AM, Derbentseva AM (2003) Degradation of soils and their recultivation. Vladivostok Univ., pp 88 (In Russian: Деградация почв и их рекультивация. Владивосток. Изд-во Дальневост. ун-та)
- Jarrah M, Mayela S, Tatarko J, Funk R, Kuka K (2020) A review of wind erosion models: data requirements, processes, and validity. *Catena* 187:104388
- Jing Z, Wang J, Zhu Y, Feng Y (2018) Effects of land subsidence resulted from coal mining on soil nutrient distributions in a loess area of China. *J Cleaner Prod* 177:350–361. <https://doi.org/10.1016/j.jclepro.2017.12.191>
- Jones RJA, Spoor G, Thomasson AJ (2003) Vulnerability of subsoils in Europe to compaction: a preliminary analysis. *Soil Tillage Res* 73(1–2):131–143. [https://doi.org/10.1016/S0167-1987\(03\)00106-5](https://doi.org/10.1016/S0167-1987(03)00106-5)
- Karlen DL, Andrews SS, Wienhold BJ, Zobeck TM (2008) Soil quality assessment: past, present and future. Publications from USDA-ARS/UNL Faculty. 1203. <https://digitalcommons.unl.edu/usdaarsfacpub/1203>
- Kayombo B, Lal R (1994) Chapter 13—responses of tropical crops to soil compaction. *Develop Agric Eng* 11:287–316. <https://doi.org/10.1016/B978-0-444-88286-8.50021-0>
- Keesstra SD, Bouma J, Wallinga J, Tittone P, Smith P, Cerdà A, Montanarella L, Quinton JN, Pachepsky Y, van der Putten WH, Bardgett RD, Moolenaar S, Mol G, Jansen B, Fresco LO (2016) The significance of soils and soil science towards realization of the United Nations Sustainable Development Goals. *Soil* 2:111–128. <https://doi.org/10.5194/soil-2-111-2016>
- Keller T, Arvidsson J (2006) Prevention of traffic-induced subsoil compaction in Sweden: experiences from wheeling experiments. *Arch Agron Soil Sci* 52(2):207–222. <https://doi.org/10.1080/03650340600631540>

- Keller T, Lamandé M (2010) Challenges in the development of analytical soil compaction models. *Soil Tillage Res* 111(1):54–64. <https://doi.org/10.1016/j.still.2010.08.004>
- Keller T, Trautner A, Arvidsson J (2002) Stress distribution and soil displacement under a rubber-tracked and a wheeled tractor during ploughing, both on-land and within furrows. *Soil Tillage Res* 68(1):39–47. [https://doi.org/10.1016/S0167-1987\(02\)00082-X](https://doi.org/10.1016/S0167-1987(02)00082-X)
- Keller T, Défossez P, Weisskopf P, Arvidsson J, Richard G (2007) SoilFlex: a model for prediction of soil stresses and soil compaction due to agricultural field traffic including a synthesis of analytical approaches. *Soil Tillage Res* 93(2):391–411. <https://doi.org/10.1016/j.still.2006.05.012>
- Keller T, Lamandé M, Peth S, Berli M, Delenne J-Y, Baumgarten W, Rabbel W, Radjai F, Rajchenbach J, Selvadurai APS, Or D (2013) An interdisciplinary approach towards improved understanding of soil deformation during compaction. *Soil Tillage Res* 128: 61–80. <https://doi.org/10.1016/j.still.2012.10.004>
- Keller T, Colombi T, Ruiz S, Manalili MP, Rek J, Stadelmann V, Wunderli H, Breitenstein D, Reiser R, Oberholzer H, Schymanski S, Romero-Ruiz A, Linde N, Weisskopf P, Walter A, Or D (2017) Long-term soil structure observatory for monitoring post-compaction evolution of soil structure. *Vadose Zone J* 16. <https://doi.org/10.2136/vzj2016.11.0118>
- Keller T, Sandin M, Colombi T, Horn R, Or D (2019) Historical increase in agricultural machinery weights enhanced soil stress levels and adversely affected soil functioning. *Soil Tillage Res* 194. <https://doi.org/10.1016/j.still.2019.104293>
- Kheir RB, Cerdan O, Abdallah C (2006) Regional soil erosion risk mapping in Lebanon. *Geomorphology* 2 (3–4):347–359
- Khitrov E, Andronov A, Bogatova E, Kotenev E (2019) Development of recommendations on environmental certification of forestry machinery drives. In: International multidisciplinary scientific geoconference: SGEM. Sofia, Bd. 19, Ausg. 3.2. <https://doi.org/10.5593/sgem2019/3.2/S14.089>
- Kirkby MJ, Irvine BJ, Jones RJA, Govers G, Boer M, Cerdan O, Daroussin J, Gobin A, Grimm M, Le Bissonnais Y, Kosmas C, Mantel S, Puigdefabregas J, van Lynden G (2008) The PESERA coarse scale erosion model for Europe. I.—Model rationale and implementation. *Eur J Soil Sci* 59(6):1293–1306. <https://doi.org/10.1111/j.1365-2389.2008.01072.x>
- Konečná J, Karásek P, Beitlerová H, Fučík P, Kapička J, Podhrázká J, Kvítek T (2020) Using WaTEM/SEDEM and HEC-HMS models for the simulation of episodic hydrological and erosion events in a small agricultural catchment. *Soil Water Res* 15:18–29
- Lafrenière MJ, Lamoureux SF (2019) Effects of changing permafrost conditions on hydrological processes and fluvial fluxes. *Earth-Sci Rev* 191:212–223. <https://doi.org/10.1016/j.earscirev.2019.02.018>
- Lal R, Hall GF, Miller FP (1989) Soil degradation: I. Basic processes. *Land Degrad Dev* 1:51–69. <https://doi.org/10.1002/ldr.3400010106>
- Lal R (2001) Soil degradation by erosion. *Land Degrad Dev* 12:519–539. <https://doi.org/10.1002/ldr.472> http://tinread.usarb.md:8888/tinread/fulltext/lal/soil_degradation.pdf
- Lal R (2020) Soil erosion and gaseous emissions. *Appl Sci* 10(8): 2784. <https://doi.org/10.3390/app10082784>
- Lewandowski TE, Forrester JA, Mladenoff DJ, Marin-Spiotta E, D’Amato AW, Palik BJ, Kolka RK (2019) Long term effects of intensive biomass harvesting and compaction on the forest soil ecosystem. *Soil Biol Biochem* 137:107572. <https://doi.org/10.1016/j.soilbio.2019.107572>
- Leys J, McTainsh G, Strong C, Heidenreich SK (2008) DustWatch: using community networks to improve wind erosion monitoring in Australia. *Earth Surf Process Landforms* 33(12):1912–1926. <https://doi.org/10.1002/esp.1733>
- Li S, Lobb DA, Lindstrom MJ, Farenhorst A (2007) Tillage and water erosion on different landscapes in the northern North American Great Plains evaluated using ¹³⁷Cs technique and soil erosion models. *CATENA* 70(3):493–505. <https://doi.org/10.1016/j.catena.2006.12.003>
- Li X, Zhao N, Jin R, Liu S, Sun X, Wen X, Wu D, Zhou Y, Guo J, Chen S, Xu Z, Ma M, Wang T, Qu Y, Wang X, Wu F, Zhou Y (2019) Internet of Things to network smart devices for ecosystem monitoring. *Sci Bull* 64(17):1234–1245. <https://doi.org/10.1016/j.scib.2019.07.004>
- Li S (2006) Tillage translocation and tillage erosion: measurement, modelling, application and validation. Doctors thesis, Department of Soil Science, University of Manitoba Winnipeg, 153 pp
- Lindstrom MJ, Nelson WW, Schumacher TE, Lemme GD (1990) Soil movement by tillage as affected by slope. *Soil Tillage Res* 17:255–264
- Lobb DA, Kachanoski RG (1999) Modelling tillage erosion in the topographically complex landscapes of southwestern Ontario, Canada. *Soil Tillage Res* 51:261–277
- Lobb DA, Kachanoski RG (1999) Modelling tillage translocation using step, linearplateau and exponential functions. *Soil Tillage Res* 51:317–330
- Lobb DA, Kachanoski RG, Miller MH (1995) Tillage translocation and tillage erosion on shoulder slope landscape positions measured using ¹³⁷Cs as a tracer. *Can J Soil Sci* 75:211–218
- Lobb DA, Kachanoski RG, Miller MH (1999) Tillage translocation and tillage erosion in the complex upland landscapes of southwestern Ontario, Canada. *Soil Tillage Res* 51:189–209
- Louwagie G, Gay SH, Burrell A (eds) (2009) Addressing soil degradation in EU agriculture; relevant processes, practices and policies: report on the Project “Sustainable Agriculture and Soil Conservation (SoCo)”. https://esdac.jrc.ec.europa.eu/ESDB_Archive/eusoils_

- [docs/other/EUR23767_Final.pdf](#). Accessed on 23 May 2020
- Lu H, Prosser IP, Moran CJ, Gallant JC, Priestley G, Stevenson JG (2003) Predicting sheetwash and rill erosion over the Australian continent. *Soil Res* 41:1037. <https://doi.org/10.1071/SR02157>
- Luti T, Segoni S, Catani F, Munafò M, Casagli N (2020) Integration of remotely sensed soil sealing data in landslide susceptibility mapping. *Remote Sens* 12 (9):1486. <https://doi.org/10.3390/rs12091486>
- Lyles L, Tatarko J (1988) Soil wind erodibility index in seven North Central States. *Transactions of the ASAE. Am Soc Agric Eng* 31(5):1396–1399. <https://doi.org/10.13031/2013.30875>
- Maucha G, Büttner G, Kosztra B (2011) European validation of GMES FTS soil sealing enhancement data. In: Halounová L (ed) *Remote sensing and geoinformation not only for scientific cooperation EARSeL*, pp 223–238
- Van der Meij WM, Temme AJAM, Wallinga J, Sommer M (2020) Modeling soil and landscape evolution: the effect of rainfall and land-use change on soil and landscape patterns. *SOIL* 6(2):337–358. <https://doi.org/10.5194/soil-6-337-2020>
- Melsbach A, Torrentó C, Ponsin V, Bolotin J, Lachat L, Prasuhn V, Hofstetter TB, Hunkeler D, Elsner M (2020) Dual-element isotope analysis of desphenylchloridazon to investigate its environmental fate in a systematic field study: a long-term lysimeter experiment. *Environ Sci Technol* 7(54):3725–4696. <https://doi.org/10.1021/acs.est.9b04606>
- Mirschel W, Wieland R, Voss S M, Ajibefun IA, Deumlich D (2006) Spatial analysis and modeling tool (SAMT). applications. *Ecol Inform* 1:77–85
- Mirschel W, Berg-Mohnicke M, Wenkel K-O, Wieland R, Köstner B (2020) LandCaRe-DSS: an interactive model-based decision support system for assessing the impacts of climate change on agriculture and agricultural landscapes. In: Mirschel W, Terleev VV, Wenkel K-O (eds) *Landscape modelling and decision support*. Springer Nature Switzerland, Cham, pp 463–494
- Mission Board (2020) *Mission Board Soil health and food (2020) Caring for soil is caring for life. Ensure 75% of soils are healthy by 2030 for healthy food, people, nature and climate*. Publications Office of the European Union, Luxembourg, 52 pp. ISBN 978-92-76-19954-0. <https://doi.org/10.2777/918775>
- Montgomery D (2007) Soil erosion and agricultural sustainability. *Proc Natl Acad Sci USA* 104:13268–13272. <https://doi.org/10.1073/pnas.0611508104>
- Morgan RPC, Rickson RJ (eds) (1995) *Slope stabilization and erosion control: a bioengineering approach*. E & FN SPON, 1st edn, 292 pp
- Mueller L, Kay BD, Hu C, Li Y, Schindler U, Behrendt A, Shepherd TG, Ball BC (2009a) Visual assessment of soil structure: Evaluation of methodologies on sites in Canada, China and Germany: Part I: Comparing visual methods and linking them with soil physical data and grain yield of cereals. *Soil Tillage Res* 103(1):178–187. <https://doi.org/10.1016/j.still.2008.12.015>
- Mueller L, Shepherd G, Schindler U, Ball BC, Munkholm LJ, Hennings V, Smolentseva E, Rukhovi O, Lukin S, Hu C (2009b) Evaluation of soil structure in the framework of an overall soil quality rating. *Soil Tillage Res* 127:74–84. <https://doi.org/10.1016/j.still.2012.03.002>
- Mueller L, Eulenstein F, Mirschel W, Antrop M, Jones M, McKenzie BM, Dronin NN, Kazakov LK, Kravchenko VV, Khoroshev A, Gerasimova M, Danowski R, Schindler U, Ruhovich O, Sychev VG, Sheudzhen AK, Couvet D, Robinson G, Blum W, Joniak T, Eisendle U, Trovato MG, Sahnjikov E, Haubold-Rosar M, Knoche D, Köhl M, Bartlett D, Hoffmann J, Römbke J, Glante F, Sumina OI, Saporov A, Bukvareva E, Terleev VV, Topaj AG, Kienast F (2019) Landscapes, their exploration and utilisation: status and trends of landscape research. In: Mueller L, Eulenstein F (eds) *Current trends in landscape research. Innovations in landscape research*. Springer, Cham, pp 105–164. https://doi.org/10.1007/978-3-030-30069-2_5
- Mullins CE, MacLeod DA, Northcote KH, Tisdall JM, Young IM (1990) Hardsetting soils: behavior, occurrence, and management. In: Lal R, Stewart BA (eds) *Advances in soil science. Advances in soil science*, vol 11. Springer, New York, NY. https://doi.org/10.1007/978-1-4612-3322-0_2
- Mulqueen J (1986) Hydrology and drainage of peatland. *Environ Geol Water Sci* 9:15–22. <https://doi.org/10.1007/BF02439882>
- Munson SM, Belnap J, Okin GS (2011) Responses of wind erosion to climate induced vegetation changes on the Colorado Plateau. *Proc Natl Acad Sci* 108:3854–3859
- Musche M, Adamescu M, Angelstam P, Bacher S, Bäck J, Buss HL, Duffy C, Flaim G, Gaillardet J, Gianakis GV, Haase P, Halada L, Kissling WD, Lundin L, Matteucci G, Meesenburg H, Monteith D, Nikolaidis NP, Pipan T, Pyšek P, Rowe EC, Roy DB, Sier A, Tappeiner U, Vilà M, White T, Zobel M, Klotz S (2019) Research questions to facilitate the future development of European long-term ecosystem research infrastructures: A horizon scanning exercise. *J Environ Manage* 250(15):109479. <https://doi.org/10.1016/j.jenvman.2019.109479>
- Naipal V, Reick C, Pongratz J, Van Oost K (2015) Improving the global applicability of the RUSLE model—adjustment of the topographical and rainfall erosivity factors. *Geosci Model Dev* 8:2893–2913. <https://doi.org/10.5194/gmd-8-2893-2015>
- Nawaz MF, Bourrié G, Trolard F (2013) Soil compaction impact and modelling. A review. *Agron Sustain Dev* 33:291–309. <https://doi.org/10.1007/s13593-011-0071-8>
- Naylor D, Sadler N, Bhattacharjee A, Graham EB, Anderton CR, McClure R, Lipton M, Hofmockel KS, Jansson JK (2020) Soil microbiomes under climate change and implications for carbon cycling. *Annu Rev*

- Environ Resour. <https://doi.org/10.1146/annurev-environ-012320-082720>
- Nearing MA, Xie Y, Liu B, Ye Y (2017) Natural and anthropogenic rates of soil erosion. *Int Soil Water Conserv Res* 5:77–84. <https://doi.org/10.1016/j.iswcr.2017.04.001>
- Nunes MR, Karlen DL, Moorman TB (2020) Tillage intensity effects on soil structure indicators: a US meta-analysis. *Sustainability* 12:2071. <https://doi.org/10.3390/su12052071>
- Nyssen J, Poesen J, Haile M, Moeyersons J, Deckers J (2000) Tillage erosion on slopes with soil conservation structures in the Ethiopian highlands. *Soil Tillage Res* 57:115–127
- Oldeman LR, Van Lynden GWJ (1997) Assessment of the status of human induced soil degradation in China. In: Uithol PWJ, Groot JJR (eds) *Proceedings workshop Wageningen-China*. Wageningen, Report 84, Wageningen December 1997, pp 101–111. <https://edepot.wur.nl/338121#page=101>. Accessed on 23 May 2020
- Oldeman LR (1992) Global extent of soil degradation. *ISRIC Bi-Annual Report 1991–1992*, pp 19–36 <https://library.wur.nl/WebQuery/wurpubs/fulltext/299739>. Accessed on 22 Nov 2020
- Oliveira FCC, Ferreira G WD, Souza JLS, Vieira MEO, Pedrotti A (2019) Soil physical properties and soil organic carbon content in northeast Brazil: long-term tillage systems effects. *Scientia Agricola* 77(4): e20180166. Epub November 04, 2019. <https://doi.org/10.1590/1678-992x-2018-0166>
- Van Oost K, Govers G, Van Muysen W, Nachtergaele J (2003b) Modelling water and tillage erosion using spatially distributed models. In: Lang A, Dikau R, Henrich K (eds) *Long term hillslope and fluvial system modelling. Lecture notes in earth sciences*, vol 101. Springer, Berlin, Heidelberg. https://doi.org/10.1007/3-540-36606-7_6
- Panagos P, Katsoyiannis A (2019) Soil erosion modelling: the new challenges as the result of policy developments in Europe. *Environ Res* 172:470–474. <https://doi.org/10.1016/j.envres.2019.02.043>
- Panagos P, Borrelli P, Poesen J, Ballabio C, Lugato E, Meusburger K, Montanarella L, Alewell C (2015) The new assessment of soil loss by water erosion in Europe. *Environ Sci Policy* 54:438–447
- Panagos P, Ballabio C, Poesen J, Lugato E, Scarpa S, Montanarella L, Borrelli P (2020) A soil erosion indicator for supporting agricultural, environmental and climate policies in the European union. *Remote Sensing* 12(9):1365
- Pandey A, Himanshu SK, Mishra SK, Singh VP (2016) Physically based soil erosion and sediment yield models revisited. *CATENA* 147:595–620
- Parsons AJ (2019) How reliable are our methods for estimating soil erosion by water? *Sci Total Environ* 676:215–221
- Peng X, Horn R (2008) Time-dependent, anisotropic pore structure and soil strength in a 10-year period after intensive tractor wheeling under conservation and conventional tillage. *J Plant Nutr Soil Sci* 171(6):936–944. <https://doi.org/10.1002/jpln.200700084>
- Penn-Bressel G (2018) Chapter II/20: reducing land take for settlements and transport infrastructures—goals and monitoring on the path to sustainable land use. In: Sychev VG, Mueller L (eds) *Novel methods and results of landscape research in Europe, Central Asia and Siberia, vol II, understanding and monitoring processes in soils and water bodies*. © FSBI “VNI Agrochemistry” 2018, pp 99–103. <https://doi.org/10.25680/5205.2018.95.71.117>. <http://vniia-pr.ru/monografii/pdf/tom2-20.pdf>. Accessed on 23 May 2020
- Pi H, Huggins DR, Abatzoglou JT, Sharratt B (2020) Modeling soil wind erosion from agroecological classes of the pacific northwest in response to current climate. *J Geophysical Res: Atmos* 125(2): e2019JD031104. <https://doi.org/10.1029/2019JD031104>
- Pierre C, Kergoat L, Hiernaux P, Baron C, Bergametti G, Rajot JL, Abdourhamane Toure A, Okin GS, Marticorena B (2018) Impacts of agro-pastoral management on wind erosion in Sahelian croplands. *Land Degrad Dev* 29: 800–811
- Pimentel D (2006) Soil erosion: a food and environmental threat. *Environ Dev Sustain* 8:119–137. <https://doi.org/10.1007/s10668-005-1262-8>
- Poesen J, Turkelboom F, Ohler I, Ongprasert AS, Vlasak K (2000) Tillage erosion in Northern Thailand: intensities and implications. *Mededelingen Koninklijke Academie Voor Overzeese Wetenschappen* 46:489–512
- Prasuhn V (2011) Soil erosion in the Swiss midlands: results of a 10-year field survey. *Geomorphology* 126 (1–2):32–41
- Prasuhn V (2020) Twenty years of soil erosion on-farm measurement: annual variation, spatial distribution and the impact of conservation programmes for soil loss rates in Switzerland. *Earth Surf Process Landforms* 1–16. <https://doi.org/10.1002/esp.4829>
- Prokop G, Jobstmann H, Schönbauer A (2011) Report on best practices for limiting soil sealing and mitigating its effects. Study contracted by the European Commission, DG Environment, Technical Report-2011–50, Brussels, Belgium, 231 pp. <https://ec.europa.eu/environment/archives/soil/pdf/sealing/Soil%20sealing%20-%20Final%20Report.pdf>. Accessed on 23 May 2020
- Quine TA, Govers G, Walling DE, Zhang X, Desmet PJJ, Zhang Y, Vandaele K (1997) Erosion processes and landform evolution on agricultural land—new perspectives from caesium-137 measurements and topographic-based erosion modelling. *Earth Surf Proc Land* 22:799–816
- Reimann T, Román-Sánchez A, Vanwalleghem T, Wallinga J (2017) Getting a grip on soil reworking—single-grain feldspar luminescence as a novel tool to quantify soil reworking rates. *Quat Geochronol* 42:1–14. <https://doi.org/10.1016/j.quageo.2017.07.002>

- Renard KG, Foster GR, Weesies GA (2001) Predicting soil erosion by water: a guide to conservation planning with the revised universal soil loss equation (RUSLE). Agriculture Handbook, p 703
- Rogger M, Agnoletti M, Alaoui A, Bathurst JC, Bodner G, Borga M, Chaplot V, Gallart F, Glatzel G, Hall J, Holden J, Holko L, Horn R, Kiss A, Kohnová S, Leitinger G, Lennartz B, Parajka J, Perdigão R, Peth S, Plavcová L, Quinton JN, Robinson M, Salinas JL, Santoro A, Szolgay J, Tron S, van den Akker JJH, Viglione A, Blöschl G (2017) Land use change impacts on floods at the catchment scale: challenges and opportunities for future research. *Earth Space Sci* 20: 5209–5219. <https://doi.org/10.1002/2017WR020723>
- Schjøning P, van den Akker JJH, Keller T, Greve M H, Lamande M, Simojoki A, Stettler M, Arvidsson J, Breuning-Madsen H (2015) Driver-pressure-state-impact-response (DPSIR) analysis and risk assessment for soil compaction—a European perspective. In: Sparks DL (ed) *Advances in agronomy*, vol 133. Elsevier, Amsterdam, pp 183–237. <https://doi.org/10.1016/bs.agron.2015.06.001>
- Schmidt J, von Werner M, Michael A (1999) Application of the EROSION 3D model to the CATSOP watershed, The Netherlands. *CATENA* 37(3–4):449–456. [https://doi.org/10.1016/S0341-8162\(99\)00032-6](https://doi.org/10.1016/S0341-8162(99)00032-6)
- Schneider F, Don A (2019) Root-restricting layers in German agricultural soils. Part I: extent and cause. *Plant Soil* 442:433–451. <https://doi.org/10.1007/s11104-019-04185-9>
- Schneider P, Meyer A, Plat K (2020) Potential of bioeconomy in urban green infrastructure. In: Keswani C (eds) *Bioeconomy for sustainable development*. Springer, Singapore, pp 251–276. https://doi.org/10.1007/978-981-13-9431-7_13
- Seitz S, Prasuhn V, Scholten T (2020) Controlling soil erosion using no-till farming systems. In: Dang Y, Dalal R, Menzies NW (eds) *No-till farming systems for sustainable agriculture*. Springer, Challenges and opportunities, pp 195–211
- Selivanovskaya SY, Galitskaya PY, Hung YT (2014) Chapter 12: the use of biological methods for toxicity evaluation of wastes and waste-amended soils. *Handbook of environment and waste management: land and groundwater pollution control*, pp 737–779
- Shainberg I, Levy GJ (1996) Infiltration and seal formation processes. In: Agassi M (ed) *Soil erosion, conservation and rehabilitation*. Marcel Dekker, New York, NY, pp 1–24
- Shu H, Hürlimann M, Molowny-Horas R, González M, Pinyol J, Abancó C, Ma J (2019) Relation between land cover and landslide susceptibility in Val d’Aran, Pyrenees (Spain): historical aspects, present situation and forward prediction. *Sci Total Environ* 693: 133557
- Siegmund N, Funk R, Koszinski S, Buschiazio D, Sommer M (2018) Effects of low-scale landscape structures on aeolian transport processes on arable land. *Aeol Res* 32:181–191. <https://doi.org/10.1016/j.aeolia.2018.03.003>
- Silveira M, Comerford N, Reddy K, Prenger J, DeBusk W (2010) Influence of military land uses on soil carbon dynamics in forest ecosystems of Georgia, USA. *Ecol Indic* 10:905–909
- Snakin VV, Krechetov PP, Kuzovnikova TA, Minashina NG, Karpachevsky LO, Alyabina IO, Gurov AF, Melchenko V, Stepichev AV, Kazantseva OF, Ananyeva ND (1992) Soil degradation assessment system. Pushchino Scientific Centre of the Russian Academy of Sciences. Research Institute of Nature, p 20 (In Russian: Снакин В.В., Кречетов П.П., Кузовникова Т.А., Минашина Н.Г., Карпачевский Л.О., Алябина И.О., Гуров А.Ф., Мельченко В., Степичев А.В., Казанцева О.Ф., Ананьева Н.Д. Система оценки степени деградации почв. Пушкино, Пушкинский научный центр РАН. ВНИИ Природы.)
- Snakin VV, Krechetov PP, Kuzovnikova TA, Alyabina IO, Gurov AF, Stepichev AV (1996) The system of assessment of soil degradation. *Soil Technol* 8(4):331–343. [https://doi.org/10.1016/0933-3630\(95\)00028-3](https://doi.org/10.1016/0933-3630(95)00028-3)
- Soane BD, Ball BC, Arvidsson J, Basch G, Moreno F, Roger-Estrade J (2012) No-till in northern, western and south-western Europe: a review of problems and opportunities for crop production and the environment. *Soil Tillage Res* 118:66–87
- Soleimani Z, Teymouri P, Bolorani AD, Mesdaghini A, Middleton N, Griffin DW (2020) An overview of bioaerosol load and health impacts associated with dust storms: a focus on the Middle East. *Atmos Environ* 223: 117187. <https://doi.org/10.1016/j.atmosenv.2019.117187>
- Srivastava A, Brooks ES, Dobre M, Elliot WJ, Wu JQ, Flanagan DC, Gravelle JA, Link TE (2020) Modeling forest management effects on water and sediment yield from nested, paired watersheds in the interior Pacific Northwest, USA using WEPP. *Sci Total Environ* 20 (701):134877. <https://doi.org/10.1016/j.scitotenv.2019.134877>
- Stanilovskaya J (2019) Landslides in permafrost zone of Russia. In: Pradhan S, Vishal V, Singh T (eds) *Landslides: theory, practice and modelling*. Advances in natural and technological hazards research, vol 50. Springer, Cham. https://doi.org/10.1007/978-3-319-77377-3_14
- Stettler M, Keller T, Weisskopf P, Lamandé M, Lassen P, Schjøning P (2014) Terranimo®—a web-based tool for evaluating soil compaction. *Landtechnik* 69 (3):132–137
- Streeter RT, Cutler NA (2020) Assessing spatial patterns of soil erosion in a high-latitude rangeland. *Land Degrad Develop*. <https://doi.org/10.1002/ldr.3585>
- Sumner ME, Miller WP (1992) Soil crusting in relation to global soil degradation. *Am J Altern Agric* 7:56–62
- Tarolli P, Sofia G, Wenfang CAO (2018) The geomorphology of the human age. In: Dellasala DA,

- Goldstein MI (eds) *Encyclopedia of the anthropocene*. Elsevier Inc., pp 35–43. <https://doi.org/10.1016/B978-0-12-809665-9.10501-4>
- Tatarko J, Wagner L, Fox F (2019) The wind erosion prediction system and its use in conservation planning. In: Wendroth O, Lascano RJ, Ma L (eds) *Bridging among disciplines by synthesizing soil and plant processes, advances in agricultural systems modelling*, vol 8. Madison, WI
- Tebebu TY, Bayabil HK, Steenhuis TS (2020) Can degraded soils be improved by ripping through the hardpan and liming? A field experiment in the Ethiopian Highlands. *Land Degrad Develop* <https://doi.org/10.1002/ldr.3588>
- Thapa BB, Cassel DK, Garrity DP (1999) Ridge tillage and contour natural grass barrier strips reduce tillage erosion. *Soil Tillage Res* 51:341–356
- Tisdall JM, Oades JM (1982) Organic matter and water-stable aggregates. *J Soil Sci* 33:141–163
- Torri D, Borselli L (2000) Water erosion. In: Sumner ME (eds) *Handbook of soil science*. CRC press, Boca Raton, London, New York, Washington DC, pp G171–G194
- UN (2015) *Agenda 2030: sustainable development goals. 17 Goals to transform our world*. <https://www.un.org/sustainabledevelopment/>. Accessed on 23 May 2020
- UNCCD (1994) *United Nations convention to combat desertification in those countries experiencing serious drought and/or desertification, particularly in Africa*. Paris, France, 54 pp
- UNDP (2019) *Combatting land degradation. Securing a sustainable future*. https://www.undp.org/content/dam/undp/library/planet/environment/Combatting_Land_Degradation%E2%80%9393Securing_A_Sustainable_Future.pdf. Accessed on 23 May 2020
- Unger PW, Kaspar TC (1994) Soil compaction and root growth: a review. *Agron J* 86:759–766
- USDA (2019) *KINEROS—the kinematic runoff and erosion model*. *Ag Data Commons*. <https://data.nal.usda.gov/dataset/kineros-kinematic-runoff-and-erosion-model>. Accessed on 23 May 2020
- Van der Meij WM, Reimann T, Vornehm VK, Temme AJAM, Wallinga J, Van Beek R, Sommer M (2019) Reconstructing rates and patterns of colluvial soil redistribution in agrarian (hummocky) landscapes. *Earth Surf Proc Land* 44:2408–2422. <https://doi.org/10.1002/esp.4671>
- Van Oost K, Govers G, Van Muysen W, Quine TA (2000b) Modeling translocation and dispersion of soil constituents by tillage on sloping land. *Soil Sci Soc Am J* 64:1733–1739
- Van Oost K, Van Muysen W, Govers G, Heckrath G, Quine TA, Poesen J (2003) Simulation of the redistribution of soil by tillage on complex topographies. *Eur J Soil Sci* 54:63–76
- Van Oost K, Govers G, Van Muysen W (2003) A process-based conversion model for caesium-137 derived erosion rates on agricultural land: an integrated spatial approach. *Earth Surf Proc Land* 28: 187–207
- Van Oost K, Govers G, Desmet P (2000a) Evaluating the effects of changes in landscape structure on soil erosion by water and tillage. *Landscape Ecol* 15:577–589. <https://doi.org/10.1023/A:1008198215674>
- Vereecken H, Pachepsky Y, Bogen H, Montzka C (2019) Upscaling issues in ecohydrological observations. In: Li X, Vereecken H (eds) *Observation and measurement of ecohydrological processes, ecohydrology*, pp 435–454. https://doi.org/10.1007/978-3-662-48297-1_14
- Verheijen FG, Jones RJ, Rickson RJ, Smith CJ (2009) Tolerable versus actual soil erosion rates in Europe. *Earth Sci Rev* 94(1–4):23–38
- Vlotman WF, Smedema LK, Rycroft DW (2020) *Modern land drainage: planning, design and management of agricultural drainage systems*. CRC press 2nd ed, 477 pp
- Walther GR, Post E, Convey P, Menzel A, Parmesan C, Beebee TJ, Bairlein F (2002) Ecological responses to recent climate change. *Nature* 416(6879): 389e395. <https://doi.org/10.1038/416389a>
- Wang Y, Zhang JH, Zhang ZH, Jia LZ (2016) Impact of tillage erosion on water erosion in a hilly landscape. *Sci Total Environ* 511:522–532
- Wang Y, Zhang ZH, Zhang JH, Liang XL, Liu X, Wang G (2020) Effect of surface rills on soil redistribution by tillage on a steep hillslope. *Geomorphology* (under revision)
- Weaver T, Dale D (1978) Trampling effects of hikers, motorcycles and horses in meadows and forests. *J Appl Ecol* 15(2):451–457. <https://doi.org/10.2307/2402604>
- Webb RH (2002) Recovery of severely compacted soils in the Mojave Desert, California, USA. *Arid Land Res Manage* 16(3):291–305
- Webb NP, Kachergis E, Miller SW, McCord SE, Bestelmeyer BT, Brown JR, Chappell A, Edwards BL, Herrick JKE, Karl JW, Leys JF, Metz LJ, Smarik S, Tatarko J, Van Zee JW, Zwicke G (2020) Indicators and benchmarks for wind erosion monitoring, assessment and management. *Ecol Indicators* 110:10588. <https://doi.org/10.1016/j.ecolind.2019.105881>
- Wenkel K-O, Berg M, Mirschel W, Wieland R, Nendel C, Köstner B (2013) *LandCaRe DSS—an interactive decision support system for climate change impact assessment and the analysis of potential agricultural land use adaptation strategies*. *J Environ Manage* 127 (Supplement):S168–S183
- Weyer T, Boeddinghaus RS (2016) Preventing soil compaction—preserving and restoring soil fertility. Including the classification key for detection and evaluation of harmful soil compaction in the field. Edited by the ministry for climate protection, environment, agriculture, nature conservation and consumer protection of the State North Rhine Westphalia, 41 pp
- Wieland R (2010) *Modell EROSION zur Berechnung der potentiellen Erosionsgefährdung im LandCaRe-DSS (Modellbeschreibung)*. In: Wenkel K-O, Berg M,

- Wieland R, Mirschel W (eds) Modelle und Entscheidungs-unterstützungssystem zur Klimafolgenabschätzung und Ableitung von Adaptionsstrategien der Landwirtschaft an veränderte Klimabedingungen (AGROKLIM-ADAPT)—Decision Support System (DSS). Forschungs-Abschlußbericht: BMBF 01 LS 05104, ZALF Müncheberg, Selbstverlag, Müncheberg, pp A6/1-A6/7
- Winnigge B (2004) Investigations of soil movement by tillage as a type of soil erosion in the young moraine soil landscape of Northeast Germany. *Arch Agron Soil Sci* 50(3):319–327
- Wischmeier WH, Smith DD (1978) Predicting rainfall erosion losses—a guide to conservation planning. In: *Agricultural handbook*, vol 537, Department of Agriculture, Washington D.C., US
- Wischmeier WH, Mannering JV (1969) Relation of soil properties to its erodibility. *Soil Sci Soc Am J* 33(1):131–137. <https://doi.org/10.2136/sssaj1969.03615995003300010035x>
- WMO (2020) Sand and dust storm warning advisory and assessment system (forecast maps). <https://public.wmo.int/en/our-mandate/focus-areas/environment/SDS/warnings>. Accessed on 23 May 2020
- Wolkowsky R, Lowery B (2008) Soil compaction: causes, concerns and cures 2008 University of Wisconsin-Extension, paper A3367, 8 pp
- Woodruff NP, Siddoway FH (1965) A wind erosion equation. *Soil Sci Soc Am Proc* 29:602–608
- Wu G-W, Liu Y-F, Cui Z, Liu Y, Shi Z-H, Yin R, Kardol P (2020) Trade-off between vegetation type, soil erosion control and surface water in global semi-arid regions: a meta-analysis. *J Appl Ecol* 57(5): 875–885. <https://doi.org/10.1111/1365-2664.13597>
- Wu Q, Wang M (2007) A framework for risk assessment on soil erosion by water using an integrated and systematic approach. *J Hydrol* 337:11–21
- Xiong M, Sun R, Chen L (2018) Effects of soil conservation techniques on water erosion control: a global analysis. *Sci Total Environ* 645:753–760
- Xu HC, Zhang JH, Wei YH, Dai JD, Wang Y (2020) Bedrock erosion due to hoeing as tillage technique in a hilly agricultural landscape, SW China. *Earth Surf Proc Land* 45:1418–1429
- Yang D, Kanae S, Oki T, Koike T, Musiak K (2003) Global potential soil erosion with reference to land use and climate changes. *Hydrol Process* 17:2913–2928. <https://doi.org/10.1002/hyp.1441>
- Yang C, Su ZA, Fan JR, Fang HD, Shi LT, Zhang JH, He ZY, Zhou T, Wang XY (2020) Simulation of the landform change process on a purple soil slope due to tillage erosion and water erosion using UAV technology. *J Mountain Sci* 17:1333–1344
- Zhang JH, Lobb DA, Li Y, Liu GC (2004) Assessment for tillage translocation and tillage erosion by hoeing on the steep land in hilly areas of Sichuan, China. *Soil Tillage Res* 75:99–107
- Zhang JH, Frielinghaus M, Tian G, Lobb DA (2004) Ridge and contour tillage effects on soil erosion from steep hillslope in the Sichuan Basin, China. *J Soil Water Conserv* 59:277–284
- Zhang JH, Nie XJ, Su ZA (2008) Soil profile properties in relation to soil redistribution by intense tillage on a steep hillslope. *Soil Sci Soc Am J* 72:1767–1773
- Zhang JH, Su ZA, Nie XJ (2009) An investigation of soil translocation and erosion by conservation hoeing tillage on steep lands using a magnetic tracer. *Soil Tillage Res* 105:177–183. <https://doi.org/10.1016/j.still.2009.07.006>
- Zhang Z, Wieland R, Reiche M, Funk R, Hoffmann C, Li Y, Sommer M (2011) Wind modelling for wind erosion research by open source computational fluid dynamics. *Ecol Inform* 6(5):316–324
- Zhang JH (2011) Tillage erosion. In: Gliński J, Horabik J, Lipiec J (eds) *Encyclopedia of agrophysics. Encyclopedia of earth sciences series*. Springer, Dordrecht. https://doi.org/10.1007/978-90-481-3585-1_173
- Zhao HL, Yi ZY, Zho RL, Zhao ZY, Zhang TH, Drake S (2006) Wind erosion and sand accumulation effects on soil properties in Horqin sandy farmland. *Inner Mongolia Catena* 65(1):71–79. <https://doi.org/10.1016/j.catena.2005.10.001>
- Zobeck TM, Van Pelt RS (2014) Wind erosion. Publications from USDA-ARS/UNL Faculty. 1409. <https://digitalcommons.unl.edu/usdaarsfacpub/1409>. Accessed on 23 May 2020
- Zuazo VHD, Pleguezuelo CRR (2009) Soil-erosion and runoff prevention by plant covers: a review. In: Lichtfouse E, Navarrete M, Debaeke P, Véronique S, Alberola C (eds) *Sustainable agriculture*. Springer, Dordrecht. https://doi.org/10.1007/978-90-481-2666-8_48



Understanding and Monitoring Chemical and Biological Soil Degradation

3

Elmira Saljnikov, Anton Lavrishchev,
Jörg Römbke, Jörg Rinklebe, Christoph Scherber,
Berndt-Michael Wilke, Tibor Tóth,
Winfried E. H. Blum, Undine Behrendt,
Frank Eulenstein, Wilfried Mirschel,
Burghard C. Meyer, Uwe Schindler,
Kairat Urazaliev, and Lothar Mueller

Abstract

Soil degradation is an exceedance of the capacity and resiliency of soil for providing functions and ecosystem services. It is a complex ongoing phenomenon threatening

humans' livelihoods and our future on earth. Knowledge gain can help to find solutions for monitoring, preventing and combating soil degradation. In this chapter we address the essence, causes, extent, features and implica-

E. Saljnikov (✉)
Institute of Soil Science, Teodora Drajzera 7, 11000
Belgrade, Serbia
e-mail: elmira.saljnikov@soilinst.rs

E. Saljnikov · F. Eulenstein · U. Schindler
Mitscherlich Academy for Soil Fertility (MITAK),
GmbH, Prof.-Mitscherlich-Allee 1, 14641
Brandenburg, Germany
e-mail: feulenstein@zalf.de

U. Schindler
e-mail: schindler@mitak.com

A. Lavrishchev
St. Petersburg State Agrarian University,
Peterburgskoye Ave. 2, 196601 St. Petersburg,
Pushkin, Russia

J. Römbke
ECT Oekotoxikologie GmbH, Böttgerstr. 2–14,
65439 Flörsheim, Germany
e-mail: j-roembke@ect.de

J. Rinklebe
School of Architecture and Civil Engineering,
Institute of Foundation Engineering, Water and
Waste Management, Laboratory of Soil and
Groundwater-Management, University of
Wuppertal, Pauluskirchstraße 7, 42285 Wuppertal,
Germany
e-mail: rinklebe@uni-wuppertal.de

C. Scherber
Centre for Biodiversity Monitoring, Zoological
Research Museum Alexander Koenig, Adenauerallee
160, 53113 Bonn, Germany
e-mail: C.Scherber@leibniz-zfmk.de

B.-M. Wilke
Department of Ecology, Chair Waste Management
and Environmental Research, TU Berlin,
Ernst-Reuter-Platz 1, 10587 Berlin, Germany
e-mail: bmwilke@tu-berlin.de

T. Tóth
Institute for Soil Sciences and Agricultural
Chemistry, Centre for Agricultural (ATK TAKI),
Budapest II. Herman O. út 15, Budapest 1025,
Hungary
e-mail: tibor@rissac.hu

W. E. H. Blum
Institute of Soil Research, University of Natural
Resources and Life Sciences, Peter-Jordan-Str. 82,
1190 Vienna, Austria
e-mail: winfried.blum@boku.ac.at

U. Behrendt · F. Eulenstein · W. Mirschel ·
L. Mueller
Leibniz-Centre for Agricultural Landscape Research
(ZALF), Eberswalder Str. 84, 15374 Müncheberg,
Germany
e-mail: ubehrendt@zalf.de

tions of various types of chemical and biological soil degradation. The aspects of chemical degradation, such as pollution, acidification, salinization, nutrient depletion and eutrophication are characterized shortly; for biological degradation, harm to soil microbiota and biodiversity, and soil organic matter depletion are considered. Progress in monitoring and modelling or forecasting these types of degradation is also shown. Soils of drylands, the Arctic and all man-made soils are hotspots of chemical and biological degradation. As chemical and biological degradation processes in the microscale are lingering and interacting, they need better awareness and monitoring approaches. Highly developed laboratory methods of soil chemical and biological analyses are existing, but screening methods that work under field conditions are comparatively rare. Biological soil degradation needs further evidence-based research and high-precision data for understanding and combating processes. Crucial questions such as calculation of carbon sequestration potential of agricultural soils and assessment of desertification processes should be better explored to bridge science-policy gaps.

Keywords

Soil degradation · Soil pollution · Acidification · Salinization · Nutrient depletion · Eutrophication · Soil microbial community · Soil organic matter · Desertification · Monitoring

B. C. Meyer
 Institut Für Geographie, Universität Leipzig,
 Johannisallee 19a, 04103 Leipzig, Germany
 e-mail: burghard.meyer@uni-leipzig.de

K. Urazaliev
 Department of Genetics, Breeding and
 Biotechnology, Kazakh National Agrarian Research
 University, Ave. Abay 8, Almaty 050010,
 Kazakhstan

3.1 Introduction

Soils of the globe are not yet sustainably managed, sufficiently protected and are subject to widespread degradation (Lal 1998; Blum 2013; Keesstra et al. 2016). About one-fifth of global soils are degraded and soil degradation continues at an annual rate of 5–10 billion hectares (Bateman and Muñoz-Rojas 2019). Lack of knowledge and data is contributing to this problem. Numerous soil functions, such as the relationship between soil quality and human and animal health, environmental quality, living standards, impacts on and from climate change to mitigate or slow down the rate of soil degradation have not yet been well studied. Data on the effects of soil degradation on global productivity and other functions and ecosystem services of soil are very approximate (Sartori et al. 2019) and vary widely between continents, countries and regions. Because soil quality attributes and indicators are not well defined and because soil quality is only one of the factors affecting food security (e.g., Horion et al. 2019), assessing and interpreting the effects of soil degradation and designing sound and effective response policies remain challenging. Another limitation is related to the differences in definitions, terminology, approaches in assessing the indicators and concepts of soil degradation (Eswaran et al. 2001; Prince and Podwojewski 2020). These differences are primarily dictated by the differences in the climatic, topographic and environmental conditions (Oldeman and van der Linden 1998; Pham et al. 2018). In addition, regional specifics, the scale and scope of the study, the anthropogenic load and perception of soil quality indicators also contribute to the differences in the approaches to assessing soil degradation. Knowledge gains and smart technologies can help to feed the global population, to manage soils sustainably and to reduce agriculture's environmental footprint (Foley et al. 2011; Hou et al. 2020; Mueller et al. 2021).

In this chapter we explain the types of soil chemical and biological degradation and their implications for soil and ecosystem health and agricultural food production. Progress in

monitoring and modelling these processes and remaining knowledge gaps in preventing and mitigating degradation and desertification are shown.

3.2 Chemical Soil Degradation

Chemical soil degradation is an irreversible disturbance of soils chemical status, diminishing soil functions and ecosystem services. Chemical degradation can occur (i) as a result of soil-forming processes under certain combinations of climate and soil parent material (primary salinization, acidification), (ii) as a direct human-induced impact of chemicals to soils (contamination, pollution), (iii) as an indirect impact on site conditions through land management (secondary salinization) or (iv) as a combination of those factors. Degraded soils are characterized by toxic chemicals interfering with processes that are important for soil health, such as nutrient availability for organisms, nutrient uptake and nutrient element mobility (Logan 1990; Tetteh 2015; Elbana et al. 2019; Dubey et al. 2020). High concentrations of chemical pollutants exceeding the buffering capacity of soil can become sources of pollution of water, air, other soils and ecosystems (Palansooriya et al. 2020).

Chemical degradation includes the deterioration of the chemical properties of the soil, depletion of nutrient reserves, secondary salinization and alkalization, or pollution with toxicants (Saha et al. 2017). Processes depend on the chemical composition, concentration and activity of pollutants, as well as the specifics of natural conditions and land use. It is manifested mainly on the soils exposed to the anthropogenic factors, e.g., agro-landscapes, influence of industrial facilities, urban zones, mining etc. Soil chemical and physicochemical properties maintain soil absorption capacity, decomposition and mineralization of organic residues, re-synthesis of mineral and organic substances, and nutrient supply to plants (Hatfield et al. 2017). The most applied indicators of chemical soil degradation are soil acidity, electrical conductivity, cation exchange capacity, plant-available nutrients, or

total concentrations of potentially toxic elements (PTE) and available/mobile forms of PTEs (Palansooriya et al. 2020).

3.2.1 Pollution

Essence and causes. Soil pollution or contamination is a soil degradation associated with the spread, accumulation and adverse biological or toxic effects of a substance (often: a mixture of various organic and inorganic substances as well as radionuclides (Scholten and Timmermans 1995; Fesenko et al. 2007; Endo et al. 2012) to soil. It is a threat to the health of not only soil organisms (microbes, plants, invertebrates) but also aboveground animals and, ultimately, humans (Saha et al. 2017; Rinklebe et al. 2019; Mensah et al. 2020). This may include pollution from local sources [such as landfills (Orlova et al. 2017), spills or factory sites] as well as diffuse or air-borne pollution such as atmospheric deposition of acidifying compounds and/or PTEs (Fig. 3.1) (Koul and Taak 2018). Special attention is given to substances that are regularly and intentionally applied in the environment [e.g., fertilizers, pesticides or veterinary medicines (e.g., antibiotics)], mainly at agricultural sites (Pan and Chu 2017; Wang and Tiedje 2020).

The flow of pollutants through soil can pass the stages of dilution, mixing, transfer, sedimentation, removal or dispersion (Derbentseva et al. 2005; Jaramaz 2018). Excessive accumulation of chemical pollutants deteriorates the physical and biological characteristics of soil and adversely affects plant growth (Gupta and Sandallo 2011). In contrast, PTEs can be taken up by organisms in aquatic and terrestrial food chains, causing directly or indirectly serious animal and, in the long run, human diseases (e.g., Khan et al. 2009; Nagaijyoti et al. 2010; Geng et al. 2019). Among anthropogenic sources, the most polluting activities are mining of minerals and fossil fuels, industrial by-products, traffic-generated PTEs, the operation of thermal power stations (TPS) as well as residential fossil fuel combustion, same as product use and consumption, waste disposal and use of agrochemicals and

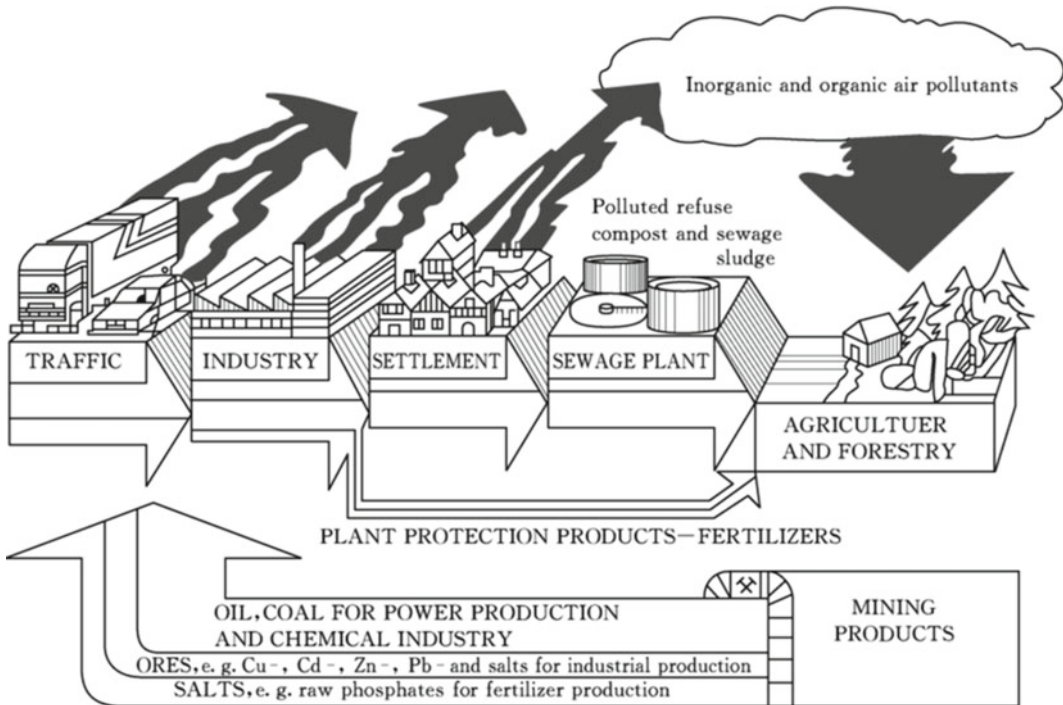


Fig. 3.1 Soil contamination through excessive use of fossil energy and raw materials (Source Blum 2013)

organic or inorganic fertilizers (e.g., Pejović et al. 2017; Raheem et al. 2018; Jaramaz 2018; Saljnikov et al. 2019; Gruszecka-Kosowska et al. 2020; Prathumratana et al. 2020). Because the term “soil contamination” is often used as a synonym for soil pollution, the Intergovernmental Technical Panel on Soils (ITPS) under the Global Soil Partnership (GSP) has formalized definitions of the two terms (FAO and ITPS 2015). Soil contamination occurs when the concentration of a chemical or substance is higher than would occur naturally but is not necessarily causing harm. Soil pollution, on the other hand, refers to the presence of a chemical or substance out of place and/or present at a higher than the normal concentration that has adverse (usually dose-dependent) effects on non-target organisms.

Extent, Features and Implications

Soil pollution comprises different elements and materials. Plastic residues, microplastics and nanomaterials came into the focus in more recent

years (Rajkovic et al. 2020; Qi et al. 2020; Yang et al. 2020; Abbas et al. 2020).

Urban soil pollution. Rapidly expanding urban and industrial areas (Khan et al. 2018; Huang et al. 2019) and the operation of greenhouses (Wang et al. 2019) pose an additional threat to soil quality by pollution with PTEs. The environmental condition of the green urban playgrounds and parks is especially in focus since they are actively attended by children (Pavlović et al. 2017; Čakmak et al. 2018, 2020) who physically come into contact with ground and soil surfaces. In the study of Pavlović et al. (2017) the highest accumulation of B, Cr, Cu, Mn and Zn was observed in the soil and the pine needles in parks which were located in proximity to big industrial and intensive transportation networks. Čakmak et al. (2018) in the study of small green areas in Belgrade city (Serbia) found that 30.7% of the green areas in the city centre had a moderate ecological risk index (RI) indicating no health risk to children. However,

increased concentrations of Zn and Cd were due to anthropogenic factors (Antoniadis et al. 2019).

Pollution of agricultural soils. Soils used for agriculture are often polluted from industrial sources via dust deposition paths (Peng et al. 2019). The use of fertilizers and agrochemicals also can be a source of pollutants in soil. Furthermore, the application of fertilizer (Nicholson et al. 1999; Bolan and Duraisamy 2003) and sewage sludge (Singh and Agrawal 2007; Raheem et al. 2018) was reported to be a source of chemical enrichment in soils. Relatively high contents of heavy metals can be found in soils under irrigation in arid regions (Otarov 2014). Phosphorus fertilizers are also a source of heavy metals (Mortvedt 1996; Xia et al. 2020) and can additionally cause radioactive contamination (Scholten and Timmermans 1995).

Another group of chemicals that act as water and soil pollutants are pesticides (Keesstra et al. 2016; Qin et al. 2018; Pan et al. 2019; Silva et al. 2019). They are a source of xenobiotics, which are often resistant to microbial degradation processes and can be toxic to organisms even at low concentrations (Steffan et al. 2018). Pesticides can accumulate in the soil, poison macro- and microorganisms, penetrate plants by absorption and eventually affect pollinator insects. They can also leach down the soil profile and contaminate

groundwater and thus drinking water sources (Sjerps et al. 2019).

Long-term, excessive and exclusive use of mineral fertilizers can affect soil structure adversely, alter the chemical structure and fungistatic activities of humic acids and thus promoting physical, chemical and biological degradation (Guo et al. 2019a; Wu et al. 2019). Pesticides can alter the composition and diversity of soil microbial communities (Sharma et al. 2019; Satapute et al. 2019; Meena et al. 2020) with largely unexplored consequential effects cascading up to higher trophic levels in soil food webs and negatively affecting soil health (Silva et al. 2019). Besides “diffuse” soil pollution, numerous kinds of locally detectable, “source-based” pollutions exist (Fang et al. 2020; Fig. 3.2).

Pollution of soils under forests. Soil pollution under forests, mainly via the air entry path (dry and wet deposition), has reached giant dimensions in all climate zones and ecosystems of the globe. In combination with other stressors, significant forest decline has occurred, coupled with strongly altered herb layer composition (invasion of nitrophilous plants), reducing forest biodiversity across all strata. Industrial plants, urban areas and traffic are the main emitters of polluted air (Lee et al. 2019), especially responsible for the deposition of reactive nitrogen species. To



Fig. 3.2 Visible signs of soil pollution on agricultural lands. Left side: Many of today’s agricultural areas were former battlefields. They are polluted by war materials and explosives, which are a risk for human’s health and life. Right side: Illegal waste disposal on a

rangeland/pasture is a risk for various organisms. If not collected and removed, plastic materials and other particles (including nanoparticles) contaminate soils in the long term and become part of the food web. Photos L. Mueller

analyse the response of forests to climate change and air pollutants, and implications for soil and groundwater sophisticated measurement systems such as lysimeters, other field sampling technologies have been developed (Müller 2016).

Monitoring and Modelling Soil Pollution

The development of measurement and monitoring methods for soil pollution is a broad area of research, technology and outreach. Its practice is ruled by national and international standards and other protocols, and it has a very advanced level in many countries.

Laboratory methods of detecting pollutants: Licensed laboratories provide soil analyses, many of them in the framework of environmental and agricultural monitoring (e.g., Poláková et al. 2018; Derevyagin 2018; Eugenio et al. 2020). As most measurement technologies are suitable to analyse pollutants of other media besides soil, e.g., water, plant tissue, air etc., sample preparation for analysis is a decisive criterion of success.

Standard analyses of agrochemistry are used for the detection of plant nutrients such as nitrogen, phosphorus, potassium, calcium, manganese etc., and their dissociates which can act as pollutants as well can be detected by standard methods such as ion-chromatography for anions (Gutorova et al. 2018a). Standard protocols for extraction methods to adapting the solubility status of elements to natural conditions of soils have been developed, but they are country-specific and often difficult to compare (Cherenok and Barkusky 2014). However, the International Standardization Organisation (ISO) has recently published some standard protocols for extraction procedures, which address, e.g., the problem of non-extractable residues (NERs) (Löffler et al. 2020). If overall element concentrations are required, for example for detecting heavy metal pollution, total solubility of elements using aqua regia and measurement by atomic absorption spectrometry (AAS) analysers is common (Davidson 2013). Organic pollutants such as mineral oil and other hydrocarbons can be detected by gas chromatography (GC) or high-performance liquid chromatography (HPLC)

(Beškoski et al. 2012), but simplified methods such as near-infrared spectroscopy (NIRS) have been developed for screening purposes (Pankratova et al. 2016). Special substances polluting soils in small doses, such as antibiotics (Pan and Chu 2017) and other organic xenobiotics (Schauss et al. 2009), are measurable by special methods such as EPR spectroscopy with the use of spin labels (Aleksandrova 2018). Special analytical methods also have been developed for cases of mixed contaminants such as hydrocarbons with heavy metals (Ding et al. 2019).

Field indication and bioassays. Though many forms of soil pollution are invisible with naked eyes, a number of bioindicative methods exist (Schubert 1985). Anthropogenic soils (Technosols, Anthrosols) showing macro-artefacts (waste, debris etc.) are often polluted and require special analyses. Mosses, lichen and fungi are particularly sensitive to contamination and can be used as bioindicators (Singh 1998). Bioassays using different kinds and indices of microflora, microfauna and higher soil-inhabiting plants and animals have been developed (Römbke et al. 2005; Griffiths et al. 2016; Bardina et al. 2018; Römbke 2018; Tang et al. 2019; Van Gestel et al. 2020). Field chemical analytical methods using test kits and simplified sample preparation are also possible, but the detection limits of the expected results compared to the threshold values must be taken into consideration (Zeiner et al. 2019). Moreover, soil ecotoxicological methods can be used for the detection of soil pollution. Their main advantage over chemical analysis is that they include possible interactions (synergy/antagonism) between chemicals and the complex soil matrix. ISO 15799–2019 and ISO 17616–2019 provide guidance on the selection and evaluation (ISO 17616) of experimental methods for the assessment of the ecotoxic potential of soils and soil materials (ISO 15799:2019-11 2019; ISO 17616:2019-11 2019).

Soil pollution is always a risk for water pollution and therefore requires a careful analysis of the risk assessment (Eulenstein et al. 2016). Figure 3.3 shows a workflow in the exploratory investigation of suspected cases of soil

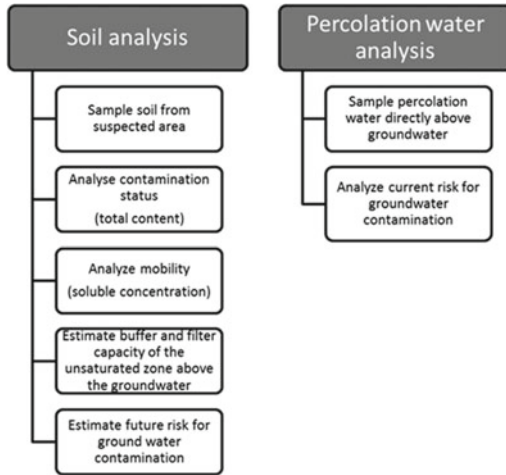


Fig. 3.3 Workflow in an exploratory investigation of suspected contamination with trace elements. Guideline of the German Federal and State Working Group for Soil Protection (LABO 2003). *Source* Godbersen et al. (2014)

contamination with trace elements (Godbersen et al. 2014).

Lysimetry. Experiments using precision lysimeters (Meißner et al. 2010; Shaheen et al. 2014; Fig. 3.4) with internal sensors and succeeding automated laboratories are high technologies for exploring transport and transformation of pollutants in soil and their transfer towards geosphere, hydrosphere, atmosphere and biosphere (Haselow et al. 2019; Schuhmann et al. 2019; Gros et al. 2020; Zhao

et al. 2020a). They are useful to calibrate ecosystem models (Wegehenkel and Mirschel 2007; Diestel et al. 2007; Groh et al. 2020) and they are an important bridge for scaling up experiments from the laboratory to the field scale (Rupp et al. 2010).

Background definition. It is crucial to separate background values from baseline values when defining the extent of contamination (Mrvić et al. 2014; Jaramaz 2018), especially in areas where environmental legislation has not yet established intervention limits for all environmental matrices (Albanese et al. 2007; Antoniadis et al. 2019; Prathumratana et al. 2020). Background values indicate geogenic natural content, while baseline values indicate the actual content of an element in the superficial environment at any given point (Reimann et al. 2005; Jaramaz 2018).

Modelling soil pollution. Soils can traditionally be considered physically as a phase system consisting of a solid phase and pores filled with water and air. The solid phase is very heterogeneous in constituents (soil texture, dead organic matter, pores, microbiota, roots) and structure (pore size, continuity, connectivity). Due to precipitation and evapotranspiration, freezing, thawing and other processes, the pore space underlays a high dynamic of water and air phases. If a contaminant enters the soil, different processes of retention (adsorption–desorption),



Fig. 3.4 Lysimeters embedded in a cropped field for agri-environmental monitoring of soil and groundwater pollution. On the right side there is the entry into the lysimeter cellar containing probes and samplers. *Photo* L. Mueller

transformation (biologically and chemically) and transport through water (convective–dispersive, mass flow solely, film flow) or in the damp phase can occur. Older models (before 1980), which describe the transport of fluids and gases in soils, consider individual processes and mainly show the translocation of contaminants; newer ones are more complex (Rao and Jessup 1982; Halm and Grathwohl 2003; Shuang et al. 2019; La Cecilia and Maggi 2020). Also, some more recent models like the SWAP-ANIMO model (Kroes and Roelsma 2007), the HERMES model (Kersebaum 2007) and the model of Fang et al. (2019) take into account the water and solute transport and consider the structure of soil and rhizosphere in more detail.

3.2.2 Acidification

Essence and causes. Soil acidification is a permanent increase of acid strength, commonly measured by a decrease in soil pH. It is observed upon the build-up of hydrogen cations that occurs when an acidic proton donor is added to the soil (e.g., nitric, sulphuric or carbonic acids) mainly derived from acid deposition. In addition, ion uptake by biota through processes such as microbial decomposition of organic matter, nitrification, nitrogen inputs and transformations (Hong et al. 2019; Liu et al. 2020a) or leaching of basic cations, such as Ca, Mg, K and Na (Xu et al. 2019a) also contribute to this process. Soil acidification is a natural process in humid regions (Posch and Kauppi 1991; Fujii 2014). It occurs slowly as a result of weathering when lichens and algae act on parent materials consisting of acidic compounds that keep dissolving as the soil develops (Chen et al. 2019). Plant roots also release protons and organic acids to chemically retrieve nutrients from the mineral soil phase (Chigira and Oyama 2000). In addition, decay of the litter from coniferous trees, such as pine, spruce and fir also contribute to soil acidification, as they contain much less basic cations than deciduous trees (e.g., Posch and Kauppi 1991; Nisbet and Evans 2014). Chen et al. (2019)

revealed by combining data from 4700 soil profiles in China that the climatic factor (temperature and precipitation) and soil type were the main factors determining the soil pH.

Important sources of soil acidification are volatile emissions of nitrogen oxides, sulphur dioxide, ammonia and other emissions to the atmosphere which are deposited as acid rains (Liu et al. 2020b). Soils under forests are landscape hotspots of deposition (Ulrich and Sumner 1991). Acid rains may pose a serious negative impact on the solubility and leaching pattern of potentially toxic elements and heavy metals (De Vries and McLaughlin 2013; Xu et al. 2019b; Fei et al. 2020).

Acidification of agricultural soils. Soil acidity (low value of pH) is one of the most sensitive indicators prone to rapid changes due to agronomic practices such as fertilization, irrigation with mineralized water, liming and manure application. In soils under agriculture, nitrogen fertilization directly promotes acidification (De Vries and Breeuwsma 1987). The main causes of anthropogenic soil acidification are overuse of acidifying fertilizers, especially pronounced on the soils having naturally low-activity clays and low organic matter content (e.g., Jones et al. 2020). In arable farming systems, ammonia-containing fertilizers are the main acidifying agent, since the added ammonia can substantially contribute to the proton loading to the soils (e.g., Guo et al. 2010; Liu et al. 2020a). When negatively charged nitrate is absorbed by plants, a negatively charged hydroxide ion is released from the plant to maintain electrical balance. If nitrate is not absorbed by plants, it can be leached down from the root zone, which means that no hydroxide ion is released from the plant to bind with a hydrogen ion. Excessive amounts of added mineral N cannot be assimilated by the soil biota or transformed into soil humus generating acidification of soil. In addition, incomplete recovery of organic anions can also add to the acidification process (Guo et al. 2010; Khan et al. 2018). Livestock manure is responsible for nearly 65% of man-made ammonia emissions, about 40% of nitrous oxide emissions and an enormous amount of methane release (Steinfeld et al. 2006).

Extent, Features and Implications

Soil acidity influences nutrient availability to plants and at the same time regulates their concentrations that under certain values of pH may become toxic (e.g., Al, Mn) or deficient (e.g., Mn, Fe and Zn) (Karlen et al. 2008; Xu et al. 2020b). Most metals such as Cd, Cu, Ni, Cr, Zn are sensitive to pH and lower pH leads to enhanced mobilization and potential migration (Rinklebe et al. 2016a,b).

Acidic agricultural soils have a number of adverse properties that limit obtaining high and stable yields as a result of decreased availability of some plant nutrients (Hou et al. 2020). Combustion of fossil fuel and solid waste, as well as the treatment of wastewater and exhausts of motor vehicles, is the next major source of sulphuric gases and nitrogen oxides (MacKenzie and Dietrich 2020). The negative consequences of acidic soils are:

- (1) Changes in the structure and activity of the microbial community, which can lead to malfunctioning of nutrient recycling
- (2) Nutrients in an acidic environment may become unavailable or deficient to plants (e.g., P, Ca, Mg, Mo)
- (3) Release of toxic elements may affect plants and microorganisms (e.g., Al, Fe, Mn) (Bowman et al. 2008) and
- (4) Heavy metals may become available to plants (e.g., Cd) (Blake and Goulding 2002).

A number of authors emphasize that soil acidity is the most important parameter of soil chemical health, as this indicator affects and determines a wide spectrum of processes in the soil such as microbial activity, nutrient availability and heavy metal immobilization or release (e.g., Robson 1989; Bolan et al. 2003). Various soil types and climatic conditions determine to a large extent the frames of natural levels of soil acidity when the specific ecosystem functions properly (Cardoso et al. 2013).

Monitoring and Modelling Acidification

Soil pH as an indicator of acidification can be measured easily in the field and laboratory (Smith

and Doran 1997). The pH values in the range of 5.2–8.2 are considered suitable for topsoils of cropland (AG Boden 2005; Mueller et al. 2007a). If pH falls below 5.5 in sandy soils, 5.8 in loamy sands and 6.1 in loamy and silty soils, liming is recommended for soils of the temperate zone (Kundler 1989). Vegetation is sensitive to the acidification status of the soil. Higher plants can be used for the bioindication of soil acidity (Ellenberg et al. 2001; Mueller et al. 2014a).

For the prediction of acidification of arable soils, a number of models were developed. The VSD + model (very simple dynamic model plus) (Posch and Reinds 2009; Bonten et al. 2016; Xu et al. 2020a) is a single-layer dynamic model based on the charge and mass balances to calculate changes in pH and element concentrations (SO₂, NO_x, NH₃) in soil solution and thereby element outputs from the root zone (Zhu et al. 2018). The VSD + model was developed for processes of organic C and N turnover and mass balances of elements, cation exchange and base cation weathering (displaying eutrophication and carbon sequestration) and was also suited to model acidification and liming processes (Xu et al. 2020b).

The 'Regional Air Pollution INformation and Simulation' (RAINS) model with different sub-models was developed by IIASA as a tool for the integrated assessment of alternative strategies to reduce acid deposition in Europe and Asia (Kauppi et al. 1987; Alcamo et al. 1990). The RAINS 7.2 model with different modules describes the pathways of emissions of sulphur dioxide, nitrogen oxides and ammonia and explores their impacts on acidification and eutrophication (IIASA 2020). The simulation model RAINS with sub-models as well as simulation by the SWAP-ORCHESTRA model (Kros et al. 2017) simulates the dynamics of nutrients and pH in the soil.

3.2.3 Salinization and Alkalinization

Essence and causes. Salinization occurs when water-soluble salts (typically composed of K⁺, Mg²⁺, Ca²⁺, Cl⁻, SO₄²⁻, CO₃²⁻, HCO₃ and Na⁺

ions) accumulate in the soil in high concentrations above 0.05–0.15%, which are generally the toxic thresholds for plants (Bazilevich and Pankova 1972).

In nature, salinization occurs due to high salt content of the parent material (weathering), discharge from groundwater or deposition of salts blown off from coastal areas and salty deserts. Increasing salt concentration results from aridity, which generates high evaporation and upwards directed water transport in the soil. Types of salinization (Fig. 3.5) in terms of the mineralogical composition of soils and severity of processes are landscape-specific (Kotenko et al. 2020). The occurrence of very alkaline landscapes is closely related to flat sedimentary landscapes. Stagnation of shallow water tables but exposure to evaporative concentration typically results in very alkaline soils (Jobbágy et al. 2017).

Salinity forms/types after Bolt and Bruggenwert (1976) are:

- (1) Soils of very high salt concentrations (saline soils, typical soil types or reference groups are *Solonchaks*)
- (2) Soils of uneven cation composition in favour of the monovalent alkali cation sodium (sodic or alkali soils, typical soil types or reference groups are *Solonetz*)

- (3) Other soils having a high pH often due to a dominance of (bi)carbonate anions (alkaline soils) (Bolt and Bruggenwert 1976; Bloem et al. 2012).

Salt-affected soils may develop both under dryland and irrigated conditions (Pla Sentís 2021), with unfavourable physical and chemical soil properties, crop production and animal and human health. Salt-affected soils may develop through natural processes (primary salinization) or can be induced by human intervention (secondary salinization). Anthropogenic salinization occurs due to human activities such as inappropriate irrigation practices, for example with mineralized irrigation water and/or insufficient drainage (e.g., Cuevas et al. 2019; Abdollahpour et al. 2020; Nguyen et al. 2020; Tanirbergenov et al. 2020) as well as contamination of soils with salt-rich waters and industrial by-products such as oil extraction and cement manufacturing, as well as road maintenance by salting (Litalien and Zeeb 2020). The processes of secondary salinization become accelerated when the soil water regime is drastically changed with the introduction of irrigation without adequate drainage (Fig. 3.5).

From a soil classification aspect, there are two groups of salt-affected soils: (1) soils with water-



Fig. 3.5 Soil profile of a Solonchak (left hand) and landscape with Solonchaks in depressions, surrounded by Solonetz and Southern Chernozems in the Kulunda Steppe of Siberia. Photos L. Mueller

soluble salts accumulated in the upper soil layer, such as Solonchaks, and (2) soil with a high content of exchangeable Na, sometimes also Mg, expressed by a Natric (sodic) horizon, such as Solonetz (IUSS Working Group WRB 2014, Fig. 3.5).

Extent, features and implications. The accumulation of salts is one of the most severe physiological threats to ecosystems since strong salinization slows down protein synthesis and inhibits plant growth and soil microorganisms (Rubio et al. 2020; Munns et al. 2020; Litalien and Zeeb 2020). Approximately 20% of the world arable land area is salt-affected, mainly located in arid and semi-arid regions (Funakawa et al. 2000; Shrivastava and Kumar 2015), while the area of salt-induced land loss is estimated to be 10 million ha each year (Szabolcs 1974), which may result that by 2050, 50% of the world's irrigated land will be affected by salinity (Bartels and Sunkar 2005; Hasanuzzaman et al. 2014).

Solonchaks cover about 260 million ha in the world according to IUSS Working Group WRB (2014). Solonetz soils mainly occur in areas with a semi-arid temperate continental climate and cover about 135 million ha worldwide (IUSS Working Group WRB 2014). Both types of soil are often locally associated (Fig. 3.5).

Accumulation of sodium ions is one of the most dangerous processes since sodification (alkalinization) is hard to reverse (Egorov et al. 1977). An excess of sodium results in the destruction of the soil structure, compaction and crusting; therefore, due to the lack of oxygen, the soil becomes incapable of sustaining either plant growth or animal life. Due to the destruction of the soil structure, these soils are more easily eroded by water and wind. In addition, salinization increases the non-permeability of deep soil layers, making it impossible to use the land for cultivation. Generally, the soils with a low filtration rate, particularly the soils with high clay content, are more sensitive to salinization processes. According to negative effects on plants, salts are divided into the highly toxic (Na_2CO_3 , NaHCO_3 , NaCl) since they easily penetrate into the cytoplasm, moderately toxic (CaCl_2 , MgCl_2 , Na_2SO_4) and less toxic (MgSO_4 , CaSO_4) classes.

When water evaporates from the soil these dissolved salts remain in the soil in high concentrations. This typically occurs in areas where excessive transpiration/evaporation can result in a concentrated accumulation of salts in near-surface horizons. The effect of salts on plants is dual in nature. On the one hand, salt accumulation in the soil increases the osmotic pressure of the soil solution, significantly reduces the availability of water for the roots, and on the other hand, some salts have a specific toxic effect on plants (due to a sharp disruption of nitrogen metabolism and the accumulation of protein breakdown products). Under natural conditions, it is difficult to distinguish between these two effects since it varies depending on the ratio of salt ions in the soil and the plant response to salinization.

Salinity causes water stress to plants because the increased osmotic potential affects water uptake (Bazrafshan et al. 2020), but crops have a different sensitivity against soil salinity. Also, salts act differently. Salinization and alkalinization also have negative effects on the carbon and nitrogen cycles of soil. Dissolved organic carbon increases with pH (Tavakkoli et al. 2015).

Most plants are non-tolerable to salt accumulation in soil. Moreover, excess concentrations of salts may leach into freshwaters, affect the diversity and richness of detritivores, macroinvertebrates, and fish (e.g., East et al. 2017), as well as lower production potential of soil (Szabolcs 1974; Saparov et al. 2008; Saparov 2014). Irrigated lands produce 1/3 of the world's food; however, about 20% of these lands are salt-affected (Shrivastava and Kumar 2015). Concentrated irrigation return flow, as well as surface and underground drainage discharge waters, often pose risk not only due to elevated concentration of irrigation water ions but also due to pesticides and toxic elements mobilized during leaching (Hillel 2000).

Monitoring and Modelling Salinization and Alkalinization

The most widely used indicator of soil salinity is the electrical conductivity of saturated soil extract (ECe) expressed in deciSiemens (or dS)

Table 3.1 Classification of salinity based on effects on crops and measurement of electrical conductivity of soil saturation extract (ECe) (Richards 1954)

ECe (mS/cm)	Class	Effect
0–2	Non-saline	Negligible
2–4	Mildly saline	Yield reduction of sensitive crops
4–8	Medium saline	Yield reduction for many crops
8–12	Very saline	Normal yields for salt-tolerant crops only
>16	Extremely saline	Reasonable crop yield for very tolerant crops only

m^{-1} with the typical threshold value of 4 dS m^{-1} between saline and non-saline soils (Table 3.1). In the laboratory or field, soil salinity can be measured with conductometers (Tóth 2018). Plant community composition is a field indicator and predictor of soil salinity and alkalinity (Tóth et al. 1997, 2008). Also, shifts in bacterial community composition of soil can serve as bioindicators of the soil salinity status (Zhao et al. 2020).

Sodium adsorption ratio (SAR) and the exchangeable sodium percentage (ESP) may be estimated from the measured concentrations of the dissolved or exchangeable cations (IUSS Working Group WRB (2014).

Measurement of soil pH is an important diagnostic criterion of soil alkalinity. HCO_3^{3-} (Na^+ , K^+ and Mg^{2+}) salts and CaCO_3 dominate in the pH range 7.0–8.5, and CO_3^{2-} salts of Na^+ and K^+ dominate above pH 8.5 (Tavakkoli et al. 2015).

Monitoring of the dynamics of salt concentrations in soil due to the intrusion of the seawater salts and decline in underground water level due to drought, advanced geophysical survey for detection and prediction of salt-affected areas such as geostatistical non-parametric technique, probability kriging, near-infrared channel and vegetation soil salinity index are promising tools to assess the risk of soil salinization and delineate different hazard zones within a field as well as for designation of soil ameliorative countermeasures (Mandal et al. 2009; Allbed and Kumar 2013; Nguyen et al. 2020; Shaddad et al. 2020). As soil surface and vegetation are very sensitive to soil salinization and alkalinization, a multitude of remote sensing approaches has been

developed for monitoring (Allbed and Kumar 2013; Zolnikov et al. 2016; Abd El-Hamid and Hong 2020). Various models have also been developed to monitor the condition of soils and the direction, extent and trend of the risk of degradation through salinization processes. For example, there are models based on numerical models of water and solute dynamics in agroecosystems (van de Craats et al. 2020), the simulation model UNSATCHEM (Schoups et al. 2006) or the integrated simulation model SALTMED (Ragab 2015), SODIC (van der Zee et al. 2014) and the integrated model of vertical water transport simulation in the soil–water–atmosphere–plant system—SWAP (van Dam et al. 1997; Chen et al. 2019).

A recent initiative of the FAO, the Global Map of Salt-affected Soils (GSSmap) suggested a country-driven approach (Omuto et al. 2020). One of the pioneer countries to prepare and publish the map according to the requirements of FAO was Hungary (Szatmári et al. 2020). This mapping did not use the old classification shown in Table 3.1 but is convertible for the lower categories. On the other hand, Ivushkin et al. 2019 was faithful to those threshold values and used remotely sensed data to monitor the increase in the salt-affected areas between 1986 and 2016 at four stages.

3.2.4 Nutrient Depletion

Essence and Causes

Nutrient depletion is a decrease in soil fertility through excessive withdrawal of essential plant nutritional elements. Different biomes differently

cycle soil nutrients depending on the predominance of abiotic and biotic factors (Sherrard et al. 2019). If not properly fertilized, agricultural land use systems result in a net removal of nutrients from the soil either by the harvested product and/or through increased losses/leaching as compared with the natural ecosystem (Tan et al. 2005; Litvinovich et al. 2019; Zhang et al. 2020). If the nutrients removed by the harvested product are not replaced either naturally through weathering and bio-geocycling or through sustainable agricultural management, many soils will be exhausted by permanent crop cultivation. Farming based on nutrient depletion is called nutrient mining. Loss of fertile topsoil layer (due to erosion) and poor land management (slash, burn, harvest of crop residues, improper fertilization,

etc.) that do not replenish the nutrients taken out of the soil by the crops diminish plant nutrition minerals (Van der Pol and Traore 1993; Tan et al. 2005; Pasley et al. 2019) (Fig. 3.6). Especially the loss of basic cations is pronounced in acid soils where calcium losses due to leaching from sod-podzolic soils are 300–400 kg per ha (Kanash et al. 2018; Lavrishchev et al. 2020), while the annual calcium removal from soil by different crop species varies from 20 to 500 kg per ha (Nebol'sin and Nebol'sina 2005).

Extent, features and implications. Nutrient depletion can occur in all farming systems that are not properly managed, monitored and controlled. This is typical for agriculture in countries with fewer resources (Tan et al. 2005). One of



Fig. 3.6 Effects of nutrient depletion due to missing or imbalanced fertilization in cropping systems. The photo shows the unfertilized plot of a long-term fertilization trial. Barley plants are weakly developed, prone to pests and diseases, have low yields and poor nutrition quality.

Because leaching of nutrients is a natural process in humid and sub-humid landscapes, crop yields are dropping permanently. Inputs of nitrogen and other elements through wet and dry deposition can mask yield dropping. *Photo* L. Mueller

the off-site effects of nutrient depletion due to intensive management is a negative succession and invasion of alien plants that can threaten the biosecurity of indigenous plants (Zhou et al. 2020a, b). In the humid zone, nutrient depletion is often associated with soil acidification and exacerbated by it.

Monitoring and modelling nutrient depletion. Nutrient depletion of soil can be measured in the framework of agrochemical monitoring of agricultural lands (Romanenkov et al. 2021) and forests (Müller 2016). Nutrient balancing is a common part of most ecosystem models (Mirschel et al. 2020).

Nutrient depletion via drainage fluxes of nutrients can be estimated for instance by the SWAP (StateWide Agricultural Production) model (Bonfante et al. 2010) or by the QUEFTS (QUantitative Evaluation of the Fertility of Tropical Soils) model (Janssens et al. 1990). The last one predicts crop yields from chemical soil characteristics, as an indicator of soil fertility.

3.2.5 Eutrophication

Essence and causes. Eutrophication is the enrichment of the environment with nutrients. Soil eutrophication in horticulture (Bai et al. 2020) and agriculture (Daniel et al. 1998) is caused by excessive inputs of plant nutrition elements, mainly of phosphorus and nitrogen, through fertilization and other input sources such as wet and dry deposition (Rodríguez and Macías 2006). Eutrophication is the opposite of nutrient depletion. Waste disposal sites are hotspots of eutrophication (Sauve and Van Acker 2020). Soil eutrophication is a particular problem in excessively livestock-dominated farming systems, which are prone to high surpluses in the nutrient budget. Factory indoor farming of pigs, poultry and ruminants is often based on imported high-energy concentrates and boosted by pharmaceuticals. The capacity of local soils to recycle manure and other remainders from animal factories is exceeded in most cases. Urban soils are

also prone to eutrophication due to human effluents, waste and nitrogen inputs by traffic. Eutrophication is often associated with soil pollution (Rashmi et al. 2020) and soil acidification (Diekmann and Dupré 1997).

Extent, Features and Implications

As eutrophication leads to potentially increased primary productivity due to enhanced availability or usage of nutrients and altered plant competitive hierarchies and does not diminish the productivity function of soil, it has largely not yet been recognized as a soil threat. However, it affects soil ecosystems, biodiversity and animal and human health. Communities of organisms and food webs shift towards nitrophilic and phosphophilic species and overall higher trophic levels (Potapov et al. 2019; Chen et al. 2020a, b, c). Eutrophication in terms of nitrogen availability and surplus could play an important role in the ongoing pollinator declines, mediated via altered functional composition of plant communities (Carvalho et al. 2020). One of the longest ecological field experiments, the Park Grass Experiment, has shown dramatic plant biodiversity effects of altered nutrient regimes (Crawley et al. 2005).

Soil eutrophication is a severe threat to all existing inland water bodies and finally, to the oceans. Common causes of eutrophication of aquatic systems are discharge (leaching and/or runoff) of nitrate or phosphate-containing detergents, fertilizers or sewage from soil (Khan and Mohammad 2014a). All this may result in accelerated accumulation of dead organisms (plant and animals) in benthic layers, thus resulting in a shortage of oxygen as well as pollution of lakes and silting coastal inlets (e.g., Khan and Mohammad 2014b), or even in contamination of drinking water with nitrates (Chorus and Bartram 1999; Eulenstein et al. 2016). Furthermore, the natural vegetation of coastal areas, bogs, meadows, forests adapted to their level of nutrition may be replaced by faster-growing species that take advantage of higher N supply, such as reed or reedgrass species (Pullin 2002). Although anthropogenic eutrophication is a relatively recent

phenomenon, its recovery may take 1000 years (Carpenter 2005).

Monitoring and Modelling Eutrophication

Many higher plants are indicators of eutrophication (Ellenberg et al. 2001). Semi-quantitatively, it can be detected by vegetation analyses (Diekmann and Dupré 1997). Also, microbial communities reflect eutrophication well (Johnson et al. 2008; Chen et al. 2020a, c). Direct thresholds of soil eutrophication in terms of permissible nitrogen and phosphorus concentrations in the soil do not exist. Instead, thresholds for surpluses of nitrogen balances are used to monitor and protect groundwater from nitrogen pollution/eutrophication (Eulenstein et al. 2016). Besides nutrient balancing, some other proven monitoring approaches of nitrogen and phosphorus in agricultural systems have been developed (Eulenstein et al. 2016). Most ecosystem models and transport models have the potential to inform about an excessive nutrient status of soil, indicating eutrophication (Mirschel et al. 2020; Preetha and Al-Hamdan 2020). Other modelling approaches refer to specific entry paths such as atmospheric deposition of eutrophicans (Bonten et al. 2016).

3.3 Biological Soil Degradation

Soil is the medium for growth, survival and development of both above- and belowground organisms. Therefore, both the living part of the soil and the dead organic substance (humus, soil organic matter) are important factors in maintaining the structure for next generations of soil biota and plant roots (e.g., Hatfield et al. 2017; Griffiths et al. 2000; Six et al. 2004). In general, the biomass of terrestrial organisms accounts for 99.87% of the total planet biomass (Bazilevich et al. 1970; Dobrovolskiy et al. 2012; Bar-On et al. 2018).

Soil ecosystems contain a large variety of animals, macro-, meso- and microfauna as well as microorganisms which are spatially distributed in the soil and litter layers (Menta 2012; Briones 2018). They all contribute significantly to the

transformation and distribution (including mixing and bioturbation) of soil organic matter (in particular in the litter- and root layers) and thus to nutrient, carbon and water cycling (Ramesh et al. 2019). Soil biota processes mediated by them can thus serve as sensitive indicators of changes in soil quality (Anderson 2003; Cajaiba et al. 2019). Moreover, edaphic fauna positively influences the porosity and aeration of the soil. Particularly earthworms are among the most important organisms in many soils of the world that contribute to soil resistance to erosion (Römbke et al. 2005; Coleman 2011; Orgiazzi and Panagos 2018), to nitrogen supply from their cast and biomass turnover (Agapit et al. 2018; Rozanova et al. 2019) and furthermore, due to their burrowing activity, to the water holding capacity of soils (Hallam and Hodson 2020). Anthropogenic factors such as cultivation, use of agrochemicals, mechanical disturbances, plant biomass removal, deforestation, irrigation, liming, drainage as well as urbanization and industrialization inversely affect the diversity and number of soil fauna (Hansen et al. 2001; Cortet et al. 2002; Jeffery and Gardi 2010; Menta 2012). Since the majority of these organisms is aerobic, the amount of porous space, pore-size distribution, surface area, and oxygen levels are also of crucial importance to their life cycles and activities (Briones 2018).

The pool and dynamics of soil organic matter (SOM) play a central role in all biological cycles on earth. Roughly half of SOM is soil organic carbon (SOC), and roughly 5% of SOM is nitrogen in the topsoil of agricultural land. The largest proportion of SOM/SOC consists of microbial necromass.

In ecosystems of the temperate zone, 55% of SOC in soils under cropping, 62% of SOC in soils under grassland and 33% of SOC in soils under forest are microbial necromass, with about two-thirds being fungal necromass and one-third bacterial necromass (Liang et al. 2019). The quantity and quality of soil organic matter is one of the most important indicators of soil quality and health (e.g., Luebbbers 2002; Obalum et al. 2017; Ramesh et al. 2019; Jensen et al. 2020). It greatly determines biological functions of soil, chemical functions (e.g., nutrient cycling) and physical

functions (soil structure, aggregation, runoff, water and air regimes etc.) (Bünemann et al. 2018; Gregorich et al. 1994; Luebbers 2002; Wiesmeier et al. 2019; Zhou et al. 2020a, b). Besides, organic carbon plays a major role in the global carbon cycle and carbon sequestration in the soil pool (Lal 2004, 2020a; Chen et al. 2019; Jia et al. 2019). Because the bulk of SOM is concentrated in the upper soil layer and because it is lighter than the mineral part of the soil, it is highly exposed to erosive actions of water and wind (Lal 2020a). However, the direct relationship between the SOC stocks and the level of changes in related ecosystem attributes is not established yet (Körshens et al. 2014; Obalum et al. 2017; Lorenz et al. 2019). Similarly, the lack of understanding of the functioning of different organic carbon pools limits predicting SOC responses to climate changes (Poeplau et al. 2020).

In the case of degradation of soil biota and SOM/SOC, soil is diminished in its capacity to provide functions. If the land is being converted from natural vegetation as forest or grassland to cropland and no measures of SOM conservation are taken, the fast decay of SOM leads to a degradation of physical, chemical and biological soil properties. This is associated with other threats such as degradation of soil structure (Tolimir et al. 2020; Jensen et al. 2020), resulting in weakened resistance and resilience to erosion and compaction, lack of nitrogen replenishment (Treseder 2008) and enhanced greenhouse gas (GHG) emissions speeding up climate change (Blankinship et al. 2011).

3.3.1 Degradation of Soil Biota and Biodiversity

Essence and causes. Degradation of soil biota and soil biodiversity negatively affects soil-mediated processes, functions and services. That includes a decrease/loss in biodiversity, both belowground and aboveground, disturbance and deterioration of the function of biota (microbes, micro-, meso- and macrofauna), with indirect cascading effects also on aboveground interaction networks. Biological soil degradation

is caused by interacting drivers of global change, including chemical and physical soil degradation.

Extensive research has been devoted to the unprecedented rate of biodiversity loss resulting from human activities (e.g., environmental pollution, deforestation, overexploitation of natural resources, habitat loss, urbanization, excess use of agrochemicals, nutrient mining etc.) (e.g., Anderson and Domsch 1990; Snakin et al. 1992; Griffiths et al. 2000; Ritz and van der Putten 2012; Guerra et al. 2020; Potapov et al. 2019; van Leeuwen et al. 2019).

Extent, Features and Implications

Soil microbiota is the most dynamic and reactive pool responsible for most of the biogeochemical processes and nutrient and carbon cycling in soil ecosystems. Microbes form an important linkage between autotrophic production (photosynthesis) and decomposition, linking above- and below-ground subsystems, e.g., in the root hair zone, with important interactions being shaped by root exudations triggering microbial processes and initializing higher trophic-level interactions in complex interactions with the surrounding medium (e.g., Holz et al. 2017).

If microbial communities and processes are altered via biological soil degradation, this can cascade up to larger spatial scales (Dobrovolskiy et al. 2012). Microbial biomass, activity (e.g., substrate-induced respiration, enzyme activities) or diversity are considered reliable indicators of subtle changes in soil quality (e.g., Brookes et al. 1982; Saljnikov-Karbozova et al. 2004; Bünemann et al. 2006; Martinez-Salgado et al. 2019; Le et al. 2019). At the same time, because of its sensitivity, the microbial pool is the first to be exposed to any climatic stress (e.g., Delgado-Baquerizo et al. 2019). Recent studies have even shown multifactorial climate change effects on microbes and food webs (Stevnbak et al. 2012). Soil microbial biodiversity and structure are depleted in response to environmental stressors, including altered taxonomic composition and pathogen prevalence (e.g., Janssens et al. 2006; Jeffery and Gardi 2010). This, in turn, disrupts the functional activity of other soil biota, e.g.,

nitrogen fixation and humus formation as well as aggregation of soil particles, while functions such as decomposition, nitrification and denitrification can be accelerated (Selivanovskaya et al. 2014). For example, Guzev and Levin (1991) found out that soil contamination causes certain changes in the microbial community through several adaptive zones.

Moreover, since soil is the largest gene bank that stores unique and effective antibiotics and drugs (Liu et al. 2012; Rodríguez-Eugenio et al. 2018), the loss of soil biodiversity due to land use change and agricultural intensification (Castro 2000; Donkova and Kaloyanova 2008; Saljnikov et al. 2014; Keesstra et al. 2016; Chen et al. 2020a, b, c) may also result in decreased control of plant, animal and human diseases (Scherber et al. 2010; Jeffery and van der Putten 2011; Wall et al. 2015). On the other hand, excess use of antibiotics in animal therapy and growth control in livestock production can result in large amounts of these antibiotics and antiparasitics ending up in metabolites not only polluting soil and wastewater (Michael et al. 2013; Danilova et al. 2020) but also affecting soil invertebrates and aboveground fauna such as dung beetles with soil-inhabiting larval stages (Scheffczyk et al. 2016). Additionally, increased soil erosion and climate-induced shifts in land use pose a considerable threat to soil biodiversity (e.g., Fernandez et al. 2009; Keesstra et al. 2016).

Landscape structure additionally affects soil biodiversity (Scherber et al. 2021a). As the conversion of forest to cropland or other

anthropogenic sites already decreases, the abundance, diversity and activity of a wide range of soil biota (Kooch et al. 2020), maintaining semi-natural landscape elements, are important for safeguarding landscape-wide soil functioning and biodiversity.

Microorganisms have shown the potential to be applied as biofertilizers or biopesticides. There is increasing interest to integrate them as alternatives to chemical products in agricultural practices and biostimulants and microbial inoculants have largely unknown effects on soils (Kaminsky et al. 2019).

Monitoring and Modelling Soil Biota and Biodiversity

Indicators and measurements. Rapid ecosystem functioning assessment methods (REFA) have been developed for quick assessments of soil processes across systems (Meyer et al. 2015; Fig. 3.7). Additionally, indicator species may be used for some particularly well-known systems (e.g., Churkina et al. 2018). Further direct biological indicators of soil health, including microbial biomass, microbial activity, pathogens, parasites, biodiversity, earthworms and overall fauna, are being developed (Lehmann et al. 2020a, b). As those indicators are site-specific, orientation values and thresholds do not yet exist in most cases..

Soil microbial communities and functional aspects can be characterized by the size of the microbial community (Tischer et al. 2019). This includes biomass and numbers, bulk activities



Fig. 3.7 Functional methods. Left: Litter-bag test with a single bag (inlet). Center: Bait-lamina test with single strips (with/without fed holes) individual strip (inlet). Right: Water-infiltration test. Photos J. Römcke

(respiration, enzyme activities), community composition (phospholipid fatty acid (PLFA), molecular profiles) as well as quantification of subsets of microbes and their activity potentials using molecular probes and soil metagenomic approaches (Lehman et al. 2015; Behrendt et al. 2016). Methods for characterizing soil microbiota community shifts include ribosomal ribonucleic acid (rRNA) amplicon sequencing and mid-infrared spectroscopy (Ricketts et al. 2020). It is important to measure not only steady-state nutrient or carbon contents but to assess the activity dynamics depending on the input, source and distribution of substrates. Therefore, it is preferable to use a complex of different biological diversity indicators and/or integrating functional indicators of biological activity. The most widely used ones are the processes of the mineralization of organic carbon and nitrogen, biological fixation of nitrogen, the activity of particular soil enzymes and microbial biomass combined with estimation of their population sizes (Fernandez et al. 2009; Thiele-Bruhn et al. 2020).

Soil microbial C and N provides a measure of the biological activity within soil and is reliably used as an indicator of soil quality (Martinez-Salgado et al. 2019) since these parameters serve as early indicators of changes in soil properties (Trasar-Capeda et al. 1998; Saljnikov et al. 2009; FAO 2019). Enzymatic activity (substrate-induced), basal respiration, the metabolic quotient (qCO_2), defined as respiration to microbial biomass ratio and microbial (genetic) diversity, are used to assess soil degradation not only because of their sensitivity to change but also of their role in nutrient cycling (e.g., Brookes et al. 1982; Bastida et al. 2008; Sheudzhen et al. 2018). Selivanovskaya et al. (2014) proposed the following criteria for the selection of the biological indicator of soil quality changes:

- (1) Sensitivity to anthropogenic impact
- (2) Close link with soil fertility parameters
- (3) Usability for the interpretation of the ongoing changes in the ecosystem observed
- (4) Convenience and benefits for land users and
- (5) Ease usage and low cost of measurement.

Bastida et al. (2006) developed a soil degradation index based on microbiological parameters such as dehydrogenase and urease activity, the content of water-soluble carbohydrates and water-soluble carbon, and respiration. Except for direct measurement of microbial respiration and biomass, their ratio as a metabolic coefficient qCO_2 proved to be a universal indicator of the ecosystem balance that reflects the ability of the microbial community to overcome external influences (e.g., Blagodatskaya et al. 2001; Kuhwald et al. 2018). Another important indicator of soil fertility is enzymatic activity, which reflects the activity of soil biota and can serve to diagnose changes occurring in it (Gutorova et al. 2018b). The processes and associated ferments that best characterize the substrate-energy exchange in soil are redox ferments (dehydrogenase, catalase); enzymes that convert nitrogen-containing compounds (protease, urease), phosphorus (nuclease, phosphatase), carbohydrates (cellulase, invertase), sulphur-containing organic compounds (arylsulfatase) (Martinez-Salgado et al. 2019; Chaer et al. 2009) β -glucosidase (Andrews et al. 2004; Stott et al. 2010). Altered dehydrogenase activity may indicate Cd toxicity to soil microorganisms in a saline environment (Filipović et al. 2020).

Snakin et al. (1996) proposed the following indicators for assessing biological soil degradation:

- Content of active microbial biomass
- Amount of pathogenic microorganisms
- Phytotoxicity measured by plant seedling tests
- Genotoxicity is measured by the increase of mutations.

Existing and needed microbial functional standards for quality assessment were summarized by Thiele-Bruhn et al. (2020). It should be noted, however, that microbial communities and functions are only one side of the coin. To assess biological soil degradation more completely, higher (eukaryotic) order taxa also need to be considered as they are linked to the microbial subsystem in a multitude of ways; responses of

meso- and macrofauna, but also of aboveground components (plants, insects) can often be easier to understand and interpret than changes in a belowground enzyme rate. Often, such analyses involve a wide range of food web components, including soil invertebrates such as collembolans, nematodes, earthworms and insects (Römbke et al. 2005; Griffiths et al. 2018; Römbke 2018; Andriuzzi et al. 2020; Scherber et al. 2021b; Figs. 3.7 and 3.8).

Overall, monitoring soil biodiversity requires a network approach covering all major components of biodiversity, from microbes to soil fauna and plants. Understanding how global change drivers such as climate change or chemical soil degradation affect interactions among taxa remains a rich source for future research, combining experimental, observational and modelling approaches.

Modelling approaches. A broad variety of specific modelling approaches to understand and explain soil microbial processes of element cycling, biodegradation, food webs and further biogeochemical processes relevant to ecosystem functionality risk assessment exist (Zhuang et al. 2011; Nagarajan et al. 2013; Xu et al. 2019a, b; Fry et al. 2019). They cover the range from species level, genome-scale metabolic models (GSMM), flux balance analysis (FBA), species distribution models (SDMs), up to more complex

community biodiversity patterns and fluxes at the ecosystem level (Gevorgyan et al. 2011; Latendresse et al. 2012; Lakshmanan et al. 2014; Xu et al. 2019a; Fry et al. 2019; White et al. 2020; Bach et al. 2020; König et al. 2020). Also, types of models developed range from mechanistic (Forbes et al. 2020) to statistical approaches characterizing biodiversity and ecotoxicity (Gelius-Dietrich et al. 2013; Roy et al. 2020). For example, Gutiérrez et al. (2020) constructed a statistical structural equation model (SEM) quantifying the effects of the experimental treatments, plant community diversity and herbicide treatment, on the performance and reproduction of a grasshopper species.

3.3.2 Soil Organic Matter Depletion

Essence and Causes

Soil organic matter (SOM) depletion in a broader sense is the reduction in the content of soil organic matter due to oxidation and mineralization. It is caused by a disturbance of the soil ecosystem, altering constellations of the factors climate, land use, vegetation, hydrology, soil texture, soil structure and others. SOM depletion in a closer sense is the loss of organic carbon in



Fig. 3.8 Field experiment for insect monitoring in an agricultural landscape. *Source* Scherber et al. 2021b, modified (Image copyrights: Laura Rose, L. Mueller)

cropping systems due to unsustainable management practices such as reduced rotations and insufficient organic and mineral fertilization.

Extent, features and implications

Organic matter of the soil consists of many constituent units that vary greatly in decay and synthesis time, in sensitivity to external influences, therefore individual SOM fractions may greatly differ in the degree of indication of soil degradation (e.g., Lorenz et al. 2019; Kholodov et al. 2020). The amount of soil organic carbon is influenced by the function of the rates of deposition and decomposition of the actual and potential SOM (Anderson et al. 1986; Gregorich et al. 1994; Lal 1998; Saljnikov et al. 2013; Ramesh et al. 2019). Labile (low molecular weight) components of SOM are considered responding faster to external influences, thus being a more sensitive indicator of soil changes (Tisdall and Oades 1982; Six et al. 2004) since it affects nutrient dynamics within a single growing season and C sequestration over extended periods of time (e.g., Gregorich et al. 1994; Saljnikov et al. 2013). However, it still remains unresolved which labile fraction is the best indicator and is usefully related to soil functions, and as such can be used as a sensitive soil quality indicator (Poeplau et al. 2018; Bünemann et al. 2018; Popov et al. 2020). Moreover, recent findings of Kuhry et al. (2020) showed that SOM in organic soils (Histels, Histosols and Turbels) has relatively slow decomposition rates, indicating that previous understanding of organic soils as highly labile should be reconsidered and requires further researching.

Reclamation of largely virgin lands for agriculture, land use changes through simplified crop rotations and intensification of agriculture have altered vegetation, hydrology, soil texture and structure, and contributed to climate warming worldwide. This has pushed and speeded up the global carbon cycle, nitrogen cycle and other ones (Lehmann et al. 2020a).

Recent trends in land use and climate change have resulted in soil organic carbon loss at a rate equivalent to 10% of the total fossil fuel

emissions for Europe as a whole. In a more sensitive climatic soil ecosystem, the loss of soil carbon in a cultivated agrosystem was 27–90% compared to natural grassland (Loke et al. 2019). Many of the cited researches showed that it is greatly influenced by agronomic practices such as tillage and cropping intensity (ploughing, manure/fertilizers, crop rotation etc.), crop residue management (higher amount of crop residues helps to maintain SOM replenishment as well as to protect soil from water and wind erosion), nutrient mining (harvesting, burning, leaching etc.). Aside from aboveground biomass, the abundance and pathway of roots contribute to better soil water and air regimes, transport of nutrients and microflora (e.g., Menta 2012). In addition, root exudates contribute to a better aggregation of soil mineral particles through cementing effect, making the soil less vulnerable to erosion (FAO 2019).

SOM (SOC) depletion has reached large dimensions in cropping systems of all soils worldwide. Even Loess soils, the most fertile soils on earth, suffer from SOM depletion. In the wheat–maize cropping zone in Northeast China, the topsoil SOC is already low, and it decreased from 52 to 24 g C (kg soil)⁻¹ during the past 150 years of cultivation (Xu et al. 2020a). To increase SOC concentration in Chernozems, the most fertile soils worldwide, under intensive farming through agricultural management seems to be difficult (Husniev et al. 2020), even through short-term fallowing (Saljnikov et al. 2015), whilst it seems to be possible by post-agricultural restoration through steppe vegetation (Kurganova et al. 2019; Ramesh et al. 2019).

SOM (SOC) depletion is a particular threat to soils of peatlands due to climate warming and human impacts of drainage and land cultivation (e.g., Mueller et al. 2007b; Inisheva et al. 2018; Gaudig and Tanneberger 2019). In tilled soils and drylands, the process of SOM depletion is often caused and accelerated by wind erosion (Chappel et al. 2019).

Since the changes in soil properties occur simultaneously in dynamic interactions (Obalum et al. 2017) studies on the fractions of soil organic matter and their dynamics should be

integrated (e.g., Obalum et al. 2017). Although a huge number of studies on the SOM transformation and loss is under discussion, and, due to difficulties in revealing the complex nature and interactions between SOM fractions (e.g., Jeffery and Gardi 2010), there are still many gaps in knowledge and understanding of the interactions between aboveground and belowground biota (Huhta 2007; Bradford and Fierer 2012; Orgiazzi and Panagos 2018; Vojnov et al. 2020), on the effect of driving factors on decomposition/accumulation rate of SOM (Jia et al. 2019), on the behaviour of individual species, communities, especially in cultivated or altered land use systems as well as comprehensive, standardized approaches to measuring the composition, diversity and function of soil biota are still lacking (Thiele-Bruhn et al. 2020). Some of the new techniques, such as molecular and genetic tools (high-throughput sequencing of ribosomal operons; shotgun metagenomics), the determination of specific microbial biomarkers using the analysis of phospholipid fatty acids (PLFA), culture-independent metagenomic approach, as well as previously existing approaches for the assessment and quantification of indicators of biological degradation, should be standardized and harmonized (Trivedi et al. 2016; Schöler et al. 2017; Muñoz-Arenas et al. 2020). The emerging use of nanomaterials for regulating soil processes needs further longer investigations and field verification since they can change soil physical, chemical and biological properties in different directions and as such may adversely affect the environmental quality (Perez-Hernandez et al. 2020).

Enhancing the amount of SOM should contribute to mitigate degradation processes and restore degraded soils by rotations and tillage (e.g., Reicosky et al. 2005; Lal 2020a), deep tillage included (Feng et al. 2020). SOM decline and restoration to climate change mitigation has reached public debates and is possibly already drifted away from evidence-based research data in terms of realistic targets (Körschens 2021). Also, debates stylizing soil as a medium for

saving the climate, distort the true image of the multiple ecosystem services (Baveye et al. 2020).

Soil Carbon Monitoring and Modelling

Knowledge about the crucial role of microbiota and its necromass on the global carbon and nitrogen cycle has grown rapidly in the past 10 years, thanks to modern analytical studies (Lehmann and Kleber 2015; Hu et al. 2020; Lehmann et al. 2020a,b). Long-term field experiments (LTEs) (Romanenkov et al. 2021; Körschens 2021) and long-term soil monitoring studies (Gubler et al. 2019) are the only true basis of hard data to assess organic matter decline in cropping systems and to derive landscape-specific realistic targets of carbon sequestration (Körschens 2021) and to calibrate carbon models (Brock et al. 2013). Results of LTEs indicate that targets of estimated potential carbon sequestration through soil management practices require a specification (Körschens 2021).

Long-term ecosystem observatories of peatlands have particular importance for understanding, monitoring and deriving restoration strategies for peatlands (Inisheva et al. 2018; Gaudig and Tanneberger 2019).

Models of the SOC cycle are experiencing a strong upswing, becoming more specific, more precise and more complex. More and more organisms and their functions are included (Woolf and Lehmann 2019; Schmitz and Leroux 2020). As the persistence of soil organic matter is an ecosystem property (Schmidt et al. 2011), models applied for prediction and simulation of impacts to soil microbiological functions are usually coupled with soil organic matter turnover models

The process-based prediction of microbial growth and activity show the DEMENT model (Allison 2014) and soil food web model (Holtkamp et al. 2011). Some newer models such as the TRIPLEX-Microbe model as a product of the integration of TRIPLEX-GHG and MEND (microbial–enzyme-mediated decomposition) evolved in an improved model representing a sensitive tool for soil biological degradation prediction. Another group of models that

incorporates microbially based mineral-associated OM, such as MIMICS (Wieder et al. 2015); CORPSE (Sulman et al. 2014); RESOM (Tang and Riley 2015) and SOMic (Woolf and Lehmann 2019) represent a new generation of models that have been further updating and optimizing to closer representation of the real situation and future trend of changes. Although existing first-order linear and nonlinear microbial models implicitly represent soil biological processes, they have certain uncertainties, depending on how much the outputs from experimental conditions correspond to the real in terms of spatial homogeneity of community and substrate, speed of microbially mediated processes etc.

For the simulation of soil carbon turnover, there are many existing and emerging models such as CANDY (Franko 1997; Franko and Witing 2020), RothC (Dungait et al. 2012; Husniev et al. 2020), Century and Yasso models

(Tupek et al. 2019), CBALANCE (Thum et al. 2020); FLUXCOM (Jung et al. 2020), MONICA (Nendel 2014, Fig. 3.9) with model algorithms taken from HERMES (Kersebaum 2007) for soil nitrogen and crop growth processes, from AGROSIM (Mirschel and Wenkel 2007) for respiration and crop growth processes and from DAISY (Hansen et al. 1991) for organic matter turn-over processes, and many other models (Brock et al. 2013; Kersebaum et al. 2007). The Lund–Potsdam–Jena General Ecosystem Simulator (LPJ-GUESS) is a sophisticated and proven process-based model of the biogeochemistry and vegetation dynamics of terrestrial ecosystems (Smith et al. 2001; Chaudhary et al. 2020) enabling forecasting climate-dependent soil carbon dynamics (Guggenberger et al. 2020).

Understanding the limitations of such predictions is highly important since the empirical outputs of the models must be extrapolated over

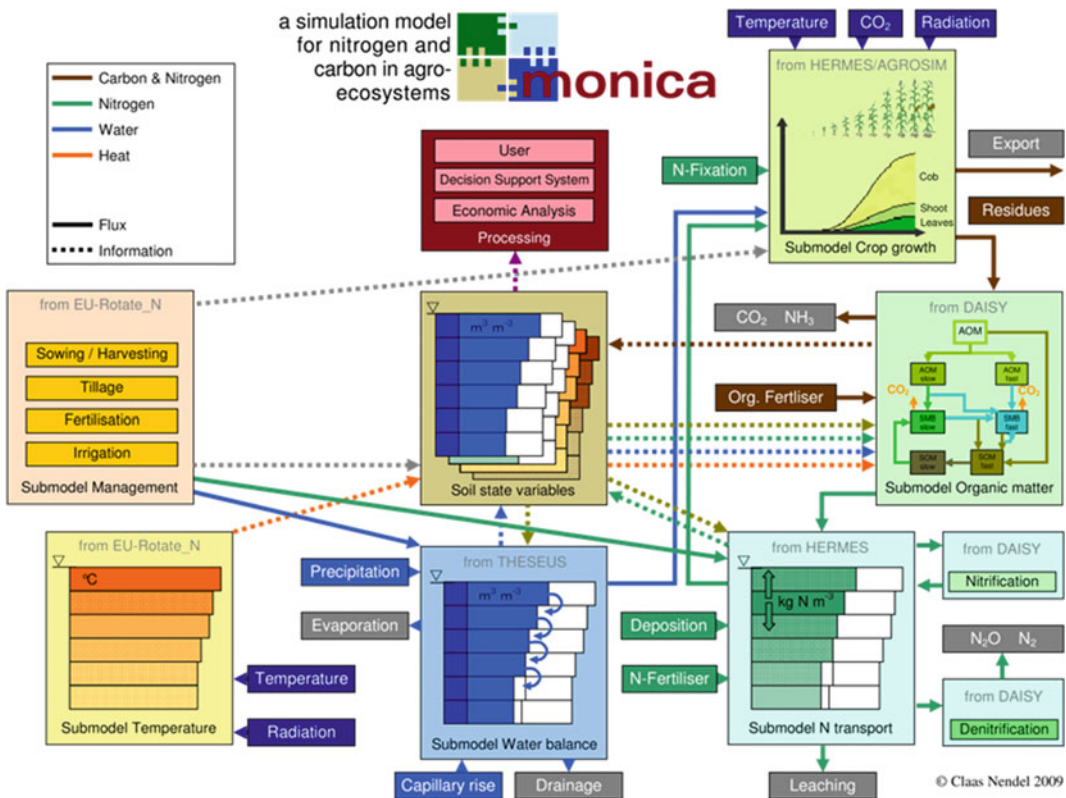


Fig. 3.9 Scheme of the MONICA model for simulation of nitrogen and carbon dynamics in agro-ecosystems *Source* Nendel 2014

space and through time to predict soil C dynamics across diverse soil conditions (Bradford and Fierer 2012). Because the current generation of the models lacks reliable projections of carbon transformations when applied on a global scale, then the real challenge is to develop the process-based simulation tool, which would represent actual and predicts realistic changes in soil biological parameters (Wieder et al. 2015) either by data integration (e.g., Hararuk et al. 2014) or by new model approaches to be generated.

The input data is obtained from long-term field experiments (Kholodov et al. 2020; Husniev et al. 2020; Romanenkov et al. 2021), from incubations and parameterized to fit plot or field-scale stock and flux observations.

3.4 Hotspots of Chemical and Biological Soil Degradation

3.4.1 Urban Soils

Progressive trend of urbanization and soil transformation. At present, approximately 54% of the global population lives in cities (UN 2014), and the proportion is increasing. An increasing trend of the urban population leads to the enhanced need for service infrastructure and other economic activities. This in turn expands the administrative boundaries of the city often at the expense of previously cultivated land as well as shrinking the urban green spaces (Norra and Cheng 2017).

More and more agricultural soils will be transformed into urban soils. Urban soils play the role of the main component of the urban geo-system, which performs a number of important environmental functions and largely determines the formation of human living conditions in the city such as for recreation, sport, small gardening, playgrounds, green lawns, ornamental plantations, protective forest belts etc.

In contrast to soils of natural and agricultural landscapes, urban soils are greatly disturbed, contaminated and transformed (Meuser 2010; Vodyanitskii and Savichev 2017) due to excavating, replacing, shifting and mixing with urban by-products. In addition, the microclimate of

urban areas is characterized by altered air and soil temperature, and elevated airborne dust deposition (Höke 2003). To date, the common outcomes of studying urban soils have elevated the value of electrical conductivity, increased K, Ca contents, have elevated values of bulk density, higher content of sand fraction, which are satellite problems of an urban environment due to urban network operations (Alekseenko and Alekseenko 2014; Adamiec et al. 2016; Čakmak et al. 2018) as well as due to the proximity of manufacturing facilities and venues mostly in sub-urban areas (Galitskova and Murzayeva 2016).

Complexity of soil degradation processes and risks. Studies on the quality of urban soils are in focus recently, therefore not much data have been accumulated (Zornoza et al. 2015; Herrmann et al. 2017; Čakmak et al. 2018; Tresch et al. 2018; Olsson et al. 2019) for comprehensive analysis. According to Čakmak et al. (2018) and other published studies, urban soils experience drastic changes in their physical, chemical and biological status due to heavy traffic load (Luo et al. 2019), lack of vegetation cover and sealing of the soil surface, human activities and materials used in the construction of pavements and buildings (Ferreira et al. 2018), use of anti-icing chemicals, recycling and disposal of wastes, application of lawn chemicals and other urban impacts. Luo et al. (2019) found that the 20% loss of labile carbon stock in near-urban environments reached down to 60 cm depths. Urban soils are characterized both by enhanced carbon stocks (Canedoli et al. 2020) and eutrophication. The maintenance of urban functioning generates far-reaching resonance in soil that inevitably lead to contamination of urban soils with heavy metals (Pavlović et al. 2017), urban debris, PAH's PCBs (Wang et al. 2019) and other pollutants originated from residential and industrial fuel combustion, traffic exhaust, power plants servicing the settlements (Höke 2003; Meuser 2010; Norra and Cheng 2017) as well as withdrawal of arable lands for urban and industrial needs. The risk of contamination of urban soils with trace elements (P, Mn, Sr, Zn, Cr, NI, Cu, As and Pb) which ultimately contaminate water (Yang et al. 2016; Jha et al.

2020) poses a real hazard to the health of urban residents and animals. Even constructing green infrastructure faces a number of interrelated environmental problems in the urban region and far away (Figs. 3.10 and 3.11).

Challenges to explore man-made soils. According to the World Reference Base for Soil Resources (IUSS Working Group WRB 2014), man-made soils are classified as Anthrosols and Technosols. However, these soils are extremely diverse requiring more detailed analysis and functional classifications (Gerasimova and Bezuglova 2019).

Green infrastructure in urban areas creates new soils and ecosystems with unexplored food webs beginning with microbial communities to be researched and understood (Joyner et al. 2019). Home gardening and urban agriculture for advancing food and nutritional security will gain greater importance in the future, but pollution must be addressed (Lal 2020b). Man-made soils, ecosystems and landscapes will dominate the Anthropocene. They must not degrade. Their performance is in our hands. We have to develop tools to explore and understand them better.

3.4.2 Soils in Drylands

Need for understanding desertification. Desertification is a degradation of drylands towards the formation of deserts. It is a very complex phenomenon occurring mostly in arid, semi-arid and dry sub-humid areas as a result of various factors, including climate change and human activities (Dregne 1977; Prince and Podwojewski 2020). It must be evaluated and combated taking into account both natural and socio-economic factors (Venkatramanan and Shah 2019). It is often associated with salinization. One of the human-induced reasons for desertification is poor land management, i.e., overgrazing leading to the deterioration of soil chemical, physical and biological properties (Figs. 3.12 and 3.13). Missing vegetation due to overgrazing can mask the possibility of bioindication and distort results.

Need of better monitoring cold deserts in Central Asia and Russia. Estimates of the state and extent of desertification have been and are still controversial, due to the lack of common understanding of the indicators to be measured and the approaches to estimate those indicators (Enne and Zucca 2000; Sterk and Stoorvogel 2020).



Fig. 3.10 The demand for potting soils as growing media for in-door and urban greening and urban horticulture is increasing. Peat mining from peat bogs is largely meeting this demand. This is conflicting with environmental targets of peatland conservation and

climate change mitigation. Potting soils made from compost seem to be an alternative but are often polluted by plastic material and other contaminants. *Photo* L. Mueller



Fig. 3.11 Peat extraction site in Northern Germany (Diepholzer Moorniederung). Photo C. Scherber



Fig. 3.12 Examples of desertification. **a** Deforestation and overgrazing as triggering factors. The photo shows a semi-arid landscape in Northern China. The occurrence of Luvisols (associated with Regosols and Cambisols) shows that the landscape has a sub-humid history. Also, the current climate is sub-humid to semi-arid, but not desert.

Apparent desertification is man-made. **b** Desertified landscape in Eastern Kazakhstan. As vegetation is sparse due to overgrazing, wind and water cause a high dynamic of landscape features. The photo shows the inner part of an erosion gully. Photos L. Mueller

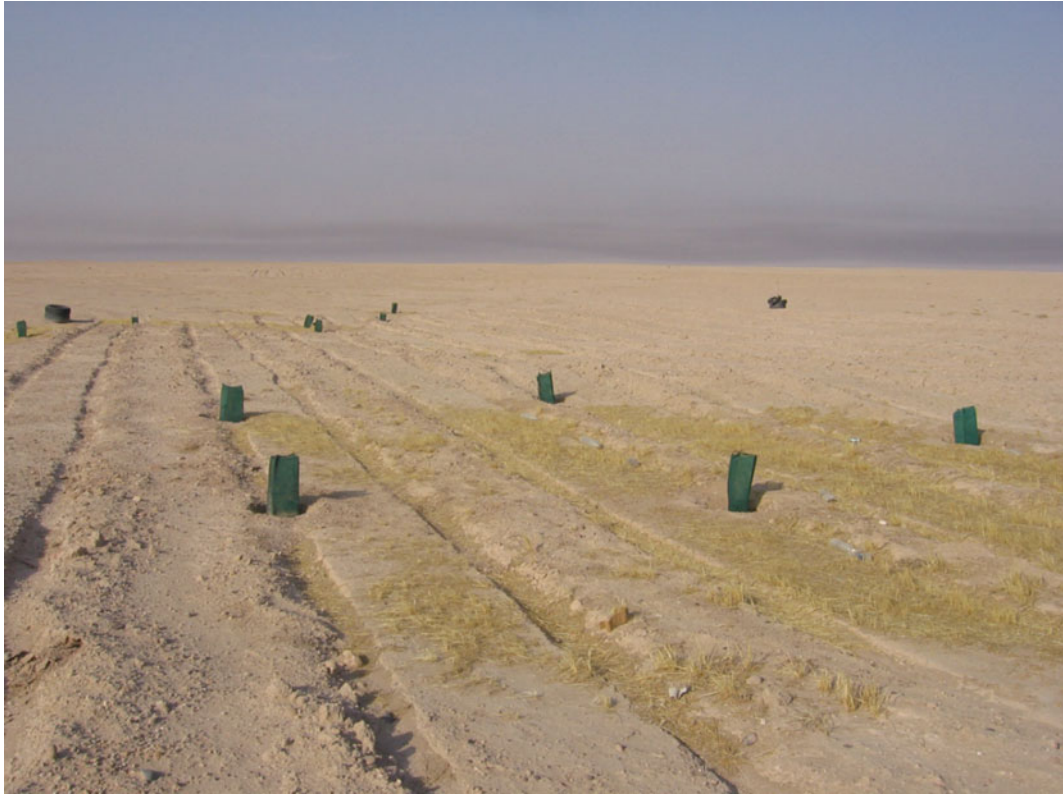


Fig. 3.13 Completely disturbed soils in the Kuwait desert. Shown are the initial stages of restoration with native vegetation. *Photo C. Scherber*

The central part of the Eurasian continent is characterized by many deserts and semi-deserts. Large parts belong to Central Asia and Russia. Drying up the Aral Sea and the formation of the Aral-Kum desert in the second half of the last century is an example of man-made desertification (Issanova and Abuduwaili 2017). Overgrazing and climate change pose a great impact on the desertification of the Central Asian drylands (Issanova and Abuduwaili 2017).

The only desert in Europe, which was formed as a result of human activities in the last century, covering about one million hectares, is located in Kalmykia, Russia (Saiko and Zonn 1997). This is a result of the uncontrolled and improper animal husbandry management initiated in the 1960s.

Meanwhile, 6.2 million hectares of agricultural land of Kalmykia are affected by various types of degradation (Dedova et al. 2020).

In Russia, for the monitoring of the state and dynamics of desertification, a system of indicators based on the combination of key indicators includes groups of geobotanical indicators, soil indicators and remote-sensing based indicators (Trofimov et al. 2015). Despite some disciplinary progress in understanding the phenomena of desertification in Russia (Schreiner and Meyer 2014; Borisov and Alekseev 2020; Novikova et al. 2020) an overall comprehensive monitoring system based on the indicator system of Trofimov et al. (2015) does not yet exist.

3.4.3 Arctic Soils

Soils of the Arctic and sub-Arctic underlay rapid transformation processes due to climate warming and permafrost thawing. Frozen soil organic matter (SOM) becomes deposited, resulting in the release of greenhouse gases (GHG) from the soil. This process is a global hotspot of SOM/SOC depletion and degradation of soil microbiota and biodiversity.

Permafrost soils of the Northern hemisphere bear around half of the global soil carbon pool and about one-fourth of this permafrost could thaw by 2100 (Davidson and Janssens 2006; Aaltonen et al. 2019).

SOM of Arctic tundra soils are in a stage of relatively early decomposition and particularly threatened (Semenchuk et al. 2019). To understand this process, different mechanical and chemical compositions of organic matter, such as particulate organic matter (POM) and clay-sized mineral-associated organic matter (MAOM) and their functional behaviour elemental, isotopic and chemical composition gain importance (Prater et al. 2020). SOM decay is associated with a certain proportion of organic nitrogen which is a potential risk for ecosystem degradation as boosting the N-cycle of these soils (Prater et al. 2020).

Many soils of the Arctic and sub-Arctic are organic (Fig. 3.14). Hugelius et al. 2020 projected that northern peatlands could shift from a current sink of atmospheric C ($0.10 \pm 0.02 \text{ Pg C}\cdot\text{y}^{-1}$) to a C source when 0.8–1.9 million km^2 of permafrost-affected peatlands will thaw. Projections of Chaudhary et al. (2020) revealed that peatlands continue to act as carbon sinks, but their capacity will be substantially reduced under a high-warming scenario after 2050.

As processes are fed back and self-reinforcing, they are not yet well understood, and projections are uncertain. For example, fires do not only boost carbon emission but change the composition of remaining carbon, mainly towards recalcitrant forms, and have implications for microbial communities and vegetation recovery (Aaltonen et al. 2019).

Increasing temperatures make relatively inaccessible C sources more available for mineralization leading to community shifts of soil microbiota (Ricketts et al. 2020). Perez-Mon et al. (2020) found different behaviour of prokaryotic communities in comparison with fungal communities regarding freeze–thaw cycles in alpine soils. Most soil microbiota community shift and their functional implications are still largely unclear.

The thawing of the permafrost constantly brings new organisms to light, e.g., Martinez et al. (2019). It could also create soils that are already biologically contaminated due to activated, previously undiscovered forms and parts of life. Some of these life forms could have the potential to destroy higher life, others could be used as agents and antagonists for new pharmaceuticals and biotechnologies (Sánchez-Otero et al. 2019). Other microbiota, plants and animals will invade the Arctic and displace current communities.

The warming Arctic increases overall pressure on soils. Arctic regions are the operational field of mining activities; thus, pollution monitoring is essential (Opekunova et al. 2020). As forestry and agriculture move northwards, monitoring herbicide degradation (Tomco et al. 2020) and many other topics of preventing soil degradation become more important for the Arctics.

3.4.4 Steppe Soils of the Eurasian Loess Belt

Soils of the Eurasian Loess belt, mainly Chernozems, Kastanozems and Phaeozems of steppes and forest-steppes, are the most fertile worldwide and have crucial importance for feeding humanity (Mueller et al. 2014c; Frühauf et al. 2020). Post World War II land reclamation in the steppes of Siberia and Kazakhstan was beneficial for food security. However, soils experienced severe degradation through erosion and humus and nutrient depletion and regionally as well salinization (Meyer et al. 1998; Schreiner and Meyer 2014; Frühauf et al. 2020; Guggenberger

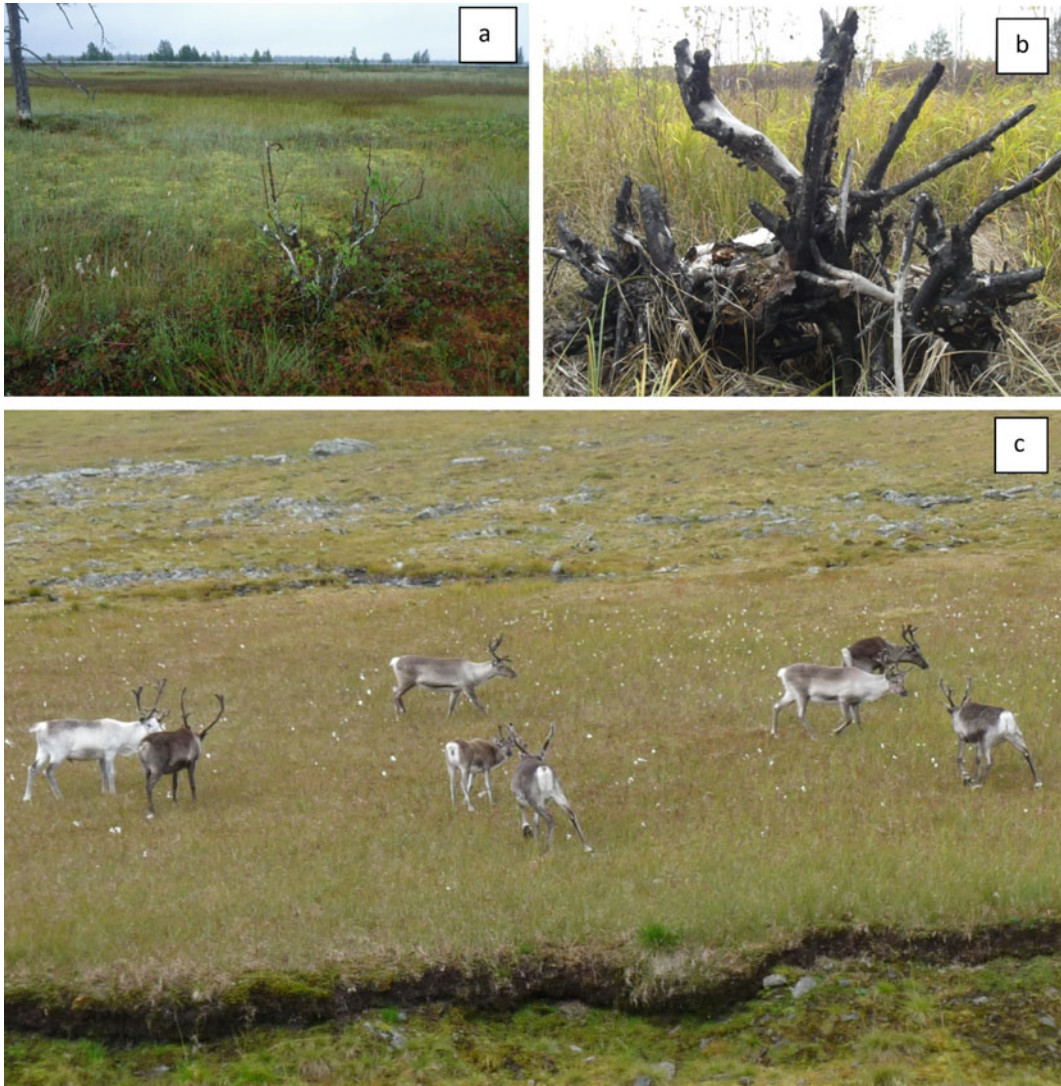


Fig. 3.14 Peatlands of the Northern Hemisphere **a, b** are facing SOM depletion processes through climate warming and fires. Thawing permafrost soils (**c**). Implications for

soil biota and biological cycles are not yet well understood. *Photos* L. Mueller

et al. 2020). It is essential to better understand the driving forces (the political, societal and technological drivers) as initials/tipping points/start or end points of change for the activity of soil degradation processes in the Loess belt (Baude et al. 2019). The same authors identified important changes during the last two centuries and degradation activity periods in soil degradation by the formulating of proxies for the performance

in natural soil production capacity and soil erosion hazards from 1750 to 2005 based on soil and landscape data and hazard modelling. The monitoring of soil degradation in the steppe regions should be embedded in a complex land degradation system understanding holding multiple indicators beyond the chemical and biological soil degradation in land degradation research (Schreiner and Meyer 2014). The time scale of

the total loss measured and modelled by meaningful indicators of soil degradation is not yet clarified appropriately by scientific methods.

Practices of sustainable intensification (SI, Pretty 2018) consisting of locally adapted conservation agriculture (Grunwald et al. 2020) are a step forward to avoid large-scale soil erosion, but cannot yet be considered as a sustainable solution for the future. Common practice is often based on large-scale spring-wheat monocultures and the application of herbicides, fungicides and pesticides. Landscape-adapted agriculture (Kiryushin 2019; Mueller et al. 2021) combined with smart locally optimized technologies (Grunwald et al. 2020), restoration of steppe in parts of the landscape (Silantjeva et al. 2020) and optimization of shelterbelts (Narozhnyaya and Chendev 2020) would be a better solution towards sustainability and multiple ecosystem services. However, there are still too many open questions and existing long-term agricultural experiments (Husniev et al. 2020; Romanenkov et al. 2020) but missing landscape experiments. Research about possible side-effects of new technologies and the complexity of soil degradation risks must play a pivotal role in those experiments.

3.5 Conclusions

1. Soils are highly dynamic and multifunctional systems of crucial importance for life on earth and the survival of humankind. Increasingly, soil degradation threatens soil's performance to meet these functions and ecosystem services.
2. Types of chemical and biological degradation of soil addressed here in particular are very complex phenomena. They are often interrelated with other types of soil degradation, such as erosion or sealing, or sometimes triggered by them.
3. Drylands and all kinds of man-made soils, in urban landscapes, in particular, are hotspots of chemical and biological degradation. Soils of high humus and carbon accumulation, such as those in the Arctics, sub-Arctics and steppes, face particular problems of biological

soil degradation with huge implications for global cycles and climate. Feature and functions of soil microbiota are not yet understood sufficiently. Thus, their performance and potential state of degradation need further attention in research.

4. Most regions of Russia and Central Asia bear those types of hotspot soils facing problems of soil as chemical and biological soil degradation are not yet understood sufficiently. Improved monitoring technologies in combination with overall soil quality assessment could help to understand and combat them better.
5. Laboratory methodologies of soil chemical and biological analyses are highly developed, and sophisticated modelling approaches are emerging. Better screening methods for field indication are desirable to avoid alienation between "laboratory/desk research" and "field research/stakeholder participation".
6. Globally, crucial topics of soil and land degradation, such as assessment of desertification and carbon sequestration potential of soil as well as the (mostly not visible) loss of belowground biodiversity, show a disconnection between science and policy. Evidence-based natural-scientific research and exactly measured data as well as the presentation of these findings in a way suitable for the respective stakeholders and the general public have to be developed. Such adapted links could help to achieve progress in understanding and combating soil degradation.

Acknowledgements Preparation of this chapter was supported by the Ministry of Education, Science and Technological Development of the Republic of Serbia (contract no. 451-03-09/2021-14/200011)

References

- Aaltonen H, Köster K, Köster E, Berninger F, Zhou X, Karhu K, Biasi C, Bruckman V, Palviainen M, Pumpanen J (2019) Forest fires in Canadian permafrost region: the combined effects of fire and

- permafrost dynamics on soil organic matter quality. *Biogeochemistry* 143:257–274. <https://doi.org/10.1007/s10533-019-00560-x>
- Abbas Q, Yousaf B, Amina Ali MU, Munir MAM, El-Naggar A, Rinklebe J, Naushad M (2020) Transformation pathways and fate of engineered nanoparticles (ENPs) in distinct interactive environmental compartments: a review. *Environ Int* 138:105646. <https://doi.org/10.1016/j.envint.2020.105646>
- Abd El-Hamid HT, Hong G (2020) Hyperspectral remote sensing for extraction of soil salinization in the northern region of Ningxia. *Model Earth Syst Environ* 6:2487–2493 (2020). <https://doi.org/10.1007/s40808-020-00829-3>
- Abdollahpour M, Rahnamaie R, Lutzenkirchen J (2020) The vulnerability of calcareous soils exposed to Mg-rich irrigation water. *Land Degrad Develop* 31(16):2295–2306. <https://doi.org/10.1002/ldr.3605>
- Adamiec E, Jarosz-Krzemińska E, Wieszała R (2016) Heavy metals from non-exhaust vehicle emissions in urban and motorway road dusts. *Environ Monitor Assessment* 188:369. <https://doi.org/10.1007/s10661-016-5377-1>
- Agapit C, Gigon A, Puga-Freitas R, Zeller B, Blouin M (2018) Plant-earthworm interactions: influence of age and proportion of casts in the soil on plant growth, morphology and nitrogen uptake. *Plant Soil* 424:49–61. <https://doi.org/10.1007/s11104-017-3544-y>
- Albanese S, De Vivo B, Lima A, Cicchella D (2007) Geochemical background and baseline values of toxic elements in stream sediments of Campania region (Italy). *J Geochem Explor* 93:21–34. <https://doi.org/10.1016/j.gexplo.2006.07.006>
- Alcamo J, Shaw R, Hordijk L (eds) (1990) The RAINS model of acidification. Science and strategies in Europe. Kluwer Academic Publishers, Dordrecht, Netherlands
- Aleksandrova ON (2018) Chapter I/34: method of epr spectroscopy with use of spin labels applied to investigation of interaction of organic xenobiotics with soil (in Russian). In: Sychev VG, Mueller L (Eds) Novel methods and results of landscape research in Europe, Central Asia and Siberia. Vol. I Landscapes in the 21th Century: Status Analyses, Basic Processes and Research Concepts. © FSBI “VNII Agrochemistry”, pp 190–194. <https://doi.org/10.25680/9569.2018.64.90.034>. <https://vniia-pr.ru/monografii/pdf/tom1-34.pdf>
- Alekseenko V, Alekseenko A (2014) The abundances of chemical elements in urban soils. *J Geochem Explor* 147:245–249. <https://doi.org/10.1016/j.gexplo.2014.08.003>
- Allbed A, Kumar L (2013) Soil salinity mapping and monitoring in arid and semi-arid regions using remote sensing technology: a review. *Adv Remote Sensing* 2:373–385
- Allison SD (2014) Modeling adaptation of carbon use efficiency in microbial communities. *Front Microbiol.* <https://doi.org/10.3389/fmicb.2014.00571>
- Anderson T (2003) Microbial eco-physiological indicators to assess soil quality. *Agr Ecosyst Environ* 98:285–293
- Anderson T-H, Domsch KH (1990) Application of eco-physiological quotients (qCO₂ and qD) on microbial biomasses from soils of different cropping histories. *Soil Biol Biochem* 22:251–255. [https://doi.org/10.1016/0038-0717\(90\)90094-G](https://doi.org/10.1016/0038-0717(90)90094-G)
- Anderson DW, Joug E, de Verity GE, Gregorich EG (1986) The effect of cultivation on the organic matter of soils of the Canada prairies. *Trans Cong Int Soc Soil Sci Hamburg* 4(9):1344–1345
- Andrews SS, Karlen DL, Cambardella CA (2004) The soil management assessment framework: a quantitative soil quality evaluation method. *SSSAJ* 68(6):1945–1962
- Andriuzzi WS, Franco ALC, Ankrom KE, Cui S, de Tomasel CM, Guan P, Gherardi LA, Sala OE, Wall DH (2020) Body size structure of soil fauna along geographic and temporal gradients of precipitation in grasslands. *Soil Biol Biochem* 140:107638. <https://doi.org/10.1016/j.soilbio.2019.107638>
- Antoniadis V, Shaheen SM, Levizou E, Shahid M, Niazi NK, Vithanage M, Ok YS, Bolan N, Rinklebe J (2019) A critical prospective analysis of the potential toxicity of trace element regulation limits in soils worldwide: are they protective concerning health risk assessment? A review. *Environ Int* 127:819–847. <https://doi.org/10.1016/j.envint.2019.03.039>
- Bach EM, Ramirez KS, Fraser TD, Wall DH (2020) Soil biodiversity integrates solutions for a sustainable future. *Sustainability* 12:2662. <https://doi.org/10.3390/su12072662>
- Bai X, Gao J, Wang S, Cai H, Chen Z, Zhou J (2020) Excessive nutrient balance surpluses in newly built solar greenhouses over five years leads to high nutrient accumulations in soil. *Agric Ecosyst Environ* 288:106717. <https://doi.org/10.1016/j.agee.2019.106717>
- Bardina TV, Kulibaba VV, Bardina VI (2018) Chapter II/30: ecotoxicity assessment of soils in industrial areas by phyto-tests (in Russian). In: Sychev VG, Mueller L (eds) Novel methods and results of landscape research in Europe, Central Asia and Siberia, vol II understanding and monitoring processes in soils and water bodies. © FSBI “VNII Agrochemistry” 2018, pp 145–149. <https://doi.org/10.25680/4700.2018.64.90.127>. <https://vniia-pr.ru/monografii/pdf/tom2-30.pdf>

- Bar-On YM, Phillips R, Milo R (2018) The biomass distribution on Earth. *PNAS* 115(25):6506–6511. <https://doi.org/10.1073/pnas.1711842115>
- Bartels D, Sunkar R (2005) Drought and salt tolerance in plants. *Crit Rev Plant Sci* 24:23–58
- Bastida F, Moreno JL, Hernández T, García C (2006) Microbiological degradation index of soils in a semiarid climate. *Soil Biol Biochem* 38(2006):3463–3473
- Bastida FZA, Hernández H, García C (2008) Past, present and future of soil quality indices: a biological perspective. *Geoderma* 147:159–171
- Bateman AM, Muñoz-Rojas M (2019) Chapter one - to whom the burden of soil degradation and management concerns. *Environ Manage Protect* 4(2019):1–22. <https://doi.org/10.1016/bs.apmp.2019.07.001>
- Baude M, Meyer BC, Schindewolf M (2019) Land use change in an agricultural landscape causing degradation of soil based ecosystem services. *Sci Total Environ* 659:1526–1536. <https://doi.org/10.1016/j.scitotenv.2018.12.455>
- Baveye PC, Schnee LS, Boivin P, Laba M, Radulovich R (2020) Soil organic matter research and climate change: merely re-storing carbon versus restoring soil functions. *Front Environ Sci*. <https://doi.org/10.3389/fenvs.2020.579904>
- Bazilevich NI, Pankova EI (1972) The experience of soil classification according to the content of toxic salts and ions. *Bull Dokuchaev Soil Res Inst* 6:63–740 (in Russian; Опыт классификации почв по содержанию токсичных солей и ионов. Бюл. Почв. ин-та им. В.В. Докучаева.)
- Bazilevich NI, Rodin LE, Rozov NN (1970) Geographical aspects of the study of biological productivity. In: *Proceedings of the V congress of the geographical society of the USSR*. Leningrad 1970, 27 pp. (In Russian: Н. И. Базилевич, Л. Е. Родин, Н. Н. Розов. - Ленинград : [б. и.], Географические аспекты изучения биологической продуктивности. Материалы V съезда географического общества СССР. Ленинград 1970. - 27 с.)
- Bazrafshan A, Shorafa M, Mohammadi MH, Zolfaghari AA, van de Craats D, van der Zee Seatm (2020) Comparison of the individual salinity and water deficit stress using water use, yield, and plant parameters in maize. *Environ Monit Assess* 192:448. <https://doi.org/10.1007/s10661-020-08423-x>
- Behrendt U, Kämpfer P, Glaeser SP, Augustin J, Ulrich A (2016) Characterisation of the N₂O producing soil bacterium *Rhizobium azooxidifex* sp. nov. *Int J Syst Evol Microbiol* 66(6):2354–2361
- Beškoski VP, Gojčić-Cvijović G, Jovančičević B, Vrvčić MM (2012) Gas chromatography in environmental sciences and evaluation of bioremediation. In: Salih B (Ed.) *gas chromatography—biochemicals, narcotics and essential oils*. InTech open, ISBN: 978–953–51–0295–3. Available from: <https://www.intechopen.com/books/gas-chromatography-biochemicals-narcotics-and-essential-oils/gas-chromatography-in-environmental-sciences-and-evaluation-of-bioremediation>. Accessed on 12 Sept 2020
- Blagodatskaya EV, Bogomolova IN, Blagodatsky SA (2001) Changing the environmental strategy of the soil microbial community initiated by glucose. *Pochvovedenie* 5:700–708 (in Russian: Изменение экологической стратегии микробного сообщества почвы, инициированной внесением глюкозы. Почвоведение 5:700–708).
- Blake L, Goulding K (2002) Effects of atmospheric deposition, soil pH and acidification on heavy metal contents in soils and vegetation of semi-natural ecosystems at Rothamsted Experimental Station, UK. *Plant Soil* 240:235–251. <https://doi.org/10.1023/A:1015731530498>
- Blankinship JC, Niklaus PA, Hungate BA (2011) A meta-analysis of responses of soil biota to global change. *Oecologia* 165(3):553–565. <https://doi.org/10.1007/s00442-011-1909-0>
- Bloem E, van der Zee Seatm, Tóth T, Hagyo A (2012) Soil salinisation. In: van Beek C, Tóth G (eds) *Risk assessment methodologies of soil threats in Europe*. pp 28–39. Status and options for harmonization for risks by erosion, compaction, salinization, organic matter decline and landslides—JRC Report EUR 24097 EN 2012, 84 pp. <https://doi.org/10.2788/47096>. https://esdac.jrc.ec.europa.eu/ESDB_Archive/eusoils_docs/other/EUR24097.pdf. Accessed on 28 Nov 2020
- Blum WEH (2013) Soil and land resources for agricultural production: general trends and future scenarios—a world-wide perspective. *Int Soil Water Conserv Res* 1(3):1–14. [https://doi.org/10.1016/S2095-6339\(15\)30026-5](https://doi.org/10.1016/S2095-6339(15)30026-5)
- AG Boden (2005) *Bodenkundliche Kartieranleitung (KA5)*, 5th edn. Hannover, 432 pp
- Bolan NS, Duraisamy VP (2003) Role of inorganic and organic soil amendments on immobilization and phytoavailability of heavy metals: a review involving specific case studies. *Aust J Soil Res* 41:533–535
- Bolan NS, Adriano DC, Curtin D (2003) Soil acidification and liming interactions with nutrient and heavy metal transformation and bioavailability. *Adv Agron* 78:215–272
- Bolt GH, Bruggenwert MGM (1976) *Soil chemistry*. Part A: basic elements. Elsevier Amsterdam, New York, p 271
- Bonfante A, Basile A, Acutis M, De Mascellis R, Manna P, Perego A, Terribile F (2010) SWAP, CropSyst and MACRO comparison in two contrasting soils cropped with maize in northern Italy. *Agric Water Manage* 97:1051–1062. <https://doi.org/10.1016/j.agwat.2010.02.010>
- Bonten LTC, Reinds GJ, Posch M (2016) A model to calculate effects of atmospheric deposition on soil acidification, eutrophication and carbon sequestration. *Environ Model Softw* 79(2016):75–84. <https://doi.org/10.1016/j.envsoft.2016.01.009>
- Borisov AV, Alekseev AO (2020) Timing and causes of the origin of the solonetz process in the

- desert–steppe soils of the southeastern russian plain. *Arid Ecosyst* 10:27–35. <https://doi.org/10.1134/S2079096120010023>
- Bowman WD, Cleveland CC, Halada L, Hresko J, Baron JS (2008) Negative impact of nitrogen deposition on soil buffering capacity. *Nat Geosci* 1:767–770
- Bradford MA, Fierer N (2012) Chapter 3.5 The biogeography of microbial communities and ecosystem processes: Implications for soil and ecosystem models. In: Wall DH, Bardgett RD, Behan-Pelletier V, Herrick JE, Jones TH, Ritz K, Six J, Strong DR, van der Putten WH (eds) *Soil ecology and ecosystem services*. Oxford Univ. Press, Oxford, U.K, pp 189–200, 424 pp. ISBN: 9780199575923
- Briones MJ (2018) The serendipitous value of soil fauna in ecosystem functioning: the unexplained explained. *Front Environ Sci*. <https://doi.org/10.3389/fenvs.2018.00149> Corpus ID: 54447820
- Brock C, Franko U, Oberholzer H-R, Kuka K, Leithold G, Kolbe H, Reinhold J (2013) Humus balancing in Central Europe—concepts, state of the art, and further challenges. *J Plant Nutr Soil Sci* 176(1):3–11. <https://doi.org/10.1002/jpln.201200137>
- Brookes PC, Powlson DS, Jenkinson DS (1982) Measurement of microbial biomass phosphorus in soil. *Soil Biol Biochem* 14:319–329. [https://doi.org/10.1016/0038-0717\(82\)90001-3](https://doi.org/10.1016/0038-0717(82)90001-3)
- Bünemann EK, Schwenke GD, Van Zwieten L (2006) Impact of agricultural inputs on soil organisms: a review. *Aust J Soil Res* 44(4):379–406. <https://doi.org/10.1071/SR05125>
- Bünemann EK, Bongiorno G, Bai Zh, Creamer RE, De Deyn G, de Goede R, Fleskens L, Geissen V, Kuyper TW, Mäder P, Pulleman M, Sukkel W, van Groenigen JW, Brussaard L (2018) Soil quality: a critical review. *Soil Biol Biochem* 120:105–125. <https://doi.org/10.1016/j.soilbio.2018.01.030>
- Cajaiba RL, Perico E, da Silva WB, Caron E, Buss BC, Dalzochio M, Santos M (2019) Are primary forest irreplaceable for sustaining Neotropical landscapes' biodiversity and functioning? Contributions for restoration using ecological indicators. *Land Degrad Develop* 31(4):508–517. <https://doi.org/10.1002/ldr.3467>
- Čakmak D, Perovic V, Kresovic M, Jaramaz D, Mrvic V, Belanovic Simic S, Saljnikov E, Trivan G (2018) Spatial distribution of soil pollutants in urban green areas (a case study in Belgrade). *J Geochem Explor* 188:308–317
- Čakmak D, Perović V, Kresović M, Pavlović DS, Pavlović MD, Mitrović M, Pavlović PV (2020) Sources and a health risk assessment of potentially toxic elements in dust at children's playgrounds with artificial surfaces: a case study in Belgrade. *Arch Environ Contam Toxicol* 1–16
- Canedoli C, Ferrè C, El Khair DA, Padoa-Schioppa E, Comolli R (2020) Soil organic carbon stock in different urban land uses: high stock evidence in urban parks. *Urban Ecosyst* 23:159–171. <https://doi.org/10.1007/s11252-019-00901-6>
- Cardoso EJBN, Vasconcellos RLF, Bini D, Miyauchi MYH, dos Santos CA, Alves PRL, de Paula AM, Nakatani AS, Pereira JdM, Nogueira MA (2013) Soil health: looking for suitable indicators. What should be considered to assess the effects of use and management on soil health? *Scientia Agricola* 70(4):274–289. <https://doi.org/10.1590/S0103-90162013000400009>
- Carpenter SR (2005) Eutrophication of aquatic ecosystems: bistability and soil phosphorus. *PNAS* 102(29):10002–10005. <https://doi.org/10.1073/pnas.0503959102>
- Carvalho LG, Biesmeijer JC, Franzén M, Aguirre-Gutiérrez J, Garibaldi LA, Helm A, Michez D, Pöyry J, Reemer M, Schweiger O, van den Michiel BL, DeVries FW, Kunin WE (2020) Soil eutrophication shaped the composition of pollinator assemblages during the past century. *Ecography* 43(2):209–221. <https://doi.org/10.1111/ecog.04656>
- Castro I (2000) Exotoxicological effects of heavy metals in the biological fixing of nitrogen in industrially contaminated soils. *Silva-Lusitana* 8(2):165–194
- Chaer G, Fernandes M, Myrold D, Bottomley P (2009) Comparative resistance and resilience of soil microbial communities and enzyme activities in adjacent native forest and agricultural soils. *Microb Ecol* 58(2):414–424
- Chappel A, NP, Leys JF, Waters CM, Orgill S, Eyres MJ (2019) Minimizing soil organic carbon erosion by wind is critical for land degradation neutrality. *Environ Sci Policy* 93:43–52. <https://doi.org/10.1016/j.envsci.2018.12.020>
- Chaudhary N, Westermann S, Lamba S, Shurpali N, Britta A, Sannel K, Schurgers G, Miller PA, Smith B (2020) Modelling past and future peatland carbon dynamics across the pan-Arctic. *Global Change Biol* 26(7):4119–4133. <https://doi.org/10.1111/gcb.15099>
- Chen D, Xue M, Duan X, Feng D, Huang Y, Rong L (2019) Changes in topsoil organic carbon from 1986 to 2010 in a mountainous plateau region in southwest China. *Land Degrad Develop* 31(6):734–747. <https://doi.org/10.1002/ldr.3487>
- Chen W, Zhou H, Wu Y, Wang J, Zhao Z, Li Y, Qiao L, Chen K, Liu G, Xue S (2020a) Direct and indirect influences of long-term fertilization on microbial carbon and nitrogen cycles in an alpine grassland. *Soil Biol Biochem* 149:107922. <https://doi.org/10.1016/j.soilbio.2020.107922>
- Chen XD, Dunfield KE, Fraser TD, Wakelin SA, Richardson AE, Condron LM (2020b) Soil biodiversity and biogeochemical function in managed ecosystems. *Soil Res* 58:1–20. <https://doi.org/10.1071/SR19067>
- Chen Q-L, Ding J, Zhu D, Hu H-W, Delgado-Baquerizo M, Ma Y-B, He J-Z, Zhu Y-G (2020c) Rare microbial taxa as the major drivers of ecosystem multifunctionality in long-term fertilized soils. *Soil Biol Biochem*

- 141:107686. <https://doi.org/10.1016/j.soilbio.2019.107686>
- Chernenok V, Barkusky D (2014) Diagnosis and optimization of phosphorus nutrition conditions of grain crops in Northern Kazakhstan. In: Mueller L, Saparov A, Lischeid G (eds) Novel measurement and assessment tools for monitoring and management of land and water resources in agricultural landscapes of Central Asia. Environmental science and engineering. Springer, Cham. https://doi.org/10.1007/978-3-319-01017-5_43
- Chigira M, Oyama T (2000) Mechanism and effect of chemical weathering of sedimentary rocks. In: Kanaori Y, Tanaka K, Masahiro C (eds) Engineering geological advances in Japan for the new millennium, developments in geotechnical engineering, vol 84. Elsevier, pp 267–278
- Chorus I, Bartram J (eds) (1999) Toxic cyanobacteria in water: a guide to their public health consequences, monitoring and management. World Health Organization. ISBN 0-419-23930-8 https://www.who.int/water_sanitation_health/resourcesquality/toxycyanobegin.pdf. Accessed on 12 Sept 2020
- Churkina GN, Rukavitsina IV, Kunanbayev KK, Yerpasheva D (2018) Chapter IV/45: Influence of long-term application of mineral fertilizers on the fungistasis of Southern Chernozems in the system of landscape adapted agriculture. In: Sychev VG, Mueller L (Eds) Novel methods and results of landscape research in Europe, Central Asia and Siberia, vol IV optimising agricultural landscapes. © FSBI “VNI Agrochemistry”, pp. 220–224. <https://doi.org/10.25680/5398.2018.72.20.310>. <https://vniia-pr.ru/monografii/pdf/tom4-45.pdf>
- Coleman DC (2011) Understanding soil processes: one of the last frontiers in biological and ecological research. *Australas Plant Pathol* 40:207–214
- Cortet J, Gillon D, Joffre R, Ourcival J-M, Poinso-Balanguier N (2002) Effects of pesticides on organic matter recycling and microarthropods in a maize field: use and discussion of the litterbag methodology. *Eur J Soil Biol* 38:261–265
- Crawley MJ, Johnston AE, Silvertown J, Dodd M, de Mazancourt C, Heard MS, Henman DF, Edwards GR (2005) Determinants of species richness in the Park Grass Experiment. *Am Nat* 165:179–192
- Cuevas J, Daliakopoulos IN, del Moral F, Hueso JJ, Tsanis IK (2019) A review of soil-improving cropping systems for soil salinization. *Agronomy* 9(6):295
- Van Dam JC, Huygen J, Wesseling JG, Feddes RA, Kabat P, van Walsum PEV, Groenendijk P, van Diepen CA (1997) Theory of SWAP Version 2.0 DLO Winand Staring Centre, Wageningen, Netherlands. <https://www.wur.nl/en/Publication-details.htm?publicationId=publication-way-333036363431>. Accessed on 12 Sept 2020
- Daniel TC, Sharpley AN, Lemunyon J L (1998) Agricultural phosphorus and eutrophication: a symposium overview. *J Environ Qual* 27(2):251–257. <https://doi.org/10.2134/jeq1998.00472425002700020002x>
- Danilova N, Galitskaya P, Selivanovskaya S (2020) Veterinary antibiotic oxytetracycline’s effect on the soil microbial community. *J Ecol Environ* 44:10. <https://doi.org/10.1186/s41610-020-00154-x>
- Davidson EA, Janssens IA (2006) Temperature sensitivity of soil carbon decomposition and feedbacks to climate change. *Nature* 440:165–173. <https://doi.org/10.1038/nature04514>
- Davidson CM (2013) Methods for the determination of heavy metals and metalloids in soils. In: Alloway B (eds) Heavy metals in soils. *Environ Pollut* 22. Springer, Dordrecht. https://doi.org/10.1007/978-94-007-4470-7_4
- De Vries W, Breeuwsma A (1987) The relation between soil acidification and element cycling. *Water Air Soil Pollut* 35(1987):293–310
- De Vries W, McLaughlin MJ (2013) Modeling the cadmium balance in Australian agricultural systems in view of potential impacts on food and water quality. *Sci Total Environ* 461:240–257
- Dedova EB, Goldvarg BA, Tsagan-Mandzhiev NL (2020) Land degradation of the republic of kalmykia: problems and reclamation methods. *Arid Ecosyst* 10:140–147. <https://doi.org/10.1134/S2079096120020043>
- Delgado-Baquerizo M, Doulier G, Eldridge DJ et al. (2019) Increases in aridity lead to drastic shifts in the assembly of dryland complex microbial networks. *Land Degrad Develop* 31(3):346–355
- Derbentseva AM, Stepanova AI, Krupskaya LT (2005) Chemical degradation of soils as affected by technogenic geochemical flows. In: Zorin AA, Kirillova AA, Krupskaya LT, Saksin BG, Derbentseva AM (eds) (In Russian: Химическая деградация почв под воздействием техногенных геохимических потоков)
- Derevyagin SS (2018) Chapter II/43: results of long-term monitoring of heavy metals in landscapes of the saratov region (In Russian). In: Sychev VG, Mueller L (Eds) Novel methods and results of landscape research in Europe, Central Asia and Siberia, vol II understanding and monitoring processes in soils and water bodies. © FSBI “VNI Agrochemistry”, pp 202–206. <https://doi.org/10.25680/5811.2018.84.19.140>. <https://vniia-pr.ru/monografii/pdf/tom2-43.pdf>
- Diekmann M, Dupré C (1997) Acidification and eutrophication of deciduous forests in northwestern Germany demonstrated by indicator species analysis. 8(6):855–864. <https://doi.org/10.2307/3237030>
- Diestel H, Zenker T, Schwartengraeber R, Schmidt M (2007) The lysimeter station at Berlin-Dahlem. In: Kersebaum KC, Hecker J-M, Mirschel W, Wegehenkel M (eds) Modelling water and nutrient dynamics in soil-crop systems: proceedings of the workshop on “Modelling water and nutrient dynamics in soil-crop systems” held on 14–16 June 2004 in Münchenberg, Germany. Dordrecht (Springer), pp 259–266
- Ding Y, Xia G, Ji H, Xiong X (2019) Accurate quantitative determination of heavy metals in oily soil by laser induced breakdown spectroscopy (LIBS) combined with interval partial least squares (IPLS).

- Anal Methods 11:3657–3664. <https://doi.org/10.1039/C9AY01030K>
- Dobrovolskiy GV, Kust GS, Sanaev VG (eds) (2012) Soils in biosphere and life of human. Monograph, Moscow, Publishing house of the Moscow State Forest University, 584 pp (In Russian: Г.В. Добровольский, Г.С. Куст, Санаев В.Г. Почвы в биосфере и жизни человека. Монография Москва. Издательство Московского государственного университета леса. 2012, 584 с)
- Donkova R, Kaloyanova N (2008) The impact of soil pollutants on soil microbial activity. In: Simeonov L, Sargsyan V (eds) Soil chemical pollution, risk assessment, remediation and security. NATO Science for Peace and Security Series. Springer, Dordrecht. https://doi.org/10.1007/978-1-4020-8257-3_6
- Dregne HE (1977) Desertification of arid lands. *J Econ Geogr* 53(4):322–331. The Human Face of Desertification
- Dregne HE (1986) Desertification of arid lands. In: El-Baz F, Hassan MHA (eds) Physics of desertification. Springer, Dordrecht
- Dubey R, Gupta DK, Sharma GK (2020) Chemical stress on plants. In: Rakshit A, Singh H, Singh A, Singh U, Fraceto L (eds) New frontiers in stress management for durable agriculture. Springer, Singapore. https://doi.org/10.1007/978-981-15-1322-0_7
- Dungait JAJ, Hopkins DW, Gregory AS, Whitmore AP (2012) Soil organic matter turnover is governed by accessibility not recalcitrance. *Glob Change Biol* 18:1781–1796. <https://doi.org/10.1111/j.1365-2486.2012.02665.x>
- East JL, Wilcut C, Pease AA (2017) Aquatic food-web structure along a salinized dryland river. *Freshw Biol* 62(4):681–694
- Egorov VV, Ivanova EN, Fridland VM (1977) Classification and Diagnosis of the soils of USSR. Moscow, Kolos pp 224 (In Russian: Классификация и диагностика почв СССР. М.: Колос, 1977. 224 с.)
- Elbana T, Gaber HM, Kishk FM (2019) Soil chemical pollution and sustainable agriculture. In: El-Ramady H, Alshaal T, Bakr N, Elbana T, Mohamed E, Belal AA (eds) The soils of Egypt. World Soils Book Series. Springer, Cham. https://doi.org/10.1007/978-3-319-95516-2_11
- Ellenberg H, Weber HE, Duell R, Wirth V, Werner W, Paulissen D (2001) Zeigerwerte von Pflanzen in Mitteleuropa: indicator values of plants in Central Europe. *Scripta Geobotanica* 18, Goettingen: Goltze, 3. ed., 262 p
- Endo S, Kimura S, Takatsuji T, Nanasawa K, Imanaka T, Shizuma K (2012) Measurement of soil contamination by radionuclides due to the Fukushima Dai-ichi Nuclear Power Plant accident and associated estimated cumulative external dose estimation. *J Environ Radioact* 111:18–27. <https://doi.org/10.1016/j.jenvrad.2011.11.006>
- Enne G, Zucca C (2000) Desertification indicators for the European Mediterranean region: state of the art and possible methodological approaches [= Indicatori di desertificazione per il Mediterraneo europeo: stato dell'arte e proposte di metodo]. http://eprints.uniss.it/3166/1/Enne_G_Libro_2000_Desertification.pdf
- Eswaran H, Lal R, Reich PF (2001) Land degradation: an overview. In: Bridges EM, Hannam ID, Oldeman LR, Pening de Vries FWT, Scherr SJ, Sompatpanit S (eds) Responses to land degradation. Proceedings of the 2nd international conference on land degradation and desertification, Khon Kaen, Thailand. Oxford Press, New Delhi, India
- Eugenio NR, Naidu R, Colombo CM (2020) Global approaches to assessing, monitoring, mapping, and remediating soil pollution. *Environ Monit Assess* 192:601. <https://doi.org/10.1007/s10661-020-08537-2>
- Eulenstein F, Saparov A, Lukin S, Sheudshen AK, Mayer WH, Dannowski R, Tauschke M, Rukhovich OV, Lana M, Schindler R, Pachikin K, Drechsler H, Cremer N (2016) Assessing and controlling land use impacts on groundwater quality. In: Mueller L, Sheudshen A, Eulenstein F (eds) Novel methods for monitoring and managing land and water resources in Siberia. Springer Water. Springer, Cham, pp 635–666. https://doi.org/10.1007/978-3-319-24409-9_29
- Fang Y, Yabusaki SB, Ahkami AH, Chen X, Scheibe TD (2019) An efficient three-dimensional rhizosphere modeling capability to study the effect of root system architecture on soil water and reactive transport. *Plant Soil* 441:33–48. <https://doi.org/10.1007/s11104-019-04068-z>
- Fang Z, Gao Y, Wu X, Xu X, Sarmah AK, Bolan N, Gao B, Shaheen SM, Rinklebe J, Ok YS, Xu S, Wang H (2020) A critical review on remediation of bisphenol S (BPS) contaminated water: efficacy and mechanisms. *Crit Rev Environ Sci Technol* 50(5):476–522. <https://doi.org/10.1080/10643389.2019.1629802>
- FAO and ITPS (2015) Status of the World's Soil Resources (SWSR)—main report. Rome, Italy, Food and Agriculture Organization of the United Nations and Intergovernmental Technical Panel on Soils, 607 pp. <http://www.fao.org/3/a-i5199e.pdf>. Accessed on 12 Sept 2020
- FAO (2019) The state of the world's biodiversity for food and agriculture. In: Belanger J, Pilling D (eds) FAO commission on genetic resources for food and agriculture assessment. Rome 572 pp. <http://www.fao.org/3/CA3129EN/CA3129EN.pdf>
- Fei J, Ma J, Yang J, Liang Y, Ke Y, Yao L, Li Y, Liu D, Min X (2020) Effect of simulated acid rain on stability of arsenic calcium residue in residue field. *Environ Geochem Health* 42:769–780. <https://doi.org/10.1007/s10653-019-00273-y>
- Feng Q, An C, Chen Z, Wang Z (2020) Can deep tillage enhance carbon sequestration in soils? A meta-analysis towards GHG mitigation and sustainable agricultural management. *Renew Sustain Energy Rev* 133: 110293. <https://doi.org/10.1016/j.rser.2020.110293>
- Fernandez JM, Plaza C, Garcia-Gil JC (2009) Biochemical properties and barley yield in a semiarid

- Mediterranean soil amended with two kinds of sewage sludge. *Appl Soil Ecol* 42(1):8–24
- Ferreira CSS, Walsh RPD, Ferreira AJD (2018) Degradation in urban areas. *Curr Opin Environ Sci Health* 5:19–25
- Fesenko SV, Alexakhin RM, Balonov MI, Bogdevitch IM, Howard BJ, Kashparov VA, Sanzharova NI, Panov AV, Voigt G, Zhuchenka YM (2007) An extended critical review of twenty years of counter-measures used in agriculture after the Chernobyl accident. *Sci Total Environ* 383(1):1–24. <https://doi.org/10.1016/j.scitotenv.2007.05.011>
- Filipović L, Romić M, Sikora S, Huić Babić K, Filipović V, Gerke HH, Romić D (2020) Response of soil dehydrogenase activity to salinity and cadmium species. *J Soil Sci Plant Nutr* 20(2):530–536. <https://doi.org/10.1007/s42729-019-00140-w>
- Foley JA, Ramankutty N, Brauman KA, Cassidy ES, Gerber JS, Johnston M, Mueller ND, O'Connell C, Ray DK, West PC, Balzer C, Bennett EM, Carpenter SR, Hill J, Monfreda C, Polasky S, Rockström J, Sheehan J, Siebert S, Tilman D, Zaks DPM (2011) Solutions for a cultivated planet. *Nature* 478:337–342. <https://doi.org/10.1038/nature10452>
- Forbes VE, Agatz A, Ashauer R, Butt RK, Capowicz Y, Duquesne S, Ernst G, Focks A, Gergs AE, Hodson M et al. (2020) Mechanistic effect modeling of earthworms in the context of pesticide risk assessment. Synthesis of the FORESEE Workshop. <https://doi.org/10.1002/ieam.4338>
- Franko U (1997) Modellierung des Umsatzes der organischen Bodensubstanz. *Arch Acker- Pfl Bodenk* 41:527–547
- Franko U, Witing F (2020) Dynamics of Soil Organic Matter in Agricultural Landscapes. In: Mirschel W, Terleev V, Wenkel KO (eds) *Landscape modelling and decision support*. Innovations in landscape research. Springer, Cham. https://doi.org/10.1007/978-3-030-37421-1_14
- Frühauf M, Schmidt G, Illiger P, Meinel T (2020) Types, occurrence and tendencies of soil degradation in the Altai Krai and the KULUNDA research region. In: Frühauf M, Guggenberger G, Meinel T, Theesfeld I, Lentz S (eds) *KULUNDA: climate smart agriculture*. Innovations in landscape research. Springer, Cham. https://doi.org/10.1007/978-3-030-15927-6_14
- Fry EL, De Long JR, Álvarez Garrido L, Alvarez N, Carrillo Y, Castañeda-Gómez L, Chomel M, Dondini M, Drake JE, Hasegawa S, Hortal S, Jackson BG, Jiang M, Lavalley JM, Medlyn BE, Rhymes J, Singh BK, Smith P, Anderson IC, Bardgett RD, Baggs EM, Johnson D. (2019) Using plant, microbe, and soil fauna traits to improve the predictive power of biogeochemical models. *Methods Ecol Evol* 10(1):146–157. <https://doi.org/10.1111/2041-210X.13092>
- Fujii K (2014) Soil acidification and adaptations of plants and microorganisms in Bornean tropical forests. *Ecol Res* 29:371–381. <https://esj-journals.onlinelibrary.wiley.com/https://doi.org/10.1007/s11284-014-1144-3>
- Funakawa S, Suzuki R, Karbozova E, Kosaki T, Ishida N (2000) Salt-affected soils under rice-based irrigation agriculture in southern Kazakhstan. *Geoderma* 97:61–85
- Gad A (2020) Qualitative and quantitative assessment of land degradation and desertification in Egypt based on satellite remote sensing: urbanization, salinization and wind erosion. In: Elbeih S, Negm A, Kostianoy A (eds) *Environmental remote sensing in Egypt*. Springer geophysics. Springer, Cham. https://doi.org/10.1007/978-3-030-39593-3_15
- Galitskova YM, Murzayeva AI (2016) Urban soil contamination. *Procedia Eng* 153:162–166. <https://doi.org/10.1016/j.proeng.2016.08.097>
- Gaudig G, Tanneberger F (2019) Peatland science and conservation: contributions of the greifswald Mire Centre, Germany. In: Mueller L, Eulenstein F (eds) *Current trends in landscape research. Innovations in landscape research*. Springer, Cham. https://doi.org/10.1007/978-3-030-30069-2_28
- Gelius-Dietrich G, Amer Desouki A, Fritzeimer CJ, Lercher MJ (2013) sybil—efficient constraint-based modelling in R. *BMC Syst Biol* 7(1):125. <https://doi.org/10.1186/1752-0509-7-125>
- Geng N, Wu Y, Zhang M, Tsang DCW, Rinklebe J, Xia Y, Lu D, Zhu L, Palansooriya KN, Kim K-H, Ok YS (2019) Bioaccumulation of potentially toxic elements by submerged plants and biofilms: a critical review. *Environ Int* 131:105015. <https://doi.org/10.1016/j.envint.2019.105015>
- Gerasimova MI, Bezuglova O (2019) Functional-environmental and properties-oriented approaches in classifying urban soils (In Memoriam Marina Stroganova). In: Vasenev II et al. (eds) *Urbanization: challenge and opportunity for soil functions and ecosystem services*. Proceedings of the 9th SUITMA Congress, January 2019. Springer series Geography, pp 4–10. https://doi.org/10.1007/978-3-319-89602-1_2
- Gevorgyan A, Bushell ME, Avignone-Rossa C, Kierzek AM (2011) SurreyFBA: a command line tool and graphics user interface for constraint-based modeling of genome-scale metabolic reaction networks. *Bioinformatics* 27(3): 433–434. <https://doi.org/10.1093/bioinformatics/btq679>
- Godbersen L., Utermann J., Duijnsveld W.H.M. (2014) Methods in the exploratory risk assessment of trace elements in the soil-groundwater pathway. In: Mueller L, Saporov A, Lischied G (eds) *Novel measurement and assessment tools for monitoring and management of land and water resources in agricultural landscapes of Central Asia*. Environmental science and engineering. Springer, Cham. https://doi.org/10.1007/978-3-319-01017-5_17
- Gregorich EG, Carter MR, Angers DA, Monreal CM, Ellert BH (1994) Towards a minimum data set to assess soil organic matter quality in agricultural soils. *Can J Soil Sci* 74(4):367–385. <https://doi.org/10.4141/cjss94-051>
- Griffiths BS, Ritz K, Bardgett RD, Cook R, Christensen S, Ekelund F, Sorensen SJ, Bååth E, Bloem J, de Ruiter PC, Dolfing J, Nicolardot B (2000) Ecosystem

- response of pasture soil communities to fumigation-induced microbial diversity reductions: an examination of the biodiversity–ecosystem function relationship. *Oikos* 90(2):279–294
- Griffiths BS, Römbke J, Schmelz R, Jänsch S, Faber J, Bloem J, Peres G, Cluzeau D, Stone D (2016) Selecting cost effective and policy-relevant biological indicators for European monitoring of soil biodiversity and ecosystem function (EcoFINDERS). *Ecol Ind* 69:213–223
- Griffiths BS, de Groot GA, Laros I, Stone D, Geisen S (2018) The need for standardisation: exemplified by a description of the diversity, community structure and ecological indices of soil nematodes. *Ecol Ind* 87:43–46. <https://doi.org/10.1016/j.ecolind.2017.12.002>
- Groh J, Diamantopoulos E, Duan X, Ewert F, Herbst M, Holbak M, Kamali B, Kersebaum K-C, Kuhnert M, Lischeid G, Nendel C, Priesack E, Steidl J, Sommer M, Pütz T, Vereecken H, Wallor E, Weber TKD, Wegehenkel M, Weihermüller L, Gerke HH (2020) Crop growth and soil water fluxes at erosion-affected arable sites: using weighing lysimeter data for model inter-comparison. *Vadose Zone J* 19(12020):e20058. <https://doi.org/10.1002/vzj2.20058>
- Gros P, Meissner R, Wirth MA, Kanwischer M, Rupp H, Schulz-Bull DR, Leinweber P (2020) Leaching and degradation of 13C2-15N-glyphosate in field lysimeters. *Environ Monit Assess* 192:127. <https://doi.org/10.1007/s10661-019-8045-4>
- Grunwald LC, Belyaev VI, Meinel T (2020) Improving efficiency of crop protection measures. A technical contribution for better weed control, less pesticide use and decreasing soil tillage intensity in dry farming regions exposed to wind erosion. In: Fröhauß M, Guggenberger G, Meinel T, Theesfeld I, Lentz S (eds) KULUNDA: climate smart agriculture. Innovations in landscape research. Springer, Cham. https://doi.org/10.1007/978-3-030-15927-6_28
- Gruszecka-Kosowska A, Baran A, Wdowin M, Mazur-Kajta K, Czech T (2020) The contents of the potentially harmful elements in the arable soils of southern Poland, with the assessment of ecological and health risks: a case study. *Environ Geochem Health* 42:419–442. <https://doi.org/10.1007/s10653-019-00372-w>
- Gubler A, Wächter D, Schwab P, Müller M, Keller A (2019). Twenty-five years of observations of soil organic carbon in Swiss croplands showing stability overall but with some divergent trends. *Environ Monitor Assess* 191 (5):277. <https://doi.org/10.1007/s10661-019-7435-y>
- Guerra CA, Rosa IMD, Valentini E et al (2020) Global vulnerability of soil ecosystems to erosion. *Landscape Ecol*. <https://doi.org/10.1007/s10980-020-00984-z>
- Guggenberger G, Bischoff N, Shibistova O, Müller C, Rolinski S, Puzanov A, Prishchepov AV, Schierhorn F, Mikutta R (2020) Interactive effects of land use and climate on soil organic carbon storage in Western Siberian steppe soils. In: Fröhauß M, Guggenberger G, Meinel T, Theesfeld I, Lentz S (eds) KULUNDA: climate smart agriculture. Innovations in landscape research. Springer, Cham. https://doi.org/10.1007/978-3-030-15927-6_13
- Guo JH, Liu XJ, Zhang YU, Shen JL et al (2010) Significant acidification in major Chinese croplands. *Science* 327:1008–1010
- Guo M, Yang B, Wang W et al (2019) Distribution, morphology and influencing factors of rills under extreme rainfall conditions in main land on the Loess Plateau of China. *Geomorphology* 345:106847. <https://doi.org/10.1016/j.geomorph.2019.106847>Notintext
- Guo Z, Zhang L, Yang W, Hua L, Cai C (2019b) Aggregate Stability under long-term fertilization practices: the case of eroded ultisols of South-Central China. *Sustainability* 11(4):1169. <https://doi.org/10.3390/su11041169>
- Gupta DK, Sandallo LM (eds) (2011) Metal toxicity in plants: perception, signalling and remediation. Springer, London
- Gutiérrez Y, Ott D, Scherber C (2020) Direct and indirect effects of plant diversity and phenoxy herbicide application on the development and reproduction of a polyphagous herbivore. *Sci Rep* 10:7300. <https://doi.org/10.1038/s41598-020-64252-5>
- Gutorova O, Sheudzhen A, Eulenstein F, Mueller L, Schindler U (2018a) Chapter I/33: Ion Chromatographic Method in Agrochemistry (In Russian: Ионхроматографический Метод в Агрохимии). In: Sychev VG, Mueller L (eds) Novel methods and results of landscape research in Europe, Central Asia and Siberia, vol I Landscapes in the 21th century: status analyses, basic processes and research concepts. © FSBI “VNI Agrochemistry”, pp 185–189. <https://doi.org/10.25680/9569.2018.64.90.033>. <https://vniia-pr.ru/monografii/pdf/tom1-33.pdf>
- Gutorova OA, Sheuzhen AK, Shkhatpatsev AK, Mueller L, Eulenstein F, Schindler U (2018b) Chapter I/37: enzymatic activity of soils in rice agrolandscapes of the Kuban Глава I/37: Ферментативная Активность Почв Рисовых Агроландшафтов Кубани. In: Sychev VG, Mueller L (Eds) Novel methods and results of landscape research in Europe, Central Asia and Siberia, vol I landscapes in the 21th century: status analyses, basic processes and research concepts. © FSBI “VNI Agrochemistry”, pp 204–208. <https://doi.org/10.25680/4199.2018.74.32.037>. <https://vniia-pr.ru/monografii/pdf/tom1-37.pdf>
- Guzev VS, Levin SV (1991) Perspectives of ecological-microbiological examination of soil conditions under anthropogenic impacts. *Soil Sci* 9:50–62. (In Russian: Перспективы эколого-микробиологической экспертизы состояния почв при антропогенных воздействиях. *Почвоведение* 9:50 – 62.)
- Hallam J, Hodson ME (2020) Impact of different earthworm ecotypes on water stable aggregates and soil water holding capacity. *Biol Fert Soils* 56:607–617
- Halm D, Grathwohl P (2003) (eds) Proceedings of the 2nd international workshop on groundwater risk assessment at contaminated sites (GRACOS) and integrated soil and water protection (SOWA), held in Tübingen, Germany, from 20 to 21 March 2003. https://doi.org/10.1007/978-3-030-15927-6_13

- publikationen.uni-tuebingen.de/xmlui/bitstream/handle/10900/48470/pdf/TGA_C69_Halm.pdf?sequence=1#page=139. Accessed on 12 Sept 2020
- Hansen S, Jensen HJ, Nielsen NE, Svendsen H (1991) Simulation of nitrogen dynamics and biomass production in winter wheat using the Danish simulation model DAISY. *Fert Res* 27(2–3):245–259
- Hansen B, Alroe HF, Kristensen ES (2001) Approaches to assess the environmental impact of organic farming with particular regard to Denmark. *Agric Ecosys Environ* 83:11–26
- Hararuk O, Xia J, Luo Y (2014) Evaluation and improvement of a global land model against soil carbon data using a Bayesian Markov chain Monte Carlo method. *J Geophys Res Biogeosci* 119:403–417. <https://doi.org/10.1002/2013JG002535>
- Hasanuzzaman M, Nahar K, Alam MM, Bhowmik PC, Hossain MA, Rahman MM, Narasimha M, Prasad V, Ozturk M, Fujita M (2014) Potential use of halophytes to remediate saline soils. *BioMed Res Int* 1–12
- Haselow L, Rupp H, Bondarovich AA, Meissner R (2019) Measurement and estimation of evapotranspiration in semi-arid grassland during the summer season in southwest Siberia. *Eur J Soil Sci* 8(3):257–266. <https://doi.org/10.18393/ejss.567359>
- Hatfield JL, Sauer TJ, Cruse RM (2017) Soil: the forgotten piece of the water, food, energy nexus. *Adv Agron* 143:1–46. <https://doi.org/10.1016/bs.agron.2017.02.001>
- Herrmann DL, Shuster WD, Garmestani AS (2017) Vacant urban lot soils and their potential to support ecosystem services. *Plant Soil* 413(1–2):45–57. <https://doi.org/10.1007/s11104-016-2874-5>
- Hillel D (2000). *Salinity management for sustainable irrigation: integrating science, environment, and economics*. The World Bank. ISBN: 978–0–8213–4773–7. <https://doi.org/10.1596/0-8213-4773-X>
- Höke S (2003) Identifizierung, Herkunft, Mengen und Zusammensetzung von Exstäuben in Böden und Substraten des Ruhrgebiets (Identification, origin, quality and composition of ex-dust in soils and substrates of the Ruhr area). *Essener Ökologische Schriften*, vol 20. Westarp Wissenschaften Verlags GmbH, Hohenwarsleben, p 141
- Holtkamp R, Van der Wal A, Kardol P, Van der Putten WH, De Ruiter PC, Dekker SC (2011) Modelling C and N mineralisation in soil food webs during secondary succession on ex-arable land. *Soil Biol Biochem* 43:251–260. <https://doi.org/10.1016/j.soilbio.2010.10.004>
- Holz M, Zarebanadkouki M, Kuzyakov Ya, Pausch J, Carminati A (2017) Root hairs increase rhizosphere extension and carbon input to soil. *Ann Bot* 121(1): 61–69. <https://doi.org/10.1093/aob/mcx127>
- Hong S, Gan P, Chen A (2019) Environmental controls on soil pH in planted forest and its response to nitrogen deposition. *Environ Res* 172:159–165. <https://doi.org/10.1016/j.envres.2019.02.020>
- Horion S, Ivits E, De Keersmaecker W, Tagesson T, Vogt J, Fensholt R (2019) Mapping European ecosystem change types in response to land-use change, extreme climate events, and land degradation. *Land Degrad Develop* 30(8):951–963. <https://doi.org/10.1002/ldr.3282>
- Hou D, O’Connor D, Igalavithana AD, Alessi DS, Luo J, Tsang DCW, Sparks DL, Yamauchi Y, Rinklebe J, Ok YS (2020) Metal contamination and bioremediation of agricultural soils for food safety and sustainability. *Nature Reviews. Earth & Environment*. 1:366–381
- Hu Y, Zheng Q, Noll L, Zhang S, Wanek W (2020) Direct measurement of the in situ decomposition of microbial-derived soil organic matter. *Soil Biol Biochem* 141:107660. <https://doi.org/10.1016/j.soilbio.2019.107660>
- Huang J, Peng S, Mao X, Li F, Guo S, Shi L, Shi Y, Yu H, Zeng G-M (2019) Source apportionment and spatial and quantitative ecological risk assessment of heavy metals in soils from a typical Chinese agricultural county. *Process Saf Environ Prot* 126:339–347. <https://doi.org/10.1016/j.psep.2019.04.023>
- Hugelius G, Loisel J, Chadburn S, Jackson RB, Jones M, MacDonald G, Marushchak M, Olefeldt D, Packalen M, Siewert MB, Treat C, Turetsky M, Voigt C, Yu Z (2020) Large stocks of peatland carbon and nitrogen are vulnerable to permafrost thaw. *PNAS* 117(34):20438–20446. <https://doi.org/10.1073/pnas.1916387117>
- Huhta V (2007) The role of soil fauna in ecosystems: a historical review. *Pedobiologia* 50:489–495
- Husniev I, Romanenkov V, Minakova O, Krasilnikov P (2020) Modelling and prediction of organic carbon dynamics in arable soils based on a 62-year field experiment in the Voronezh Region, European Russia. <https://doi.org/10.20944/preprints202009.0176.v1>
- IIASA (2020) The RAINS 7.2 model of air pollution. <https://user.iiasa.ac.at/~schoepp/doc/manual/intro.htm#Amann%20Bertok%20Cofala%2096>
- Inisheva LI, Porokhina EV, Sergeeva MA (2018) Chapter I/24: long-term stationary research in peat landscapes (in Russian). In: Sychev VG, Mueller L (eds) *Novel methods and results of landscape research in Europe, Central Asia and Siberia, vol I landscapes in the 21th century: status analyses, basic processes and research concepts*. © FSBI “VNIi Agrochemistry”, pp 141–146. <https://doi.org/10.25680/2326.2018.41.15.024>. <https://vniia-pr.ru/monografii/pdf/tomI-24.pdf>
- ISO 15799:2019–11 (2019) Soil quality—Guidance on the ecotoxicological characterization of soils and soil materials. <https://www.iso.org/standard/70770.html>. Accessed on 15 Feb 2021
- ISO 17616:201911 (2019) Soil quality—Guidance on the choice and evaluation of bioassays for ecotoxicological characterization of soils and soil materials. <https://www.iso.org/standard/73592.html>. Accessed on 15 Feb 2021
- Issanova G, Abuduwaili J (2017) Aeolian processes as dust storms in the deserts of Central Asia and

- Kazakhstan. Springer Nature Singapore Pte Ltd. <https://doi.org/10.1007/978-981-10-3190-8>
- IUSS Working Group WRB (2014) World reference base for soil resources 2014. In: Schad P, van Huyssteen C, Micheli E (eds) World soil resources reports No. 106. FAO, Rome, 189 p. ISBN 978-92-5-108369-7
- Ivushkin K, Bartholomeus H, Bregt AK, Pulatov A, Kempen B, De Sousa L (2019) Global mapping of soil salinity change. *Remote Sens Environ* 231:111260. <https://doi.org/10.1016/j.rse.2019.111260>
- Janssen BH, Guiking FCT, van der Eijk D, Smaling EMA, Wolf J, van Reuler H (1990) A system for quantitative evaluation of the fertility of tropical soils (QUEFTS). *Geoderma* 46:299–318
- Janssens J, Deng Z, Sonwa D, Torrico JC, Mulindabigwi V, Pohlen J (2006) Relating agro-climax of orchards to eco-climax of natural vegetation. *Acta Horticulturae* 707:181–186
- Jaramaz D (2018) The impact of anthropogenic pollution on soil degradation at wide area of Bor City. Doctoral thesis, Faculty of Forestry, University of Belgrade, Serbia
- Jeffery S, van der Putten WH (2011) Soil-Borne human diseases 1–56. <https://doi.org/10.2788/37199>
- Jeffery S, Gardi C (2010) Soil biodiversity under threat—a review. *Acta Soc Zool Bohem* 74:7–12
- Jensen JL, Schjønning P, Watts CW, Christensen BT, Obour PB, Munkholm LJ (2020) Soil degradation and recovery—changes in organic matter fractions and structural stability. *Geoderma* 364:114181. <https://doi.org/10.1016/j.geoderma.2020.114181>
- Jha P, Banerjee S, Bhuyan P, Sudarshan M, Dewanji A (2020) Elemental distribution in urban sediments of small waterbodies and its implications: a case study from Kolkata, India. *Environ Geochem Health* 42:461–482. <https://doi.org/10.1007/s10653-019-00377-5>
- Jia Y, Kuzyakov Y, Wang G, Tan W, Zhu B, Feng X (2019) Temperature sensitivity of decomposition of soil organic matter fractions increases with their turnover time. *Land Degrad Develop* 31(5):632–645. <https://doi.org/10.1002/ldr.3477>
- Jobbágy EG, Tóth T, Nosoletto MD, Earman S (2017) On the fundamental causes of high environmental alkalinity (pH \geq 9): an assessment of its drivers and global distribution. *Land Degrad Dev* 28(7):1973–1981
- Johnson NC, Rowland DL, Corkidi L, Allen EB (2008) Plant winners and losers during grassland n-eutrophication differ in biomass allocation and mycorrhizas. *Ecol* 89(10):2868–2878. <https://doi.org/10.1890/07-1394.1>
- Jones C, Engel R, Olson-Rutz K (2020) Soil acidification in the semiarid regions of North America's Great Plains. *Crops Soils* 52(2):28–56. <https://doi.org/10.2134/cs2019.52.0211>
- Joyner JL, Kerwin J, Deeb M, Lozefski G, Prithiviraj B, Paltseva A, McLaughlin J, Groffman P, Cheng Z, Muth TR (2019) Green infrastructure design influences communities of urban soil bacteria. *Front Microbiol*. <https://doi.org/10.3389/fmicb.2019.00982>
- Jung M, Schwalm C, Migliavacca M, Walther S, Camps-Valls G, Koirala S, Anthoni P, Besnard S, Bodesheim P, Carvalhais N, Chevallier F, Gans F, Goll DS, Haverd V, Köhler P, Ichii K, Jain AK, Liu J, Lombardozzi D, Nabel JEMS, Nelson JA, O'Sullivan M, Pallandt M, Papale D, Peters W, Pongratz J, Rödenbeck C, Sitch S, Tramontana G, Walker A, Weber U, Reichstein M (2020) Scaling carbon fluxes from eddy covariance sites to globe: synthesis and evaluation of the FLUXCOM approach. *Biogeosciences* 17:1343–1365. <https://doi.org/10.5194/bg-17-1343-2020>
- Kaminsky LM, Trexler RV, Malik RJ, Hockett KL, Bell TH (2019) The inherent conflicts in developing soil microbial inoculants. *Trends Biotechnol* 37(2):140–151. <https://doi.org/10.1016/j.tibtech.2018.11.011>
- Kanash EV, Litvinovich AV, Kovleva AO, Osipov YuA, Saljnikov E (2018) Grain production and optical characteristics in three wheat (*Triticum aestivum* L.) Varieties under liming and nitrogen fertilization. *Agricultural Biology* 53(1):61–71. doi: <https://doi.org/10.15389/agrobiol.2018.1.61eng>
- Karlen DL, Andrews SS, Wienhold BJ, Zobeck TM (2008) Soil Quality Assessment: Past, Present and Future. Publications from USDA-ARS / UNL Faculty. 1203. <https://digitalcommons.unl.edu/usdaarsfacpub/1203>
- Kauppi P, Kamari J, Posch M, Kauppi L, Matzner E (1987) Acidification of forest soils: model development and application for analyzing impacts of acidification in Europe. Laxenburg, Novographic, Vienna, Austria, <http://pure.iiasa.ac.at/id/eprint/2766/1/RR-87-05.pdf>, accessed on Sept 12, 2020
- Keesstra SD, Bouma J, Wallinga J, Tittonell P, Smith P, Cerdà A, Montanarella L, Quinton JN, Pachepsky Y, van der Putten WH, Bardgett RD, Moolenaar S, Mol G, Jansen B, Fresco LO (2016) The significance of soils and soil science towards realization of the United Nations Sustainable Development Goals. *Soil* 2:111–128. <https://doi.org/10.5194/soil-2-111-2016>
- Kersebaum KC, Hecker J-M, Mirschel W, Wegehenkel M (eds.) (2007) Modelling water and nutrient dynamics in soil-crop systems: proceedings of the workshop on “Modelling water and nutrient dynamics in soil-crop systems” held on 14–16 June 2004 in Müncheberg, Germany. Dordrecht (Springer), 271pp
- Kersebaum KC (2007) Modelling nitrogen dynamics in soil-crop systems with HERMES. In: Kersebaum KC, Hecker J-M, Mirschel W, Wegehenkel M (eds) Modelling water and nutrient dynamics in soil-crop systems: proceedings of the workshop on “Modelling water and nutrient dynamics in soil-crop systems” held on 14–16 June 2004 in Müncheberg, Germany. Dordrecht (Springer), pp 147–160
- Khan NI, Owens G, Bruce D, Naidu R (2009) Human arsenic exposure and risk assessment at the landscape

- level: a review. *Environ Geochem Health* 31:143–166. <https://doi.org/10.1007/s10653-008-9240-3> PMID: 19172401
- Khan MN, Mohammad F (2014a) Eutrophication: Challenges and Solutions. In: Ansari AA, Gill SS (eds) *Eutrophication: causes, consequences and control*. Springer Science+Business Media Dordrecht. <https://doi.org/10.1007/978-94-007-7814-6-1>
- Khan MN, Mohammad F (2014b) Eutrophication of Lakes. In: Ansari AA, Gill SS (eds) *Eutrophication: challenges and solutions, vol II of eutrophication: causes, consequences and control*. Springer Science+Business Media Dordrecht. <https://doi.org/10.1007/978-94-007-7814-6-5>
- Khan MN, Mobin M, Abbas ZK, Alamri SA (2018) Fertilizers and their contaminants in soils, surface and groundwater. In: DellaSala DA, Goldstein MI (eds) *The encyclopedia of the anthropocene, vol 5*. Elsevier, Oxford, pp 225–240
- Kholodov VA, Yaroslavtseva NV, Farkhodov YR, Yashin MA, Lazarev VI, Iliyn BS, Philippova OI, Volikov AB, Ivanov AL (2020) Optical properties of the extractable organic matter fractions in typical chernozems of long-term field experiments. *Eurasian Soil Sci.* 53:739–748. <https://doi.org/10.1134/S1064229320060058>
- Kiryushin VI (2019) The management of soil fertility and productivity of agrocenoses in adaptive-landscape farming systems. *Eurasian Soil Sci* 52:1137. <https://doi.org/10.1134/S1064229319070068>
- König S, Vogel H-J, Harms H, Worrich A (2020) Physical, chemical and biological effects on soil bacterial dynamics in microscale models. *Front Ecol Evol.* <https://doi.org/10.3389/fevo.2020.00053>
- Kooch Y, Ehsani S, Akbarini M (2020) Stratification of soil organic matter and biota dynamics in natural and anthropogenic ecosystems. *Soil Tillage Res* 200:10462. <https://doi.org/10.1016/j.still.2020.104621>
- Körshens M, Albert E, Baumecker M, Ellmer F, Grunert M, Hoffmann S, Kismanyoky T, Kubat J, Kunzova E, Marx M, Rogasik J, Rinklebe J, Rühlmann J, Schilli C, Schröter H, Schoetter S, Schweizer K, Toth Z, Zimmer J, Zorn W (2014) Humus and climate change—results of 15 long-term experiments (Humus und Klimaänderung - Ergebnisse aus 15 langjährigen Dauerfeldversuchen). *Arch Agron Soil Sci* 60(11):1485–1517. <https://doi.org/10.1080/03650340.2014.892204>
- Körshens M (2021) Chapter 8. Long-term field experiments (LTEs)—importance, overview, soil organic matter. In: Mueller L, Sychev VG, Dronin NM, Eulenstein F (eds) *Exploring and optimizing agricultural landscapes. Innovations in landscape research*. Springer, Cham, in print ISBN 978-3-030-67448-9
- Kotenko ME, Sorokin AE, Savich VI, Podvolovskaya GB, Shima M (2020) Change in soil salination in time and in space. *Plodorodie* 1(112). <http://plodorodie-j.ru/journal/2020/1-2020/2020-1-43-48.html> (In Russian: М.Е. Котенко, А.Е. Сорокин, В.И. Савич, Г.Б. Подволоцкая, Мохаммади Шима (2020) Изменение засоления почв во времени и в пространстве)
- Koul B, Taak P (2018) Soil pollution: causes and consequences. In: *Biotechnological strategies for effective remediation of polluted soils*. Springer, Singapore. https://doi.org/10.1007/978-981-13-2420-8_1
- Kroes J, Roelsma J (2007) Simulation of water and nitrogen flows on field scale: application of the SWAP-ANIMO model for the Müncheberg data set. In: Kersebaum KC, Hecker J-M, Mirschel W, Wegehenkel M (eds) *Modelling water and nutrient dynamics in soil-crop systems: proceedings of the workshop on “Modelling water and nutrient dynamics in soil-crop systems” held on 14–16 June 2004 in Müncheberg, Germany*. Dordrecht (Springer), pp 111–128
- Kros J, Mol-Dijkstra JP, de Vries W, Fujita Y, Witte JPM (2017) Comparison of model concepts for nutrient availability and soil acidity in terrestrial ecosystems. KWR2017.053 Wageningen University and Research. <https://edepot.wur.nl/428560>
- Kuhry P, Bárta J, Blok D, Elberling B, Faucherre S, Hugelius G, Jørgensen CJ, Richter A, Šantrůčková H, Weiss N (2020) Lability classification of soil organic matter in the northern permafrost region. *Biogeosciences* 17:361–379. <https://doi.org/10.5194/bg-17-361-2020>
- Kuhwald M, Thomas C, Becker J, Berger A, Duttman R (2018) Chapter I/32: a new approach for soil respiration measurements in laboratory. In: Sychev VG, Mueller L (eds) *Novel methods and results of landscape research in Europe, Central Asia and Siberia, vol I landscapes in the 21st century: status analyses, basic processes and research concepts*. © FSBI “VNII Agrochemistry”, pp 180–184. <https://doi.org/10.25680/5884.2018.95.45.032> <https://vniia-pr.ru/monografii/pdf/tom1-32.pdf>
- Kundler P (1989) *Erhöhung der Bodenfruchtbarkeit*, VEB Deutscher Landwirtschaftsverlag Berlin, 1st edn, 452 pp
- Kurganova I, Merino A, Lopes de Gerenyu V, Barros N, Kalinina O, Gianì L, Kuzyakov Y (2019) Mechanisms of carbon sequestration and stabilization by restoration of arable soils after abandonment: a chronosequence study on Phaeozems and Chernozems. *Geoderma* 354:113882
- La Cecilia D, Maggi F (2020) Influential sources of uncertainty in glyphosate biochemical degradation in soil. *Math Comput Simulat* 175:121–139. <https://doi.org/10.1016/j.matcom.2020.01.003>
- LABO (2003) *Bund/Länder Arbeitsgemeinschaft Bodenschutz: Arbeitshilfe Sickerwasserprognose bei Orientierenden Untersuchungen*. http://www.labo-deutschland.de/documents/SiWaPrognose-120903_91f.pdf. Accessed on Oct 10, 2020

- Lakshmanan M, Koh G, Chung BK, Lee DY (2014) Software applications for flux balance analysis. *Brief Bioinform* 15(1):108–122. <https://doi.org/10.1093/bib/bbs069>
- Lal R (2004) Soil carbon sequestration impacts on global climate change and food security. *Science* 304:1623–1627. <https://doi.org/10.1126/science.1097396>
- Lal R (2020a) Soil erosion and gaseous emissions. *Appl Sci* 10(8):2784. <https://doi.org/10.3390/app10082784>
- Lal R, Hall GF, Miller FP (1989) Soil degradation: I. Basic processes. *Land Degrad Develop* 1:51–69. <https://doi.org/10.1002/ldr.3400010106>
- Lal R (1998) Soil erosion impact on agronomic productivity and environment quality. *Crit Rev Plant Sci* 17(4):319–464
- Lal R (2001) Soil degradation by erosion. *Land Degrad Dev* 12:519–539. <https://doi.org/10.1002/ldr.472>. http://tinread.usarb.md:8888/tinread/fulltext/lal/soil_degradation.pdf Not in text
- Lal R (2020b) Home gardening and urban agriculture for advancing food and nutritional security in response to the COVID-19 pandemic. *Food Sec* (2020). <https://doi.org/10.1007/s12571-020-01058-3>
- Latendresse M, Krummenacker M, Trupp M, Karp PD (2012) Construction and completion of flux balance models from pathway databases. *Bioinformatics* 28:388–396. <https://doi.org/10.1093/bioinformatics/btr681>
- Lavrishchev A, Litvinovich A, Pavlova O, Vladimir B (2020) Effect of liming of sod-podzolic soils with by-products of steel production on soil acidity and composition of wash water (column experiments). *Zemljiste i Biljka* 69(2):68–81. http://www.sdpz.rs/images/casopis/2020/zib_69_2_75.pdf
- Le HT, Rochelle-Newall E, Ribolzi O, Janeau JL, Huon S, Latschack K, Pommier T (2019) Land use strongly influences soil organic carbon and bacterial community export in runoff in tropical uplands. *Land Degrad Develop* 31(1):118–132. <https://doi.org/10.1002/ldr.3433>
- Lee CS, Jung S, Lim BS, Kim AR, Lim CH, Lee H (2019) Forest decline under progress in the urban forest of Seoul. *Central Korea Intech Open*. <https://doi.org/10.5772/intechopen.86248>
- Van Leeuwen JP, Creamer RE, Cluzeau D, Debejak M, Gatti F, Henriksen C, Kuzmanovski V, Menta C, Peres G, Picaud C, Saby N, Trajanov A, Trinsoutrot-Gattin I, Visioli G, Rutgers M (2019) Modeling of soil functions for assessing soil quality: soil biodiversity and habitat provisioning. *Front Environ Sci* 7:113. <https://doi.org/10.3389/fenvs.2019.00113>
- Lehman RM, Cambardella CA, Stott DE, Acosta-Martinez V, Manter DK, Buyer JS, Maul JE, Smith JL, Collins HP, Halvorson JJ, Kremer RJ, Lundgren JG, Ducey TF, Jin VL, Karlen DL (2015) Understanding and enhancing soil biological health: the solution for reversing soil degradation. *Sustainability* 7(1):988–1027. <https://doi.org/10.3390/su7010988>
- Lehmann J, Bossio DA, Kögel-Knabner I, Rillig MC (2020) The concept and future prospects of soil health. *Nat Rev Earth Environ* 1:544–553. <https://doi.org/10.1038/s43017-020-0080-8>
- Lehmann J, Hansel CM, Kaiser C, Kleber M, Maher K, Manzoni S, Nunan N, Reichstein M, Schimel JP, Torn MS, Wieder WR, Kögel-Knabner I (2020) Persistence of soil organic carbon caused by functional complexity. *Nat Geosci* 13:529–534. <https://doi.org/10.1038/s41561-020-0612-3>
- Lehmann J, Kleber M (2015) The contentious nature of soil organic matter. *Nature* 528(2015):60–68. <https://doi.org/10.1038/nature16069>
- Liang C, Amelung W, Lehmann J, Kästner M (2019) Quantitative assessment of microbial necromass contribution to soil organic matter. *Global Change Biol* 5(11):3578–3590. <https://doi.org/10.1111/gcb.14781>
- Litalien A, Zeeb B (2020) Curing the earth: a review of anthropogenic soil salinization and plant-based strategies for sustainable mitigation. *Sci Total Environ* 698:134235. <https://doi.org/10.1016/j.scitotenv.2019.134235>
- Litvinovich A, Salaev I, Pavlova O, Lavrishchev A, Bure V, Saljnikov E (2019) Utilization of large-sized dolomite by-product particles and losses of cations from acidic soil. *Commun Soil Sci Plant Anal*. <https://doi.org/10.1080/00103624.2019.1589490>
- Liu M, Song Yu, Xu T, Xu Zh, Wang T, Yin L, Jia X, Tang J (2020a) Trends of precipitation acidification and determining factors in China during 2006–2015. *J Geophys Res Atmos* 125(6):e2019JD031301. <https://doi.org/10.1029/2019JD031301>
- Liu X, Shi H, Bai Z, Liu X, Yang B, Yan D (2020b) Assessing soil acidification of croplands in the poyang lake basin of China from 2012 to 2018. *Sustainability* 12:3072. <https://doi.org/10.3390/su12083072>
- Liu D et al. (2012) Occurrence, fate, and ecotoxicity of antibiotics in agro-ecosystems. A review. *Agron Sustain Develop* Springer Verlag, EDP Sciences, INRA, 32(2):309–327. <https://doi.org/10.1007/s13593-011-0062-9>
- Löffler D, Hatz A, Albrecht D, Fligg M, Hogeback J, Ternes TA (2020) Determination of non-extractable residues in soils: Towards a standardised approach. *Environ Poll* 259:113826.
- Logan TJ (1990) Chemical degradation of soil. In: Lal R, Stewart BA (eds) *Advances in soil science*, vol 11. Springer, New York, NY. <https://doi.org/10.1007/978-1-4612-3322-0>
- Loke PF, Kotze E, du Preez CC, Twigge L (2019) Dynamics of soil carbon concentrations and quality induced by agricultural land use in Central South Africa. *SSSAJ Soil Chem* 83(2):366–379. <https://doi.org/10.2136/sssaj2018.11.0423>
- Lorenz K, Lal R, Ehlers K (2019) Soil organic carbon stock as an indicator for monitoring land and soil degradation in relation to United Nations' sustainable development goals. *Land Degrad Develop* 30(7):824–838

- Luebbers F (2002) Soil organic matter stratification ratio as an indicator of soil quality. *Soil Tillage Res* 66 (2):95–106
- Luo Y, Li Q, Wang Ch, Li B, Stomph T-J, Yang J, Tao Q, Yuan S, Tang X, Ge J, Yu X, Peng Y, Xu Q, Zheng G (2019) Negative effects of urbanization on agricultural soil easily oxidizable organic carbon down the profile of the Chengdu Plain, China. *Land Degrad Develop* 31(3):401–416. <https://doi.org/10.1002/ldr.3458>
- MacKenzie MD, Dietrich ST (2020) Atmospheric sulfur and nitrogen deposition in the Athabasca oil sands region is correlated with foliar nutrient levels and soil chemical properties. *Sci Total Environ* 711(1):134737. <https://doi.org/10.1016/j.scitotenv.2019.134737>
- Mandakh N, Tsogetbaatar J, Dash D, Khodolmor S (2016) System of indicators and evaluation of desertification in Mongolia. *Arid Ecosystems* 22-1(66):93-105. (In Russian: Система индикаторов и оценка опустынивания в Монголии. Аридные экосистемы)
- Mandal AK, Sharma RC, Singh G (2009) Assessment of salt affected soils in India using GIS. *Geocarto Int* 24:437–456
- Martinez MA, Woodcroft BJ, Espinoza JCI, Zayed AA, Singleton CM, Boyd JA, Li Y-F, Purvin S, Maughan H, Hodgkins SB, Anderson D, Sederholm M, Temperton B, Bolduc B, Saleska SR, Tyson GW, Rich VI (2019) Discovery and ecogenomic context of a global Caldiseica-related phylum active in thawing permafrost, *Candidatus Cryoserica phylum* nov., *Ca. Cryoserica* class nov., *Ca. Cryosericales* ord. nov., *Ca. Cryoseriaceae* fam. nov., comprising the four species *Cryosericum septentrionale* gen. nov. sp. nov., *Ca. C. hinesii* sp. nov., *Ca. C. odellii* sp. nov., *Ca. C. terrychapinii* sp. nov. *Syst Appl Microbiol* 42(1):54–66. <https://doi.org/10.1016/j.syapm.2018.12.003>
- Martinez-Salgado MM, Gutiérrez-Romero V, Janssens M, Ortega-Blu R (2019) Biological soil quality indicators: a review. In: Mendez-Vilas A (ed) *Current research, technology and education topics in applied microbiology and microbial biotechnology*, pp 319–328.
- Meena RS, Kumar S, Datta R, Lal R, Vijayakumar V, Brtnicky M, Sharma MP, Yadav GS, Jhariya MK, Jangir CK, Pathan SI, Dokulilova T, Pecina V, Marfo TD (2020) Impact of agrochemicals on soil microbiota and management: a review. *Land* 9(2):34. <https://doi.org/10.3390/land9020034>
- Meißner R, Prasad MNV, Du Laing G, Rinklebe J (2010) Lysimeters application for measuring the water and solute fluxes with high precision. *Curr Sci* 99(5):601–607
- Mensah AK, Marschner B, Shaheen SM, Wang S-L, Rinklebe J (2020) Arsenic contamination in abandoned and active gold mine spoils in Ghana: geochemical fractionation, speciation, and assessment of the potential human health risk. *Environ Pollut* 261. <https://doi.org/10.1016/j.envpol.2020.114116>
- Menta C (2012) Soil fauna diversity—function. Soil degradation, biological indices, soil restoration, biodiversity conservation and utilization in a diverse world. *Gbolagade Akeem Lameed*, IntechOpen. <https://doi.org/10.5772/51091>
- Meuser H (2010) Assessment of urban soils. In: *Contaminated urban soils. Environmental pollution*, vol 18. Springer, Dordrecht. https://doi.org/10.1007/978-90-481-9328-8_7
- Meyer BC, Schreiner V, Smolentseva EN, Smolentsev BA (2008) Indicators of desertification in the Kulunda Steppe in the south of Western Siberia. *Arch Agron Soil Sci* 54(6):585–603. <https://doi.org/10.1080/03650340802342268>
- Meyer ST, Koch C, Weisser WW (2015) Towards a standardized rapid ecosystem function assessment (REFA). *Trends Ecol Evol* 30:390–397
- Michael I, Rizzo L, McArdell CS, Manai CM, Merline C, Schwartz T, Dagot C, Fatta-Kassinosa D (2013) Urban wastewater treatment plants as hotspots for the release of antibiotics in the environment: a review. *Water Res* 47(3):957–995. <https://doi.org/10.1016/j.watres.2012.11.027>
- Mirschel W, Wenkel K-O (2007) Modelling soil-crop interactions with AGROSIM model family. In: Kersebaum KC, Hecker J-M, Mirschel W, Wegehenkel M (eds) *Modelling water and nutrient dynamics in soil-crop systems: proceedings of the workshop on “Modelling water and nutrient dynamics in soil-crop systems” held on 14–16 June 2004 in Müncheberg, Germany*. Dordrecht (Springer), pp 59–73
- Mirschel W, Berg-Mohnicke M, Wieland R, Wenkel K-O, Terleev VV, Topaj AG, Müller L (2020) Modelling and simulation of agricultural landscapes. In: Mirschel W, Terleev VV, Wenkel K-O (eds) *Landscape modelling and decision support, innovations in landscape research*. Springer Nature Switzerland, Cham. https://doi.org/10.1007/978-3-030-37421-1_1
- Mortvedt JJ (1996) Heavy metal contaminants in inorganic and organic fertilizers. In: Rodriguez-Barrueco C (eds) *Fertilizers and environment. Developments in plant and soil sciences*, vol 66. Springer, Dordrecht. https://doi.org/10.1007/978-94-009-1586-2_2
- Mrvic V, Lj K-K, Sikirić B, Delić D, Jaramaz D (2014) Methods for the assessment of background limits of Cd and Cr in the soil of Moravički district. *Bull Faculty Forestry* 109:137–148. <https://doi.org/10.2298/GSF1409137M>
- Mueller L, Wirth S, Schulz E, Behrendt A, Höhn A, Schindler U (2007a) Implications of soil substrate and land use for properties of fen soils in North-East Germany Part I: Basic soil conditions, chemical and biological properties of topsoils. *Arch Agron Soil Sci* 53(2):113–126. <https://doi.org/10.1080/03650340701224823>
- Mueller L, Schindler U, Ball BC, Smolentseva E, Sychev VG, Shepherd TG, Qadir M, Helming K, Behrendt A, Eulenstein F (2014a) Productivity potentials of the global land resource for cropping and grazing. In: Mueller L, Saporov A, Lischeid G (eds) *Novel measurement and assessment tools for monitoring and management of land and water*

- resources in agricultural landscapes of Central Asia. Springer International Publishing, Cham. Environmental Science and Engineering, pp 115–142. https://doi.org/10.1007/978-3-319-01017-5_6
- Mueller L, Schindler U, Behrendt A, Eulenstein F, Dannowski R (2007b) The Muencheberg soil quality rating (SQR). Field manual for detecting and assessing properties and limitations of soils for cropping and grazing. http://www.zalf.de/de/forschung_lehre/publikationen/Documents/Publikation_Mueller_L/field_mueller.pdf. Accessed on 12 Sept 2020
- Mueller L, Behrendt A, Shepherd TG, Schindler U, Ball BC, Khudyaev S, Kaiser T, Dannowski R, Eulenstein F (2014b) Simple field methods for measurement and evaluation of grassland quality. In: Mueller L, Saporov A, Lischeid G (eds) Novel measurement and assessment tools for monitoring and management of land and water resources in agricultural landscapes of Central Asia. Springer International Publishing, Cham, pp 199–222. https://doi.org/10.1007/978-3-319-01017-5_11
- Mueller L, Suleimenov M, Karimov A, Qadir M, Saporov A, Balgabayev N, Helming K, Lischeid G (2014c) Land and water resources of Central Asia, their utilisation and ecological status. In: Mueller L, Saporov A, Lischeid G (eds) Novel measurement and assessment tools for monitoring and management of land and water resources in agricultural landscapes of Central Asia. Environ Sci Eng. https://doi.org/10.1007/978-3-319-01017-5_1
- Mueller L, Eulenstein F, Mirschel W, Schindler U, Sychev VG, Rukhovich OV, Sheudzen AK, Romanenkov V, Lukin SM, McKenzie BM, Jones M, Dannowski R, Blum WEH, Saljnikov E, Saporov A, Pachikin K, Hennings V, Scherber C, Hoffmann J, Antrop M, Garibaldi L, Gómez Carella DS, Augstburger H, Schwilch G, Angelstam P, Manton M, Dronin NM (2021) Chapter 3: optimizing agricultural landscapes: measures towards prosperity and sustainability. In: Mueller L, Sychev VG, Dronin NM, Eulenstein F (eds) Exploring and optimizing agricultural landscapes. Innovations in landscape research. Springer, Cham, in print ISBN 978–3–030–67448–9
- Müller J (2016) Methods for measuring water and solute balances in forest ecosystems. In: Mueller L, Sheudshen A, Eulenstein F (eds) Novel methods for monitoring and managing land and water resources in Siberia. Springer Water. Springer, Cham. https://doi.org/10.1007/978-3-319-24409-9_15
- Munns R, Passioura JB, Colmer TD, Byrt CS (2020) Osmotic adjustment and energy limitations to plant growth in saline soil. New Phytol 225(3):1091–1096. <https://doi.org/10.1111/nph.15862>
- Muñoz-Arenas LC, Fusaro C, Hernández-Guzmán M, Dendooven L, Estrada-Torres A, Navarro-Noya Y-E (2020) Soil microbial diversity drops with land-use change in a high mountain temperate forest: a metagenomics survey. Environ Microbiol Rep 12(2):185–194. <https://doi.org/10.1111/1758-2229.12822>
- Muratchaeva PM, Khabibov S (2013) Regulatory of the manifestation of digressions in the ephemeral-wormwood communities of the Tersko-Kuma lowland. Arid Ecosyst 19(1):67–77. (In Russian: Муратчаева П.М.-С., Хабибов. 2013. О закономерностях проявления дигрессий в эфемерово-полюнных сообществах Терско-Кумской низменности. Аридные экосистемы.) Nicht im Text.
- Nagajyoti PC, Lee KD, Sreekanth VM (2010) Heavy metals, occurrence and toxicity for plants: a review. Environ Chem Lett 8:199–216
- Nagarajan H, Embree M, Rotaru A-E, Shrestha PM, Feist AM, Palsson BÖ, Lovley DR, Zengler K (2013) Characterization and modelling of interspecies electron transfer mechanisms and microbial community dynamics of a syntrophic association. Nat Commun 4: ncomms 3809
- Narozhnyaya AG, Chendev YuG (2020) The study of the modern ecological state of shelterbelts using GIS and remote sensing data InterCarto. InterGIS. GI support of sustainable development of territories: proceedings of the international conference, vol 26. Part 2. . Moscow University Press, Moscow, pp 54–65. <https://doi.org/10.35595/2414-9179-2020-2-26-54-65> (In Russian Изучение Современного Экологического Состояния Лесных Полос с Использованием ГИС и ДДЗ) <http://intercarto.msu.ru/jour/articles/article780.pdf>
- Nebol'sin AN, Nebol'sina ZP (2005) Theoretical bases of soil liming. St. Petersburg, 252 pp. (in Russ. Небольсин А.Н., Небольсин З.П. (2005) Теоретические основы известкования почв. СПб.: ЛНИИСХ, 2005. - 252 с)
- Nendel C (2014) MONICA: a simulation model for nitrogen and carbon dynamics in agro-ecosystems. In: Mueller L, Saporov A, Lischeid G (eds) Novel measurement and assessment tools for monitoring and management of land and water resources in agricultural landscapes of Central Asia. Environmental science and engineering. Springer, Cham. https://doi.org/10.1007/978-3-319-01017-5_23
- Nguyen KA, Liou YA, Tran HP, Hoang PP, Nguyen TH (2020) Soil salinity assessment by using near-infrared channel and Vegetation Soil Salinity Index derived from Landsat 8 OLI data: a case study in the Tra Vinh Province, Mekong Delta, Vietnam. Prog Earth Planet Sci 7:1. <https://doi.org/10.1186/s40645-019-0311-0>
- Nicholson FA, Chambers BJ, Williams JR, Unwin RJ (1999) Heavy metal content in livestock feeds and animal manures in England and Wales. Sci Total Environ 311:205–219
- Nisbet TR, Evans CD (2014) Forestry and surface water acidification. Forestry Commission. ISBN 9780855389000. OCLC 879011334. https://www.forestresearch.gov.uk/documents/352/FCRN016_46PkeE8.pdf. Accessed on 12 Sept 2020
- Norra S, Cheng Z (2017) Urban soils contamination. In: Levin MJ, Kim KHJ, Morel JL, Burghardt W, Charzynski P, Shaw RK (eds) In behalf of IUSS

- working group SUITMA: soils within cities. Catena-Schweizerbart, Stuttgart, pp 35–42
- Novikova NM, Volkova NA, Ulanova SS, Chemidov MM (2020) Change in vegetation on meliorated solonchic soils of the Peri-Yergenian plain over 10 years (Republic of Kalmykia). *Arid Ecosyst* 10:194–202. <https://doi.org/10.1134/S2079096120030051>
- Obalum SE, Chibuike GU, Peth S, Ouyang Y (2017) Soil organic matter as sole indicator of soil degradation. *Environ Monitor Assess* 189(4). <https://doi.org/10.1007/s10661-017-5881-y>
- Oldeman LR, Van Lynden GWJ (1998) Revisiting the GLASOD methodology. In: Lal R, Blum WH, Valentine C, Steward BR (eds) *Methods for assessment of soil degradation* CRC press, pp 423–440, 555
- Olsson L, Barbosa H, Bhadwal S, Cowie A, Delusca K, Flores-Renteria D, Hermans K, Jobbager E, Kurz W, Li D, Sonwa DJ, Stringer L, (2019) Chapter 4 land degradation. In: Shukla PR, Skea J, Calvo Buendia E, Masson-Delmotte V, Pörtner H-O, Roberts DC, Zhai P, Slade R, Connors S, van Diemen R, Ferrat M, Haughey E, Luz S, Neogi S, Pathak M, Petzold J, Portugal Pereira J, Vyas P, Huntley E, Kissick K, Belkacemi M, Malley J (eds) *Climate change and land: an IPCC special report on climate change, desertification, land degradation, sustainable land management, food security, and greenhouse gas fluxes in terrestrial ecosystems*, pp 345–436. <https://www.ipcc.ch/site/assets/uploads/2019/11/SRCL-Full-Report-Compiled-191128.pdf>. Accessed on 12 Sept 2020
- Omuto CT, Vargas RR, El Mobarak AM, Mohamed N, Viatkin K, Yigini Y (2020) Mapping of salt-affected soils. *Technical Manual*; FAO: Rome, Italy
- Opekunova M, Opekunov A, Elsukova E, Kukushkin S, Janson S (2020) Comparative analysis of methods for air pollution assessing in the Arctic mining area. *Atmos Poll Res*. <https://doi.org/10.1016/j.apr.2020.08.017>
- Orgiazzi A, Panagos P (2018) Soil biodiversity and soil erosion: it is time to get married. *Glob Ecol Biogeogr* 27(10). <https://doi.org/10.1111/geb.12782>
- Orlova T, Melnichuk A, Klimenko K, Vitvitskaya V, Popovych V, Dunajeva I, Terleev V, Nikonov A, Togo I, Volkova Y, Mirschel W, Garmanov V (2017) Reclamation of landfills and dumps of municipal solid waste in a waste management system: methodology and practice. In: *IOP conference series: earth and environmental science* 90, 1, Article No.: 012110, 13 p. <https://doi.org/10.1088/1755-1315/90/1/012110>
- Otarov A (2014) Concentration of heavy metals in irrigated soils in Southern Kazakhstan. In: Mueller L, Saporov A, Lischeid G (eds) *Novel measurement and assessment tools for monitoring and management of land and water resources in agricultural landscapes of Central Asia*. Environmental science and engineering. Springer, Cham. https://doi.org/10.1007/978-3-319-01017-5_41
- Palansooriya KN, Shaheen SM, Chen SS, Tsang DCW, Hashimoto Y, Hou D, Bolan NS, Rinklebe J, Ok YS (2020) Soil amendments for immobilization of potentially toxic elements in contaminated soils: a critical review. *Environ Int* 134. <https://doi.org/10.1016/j.envint.2019.105046>
- Pan M, Chu LM (2017) Fate of antibiotics in soil and their uptake by edible crops. *Sci Total Environ* 599–600:500–512
- Pan X-L, Dong F-S, Wu X-H, Xu J, Liu X-G, Zheng Y-Q (2019) Progress of the discovery, application, and control technologies of chemical pesticides in China. *J Integr Agric* 18(4):840–853. [https://doi.org/10.1016/S2095-3119\(18\)61929-X](https://doi.org/10.1016/S2095-3119(18)61929-X)
- Pankratova KG, Shchelokov VI, Stupakova GA, Sychev VG (2016) Study of the suitability of NIR spectroscopy for monitoring the contamination of soils with oil products. In: Mueller L, Sheudshen A, Eulenstein F (eds) *Novel methods for monitoring and managing land and water resources in Siberia*. Springer Water. Springer, Cham. https://doi.org/10.1007/978-3-319-24409-9_13
- Pasley HR, Cairns JE, Camberato JJ, Vyn TV (2019) Nitrogen fertilizer rate increases plant uptake and soil availability of essential nutrients in continuous maize production in Kenya and Zimbabwe. *Nutr Cycl Agroecosyst* 115:373–389. <https://doi.org/10.1007/s10705-019-10016-1>
- Pavlović M, Pavlović D, Kostić O, Jarić S, Čakmak D, Pavlović P, Mitrović M (2017) Evaluation of urban contamination with trace elements in city parks in Serbia using pine (*Pinus nigra* Arnold) needles, bark and urban topsoil. *Int J Environ Res* 11:625–639. <https://doi.org/10.1007/s41742-017-0055-x>
- Pejović M, Bajat B, Gospavić Z, Saljnikov E, Kilibarda M, Čakmak D (2017) Layer-specific spatial prediction of As concentration in copper smelter vicinity considering the terrain exposure. *J Geochem Explor* 179:25–35. <http://grafar.grf.bg.ac.rs/handle/123456789/821>
- Peng H, Chen Y, Weng L, Ma J, Ma Y, Li Y, Islam MdS (2019) Comparisons of heavy metal input inventory in agricultural soils in North and South China: a review. *Sci Total Environ* 660:776–786. <https://doi.org/10.1016/j.scitotenv.2019.01.066>
- Perez-Hernandez H, Fernandez-Luqueno F, Huerta-Lwanga E, Huerta-Lwanga D (2017) Layer-specific spatial prediction of As concentration in copper smelter vicinity considering the terrain exposure. *J Geochem Explor* 179:25–35. <http://grafar.grf.bg.ac.rs/handle/123456789/821>
- Perez-Hernandez H, Fernandez-Luqueno F, Huerta-Lwanga E, Huerta-Lwanga D (2017) Layer-specific spatial prediction of As concentration in copper smelter vicinity considering the terrain exposure. *J Geochem Explor* 179:25–35. <http://grafar.grf.bg.ac.rs/handle/123456789/821>
- Perez-Hernandez H, Fernandez-Luqueno F, Huerta-Lwanga E, Huerta-Lwanga D (2017) Layer-specific spatial prediction of As concentration in copper smelter vicinity considering the terrain exposure. *J Geochem Explor* 179:25–35. <http://grafar.grf.bg.ac.rs/handle/123456789/821>
- Perez-Hernandez H, Fernandez-Luqueno F, Huerta-Lwanga E, Huerta-Lwanga D (2017) Layer-specific spatial prediction of As concentration in copper smelter vicinity considering the terrain exposure. *J Geochem Explor* 179:25–35. <http://grafar.grf.bg.ac.rs/handle/123456789/821>
- Perez-Hernandez H, Fernandez-Luqueno F, Huerta-Lwanga E, Huerta-Lwanga D (2017) Layer-specific spatial prediction of As concentration in copper smelter vicinity considering the terrain exposure. *J Geochem Explor* 179:25–35. <http://grafar.grf.bg.ac.rs/handle/123456789/821>
- Perez-Hernandez H, Fernandez-Luqueno F, Huerta-Lwanga E, Huerta-Lwanga D (2017) Layer-specific spatial prediction of As concentration in copper smelter vicinity considering the terrain exposure. *J Geochem Explor* 179:25–35. <http://grafar.grf.bg.ac.rs/handle/123456789/821>
- Perez-Hernandez H, Fernandez-Luqueno F, Huerta-Lwanga E, Huerta-Lwanga D (2017) Layer-specific spatial prediction of As concentration in copper smelter vicinity considering the terrain exposure. *J Geochem Explor* 179:25–35. <http://grafar.grf.bg.ac.rs/handle/123456789/821>
- Perez-Hernandez H, Fernandez-Luqueno F, Huerta-Lwanga E, Huerta-Lwanga D (2017) Layer-specific spatial prediction of As concentration in copper smelter vicinity considering the terrain exposure. *J Geochem Explor* 179:25–35. <http://grafar.grf.bg.ac.rs/handle/123456789/821>
- Perez-Hernandez H, Fernandez-Luqueno F, Huerta-Lwanga E, Huerta-Lwanga D (2017) Layer-specific spatial prediction of As concentration in copper smelter vicinity considering the terrain exposure. *J Geochem Explor* 179:25–35. <http://grafar.grf.bg.ac.rs/handle/123456789/821>
- Perez-Hernandez H, Fernandez-Luqueno F, Huerta-Lwanga E, Huerta-Lwanga D (2017) Layer-specific spatial prediction of As concentration in copper smelter vicinity considering the terrain exposure. *J Geochem Explor* 179:25–35. <http://grafar.grf.bg.ac.rs/handle/123456789/821>
- Perez-Hernandez H, Fernandez-Luqueno F, Huerta-Lwanga E, Huerta-Lwanga D (2017) Layer-specific spatial prediction of As concentration in copper smelter vicinity considering the terrain exposure. *J Geochem Explor* 179:25–35. <http://grafar.grf.bg.ac.rs/handle/123456789/821>
- Perez-Hernandez H, Fernandez-Luqueno F, Huerta-Lwanga E, Huerta-Lwanga D (2017) Layer-specific spatial prediction of As concentration in copper smelter vicinity considering the terrain exposure. *J Geochem Explor* 179:25–35. <http://grafar.grf.bg.ac.rs/handle/123456789/821>
- Perez-Hernandez H, Fernandez-Luqueno F, Huerta-Lwanga E, Huerta-Lwanga D (2017) Layer-specific spatial prediction of As concentration in copper smelter vicinity considering the terrain exposure. *J Geochem Explor* 179:25–35. <http://grafar.grf.bg.ac.rs/handle/123456789/821>
- Perez-Hernandez H, Fernandez-Luqueno F, Huerta-Lwanga E, Huerta-Lwanga D (2017) Layer-specific spatial prediction of As concentration in copper smelter vicinity considering the terrain exposure. *J Geochem Explor* 179:25–35. <http://grafar.grf.bg.ac.rs/handle/123456789/821>
- Perez-Hernandez H, Fernandez-Luqueno F, Huerta-Lwanga E, Huerta-Lwanga D (2017) Layer-specific spatial prediction of As concentration in copper smelter vicinity considering the terrain exposure. *J Geochem Explor* 179:25–35. <http://grafar.grf.bg.ac.rs/handle/123456789/821>
- Perez-Hernandez H, Fernandez-Luqueno F, Huerta-Lwanga E, Huerta-Lwanga D (2017) Layer-specific spatial prediction of As concentration in copper smelter vicinity considering the terrain exposure. *J Geochem Explor* 179:25–35. <http://grafar.grf.bg.ac.rs/handle/123456789/821>
- Perez-Hernandez H, Fernandez-Luqueno F, Huerta-Lwanga E, Huerta-Lwanga D (2017) Layer-specific spatial prediction of As concentration in copper smelter vicinity considering the terrain exposure. *J Geochem Explor* 179:25–35. <http://grafar.grf.bg.ac.rs/handle/123456789/821>
- Perez-Hernandez H, Fernandez-Luqueno F, Huerta-Lwanga E, Huerta-Lwanga D (2017) Layer-specific spatial prediction of As concentration in copper smelter vicinity considering the terrain exposure. *J Geochem Explor* 179:25–35. <http://grafar.grf.bg.ac.rs/handle/123456789/821>
- Perez-Hernandez H, Fernandez-Luqueno F, Huerta-Lwanga E, Huerta-Lwanga D (2017) Layer-specific spatial prediction of As concentration in copper smelter vicinity considering the terrain exposure. *J Geochem Explor* 179:25–35. <http://grafar.grf.bg.ac.rs/handle/123456789/821>
- Perez-Hernandez H, Fernandez-Luqueno F, Huerta-Lwanga E, Huerta-Lwanga D (2017) Layer-specific spatial prediction of As concentration in copper smelter vicinity considering the terrain exposure. *J Geochem Explor* 179:25–35. <http://grafar.grf.bg.ac.rs/handle/123456789/821>
- Perez-Hernandez H, Fernandez-Luqueno F, Huerta-Lwanga E, Huerta-Lwanga D (2017) Layer-specific spatial prediction of As concentration in copper smelter vicinity considering the terrain exposure. *J Geochem Explor* 179:25–35. <http://grafar.grf.bg.ac.rs/handle/123456789/821>
- Perez-Hernandez H, Fernandez-Luqueno F, Huerta-Lwanga E, Huerta-Lwanga D (2017) Layer-specific spatial prediction of As concentration in copper smelter vicinity considering the terrain exposure. *J Geochem Explor* 179:25–35. <http://grafar.grf.bg.ac.rs/handle/123456789/821>
- Perez-Hernandez H, Fernandez-Luqueno F, Huerta-Lwanga E, Huerta-Lwanga D (2017) Layer-specific spatial prediction of As concentration in copper smelter vicinity considering the terrain exposure. *J Geochem Explor* 179:25–35. <http://grafar.grf.bg.ac.rs/handle/123456789/821>
- Perez-Hernandez H, Fernandez-Luqueno F, Huerta-Lwanga E, Huerta-Lwanga D (2017) Layer-specific spatial prediction of As concentration in copper smelter vicinity considering the terrain exposure. *J Geochem Explor* 179:25–35. <http://grafar.grf.bg.ac.rs/handle/123456789/821>
- Perez-Hernandez H, Fernandez-Luqueno F, Huerta-Lwanga E, Huerta-Lwanga D (2017) Layer-specific spatial prediction of As concentration in copper smelter vicinity considering the terrain exposure. *J Geochem Explor* 179:25–35. <http://grafar.grf.bg.ac.rs/handle/123456789/821>
- Perez-Hernandez H, Fernandez-Luqueno F, Huerta-Lwanga E, Huerta-Lwanga D (2017) Layer-specific spatial prediction of As concentration in copper smelter vicinity considering the terrain exposure. *J Geochem Explor* 179:25–35. <http://grafar.grf.bg.ac.rs/handle/123456789/821>
- Perez-Hernandez H, Fernandez-Luqueno F, Huerta-Lwanga E, Huerta-Lwanga D (2017) Layer-specific spatial prediction of As concentration in copper smelter vicinity considering the terrain exposure. *J Geochem Explor* 179:25–35. <http://grafar.grf.bg.ac.rs/handle/123456789/821>
- Perez-Hernandez H, Fernandez-Luqueno F, Huerta-Lwanga E, Huerta-Lwanga D (2017) Layer-specific spatial prediction of As concentration in copper smelter vicinity considering the terrain exposure. *J Geochem Explor* 179:25–35. <http://grafar.grf.bg.ac.rs/handle/123456789/821>
- Perez-Hernandez H, Fernandez-Luqueno F, Huerta-Lwanga E, Huerta-Lwanga D (2017) Layer-specific spatial prediction of As concentration in copper smelter vicinity considering the terrain exposure. *J Geochem Explor* 179:25–35. <http://grafar.grf.bg.ac.rs/handle/123456789/821>
- Perez-Hernandez H, Fernandez-Luqueno F, Huerta-Lwanga E, Huerta-Lwanga D (2017) Layer-specific spatial prediction of As concentration in copper smelter vicinity considering the terrain exposure. *J Geochem Explor* 179:25–35. <http://grafar.grf.bg.ac.rs/handle/123456789/821>
- Perez-Hernandez H, Fernandez-Luqueno F, Huerta-Lwanga E, Huerta-Lwanga D (2017) Layer-specific spatial prediction of As concentration in copper smelter vicinity considering the terrain exposure. *J Geochem Explor* 179:25–35. <http://grafar.grf.bg.ac.rs/handle/123456789/821>
- Perez-Hernandez H, Fernandez-Luqueno F, Huerta-Lwanga E, Huerta-Lwanga D (2017) Layer-specific spatial prediction of As concentration in copper smelter vicinity considering the terrain exposure. *J Geochem Explor* 179:25–35. <http://grafar.grf.bg.ac.rs/handle/123456789/821>
- Perez-Hernandez H, Fernandez-Luqueno F, Huerta-Lwanga E, Huerta-Lwanga D (2017) Layer-specific spatial prediction of As concentration in copper smelter vicinity considering the terrain exposure. *J Geochem Explor* 179:25–35. <http://grafar.grf.bg.ac.rs/handle/123456789/821>
- Perez-Hernandez H, Fernandez-Luqueno F, Huerta-Lwanga E, Huerta-Lwanga D (2017) Layer-specific spatial prediction of As concentration in copper smelter vicinity considering the terrain exposure. *J Geochem Explor* 179:25–35. <http://grafar.grf.bg.ac.rs/handle/123456789/821>
- Perez-Hernandez H, Fernandez-Luqueno F, Huerta-Lwanga E, Huerta-Lwanga D (2017) Layer-specific spatial prediction of As concentration in copper smelter vicinity considering the terrain exposure. *J Geochem Explor* 179:25–35. <http://grafar.grf.bg.ac.rs/handle/123456789/821>
- Perez-Hernandez H, Fernandez-Luqueno F, Huerta-Lwanga E, Huerta-Lwanga D (2017) Layer-specific spatial prediction of As concentration in copper smelter vicinity considering the terrain exposure. *J Geochem Explor* 179:25–35. <http://grafar.grf.bg.ac.rs/handle/123456789/821>
- Perez-Hernandez H, Fernandez-Luqueno F, Huerta-Lwanga E, Huerta-Lwanga D (2017) Layer-specific spatial prediction of As concentration in copper smelter vicinity considering the terrain exposure. *J Geochem Explor* 179:25–35. <http://grafar.grf.bg.ac.rs/handle/123456789/821>
- Perez-Hernandez H, Fernandez-Luqueno F, Huerta-Lwanga E, Huerta-Lwanga D (2017) Layer-specific spatial prediction of As concentration in copper smelter vicinity considering the terrain exposure. *J Geochem Explor* 179:25–35. <http://grafar.grf.bg.ac.rs/handle/123456789/821>
- Perez-Hernandez H, Fernandez-Luqueno F, Huerta-Lwanga E, Huerta-Lwanga D (2017) Layer-specific spatial prediction of As concentration in copper smelter vicinity considering the terrain exposure. *J Geochem Explor* 179:25–35. <http://grafar.grf.bg.ac.rs/handle/123456789/821>
- Perez-Hernandez H, Fernandez-Luqueno F, Huerta-Lwanga E, Huerta-Lwanga D (2017) Layer-specific spatial prediction of As concentration in copper smelter vicinity considering the terrain exposure. *J Geochem Explor* 179:25–35. <http://grafar.grf.bg.ac.rs/handle/123456789/821>
- Perez-Hernandez H, Fernandez-Luqueno F, Huerta-Lwanga E, Huerta-Lwanga D (2017) Layer-specific spatial prediction of As concentration in copper smelter vicinity considering the terrain exposure. *J Geochem Explor* 179:25–35. <http://grafar.grf.bg.ac.rs/handle/123456789/821>
- Perez-Hernandez H, Fernandez-Luqueno F, Huerta-Lwanga E, Huerta-Lwanga D (2017) Layer-specific spatial prediction of As concentration in copper smelter vicinity considering the terrain exposure. *J Geochem Explor* 179:25–35. <http://grafar.grf.bg.ac.rs/handle/123456789/821>
- Perez-Hernandez H, Fernandez-Luqueno F, Huerta-Lwanga E, Huerta-Lwanga D (2017) Layer-specific spatial prediction of As concentration in copper smelter vicinity considering the terrain exposure. *J Geochem Explor* 179:25–35. <http://grafar.grf.bg.ac.rs/handle/123456789/821>
- Perez-Hernandez H, Fernandez-Luqueno F, Huerta-Lwanga E, Huerta-Lwanga D (2017) Layer-specific spatial prediction of As concentration in copper smelter vicinity considering the terrain exposure. *J Geochem Explor* 179:25–35. <http://grafar.grf.bg.ac.rs/handle/123456789/821>
- Perez-Hernandez H, Fernandez-Luqueno F, Huerta-Lwanga E, Huerta-Lwanga D (2017) Layer-specific spatial prediction of As concentration in copper smelter vicinity considering the terrain exposure. *J Geochem Explor* 179:25–35. <http://grafar.grf.bg.ac.rs/handle/123456789/821>
- Perez-Hernandez H, Fernandez-Luqueno F, Huerta-Lwanga E, Huerta-Lwanga D (2017) Layer-specific spatial prediction of As concentration in copper smelter vicinity considering the terrain exposure. *J Geochem Explor* 179:25–35. <http://grafar.grf.bg.ac.rs/handle/123456789/821>
- Perez-Hernandez H, Fernandez-Luqueno F, Huerta-Lwanga E, Huerta-Lwanga D (2017) Layer-specific spatial prediction of As concentration in copper smelter vicinity considering the terrain exposure. *J Geochem Explor* 179:25–35. <http://grafar.grf.bg.ac.rs/handle/123456789/821>
- Perez-Hernandez H, Fernandez-Luqueno F, Huerta-Lwanga E, Huerta-Lwanga D (2017) Layer-specific spatial prediction of As concentration in copper smelter vicinity considering the terrain exposure. *J Geochem Explor* 179:25–35. <http://grafar.grf.bg.ac.rs/handle/123456789/821>
- Perez-Hernandez H, Fernandez-Luqueno F, Huerta-Lwanga E, Huerta-Lwanga D (2017) Layer-specific spatial prediction of As concentration in copper smelter vicinity considering the terrain exposure. *J Geochem Explor* 179:25–35. <http://grafar.grf.bg.ac.rs/handle/123456789/821>
- Perez-Hernandez H, Fernandez-Luqueno F, Huerta-Lwanga E, Huerta-Lwanga D (2017) Layer-specific spatial prediction of As concentration in copper smelter vicinity considering the terrain exposure. *J Geochem Explor* 179:25–35. <http://grafar.grf.bg.ac.rs/handle/123456789/821>
- Perez-Hernandez H, Fernandez-Luqueno F, Huerta-Lwanga E, Huerta-Lwanga D (2017) Layer-specific spatial prediction of As concentration in copper smelter vicinity considering the terrain exposure. *J Geochem Explor* 179:25–35. <http://grafar.grf.bg.ac.rs/handle/123456789/821>
- Perez-Hernandez H, Fernandez-Luqueno F, Huerta-Lwanga E, Huerta-Lwanga D (2017) Layer-specific spatial prediction of As concentration in copper smelter vicinity considering the terrain exposure. *J Geochem Explor* 179:25–35. <http://grafar.grf.bg.ac.rs/handle/123456789/821>
- Perez-Hernandez H, Fernandez-Luqueno F, Huerta-Lwanga E, Huerta-Lwanga D (2017) Layer-specific spatial prediction of As concentration in copper smelter vicinity considering the terrain exposure. *J Geochem Explor* 179:25–35. <http://grafar.grf.bg.ac.rs/handle/123456789/821>
- Perez-Hernandez H, Fernandez-Luqueno F, Huerta-Lwanga E, Huerta-Lwanga D (2017) Layer-specific spatial prediction of As concentration in copper smelter vicinity considering the terrain exposure. *J Geochem Explor* 179:25–35. <http://grafar.grf.bg.ac.rs/handle/123456789/821>
- Perez-Hernandez H, Fernandez-Luqueno F, Huerta-Lwanga E, Huerta-Lwanga D (2017) Layer-specific spatial prediction of As concentration in copper smelter vicinity considering the terrain exposure. *J Geochem Explor* 179:25–35. <http://grafar.grf.bg.ac.rs/handle/123456789/821>
- Perez-Hernandez H, Fernandez-Luqueno F, Huerta-Lwanga E, Huerta-Lwanga D (2017) Layer-specific spatial prediction of As concentration in copper smelter vicinity considering the terrain exposure. *J Geochem Explor* 179:25–35. <http://grafar.grf.bg.ac.rs/handle/123456789/821>
- Perez-Hernandez H, Fernandez-Luqueno F, Huerta-Lwanga E, Huerta-Lwanga D (2017) Layer-specific spatial prediction of As concentration in copper smelter vicinity considering the terrain exposure. *J Geochem Explor* 179:25–35. <http://grafar.grf.bg.ac.rs/handle/123456789/821>
- Perez-Hernandez H, Fernandez-Luqueno F, Huerta-Lwanga E, Huerta-Lwanga D (2017) Layer-specific spatial prediction of As concentration in copper smelter vicinity considering the terrain exposure. *J Geochem Explor* 179:25–35. <http://grafar.grf.bg.ac.rs/handle/123456789/821>
- Perez-Hernandez H, Fernandez-Luqueno F, Huerta-Lwanga E, Huerta-Lwanga D (2017) Layer-specific spatial prediction of As concentration in copper smelter vicinity considering the terrain exposure. *J Geochem Explor* 179:25–35. <http://grafar.grf.bg.ac.rs/handle/123456789/821>
- Perez-Hernandez H, Fernandez-Luqueno F, Huerta-Lwanga E, Huerta-Lwanga D (2017) Layer-specific spatial prediction of As concentration in copper smelter vicinity considering the terrain exposure. *J Geochem Explor* 179:25–35. <http://grafar.grf.bg.ac.rs/handle/123456789/821>
- Perez-Hernandez H, Fernandez-Luqueno F, Huerta-Lwanga E, Huerta-Lwanga D (2017) Layer-specific spatial prediction of As concentration in copper smelter vicinity considering the terrain exposure. *J Geochem Explor* 179:25–35. <http://grafar.grf.bg.ac.rs/handle/123456789/821>
- Perez-Hernandez H, Fernandez-Luqueno F, Huerta-Lwanga E, Huerta-Lwanga D (2017) Layer-specific spatial prediction of As concentration in copper smelter vicinity considering the terrain exposure. *J Geochem Explor* 179:25–35. <http://grafar.grf.bg.ac.rs/handle/123456789/821>
- Perez-Hernandez H, Fernandez-Luqueno F, Huerta-Lwanga E, Huerta-Lwanga D (2017) Layer-specific spatial prediction of As concentration in copper smelter vicinity considering the terrain exposure. *J Geochem Explor* 179:25–35. <http://grafar.grf.bg.ac.rs/handle/123456789/821>
- Perez-Hernandez H, Fernandez-Luqueno F, Huerta-Lwanga E, Huerta-Lwanga D (2017) Layer-specific spatial prediction of As concentration in copper smelter vicinity considering the terrain exposure. *J Geochem Explor* 179:25–35. <http://grafar.grf.bg.ac.rs/handle/123456789/821>
- Perez-Hernandez H, Fernandez-Luqueno F, Huerta-Lwanga E, Huerta-Lwanga D (2017) Layer-specific spatial prediction of As concentration in copper smelter vicinity considering the terrain exposure. *J Geochem Explor* 179:25–35. <http://grafar.grf.bg.ac.rs/handle/123456789/821>
- Perez-Hernandez H, Fernandez-Luqueno F, Huerta-Lwanga E, Huerta-Lwanga D (2017) Layer-specific spatial prediction of As concentration in copper smelter vicinity considering the terrain exposure. *J Geochem Explor* 179:25–35. <http://grafar.grf.bg.ac.rs/handle/123456789/821>
- Perez-Hernandez H, Fernandez-Luqueno F, Huerta-Lwanga E, Huerta-Lwanga D (2017) Layer-specific spatial prediction of As concentration in copper smelter vicinity considering the terrain exposure. *J Geochem Explor* 179:25–35. <http://grafar.grf.bg.ac.rs/handle/123456789/821>
- Perez-Hernandez H, Fernandez-Luqueno F, Huerta-Lwanga E, Huerta-Lwanga D (2017) Layer-specific spatial prediction of As concentration in copper smelter vicinity considering the terrain exposure. *J Geochem Explor* 179:25–35. <http://grafar.grf.bg.ac.rs/handle/123456789/821>
- Perez-Hernandez H, Fernandez-Luqueno F, Huerta-Lwanga E, Huerta-Lwanga D (2017) Layer-specific spatial prediction of As concentration in copper smelter vicinity considering the terrain exposure. *J Geochem Explor* 179:25–35. <http://grafar.grf.bg.ac.rs/handle/123456789/821>
- Perez-Hernandez H, Fernandez-Luqueno F, Huerta-Lwanga E, Huerta-Lwanga D (2017) Layer-specific spatial prediction of As concentration in copper smelter vicinity considering the terrain exposure. *J Geochem Explor* 179:25–35. <http://grafar.grf.bg.ac.rs/handle/123456789/821>
- Perez-Hernandez H, Fernandez-Luqueno F, Huerta-Lwanga E, Huerta-Lwanga D (2017) Layer-specific spatial prediction of As concentration in copper smelter vicinity considering the terrain exposure. *J Geochem Explor* 179:25–35. <http://grafar.grf.bg.ac.rs/handle/123456789/821>
- Perez-Hernandez H, Fernandez-Luqueno F, Huerta-Lwanga E, Huerta-Lwanga D (2017) Layer-specific spatial prediction of As concentration in copper smelter vicinity considering the terrain exposure. *J Geochem Explor* 179:25–35. <http://grafar.grf.bg.ac.rs/handle/123456789/821>
- Perez-Hernandez H, Fernandez-Luqueno F, Huerta-Lwanga E, Huerta-Lwanga D (2017) Layer-specific spatial prediction of As concentration in copper smelter vicinity considering the terrain exposure. *J Geochem Explor* 179:25–35. <http://grafar.grf.bg.ac.rs/handle/123456789/821>
- Perez-Hernandez H, Fernandez-Luqueno F, Huerta-Lwanga E, Huerta-Lwanga D (2017) Layer-specific spatial prediction of As concentration in copper smelter vicinity considering the terrain exposure. *J Geochem Explor* 179:25–35. <http://grafar.grf.bg.ac.rs/handle/123456789/821>
- Perez-Hernandez H, Fernandez-Luqueno F, Huerta-Lwanga E, Huerta

- perspectives. In: Taleisnik E, Lavado RS (eds) *Saline and Alkaline soils in Latin America*. Springer, Cham. https://doi.org/10.1007/978-3-030-52592-7_1
- Poeplau C, Sigurdsson P, Sigurdsson BD (2020) Depletion of soil carbon and aggregation after strong warming of a subarctic Andosol under forest and grassland cover. *SOIL* 6:115–129. <https://doi.org/10.5194/soil-6-115-2020,2020>
- Poeplau C, Don A, Six J, Kaiser M, Benbi D, Chenu C, Croturo F, Derrien D, Gioacchini P, Grand S, Gregorich E, Griepentrog M, Gunina A, Haddix M, Kuzyakov Y, Kühnel A, Macdonald LM, Soong J, Trigalet S, Vermeire M-L, Rovira P, Wesemael B, Wiesmeier M, Yeasmin S, Yevdokimov I, Nieder R (2018) Isolating organic carbon fractions with varying turnover rates in temperate agricultural soils: a comprehensive method comparison. *Soil Biol Biochem* 125:10–26. <https://doi.org/10.1016/j.soilbio.2018.06.025>
- Poláková Š, Sánka M, Vácha R (2018) Chapter II/39: assessment of contaminants in agricultural soils in the Czech Republic. In: Sychev VG, Mueller L (eds) *Novel methods and results of landscape research in Europe, Central Asia and Siberia, vol II understanding and monitoring processes in soils and water bodies*. © FSBI “VNII Agrochemistry”, pp. 185–189. <https://doi.org/10.25680/7849.2018.50.65.136>. <https://vniia-pr.ru/monografii/pdf/tom2-39.pdf>
- Popov A, Kholostov G, Sazanova E, Simonova J, Tsvika K (2020) Characteristics of the qualitative composition of soil organic matter: problems and solutions. *Zemljiste i Biljka* 69(2):26–37. http://www.sdpz.rs/images/casopis/2020/zib_69_2_72.pdf
- Posch M, Kauppi L (1991) Potential for acidification of forest soils in Europe. In: Brouwer FM, Thomas AJ, Chadwick MJ (eds) *Land use changes in Europe*. The GeoJournal Library, vol 18. Springer, Dordrecht. https://doi.org/10.1007/978-94-011-3290-9_15
- Posch M, Reinds GJ (2009) A very simple dynamic soil acidification model for scenario analyses and target load calculations. *Environ Model Softw* 24 (2009):329–340
- Potapov AM, Klarner B, Sandmann D, Widyastuti R, Scheu S (2019) Linking size spectrum, energy flux and trophic multifunctionality in soil food webs of tropical land-use systems. *J Anim Ecol*. <https://doi.org/10.1111/1365-2656.13027>
- Prater I, Zubrzycki S, Buegger F, Zoor-Füllgraff LC, Angst G, Dannenmann M, Mueller CW (2020) From fibrous plant residues to mineral-associated organic carbon the fate of organic matter in Arctic permafrost soils. *Biogeosciences* 17:3367–3383. <https://doi.org/10.5194/bg-17-3367-2020>
- Prathamratana L, Kim R, Kim K (2020) Lead contamination of the mining and smelting district in Mitrovica, Kosovo. *Environ Geochem Health* 42:1033–1044. <https://doi.org/10.1007/s10653-018-0186-9>
- Preetha PP, Al-Hamdan AZ (2020) Developing nitrate-nitrogen transport models using remotely-sensed geospatial data of soil moisture profiles and wet depositions. *J Environ Sci Health, Part A* 55(5):615–628. <https://doi.org/10.1080/10934529.2020.1724503>
- Pretty J (2018) Intensification for redesigned and sustainable agricultural systems. *Science* 362(6417): eaav0294. <https://doi.org/10.1126/science.aav0294>
- Prince SD, Podwojewski P (2020) Desertification: inappropriate images lead to inappropriate actions. *Land Degrad Develop* 31(6):677–682. <https://doi.org/10.1002/ldr.3436>
- Pullin AS (2002) *Conservation biology*. Cambridge University Press. ISBN 978–0–521–64482–2
- Qi Y, Ossowicki A, Yang X, Lwanga EH, Dini-Andreote F, Geissen V, Garbeva P (2020) Effects of plastic mulch film residues on wheat rhizosphere and soil properties. <https://doi.org/10.1016/j.jhazmat.2019.121711>
- Qin P, Wang H, Yang X, He L, Müller K, Shaheen SM, Xu S, Rinklebe J, Tsang DCW, Ok YS, Bolan N, Zhaoliang S, Che L, Xu X (2018) Bamboo- and pig derived biochars reduce leaching losses of dibutyl phthalate, cadmium, and lead from co-contaminated soils. *Chemosphere* 198:450–459. <https://doi.org/10.1016/j.chemosphere.2018.01.162>
- Ragab R (2015) Integrated management tool for water, crop, soil and N-fertilizers: the SALTMED model. *Irrig Drain* 64:1–12
- Raheem A, Sikarwar VS, He J, Dastyar W, Dionysiou DD, Wang W, Zhao M (2018) Opportunities and challenges in sustainable treatment and resource reuse of sewage sludge: a Review. *Chem Eng J* 337:616–641. <https://doi.org/10.1016/j.cej.2017.12.149>
- Rajkovic S, Bornhöft NA, van der Weijden R, Nowack B, Adam V (2020) Dynamic probabilistic material flow analysis of engineered nanomaterials in European waste treatment systems. <https://doi.org/10.1016/j.wasman.2020.05.032>
- Ramesh T, Bolan NS, Kirkham MB, Wijesekara H, Kanchikerimath M, Rao CS, Sandeep S, Rinklebe J, Ok YS, Choudhury BU, Wang H, Tang C, Wang X, Song Z, Freeman OW (2019) Soil organic carbon dynamics: impact of land use changes and management practices: a review. *Adv Agron* 159(156):1–107
- Rao PSC, Jessup RE (1982) Development and verification of simulation models for describing pesticide dynamics in soils. *Ecol Modell* 16(1):67–75. [https://doi.org/10.1016/0304-3800\(82\)90073-4](https://doi.org/10.1016/0304-3800(82)90073-4)
- Rashmi I, Roy T, Kartika KS, Pal R, Coumar V, Kala S, Shinoji KC (2020) Organic and inorganic fertilizer contaminants in agriculture: impact on soil and water resources. In: Naem M, Ansari A, Gill S (eds) *Contaminants in agriculture*. Springer, Cham, pp 3–41. https://doi.org/10.1007/978-3-030-41552-5_1
- Reicosky DC, Lindstrom MJ, Schumacher TE (2005) Tillage induced CO₂ loss across an eroded landscape. *Soil Tillage Res* 81:183–194
- Reimann C, Filzmoser P, Garrett RG (2005) Background and threshold: critical comparison of methods of determination. *Sci Total Environ* 346(1–3):1–16. <https://doi.org/10.1016/j.scitotenv.2004.11.023>

- Richards LA (ed) (1954) Diagnosis and improvement of saline and alkali soils. Agricultural hand book 60. U.S. Dept. of Agriculture, Washington D.C., 160 p
- Ricketts MP, Matamala R, Jastrow JD, Antonopoulos DA, Koval J, Ping C-L, Liang C, Gonzalez-Meler MA (2020) The effects of warming and soil chemistry on bacterial community structure in Arctic tundra soils. *Soil Biol Biochem* 148:107882. <https://doi.org/10.1016/j.soilbio.2020.107882>
- Rinklebe J, Shaheen SM, Frohne T (2016a) Amendment of biochar reduces the release of toxic elements under dynamic redox conditions in a contaminated floodplain soil. *Chemosphere* 142:41–47
- Rinklebe J, Shaheen SM, Schroeter F, Rennert T (2016b) Exploiting biogeochemical and spectroscopic techniques to assess the geochemical distribution and release dynamics of chromium and lead in a contaminated floodplain soil. *Chemosphere* 150:390–397
- Rinklebe J, Antoniadis V, Shaheena SM, Rosche O, Altermann M (2019) Health risk assessment of potentially toxic elements in soils along the Central Elbe River, Germany. *Environ Int* 126:76–88. <https://doi.org/10.1016/j.envint.2019.02.011>
- Ritz K, van der Putten WH (2012) The living soil and ecosystem services. In: Wall DH (ed) *Soil ecology and ecosystem services*. Oxford University Press, UK, pp 5–7
- Robson AD (1989) *Soil acidity and plant growth*. Academic Press, Sydney, pp 139–165
- Rodríguez L, Macías F (2006) Eutrophication trends in forest soils in Galicia (NW Spain) caused by the atmospheric deposition of nitrogen compounds. *Chemosphere* 63(9):1598–1609. <https://doi.org/10.1016/j.chemosphere.2005.08.072>
- Rodríguez-Eugenio N, McLaughlin M, Pennock D (2018) *Soil Pollution: a hidden reality*. FAO, Rome, p 142
- Romanenkov VA, Rukhovich OV, Belichenko MV (2021) Chapter 21: ggeographical network of long-term experiments with fertilizers in the agroecological monitoring system of Russia. In: Mueller L, Sychev VG, Dronin NM, Eulenstein F (2021) (eds) *Exploring and optimizing agricultural landscapes*. Innovations in landscape research. Springer, Cham, in print ISBN 978–3–030–67448–9
- Römbke J, Jänsch S, Didden W (2005) The use of earthworms in ecological soil classification and assessment concepts. *Ecotoxicol Environ Safety* 62(2):249–265
- Römbke J (2018) Chapter I/71: monitoring the biological quality of soil based on the structure and functions of soil organism communities. In: Sychev VG, Mueller L (eds) *Novel methods and results of landscape research in Europe, Central Asia and Siberia, vol I landscapes in the 21th Century: status analyses, basic processes and research concepts*. © FSBI “VNII Agrochemistry”, pp 367–372. <https://doi.org/10.25680/1244.2018.27.50.071>. <https://vniia-pr.ru/monografii/pdf/tom1-71.pdf>
- Roy J, Ojha PK, Carnesecchi E, Lombardo A, Roy K, Benfenati E (2020) First report on a classification-based QSAR model for chemical toxicity to earthworm. *J Hazardous Mater* 386:121660. <https://doi.org/10.1016/j.jhazmat.2019.121660>
- Rozanova OL, Tsurikov SM, Tiunov AV, Semenina EE (2019) Arthropod rain in a temperate forest: intensity and composition. *Pedobiologia* 75:52–56. *Analysis. Sustainability* 12:2071. <https://doi.org/10.3390/su12052071>
- Rubio F, Nieves-Cordones M, Horie T, Shabala S (2020) Doing ‘business as usual’ comes with a cost: evaluating energy cost of maintaining plant intracellular K⁺ homeostasis under saline conditions. *New Phytologist* 225(3):1097–1104 <https://doi.org/10.1111/nph.15852>
- Rupp H, Rinklebe J, Bolze S, Meissner R (2010) A scale-dependent approach to study pollution control processes in wetland soils using three different techniques. *Ecol Eng* 36:1439–1447
- Saha JK, Selladurai R, Coumar MV, Dotaniya ML, Kundu S, Patra AK (2017) *Soil pollution-an emerging threat to agriculture*. Springer Singapore. Print ISBN: 978–981–10–4273–7, Electronic ISBN: 978–981–10–4274–4
- Saiko TA, Zonn IS (1997) Europe’s First Desert. In: Glantz MH, Zonn IS (eds) *Scientific, environmental, and political issues in the circum-caspian Region*. NATO ASI Series (Series 2: Environment), vol 29. Springer, Dordrecht. https://doi.org/10.1007/978-94-011-5502-1_13
- Saljnikov E, Čakmak D, Akshalov K, Mrvic V (2009) Effect of different cropping technologies on SOM in chernozem of semi-arid zone. *Zemljiste I Biljka* 58(1):25–34
- Saljnikov E, Čakmak D, Muhanbet A, Kresovic M (2014) Biological indices of soil organic matter in long-term fertilization experiment. *Zemljiste i Biljka* 63(2):11–20
- Saljnikov E, Mrvic V, Čakmak D, Jaramaz D, Perovic V, Antic-Mladenovic S, Pavlović P (2019) Pollution indices and sources apportionment of heavy metal pollution of agricultural soils near the thermal power plant. *Environ Geochem Health* 5–15. <https://doi.org/10.1007/s10653-019-00281-y> Online ISSN 1573-2983
- Saljnikov E, Čakmak D, Rahimgalieva S (2013) Soil organic matter stability as affected by land management in steppe ecosystem. Chapter 10. In: Hernandez Soriano MC (ed) *Soil processes and current trends in quality assessment*. Belgium, INTECH Open Access Publisher, pp 269–310. ISBN 980–953–307–671–8. p. 434
- Saljnikov E, Rakhimgaliyeva S, Raymbek A, Tosic S, Mrvic V, Sikiric B, Pachikin K (2015) Effect of fallowing on soil organic matter characteristics on wheat monoculture in arid steppes of northern Kazakhstan. *Zemljiste i Biljka* 64(2):17–26 http://www.sdpz.rs/images/casopis/2015/ZIB_vol64_no2_2015_pp17-26.pdf
- Saljnikov-Karbozova E, Funakawa S, Akhmetov K, Kosaki T (2004) Soil organic matter status of Mollisols soil in North Kazakhstan: effects of summer fallow. *Soil Biol Biochem* 36:1373–1381

- Sánchez-Otero MG, Quintana-Castro R, Domínguez-Chávez JG, Peña-Montes C, Oliart-Ros RM (2019) Unique microorganisms inhabit extreme soils. In: Kumar , Sharma S (eds) *Microbes and enzymes in soil health and bioremediation, microorganisms for sustainability*, vol 16. Springer, Singapore. https://doi.org/10.1007/978-981-13-9117-0_3
- Sanders D (2020) The salinity challenge. *New Phytol* 225 (3):1047–1048. <https://doi.org/10.1111/nph.16357>
- Santini M, Caccamo G, Laurenti A (2010) A multi-component GIS framework for desertification risk assessment by an integrated index. *Appl Geogr* 30 (3):394–415
- Saparov A, Dzalankuzov T, Umbetayev I, Suleimenov B (2008) Effect of irrigation on salinization of light grey soils. *Soil Science and Agrochemistry* 3:72–76 (In Russian: Влияние орошения на засоление светлых сероземов. *Почвоведение и агрохимия* 2008, 3:72–76)
- Saparov A (2014) Soil resources of the Republic of Kazakhstan: current status, problems and solutions. In: Mueller L, Saparov A, Lischeid G (eds) *Novel measurement and assessment tools for monitoring and management of land and water resources in agricultural landscapes of Central Asia*. Environmental science and engineering. Springer, Cham. https://doi.org/10.1007/978-3-319-01017-5_2
- Sartori M, Philippidis G, Ferrari E, Borrelli P, Lugatod E, Montanarella L, Panagos P (2019) A linkage between the biophysical and the economic: Assessing the global market impacts of soil erosion. *Land Use Policy* 86:299–312. <https://doi.org/10.1016/j.landusepol.2019.05.014>
- Satapute P, Kamble MV, Adhikari SS, Jogaiah S (2019) Influence of triazole pesticides on tillage soil microbial populations and metabolic changes. *Sci Total Environ* 651:2334–2344. <https://doi.org/10.1016/j.scitotenv.2018.10.099>
- Sauve G, Van Acker K (2020) The environmental impacts of municipal solid waste landfills in Europe: a life cycle assessment of proper reference cases to support decision making. *J Environ Managem* 261:110216. <https://doi.org/10.1016/j.jenvman.2020.110216>
- Schauss K, Focks A, Heuer H, Kotzerke A, Schmitt H, Thiele-Bruhn S, Smalla K, Wilke BM, Matthies M, Amelung W, Klasmeier J, Schloter M (2009) Analysis, fate and effects of the antibiotic sulfadiazine in soil ecosystems. *TrAC Trends Anal Chem* 28(5):612–618. <https://doi.org/10.1016/j.trac.2009.02.009>
- Scheffczyk A, Floate K, Blanckenhorn W, Dühring R-A, Klockner A, Lahr J, Lumaret J-B, Salamon J-A, Tixier T, Wohde M, Römbke J (2016) Non-target effects of ivermectin residues on earthworms and springtails dwelling beneath dung of treated cattle: examination in a ringtest in four countries. *Environ Toxicol Chem* 35:1959–1969
- Scherber C, Eisenhauer N, Weisser WW, Schmid B, Voigt W, Fischer M, Schulze ED, Roscher C, Weigelt A, Allan E, Beler H, Bonkowski M, Buchmann N, Buscot F, Clement LW, Ebeling A, Engels C, Halle S, Kertscher I, Klein AM, Koller R, König S, Kowalski E, Kummer V, Kuu A, Lange M, Lauterbach D, Middelhoff C, Migunova VD, Milcu A, Müller R, Partsch S, Petermann JS, Renker C, Rottstock T, Sabais A, Scheu S, Schumacher J, Temper-ton VM, Tschardt T (2010) Bottom-up effects of plant diversity on multitrophic interactions in a biodiversity experiment. *Nature* 468:553–556
- Scherber C, Beduschi T, Tschardt T (2021a) Chapter 19: a grid-based sampling approach to insect biodiversity monitoring in agricultural landscapes. In: Mueller L, Sychev VG, Dronin NM, Eulenstein F (eds) *Exploring and optimizing agricultural landscapes*. Innovations in landscape research. Springer, Cham, in print ISBN 978–3–030–67448–9
- Scherber C, Brandmeier J, Everwand G, Karley AJ, Kiær LP, Meyer M, Ott D, Reininghaus H, Tschardt T (2021b) Chapter 20: using field experiments to inform biodiversity monitoring in wgricultural landscapes. In: Mueller L, Sychev VG, Dronin NM, Eulenstein F (eds) *Exploring and optimizing agricultural landscapes*. Innovations in landscape research. Springer, Cham, in print ISBN 978–3–030–67448–9
- Schmidt M, Torn M, Abiven S, Dittmar Z, Guggenberger G, Janssens IA, Kleber M, Kögel-Knabner I, Lehmann J, Manning DAC, Nannipieri P, Rasse DP, Weiner S, Trumbore SE (2011) Persistence of soil organic matter as an ecosystem property. *Nature* 478:49–56. <https://doi.org/10.1038/nature10386>
- Schmitz OJ, Leroux SJ (2020) Food webs and ecosystems: linking species interactions to the carbon cycle. *Ann Rev Ecol Syst* 51. <https://doi.org/10.1146/annurev-ecolsys-011720-104730>
- Schöler A, Jacquiod S, Vestergaard G, Schulz S, Schloter M (2017) Analysis of soil microbial communities based on amplicon sequencing of marker genes. *Biol Fert Soils* 53:485–489
- Scholten LC, Timmermans CWM (1995) Natural radioactivity in phosphate fertilizers. *Fert Res* 43:103–107. <https://doi.org/10.1007/BF00747688>
- Schoups G, Hopmans JW, Tanji KK (2006) Evaluation of model complexity and space–time resolution on the prediction of long-term soil salinity dynamics, western San Joaquin Valley, California. *Hydro Process* 20 (13):2647–2668. <https://doi.org/10.1002/hyp.6082>
- Schreiner V, Meyer BC (2014) Indicators of land degradation in steppe regions: soil and morphodynamics in the Northern Kulunda. In: Mueller L, Saparov A, Lischeid G (eds) *Novel measurement and assessment tools for monitoring and management of land and water resources in agricultural landscapes of Central Asia*. Environmental science and engineering. Springer, Cham. https://doi.org/10.1007/978-3-319-01017-5_33
- Schubert R (ed)(1985) *Bioindikation in terrestrischen Ökosystemen*. Gustav Fischer Verlag Jena, 327 pp
- Schuhmann A, Klammler G, Weiss S, Gans O, Fank J, Haberhauer G, Gerzabek MH (2019) Degradation and leaching of bentazone, terbuthylazine and S-metolachlor and some of their metabolites: A long-

- term lysimeter experiment. *Plant Soil Environ* 65: 273–281. <https://doi.org/10.17221/803/2018-PSE>
- Selivanovskaya SY, Galitskaya PY, Hung YT (2014) Chapter 12: the use of biological methods for toxicity evaluation of wastes and waste-amended soils. In: *Handbook of environment and waste management: land and groundwater pollution control*, pp 737–779
- Semenchuk PR, Krab EJ, Hedenström M, Phillips CA, Ancin-Murguzur FJ, Cooper EJ (2019) Soil organic carbon depletion and degradation in surface soil after long-term non-growing season warming in High Arctic Svalbard. *Sci Total Environ* 646:158–167. <https://doi.org/10.1016/j.scitotenv.2018.07.150>
- Shaddad SM, Buttafuoco G, Castrignano A (2020) Assessment and mapping of soil salinization risk in an Egyptian field using a probabilistic approach. *Agronomy* 10(1):85. <https://doi.org/10.3390/agronomy10010085>
- Shaheen SM, Rinklebe J, Rupp H, Meissner R (2014) Lysimeter trials to assess the impact of different flood-dry-cycles on the dynamics of pore water concentrations of As, Cr, Mo and V in a contaminated floodplain soil. *Geoderma* 228–229:5–13
- Sharma A, Kumar V, Shahzad B, Tanveer M, Singh Sidhu GP, Handa N, Kohli SK, Yadav P, Bali AS, Parihar RD, Dar OI, Singh K, Jasrotia S, Bakshi P, Ramakrishnan M, Kumar S, Bhardwaj R, Thukral AK (2019) Worldwide pesticide usage and its impacts on ecosystem. *Springer Nat Appl Sci* 1:1446. <https://doi.org/10.1007/s42452-019-1485-1>
- Sherrard ME, Elgersma K, Koos JMA, Kokemuller CM, Dietz HE, Glidden AJ, Carr CM, Cambardella CA (2019) Species composition influences soil nutrient depletion and plant physiology in prairie agroenergy feedstocks. *Ecosphere* 10(7):e02805. <https://doi.org/10.1002/ecs2.2805>
- Sheudzhen AK, Gutorova OA, Onishchenko LM, Isipov MA, Esipenko SV (2018) Chapter 170: microflora and biological activity of leached Chernozem in a plain agrolandscape after long-term application of mineral fertilizers (Микрофлора и биологическая активность чернозема выщелоченного равнинного агроландшафта при длительном применении минеральных удобрений) In: Sychev VG, Mueller L (eds) *Novel methods and results of landscape research in Europe, Central Asia and Siberia, vol I landscapes in the 21th century: status analyses, basic processes and Research Concepts*. © FSBI “VNI Agrochemistry” 2018, pp 362–367. <https://doi.org/10.25680/1533.2018.90.54.070>. <https://vniia-pr.ru/monografii/pdf/tom1-70.pdf>
- Shrivastava P, Kumar R (2015) Soil salinity: a serious environmental issue and plant growth promoting bacteria as one of the tools for its alleviation. *Saudi J Biol Sci* 22:123–131
- Shuang X, Zhang W, Hamza J (2019) A new model approach for reactive solute transport in dual-permeability media with depth-dependent reaction coefficients. *J Hydrol* 577:123946. <https://doi.org/10.1016/j.jhydrol.2019.123946>
- Silantyeva MM, Terekhina TA, Elesova NV, Ovcharova NV, Kornievskaya TV (2020) Possibility of natural steppe cover restoration and its biodiversity expansion. In: Frühauf M, Guggenberger G, Meinel T, Theesfeld I, Lentz S (eds) *KULUNDA: climate smart agriculture. Innovations in landscape research*. Springer, Cham. https://doi.org/10.1007/978-3-030-15927-6_30
- Silva V, Mol HGJ, Zomer P, Tienstra M, Ritsema CJ, Geissen V (2019) Pesticide residues in European agricultural soils: a hidden reality unfolded. *Sci Total Environ* 653:1532–1545. <https://www.sciencedirect.com/science/article/pii/S0048969718343420>
- Singh RP, Agrawal M (2007) Effect of sewage sludge amendmen on heavy metal accumulation and consequent responses of *Beta Vulgaris* plant. *Chemosphere* 67:2229–2240
- Singh BR (1998) Soil pollution and contamination. In: Lal R, Blum WH, Valentine C, Steward BA (eds) *Advances in soil science. Methods for assessment of soil degradation*. CRC Press Boca Raton, pp 279–299
- Six J, Bossuyt H, De Gryze S, Deneff K (2004) A history of research on the link between (micro) aggregates, soil biota, and soil organic matter dynamics. *Soil till Res* 79:7–31
- Sjerps RMA, Kooij PJJ, van Loon A, Van Wezel AP (2019) Occurrence of pesticides in Dutch drinking water sources. *Chemosphere* 235:510–518
- Smith B, Prentice IC, Sykes MT (2001) Representation of vegetation dynamics in the modelling of terrestrial ecosystems: comparing two contrasting approaches within European climate space. *Glob Ecol Biogeogr* 10:621–637. <https://doi.org/10.1046/j.1466-822X.2001.t01-1-00256.x>
- Smith JL, Doran JW (1997) Chapter 10. Measurement and use of pH and electrical conductivity for soil quality analysis. In: Doran JW, Jones AJ (eds) *Methods for assessing soil quality*, vol 49, pp 169–185. <https://doi.org/10.2136/sssaspecpub49.c10>
- Snakin VV, Krechetov PP, Kuzovnikova TA, Alyabina IO, Gurov AF, Stepichev AV (1996) The system of assessment of soil degradation. *Soil Technol* 8(4):331–343. [https://doi.org/10.1016/0933-3630\(95\)00028-3](https://doi.org/10.1016/0933-3630(95)00028-3)
- Snakin VV, Krechetov PP, Kuzovnikova TA, Minashina NG, Karpachevsky LO, Alyabina IO, Gurov AF, Melchenko V, Stepichev AV, Kazantseva OF, Ananyeva ND (1992) Soil degradation assessment system. Pushchino Scientific Centre of the Russian Academy of Sciences. Research Institute of Nature. p 20 (In Russian: Снакин В.В., Кречетов П.П., Кузовникова Т.А., Минашина Н.Г., Карпачевский Л.О., Алябина И.О., Гуров А.Ф., Мельченко В., Степичев А.В., Казанцева О.Ф., Ананьева Н.Д. Система оценки степени деградации почв. Пушкино, Пушкинский научный центр РАН. ВНИИ Природы.)
- Steffan JJ, Brevik EC, Burgess LC, Cerdà A (2018) The effect of soil on human health: an overview. *Eur J Soil*

- Sci 69(1):159–171. <https://doi.org/10.1111/ejss.12451>. Epub 2017 Jul 17. PMID: 29430209; PMCID: PMC5800787.
- Steinfeld S, Gerber P, Wassenaar T, Castel V, Rosales M, de Haan C (2006) “Livestock's long shadow: environmental issues and options”. Food and agriculture organization of the United Nations. <http://www.fao.org/3/a0701e/a0701e00.htm>. Accessed on 12 Sept 2020
- Sterk G, Stoorvogel JJ (2020) Desertification-scientific versus political realities. *Land* 2020(9):156. <https://doi.org/10.3390/land9050156>
- Stevnbak K, Scherber C, Gladbach DJ, Beier C, Mikkelsen TN, Christensen S (2012) Interactions between above- and belowground organisms modified in climate change experiments. *Nat Climate Change* 2:805–808
- Stott DE, Andrews SS, Liebig MA, Wienhold BJ, Karlen DL (2010) Evaluation of β-glucosidase activity as soil quality indicator for the soil management assessment framework (SMAF). *Soil Sci Soc Am J* 74:107–119
- Sulman BN, Phillips RP, Oishi AC, Shevliakova E, Pacala SW (2014) Microbe-driven turnover offsets mineral-mediated storage of soil carbon under elevated CO₂. *Nat Clim Change* 4:1099–1102
- Szabolcs I (1974) Salt affected soils in Europe. MartinusNijhoff, The Hague, p 63
- Szatmári G, Bakacsi Z, Laborczi A, Petrik O, Pataki R, Tóth T, Pásztor L (2020) Elaborating Hungarian segment of the global map of salt-affected soils (GSSmap): national contribution to an international initiative. *Remote Sensing* 12:4073. <https://doi.org/10.3390/rs12244073>
- Tan Z, Lal R, Wiebe K (2005) Global soil nutrient depletion and yield reduction. *J Sustain Agric* 26(1). https://doi.org/10.1300/J064v26n01_10
- Tang J, Zhang J, Ren L, Zhou Y, Gao J, Luo L, Yang Y, Peng Q, Huang H, Chen A (2019) Diagnosis of soil contamination using microbiological indices: a review on heavy metal pollution. *J Environ Manage* 242:121–130. <https://doi.org/10.1016/j.jenvman.2019.04.061>
- Tang J, Riley WJ (2015) Weaker soil carbon-climate feedbacks resulting from microbial and abiotic interactions. *Nat Clim Change* 5:56–60
- Tanirbergenov S, Saljnikov E, Suleimenov B, Saparov A, Cakmak D (2020) Salt affected soils under cotton-based irrigation agriculture in southern Kazakhstan. *Zemljiste i Biljka* 69(2):1–14. http://www.sdpz.rs/images/casopis/2020/zib_69_2_70.pdf
- Tavakkoli E, Rengasamy P, Smith E, McDonald GK (2015) The effect of cation–anion interactions on soil pH and solubility of organic carbon. *Eur J Soil Sci* 66(6):1054–1062. <https://doi.org/10.1111/ejss.12294>
- Tetteh RN (2015) Chemical soil degradation as a result of contamination: a review. *J Soil Sci Environ Manage* 6(11):301–308. <https://doi.org/10.5897/JSEEM15.0499>. ISSN 2141–2391 <https://academicjournals.org/journal/JSEEM/article-full-text-pdf/A3847D356736>. Accessed on 12 Sept 2020
- Thiele-Bruhn S, Schloter M, Wilke B-M, Beaudette LA, Martin-Laurent F, Cheviron N, Mougou C, Römbke J (2020) Identification of new microbial functional standards for soil quality assessment. *SOIL* 6:17–34. <https://doi.org/10.5194/soil-6-17-2020>
- Thum T, Nabel J, Tsuruta A, Aalto T, Dlugokencky EJ, Liski J, Lujkx IT, Markkanen T, Pongratz J, Yoshida Y, Zaehle S (2020) Evaluating two soil carbon models within a global land surface model using surface and spaceborne observations of atmospheric CO₂ mole fractions. *Biogeosciences*. EGU Discussions. <https://www.biogeosciences-discuss.net/bg-2020-7/bg-2020-7.pdf>
- Tischer A, Sehl L, Meyer U-N, Kleinebecker T, Klaus V, Hamer U (2019) Land-use intensity shapes kinetics of extracellular enzymes in rhizosphere soil of agricultural grassland plant species. *Plant Soil* 437:215–239
- Tisdall JM, Oades JM (1982) Organic matter and water-stable aggregates. *J Soil Sci* 33:141–163
- Tolimir M, Kresović B, Životić L et al (2020) The conversion of forestland into agricultural land without appropriate measures to conserve SOM leads to the degradation of physical and rheological soil properties. *Sci Rep* 10:13668. <https://doi.org/10.1038/s41598-020-70464-6>
- Tomco PL, Seefeldt SS, Rodriguez-Baisi K, Hatton JJ, Duddleston KN (2020) Sub-arctic field degradation of metsulfuron-methyl in two Alaskan soils and microbial community composition effects. *Water Air Soil Pollut* 231:157. <https://doi.org/10.1007/s11270-020-04528-8>
- Tóth T, Kertész M, Guerra LC, Labrada JL, Machado BP, Fonseca PC, Martínez MN (1997) Plant composition of a pasture as a predictor of soil salinity. *Revista de biología* 45(4). <https://revistas.ucr.ac.cr/index.php/rbt/article/download/21443/21659>, accessed on Sept 12, 2020
- Tóth T, Schaap Mg, Molnár Z (2008) Utilization of soil-plant interrelations through the use of multiple regression and artificial neural network in order to predict soil properties in Hungarian solonchic grasslands. *Cereal research communications*, vol 36, Supplement: Proceedings of the VII. Alps-Adria Scientific Workshop, 28 April–2 May 2008, Stara Lesna, Slovakia, pp. 1447–1450
- Tóth T (2018) Chapter II/67: methods for quantifying and monitoring soil salinity, sodicity and alkalinity. In: Sychev VG, Mueller L (eds) *Novel methods and results of landscape research in Europe, Central Asia and Siberia*, vol II understanding and monitoring processes in soils and water bodies. © FSBI “VNI Agrochemistry”, pp. 145–149. <https://doi.org/10.25680/4650.2018.47.53.164>, <https://vniia-pr.ru/monografii/pdf/tom2-67.pdf>
- Trasar-Capeda C, Leiros C, Gil-sotres F, Seoane S (1998) Towards a biochemical quality index for soils: an expression relating several biological and biochemical properties. *Biol Fertil Soils* 26:100–106
- Tresch S, Moretti M, Le Bayon R-C, Mäder P, Zanetta A, Frey D, Stehle B, Kuhn A, Munyangabe A,

- Fliessbach A (2018) Urban soil quality assessment—a comprehensive case study dataset of Urban garden soils. *Front Environ Sci*. <https://doi.org/10.3389/fenvs.2018.00136>
- Treseder KK (2008) Nitrogen additions and microbial biomass: a meta-analysis of ecosystem studies. *Ecol Lett* 11:1111–1120. <https://doi.org/10.1111/j.1461-0248.2008.01230.x>
- Trivedi P, Delgado-Baquerizo M, Anderson IC, Singh BK (2016) Response of soil properties and microbial communities to agriculture: implications for primary productivity and soil health indicators. *Front Plant Sci* 7:990. <https://doi.org/10.3389/fpls.2016.00990>
- Trofimov IA, Trofimova LS, Yakovleva EP (2015) Remote indicators of land desertification. *Arid Ecosyst* 21(1)(62):36–40. (In Russian: Дистанционные индикаторы опустынивания земель. Аридные Экосистемы, 2015 том 21, № 1 (62), с. 36–40)
- Tupek B, Launiainen S, Peltoniemi M, Sievänen R, Perttunen J, Kulmala L, Penttilä T, Lindroos A-J, Hashimoto S, Lehtonen A (2019) Evaluating CENTURY and Yasso soil carbon models for CO₂ emissions and organic carbon stocks of boreal forest soil with Bayesian multi-model inference. *Eur J Soil Sci* 70(4):847–858. <https://doi.org/10.1111/ejss.12805>
- Ulrich B, Sumner ME (eds)(1991) An ecosystem approach to soil acidification. *Soil Acidity*, Springer, Berlin, Heidelberg (1991), pp 28–79
- UN (2014) United nations, Department of economic and social affairs, population division. *World Urbanization Prospects. The 2014 Revision, Highlights*. <https://population.un.org/wup/Publications/Files/WUP2014-highlights.pdf>. Accessed on 12 Sept 2020
- Van de Craats D, van der Zee S, Sui CH, van Asten PJA, Cornelissen P, Leijnse A (2020) Soil sodicity originating from marginal groundwater. *Vadose Zone J* 19(1):e20010. <https://doi.org/10.1002/vzj2.20010>
- Van der Pol F, Traore B (1993) Soil nutrient depletion by agricultural production in Southern Mali. *Fert Res* 36:79–90. <https://doi.org/10.1007/BF00749951>
- Van der Zee S, Shah S, Vervoort R (2014) Root zone salinity and sodicity under seasonal rainfall due to feedback of decreasing hydraulic conductivity. *Water Resour Res* 50:9432–9446. <https://doi.org/10.1002/2013WR015208>
- Van Gestel CAM, Mommer J, Montanarella L, Pieper S, Coulson M, Totschki A, Rutgers M, Focks A, Römbke J (2020) Soil biodiversity: state-of-the art and possible application in chemical risk assessment. *Integr Environ Assess Manag (IEAM)* <https://doi.org/10.1002/ieam.4371>
- Venkatramanan V, Shah S (2019) Climate smart agriculture technologies for environmental management: the intersection of sustainability, resilience, wellbeing and development. In: Shah S, Venkatramanan V, Prasad R (eds) *Sustainable green technologies for environmental management*. Springer, Singapore
- Vodyanitskii YN, Savichev AT (2017) Magnetite contamination of urban soils in European Russia. *Ann Agrarian Sci* 15(2):155–162. <https://doi.org/10.1016/j.aasci.2017.05.020>
- Vojnov B, Šeremešić S, Čupina B, Đorđe Krstić Đ, Vujić S, Živanov M, Pavlović S (2020) Sadržaj labilne organske materije černozema u sistemu zaoravanja međuuseva i naknadne setve jarih useva. *Zemljiste I Biljka* 69(2):82–94. http://www.sdpz.rs/images/casopis/2020/zib_69_2_76.pdf
- Wall DH, Nielsen UN, Six J (2015) Soil biodiversity and human health. *Nature*. <https://doi.org/10.1038/nature15744>
- Wang F, Tiedje JM (2020) Antibiotic resistance in soil. In: Manaia C, Donner E, Vaz-Moreira I, Hong P (eds) *Antibiotic resistance in the environment. The handbook of environmental chemistry*, vol 91. Springer, Cham. https://doi.org/10.1007/698_2020_562
- Wang Ch, Wang J, Zhou Sh Tang J, Jia Z, Ge L, Li Y, Wu S (2019) Polycyclic aromatic hydrocarbons and heavy metals in urban environments: Concentrations and joint risks in surface soils with diverse land uses. *Land Degrad Develop* 31(3):383–391 <https://doi.org/10.1002/ldr.3456>
- Wegehenkel M, Mirschel W (2007) Application and validation of the models THESEUS and OPUS with two experimental data sets. In: Kersebaum KC, Hecker J-M, Mirschel W, Wegehenkel M (eds) *Modelling water and nutrient dynamics in soil-crop systems: proceedings of the workshop on “Modelling water and nutrient dynamics in soil-crop systems” held on 14–16 June 2004 in Müncheberg, Germany*, pp. 37–49. Dordrecht (Springer)
- White HJ, León-Sánchez L, Burton VJ, Cameron EK, Caruso T, Cunha L, Dirilgen T, Jurburg SD, Kelly R et al (2020) Methods and approaches to advance soil macroecology. *Glob Ecol Biogeogr*. <https://doi.org/10.1111/geb.13156>
- Wieder WR, Allison SD, Davidson EA, Georgiou K, Hararuk O, He Y, Hopkins F, Luo Y, Smith MJ, Sulman B, Todd-Brown K, Wang Y-P, Xia J, Xu X (2015) Explicitly representing soil microbial processes in Earth system models. *Glob Biochem Cycles* 29(10):1782–1800. <https://doi.org/10.1002/2015GB005188>
- Wiesmeier M, Urbanski L, Hobbey E, Lang B, von Lützw M, Marin-Spiotta E, van Wesemael B, Rabot E, Ließ M, Garcia-Franco N, Wollschläger U, Vogel H-J, Kögel-Knabner I (2019) Soil organic carbon storage as a key function of soils: a review of drivers and indicators at various scales. *Geoderma* 333:149–162. <https://doi.org/10.1016/j.geoderma.2018.07.026>
- Woolf D, Lehmann J (2019) Microbial models with minimal mineral protection can explain long-term soil organic carbon persistence. *Sci Rep* 9:6522 (2019). <https://doi.org/10.1038/s41598-019-43026-8>
- Wu Q, Wang M (2007) A framework for risk assessment on soil erosion by water using an integrated and systematic approach. *J Hydrol* 337:11–21. Not in text.
- Wu M, Wei S, Liu J, Liu M, Jiang C, Li Z (2019) Long-term mineral fertilization in paddy soil alters the

- chemical structures and decreases the fungistatic activities of humic acids. *Eur J Soil Sci* 70(4):776–785. <https://doi.org/10.1111/ejss.12778>
- Xia Y, Zhang M, Tsang DCW, Geng H, Lu D, Zhu L, Igalavithana AD, Dissanayake PD, Rinklebe J, Yang X, Ok YS (2020) Recent advances in control technologies for non-point source pollution with nitrogen and phosphorous from agricultural runoff: current practices and future prospects. *Appl Biol Chem* 63(1):8. <https://doi.org/10.1186/s13765-020-0493-6>
- Xu X, Zarecki R, Medina S, Ofaim S, Liu X, Chen C, Hu S, Brom D, Gat D, Porob S, Eizenberg H, Ronen Z, Jiang J, Freilich S (2019) Modeling microbial communities from atrazine contaminated soils promotes the development of biostimulation solutions. *ISME J* 13:494–508. <https://doi.org/10.1038/s41396-018-0288-5>
- Xu H, Demetriades A, Reimann C, Jiménez JJ, Filser J, Zhang C (2019) Identification of the co-existence of low total organic carbon contents and low pH values in agricultural soil in north-central Europe using hot spot analysis based on GEMAS project data. *Sci Total Environ* 678:94–104
- Xu D, Carswell A, Zhu Q, Zhang F, de Vries W (2020) Modelling long-term impacts of fertilization and liming on soil acidification at Rothamsted experimental station. *Sci Total Environ* 713:136249. <https://doi.org/10.1016/j.scitotenv.2019.136249>
- Xu X, Pei J, Xu Y, Wang J (2020) Soil organic carbon depletion in global Mollisols regions and restoration by management practices: a review. *J Soils Sediments* 20:1173–1181. <https://doi.org/10.1007/s11368-019-02557-3>
- Yang C, Wu Y, Zhang F, Liu L, Pan R (2016) Pollution characteristics and ecological risk assessment of heavy metals in the surface sediments from a source water reservoir. *Chem Speciat Bioavailab* 28(1–4):133–141. <https://doi.org/10.1080/09542299.2016.1206838>
- Yang X, Guo X, Huang S, Xue S, Meng F, Qi Y, Cheng W, Fan T, Lwanga EH, Geissen V (2020) Microplastics in soil ecosystem: insight on its fate and impacts on soil. *Quality*. https://doi.org/10.1007/698_2020_458
- Zeiner M, Pirkl R, Juranović Cindrić I (2019) Field-Tests versus laboratory methods for determining metal pollutants in soil extracts. *Soil Sediment Contam Int J* 29(1):53–68. <https://doi.org/10.1080/15320383.2019.1670136>
- Zhang X, Davidson EA, Zou T, Lassaletta L, Quan Z, Li T, Zhang W (2020) Quantifying nutrient budgets for sustainable nutrient management. *Global Biogeochem Cycles* 34: e2018GB006060. <https://doi.org/10.1029/2018GB006060>
- Zhao Q, Bai J, Gao Y, Zhao H, Zhang G, Cui B (2020a) Shifts in the soil bacterial community along a salinity gradient in the Yellow River Delta. *Land Degrad Develop*. <https://doi.org/10.1002/ldr.3594>
- Zhao L, Shanguan Y, Yao N, Sun Z, Ma J, Hou H (2020b) Soil migration of antimony and arsenic facilitated by colloids in lysimeter studies. *Sci Total Environ* 728(1):138874. <https://doi.org/10.1016/j.scitotenv.2020.138874>
- Zhou M, Liu C, Wang J, Meng Q, Yuan Y, Ma X, Liu X, Zhu Y, Ding G, Zhang J, Zeng X, Du W (2020a) Soil aggregates stability and storage of soil organic carbon respond to cropping systems on Black Soils of Northeast China. *Sci Rep* 10:265. <https://doi.org/10.1038/s41598-019-57193-1>
- Zhou X, Zhu H, Wen Y, Goodale UM, Zhu Y, Yu S, Li C, Li X (2020b) Intensive management and declines in soil nutrients lead to serious exotic plant invasion in *Eucalyptus* plantations under successive short-rotation regimes. *Land Degrad Develop* 31(3):297–310. <https://doi.org/10.1002/ldr.3449>
- Zhu Q, Liu X, Hao T, Zeng M, Shen J, Zhang F, De Vries W (2018) Modeling soil acidification in typical Chinese cropping systems. *Sci Total Environ* 613–614:1339–1348
- Zhuang K, Izallalen M, Mouser P, Richter H, Risso C, Mahadevan R, Lovley DR (2011) Genome-scale dynamic modeling of the competition between *Rhodospirillum rubrum* and *Geobacter* in anoxic subsurface environments. *ISME J* 5:305–316
- Zolnikov ID, Glushkova NV, Smolentseva EN, Chupina DA, Pchelnikov DV, Lyamina VA (2016) GIS and remote sensing data-based methods for monitoring water and soil objects in the steppe biome of Western Siberia. In: Mueller L, Sheudshen A, Eulenstein F (eds) *Novel methods for monitoring and managing land and water resources in Siberia*. Springer Water, Springer, Cham. https://doi.org/10.1007/978-3-319-24409-9_9
- Zornoza R, Acosta JA, Bastida F, Domínguez SG, Toledo DM, Faz A (2015) Identification of sensitive indicators to assess the interrelationship between soil quality, management practices and human health. *Soil* 1:173–185. <https://doi.org/10.5194/soil-1-173-2015>



Classification and Causes of Soil Degradation by Irrigation in Russian Steppe Agrolandscapes

4

Vladimir G. Mamontov

Abstract

This chapter covers the causes of soil degradation in irrigated agrolandscapes of Russia. The most significant causes are the extensive use of irrigated arable land and the unfavourable chemical composition of irrigation water. This is especially pronounced in the absence of land reclamation measures. As yet, there is no accepted classification of soil degradation due to irrigation. In this chapter, a classification for the degradation of irrigated soils was developed. Five types were proposed, divided into sub-types. Physical degradation includes the deflation and reorganisation of the soil mass. Chemical degradation suggests the unbalanced removal of biophilic elements or the excessive accumulation of harmful substances. Physico-chemical degradation manifests in negative changes in the soil absorption complex (SAC), which triggers other negative changes. Biological degradation is associated with a decreased content of organic matter in soil and unfavourable biota succession. Hydrological degradation occurs due to negative changes in the soil water regime. The

degradation degree indicates how intensively the degradation processes manifest, while the speed of degradation shows the activity of negative changes over time. The nature of the degradation reflects the specificity of the degradation processes. The reversibility of degradation indicates a soil's ability to restore its original properties. The resistance of soil to degradation is an indicator for the soil's ability to maintain its productive and environmental functions.

Keywords

Irrigation degradation · Degradation classification · Soil salinisation · Degradation speed · Degradation nature

4.1 Introduction: Soil Degradation in Russian Steppe Agrolandscapes

The current state of the biosphere is characterised by an ever-increasing anthropogenic load on the environment. One such anthropogenic impact on the soil cover is irrigation. A widespread use of irrigation in agriculture is associated with natural needs to produce sufficient food, forage and fibre in a number of regions. In steppe landscapes, due to the lack of precipitation, it is almost impossible to create highly productive agricultural landscapes without irrigation. Irrigation makes it

V. G. Mamontov (✉)
Department of Soil Science, Geology and Landscape Science, Russian State Agrarian University—
Moscow Timiryazev Agricultural Academy,
Pryanishnikov street, 6, 127550 Moscow, Russia
e-mail: mamontov1954@inbox.ru

possible to quickly deal with the moisture deficit in the soil and provides favourable conditions for the growth and development of crops. The effectiveness of irrigation has also been proven in areas with a relatively high amount of precipitation. However, the level of the anthropogenic load on the soil multiplies under intensive irrigation due to a significant change in soil properties and regimes, and often leads to negative consequences, such as the degradation of irrigated soils.

The degradation of arable soil is a serious problem as it is accompanied by a number of negative consequences:

- changes in the qualitative and quantitative characteristics of migration flows;
- changes in the ratio between surface and groundwater flow, favouring an increase in the former;
- increased evapotranspiration and therefore negative changes in the microclimate;
- desiccation and degradation of vegetation;
- increasing erosion and deflation.

These and other phenomena and processes cause changes in the intensity and direction of the flow of biogeochemical substances and energy, which leads to the disruption of intralandscape bonds and makes natural landscapes unsustainable. On the soils subject to degradation, the effectiveness of agrotechnical and agrochemical measures decreases. Therefore, cultivated plants cannot fully realise their biological potential. The lack of adequate cultivation techniques prevents the creation of balanced, highly productive agricultural landscapes. The development of appropriate criteria for the diagnosis and assessment of soil degradation has recently become one of the main priorities in soil ecology research.

To date, considerable experience has been gained in assessing and classifying soil degradation, identifying the factors that determine soil resistance to degradation (Karmanov and Bulgakov 1998; Khitrov 1998; Kiryushin 1998; Jie

et al. 2002; Soil degradation and protection 2002; Braimoh and Vlek 2008; Mamontov 2013; Bilgili et al. 2018; FAO 2019; Ahmad et al. 2020; Olsson et al. 2019; Yousefi et al. 2020; Mohammed et al. 2020). However, in general, this problem requires further study, since soil degradation continues to affect crop productivity and environmental sustainability. The last statement applies to both the conceptual framework and quantitative parameters, which allow various aspects of this phenomenon to be evaluated.

The negative transformation of the properties and regimes of the soil can be a consequence of both natural processes and human impact. The changes caused by natural processes (e.g. climate change) occur largely independently of human beings. Therefore, it seems inappropriate to treat them as degradation (Khitrov 1998), because we are dealing with the evolution of the soil under altered natural conditions. When all the natural soil formation factors (except vegetation) remain more or less stable, but the soil parameters deteriorate, the anthropogenic factor should be considered the cause of soil degradation.

The term “soil degradation” should be applied to a steady deterioration in the soil’s composition, properties and regimes as a result of human activity, accompanied by the partial or complete loss of its environmental and productive functions. The most important cause of anthropogenic soil degradation is the direction and intensity of anthropogenic impact being incompatible with the genetic characteristics of the soil (Mamontov 2013). The mechanisms that determine the degradation of agricultural soil are due to changes in the ratio and intensity of soil processes, and anthropogenic processes that differ from natural ones (Kiryushin 1998). Globally, the degradation of arable land is leading to a decrease in soil fertility, productivity and the quality of agricultural products. Meanwhile, production costs are increasing and the environmental situation is deteriorating, not only within individual agrolandscapes, but also in adjacent areas, including water basins (Karlen and Rice 2015).

4.2 Causes for the Degradation of Irrigated Soils in Agricultural Landscapes

There are various reasons for unfavourable changes in the properties and regimes of irrigated soils. Some of them are similar to the causes for degradation in non-irrigated agricultural landscapes, while others only appear in the case of irrigation. At the same time, there are many problems in the management of dry farming, which manifest more intensively, with serious consequences, as a result of irrigation. First, degradation processes mainly develop with the extensive use of irrigated soils. Negative changes in the properties and regimes of soils caused by changes in the conditions of soil formation and the nature of migration processes are consequences of:

- long-term/continuous cultivation of row crops;
- non-compliance with agricultural technology;
- insufficient or unbalanced fertilisation;
- permanent over-irrigation;
- inappropriate quality of irrigation water;
- lack of preventive melioration measures.

In the Russian Federation, the main areas of irrigated land have Chernozem and Kastanozem soils (WRB 2015), which are of great importance. These soils were formed under a non-percolating water regime and insufficient moisture with an absolute predominance of aerobic conditions.

Sporadic irrigation using low irrigation rates, as a rule, does not significantly affect the direction of soil formation processes. When ground water level does not rise and the quality of irrigation water is satisfactory, then the properties of irrigated soils do not noticeably change (Minhas et al. 2020). However, with intensive irrigation the situation changes significantly, especially when the agricultural lands are used widely and intensively or the quality of the irrigation water and drainage is poor (Kanzari et al. 2020; Tanirbergenov et al. 2020).

With intensive irrigation, the frequency of wetting and draining cycles in the soil increases, with a periodic percolation of moisture. This leads to an increase in moisture reserves in the “dead horizon” and penetration into the lower horizons of the soil (Rozanov 1989). On average, about 10% of the total consumed water is lost to infiltration, thus replenishing the groundwater and causing an increase in its level (Mosienko and Chumakova 1990). Various water-soluble elements and compounds, including calcium ions and nutrients, are lost from the upper part of the irrigated soil with leaching water (Mosienko and Chumakova 1990; Stockle 2007; Hillel et al. 2008; Foster et al. 2018). Moreover, short term but frequent over-irrigation during hot seasons creates anaerobic conditions. This leads to a transformation in the composition of the soils, similar to the effect of gley formation (gleying). Iron, aluminium, calcium and other elements are transformed into a mobile form, while an organic part of the soil undergoes negative changes (Zaydelman 2016).

The functioning of microflora is closely related to the nature of soil moistening. At a soil moisture content of 90% of the maximum field moisture capacity, the amount of denitrification increases 20 times compared with non-irrigated soil. The amount of anaerobic bacteria of the genus *Clostridium pasteurianum* increases seven times (Andreiuk et al. 1988). It is notable that irrigation changes the composition of microflora, increasing the amount and at the same time prolonging the period of active functioning due to the additional supply of water in the summer months. This accelerated activity of soil biota intensifies the mineralisation of soil organic matter. Thus, during irrigation, due to the lack of organic substrate for the growth of microbes, depletion of organic matter in the soil can occur.

The quality (chemical composition) of irrigation water is of great importance because the salt regime and physico-chemical properties of irrigated soils directly depend on it. In the study, Chernozems and Kastanozems were characterised by the bicarbonate-calcium composition of the soil solution with a total mineralisation of

about 1 g/L^{-1} with a predominance of calcium. The ratio of Ca/Na was about 26, and Ca/Na+Mg was 2.6 (Table 4.1) (Panov and Mamontov 2001).

The chemical composition presented here ensures the stability of the soil absorption complex (SAC) and contributes to the formation of well-defined soil properties. The concentration of calcium ions accounted for 70–85% of the sum of exchangeable cations. The saturation of soil solutions with bicarbonate and to some extent calcium sulphate led to a neutral pH, the coagulation of humic substances, the formation of new humic substances and organo-mineral and mineral colloids. Also importantly, it helped the soil form an agronomically valuable waterproof structure. In the water from the main irrigation sources, the ratios of those elements were much lower. For Ca/Na ratio, it was 0.4–2.1 and for Ca/Na+Mg it was 0.2–1.1. This implies that the chemical composition of even the highest quality irrigation water (the Volga, the Don and the Kuban Rivers) does not correspond to the chemical composition of the soil solutions circulating in non-saline and non-alkaline Chernozem and Kastanozem soils. This may indicate that, over time, the chemical composition of soil solutions will be similar to the composition of the irrigation water, which can cause negative changes in the properties and regimes of these soils.

When freshwater is used for irrigation, the chemistry of soil solutions varies according to the intensity of the irrigation. With intensive irrigation, the soil solution is diluted 1.5–3 times or more, and the calcium carbonate and calcium sulphate are removed from the upper part of the soil. Lysimetric studies have shown that under non-irrigated conditions in the summer period, the substances' migration in Chernozem and Kastanozem soils was practically not observed. Meanwhile, with irrigation, the removal of mineral compounds from the plough layers of these soils varied from 10 to 113 kg/ha^{-1} , where 45 to 75% of the dissolved elements was calcium (Table 4.2).

These changes affected not only calcium compounds in the liquid phase but also the labile part of carbonate accumulations (pellicles, mould, veins and streaks). The entire carbonate soil layer was restructured when the stable carbonate aggregates (“white eyes”) were replaced by the mobile migrated forms (pellicles and streaks). The mobile forms of carbonates were also found in deeper horizons compared to the non-irrigated soils. The removal of calcium with downward migration flows was not fully compensated for by its movement to the upper part when the soil dried between irrigations. Obviously, the process of leaching had been accelerated in intensively irrigated soils. Leaching was accompanied by the accumulation of carbonate

Table 4.1 Chemical composition of soil solutions and irrigation water (average, mmol-eql^{-1}) (Panov and Mamontov 2001)

Soil, Source of irrigation	Sum of salts, g/L^{-1}	HCO_3^-	Cl^-	SO_4^{2-}	Ca^2_+	Mg^2_+	Na^+	Ca^2_+ Na^+	Ca^{2+} Mg^{2+} $+$ Na^+
Chernozem	0.88	6.6	1.3	1.5	7.7	2.7	0.3	25.7	2.6
Volga River	0.38	2.7	1.4	1.3	3.0	1.0	1.4	2.1	1.1
Don River	0.41	2.7	1.7	1.4	2.3	1.4	2.0	1.2	0.7
Kuban River	0.37	2.7	1.0	1.4	2.8	1.0	1.3	2.2	1.2
Egorlyk River	1.66	3.0	6.5	20.7	7.6	10.5	14.4	0.5	0.3
Veselovskoye Reservoir	1.59	3.3	15.2	12.5	6.0	8.3	17.0	0.4	0.2
Taganrog Bay	2.20	2.4	25.6	8.0	3.8	6.8	25.8	0.2	0.1
Drainage water	1.20	6.6	2.6	8.1	3.7	4.1	9.6	0.4	0.3

Table 4.2 Composition of lysimetric leachates of irrigated Chernozem and Kastanozem soil, (Panov and Mamontov 2001)

Land use	Depth	pH	Ca	Mg	Na	K	Fe	Si	Sum of elements
	cm		mg/L ⁻¹						
Chernozems									
Row crops	30	7.4	44.0	6.9	9.7	3.1	0.2	2.5	66.4
	55	7.6	72.7	9.1	11.4	5.7	1.6	1.6	102.1
Perennial grasses	30	7.4	83.4	44.5	10.1	3.2	Traces	4.1	145.3
	55	7.7	167.7	33.8	15.8	4.3	0.1	2.3	224.0
Kastanozems									
Row crops	30	7.1	37.0	10.9	8.3	2.7	0.7	2.5	62.1
	58	7.4	57.3	21.8	9.6	7.1	1.7	3.6	101.1
Perennial grasses	30	7.5	68.3	38.1	10.8	3.8	0.1	4.8	125.9
	58	7.8	76.2	29.3	13.2	4.1	Traces	3.1	125.9

moving downward, and in a relatively short period of irrigation it reached a soil depth of 20–50 cm. Presumably, after 10–15 years of intensive irrigation, the soil may almost completely lose all free carbonates from the upper 20–30-cm layer. Under conditions of this kind, the concentration of calcium in the soil solution decreases, and the sodium increases. This type of change in the chemical composition of the soil solution reduces its coagulating ability, which creates certain prerequisites for increasing the dispersion of the soil mass.

Another situation arises with moderate freshwater irrigation, when an additional amount of water entering the soil circulates exclusively within the natural moisture circulation. In this case, the irrigation water does not touch the “dead horizon” and, most importantly, does not affect the inert accumulations of easily soluble salts located at a particular depth in the soil. In the latter case, a positive calcium balance is formed in irrigated soils due to its intake with irrigation water. In this irrigation scenario, in 20–40 years, the scale of calcium accumulation in the soil can be assessed quantitatively and qualitatively.

The concentration of soil solutions often increases to critical values in the case of irrigation with saline water. In our study, sodium and magnesium chlorides, sulphates and bicarbonates that were applied with irrigation water dominated

in the ionic composition of the soil. Depending on the nature of the irrigation, soluble salts accumulated either in the upper part of the soil profile or in the underlying horizons (Tables 4.3 and 4.4). The accumulation of water-soluble salts from irrigation water led to the formation of soils which were saline to varying degrees. The salinisation process was especially active at a groundwater level exceeding the critical point (FAO 2008; Hillel et al. 2008; Pankova 2008; Brinck and Frost 2009; Minashina 2009; Lyubimova et al. 2012; Cucci and Lacolla 2013; Zaydelman 2014; Lekakis and Antonopoulos 2015; Machekposhti et al. 2017). In this case, in the areas with an evaporative hydromorphic regime, not only readily soluble salts but also gypsum and carbonates accumulated in plough layers (Table 4.5).

The sources of salinity were both the groundwater and the gypsum-carbonate accumulations located in the deep soil layers. Under automorphic conditions, they practically do not affect the upper part of the soil profile (Pankov and Konyushkova 2014).

When the groundwater level rises and passes through the carbonate- and gypsum-bearing layers, it is saturated with CaSO₄ and CaCO₃. When moisture evaporated, these salts precipitated, accumulating in the upper part of the soil in appreciable quantities. Secondary salinisation,

Table 4.3 Effect of short-term irrigation with alkaline water (1.17 g/L^{-1}) on Kastanozem (Mamontov 2013)

Horizon, depth, cm	Plough layer 0–20	B ₁ 30–40	B ₂ 52–62
Non-irrigated soil			
Amount of salts, %	0.025	0.068	0.087
Water-soluble Na, mmol-eq/100 g ⁻¹ of soil	0.05	0.16	0.34
Water-soluble sulphate ion, mmol-eq/100 g of soil	0.18	0.49	0.62
Irrigated soil			
Amount of salts, %	0.364	0.348	0.162
Water-soluble Na, mmol-eq/100 g ⁻¹ of soil	2.48	2.17	0.91
Water-soluble sulphate ion, mmol-eq/100 g ⁻¹ of soil	2.56	2.35	1.66

Table 4.4 Effect of long-term intensive irrigation with neutral water (1.94 g/L^{-1}) on Kastanozem soil (Mamontov 2013)

Depth, cm	0–20	20–40	40–60	60–80	80–100
Non-irrigated soil					
Amount of salts, %	0.047	0.066	0.077	0.098	0.142
Water-soluble Na, mmol-eq/100 g ⁻¹ of soil	0.21	0.19	0.20	0.31	0.53
Water-soluble Cl, mmol-eq/100 g ⁻¹ of soil	0.12	0.16	0.21	0.43	0.67
Irrigated soil					
Amount of salts, %	0.070	0.073	0.099	0.162	0.267
Water-soluble Na, mmol-eq/100 g ⁻¹ of soil	0.45	0.40	0.63	1.12	2.43
Water-soluble Cl, mmol-eq/100 g ⁻¹ of soil	0.41	0.52	0.67	1.06	2.15

Table 4.5 Soluble salts in 0–200 cm and carbonates in 0–20 cm and depth of secondary local accumulations of gypsum in Chernozem depending on the irrigation conditions (Ryskov and Gurov 1987)

Irrigation, groundwater level (GWL)	Amount of ions, mEq/100 g ⁻¹ of soil				Gypsum accumulation, %		CaCO ₃ , %
	HCO ₃ ⁻	Cl ⁻	SO ₄ ²⁻	Na ⁺	0–10 cm	0–20 cm	
Non-irrigated, GWL 10 m	0.55	0.09	0.13	0.10	0	0	0.32
Irrigated, GWL 3–7 m	0.60	0.14	0.18	0.16	63	63	0.30
Irrigated, GWL 2–3 m	0	0	0	0	64	79	0.68
Irrigated, GWL < 2 m	0.55	0.75	5.10	3.15	60	100	2.0–5.0

Note GWL—ground water level

caused by irrigation due to the raised level of groundwater or due to salt intake, is a serious problem. According to Brinck and Frost (2009), 10 million hectares of irrigated land are lost annually in the world. Due to the salinisation of

irrigated soils, the content of sodium ions increases significantly, creating real prerequisites for the further alkalisiation process.

When the salt concentration in irrigation water exceeds 1 g/L^{-1} , the concentration of

exchangeable sodium and magnesium in the SAC increases (Rozanov 1989; Buckland et al. 2002; Herrero and Covetta 2005; Lozovitsky 2005; FAO 2008; Mamontov 2013; Minashina 2011; Cucci and Lacolla 2013; Kirankumar et al. 2015; Lekakis and Antonopoulos 2015). As a result, initially non-alkaline soils turn into slightly, moderately and strongly alkaline soils containing sharply increased amounts of exchangeable sodium and magnesium in the soil absorption complex (Table 4.6).

Moreover, poorly mineralised (1 g/L^{-1}) alkaline irrigation water containing free sodium bicarbonates and sodium carbonates had a very negative impact on soils (Table 4.7). In the case of irrigation with alkaline water, the sodium was absorbed by soil colloids as a result of calcium precipitation as CaCO_3 . This led to the deterioration of the soils' physico-chemical properties due to alkalinisation (Brinck and Frost 2009). Within a few years of irrigation with this type of water, the content of exchangeable Na reached 10–15% and more in the soil CEC.

Irrigation with saline water most negatively manifests under the extensive use of arable lands. The violation of irrigation water standards, a poor quality of water, a lack of preventive amelioration measures, the inadequate use of fertilisers and a lack of perennial grasses in crop rotation, all led to the rapid salinisation and alkalinisation of irrigated soils in 3–5 years. Currently, 23% and 39% of cultivated land are

considered saline and solonetzic (Essington 2004; Qadir et al. 2006). Irrigation also influenced the soil organic matter due to a change in the hydrothermal regime followed by a change in the way the soil biota functioned (Lozovitsky 2012; Panov and Mamontov 2001; Mamontov 2013) (Table 4.8).

The fastest negative changes in soil organic matter occurred under irrigation with alkaline water (Table 4.9). The decrease in the content and reserves of humus and humin indicates a weakened connection of humus substances with the mineral part of the soil.

There was not only a decrease in the content of humic acids, but also adverse changes in their composition and properties. These changes led to the loss of a significant part of their labile components of nitrogen-containing groups, the enrichment with inert cyclic components and the loss of their adhesiveness. The soil structure also underwent a negative transformation due to irrigation (Table 4.10).

The negative effect of irrigation was manifested in increased cloddiness and a decrease in the number and average diameter of agronomically valuable and water-resistant aggregates. The adverse changes in the soil structure were most pronounced with the extensive use of irrigated land and the use of saline water for irrigation. Cockroft and Olsson (2000), and Emdad et al. (2006) reported similar results. These negative transformations of the soil

Table 4.6 Effect of long-term irrigation with sodium-chloride saline water (1.54 g/L^{-1}) on physico-chemical properties of Kastanozem (Mamontov 2013)

Horizon	pH	Exchangeable cations					
		Ca ²⁺	Mg ²⁺	Na ⁺	Ca ²⁺	Mg ²⁺	Na ⁺
		Mg-eq/100 g ⁻¹ of soil			% of CEC		
Non-irrigated soil							
0–20	7.2 ± 0.1	16.04 ± 0.12	4.25 ± 0.13	0.46 ± 0.05	77.3	20.5	2.2
20–40	7.2 ± 0.1	16.12 ± 0.20	4.33 ± 0.19	0.48 ± 0.03	77.0	20.7	2.3
40–60	7.3 ± 0.1	16.49 ± 0.24	5.36 ± 0.31	0.50 ± 0.05	73.8	24.0	2.2
Irrigated soil							
0–20	7.3 ± 0.1	14.36 ± 0.21	4.36 ± 0.05	0.92 ± 0.03	73.1	22.2	4.7
20–40	7.3 ± 0.1	14.23 ± 0.19	5.33 ± 0.08	0.94 ± 0.06	69.4	26.0	4.6
40–60	7.4 ± 0.1	15.80 ± 0.17	5.29 ± 0.13	0.86 ± 0.06	72.0	24.1	3.9

Table 4.7 Effect of 4-year irrigation with alkaline mineralised water on physico-chemical properties of Kastanozem (Mamontov 2013)

Horizon	pH	Exchangeable cations					
		Ca ²⁺	Mg ²⁺	Na ⁺	Ca ²⁺ ₊	Mg ²⁺ ₊	Na ⁺
		mg-eq/100 g ⁻¹ of soil			% of CEC		
Non-irrigated soil							
Plough layer	7.1 ± 0.1	19.2 ± 0.4	7.9 ± 0.3	0.5 ± 0.1	69.6	28.6	1.8
B ₁	7.1 ± 0.1	19.8 ± 0.3	7.7 ± 0.3	0.7 ± 0.1	70.2	27.3	2.5
B ₂	7.4 ± 0.2	19.5 ± 0.5	7.7 ± 0.4	0.7 ± 0.1	69.9	27.6	2.5
Irrigated soil, water mineralisation 1.17 g/L ⁻¹ , pH = 8.5							
Plough layer	7.8 ± 0.3	17.3 ± 0.6	8.7 ± 0.3	2.8 ± 0.3	60.1	30.2	9.7
B ₁	7.8 ± 0.4	18.8 ± 0.6	8.7 ± 0.4	2.2 ± 0.3	63.3	29.3	7.4
B ₂	7.6 ± 0.2	19.0 ± 0.5	7.7 ± 0.3	0.9 ± 0.1	68.8	27.9	3.3

Table 4.8 Effect of irrigation with freshwater on humus composition in southern Chernozem, % of soil mass (Pilgunova and Grigorieva 1983)

Horizon, depth, cm	C total %	C humic acids	C fulvic acids	Humin	C ha/C fa
	% of soil mass				
Non-irrigated Chernozem					
Plough layer 0–30	1.90	1.05	0.39	0.47	2.69
AB 30–61	0.99	0.49	0.18	0.23	2.72
Irrigated chernozem (19 years)					
Plough layer 0–31	1.54	0.61	0.59	0.38	1.15
AB 31–59	0.86	0.28	0.36	0.19	0.77

Table 4.9 Effect of irrigation on organic matter in Kastanozem (Mamontov 2013)

Horizon, depth, cm	Humus, %	Humus reserves, th ⁻¹	C humic acids, %	C fulvic acids, %	Humin	C ha/C fa
Non-irrigated soil						
Plough layer 0–20	2.53	61	0.51	0.25	0.71	2.04
B ₁ 20–40	1.89	48	0.36	0.19	0.54	1.89
Irrigated soil, irrigation water mineralisation 1.17 g/L-1, pH 8.5						
Plough layer 0–20	2.02	50	0.38	0.26	0.53	1.46
B ₁ 20–40	1.72	44	0.31	0.23	0.46	1.35

structure were accompanied by the appearance and accumulation of water-peptised silt. In the irrigated soils, the easily water-peptised fine

particles had a negative effect on the soil's physical properties (Chizhikova et al. 2011; Mamontov 2013).

Table 4.10 Changes in aggregation state and content of water-peptised silt in irrigated Chernozem and Kastanozem (Mamontov 2013)

Diameter (mm) of aggregates > 0.25 mm	Diameter (mm) of aggregates > 0.25 mm–10 mm	Agron. valuable aggregates, %	Structural coefficient	Waterproof units, %	Diameter of water-stable aggregates, mm	Water-peptised silt, %
Non-irrigated Chernozem						
5.38	4.13	70.0	2.3	73.8	1.07	1.1
Chernozem irrigated with freshwater, crop rotation includes perennial grasses						
5.71	3.16	53.0	1.1	65.3	0.86	2.5
Chernozem irrigated with freshwater, permanent corn						
6.33	2.37	35.8	0.6	57.6	0.75	3.3
Kastanozem non-irrigated						
4.18	2.68	64.1	1.8	48.7	1.05	3.07
Kastanozem, water mineralisation 1.54 g/L ⁻¹ , crop rotation includes perennial grasses						
4.84	1.74	41.2	0.7	37.5	0.68	6.89
Kastanozem, water mineralisation 1.54 g/L ⁻¹ , permanent winter wheat						
5.60	1.49	32.3	0.5	26.0	0.60	8.16

The reasons for the degradation of structure in irrigated soils were:

- destructive impact of irrigation water on the soil during long-term and intensive irrigation;
- harmful effect of the air trapped in aggregates during intensive irrigation of dry soils;
- excessive use of heavy agricultural equipment;
- tillage of highly humid soil;
- peptising effect of sodium ions in irrigation water;
- unfavourable calcium regime;
- mineralisation of organic substances holding aggregates and
- extensive use of irrigated arable land.

The degradation of the soil structure might also be due to the initially low resistance to the irrigation impact, which was determined by soil genetic characteristics. Usually, the negative changes at the aggregate level of the soil structure are accompanied by an increase in the density of irrigated soils. The plough layer of non-irrigated Chernozem and Kastanozem soils

typically has a bulk density in the range of 1.1–1.25 g/cm⁻³. With irrigation, the density eventually increases to 1.30–1.45 g/cm⁻³ and higher, and the compaction extends to a soil depth of 50–80 cm (Cockroft and Olsson 2000; Oster 2004; Emdad et al. 2006; Gurbanov 2010; Dubovik 2012; Mamontov 2013). The overall manifestation of the destruction of soil texture, over-consolidation and gleying is accompanied by an increase in the hydrophilicity of fine particles with a tendency to soil thixotropy. This in turn may lead to eventual consolidation—a process that cannot be unequivocally diagnosed but that periodically manifests in irrigated soils, indicating the extreme degree of their physical degradation.

The mineralogical composition also undergoes changes in irrigated soils as the minerals in the montmorillonitic group and the mica-smectite components of the interlayer transition to a highly dispersed state. This contributes to their more active destruction, especially when alkaline water is used for irrigation. Chizhikova et al. (1992) also identified the phenomenon of hydromicatisation of the silt fraction, which,

along with a decrease in the humus content, leads to a decrease in the soil exchange capacity.

In irrigated soils, one type of degradation usually causes adverse changes in other soil properties. For example, a decrease in the humus content leads to a decrease in CEC and the deterioration of the soil structure, because humic substances are one of the main aggregating agents of soil. Meanwhile, alkalisation is accompanied by the dispersion of the soil mass, the destruction of the soil structure and a decrease in the humus content because the solubility of humic substances increases and they become more accessible to microorganisms.

4.3 Classification of Irrigation Degradation in Agricultural Landscapes

Soil degradation phenomena have a varying nature and degree of manifestation. They can be found at almost all levels of the soil structural organisation. There is no generally accepted classification of soil degradation yet, although various options have been proposed (Karmanov and Bulgakov 1998; Kiryushin 1998; Khitrov 1998; Soil degradation and protection 2002; Braimoh and Vlek 2008). For irrigated soils, degradation processes can be classified into five types (Table 4.11).

4.3.1 Physical Degradation

Physical degradation includes processes involving the mechanical removal of soil material (irrigation-induced erosion, preparation activities) and reorganisation of the soil mass (overcompaction, destruction of soil texture, compaction caused by chemical processes). The consequence of physical soil degradation is the deterioration of the soil's water-air regime, which affects its physical and physico-mechanical properties. As a result of irrigation-induced erosion or preparation activities, the other soil parameters also may deteriorate (decrease in depth of organic layer, decrease in

content and reserves of humus, nitrogen, labile organic matter, while the free carbonates and other elements are involved in the plough layer).

4.3.2 Chemical Degradation

During chemical soil degradation, the soil is depleted of mobile and fixed nitrogen, phosphorous, potassium and other important biophilic elements. This is commonly observed under extensively irrigated lands. In addition, chemical degradation is associated with an excess accumulation of easily and poorly soluble salts coming from groundwater or irrigation water (secondary salinisation) and the accumulation of heavy metals, radionuclide and synthetic compounds of organic nature (soil pollution).

Chemical degradation has a negative effect on plants' uptake of water and macro- and micronutrients, while individual ions and compounds can have a toxic effect on crops. In addition, chemical degradation affects the functioning of the soil biota and processes of humification.

4.3.3 Physico-Chemical Soil Degradation

Physico-chemical soil degradation is determined by negative changes in the composition of the soil absorption complex. In the irrigated Chernozem and Kastanozem soils, the physico-chemical degradation most often occurs due to accumulation of exchangeable sodium in the SAC. As a result, the reaction of the soil solution worsens; the dispersion of the organic and mineral parts of the soil increases due to alkalisation. The negative changes associated with soil acidification occur to a much lower extent in irrigated soils.

4.3.4 Biological Soil Degradation

Biological soil degradation includes biochemical processes that cause soil to be depleted of its

Table 4.11 Degradation classification for irrigated soil

	Degradation types				
	Physical	Chemical	Physico-chemical	Biological	Hydrological
Degradation factors	Degradation groups				
	- Overconsolidation - Soil texture destruction - Consolidation caused by chemical processes - Irrigation-induced erosion - Planning-based degradation	- Irrigation-induced salinity - Depletion - Chemical pollution	- Irrigation-induced alkalisation - Magnesium-based alkalinity - Reduction of CEC and buffering - Alkalisation and acidification	- Humus reduction - Soil fatigue - Unfavourable biota succession - Deterioration of biological and enzyme activity	- Over-wetting - Waterlogging
Degradation degree*	1. Weak—<10% 2. Moderate—10–25% 3. Strong—26–50% 4. Very strong— >50%				
Degradation rate	1. Slow > 20 years 2. Accelerating—10–20 years 3. Fast—<10 years				
Degradation nature	1. Gradual 2. Abrupt				
Degradation resistance	1. High 2. Moderate 3. Low				
Reversibility of degradation	1. Reversible 2. Partially reversible 3. Virtually irreversible				

* The magnitude of the deviation in a property from the initial state or in comparison with the reference soil

organic matter and leads to a deterioration in the quality of its composition (dehumification). This also includes negative changes in the number and the species diversity of soil biota, as well as the accumulation of phytotoxic substances of organic nature, which are decomposition products of the crop residues and metabolism of living organisms (soil fatigue). In most cases, biological degradation develops because of an environmental discrepancy between the soil environment and the plant community, which affect it unilaterally. Biological degradation significantly reduces soil fertility and makes it impossible to successfully cultivate crops in highly specialised crop rotations or in monocultures.

4.3.5 Hydrological Soil Degradation

Hydrological soil degradation develops when excess moisture accumulates within the soil profile, originating from irrigation and groundwater. In the case of irrigation, the water periodically stagnates on the soil surface due to excessive irrigation, a poor-quality field surface, or poor filtration conditions (over-wetting). In the case of groundwater, the moisture enters the soil profile from nearby groundwater (waterlogging). The anaerobic conditions cause negative changes in the organic and mineral parts of the soil that are accompanied by the gley formation process.

Multiple types of degradation often occur together in irrigated soils. For example,

waterlogging is usually followed by the secondary salinisation and alkalinisation of irrigated soils, and by negative changes in their physical properties. In addition, the development of one type of degradation may initiate negative processes characteristic of another type of degradation. In particular, biological degradation manifested in dehumification entails the destruction of irrigated soils and a decrease in their exchange and buffering capacities. All this greatly complicates the use of land and reclamation practices.

4.3.6 Degree of Degradation

The degree of degradation varies from weak to very strong. It is characterised by properties deviating from their initial state or in comparison with the reference soil. The degree of degradation can be expressed with the help of both absolute and relative indicators. However, for many types of degradation, such scales have not been developed. In some cases, the degree of soil degradation is assessed based on yield reduction. However, this approach is unlikely to be valid, since a decrease in yield may not occur in the initial stages of soil degradation. For example, when the level of groundwater initially rises, an increase in yield can even be observed as plants use additional moisture from the capillary edges. Subsequently, as a result of salinisation, alkalinisation, gleying and other negative processes, there is a significant deterioration in soil fertility and a sharp decrease in the productivity of irrigated land. Therefore, to assess the degree of degradation it is mainly necessary to use indicators characterising soil properties and yield data as corrective measures. The classification of the degree of degradation given in Table 4.11 is very general, and evaluation criteria are probably required for each type of degradation. Thus, in characterising sodium alkalinisation, different countries can use their specific methodological approaches, methods and criteria for evaluating alkaline soils formed as a result of secondary

salinisation (Shishov and Pankova 2006; Richards 1968), etc. It should also be borne in mind that changes in individual soil parameters can occur not as a result of degradation per se, but as a result of a new hydrothermal regime.

4.3.7 Rate of Degradation

The rate of degradation characterises the intensity of the increase in negative changes over time, which is assessed by monitoring irrigated soils. The rates of development of different types of degradation vary significantly. This depends on the soil's resistance to each type of degradation and the intensity of the factor causing the degradation changes. Secondary salinisation and alkalinisation of irrigated soils occur relatively quickly during irrigation with saline waters. The higher the degree of mineralisation in the irrigation water, the more actively these processes take place. The destruction of soil texture occurs with less intensity, and a significant amount of time is required for a clear manifestation of compaction caused by a chemical process. The latter is especially true during irrigation with freshwater.

4.3.8 Nature of Degradation

The nature of the degradation characterises how the degradation process specifically manifests. In some cases, soil degradation can develop gradually, with a more or less uniform increase in negative changes over time until it reaches a maximum under the given conditions. Therefore, in particular, secondary salinisation and alkalinisation, biochemical dehumification and other types of degradation occur in a similar way in soils irrigated with saline waters.

In other cases, the manifestation of the degradation may be intermittent. At the initial stages, due to the buffer properties of the soil, the negative effects of degradation may not be detected or may manifest to a very low degree.

Then, after passing the critical point, the soil sharply degrades or acquires a much higher degree of degradation compared with the period when its protective mechanisms were still active.

4.3.9 Reversibility of Degradation

The reversibility of degradation is the ability to restore soil properties which were modified or lost as a result of degradation processes. Some types of degradation (depletion, weak alkalisation, adverse pH of soil, etc.) can be eliminated in a relatively short time. Relatively simple agrochemical techniques and chemical reclamation, and changing the nature of the land use, quickly restore the properties of the soil to the level of non-degraded or reference analogues. Eliminating the consequences of certain types of degradation (irrigation-induced erosion, compaction caused by a chemical process, pollution with heavy metals and radionuclide) is a difficult and extremely problematic task in the short term. Especially when these types of degradation are strongly developed, they can become irreversible. Although the development of some degradation processes (waterlogging, strong alkalinity, high loss of humus, de-structuring) can be eliminated through various reclamations, their residual effects can persist for a long time. In particular, after exchangeable sodium is removed from the SAC of the soils subjected to strong alkalisation, increased dispersion, poor structure and a tendency to crust formation are retained due to the alkaline lyophilisation of colloids. This is the partial reversibility of the process.

4.3.9.1 Resistance to Degradation

Resistance to degradation is the soil's ability to withstand external influences while maintaining its production and environmental functions. Soils' resistance to different types of degradation varies. Therefore, a detailed assessment of changes in soil properties under the influence of irrigation is necessary.

4.4 Conclusion and Outcomes

1. Based on an analysis of the characteristics and effects of soil degradation caused by irrigation in the steppe agrolandscapes of Russia, a conceptual framework for the classification has been developed.
2. The framework covers five degradation types (physical, chemical, physico-chemical, biological, hydrological) and their factors, and categories of degree, rate, nature, resistance and reversibility of degradation.
3. The framework has the potential to be applied for monitoring and mapping soil degradation caused by irrigation.

References

- Ahmad NSBN, Safiah FBM, Yusoff YM, Didams G (2020) A systematic review of soil erosion control practices on the agricultural land in Asia. *Int Soil Water Cons Res* 8(2):103–115. <https://doi.org/10.1016/j.iswcr.2020.04.001>
- Andreiuk AI, Iutinskaya GA, Dulgerov AN (1988) Soil microorganisms and intensive farming. Kiev, p 189 (Почвенные микроорганизмы и интенсивное земледелие, Киев, 189 стр)
- Bilgili AV, Yeşilnacar İ, Akihiko K, Nagano T, Aydemir A, Hızlı HS, Bilgili A (2018) Post-irrigation degradation of land and environmental resources in the Harran plain, southeastern Turkey. *Environ Monit Assess* 190(11):660. <https://doi.org/10.1007/s10661-018-7019-2>
- Braimoh AK, Vlek PLG (eds.) (2008) Land use and soil resources. Springer, Heidelberg, Germany, pp 1–7. <https://doi.org/10.1002/ldr.881>
- Brinck E, Frost C (2009) Evaluation of amendments used to prevent sodification of irrigated fields. *Appl Geochem* 24(11):2113–2122. <https://doi.org/10.1016/j.apgeochem.2009.09.001>
- Buckland GD, Bennett DR, Mikalson DE, de Jong E, Chang C (2002) Soil salinisation and sodification from alternate irrigations with saline-sodic water and simulated rain. *Can J Soil Sci* 82:297–309. <https://doi.org/10.4141/S01-080>
- Chizhikova NP, Baranovskaya VA, Khitrov NB (2011) The effect of long-term irrigation on the state of aggregation and mineralogical composition of the silt fraction of Kastanozems in the trans-Volga region (Влияние длительного орошения на степень агрегированности и минералогический состав илистой фракции темно-каштановых почв Заволжья). *Pochvovedenie* 8:978–994

- Cockroft B, Olsson KA (2000) Degradation of soil structure due to coalescence of aggregates in no-till, no traffic bed in irrigated crops. *Aust J Soil Res* 38:67–70
- Cucci G, Lacolla G (2013) Irrigation with saline-sodic water: effects on two clay soils. *Ital J Agron* 8:94–101. <https://www.agronomy.it/index.php/agro/article/view/ija.2013.e13/643>
- Dubovik EV (2012) Influence of sprinkling irrigation on the macrostructure of typical Chernozem (Влияние дождевания на макроструктуру чернозема типичного). *Pochvovedenie* 3:350–335
- Emdad MR, Shahabifar M, Fardad H (2006) Effect of different water qualities on soil physical properties. In: 10th international water technology conference, IWTC10, Alexandria, Egypt, pp 647–652. https://www.researchgate.net/publication/237742441_EFFECT_OF_DIFFERENT_WATER_QUALITIES_ON_SOIL_PHYSICAL_PROPERTIES. Accessed on 7 March 2021
- Essington ME (2004) Soil and water chemistry: an integrative approach. CRC Press LLC, Boca Raton
- FAO (2008) Management of irrigation-induced salt-affected soils. *FAO Soils Bulletin*, No. 39, United Nations Food and Agriculture Organisation, Rome, Italy
- FAO (2019) Proceedings: global symposium on soil erosion. 15–17 May 2019. FAO, Rome. <http://www.fao.org/3/ca5582en/CA5582EN.pdf>. Accessed on 7 March 2021
- Foster S, Pulido-Bosch A, Vallejos A, Molina L, Llop A, MacDonald AM (2018) Impact of irrigated agriculture on groundwater-recharge salinity: a major sustainability concern in semi-arid regions, *Hydrogeology J* 26 (8):2781–2791. <https://doi.org/10.1007/s10040-018-1830-2>. <https://core.ac.uk/download/pdf/196583203.pdf>
- Gurbanov EA (2010) Soil degradation resulted from erosion caused by furrow irrigation (Деградация почв в результате эрозии при поливе по бороздам). *Pochvovedenie* 12:1494–1500
- Herrero J, Covetta OP (2005) Soil salinity changes over 24 years in a Mediterranean irrigated district. *Geoderma* 125:287–308. <https://doi.org/10.1016/j.geoderma.2004.09.004>
- Hillel D, Braimoh AK, Vlek PLG (2008) Soil degradation under irrigation. In: Braimoh AK, Vlek PLG (eds) *Land use and soil resources*. Springer, Dordrecht, pp 101–119. https://doi.org/10.1007/978-1-4020-6778-5_6
- Jie C, Jing-Zhang C, Man-Zhi T, Zi-Tong G (2002) Soil degradation: a global problem endangering sustainable development. *J Geog Sci* 12(2):243–252. <https://doi.org/10.1007/BF02837480>
- Kanzari S, Daghari I, Šimůnek J et al. (2020) Simulation of water and salt dynamics in the soil profile in the semi-arid region of Tunisia-Evaluation of the irrigation method for a tomato crop. *Water* 12(6):1594. <https://doi.org/10.3390/w12061594>
- Karlen DL, Rice CW (2015) Soil degradation: will humankind ever learn? *Sustainability* 7(9):12490–12501. <https://doi.org/10.3390/su70912490>
- Karmanov II, Bulgakov DS (1998) Soil Degradation: suggestions for improving terms and definitions. (Деградация почв: предложения по совершенствованию терминов и определений). Anthropogenic degradation of soil cover and measures for its prevention (Антропогенная деградация почвенного покрова и меры ее предупреждения). Moscow, Russian Academy of Agricultural Sciences 1:5–7
- Khitriv NB (1998) Soil and soil cover degradation: concepts and approaches to obtaining estimates (Деградация почв и почвенного покрова: понятия и подходы к получению оценок). Anthropogenic degradation of soil cover and measures for its prevention, Moscow, Russian Academy of Agricultural Sciences 1:20–26. (Антропогенная деградация почвенного покрова и меры ее предупреждения)
- Kirankumar S, Nagaraja MS, Suma R, Alur AS (2015) Extent of soil sodification as influenced by different irrigation water sources in a typical black soil of Karnataka. *An Asian J Soil Sci* 10(1):154–157. <https://doi.org/10.15740/HAS/AJSS/10.1/154-157>
- Kiryushin VI (1998) The methodology for assessing and preventing soil degradation and agrolandscapes (О методологии оценки и предотвращения деградации почв и агроландшафтов). Anthropogenic degradation of soil cover and measures for its prevention (Антропогенная деградация почвенного покрова и меры ее предупреждения). Moscow, Russian Acad Agric Sci 1:8–10
- Lekakis EH, Antonopoulos VZ (2015) Modeling the effects of different irrigation water salinity on soil water movement, uptake and multicomponent solute transport. *J Hydrol* 530:431–446. <https://doi.org/10.1016/j.jhydrol.2015.09.070>
- Lozovitsky PS (2005) Changes in the properties of dark Chestnut soil under the conditions of prolonged irrigation by the example of the Kakhovskaya irrigation system. *Pochvovedenie* 5:620–633 (Изменение свойств темно-каштановой почвы в условиях длительного орошения на Каховской оросительной системе)
- Lozovitsky PS (2012) Monitoring of soil humus condition of the Ingulets irrigation system. *Pochvovedenie* 3:336–349. (Мониторинг гумусового состояния почв Ингулецкой оросительной системы)
- Lyubimova IN, Motuzov VYa, Bondarev AG (2012) Changes in virgin and postirrigation soils of Solonetz complexes of the Privolzhskaya sandy ridge depending on the depth of the groundwater. In: *Degradation of rain-fed and irrigated Chernozem soils under the conditions of waterlogging and melioration*. Nauchnye Trudy, Moscow: APR, pp 107–125. (Изменение целинных и постирригационных почв солонцовых комплексов Приволжской песчаной гряды в зависимости от глубины залегания грунтовых вод)

- Machekposhti MF, Shahnasari A, Ahmadi MZ, Aghajani G, Ritzema H (2017) Effect of irrigation sea water soil salinity and yield of oleic sunflower. *Agric Water Manag* 188(1):69–78. <https://doi.org/10.1016/j.agwat.2017.04.002>
- Mamontov VG (2013) Irrigated Chernozem and Chestnut soils: composition, properties, transformation processes (Орошаемые черноземы и каштановые почвы: состав, свойства, процессы трансформации). Timiryazev State Agrarian Academy, RGAU-MTAA p, Moscow, p 290
- Minashina NG (2009) Problems of soil irrigation in the steppes of southern Russia and the solution possibilities based on the analysis of production experience 1950–1990. *Pochvovedenie* 7:865–874 (Проблемы орошения почв степей юга России и возможности их решения на основе анализа производственного опыта 1950–1990)
- Minashina NG (2011) Irrigation waters with a high content of magnesium and its role in the degradation Chernozem in southeastern Europe. *Pochvovedenie* 5:564–571. (Оросительные воды с повышенным содержанием магния и их роль в деградации черноземов на юго-востоке Европы)
- Minhas PS, Ramos TB, Ben-Gal A, Pereira LS (2020) Coping with salinity in irrigated agriculture: crop evapotranspiration and water management issues. *Agric Water Manag* 227:105832. <https://doi.org/10.1016/j.agwat.2019.105832>
- Mohammed S, Alsafadi K, Talukdar S, Kiwan S, Hennawi S, Alshihabi O, Sharaf M, Harsanyie E (2020) Estimation of soil erosion risk in southern part of Syria by using RUSLE integrating geo informatics approach. *Remote Sens Appl Soc Environ* 20:100375. <https://doi.org/10.1016/j.rsase.2020.100375>
- Mosienko NA, Chumakova LN (1990) Water regime of Chestnut soils in the Zavolzhye. *Pochvovedenie* 4:60–65 (Водный режим каштановых почв Заволжья)
- Olsson L, Barbosa H, Bhadwal S, Cowie A, Delusca K, Flores-Renteria D, Hermans K, Jobbagy E, Kurz W, Li D, Sonwa DJ, Stringer L (2019) Land degradation. In: Shukla PR, Skea J, Calvo Buendia E, Masson-Delmotte V, Pörtner H-O, Roberts DC, Zhai P, Slade R, Connors S, van Diemen R, Ferrat M, Haughey E, Luz S, Neogi S, Pathak M, Petzold J, Portugal Pereira J, Vyas P, Huntley E, Kissick K, Belkacemi M, Malley J (eds) *Climate change and land: an IPCC special report on climate change, desertification, land degradation, sustainable land management, food security, and greenhouse gas fluxes in terrestrial ecosystems*. https://www.ipcc.ch/site/assets/uploads/sites/4/2019/11/07_Chapter-4.pdf. Accessed on 7 March 2021
- Oster JD (2004) Amendment use to mitigate the adverse effects of sodic water. In: *Proceedings of the international conference on sustained management of sodic lands extended summaries*, UPCAR Lucknow India, pp 89–91
- Pankova EI (2008) Critical analysis of the history of irrigation development in the Soviet Union. *Pochvovedenie* 9:1138–1140. (Критический анализ истории развития орошения в Советском Союзе)
- Panov NP, Mamontov VG (2001) Soil processes in irrigated Chernozem and Chestnut soils and degradation prevention measures. Moscow, Russian State Agrarian University, pp. 253f. (Почвенные процессы в орошаемых черноземах и каштановых почвах и пути предотвращения их деградации).
- Pilgunova MY, Grigorieva EE (1983) Particular qualities of the humus condition of irrigated southern Chernozem soils. *Pochvovedenie* 1:22–29 (Особенности гумусного состояния орошаемых южных черноземов).
- Qadir M, Noble AD, Schubert S, Thomas RJ, Arslan A (2006) Sodicy-induced land degradation and its sustainable management: problems and prospects, *Land Degrad. Develop* 17:661–676. <https://doi.org/10.1002/ldr.751>
- Richards LA (ed) (1968) *Diagnosis and improvement of saline and alkaline soils*. Agriculture Handbook, New Delhi, p 160
- Rozanov BG (ed) (1989) *Irrigated Chernozem soils*. Moscow, Moscow State University, pp. 240f. (Орошаемые черноземы. Москва, МГУ).
- Ryskov YG, Gurov AF (1987) The role of irrigation in the modern evolution of terraced Chernozems of the Nizhny Don. *Pochvovedenie* 12:81–88. (Роль орошения в современной эволюции террасовых черноземов Нижнего Дона)
- Shishov LL, Pankova EI (eds) (2006) *Saline soils of Russia*. IKC Akademkniga, p 854 (Засоленные почвы России).
- Soil degradation and protection (2002) Moscow, Moscow State University, p 654f. (Деградация и охрана почв).
- Stockle CO (2007) Environmental impact of irrigation: a review. State of Washington Water Research Center, Washington State University. <http://citeserx.ist.psu.edu/viewdoc/download?doi=10.1.1.488.4861&rep=rep1&type=pdf>. Accessed on 7 March 2021
- Tanirbergenov S, Saljnikov E, Suleimenov B, Saparov A, Čakmak D (2020) Salt affected soils under cotton-based irrigation agriculture in southern Kazakhstan. *Zemljiste I Biljka* 69(2):1–14. <https://doi.org/10.5937/ZemBilj2002001T>. http://www.sdpz.rs/images/casopis/2020/zib_69_2_70.pdf
- WRB (2015) *World reference base for soil recourses*. Food and Agriculture Organization of the United Nations, Rome, p 2015
- YeI P, Konyushkova MV (2014) Effect of global warming on soil salinity of the arid regions. *Russ Agric Sci* 39(5–6):464–467. <https://doi.org/10.3103/S1068367413060165>
- Yousefi S, Pourghasemi HR, Avand M, Janizadeh S, Tavangar S, Santosh M (2020) Assessment of land degradation using machine-learning techniques: a case of declining rangelands. *Land Degr Devel: Early View*. <https://doi.org/10.1002/ldr.3794>

Zaydelman FR (2014) Degradation of meliorated soils in Russia and neighbouring countries as a result of changes in water regime and methods of protection. Voronezh, Kvarta, p 269f. (Деградация мелиорированных почв России и сопредельных стран в результате изменения их водного режима и способы защиты).

Zaydelman FR (2016) Gley formation is a global soil-forming process. Process theory and Practice. Voronezh, Kvarta, pp. 328f. (Глееобразование – глобальный почвообразовательный процесс. Теория процесса и практика применения).



Desertification in Western Siberia: Identification, Assessment and Driving Forces in Temporal Scale

5

V. Schreiner and Burghard C. Meyer

Abstract

Desertification factors in the dry sub-humid regions of Russia have not yet been sufficiently studied from a systemic point of view. The Northern Kulunda Steppe is a typical inner continental steppe on the southern border of the West Siberian Plain. It is an intensively used landscape and arable land covers an area of 90% of the total land surface. The main objectives of this study were (1) to evaluate existing “desertification assessment systems” based on of post-Soviet/Russian and European approaches, (2) to develop a comprehensive regionally adapted system of indicators and identify desertification processes in the Northern Kulunda Steppe and (3) to analyse the driving forces behind these and their variation in temporal scale. Based on change detection thresholds, 16 biophysical indicators and 18 socio-economic processes were analysed and assessed to

produce a systematic and reliable description of the regional desertification process. To shed light on the desertification processes, regional geocological prerequisites and the main climatic and anthropogenic factors causing desertification were determined. The results on the interdependence of causal factors were used to create a better model for describing the temporal development of desertification processes. Analysis of the indicators resulted in (1) critical discussion about the applicability of Russian and European indicator systems, (2) the identification and refined description of the desertification process, (3) a description of the relationships between factors affecting the steppe regions and the variation of driving forces on a temporal scale and (4) evidence that the desertification processes affecting the steppe regions of the south of Western Siberia lead to the adaptation of environmental and socio-economic components.

Keywords

Western Siberia · Steppe ecosystems · Desertification · Indicator framework · Biophysical indicators · Socio-economic indicators · Driving forces · Complex monitoring

V. Schreiner (✉)

Institute of Geosciences and Geography,
Martin-Luther-University Halle-Wittenberg,
Von-Seckendorff-Platz 4, 06120 Halle, Germany
e-mail: vera.schreiner@geo.uni-halle.de

B. C. Meyer

Department of Physical Geography and Geoecology,
Institute of Geography, Leipzig University,
Johannisallee 19a, 04103 Leipzig, Germany
e-mail: burghard.meyer@uni-leipzig.de

5.1 Introduction

Desertification studies have been carried out since the 1970s to analyse and better understand what is one of the most important environmental problems of our time in dryland areas. The term “desertification” was formulated in 1949, when the main focus was on describing environmental changes since the Neolithic (Spooner 1989). Various past cultures fought this undesirable problem, such as the Sumerians (5000 BP), the Mayans (1000 BP) and other civilisations (Jacobsen and Adams 1958; Bosselmann 1992; Warner 2004). Today, more than one billion people in over 110 countries are affected by the social, economic and environmental problems caused by desertification (GIZ 2013). The main causes of desertification are primarily analysed today in the context of the anthropogenic impact on the natural environment and extreme fluctuations in the climate system (Meckelein 1983; Mensching 1979, 1990; Ibrahim 1978, 1992; Thomas and Middleton 1994; UNSD 2012, Cherlet et al. 2018; IPBES 2018; Emadodin et al. 2019; Abdullahi and Cheri 2020). The cause (and a key control variable) for any start of a desertification process is an anthropogenic impact on natural, undisturbed ecosystems. Such impacts disturb ecosystems’ natural potential for self-regeneration and resilience due to the risk of system changes and destruction (Mensching 1979, 1990; Baumhauer 2011; Kosmas et al. 2016; Whitford and Duval 2020). Ongoing desertification is regarded as one of the main causes of instability in regional governance and economic systems (ME Assessment 2005, Egidi et al. 2020; Xie et al. 2020). In the face of a growing population, and in order to protect natural resources and food security, many governments and international scientific societies are working to understand, monitor and solve associated problems.

Scientific approaches in studies on desertification should address the problems of:

- Lacking scientific knowledge on the multiple, complex relationships between the system’s

components of meteorological, climatologic, environmental and anthropogenic processes. This problem is associated with correlation of the causes and effects and, at the same time based on well-known initial factors and processes in the physical, socio-economic and management systems.

- The fact that the significance and specificity of the sets of indicators used to measure and monitor desertification have a more or less unknown quality, since cause-effect relationships and cause-effect networks are statistically analysed using several indicators, rather than fully verified cause-and-effect relationships, ignoring various aspects which affect systems.
- Regional (geographical) differences in the highly complex cause-effect correlations (Baumhauer 2011), which lead to detailed regional studies and regional indicator systems for elucidating the biophysical and socio-economic factors of desertification.
- The fact that the most detailed studies in the field of desertification research and the measures designed to prevent and solve the problem of desertification have been developed in heavily affected regions of the world (e.g. in the Sahel), ignoring industrialised countries such as the former Soviet Union/Russia and other cold regions.

The terms “soil degradation” and “land degradation” are commonly used synonymously. It should be emphasised that the soil degradation mainly affects in situ soils, and land degradation implies a wider range of degradation of the functioning and provision of ecosystems and ecosystem services. Desertification is defined as land degradation in arid, semi-arid and dry sub-humid regions (Fig. 5.1). Desertification is therefore a region-specific type of land degradation involving multiple indicators and process systems, such as the soil degradation system (GIZ 2011; Schreiner 2017). As unsustainable land use causes both land degradation and soil degradation in all climatic zones around the world, this is not considered a problem only

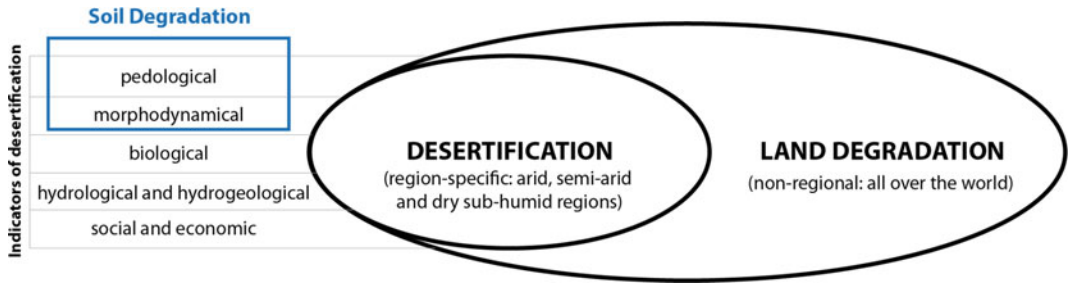


Fig. 5.1 Systematic model of the interdependencies of desertification, land degradation and soil degradation (GIZ 2011, adapted)

specific to dryland areas (DSD 2009, Mirzabaev et al. 2019).

In this study, we used the following definition of the term “desertification”: a permanent and irreversible land degradation in environmentally sensitive and geo-ecologically predetermined regions with arid, semi-arid and dry sub-humid climates caused by anthropogenic impacts on ecosystems and extreme climatic conditions (climate change) that are stronger/higher than the capacity of the system resilience (Schreiner 2017).

Based on this scientific context the aim of this study was to:

- shed light on desertification factors of the Northern Kulunda Steppe by identifying basic geoecological factors and analysing anthropogenic and climatic causes;
- develop integrated regional indicator systems to describe desertification based on a comparative analysis of European and post-Soviet methodological scientific methods;
- assess selected indicators to identify desertification and
- describe the temporal steps of the drivers of desertification processes in the study area.

5.2 Study Area

The south of West Siberia is not in the focus of land degradation and desertification research in Russia. Semiarid areas of Western Siberia

(especially the South Kulunda Steppe) have been studied in detail regarding the processes associated with the indicators of desertification, such as deflation and water erosion (Rudskij 1996, 2000; Tanasienko et al. 1999; Meinel 2002; Paramonov et al. 2003; Paramonov 2012; Kulunda-Projekt 2012). For the area studied, located in the dry sub-humid steppe, the determinants of desertification have not yet been studied in detail. The selection criteria for the study area were based on the definition of desertification, the aim being to elucidate the geoecological predisposition and anthropogenic and climatic factors behind it:

- The area in the Northern Kulunda Steppe has an average aridity index of 0.6 and is a dry sub-humid region as classified in UNCCD dryland categories. The territory is a typical grassy steppe, not a type of desert steppe.
- The area is one of the most heavily affected by climate change. The average annual temperature increase in the last 100 years was 0.3–0.6 °C globally and 0.9 °C in Russia (Jagudin 2003). The average annual temperature increase determined in Western Siberia over the past 40 years was 0.31 °C (Roshydromet 2016).
- Another criterion for choosing this area was that the location underwent the planned transformation of the steppe in Western Siberia in the past. In such regions, large-scale disasters related to land degradation occurred. The degradation was caused by overcultivation, overgrazing, the devastation of woody vegetation and inadequate water management

(Meyer et al. 2008). Approximately, 80% of the study area is agricultural land.

- The lack of data on desertification in the northern part of Kulunda played a key role in choosing the study site.

5.2.1 Regional Geocological Preconditions

Northern Kulunda is a typical inner continental grass steppe that is not influenced by the sea. It is located on the southern edge of the West Siberian Plain and features about 90% arable and urban land. The steppe is not strongly affected by mountains, and its continental location is characterised by the influence of dry Arctic, subtropical and continental air circulation, with mostly southern winds. The wind often transports aeolian salts, blown out of the plains and depressions in Kazakhstan and Central Asia and deposited by rain and as dry deposits. The geocological predisposition of the typical dry steppes of West Siberia can be described as follows:

Climate: The average annual aridity index is 0.6 (dry sub-humid climate). During the vegetation period, the semi-arid climate is characterised by an aridity index of 0.4–0.35. The annual precipitation value is around 240–320 mm (Kravzov and Donukalova 1996; AKS 1966).

Relief and geomorphology: Kulunda is located geologically in an undrained endorheic basin at an altitude of 100–120 m north and does not have a strongly structured relief (Atlas, 2002). The most important geomorphological reliefs are long southwest-facing hills (Griva) with a height of about 4–5 m and a length of often from 1 to 3 km. Numerous shallow lakes are located in the depressions (Kravzov and Donukalova 1996).

Soil: The zonal soils of Kulunda are typical black soils (humus-rich Chernozems) with a local pattern of alluvial soils, boggy areas and salt-affected or salt-dominated soils (e.g. Solonetz and Solonchak soils) distributed depending on

the position on the relief (Meyer et al. 2008; Smolnzeva et al. 2007).

Hydrology and hydrogeology: The water system network is sparsely developed in the Kulunda catchments, only covering 0.10 km² (Atlas 2002; Meyer et al. 2008). The rivers and creeks dry out in the form of an internal delta in a geological depression containing several lakes. The groundwater tables are usually at a depth of 0.5–10 m below the surface (Paramonov et al. 2003; Kasanzev and Magaeva 2003) (Fig. 5.2).

Flora and fauna: The natural steppe vegetation was totally modified during the steppe conversion. During this process the cultural landscape was developed. Some remains of steppe grass vegetation are located at the edges between the depressions and the Griva Hills, in small areas around lakes and swamps (Meyer et al. 2008).

Land use: Today, Northern Kulunda is dominated by 79–80% agricultural land, made up of 52–55% arable land, 10–17% hayfields and 31–35% pastures (Smolnzeva et al. 2007). At the end of the twentieth and the beginning of the twenty-first century, the steppe landscapes of the Kulunda Region underwent major land use changes. Hese et al. (2020) reported that the area of cultivated land in the Kulunda Steppes increased until 1989 by almost 1 million hectares due to a decrease in the area of pastures and steppes, then decreased by 500,000 hectares by 2013/2014 due to an increase in the area of pastures and steppes.

Socio-economy and demography: The dominant economic sectors are agriculture, health/education and trade (Atlas 2002), with 22–50% of employees working in the agricultural sector (Passport BR. 2015a). The population density is very low at about 7–8 inhabitants per km².

5.3 Analysis of Data and Approaches

The study focused on regional and local investigations based on published regional statistics, papers and scientific investigations on Western

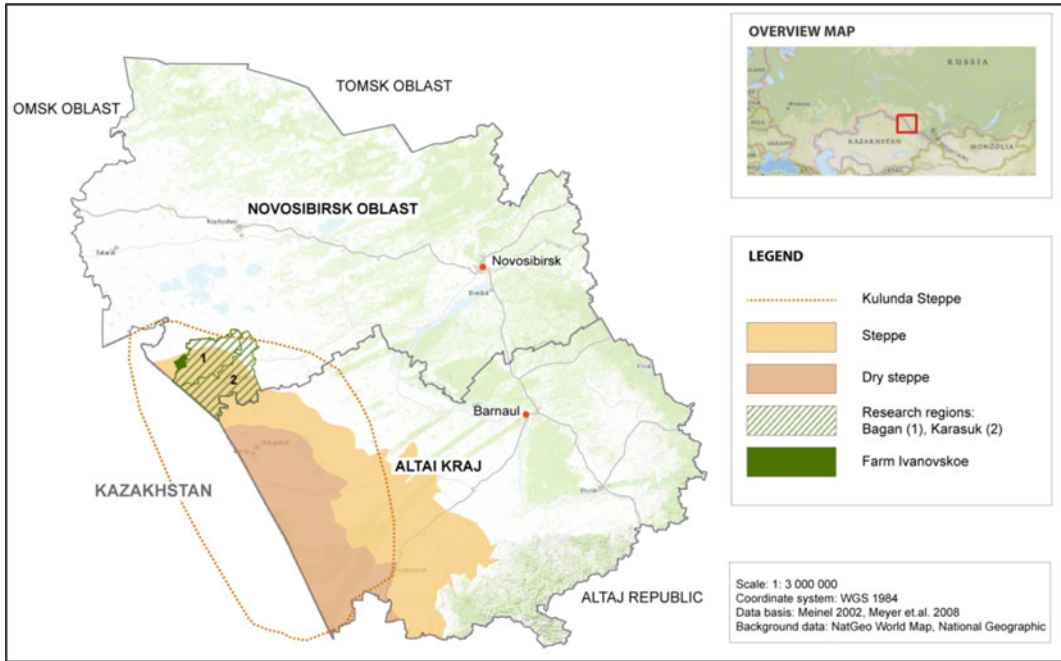


Fig. 5.2 Study area in the Kulunda steppe—research sites in Bagan and Karasuk Regions and Ivanovskoe farm (Schreiner 2017)

Siberia and the Kulunda Steppe. Some data are based on field research in Russia. Some of the materials used are based on questionnaires and field mapping. The methodology chosen to assess the wide range of indicators was based on data from local and regional studies, data from standardised climate data and documents from regional authorities, published statistics and a general analysis of the media. The methods applied to study various analysed data were field mapping, map interpretation (especially for the time series analysis) and the analysis of differences to characterise the changes in the processes. The multilevel information used was based on geographic information systems and remote sensing methods.

Indicators of different spatial scales were used to identify desertification and land degradation factors. The following approach was applied: (1) selection of general desertification indicators; (2) development of a regional indicator system and (3) investigation on data availability at

different scales. The local analysis was also based on field survey information and the newly interpreted data from the Siberian Academy of Sciences in Novosibirsk. According to the UNCCD definition of desertification and land degradation, indicators should include factors that are affected by the climate and human activity (UNCCD 2012). It was assumed that, following the principles of natural processes, anthropogenic impacts would be relatively rapid and have a major influence on the dynamics initiated by the conversion of the vegetation cover. Climatic dynamic factors also have an impact, but over a longer period of time. Problems arise when, for example, in terms of morphodynamics, quasi-natural processes (e.g. wind or erosive rains) are activated that affect soils due to changes in the vegetation cover of arable land (Schreiner 2017). Finally, it should be emphasised that in order to compare the status before the steppe conversion and the status quo of the desertification process, at least two time steps are always studied.

5.3.1 Evaluation of Current “Desertification Assessment Systems”

The main basis for any indicator system development is knowledge about the evaluation of existing “desertification assessment systems” including the methodology used, based on post-Soviet/Russian and European methodological approaches.

The identification and assessment of desertification-related damage in Russia and in post-Soviet countries focused on the dryland areas of Siberia and Central Asia (Charin et al. 1987; Kust 1999; Kust and Andreeva 2006; NPDBO 2000; Paramonov et al. 2003; OZZR 2009).

The studies cited above used methods and indicator systems as summarised below:

- limited to morphodynamic/pedological, hydrological/pedological or biological aspects of desertification (the latter simplified to botanical analysis);
- often simplify the desertification process by taking a selective approach to soil degradation, describing a strong and well-developed desertification process, ignoring or not identifying the initial phases of desertification;
- do not always distinguish between primary and secondary salinisation of soils;
- simply include only the biophysical factors of desertification and are therefore not suitable for the inclusion of socio-economic changes and measures to adapt to environmental changes.

In Europe, the indicator systems developed for identifying and assessing desertification differ from the systems developed in the post-Soviet countries in Central Asia: they are based on a much more complex and multi-disciplinary scientific approach and are focused on sustainability indicators. They include the Pressure-State-Response (PSR) model, OECD (1993, 2003); the Driving Force-State-Response (DSR) model; the Drivers-Pressures-State-Impact-Response model (DPSIR, an extension of the PSR model

developed by the OECD), EEA (1999) and the AEZR model (Aktivitäten-Einwirkungen-Zustand-Reaktionen) by the ECOLOG Institute (2011). The latter model strongly emphasises the socio-economic and management aspects of the problems of desertification.

The AEZR approach is based on the PSR and DSR models and ranks the social and economic dimensions according to the environmental dimensions (ECOLOG Institute 2011). The European desertification indicator systems cannot easily be transferred to Russia without considerable modification. This is due to their scientific basis: they were formulated previously for developing countries such as the Sahel Region. The identification of desertification in industrialised countries should summarise some indicators, as well as add specific indicators related to land use.

5.3.2 Development of a Regionally Adapted Indicator System

Analysis of the potential applicability of the individual post-Soviet/Russian or European desertification monitoring or assessment systems revealed an urgent need for changes and modifications when developing a new system for application in the Kulunda Steppe. The new system was developed to include geo-environmental factors specific to the region, as well as integrating specific causes and initial parameters and identifying new factors.

Thus, the theoretical and methodological basis of the following tables is the methods used by European, especially German, scientists and organisations that publish important information for describing and assessing desertification processes, such as Mensching (1990), Ibrahim (1992), UNCCD (2001), Rubio and Recatal (2006), Kosmas et al. (2013), and the publications from Russia mentioned above (Charin et al. 1987; Kust 1999; Kust and Andreeva 2006; NPDBO 2000; Paramonov et al. 2003; OZZR 2009).

The system of desertification indicators in the Kulunda Steppe is divided into four groups

indicating changes in land use determined by biophysical processes, and one large group of indicators determined by socio-economic processes.

The framework of indicators in Table 5.1 firstly integrates the following geocological factors: (a) vegetation cover, (b) plant community, (c) plants unusable for pasture, (d) biomass, (e) natural production, (f) expansion of C4 plants, (g) biological invasion of species, (h) upper groundwater table, (i) drying rivers and lakes, (j) soil and water salinisation, (k) deflation, (l) soil erosion, (m) degradation of the upper soil horizon, (n) loss of organic matter, (o) loss of nutrients and (p) accumulation of sand and gravel in the topsoil (Table 5.1). These indicators have been selected to describe the various processes of land degradation. The literature cited in our study should provide an introduction to the regional data and to the research methodologies of each of the indicators. It is important to state that while survey studies for the Kulunda Steppe are available for each indicator, detailed local investigations in larger areas have not been carried out. The local biophysical investigations were based on studies by Smolenzev et al. (2004) and the expedition report by Koroljuk (2005). Survey studies by other authors that integrate multiple indicators of land degradation cannot yet be applied to the Kulunda Steppe (Schreiner and Meyer 2018; Meyer et al. 2008).

5.3.3 Identification and Analysis of Desertification Processes in the Northern Kulunda Steppe as a Systemic Problem

The choice of meaningful indicators to determine desertification was identified for the regional system of the Kulunda Steppe. 16 biophysical and 18 socio-economic processes were separated and minimally specified for two temporal ecosystem states. The reference time step is a more or less natural grass steppe before conversion to agricultural land during new developments in the 1950s. The second time step was

determined by the state of the ecosystem in the first decade of the twenty-first century and is summarised here:

- The main results can be summed up in the identification of 29 individual desertification processes.
- Fourteen biophysical desertification factors were found to be identified in Northern Kulund, often significantly and clearly, and only two biophysical indicators were not clearly identified (the groundwater table was not used due to the lack of data and dispersion of the C4 plants, and a lack of studies; Table 5.2).
- The ecological problems of desertification are explained by many, but not all socio-economic indicators. One of the key reasons may be the growing financial subsidisation of Russian farms in the first decade of the twenty-first century. The Russian government pays subsidies in the form of seasonally reduced fuel prices, crop insurance, direct payments of loan rates, assistance to families and more. Analysis of the indicators showed that the usual socio-economic indicators of desertification do not explain the existing desertification state, since the main problems are absent in the time span studied in Kulunda, in contrast to other studies conducted in Africa.
- Important regional social indicators were found to describe the processes caused by desertification. Migration balances and migration rates are interpreted as revealing an important depopulation problem in rural areas, which may indicate a deterioration in the quality of life due to desertification. Another factor overlaps this interpretation: a large group of migrants moved to Germany in around 2000.

Analysis of individual indicators (in Table 5.2) in the context of the causes and interdependencies between the indicators revealed that ecological and socio-economic systems in the study area are adapted to the measures potentially protecting against

Table 5.1 Groups of indicators for assessing desertification and their measurement units (Schreiner 2017)

Processes	Group of indicators	Indicators [<i>measuring unit</i>]
Biophysical processes	Biological (8)	(1) Vegetation cover [(%)], (2) Species composition of plant communities [<i>species number, abundance</i>], (3) Production and stock of biomass [<i>t/ha/year, biomass C stock in t</i>], (4) Vitality of vegetation [<i>NDVI</i>], (5) Invasive species, biological invasion [<i>number of invasive species</i>], (6) Non-usable plants (in pasture) [<i>number of plant species, cover (%)</i>], (7) Quality of forest stands [<i>age of forest stands, functionality of wind buffer strips</i>], (8) Spread of C4 plants [<i>number of C4 plants</i>],
	Hydrological and hydro-geological (3)	(9) Ground water [<i>level of first upper ground water level/layer (m)</i>], (10) Degradation of hydrological resources [<i>lake surface area (km²), Run off (m³), salt concentration (mg/l)</i>], (11) Soil salinisation [<i>affectability (ha, km²)</i>],
	Morphodynamical (2)	(12) Aeolian activity [<i>affectability (ha, km²)</i>], (13) Fluvial activity [<i>affectability (ha, km²)</i>],
	Pedological (3)	(14) A horizon [<i>cm</i>], (15) Humus (organic material) and nutrient content [<i>content in %</i>], (16) Skeletisation of the A horizon [<i>amount of clay and fine material fractions (%)</i>],
Socio-economic processes	Social (6)	(17) Transnational and international migration [<i>net migration, migration ratio</i>], (18) Concentration of the population in the central towns caused by internal migration [<i>urban/rural population (%)</i>], (19) Abandoned settlements and small settlements [<i>number</i>], (20) Birth rate [<i>birth rate</i>], (21) Age structure of the population [<i>average age of population, number of retirees per 100 persons of working age</i>], (22) Health problems caused by desertification [<i>health disorders, neoplasm, anomalies (n, %)</i>],
	Economic (12)	(23) Harvest of main crops (cash crops) [<i>harvest (dt/ha)</i>], (24) Fodder availability; change of animal husbandry technology from grazing to full-year stabling [<i>fodder (t/ha)</i>], (25) Livestock, changes in livestock breeding [<i>livestock, animal density, number of cattle</i>], (26) Arable land and change from arable land to meadow/pasture and vice versa [<i>arable land, area of meadows and pasture</i>], (27) Employment structure of the population [<i>number of employees in agricultural sector</i>], (28) Farms [<i>number</i>], (29) Income [<i>roubles per month</i>], (30) Water deficit for domestic use [<i>number and depth of new wells</i>], (31) Application of pesticides and mineral fertilisers [<i>amount used (t/ha/year)</i>], (32) Quality of windbreak management [<i>new planting and follow-up planting (ha/year)</i>], (33) Change of major agricultural economic activities from agriculture to factory animal farming [<i>agricultural land, animal stock</i>], (34) Irrigated area [<i>irrigated land, ha</i>]

Table 5.2 Identification of individual desertification processes in the study area

	Group of indicators	Indicators	Spatial scale of indicator; data quality	Trend indicating desertification: trend in the study area
B I O - P H Y S I C A L P R O C E S S E S	Biological (8)	(1) Vegetation cover (2) Species composition of plant communities (3) Production and stock of biomass (4) Vitality of vegetation (5) Invasive species, biological invasion (6) Non-usable plants (in pasture) (7) Quality of forest stands (8) Spread of C4 plants	(1) RA; III (2) RA; III (3) SW; II (4) NK; II (5) NK; III (6) SW; II (7) SK; III (8) SW; I	(1) Decrease: Decrease (2) Decrease: Decrease (3) Decrease: Decrease (4) Decrease: Decrease (5) Increase: Increase (6) Increase: Increase (7) Increase: Increase (age) Decrease: Decrease (functionality) (8) Increase: Increase
	Hydrological and hydro-geological (3)	(9) Ground water (10) Degradation of hydrological resources (11) Soil salinisation	(9) NK; I (10) RA; III (11) RA; II	(9) Decrease: Decrease (10) Decrease: Decrease (area) Decrease: Decrease (runoff) Increase: Increase (salt content.) (11) Increase: Increase
	Morphodynamical (2)	(12) Aeolian activity (13) Fluvial activity	(12) RA; III (13) RA; II	(12) Increase: Increase (13) Increase: No trend
	Pedological (3)	(14) A horizon (15) Humus (organic material) and nutrient content (16) Skeletisation of the A horizon	(14) RA; III (15) RA; III; (16) RA; III	(14) Decrease: Decrease (15) Decrease: Decrease (16) Decrease: Decrease
S O C I O - E C O N O M I C P R	Social (6)	(17) Transnational and international migration (18) Concentration of the population in the central towns caused by internal migration (19) Abandoned settlements and small settlements (20) Birth rate (21) Age structure of the population (22) Health problems caused by desertification	(17) NK; III (18) NK; III (19) NK; III (20) NK; III (21) NK; III (22) NK; II	(17) Increase: Decrease (18) Increase: Increase (19) Increase: Increase (20) Decrease: Decrease (21) Increase: Increase (22) Increase: Increase
	Economic (12)	(23) Harvest of main crops (cash crops) (24) Fodder availability; change in the animal husbandry technology from grazing to full-year stabling	(23) SK; II (24) RA; II (25) RA; ← (26) NK; III	(23) Decrease: Decrease (24) Decrease: Decrease

(continued)

Table 5.2 (continued)

	Group of indicators	Indicators	Spatial scale of indicator; data quality	Trend indicating desertification: trend in the study area
O C E S S E S		(25) Livestock, changes in livestock breeding (26) Arable land and change in arable land to meadow/pasture and vice versa (27) Employment structure of the population (28) Farms (29) Income (30) Water deficit for domestic use (31) Application of pesticides and mineral fertilisers (32) Quality of windbreak management (33) Change of major agricultural economic activities from agriculture to factory animal farming (34) Irrigated area	(27) NK; III; (28) NK; III; (29) NK; III; (30) NK; II (31) SK; III (32) SK; III (33) RA; III (34) NK; III	(25) Decrease: Increase (26) Decrease: Decrease (27) Decrease: Decrease (28) Decrease: No trend (29) Decrease: Increase (30) Increase: Increase (31) Decrease: Decrease (32) Decrease: Decrease (33) Decrease: Decrease (agric. land) Increase: Increase (animal stock) (34) Increase: Increase

desertification, accompanied by changing environmental conditions. Indicators of adaptation include the spread of C4 plants, natural biological invasion, the expansion of irrigated agricultural area, a change in the specialisation of arable agriculture using a large-scale livestock system, and the replacement of the main agricultural land with livestock.

(a) The spatial scale of the indicators: *SW* South of West Siberia, *SK* Southern Kulunda Steppe, *NK* Northern Kulunda Steppe, *RA* “Ivanovskoe” Research Area Farm.

(b) Data quality related to identification of the desertification indicators:

← the reverse trend of the analysed data; no significant desertification was found; *I* difficult to identify: lack of reliable scientific studies; lack of identification of the process indicator, lack of information in local newspapers, validation is only true based on samples and laboratory results; *II* limited identification: few studies are available;

multiple descriptions in local and regional newspapers but not in historical scientific literature, validated by their own field survey; *III* clearly and reliably identified: numerous scientific studies on the subject are available on the basis of detailed projects and studies. The indicator process is clearly found

(c) Trend indicating desertification

Trend indicating desertification (decrease, increase, no trend)

Trend in the study area (decrease, increase, no trend)/(short interpretation of the trend)

5.3.4 Selected Biophysical Desertification Indicators

Indicators of soil degradation, including issues such as loss and degradation of the upper soil horizons, loss of organic matter, a decrease in

clay and silt fractions in the A horizon, are often associated with an increase in sandy and skeleton soil fractions, as well as indicators revealing morphodynamics (such as deflation and water erosion) and soil salinisation problems (hydrological-pedological indicator). Below are some selected results.

A change in balance or a disturbance in the stability of the soil system is caused by morphodynamic processes such as deflation and soil erosion by water. The scientific literature on qualitative and quantitative measurements of water erosion and soil vulnerability assessment for Northern Kulunda showed strong differences in terms of the published results, mainly due to the diverse spatial scale, from subcontinental, regional and local studies. On a subcontinental scale, data are available from the International Soil Reference and Information Centre (ISRIC), including a map of soil degradation (GLASOD 1991). This map erroneously indicates water erosion as the most important aspect of soil degradation in Northern Kulunda. This is in contrast with a sub-regional programme to prevent desertification in the Altai and Novosibirsk Regions (NPDBO 2000) that was published after implementation of the UNEP project by the Centre for International Projects of Russia and the All-Russian Institute of Agroforestry Melioration (1997–2000) in the West Siberian Steppes. The results of this project showed that the processes caused by water erosion were insignificant in Northern Kulunda.

During this study, soil investigations carried out on a local level from 2004 to 2006 revealed the primary loss of the upper horizon by deflation, and in some places also water erosion problems.

5.3.4.1 Deflation

Precondition: The mean annual snow cover in Northern Kulunda is caused by low levels of winter precipitation and strong snow transport by wind only to a depth of 20 cm. In the winter, the soil is often deeply frozen to a depth of 1.5–2 m (Meyer et al. 2008), causing some winter deflation processes in the low-snow winters (Paramonov et al. 2003). The dominant southwest wind direction means that strong wind with a

speed above 15 ms^{-1} occurs 51–100 days a year (Jaschutin 1999).

Northern Kulunda is only a slightly inclined plain, and is open to emerging storms initiating sand and dust storms (Mezosi et al. 2015). Local studies by Smolenzeva et al. (2007) on a research area of 1400 ha in Northern Kulunda revealed that the deflation process was still active on 16% of the arable land. The deflation process in this area was initiated by the transformation of the steppe in 1955–1956. Many anti-wind erosion measures created subsequently, such as hedgerows, were not capable of stopping the deflation processes. Sites strongly affected by deflation, with dunes at the field edges and minor vegetation cover of only 10% in June (Meinel 2002), are often observed in areas without hedgerow systems or in areas with insufficiently planned protective elements (Smolenzeva et al. 2007).

5.3.4.2 Water Erosion

Little water erosion research on Northern Kulunda is available in the literature. Morphological forms of water erosion are rarely found here because of the very low degree of the slope ($<0.3^\circ$), and low precipitation (243–313 mm). Our observations during fieldwork in 2003–2005 identified water erosion in Northern Kulunda in the form of rill to gully erosion (Fig. 5.3). On a research farm in Ivanovskoe, seven sites were exposed to gully erosion, with a total length of more than 3 km (Smolenzeva et al. 2007), mainly in the immediate vicinity of lakes and covered by pastures. This gully-type erosion was caused by changes in the water level, salt dynamics, damage to the vegetation cover of the pastures by livestock and, finally, snowmelt erosion in spring (Schreiner 2017). This gully water erosion reduces the quality and value of pastures. The eroded soil is transported into nearby shallow lakes (Smolenzeva et al. 2007). Figure 5.3 clearly demonstrates the accumulation of salt on the shoreline and the form of erosion.

5.3.4.3 Soil Salinity

Soil salinity is an important subject among the hydrological indicators of desertification (Mensching 1990). General soil salinity is a



Fig. 5.3 Gully erosion developments around Bagan Lake (Schreiner 2017) (satellite image: Landsat, 08.09.2003, images: Meyer (2003), Schreiner (2005))

hydrological/pedological indicator. The soil salinisation processes of Northern Kulunda are affected not only by the typical imbalance of irrigation and drainage that is typical of desertification processes. Irrigated arable land only makes up 0.17–2.64% of the Karasuk and Bagan Regions (Gos. Doklad Pochva No. 2008, 2013).

However, soil salinisation is very active in Kulunda, caused by near-surface groundwater with a high salt content and an area percentage of salt-dominated soils of 20–25% (Meyer et al. 2008). As well as resulting from the drying of several lakes, the salt-dominated soils (the soils here are locally called Sor Solonchak) are often

found in the areas of former lakes. Areas with solonchak soils increased by 50% between 1982 and 2007 (Smolenzeva et al. 2007).

The type and intensity of soil degradation is described based on soil indicators. The indicators of this group are (1) loss of the upper soil horizon; (2) loss of organic carbon (loss of humus) and (3) reduction of clay and silt fraction in the upper soil horizon/skeletisation. The ploughing of humus-rich steppe soils also negatively changed typical deeper humus-rich soil horizons, reducing the depth of organic horizons and resulting in an overall lower humus content (Meinel 2002; Meyer et al. 2008). At the same time, frequent harrowing can intensify the mineralisation of soil carbon and crop residues (Scheffer et al. 1992). As a result of the erosion processes, soil humus and fine soil particles are relocated.

The **depth of the upper soil horizon** (A horizon) decreases with the steppe conversion by around 50% (Rudskij 1996, 2000). The depth of the humus horizon in Northern Kulunda is still around 26 cm. This is directly related to the level of soil erosion. The more active the deflation process, the shallower the remaining humus layer (Smolenzev et al. 2004). It has been estimated that the active deflation processes caused by the use of arable land have reduced the depth of the humus horizon by 12–22 cm (Meyer et al. 2008). Meinel (2002) also reported a strong degradation of the A horizon of arable soils compared with native southern Chernozem soils.

Another related desertification problem in the Kulunda is **dehumification**. Since the time of the steppe conversion, the humus content has decreased from 4–6% to 1.5–2% (Jushakov 1999). Around 10% of the arable soils in Northern Kulunda contain less than 1.3% humus (Smolenzev et al. 2004). The same authors found that the average humus content in the soils of Northern Kulunda is 2.2–2.5%. The total loss of humus in the Western Siberian steppes and forest steppes in the period 1940–2000 was calculated at 1010 million tonnes of carbon (Titlianova 2000).

The assessment of the selected indicators is used as a basis for describing and explaining the

temporal steps of the desertification processes. Process models have been developed to structure the causal chains and interdependencies between the initial factors and indicator processes. However, the biophysical and socio-economic factors of desertification are worked out separately in the study by Schreiner (2017).

5.4 Driving Forces and Variation in Temporal Scale

As described earlier, the initial factors behind the desertification process in Northern Kulunda are determined and accelerated by climate warming and steppe transformation due to land use change since the 1950s (anthropogenic drivers).

5.4.1 Climate Change

Data from four climate stations in the vicinity of the Kulunda have been analysed to shed light on changes in climate elements. The 1998–2013 period (Meteo 2013) was analysed based on data measured every 4–6 h. Climatological reference periods for the analysis of climate change between 1891–1964 and 1951–1964 were freely available from the meteorological data (SpK 1977). The analysed parameters were generalised to produce the mean annual and average monthly precipitation, average annual and monthly air temperature, and average annual and average monthly wind speed.

Analysis of the monthly precipitation and average monthly temperature showed a strong increase in temperature with a constant and unchanged amount of precipitation, indicating the aridification process in the research areas (Table 5.3). The increase in precipitation is significant in winter (85%) and not in summer (8.2%), which results in an increased risk of wind erosion (due to the late spring and summer). A strong change in the inter-annual distribution of precipitation was observed. The statistical analysis of the temperature indicates that the temperature increases in all time periods of the year by approximately 0.4 °C over 10 years. The

Table 5.3 Trends of temperature increase, 1998–2014, compared with the reference period 1951–1964 (Schreiner 2017; Data: SpK 1977; METEO 2013)

Month	I	II	III	IV	V	VI	VII	VIII	IX	X	XI	XII
t Increase (°C)	1.07	2.23	5.49	4.6	2.54	1.75	0.25	0.65	0.96	1.87	3.55	1.31
	■	■	■	■	■	■	■	■	■	■	■	■
	■	■	■	■	■	■	■	■	■	■	■	■
	■	■	■	■	■	■	■	■	■	■	■	■
p Increase (mm)	1.7	7.8	8.7	0.5	5.5	5.9	37.5	-10.7	-3.5	-0.1	6.8	-0.1
	■	■	■	■	■	■	■	■	■	■	■	■
	■	■	■	■	■	■	■	■	■	■	■	■
	■	■	■	■	■	■	■	■	■	■	■	■

t: mean average temperature increase from the three weather stations Karasuk, Bagan and Michajlovskoe;
p: mean average precipitation from the Karasuk weather station

months with a substantially increased temperature are March and April, indicating an average monthly increase by 4–5.7 °C compared to the data of the reference period (Schreiner 2017).

5.4.2 Anthropogenic Causes

The main driver of anthropogenic desertification in Northern Kulunda is the intensification of land use in the 1950s. The intensification was focused on the transformations of the steppe, deforestation in the steppe, the lack of water management and the use of pastures without adapting the plot (overgrazing on the remaining few pastures). The factors have been described in detail in this chapter.

5.4.3 Temporal Model on Desertification and Land Use Change

The temporal analysis on the interconnections of the processes of ecological and socio-economic systems is based on 34 indicators and generalised for desertification in the Kulunda Steppe. The temporal input–output model is demonstrated in Fig. 5.4.

The main cause for desertification processes starting is the large-scale use of arable land, replacing the natural steppes, that took place in the second land reclamation campaign by the Russian administration from 1954 to 1960. At the same time and in parallel, the climate began to change towards climate warming. The transition of steppe land use to large-scale arable plots for a few years of ploughing and the growing of a few cash crops led to the collapse of local and regional production capacities. Only 5 years after the land reclamation, soil deflation resulted in disasters, e.g. in mobilised sand dunes (Interview 2005). This caused 45% of the soils to be classified as strongly eroded (Vologshina and Smolenzev 2003).

Irrigation projects were abandoned after several years due to large-scale salinisation problems. The land use was intensified by the agricultural authorities between 1965 and 1980. Intensification measures were applied such as new technologies and land machinery, mineral fertilisers, new crop rotations and a new distribution of wind protection buffer strips (hedge-rows) (Meinel 2002). The listed countermeasures slowed down the desertification processes but not the changes in the ecosystem and climate warming. The process of deflation was generally stopped during that time.

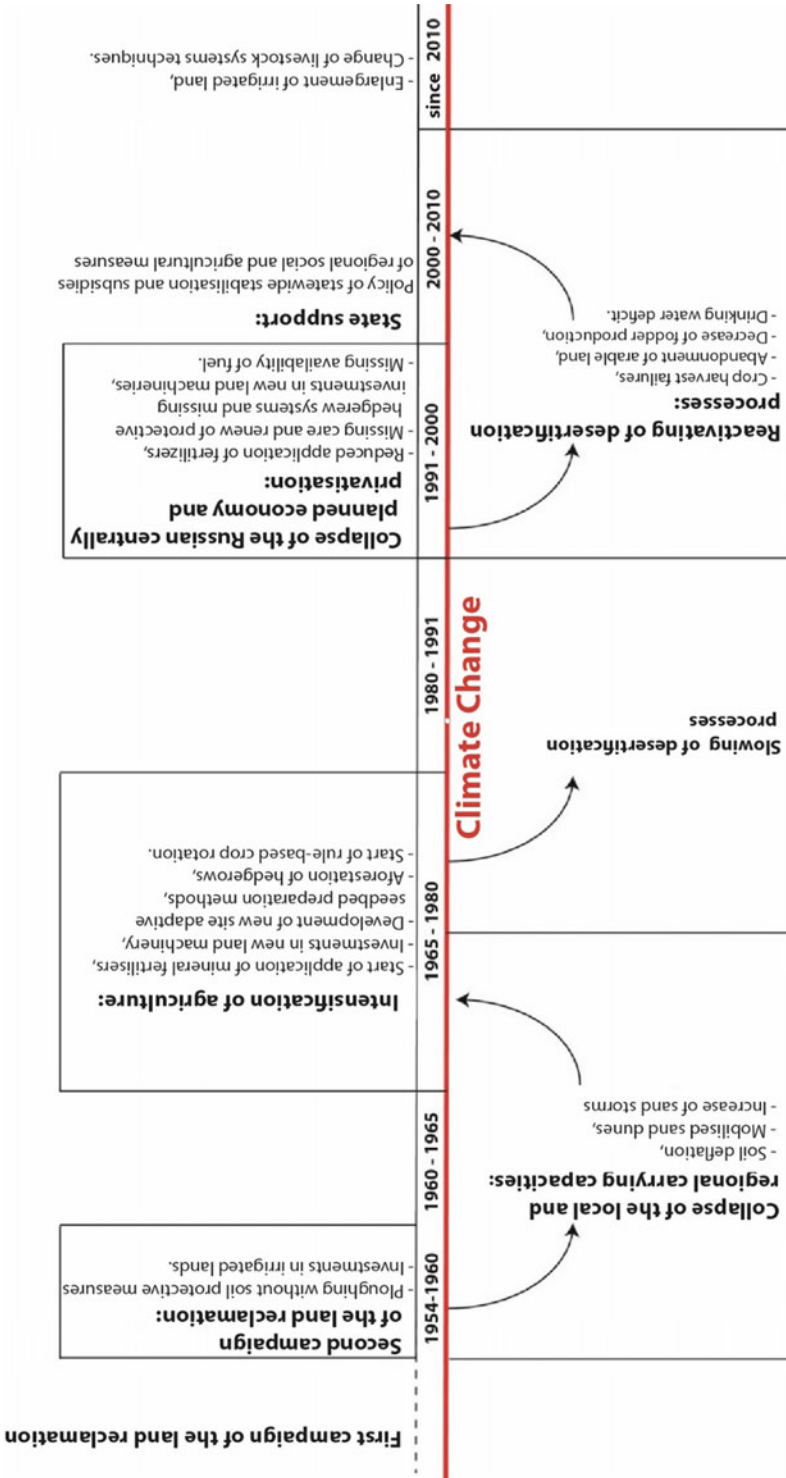


Fig. 5.4 Temporal input–output model summarising the changes in desertification processes in the Northern Kulunda Steppe which began in the 1950s (Schreiner 2017)

Subsequent major changes in land use were caused by privatisation and the reorganisation of farms in the 1990s after the collapse of the centrally planned Russian economy, which led to a decrease in desertification mitigation activities. The changes reduced investment in the organisation of hedge replanting, protecting and trimming, and decreased the use of fertilisers, which led to the losses of humus caused by the constant use of non-sustainable management techniques and outdated agricultural machinery. The desertification processes resumed during this period of time.

During the first decade of the twenty-first century, the Russian government substantially subsidised the agricultural sector. The investments were directed to the social sector in order to obtain short-term benefits and ignore the current desertification processes. The abandonment of arable land, frequent crop failures and a lack of fuel led to a new problem of desertification and a structural change in farm investments from arable farming to mass production of livestock. This resulted in an increase in the area of meadows and pastures, a change of management in livestock production, and the modernisation and expansion of irrigated land (Schreiner 2017). Active soil protection measures were not the focus of land use management, prompting the resumption of soil degradation in the 1990s. Russia's generally positive economic development was evidently not positively oriented towards the agricultural sector of Western Siberia. This sector is still undergoing a crisis and management reorganisation. The number of livestock at the Ivanovskoe farm doubled from 2001 to 2005 (Interview 2005; Administratsia IS 2014). The livestock brought in 70% of the economic turnover and the crop production only 30% (Administratsia IS 2014). One positive point is the rapid increase in the area of pastures and meadows, resulting in an increase in agricultural area by 20% from 2005 to 2014 (Passport IV 2015b). Due to the very high grazing intensity, large-scale degradation of pastures is observed (Paramonov et al. 2003).

After a period of traditional nomadism, ongoing arable land use began in the 1950s as

part of the steppe transformation policy. Soil protection measures were not applied in the first 10–15 years of implementation (Meinel 2002). This led to wind erosion, significantly degrading 30% of the new arable land by 1963 (Wein 1999). From 1965 to 1980, agricultural activities intensified, including the use of mineral fertilisers and crop rotation systems, the concept of irrigation schemes and the planting and management of hedgerow systems (Meinel 2002). After 1989, as a result of the collapse of the centrally planned economy, the agriculturally based rural economy in the Kulunda Region was in crisis. As a result, the lack of investments in fertilisers, fuel, technology or spare parts, the lack of management in land and water protection, including the replanting of hedgerows, and the apparent loss of humus caused by unsustainable cereal production, re-initiated the degradation and desertification processes.

5.5 Discussion

The development and application of indicators on the southern borders of the West Siberian Plain in the Northern Kulunda Steppe showed that the existing Russian and European indicator systems have limitations in terms of regional applicability. In contrast to our results, the Russian indicator systems examined explain only the final levels of degradation. They focus on soil indicators, not taking into account other biophysical factors and ignoring the socio-economic aspects of desertification processes. The analysed European indicator systems were mainly worked out for developing countries. It is concluded that none of the listed indicator systems is applicable in the Kulunda Region without considerable modification.

The presented indicator system for Northern Kulunda includes four groups of land use change revealed by biophysical indicators and one large group of drivers of socio-economic indicators applicable to an industrialised country. The analysis was applied to 34 indicators, which resulted in 29 desertification processes being identified. Most of the biophysical processes of

desertification were clearly identified. The socio-economic consequences of biophysical desertification caused by changes and modifications by Russian regional and agricultural policies and the subsidy measures in the first decade of the twenty-first century are not clearly measurable. Analysis of the biophysical and socio-economic systems showed a systemic reaction caused by desertification and environmental change, as well as systemic adaptation. The primary (initial) factor behind desertification in the Northern Kulunda Steppe was clearly the large-scale transformation of land use into arable land, which caused significant changes in vegetation, soil and water management in the 1950s.

Changes in the components of the biophysical and socio-economic systems shown in the framework of the indicator system indicate that landscape degradation and desertification in Northern Kulunda are caused by natural and social processes (Schreiner 2017; Schreiner and Meyer 2018). Strong evidence was found regarding land use change. The collapse of Soviet agriculture around 1990 initiated the emergence of a number of new processes that contributed to desertification. At the same time, climate change led to a modification of the natural system components and a sharp reduction in the total population occurred. Nevertheless, the agricultural organisational structures inherited from the collective farm system still dominate. A second major land use system change towards landscape degradation is analysed as a result of the collapse of the kolkhoz system, caused by changes in multiple parameters. The main change in the system was the transformation of the steppe.

The first change in the system caused by the steppe transformation was followed by the intensification of agriculture in 1965–1980. This led to an increased use of fertilisers, new tillage technologies, improved crop rotation and planting of windbreaks (hedgerows) to avoid dust bowl syndrome. During the same period, there was a slowdown in land degradation. Since the second systems changed in the early 1990s, the analysed indicators have revealed a new type of desertification process caused by a significant

deficit in hedgerow maintenance, coupled with increased soil degradation caused by a lack of land management and fertilisation techniques. Wind erosion and the content of salt have increased and the vegetation structure has changed due to the changes in water balances on landscape scale. At the same time, agriculture in dryland has been gradually replaced by livestock farming subsidised by the Russian government, in an ongoing process. The landscape is left without necessary management investment.

Climatic changes are triggering an array of global transformations in terms of socio-economic, environmental and land use aspects (Sanzheev et al. 2020; Li et al. 2020; Lyu et al. 2021). Meanwhile, anthropogenic pressures are intensifying the negative effects of climate-induced changes (Kulik et al. 2020). Zolotkrylin (2019) explain that the formation of deserted “islands” in arid regions of Russia and Mongolia is largely due to the excessive anthropogenic pressure placed on arid pastures (overgrazing), as well as natural factors such as regularly occurring seasonal droughts.

5.6 Conclusions

The 16 biophysical and 18 socio-economic indicators which were analysed revealed numerous complex changes, many of which are not yet fully understood. In the Northern Kulunda Region, biophysical indicators clearly demonstrated desertification and landscape degradation due to a variety of land degradation processes. The socio-economic indicators also indicate degradation, but comprehensive economic, social and governmental adaptation cannot be fully compared with case studies in Africa or Central Asia taken from the literature. Finally, problems related to the quality and availability of data have reduced the applicability of a more sophisticated indicator approach: measurements in Western Siberia typically focused on only one aspect/system component, which can make it hard to apply the approach to the entire system.

A complex system-oriented understanding is necessary for a further and better understanding

of landscape degradation processes. This may include the relationships between driving forces and system behaviour and possibly also other indicators, including soil microbiology, as well as detailed studies of changes in the landscape water balance. The processes of primary and secondary salt accumulation should be better aligned with water chemistry and water management approaches designed to address the observed and predicted drying over most of the Kulunda Steppe.

References

- Administratsia IS (Administratsia "Ivanovskoe") (2014) <http://www.ivanovski.ru/sotchialnaya/selhoz> (in Russian)
- AKS (1966) *Agroklimatichesky spravochnik po jugozapadnym rayonam Novosibirskoy oblasti* (Chistoozerny, Kupinsky, Bagansky, Karasuksky), Novosibirskaya hydrometeorologicheskaya observatorija, Novosibirsk (in Russian)
- Atlas (2002) *Atlas Novosibirskoy oblasti*, Novosibirsk, p 56 (in Russian). ISBN 5-85120-129-0
- Abdullahi M, Cheri I (2020) Managing ecological challenges in Nigeria: effects of desertification on food security in Yusufari local government area of Yobe state, Nigeria, pp 411–430. In: Ododo SE, Tijani AI, Vogels R (eds) *Chapter in cultural sustainability, performance and the sustainable development goals in time of crisis*. CSPCS, Publication Office of the European Union, Luxembourg
- Baumhauer R (2011) *Beschleunigung der Desertifikation*. In: Lozan JL, Graßl H, Hupfer P, Menzel L, Schönwiese CD (Eds) *Warnsignal Wasser – Genug Wasser für alle*, 3rd edn. Hamburg, pp 368–374
- Bosselmann K (1992) *Im Namen der Natur*. Bern, Scherz Verlag, *Der Weg zum ökologischen Rechtsstaat*
- Charin N, Nechaeva N, Nikolaev V et al (1987) *Metodicheskie osnovy izuchenija i kartografirovanija prozessov opustynivanja (na primere aridnyh territory Turkmenistana)*, Ashgabat, 102 pp. (in Russian)
- Cherlet M, Hutchinson C, Reynolds J, Hill J, Sommer S, von Maltitz G (2018) *World atlas of desertification*
- DSD (Dryland Science for Development Consortium) (2009) *Integrated methods for monitoring and assessing desertification/land degradation processes and drivers (land quality)*. In: *White paper of the DSD working group 1*, Version 2, 19 August 2009 (draft) http://dsd-consortium.jrc.ec.europa.eu/documents/WG1_White-Paper_Draft-2_20090818.pdf
- EEA/European Environment Agency (1999) *Environmental indicators: typology and overview*, EEA technical report no. 25: 19 pp.
- ECOLOG-Institut (2011) *Indikatoren für eine nachhaltige Entwicklung*. <http://www.indikatoren.ecolog-institut.de/Konzept.htm>
- Egidi G, Salvati L, Cudlín P, Salvia R, Romagnoli M (2020) A new 'Lexicon' of land degradation: toward a holistic thinking for complex socioeconomic issues. *Sustainability* 12:4285. <https://doi.org/10.3390/su12104285>
- Emadodin I, Reinsch T, Taube F (2019) Drought and Desertification in Iran. *Hydrology* 6(3):66. <https://doi.org/10.3390/hydrology6030066>
- GIZ (Deutsche Gesellschaft für internationale Zusammenarbeit) (2011) *Kommentiertes Glossar zum Themenbereich Desertifikationsbekämpfung und nachhaltiges Landmanagement*, p 36
- GIZ (2013) *Desertifikationsbekämpfung. Deutschlands Engagement im Rahmen der internationalen Zusammenarbeit zur Umsetzung der Konvention der vereinten Nationen*, p 12
- GLASOD (1991) *Global assessment of human-induced soil degradation*. UNEP/ISRIC. <http://www.isric.org/projects/global-assessment-human-induced-soil-degradation-glasod> ; dataset: <https://data.isric.org/geonetwork/srv/eng/catalog.search#/metadata/9e84c15e-cb46-45e2-9126-1ca38bd5cd22>
- Gos. Doklad Pochva No (2008) *State report on soils in the Novosibirsk region in 2007*. http://www.to54.rosreestr.ru/kadastr/zemli_nso08/ (in Russian)
- Gos. Doklad Pochva No (2013) *State Report on Soils in the Novosibirsk Region in 2012*. http://www.to54.rosreestr.ru/kadastr/zemli_nso/ (in Russian)
- Hese S, Kurepina N, Walde I, Tsimbalei YM, Plutalova TG (2020) Earth observation and map-based land-use change analysis in the Kulunda Steppe since the 1950s. In: Frühauf M, Guggenberger G, Meinel T, Theesfeld I, Lentz S (eds) *KULUNDA: climate smart agriculture. Innovations in landscape research*. Springer, Cham. https://doi.org/10.1007/978-3-030-15927-6_9
- Ibrahim F (1978) *Desertifikation, Wüstenbildung – ein weltweites Problem*. 32 pp., 18 Transparente; Düsseldorf (Hagemann)
- Ibrahim F (1992) *Gründe des Scheiterns der bisherigen Strategien zur Bekämpfung der Desertifikation in der Sahelzone*. *Geomethodica.*, 17, Basel, pp 71–93. ISBN 3-905 141-54-X
- Interview (2005) *Interview with the mayor of Ivanovskoe Simanchuk A*
- IPBES (2018) *The IPBES assessment report on land degradation and restoration*. In: Montanarella L, Scholes R, Brainich A (eds) *Secretariat of the intergovernmental science-policy platform on biodiversity and ecosystem services*, Bonn, Germany. 744 pp. <https://doi.org/10.5281/zenodo.3237392>
- Jacobsen T, Adams R (1958) *Salt and silt in ancient Mesopotamian agriculture*. *Science* 128:1251–1258
- Jagudin R (2003) *Pospel li vinograd v Bagane*. *Novosibirskii Hydrometcentr, Sovetskaia Sibir* 24(03):2003

- Jaschutin N (1999) Agrarnij potencial Altaja. Altaiskij Gosudarstvennyj Agrarnij Universitet, Barnaul (in Russian)
- Jushakov A (1999) Posledstvia agrarnogo osvoenia stepy Sibiri [Consequences of land reclamation of the steppe zone in Siberia]. *Stepnoi Bull* 3–4, Novosibirsk (in Russian)
- Kasanzev V, Magaeva L (2003) Antropogenaia degradacija prirodnih system na jube Zapadnoj Sibiri. In: *Pochvy Sibiri, Krasnojarsk*, pp 62–64 (in Russian)
- Koroljuk (2005) Field data of the Expedition to Kulunda steppe and the Ivanovskoe farm in the year of 2005 of Botanical Institute of SBRAS (not published)
- Kosmas C, Kairis O et al (2013) Evaluation and selection of indicators for land degradation and desertification monitoring: types of degradation, causes, and implications for management. *Environ Manage* 54(5):951–970
- Kosmas C, Karamesouti M, Kounalaki K, Detsis V, Penny Vassiliou P, Salvati L (2016) Land degradation and long-term changes in agro-pastoral systems: an empirical analysis of ecological resilience in Asteroussia—Crete (Greece), *Catena*, vol 147, 196–204 pp. <https://doi.org/10.1016/j.catena.2016.07.018>
- Kravzov VM, Donukalova RP (1996) *Geografija Novosibirskoy oblasti. Uchebnoe posobiye*, Novosibirsk: M.: Tasis, p 137 (in Russian). ISBN5-85826-015-2
- Kulik KN, Petrov VI, Yuferev VG et al (2020) Geoinformational analysis of desertification of the Northwestern Caspian. *Arid Ecosyst* 10:98–105. <https://doi.org/10.1134/S2079096120020080>
- Kulunda Project (2012). <http://www.kulunda.eu>
- Kust G (1999) *Opustynivanie: Printsipy ekologo-geneticheskoy otsenki i kartografirovaniya*. 362 pp (in Russian)
- Kust G, Andreeva O (2006) Geographicheskoe rayonirovanie opustynivaniya poluzasuschlivoj i zasuschlivoj zon Rossii). *Doklady Po Ekologicheskomu Pochvovedeniju* 2:21–52 (in Russian)
- Li P, Zang Y, Ka F, Chan S et al. (2020) Desertification and its control along the route of China’s belt and road initiative: a critical review. *Authorea*. <https://doi.org/10.22541/au.159818324.44925559>
- Lyu X, Li X, Wang H, Gong J, Li S, Dou H, Dang D (2021) Soil wind erosion evaluation and sustainable management of typical steppe in Inner Mongolia, China. *J Environ Manag* 277. <https://doi.org/10.1016/j.jenvman.2020.111488>
- ME Assessment [Millennium Ecosystem Assessment] (2005) *Ecosystems and human well-being: desertification synthesis*. World Resources Institute, Washington, DC. <http://www.millenniumassessment.org/documents/document.355.aspx.pdf>
- Meckelein W (1983) Die Trockengebiete der Erde, Reserveräume für die wachsende Menschheit? In: *Colloquium geographicum* 17:25–58, Bonn
- Meinel T (2002) *Die geökologische Folgewirkungen der Steppenumbrüche in den 50er Jahren in Westsibirien*. Dissertation. Halle
- Mensching HG (1979) Desertifikation, ein aktuelles geographisches Forschungsproblem. *Geogr. Rundschau* 31(9):350–355, Hamburg
- Mensching H (1990) *Desertifikation. Ein weltweites Problem der ökologischen Verwüstung in den Trockengebieten der Erde*, Wissenschaftlicher Buchgesellschaft, Darmstadt
- Meteo (Wetterdienst) (2013). <http://meteo.infospace.ru/>
- Meyer B, Schreiner V, Smolenzeva E, Smolenzev B (2008) Indicators of desertification in the Kulunda steppe in the south of Western Siberia. *Arch Agron Soil Sci* 54(6):585–603. <https://doi.org/10.1080/03650340802342268>
- Mezosi G, Blanka V, Bata T, Kovács F, Meyer B (2015) Estimation of regional differences in wind erosion sensitivity in Hungary. *Nat Hazard* 15(1):197–207
- Mirzabaev A, Wu J, Evans J, García-Oliva F, Hussein IAG, Iqbal MH, Kimutai J, Knowles T, Meza F, Nedjraoui D, Tena F, Türkeş M, Vázquez RJ, Weltz M (2019) Desertification. In: *Climate change and land: an IPCC special report on climate change, desertification, land degradation, sustainable land management, food security, and greenhouse gas fluxes in terrestrial ecosystems* [P.R. Shukla, J. Skea, E. Calvo Buendia, V. Masson-Delmotte, H.-O. Pörtner, D.C. Roberts, P. Zhai, R. Slade, S. Connors, R. van Diemen, M. Ferrat, E. Haughey, S. Luz, S. Neogi, M. Pathak, J. Petzold, J. Portugal Pereira, P. Vyas, E. Huntley, K. Kissick, M. Belkacemi, J. Malley, (eds.)]. (In press)
- NPDBO (2000) *Subregionalnaya nacionalnaya programma deistvi po borbe s opustynivaniem (NPDBO) dlja Zapadnoj Sibiri (Subregional action programme to combat desertification in Western Siberia)*, Volgograd, 235 pp.
- OECD (1993) *OECD core set of indicators for environmental performance reviews. A synthesis report by the group on the state of the environment*. OECD, Paris, 35 pp.
- OECD (2003): *OECD Environmental Indicators. Development, measurement and use. Reference paper*, p 37
- OZZR (2009) *Opustynivanie zasuschlivoj zemel Rossii: novye aspekty analiza, rezultaty, problemy*. Rossijskaya akademija nauk, Institut geografii, Moskva: *Tovarischestvo nauchnyh izdany KMK*, pp 298 (in Russian)
- Paramonov E, Ischutin J, Simonenko A (2003) *Kulundinskaya step: problem opustynivaniya*. [Kulunda steppe: the problem of desertification]. Altaj Universitet, Barnaul, 137 pp (in Russian), ISBN 5-7904-0222-4
- Paramonov E (2012) *Itogi inventarizacii zaschitnyh lesnyh nasazhdenij v Altaiskom krae, vesti Altaiskogo gosudarstvennogo universiteta* 8(94):58–62 (in Russian)
- Passport IV (2015a) *Pasport Ivanovskogo selsoveta za 2014 god*, 8 pp <http://ivanovski.ru/card/pasportmo>
- Passport BR (2015b) *Pasport Baganskogo rajona za 2014 god*. http://www.econom.nso.ru/deyatelnost/territ_razv/pp/bagansky.aspx

- Roshydromet (2016) Doklad ob osobennostyah klmata territorii Rossiskoy Federazii za 2015. Moscow, p 67
- Rubio JL, Recatala L (2006) The relevance and consequences of Mediterranean desertification including security aspects. In: Kepner WG, Rubio JL, Mouat DA, Pedrazzini F (eds) *Desertification in the mediterranean region: a security issue*. Springer, The Netherlands, pp 133–165
- Rudskij V (1996) Altaj. Ekologo-geograficheskie osnovy prirodopolzovania. Barnaul, p 240 (in Russian)
- Rudskij V (2000) Prirodopolzovanie v gornich stranah (na primere Altaja i Sajan), Nauka, Novosibirsk, p 207 (in Russian)
- Sanzheev ED, Mikheeva AS, Osodoev PV, Batomunkuev VS, Tulokhonov AK (2020) Theoretical approaches and practical assessment of socio-economic effects of desertification in mongolia. *Int J Environ Res Public Health* 17(11):4068. <https://doi.org/10.3390/ijerph17114068>
- Scheffer P, Blume HP, Brümmer G (1992) *Lehrbuch der Bodenkunde*. Ferdinand Enke, Stuttgart, p 491
- Schreiner V (2017) Indikatoren und Prozessmodelle der Desertifikation – am Beispiel der nördlichen Kulundasteppe in Westsibirien. Thesis, Universität Leipzig, Institut für Geographie, p 231
- Schreiner V, Meyer B (2018) Chapter II/69: Indicator System and Assessment of Desertification Processes within the Northern Kulunda Steppe in Western Siberia. In: Sychev VG, Mueller L (eds) *Novel methods and results of landscape research in Europe, Central Asia and Siberia: Monograph in 5 Volumes; vol II Understanding and monitoring processes in soils and water bodies*. Moscow: FGBNU “VNII agrochimii”, pp 319–323. <https://doi.org/10.25680/6604.2018.72.10.166>
- Smolenzev B, Smolenzeva E, Fedorov P (2004) K problem opustynivania Severnoi Kulundi. Materiali IV siezda Dokuchaevskogo obschestva pochvovedov. [The problem of desertification in Northern Kulunda]. In: *Proceedings of the 4th congress of the Dokuchaev Society of Soil Scientists*, vol 2, Novosibirsk, pp 214–215 (in Russian)
- Smolenzeva E, Smolenzev B, Meyer B (2007) Prichiny i indikatory opustynivania v severnoy Kulunde. Materialy mezhdunarodnoy nauchnoy konferenzii po borbe s opustynivaniem. Abakan, pp 73–79
- SpK (1977) *Spravochnik po klimatu SSSR*, Vypusk 20, Tomskaya, Novosibirskaya, Kemerovskaya oblasti i Altaiskiy kraj, Part 2, Book 1, Atmosfernnye osadki, Novosibirsk, 1977 (in Russian)
- Spooner B (1989) Desertification: the historical significance. In: Huss Ashmore R, Katz SH (eds) *African food systems in crises: part one: microperspectives*. New York, pp 111–162
- Tanasienko A, Putilin A, Artamonova V (1999) Ekologicheskie aspekty erozionnih prozessov. Analiticheski obzor. [Ecological aspects of the erosion processes. Analytic overview]. Institute of Soil Science and Agrochemistry. *Ekologia* 55, Novosibirsk, p 98 (in Russian). ISBN5-7692-0254-8
- Thomas D, Middleton N (1994) *Desertification: exploding the myth*. Wiley, Chichester
- Titlanova A (2000) Osvoenie lesostepnoi i stepnoi zon Zapadnoy Sibiri uvelichilo emissiyu ugleroda. *Stepnoi Bull* 8, Novosibirsk (in Russian)
- UNCCD (United Nations Convention to Combat Desertification) (2001) World map of desertification. In: *Petermanns Geographische Mitteilungen*, vol 4/2001 *Degradation—Desertifikation*, Klett-Perthes, Gotha
- UNCCD (United Nations Convention to Combat Desertification) (2012) *Desertification: a visual synthesis*, p 48
- UNSD (United Nations Statistics Division) (2012) *Environment glossary*. <http://unstats.un.org/unsd/environment/gl/gesform.asp?getitem=328>
- Vologshina O, Smolenzev B, Ditz L (2003) Izmenenie struktury pochvennogo pokrova pod vliyaniem antropogenogo faktora. [Change of the structure of the soil cover by anthropogenic factors]. *Tomsk, Vestnik TGU* 7, pp 57–63 (in Russian). ISBN 0180-78360
- Warner T (2004) *Desert meteorology*. Cambridge University Press, Cambridge, p 595
- Wein N (1999) *Sibirien. Geographische Strukturen, Entwicklungen, Probleme*. Gotha: Klett-Perthes, p 248
- Whitford WG, Duval BD (2020) Chapter 12—Desertification. In: *Ecology of desert systems* (2nd ed). Academic Press, pp 371–395. <https://doi.org/10.1016/B978-0-12-815055-9.00012-6>
- Xie H, Zhang Y, Wu Z, Lv T (2020) A Bibliometric analysis on land degradation: current status, development, and future directions. *Land* 9(1):28. <https://doi.org/10.3390/land9010028>
- Zolotokrylin AN (2019) Global warming, desertification/ degradation, and droughts in arid regions. *Izvestiya Rossiiskoi akademii nauk. Seriya geograficheskaya* 1:3–13. <https://doi.org/10.31857/S2587-5566201913-13>. <https://journals.eco-vector.com/2587-5566/article/view/11569>



Environmental and Economic Assessment of Land Degradation in Different Regions of the Russian Plain

Oleg Makarov, Anton Strokov, Evgeny Tsvetnov, Dina Abdulkhanova, Vladislav Kudelin, and Nina Marakhova

Abstract

Widespread soil degradation processes (erosion, dehumidification, loss of nutrients, and acidification) have been observed in the Central Russian Plain. An environmental and economic analysis of land degradation was carried out in three regions of the Central Russian Plain (Belgorod, Tula and Lipetsk) assessing the effects of action and inaction, and analysing the soil nutrient balance. The results show that all three regions experienced an increase in ecosystem values during the

2001–2009 period in respect of the growth of forest area. At the same time, the area under cropland decreased, which was followed by growth in crop yields. This increase in productivity has not been adequately compensated for by fertilisation, which could lead to high costs for combating land degradation in the future, especially in the Tula region. Therefore, an additional analysis correlating the factors of land degradation and the soil nutrient balance was carried out for Tula. Spatial and dynamic models in Tula showed that the increase in the cultivated area was directly correlated with the increase in the area of degraded land. This could be due to the depletion of soil fertility as a result of an insufficient use of mineral and organic fertilisers. The negative balance of nutrients found in the soils of the Tula region in the 1995–2014 period was due to inappropriate management of agriculture in the region studied. In all the regions studied, from 2001 to 2009, the abandonment of a significant proportion of unprofitable arable land was identified, followed by overgrowing with woody vegetation. The increase in forested areas in these regions has increased the value of ecosystem services. Statistical modelling showed that the cost of inaction in the surveyed regions was higher than the cost of action against land degradation (6- and 30-year perspectives). Thus, the application of the action/inaction assessment method has

O. Makarov (✉)

Faculty of Soil Science, Lomonosov Moscow State University, Leninskie Gory, GSP-1, Leninskie Gory, 1–12, 119991 Moscow, Russia

O. Makarov · E. Tsvetnov · D. Abdulkhanova · V. Kudelin · N. Marakhova

Educational and Experimental Soil-Ecological Center, Lomonosov Moscow State University, Moscow region, Solnechnogorsk district, p/o Udarny, poselok Chashnikovo, 141592 Moscow, Russia

e-mail: ecobox@mail.ru

A. Strokov

Russian Presidential Academy of National Economy and Public Administration, Prospekt Vernadskogo, 82-1, 119571 Moscow, Russia

e-mail: strokov-as@ranepa.ru

E. Tsvetnov

Lomonosov Moscow State University Eurasian Center For Food Security, GSP-1, Leninskie Gory, 1–12, 119991 Moscow, Russia

shown that the restoration of land productivity and the maintenance of ecosystem services are economically viable.

Keywords

Land degradation · Soil fertility · Crop production · Intensification · Mineral and Organic fertilisers · Ecosystem services

6.1 Introduction

Assessing the extent to which economic factors influence changes in soil fertility is an important part of a modern agricultural economy (Nkonya et al. 2016; Farquharson et al. 2008; Barbier 1998). Using economic and mathematical modelling, it was possible to assess the impact of various factors on the degradation of croplands (Nkonya et al. 2011). The most statistically significant factors are the gross domestic product, precipitation, intensification of crop production and population density. Depending on the country or region, the links between land degradation and economic indicators can be both direct and indirect. In Latin America, an intensification of agricultural production, and in particular, an increase in the amount of mineral fertilisers per unit of arable land, contributed to an increased growth of vegetation which can be interpreted as an increase in soil fertility. In North America, by contrast, the intensification of production has led to environmental pollution and land degradation (Nkonya et al. 2011). In general, land degradation is a complex phenomenon which can occur in the periods of both economic growth and decline in a region. For example, land degradation has led to higher food prices (Von Braun et al. 2013) and caused a decline in the global ecosystem services, such as carbon sequestration in soils (Lal 2004). At the same time, the negative consequences of land degradation are especially acute for the poorest segments of the population (Nachtergaele et al. 2010).

The theoretical basis behind the economic assessment of land degradation was developed

by the International Food Policy Research Institute (IFPRI) and the University of Bonn. Their achievements are presented in a number of publications (Von Braun and Gerber 2012; Von Braun et al. 2012). Joachim von Braun from Bonn University and his team created a methodology based on comparing economic indicators of crop production with sustainable land management and traditional land use, known as action/inaction assessment (Von Braun et al. 2012; Nkonya et al. 2016). There is also a modification of this methodology, designed to assess the feasibility of restoration work (reclamation) on degraded lands. The technique is based on determining the benefits of action versus inaction in relation to the reclamation programme (Bondarenko 2016). Despite the particular relevance, the problems of economic preconditions/consequences of land degradation are still insufficiently studied both globally and in the Russian Federation. In the Russian Federation, a study on the relationship between land degradation and economic factors (primarily crop production) is the most interesting at a regional scale, as it offers great potential for managing agro-industrial complexes.

Recent studies have shown that soil erosion in Russia has decreased compared to Soviet times (Golosov et al. 2018; Wuepper et al. 2020) due to an increase in abandoned land and a decrease in arable land. Also, some studies have shown that the level of erosion in Russia is relatively lower than in other countries (Sartori et al. 2019). These studies have mainly focused on large-scale analysis of erosion processes in Russia without any specific details at the regional level. Sorokin et al. (2016) used an interdisciplinary approach to assess the cost of action versus inaction on land degradation at large-scale (national), regional and farm levels in Russia. This allowed us to see how the economics of agricultural and other activities are interrelated with soil properties, dynamics and the cost of ecosystem services. We continued the analysis of the results reported by Sorokin et al. (2016) and supplemented them with a more detailed analysis for three regions of the Russian Plain. The difference to our approach is not only in the analysis of the dynamics of changes in

land use and the cost of ecosystem services but also the deeper analysis of the dynamics of arable land, the intensity of arable land use and the balance of nutrients in the soil.

Our focus was on Chernozem soils in the territories of Belgorod, Lipetsk and Tula, which are large industrial and agricultural regions of the Central Russian Plain. The total population of these regions as of 01 January 2020 was nearly 4.26 million people (with the rural population making up a little less than one third (ROSSTAT 2010, 2020)). The main driver of agricultural production in the territories studied is agricultural holdings (large vertically and horizontally integrated agricultural enterprises). They are large structures capable of conducting cost-effective production, which, however, are not always environmentally sustainable. The area with Chernozem soils occupies about 77% in the Belgorod region, 90% in the Lipetsk region and 50% in the Tula region. In Belgorod, typical, leached and ordinary Chernozems predominate, while podzolised, leached and typical Chernozems are common in the Lipetsk and Tula regions (Shoba 2011; Lukin 2016; Rybalsky et al. 2004; Dobrovolsky and Shoba 2001).

The goal of this study was an environmental and economic assessment of land degradation in the Belgorod, Lipetsk and Tula regions. The subjects studied were (1) relationship between land degradation and economic/agricultural indicators in the region; and (2) environmental and economic assessment of action/inaction on degraded lands.

The article consists of three (analytical) research approaches. Firstly, for each of the three regions, we tried to identify cases of land use change during the relatively short period from 2001 to 2009, which was a period of economic growth in Russia (compared to the recession of the 1990s) and at the same time saw a period of sharp increases in world prices on food products in 2006–2008, which, in our opinion, may have affected the growth of arable land. Secondly, after identifying land use changes, we measured the losses and benefits of ecosystem services on different land types using the Total Economic Value (TEV) approach and for each region as a

whole to see which soil type most contributed to the changes in ecosystem services. Thirdly, we measured the soil nutrient balance for each region, especially arable land, to see if nutrient input (for NPK only) compensated for the nutrient uptake by the main agricultural crops. And finally, for one region (Tula oblast), an additional experiment was carried out to check what factors influence the soil nutrient balance.

6.2 Materials and Methods

The widespread degradation processes in these regions studied are erosion, dehumidification and loss of nutrients, and acidification. In addition, some areas in the regions are contaminated with Cs-137 as a result of the Chernobyl accident in 1986 (Lukin 2016; Rybalsky et al. 2004; Dobrovolsky and Shoba 2001). Assessing land degradation is a complex issue requiring the collection of data from different sources and the analysis of different types of variables, sometimes aggregated for different scales and different time periods (Nkonya et al. 2016). At the same time, there is still a need to study the dynamics and factors of land degradation for countries and territories that have specific historical, cultural and development problems (Sartori et al. 2019; Wuepper et al. 2020).

To analyse the dynamics and driving forces behind land degradation in Russia, much more research is focused on the environmental side of the problem, such as the dynamics and extent of soil erosion (Krasilnikov et al. 2016, Litvin et al. 2017, Golosov et al. 2018, Ivanov 2018), than the economic factors of degradation (Sorokin et al. 2016; Prishchepov et al. 2013), and to some extent Wuepper et al. (2020). Thus, one of the goals of our approach in this chapter was to show several examples of how the economic (monetary) valuation of land degradation problems and regional cases can be related to the use of different types of data (at the regional or district level) with data from different sources (GIS maps, official statistics, primary farmer data). All this is applied in a relatively small area (in comparison with Russia and even the entire

Russian Plain) covering three regions of the Central Chernozemic Region of Russia—the Belgorod, Lipetsk and Tula regions.

Our second goal was to analyse the dynamics of land degradation in terms of land use change over a relatively short period of time (2001–2009), when Russia experienced recovery from the economic reforms of the 1990s and agricultural collapse, and was also supported by higher prices for agricultural products that contributed to the growth of farm income.

The ecological and economic assessment of land degradation comprised two groups of methods:

- (1) Factor correlation and regression analysis to identify the interdependence of economic indicators and land degradation (Weinstein 1967; Kovalev 1998) (only for the Tula region);
- (2) Land degradation assessment based on the comparison of economic indicators of agricultural production with sustainable land management and traditional land use (“action/inaction assessment”) (for all regions studied).

Factor correlation and regression analysis reveals links between indicators of economic activity, when the relationship between them is not strictly functional and distorted by the influence of extraneous, random factors (Ferster and Reinz 1983). In our case, it included the use of two types of models: (1) spatial and (2) dynamic.

The spatial model involved collection of data by region (municipality) over a 1-year period. The dynamic model studied a region as a single object and was focused on the analysis and comparison of factors for a certain period of time.

The area of degraded land (in the spatial model) and the fertility balance (in the dynamic model) were used as indicators of land degradation. Various economic indicators were used as independent variables.

The independent variables in these models were economic indicators of agricultural activities indirectly used in assessing land degradation: yield, crop area, fallow ratio, crop production costs, cost of mineral and organic fertilisers,

labour, income, profitability, etc. The source of information for assessing land degradation was a database compiled from the analysis of statistical materials (Stolbovoy et al. 1999).

Statistical data processing resulted in the following linear-logarithmic equations:

$$\ln(y) = \text{const} + a * \ln(x_1) + b * \ln(x_2) \dots + n * \ln(x_n) \quad (6.1)$$

where y is a dependent variable indicating the level of land degradation (or soil fertility balance coefficient in the dynamic model) and x is the factors affecting land degradation.

The results included correlation coefficients, coefficients of determination, the Durbin–Watson criterion, elasticity β , t -statistics and their significance. These factors show the relationship between land degradation and economic indicators. They also express the degree to which selected factors describe the variability of the dependent variable, and the statistical significance of the factors.

The action/inaction assessment approach uses two methods—a simplified one based on the change in land-use, and another not using that change. The simplified method, used in this study, is based on estimating the change in the value of land following a land use or land cover change (LUCC) (e.g. when forest changes to cropland or perennial plantings to pastures). The cost of action taken to return the most productive vegetation is compared with the cost of inaction, i.e. passively waiting when the ecosystem productivity annually drops to a certain value. The decrease in land value is considered as land degradation and calculated by the Eq. (6.2):

$$C_{LUCC} = \sum_i^K (\Delta a_i * p_1 - \Delta a_i * p_2) \quad (6.2)$$

where C_{LUCC} is the cost of land degradation due to changes in LUCC; a_i is land area 1, which is replaced by land area 2; and p_1 and p_2 are the total economic value (TEV) of landscapes 1 and 2, respectively.

The cost of inaction is the sum of annual degradation losses (Eq. 6.3):

$$CI_i = \sum_{t=1}^T C_{LUCC} \tag{6.3}$$

where CI_i is the cost of inaction under vegetation i .

The cost of action against changes in the LUCC was determined as Eq. (6.4):

$$CTA_i = A_i \frac{1}{\rho^t} \left\{ z_i + \sum_{t=1}^T (x_i + p_j x_j) \right\} \tag{6.4}$$

where CTA_i is the cost of restoring high-value vegetation i ; p^t is the discount factor for the land user; A_i is an area of high-value vegetation i , which was replaced by low-value vegetation j ; z_i is the cost of establishing high-value vegetation i ; x_i is the value of caring for vegetation i until its maturity; x_j is the productivity of low-value vegetation j per hectare; p_j is the cost of low-value vegetation j per unit (e.g. per tonne); t is the time in years, and T is the timetable for planning in land degradation decisions. $P_j x_j$ represents the value of the benefits lost from not using the low-value vegetation j which is being replaced.

Applying the von Braun method, changes in land use and vegetation cover (based on the normalised difference vegetation index, NDVI)

in these regions from 2001 to 2009 were studied using MODIS remote sensing (Moderate Resolution Imaging Spectroradiometer) (Sorokin et al. 2016). The study did not use the traditional division of land use categories (Land Code 2001) but instead used so-called “land use types” provided by MODIS (forest, shrub, pastures, crops, young forest, abandoned fallow lands and wetlands). The difference between our work and that of Sorokin et al. (2016) is that we conduct a more detailed regional analysis of the three regions.

6.3 Economic Assessment of Land Degradation

6.3.1 Belgorod Region

An analysis of changes in different land use areas in the Belgorod region in 2009 compared with 2001 showed that the most significant decrease was found for the pastures, while the largest increase occurred for the areas of young forests (Table 6.1). This confirms that croplands were abandoned during that period due to non-profitable agricultural lands and bankruptcy among dairy farms, followed by fields being overgrown with woody vegetation.

Based on the assessment of changes in land use, the Belgorod region has a negative growth rate of ecosystem services (−3.5 million dollars).

Table 6.1 Changes in land use and the total cost of ecosystem services in the Belgorod region (2001–2009)

Land use	Change in land area relative to 2001		Change in the value of ecosystem services, millions of dollars (USD)
	ha	%	
Forest	+1421 ^a	+1	+4.3
Shrub	−1257	−29	−2.0
Pastures	−3813	−49	−10.9
Crops	+233	0	+0.2
Young forest	+3553	+23	+5.6
Barren lands	−55	−7	0.0
Water	−82	−15	−0.7
Total			−3.5

^a+ increase; − decrease

Table 6.2 Economic assessment of land degradation in Belgorod region

No	Results of the evaluation (2018)	Value of the index
1	Economic assessment of land degradation, including all ecosystem services, billions of USD	0.058
2	Economic assessment of land degradation, for the loss of agricultural production, billions of dollars. USD	0.0188
3	Cost of action against degradation—for 6 years, billions of USD	0.170
4	Cost of action against degradation—for 30 years, billions of USD	0.173
5	Cost of inaction against degradation—for 6 years, billions of USD	0.415
6	Cost of inaction against degradation—for 30 years, billions of USD	0.8989
7	Ratio of the cost of inaction to the cost of action—for 6 years	2.43
8	Ratio of the cost of inaction to the cost of action—for 30 years	5.20

This was due to a significant decrease in the area of pastures, which are more sustainable from an environmental point of view compared to crops.

Due to a decrease in the overall productivity of vegetation, which led to a decrease in the NDVI during the study period, the area of degraded land (428,635 ha) in Belgorod was greatly improved (4,182 ha).

The calculations showed (Table 6.2) that the cost of inaction in Belgorod was higher than the cost of action against degradation, both for the 6- and 30-year perspectives (2.43 and 5.20 times higher, respectively). This means that reclaiming (improving) land productivity and supporting ecosystem services is economically feasible (Farquharson et al. 2008; Barbier 1998; Nkonya et al. 2011; Savin et al. 2010).

By the beginning of the 2000s, the degradation of soils and land in the Russian Federation had reached a significant scale (Bondarenko 2016): erosion, nutrient depletion, dehumidification, acidification of croplands, overgrowing of croplands with woody vegetation and a decrease in pasture areas. In the Belgorod region, these processes are still manifesting, although they have been quite successfully mitigated (especially soil erosion) (Lukin 2016). Figure 6.1 shows changes in the soil nutrient balance on cropland of different agricultural organisations in the Belgorod region. The scientifically sound restoration of land productivity in the Belgorod

region resulted in sustainable growth in regional agriculture. As a result, between 2010 and 2015, the actual prices of crop production in the Belgorod region increased by 122.3%, (120.0 billion rubles) and in 2015 amounted to 218.1 billion rubles, which is 4.3% of the total value of agricultural production in Russia (Lukin 2016). These achievements brought the Belgorod region to third place in terms of agricultural production in the Russian Federation (after the Krasnodar and Rostov regions).

The agricultural development of arable lands in the Belgorod region led to a greater extraction of the main soil nutrients due to the increased crop yield (Fig. 6.1). The green line in Fig. 6.1 shows that from 2001 to 2009, the share of nutrients from chemical and organic fertilisers covered only 60–65% of nutrient extraction, a figure which dropped to 53% over a short period due to the high market cost of fertilisers. In 2010, there was a drought and the yield dropped. However, in 2011 the share of nutrients applied began to increase due to the extensive use of pig and poultry manure in the Belgorod region. Thus, by 2014, the nutrient application rate reached almost 90% of the nutrient production by crops.

Although there was a loss of ecosystem services in the Belgorod region between 2001 and 2009, from Table 6.1, we can see that their restoration is economically feasible. Table 6.2

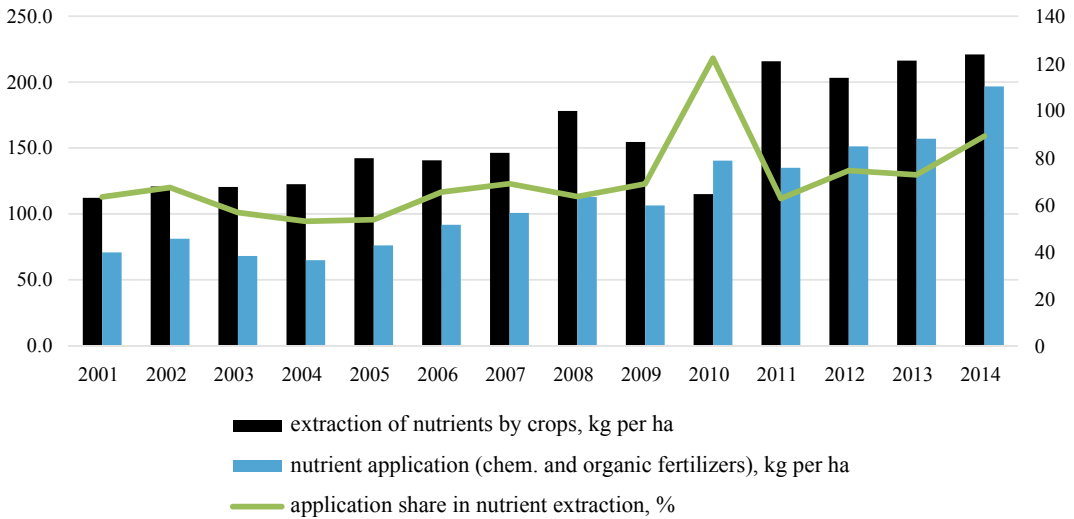


Fig. 6.1 Nutrient balance (NPK) in soils of cropland of agricultural organisations in Belgorod (calculated by authors using Rosstat (Russian Statistics) data and nutrient extraction data from Sutchev et al. 2015, and Mineev 2001). The black bar shows the harvest of main

nutrients from soil with yield. The blue bar indicates the application of nutrients in the form of chemical and organic fertilisers. The green line is the share of the applied nutrients in the volume removed by harvesting

shows that remediation costs are economically achievable, and the dynamics of nutrients in arable lands (Fig. 6.1) shows that the soil nutrient balance has become an important item on the region's agenda in recent years. In the future, the Belgorod region plans to improve the use of lime on arable land and solve the problems of erosion (Lukin 2016).

6.3.2 Lipetsk Region

Table 6.3 show the changes in the different land use areas and the corresponding value of ecosystem services in 2009 compared to 2001 in the Lipetsk region. The most significant decrease was found for the area with young forest (an area 5–10% of which is occupied by forest trees). These young forests were transformed into mature forest (50–60% of area occupied by trees). Therefore, the most significant growth was found for the land occupied by mature forests.

The remote sensing outputs indicated cropland abandonment followed by overgrowing with woody vegetation. Table 6.3 also shows an estimate of the cost of land use change. In the Lipetsk region, a small positive growth rate was

observed in ecosystem services, due to the above-mentioned increase in the area of forests that intensively absorb greenhouse gases.

Table 6.4 presents the sum of all land uses where the NDVI decreased (degraded lands occupied 112,755 ha), while the area with increased NDVI occupied 44,878 ha. Table 6.6 presents the growth in bioproductivity within each allocated land use group, and Table 6.3 shows the transition from one land use group to another. Thus, in the Lipetsk region, the area of degraded lands (decrease in bioproductivity) significantly exceeded the area of the land with increased bioproductivity between 2001 and 2009. This trend is a good reflection of the situation in agriculture in Russia in the early 2000s (Dobrovolsky 2002).

The calculations showed that the cost of inaction in the Lipetsk was higher than the cost of action against degradation (for both the 6-year and the 30-year perspectives) (Table 6.5). This means that the reclamation of land productivity and support of ecosystem services are economically reasonable in this region (Nkonya et al. 2011, 2016; Von Braun et al. 2013).

This conclusion was supported by the outputs of practical activities in the region. Recently, in

Table 6.3 Changes in land use and the total cost of ecosystem services in the Lipetsk region (2001–2009)

Land use	Change in land area relative to 2001		Change in the value of ecosystem services, millions of US dollars
	ha	%	
Forest	+8268 ^a	+5	+24.9
Shrub	+1271	+251	+2
Pastures	+328	+6	+0.9
Crops	−3239	−0.1	−2.8
Young forest	−5658	−45	−9
Barren lands	−41	−75	−0.01
Wetlands	−929	−36	−7.9
Total			+8.2

^a+ increase; − decrease

Table 6.4 Dynamics of the degraded and reclaimed lands area in the Lipetsk region (2001–2009)

Region	Area of degraded land	Area of reclaimed land	Ratio of degraded to reclaimed land
Lipetsk region	112,755 ha	44,878 ha	2.5

Table 6.5 Economic assessment of land degradation in the Lipetsk region

Lipetsk region	Billions of US dollars
Economic assessment of land degradation, for all ecosystem services	0.040
Economic assessment of degraded land, only for the loss of crop production	0.017
Cost of action against degradation—for 6 years	0.118
Cost of action against degradation—for 30 years	0.120
Assessment of opportunities (i.e. the cost of goods and services in the current land use)	0.105
Cost of inaction against degradation—for 6 years	0.289
Cost of inaction against degradation—for 30 years	0.625
Ratio of inaction to action for 6 years	2.440
Ratio of inaction to action for 30 years	5.210

the Lipetsk region, positive dynamics were observed in the growth of cropland productivity associated with an increase in the use of mineral and organic fertilisers, and chemical ameliorants (Table 6.6). From 2000 to 2004, only about 30 kg/ha^{−1} of mineral fertilisers, 1 t/ha^{−1} of organic fertilisers and 20 to 40 kg/ha^{−1} of ameliorants were applied. However, currently, about 90 kg/ha^{−1} of mineral fertilisers, more than 3 t/ha^{−1} of organic fertilisers and about 100 kg/ha^{−1} of ameliorants are used in this region. Consequently, the productivity of arable

land has increased from 1.4 to 3.0 tonnes of grain per hectare (Federal Government Agency 2020).

Figure 6.2 shows a general picture of the soil nutrient balance in the Lipetsk region over the observed period, revealing the effect of the large increase in crop yield on soil productivity (Table 6.6). Table 6.6 only shows the yields of cereals from 57% of the arable area in 2001, from 70% in 2009 and from 60% in 2014, whereas Fig. 6.2 shows the nutrient uptake by several major crops—cereals, forage grasses, sunflowers, sugar beets, potatoes and vegetables.

Table 6.6 Effect of fertilisation and amelioration on the productivity of arable land in the Lipetsk region (Federal Government Agency 2020)

Years	Application of fertilisers and ameliorants			Yield, kg of grain per ha
	Mineral (kg/ha ⁻¹)	Organic (t/ha ⁻¹)	CaCO ₃ (kg/ha ⁻¹)	
2000	35	0.8	21	1410
2001	31	0.9	44	1750
2002	35	1.1	30	1900
2003	43	1.1	30	2120
2004	43	1.2	44	2170
2005	57	1.8	44	2310
2006	73	2	44	2310
2007	72	2.4	35	2310
2008	80	2.8	43	3320
2009	71	3.1	44	3140
2010	77	2.4	119	1600
2011	84	3.2	98	2980
2012	92	3.4	87	3060
2013	82	3.2	55	3340
2014	86	3.1	95	3000

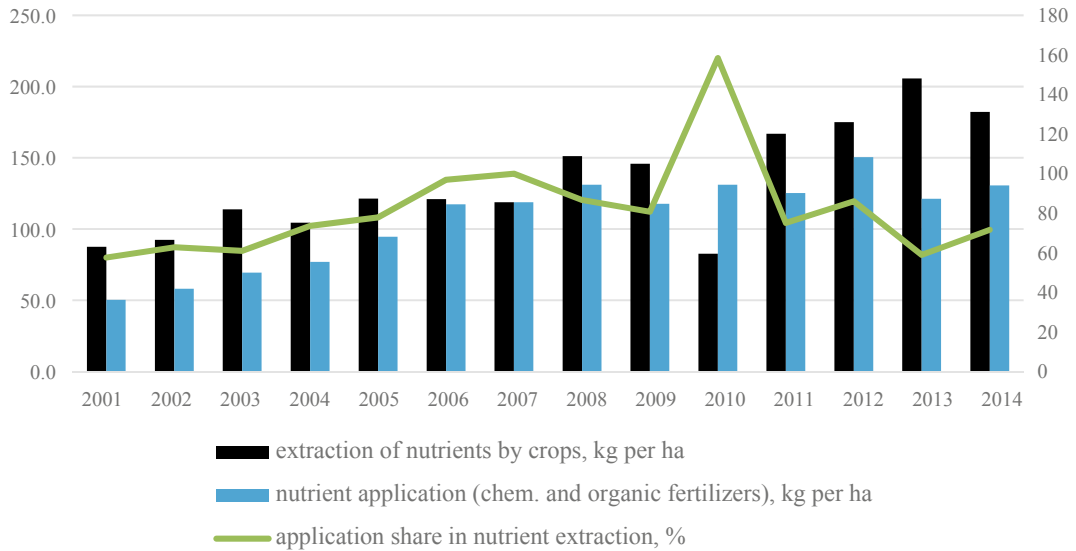


Fig. 6.2 Nutrient balance (NPK) in arable soils of the Lipetsk region (calculated by the authors using Rosstat (Russian Statistics) data and nutrient uptake data from Sutchev et al. 2015 and Mineev 2001). The black bar shows the harvest of main nutrients from soil with yield.

The blue bar indicates the application of nutrients in the form of chemical and organic fertilisers. The green line is the share of the applied nutrients in the volume removed by harvesting

Agricultural development in the Lipetsk region has led to an increase in nutrient consumption (NPK) with increasing crop yields. The green line in Fig. 6.2 shows that from 2001 to 2009, the share of nutrients from chemical and organic fertilisers increased from 58 to 81% of the total extracted nutrients. In 2010, there was a drought, the yield fell, and as of 2011 the share of fertilisation began to decline. Thus, by 2014, the fertiliser application rate had dropped to almost 72% of the nutrient extraction by crops (similar to 2004).

Between 2001 and 2009, the Lipetsk Oblast saw an increase in the value of ecosystem services (Table 6.3), mainly due to an increase in the forest area. Through detailed arable land dynamics and agricultural development analysis, we found that a decrease in arable land was followed by an increase in yields, and for some time, the nutrient balance in the soil matched this increase. But since 2011, plant nutrient extraction has increased and no rate-based fertilisation has followed, which could lead to future soil fertility problems. Therefore, the cost of action to combat land degradation is particularly important for this region.

Thus, we see that, in contrast to the Belgorod region, in Lipetsk, two different movements (dynamics) in the balance of soil nutrients were observed—positive from 2001 to 2009, and negative from 2011 to 2014. This means that, while the Belgorod region has already begun to take action to combat land degradation (especially with regard to arable land), Lipetsk agricultural and soil policy was lagging behind, which could lead to action being more costly if not taken soon.

6.3.3 Tula Region

6.3.3.1 Factor Correlation and Regression Analysis

Spatial Model

The spatial model of the region included economic indicators for 23 districts of the Tula region. The area of degraded land was used as an

indicator of land degradation (Stolbovoy et al. 1999), and various economic indicators were used as independent variables. Table 6.7 presents six linear-logarithmic equations of type (1).

The spatial regressions showed that all presented equations (except the third and fifth) have sufficiently strong correlation and high determination coefficients. This means that the variability of the dependent variable is relatively well described by the selected factors. In the first, second, third and fifth equations, a small positive autocorrelation was observed, i.e. the factors were interdependent. This occurred due to the relatively small number of observations (Eqs. 6.2 and 6.3) and the nature of the selected indicators. In the fourth and sixth equations, the Durbin–Watson coefficient was close to 2, which means there was no autocorrelation between the selected factors.

The costs of crop production, fertiliser and labour had positive ratios. This is also likely associated with the increased intensity of land exploitation, which led to land degradation. At the same time, the cost of production of potato and other crops had a negative coefficient, which may be due to the cost of the measures for combating land degradation. The growth of the sown area is directly correlated with the growth of degraded land. This may be due to soil depletion as a result of the insufficient use of fertilisers.

Dynamic Model

The dynamic model included economic indicators of the Tula region from 1995 to 2014. The soil fertility balance was used as an indicator of land degradation, and various economic indicators were used as independent variables. Table 6.8 presents the six linear-logarithmic equations of type (1), where all equations (except the third and sixth) have relatively high correlation and determination coefficients. Therefore, the variability of the dependent variable is relatively fully described by the selected factors. In the first and second equations, a small positive autocorrelation was observed, indicating the independence of the factors. This is due to the nature of the selected indicators. In the third and

Table 6.7 Results of the spatial regression model in the Tula region in 1995

Variable	Coefficients of correlation, determination, Durbin-Watson	Elasticity coefficients of the equation (beta)	t-statistics	Significance of t-statistics
1	2	3	4	5
<i>Equation 6.1</i>	$R = 0.816$ $R^2 = 0.666$ $DW = 2.064$			
Constant		-6.289	-1.844	^b
Costs of crop production		1.195	4.364	^c
Sown area		0.206	0.801	
<i>Equation 6.2</i>	$R = 0.724$ $R^2 = 0.525$ $DW = 2.036$			
Constant		1.531	0.804	
Crop income		0.541	4.625	^c
Abandoned fallow land		-0.019	-0.616	
<i>Equation 6.3</i>	$R = 0.686$ $R^2 = 0.470$ $DW = 2.107$			
Constant		-2.095	-0.669	
Cost of fertilisers		0.639	2.583	^c
Labour costs		0.185	0.655	
<i>Equation 6.4</i>	$R = 0.922$ $R^2 = 0.851$ $DW = 1.768$			
Constant		-1.49	-0.556	
Grain yield		0.725	3.074	^c
Cost of grain production		-0.204	-0.633	
Grain sown area		0.541	2.172	^c
<i>Equation 5</i>	$R = 0.500$ $R^2 = 0.250$ $DW = 2.772$			
Constant		9.887	5.698	^c
Potato income		0.401	0.712	
Cost of potato production		-0.279	-2.428	^c
of potato crop		-0.139	-0.215	
<i>Equation 6</i>	$R = 0.827$ $R^2 = 0.684$ $DW = 1.972$			
Constant		1.527	0.57	
Other costs		-0.883	-3.582	^c
Cost of fertilisers		0.061	0.269	
Labour cost		0.878	4.241	^c

^c—significance of t-statistic coefficients at 1% level; the dependent variable is the size of degraded agricultural land (n = 23 in each equation)

fourth equations, the Durbin–Watson coefficient was close to 2, which means that there is no autocorrelation between the selected factors.

The yields of potato and grain have negative coefficients: with their growth, the balance of fertility decreases, which may be due to the soil

Table 6.8 Regression analyses of the dynamic models for the Tula region (1995–2014)

Variable	Coefficients of correlation, determination, Durbin-Watson	Elasticity coefficients of the equation (beta)	t-statistics	Significance of t-statistics
1	2	3	4	5
<i>Equation 1</i>	$R = 0.855$ $R^2 = 0.731$ $DW = 2.113$			
<i>Constant</i>		3.639	3.115	^c
Crop production income		-0.37	-4.731	^c
Crop production cost		0.173	4.291	^c
<i>Equation 2</i>	$R = 0.910$ $R^2 = 0.828$ $DW = 2.220$			
<i>Constant</i>		4.012	4.68	^c
Sown area		0.977	6.38	^c
Labour costs		-0.303	-3.632	^c
<i>Equation 3</i>	$R = 0.760$ $R^2 = 0.557$ $DW = 1.142$			
<i>Constant</i>		4.595	2.317	^c
Crop production cost		0.219	1.968	^b
Cost of mineral fertilisers		-0.383	-2.537	^c
Cost of organic fertilisers		0.072	1.035	
<i>Equation 4</i>	$R = 0.946$ $R^2 = 0.895$ $DW = 1.858$			
<i>Constant</i>		9.184	6.377	^c
Grain yield		-0.754	-5.649	^c
Sown area		0.871	10.211	^c
<i>Equation 5</i>	$R = 0.913$ $R^2 = 0.834$ $DW = 1.385$			
<i>Constant</i>		3.726	4.217	^c
Potato yield		-0.148	-6.807	^c
Crop production cost		0.112	3.381	^c
<i>Equation 6</i>	$R = 0.522$ $R^2 = 0.273$ $DW = 0.643$			
<i>Constant</i>		5.314	4.065	^c
Fallow land		0.13	1.877	^b
Cost of fertilisers		-0.239	-1.402	^a

^c—significance of t-statistic coefficients at 1% level; ^b—significance of t-statistic coefficients at 5% level; ^a—significance of t-statistic coefficients at 10% level;—the coefficient is not statistically significant and does not affect the dependent variable in the equation; the dependent variable is an index of balance of soil fertility (n = 20 in each equation)

depletion. In addition, a negative beta-coefficient (elasticity) revealed an increase in crop production and a decrease in the soil fertility balance due to the intensification of agriculture. At the same time, the costs of labour and mineral fertilisers also have negative coefficients.

The sown area had a positive correlation with the soil fertility balance. This was probably due to the cost of organic fertilisers, which also had a positive coefficient. Abandoned fallow lands had a positive coefficient, which confirms the hypothesis of a positive correlation between land degradation and the intensification of agricultural production.

6.3.3.2 Action/Inaction Estimation Method

Table 6.9 shows changes in the dynamics of different land use areas in the Tula region during 2001–2009. Despite a significant reduction in cultivated areas and pastures, the highest growth was observed in the transition from pastures to forests. This confirms the fact that many non-profitable croplands were abandoned, with subsequent overgrowth by woody vegetation.

Analysing the relative indicators of changes in land use areas for the specified period (2001–2009) in the Tula region, a noticeable decrease in the areas of water bodies, pastures and shrubs was observed. The most negative factor was a significant reduction in the area of water bodies

(71%), which pose a threat not only to the surrounding ecosystems but also to public life.

Our results show that there has been an overall increase in ecosystem services due to an increase in forest area, which has one of the highest values for ecosystem services. There was also an increase in the area of degraded land in the Tula region, while the area of reclaimed land did not improve (Table 6.10).

The calculations in Table 6.11 show that the cost of inaction was higher than the cost of action against degradation (both for the 6-year and 30-year perspectives). This supports the viability of economic investment in restoring land productivity and ecosystem services, although the real benefits will only be visible with a longer perspective.

The data from Table 6.11 shows that, of the three Chernozem soil regions which were studied, the ratio of inaction vs. action is the highest in the Tula region. One of the reasons for this could be very slow agricultural development characterised by low yields and only a minor recovery of the soil nutrient balance (Fig. 6.3).

This indicates that the soil degradation situation is less favourable in Tula than in the other two regions. In the Belgorod and Lipetsk regions, varieties of more productive crops are used, which extract an average of 200 kg of the main nutrients (NPK) per hectare per year from the soil, while in Tula, only 120 kg of nutrients are

Table 6.9 Changes in different land use areas in the Tula region (2001–2009)

Land use	Change in land area relative to 2001		Change in the value of ecosystem services, millions of US dollars
	ha	%	
Forest	+44,755 ^a	+15	+135
Shrub	–588	–15	–1
Pastures	–27,932	–18	–80
Crops	–8637	0	–7
Young forest	–6450	–66	–10
Barren lands	0	0	0
Wetlands	–1148	–71	–10
Total			+26

^a+ increase; – decrease

Table 6.10 Dynamics of degraded and reclaimed lands in the period from 2001 to 2009

Region	Area of degraded land	Area of reclaimed land	Ratio of degraded to reclaimed lands (%)
Tula region	114,176 ha	0 ha	0

Table 6.11 Economic assessment of land degradation in Tula region

Tula region	Billions of US dollars
Economic assessment of land degradation for all ecosystem services	0.21
Economic assessment of degraded land, (loss of crop production)	0.06
Cost of action against degradation—for 6 years	0.51
Cost of action against degradation—for 30 years	0.51
Assessment of opportunities (i.e. cost of services in the current land use)	0.45
Cost of inaction against degradation—for 6 years	1.48
Cost of inaction against degradation—for 30 years	3.20
Ratio of inaction to action for 6 years	2.93
Ratio of inaction to action for 30 years	6.24

The ratio of the cost of inaction to the cost of action, dimensionless

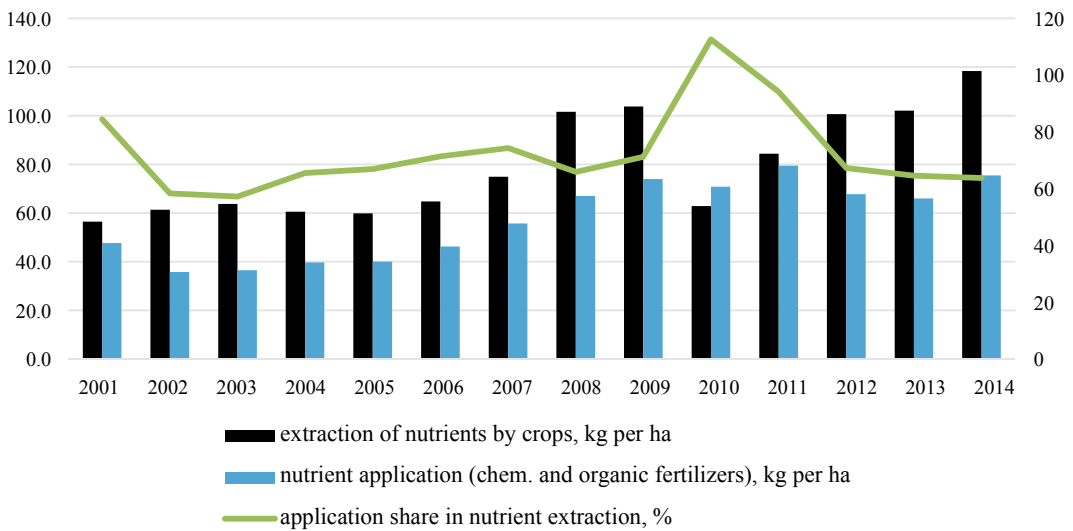


Fig. 6.3 Nutrient balance (NPK) in arable soils in Tula region (calculated by the authors using Rosstat (Russian Statistics) data and nutrient uptake data from Sutchev et al. 2015 and Mineev 2001). The black bar shows the harvest of main nutrients from soil with yield. The blue

bar indicates the application of nutrients in the form of chemical and organic fertilisers. The green line is the share of the applied nutrients in the volume removed by harvesting

harvested with crops. At the same time, fertiliser application rates are also lower in Belgorod and Lipetsk than in the Tula region.

6.4 Comparison of Economic Variables on Land Degradation in Regions Studied

The data from Sorokin et al. (2016) showed that part of the land was still abandoned, while the forest area was increasing, thus increasing ecosystem services, as measured by the total economic value method (Turner et al. 1994; de Groot et al. 2012). Our study focused on the arable lands that are specialised in crop production. Interestingly, in Belgorod, the smallest reduction in planted areas during this period was

associated with good organisational policies, while in Tula and Lipetsk, a slight reduction in planted areas was accompanied by an increased level of yield (Table 6.12). This probably happened against the backdrop of low yields in the economically critical years of the 1990s and the subsequent recovery period.

The analysis of the results showed that the increase in yield and TEV growth on arable land is still constrained by the growth of forest area and the corresponding TEV for forests, which leaves many questions about how soil degradation proceeds, especially on arable land. And here we have the third part of our goal—to identify the driving force behind land degradation using farm data. We managed to do this only for 1 region: Tula.

Table 6.12 Selected variables for comparison of land degradation indicators and drivers of change in the studied Belgorod, Lipetsk and Tula regions

Time span	Variable	Unit	Belgorod	Lipetsk	Tula	Table number
2001–2009	Cropland change	Hectare	233	–3239	–8637	Tables 1, 3, 11 respectively for particular region
2001–2009	Cropland change relative to 2001	Percentage	0.00	–0.10	0.00	Tables 1, 4, 12
2001–2009	TEV change only on cropland	Million USD	0.20	–2.80	–7.00	Tables 1, 5, 13
2001–2009	Grain yield change relative to 2001	percentage	106.14	149.37	147.92	Authors' estimates
2009	Grain yield	Tonnes per hectare	2.94	3.57	2.84	Authors' estimates
2014	Compensation for nutrients in the soil with fertilisers	% of nutrient uptake	90.00	72.00	64.00	Figures 1, 2 and 3,
1995–2014	Elasticity of cropland soil fertility by grain yield	n.a	n.a	n.a	–0.75	Table 10
1995–2014	Elasticity of crop soil fertility by sown area	n.a	n.a	n.a	0.87	Table 10
1995	Elasticity of land degradation by grain yield	n.a	n.a	n.a	0.73	Table 9
1995	Elasticity of land degradation by grain sown area	n.a	n.a	n.a	0.54	Table 9

Source calculated by the authors

For the Tula region (north of Belgorod and Lipetsk), we made two models due to the different data capacity. The first model was built using district-level data from Stolbovoy et al. (1999), which show the proportion of agricultural land in the district that is affected by soil degradation. Then we added the data collected by the primary agricultural organisations for 1995 from the Russian Statistical database, also aggregated at the municipal level. The collected data was rich in various variables for costs, incomes, yields and acreage. The first regression developed based on these data showed that extensive development factors such as large croplands contribute to land degradation.

The second regression was carried out at the regional level of Tula for the dynamic period 1995–2014. Here, a variable depending on the balance of soil fertility was used, calculated based on Rosstat data, which showed the amount of nutrients (nitrogen, phosphorus and potassium) that were removed from the soil by the crop and how they were balanced by mineral and organic substances from fertilisers. Our results showed that the dynamic balance of soil fertility in the arable land of Tula was driven by low yields and low incomes. The yield of potatoes and grains had negative coefficients, i.e. as the yield increases, the balance of fertility decreases, which may be associated with depletion of the soil. In addition, a negative beta-coefficient (elasticity) showed the income from crop production and decreased soil fertility balance due to agricultural intensification. At the same time, labour and fertiliser costs also have negative coefficients.

The relatively high level of the current state of agricultural production in the Belgorod and Lipetsk regions confirmed the adequacy of the environmental and economic analysis. In the Tula region, the costs of crop production, fertilisers and labour have positive coefficients, due to an increase in the land use intensity, which caused their degradation. Negative coefficients in the cost of potato may be due to the costs of measures to combat land degradation. An increase in sown areas was directly correlated with the growth of degraded land, due to soil

depletion caused by insufficient fertiliser application. Our data analysis showed that the fallow lands had a direct correlation with the soil fertility, which confirms the hypothesis of a close link between land degradation and the intensification of agricultural production.

Finally, we calculated the balance of soil nutrients in all three regions, comparing the removal of basic soil nutrients (NPK) by crops and how much (what proportion) of the removed nutrients are compensated for by the application of chemical and organic fertilisers. Our results show that the Belgorod and Lipetsk regions use the best high-yielding varieties, which consume more nutrients from the soil, but that at the same time, agricultural producers, following local policies, try to compensate for this loss of nutrients by applying more fertilisers. While the Tula region is developing at a low rate and has low yields with an average nutrient compensation by fertilisers of 60%, which makes this region a kind of outsider among these three. This is also supported by the estimated cost of the “action” versus the “inaction” method, where the ratio for Tula is higher than for Belgorod and Lipetsk. This situation paves the way for a more difficult and costly path to future recovery in the Tula region. Generally, the cost of inaction in the regions studied was higher than the cost of action against land degradation (in 6- and 30-year perspectives), implying the economic feasibility of restoring (improving) land productivity and supporting ecosystem services.

6.5 Conclusion

The proposed “action” and “inaction” methods proved to be effective in assessing soil degradation using land-based economic indicators. It made it possible to assess the economic feasibility of investing in the restoration of land productivity in the region, and in supporting ecosystem services, in the 6- and 30-year perspectives. Taking the example of the regions studied in the Central Russian Plain on Chernozem soils, it was possible to show the active development of land degradation processes and a

decrease in their productivity in the 2000s. The current successful crop production in these territories testifies to the high efficiency of the Russian economic policy in supporting crop production and combating land degradation.

However, although the Chernozem soils are considered highly fertile and productive compared to other soil types, their intensive exploitation for the economic growth of the region can result in the onset of degradation in these soils. Therefore, further studies and investigation should be focused on measures to prevent soil degradation and help improve the nutrient balance on arable lands. As Russian agricultural policy proposes to increase its agricultural exports, the potential pressure on soils is likely to increase in the immediate future, especially in such favourable climate conditions as the Chernozem (Black soil) region of Russia. In this regard, the use of intensive agricultural technologies can lead to agrodepletion, erosion and soil compaction even in these highly fertile soils. To combat all these risks, an economic assessment of sustainable soil practices should be a top priority.

Another priority is organising and collecting soil data and economic data. Russia still lacks a proper system for collecting data on sustainable agricultural technologies. To improve this, it is necessary to make changes in statistical recordings for different types of farms. This can be useful when organising interdisciplinary research in which data on soil and economics are presented equally. The application of the “action” and “inaction” assessment method should be proposed for an in-depth analysis of the situation in the region studied in the future, simulating an increasing agrogenic load on the soil cover and attracting a wider range of ecosystem services of soils and other natural components. In fact, using the land degradation economics method, it is possible to create a system for monitoring the risk of land degradation not only at the present but also in the distant future.

Acknowledgements The work was supported by RFBR grant # 18-010-00775a.

References

- Barbier EB (1998) The economics of environment and development: selected essays. Edward Elgar, London. p 540
- Bondarenko EV (2016) Experience of accounting for ecosystem services of soil in assessing land degradation (for example, UO PEP Moscow State University). Extended abstract of candidate’s thesis, Moscow, p 24 (Бондаренко Е.В. Опыт учета экосистемных услуг почвы при оценке деградации земель (на примере УО ПЭП МГУ). Автореферат кандидатской диссертации, Москва, стр. 24)
- de Groot R, Brander L, van der Ploeg S et al (2012) Global estimates of the value of ecosystems and their services in monetary units. *Ecosyst Serv* 1(1):50–61. <https://doi.org/10.1016/j.ecoser.2012.07.005>
- Dobrovolsky GV (ed) (2002) Soil degradation and protection. Publishing House of Moscow State University, Moscow. p 658 (Добровольский Г.В. Деградация и защита почв. Издательство МГУ, Москва. 658 с.)
- Dobrovolsky GV, Shoba SA (eds) (2001) Assessment and ecological control of the environment (on the example of Tula region). Publishing House of Moscow State University, Moscow, p 256 (Добровольский Г.В., Шоба С.А. Оценка и экологический контроль окружающей среды (на примере Тульской области). Издательство МГУ, Москва, с. 256)
- Farquharson RJ, Cacho OJ, Mullen JD, Schwenke GD (2008) An economic approach to soil fertility management for wheat production in North-Eastern Australia. *Agric Econ* 38(2):181–192. <https://doi.org/10.1111/j.1574-0862.2008.00292.x>
- Federal Government Agency (2020) Impact of soil cultivation on the productivity of arable land in the Lipetsk region (Влияние окультуренности почв на продуктивность пашни Липецкой области). <https://agrohim48.ru/articles/vliyanie-okulturennosti-pochv-na-produktivnost-pashni-lipeczkoy-oblasti.html>. Accessed 7 March 2021
- Ferster E, Reinz B (1983) Methods of correlation and regression analysis. Finance and statistics, Moscow, p 304 (translated from German: Ферстер Э., Рейнц Б. Методы корреляционного и регрессионного анализа. Финансы и статистика, Москва, стр 304)
- Golosov V, Yermolaev O, Litvin L, Chizhikova N, Kiryukhina Z, Safina G (2018) Influence of climate and land use changes on recent trends of soil erosion rates within the Russian Plain. *Land Degrad Develop* 29:2658–2667. <https://doi.org/10.1002/ldr.3061>
- Ivanov MA (2018) Changes of cropland area in the river basins of the European part of Russia for the period 1985–2015 years, as a factor of soil erosion dynamics. *IOP Conf Ser Earth Environ Sci* 107:012010. <https://doi.org/10.1088/1755-1315/107/1/012010>
- Kovalev VV (1998) Financial analysis. Finance and statistics, Moscow, p 512 (Ковалев В.В.

- Финансовый анализ. Финансы и статистика, Москва, с. 512)
- Krasilnikov P, Makarov O, Alyabina I, Nachtergaele F (2016) Assessing soil degradation in northern Eurasia. *Geoderma Reg* 7(1):1–10. <https://doi.org/10.1016/j.geodrs.2015.11.002>
- Lal R (2004) Carbon sequestration in dryland ecosystems. *Environ Manage* 33(4):528–544. <https://doi.org/10.1007/s00267-003-9110-9>
- Land Code (2001) Federal law (25.10.2001 N 136-Fl) Land code of the Russian Federation (edition of 03.07.2016) Adopted by the State Duma on September 28th, 2001. Approved by the Federation Council on October 10th, 2001 (Земельный кодекс 2001г. Федеральный закон (25.10.2001 N 136-Фл) «Земельный кодекс Российской Федерации» (редакция от 03.07.2016 г.)
- Litvin LF, Kiryukhina ZP, Krasnov SF et al (2017) Dynamics of agricultural soil erosion in European Russia. *Eurasian Soil Sci* 50:1344. <https://doi.org/10.1134/S1064229317110084>
- Lukin SV (2016) Agroecological status and productivity of soils in Belgorod region. Constanta, Belgorod, p 344 (Лукин С.В. Агроэкологическое состояние и продуктивность почв Белгородской области. Константа, Белгород, с. 344)
- Mineev VG (2001). *Agrochemistry textbook*. Lomonosov Moscow State University (Минеев В.Г. Учебник по агрохимии. Московский государственный университет им. М.В. Ломоносова)
- Nachtergaele F, Petri M, Biancalani R, Van Lynden G, Van Velthuisen H (2010) *Global Land Degradation Information System (GLADIS)*. Beta version. An information database for land degradation assessment at global level. Land degradation assessment in Drylands technical report No 17. Food and Agriculture Organisation of the United Nations, Rome
- Nkonya E, Gerber N, Baumgartner P, von Braun J, De Pinto A, Graw V, Kato E, Kloos J, Walter T (2011) The economics of land degradation: toward an integrated global assessment, vol 66, *Development economics and policy series*. Peter Lang GmbH, Frankfurt, p 262
- Nkonya E, Mirzabaev A, von Braun J (eds) (2016) *Economics of land degradation and improvement—a global assessment for sustainable development*. Springer, Netherlands, p 686
- Prishchepov AV, Muller D, Dubinin M, Baumann M, Radeloff VC (2013) Determinants of agricultural land abandonment in post-Soviet European Russia. *Land Use Policy* 30(1):873–884. <https://doi.org/10.1016/j.landusepol.2012.06.011>
- РОССТАТ (2020) Estimated resident population as of January 1, 2020 and on average for 2019. Rosstat. Date of treatment: retreated November 26, 2020 (Оценка численности постоянного населения на 1 января 2020 года и в среднем за 2019 год. Росстат). <https://showdata.gks.ru/report/278928/>. Accessed 7 March 2021
- ROSSTAT (2010) https://rosstat.gov.ru/free_doc/new_site/perepis2010/croc/perepis_itogi1612.htm. Accessed 7 March 2021
- Rybalsky NG, Gorbатовsky VV, Yakovlev AS (eds) (2004) *Natural resources and environment of the Russian Federation regions*. Central Federal district: Lipetsk region. NIA-Priroda, Moscow, p 596 (Рыбальский Н.Г., Горбатовский В.В., Яковлев А.С. Природные ресурсы и окружающая среда регионов Российской Федерации. Центральный федеральный округ: Липецкая область. НИА-Природа, Москва, с. 596)
- Sartori M, Philippidis G, Ferrari E, Borrelli P, Lugato E, Montanarella L, Panagos P (2019) A linkage between the biophysical and the economic: assessing global market impacts of soil erosion. *Land Use Policy* 86:299–312. <https://doi.org/10.1016/j.landusepol.2019.05.014>
- Savin I Yu, Bartalev SA, Lupyan EA, Tolpin VA, Khvostikov SA (2010) Yield forecasting based on satellite data: opportunities and perspectives. *Current problems in remote sensing of the Earth from space* 7 (3):275–285 (Савин И.Ю., Барталев С.А., Лупян Е.А., Толпин В.А., Хвостиков С.А. Прогнозирование урожайности по спутниковым данным: возможности и перспективы. Актуальные проблемы дистанционного зондирования Земли из космоса 7 (3):275–285
- Shoba SA (ed) (2011) *National Atlas of soils of the Russian Federation*. Astrel, Moscow, p 632 (Шоба С.А. (под ред.) Национальный атлас почв Российской Федерации. Москва, Астрель, 632 с.)
- Sorokin A, Bryzzhev A, Strokov A, Mirzabaev A, Johnson T, Kiselev S (2016) The economics of land degradation in Russia. In: Nkonya E, Mirzabaev A, von Braun J (eds) *Economics of land degradation and improvement—a global assessment for sustainable development*. Springer, Cham, pp 541–576. https://doi.org/10.1007/978-3-319-19168-3_18
- Stolbovoy VS, SavinIYu SBV, Sizov VV, Ovechkin SV (1999) The geoinformation system on soil degradation in Russia. *Eurasian Soil Sci* 5:646–651
- Sutchev VG, Esaulko AN, Ageev VV, Podkolzin AI, Sigada MS (2015) Peculiar features of using fertilizers for growing crops in Stavropol region (Сычѳв В. Г., Есаулко АН, Агеев ВВ, Подколзин АИ, Сигада МС. Особенности применения систем удобрений под сельскохозяйственные культуры в Ставропольском крае. Вестн. АПК Ставрополя. № 2:53–67)
- Turner RK, Pearce D, Bateman I (1994) *Environmental economics*. Harvester Wheatsheaf, London
- Von Braun J, Gerber N (2012) The economics of land and soil degradation—toward an assessment of the costs of inaction. In: Lal R, Lorenz K., Hüttl RF, Schneider BU, von Braun J (eds) *Recarbonisation of the biosphere*. Springer, Netherlands, pp 493–516
- Von Braun J, Gerber N, Mirzabaev A, Nkonya E (2012) The economics of land degradation. An issue paper for global soil week 08–22 Nov 2012. Berlin, p 30

- Von Braun J, Gerber N, Mirzabaev A, Nkonya E (2013) The economics of land degradation, ZEF working paper No 109. Center for Development Research, Bonn, p 35
- Weinstein AI (1967) Methodology of short-term forecast of grain yield. USSR Academy of Sciences, Moscow, p 13 (Вайнштейн А.И. Методика краткосрочного прогноза урожая зерновых. Академия наук СССР, Москва, с.13)
- Wuepper D, Borrelli P, Mueller D, Finger R (2020) Quantifying the soil erosion legacy of the Soviet Union. *Agric Syst* 185. <https://doi.org/10.1016/j.agsy.2020.102940>



Measurement and Assessment of Snowmelt Erosion in Western Siberia

7

Alexander S. Chumbaev
and Anatoly A. Tanasienko

Abstract

Snowmelt erosion is the most destructive type of soil degradation in the dissected territories of Western Siberia. More than 50% of all Siberian farmlands are subject to erosion to various degrees. Issues related to the processes and consequences of soil erosion are a serious problem for both scientists and farmers. The purpose of this work is to present the main methods and devices used to define the quantity and quality of snowmelt water surface runoff and the damage caused by the snowmelt soil erosion. In Western Siberia, one of the main factors of erosion is snow cover, which forms and accumulates for up to five consecutive months. The water content in snow ranges from 65 mm in very low-snow winters to 255 mm in extremely high-snow winters. To measure soil erosion during the snowmelt, field methods were used to determine parameters such as the meltwater runoff volume, number of days with active meltwater drainage, water flow temperature and turbidity

of the snowmelt waters. Diagnostic signs of the effects of soil erosion after snowmelt included the volume of the soil solid phase removed by meltwater and the change in thickness of the humus horizon. The losses from erosion after winters with different amounts of snow were: solid phase of the soil—from 1 to 11 t/ha⁻¹, carbon—from 5 to 1000 kg⁻¹, and nitrogen—from 1 to 55 kg⁻¹. The described methods for studying soil erosion during the snowmelt are simple to use and do not require expensive equipment in the field.

Keywords

Soil erosion · Snowmelt surface runoff · Slope gradient · Western Siberia · Soil loss · Humus and nutrient removal · Chernozem transformation

A. S. Chumbaev (✉) · A. A. Tanasienko
Institute of Soil Science and Agrochemistry, Siberian
Branch of Russian Academy of Sciences (ISSA SB
RAS), Lavrentieva Avenue 8/2, 630090
Novosibirsk, Russia
e-mail: chumbaev@issa-siberia.ru

A. A. Tanasienko
e-mail: tanasienko@issa-siberia.ru

7.1 Introduction

The land degradation process due to the rate of soil loss exceeding the soil formation contributed to the formation of the modern physical landscape (Alewell et al. 2015). Soil erosion is among the eight soil threats listed in the Soil Thematic Strategy of the European Commission (Panagos et al. 2015). Erosion is the most common and dangerous type of soil degradation in the world. Soil degradation is inherently a gradual process, and the consequences are not always

obvious until damage is done. Erosion processes have disastrous consequences for humans and the environment, since they threaten the existence of soil as the main means of agricultural production and an indispensable component of the biosphere (Dobrovolskii 1997). The current rates of soil degradation continue to exceed the rates of soil formation, and soil degradation is jeopardising basic food production capabilities in certain parts of the world, even in the short term (Scherr 1999). Globally, 80% of agricultural land is subject to moderate and severe erosion, with soil loss of about 30 t ha⁻¹ per year on average (Pimentel 2006). Soil erosion reduces agricultural productivity and is estimated to reduce global gross annual agricultural output by 10% (Lal 1998).

Soil erosion is clearly affected by the amount and intensity of precipitation (Li and Fang 2016; Shi et al. 2020). Particularly, in mid-high latitudes and cold regions such as the northern parts of North America, Europe, Russia and northeast China, soil erosion depends predominantly on the climate (Edwards et al. 1998) and vegetation characteristics (Maltsev and Yermolaev 2019). Seasonal variations characterise the degree of snowmelt soil erosion due to the increasing surface runoff caused by melting snow in early spring and intense rainfall in summer (Lal 1998; Tanasienko 2003; Tanasienko et al. 2009; Ouyang et al. 2017; Wu et al. 2018). Snowmelt-induced gully erosion is one of the most harmful forms of degradation, particularly on arable lands (Maltsev and Yermolaev 2020; Xu et al. 2019). In addition, repeated freeze–thaw cycles significantly contribute to gully erosion (Luffman and Nandi 2019). Different factors contribute to meltwater erosion, including the slope gradient and flow rate (Shi et al. 2020); the topography and microtopography (Barneveld et al. 2019); climatic factors (temperature and the amount, rate and repeatability of snow melting) (Luffman and Nandi 2019; Tanasienko et al. 2019; Xu et al. 2019); the type of vegetation (Maltsev and Yermolaev 2020); and the depth of frost penetration, slaking and other aspects (Barneveld et al. 2019).

In Western Siberia (Russia), Chernozem soils (13.3 million ha) occupy the southern part, over a relatively flat territory that is completely cultivated with crops (10.7 million ha, Khmelev, Tanasienko et al. 2009). The further expansion of arable land is possible only on soils located on slopes. Slopes with gradients exceeding 3° are more susceptible to erosion than flat lands. Approximately 30% of these sloped lands are located on the northern slopes, while 50% are located on the southern slopes. On average, 10% of all arable land is located on slopes with a gradient of 6–9°, and approximately 5% is located on slopes with a gradient exceeding 9°. Soils on such slopes are exposed to very strong sheet erosion. Predsairye, Priobye and the Kuznetsk Depression are areas in the southeast of Western Siberia with almost 2.5 million hectares of arable land. More than 60% of these soils are Chernozems. About 20% of the arable land of this region has already been eroded to varying degrees. Therefore, the study of erosion processes and the causes of their various developments in this area appear to be highly relevant.

Despite advances in understanding rain erosion, the issues of snowmelt erosion remain poorly investigated. In particular, the relationships between rainfall, snowmelt water and water discharge on the deep and long-term frozen soils of Western Siberia are not fully understood. The mechanisms governing the detachment and sedimentation of soil particles are also poorly understood. There is also scant information on field observations in the zones of snowmelt erosion. Thus, the specific objectives of this study were to identify and assess the causes of the development of erosion processes and their impact on soils of Chernozems in years with different amounts of snow in the southeast of Western Siberia.

7.2 Study Regions and Relief Characteristics

The study area is located in Western Siberia and is a zone containing extremely fertile Chernozem soils and intensive agriculture. The regions

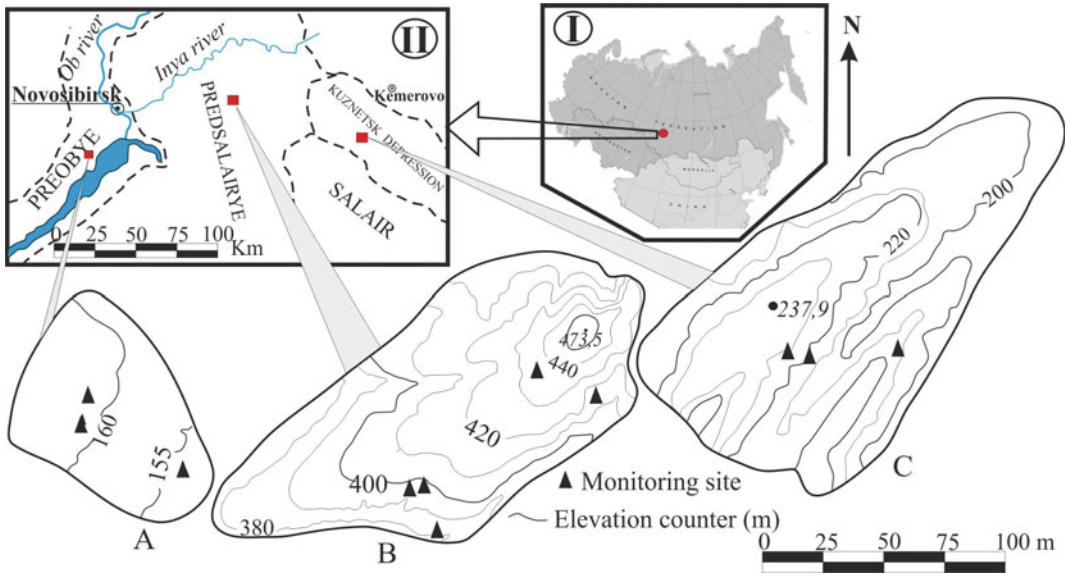


Fig. 7.1 Map of monitoring sites at Priobye (a), Predsairye (b) and the Kuznetsk Depression (c). The insert shows the location of the study area in Russia (I), southern Western Siberia (II) (Tanasienko et al. 2011)

studied include Novosibirsk (Predsairye and Priobye) and the Kuznetsk Depression (Kemerovo region) (Fig. 7.1). The areas differ in terms of their geomorphological and climatic characteristics and soils.

Predsairye is a flat, partly hilly, highly incised plain, located in a forest steppe zone. Arable land occupies more than 60% of all agricultural land, or approximately 800,000 ha; 23% of this territory is already eroded to a slight to moderate degree. The very high horizontal and vertical incision of the territory promotes erosive processes (Barneveld et al. 2019). Within Predsairye, subareas with varying degrees of erosion are easily distinguishable. The most severe erosion processes in Predsairye were observed in the Bugotac Hills subarea, which is a series of small hills extending in a northeastern direction.

The hill height is 480 m above sea level. The horizontal incision of this territory is the greatest for Predsairye and ranges from 1.5 to 2.2 km km⁻¹; the vertical incision is 75–100 m. Due to the strong incision of the territory, the basic landscape elements are slopes with gradients of 9–12° near the watershed area and 25–30° closer to gullies. The convex slopes are predominant

forms in this region; therefore, the greatest intensity of water discharge mainly occurs in the middle and bottom portions of the long slopes. Slopes with a southerly aspect are the steepest, while slopes with a northerly aspect are fairly steep and therefore less subject to erosion processes. The Bugotac Hills are classified as a territory with a very high risk of erosion.

The Kuznetsk Depression is also located in the forest steppe zone, with a strongly incised relief. The horizontal incision varies from 0.6 to 0.8 km km⁻¹ in the west of the depression and from 1.0 to 2.6 km km⁻¹ in the rest of the territory, while in some agricultural areas, the horizontal incision reaches 3.3–3.5 km km⁻¹. The vertical incision of the territory is similar to Predsairye (75–100 m). Due to such incisions, the watersheds occupy approximately 20% of the territory. In the incised parts of the depression, arable land occupies slightly more than 1 million ha, 15% of which is eroded from a slight to a moderate degree.

Priobye is located in a transition from a forest steppe to a steppe zone with absolute heights of 130–310 m, good natural drainage, an absence of primary salinity and deep ground waters (10–

15 m). Priobye's relief has a slight horizontal incision of 0.6–0.8 km km⁻¹. The watersheds are flat and occupy nearly 40% of the territory. The slope steepness in the watersheds ranges from 15° to 30° and that near gullies reaches 25–30°, indicating a significant erosion hazard in the territory. Of 180,000 ha of arable land, 15% are already eroded to a slight or moderate degree. Thus, this territory was classified as at a moderate risk of erosion (Nikitenko 1963).

7.3 Key Plot Characteristics

The theory of studying erosion is based on general models of the development of the biosphere and landscape elements. Studies of erosion processes should be based on a systematic approach using the principle of landscape catenae, and the method of field observations is the main tool for their study. To study the development of soil erosion in Western Siberia, it is advisable to place key plots in various landscape positions: near watersheds (non-eroded or virgin soils); in transluvial positions (weakly, moderately and strongly eroded soils) and in transaccumulative positions (accumulated soils).

Our studies of the factors and the process of erosion were carried out mainly on the slopes with a southeastern exposure, since these slopes are most susceptible to erosion. According to the principles of landscape catenae, non-eroded soils occupy a flat watershed, below which there are relatively long (600–800 m) dissected slopes. The upper boundary of weakly eroded soils ran approximately 150 m from the boundary with the watershed, and the lower one reached 300–350 m from this boundary. Areas with a slope of 3–6° were occupied by moderately eroded soils. Below the slope, strongly eroded soils were found with an upper boundary at 450–500 m from the watershed boundary. The southeastern slope ranged from 7 to 9°.

On the slopes, along with erosion processes, accumulative processes also took place. At the bottom of the erosion furrow, from the moment of its formation, a partial accumulation begins (Makaveev 1955). In this case, there are three

zones of sediment accumulation. The first is arable land, where there is intense deposition of sediments in places where the slopes go down below the confluence of temporary streams, in front of natural and artificial barriers. Golosov (1988) made the assumption that on average, up to 20% of the soil carried by the thawed soil from the slopes settles within the watersheds.

The second zone of accumulation is below the border of agricultural lands. Here, the soil material is re-deposited due to the dispersion of the water flow at the field exit and due to the increased roughness of the underlying surface. Fan formation occurs due to its expanding and removing the outer edge from the arable land. In this zone, depending on the rate of flushing, 10–75% of sediment is retained. First of all, particles drawn in by the flow accumulate, the proportion of which increases with an increase in the genuine roughness of the underlying surface. The remaining sediments are carried by the stream to ground-covered areas with slopes of 30 m or more from the borders of agricultural fields (third zone). In this zone, the depth of sediments depends on the turbidity of meltwater. Thus, in the process of erosion, the soil-removing material partially accumulates in the lower parts of the slopes, where mainly semi-hydromorphic soils are formed. In this part, in most cases, the humus horizons are 50% thicker than in upland soils. To obtain a representative material, it was necessary to select a highly dissected area of 1–1.5 km² followed by a geographical survey using both a comparative–geographical method and an analysis of the soil cover structure to determine the soil geochemical characteristics within the landscape.

7.4 Climatic Conditions of Study Sites as Related to Snowmelt Erosion

Precipitation in Western Siberia in the warm period is 200–350 mm, but only heavy rain has an erosive effect. However, since precipitation occurs in Western Siberia in a narrow time interval, on an annualised basis, summer

precipitation causes short-term soil erosion. Due to the partial protection of the soil by plants, the erosion effect from heavy rains is much weaker than from the snowmelt water in spring. In Western Siberia, soil erosion develops mainly under the influence of meltwaters, since the cold period lasts up to 6 months, and fallen snow with a depth of 70–200 mm melts in a very short time (on average 5–7 days). The development of soil erosion in this area depends on (1) the air temperature in both cold and snow melting periods; (2) the amount of solid precipitation in the cold period of the year (November–March); (3) soil moisture before winter and immediately before snow melting; (4) the depth of soil freezing; and (5) weather conditions of snowmelts.

7.4.1 Air Temperature in Pre-winter, Winter and Early Spring

One of the main factors that determine the depth and duration of soil freezing is the air temperature before the winter, during the winter and in early spring. In Western Siberia, the pre-winter period is the period from the moment the average daily air temperature passes 0 °C until the establishment of a stable snow cover. Winter (cold period) is the period from November to March, when the average daily air temperature is below 0 °C, and a permanent snow cover forms on the soil surface. Early spring is the period from the last 10 days of March to the second 10 days of April, when the daytime air temperature rises above 0 °C, and the night-time temperature remains below zero. By the end of early spring, the average daily air temperatures rise above freezing point.

In the study area, the air temperature in the first half of October is predominantly above freezing. However, in other years, average daily air temperatures sometimes remain stably below 0 °C before the formation of permanent snow cover. In this case, the upper 30 cm layer of arable soil quickly freezes, and the deep snow formed by mid-December is no longer able to prevent the subzero temperatures from penetrating deep into the soil. During such cold periods,

arable soils can freeze deeper than 160 cm. The air temperature remains significantly below zero without thaws throughout the entire cold period (November–March).

The coldest month is January, but in spring there are frequent frosts, since the spring rise in air temperature is often interrupted by a sudden (but short) sharp cold snap. Thus, the air temperature is observed to be relatively low (but above 0 °C) in April in very snowy winters in Predsairye and the Kuznetsk Depression (+0.8 and +0.7 °C, respectively).

As shown in Table 7.1, both in the cold period and in early spring, the lowest air temperature was recorded in the Kuznetsk Depression. This can be explained by the fact that this geomorphological region is located in the east of Western Siberia. Also, the end of the cold period (March) in this area is always characterised by an air temperature well below zero, from –7.1 to –11.7 °C, despite the snowy winter. In addition, the cold period in the Kuznetsk Depression is about 10–15 days longer than in Predsairye and Priobye.

The air temperature in individual months with different periods of snowiness varies greatly (Fig. 7.2). The measured data showed that the Kuznetsk Depression was the coldest site; there, the sum of subzero air temperatures ranged from –2115 to –2660 °C in each hydrological year. Winter in Predsairye was warmer than in the Kuznetsk Depression. These data may indicate deep and severe freezing of the soil in winters with very shallow snow and very snowy winters. This is one of the reasons for the formation of meltwater surface runoff in spring.

Thus, the less snow falls in November and, in general during the cold period of the hydrological year, and the lower the subzero air temperatures on these dates, the deeper the arable soil freezes. Conversely, a deeper snow cover and relatively low frequency of subzero air temperatures in the pre-winter period lead to a warmer soil profile. The depth of freezing of forest steppe soils ranges from 220 cm in very low-snow winters to 90 cm in very snowy winters, i.e. depending on the snowiness of the hydrological

Table 7.1 Average long-term air temperature in different hydrological years in the pre-winter, winter and early spring periods

Weather station (WIGOS Station Identifier ^a) Data for years	Characteristics of hydrological years	n	Average monthly air temperature (°C)											
			Months											
			X	XI	XII	I	II	III	IV					
<i>Predslaitrye</i>														
TOGUCHIN (0-20.000-0-29,636) 1960–2018	Very low-snow	4	3.7 ± 0.9	-8.0 ± 1.2	-14.6 ± 1.4	-19.2 ± 0.8	-16.2 ± 1.1	-7.1 ± 2.1						3.6 ± 0.7
	Low-snow	10	1.1 ± 0.8	-6.7 ± 1.0	-13.7 ± 1.1	-14.1 ± 1.3	-16.0 ± 1.3	-9.0 ± 0.9						1.4 ± 0.7
	Normal-snow	19	1.3 ± 0.6	-8.7 ± 0.8	-14.3 ± 0.9	-17.5 ± 0.8	-14.9 ± 0.9	-8.3 ± 0.7						1.3 ± 0.6
	High-snow	17	2.5 ± 0.3	-7.0 ± 0.9	-13.8 ± 1.1	-17.1 ± 1.4	-15.4 ± 1.1	-6.9 ± 0.7						1.9 ± 0.9
	Very high-snow	8	0	-6.2 ± 1.4	-15.3 ± 2.9	-18.0 ± 2.8	-15.7 ± 2.3	-9.0 ± 1.2						0.8 ± 0.6
<i>Priobyie</i>														
ORDYNSKOE (0-20.000-0-29,726) 1956–1988; 2006–2017	Very low-snow	5	-	-4.4 ± 1.3	-14.8 ± 1.4	-14.2 ± 0.8	-17.3 ± 1.5	-8.9 ± 2.3						2.3 ± 0.3
	Low-snow	6	-	-6.6 ± 1.2	-16.4 ± 1.5	-15.0 ± 1.3	-16.5 ± 1.3	-8.9 ± 1.2						3.6 ± 1.0
	Normal-snow	15	-	-7.9 ± 1.1	-15.1 ± 1.3	-18.3 ± 1.4	-19.2 ± 0.8	-8.2 ± 0.8						2.6 ± 0.7
	High-snow	12	-	-7.0 ± 1.3	-11.8 ± 1.2	-18.6 ± 1.4	-14.0 ± 1.0	-8.2 ± 0.8						5.2 ± 0.8
	Very high-snow	6	-	-5.0 ± 1.1	-14.0 ± 2.6	-18.3 ± 2.2	-16.0 ± 1.7	-9.3 ± 1.3						2.2 ± 1.5
<i>Kuznetsk depression</i>														
KEMEROVO (0-20.000-0-29,642) 1951–1990	Very low-snow	6	-	-10.3 ± 2.7	-14.2 ± 0.7	-16.1 ± 1.7	-16.1 ± 2.5	-6.0 ± 1.2						-0.1 ± 1.1
	Low-snow	12	-	-9.5 ± 1.2	-14.9 ± 1.2	-16.4 ± 0.9	-16.0 ± 0.9	-10.4 ± 0.5						0.5 ± 0.8
	Normal-snow	8	-	-12.1 ± 1.9	-19.3 ± 2.1	-18.6 ± 0.7	-18.9 ± 0.9	-10.1 ± 1.1						1.7 ± 0.7
	High-snow	8	-	-7.1 ± 1.6	-16.1 ± 1.5	-19.9 ± 1.5	-16.5 ± 1.1	-8.7 ± 0.7						1.3 ± 1.1
	Very high-snow	4	-	-12.3 ± 1.3	-14.1 ± 3.0	-22.2 ± 1.0	-14.4 ± 2.3	-7.5 ± 1.5						-0.8 ± 1.6

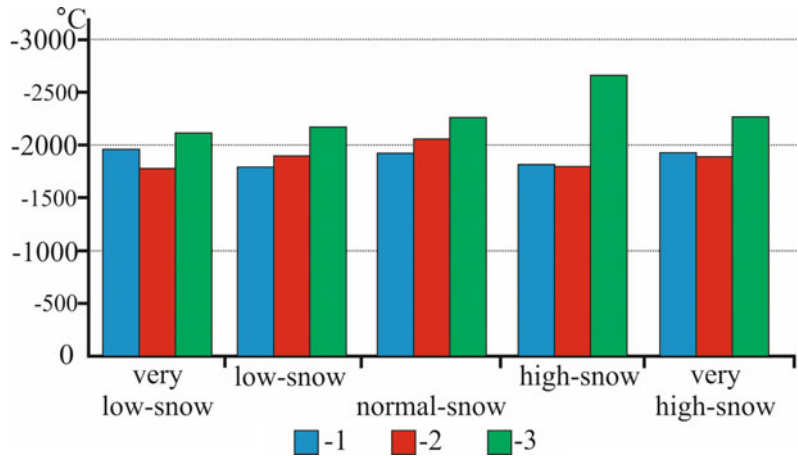
Here and in the other tables: *n* is a number of measurements (years), *Range* is the minimum to maximum values, referring to the whole data pool,

M is an arithmetic mean, *m* is a standard deviation, σ is a mean-square deviation and *V* is a coefficient of variation.

Data for 1956–1960 were from the Reference Book on the Climate of the USSR (1977), those for 1961–1990 from Meteorological Monthly (1966–1990), 1991–2018 data were obtained by the authors

^aWIGOS Station Identifier is the weather station's number in the World Meteorological Organization's Integrated Global Observing System (OSCAR/Surface 2019)

Fig. 7.2 Distribution of subzero air temperatures during the cold period (November–March) in different hydrological years ($^{\circ}\text{C}$), 1—Predsalaïrye; 2—Priobye; 3—Kuznetsk Depression



year, the freezing depth of Chernozem soils can more than double.

The average annual data on air temperature in the Kuznetsk Depression, Predsalaïrye and Priobye were calculated using data from Internet sources (Weather archive. <https://rp5.ru>, <http://aisori.meteo.ru/ClimateR>) and specialised reference books (USSR Climate Handbook 1977). Since 2005, air temperatures have been recorded at key points in Predsalaïrye using autonomous temperature recorders (Thermochron iButton Device 2019). A wooden pole was installed on the thermometric plot, on which a temperature recorder was installed at a height of 2 m from the soil surface. The air temperature recorder was protected from direct sunlight. The temperature recorders were programmed to measure the temperature at regular intervals. In total, over the cold period of a hydrological year and a period of snowmelt (November–April), more than 1000 data points on temperature were obtained.

7.4.2 Precipitation During the Winter

Solid precipitation in Predsalaïrye, Priobye and the Kuznetsk Depression falls unevenly during the cold period (Table 7.2). In these regions, regardless of the winter snowfall, the greatest amount of precipitation falls in November, and the least in February. Based on the changes in the amount of solid precipitation during the cold

period (50–220 mm), we identified six types of snowiness in the cold period of the hydrological year. If less than 65 mm of solid precipitation falls during the cold period, the year is classified as a very low-snow year. If the amount of precipitation during the cold period ranges from 65 to 95 mm, the year is classified as a low-snow year. A year with 95–125 mm of solid precipitation during the cold period is referred to as a normal-snow year. A year with 125–155 mm is considered to be a high-snow year. In the study area, during the last 15 years, cold periods prevailed with solid precipitation from 155 to 185 mm, i.e. very high-snow years. During our research, we observed winter periods with snow accumulation of more than 185 mm. We have characterised such cold periods as extremely high-snow years.

According to our research, as well as the Reference Book on the Climate of the USSR (1977), November in very low-snow and low-snow years in any region of Western Siberia was characterised by a fairly low amount of solid precipitation below 16–25 mm. In normal and high-snow years, the snow water equivalent (SWE) increased to 28–30 mm, and in years with very high snow, it rose to 42–60 mm. Therefore, at the beginning of the cold period, in very low-snow and low-snow years, the amount of solid precipitation was half that in very high-snow years.

However, given that in November in very low-snow years, the sum of subzero air

Table 7.2 Precipitation in the pre-winter, winter and early spring periods in different hydrological years

Characteristics of hydrological year		Average monthly precipitation, mm											
n	X	XI	XII	I	II	III	IV	III	II	I	XI	XII	X
<i>Predsalairye</i>													
Toguchin weather station (1938–2017)													
Very low-snow	4	50.9 ± 7.5	19.3 ± 3.1	9.4 ± 1.8	11.0 ± 2.9	6.8 ± 2.2	15.4 ± 4.3	20.6 ± 6.3	6.8 ± 2.2	11.0 ± 2.9	19.3 ± 3.1	9.4 ± 1.8	50.9 ± 7.5
Low-snow	23	39.3 ± 3.4	22.8 ± 1.5	22.0 ± 2.1	17.3 ± 1.5	8.9 ± 1.0	10.0 ± 1.0	26.6 ± 3.0	8.9 ± 1.0	17.3 ± 1.5	22.8 ± 1.5	22.0 ± 2.1	39.3 ± 3.4
Normal-snow	24	36.7 ± 3.2	34.1 ± 2.3	28.7 ± 3.1	16.9 ± 1.8	15.1 ± 1.5	14.7 ± 1.5	23.7 ± 2.6	15.1 ± 1.5	16.9 ± 1.8	34.1 ± 2.3	28.7 ± 3.1	36.7 ± 3.2
High-snow	17	46.1 ± 2.7	47.2 ± 3.5	36.5 ± 4.1	16.8 ± 2.1	16.1 ± 3.0	21.6 ± 2.6	26.5 ± 3.1	16.1 ± 3.0	16.8 ± 2.1	47.2 ± 3.5	36.5 ± 4.1	46.1 ± 2.7
Very high-snow	7	48.0 ± 8.7	46.0 ± 6.3	39.1 ± 3.9	33.7 ± 6.0	23.0 ± 2.4	22.9 ± 4.7	25.7 ± 4.1	23.0 ± 2.4	33.7 ± 6.0	46.0 ± 6.3	39.1 ± 3.9	48.0 ± 8.7
Extremely-high-snow	4	59.5 ± 12.2	48.3 ± 3.8	46.2 ± 5.5	31.8 ± 8.1	32.2 ± 2.1	32.8 ± 2.5	18.7 ± 0.5	32.2 ± 2.1	31.8 ± 8.1	48.3 ± 3.8	46.2 ± 5.5	59.5 ± 12.2
<i>Priobye</i>													
Ordynskoe weather station (1936–1988; 2006–2017)													
Very low-snow	8	24.1 ± 2.5	17.9 ± 2.1	13.7 ± 2.6	8.2 ± 0.3	7.1 ± 1.4	11.5 ± 3.3	20.0 ± 4.3	7.1 ± 1.4	8.2 ± 0.3	17.9 ± 2.1	13.7 ± 2.6	24.1 ± 2.5
Low-snow	10	34.6 ± 5.5	21.2 ± 1.1	23.1 ± 2.2	13.2 ± 2.0	5.3 ± 1.1	11.2 ± 1.2	18.2 ± 4.8	5.3 ± 1.1	13.2 ± 2.0	21.2 ± 1.1	23.1 ± 2.2	34.6 ± 5.5
Normal-snow	26	37.9 ± 3.0	26.6 ± 2.2	26.1 ± 2.3	20.8 ± 1.8	17.1 ± 1.3	14.9 ± 1.8	25.5 ± 2.7	17.1 ± 1.3	20.8 ± 1.8	26.6 ± 2.2	26.1 ± 2.3	37.9 ± 3.0
High-snow	11	41.7 ± 7.3	47.9 ± 6.0	27.8 ± 4.0	27.8 ± 4.0	20.3 ± 3.4	18.8 ± 2.8	23.7 ± 3.8	20.3 ± 3.4	27.8 ± 4.0	47.9 ± 6.0	27.8 ± 4.0	41.7 ± 7.3
Very high-snow	4	40.3 ± 3.7	50.0 ± 7.2	33.3 ± 9.2	37.5 ± 5.4	25.0 ± 5.4	22.7 ± 4.2	23.8 ± 6.4	25.0 ± 5.4	37.5 ± 5.4	50.0 ± 7.2	33.3 ± 9.2	40.3 ± 3.7
<i>Kuznetsk depression</i>													
Kemerovo weather station (1938–2017)													
Very low-snow	19	25.7 ± 3.3	27.6 ± 3.2	12.7 ± 1.5	9.5 ± 1.0	6.8 ± 0.9	7.0 ± 1.0	17.0 ± 1.8	6.8 ± 0.9	9.5 ± 1.0	27.6 ± 3.2	12.7 ± 1.5	25.7 ± 3.3
Low-snow	17	25.9 ± 3.9	22.2 ± 1.7	19.3 ± 1.7	17.1 ± 2.2	10.4 ± 1.4	8.8 ± 1.2	19.5 ± 4.6	10.4 ± 1.4	17.1 ± 2.2	22.2 ± 1.7	19.3 ± 1.7	25.9 ± 3.9
Normal-snow	8	37.2 ± 4.4	33.8 ± 3.2	24.1 ± 4.3	24.1 ± 4.5	15.0 ± 3.0	12.9 ± 3.0	16.1 ± 2.7	15.0 ± 3.0	24.1 ± 4.5	33.8 ± 3.2	24.1 ± 4.3	37.2 ± 4.4
High-snow	14	10.0 ± 11.5	42.4 ± 3.9	33.0 ± 2.6	25.4 ± 3.2	16.7 ± 2.6	18.2 ± 2.2	23.0 ± 5.9	16.7 ± 2.6	25.4 ± 3.2	42.4 ± 3.9	33.0 ± 2.6	10.0 ± 11.5
Very high-snow	13	–	48.6 ± 3.1	45.9 ± 3.6	27.0 ± 3.2	23.0 ± 2.8	22.6 ± 3.6	–	23.0 ± 2.8	27.0 ± 3.2	48.6 ± 3.1	45.9 ± 3.6	–

temperatures in Predsairyie and the Kuznetsk Depression ranged from -240 to -295 °C, in practice the shallow snow cover did not protect the soil from subzero temperatures. Within the forest steppe zone of the southeast of Western Siberia, the period during which permanent snow cover is established has a great influence on the formation of snowmelt water surface runoff and, as a consequence, on the water regime of eroded Chernozems. The formation of the first temporary snow cover occurs at the beginning of the pre-winter period. This period often coincides with a steady air temperature transition through 0 °C towards subzero temperatures. It should be mentioned that the prolonged pre-winter phase leads to the unhindered penetration of subzero temperatures into the soil profile. According to 'Meteorological Monthly' (1966–1990), snow most often falls on frozen soils in Priobye (71%), and in Predsairyie and the Kuznetsk Depression (62%).

The formation of permanent snow cover is determined by the conditions of the underlying surface. If snow falls on thawed soil with a surface temperature varying from 3 to 5 °C, the snow melts relatively quickly and replenishes moisture in the upper part of the humus horizon. In this case, the gap between the appearance of the first snow and the formation of a stable snow cover is quite significant. If the first snow falls on the surface of frozen soil, then the formation of stable snow cover is controlled only by the weather conditions at that time of the year. Therefore, in the pre-winter period, when determining the moisture in the profile of non-eroded and eroded soils, one should take into account factors such as the beginning of the formation of stable snow cover.

The distribution of snow also depends on the frequency of snowstorms, which contributes to a considerable transfer and a greater compaction of snow. Freshly fallen snow is usually blown off flat and convex relief elements and accumulates in depressions and by ridges. Snowfall reaches its maximum values in Western Siberia at the end of February and beginning of March, when wind activity increases markedly. Our studies of the distribution of snow cover were performed on

slopes with southeast exposures as these slopes are most susceptible to erosion processes. Since Predsairyie and the Kuznetsk Depression are characterised by a marked horizontal and vertical division of the territory, the distribution of snow here plays an important role in the development of soil erosion. On the erosive catena, the maximum thickness of the snow cover is inherent in the eluvial position of the landscape (watershed space). This part of the catena is always dominated by non-eroded soils, which in our study are represented by virgin and arable lands.

The presence or absence of vegetation also strongly affects the distribution of snow cover. Thus, the virgin land located on the slope with southern exposure is characterised by a greater snow cover than arable land occupying an eluvial landscape position. For example, in the Predsairyie region during the high-snow period in 2008/2009 and in the extremely high-snow years of 2014/2015, the depth of snow cover in the virgin lands was 20% higher than in the catchment area occupied by arable non-eroded soil. The southern arable slopes, regardless of the snowiness of the hydrological year, always accumulate less snow than flattened non-eroded areas and especially slopes with a cold orientation (Rikhter 1945).

Studying the snowmelt water runoff requires accurate information about the snow water equivalent (SWE), which is the total amount of water in solid and liquid forms before the spring flood. The distribution of snow cover and SWE were determined by continuous snow surveys before the snow melted (in the south of Western Siberia, the second and third 10-day periods in March) along parallel routes crossing the catchment every 100 m. The height of the snow cover was determined with a metal snow scale (160 cm long) every 5 m. The density of the snow cover (g cm^{-3}) and the water equivalent of snow (mm) were determined using a BC-1 snow gauge every 100 m in duplicate (Fig. 7.3). The snow gauge records the snow water equivalent at a specific observation point, as well as the height of the snow cover.

Using data on snow water and snow depth, the snow density was calculated. The SWE in the

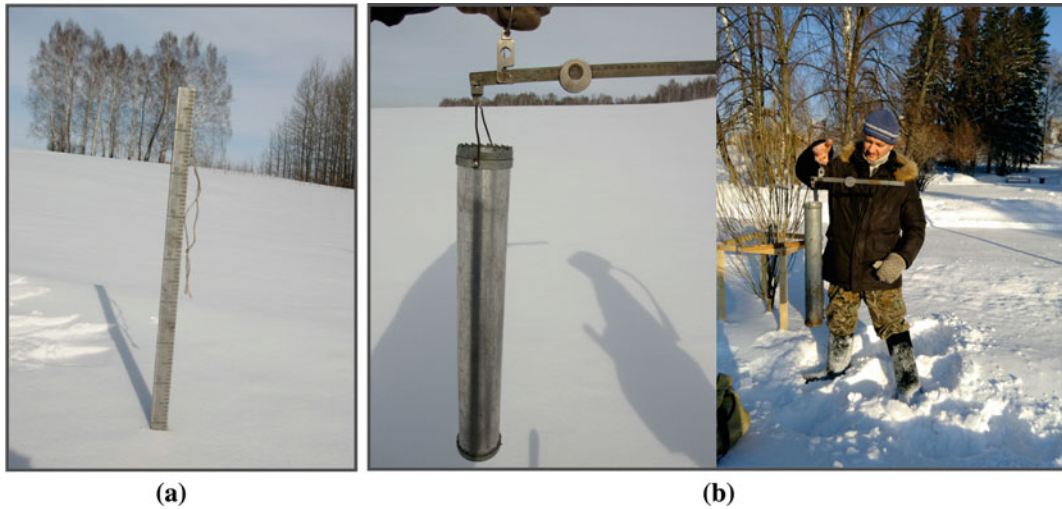


Fig. 7.3 Determining the snow depth with a metal snow scale (a) and calculating the snow water equivalent (SWE) by BC-1 (b) during the snow survey stage

catchment area was determined by multiplying the arithmetic mean of the snow density by the average snow depth on a particular element of the catchment area (Chumbaev and Tanasienko 2016).

7.4.3 Soil Moisture in the Pre-winter Period, During the Melting of Snow

To detect whether vaporous moisture was frozen in the lower part of the soil profile during the cold period of the hydrological year, and to register the redistribution of moisture along the soil profile, it was necessary to determine the amount of moisture in the profiles of non-eroded and eroded soils in the autumn–winter period. Volumetric soil

Fig. 7.4 Soil sampling for water content



samples were taken at three positions on each plot at different depths in steps from 10 cm to 1.5 m (Fig. 7.4). The moisture content of soil samples was analysed in the laboratory by drying at 105 °C to a constant weight (Vadyunina and Korzhagina 1961). Control measurements of soil moisture were carried out immediately before the snow began to melt. After the meltwater surface runoff appeared at the control points, the soil moisture was measured twice a day (morning and evening). When the snow had finished melting, the amount of moisture entering the soil profile with surface runoff was calculated.

The total soil moisture consumption after harvest had decreased. This was due, on the one hand, to the lack of moisture transpiration by cultivated plants, and on the other, to autumn air temperatures not exceeding 10–15 °C. It is desirable for precipitation of 70–90 mm to be retained in September–October in the Chernozem profile at eluvial and transluvial positions of the landscape. The low intensity of precipitation enables it to be fully absorbed by the soil (Tanasienko et al. 2019). The maximum moisture content at a depth of 1.5 m (on average 450 mm) in the pre-winter was found in non-eroded Chernozems (virgin and arable soils) in Predsairyie (Table 7.3). In the eroded soils, it was 104–129 mm less. The largest pre-winter moisture content was found in the slightly drifting soils located on the slope plume. The Priobye site is a transition from a forest steppe to steppe zone. Consequently, the atmospheric humidity during the cold period of the hydrological year should be much less than in the Predsairyie region. In Priobye, a large moisture deficit was observed both on the eroded and non-eroded arable land in the pre-winter period, ranging from 44 to 62 mm over the years of the study. The water content in the snow in Priobye has fluctuated sharply over the past 80 years (from 57 mm in low-snow years to 181 mm in very high-snow years). Comparison with the autumn moisture content leads us to conclude that under favourable conditions during the snow melting period, practically all meltwater can be absorbed by the profile of arable Chernozems. Non-eroded and eroded

Chernozems of the Kuznetsk Depression showed the lowest amount of autumn soil moisture. By the time a permanent snow cover is created in these soils, a significant moisture deficit is formed, which ranges from 50 to 100 mm.

The soils in Western Siberia remain frozen when the snow starts to melt. It is only when the snow cover is destroyed and thawing patches form that they begin to thaw during the day. A gradual increase in the daytime air temperature and the duration of sunshine leads to deep thawing and the saturation of soil with the meltwater. Complete thawing of the soil in the study region was observed 7–15 days after the disappearance of snow cover. In the soils of Western Siberia, despite the high-snow reserves, after snow melting, there can be both an increase in moisture and a deficit in the soils. We calculated the moisture reserves as the moisture content in the soil layers before and after snowmelt. As can be seen from Table 7.4, after the snow melts in any region of southeast Western Siberia, most of the moisture accumulates in the upper 50-cm soil layer. Total moisture in the upper 50 cm soil layer of virgin lands increases by an average of 20 mm in comparison with autumn. However, in the deep layers of virgin soils in Priobye and the Kuznetsk Depression, the spring total moisture is practically equal to the autumn. In non-eroded arable Chernozems, the accumulation of moisture was recorded in all layers. The non-eroded Chernozems in the Kuznetsk Depression absorbed twice as much meltwater as the Chernozems of Priobye. The relatively small absorption of meltwater by the Chernozems of Priobye is explained by the small amount of snow, the moderately loamy soil texture and the low humus content, which contributed to the soil's good water-holding capacity.

In our study, with an increase in winter snowfall in a 1.5 m layer of weakly eroded Chernozems in Predsairyie, Priobye, and the Kuznetsk Depression, spring moisture increased from 290 to 370 mm. The reason for this wide data distribution is the different accumulation of moisture in the soil in the pre-winter period. The high initial moisture content in the soil profile in

Table 7.3 Pre-winter moisture reserves^a and field water capacity (FWC) in the profile of Chernozems in normal-snow hydrological years in southeast Western Siberia

Degree of soil erosion, type of land use	Layer (cm)	Statistical parameters			FWC (mm)
		<i>n</i>	Range (mm)	$M \pm m$ (mm)	
<i>Predsalairye (1999–2012)</i>					
Non-eroded, virgin land	0–50	10	149–236	187 ± 9.2	157
	50–100	10	108–178	137 ± 6.4	135
	100–150	10	104–149	134 ± 7.2	133.8
Slightly eroded, ploughland	0–50	10	108–147	130 ± 4.9	154
	50–100	10	69–150	100 ± 8.4	139.8
	100–150	10	64–130	99 ± 6.6	130.8
Strongly eroded, fallow	0–50	10	123–175	144 ± 5.1	145
	50–100	10	73–130	93 ± 6.7	119.2
	100–150	10	76–178	114 ± 6.8	92.6
<i>Priobye (1984–1987)</i>					
Non-eroded, virgin land	0–50	6	116–169	135 ± 6.8	149
	50–100	6	69–115	96 ± 8.5	120
	100–150	6	58–97	86 ± 6.5	109
Non-eroded, ploughland	0–50	6	116–164	136 ± 6.8	146
	50–100	6	78–127	90 ± 7.5	111
	100–150	6	73–132	86 ± 9.5	107
Slightly eroded, ploughland	0–50	14	91–149	123 ± 5.5	146
	50–100	14	60–126	87 ± 5.3	104
	100–150	14	53–137	85 ± 6.5	100
Slightly drifted ^b , ploughland	0–50	3	179–229	203 ± 1.5	160
	50–100	3	143–157	148 ± 4.5	115
	100–150	3	132–164	151 ± 9.7	125
<i>Kuznetsk Depression (1968–1979)</i>					
Non-eroded, virgin land	0–50	8	130–206	165 ± 9.3	206
	50–100	8	87–162	114 ± 9.4	155
	100–150	8	101–174	122 ± 8.7	143
Non-eroded, Ploughland	0–50	9	111–201	149 ± 9.2	192
	50–100	9	90–160	122 ± 6.3	154
	100–150	9	109–155	129 ± 5.5	143
Slightly eroded, ploughland	0–50	11	123–204	153 ± 8.0	151
	50–100	11	80–136	114 ± 5.0	143
	100–150	11	86–137	110 ± 4.2	138
Moderately eroded, ploughland	0–50	11	107–195	136 ± 9.2	156
	50–100	11	86–142	113 ± 4.8	141
	100–150	11	112–137	124 ± 3.1	135

(continued)

Table 7.3 (continued)

Degree of soil erosion, type of land use	Layer (cm)	Statistical parameters			FWC (mm)
		<i>n</i>	Range (mm)	$M \pm m$ (mm)	
Strongly eroded, ploughland	0–50	9	104–176	131 ± 7.7	153
	50–100	9	75–133	106 ± 5.7	151
	100–150	9	88–124	106 ± 3.6	135
Slightly drifted, ploughland	0–50	9	124–201	165 ± 12.4	177
	50–100	9	110–178	136 ± 7.7	143
	100–150	9	145–181	164 ± 4.5	146

^aMoisture reserves are the moisture content in the soil layers before and after snowmelt; ^bSlightly drifted soils are located in the lower position (bottom part) of catenae, where the solid component of the surface meltwater runoff accumulates; FWC is the field water capacity

Table 7.4 Spring moisture reserves^a in the profile of Chernozems before snowmelt (before the line) and their increase after snow melting (beyond the line) (mm)

Layer (cm)	Degree of soil erosion					
	Non-eroded		Slightly eroded	Moderately eroded	Strongly eroded	Slightly drifted
	Virgin land	Plough land				
<i>Predsalairye</i>						
	<i>n-10</i>	<i>n-4</i>	<i>n-11</i>	–	<i>n-11</i>	–
0–50	214/27	189/0	166/36	–	176/32	–
50–100	158/21	127/-2	102/2	–	144/51	–
100–150	146/12	126/0	116/17	–	141/27	–
0–150	518/60	442/-2	384/55	–	461/110	–
<i>Priobye</i>						
	<i>n-6</i>	<i>n-6</i>	<i>n-14</i>	<i>n-3</i>	–	<i>n-3</i>
0–50	148/13	165/29	165/40	142/46	–	189/-14
50–100	95/-1	100/10	98/11	78/25	–	133/-15
100–150	82/-4	91/-3	88/3	69/4	–	138/-13
0–150	325/8	356/36	349/54	289/75	–	460/42
<i>Kuznetsk depression</i>						
	<i>n-8</i>	<i>n-9</i>	<i>n-11</i>	<i>n-11</i>	<i>n-9</i>	<i>n-9</i>
0–50	188/23	197/48	153/0	151/15	137/6	182/17
50–100	109/-5	138/16	107/-7	102/-11	106/0	142/6
100–150	117/-5	127/-2	109/-1	108/-16	101/-5	148/-16
0–150	414/13	462/62	369/-8	361/-8	344/1	472/7

^aMoisture reserves are the moisture content in the soil layers before and after snowmelt

autumn and its rather deep and severe freezing during the cold period of the hydrological year have a negative impact on the addition of

moisture during the snow-melting period. In the southeast of Western Siberia, by the end of snowmelt, the soil thaws to a maximum of

40 cm. Deeper than this, regardless of the winter snowfall, soils are frozen and are not able to absorb more water. Therefore, the increase in the moisture reserve when the snow finishes melting depends on the initial soil moisture in the autumn and the depth of the thawed layer in the spring.

The eroded soils of Predsairye, Priobye and the Kuznetsk Depression have different water storage capacities in the pre-winter period. The highest values of this indicator (about 100 mm) were observed on the strongly eroded Chernozems in the Kuznetsk Depression, the smallest (51 mm) on the slightly eroded Chernozems of Predsairye. When the snow melts, the soil on the slopes thaws to a depth of no more than 40 cm: thus, even with a significant spring moisture deficit, they are not able to absorb the amount of meltwater contained in the snow. Consequently, by using data on the pre-winter moisture in the soil profile, it was possible to predict both the accumulation of meltwater in the soil profile and the volume of surface runoff of this water.

7.4.4 Depth of Soil Freezing

The term ‘permafrost regime’ includes the rate of freezing and thawing of the profile, the depth of penetration and the duration of subzero temperatures at different depths, the depth of the seasonal layer of permafrost, etc. All these parameters depend mainly on three factors mentioned above: the air temperature in the cold period, the amount of solid precipitation (height of snow cover) and the degree of soil moisture before freezing. In Western Siberia, snow cover is the most powerful factor. According to Rikhter (1945), the snow layer breaks the heat exchange in the soil-air system into two independent fragments: the stronger the snow cover, the more the air and soil begin to differ in temperature. Therefore, the effect of snow cover on the temperature regime of Chernozems can vary from year to year. In very low- and low-snow

hydrological years, relatively shallow snow cover is formed in November, mainly until the end of the month. As a result, subzero temperatures actively penetrate deep into the soil. During this period, the temperature of 0 °C penetrates into the soils of Predsairye and the Kuznetsk Depression to a depth of 30–40 cm. Significant precipitation in the form of snow in snowy and very snowy years in November (>40 mm), even against the background of significant subzero air temperatures, has a positive effect on soil freezing in the southeast of Western Siberia (freezing up to 20 cm). In both Predsairye and the Kuznetsk Depression, in December, there is slightly less precipitation than in November (Table 7.2) and the atmosphere during this period cools much more strongly, which stimulates the active penetration of subzero temperatures deep into the soil. As a result, at the end of December, at a depth of 80 cm, the temperature is fixed at –2 °C, and in the 0–10 cm layer it drops to –6 °C. In January and February, in very low-snow hydrological years in Predsairye and the Kuznetsk Depression, an extremely small amount of snow falls against the background of a very low air temperature. During these 2 months, 20–30 mm of precipitation falls, and the average air temperature is –18 °C. Such extreme climatic conditions can greatly affect the depth of soil freezing. At the end of February, the zero isotherms are established at a depth of 180 cm, and at a depth of 70 cm, the temperature can drop to –2 °C. The air temperature in March rises in comparison with February by about –10 °C, so soil freezing slows down significantly. The rate of soil freezing in very low-snow hydrological years in November reaches 2 cm per day, and in March it slows down to 0.6 cm per day. In April, the air temperature rises above zero (>1 °C) and the snowless soil begins to thaw quickly.

The soil temperature regime in Priobye differs from the soils of the forest steppe. In the Chernozems of the forest steppe, the freezing depth is closely related to the air temperature and the height of the snow cover, while in the

Chernozems of Priobye, this is not the case. This can probably be explained by the extreme dryness of the soil in the pre-winter period (Table 7.3). During dry periods of vegetation, amount of moisture in the 0–50 cm layer in the pre-winter period are even lower than the capillary rupture humidity, which indicates that the soil profile dries out to a very high degree. It is known that the drier the soil profile, the deeper the subzero temperatures penetrate. Consequently, the significant aridity of Priobye soil means that, regardless of the snowiness of the winter period, the soil freezes deeply and strongly under the influence of subzero air temperatures.

The soils of the Kuznetsk Depression are characterised by the maximum freezing depth among the Chernozems of the southeast of Western Siberia (Table 7.5). In very low-snow winters, these soils freeze to almost 210 cm. The

depth of their freezing in very snowy years is 2.7 times less than in very low-snow years. In very low-snow winters, the soils of Predsairye are characterised by a smaller depth of freezing (by about 1/3) compared to the Kuznetsk Depression. However, in very high-snow winters, the soils of Predsairye freeze deeper than the Kuznetsk Depression.

The soil temperature in the key plots during the cold period was studied based on the time/temperature charts that were built in the autumn. We obtained reliable temperature data from small (coin-sized) electronic temperature recorders (Thermochron iButton Device 2019). To study the temperature regime of the arable soil layer (soil surface and at depths of 5, 10, 15 and 20 cm) the temperature recorders were placed in individual protective pots and then placed in the soil. To check the temperature of the subsurface layers, several holes with a

Table 7.5 The depth of freezing of Chernozems in different hydrological years

Characteristics of hydrological years	n	Statistical parameters			
		Range (cm)	$M \pm m$ (cm)	δ (cm)	V (%)
<i>Predsairye (1950–2017)</i>					
Very low-snow	3	150–180	163 ± 8.8	15.3	9
Low-snow	13	110–171	145 ± 5.6	20.2	14
Normal-snow	25	15–181	129 ± 8.1	40.5	31
High-snow	12	70–160	120 ± 10.5	36.4	30
Very high-snow	12	25–175	112 ± 13.6	47.2	42
Extremely high-snow	2	20–30	25	–	–
<i>Priobye (1941–1990)</i>					
Very low-snow	8	73–240	134 ± 23.4	66.2	49
Low-snow	13	53–246	143 ± 19.6	70.5	49
Normal-snow	22	52–260	184 ± 12.2	56.9	31
High-snow	5	76–227	157 ± 28.9	64.7	41
Very high-snow	1	–	213	–	–
<i>Kuznetsk depression (1950–1987)</i>					
Very low-snow	7	139–286	207 ± 19.8	54.3	26
Low-snow	11	40–248	180 ± 17.0	56.4	31
Normal-snow	6	125–215	154 ± 14.1	36.4	22
High-snow	7	30–132	93 ± 12.7	33.4	36
Very high-snow	3	10–125	75 ± 26.6	46.0	61

diameter of 5 cm were drilled at a depth of 40, 60, 80, 100, 120, 140 and 160 cm. The temperature recorders were fixed on the lower end of plastic pipes with a metal cover and then placed on the bottom of the hole in close contact with the soil. A wooden bar was inserted into the plastic pipe, isolating the thermostat from water and heat.

The temperature recorders were initially programmed to measure the temperature at regular intervals. The rate of frost penetration into the soils of Western Siberia, depending on weather conditions, can range from 1 to 6 cm per day. It is very important to determine when frost starts to penetrate the soil. But it is more important to record the moment the soil begins to thaw in the spring and to monitor the daily dynamics of soil temperatures at different depths during snow melting. The daily range of air temperatures during snow melting in this region is large, from +16 °C during the day, to – 15 °C at night (Tanasienko 2003). Therefore, the recorders were programmed with a measurement interval of 3 h. Free gravitational moisture in the soil freezes at 0 °C. Therefore, we considered the depth of soil freezing equal to the depth of the soil profile with a temperature of 0 °C and below.

7.4.5 Weather Conditions During the Snowmelt Period

In the south of Western Siberia, during the snow melting, high air temperatures and direct solar radiation have the greatest impact. According to Rutkovskaya (1962), spring weather conditions in the south of Western Siberia are divided into three types: (1) radiative, (2) advective and (3) mixed radiative–advective and advective–radiative. The duration of snowmelt, the intensity of runoff and the removal of soil material on the slopes depends on the type of spring weather.

Radiative conditions are characterised by sunny, calm weather with a rapid increase in daytime air temperatures above 0 °C and the persistence of subzero temperatures at night, plus, as a rule, an increase (during snow melting) in the intra-soil ice layer. This type of spring

weather occurs in 30% of cases. Snowmelt of this kind is characterised by high moduli and the largest volumes of surface drainage and soil leaching over a fairly short period (4–7 days).

The advective type of spring weather is characterised by a gradual increase in daytime temperatures above 0 °C and the persistence of subzero night-time temperatures. The predominance of low and high cloudiness in the daytime determines the long period of snow melting (18–27 days). With such a prolonged melting of snow, the intra-soil ice barrier is destroyed, and by the end of the melting, the temperature of the soil profile has risen above 0 °C (Tanasienko and Chumbaev 2010). Surface runoff under such conditions is minor. This type of spring weather occurs in 15–20% of cases.

The radiative–advective and advective–radiative subtypes of spring weather are characterised by a gradual increase in daytime air temperatures above 0 °C and night temperatures well below zero. A return of subzero daytime air temperatures is also possible. This can last 1–5 days, and can be repeated several times during the same spring period. These subtypes of spring snowmelt are usually cloudy or windy with clear spells. The frequency of this weather is 30–35%. This subtype of snowmelt lasts 10–14 days with a high runoff coefficient (0.55–0.65).

7.5 Field Measurements of the Main Components of the Soil Erosion Process

The number of days with an active meltwater surface runoff, the volume of meltwater runoff and the daytime air temperature during the period of snow melting, as well as the amount of the solid phase of the soil washed away by meltwater, are the most important indicators when studying the process of soil erosion and are determined directly in the field.

Meltwater surface runoff was studied both at temporary runoff sites (average area of 500 m²) and at elementary catchments (depressions) in a small area (10–15 ha) (Fig. 7.5). In the study of the snowmelt runoff and the washout of the solid



Fig. 7.5 Surface runoff on short-term runoff section (a) and on elementary catchments (b)

phase of the soil, runoff sections of different lengths were used (from 20–30 m to 300–400 m and more). Studies by Orlov (1977) showed that in the forest steppe zone of Western Siberia on convex–concave slopes, the optimal length of runoff sections is 100–150 m. The advantage of the runoff section is that the amount of surface meltwater can be determined with great confidence, but quite often the loss of the solid component of the flow is distorted.

The runoff depth is the amount of water flowing from an elementary catchment for any period, expressed in a layer (mm) which is evenly distributed over the areas (Taratunin 2008). An area of 1 ha with a runoff depth of 1 mm holds 10,000 L of water. To determine the depth of snowmelt runoff, the runoff intensity was measured, i.e. the amount of water (mm) generated by melting snow per unit of time. The flow rate was expressed in litres per second per ha ($l\ s^{-1}\ ha^{-1}$).

With the help of a measuring cylinder (1 L) and a stopwatch, the depth of the snowmelt runoff was determined at intervals of one hour. First, the intensity of the runoff was determined by recording the time (in seconds) required to fill the measuring cylinder with meltwater. The runoff intensity ($l\ s^{-1}$) was multiplied by the corresponding coefficients to calculate the runoff depth per hectare (Chumbaev and Tanasienko 2016).

On an elementary watershed of 10–15 ha, the volume of snowmelt runoff was determined in

the lower part of the narrow drainage. Knowing the depth, width and speed of the water flow per time unit in a narrow open drainage and elementary catchment, the intensity of the snowmelt runoff was calculated. The depth and width of the water flow in a narrow open drain was measured using a ruler or a metal snow scale. Traditionally, water flow can be determined by placing light pieces of material (such as foam) in a water stream and determining the time it takes to travel a certain distance through the stream of water. All measurements were repeated 3–5 times.

The day with the first signs of meltwater surface runoff (a drop in the drainage level or a water layer on the soil surface in the lower part of the runoff trench) is marked as the first day of active surface runoff. The last day of the snowmelt water surface runoff is considered the day when the meltwater on the slope studied is not observed either in the areas of temporary runoff or in the runoff depression.

The climate in the southeast of Western Siberia determined the temperature regime of the Chernozem soils which were studied, and especially the freezing and thawing processes, which largely determine the course of elementary soil formation, the nature of the moisture behaviour in the soil profile, and other processes. In particular, as suggested by Khmelev and Tanasienko (1983), intense freezing and late thawing of Chernozems negatively affects their water regime. Since the moisture capacity of these soils is very low due to the presence of permafrost in

Table 7.6 Snow water equivalent and surface runoff in different hydrological years

Characteristics of hydrological years	n	Snow water equivalent		Surface runoff		Runoff coefficient
		Range (mm)	M (mm)	Range (mm)	M (mm)	
<i>Predsalairye</i>						
Very low-snow	1	–	56	–	45	0.80
Low-snow	5	1–67	39	1–74	41	0.51
Normal-snow	13	96–124	111	2–87	55	0.50
High-snow	13	135–155	146	19–111	68	0.46
Very high-snow	7	160–185	172	1–130	71	0.41
Extremely high-snow	2	187–210	198	89–142	115	0.58
<i>Priobye</i>						
Very low-snow	4	18–71	50	2–45	27	0.54
Low-snow	3	78–87	84	35–47	41	0.49
Normal-snow	4	92–99	96	48–70	60	0.62
High-snow	3	109–119	113	58–78	69	0.61
Very high-snow	3	129–149	138	60–91	73	0.53
<i>Kuznetsk depression</i>						
Very low-snow	1	–	58	–	0	0
Low-snow	2	–	60	–	33	0.55
Normal-snow	1	–	90	–	58	0.64
High-snow	1	–	115	–	75	0.65
Very high-snow	2	105–283	194	74–191	132	0.68

the soil profile during snow melting, large losses of meltwater with surface runoff occur on highly dissected terrain (Table 7.6).

The reason for the high meltwater surface runoff in very low-snow winters in Predsalairye, and especially in Priobye, is the low permeability of frozen soils due to their very deep and strong freezing (160–207 cm). Previous studies have shown that for frozen or unfrozen soils, permeability decreased with increasing soil moisture, but the effect of moisture on the infiltration rate decreased over time (Bodman and Colman 1944; Kuznik 1962). As the freezing depth decreases, the meltwater surface runoff gradually decreases.

Removal of the solid phase of the soil depends, firstly, on the permeability of the soil during snow melting, and secondly, on the intensity of snow melting. In the Chernozems of southeast Western Siberia, when the snow starts

to melt, large reserves of cold accumulate (Tanasienko 2003); therefore, these soils are practically waterproof. Moreover, during the melting of snow at night, frosts often reach -10°C , therefore the soil which has thawed during the day freezes again at night, making it impossible for the soil to fully absorb the meltwater.

The intensity of the erosion processes during snow melting characterises the amount of the soil solid phase in the runoff from the upper soil layer of the slopes. According to the studies by Maltsev and Yermolaev (2020), in the basins of small rivers in the European territory of Russia, erosion from melting snow is only $260 \text{ kg/ha}^{-1} \text{ year}^{-1}$. Our long-term studies have shown that from 0 to 150 kg/ha^{-1} of soil material is removed from non-eroded arable soils (Tanasienko 2003). This insignificant removal of the solid phase of

Chernozems with a significant snowmelt water surface runoff can be explained by the location of these soils in combined watersheds, where the surface runoff begins and therefore still has a low kinetic energy.

Slightly eroded soils are located below the watershed line, where the slope gradient is 3°. With an increase in the gradient in low-snow winters, the surface runoff on slightly eroded Chernozems does not exceed 40 mm (Table 7.6) with the washout of the soil material 2 t/ha⁻¹. In Priobye and the Kuznetsk Depression, in very low-snow and low-snow hydrological years, the removal of the soil solid phase on slightly eroded Chernozem ranges between 0 and 4 t/ha⁻¹, which is taken as the permissible value of erosion (Zaslavsky 1979). An increase in meltwater by 15–20 mm in normal-snow years significantly affects the amount of soil material removed by meltwater flows (Table 7.7). After high-snow winters, a large snowmelt water surface runoff was observed, which, leads to a significant removal of the solid component (5–10 t/ha⁻¹). Its value for weakly eroded Chernozems in Predsairye, Priobye and the Kuznetsk Depression was diagnosed as average. In a very high-snow years, depending on the weather conditions during the snow melting, surface runoff can reach enormous values (up to 190 mm). Snow melting can occur in a relatively short time, which

predetermines a large daily flow rate, approaching a strong removal of the solid phase of weakly eroded Chernozems which are resistant to erosion (up to 20 t/ha⁻¹).

The question is: How can the annual loss of the soil solid phase be estimated depending on the snowiness of the hydrological year? If we take into account that, on average, 1 mm of the humus horizon of the soils studied has a mass of 9.0–10.4 t/ha⁻¹ (Khmelev and Tanasienko 2009), then soil loss in very low-snow, low-snow and normal-snow years does not reach even 0.5 mm. In high-snow and very high-snow years, the loss of the solid phase of the soil increases sharply and ranges from 4.5 to almost 20 t/ha⁻¹, i.e. fluctuates between 0.4 and 1.9 mm per year. Consequently, if in the very low-, low-, normal- and high-snow years (the share of which in the long-term climate cycle is more than 60%), the amount of washable arable soils is determined by their resistance to erosion, then in the very high-snow years the main factors of soil erosion are weather conditions during snowmelt and soil tillage. At this rate of solid-phase removal, in the absence of anti-erosion measures, these slopes can lose 20–22 cm in 100 years, which corresponds to half of the humus horizon.

The temperature of the meltwater directly affects the rate of soil thawing and thus these soils' ability to absorb meltwater. The higher the

Table 7.7 Loss of soil solid phase by meltwaters from slightly eroded Chernozems in different hydrological years

Characteristics of hydrological years	Predsairye			Priobye			Kuznetsk Depression		
	<i>n</i>	<i>Range</i> (t/ha)	<i>M</i> (t/ha)	<i>n</i>	<i>Range</i> (t/ha)	<i>M</i> (t/ha)	<i>n</i>	<i>Range</i> (t/ha)	<i>M</i> (t/ha)
Very low-snow	1	–	4.1	4	0–1.4	0.9	1	–	0
Low-snow	5	0.2–3.3	2.9	3	0.8–3.0	1.9	1	–	0.8
Normal-snow	13	1.0–28.3	7.6	4	1.4–6.1	3.9	1	–	1.4
High-snow	13	0.6–12.1	5.0	4	8.5–11.9	10.2	2	1.3–3.9	2.6
Very high-snow	7	0.3–28.8	8.6	4	1.4–14.2	9.9	2	9.0–9.7	9.3
Extremely high-snow	2	1.1–1.5	1.3	–	–	–	–	–	–

temperature of the meltwater, the greater the thickness of the thawed arable layer, which is in a so-called thixotropic (liquid) state due to oversaturation with meltwater. The temperature was recorded by an autonomous 'Termochron' thermometer while simultaneously measuring the hourly volume of meltwater runoff in the lower parts of the temporary runoff areas and runoff gutters.

7.6 Assessment of Soil Erosion Effects

Erosion is the process of destruction of rocks and soils by water flow, the movement of products of destruction and their re-deposition. To assess the consequences of soil erosion, it is necessary to determine the amount of soil material captured by meltwater from the fields. For this, the hourly turbidity of the water flow at the bottom of the drain gutter was determined, accompanied by checks at temporary runoff sites. The turbidity of the water flow characterises a decrease in the transparency of the water due to the presence of fine inorganic and organic suspensions. The turbidity of the meltwater was determined in the laboratory on an hourly basis using field samples taken from the experimental runoff plot using a 1 L measuring cylinder. The snowmelt water from a cylinder was transferred into a plastic jar and delivered to the laboratory. On the same day, the soil solid phase was separated from the liquid by filtration or centrifugation. For further analysis, the filtered water was placed in a refrigerator. The filtrate was weighed and the amount of solid phase in the soil was determined per litre of snowmelt water sample. The turbidity was evaluated in grammes per litre of water (g/l). Then, the amount of solid sediment washed off by meltwater per hour and per day was calculated. At the end of the snowmelt period, the data were summarised and the amount of solid phase displaced by meltwater over the entire period of snow melting was calculated.

In Western Siberia, erosion processes are intensifying due to the long-term use of

Chernozems on the slopes nowadays. The conditions of the erosion process revealed that neither snow water nor abundant precipitation indicates the severity of erosion. They only create the conditions for the formation of surface runoff of meltwater and rainwater. The intensity of the development of erosion processes can be judged by the amount of the soil solid phase in the snowmelt water runoff and the humus content in them. To assess the intensity of soil washout, Zaslavsky (1979) proposed the following scale, based on the annual removal of the solid phase of the soil: low washout—annual soil loss of 2–5 t/ha⁻¹; medium—5–10 t/ha⁻¹; strong—10–20 t/ha⁻¹ and very strong—average annual soil losses exceeding 20 t/ha⁻¹.

A common criterion for assessing the susceptibility of soil to erosion is the scale of the decrease in the thickness of the upper (humus) horizons of the Chernozem profile. In assessing the degree of soil erosion in Western Siberia, virgin soil was taken as the reference. In these soils, the upper, most humified part of the profile consists of a complete set of genetic horizons: Ah – AhB – B. If the thickness of Ahp + Ah horizons of arable soils on the slopes is less than the same reference horizon, then such soils are considered to be slightly eroded. When the AhB horizon partially enters the arable layer, these soils are moderately eroded. When the arable layer consists of a mixture of Ah, AhB and B horizons, this means that the initial horizon Ah has been eroded and such soils are strongly eroded.

Solid runoff products contain various amounts of the biogenic elements involved in the formation of soil structure and provide nutrients for cultivated crops, with organic carbon nitrogen, phosphorus, sodium, calcium and magnesium being the major nutrients (Coble et al. 2019; Hoffman et al. 2019; Wilson et al. 2019; Rasmussen et al. (2020). According to Nearing et al. (2017), soil erosion is the source of 80% of the total phosphorus and 73% of the total nitrogen in waterways in the United States. The same nutrients are present in the liquid phase of surface runoff. Their especially high content was

observed in the initial and final phases of runoff, when the time of contact of meltwater with the surface of slightly thawed soils is greatest.

In the light of climate warming, particularly in the cold regions, the export of dissolved organic carbon with the snowmelt has become a serious hazard (Meingast et al. 2020) to soil fertility. Almost every year, meltwater washes away a significant amount of water-soluble humus, mainly represented by mobile humic acids and calcium, which play an important role in soil formation, acting as organic and mineral adhesives (Kononova 1951). The amount lost increases many times with an increase in the equivalent of snow water and the amount of surface meltwater runoff. The washing out of soluble calcium and humus weakens the bonds between soil aggregates and creates the conditions for the subsequent separation of these aggregates by the surface waters when the kinetic energy of the flow is high.

The losses of water-soluble humus in various regions of Western Siberia in different hydrological years are given in Fig. 7.6. Naturally, the lowest losses of water-soluble carbon were observed in very low-snow winters. In the low-snow hydrological years with small losses of snowmelt waters, carbon removal from the soils of Priobye remains almost at the same level: twice the level as from the Predsairye soils. The latter have low losses of water-soluble carbon in the low-snow hydrological years, and a neutral reaction of the arable soil layer. In normal-snow hydrological years, carbon removal by snowmelt

waters in all regions of Western Siberia was almost the same.

In high-snow hydrological years, the removal of carbon by meltwater was almost the same in all regions of Western Siberia, while in very high-snow years, the difference increases significantly. Thus, for example, the removal of water-soluble carbon from the Chernozems of Predsairye and Priobye in a very high-snow year was 7 and 4 times greater, respectively, than in a low-snow year, and almost twice as high as in a high-snow year. Losses of organic carbon with meltwater from the Chernozems of the Kuznetsk Depression in very high-snow years were almost 1.5 times greater than in similar years in Priobye and Predsairye. This large removal of carbon can only be explained by the fact that the Chernozems of the Kuznetsk Depression contain a very large amount of carbon in the arable layer (5.5%), while in similar soils of Predsairye and Priobye, the content of this element is much lower (4.5 and 3.5%, respectively). In addition to the losses of water-soluble carbon, mineral nitrogen and phosphorus are lost concurrently. The nitrogen content in the meltwater was insignificant, however, given that, on average, 850 m³ of meltwater flows from the soil surface of Predsairye and the Kuznetsk Depression annually: the loss of this element reaches almost 2 kg/ha⁻¹ (Fig. 7.7).

The nitrogen content in the solid component of surface runoff was from 0.4 to 0.7% on average. A significant removal of nitrogen from the solid phase of the soil led to a sharp decrease

Fig. 7.6 Carbon loss from slightly eroded Chernozems with liquid and solid component of meltwater surface runoff in Predsairye (1), Priobye (2) and the Kuznetsk Depression (3) sites

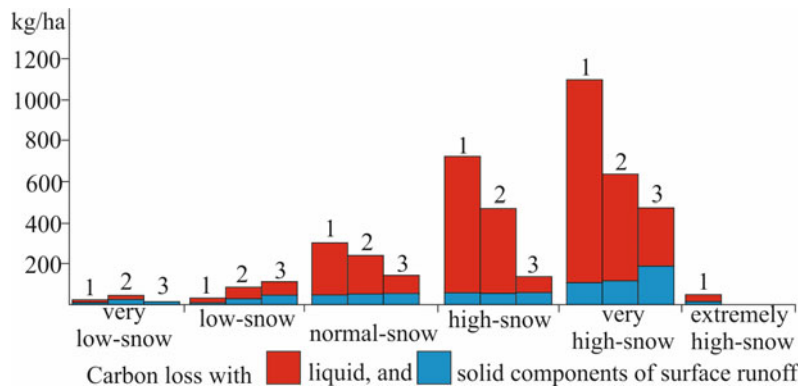
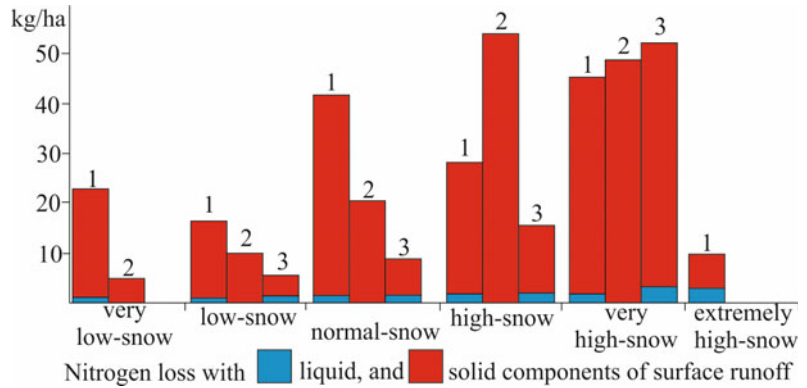


Fig. 7.7 Nitrogen loss from slightly eroded Chernozems with liquid and solid components of meltwater surface runoff in Predsairrye (1), Priobye (2), Kuznetsk Depression (3)



in the amount in the profile of eroded soils. The nitrogen concentration in solid runoff was approximately 0.1–0.2% higher than in the arable layer of slightly eroded Chernozems (Tanasienko et al. 2016). Calculations show that in these soils the annual removal of nitrogen from solid runoff, depending on the snowiness of the hydrological year, was between 15–50 kg/ha⁻¹. Absolute nitrogen losses due to erosion during the period of intense anthropogenic impact on the soil of slopes reached 6.6 t/ha⁻¹ for slightly eroded Chernozems, 12.2 t/ha⁻¹ for moderately eroded Chernozems and 15.5 t/ha⁻¹ for strongly eroded Chernozems.

A decrease in the depth of the humus horizon under the influence of erosion processes led to a regular decrease in the content of total phosphorus. Since the maximum amount of biogenic elements is concentrated in the upper part of the humus layer, during the meltwater surface runoff, their losses occur together with the solid phase of the soil. As a rule, in very low-snow and low-snow hydrological years, the removal of gross phosphorus is low (no more than 5 kg/ha⁻¹ annually). Losses of phosphorus with a solid runoff of meltwater in normal-snow winters in the Kuznetsk site were almost three times greater than in low-snow winters. The annual loss of phosphorus in very high-snow years exceeded 30 kg/ha⁻¹, twice as much as after high-snow winters.

Our results showed that in the Chernozems at higher elevations, a general increase in moisture content can provide a periodic type of leaching

regime with more frequent soil moistening in early spring. Due to the significant surface runoff of snowmelt water, the accumulation of moisture in the slope is sharply reduced, which affects their water regime. In weakly eroded soils, the water regime formed is the non-leaching type, and in highly eroded soils, the so-called ‘drainage’ type. Due to the influx of moisture with surface runoff to the reclaimed soils, they periodically form a leaching water regime. The soils of the sloping territories of Predsairrye, Priobye and the Kuznetsk Depression, regardless of the snowiness of a hydrological year, freeze for more than five months, which significantly limits the absorption of snowmelt water and stimulates significant surface runoff.

Almost all Chernozem soils of Western Siberia have been cultivated for a long time; therefore, they should be considered anthropogenically transformed soils. From 30 to 130 mm of meltwater, large areas of slopes are lost annually as a result of surface runoff, causing an intensive development of erosion processes, accompanied by the loss of 1–5 tonnes per ha of soil material, and lower amounts of humus, nitrogen and phosphorus.

7.7 Conclusions

- Due to the strong impact of erosion on the slope soils, the initially highly humified full-profile Chernozems were transformed into

moderately and slightly humified soils in the southeast of Western Siberia. On the slopes of any exposure, a decrease in the thickness of the humus horizon, which exceeds the level of natural variability, indicated the formation of eroded soils.

- Ploughing of virgin lands, unregulated surface runoff, flushing, transport and re-deposition of the soil solid phase by snowmelt flows (mostly) resulted in the formation of elementary soil areas that differ from those on the elevated lands. An increase in thickness in the lower positions of the landscape (slope paths) indicates the appearance of eroded (stratified) soils.
- The concentration of water-soluble humus and nutrients in meltwater depended both on the humus content in the depth of arable layer and on the amount of pre-winter moisture in the soil profile.
- The formation of a permanent snow cover late in the year promoted the free penetration of sub-zero temperatures into the soil profile, affecting the soil's water and temperature regime.
- Analysis of long-term data on the amount of solid precipitation falling in different hydrological years in Predsalaurye, Priobye and the Kuznetsk Depression showed that the significant amount of snow accumulating annually is sufficient to form surface runoff and erode the solid phase of arable slopes.
- The methods proposed for studying soil erosion during snowmelt are simple to use and do not require the use of expensive equipment in the field.

Acknowledgements This work is based on the results of the research work carried out according to the state assignment of ISSA SB RAS. This study was financed by the Ministry of Science and Higher Education of the Russian Federation. We would like to thank our colleagues from the ISSA SB RAS laboratory of soil physical processes for their cooperation and support during the investigations.

References

- Alewell C, Egli M, Meusburger K (2015) An attempt to estimate tolerable soil erosion rates by matching soil formation with denudation in Alpine grasslands. *J Soils Sediments* 15(6):1383–1399. <https://doi.org/10.1007/s11368-014-0920-6>
- Barneveld RJ, van der Zee SEATM, Stolte J (2019) Quantifying the dynamics of microtopography during a snowmelt event. *Earth Surf Process Land* 44(13). <https://doi.org/10.1002/esp.4678>
- Bodman GB, Colman EA (1944) Moisture and energy conditions during downward entry of water into soils. *Soil Sci Soc Am Proc* 8:116–122. <https://doi.org/10.2136/sssaj1944.036159950008000C0021x>
- Chumbaev AS, Tanasienko AA (2016). Measuring snowmelt in Siberia: causes, process and consequences. Novel methods for monitoring and managing land and water resources in Siberia. Springer, pp 213–231. https://doi.org/10.1007/978-3-319-24409-9_7
- Coble AA, Marcarelli AM, Kane ES (2019) Year-round measurements reveal seasonal drivers of nutrient uptake in a snowmelt-driven headwater stream *Freshwater Sci.* 38:156–69. <https://doi.org/10.1086/701733>
- Dobrovolskii GV (1997) Quiet crisis of the planet (Тихий кризис планеты). *Herald of the Russian Academy of Sciences.* 67(4):313–320 (Добровольский Г.В. Тихий кризис планеты. *Вестник Российской академии наук*, 67(4): 313–320)
- Edwards L, Richter G, Bernsdorf B, Schmidt RG, Burney J (1998) Measurement of rill erosion by snowmelt on potato fields under rotation in Prince Edward Island (Canada). *Can J Soil Sci* 78(3):449–458. <https://doi.org/10.4141/S97-053>
- Golosov VN (1988) Erosion-accumulation processes and sediment balance in the Protva's river basin. *Moscow Univ Bull* 6:19–25 (Эрозионно-аккумулятивные процессы и баланс наносов в бассейне р. Протвы)
- Hoffman AR, Polebitski AS, Penn MR, Busch DL (2019) Long-term variation in agricultural edge of field phosphorus transport during snowmelt, rain, and mixed runoff events. *J Environ Qual.* 48(4). Special Section: Agric Water Qual Cold Environ. <https://doi.org/10.2134/jeq2018.11.0420>
- Khmelev VA, Tanasienko AA (1983) Chernozems of the Kuznetsk depression. Nauka Publisher, 256 pp. (Черноземы Кузнецкой котловин)
- Khmelev VA, Tanasienko AA (2009) Soil resources of the Novosibirsk region and ways of their rational use. SB RAS Publisher, Novosibirsk. 349 p. ISBN: 978-5-7692-1049-5 (Почвенные ресурсы Новосибирской области и пути их рационального использования) <https://elibrary.ru/download/16447274.pdf>
- Kononova MM (1951) Problems of soil humus and modern tasks of its study. AS USSR Publishing. 390 pp. (Проблемы почвенного гумуса и современные задачи его изучения)
- Kuznik IA (1962) Agroforest reclamation activities, spring runoff and soil erosion. *Gidrometeoizdat*, 220

- pp. (Агролесомелиоративные мероприятия, весенний сток и эрозия почв)
- Lal R (1998) Soil erosion impact on agronomic productivity and environment quality. *Crit Rev Plant Sci* 17 (4):319–464. <https://doi.org/10.1080/07352689891304249>
- Li Z, Fang H (2016) Impacts of climate change on water erosion: a review. *Earth Sci Rev* 163:94–117. <https://doi.org/10.1016/j.earscirev.2016.10.004>
- Luffman I, Nandi A (2019) Freeze-thaw induced gully erosion: a long-term high-resolution analysis. *Agronomy* 9:549. <https://doi.org/10.3390/agronomy9090549>
- Макавеев НИ (1955) Riverbed and erosion in its basin (Русло реки и эрозия в ее бассейне). *Pub Acad Sci of USSR*. 346 pp. (Макавеев Н.И. Русло реки и эрозия в ее бассейне. Труды Акад. наук СССР. 346 с.)
- Maltsev K, Yermolaev O (2020) Assessment of soil loss by water erosion in small river basins in Russia. *CATENA* 195. <https://doi.org/10.1016/j.catena.2020.104726>
- Maltsev KA, Yermolaev OP (2019) Potential soil loss from erosion on arable lands in the European part of Russia. *Eurasian Soil Sc* 52:1588–1597. <https://doi.org/10.1134/S106422931912010X>
- Meingast KM, Kane ES, Coble AA, Marcarelli AM, Toczydlowski D (2020) Climate, snowmelt dynamics and atmospheric deposition interact to control dissolved organic carbon export from a northern forest stream over 26 years. *Environ Res Lett* 15(10). <https://doi.org/10.1088/1748-9326/ab9c4e>
- Meteorological Monthly (1966–1990) Main administration of the hydrometeorological service under the council of ministers of the USSR. Western Siberian Office, Novosibirsk, vol 20. (Метеорологический ежемесячник. Гл. упр. гидрометеоролог. службы при Совете министров СССР. Зап.-Сиб. упр. гидрометеоролог. службы)
- Nearing M, Xie Y, Liu B, Ye Y (2017) Natural and anthropogenic rates of soil erosion. *Int Soil Water Conserv Res* 5:77–84. <https://doi.org/10.1016/j.iswcr.2017.04.001>
- Nikitenko FA (1963) Loess in Novosibirsk preobye and its geoengeineering characterisation. *Proc Novosibirsk Inst of Railway Transp Engng*. Novosibirsk 34:7–287 (Лёссовые породы Новосибирского Приобья и их инженерно-геологическая характеристика)
- Orlov AD (1977) Surface runoff of melt water and soil washout in the forest-steppe zone of Western Siberia. Eroded soils and ways to increase their productivity. Nauka Publisher. pp 23–49. (Поверхностный сток талых вод и смыв почв в лесостепной зоне Западной Сибири)
- OSCAR/Surface. <https://oscar.wmo.int/surface/index.html/>. Accessed 7 March 2021
- Ouyang W, Gao X, Wei P, Gao B, Lin C, Hao F (2017) A review of diffuse pollution modeling and associated implications for watershed management in China. *J Soils Sediments* 1:1–10. <https://doi.org/10.1007/s11368-017-1688-2>
- Panagos P, Borrelli P, Poesen J, Ballabio C, Lugato E, Meusburger K, Montanarella L, Alewell C (2015) The new assessment of soil loss by water erosion in Europe. *Environ Sci Policy* 54:438–447. <https://doi.org/10.1016/j.envsci.2015.08.012>
- Pimentel D (2006) Soil erosion: A food and environmental threat. *Environ Dev Sustain* 8:119–137. <https://doi.org/10.1007/s10668-005-1262-8>
- Rasmussen LH, Ambus P, Zhang W, Jansson PE, Michelsen A, Elberling B (2020) Slope hydrology and permafrost: the effect of snowmelt N transport on downslope ecosystem, EGU general assembly 2020, Online, 4–8 May 2020, EGU2020–2927. <https://doi.org/10.5194/egusphere-egu2020-2927>
- Rikhter GD (1945) Snow cover, its formation and properties (Снежный покров, его формирование и свойства) *Pub. Acad. of Sci. of USSR*, 120 pp. (in Russian). <http://www.webgeo.ru/books/Rikhter1945SnezhnyyPokrovEgoFormirovaniyeSvoystva.pdf>. Accessed 7 March 2021
- Rutkovskaya NV (1962) Snowmelting in the southeastern part of West Siberian plain. In: Rikhter (ed) *Snow cover: distribution and role in national economy*. USSR Acad Sci, Moscow, pp 104–113, (Таяние и сход снежного покрова на юго-востоке Западно-Сибирской низменности)
- Scherr SJ (1999) Soil degradation: A threat to developing-country food security by 2020? *Intl Food Policy Res Inst* 63 pp. ISBN 0-89629-631-8 <http://cdm15738.contentdm.oclc.org/utills/getfile/collection/p15738coll2/id/125787/filename/125818.pdf> accessed on March 7, 2021
- Shi X, Zhang F, Wang L, Jagirani MD, Zeng C, Xiao X, Wang G (2020) Experimental study on the effects of multiple factors on spring meltwater erosion on an alpine meadow slope. *Int'l Soil Water Conser Res* 8 (2):116–123. <https://doi.org/10.1016/j.iswcr.2020.02.001>
- Specialized data for climate research. <http://aisori.meteo.ru/ClimateR>. Accessed 7 March 2021
- Tanasienko AA (2003) Specific features of soil erosion in Siberia. SB RAS Publishing, Novosibirsk, 173 pp. (Специфика эрозии почв в Сибири)
- Tanasienko AA, Yakutina OP, Chumbaev AS (2009) Snowmelt runoff parameters and geochemical migration of the elements in the dissected forest-steppe of West Siberia. *CATENA* 78(2):122–128. <https://doi.org/10.1016/j.catena.2009.03.008>
- Tanasienko AA, Chumbaev AS (2010) Conditions of the formation of ice barriers in eroded Chernozems of

- Western Siberia. *Eurasian Soil Sci* 43(4):417–426. <https://doi.org/10.1134/S1064229310040071>
- Tanasienko AA, Yakutina OP, Chumbaev AS (2011) Effect of snow amount on runoff, soil loss and suspended sediment during periods of snowmelt in southern West Siberia. *CATENA* 87:45–51. <https://doi.org/10.1016/j.catena.2011.05.004>
- Tanasienko AA, Yakutina OP, Chumbaev AS (2016) Content of nitrogen in eroded and non-eroded chernozems and products of sediments and runoff of dissected territory of West Siberia. *Problemy agrohimii i ekologii* 3:39–46. (Содержание азота в нарушенных и ненарушенных черноземах и продуктах твердого и жидкого стока расчлененной территории Западной Сибири) https://elibrary.ru/download/elibrary_26508328_52016885.pdf accessed on March 7, 2021
- Tanasienko AA, Chumbaev AS, Yakutina OP et al (2019) The impact of climatic humidity of the southeastern part of Western Siberia on spring deficit of moisture in the profiles of eroded chernozems. *Eurasian Soil Sc* 52:935–944. <https://doi.org/10.1134/S1064229319080143>
- Taratunin AA (2008) *Inundations in Russian Federation*. FGUP RosNIIVKH Publishing, Ekaterinburg, 432 pp. (Наводнения на территории Российской Федерации)
- Thermochron iButtonDevice (2019). <https://www.maximintegrated.com/en/products/ibutton/data-loggers/DS1921G.html>. Accessed 7 March 2021
- USSR Climate Handbook (1977) Novosibirsk 20(2):378 (Справочник по климату СССР)
- Vadyunina AF, Korchagina ZA (1961) *Methods of research of physical properties of soils and grounds*. State publisher ‘The higher school’, Moscow 346 pp. (Методы исследования физических свойств почв и грунтов)
- Weather archive. <https://rp5.ru/>. Accessed 7 March 2021
- Wilson H, Elliott J, Macrae M, Glenn A (2019) Near-surface soils as a source of phosphorus in snowmelt runoff from cropland. *J Environ Qual* 48(4), Special section: agricultural water quality in cold environment. <https://doi.org/10.2134/jeq2019.04.0155>
- Wu Y, Ouyang W, Hao Z, Yang B, Wang L (2018) Snowmelt water drives higher soil erosion than rainfall water in a mid-high latitude upland watershed. *J Hydrol* 556:438–448. <https://doi.org/10.1016/j.jhydrol.2017.11.037>
- Xu J, Li H, Liu X, Hu W, Yang Q, Hao Y, Zhen H, Zhang X (2019) Gully erosion induced by snowmelt in northeast china: a case study. *Sustainability* 11:2088. <https://doi.org/10.3390/su11072088>
- Zaslavsky MN (1979) *Soil erosion*. “Mysl” Publisher, 245 pp. (Эрозия почв. Мысль с. 245)



The Potential Impact of Climate Change and Land Use on Future Soil Erosion, Based on the Example of Southeast Serbia

Veljko Perović, Dragan Čakmak,
Miroslava Mitrović, and Pavle Pavlović

Abstract

Soil erosion caused by climate change and changes in land use increases or decreases depending on the geographic location, climate scenarios, precipitation patterns, topographic potential, and land management practices. For this reason, the impact of climate change on soil erosion needs to be analysed at the regional and/or local levels. Bearing in mind that climate and land use will change in the future, the purpose of this chapter is to quantify the current intensity of soil erosion, taking the Vranjska Valley (southern Serbia) as an example, to simulate soil losses for 2050 and 2100 due to changes in climate and land use, and to analyse the spatial and temporal grouping of clusters of soil loss for 2015 and 2100. The Integrated Valuation of Ecosystem Services and Tradeoffs (InVEST) of the sediment delivery ratio (SDR) model integrated with the EBU-POM (Eta Belgrade University-Princeton Ocean Model) regional climate model was used with the aim of quantifying

erosion intensity in the Vranjska Valley region. The results of research in the Vranjska Valley region show that average erosion intensity during 2015 amounted to $5.33 \text{ t ha}^{-1} \text{ yr}^{-1}$. According to the A1B scenario, average annual soil loss is expected to fall for the two periods in the future, by 6.6% (2050) and 41.8% (2100), mainly as a result of a reduction in the rainfall erosivity factor. Measures which could protect soil effectively in the future include reforestation with drought-resistant species, soil conservation, no-till practices, and an evaluation of current erosion models.

Keywords

Climate change · Soil erosion · Land use · Scenario analysis · Clustering

8.1 Introduction

The problems caused by climate change are one of the challenges of the modern era and demand an active approach to mitigate the consequences. Measuring and analysing temperatures on Earth over the past million years has provided a general pattern for changes in climate arising from natural phenomena such as volcanic activity, fluctuations in solar energy or increases in the concentrations of greenhouse gases in the atmosphere. However, today it is believed that human

V. Perović (✉) · D. Čakmak · M. Mitrović · P. Pavlović
Department of Ecology, Institute for Biological Research 'Siniša Stanković' – National Institute of the Republic of Serbia, University of Belgrade, Bulevar despota Stefana 142, 11060 Belgrade, Serbia
e-mail: veljko.perovic@ibiss.bg.ac.rs

activities (e.g. fossil fuel combustion, crop fertilisation, deforestation, animal husbandry, and the release of chemicals) are the dominant causes of the climatic changes that have been observed over the past half century. In fact, the Intergovernmental Panel on Climate Change (IPCC) points to an increase in average global land and ocean temperatures of 0.85 °C between 1880 and 2012 in its Fifth Assessment Report (IPCC 2014). Moreover, it has been noted that the period from 1983 to 2012 was the warmest in the last 800 years, and that if carbon dioxide levels double by 2040, the temperature will increase by 2.8 ± 1.2 °C. In addition to global warming and all the processes and phenomena that accompany it, such as more frequent droughts, heat waves, floods, and soil erosion, we also face air pollution, soil degradation and contamination, desertification processes, systematic destruction of forests, the reduction of useable fresh water resources, the reduction of biodiversity, threats to marine fish stocks, and the emergence of new diseases, which will all result in a food shortages in certain regions (Kadović et al. 2013).

Research to date has shown that the combined effects of changes in land use and climate have the greatest impact on ecosystem changes, including a reduction in biodiversity and ecosystem services (Oliver and Morecroft 2014; Peng et al. 2020). Namely, future climate changes will affect the composition of plant species, especially any species that are sensitive to temperature and/or humidity and have limited migration potential (Bakkenes et al. 2006). Today, human activities are the primary source of changes in land use. Climate change is expected to enhance and accelerate impacts on the land, hydrological and climatic regimes, and increase species vulnerability (Staud et al. 2013; Grimm et al. 2013).

Climate change mainly affects soil erosion through changes in rainfall intensity and temperature. These effects may be positive or negative; however, they are difficult to predict accurately (Li and Fang 2016). In particular, an altered temperature and precipitation regime will affect soil erosion, soil fertility, biomass

production, the loss of organic matter, infiltration rates, moisture levels in soil, land use, and crop management, all of which has an impact on environmental sustainability (Lal et al. 2011; Pavlović et al. 2017; Perović et al. 2021). It is particularly important to highlight that erosion of the surface soil layer leads to a reduction in the amount of organic matter, which has a general impact on soil fertility. Its loss results in the deterioration of soil structure and a decrease in the soil's water-holding capacity, which can increase the risk of flooding and the occurrence of landslides. In addition, soil erosion can have a major impact on the migration of heavy metals, fertilisers, and pesticides, which are found in sediments, leading to eutrophication and a possible negative impact on the global carbon, nitrogen, and phosphorus cycles.

The use of remote sensing methods and geographical information science (GIS) makes soil erosion analysis more accessible and precise compared to conventional techniques (Irvem et al. 2007; Perović et al. 2013). In this respect, the erosion modelling process is a significant step towards solving environmental problems in the future (Mullan et al. 2012), and it is becoming an increasingly important tool in creating erosion maps as conventional methods for determining soil conservation action (Du et al. 2016). Several such erosion models exist that help predict soil loss and estimate soil erosion risk, including the Universal Soil Loss Equation (USLE) (Wischmeier and Smith 1978), the Revised Universal Soil Loss Equation (RUSLE) (Renard et al. 1997), the Pan-European Soil Erosion Risk Assessment (PESERA) (Kirkby et al. 2004, 2008), WaTEM-SEDEM (Van Oost et al. 2000; Van Rompaey et al. 2001), the Water Erosion Prediction Project (WEPP) (Flanagan and Nearing 1995), the Soil and Water Assessment Tool (SWAT) (Arnold et al. 1998), and the European Soil Erosion Model (EUROSEM) (Morgan et al. 1998). Numerous studies have aimed to analyse the impact of future climate change on soil erosion using various erosion models (Zhang et al. 2009; Bosco et al. 2009; Litschert et al. 2014; Routschek et al. 2014; Serpa et al. 2015; Khare

et al. 2016). In general, such studies reveal the relationship between soil erosion intensity and climate change to be a non-linear spatial and temporal one (Jones et al. 2009).

On the basis of possible climate scenarios, it is possible to develop specific adaptation measures. Adaptation to climate change crosses the boundaries of science, society, and politics, with various spatial and temporal issues to consider such as the social aspect, financial resources, the political context, public awareness, and scientific uncertainty (Carlson and McCormick 2015; Enríquez-de-Salamanca et al. 2017).

Given that climate and land use can potentially change in the future, the purpose of this chapter is to consider the possible effects of climate change and land use change on soil erosion, using the example of the Vranjska Valley (Southern Serbia). The objectives of the research were to estimate the current soil loss in the study area, to simulate soil loss due to changes in climate and land use in 2050 and 2100, and to analyse the spatial and temporal grouping of soil loss clusters for 2015 and 2100.

8.2 Materials and Methods

8.2.1 Study Area

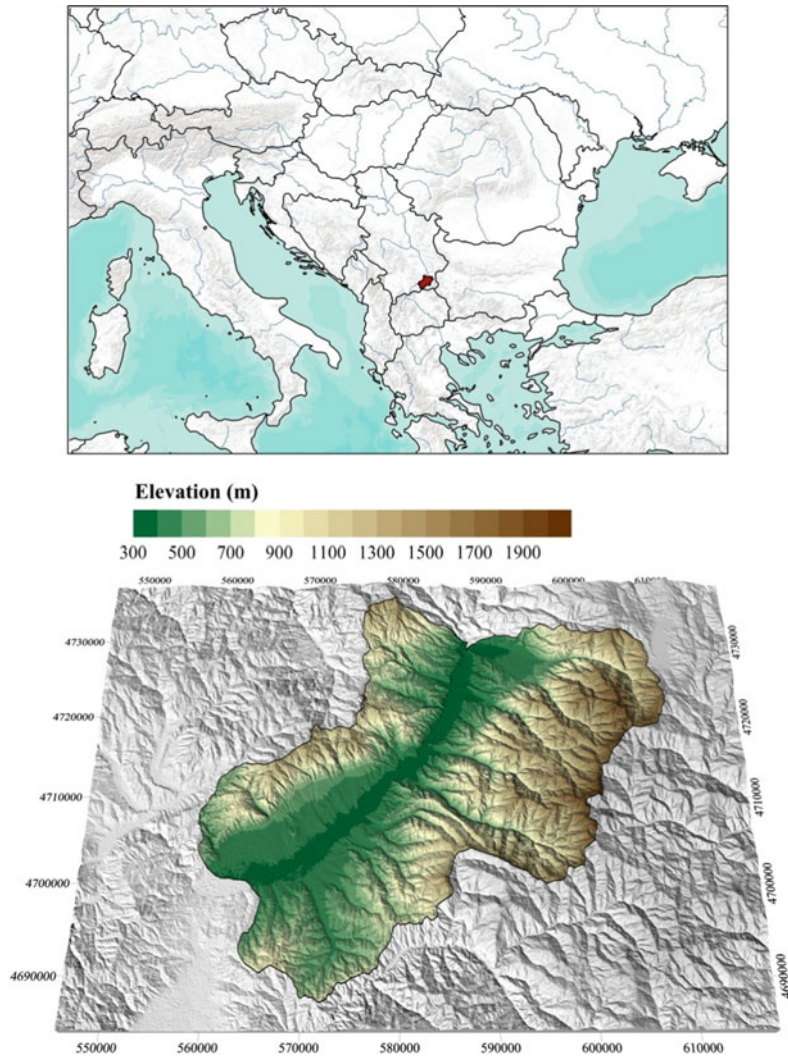
The Vranjska Valley is an extensive area located in the upper reaches of the Južna Morava river in the south of Serbia (Fig. 8.1). It extends predominantly from the south-west towards the north-east, between 42° 19' N–42° 45' N and 21° 42' E–22° 19' E, with an average altitude of 789.51 m ASL.

The hydrographical network of the Vranjska Valley is extremely arborescent. The largest river in this region is the Južna Morava, which has 73 tributaries, including the Vrla, Vranjsko-Banjska, Kozarska, and Trnovačka Rivers. Almost all the rivers originate beneath the mountain peaks, with upper courses characterised by large drops in their longitudinal profiles, deeply cut riverbeds with steep sides, and the frequent presence of rocky blocks. The geological composition of the Vranjska Valley is mainly groups of disturbed

and highly fractured crystalline schists, prone to weathering, particularly in the surface areas of steep, bare slopes. Only small areas were formed from volcanic rocks and tuffs, sedimentary rocks, diluvium, and alluvium. A variety of soil types have formed in the study area due to the relief, climate, geological composition and vegetation, and anthropogenic activity. Different types of oak forest dominate the study area, including thermophilic oak communities with pubescent oak (*Quercus pubescens* Willd.), which are very rarely found in other parts of Serbia; here, they play a significant role and are widely distributed (Mišić et al. 1985). Another special characteristic of this area that deserves mention is the presence of specific polydominant and depleted forest communities in which three Tertiary relict species were found: *Corylus colurna* L., *Ostrya carpinifolia* Scop., and *Acer intermedium* Panč. (Dinic et al. 2000).

8.2.2 Climate Change Scenarios

The simulations used in climate models employ socio-economic scenarios which offer an insight into projected future concentrations of greenhouse gases (GHGs) and estimated future vulnerability to climate change (Carter et al. 2007). Creating such scenarios requires projections for expected population levels, economic activity, management structures, social values, and possible technological changes in the region that is the topic of research. In this study, simulation of changes in climate parameters was conducted using the Eta Belgrade University–Princeton Ocean Model (EBU-POM) (Djurdjević and Rajković 2008, 2012), which arose from coupling a regional atmospheric model and an oceanic model and is used in the simulation of climate parameters according to a given scenario. The integration covers the period between 1951 and 2100. Observed concentrations of greenhouse gases were used for the 1951–2000 period, following 20C3M protocol, while the post-2000 period is presented through the A1B scenario (Nakicenovic and Swart 2000). The A1 group of scenarios describes a future world conditioned by

Fig. 8.1 The study area

very fast economic growth and the rapid introduction of new and efficient technologies. The basic premise for these scenarios is the linking of regions, the building of technical capacities, and growing cultural and social interaction. The A1 scenario develops into three sub-groups, which describe possible directions of technological change, with the A1B scenario emphasising the balanced use of all energy sources (IPCC 2007).

Compared to the results of other climate models used across Europe, the results of the EBU-POM model are within the mid-range of possible scenarios. In Serbia, changes in climate characteristics were assessed using the EBU-

POM model based on the results of the IPCC's climate modelling, according to the most frequently used scenarios: the SRES A1B scenario (Fig. 8.2) and the SRES A2 scenario. Concentrations of CO₂ at the end of the century are around 690 ppm for the A1B scenario and approximately 850 ppm for the A2 scenario, which is almost twice as much as current levels of CO₂ at 387 ppm. According to the A1B scenario, the average annual air temperature in Serbia is expected to increase by 3.4–3.8 °C by the end of the century, while precipitation levels will decrease by around 12–15% compared to the reference period of 1961–1990 (Djordjević and

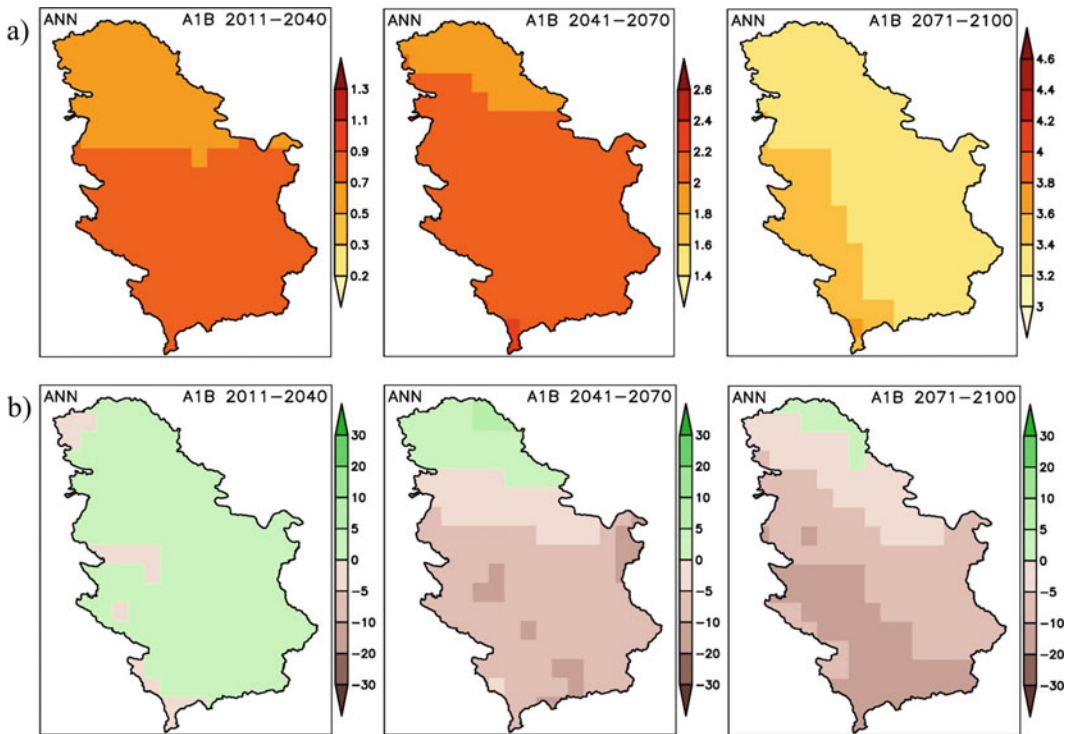


Fig. 8.2 Figures for **a** annual mean temperature and **b** precipitation change for selected future time periods (Rajković et al. 2013)

Rajković 2008, 2012). Future air temperature forecasts have also been analysed for the Danube River Basin (DRB), (ICPDR 2018). The results of this analysis reveal that the mean daily air temperature for the period 2021–2050 will increase by 0.5–4 °C by the end of the period depending on the region, while the expected increase in daily temperatures by the end of the second period (2071–2100) is 2.8–6.0 °C. Moreover, a reduction in precipitation of about 5% is expected in the DRB, while in the more distant future, forecasts suggest a reduction between 5%–10% (ICPDR 2018). In these altered climatic conditions, certain social changes are almost inevitable, such as population migration due to changes in agricultural and industrial areas, the outbreak of new diseases and starvation, and possible conflicts over the remaining land and water.

It is clear that the negative consequences of climate change will also have a significant impact on the Serbian economy, inflicting significant damage and losses. It is estimated that the total material damage caused by extreme climatic and weather conditions since 2000 is more than 5 billion euros, with more than 70% of these losses due to drought and high temperatures. Another major cause of the significant losses is floods, which caused huge damage in 2014. It is estimated that restoration in the afflicted region will cost around 1.35 billion euros (Jovović and Jovičić 2017).

In this work, to study the effects of climate change and changes in land use, time series of annual accumulated precipitation were used. Based on the simulation results for the predicted precipitation distribution, the changes in the rainfall erosivity factor (R) and crop-management factor (C) were calculated, as well

Table 8.1 Overview of the InVEST SDR inputs and outputs

Input	Type	Output	Type
Rainfall erosivity index (R)	.tiff	parameter log	.txt
Soil erodibility (K)	.tiff	rkls (tonnes/pixel)	.tiff
Digital elevation model (DEM)	.tiff	sed_export.tif (tonnes/pixel)	.tiff
Land use/land cover (LULC)	.tiff	stream (pixel mask)	.tiff
Watersheds	.shp	stream_and_drainage (pixel mask)	.tiff
Lucode	Decimal	usle (tonnes/pixel)	.tiff
C factor	Decimal	sed_retention (tonnes/pixel)	.tiff
P factor	Decimal	sed_retention_index (tonnes/pixel)	.tiff
Threshold Flow Accumulation	Integer	watershed_results_sdr	.shp
Borselli k parameter	Decimal	sed_export (tonnes/watershed)	.tiff
Borselli IC0 parameter	Decimal		
Max SDR Value	Decimal		

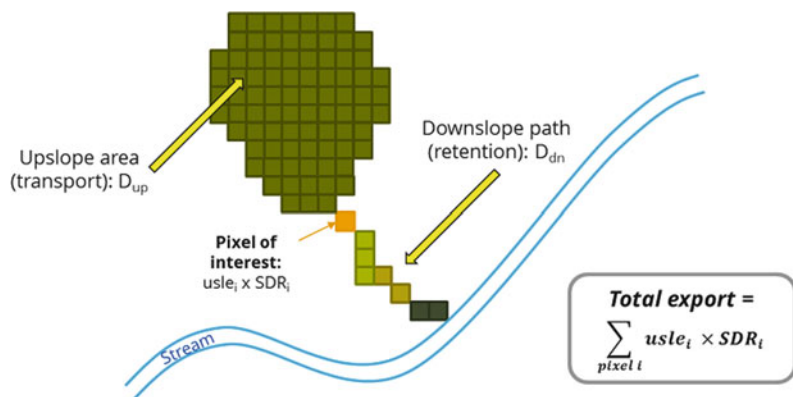
as the prediction of future changes in soil loss in the Vranjska Valley region (Table 8.1).

8.2.3 Model Setup and Input Data

InVEST (Integrated Valuation of Ecosystem Services and Tradeoffs) is a group of spatially oriented tools which allow the interaction between various ecological and economic components to be assessed. Some of the most important tools are sediment transport modelling, carbon modelling, crop pollination modelling,

and seasonal water yield modelling. Based on the topography, climate, soil type, and land use, the InVEST Sediment Delivery Ratio (SDR) model calculates the intensity of erosion processes, mainly in rural areas (Grafius et al. 2016). The average annual amount of eroded sediment, i.e. soil loss, is calculated for each pixel first using the algorithm and then the sediment delivery ratio (SDR); the latter represents the proportion of soil loss that reaches a stream (Hamel et al. 2015; Fig. 8.3). This approach was proposed by Borselli et al. (2008) and later applied by others (Cavalli et al. 2013; López Vicente et al. 2013;

Fig. 8.3 Conceptual approach used in the model (Hamel et al. 2015)



Sougnéz et al. 2011). The raster format, which is increasingly used in the analysis of erosion processes, simplifies the synthesis and more accurate interpretation of spatially distributed data (Perović et al. 2016). As such, the dominant data available with this model are data on climate, soil, topography, land use, etc. Detailed information on data preparation and the methodology applied in the InVEST SDR model can be found in the works by Perović et al. (2018, 2019).

Average annual soil loss was calculated using the following Eq. (8.1):

$$\text{soil loss} = R_i \cdot K_i \cdot LS_i \cdot C_i \cdot P_i \quad (8.1)$$

where R_i is the rainfall erosivity ($\text{MJ mm (ha hr)}^{-1}$); K_i is the soil erodibility ($\text{tonnes ha hr (MJ ha mm)}^{-1}$); LS_i is the slope length-gradient factor; C_i is the crop-management factor, and P_i is the support practice factor.

8.2.4 Differential Local Moran's I Statistics

The differential local Moran's I method is a natural extension of Moran's I statistics and represents calculated spatial patterns of changes in attributed values between two different points in time (Anselin 2016). The form of the differential local Moran's I is as follows:

$$I_i = z(V_{it_2} - V_{it_1}) \sum_j w_{ij} z(V_{jt_2} - V_{jt_1}) \quad (8.2)$$

where $z(V_{it_2} - V_{it_1})$ and $(V_{jt_2} - V_{jt_1})$ are the normalised values of the changes in v from time t_1 to t_2 . Conditional random permutations are used in the simulation process. To compare the two time periods, the attribute can be normalised by the length of two periods (Fan et al. 2018), which gives the following:

$$I_i = z\left(\frac{V_{it_2}}{L_{t_2}} - \frac{V_{it_1}}{L_{t_1}}\right) \sum_j w_{ij} z\left(\frac{V_{jt_2}}{L_{t_2}} - \frac{V_{jt_1}}{L_{t_1}}\right) \quad (8.3)$$

where L_{t_2} and L_{t_1} are the lengths of the two periods.

In this chapter, the spatial and temporal dynamics of soil loss were analysed for the Vranjska Valley region for the period between 2015 and 2100. This time series made it possible to identify change patterns and interpret the spatial dynamics of soil loss better. The differential local Moran's I method was tested using 999 permutations and the significance level was 0.05.

8.2.5 Land Use

8.2.5.1 Current Land Use

Forests cover most of the region of the Vranjska Valley (60.43% of the surface area), only 3.07% of which are degraded forests (Fig. 8.4). Beech forests are found on slopes of 4.3–57.9%, while oaks are on slopes of up to 46.6%. In terms of productive land, the most common categories are meadow and pasture, as well as arable land, which together accounts for 34.27% of the region. They are found on slopes of 5.6–65.9%. Meadows are found at altitudes of up to 500 m, most frequently on the northern exposures and gentle slopes. Arable land is mainly located in the lower areas of the region, i.e. in extended river valleys, but can also be found at higher altitudes, often on steeper slopes where conditions do not actually allow field crops to be cultivated. Negative population migration leads to the spontaneous development of vegetation and the formation of meadows and pastures on abandoned arable land. Orchards and meadows only account for 1.49% of the total area and are predominantly found on south- and south-western-facing slopes at altitudes up to 1000 m ASL, usually on slopes of 4.3–41.2%. These areas are usually small plots of land in populated areas of the river basin, where orchards and vineyards are poorly cultivated and maintained (Braunović 2013; Perović 2015).

8.2.5.2 Land Use Change Scenario

Soil erosion and sediment yield in Europe are important topics on political agendas (Ward et al. 2009) and for policy-makers at the local, national and European levels (Van Rompaey et al. 2005).

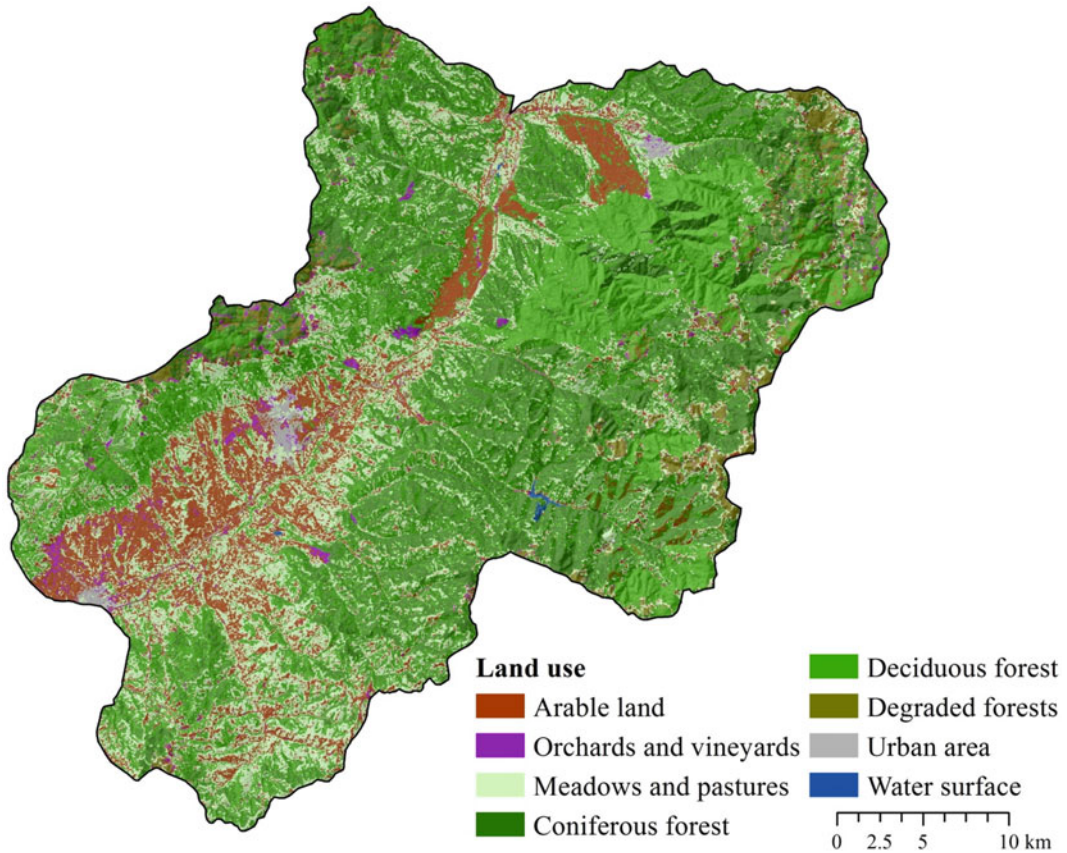


Fig. 8.4 Land use (modified by Perović et al. 2019)

In Western Europe, these issues are taking on ever greater significance due to the negative effects of climate change that are expected in the future. An approach based on the IPCC scenarios is being employed to develop an overview of probable changes in land use in Europe. However, in view of the fact that the focus of these scenarios is not based on land use systems, agriculture, and rural development, there is a lack of regionally developed high-resolution elements that are needed for land use modelling. As a result, the “Continental Market” and “Global Cooperation” land use change scenarios are most commonly used, corresponding to the Special Report on Emissions Scenarios (SRES) scenarios.

To date, studies have shown that changes in plant phenology, range and species distribution, and changes in composition and interaction

within communities, including changes in the structure and dynamics of ecosystems, are due to climate change (Walther et al. 2002). This can affect species diversity in several ways. Species can tend to head to areas with a more favourable climate, within certain tolerance limits, which results in changes in their distribution, while species with low tolerance can adapt or modify under altered climatic conditions, creating a new spectrum of species. Generally speaking, species are faced with two options—to adapt to the altered habitat conditions or to disappear from their habitats (Graves and Reavey 1996).

In Serbia to date, no studies have been conducted examining how climate change affects vegetation. However, Mihailović et al. (2015) conducted an analysis of climate change based on altitude zones in accordance with the Köppen classification (Köppen 1936), under the A1B and

A2 SRES climate change scenarios for the 2001–2030 and 2071–2100 periods, applying the EBU-POM regional climate model. As generally known, Köppen created a climate classification system based on empirical observations, using monthly temperatures and precipitation levels to determine the boundaries of different types of climate. Most Köppen applications use mapping of the geographical distribution of climate and vegetation parameters using long-term climate datasets (Chen et al. 2013). Thus, this study used the Köppen classification integrated with altitude zones when creating scenarios for possible changes in vegetation distribution up to 2100. In Serbia, compared to the reference period of 1961–1990, the dominant climate zone is *Cfbwx*”, which covers 81.0% of the country’s territory, extending from north to south. In the southwestern and southeastern regions, there is a transition to the *Dfbwx*” climate zone (18.2%), while the ET zone, i.e. a polar and alpine climate, is found in the high mountains of the south-west (0.2%). Finally, there are isolated spots of the *Cfwax*” climate type (0.6%) in eastern Serbia (Mihailović et al. 2015).

8.3 Results and Discussion

8.3.1 Effects of Changes in the Rainfall Erosivity Factor

The numerical value of the R factor quantifies the effect of the impact of raindrops, but also provides relevant information on the quantity and speed of runoff after a rain event (Kadović 1999). This is why the R factor is the most frequently used index for quantifying precipitation and is represented in many erosion models, such as USLE, RUSLE, and WaTEM SEDEM. Precipitation frequency and intensity have a primary effect on soil erosion, sediment delivery and landscape (Burt et al. 2016); they vary in different parts of the world and can increase or decrease at the regional and global level (Li and Fang 2016), meaning that soil erosion can

increase or decrease depending on local climatic and ecological conditions.

Based on the A1B climate scenario, the distribution of precipitation was predicted for the Vranjska Valley region and R factor values were calculated for 2015, 2050, and 2100. R factor values for 2015 ranged from 625.44 to 657.85 MJ mm ha⁻¹ h⁻¹ yr⁻¹, with a mean value of 632 MJ mm ha⁻¹ h⁻¹ yr⁻¹ (Perović et al. 2019), (Fig. 8.5).

Based on data from 3625 rainfall erosivity stations distributed across 63 countries throughout the world, the estimated global mean rainfall erosivity factor was calculated as being 2,190 MJ mm ha⁻¹ h⁻¹ yr⁻¹. In terms of continents, South America was estimated to have the highest mean R factor (5,874 MJ mm ha⁻¹ h⁻¹ yr⁻¹), followed by Africa (3,053 MJ), Asia and the Middle East (1,487 MJ mm ha⁻¹ h⁻¹ yr⁻¹), and Oceania (1,675 MJ mm ha⁻¹ h⁻¹ yr⁻¹), (Panagos et al. 2017a, b).

The results obtained for the Vranjska Valley region are in accordance with estimated rainfall erosivity based on high-temporal-resolution precipitation data in Europe, where there is a wide range of rainfall erosivity, from 51.4 to 6228.7 MJ mm ha⁻¹ h⁻¹ yr⁻¹, with a mean value of 722 MJ mm ha⁻¹ h⁻¹ yr⁻¹. This is due to substantial variations in climate and terrain across the 4.4 million km² area (Panagos et al. 2015a, b), (Fig. 8.6a). The R factor values obtained in this study fall within the same range of values as for other countries in the region, e.g. Bulgaria (a mean value of 695.0 MJ mm ha⁻¹ h⁻¹ yr⁻¹), Romania (a mean value of 785.0 MJ mm ha⁻¹ h⁻¹ yr⁻¹) and Hungary (a mean value of 683.3 MJ mm ha⁻¹ h⁻¹ yr⁻¹), (Panagos et al. 2015a, b).

Predictions for the Vranjska Valley region suggest that R factor values will have decreased in 2050 by 6.33% compared to 2015. Specifically, simulated R factor values range from 589.12 to 608.96 MJ mm ha⁻¹ h⁻¹ yr⁻¹, with a mean value of 592 MJ mm ha⁻¹ h⁻¹ yr⁻¹ (Perović et al. 2019), (Fig. 8.5). In EU countries, the Joint Research Centre (JRC2017) forecasts a change in rainfall erosivity by 2050, predicting an increase in northern Europe (the coasts of the

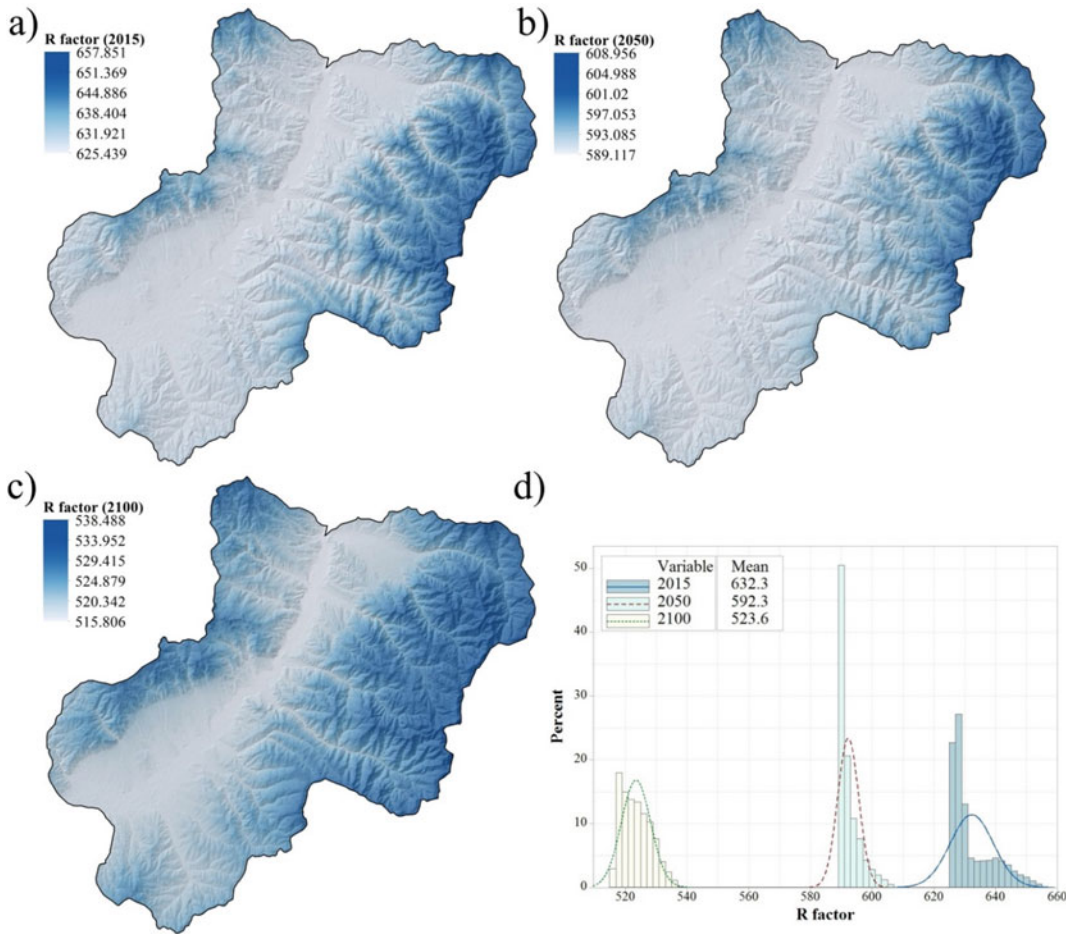


Fig. 8.5 The R factor for **a** 2015, **b** 2050, and **c** 2100, and **d** a histogram for R factor distribution (modified by Perović et al. 2019)

North Sea and the English Channel), the Alps, northwestern France and eastern Croatia. On the other hand, a decline in rainfall erosivity has been predicted for the Nordic countries (particularly Finland and Sweden) and for parts of Poland. Small changes are expected in central Europe (particularly in Slovakia and western Poland), while the Mediterranean Basin exhibits mixed trends with predictions for the Adriatic Sea region (the coasts of Italy, Slovenia, and Croatia), western Greece, and parts of Bulgaria and Romania suggesting a significant reduction in rainfall erosivity (Panagos et al. 2017a, b, Fig. 8.6b). With this in mind, R factor estimates for 2050 for the Vranjska Valley region can be considered realistic.

Estimates for 2100 for the Vranjska Valley reveal a further reduction in the R factor, which will range from 515.80 to 538.49 $\text{MJ mm ha}^{-1} \text{h}^{-1} \text{yr}^{-1}$ with a mean value of 523 $\text{MJ mm ha}^{-1} \text{h}^{-1} \text{yr}^{-1}$ (Perović et al. 2019), (Fig. 8.5). The study by Perović et al. (2019) showed that the R factor values will drop on average by 17.19% compared with 2015. These results are in line with the forecasts outlined in the Second National Communication on Climate Change of the Republic of Serbia, which states that no major changes in precipitation levels are expected up to the mid-twenty-first century; however, by the end of the century a more significant reduction in rainfall is expected, with changes expected to be from -10 to -15% in central

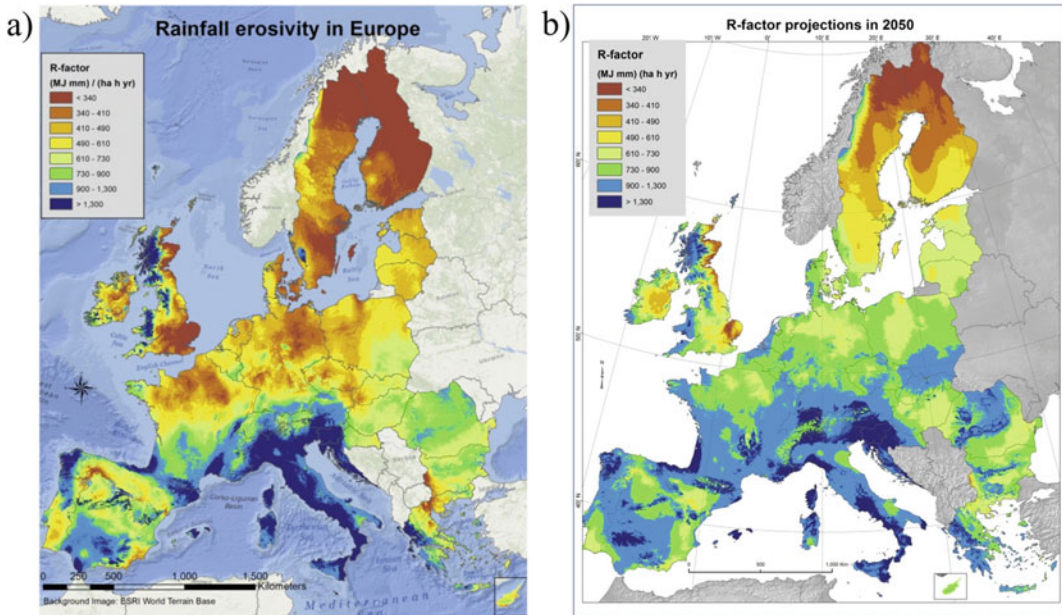


Fig. 8.6 Map of rainfall erosivity in Europe: **a** 2015 and **b** 2050 (Panagos et al. 2015a, b, 2017a, b)

Serbia (Kadović et al. 2013). Estimates of the R factor for the Vranjska Valley are consistent with general trends in precipitation reduction in this part of the world (Brankovic et al. 2013; Gajic-Capka et al. 2017; Tomozeiu et al. 2005; Tayanc et al. 2009).

8.3.2 Effects of Changes in the Crop-Management Factor

The vertical distribution of forests also corresponds to climate altitudinal zones. According to the map of potential vegetation in Serbia (Fukarek and Jovanović 1983), the Vranjska Valley region, in a broad sense, is characterised by oak forest belts consisting of Hungarian oak, Austrian oak and sessile oak forests at an altitude of up to 1100 m and different variations of beech forest between 400 and 1300 m ASL, relict vegetation in gorges of Moesian provenance, and poplar and willow woods in the river valleys.

According to the A1B scenario, the Serbian climate will be warmer and drier in the future. Estimates suggest that between 2001 and 2030, the whole of Serbia, meaning the Vranjska

Valley region as well, will experience an upward shift in the Cfwax" climate zone by 10 m, while the Cfwbx" climate zone will shift upwards by 100 m, potentially resulting in certain changes in forest vegetation composition and thus also land cover (Mihailovic et al. 2015). However, between 2071 and 2100, according to the same scenario, the Cfwax" climate zone will expand upwards by 685 m into large areas of the current Cfwbx" zone, which will in turn shift upwards by 800 m. Meanwhile, the Dfwbx" zone will shift 100 m upwards for the period between 2001 and 2030, and 400 m upwards between 2071 and 2100 (Perović et al. 2019). This will result in significant changes in the composition of forest vegetation and also in vegetation cover in general.

Changes in land use in Europe before 2050 will be negligible because of the species' adaptation potential, phenotypic plasticity, and non-linear shifts (Benot et al. 2013; Oliver and Morecroft 2014; Schirpke et al. 2017). The greatest changes in vegetation are predicted to be witnessed in northern Europe, where more than 35% of plant species will be invasive by 2100, while in southern Europe up to 25% of current

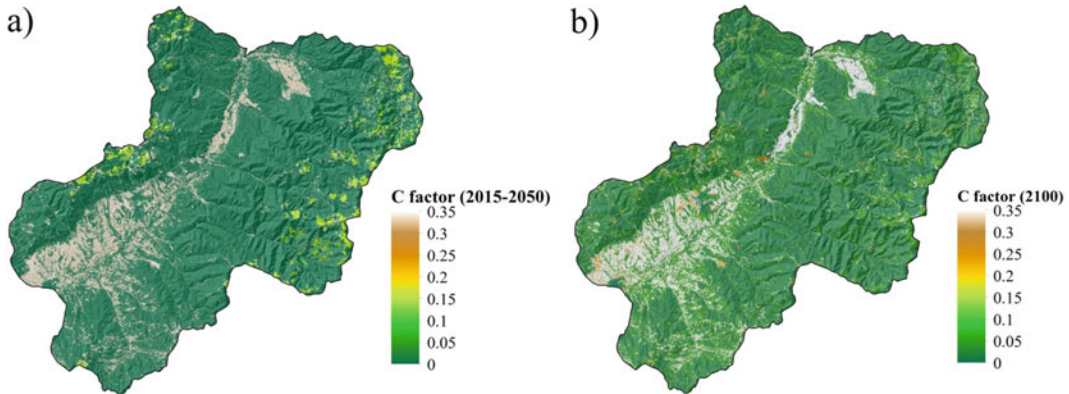


Fig. 8.7 C factor values for **a** 2015–2050 and **b** 2100 (modified by Perović et al. 2019)

plant species will disappear (Bakkenes et al. 2006). In relation to this, C factor values for 2015 and 2050 were identical; on the other hand, they changed by 2100, reflecting the predicted climatic conditions in that period. Hence, for example, where the slopes are at their steepest and soil quality is lowest, mainly close to rivers, arable land will be replaced by shrub land. In addition, on steeper slopes and at lower altitudes, it is predicted that arable land will be replaced by grassland with C factor values between 0.01 and 0.05, and 0.2 in extreme conditions (Perović et al. 2019; Fig. 8.7). This scenario is in line with global and local predictions forecasting a significant reduction in productive (arable) soil and an increase in surfaces classed as unmanaged or abandoned land (Harrison et al. 2019). In addition, we predict that existing forested areas will undergo a transition into young forest communities, which will be less protected from soil erosion and where C factor values will reach 0.01. The dynamics of change in mountain forest ecosystems due to climate change will significantly impact the variable competitiveness of plant species and their later distribution, and also the structure and composition of mountain forests (Lexer et al. 2002). Specifically, certain forest belts will respond to temperature increases by shifting to higher altitudes with favourable micro-locations (Peñuelas et al. 2007).

The scenario for the Vranjska Valley region is in line with some of the general trends predicted

for Europe. Namely, according to estimates by Ewert et al. (2005), the use of highly developed technologies in agricultural production in the countries of Western Europe will result in a continuing increase in yields, which will be further accelerated by the increases in temperature and concentrations of carbon dioxide. On the other hand, in the Mediterranean region and the countries of southeastern European, cereal yields are expected to fall (IPCC 2007). Furthermore, it is predicted that the greatest threat to crops in this part of Europe will occur during the summer months due to high temperatures and drought (Iglesias et al. 2007), with yields falling by up to 20% (Ciscar et al. 2018), which will inevitably lead to economic and ecological crisis caused by climate change (Bucak et al. 2017).

8.3.3 Effects of Changes in Soil Erosion

Soil erosion represents a huge ecological threat to the sustainability and production capacity of agriculture in many tropical and subtropical regions of the world. Average soil losses on our planet range from $6.5 \text{ t ha}^{-1} \text{ yr}^{-1}$ (Naipal et al. 2015) to $10.2 \text{ t ha}^{-1} \text{ yr}^{-1}$ (Yang et al. 2003). Even the lowest estimated soil erosion rate of $3 \text{ t ha}^{-1} \text{ yr}^{-1}$ (in Australia) is above tolerable loss thresholds. These authors state that almost 60% of current soil erosion is caused by human

activity. Analysis of annual soil loss connected to different types of land use in four global climate zones revealed that bare land has the highest mean loss values, ranging from 10.6 to 109.2 t ha⁻¹ yr⁻¹, followed by cropland (3.9–41.8 t ha⁻¹ yr⁻¹), orchards (23.5 t ha⁻¹ yr⁻¹), grassland (0.3–3.6 t ha⁻¹ yr⁻¹), shrubland (0.3–1.57 t ha⁻¹ yr⁻¹) and forests (0.2–0.6 t ha⁻¹ yr⁻¹), (Xiong et al. 2019). With the intensification of agricultural production that commenced in the last century, it is estimated that potential soil erosion will increase by approximately 17%. Average soil loss in Europe amounts to 2.46 t ha⁻¹ yr⁻¹, while average soil loss on arable land is 2.67 t ha⁻¹ yr⁻¹ (Panagos et al. 2015a, b). Permanent crops have a high soil loss rate of 9.47 t ha⁻¹ yr⁻¹ because the majority of vineyards and olive trees are to be found in the hilly Mediterranean regions of Europe. The average annual soil loss in pastures is 2.02 t ha⁻¹ yr⁻¹, while heterogeneous agricultural areas have an average loss of 4.21 t ha⁻¹ yr⁻¹. The highest mean annual soil losses have been recorded in Italy (8.46 t ha⁻¹ yr⁻¹), Slovenia (7.43 t ha⁻¹ yr⁻¹), and Austria (7.19 t ha⁻¹ yr⁻¹), while the lowest are in Finland (0.06 t ha⁻¹ yr⁻¹), Estonia (0.21 t ha⁻¹ yr⁻¹) and Holland (0.27 t ha⁻¹ yr⁻¹) (Panagos et al. 2015a, b). Average soil loss in the countries of the Western Balkans amounts to 7.13 t ha⁻¹ yr⁻¹ (with a maximum in Albania of 18.7 t ha⁻¹ yr⁻¹), while total soil loss (produced sediments) is 141,106 tonnes, which represents 7.6% of the total soil loss in Europe (Blinkov 2015). Soil erosion is one of the most significant causes of land degradation in Serbia, and resulting problems lead to economic losses in the sectors of agriculture and forestry and might pose a direct or indirect threat to people or property (Perović et al. 2012). The total average annual gross erosion in Serbia is 37,249,975.0 m³, or 421.57 m³ km⁻², while annual sediment transport is 9,350,765.0 m³ and specific annual sediment transport is 105.80 m³ km⁻². Based on a soil thickness of 20 cm, this means that around 20,525 ha are endangered on an annual basis (Ristić et al. 2017).

In the region of eastern Serbia (the Vranjska Valley), average erosion intensity during 2015

amounted to 5.33 t ha⁻¹ yr⁻¹ (Fig. 8.8) (Perović et al. 2019), which means the area is under little threat according to the FAO-PNUMA-UNESCO (1980) classification. Even so, in certain parts of the valley, soil erosion has surpassed the tolerable rates of loss that are characteristic for Europe (Verheijen et al. 2012) and can pose a serious problem for soil productivity.

Average soil losses in the Vranjska Valley region obtained by using the InVEST SDR model are in line with earlier research using the Erosion Potential Method, EPM (Gavrilović 1970, 1972, 1988). The mean erosion coefficient obtained was $Z = 0.24$, which classifies the Vranjska Valley as a region of weak erosion intensity. In addition, the Z coefficients for 17 basins within the valley fall into the same category, ranging from 0.21 to 0.36 (Braunović 2013). It should be noted that this region can also be categorised as one of weak intensity soil erosion following data on erosion losses measured at the experimental area of Vlasina, which is located in the northeastern part of the valley; all the data on soil loss over a research period of five years was below the lower tolerable erosion threshold of 2.5 t ha⁻¹ yr⁻¹ (Djorović 1974). High and very high intensity erosion mainly occurs in the hilly and mountainous areas of the valley, particularly in the eastern part (Fig. 8.8). High soil erodibility, steep slopes, degraded forests, and inappropriate land use have all contributed to wide-scale erosion in this region, particularly at the Prvonek reservoir watershed. The application of three erosion models established that there were significant soil losses at this watershed. According to the USLE model, annual soil losses ranged from 0 to 522.01 t ha⁻¹ yr⁻¹, with an average level of 17.63 t ha⁻¹ yr⁻¹; according to the PESERA model, they were between 0 and 147.61 t ha⁻¹ yr⁻¹, with an average level of 16.68 t ha⁻¹ yr⁻¹; and according to the WaTEM/SEDEM model, they averaged 18.23 t ha⁻¹ yr⁻¹ (Perović 2015).

A decrease in precipitation leads to improved infiltration of water into the soil and thus reduced runoff and soil erosion (Zabaleta et al. 2014; Serpa et al. 2015). Changes of 1% in precipitation can cause a 1.7% change in soil erosion

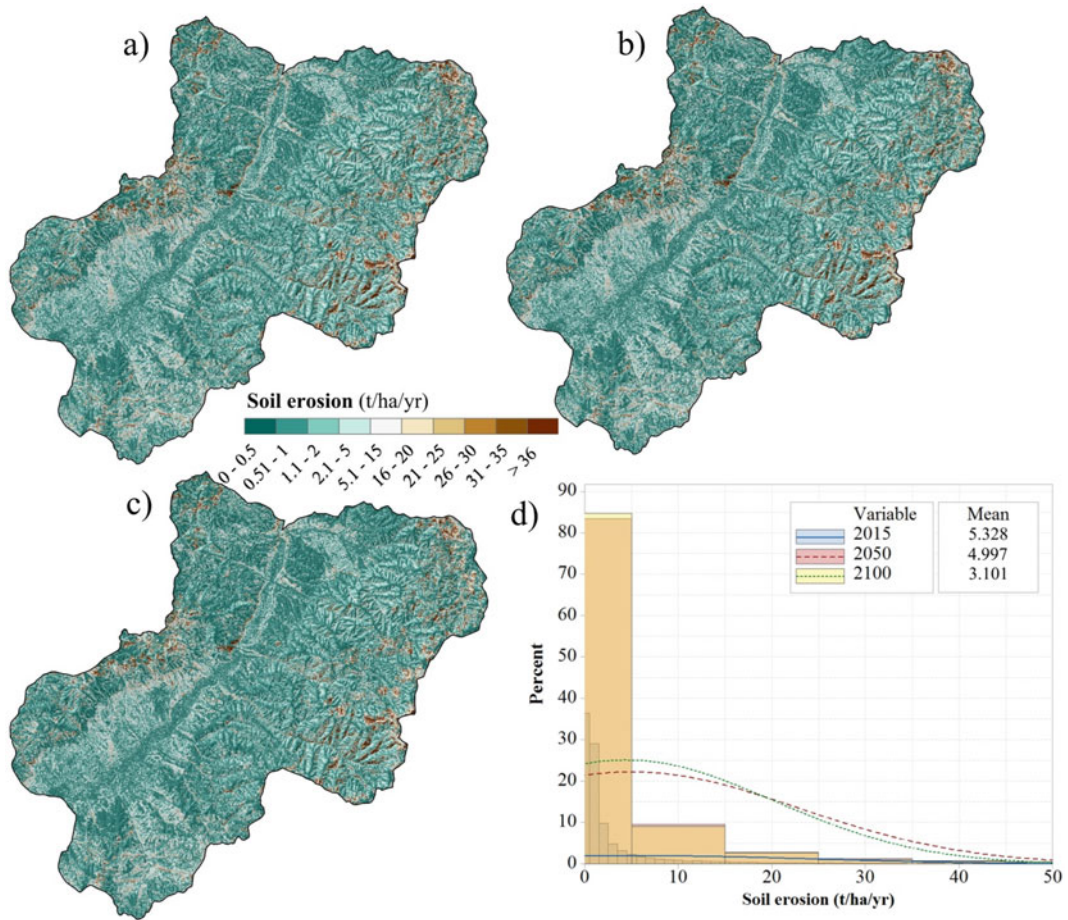


Fig. 8.8 Soil erosion for **a** 2015, **b** 2050, and **c** 2100, and **d** a histogram (modified by Perović et al. 2019)

intensity (Pruski and Nearing 2002). Bearing this in mind, soil erosion is predicted to fall to $4.98 \text{ t ha}^{-1} \text{ yr}^{-1}$ by 2050 (Perović et al. 2019). Moreover, as a result of land use changes and a reduction in the R factor, it has been estimated that the average soil erosion intensity will fall to $3.10 \text{ t ha}^{-1} \text{ yr}^{-1}$ by 2100 (Fig. 8.8), which means that the average soil loss will fall by 41.84% compared to the 2015 baseline level (Perović et al. 2019).

The results obtained from our research are in accordance with those found in recently published studies, which confirm a reduction in runoff and sediment production by the end of the

century (Bangash et al. 2013; Routschek et al. 2014; Serpa et al. 2015; Rodriguez-Lloveras et al. 2016), particularly in southern Europe (Dadson et al. 2010). In addition, erosion processes are predicted to increase by 14% in most parts of the world, while in terms of continents, only Europe and North America will experience a fall (Yang et al. 2003).

There is still uncertainty regarding the specific mechanisms of the effects of climate change on soil erosion in different parts of the world. Li and Fang (2016), analysing 205 studies investigating the impact of climate change on soil erosion from across the whole world, established that in 136

cases erosion rates will increase in the future, in 55 cases they will decrease, and in 14 cases they will not change at all.

8.3.4 Spatial Distribution of Soil Erosion Variables

Analysis using differential Moran's I illustrates the spatial distribution of significant spatial clusters of soil loss between 2015 and 2100 (Fig. 8.9a, b). Generally speaking, the effects of soil loss on the Vranjska Valley region can be categorised with two types of cluster: High-High and Low-Low. High-High clusters represent above-average changes during the analysed period compared to local observations, with the significant level at $p < 0.05$ (Fig. 8.9a, b). Hence, our research showed that there will be a geographic dislocation primarily of forest ecosystems, but also a change in the structure of certain plant communities, while new communities will appear and others will disappear. This relates primarily to oak forests, which cover the majority of the region and whose vulnerability stems from their being highly dependent on underground water, the amount of which will decrease constantly throughout the twenty-first century. In addition, a reduction in forest ecosystems is also expected due to longer periods

of drought, increased frequency and intensity of forest fires, and outbreaks of diseases and pests (Lindner et al. 2010).

Forest vegetation creates conditions for the accumulation of litter on soil, which significantly increases the retention of rainwater and water from melting snow (Kostadinov 2008), hence decreasing soil erosion. In this sense, climate change will lead to the accelerated decomposition of organic matter, a key process in the sustainability of forests. Namely, high temperatures and low moisture levels can drastically limit the growth and activity of microorganisms (Gauquelin et al. 2018). For these reasons, high-high clusters can be seen in those areas where larger soil losses were established and expected (Figs. 8.9a, b).

On the other hand, low-low clusters show below-average changes and are mainly present in flat and gently sloping areas, i.e. in those areas which had relatively higher soil losses in 2015 (Figs. 8.9a, b). Regional climatic conditions are a key factor in agricultural productivity because plants' metabolic processes are regulated by variables such as temperature, sunlight, carbon dioxide, and water availability (Chaves et al. 2003). In particular, the reduction in agricultural areas in the Vranjska Valley will accelerate an increase in the mean annual soil temperature of 3.8 °C and a reduction in mean annual soil

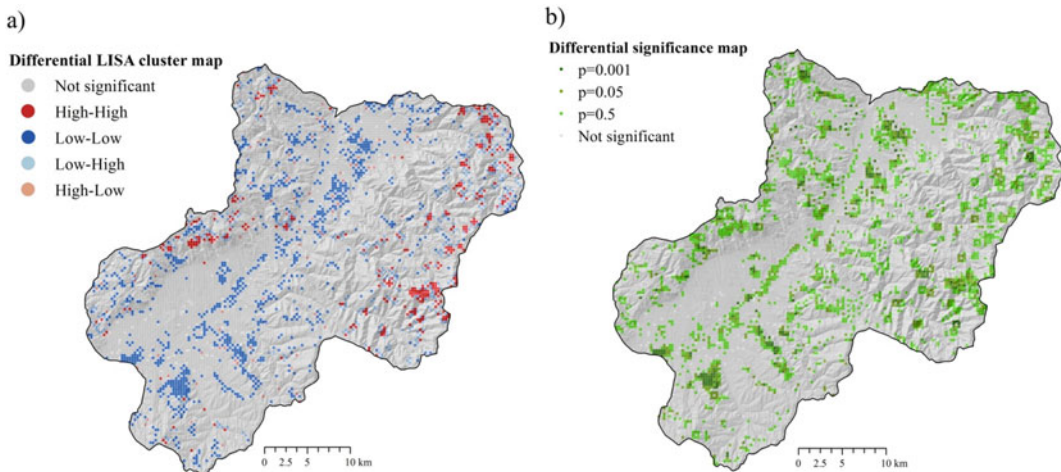


Fig. 8.9 Differential local Moran's I analysis (2015–2100)

moisture of 11.3%, as is expected in Serbia (Mihailovic et al. 2016). However, of the climate factors mentioned, water availability is the most important for agricultural production. In this regard, the annual median river flow is expected to decrease. An expected reduction of up to 30% has been simulated (2 °C warming scenario) for southern Europe, while during the summer months the flow will decrease by more than 30% (Ciscar et al. 2018). These results are in accordance with findings in studies by Lopez-Moreno et al. (2008), Zabaleta et al. (2014), and Stigter et al. (2014), which suggest that a climate change-induced reduction in precipitation will result in a decrease in the availability of surface water. As water availability will be greatly impacted by future climate change, it is assumed that this will result in enormous consequences for agriculture in the Vranjska Valley and the wider region. In the altered climate conditions, such areas will decrease, along with their fertility, due to thermal stress and the lack of available water, leading to a reduction in soil loss (Perović et al. 2019).

8.3.5 Adaptation to Climate Change

Assessing vulnerability to climate change and planning how to adapt to it are extremely complex processes which require analyses of all sectors of society and the involvement of numerous experts. As the global climate grows warmer, maintaining the structure and function of forest and agricultural soils is a key challenge. Every plant species has an optimum temperature range for development, meaning that any future rise in temperatures will change the species balance and distribution patterns. Furthermore, changes in the precipitation regime and levels will inhibit the regeneration of plant species, particularly in the Mediterranean region (Bravo et al. 2017). In this regard, cultivating mixed forests could provide important means of adapting to climate change and maintaining ecosystem services (Gamfeldt et al. 2013; Jactel et al. 2017; Vilà-Cabrera et al. 2018). The results of research in this field up to now have shown that drought-

resistant species, such as sessile oak (*Quercus petraea*), pubescent oak (*Quercus pubescens*), and Scots pine (*Pinus sylvestris*), can survive at lower altitudes across Europe, while the vertical distribution of other species such as beech (*Fagus sylvatica*), sycamore maple (*Acer pseudoplatanus*), lime (*Tilia* sp.), elm (*Ulmus* sp.) and silver fir (*Abies alba*) will probably be reduced. In addition, the distribution of species from (sub-)Mediterranean regions such as holm oak (*Quercus ilex*), hop hornbeam (*Ostrya carpinifolia*), and cork oak (*Quercus suber*) will spread towards the north (EEA 2017). The expansion of existing areas of agroforestry systems and the establishment of new ones could support measures to mitigate the effects of climate change, particularly in continental Europe (Hernández-Morcillo et al. 2018). The adoption of certain crop-management measures, primarily changing the planting dates and introducing cultures that require less moisture, can help reduce negative responses to climate change. A decrease in the yield of wheat and corn can be expected if the temperature rises by 2 °C in combination with a lack of precipitation during the vegetation period. This will thus affect the economic efficiency of production and price stability, making it necessary to switch to crops that better adapt to changing conditions or move existing crops to higher altitudes (Torquebiau et al. 2016).

Approaches to soil conservation planning based on generally accepted principles should be re-evaluated in light of this information on current and future climate change. In this context, changes in the planning of soil conservation systems will require the identification and quantification of threshold values for soil erosion tolerance, the determination of the probability of precipitation of sufficient intensity causing damage beyond these threshold levels, and the planning and design of conservation systems that play a protective role in vulnerable times and during particular events in a particular region (SWCS 2003). Adaptation measures for cultivated soils are necessary to maintain soil structure and fertility. For example, a proposal for appropriate changes in tilling practices (minimum or zero tillage), which involves leaving

crop residues on the soil surface, will help maintain the quality of soil, protect it from erosion, and lead to more efficient water infiltration (Ortiz et al. 2008; Saljnikov et al. 2014). Therefore, current erosion models need to be improved or replaced with alternatives that will allow researchers to incorporate the probability of extreme events in their recommendations to reduce soil erosion, surface runoff, and water pollution.

It must be borne in mind that it will take 3–10 years to provide new areas and to acquire new varieties, and 50–100 years to implement large investment projects, such as changes in infrastructure and changes in production based on new crops (Reilly 1997). Therefore, adaptation measures should begin today.

8.4 Conclusions

Soil erosion caused by climate change can increase or decrease depending on the geographic location, climate scenarios, precipitation patterns, topographic potential, and land management practices. Hence, the impact of climate change on soil erosion needs to be analysed at the regional and/or local levels.

In this chapter, the results of the InVEST SDR model, integrated with the EBU-POM regional climate model, have been presented and discussed, showing them to be reliable tools for predicting the effects of changes in climate and land use when assessing soil losses. The results of this study suggest that there will be a decrease in soil erosion in southeastern Europe, primarily due to the reduction in total rainfall. Specifically, it has been established that a reduction in the rainfall erosivity factor (in the range of 6.33–17.19%), as well as changes in the crop-management factor, will lead to a decrease in soil loss by 6.57% for the 2050 scenario and by 41.84% for the 2100 scenario.

The integrated spatial modelling approach applied in this study, which combines the effects of climate change and land use, can contribute to a more accurate and realistic assessment of future changes in soil erosion in Serbia.

In this chapter, possible uncertainties have not been analysed, primarily regarding the choice of the climate model, the choice of climate scenarios, the impact of extreme climatic events, the choice of socio-economic patterns of change, etc. Of course, for a complete assessment of the possible effects of climate change on soil erosion, it is necessary to include the interaction of these factors to make predictions more accurate. In addition, it is necessary to improve existing erosion models and/or replace them with new ones which allow climate models and land use change models to be integrated and thus give a more realistic picture of the processes affecting soil erosion in a certain place.

Acknowledgements This work was supported by the Ministry of Education, Science and Technological Development of Serbia, grant no. 451-03-9/2021-14/200007.

References

- Anselin L (2016) GeoDa Workshop 2: updated 2016. https://geodacenter.github.io/docs/geoda_1.8_2.pdf. Accessed 15 April 2021
- Arnold JG, Srinivasan R, Muttiah RS, Williams JR (1998) Large area hydrologic modeling and assessment: Part I. Model development. *J Am Water Resour Assoc* 34(1):73–89. <https://doi.org/10.1111/j.1752-1688.1998.tb05961.x>
- Bakkenes M, Eickhout B, Alkemade R (2006) Impacts of different climate stabilisation scenarios on plant species in Europe. *Glob Environ Change* 16(1). ISSN 19–28:0959–3780. <https://doi.org/10.1016/j.gloenvcha.2005.11.001>
- Bangash RF, Passuello A, Sanchez-Canales M, Terrado M, López A, Elorza FJ, Ziv G, Acuña V, Schuhmacher M (2013) Ecosystem services in mediterranean river basin: climate change impact on water provisioning and erosion control. *Sci Total Environ* 458–460:246–255. <https://doi.org/10.1016/j.scitotenv.2013.04.025>
- Benot M, Saccone P, Vicente R, Pautrat E, Morvan-Bertrand A, Decau M, Grigulis K, Prud'homme M, Lavorel S (2013) How extreme summer weather may limit control of *Festucapaniculata* by mowing in subalpine grasslands. *Plant Ecology Divers* 6:393–404. <https://doi.org/10.1080/17550874.2013.784818>
- Blinkov I (2015) Review and comparison of water erosion intensity in the western Balkans and EU countries. *Sect Nat Math Biotech Sci*. ISSN: 1857–9027. <https://doi.org/10.20903/csnmbs.masa.2015.36.1.63>

- Borselli L, Cassi P, Torri D (2008) Prolegomena to sediment and flow connectivity in the landscape: a GIS and field numerical assessment. *CATENA* 75(3):268–277. <https://doi.org/10.1016/j.catena.2008.07.006>
- Bosco C, Rusco E, Montanarella L, Panagos P (2009) Soil erosion in the Alpine area: risk assessment and climate change. *Stud Trent Sci Nat* 85:117–123. https://esdac.jrc.ec.europa.eu/ESDB_Archive/eusoils_docs/Pub/soil_erosion_in_the_alpine_area.pdf. Accessed 15 April 2021
- Brankovic C, Güttler I, Gajic-Capka M (2013) Evaluating climate change at the Croatian Adriatic from observations and regional climate models' simulations. *Clim Dyn* 41:2353. <https://doi.org/10.1007/s00382-012-1646-z>
- Braunović S (2013) Effects of erosion control works on the state of erosion in Grdelička klisura and Vranjska kotlina. The doctoral dissertation. University of Belgrade, Faculty of Forestry, Belgrade, Serbia (in Serbian: Efekti protiverozionih radova na stanje erozije u Grdeličkoj klisuri I Vranjskoj kotlini, doktorska disertacija)
- Bravo F, del Río M, Bravo-Oviedo A, Ruiz-Peinado R, del Peso C, Montero G (2017) Forest carbon sequestration: the impact of forest management. *Managing forest ecosystems: the challenge of climate change*. Springer International Publishing, pp 251–276. <https://doi.org/10.1007/978-3-319-28250-3>
- Bucak T, Trolle D, Andersen HE, Thodsen H, Erdoğan Ş, Levi EE, Filiz N, Jeppesen E, Beklioglu M (2017) Future water availability in the largest freshwater Mediterranean lake is at great risk as evidenced from simulations with the SWAT model. *Sci Total Environ* 581–582:413–425. <https://doi.org/10.1016/j.scitotenv.2016.12.149>
- Burt T, Boardman J, Foster I, Howden N (2016) More rain, less soil: long-term changes in rainfall intensity with climate change. *Earth Surf Process Landf* 41:563–566. <https://doi.org/10.1002/esp.3868>
- Carlson K, McCormick S (2015) American adaptation: social factors affecting new developments to address climate change. *Glob Environ Chang* 35:360–367. <https://doi.org/10.1016/j.gloenvcha.2015.09.015>
- Carter TR, Jones RN, Lu X, Bhadwal S, Conde C, Mearns LO, O'Neill BC, Rounsevell MDA, Zurek MB (2007) New assessment methods and the characterisation of future conditions. *climate change 2007: impacts, adaptation and vulnerability*. In: Parry ML, Canziani OF, Palutikof JP, van der Linden PJ, Hanson CE (eds) Contribution of working group II to the fourth assessment report of the intergovernmental panel on climate change. Cambridge University Press, Cambridge, UK, 133–171. <https://www.ipcc.ch/site/assets/uploads/2018/02/ar4-wg2-chapter2-1.pdf>. Accessed 15 April 2021
- Cavalli M, Trevisani S, Comiti F, Marchi L (2013) Geomorphometric assessment of spatial sediment connectivity in small Alpine catchments. *Geomorphology* 18831–41. <https://doi.org/10.1016/j.geomorph.2012.05.007>
- Chaves MM, Maroco JP, Pereira JS (2003) Understanding plant responses to drought—from genes to the whole plant. *Func Plant Bio* 30:239–264. <https://doi.org/10.1071/FP02076>
- Chen D, Chen HW (2013) Using the Köppen classification to quantify climate variation and change: an example for 1901–2010. *Environ Dev* 6:69–79. <https://doi.org/10.1016/j.envdev.2013.03.007>
- Ciscar JC, Ibarreta D, Soria A, Dosio A, Toreti A, Ceglar A, Fumagalli D, Dentener F, Lecerf R, Zucchini A et al (2018) Climate impacts in Europe: final report of the JRC PESETA III project, EUR 29427 EN, Publications Office of the European Union, Luxembourg. ISBN 978-92-79-97218-8. <https://doi.org/10.2760/93257>, JRC112769
- Dadson S, Irvine B, Kirkby M (2010) Effects of climate change on soil erosion: estimates using newlyavailable regional climate model data at a pan-European scale. *Geophys Res Abstract* 12, EGU2010-7047. <https://meetingorganizer.copernicus.org/EGU2010/EGU2010-7047.pdf>
- Dinić A, Jovanović V, Mišić V (2000) Forest vegetation around Vranjska Banja. In: 6th symposium on the flora of southeastern Serbia and neighbouring regions, Vrnjačka Banja, pp 95–101
- Djorović M (1974) Soil and water losses due to erosion from different soil types in SR Serbia. Doctoral dissertation, Faculty of Agriculture, Zemun (in Serbian)
- Djurdjević V, Rajković B (2008) Verification of a coupled atmosphere–ocean model using satellite observations over the Adriatic Sea. *Annales De Geophysique* 26:1935–1954. <https://doi.org/10.5194/angeo-26-1935-2008>
- Djurdjević V, Rajković B (2012) Development of the EBU-POM coupled regional climate model and results from climate change experiments. In: Mihailovic DT, Lalic B (eds) *Advances in environmental modeling and measurements*. Nova Science Publishers Inc., New York, USA, pp 23–32
- Du H, Dou S, Deng X, Xue X, Wang T (2016) Assessment of wind and water erosion risk in the watershed of the Ningxia-Inner Mongolia Reach of the Yellow River, China. *Ecological Indicators* 67:117–131, ISSN 1470-160X. <https://doi.org/10.1016/j.ecolind.2016.02.042>
- Enriquez-de-Salamanca Á, Díaz-Sierra R, Martín-Aranda RM, Santos MJ (2017) Environmental impacts of climate change adaptation. *Environ Impact Assess Rev* 64:87–96. ISSN 0195–9255. <https://doi.org/10.1016/j.eiar.2017.03.005>
- European Environment Agency (2017) Climate change, impacts and vulnerability in Europe 2016, An indicator-based report ISBN 978-92-9213-835-6. ISSN 1977–8449. <https://doi.org/10.2800/534806>
- Ewert F, Rounsevell MDA, I, Reginster MJ Metzger, R Leemans (2005) Future scenarios of European agricultural land use I. Estimating changes in crop productivity. *Agr Ecosyst Environ* 107:101–116. <https://doi.org/10.1016/j.agee.2004.12.003>

- Fan Y, Zhu X, She B, Guo W, Guo T (2018) Network-constrained spatio-temporal clustering analysis of traffic collisions in Jianghan District of Wuhan. *China Plos ONE* 13(4). <https://doi.org/10.1371/journal.pone.0195093>
- FAO-PNUMA-UNESCO (1980) Metodología provisional para la evaluación de la degradación de los suelos [Provisional methodology to evaluate soil erosion]. Food and Agricultural Organization of the United Nations, Rome. ISBN: 9253008695, p 86
- Flanagan DC, Nearing MA (1995) USDA water erosion prediction project: hillslope profile and watershed model documentation, NSERL Report No. 10, USDA-ARS National Soil Erosion Research Laboratory, West Lafayette, In 47907-1194
- Fukarek P, Jovanović B (1983) Map of natural potential vegetation 1:1,000,000. Skopje: Scientific Council for the vegetation map of Yugoslavia, Faculty of Forestry
- Gajic-Capka M, Güttler I, Cindric K, Brankovic C (2017) Observed and simulated climate and climate change in the lower Neretva river basin. *J Water Clim.* <https://doi.org/10.2166/wcc.2017.034>
- Gamfeldt L, Snäll T, Bagchi R, Jonsson M, Gustafsson L, Kjellander P, Ruiz-Jaen MC, Fröberg M, Stendahl J, Philipson CD, Mikusiński G, Andersson E, Westerglund B, Andrén H, Moberg F, Moen J, Bengtsson J (2013) Higher levels of multiple ecosystem services are found in forests with more tree species. *Nat Commun* 4(1). <https://doi.org/10.1038/ncomms2328>
- Gauquelin T, Michon G, Joffre R, Duponnois R, Génin D, Fady B, Bou Dagher-Kharrat M, Derridj A, Slimani S, Badri W et al (2018) Mediterranean forests, land use and climate change: a social-ecological perspective. *Reg Environ Chang* 18:623–636. <https://doi.org/10.1007/s10113-016-0994-3>
- Gavrilovic S (1970) Savremeni način I proračunavanja bujičnih nanosa I izrada karata erozije. In: *Erozija, bujičnitokoviirečninanos (Erosion, Torrents and Alluvial Deposits)*. Jugoslovenski komitet za međunarodnu hidrološku deceniju, Belgrade, pp 85–100 (in Serbian)
- Gavrilovic S (1972) Inženjering o bujičnim tokovima I eroziji (Engineering of Torrents and Erosion). *Izgradnja*, Belgrade, p 292 (in Serbian)
- Gavrilovic S (1988) The use of empirical method (erosion potential method) for calculating sediment production and transportation in unstudied or torrential streams. In: White WR (ed) *International conference on river regime*. Wiley, Chichester, pp 411–422
- Grafius DR, Corstanje R, Warren PH et al (2016) *Landscape Ecol* 31:1509. <https://doi.org/10.1007/s10980-015-0337-7>
- Graves J, Reavey D (1996) *Global environmental change: plants, animals and communities*. Publisher, Longman Pub Group
- Grimm NB, Staudinger MD, Staudt A, Carter SL, Chapin FS, Kareiva P, Ruckelshaus M, Stein B (2013) Climate change impacts on ecological systems: introduction to a US assessment. *Front Ecol Environ* 11:456–464. <https://doi.org/10.1890/120310>
- Hamel P, Chaplin-Kramer R, Sim S, Mueller C (2015) A new approach to modelling the sediment retention service (InVEST 3.0): Case study of the Cape Fear catchment, North Carolina, USA. *Sci Total Environ* 524–525:166–177. <https://doi.org/10.1016/j.scitotenv.2015.04.027>
- Harrison PA, Dunford RW, Holman IP, Cojocaru G, Madsen MS, Chen PY, Pedde S, Sandars D (2019) Differences between low-end and high-end climate change impacts in Europe across multiple sectors. *Reg Environ Chang.* <https://doi.org/10.1007/s10113-018-1352-4>
- Hernández-Morcillo M, Burgess P, Mirck J, Pantera A, Plieninger T (2018) Scanning agroforestry-based solutions for climate change mitigation and adaptation in Europe. *Environ Sci Policy* 80:44–52. ISSN 1462–9011. <https://doi.org/10.1016/j.envsci.2017.11.013>
- ICPDR (2018) Integrating and editing new scientific results in climate change research and the resulting impacts on water availability to revise the existing adaptation strategies in the Danube River basin. Department of Geography, Munich, Germany. https://www.icpdr.org/main/sites/default/files/nodes/documents/danube_climate_adaptation_study_2018.pdf. Accessed 15 April 2021
- Iglesias A, Avis K, Benzie M, Fisher P, Harley M, Hodgson N, Horrocks L, Moneo M, Webb J (2007) Adaptation to climate change in the agricultural sector. AEA Energy & Environment. Universidad de Politécnica Madrid. Report to EC-DG Agriculture and rural development, p 245. https://ec.europa.eu/info/sites/info/files/food-farming-fisheries/key_policies/documents/ext-study-adapt-climate-change-full-text_2007_en.pdf. Accessed 15 April 2021
- IPCC (2007) Summary for policymakers. In: Parry ML, Canziani OF, Palutikof JP, van der Linden PJ, Hanson CE (eds) *Climate change 2007: impacts, adaptation and vulnerability. Contribution of working group II to the fourth assessment report of the intergovernmental panel on climate change*. Cambridge University Press, Cambridge, UK, pp 7–22
- IPCC (2014) Summary for policymakers. In: Edenhofer O, Pichs-Madruga R, Sokona Y, Farahani E, Kadner S, Seyboth K, Adler A, Baum L, Brunner S, Eickemeier P, Kriemann B, Savolainen J, Schlömer S, von Stechow C, Zwickel T, Minx JC (eds) *Climate change 2014: mitigation of climate change. Contribution of working group III to the fifth assessment report of the intergovernmental panel on climate change*. Cambridge University Press, Cambridge, United Kingdom and New York, NY, USA
- Irvem A, Topaloglu F, Uygur V (2007) Estimating spatial distribution of soil loss over Seyhan river basin in Turkey. *J Hydrol* 336(1–2):30–37. <https://doi.org/10.1016/j.jhydrol.2006.12.009>
- Jactel H, Bauhus J, Boberg J, Bonal D, Castagneyrol B, Gardiner B, Gonzalez-Olabarria JR, Koricheva J, Meurisse N, Brockerhoff EG (2017) Tree diversity drives forest stand resistance to natural

- disturbances. *Current Forestry Reports* 3(3):223–243. <https://doi.org/10.1007/s40725-017-0064-1>
- Jones A, Stolbovov V, Rusco E et al (2009) Climate change in Europe. 2. Impact on soil. *A Rev Agron Sustain Dev* 29:423. <https://doi.org/10.1051/agro:2008067>
- Jovović A, Jovičić B (2017) Strategija komunikacije za oblast klimatskih promena. Misija OEBS-a u Srbiji. ISBN 978-86-6383-064-6
- Kadović R, Đurđević V, BelanovićSimić S, Todosijević M (2013) Regional climate model: impact of climate change for soil erosion and conservation in Central Serbia. In: International conference on water resources and climate change, “Jaroslav Cerni” Research Institute, Belgrade, p 138
- Kadović R (1999) Anti-erosion agrosystems, Faculty of Forestry, Belgrade. ISBN 86-7299-046-3 (in Serbian), p 454
- Khare D, Mondal A, Kundu S., Mishra PB (2016) Climate change impact on soil erosion in the Mandakini River Basin, North India. *Appl Water Sci*. <https://doi.org/10.1007/s13201-016-0419-y>
- Kirkby MJ, Irvine BJ, Jones RJA, Govers G, and PESERA team (2008) The PESERA coarse scale erosion model for Europe. Model rationale and implementation. *Eur J Soil Sc* 59(6):1293–1306
- Kirkby MJ, Jones RJA, Irvine B, Gobin A, Govers G, Cerdan O, Van Rompaey AJJ, Le Bissonnais Y, Daroussin J, King D, Montanarella L, Grimm M, Vieillefont V, Puigdefabregas J, Boer M, Kosmas C, Yassoglou N, Tsara M, Mantel S, Van Lynden GJ, Huting J (2004) European Soil Bureau Research Report No.16, EUR 21176, 18 pp. and 1 map in ISO B1 format. Office for Official Publications of the European Communities, Luxembourg
- Köppen W (1936) Das geographische system der Klimate. In: Köppen W, Geiger G (eds.) *Handbuch der Klimatologie*. I. C. Gebr, Borntraeger, pp 1–44
- Lal R, Delgado JA, Groffman PM, Millar N, Dell C, Rotz A (2011) Management to mitigate and adapt to climate change. *J Soil Water Conserv* 66:276–285. <https://doi.org/10.2489/jswc.66.4.276>
- Lexer MJ, Hoßnninger K, Scheifinger H, Matulla C, Groll N, Kromp-Kolb H, Schadauer K, Starlinger F, Englisch M (2002) The sensitivity of Austrian forests to scenarios of climatic change: a large-scale risk assessment based on a modified gap model and forest inventory data. *For Ecol Manage* 162:53–72. [https://doi.org/10.1016/S0378-1127\(02\)00050-6](https://doi.org/10.1016/S0378-1127(02)00050-6)
- Li Z, Fang H (2016) Impacts of climate change on water erosion: a review. *Earth-Sci Rev* 163:94–117. ISSN 0012–8252. <https://doi.org/10.1016/j.earscirev.2016.10.004>
- Lindner M, Maroschek M, Netherer S, Kremer A, Barbati A, Garcia Gonzalo J, Seidl R, Delzon S, Corona P, Kolström M, Lexer MJ, Marchetti M, (2010) Climate change impacts, adaptive capacity, and vulnerability of European forest ecosystems. *For Ecol Manage* 259:698–709. <https://doi.org/10.1016/j.foreco.2009.09.023>
- Litschert SE, Theobald DM, Brown TC (2014) Effects of climate change and wildfire on soil loss in the Southern Rockies Ecoregion. *CATENA* 118:206–219. <https://doi.org/10.1016/j.catena.2014.01.007>
- López-Moreno JI, Beniston M, García-Ruiz JM (2008) Environmental change and water management in the Pyrenees: facts and future perspectives for Mediterranean mountains. *Global Planet Chang* 61:300–312. <https://doi.org/10.1016/j.gloplacha.2007.10.004>
- López-Vicente M, Poesen J, Navas A, Gaspar L (2013) Predicting runoff and sediment connectivity and soil erosion by water for different land use scenarios in the Spanish Pre-Pyrenees. *CATENA* 10262–73. <https://doi.org/10.1016/j.catena.2011.01.001>
- Mihailovic DT, Dreskovic N, Arsenic I, Ciric V, Djurdjevic V, Mimic G, Pap I, Balaz I (2016) Impact of climate change on soil thermal and moisture regimes in Serbia: an analysis with data from regional climate simulations under SRES-A1B. *Sci Total Environ* 571:398–409. <https://doi.org/10.1016/j.scitotenv.2016.06.142>
- Mihailovic DT, Lalic B, Dreskovic N, Mimic G, Djurdjevic V, Jancic M (2015) Climate change effects on crop yields in Serbia and related shifts of Köppen climate zones under the SRES-A1B and SRES-A2. *Int J Climatol* 35:3320–3334. <https://doi.org/10.1002/joc.4209>
- Mišić V, Dinić A, Jovanović V, Kalinić M (1985) Specificity of woodland vegetation in southern Serbia in the area from Vranje to Preševo. Collection of papers from the Symposium “One hundred years of flora around Niš”, Niš: 73–80 (in Serbian)
- Morgan RPC, Quinton JN, Smith RE, Govers G, Poesen J, Auerswald K, Chisci G, Torri D, Styczen ME (1998) The European Soil Erosion Model (EUROSEM): a dynamic approach for predicting sediment transport from fields and small catchments. *Earth Surf Proc Land* 23(6):527–544
- Mullan D, Favis-Mortlock D, Fealy R (2012) Addressing key limitations associated with modelling soil erosion under the impacts of future climate change. *Agric Forest Meteorol* 156:18–30. ISSN 0168–1923. <https://doi.org/10.1016/j.agrformet.2011.12.004>
- Naipal V, Reick C, Pongratz J, Van Oost K (2015) Improving the global applicability of the RUSLE model—adjustment of the topographical and rainfall erosivity factors. *Geosci Model Dev* 8:2893–2913. <https://doi.org/10.5194/gmd-8-2893-2015>
- Nakicenovic N, Swart R (2000) Special report on emissions scenarios. In: A special report of working group III of the intergovernmental panel on climate change. Cambridge University Press, Cambridge, United Kingdom and New York, NY, USA, p 599
- Oliver TH, Morecroft MD (2014) Interactions between climate change and land use change on biodiversity: attribution problems, risks, and opportunities. *Wires Clim Change* 5:317–335. <https://doi.org/10.1002/wcc.271>

- On water eutrophication in Xiaojiang River basin. *J Soil Water Conserv* 24(4):31. <https://doi.org/10.1109/ICMSS.2010.5577555>
- Ortiz R, Sayre KD, Govaerts B, Gupta R, Subbarao GV, Ban T, Hodson D, Dixon JM, Ortiz-Monasterio JI, Reynolds M (2008) Climate change: can wheat beat the heat? *Agri Ecosys Environ* 126:46–58. <https://doi.org/10.1016/j.agee.2008.01.019>
- Panagos P, Ballabio C, Borrelli P, Meusburger K, Klik A, Rousseva S, Tadic MP, Michaelides S, Hrabalíková M, Olsen P, Aalto J, Lakatos M, Rymaszewicz A, Dumitrescu A, Beguería S, Alewell C (2015a) Rainfall erosivity in Europe. *Sci Total Environ* 511:801–814. <https://doi.org/10.1016/j.scitotenv.2015.01.008>
- Panagos P, Borrelli P, Poesen J, Ballabio C, Lugato E, Meusburger K, Montanarella L, Alewell C (2015b) The new assessment of soil loss by water erosion in Europe. *Environ Sci & Policy* 54:438–447. <https://doi.org/10.1016/j.envsci.2015.08.012>
- Panagos P, Ballabio C, Meusburger K, Spinoni J, Alewell C, Borrelli P (2017a) Towards estimates of future rainfall erosivity in Europe based on REDES and WorldClim datasets, *J Hydrol* 548:251–262. ISSN 0022–1694. <https://doi.org/10.1016/j.jhydrol.2017.03.006>
- Panagos P, Borrelli P, Meusburger K, Yu B, Klik A, Lim KJ, Yang JE, Ni J, Miao C, Chattopadhyay N, Sadeghi SH, Hazbavi Z, Zabihi M, Larionov GA, Krasnov SF, Garobets A, Levi Y, Erpul G, Birkel C, Hoyos N, Naipal V, Oliveira PTS, Bonilla CA, Meddi M, Nel W, Dashti H, Boni M, Diodato N, Van Oost K, Nearing MA, Ballabio C (2017b) Global rainfall erosivity assessment based on high-temporal resolution rainfall records. *Sci Rep* 7:4175. <https://doi.org/10.1038/s41598-017-04282-8>
- Pavlović P, Kostić N, Karadžić B, Mitrović M (2017) The soils of Serbia. Springer Science+Business Media Dordrecht. <https://doi.org/10.1007/978-94-017-8660-7>, PrintISBN978-94-017-8659-1, OnlineISBN978-94-017-8660-7
- Peng J, Tian L, Zhang Z, Zhao Y, Green S, Quine T, Liu H, Meersmans J (2020) Distinguishing the impacts of land use and climate change on ecosystem services in a karst landscape in China. *Ecosyst Serv* 46. <https://doi.org/10.1016/j.ecoser.2020.101199>
- Peñuelas J, Ogaya R, Boada MS, Jump A (2007) Migration, invasion and decline: changes in recruitment and forest structure in a warming-linked shift of European beech forest in Catalonia (NE Spain). *Ecography* 30:829–837. <https://doi.org/10.1111/j.2007.0906-7590.05247.x>
- Perović V, Djordjević A, Lj Z, Nikolić N, Kadović R, Belanović S (2012) Soil erosion modeling in the complex terrain of Pirot municipality. *Carpathian J Earth and Environ Sci* 7(2):93–100
- Perović V, Lj Z, Kadović R, Djordjević A, Jaramaz D, Mrvic V, Todorovic M (2013) Spatial modelling of soil erosion potential in a mountainous watershed of South-eastern Serbia. *Environ Earth Sci* 68(1):115–128. <https://doi.org/10.1007/s12665-012-1720-1>
- Perović V (2015) Assessment of soil erosion potential by application of USLE and PESERA models on the territory of Prvonek catchment. Doctoral Dissertation, University of Belgrade, Faculty of Forestry, UDC: 630*116.2/3:519.876.5 (497.11 Prvonek) (043.3)
- Perović V, Jaramaz D, Lj, Životić, Čakmak D, Mrvić V, Milanović M, Saljnikov E (2016) Design and implementation of webgis technologies in evaluation of erosion intensity in the municipality of NIS (Serbia). *Environ Earth Sci* 75:211–221. <https://doi.org/10.1007/s12665-015-4857-x>
- Perović V, Jakšić D, Jaramaz D, Koković N, Čakmak D, Mitrović M, Pavlović P (2018) Spatio-temporal analysis of land use/land cover change and its effects on the soil erosion (Case study in the Oplenac wine-growing district, Serbia). *Environ Monit Assess.* <https://doi.org/10.1007/s10661-018-7025-4>
- Perović V, Kadović R, Djurdjević V, Braunović S, Čakmak D, Mitrović M, Pavlović P (2019) Effects of changes in climate and land use on soil erosion: a case study of the Vranjska Valley. Serbia. *Reg Environ Change* 19:1035–1046. <https://doi.org/10.1007/s10113-018-1456-x>
- Perović V, Kadović R, Đurđević V, Pavlović D, Pavlović M, Čakmak D, Mitrović M, Pavlović P (2021) Major drivers of land degradation risk in Western Serbia: current trends and future scenarios. *Ecol Ind* 123. <https://doi.org/10.1016/j.ecolind.2021.107377>
- Pruski FF, Nearing MA (2002) Runoff and soil-loss responses to changes in precipitation: a computer simulation study. *J Soil Water Conserv* 57(1):7–16
- Rajković B, Vujadinovic M, Vukovic A (2013) Report on revisited climate change scenarios including review on applied statistical method for removing of systematic model errors, with maps of temperature, precipitation and required climate indices changes; Second national communication of the Republic of Serbia under the United Nations framework convention on climate change. MERZ, Belgrade, Serbia. <http://haos.ff.bg.ac.rs/climatedb-srb/>. Accessed 21 July 2018
- Reilly J (1997) Changement de climat, agriculture globale et vulnérabilité régionale. Chapitre 10 de Changement du Climat et Production Agricole: Effets Directs et Indirects du Changement des Processus Hydrologiques, Pédologiques et Physiologiques des Végétaux, FAO, Rome et Polytechnica, Paris. <http://www.fao.org/3/w5183f/w5183f0c.htm>. Accessed 15 April 2021
- Renard KG, Foster, GR, Weesies GA, McCool DK, Yoder DC (1997) Predicting soil erosion by water: a guide to conservation planning with the Revised Universal Soil Loss Equation (RUSLE). Agriculture Handbook No. 703. U.S. Department of Agriculture, Agricultural Research Service, Washington, District of Columbia, USA. https://www.ars.usda.gov/ARUserFiles/64080530/RUSLE/AH_703.pdf. Accessed 15 April 2021
- Ristić R, Dragović N, Stajić B, Radić B, Vulević T (2017) Overview of the natural resource management in the Republic of Serbia. In: Chapter B6, Natural resource management in Southeast Europe: forest, soil and

- water. Published by: Deutsche Gesellschaft für Internationale Zusammenarbeit (GIZ), GmbH. ISBN 978-608-4536-07-9
- Rodriguez-Lloveras X, Buytaert W, Benito G (2016) Land use can offset climate change induced increases in erosion in Mediterranean watersheds. *CATENA* 143. ISSN 244–255:0341–8162. <https://doi.org/10.1016/j.catena.2016.04.012>
- Routschek A, Schmidt J, Kreienkamp F (2014) Impact of climate change on soil erosion—a high-resolution projection on catchment scale until 2100 in Saxony/Germany. *CATENA* 121. ISSN 99-109:0341-8162. <https://doi.org/10.1016/j.catena.2014.04.019>
- Saljnikov E, Saljnikov A, Rahimgalieva S, Cakmak D, Kresovic M, Mrvic V, Dzhalankuzov T (2014) Impact of Energy Saving Cultivations on Soil Parameters in Northern Kazakhstan. 77:35–41. <https://doi.org/10.1016/j.energy.2014.03.042>
- Schirpke U, Kohler M, Leitinger G, Fontana V, Tasser E, Tappeiner U (2017) Future impacts of changing land-use and climate on ecosystem services of mountain grassland and their resilience. *Ecosyst Serv* 26. ISSN 79–94:2212–2416. <https://doi.org/10.1016/j.ecoser.2017.06.008>
- Serpa D, Nunes JP, Santos J, Sampaio E, Jacinto R, Veiga S, Lima JC, Moreira M, Corte-Real J, Keizer JJ, Abrantes N (2015) Impacts of climate and land use changes on the hydrological and erosion processes of two contrasting Mediterranean catchments. *Sci Total Environ* 538:64–77. ISSN 0048–9697. <https://doi.org/10.1016/j.scitotenv.2015.08.033>
- Sougnéz N, van Wesemael B, Vanacker V (2011) Low erosion rates measured for steep sparsely vegetated catchments in southeast Spain. *CATENA* 84(1–2):1–11. <https://doi.org/10.1016/j.catena.2010.08.010>
- Staudt A, Leidner AK, Howard J et al (2013) The added complications of climate change: understanding and managing biodiversity and ecosystems. *Front Ecol Environ* 11:494–501
- Stigter TY, Nunes JP, Pisani B, Fakir Y, Hugman R, Li Y, Tomé S, Ribeiro L, Samper J, Oliveira R, Monteiro JP, Silva A, Tavares PCF, Shapouri M, da Fonseca L, Cancela, El Himer H (2014) Comparative assessment of climate change and its impacts on three coastal aquifers in the Mediterranean. *Reg Environ Change* 14 (S1):41–56. <https://doi.org/10.1007/s10113-012-0377-3>
- SWCS (2003) Conservation implications of climate change: soil erosion and runoff from cropland. A Report from the Soil and Water Conservation Society, January 2003. Iowa
- Tayanc M, Im U, Dogruel M, Karaca M (2009) Climate change in Turkey for the last half century. *Clim Change* 94:483–502. <https://doi.org/10.1007/s10584-008-9511-0>
- Tomozeiu R, Stefan S, Busuioc A (2005) Winter precipitation variability and largescale circulation patterns in Romania. *Theoret Appl Climatol* 81:193–201. <https://doi.org/10.1007/s00704-004-0082-3>
- Torquebiau E, Tissier J, Grosclaude JV (2016) How climate change reshuffles the cards for agriculture. In: Torquebiau E (ed) *Climate change and agriculture worldwide*. Springer, pp 1–16. https://doi.org/10.1007/978-94-017-7462-8_1
- Van Oost K, Govers G, Desmet PJJ (2000) Evaluating the effects of changes in landscape structure on soil erosion by water and tillage. *Landscape Ecol* 15:577–589. <https://doi.org/10.1023/A:1008198215674>
- Van Rompaey A, Verstraeten G, Van Oost K, Govers G, Poesen J (2001) Modelling mean annual sediment yield using a distributed approach. *Earth Surf Proc Land* 26(11):1221–1236. <https://doi.org/10.1002/esp.275>
- Van Rompaey A, Bazzoffi P, Jones RJA, Montanarella L (2005) Modeling Sediment Yields in Italian Catchments *Geomorphology* 65:157–169. <https://doi.org/10.1016/j.geomorph.2004.08.006>
- Verheijen FGA, Jones RJA, Rickson RJ, Smith CJ, Bastos AC, Nunes JP, Keizer JJ (2012) Concise overview of European soil erosion research and evaluation. *Acta Agric Scand Sect B Soil Plant Sci* 62:185–190. <https://doi.org/10.1080/09064710.2012.697573>
- Vilà-Cabrera A, Coll L, Martínez-Vilalta J, Retana J (2018) Forest management for adaptation to climate change in the Mediterranean basin: a synthesis of evidence. *Forest Ecol Manage* 407:16–22. ISSN 0378-1127. <https://doi.org/10.1016/j.foreco.2017.10.021>
- Walther GR, Post E, Convey P, Menzel A, Parmesan C, Beebee TJ, Bairlein F (2002) Ecological responses to recent climate change. *Nature* 416 (6879), 389e395. <https://doi.org/10.1038/416389a>
- Ward PJ, van Balen RT, Verstraeten G, Renssen H, Vandenberghe J (2009) The impact of land use and climate change on late Holocene and future suspended sediment yield of the Meuse catchment. *Geomorphology* 103(3):389–400. <https://doi.org/10.1016/j.geomorph.2008.07.006>
- Wischmeier WH, Smith DD (1978) Predicting rainfall erosion losses: a guide to conservation planning. *Agriculture Handbook No. 537*. USDA/Science and Education Administration, US. Govt. Printing Office, Washington, DC. 58 pp.
- Yang D, Kanae S, Oki T, Koike T, Musiak K (2003) Global potential soil erosion with reference to land use and climate changes. *Hydrol Process* 17:2913–2928. <https://doi.org/10.1002/hyp.1441>
- Zabaleta A, Meaurio M, Ruiz E, Antigüedad I (2014) Simulation climate change impact on runoff and sediment yield in a small watershed in the Basque Country, Northern Spain. *J Environ Qual* 43:235–245. <https://doi.org/10.2134/jeq2012.0209>
- Zhang XC, Liu WZ, Li Z, Zheng FL (2009) Simulating site-specific impacts of climate change on soil erosion and surface hydrology in southern Loess Plateau of China. *CATENA* 79:237–242. <https://doi.org/10.1016/j.catena.2009.01.006>



Ground-Based Dust Deposition Monitoring in the Aral Sea Basin

9

Michael Groll, Christian Opp, Oleg Semenov,
Gulnura Issanova, and Alexander Shapov

Abstract

The ground-based monitoring of dust deposition is an essential tool for the long-term evaluation of the aeolian processes involved in sediment transport in arid regions. It offers valuable insights into the spatio-temporal dynamics of the dust distribution and grants access to the deposited material for further analyses. Central Asia in general and the Aral Sea Basin, in particular, is an arid region that largely contributed to the aeolian transport of dust from natural and anthropogenic sources over long distances. The shrinking Aral Sea itself has become a global symbol for the overexploitation of limited water resources. Its artificial desiccation has led to the emergence of a new salty desert, the Aralkum. Exposed to severe wind erosion, the lake bed sediments are transported over hundreds of kilometers as white sand and dust storms, negatively affect-

ing the Turan lowland surrounding the Aralkum. Passive dust deposition samplers were installed at 23 meteorological stations throughout the Turan lowland to monitor and evaluate the temporal and spatial dust dynamics between 2006 and 2012 and assess the grain size distribution, mineralogical and chemical properties of the deposited material. The dust deposition increased over time, which correlates with a decreasing trend in precipitation, increasing wind speeds, and a shift toward northern winds. More than 50% of all dust samples collected exceed the health-based deposition threshold, and the most intense dust storm events reached ground level deposition rates of up to 150 g m^{-2} per hour. The grain size analysis showed that most of the material deposited in 3 m height was part of the PM_5 group with average regional grain diameters between 0.0018 and 0.0129 mm. Coarser material was deposited in spring and summer throughout the study period. The average annual grain diameter increased from 0.0019 mm in 2006 to 0.0141 mm in 2012. Quartz, calcite, and dolomite were the main mineral components in the Central Asian dust samples, and the Aralkum and Karakum samples showed the most significant similarity. A slightly different composition characterized the Kyzylkum dust, but overall all Central Asian dust samples could easily be separated from dust samples from dust source regions in Asia. The

M. Groll (✉) · C. Opp
Department of Geography, University of Marburg,
Deutschhausstr. 10, 35037 Marburg, Germany
e-mail: mgroll@gmx.net

O. Semenov · A. Shapov
Kazakh Research Institute for Ecology and Climate
(KAZNIIIEK), Pr. Sejfulin 597, 480072 Almaty,
Kazakhstan

G. Issanova
Research Centre of Ecology and Environment of
Central Asia, 050060 Almaty, Kazakhstan

differences between the Central Asian dust sources are more pronounced on the level of their chemical composition. The Aralkum samples show a greater similarity to the samples from the Kyzylkum and samples collected in Central Xinjiang, Inner Mongolia, and the Western Sahara. Combining different analytical methods allows for a detailed characterization of the different dust source regions and can be used to track this dust over greater distances. This study showed the impact of the Aralkum, but also that the Kyzylkum is a far more active dust source. Concerning climate change and increasing aridity in the region, the aeolian dust transport will continue to increase, making a widespread monitoring program even more critical.

Keywords

Central Asia · Aral Sea · Aralkum · Desertification · Dust · Aeolian processes · Dust deposition · Grain size · Minerals · Chemical composition · Long-term monitoring

9.1 Introduction

Central Asia is a large, varied, and landlocked region in the Eurasian heartland, characterized by the high mountains of the Pamir and the Tian Shan as well as by the arid Turan lowland. Water, the most precious resource of this region, flows from the glaciated upper mountain regions (the Central Asian water towers) into the Aral Sea following two main paths—the Amudarya and the Syrdarya Rivers (Chub et al. 2002; Opp 2005). Over the centuries, these two rivers have led to the development of rich cultures in the land between both streams—the so-called Transoxania (=the land beyond the Oxus, which is an older name for the Amudarya) (Soucek 2000; Dukhovny and de Schutter 2011). Oases cities like Penjikent, Samarkand, Bukhara, or Khiva thrived due to the favorable continental climate, the abundance of water provided by the rivers, and their location along the Silk Road, connecting China to Constantinople (Soucek 2000;

Beckwith 2009). Irrigation farming has always played an essential role in this region as remnants of medieval water use infrastructure in the Aral Sea Basin, like sardobas, confirm still today (Dukhovny and de Schutter 2011; Khasanov 2016). The Soviet administration overturned the traditional equilibrium of resource availability and land use and the rapid expansion of the irrigation schemes in the Turan lowland (Matley 1970; Micklin 1988; Saiko and Zonn 2000) led to a wide range of ecological and socio-economic problems. Soil salinization and soil degradation (Saiko and Zonn 2000; Kitamura et al. 2006; Hbirkou et al. 2011; Kulmatov et al. 2018) feature prominently alongside water pollution (Kiyatkin et al. 1990; Aparin et al. 2006; Alihanov 2008; Kulmatov and Hojamberdiev 2010; Umarov 2013; Groll et al. 2015) and failing fisheries (Petr et al. 2004; Karimov et al. 2009; Groll et al. 2017). The overexploitation of the limited water resources is at the heart of this complex system failure. The desiccation of the Aral Sea itself, once the world's fourth-largest inland lake, has become a global symbol for the negative impacts of unsustainable resource management (Saiko and Zonn 2000; Opp 2005). Between the middle of the twentieth century and the present day, the Aral Sea surface area shrank from once 68,000 km² to roughly one-tenth (Micklin 1988, 2010, 2016; Dukhovny 2008), exposing more than 60,000 km² of lakebed sediments to severe wind erosion, forming a new desert, called the Aralkum (Indoitu et al. 2012; Groll et al. 2013). The Aral Sea has been a sink for the contents of the Amudarya and Syrdarya water—from suspended solids and heavy metals, to fertilizers, leached salts, and chemical waste products (Micklin 1988; Zetterström 1999; O'Hara et al. 2000; Wish-Wilson 2002; Wiggs et al. 2003; Létolle et al. 2005; Kulmatov and Hojamberdiev 2010). This cocktail of chemical compounds, deposited in the lake bed sediments for decades, has become accessible to the eroding forces of the wind, potentially mobilizing these pollutants and distributing them across a large region.

Analyzing these transport processes and monitoring their temporal and spatial dynamics is

an essential task for evaluating the impact the Aralkum dust can have on soils, agriculture, livestock, or human health. Due to the size (1.5 million km²) and inaccessibility of the Turan lowland and the harshness of the regional climate, remote sensing methods are the tool of choice for this type of monitoring (Washington et al. 2003; Orlovsky et al. 2005; Spivak et al. 2009, 2012; Indoitu et al. 2012, 2015; Issanova et al. 2015; Shen et al. 2016). But remote analytical methods can only go so far and need to be complemented by ground-based monitoring that can determine reliable data about measured deposition rates, grain size composition, and the mineralogical/chemical characterization of the deposited dust.

9.2 Study Design

Setting up and maintaining such a widespread network of monitoring sites is an ambitious task, and it took a large EU project (Central Asian Long-Term Ecological Research—CALTER) to implement it. The ground-based dust monitoring was just one aspect of the CALTER project, utilizing a total of 23 meteorological stations in Kazakhstan, Turkmenistan, and Uzbekistan (Fig. 9.1). The dust study presented here was also carried out closely with the UNESCO KHOREZM and the LUCA (Land Use and Human Welfare in Central Asia) projects (Manschadi et al. 2011; Opp et al. 2017) for an increased temporal scope of the data collection.

Monthly dust samples were collected between 2006 and 2012 in 3 m height, using passive deposition samplers of an inverted Frisbee design (Fig. 9.1). This kind of samplers has a long tradition in Central Asia, as they are reliable and easy to maintain (O'Hara et al. 2000; Tolkacheva 2000; Wiggs et al. 2003; Orlovsky et al. 2004). Additional samplers were installed and manually exposed specifically to collect dust material during dust storm events (defined by a visibility of less than 1 km). Supplemental measurement campaigns conducted during dust storms in the Kazakh part of the research area provided

additional information on the vertical dust profile between 0.25 and 16 m (Semenov 2011, 2012).

All collected dust samples were weighted, and prepared for further analyses. These included a grain size composition assessment using microscope diameter measurements, determining the mineral composition using wavelength dispersive X-ray diffraction (Debye and Scherrer 1916), and assessing the chemical composition of the dust samples using atomic absorption spectroscopy and X-ray fluorescence (Glocker and Schreiber 1928).

The resulting data sets were grouped by source region (see Fig. 9.1) and analyzed statistically using the meteorological parameters monthly mean air temperature, monthly total precipitation, monthly mean and max wind speed, and monthly dominant wind direction.

9.3 Results

9.3.1 Meteorological Characteristic

The Turan lowland is characterized by a highly continental and arid climate with hot summers (seasonal average: 28.2 °C; July: 29.0 °C) and cold winters (−3.6 °C; January: −7.1 °C). The average air temperature across all stations between 2006 and 2012 was 13.9 °C, with the Kyzylkum region having the highest average temperature (regional average: 15.0 °C; Beruniy: 16.2 °C). The Aralkum was characterized by the lowest average temperature (regional average: 11.9 °C; Jaslyk: 11.3 °C), caused by the mitigating effects of the (shrinking) water body of the lake. During the study period, the average air temperatures have shown no significant temperature trends. But, of course, the study period has been too short to observe long-term temperature trends thoroughly. Data from the Global Historical Climate Network (GHCN, www.ncdc.noaa.gov 2013) show a drastic increase in the average air temperature in the Turan lowland since the late nineteenth century. For instance, Jizzakh in Central Uzbekistan had a T_{avg} of 14.1 °C during the 1880s and 15.3 °C during the 2000s, while

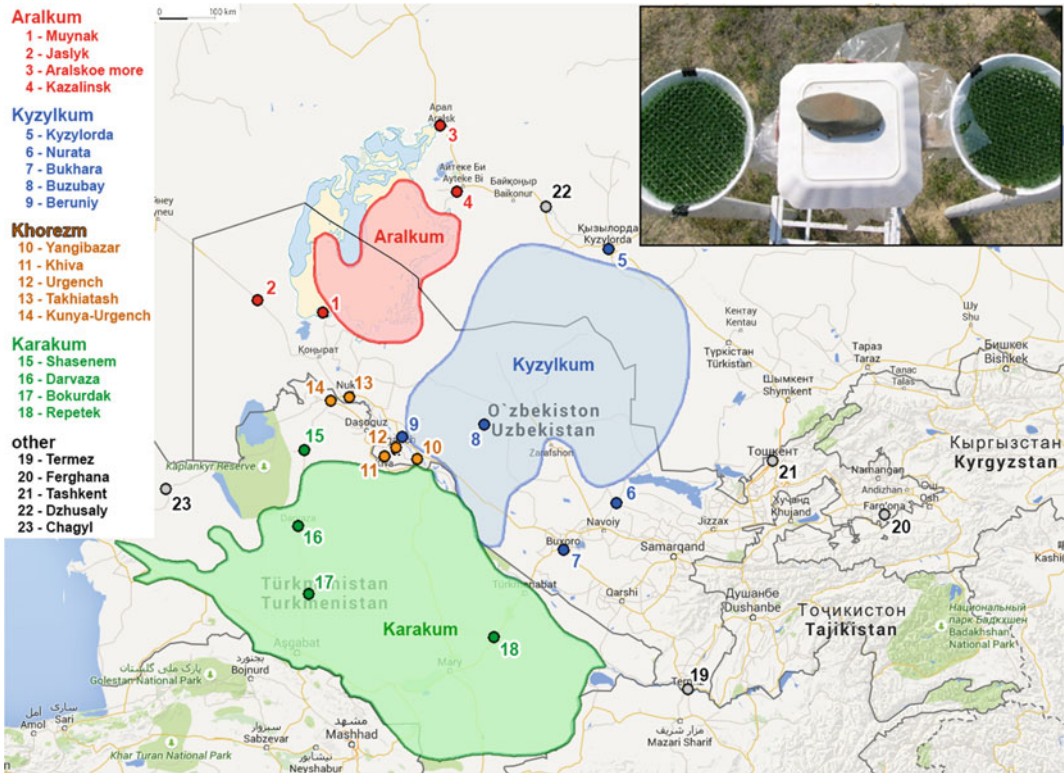


Fig. 9.1 Location of the dust samplers in the significant Central Asian dust sources (base map: Google Maps 2017; photo: Ch. Opp 2008)

Kazalinsk showed an increase from 7.8 to 9.8 °C during the same period. Close to the Aral Sea, the temperature increase was even more dramatic, even though the measurements do not reach back to the late nineteenth century. In Aralskoe More, at the shore of the small Aral in Kazakhstan, the average air temperature in the 1900s was 6.8 °C, and hundred years later, this average had risen to 9.23 °C. In Jaslyk and Muynak, the temperatures increased from 9.5 to 10.6 °C during the 1960s, to 11.3 and 12.4 °C during the study period of this project. This increase indicates that the desiccation of the Aral Sea since the 1970s enhances the upward temperature trend observable in the Turan lowland.

The average precipitation in the study area was 82.1 mm per year, with a maximum occurring during winter and spring (9.4 mm and 8.8 mm per month, respectively) (Opp et al. 2019). The months with the highest average

precipitation were March (10.7 mm) and November (9.9 mm). Summer months are particularly arid in the Turan lowland, with just 3.1 mm per month. A considerable decrease of the annual precipitation (from 109.3–66.5 mm) was detected during the study period. The rainfall distribution also showed a fundamental spatial component which ranged from 66 to 105 mm (for the Aralkum stations Muynak and Jaslyk) (Opp et al. 2019). Overall the Kyzylkum region was characterized by a higher precipitation than even the non-desert region Khorezm (94.1–79.8 mm).

The average wind speed data recorded at the meteorological stations showed a wide range from 0.6 m s⁻¹ in Yangibazar (Khorezm) to 8.2 m s⁻¹ in Buzubay (Kyzylkum). The overall average across all stations was 3.2 m s⁻¹ and showed low seasonal variability (from 2.2 m s⁻¹ in October to 4.4 m s⁻¹ in February and June)

(Opp et al. 2019). On the other hand, the inter-annual dynamic was considerable and ranged from 0.5 m s^{-1} in 2005 to 4.2 m s^{-1} in 2009, with a general trend of increasing wind speeds. This increase of the recorded wind speeds goes hand in hand with both the higher air temperature (leading to more intense air pressure gradients) and the lower precipitation (leading to reduced vegetation cover and surface roughness) (Albini 1981; Wasson and Nanninga 1986; Munson et al. 2011; Kim et al. 2017).

Across all stations and years from 2006 to 2010, 39.9% of all months were dominated by eastern winds, followed winds from the South and North (30.5% and 27.2%, respectively) (Opp et al. 2019). Western winds only occurred during 2.3% of all recorded months. But there were notable spatial differences within the Turan lowland: In the Karakum and Aralkum, eastern winds were dominant (73.3 and 68.8%) while winds from the South were hardly detected (Karakum: 0%; Aralkum: 2.1%). In Khorezm eastern winds were recorded less frequently than winds from the South (24.4–50.0%), and northern winds dominated the Kyzylkum (62.2%). The dominant wind direction at the stations shifted throughout the year. These shifts showed an undulating pattern with winds from southern directions being strongest during winter and autumn, while winds from the North were most frequent during winter and summer. Eastern winds dominated during spring and summer, while western winds were detected too infrequently for any pattern (Opp et al. 2019). The temporal pattern of the dominant wind directions also changed during the study time. Southern winds were considerably more frequent from 2006 to 2008, while the reverse was true for northern winds. This dynamic indicates larger spatial and temporal patterns of the regional circulation systems (up to the North Atlantic Oscillation; Aizen et al. 1997; Small et al. 1999; Lioubimtseva et al. 2005; Orlovsky et al. 2005; Chen et al. 2008; Li et al. 2008) affecting the study area.

9.3.2 Spatial and Temporal Dust Deposition Dynamics

The average dust deposition intensity across all 23 meteorological stations in the Turan lowland included in this study for 2006–2012 was 117.2 kg ha^{-1} per month, which equals 11.7 g m^{-2} per month (Opp et al. 2019). The highest average monthly deposition rate was detected in the Kyzylkum region with 247.7 kg ha^{-1} per month, or more than two times the Turan lowland average (Table 9.1). 52% of all samples collected in the Kyzylkum exceeded the long-term dust deposition threshold of 10.5 g m^{-2} per month. This threshold is based on clinical research and related to respiratory diseases (BMU 2002). The man-made Aralkum ranked second behind the Kyzylkum, with an average deposition intensity of 151.5 kg ha^{-1} per month and 45% of all samples exceeding the health threshold. The stations in the Karakum, the largest desert in the Aral Sea Basin, registered an average deposition rate of 125.2 kg ha^{-1} per month and a threshold excess of 40.5% (Table 9.1). But even though these values were much smaller than the ones measured in the other two dust source regions, the Karakum still is a significant dust source, especially as 0% of the samples collected there had a deposition rate of less than 10 kg ha^{-1} per month and only 10.8% of all monthly samples stayed below 25 kg ha^{-1} month. These values were much higher in the Kyzylkum and Aralkum (15.3 and 21.4% for the Kyzylkum and 10.8 and 26.7% for the Aralkum) and in the parts of the study area, which are no permanent dust sources (25.7 and 46.1% in Khorezm and 60.6 and 87.9% across all other stations). Khorezm was included as a separate region in this study as it is a densely populated and vital agricultural center in the lower Amu Darya River Basin. Due to its location between the three significant deserts in the Turan lowland, Khorezm is especially prone to the impacts of aeolian dust and is heavily affected by the Aral Sea desiccation. Khorezm showed the lowest

deposition intensity (60.9 kg ha^{-1} per month or 6.1 g m^{-2} per month) in the Turan lowland. Still, even here, more than one-fifth of all sampled months (21.3%) had to be considered potentially harmful for the respiratory system (Table 9.1). Comparing these four regions within the Turan lowland with the “other” meteorological stations included in this study (e.g., Tashkent or Fergana) shows that the aeolian dust processes are concentrated on the arid Central Asian lowlands (Opp et al. 2019). Stations closer to the mountainous eastern parts of Central Asia and those further away from the significant dust sources showed much lower dust deposition rates. Only 3% of all samples from these other parts of the Aral Sea Basin exceeded the health-based deposition threshold.

The temporal analysis of the dust samples showed that the dust deposition rate was highest during fall and spring (122.4 kg ha^{-1} per month and 115.1 kg ha^{-1} per month, respectively) and slightly lower during the summer and winter months (108.7 kg ha^{-1} per month and

110.3 kg ha^{-1} per month, respectively). However, the health threshold excess was elevated during the cold season (37% in winter and spring, compared to 27% in summer and fall; Table 9.1). This shows that even though the dust deposition follows seasonal patterns, the aeolian sediment transport is a fundamental problem throughout the year (Opp et al. 2019).

Between 2006 and 2012, the overall intensity of the dust transport increased from 108.4 kg ha^{-1} per month to 195.6 kg ha^{-1} per month (Table 9.1).

This increase in dust activity is closely related to the decrease of precipitation, the increase of the wind speed, and potentially the shift to northern wind directions discussed earlier. But the time frame of this deposition monitoring is too short to conclude a long-term trend from the detected increase of the dust deposition intensity or to pinpoint climate change or the desiccation of the Aral Sea as its reasons. Such analyses would require a much more extended sampling period.

Table 9.1 Summary of the regional and seasonal dust deposition distribution and grain size averages in the Turan lowland

All dust samples without dust storm events	Avg. dust deposition (kg ha^{-1} per month)	% of samples exceeding the health care threshold ($10.5 \text{ g m}^{-2} \text{ month}^{-1}$) (%)	Avg. grain size diameter (in mm)
Aralkum	151.5	45.0	0.0129
Karakum	125.2	40.5	0.0018
Kyzylkum	247.7	52.0	0.0142
Khorezm	60.9	21.3	0.0042
All data	117.2	34.8	0.0051
2006	108.4	38.7	0.0019
2007	42.2	13.6	0.0020
2008	61.1	7.4	0.0094
2009	89.2	21.8	0.0207
2010	155.4	45.8	0.0200
2011	168.6	55.9	0.0213
2012	195.6	50.8	0.0141
Spring	115.1	36.9	0.0065
Summer	108.7	27.7	0.0061
Fall	122.4	27.1	0.0035
Winter	110.3	36.8	0.0034

9.3.3 Grain Size Composition of the Dust Samples and the Vertical Dust Profile

The grain size analysis showed that the majority of the material deposited in 3 m height (85.8–97.6% in the four regions of the study area) was part of the PM₅ group (fine silt and clay particles; <0.0063 mm) and that the average grain diameter ranged between 0.0018 and 0.0129 mm (Table 9.1; Fig. 9.2). The Karakum is characterized by a unique and much finer grain size composition, while the other three regions are very similar to each other (Fig. 9.2). The grain size averages across all sampling sites also show a seasonal dynamic as the deposited material is coarser in spring and summer than in winter. Still, even in March, the percentage of PM₅ material remains above 80%. The average grain diameter increased from 0.0019 mm in 2006 to 0.0141 mm in 2012 (with a maximum of 0.0214 mm in 2011) throughout the study period. This increase coincides with the recorded increase of the wind speed (from 1.3 m s⁻¹ average wind speed during the first three years of the study period to 3.6 m s⁻¹ during the last three years) and the average dust deposition rate increase detected during the same period.

The dominance of PM₅ material in the deposited dust samples further emphasizes the adverse effects this dust can have on the respiratory system as such fine particles can effortlessly enter and damage human and animal lung tissue as well as plant stomata (St. Amand et al. 1986, Gill and Cahill 1991; Zetterström 1999; Arimoto 2001; Kunii et al. 2003; Wiggs et al. 2003; Létolle et al. 2005; Ochmann and Nowak 2009; McPherson 2012; Abuduwaili et al. 2015; Squires 2016; Hatami et al. 2017; Sett 2017; Kameswaran et al. 2019). But this PM₅ dominance is also just a snapshot, as the dust samples have been collected at 3 m height to minimize the effects of local dust transport. The actual dust deposition on the land surface differs from the samples collected at 3 m height considerably, as the analysis of samples collected during a dust storm event near Aralsk (Kazakhstan) in July

1983 reveals (Fig. 9.3). The dust data shows that the deposition of material in 3 m height is just 8.8% of the material deposited 0.25 m above ground. The most intense dust storm detected during the project duration was recorded in Buzubay in September of 2009 and with an hourly deposition intensity in 3 m height of 13.4 g m⁻² (Fig. 9.2), equal to approximately 150 g m⁻² per hour close to the ground surface. The grain size composition shows a similar vertical profile (Fig. 9.3), with the larger and heavier grains detected closer to the ground and the finer grains dominating in greater heights. The average of all dust samples collected in 3 m fits very well into this profile, with 77.5% of all grains belonging to the clay size class (<0.002 mm) and only 6.9% to the fine sand class (>0.063 mm) or larger. Following this data, the percentage of PM₅ dust material on the land surface would be closer to 20–25%, while more than one-third could be sand (>0.063 mm). And while sand is far less problematic for the respiratory system, it can, when mobilized during high wind speeds, lead to substantial damage to plants due to physical abrasion (Genis et al. 2013; Hagen and Casada 2013; Gonzales et al. 2017; Santra et al. 2017).

9.3.4 Mineralogical and Chemical Characterization of the Dust Samples

The mineral composition of the dust samples enables a primary regional differentiation of the Turan lowland as different geological formations characterize the other dust source regions. Dust from the Aralkum and the Karakum contained a very similar mineralogical spectrum. Quartz, calcite, and dolomite were detected in the samples of both areas in nearly identical percentages (25.2, 25.2, and 15.2% for a total of 65.59% in the Aralkum; 24.7, 24.7%, and 15.9% for a total of 65.24% in the Karakum). But there are differences as well. The Aralkum dust samples contain hardly any illite (0.56%) and showed the highest microcline concentration across all dust source regions (4.97%). The dust from the

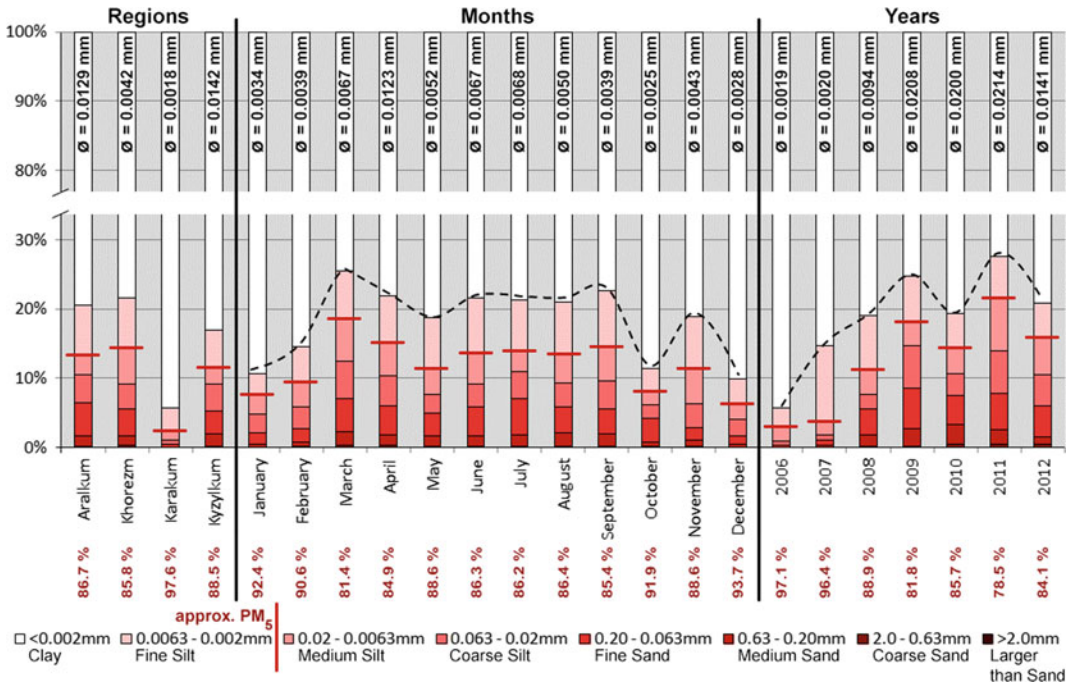


Fig. 9.2 Effect of the sampling height (from 25 cm to 16 m above ground) on dust deposition rate, grain size distribution, and mineralogical composition (data collected during a dust storm event near Aralsk in July 1983)

Karakum, on the other hand, contained only 1% orthoclase but the highest concentrations of albite (24.67%) and illite (3.84%). The Kyzylkum is characterized by a very different mineral composition with an even spread of quartz, calcite, albite, dolomite, and orthoclase. The two latter minerals were far more common (18.8% each) in the Kyzylkum samples than in the other regions, while quartz and calcite had the lowest percentages across all regions. The densely populated agricultural center Khorezm, located in-between the three deserts in this region, was characterized by the highest rates of quartz (34.5%) and calcite (29.3%) and the lowest values for dolomite (9.7%). Chinese dust samples analyzed by Feng et al. (2001) showed a similar mineralogical composition, with the samples from the Karakum and Aralkum regions being a very close match to the dust gathered in the Taklimakan desert (Luntai). Dust from Inner Mongolia and north-eastern China (Beijing), on the other hand, showed a very different characteristic (quartz + calcite + dolomite were at 52% and

48%, respectively). Thus, these results act as a mineralogical fingerprint, separating the Central Asian dust sources from other sources in Asia. But they also give insights into the health risk that this mineral composition poses in aeolian dust of mostly PM₅ size. Especially quartz, albite, and illite have a high potential of causing respiratory diseases (Oakes et al. 1982; Aranyi et al. 1983; Tursonov 1989; Osornio-Vargas et al. 1991; Dumortier et al. 1994; Seldén et al. 2001; Dai et al. 2008; Hussain et al. 2008; Taunton et al. 2010; Neghab et al. 2012; Tang et al. 2013; Garcia-Chevesich et al. 2014). These diseases are one of the leading health concerns in the Aral Sea region (especially in Karakalpakstan and Khorezm) (Tursunov 1989; O’Hara et al. 2000; Orlovsky et al. 2001; Chiba et al. 2003; Bennion et al. 2007; Kulmatov and Soliev 2009; Crighton et al. 2011).

Just as with the dust deposition rate and the grain size composition, the mineralogical characterization of the collected dust heavily depends on the sampling height, and the results discussed

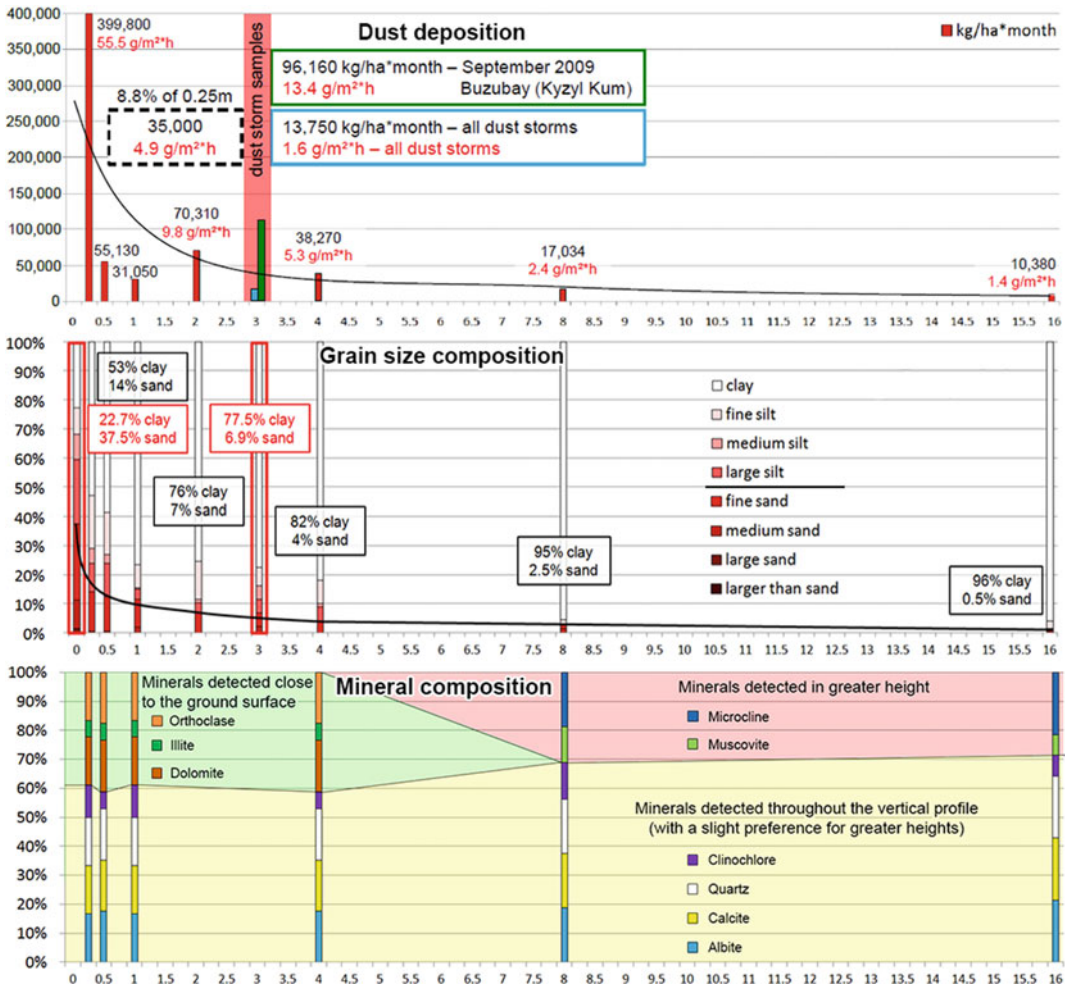


Fig. 9.3 Regional, monthly, and annual variability of the dust deposition sample grain size distribution, based on samples collected in 3 m height

here are only valid for dust samples collected at 3 m height. The mineralogical analysis of the 1983 dust storm samples (Fig. 9.3) showed that certain minerals (clinochlore, quartz, calcite, and albite) were evenly distributed across the vertical dust profile. But other minerals were only found closer to the ground (orthoclase, illite, and dolomite) or in greater heights (microcline and muscovite). This distribution is directly related to the density of the detected minerals. The minerals only found near the ground have an average density of 2.798 g m^{-3} . In comparison, the evenly distributed group has a density of 2.662 g m^{-3} , and the minerals found only in

greater heights have an average density of 2.601 g m^{-3} .

The mineral composition of the Central Asian dust samples results reveal that SiO_2 is the most common compound detected (on average 56.3%), followed by CaO (8.86%) and Al_2O_3 (7.8%). And while the mineralogical characterization of the Aralkum showed the most significant similarity to the Karakum, the analysis of the chemical composition groups the Aralkum and the Kyzylkum together. Both were characterized by above-average concentrations of SiO_2 (60.1% and 61.4%, respectively) and CaO (11.7% and 13.4%, respectively), while the

Karakum samples showed above-average concentrations of Al_2O_3 (8.7%) and below-average concentrations of CaO (6.4%). More pronounced differences were detected in the minor compounds and the trace elements. The Aralkum dust samples, for instance, were characterized by a much higher concentration of SO_3^{2-} compared to the Karakum and Kyzylkum (2,365 ppm vs. 232 and 512 ppm). Khorezm also showed a high value for SO_3^{2-} (1,681 ppm) and had the highest concentration of P_2O_5 (1,857 ppm compared to 1,074 ppm in the Aralkum, 866 ppm in the Karakum, and 465 ppm in the Kyzylkum). The high concentrations of phosphor in Khorezm and the Aralkum samples reflect the strong anthropogenic impact of local agricultural dust sources (Khorezm) and the accumulation of agrochemicals in the Aral Sea sediments.

Comparing the mineralogical composition of the collected dust samples with results from other studies is a valuable tool for a first regional fingerprinting of the dust origin. Still, this kind of analysis delivers far more accurate and reliable results on the level of chemical compounds. For that step, the following ratios were calculated and compared to data from other dust sources: $\text{K}_2\text{O}/\text{SiO}_2$ (K/S-Ratio); $\text{SiO}_2/\text{Al}_2\text{O}_3$ (S/A-Ratio); $\text{K}_2\text{O}/\text{Al}_2\text{O}_3$ (K/A-Ratio); $(\text{Na}_2\text{O} + \text{K}_2\text{O})/\text{SiO}_2$ (NK/S-Ratio). Khorezm and the Karakum showed very similar results for the first three ratios (K/S: 0.0301 and 0.0305; S/A: 6.74 and 6.6; K/A: 0.2031 and 0.2012), indicating a robust chemical connection, either due to similar geology or because of a more substantial influence of dust from the Karakum and the nearby exposed floodplain of the Amu Darya on Khorezm. The samples from these two regions were also comparable to Central Xinjiang, Inner Mongolia, and the Western Sahara (Feng et al. 2001; Moreno et al. 2006). The Aralkum dust samples, on the other hand, were closer to the Kyzylkum samples and these two regions shared similarities with dust collected in Midwestern and Central China as well as with Southern Xinjiang (Feng et al. 2001; Ta et al. 2003).

These results show that the four regions included in this study, even though they are close to each other, are exposed to the same climate,

and have a similar geological background, show distinct differences in the collected dust samples. These reflect general physical characteristics (e.g., the much smaller average grain diameter in the Karakum) and anthropogenic influences (e.g., concentrations of phosphor in Khorezm and the Aralkum). These differences result in a unique fingerprint for each region. These fingerprints can be used to trace the dust from the three primary dust sources in the Turan lowland—the Karakum, the Kyzylkum, and the Aralkum. Continuing this long-term ground-based dust monitoring research would allow a more accurate assessment of the often proclaimed health risk related to dust from the Aralkum.

9.4 Conclusion

The meteorological results show an increase in the mean air temperature and wind speed, while the annual precipitation decreased during this study. This decrease led to an increase in the average monthly dust deposition rates and the average grain size of the deposited material throughout the Aral Sea Basin. Overall the dust deposited in the passive collectors was dominated by fine grains (clay and fine silt = PM_{10}) and consisted mainly of quartz, calcite, albite, and dolomite. In its mineralogical composition, the dust collected in the Turan lowland shared certain similarities with dust from Northwestern China (Taklamakan, Kunlun), but also to Midwestern China, Inner Mongolia, and even the Western Sahara. However, the four regions within the Turan lowland analyzed in this study showed distinctive temporal, physical, and chemical differences based on their geology, vicinity to each other, and location within the Central Asian atmospheric circulation system. As an emerging new dust source, the Aral Kum showed the fastest increase of the deposition rates and at times surpassed the Kyzylkum as the primary dust source in the Aral Sea Basin. With the expected reduction of water availability and the continuously growing demand for water in the Aral Sea Basin, the Aral Kum is here to stay and will continue to affect the western part of the

Turan lowland. Based on the mineralogical and chemical composition of the Aral Sea lakebed sediments, continued long-term monitoring not only of the aeolian transport of these mobilized sediments but also of their impacts on human health, livestock, and arable land is strongly advised, as only the detailed knowledge about the quantity and quality of the dust and its spatial and temporal dynamic can provide the means to mitigate its adverse effects.

References

- Abuduwaili J, Zhaoyong Z, Qing J, Wei L (2015) The disastrous effects of salt dust deposition on cotton leaf photosynthesis and the cell physiological properties in the Ebinur basin in Northwest China. *PLoS ONE* 10 (5):24, e0124546. <https://doi.org/10.1371/journal.pone.0124546>
- Aizen V, Aizen E, Melack J, Dozier J (1997) Climatic and hydrologic changes in the Tien Shan Central Asia. *J Clim* 10:1393–1404. [https://doi.org/10.1175/1520-0442\(1997\)010%3c1393:CAHCIT%3e2.0.CO;2](https://doi.org/10.1175/1520-0442(1997)010%3c1393:CAHCIT%3e2.0.CO;2)
- Albini F (1981) A phenomenological model for wind speed and shear stress profiles in vegetation cover layers. *J Applied Meteor* 20:1325–1335. <https://www.jstor.org/stable/26180303>
- Alihanov B (2008) About a condition of environment and use of natural resources in Republic of Uzbekistan (The Retrospective Analysis for 1988–2007). National Report of the State Committee for Nature Protection of the Republic of Uzbekistan, Tashkent (Алиханов Б. О состоянии окружающей среды и использовании природных ресурсов в Республике Узбекистан (ретроспективный анализ за 1988–2007 гг.). Национальный отчет Государственного комитета по охране природы Республики Узбекистан, Ташкент) (in Russian)
- Aparin V, Kawabata Y, Ko S, Shiraishi K, Nagai M, Yamamoto M, Katayama Y (2006) Evaluation of geocological status and anthropogenic impact on the Central Kyzylkum Desert (Uzbekistan). *J Arid Land Stud* 15:129–133. <https://ci.nii.ac.jp/naid/10017555932/en/>
- Aranyi C, Graf JL, O'Shea WJ, Graham JA, Miller FJ (1983) The effects of intratracheally administered coarse mode particles on respiratory tract infection in mice. *Toxicol Lett* 19:63–72. [https://doi.org/10.1016/0378-4274\(83\)90263-1](https://doi.org/10.1016/0378-4274(83)90263-1)
- Arimoto R (2001) Eolian dust and climate – relationships to source, tropospheric chemistry, transport and deposition. *Earth Sci Rev* 54:29–42. [https://doi.org/10.1016/S0012-8252\(01\)00040-X](https://doi.org/10.1016/S0012-8252(01)00040-X)
- Beckwith C (2009) *Empires of the silk road—a history of Central Eurasia from the Bronze Age to the present*. Princeton University Press, 472 pp.
- Bennion P, Hubbard R, O'Hara S, Wiggs G, Wegerdt J, Lewis S, Small I, van der Meer J, Upshur R (2007) The impact of airborne dust on respiratory health in children living in the Aral Sea region. *Int'l J Epidemiol* 36:1103–1110. <https://doi.org/10.1093/ije/dym195>
- BMU – Bundesministerium für Umwelt, Naturschutz und Reaktorsicherheit (2002) Erste Allgemeine Verwaltungsvorschrift zum Bundes- Immissionsschutzgesetz (Technische Anleitung zur Reinhaltung der Luft – TA Luft) vom 24. Juli 2002 (first common regulation for the federal immission protection law (technical regulation air), issued on the 24th of July 2002 by the German federal ministry for environment, nature protection and reactor safety). *Gemeinsames Ministerialblatt* vom 30. Juli 2002 (25–29) Cologne:511–605
- Chen F, Yu Z, Yang M, Ito E, Wang S, Madsen D, Huang X, Zhao Y, Sato T, Birks H, Boomer I, Chen J, Chengbang A, Wünnemann B (2008) Holocene moisture evolution in arid Central Asia and its out-of-phase relationship with Asian monsoon history. *Quar Sci Rev* 27:351–364. <https://doi.org/10.1016/j.quascirev.2007.10.017>
- Chiba M, Caypil W, Inaba Y (2003) Environmental disruption and human health—reduction of the Aral Sea and the resident's health problem. *Trans Biomed Health* 7:163–169. <https://doi.org/10.2495/EHR030171>
- Chub V, Agaltseva S, Myagkrov S (2002) Climate change impact on the rivers runoff for the Central Asian River. In: Proceedings of the international conference on hydrology and watershed management with the focal theme on water quality and conservation, vol 2, pp 252–257. <https://www.tib.eu/en/search/id/BLCP:CN051398323/Climate-Change-Impact-on-the-Rivers-Runoff-for?cHash=d40881ffcad01f2296be4d236d2fde4d>
- Crighton EJ, Barwin L, Small I, Upshur R (2011) What have we learned? A review of the literature on children's health and the environment in the Aral Sea area. *Int'l J Public Health* 56:125–138. <https://doi.org/10.1007/s00038-010-0201-0>
- Dai S, Tian L, Chou C-L, Zhou Y, Zhang M, Zhao L, Wang J, Yang Z, Cao H, Ren D (2008) Mineralogical and compositional characteristics of late Permian coals from an area of high lung cancer rate in Xuan Wei, Yunnan, China—occurrence and origin of quartz and chamosite. *Int'l J Coal Geol* 76:318–327. <https://doi.org/10.1016/j.coal.2008.09.001>
- Debye P, Scherrer P (1916) Interferenzen an regellos orientierten Teilchen im Röntgenlicht (Interference on Unaligned Particles in X-Rays). *Nachrichten von der Gesellschaft der Wissenschaften Göttingen*, 1–15
- Dukhovny V (ed) (2008) *Comprehensive remote sensing and ground based studies of the dried Aral Sea bed*. SIC ICWC, Tashkent, 173 pp.

- Dukhovny V, de Schutter J (2011) *Water in Central Asia—past, present, future*. CRC Press/Balkema, 408 pp.
- Dumortier P, de Vuyst P, Yernault JC (1994) Comparative analysis of inhaled particles contained in human bronchoalveolar lavage fluids, lung parenchyma and lymph nodes. *Environ Health Perspect* 102(5):257–259. <https://doi.org/10.1289/ehp.94102s5257>
- Feng Q, Endo KN, Cheng GD (2001) Dust storms in China—a case study of dust storm variation and dust characteristics. *Bull Eng Geol Env* 61:253–261. <https://doi.org/10.1007/s10064-001-0145-y>
- García-Chevesich PA, Alvarado S, Neary DG, Valdes R, Valdes J, Aguirre JJ, Mena M, Pizarro R, Jofré R, Vera M, Olivares C (2014) Respiratory disease and particulate air pollution in Santiago Chile—contribution of erosion particles from fine sediment. *Environ Poll* 187:202–205. <https://doi.org/10.1016/j.envpol.2013.12.028>
- Genis A, Vulfson L, Ben-Asher J (2013) Combating wind erosion of sandy soils and crop damage in the coastal deserts—wind tunnel experiments. *Aeol Res* 9:69–73. <https://doi.org/10.1016/j.aeolia.2012.08.006>
- Gill T, Cahill T (1991) Playa-generated dust storms from Owens lake. In: Hall C, Doyle-Jones V, Widawski B (eds) (1991) *WMRS symposium volume 4—the history of water: Eastern Sierra Nevada, Owens Valley, White-Inyo Mountains*, pp 63–73
- Glocker R, Schreiber H (1928) Quantitative Röntgenspektralanalyse mit Kalterregung des Spektrums (quantitative X-ray spectral analysis through cold stimulation of the spectrum). *Ann Phys* 390:1089–1102
- Gonzales HB, Casada ME, Hagen LJ, Tatarko J, Maghirang RG (2017) Sand transport and abrasion within simulated standing vegetation. *Trans ASABE* 60(3):791–802
- Google Maps (2017) Topographical map of Central Asia. www.google.com/maps. Accessed 15 Dec 2017
- Groll M, Opp C, Aslanov I (2013) Spatial and temporal distribution of the dust deposition in Central Asia—results from a long term monitoring program. *Aeol Res* 9:49–62. <https://doi.org/10.1016/j.aeolia.2012.08.002>
- Groll M, Opp C, Kulmatov R, Ikramova M, Normatov I (2015) Water quality, potential conflicts and solutions—an upstreamdownstream analysis of the transnational Zarafshan River (Tajikistan, Uzbekistan). *Environ Earth Sci* 73:743–763. <https://doi.org/10.1007/s12665-013-2988-5>
- Groll M, Kulmatov R, Mullabaev N, Opp C, Kulmatova D (2017) Rise and decline of the fishery industry in the Aydarkul-Arnasay Lake System (Uzbekistan)—effects of reservoir management, irrigation farming and climate change on an unstable ecosystem. *Environ Earth Sci* 75:921. <https://doi.org/10.1007/s12665-016-5691-5>
- GHCN (2013) www.ncdc.noaa.gov The Global historical climate network database. <http://www.ncdc.noaa.gov/oa/climate/ghcndaily/> Accessed 12 Feb 2013
- Hagen LJ, Casada ME (2013) Effect of canopy leaf distribution on sand transport and abrasion energy. *Aeol Res* 10:37–42. <https://doi.org/10.1016/j.aeolia.2013.01.005>
- Hatami Z, Moghaddam P, Rashki A, Mahallati M, Khaniani B (2017) Effects of dust deposition from two major dust source regions of Iran on wheat (*triticum aestivum* L.) production. *Int’l J Environ Stud* 74(6):991–1000. <https://doi.org/10.1080/00207233.2017.1356630>
- Hbirkou C, Martius C, Khamzina A, Lamers J, Welp G, Amelung W (2011) Reducing topsoil salinity and raising carbon stocks through afforestation in Khorazm, Uzbekistan. *J Arid Environ* 75:146–155. <https://doi.org/10.1016/j.jaridenv.2010.09.018>
- Hussain MY, Yousuf M, Islam-ud-Din IM (2008) A pollutant of environment—qualification, quantification and characterization of airborne particulates. *Pakistan J Agric Sci* 45(1):116–118
- Indoitu R, Orlovsky L, Orlovsky N (2012) Dust storms in Central Asia—spatial and temporal variations. *J Arid Environ* 85:62–70. <https://doi.org/10.1016/j.jaridenv.2012.03.018>
- Indoitu R, Kozhoridze G, Batyrbaeva M, Vitkovskaya I, Orlovsky N, Blumberg D, Orlovsky L (2015) Dust emission and environmental changes in the dried bottom of the Aral Sea. *Aeolian Res* 17:101–115. <https://doi.org/10.1016/j.aeolia.2015.02.004>
- Issanova G, Abuduwaili J, Kaldybayev A, Semenov O (2015) Dedova T (2015) Dust storms in Kazakhstan—frequency and division. *J Geol Soc Ind* 3:348–358. <https://doi.org/10.1007/s12594-015-0224-5>
- Kameswaran S, Gunavathi Y, Krishna P (2019) Dust pollution and its influence on vegetation—a critical analysis. *Res J Life Sci, Bioinform, Pharmac Chem Sci* 5(1):341–363. <http://www.rjlbpcsc.com/article-pdf-downloads/2019/24/487.pdf>
- Karimov B, Kamilov B, Upare M, van Anrooy R, Bueno P, Shokhimardonov D (2009) *Inland capture fisheries and aquaculture in the Republic of Uzbekistan—current status and planning*. FAO Fisheries and Aquaculture Circular No. 1030/1, SEC/C1030/1, Rome:124 pp.
- Khasanov A (2016) About several infrastructure constructions of the Great Silk Road. *Int’l J Innov Sci Eng Technol* 3(6):295–299. http://ijiset.com/vol3/v3s6/IJISSET_V3_I6_40.pdf
- Kim D, Chin M, Remer L, Diehl T, Bian H, Yu H, Brown M, Stockwell W (2017) Role of surface wind and vegetation cover in multi-decadal variations of dust emission in the Sahara and Sahel. *Atmos Environ* 148:282–296. <http://www.sciencedirect.com/science/article/pii/S1352231016308585?via%3Dihub>

- Kiyatkin A, Shaporenko S, Sanin M (1990) Water and salt regime of the Arnasai Lakes. *Gidrotekhnicheskoe Stroitel'stvo* 3:172–177 (Кияткин А, Шапоренко С, Санин М. Водно-солевой режим Арнасайских озер. *Гидротехническое строительство* 3:172–177)
- Kitamura Y, Yano T, Honna T, Yamamoto S, Inosako K (2006) Causes of farmland salinization and remedial measures in the Aral Sea basin—research on water management to prevent secondary salinization in rice-based cropping system in arid land. *Agric Water Manag* 85:1–14. <https://doi.org/10.1016/j.agwat.2006.03.007>
- Kulmatov R, Hojamberdiev M (2010) Speciation analyses of heavy metals in the transboundary Rivers of Aral Sea basin: Amudarya and Syrdarya rivers. *J Environ Sci Eng* 4(8):36–45
- Kulmatov R, Soliev I (2009) The crisis of Aral Sea and health of the population in the disaster zone. In: *Proceedings of the 13th World Lake conference*, p 10
- Kulmatov R, Groll M, Rasulov A, Soliev I, Romic M (2018) Status quo and present challenges of the sustainable use and management of water and land resources in Central Asia irrigation zones—the example of the Navoi region (Uzbekistan). *Quat Int* 464:396–410. <https://doi.org/10.1016/j.quaint.2017.11.043>
- Kunii O, Hashizume M, Chiba M, Sasaki S, Shimoda T, Caypi I, Dauletbaev D, (2003) Respiratory symptoms and pulmonary function among school-age children in the Aral Sea region. *Arch Environ Health* 58:676–682. <https://doi.org/10.3200/AEOH.58.11.676-682>
- Létolle R, Aladin N, Filipov I, Boroffka N (2005) The future chemical evolution of the Aral Sea from 2000 to the years 2050. *Mitig Adap Strat Global Change* 10:51–70. <https://doi.org/10.1007/s11027-005-7830-2>
- Li J, Yu R, Zhou T (2008) Teleconnection between NAO and climate downstream of the Tibetan plateau. *J Clim* 21:4680–4690. <https://doi.org/10.1175/2008JCLI2053.1>
- Lioubimtseva E, Cole R, Adams J, Kapustin G (2005) Impacts of climate and land-cover changes in arid lands of Central Asia. *J Arid Environ* 62:285–308. <https://doi.org/10.1016/j.jaridenv.2004.11.005>
- Manschadi A, Lamers J, Conrad C, Khamzina A, Tischbein B, Hassan M, Djanibekov N, Franz J, Rücker G, Kuzmits B, van der Veen A, Vlek P (2011) Economic and ecological restructuring of land and water use in the region Khorezm—status report—ZEF/UNESCO project phase III (2007–2011), p 16. https://www.zef.de/fileadmin/webfiles/downloads/projects/khorezm/downloads/Publications/wps/ZEF-UZ-WP01_proposal.pdf
- Matley I (1970) The Golodnaya steppe—a Russian irrigation venture in Central Asia. *Geogr. Rev* 60 (3):328–346. <https://www.jstor.org/stable/214037>
- McPherson M (2012) Subsurface ventilation engineering—Chapter 19—the hazardous nature of dusts, online publication. <http://www.mvsengineering.com>. Accessed 15 Apr 2012
- Micklin P (1988) Desiccation of the Aral Sea—a water management disaster in the Soviet Union. *Science* 241:1170–1176. <https://doi.org/10.1126/science.241.4870.1170>
- Micklin P (2010) The past, present, and future Aral Sea. *Lakes Reserv Res Manag* 15:193–213. <https://doi.org/10.1111/j.1440-1770.2010.00437.x>
- Micklin P (2016) The future Aral Sea—hope and despair. *Environ Earth Sci* 75:844. <https://doi.org/10.1007/s12665-016-5614-5>
- Moreno T, Querol X, Castillo S, Alastuey A, Cuevas E, Herrmann L, Mounkaila M, Elvira J, Gibbons W (2006) Geochemical variations in Aeolian mineral particles from the Sahara-Sahel dust corridor. *Chemosphere* 65:261–270. <https://doi.org/10.1016/j.chemosphere.2006.02.052>
- Munson S, Belnap J, Okin G (2011) Responses of wind erosion to climate-induced vegetation changes on the Colorado Plateau. *PNAS* 108(10):3854–3859. <https://doi.org/10.1073/pnas.1014947108>
- Neghab M, Abedini R, Soltanzadeh A, Kashkooli AI, Ghayoomi SMA (2012) Respiratory disorders associated with heavy inhalation exposure to dolomite dust. *Iranian Red Crescent Med J* 14(9):549–557. PMID: 23115717; PMCID: PMC3482327
- Oakes D, Knight DK, Wusteman M, McDonald JC (1982) Respiratory effects of prolonged exposure to gypsum dust. *Ann Occup Hyg* 26(1–4):833–840 PMID: 7181310
- Ochmann U, Nowak D (2009) Inhalationsbedingte chemische Lungenschädigung (Inhalation-induced chemical pulmonary damage). *Pneumologie* 6:22–29. <https://doi.org/10.1007/s10405-008-0229-5>
- O'Hara S, Wiggs G, Mamedov B, Davidson G, Hubbard R (2000) Exposure to airborne dust contaminated with pesticide in the Aral Sea region. *Lancet* 355 (9204):627–628. [https://doi.org/10.1016/S0140-6736\(99\)04753-4](https://doi.org/10.1016/S0140-6736(99)04753-4)
- Opp C (2005) Desertification in Uzbekistan. *Geographische Rundschau International Edition* 1(2):12–20. https://www.researchgate.net/publication/303244313_Desertification_in_Uzbekistan
- Opp C, Groll M, Aslanov I, Lotz T, Vereshagina N (2017) Aeolian dust deposition in the southern Aral Sea region (Uzbekistan)—ground-based monitoring results from the LUCA project. *Quatern Int* 429:86–99. <https://doi.org/10.1016/j.quaint.2015.12.103>
- Opp C, Groll M, Semenov O, Vereshagina N, Khamzina A (2019) Impact of the Aral Sea syndrome—the Aralkum as a man—made dust source. *E3S Web of Conference* 99 (2019) 03003. <https://doi.org/10.1051/e3sconf/20199903003>
- Orlovsky N, Radzinsky V, Orlovsky L (2001) Desertification and population health in the Turkmenistan part of the Aral Sea region. *Trans Biomed Health* 5:267–276. <https://www.witpress.com/library/wit-transactions-on-biomedicine-and-health/5/3801>
- Orlovsky L, Tolkacheva G, Orlovsky N, Mamedov B (2004) Dust storms as a factor of atmospheric air

- pollution in the Aral Sea basin. *Air Poll* 12:353–362. <https://www.witpress.com/elib/transaction-on-ecology-and-the-environment/74/12460>
- Orlovsky L, Orlovsky N, Durdyyev A (2005) Dust storms in Turkmenistan. *J Arid Environ* 60:83–97. <https://doi.org/10.1016/j.jaridenv.2004.02.008>
- Osornio-Vargas AR, Hernández-Rodríguez NA, Yáñez-Buruel AG, Ussler W, Overby LH, Brody AR (1991) Lung cell toxicity experimentally induced by a mixed dust from Mexicali, Baja California, Mexico. *Environ Res* 56:31–47. [https://doi.org/10.1016/S0013-9351\(05\)80107-0](https://doi.org/10.1016/S0013-9351(05)80107-0)
- Petr T, Ismukhanov K, Kamilov B, Umarov P (2004) Irrigation systems and their fisheries in the Aral Sea Basin, Central Asia. In: Robin L, Petr T (eds) Sustaining livelihoods and biodiversity in the new millennium. Proceedings of the FAO and Mekong River commission conference, 11.-14.02.2003, Phnom Penh. RAP Publication 17/2004, 27pp, <http://www.fao.org/3/ad526e0i.htm#bm18>
- Saiko T, Zonn I (2000) Irrigation expansion and dynamics of desertification in the Circum-Aral region of Central Asia. *Appl Geogr* 20:349–367. [https://doi.org/10.1016/S0143-6228\(00\)00014-X](https://doi.org/10.1016/S0143-6228(00)00014-X)
- Santra P, Moharana PC, Kumar M, Soni ML, Pandey CB, Chaudhari SK, Sikka AK (2017) Crop production and economic loss due to wind erosion in hot arid ecosystem of India. *Aeol Res* 28:71–82. <https://doi.org/10.1016/j.aeolia.2017.07.009>
- Seldén AI, Berg NP, Lundgren EAL, Hillerdal G, Wik NG, Ohlson C-G, Bodin LS (2001) Exposure to tremolite asbestos and respiratory health in Swedish dolomite workers. *Occup Environ Med* 58:670–677. <https://www.jstor.org/stable/27731569>
- Semenov O (2011) Introduction to the experimental Meteorology and Climatology of Sand Storms. *Almaty*:580 pp (Семенов О. Введение в экспериментальную метеорологию и климатологию песчаных бурь. Алматы, с. 580)
- Semenov O (2012) Dust storms and sandstorms and aerosol long-distance transport. In: Breckle S, Wucherer W, Dimeyeva L, Ogar N (Eds) *Aralkum—a man-made desert*. Springer, Ecological Studies 218:73–82
- Sett R (2017) Responses in plants exposed to dust pollution. *Hortic Int'l J* 1(2):53–56. <https://doi.org/10.15406/hij.2017.01.00010>
- Shen H, Abuduwaili J, Samat A, Ma L (2016) A review on the research of modern Aeolian dust in Central Asia. *Arab J Geosci* 9:625. <https://doi.org/10.1007/s12517-016-2646-9>
- Small E, Giorgi F, Sloan L (1999) Regional climate model simulation of precipitation in Central Asia—mean and interannual variability. *J Geophys Res* 104:6563–6582. <https://doi.org/10.1029/98JD02501>
- Soucek S (2000) *A history of inner Asia*. Cambridge University Press:369pp
- Spivak L, Terekhov A, Vitkovskaya I, Batyrbayeva M (2009) Analysis of changes of the zone of formation of salt-dust storms from the drained bottom of the Aral Sea with using the long-term satellite data. *Curr Prob Remote Sens Earth Space* 2(6):193–202
- Spivak L, Terechov A, Vitkovskaya I, Batyrbayeva M, Orlovsky L (2012) Dynamics of dust transfer from the desiccated Aral Sea bottom analysed by remote sensing. In: Breckle S-W, Wucherer W, Dimeyeva L, Ogar N (eds) *Aralkum—a man-made desert*. *Ecol Stud* 218:97–106
- Squires V (2016) Dust particles and aerosols—impact on biota—a review (part I). *J Rangeland Sci* 6(1):82–90. http://www.rangeland.ir/article_520467.html
- St. Amand P, Mathews L, Gaines C, Reinking R (1986) Dust storms from Owens and Mono valleys, California. Naval Weapons Center Technical Publication 6731:79
- Ta W, Xiao Z, Qu J, Yang G, Wang T (2003) Characteristics of dust particles from the desert Gobi area of northwestern China during dust-storm periods. *Environ Geol* 43:667–679. <https://doi.org/10.1007/s00254-002-0673-1>
- Tang J, Dong F, Dai Q, Deng Y (2013) Characterization of atmosphere PM_{2.5} and Dustfall in Xining (China). *Key Eng Mater* 562–565:1422–1427
- Taunton AE, Gunter ME, Druschel GK, Wood SA (2010) Geochemistry in the lung—reaction-path modeling and experimental examination of rock-forming minerals under physiologic conditions. *Am Mineral* 95:1624–1635. https://pdfs.semanticscholar.org/682e/8532234e63e9fb31ae2c861cc92b8fe71ee7.pdf?_ga=2.177283237.128734785.1608109693-561507554.1607864254
- Tolkacheva G (2000) Guidance for monitoring of dry atmospheric fallings in the Central Asian Region. SANIGMI report, Tashkent
- Tursunov AA (1989) The Aral Sea and the ecological situation in Central Asia and Kazakhstan. *Gidrotekhnicheskoe Stroitel'stvo* 6:15–19 (Турсунов А.А. Аральское море и экологическая ситуация в Центральной Азии и Казахстане. Гидротехническое строительство 6: 15–19)
- Umarov N (2013) About a condition of environment and use of natural resources in Republic of Uzbekistan (The Retrospective Analysis for 2008–2011). National Report of the State Committee for Nature Protection of the Republic of Uzbekistan, Tashkent (Умаров Н. О состоянии окружающей среды и использовании природных ресурсов в Республике Узбекистан (Ретроспективный анализ за 2008–2011 годы). Национальный отчет Государственного комитета по охране природы Республики Узбекистан, Ташкент)
- Washington R, Todd M, Middleton NJ, Goudie AS (2003) Duststorm source areas determined by the total ozone monitoring spectrometer and surface

- observations. *Ann Assoc Am Geogr* 93(2):297–313. <https://doi.org/10.1111/1467-8306.9302003>
- Wasson R, Nanninga P (1986) Estimating wind transport of sand on vegetated surfaces. *Earth Surf Proc Land* 11:505–514. <https://doi.org/10.1002/esp.3290110505>
- Whish-Wilson P (2002) The Aral Sea environmental health crisis. *J Rural Remote Environ Health* 1:29–34. <http://jrtp.h.jcu.edu.au/vol/v01whish.pdf>
- Wiggs G, O'Hara S, Mamedov B (2003) Wind erosion and dust deposition in the Aral Sea Region—possible consequences of unsustainable human activity. In: Alsharhan A, Wood W, Goudie A, Fowler A, Abdelatif E (eds) *Desertification in the third millenium*, Swets and Zeitlinger B.V:291–298
- Zetterström R (1999) Child health and environmental pollution in the Aral Sea region in Kazakhstan. *Acta Paediatr Suppl* 429:49–54. <https://doi.org/10.1111/j.1651-2227.1999.tb01290.x>



How Does Tillage Accelerate Soil Production and Enhance Soil Organic Carbon Stocks in Mudstone and Shale Outcrop Regions?

10

Jianhui Zhang, Yong Wang, Jiadong Dai,
and Haichao Xu

Abstract

In the academic community, tillage has become a subject of research in environmental change as it is closely associated with the global stocks of soil carbon, the largest terrestrial organic carbon pool. However, tillage's impacts on the soil mass are unknown and the role of tillage in the global carbon cycle is intensely debated worldwide. It is still not known how soil eroded by prior natural processes and human activities is offset by tillage, or how soil production is controlled by tillage. Using a physical tracer method, the tillage-induced flux and translocation rate of rock fragments were estimated on the Regosol hillside of the Sichuan Basin, China, where there are extensive mudstone and shale outcrops. There, we found that tillage in the fields artificially accelerates soil production by crushing bedrock to increase the soil matrix.

Tilling into bedrock takes place as the soil mass is the minimum required for basic grain production. Tillage caused bedrock fragmentation and accelerated soil production/formation by increasing the soil matrix: the resultant rock fragments are incorporated into the soil layers in the Regosol areas with mudstone and shale outcrops. Our results indicate that tillage and associated tillage erosion can play a positive role in soil production, agricultural productivity, and carbon sequestration in the sloped landscapes of Sichuan, China.

Keyword

Soil erosion · Tillage erosion · Bedrock fragmentation · Mechanical tracer experiment · Soil production · SOC sequestration

J. Zhang (✉) · Y. Wang · J. Dai · H. Xu
Institute of Mountain Hazards and Environment,
Chinese Academy of Sciences and Ministry of Water
Conservancy, Chengdu 610041, China
e-mail: zjh@imde.ac.cn

Y. Wang
e-mail: wangyong2015@sicau.edu.cn

Y. Wang
College of Water Conservancy and Hydropower
Engineering, Sichuan Agricultural University, Ya'an
625014, China

10.1 Introduction

Soils form the basis for food production and simultaneously support environmental sustainability. As a result, soil production is an indispensable aspect of the maintenance of soil resources and is directly associated with human prosperity and survival, especially in the case of intensive soil erosion. In recent decades, the effects of tillage on soil erosion have attracted much more attention among scientists, policy-makers, and decision-makers. The titles of

publications around the world regarding the impacts of tillage on soil resources are almost entirely dominated by negative views. In recent years, however, no-tillage or minimum tillage have become the subject of research in environment change in the academic community, as it is closely associated with global soil C stocks, the largest terrestrial organic C pool. A few well-reputed journals such as *Nature* (Buffett 2012; Six 2013; Paustian et al. 2016), *Science* (Lal 2004; Renwick et al. 2004; Van Oost et al. 2004, 2007), and *Nature Climate Change* (Powelson et al. 2014) have published relevant studies dealing with the relationship between tillage/no-tillage and C sequestration, showing that tillage's impacts on the global C cycle are a subject of intense worldwide debate.

Thirty-three percent (33%) of the soils in the world are estimated to be in the process of degradation (Wall and Six 2015). Agricultural soil erosion due to human activities is degrading soil faster than it is naturally formed (about 1000 years to form a 1 cm-thick layer of soil), which severely threatens human welfare over the next century (Amundson et al. 2015). The world's soils are thought of as the largest terrestrial organic C pool, up to 2,400 Pg C at a soil thickness of 2 m, which is twice the amount in the atmosphere (~ 830 Pg C) (Batjes 1996; Ciais et al. 2013). This means that a slight increase in the net soil C stock can considerably improve the C sink potential. If appropriate agricultural practices are adopted, a substantial increase in soil C stocks will become possible, diminishing soil GHG emissions (Paustian et al. 2016).

One approach to enhancing C stocks is to enlarge the below-ground biomass by making it possible for root systems to become larger and deeper, thus increasing the plant C input (Hurd 1974; Kell 2012; Lynch and Wojciechowski 2015). Improving rooting depths and soil structure, for example, through deep ploughing, is another important agricultural practice in which the distribution of soil C can be extended to a greater depth (Jobba'gy and Jackson 2000; Lal 2004; Mueller et al. 2013; Alcántara et al. 2016). These approaches have the potential to significantly increase C sequestration in soil. To attain

either or both goals, nevertheless, one important premise for soils with a shallow layer (such as Regosols) is that soil layer thickness needs to be enlarged to create enough space for root system expansion and deep ploughing.

In China, there is a widespread distribution of Regosols (also popularly referred to as "purple soils" due to their color in China). These were mainly derived from mudstone and shale of the Triassic, Jurassic, Cretaceous, and Tertiary periods (Du et al. 2013). These soils cover an area of over 20 million hectares distributed across 16 provincial regions of China, including Sichuan, Yunnan, Guizhou, Guangxi, Guangdong, Hunan, Hubei, Anhui, Jiangxi, Fujian, Zhejiang, Henan, Shanxi, Jiangsu, and Hainan, of which the Sichuan province takes up the largest part of the total area (He 2003). Soil organic carbon stocks are estimated to have increased in Chinese croplands over a period of a few decades (Luo et al. 2010; Zhao et al. 2018). In southwest China, where Regosols are distributed over a large region, soil organic carbon (SOC) stocks in croplands increased by $5.49 \text{ Mg C ha}^{-1}$ over the three decades from 1980 to 2011 at a rate of $0.183 \text{ Mg C ha}^{-1} \text{ yr}^{-1}$ (Zhao et al. 2018). What has led to this improvement in SOC stocks? The study reported that deepening plough layers can increase SOC sequestration in the croplands of China (Zhao et al. 2018). From another point of view, the eroded soil may be replenished by the newly formed soils derived from the underlying sediment, parent material, or bedrock. However, it should be emphasized that the pace of this replenishment process was poorly known (Montgomery 2007), and more importantly, how it is replenished remains unknown (e.g., by natural or artificial processes).

Overall, previous viewpoints have been that tillage causes soil aggregate disintegration, a decline in SOC decline, and an increase in soil erodibility (Takken et al. 2001; Mishra et al. 2010; Abdollahi et al. 2014; Kumar et al. 2014; Wang et al. 2015; Rocha Junior et al. 2016), resulting in soil deterioration and soil loss. Can any aspect of tillage play a positive role in stopping or reversing the trend towards soil loss, and enhancing SOC stocks? Here, we seek the

mechanism which has prompted soil production, offset eroded soils, and raised the SOC pool on a regional scale.

10.2 Materials and Methods

Location and soil. The study site was located in the east of the Sichuan Basin (30° 26' N, 104° 28' E) with an altitude ranging from approximately 400–600 m above sea level (Fig. 10.1). This area has a subtropical humid climate with a mean annual temperature of 17.4 °C and a mean annual rainfall of 872 mm. The dominant crops on cultivated land are commonly wheat (*Triticum aestivum* L), corn (*Zea mays* L), and sweet potato (*Ipomoea batatas* Lam). The soil, derived from mudstone and shale of the Jurassic period, was classified as a Regosol in accordance with FAO taxonomy (FAO 1988). The soil texture is identified as loam with 9–11% clay, 45–47% silt, and 42–46% sand, and the soil organic carbon (SOC) has a concentration of 7.6–8.6 g kg⁻¹, according to the data on typical soils (Dai et al. 2021). Soil layer thicknesses are commonly within 20–50 cm deep and show an increasing depth from the topslope to toeslope positions. In most upslope positions, there are shallow soil layers resulting predominantly from severe soil erosion by tillage and water. A major tillage operation generally occurs before winter wheat sowing, with a minor tillage operation during sweet potato harvesting. Hoeing tillage, a conventional tillage practice, is performed by local farmers, starting from the bottom and ending at the top of the hill-slope. In the course of tillage, soil is turned over and pulled down in the opposite direction to the operator's direction of travel, and moves downhill under the forces of drag and gravity.

In long-term agricultural practice, originally long slopes were dissected into short slope segments with a slope length of generally 10 to 20 m to diminish water erosion and facilitate field management (Fig. 10.2). Soil-covered bedrock had slope gradients ranging from 0.09 to 0.47 m m⁻¹. Soils derived from Jurassic mudstone and shale are commonly thought of as being

fertile with mineral nutrients of P and K derived from bedrock (Zhu et al. 2008). The formation of soils can be substantially promoted by human activities, such as tillage, cropping, fertilization, and land reclamation (Wei et al. 2006).

Tillage procedure and measurements. To increase the soil matrix, bedrock fragmentation by tillage generally occurs at upper slope positions where there is a shallow soil layer. A physical tracer method, referred to as the gravel tracing technique, was used to determine how tillage affected the downslope translocation of rock fragments at the three depths of bedrock fragmentation (2, 4, and 6 cm) and under the three soil cover thicknesses (0, 6, and 10 cm) (Fig. 10.3). Small pieces of gravel of approximately 2 cm in diameter, in a contrasting color and numbering, were applied to track the tillage-induced movement of rock fragments and soils. Along the contour of the experimental plots, a series of small holes 6 cm in depth and 2 cm in diameter were made at 10 cm intervals in bedrock using a portable drill. One to three small pieces of gravel were put into the holes as tracers in a vertical arrangement according to the designed bedrock-crushing depths of 2–6 cm, respectively. The positions of the holes were marked with small sticks, and soil layers were recovered up to the designed thicknesses with an original soil bulk density. Immediately above each of the bedrock holes which were made, three to five small pieces of gravel were vertically inserted into the soil at depths of 6–10 cm depending on the thickness of the soil cover. The plots were tilled in a conventional way, in that the farmers tilled their fields with a hoe. Hoeing tillage was performed with 6, 12, and 16 cm tillage depths, respectively. When the plots had been thoroughly tilled, the positions and numbering of the small pieces of gravel were each measured and recorded. The tracer positions were detected by means of the Cartesian coordinate (x, y, z) system. The reliability of the gravel tracing technique has been confirmed by the bedrock dyeing tracing method, which is considered to be of high accuracy; it enables the movement of rock fragments themselves to be observed (Xu et al. 2020).

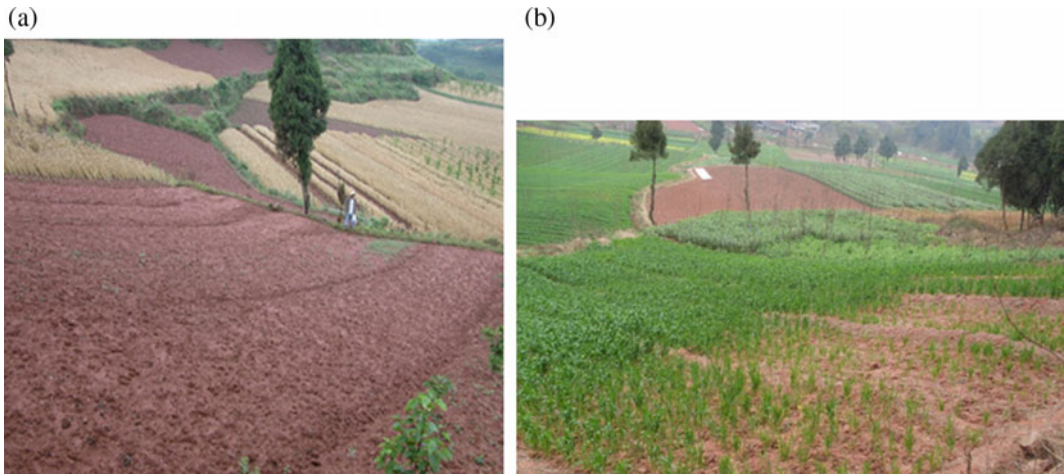


Fig. 10.1 An agricultural landscape showing short slopes derived from original long slopes (a); weaker wheat growth at upper slope than at lower slope positions on the hill-slope due to intensive tillage erosion (b)

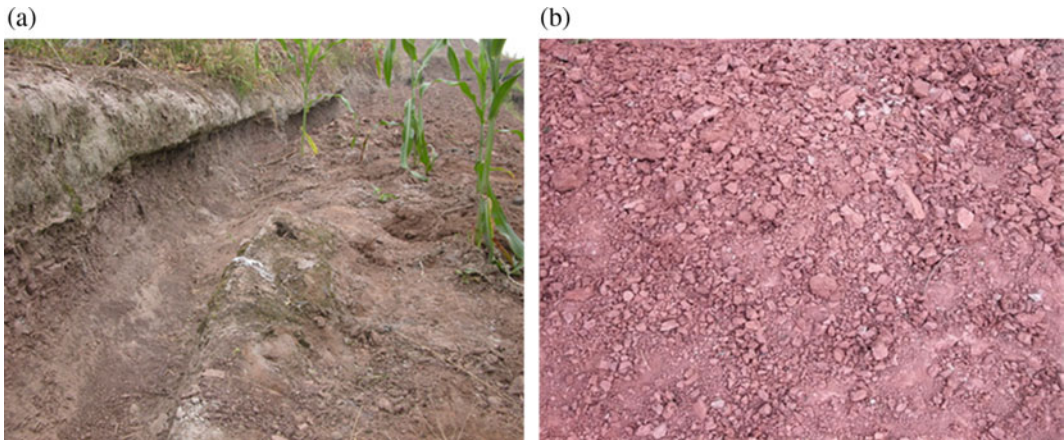


Fig. 10.2 Concave formation and bedrock exposure on the hilltop due to intensive tillage erosion (a); appearance of rock fragments freshly crushed from bedrock by tillage on the soil surface (b)

The rock fragment flux induced by tillage was estimated based on controlled bedrock-crushing depths and bedrock bulk densities. The designed hoeing depth needed to be fixed for each operation in the experiments, therefore a device was used to control the hoeing depth precisely in this study (Xu et al. 2020).

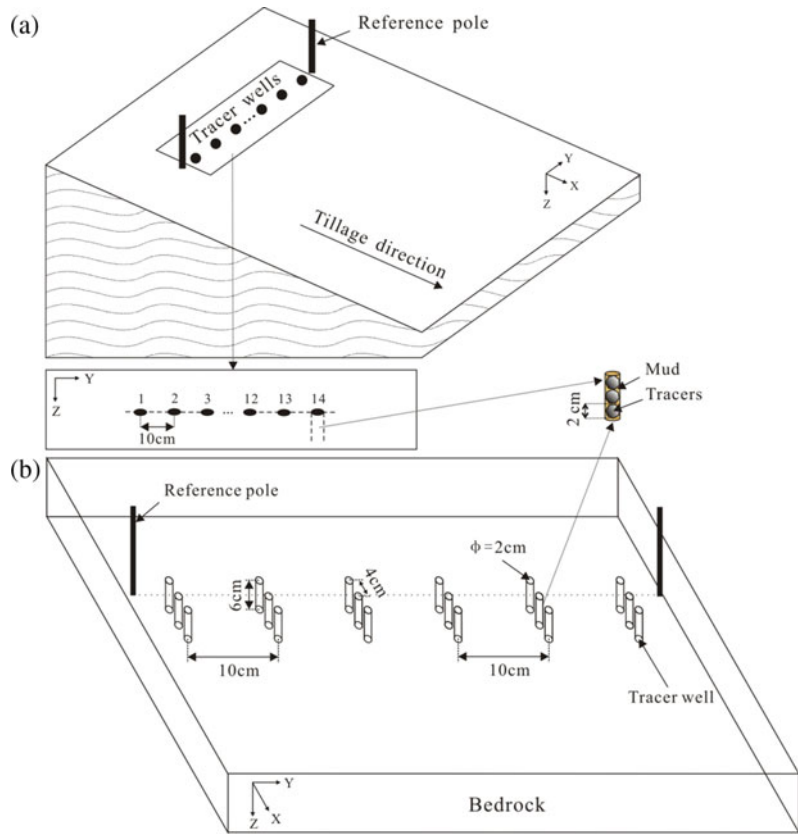
Calculation of erosion rates and flux The displacement distance of the rock fragments was estimated by measuring the distribution of tracers translocated by tillage, expressed as:

$$D = \frac{1}{mn} \sum_{i=1}^m \sum_{j=1}^n (D_{ij}) \quad (10.1)$$

where D is the mean translocation distance of the rock fragments moving downhill (m); D_{ij} is the displacement distance of the i, j th tracer moved downhill, and m and n are the row number and column number of the tracers, respectively.

The tillage translocation rates of rock fragments can be calculated as:

Fig. 10.3 Schematic diagram of the gravel tracing technique showing downslope translocation of rock fragments due to bedrock fragmentation induced by tillage: **a** a setup of tracers on the slope, and **b** an in-depth view of the experimental setup in the bedrock



$$Q = D \cdot \rho \cdot d \quad (10.2)$$

where Q is the unit transport rate for one downhill-tillage pass per unit of width (kg m^{-1} tillage pass $^{-1}$); ρ is the bulk density of bedrock (kg m^{-3}); d is the depth to which the bedrock is cut by tillage (m).

Bedrock erosion rates by tillage were estimated as the downslope translocation of rock fragments per unit of slope width divided by the slope length over which the rock fragments were lost. Bedrock erosion rates can be estimated as:

$$R = 10 \cdot Q/L \quad (10.3)$$

where R is the bedrock erosion rate (Mg ha^{-1} tillage pass $^{-1}$) and L is the downslope length (m).

The rock fragment flux was calculated as the mass of rock fragments derived from bedrock per unit of area covered by tillage, which can be expressed as:

$$F = l \cdot \rho \cdot d \quad (10.4)$$

where F is the rock fragment flux for a single downhill tillage operation per unit of width (kg m^{-1} tillage pass $^{-1}$); l is the slope length of bedrock crushed by tillage (m).

Data on other measurements. The data on soil erosion rates by tillage, ^{137}Cs inventories, and SOC concentrations were obtained from previous publications related to the soils in this study.

10.3 Results and Discussion

10.3.1 Why is a Certain Soil Layer Thickness Always Maintained Despite Severe Soil Erosion at a Rate of Approximately $5000 \text{ t km}^{-2} \text{ yr}^{-1}$?

The soil mass has not been reduced during long-term agricultural practice despite intense agriculture accompanied by severe soil erosion in the hillside landscapes. The most intuitive explanation is that a certain soil layer thickness always remains under severe soil erosion in the Regosol areas with mudstone and shale outcrops. The results obtained by a variety of methods showed that average soil erosion rates are $5036 \text{ t km}^{-2} \text{ yr}^{-1}$, ranging from $3615 \text{ t km}^{-2} \text{ yr}^{-1}$ ($2936\text{--}4164 \text{ t km}^{-2} \text{ yr}^{-1}$) using the runoff plot method (Li et al. 1995; Liu et al. 2007; Dong et al. 2009) to $6456 \text{ t km}^{-2} \text{ yr}^{-1}$ ($6011\text{--}6865 \text{ t km}^{-2} \text{ yr}^{-1}$) using the ^{137}Cs tracing method (Wen et al. 2002; Wang et al. 2003). In this case, the soil should have been eroded completely after 52 years (presuming the soil bulk density is 1300 kg m^{-3}) for a 20-cm-thick soil, resulting in widely exposed bedrock at upslope positions. However, we find that a certain soil layer thickness (generally 20 cm) always exists, even in the most severely eroded areas such as those upslope where intense tillage erosion occurs.

Little attention has been paid to the mechanism of soil production in areas with mudstone and shale outcrops, but this relevant phenomenon has existed since the beginnings of agricultural cultivation. It is largely due to this action that it has been possible to sustain soil resources and soil productivity to date and therefore provide subsistence for the inhabitants in these regions. In these agricultural regions, bedrock is crushed by tillage and incorporated into eroding soil to compensate for soil loss. This is referred to as bedrock fragmentation. Among the most commonly adopted practices is bedrock fragmentation by tillage in regions of intensive agriculture.

Rock fragments induced by this action provide a soil matrix which develops into soil over a certain period of time, as well as nutrients which can contribute to newly formed soil. Bedrock fragmentation and the incorporation of the rock fragments into the soil take place under the combined circumstances of both soft bedrock and severe soil erosion. Tillage is an essential driving factor behind this action, which is a response to the impacts of natural and human factors.

10.3.2 What is the Result of the Balance Between the Gain of Bedrock-Derived Rock Fragments and Soil Loss Due to Tillage?

A hill-slope is divided into upper, middle, and lower slope segments, and bedrock fragmentation normally occurs in the upper slope positions, generally up to 1/3 of the slope length. The rock fragment flux was estimated to be 144.6, 289.2, and $433.8 \text{ Mg ha}^{-1} \text{ tillage pass}^{-1}$ for bedrock-crushing depths of 0.02 m, 0.04 m, and 0.06 m, respectively, based on a bedrock bulk density of 2169 kg m^{-3} . Rock fragments are also translocated downslope in the process of bedrock fragmentation by tillage, similar to soil translocation by tillage on the hillside. The translocation rates of rock fragments were measured as $7.91\text{--}27.09 \text{ kg m}^{-1} \text{ tillage pass}^{-1}$ with a mean of $16.55 \text{ kg m}^{-1} \text{ tillage pass}^{-1}$ (in the case of bare bedrock fragmentation), equivalent to a bedrock erosion rate of $11.03 \text{ Mg ha}^{-1} \text{ tillage pass}^{-1}$ (presuming the slope length averages 15 m). The soil matrix obtained by bedrock fragmentation was $96.3\text{--}374.9 \text{ Mg ha}^{-1} \text{ tillage pass}^{-1}$ with a mean of $235.7 \text{ Mg ha}^{-1} \text{ tillage pass}^{-1}$. In the case of overlying soil layers (0.06–0.10 m thick) and the maximum hoeing depth of bedrock (0.06 m), the net gain of soil matrix reached $378.3\text{--}379.1 \text{ Mg ha}^{-1} \text{ tillage pass}^{-1}$ with a mean of $378.7 \text{ Mg ha}^{-1} \text{ tillage pass}^{-1}$ (Table 10.1). Hence, even considering the occurrence of rock

fragment translocation, a net gain of rock fragments at the point of tillage operations appears to be found. A balance between an increase in the soil matrix and a loss of soil may arise when the two processes (bedrock erosion and soil erosion by tillage) occur simultaneously. The experimental results described above showed that the gain of rock fragments is far greater than the soil translocated by tillage, compared with soil translocation rates of 24.01–75.43 Mg ha⁻¹ tillage pass⁻¹ with a mean of 42.50 Mg ha⁻¹ tillage pass⁻¹ (Zhang et al. 2004). Taking the 0.02 m bedrock-crushing depth as an example, the implementation of bedrock fragmentation by tillage once every 2 years can offset soil loss due to tillage erosion. In the case of overlying soil layers (0.06–0.10 m thick) and a maximum hoeing depth of bedrock (0.06 m), the soil matrix obtained by bedrock fragmentation can offset soil loss of approximately 9 years (Table 10.1). In practice, major soil tillage occurs once a year, but bedrock fragmentation by tillage depends on soil erosion rates, with a frequency of once in a few years.

10.3.3 Does Tillage Play a Positive or Negative Role in SOC Sequestration for mudstone- and Shale-Derived Soil Regions?

Figure 10.4 shows that the ¹³⁷Cs concentrations of severely eroded soils (0.442–0.956 Bq kg⁻¹ with a mean of 0.736 Bq kg⁻¹) were markedly lower than those of less eroded soils (1.393–2.60 Bq kg⁻¹ with a mean of 2.063 Bq kg⁻¹), but those two types of soils have a similar SOC concentration (7.13–7.63 g kg⁻¹ with a mean of 7.38 g kg⁻¹ for the former and 7.30–7.40 g kg⁻¹ with a mean of 7.35 g kg⁻¹ for the latter) (Fig. 10.5). This is attributed to the dynamic replacement of SOC by crop residues in tillage-eroded areas (upslope and convex positions) (Stallard 1998; van Oost et al. 2004), and a constantly large soil pool is maintained for accommodating external C (mainly crop C). This

process is closely associated with the mechanism of tillage erosion. Deposition induced by tillage erosion can protect SOC from decomposition by burial in concave (or lower slope) landscape positions. Upslope soil, which is replenished and rejuvenated by incoming rock fragments, can attain the goal of a constantly large soil pool, as mentioned above. Moreover, bedrock contains an extremely small amount of OC, with a concentration ranging from 0.03 to 0.21 C g kg⁻¹, averaging 0.094 C g kg⁻¹ (Li 1991), which is conducive to external C sequestration in soil when the soil matrix derived from rock fragments increases. Hence, SOC not only does not decline as was previously believed, but also rises to a certain extent (Luo et al. 2010; Zhao et al. 2018). The mechanism of soil maintenance in the Regosol regions is different from that in the well-developed soil regions, and soil productivity is characterized by the rapid artificial replenishment of soil material, instead of preserved and increasing soil aggregates as commonly believed.

Less intensive tillage in croplands can be beneficial to sequestering SOC, and the conversion of croplands to grasslands enhances the sequestration of soil organic carbon (Ogle et al. 2005; Baer et al. 2010; Zhang et al. 2014). However, SOC increases due to no-tillage in soil surface layers are offset by SOC losses in deeper layers (Six et al. 2004; Powlson et al. 2014). Thus, the positive roles of no-tillage in SOC sequestration are widely overstated (Buffett 2012; Six 2013; Powlson et al. 2014). Additional studies have reported that tillage erosion leads to C sequestration with a rate of 10 g C m⁻² yr⁻¹ (van Oost et al. 2004); on the other hand, 100% conversion to no-till farming is projected to produce a potential carbon sequestration rate of 10 to 40 g C m⁻² yr⁻¹ (Smith et al. 1998; Smith 2004). Hence, the C sequestration potential of tillage is of the same order of magnitude as that of no-till. The results of this study confirm that tillage plays an important role in enhancing SOC stocks in croplands.

Tillage erosion leads to an increase in SOC stocks in the landscape, as stated above, but water erosion diminishes SOC stocks in the landscape. On the other hand, tillage erosion may

Table 10.1 Tillage-created rock fragment flux and net gain of soil matrix under bare bedrock and soil-covered bedrock

Hoeing tillage depth (m)	Soil cover thickness (m)	Translocation rate of rock fragment (kg ha ⁻¹ tillage pass ⁻¹)		Bedrock erosion rate by tillage ^a (Mg ha ⁻¹ tillage pass ⁻¹ , A)		Soil erosion rate by tillage ^b (Mg ha ⁻¹ tillage pass ⁻¹ , B)		Rock fragment flux (Mg ha ⁻¹ tillage pass ⁻¹ , C)	Net gain of soil matrix ^c (Mg ha ⁻¹ t tillage pass ⁻¹ , D)	Equivalent years of offsetting soil loss by tillage
		Range	Mean	Range	Mean	Range	Mean			
<i>Bare bedrock</i>						24.01–75.43	42.50			
0.02	0	7.91–9.5	8.67	5.27–6.33	5.78			144.6	96.3	2.3
0.04	0	10.86–19.68	16.43	7.24–13.12	10.95			289.2	235.8	5.5
0.06	0	19.08–27.09	24.55	12.72–18.06	16.37			433.8	374.9	8.8
Sub-mean	0		16.55		11.03			289.2	235.7	5.5
<i>Soil-covered bedrock</i>										
0.12	0.06	14.61–23.10	19.46	9.74–15.40	12.98			433.8	378.3	8.9
0.16	0.10	14.67–21.49	18.26	9.78–14.33	12.17			433.8	379.1	8.9
Sub-mean	0.08		18.86		12.58			433.8	378.7	8.9
Mean			17.47		11.65			347.0	292.9	6.9

^aBedrock erosion rate by tillage is calculated by assuming a slope length of 15 m

^bThe data are after Zhang et al. (2004)

^cD = C – A – B

interact with water erosion in specific landscape conditions. What is the result if the two processes occur simultaneously with an interaction between the two? Tillage erosion apparently only accelerates water erosion if the two processes create a similar magnitude of soil redistribution, i.e., tillage erosion rates are equivalent to water erosion rates. The greater the difference between the two, the weaker the resultant effects of the interaction between them (Zhang et al. 2012). In practice, long slopes have been dissected into short slopes for the past few decades in Regosol regions, leading to greater tillage erosion rates than water erosion rates in the hillside areas. Recent studies suggest that tillage erosion exceeds water erosion in the hilly landscape, with 64–71% for the former and 29–36% for the latter (Zhang et al. 2012). This is attributed to the fact that tillage

erosion rates are negatively proportional to the slope length, contrary to water erosion rates (Lindstrom et al. 1990; Zhang et al. 2004).

In upper slope areas, eroded soil (mainly induced by tillage erosion) is replaced by the conversion of incoming rock fragments into new soils. In lower slope areas, tillage-translocated soil accumulates. This offsets soil loss by water, which mainly occurs here in the form of rill and sheet erosion. The greater the soil loss in lower slope positions, the more intense the soil tillage erosion in the upper slope positions. This leads to greater human-driven bedrock fragmentation in upper slope positions to offset the soil loss there. Yet, the soil mass of the hill-slope is approximately maintained in a dynamic balance between the soil matrix entering the hill-slope (soil layer) and the soil leaving the hill-slope. Hence, at the

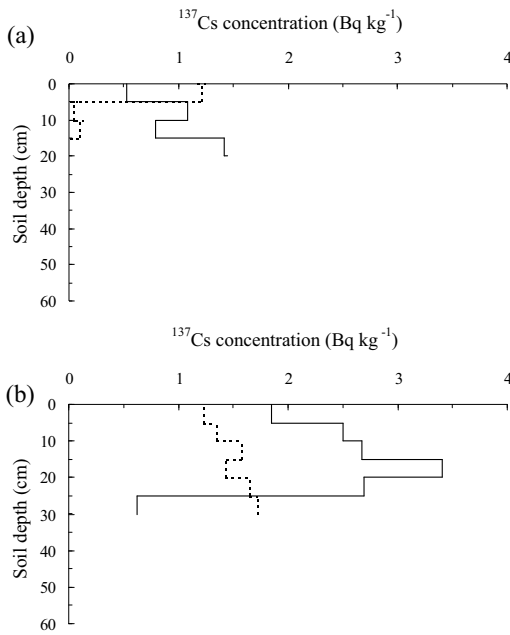


Fig. 10.4 Depth distribution of ^{137}Cs at different landscape positions in the toposequence: **a** top position, and **b** toe position. Dotted and full lines represent the upper and lower parts of the slope, respectively (After Zhang et al. 2012)

hill-slope scale, little net soil loss can be found, as the total soil mass is unchanged or slightly increased. Seen from a larger scale than the hill-slope, however, a net soil loss from the hill-slope landscape is inevitable irrespective of the relative magnitudes of the two erosion processes. In such cases, sediments from the hill-slope are transported to depressions, leading to the physical protection of SOC buried with sediments off the hill-slope (Stallard 1998; Renwick et al. 2004; Van Oost et al. 2007; Yue et al. 2016). This action has a beneficial and positive effect on terrestrial carbon sequestration. A few studies, one of which dealt with the Regosol regions of China, have identified soil erosion as a net sink of atmospheric CO_2 at the regional scale or above (Van Oost et al. 2007; Quine and Van Oost 2007; Yue et al. 2016).

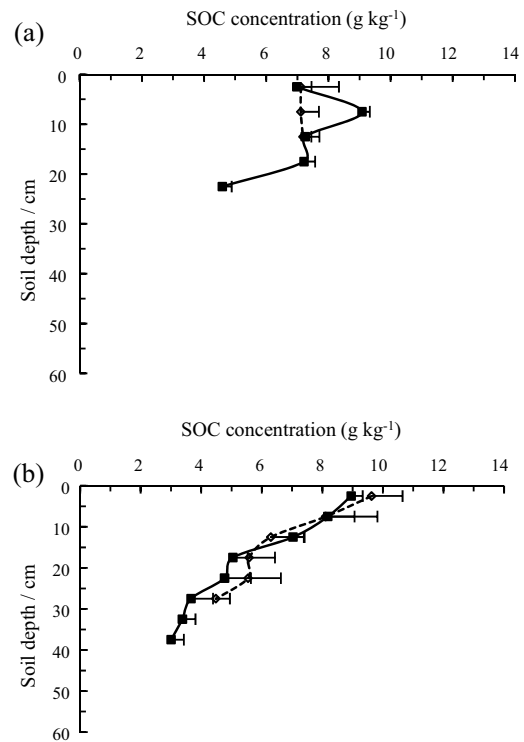


Fig. 10.5 Depth distribution of SOC at different landscape positions in the toposequence: **a** top position, and **b** toe position. Dotted and full lines represent the upper and lower parts of the slope, respectively (After Zhang et al. 2012)

10.4 Conclusions

In summary, tillage in the fields artificially accelerates soil formation by crushing bedrock to increase the soil matrix. Soil loss is largely offset by tillage through bedrock fragmentation and the conversion of resultant rock fragments into soil. When soil erosion by conventional tillage and other practices reaches a limitation of the soil layer thickness (equivalent to a plough layer, generally 15–20 cm) below which the fundamental soil productivity can be heavily restricted, tilling into bedrock to obtain soil matrix is a strong, passive response to soil loss under the

circumstance of limited soil conservation measures. For the soil itself, tillage-induced soil translocation enhances SOC stocks in sloping lands by protecting SOC in depressions, and dynamically replacing SOC with fresh crop residue in convex areas. It is suggested that tillage accelerates soil production to compensate for intensive erosion and significantly contributes to the enhancement of SOC stocks in Regosol regions. This tillage mechanism would have an important implication when it comes to understanding the global C cycle under intense agricultural practice.

Acknowledgements The authors wish to acknowledge the financial support for this study provided by the National Natural Science Foundation of China (41877069 and 41701324), and the Major Science and Technology Special Project of Sichuan Province (Grant 2018SZDZX0034).

References

- Abdollahi L, Schjonning P, Elmholt S, Munkholm LJ (2014) The effects of organic matter application and intensive tillage and traffic on soil structure formation and stability. *Soil Tillage Res* 136:28–37
- Alcántara V, Don A, Well R, Nieder R (2016) Deep ploughing increases agricultural soil organic matter stocks. *Glob Change Biol* 22:2939–2956. <https://doi.org/10.1111/gcb.13289>
- Amundson R, Berhe AA, Hopmans JW, Olson C, Szein AE, Sparks DL (2015) Soil and human security in the 21. *Science* 348:647
- Baer SG, Meyer CK, Bach EM, Klopff RP, Six J (2010) *Ecosphere* 1, art5. <https://doi.org/10.1890/ES10-00004.1>
- Batjes NH (1996) Total carbon and nitrogen in the soils of the world. *Eur J Soil Sci* 47:151–163
- Buffett HG (2012) Reaping the benefits of no-tillage farming. *Nature* 484:455
- Ciais P, Sabine C, Bala G, Bopp L, Brovkin V, Canadell J, Chhabra A, DeFries R, Galloway J, Heimann M, Jones C, Le Quéré C, Myneni RB, Piao S, Thornton P (2013) Carbon and other biogeochemical cycles. In: Stocker TF et al (eds) *Climate change 2013: the physical science basis. Contribution of working group I to the fifth assessment report of the intergovernmental panel on climate change*, pp 465–570. Cambridge Univ. Press
- Dai JD, Zhang JH, Xu HC, Wang Y, Zhang GM, Xu YT, Hu XJ (2021) Effects of bedrock erosion by tillage on architectures and hydraulic properties of soil and near-surface bedrock. *Sci Total Environ* (in press)
- Dong YP, Lu HS, Zhang QG, Yan LJ (2009) Soil erosion of slopland in the the Yangtze Three Gorges Reservoir areas. *J Univ Jinan (Sci Tech)* 23:90–93 (in Chinese)
- Du J, Luo Y, Zhang W, Xu C, Wei C (2013) Major element geochemistry of purple soils/rocks in the red Sichuan Basin, China: implications of their diagenesis and pedogenesis. *Environ Earth Sci* 69:1831–1844. <https://doi.org/10.1007/s12665-012-2019-y>
- FAO (1988) Soil map of the world, Revised legend. World Soil Resources Report 60, FAO, Rome
- He YR (2003) Purple soils in China (2). Chinese Science Press, Beijing, p 2 (in Chinese)
- Hurd EA (1974) Phenotype and drought tolerance in wheat. *Agric Meteorol* 14:39–55
- Jobba'gy EG, Jackson RB, (2000) The vertical distribution of soil organic carbon and its relation to climate and vegetation. *Ecol Appl* 10:423–436
- Kell D (2012) Large-scale sequestration of atmospheric carbon via plant roots in natural and agricultural ecosystems: why and how. *Philos Trans Roy Soc b: Biol Sci* 367:1589–1597
- Kumar S, Nakajima T, Mbonimpa EG, Gautam S, Somireddy UR, Kadono A, Lal R, Chintala R, Rafique R, Fausey N (2014) Long-term tillage and drainage influences on soil organic carbon dynamics, aggregate stability and corn yield. *Soil Sci Plant Nutr* 60:108–118
- Lal R (2004) Soil carbon sequestration impacts on global climate change and food security. *Science* 304:1623–1627
- Li QY, Jiang SQ, Sun HC (1995) Determination of surface erosion of the small watersheds in the hilly area of purple soils in the Upper reaches of the Yangtze River. *J Yangtze River Sci Res Inst* 12:51–56 (in Chinese)
- Li ZM (1991) Purple soils in China (1). Chinese Science Press, Beijing, pp 26–39 (in Chinese)
- Lindstrom MJ, Nelson WW, Schumacher TE, Lemme GD (1990) Soil movement by tillage as affected by slope. *Soil Tillage Res* 17:255–264
- Liu DH, Zhao XJ, Cao JC, Liu M, Wang CT, Mao SC (2007) Impacts and mechanism of Eulaliopsis Binata hedgerow system on soil and water losses control in purple hilly area in Sichuan basin. *Southwest China J Agric Sci* 20:439–442 (in Chinese)
- Luo HL, Wang HP, Chen H (2010) Change of farmland soil organic carbon density in hilly area of central Sichuan Basin in the last 25 years—a case study of Yangting County, Sichuan Province. *J Mt Sci* 28:211–216 (in Chinese)
- Lynch JP, Wojciechowski T (2015) Opportunities and challenges in the subsoil: pathways to deeper rooted crops. *J Exp Bot* 66:2199–2210
- Mishra U, Ussiri DAN, Lal R (2010) Tillage effects on soil organic carbon storage and dynamics in Corn Belt of Ohio USA. *Soil and Tillage Research* 107:88–96
- Montgomery DR (2007) Soil erosion and agricultural sustainability. *Proc Natl Acad Sci USA* 104:13268–13272

- Mueller L, Shepherd G, Schindler U, Ball BC, Munkholm LJ, Hennings V, Smolentseva E, Rukhovic O, Lukin S, Hu C (2013) Evaluation of soil structure in the framework of an overall soil quality rating. *Soil Tillage Res* 127:74–84
- Ogle SM, Breidt FJ, Paustian K (2005) Agricultural management impacts on soil organic carbon storage under moist and dry climatic conditions of temperate and tropical regions. *Biogeochemistry* 72:87–121
- Paustian K, Lehmann J, Ogle S, Reay D, Philip RG, Smith P (2016) Climate-smart soils. *Nature* 532:49–57
- Powlson DS, Stirling CM, Jat ML, Gerard BG, Palm CA, Sanchez PA, Cassman KG (2014) Limited potential of no-till agriculture for climate change mitigation. *Nat Clim Chang* 4:678–683
- Quine TA, Van Oost K (2007) Quantifying carbon sequestration as a result of soil erosion and deposition: retrospective assessment using caesium-137 and carbon inventories. *Glob Change Biol* 13:2610–2625
- Renwick WH, Smith SV, Sleezer RO, Buddemier RW (2004) Comments on managing soil carbon. *Science* 305:1567
- Rocha Junior PR, Bhattharai R, Fernandes RBA, Kalita PK, Andrade FV (2016) Soil surface roughness under tillage practices and its consequences for water and sediment losses. *J Soil Sci Plant Nutr* 4:1065–1074
- Six J (2013) Spare our restored soil. *Nature* 498:180–181
- Six J, Ogle SM, Breidt FJ, Conant RT, Mosier AR, Paustian K (2004) The potential to mitigate global warming with no-tillage management is only realized when practised in the long term. *Glob Change Biol* 10:155–160
- Smith P (2004) Carbon sequestration in croplands: the potential in Europe and the global context. *Eur J Agron* 20:229–236
- Smith P, Powlson DS, Glendining MJ, Smith JOU (1998) Preliminary estimates of the potential for carbon mitigation in European soils through no-till farming. *Glob Change Biol* 4:679–685
- Stallard RF (1998) Terrestrial sedimentation and the carbon cycle: Coupling weathering and erosion to carbon burial. *Global Biogeochem Cycles* 12:231–257
- Takken I, Govers G, Jetten V, Nachtergaele J, Steegen A, Poesen J (2001) Effects of tillage on runoff and erosion patterns. *Soil Tillage Res* 61:55–60
- Van Oost K, Govers G, Quine TA, Heckrath G (2004) Comment on managing soil carbon. *Science* 305:1567b
- Van Oost K, Quine TA, Govers G, De Gryze S, Six J, Harden JW, Ritchie JC, McCarty GW, Heckrath G, Kosmas C, Giraldez JV, da Silva JRM, Merckx R (2007) The impact of agricultural soil erosion on the global carbon cycle. *Science* 318(5850):626–629
- Wall DH, Six J (2015) Give soils their due. *Science* 347(6223):695
- Wang YK, Wen AB, Zhang XB (2003) Study of soil erosion on cultivated slope land in severe soil loss regions of upper reaches of Yangtze River basin using ^{137}Cs technique. *J Soil Water Conserv* 17:77–80 (in Chinese)
- Wang Y, Zhang JH, Zhang ZH (2015) Influences of intensive tillage on water-stable aggregate distribution on a steep hillslope. *Soil Tillage Res* 151:82–92
- Wei CF, Ni JP, Gao M, Xie D, Hasegawa S (2006) Anthropogenic pedogenesis of purple rock fragments in Sichuan basin, China. *CATENA* 68:51–58
- Wen AB, Zhang XB, Wang YK, Feng MY, Zhang YY, Xun JY, Bai LX, Huo TR, Wang JW (2002) Study on soil erosion rates using ^{137}Cs technique in Upper Yangtze River. *J Soil Water Conserv* 16:1–3 (in Chinese)
- Xu HC, Zhang JH, Wei YH, Dai JD, Wang Y (2020) Bedrock erosion due to hoeing as tillage technique in a hilly agricultural landscape, SW China. *Earth Surf Proc Land* 45:1418–1429
- Yue Y, Ni J, Ciais P, Piao S, Wang T, Huang M, Borthwick AGL, Li T, Wang Y, Chappell A, Van Oost K (2016) Lateral transport of soil carbon and land-atmosphere CO_2 flux induced by water erosion in China. *Proc Natl Acad Sci USA* 115:4045–4050
- Zhang JH, Li FC, Wang Y, Xiong DH (2014) Soil organic carbon stock and distribution in cultivated land converted to grassland in a subtropical region of China. *Environ Manage* 53:274–283
- Zhang JH, Lobb DA, Li Y, Liu GC (2004) Assessment of tillage translocation and tillage erosion by hoeing on the steep land in hilly areas of Sichuan, China. *Soil Tillage Res* 75:99–107
- Zhang JH, Ni SJ, Su ZA (2012) Dual roles of tillage erosion in lateral SOC movement in the landscape. *Eur J Soil Sci* 63:165–176
- Zhao YC, Wang MY, Hu SJ, Zhang XD, Ouyang Z, Zhang GL, Huang B, Zhao SW, Wu JS, Xie DT, Zhu B, Yu DS, Pan XZ, Xu SX, Shi XZ (2018) Economics- and policy-driven organic carbon input enhancement dominates soil organic carbon accumulation in Chinese croplands. *Proc Natl Acad Sci USA* 115:4045–4050
- Zhu B, Wang T, You X, Gao MR (2008) Nutrient release from weathering of purplish rocks in the Sichuan basin, China. *Pedosphere* 18:257–264



Risks and Permissible Rates of Soil Erosion in the Agrolandscapes of the Crimea

11

Elena I. Ergina and Vladimir O. Zhuk

Abstract

The chapter presents the study of soil erosion on the arable slopes of the Crimean peninsula. The paper analyses the climatic conditionality of erosion processes. Based on an array of chronological soil data, a mathematical modelling of the formation of the humus horizon was performed. An assessment was made of the permissible rates of erosion as a criterion for managing erosion neutrality on the peninsula. Calculations based on the models developed show that, in arid regions with Kastanozems and Chernozems, the highest rates of soil formation were observed on the eroded soils of the wetter slopes with a northern exposure. Regional features of climate dynamics led to an intensification of the erosion degradation processes affecting soils and landscapes of the Crimean Peninsula. In the foothills and mountainous areas and on the southern coast of the Crimean peninsula, where a significant amount of rainfall occurs, the amount of solar radiation acts as a limiting factor. For a quantitative assessment of the rate of soil formation, the most accurate method was based on an assessment of the

rate of formation of the humus horizon over time.

Keywords

Erosion · Climate · Permissible rate · Chronological soil studies · Soil formation

11.1 Introduction

The long-term economic use of the territory of the Crimean Peninsula has led to a significant transformation of its natural landscapes. This process reached its greatest scale from the second half of the nineteenth century to the first half of the twentieth century, during which an agricultural impact on the soil prevailed. Almost all available lands were cultivated, many of which were unproductive and have been abandoned today. This rapid change in natural landscapes led the development of intensive erosion processes and the degradation of soil. Intensive agricultural land use contributed to the formation of agrolandscapes on the peninsula, i.e. specifically agricultural landscapes, where agrocenoses supplanted natural vegetation on a large area. The total land area of the Crimean Peninsula is 2,608,100 ha. The share of agricultural land is 68.7% (1,792,500 ha) including 1,271,600 ha of arable lands, which are the most heavily affected

E. I. Ergina (✉) · V. O. Zhuk
Taurida Academy Subdivision, Vernadsky Crimean
Federal University, 4 Vernadsky Ave, Simferopol,
Republic of Crimea, Russia

by transformations and destruction (Report 2015).

To develop measures to stabilise the processes of land erosion in a particular territory, it is necessary to quantitatively determine the ratio of the erosion rate and its permissible speed limit. Currently, there are methodological approaches for assessing the rate of soil loss due to erosion (Svetlichny et al. 2004), but a quantitative assessment of the permissible rate has not been developed to the necessary degree.

It is extremely important to tackle the problem of anti-erosion measures for agricultural landscapes, on the basis of mathematical models of the relationship between processes of soil erosion and self-restoration. Studies by Lisetskii (2000), Goleusov and Lisetskii (2005), Cherny (1996, 1999), Ergina (2017a), Ergina et al. (2018) and others have promoted a better understanding of the problems which occur when determining permissible rates of soil erosion. Recently, numerous studies have been carried out on how soils' composition and properties are transformed under the influence of agricultural use. However, there are few studies on soil evolution under the influence of modern "modified" conditions, especially for the Crimean peninsula (Lisetskii and Ergina 2010; Lisetskii et al. 2013; Ergina 2017b; Ergina et al. 2018).

Studying the characteristics of soil formation over time is relatively complicated, although the methodological limitations of such studies can be solved by using models that describe the characteristics of soil formation over time. The main soil formation models can be grouped into factorial, energy and mass-balance models (Minsny et al. 2008). Various quantitative models of soil formation processes created by domestic and foreign scientists have paid considerable attention to the mathematical modelling of the thickness of humus horizon. Recently, due to the accumulation of chronological information on the soil, soil science has acquired the ability to carry out modelling and verify the results of mathematical models of soil properties (Dietrich et al. 2003; Godd ris et al. 2006; Dessert et al. 2003; Hoosbeek and Bryant 1992; Kirkby 1985; Ergina 2017b). Building mathematical models of

soil formation over time has become a promising area of research. The purpose of this work is thus to assess the current state of the soil erosion risk and determine the permissible erosion rates in the territory of the Crimean peninsula based on models simulating the formation of a humus soil horizon over time.

11.2 Materials and Methods

11.2.1 Characteristics of the Territory

The spatial distribution of the soils in the main part of the Crimean peninsula was determined by bioclimatic factors, though it was significantly complicated by the geology and geomorphology of the territory. The specifics of soil formation in the Crimean peninsula were mainly determined by its location on the border of the temperate and subtropical zones, and at the junction of the Scythian Platform and the Alpine geosynclinal region of the Crimean Mountains. The interaction of soil formation factors occurred in a kind of orographic landscape: 75% of the territory is flat and 25% is mountainous.

The territory of the Crimean peninsula is characterised by a mild climate with a significant amount of sunshine, relatively mild winters, hot summers and a deficit of atmospheric moisture in almost the entire territory. The spatial variability of the air temperature is quite significant. The lowest average monthly air temperature of -4.0°C in January–February was observed in mountainous areas, and the highest of about $+5^{\circ}\text{C}$ on the south coast. In July–August, the temperature is the highest on an annualised basis on most of the territory: $+23$ – $+24^{\circ}\text{C}$, and $+16^{\circ}\text{C}$ in the mountains (Climate Atlas 2000). Influenced by the Black Sea, the autumn air temperature is much higher than that of spring, especially on the southern coast of Crimea, since the precipitation pattern is formed under the influence of atmospheric circulation in the southern part of the East European Plain. The yearly precipitation varies from 250 to 300 mm in the steppe areas, and in the mountains as much as 1000 mm and more. The amount of moisture evaporation is 744–

855 mm, which is almost twice the amount of precipitation in most of the peninsula (Climate Atlas 2000). The moisture coefficient is 0.34–0.47 (Modern landscapes 2009). In summer, most of the precipitation occurs in the form of showers, most of which run off from the surface of the catchment area and lead to the manifestation of water erosion.

The zonal soils in the Crimean plain are Chernozem and Kastanozem (WRB 2015). Rendzic Leptosols are found on the Tarkhankut peninsula and in some places in the central part of the Crimean plain. Significant areas of hydromorphic plains along the coast, in the Prisivashie, on the Kerch Peninsula, are occupied by Solonetz and Solonchaks. In the lower belt of the northern part of the Crimean Mountains, Chernozems are found in combination with Rendzic Leptosols; on the ridges, they are found with Mollic Leptosols alternating with outcrops of limestone (Dragan 2004). Cambisols dominate in the upper belt of the southern macroslope of the Main Ridge. Phaeozem prevails in the lower part of the southern coast of Crimea. A more detailed analysis of the physiographic conditions of soil formation in the Crimea is presented in Table 11.1.

11.2.2 Methods and Objects of Investigation

The main approach used to study soil evolution is the chronological method. Chronologically, soil series vary from tens to hundreds and thousands of years, as evidenced from previous field studies (Ergina 2017a; Ergina et al. 2018; Lisetskii and Ergina 2010; Lisetskii 2019). The timeline can be converted to a chrono-function or model that can be used to describe changes in soil properties over time.

One important aspect of studying soil chronologically is determining the **permissible rate of soil erosion** (PRE). Effective erosion control is possible only if the current erosion rates are equal to or lower than a predetermined level, which theoretically allows a balance to be maintained between the rate of erosion losses and

the intensity of soil formation. This criterion is based on the principle of maintaining soil fertility reserves at the current level. Its quantitative assessment is primarily a soil geography problem, the solution to which is based on an assessment of soil formation factors and especially their changes over time. Determining the above characteristics is a necessary step in the development of soil management models.

An analysis of existing approaches used to determine the permissible rate of soil erosion shows that the most reasonable ways to determine the PREs are those that take into account the rate of soil formation (Svetlichny et al. 2004).

Determined this way, indicators of the permissible erosion rate make it possible to assess how natural conditions and economic activity influence erosion. These indicators can serve as quantitative criteria in the development of measures for anti-erosion control on agricultural landscapes, as an integral part of monitoring the soil cover. This is possible only if there is a transition from subjective design and management to objective calculations using mathematical modelling methods.

To assess the rate of formation of the humus horizon to justify the permissible erosion losses of the soil, quantitative characteristics of soil formation over time are necessary. If daily, chronological series of soils are collected, the process of soil formation can be studied by examining soils of different ages.

Chronological studies of the Crimean peninsula's soils have included, above all, a range of objects (settlements, defensive walls, barrows), reliably dated by archaeological and historical methods in the date range from fourteenth BC to nineteenth AD. The soils here have been formed on the turf surfaces from the fifteenth to twentieth centuries (residential and farm buildings, war trenches, man-made dumps of rocks, etc.). As a result, the following areas were identified for the study of newly formed soils:

- remnants of multi-temporal settlements on the southern coast of Crimea;
- ramparts and ancient settlements of the Kerch Peninsula;

Table 11.1 Characteristics of modern soil formation factors on the Crimean peninsula

Natural landscapes	Altitude asl, m	Mean January temperature, ° C	Mean July temperature, °C	Sum of temperatures >10 °C	Rainfall, mm	Moisture coefficient (by Ivanov 1949)	Soil types (WRB 2015)
Semi-desert wormwood-fescue steppes	0–40	0.0– – 3.0	22.7–23.7	3280–3400	300–400	0.32–0.38	Solonetz, Solonchak, Kastanozems
Typical poor-grassy feathering-fescue steppes	40–150	–0.6– –0.9	22.0–23.7	3280–3335	360–440	0.34–0.47	Chernozems
Oak and juniper-pine forests of the Southern Coast	0–600	–1.4– +4.4	19.9–24.4	3655–3940	248–751	0.46	Phaeozems, Cambisols, Rendzic Leptosols
Forest-steppe zone, foothills of the main ridge of the Crimean Mountains	0–600	–1.2– +2.5	21.0–23.0	3000–3545	375–600	–	Luvic Chernozems, Rendzic Leptosols, Cambisols
Forests of the southern macroslope of the mountains	400–1500	– 0.9– – 1.2	19.3–17.0	2655–2700	654–925	0.60–1.10	Cambisols, Leptosols
Forests of the northern macroslope of the mountains	1200–1300	–0.8– –1.5	16.8–19.5	2500–2800	487–761	0.70–1.0	Cambisols
Mountain meadows and mountain forest (Yayla)	600–1500	–3.0– –3.9	15.4– 16.4	2000	600–1200	1.00–1.80	Leptosols, Mollic Leptosols

- remnants of ancient settlements of the western and north-western Crimea;
- mediaeval cave cities;
- land plots of the ancient Greek chora (χώρα) in the territory of the Heracles Peninsula;
- archaeological sites of different ages in the steppe and foothills of the Crimean Mountains; and
- Military landscapes and areas of recent soil formation.

The spatial localisation of the study objects is presented in Fig. 11.1.

Chronological soil studies covered the territories with Kastanozems, Chernozems, Rendzic Leptosols, Cambisols and Phaeozems (WRB 2015). For the correct use of the rate of formation of the humus horizon in justifying the

permissible erosion losses of the soil, the following methodological stages are proposed:

- Determination of the rate of soil formation with differentiated estimates of permissible erosion losses;
- Determination of the formation of humus horizon in the modern combination of soil formation factors.

The first issue can be implemented by mathematically modelling the soil formation process over time, using the data obtained from chronological soil studies. These data also serve as the next step to resolve the second issue. Existing pedogenetic research methods provide the theoretical basis for this kind of research.

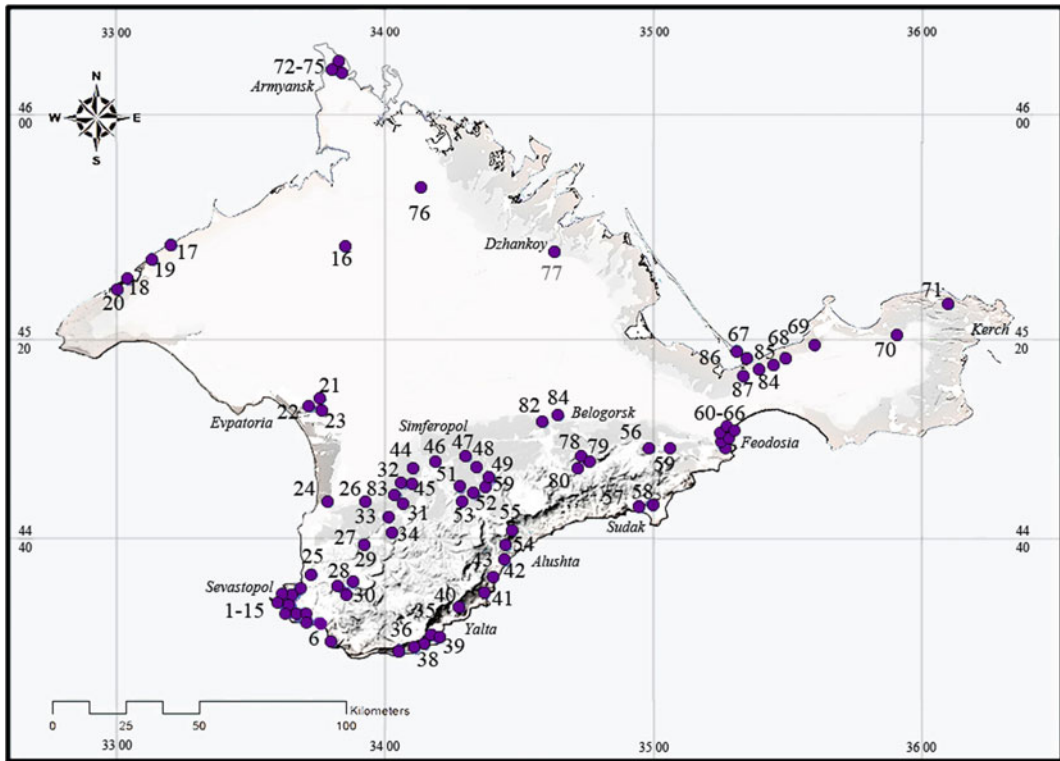


Fig. 11.1 Objects of chronological soil studies (Ergina 2017b; Lisetskii and Ergina 2010). **Map legend:** Circles indicate objects of chronological soil research. Digits—uneven-aged soils on dated surfaces: 1—The embankment of an eighteenth-century artillery battery; 2—Chembalo Fortress fifteenth-century; 3—Chersonese, the tenth-century ruins; 4—Heracles Peninsula, zonal soil; 5—Heracles Peninsula, soil-forming rock; 6—Cape Aya; 7–14—Heracles Peninsula, fortifications from the fifth–fourth century BC; 15—Heracles Peninsula, arable land; 16—Grishino, quarry waste dump; 17—Mezhvodnoe, settlement fifth–fourth century BC; 18—Panskoe settlement, fourth–third century BC; 19—Yarylgachskoe settlement, fourth–third century BC; 20—Kalos–Limena first century AD fortifications; 21—Garshino, settlement from fourth–third century BC; 22—Kara-Tobe, a site of ancient settlement from the second century; 23—environs of Evpatoria, Second World War pillboxes; 24—Ust-Alminsky settlement, third century AD; 25—Chersonese, wall of fifteenth-century house; 26—Alma-Kermen, settlement, second–third century AD; 27—Syuyrenskaya fortress fifteenth-century AD; 28—village of Kholmovka, Second World War trenches; 29—Eski-Kerman, cave city third century AD; 30—Mangup, cave city from fifteenth-century AD; 31—Bakla, cave city from fifteenth-century AD; 32—Tash-Dzhargan, settlement from second–third century BC; 33—Chufut-Kale, fifteenth-century cave city; 34—Kyz-Kerman, fifteenth-century cave city; 35—Krestovaya Mountains, tenth-century; 36—Ay-Todor, fifteenth-century monastery; 37—Issar-Kaya, fifteenth-century fortress; 38—Charax, Roman wall from first

century AD; 39—Kharaks, “Taurus” wall fifth–fourth century BC.; 40—Gelin-Kaya, fifteenth-century fortress; 41—Artek, tenth-century settlement; 42—Cape Plaka, remains of a fifteenth-century church; 43—Aluston, fortress, fifteenth-century; 44—Krasnoye, settlement fifth–fourth century BC; 45—Scythian Naples, ancient settlement, third century AD; 46—Simferopol, dumps for 20 years; 47—the outskirts of Simferopol, dumps for 20 years; 48—Jalman, fifteenth-century settlement; 49—Dolgorukovskaya Yayla, settlement from fifth–fourth century BC; 50—the village of Druzhnoye, Dolgorukovskaya Yayla fifth–fourth century BC; 51—Pionerskoye, fifteenth-century settlement; 52—Kizilkobinsky tract, settlement seventh century AD; 53—Mamut-Sultan, settlement third century AD; 54—Funa, fifteenth-century fortress; 55—Demerdzhi, Second World War trenches; 56—Trinity Paraskeviivsky monastery, ruins from the early twentieth century; 57—Sudak, a fortress from the fourteenth century; 58—Sudak fortress, the ruins of the eighteenth-century barracks; 59—Surb Khach, eighteenth-century monastery; 60—Theodosius: Kaffa, fortress wall from the fifteenth-century; 61—Aivazovsky, remnants of the eighteenth-century water supply system; 62—Northern slopes of Tepe-Oba, ruins from the nineteenth century; 63—Feodosia, ruins of the early twentieth century bridge; 64—Tepe-Oba, ruins from the nineteenth century; 65—nineteenth century crypt ruins; 66—Quarantine, fifteenth-century ruins; 67—Arabat fortress, ruins from the eighteenth-century; 68—Semisotka, Second World War anti-tank ditch; 69—Semenovka, eighteenth-century settlement; 70—Uzunlarsky defensive wall from

the first century AD; 71—Cape Zyuk, Zenonov Chersonesos, hillfort from second century AD; 72—Perekop ramparts, earthen fortress Or-Kapu, beginning of the nineteenth century; 73—early nineteenth century stone fortress on the shores of Karkinitzky Bay; 74—remnants of the Second World War bunker on the shores of Karkinitzky Bay; 75—waste dumps of the trenches of the Second World War “Armyansk bridge head”; 76—embankment of the North Crimean Canal; 77—embankment of the North Crimean Canal; 78—remnants of a

partisan dugout from the Second World War; 79—remains of buildings, Kok-Asan, mid-twentieth century; 80—Mid-twentieth century timber dryer ruins; 81—dump for “Failure” quarry, late twentieth century; 82—dumps for a quarry in Ak-Kai from the late twentieth century; 83—man-made technical forest terraces of the mid-twentieth century; 84—remnants of the long-term Second World War defensive point at the Arabat Spit; 85—late twentieth century quarry dumps; 86—Arabat Spit sandbar; 87—Ak-Monai ramparts, seventh century BC

To obtain a universal method for determining the rate of soil formation in the Crimean Peninsula, which is characterised by soil cracking and various combinations of soil formation factors, it is necessary to build a system of mathematical models for specific environmental and soil conditions.

To establish the exact start time of soil formation, published data, field reports by the Research Institute of Archaeology of the Crimea of the Russian Academy of Sciences and cartographic material were used.

Studies of the morphological soil structure of the archaeological sites were carried out in soil sections, revealing a set of newly formed soil horizons after the end of their existence (for residential areas) or the last filling (for earthen mounds).

When modelling the formation of the soil humus horizon over time (sum of horizons A and AB), a depth coefficient to the humus horizon was introduced. This leads to an increase in the horizon density to an equilibrium density of 1.2 g cm^{-3} .

To characterise the climatic conditions of soil erosion processes, data from the archives of the Institute of Hydrometeorology and Environmental Monitoring of Crimea were used.

11.3 Results and Discussion

11.3.1 Regional Features of Erosion on the Territory of the Crimean Peninsula

Most of the Crimean soil resources were transformed as a result of their agricultural use, with

erosion destruction processes prevailing. Thus, according to 2017 data, 60.3% of the arable land underwent severe erosion in the Crimea. In the Crimean plain, in addition to water erosion, almost half of the arable land is exposed to wind erosion (Tables 11.2, 11.3) (Ergina et al. 2018).

Because significant areas of slopes (up to and including $9\text{--}10^\circ$) are subject to ploughing in Crimea, they are subject to an intensive erosion processes. Recently, in the territory studied, eroded lands were identified by gradient: slopes of $1\text{--}2^\circ$ made up 60,000 ha or 3.7% of the total agricultural land; slopes of $2\text{--}3^\circ$ made up 29,300 ha (2.4%); slopes of $3\text{--}5^\circ$ made up 20,130 ha (1.6%); slopes of $5\text{--}7^\circ$ made up 1,680 ha (1.7%); and slopes $>7^\circ$ made up 900 ha (0.06% of the total agricultural land) (Ergina et al. 2018).

The manifestation of accelerated erosion on the peninsula which has been observed in recent years occurred not only due to the intensive agricultural development of the territory, but also due to the factors caused by modern climatic trends.

The most common meteorological factors affecting the intensification of erosion processes on the peninsula are strong winds and heavy rains, which lead to the development of water and wind erosion. In the steppe regions, an average of 22.7 tonnes of soil per hectare are lost to wind annually, which is more than 20 million tonnes of the entire arable land of the peninsula. Wind erosion is most intense in the Krasnoperekopsky, Nizhniyorsky, Razdolnensky, Saksy, Simferopol and Chernomorsky regions (Ergina et al. 2018).

Recently, an increase has been recorded of up to 18% of the precipitation norm for the period from 1985 to 2015 in the Crimean plain (Ergina et al. 2018). An increase in precipitation is

Table 11.2 Structure of the arable lands at risk of degradation

Name of municipality/district	Arable land subject to erosion, %	Arable land, %	Afforested arable land, %
Bakhchisaray	79.2	45.8	25.5
Belogorsky	83.3	72.5	5.4
Dzhankoisky	56.7	85.0	0
Kirovsky	44.0	79.8	3.4
Krasnogvardeisky	61.1	91.3	1.1
Krasnoperekopsky	48.3	93.2	2.9
Leninsky	51.2	76.3	3.5
Nizhnhorsky	31.0	92.7	2.3
Pervomaisky	37.6	84.0	0
Razdolnensky	70.9	83.3	15.9
Saksky	70.2	90.2	0
Simferopol	73.5	69.3	2.7
Sovetsky	54.3	97.7	0
Chernomorsky	82.7	99.9	5.6

predicted throughout the peninsula. In the Crimea, an average of 80–85% of the annual precipitation falls as rain. The share of solid precipitation is less than 10%, and mixed precipitation comprises 5–10%. In the mountains, the share of liquid precipitation decreases (Prudko and Adamenko 2011; Ergina and Zhuk 2017, 2018, 2019). The increase in precipitation is due to showers, which also cause water erosion. This

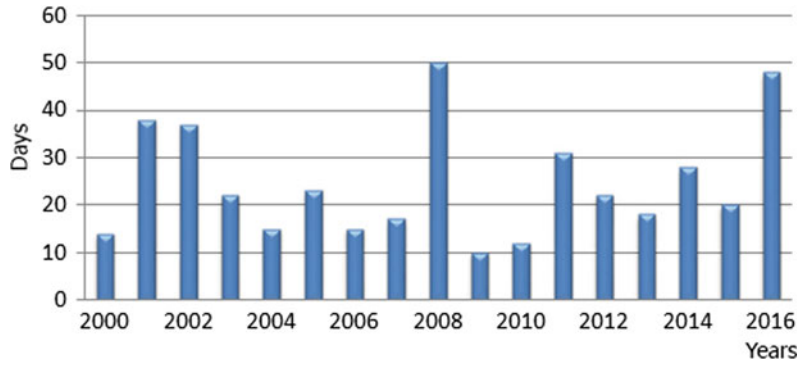
trend for landscapes at risk of erosion may have disastrous consequences in the future.

An increase in wind speed will increase dust storms. Over the past 16 years, the number of days with a wind speed of more than 15 m/s has increased significantly (Fig. 11.2), and an increase in the maximum wind speed has also been observed. For example, a wind speed of 33 m/s⁻¹ in Simferopol over the past 16 years has been observed twice, in 2007 and 2012 (Fig. 11.3).

Table 11.3 Types of land-use areas subject to water and wind erosion

Types of agricultural land	Wind erosion		Water erosion		Joint impact	
	Total hectares	% of the type of land	Total hectares	% of the type of land	Total hectares	% of the type of land
Arable land	823.2	66.0	96.0	7.6	31.8	2.5
Perennial plantations	46.8	37.4	10.8	8.6	0.3	0.2
Deposits	–	–	–	–	–	–
Hayfields	–	–	–	–	–	–
Pastures	247.2	62.2	92.5	23.3	15.8	4.0
Total agricultural land	1117.2	63.1	199.3	11.3	47.9	2.7

Fig. 11.2 Number of days with strong wind per year (Simferopol weather station) (Ergina and Zhuk 2017)



The highest wind speeds and the number of days with strong winds (over 15 m/s^{-1}) were observed at the end of winter and in early spring, and the lowest speeds were seen in summer (Ergina and Zhuk 2017). Most often, these winds are in a northeastern or western direction (Fig. 11.4). This leads to most dust storms occurring in the Crimean plain and the foothills of the Crimean Mountains at this time of the year. This destroys the upper, most fertile soil layer (given that the movement of light soil particles already occurs at a wind speed of $3\text{--}4 \text{ m/s}^{-1}$). Heavy loam soils that can be affected by a wind speed of approximately $>6 \text{ m/s}^{-1}$ are considered more resistant to soil deflation.

The frequency of strong winds in different parts of the Crimea is different. The most frequent strong winds are observed in the yaylas (highland pastures) of the Crimean Mountains, the least frequent in some areas of the southern coast. In recent years, there has been an increase in the number of days with strong wind in the foothills of the Crimea. According to the Crimean Hydrometeorology and

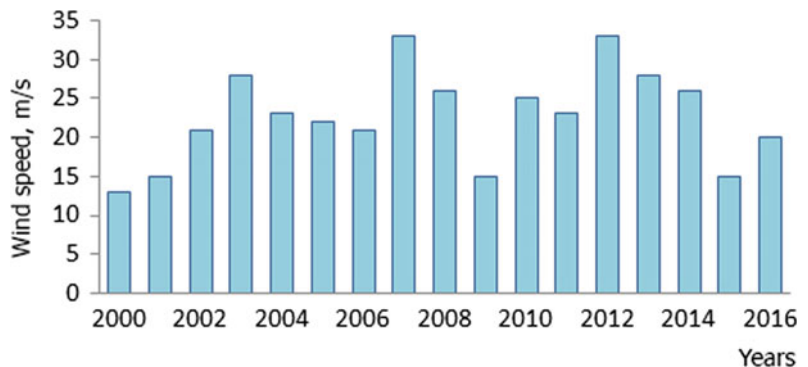
Environmental Monitoring Institute, between 2010 and 2015, there were days with a wind speed of more than 25 m/s^{-1} at each of the weather stations of the Crimea (Fig. 11.5).

At a wind speed of more than 25 m/s^{-1} , dust storms can occur not only on fields not covered by vegetation, but also on poorly developed winter crops and early spring crops. In this case, the soil from 3 to 10 cm can be blown off within a few days. In general, trends in the dynamics of wind are polynomial in nature and reflect the cyclical nature of the peninsula's climate.

Another pronounced feature of climate change in the Crimea is an increase (of about $3 \text{ }^\circ\text{C}$) in the minimum values of the average daily air temperature in the cold months of the year. As a result, a decrease was observed in the range of air temperature variability during this period (with the exception of the southern coast with its pronounced sub-Mediterranean climate).

According to forecasts on the plains and the foothills of the Crimea, this trend will continue in the coming years (Ergina et al. 2018). This will

Fig. 11.3 Dynamics of the maximum wind speed (Simferopol meteorological station) (Ergina and Zhuk 2017)



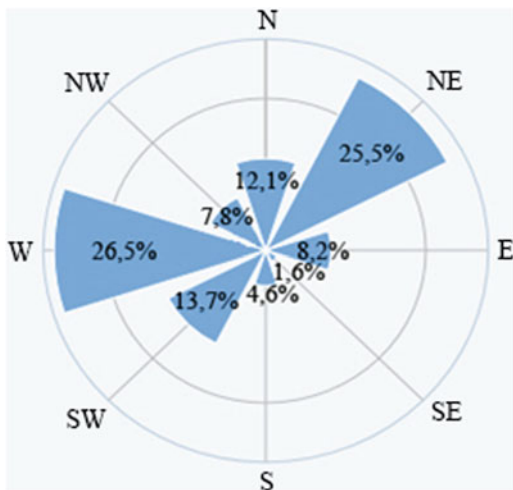


Fig. 11.4 Likelihood of strong winds in various directions (Simferopol weather station) (Ergina and Zhuk 2017)

lead to an increase in the number of winter thaws and, as a consequence, a change in the structure of the soil, the loss of its agronomically valuable aggregates and a decrease in resistance to erosion.

11.3.2 Simulation of Permissible Erosion Rates

According to theoretical concepts (Lisetskii 2000; Lisetskii and Ergina 2010; Ergina 2017a, b), the formation of the soil humus horizon over time occurs in accordance with the model:

$$H = Hg \cdot \exp(-\exp(a + \lambda \cdot T)) \quad (11.1)$$

where H—thickness of humus soil horizon, mm; Hg—maximum thickness of humus horizon, mm; a—constant of the initial state of soil formation; λ—coefficient of the bioclimatic features of soil formation; T—time of soil formation, years.

Chernozem and Kastanozem soils prevail in most of the Crimean plain, and in the southeast of the Tarkhankut peninsula, they were formed on loose, mainly loess rocks and red-brown Pliocene clays, Sarmatian and Maikop saline clays. For these soils, the model is:

$$H = 341 \cdot \exp(-\exp(0.7 - 0.003 \cdot T)) \quad (11.2)$$

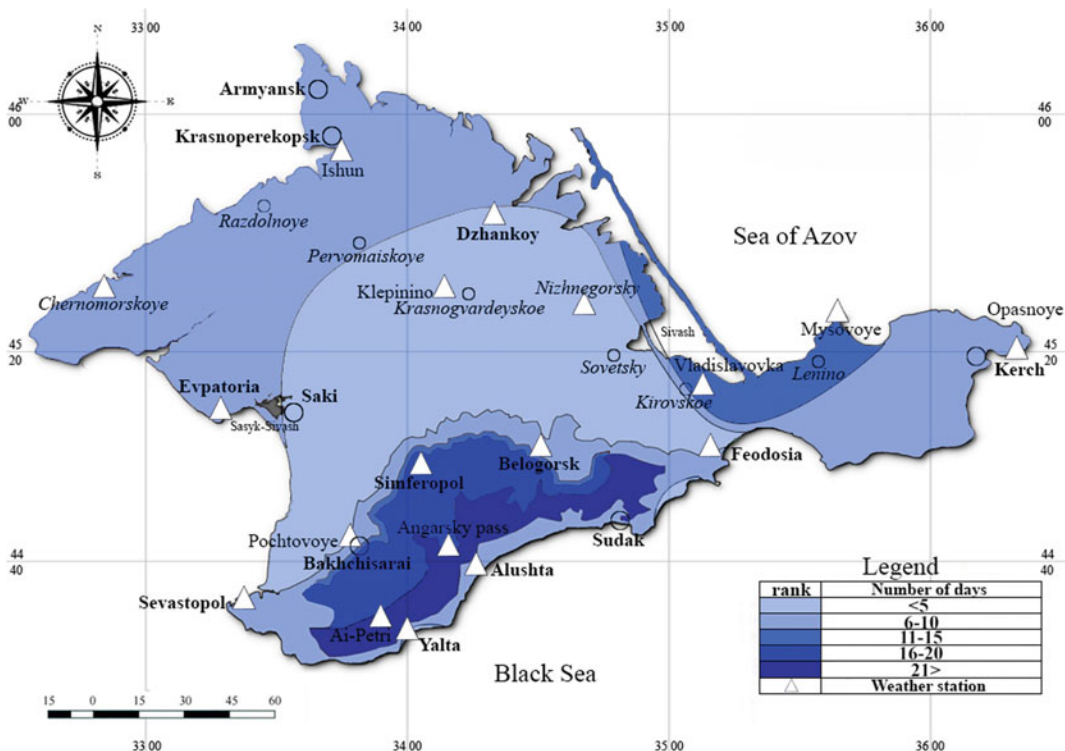


Fig. 11.5 Number of days with a wind speed of more than 25 m/s on the territory of the Crimean peninsula

In the foothill steppe vegetation on carbonate rocks in a semi-arid climate, Chernozemic soil types were formed. Chernozem was formed on rubble-stony weathering products of limestone, marl and pebble deposits, while Rendzic Leptosol was formed on depleted eluvium and carbonate materials. In the forest-steppe and steppe of the key areas, the model for the formation of the humus horizon of the soils formed on carbonate rocks on eluvium is:

$$H = 436 \cdot \exp(-\exp(0.98 - 0.001 \cdot T)) \quad (11.3)$$

Mollic Leptosols were formed on hard rocks and Cambisols on sands in the upper belt of the south macroslope of the main ridge. The southern coast of the Crimea is represented with Phaeozems. The model describing the formation of the humus horizon of these soils is:

$$H = 350.5 \cdot \exp(-\exp(0.7 - 0.001 \cdot T)) \quad (11.4)$$

The speed of formation of the humus soil horizon (G_c) after the arithmetical transformations of the model (2) takes the form (Ergina 2017a,b):

$$G_c = (-\lambda) \cdot H \cdot \exp(a + \lambda \cdot T) \cdot \exp(-\exp(a + \lambda \cdot T)) \quad (11.5)$$

The obtained models suppose that in the steppe regions of the Crimea, at the initial stages of soil formation on loose rocks which are 10 to 50 years old, the rate of soil formation reaches maximum values of 0.8–1.2 mm per year. Later, the rate of formation of the humus horizon decreases significantly, from 0.8 mm/year⁻¹ after 100 years from the beginning of soil formation to 0.2 mm/year⁻¹ after 200 years. During this period, there is probably a restructuring of the rate of the mechanisms of formation of the humus horizon.

The rate of formation of the humus horizon in the later phase of development ranges from 0.37

of the maximum value after 200 years to 0.09–0.02 mm per year in 1000–1500 years. After 2000 years, the process of stabilisation of the humus horizon formation begins (the rate decreases to 0.005 mm per year).

Within 40–50 years, the rate of formation of humus horizon of the soils formed on hard rocks, including those of carbonate origin, reaches maximum values up to 0.63–0.64 mm per year. This is much lower than the rate of soil formation on loose substrates in the Crimean steppe. In soils more than 100 years old, the rate of formation of the humus horizon naturally decreases from 0.4 to 0.07 mm per year.

Analyses of the rates of soil formation on hard rocks suggest that during the period of soil formation lasting 1000 years, the rates of formation of the humus horizon reach maximum values of 0.16 mm per year. In the period of 1500–4000 years, the rate decreases (0.14–0.02 mm per year) and only stabilises after 5000 years.

11.3.3 Geographical Analysis of Soil Formation Rates

To develop measures to combat erosion in the Crimea, it is necessary to use data on the rate of soil formation in slope areas. In the Crimea, significant land areas are located on the slopes of various gradients and exposures. All slopes with gradients up to 9–10° are cultivated for various agricultural crops. Slopes of 10–20° are occupied by perennial plantings (gardens, vineyards, forest, shrubs and pastures). Slopes of 20–21° are forested. Steep slopes exceeding 20–25° are used only partially for vineyards in the southern slopes of the main ridge of the Crimean Mountains. An increase in slope steepness from 7 to 14° increases the wash-off by 4.5 times; from 8 to 16° by 3.2 times; from 9 to 18° by 2.6 times; and from 11 to 22° by 2.1 times. A twofold increase in the length of the slope leads to an increase in wash-off by 2–2.4 times.

Soils destroyed by erosion cannot be restored to their original state due to the low rates of

compensatory soil formation. With the prolonged use of erosion-prone land, the soil can achieve optimal fertility. This is only possible if an autochthonous soil formation trend is present, which is characterised by the soil climax (quasi-climax), that is, a situation of quasi-equilibrium with the environment (Targulian 1982). Under such conditions, the rate of soil formation should always be higher than the rate of erosion. In modern production conditions, for average values of soil formation on slopes, lands (G_c , t/ha^{-1}) and surface erosion (W , t/ha^{-1}), this statement takes the form (Svetlichny et al. 2004):

$$(G_c - W) > 0 \quad (11.6)$$

Using approaches based on modelling by analogy, we can calculate the soil formation rates for eroded soils, where the washed-off soils are soils at a certain stage of development, since the rate of soil formation of the washed-off soils is negligible: a few tenths of a millimetre per year. Accurate calculations of the rate of soil formation will require multiple measurements and will be determined only after a few centuries.

Above, there is a discussion on the approach used to determine the rates of soil formation in upland conditions (Model 5).

The hydrothermal conditions of soil formation on the slopes differ from its upland analogues as follows:

$$G_c/G_n = Q_c/Q_n \quad (11.7)$$

where G —soil formation rate (c —on the slope, n —on the watershed); Q —energy cost for soil formation (c —on the slope, n —on the watershed).

Q was calculated with the equation proposed by Volobuev (1974):

$$Q = 41,868 \left[R \cdot e^{-18.8 \frac{R^{0.73}}{P}} \right], \quad (11.8)$$

where R —radiation balance, $ccal/cm^{-2}/year$; P —annual precipitation, mm ; Q —annual energy

cost for soil formation, after conversion of the units to the SI system in $MJ/m^2/year$:

Consequently:

$$G_c = (G_n \cdot Q_c)/Q_n \quad (11.9)$$

Taking into account the corrections to the microclimatic features when calculating the energy cost of soil formation on slopes, we obtain a mathematical model of the rate of soil formation in virgin conditions for slopes of various exposures and gradients:

$$G_c = G_n(41,87R \cdot kr \cdot \exp(-18.8 \cdot ((R \cdot kr)^{0.73}/P_0 \cdot k_0)))/Q_n \quad (11.10)$$

where G —soil formation rate (c —on the slope, n —on the watershed); Q —energy cost for soil formation (c —on the slope, n —on the watershed); kr —coefficient for slope exposure and gradient; P_0 —amount of precipitation on the watershed site (mm); $k_0 = \gamma \cdot kr$, where γ —empirical parameter.

Given the exponential law of the formation of the humus horizon, it can be assumed that eroded soils are similar to younger soils. The latter are at a certain stage of development and have not reached a state of quasi-equilibrium with soil formation factors. Following this approach, soil formation rates (permissible erosion rates) are calculated for soils of varying degrees of wash-off (Table 11.4). Based on the degree of soil erosion, the soils were classified as: 1—not eroded; 2—slightly eroded; 3—moderately eroded; and 4—strongly eroded. The criterion for determining the degree of a soil's susceptibility to erosion was the magnitude of the decrease in the thickness of the humus horizon in relation to its maximum thickness. Slightly eroded soils are soils that have lost 30% of the maximum soil depth. Moderately eroded soils lost up to 50% of the maximum depth, and in highly eroded soils, up to 75% of the soil layer was lost by wash-off (Ergina et al. 2018).

An analysis of Table 11.4 shows that, *ceteris paribus*, in the dry regions with Kastanozems and

Table 11.4 Soil formation rates for the Crimea ($t/ha^{-1} \text{ year}^{-1}$, with a bulk density of soil of 1.2 g cm^{-3})

No	Soils	Eroded	Northern exposure			Southern exposure			Eastern/western exposure		
			Slope (°)			Slope (°)			Slope (°)		
			0–8	9–12	13–20	0–8	9–12	13–20	0–8	9–12	13–20
1	Kastanozems, Chernozems	1	0	0	0	0	0	0	0	0	0
		2	0.9	0.9	0.8	0.9	0.9	0.9	0.9	0.9	0.9
		3	1.5	1.4	1.3	1.4	1.5	1.5	1.5	1.5	1.4
		4	2.3	2.2	2.1	2.2	2.2	2.3	2.3	2.3	2.2
2	Chernozems, Rendzic Leptosols	1	0	0	0	0	0	0	0	0	0
		2	0.7	0.7	0.7	0.7	0.7	0.7	0.7	0.7	0.7
		3	1.2	1.1	1.0	1.1	1.1	1.1	1.2	1.2	1.1
		4	1.7	1.6	1.5	1.6	1.7	1.7	1.7	1.7	1.6
3	Cambisols	1	0	0	0	0	0	0	0	0	0
		2	0.8	0.8	1.2	0.8	0.8	0.9	0.8	0.8	0.8
		3	1.4	1.3	1.2	1.4	1.4	1.4	1.4	1.4	1.3
		4	1.9	1.8	1.7	1.9	1.9	1.9	1.9	1.9	1.8
4	Phaeozems	1	0	0	0	0	0	0	0	0	0
		2	1.0	1.0	0.9	1.0	1.0	1.0	1.0	1.0	1.0
		3	1.8	1.7	1.6	1.8	1.9	1.9	1.8	1.8	1.8
		4	2.5	2.4	2.2	2.5	2.5	2.6	2.5	2.5	2.5

Chernozems, the highest soil formation rates are observed on eroded soils of a more humid northern exposure. In the foothills and mountainous areas and on the southern coast of the Crimea, where a significant amount of rainfall occurs, the amount of solar radiation acts as a limiting factor. Therefore, the highest soil formation rates are observed on the southern slopes. These patterns are most pronounced on steep slopes.

The average annual losses of the fertile soil layer due to erosion in the northern Crimea were 1.8 to 5.3 t/ha^{-1} ; in the northwest and west Crimea, and in the Kerch Peninsula, the soil losses were 12–15 t/ha^{-1} ; and in the foothill Crimea, losses were 16–22 t/ha^{-1} . The maximum values of soil losses, at 46.5 t/ha^{-1} , were in the mountainous Crimea (Ergina et al. 2018). A comparative analysis of these data with the calculated values suggests that the processes of

accelerated anthropogenic erosion in the Crimea have the parameters of a full-scale environmental catastrophe.

11.4 Conclusions

The results of field studies on changes in the depth of the humus horizon over time are given for four selected Crimean soils. When approximating data exponentially, the highest rates of formation of the humus horizon were observed at the first stages of profile formation. Calculations based on the obtained models show that, ceteris paribus, in arid regions with Kastanozems and Chernozems, the highest rates of soil formation were observed on eroded soils with a wetter northern exposure. In the foothills and mountainous areas and on the south coastal Crimea, where a significant amount of rainfall occurs, the

amount of solar radiation acts as a limiting factor. Therefore, the highest soil formation rates were observed on the slopes with a southern exposure, on the steepest slopes.

The processes of accelerated anthropogenic soil erosion in the world and in Russia are currently a full-scale environmental catastrophe. In particular, 1,117,200 ha (63% of the total area of agricultural lands) are affected by water erosion in the Crimea, including 823,200 ha of arable land. In this case, land use optimisation is only possible based on maintaining a non-negative balance between soil formation rates (permissible erosion rates) and erosion rates. For a quantitative assessment of the rates of soil formation, the most accurate method was based on an assessment of the rate of formation of the humus horizon over time.

We advocate the installation of a detailed monitoring system for soil erosion and local farmland management plans with measures that reduce erosion to a level that does not exceed the soil formation rate.

References

- Climate Atlas of Crimea: (Климатический атлас Крыма) (2000) Supplement to the scientific practical discussion analytical collection of papers "Questions of Development of Crimea". Authored and Compiled by I.P. Ved', Simferopol: Tavriya-Plus
- Cherny SG (1999) Estimation of permissible erosion rate for soils of the Steppe of Ukraine (Склоновые орошаемые агроландшафты: эрозия, почвообразование, рациональное использование). *Ukrainian Geograph J* 4:22–27
- Cherny SG (1996) Slope irrigated agrolandscapes: erosion, soil formation, rational use (Склоновые орошаемые агроландшафты: эрозия, почвообразование, рациональное использование). Kherson, Borisfen, 171 p
- Dessert C, Dupre B, Gaillardet J, Francois LM, Allegre CJ (2003) Basalt weathering laws and the impact of basalt weathering on the global carbon cycle. *Chem Geol* 202:257–273. <https://doi.org/10.1016/j.chemgeo.2002.10.001>
- Dietrich WE, Bellugi D, Heimsath AM, Roering JJ, Sklar L, Stock JD (2003) Geomorphic transport laws for predicting the form and evolution of landscapes. In: Wilcock P, Iverson R (eds) *Prediction in Geomorphology*. AGU Geophysical Monograph Series, vol 135, pp 103–132
- Dragan NA (2004) Soil resources of Crimea (Почвенные ресурсы Крыма). Simferopol, Dolya, 208 p
- Ergina EI, Gorbunov RV, Scherbina AD (2018) Geographical analysis of permissible rates of soil erosion in the agricultural landscapes of the Crimean peninsula (Географический анализ допустимых норм эрозии почв в агроландшафтах Крымского полуострова). Simferopol, Publisher, Arial, p 180
- Ergina EI, Zhuk VO (2017) The influence of current climate trends on the state of erosion dangerous agrolandscapes and the assessment of the soil-forming potential of natural factors in the Crimea (Влияние современных тенденций климата на состояние эрозионноопасных агроландшафтов и оценка почвообразующего потенциала природных факторов Крыма). *Proc Orenburg State Agrarian Univ* 3 (65):175–178. <https://cyberleninka.ru/article/n/vliyanie-sovremennyh-tendentsiy-klimata-na-sostoyanie-erozionno-opasnyh-agrolandshaftov-i-otsenka-pochvoobrazuyuschego-potentsiala>. Accessed 7 March 2021
- Ergina EI, Zhuk VO (2018) On the growth of dangerous and elemental hydrometeorological phenomena on the Crimean peninsula (Интенсификация опасных и стихийных гидрометеорологических явлений на Крымском олуострове). *Proceedings of higher educational institutions. North Caucasus region. Ser Nat Sci* 1(197):68–74
- Ergina EI, Zhuk VO (2019) Spatiotemporal variability of the climate and dangerous hydrometeorological phenomena on the Crimean Peninsula. *Russ Meteorol Hydrol* 44(7):494–500. <https://doi.org/10.3103/S1068373919070082>
- Ergina EI (2017a) Modeling of the development of humus horizons in soils of Crimea. *Eurasian Soil Sci* 50 (1):14–19. <https://doi.org/10.1134/S1064229317010069>. Accessed 20 March 2019
- Ergina EI (2017b) Spatio-temporal patterns of the processes of modern soil formation on the Crimean peninsula (Пространственно-временные закономерности процессов современного почвообразования на Крымском полуострове). Simferopol. Publisher: "Arial", p. 224
- Goddéris Y, Francois LM, Probst A, Schott J, Moncoulon D, Labat D (2006) Modelling weathering processes at the catchment scale: the WITCH numerical model. *Geochim Cosmochim Acta* 70:1128–1147. <https://doi.org/10.1016/j.gca.2005.11.018>
- Goleusov PV, Lisetskii FN (2005) Reproduction of soil in anthropogenic landscapes of forest-steppe (Воспроизводство почв в антропогенных ландшафтах лесостепи). Belgorod State University, p. 232
- Hoosbeek MR, Bryant RB (1992) Towards the quantitative modeling of pedogenesis a review. *Geoderma* 55:183–210. <https://www.sciencedirect.com/science/article/pii/001670619290083J> Accessed 7 March 2021
- Ivanov NN (1949) Landscape and climatic zones of the Earth (Ландшафтно-климатические зоны земного шара). *Zap Geogr Soc* 1:228

- Kirkby MJ (1985) A basis for soil profile modelling in a geomorphic context. *J Soil Sci* 36(1):97–121. <https://doi.org/10.1111/j.1365-2389.1985.tb00316.x> Accessed 7 March 2021
- Lisetskii FN (2000) Spatio-temporal organisation of agrolandscapes (Пространственно–временная организация агроландшафтов. Belgorod State University, Белгородский Государственный университет), p 301
- Lisetskii FN, Ergina EI (2010) Soil development on the Crimean peninsula in the late Holocene. *Eurasian Soil Sci* 43(6):601–613. <https://doi.org/10.1134/S1064229310060013> Accessed 7 March 2021
- Lisetskii FN, Stolba VF, Ergina EI, Rodionova ME, Terekhin EA (2013) Post-agrogenic evolution of soils in ancient Greek land use areas in the Herakleian peninsula, southwestern Crimea. *The Holocene* 23(4):504–514. <https://doi.org/10.1177/0959683612463098>. Accessed 7 March 2021
- Lisetskii F (2019) Estimates of soil renewal rates: applications for anti-erosion arrangement of the agricultural landscape. *Geosciences* 9(6):266. <https://doi.org/10.3390/geosciences9060266>
- Minasny B, McBratney AB, Salvador-Blanes S (2008) Quantitative models for pedogenesis: a review. *Geoderma* 144:140–157. <https://doi.org/10.1016/j.geoderma.2007.12.013>
- Modern landscapes of the Crimea and Adjacent Territories (2009) (Современные ландшафты Крыма и сопредельных территорий). I.: Pozachenuk EA (ed). Simferopol, Business-Inform, p 672
- Prudko OI, Adamenko TI (2011) Agroclimatic guide to the Crimea (Агроклиматический справочник по АР Крым). TI Simferopol, Tavrida, p 342
- Report on the state and environmental protection in the Republic of Crimea in 2015 (Доклад о состоянии и охране окружающей среды на территории Республики Крым в 2015 год) http://meco.rk.gov.ru/rus/file/Doklad_o_sostojanii_i_ohrane_okruzhajushhej_sredy_Respubliki_Krym_v_2015.pdf. Accessed 7 March 2021
- Svetlichny AA, Cherny SG, Schwabs GI (2004) Erosion: theoretical and applied aspects (Эрозиоведение: теоретические и прикладные аспекты) Monograph. University Edition, Sumy, p 410
- Targulian VO (1982) Soil development over time (Развитие почв во времени). Nauka, Problems of soil science. Moscow, pp 108–113
- Volobuev VR (1974) Introduction to the energetics of soil formation (Введение в энергетику почвообразования). Nauka p, Moscow, p 128
- WRB (2015) World reference base for soil resources 2014. Food and Agriculture Organization of the United Nations, Rome, p 2015



Effect of Deer Browsing and Clear-Cutting of Trees on Soil Erosion in a Forest Ecosystem in Japan

Nanami Murashita, Atsushi Nakao, Keiko Nagashima, and Junta Yanai

Abstract

Soil erosion is an emerging concern threatening sustainability of forest ecosystems. In case of Japan, one of the driving forces of accelerating soil erosion is heavy deer browsing and trampling. To investigate the effect of deer and clear-cutting on soil erosion, we set up three experimental plots at a slope (24° – 27°) of a forest ecosystem with high density of deer, i.e., the fenced plot [F], the non-fenced plot [NF], and the fenced + clear-cut plot [F + C]. The amounts of eroded soil, surface runoff, and loss of nutrients were measured in each experimental plot for 1 year. The amount of eroded soils were in the order of F ($1.81 \text{ t ha}^{-1} \text{ yr}^{-1}$) $< F + C$ ($5.09 \text{ t ha}^{-1} \text{ yr}^{-1}$) $< NF$ ($7.71 \text{ t ha}^{-1} \text{ yr}^{-1}$), suggesting that both deer and clear-cutting accelerated soil erosion. The amount of surface runoff also increased in the order of $F < F + C < NF$. In addition, the bulk density increased, whereas permeability coefficient decreased in the NF plot. This result would be due to the compaction by deer trampling. The amount of eroded soils in each experimental plot positively correlated with rainfall (mm) and rain-

fall peak intensity ($\text{mm } 10 \text{ min}^{-1}$) ($p < 0.01$). As the rainfall and rainfall peak intensity increased, the amount of eroded soil increased proportionally in all plots. However, the erodibility to the same rainfall in three plots was different. The loss of carbon and nitrogen from the slope also increased in the order of $F < F + C < NF$, and most of loss ($>93\%$) was derived from the loss of soil particles. In conclusion, we should conserve the forest ecosystems through preventing soil erosion because heavy deer browsing and trampling and clear-cutting of trees would lead to the accelerated soil erosion and loss of nutrients.

Keywords

Deer · Tree cutting · Rainfall · Nutrient loss · Soil degradation

12.1 Introduction

Soil erosion is an emerging concern threatening sustainability of ecosystems (Lal 2014). Increased erosion leads to a significant loss of the topsoil, which leads to a decline in ecological function or soil fertility (Holz et al. 2015). Excessively eroded soils transported to watersheds cause degradation of streams and river habitats such as fish and macroinvertebrates, or eutrophication of freshwater resources and

N. Murashita · A. Nakao · K. Nagashima · J. Yanai (✉)
Kyoto Prefectural University, 1-5 Shimogamo Hangicho, Sakyo-ku, Kyoto 606-8522, Japan
e-mail: yanai@kpu.ac.jp

coastal estuaries, thereby seriously changing the biodiversity of water ecosystems (Choi et al. 2017). Strategies are required to mitigate soil erosion based on comprehensive understanding of the factors controlling the intensity of soil erosion. Important factors to control soil erosion (i.e., erosion factors) include the climatic, hydrological, topographic, soil, geological, and vegetation conditions (Lv et al. 2012). Nowadays, in Japan, the quality of climatic and vegetation conditions is rapidly changing, which can cause accelerated soil erosion.

Concerning climatic condition, the rainfall intensity, as represented by the number of days with heavy rain ($>100 \text{ mm day}^{-1}$), has clearly increased in Japan over the past century (Fujibe et al. 2006). This trend seems to be continuing in the 2010s (Ministry of the Environmental Government of Japan 2018). Although the amount of rainfall does not show a clear increasing trend, climate models estimate more than 10% increase of rainfall intensity in this century (Kimoto et al. 2005). These long-term changes in weather patterns in the mid-to-high latitudes of the Northern Hemisphere are likely due to increased greenhouse gas emissions (Ehhalt et al. 2001). The higher the rainfall intensity, the greater the soil erosion (Nishigaki et al. 2016; Piacentini et al. 2018).

More importantly, although less focused, concerning the vegetation condition, especially in forest regions, the reduction understory vegetation cover on the land surface is increasingly enhanced by deer browsing (Nomiya et al. 2002; Nishizawa et al. 2016), which is also believed to accelerate soil erosion. The population of the sika-deer, *Cervus nippon*, has increased drastically since the late twentieth century. For example, Tsujino et al. (2004) reported that the population has increased almost 20-fold between 1988 and 2001 on Yakushima Island in Japan. This overpopulation can be explained by the extinction of the Japanese wolf *Canis lupus hodophilax* in 1905, a decrease in the amount of snow due to global warming, decrease in the number of hunters, reduction, and aging of the population in rural areas, etc. (Takatsuki 2009). Furthermore, intensively-planted *Cryptomeria*

japonica and *Chamaecy parisobtusa* for logging after World War II were left without thinning, which led to a decrease in the lighting of the lower tier and therefore decrease in the understory vegetation in wide areas of mountainous regions in Japan (Takatsuki 2009). This situation prompted deer to move into the secondary deciduous forests close to the border between mountain foothills and agricultural fields. Although the disturbance effects of deer overpopulation were broadly investigated, especially in relation to vegetation or other biota (Horsley et al. 2003; Niwa et al. 2011), a relatively small number of studies have focused on their adverse effects on soil conditions.

Secondary deciduous forests are at risk not only from deer browsing, but also widely susceptible to the oak wilt disease from the second half of the twenties century, which causes the mass mortality of *Quercus serrata* and *Quercus variabilis* (Kubono and Ito 2002). To reduce mass mortality and to re-establish the oak forest, a small-scale clear-cutting is recommended to enhance sprouting (Kuroda et al. 2012). Although clear-cutting can be effective in reestablishment of forest vegetation, it can potentially increase soil erosion.

The objective of this study, therefore, was to investigate the effect of deer and clear-cutting on soil erosion in secondary deciduous forest in Japan. To compare these effects, we established three different experimental plots on the same slope area with representative secondary deciduous forest vegetation: (1) fenced plot to exclude deer or other animals as a control, (2) un-fenced plot where deer or other animals can walk around, and (3) fenced plus clear-cut plot.

12.2 Materials and Methods

12.2.1 Study Site

The study site ($35^{\circ}05' \text{ N}$, $135^{\circ}78' \text{ E}$) was located in Sakuranomori of Takaragaike Park, Kyoto prefecture, Japan (Fig. 12.1). Main soil type here is Typic Dystrudept (Soil Survey Staff 2014). The geology was chart from GeomapNavi

(<https://gbank.gsj.jp/geonavi/>), with minor amounts of siliceous shale and bedded siliceous claystone. The mean annual rainfall and temperature recorded at the nearest meteorological office are 1491 mm and 15.9 °C, respectively, as averaged from 1981 to 2010 (Japan Meteorological Agency 2017). The climate of the study site was classified as Cfa (humid temperate climate) according to Köppen climate classification. Although main vegetation type was secondary deciduous tree, forest ecosystems in this park have been recently disturbed mainly due to heavy deer browsing and oak wilt disease (Nagashima 2017). Since around 2008, the understory vegetation such as *Rhododendron reticulatum* and bamboo grass largely reduced their population due to browsing and debarking by deer reflecting their explosive increase of the individual density as high as 48 heads km⁻² (Noda and Ogawa 2017, personal communication). Since around 2010, Japanese oak such as *Quercus serrata* and *Q. variabilis* decreased due to rapid expansion of Japanese oak wilt (Kyoto City Greening Association 2015). In contrast, several species of lower tier tree such as deer's unpalatable species (e.g., *Ilex pedunculosa* and *Mallotus Japonicus*) and alien species (e.g., *Triadica sebifera*) have increased their population (Nagashima 2015).

12.2.2 Experimental Design

We set up three adjacent experimental plots of 30 m × 10 m each on the west-facing slope with the slope angle of 24° to 27° in Takaragaike Park in December 2015; (1) fenced plot to protect vegetation from deer (F), (2) not fenced plot (NF), and (3) fenced plus clear-cut plot (F + C). In the F + C plot, all trees higher than 50 cm were once cleared in 2015 (Fig. 12.2). Then, a soil erosion monitoring plot of 2 m × 1.5 m (hereinafter called 'erosion devise') was set up in each experimental devise in December 2016 (Fig. 12.3). A rain gauge (TE 525 MM: Campbell Scientific, USA) and a thermometer (CS

215: Campbell Scientific, USA) were set up in F + C plot. Changes over time in precipitation and temperature were recorded every 1 min with a data logger (CR 1000: Campbell Scientific, USA), respectively. Quadruplicate litter traps with a length of 50 cm and a width of 50 cm (0.25 m²) were also set up in each experimental plots. The survey period was one year: from December 2016 to December 2017. In addition, a time-domain reflectometry (TDR; CS616: Campbell Scientific, USA) was set up at sub-surface soil (15–30 cm) in each experimental plot and measured soil water content every a minute from April 2017 to December 2017.

12.3 Materials and Methods

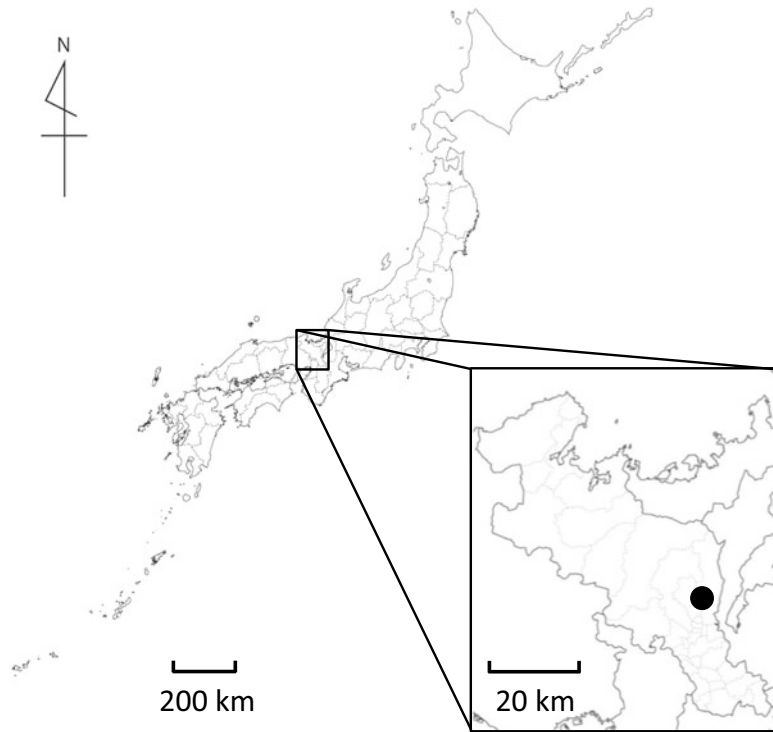
12.3.1 Permeability and Bulk Density of Surface Soil

Surface soils (0 to 5 cm) were collected using soil cores, i.e., 100 cm³ stainless sampling tube (DIK-1801, Daiki Rika Kogyo, Japan) at five points outside of the erosion device in each experimental plot. Sampling dates for F, NF, and F + C were March 2017, February 2017, and December 2016. The core samples were firstly tested on a soil permeability measurement device (DIK-II, Daiki Rica Kogyo, Japan) to determine the permeability coefficient by using the constant water level method. In this method, the permeability coefficient was calculated using the following formula (Eq. 12.1) based on Darcy equation:

$$K = qL/Aht \quad (12.1)$$

where K is the permeability coefficient (cm s⁻¹), q is the volumetric flux (cc), L is the thickness of the sample (cm), A is the cross-sectional area of the sample (cm²), h is the position difference (cm), and t is the time (s). Bulk density of the sample (g cm⁻³) was then measured by weighing the core samples after drying at 110 °C for 24 h.

Fig. 12.1 Location of the study site



12.3.2 The Amount of Surface Runoff, Eroded Soil, and Litter Fall

A stainless steel collector (Fig. 12.3) was used to intercept both eroded soils and surface runoff from a 3 m² upper slope plot with a slope length of 2.0 m and a width of 1.5 m. Surface runoff was stored in the two buckets connected with the steel collector, whereas eroded soils were either settled on the collector or leached down to the upper bucket. Both the eroded soils and surface runoff were collected about every 2 weeks and weighed individually. The eroded soils were firstly sieved to <2 mm. A portion of the samples was further sieved into four fractions (<20 μm, 20–50 μm, 50–200 μm, and 200–2000 μm). The sieving was carried out without organic matter decomposition, sonication, and pH adjustment, thereby maintaining original structure of soil aggregates. Therefore, aggregate particles were collected in addition to single particles in each particle size fraction. The amount of eroded soil

(<2 mm) and rainfall during each sampling period were used to calculate the amount transported per 1 ml of rainfall (i.e., soil transport rate [$\text{g m}^{-1} \text{mm}^{-1}$]) (Miura et al. 2002), which is useful to compare the erosion rates with those previous reported in the other forest regions in Japan. Litterfall were collected once a month and weighed after drying at 80 °C for 2 days.

12.3.3 The Amount of Carbon, Nitrogen, and Phosphorus Loss

Each fraction of the eroded soil was milled in a mortar and dried overnight at 110 °C. Approximately 100 mg was precisely weighed in a quartz boat and then the total carbon and nitrogen content was quantified by the dry combustion method using an NC analyzer (Sumigraph NC-95A: Sumika Chemical Analysis Service, Japan) coupled with a gas chromatograph (GC-8A: Shimadzu, Japan). The <20 μm and 200–

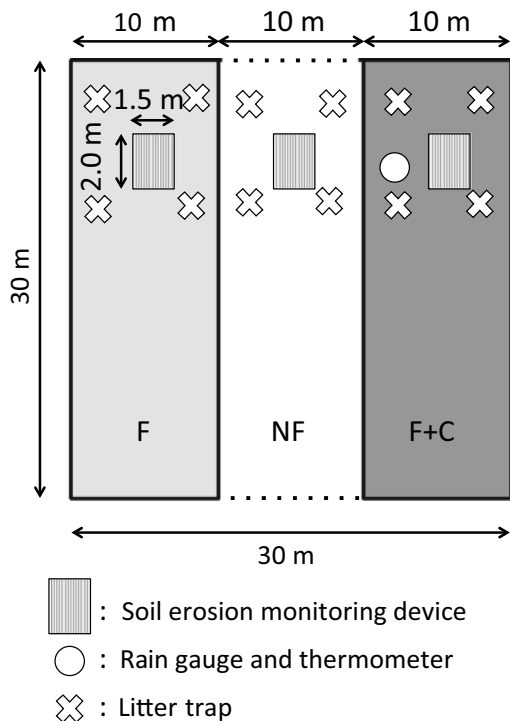


Fig. 12.2 Design of the experimental plots. F plot was without deer . NF plot was with deer . F + C plot was without deer and with clear-cutting

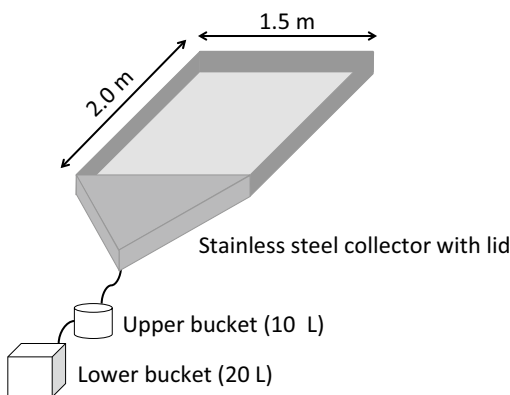


Fig. 12.3 Design of the soil erosion monitoring

2000 μm fractions we restored separately according to each sampling. The 20–50 μm and 50–200 μm fractions were, however, mixed into one composite after measuring the weight of each fraction. The surface runoff was filtered

through a 0.45 μm membrane filter to remove suspended soil and impurities. The contents of dissolved carbon and total nitrogen were then quantified by the combustion oxidation method using total organic carbon meter (TOC-VC_{SH}, TNM-1; Shimadzu, Japan). The eroded soil (all fractions) collected on November 2017 was milled in a mortar. The samples were filled into an aluminum ring ($\phi 22\text{ mm}$), and form pellets by pressing at 500 gkf cm^{-2} using hydraulic press. Then, the total amount of phosphorus was quantified using an energy dispersive X-ray fluorescence spectrometer (SPECTRO XEPOS C, Germany).

12.3.4 The Amount of Nitrogen and Phosphorus Input

Litters in the quadruplicate traps were mixed together, cut, and milled in a mortar. Approximately 20 mg was precisely weighed in a quartz boat and then the total nitrogen content was quantified by the dry combustion method using an NC analyzer (Sumigraph NC-95A; Sumika Chemical Analysis Service, Japan) coupled with a gas chromatograph (GC-8A; Shimadzu, Japan). A 0.3 g of the milled litter sample was heated with 5 ml of nitric acid for complete decomposition. The total phosphorus of digested samples was measured by molybdenum-blue methods using spectrophotometer at 712 nm.

12.3.5 Tree Census

The standing dead trees were removed before setting three plots to understand its effect on vegetation recovery and to avoid risks of dead trees falling and endangering citizens visiting the Takaragaike Park. The treatments were conducted in November 2015. Each experimental plot was further subdivided into upper, middle, and lower 10 m \times 10 m subplot, based on its location at the slope. In this study, we will show the results of tree censuses for trees smaller than 1.2 m observed in the upper subplot in 2016 and 2018.

12.4 Results

12.4.1 Bulk Density and Permeability Coefficient

Average values of bulk density and permeability coefficient for the surface soils at the F, NF, and F + C plots are shown in Fig. 12.4. The bulk density differed in the order: F ($0.62 \pm 0.15 \text{ g cm}^{-3}$) < F + C ($0.80 \pm 0.11 \text{ g cm}^{-3}$) < NF ($1.04 \pm 0.04 \text{ g cm}^{-3}$), whereas the permeability coefficient differed between the treatment plot in the reverse order: F ($6.26 \times 10^{-2} \pm 0.01 \text{ cm s}^{-1}$) > F + C ($2.21 \times 10^{-2} \pm 0.01 \text{ cm s}^{-1}$) > NF ($1.50 \times 10^{-2} \pm 0.01 \text{ cm s}^{-1}$). While not significant, the lower bulk density was associated with the higher value of the permeability coefficient.

12.4.2 Soil Water Content

The water contents in subsurface soil (15–30 cm) throughout the whole period are shown in Fig. 12.5. Although a sharp increase in the soil water content was observed immediately after rainfall in all plots, the highest peak was shown by the NF plot in most cases. Furthermore, the NF plot showed the slowest decreasing rate in soil water content from the peak almost throughout the entire period. In other words, the NF plot had the worst drainage condition.

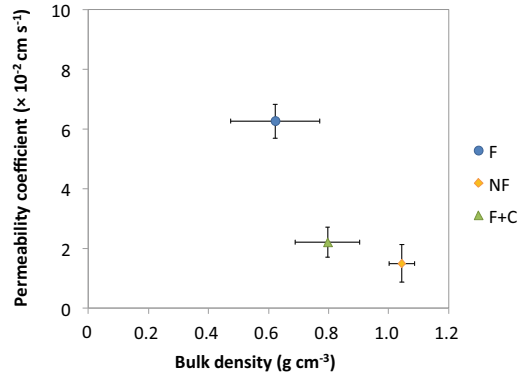


Fig. 12.4 Relationship between bulk density and permeability coefficient of the surface soils (Error bars represent standard errors)

12.4.3 Amount of Surface Runoff and Eroded Soil

The amount of eroded soil and surface runoff during each sampling period are shown in Table 12.1. Although the eroded soils were successfully collected through the whole period, the surface runoff sometimes overflowed from the storage container especially during intensive precipitation, which may cause a considerable underestimation.

Such an intensive precipitation was frequent from June to October, whereas sporadic in other seasons. Seasonal variation of the surface runoff was similar among F, NF, and F + C plots. The annual total surface runoff was in the following

Fig. 12.5 Seasonal changes in soil water content of the experimental plots

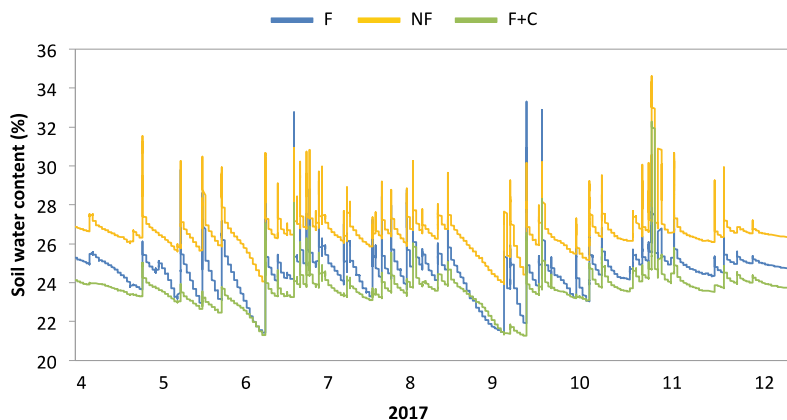


Table 12.1 Rainfall, amounts of surface runoff and eroded soil, and transport rate of soil for individual sampling periods (* over flow period)

Sampling date (m/d/yr)	Period (day)	Rainfall (mm)	Amount of surface runoff (t ha ⁻¹)			Amount of eroded soil (kg ha ⁻¹)			Transport rate of soil (g m ⁻¹ mm ⁻¹)		
			F ^a	NF ^a	F + C ^a	F	NF	F + C	F	NF	F + C
12/29/16	19	85.7	43.8	42.2	29.7	19.6	107.2	50.3	0.05	0.25	0.12
1/16/17	21	28.2	21.2	14.8	17.3						
2/2/17	18	60.0	42.7*	43.7*	14.2	6.7	16.4	28.3	0.02	0.04	0.06
2/17/17	15	36.5	14.0	13.8	31.0						
3/7/17	18	24.0	13.8	9.9	20.7	20.9	133.0	83.5	0.07	0.44	0.28
3/22/17	15	38.1	22.5	23.0	34.5	7.7	42.2	45.4	0.04	0.22	0.24
4/4/17	13	18.7	12.4	8.5	12.9	16.6	159.7	57.5	0.18	1.71	0.62
4/21/17	19	121.6	58.7	75.0*	76.7*	69.7	815.6	310.9	0.11	1.34	0.51
5/8/17	17	17.6	13.2	27.8	6.3	37.7	155.1	46.4	0.43	1.76	0.53
5/22/17	14	30.3	31.3	75.7*	55.3	52.1	251.9	68.7	0.34	1.66	0.45
6/5/17	14	34.7	68.5	118.5*	117.3*	172.0	194.0	110.2	0.98	1.12	0.64
6/19/17	14	29.8	33.2	75.1	78.7	36.5	139.4	41.6	0.24	0.94	0.28
7/3/17	14	166.6	126.5	133.2	151.0*	193.7	1097.5	1033.7	0.23	1.32	1.24
7/18/17	15	115.3	78.7*	76.0*	85.8*	188.2	824.6	775.3	0.33	1.43	1.34
7/31/17	13	40.1	58.7	77.0*	76.0*	62.2	195.0	305.4	0.31	0.97	1.52
8/14/17	14	126.8	79.0*	92.0*	82.0*	167.2	738.6	607.2	0.26	1.17	0.96
8/28/17	14	43.0	35.0	41.0	70.3	64.8	195.8	335.8	0.30	0.91	1.56
9/11/17	14	20.5	29.5	42.8	49.8	24.7	72.9	36.5	0.24	0.71	0.36
9/22/17	11	122.0	17.8*	77.7*	77.0*	221.3	956.7	785.7	0.36	1.57	1.29
10/10/17	18	93.4	81.0*	77.5*	77.5*	108.1	434.7	57.5	0.23	0.93	0.12
10/24/17	14	191.6	78.2	77.7	76.7	190.9	742.6	201.3	0.20	0.78	0.21
11/6/17	13	77.4	48.8*	75.9*	79.2*	90.0	281.9	72.8	0.23	0.73	0.19
11/20/17	14	37.7	25.8	78.2*	26.1	39.8	94.6	31.1	0.21	0.50	0.17
12/4/17	14	8.8	3.6	7.3	3.3	22.0	56.9	8.7	0.50	1.29	0.20
Total (yr ⁻¹)	365	1568.4	1037.8	1384.2	1349.3	1812.3	7706.0	5093.9	–	–	–
Average	–	–	–	–	–	–	–	–	0.27	0.99	0.59

^aF: Fenced plot, NF: not fenced plot, F + C: fenced plus clear-cut plot

order: F plot (1.04×10^3 t ha⁻¹) < F + C plot (1.35×10^3 t ha⁻¹) < NF plot (1.38×10^3 t ha⁻¹). Seasonal changes in the amount of eroded soil at the F, NF, and F + C plots are plotted in Fig. 12.6, together with the changes in precipitation. Increasing or decreasing trend in the amount of eroded soil was similar among three plots; greater erosion was frequently observed from July to October, well corresponding to the amount of precipitation at each period

(Fig. 12.6). The annual total eroded soil was largely different in the following order: F plot (1.81 t ha⁻¹) < F + C plot (5.09 t ha⁻¹) < NF plot (7.71 t ha⁻¹). On the NF and F + C plots, a significantly larger amount of eroded soil is recorded than that on the F plot, for almost the entire period. The average soil transport rate was also in the following order: F plot (0.27 g m⁻¹ mm⁻¹) < F + C plot (0.59 g m⁻¹ mm⁻¹) < NF plot (0.99 g m⁻¹ mm⁻¹). Especially, the soil

Fig. 12.6 Seasonal changes in the amount of eroded soil of the experimental plots and the rainfall

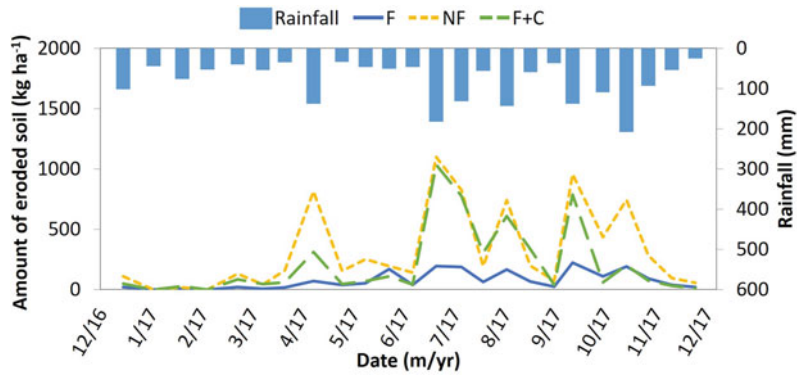


Table 12.2 The amounts (annual total, $n = 1$) and the percentages (average value \pm standard deviation, $n = 24$) of particle size distribution (<2 mm) of the eroded soil in each experimental plot

Particle size distribution						
	F		NF		F + C	
	(kg ha ⁻¹)	(%)	(kg ha ⁻¹)	(%)	(kg h ⁻¹)	(%)
< 20 urn	125	8.4 \pm 6.3	938	12.0 \pm 5.5	535	11.0 \pm 6.7
20–50 nm	66.1	4.4 \pm 2.6	376	4.6 \pm 1.4	292	5.0 \pm 1.6
50–200 nm	216	13.5 \pm 6.7	879	11.0 \pm 2.7	699	13.1 \pm 4.0
200–2000 nm	1405	73.7 \pm 13.6	5513	72.5 \pm 8.6	3568	71.0 \pm 10.3
Total	1812	100	7706	100	5094	100

transport rate in the NF and F + C plots was also clearly higher than that in the F plot throughout the period (Table 12.1).

12.4.4 Size Distribution of Eroded Soil

Particle size distributions of the eroded soil (<2.0 mm) between <20 μm , 20–50 μm , 50–200 μm , and 200–2000 μm are shown in Table 12.2. The particle size distribution was basically similar among the F, NF, and F + C plots. Weight percentage of 200 to 2000 μm fraction, which was supposed to consist mainly of the macroaggregate, was above 70% in all experimental plots. The proportion of 200 to 2000 μm fraction in the F + C plot was the smallest among the three experimental plots.

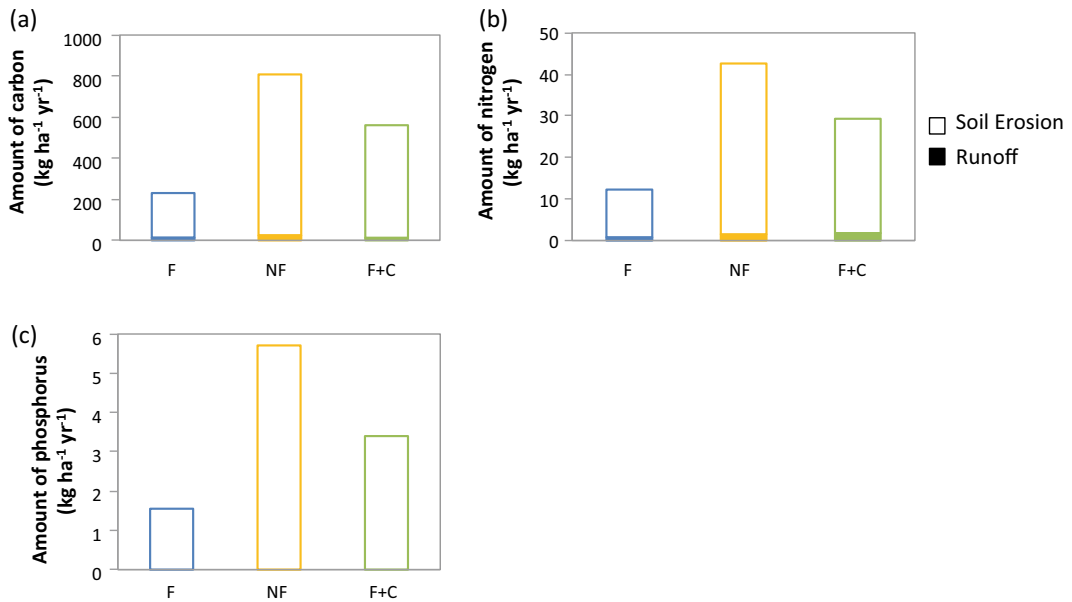
12.4.5 Carbon, Nitrogen, and Phosphorus Loss via Surface Runoff and Eroded Soil

Table 12.3 shows the average concentration of carbon and nitrogen in the eroded soil and surface runoff at the experimental plots. In the case of eroded soil, the highest concentrations of carbon and nitrogen were observed in the F plot, while their lowest concentrations were observed in the NF plot. In contrast to eroded soil, the highest concentration of carbon in the surface runoff was observed in the NF plot, whereas the nitrogen concentration was highest in the F + C plot. The lowest concentrations of both carbon and nitrogen were observed in the F plot.

The total amount of carbon, nitrogen, and phosphorus lost annually in the eroded soils and

Table 12.3 Concentration of the nutrients in the eroded soil and surface runoff

	Concentration in the eroded soil (g kg^{-1})			Concentration in the surface runoff (mg l^{-1})		
	F	NF	F + C	F	NF	F + C
Carbon	122.4	100.8	104.2	13.2	17.1	14.4
Nitrogen	6.5	5.1	5.4	0.9	1.2	1.8

**Fig. 12.7** Total amount of annual loss of **a** carbon, **b** nitrogen, and **c** phosphorus by soil erosion and runoff

surface runoff are shown in Fig. 12.7. The amount of carbon differed among the experimental plots in the following order: F plot ($231 \text{ kg ha}^{-1} \text{ yr}^{-1}$) < F + C plot ($562 \text{ kg ha}^{-1} \text{ yr}^{-1}$) < NF plot ($825 \text{ kg ha}^{-1} \text{ yr}^{-1}$). The relative contribution of eroded soil to total carbon corresponded to 94, 98, 97%, respectively. The amount of nitrogen differed among the experimental plots in the following order: F plot ($12 \text{ kg ha}^{-1} \text{ yr}^{-1}$) < F + C plot ($30 \text{ kg ha}^{-1} \text{ yr}^{-1}$) < NF plot ($43 \text{ kg ha}^{-1} \text{ yr}^{-1}$). Relative contribution of eroded soil to the total nitrogen corresponded to 93, 94, 96%, respectively. The amount of phosphorus differed among the experimental plots in the following order: F plot ($1.5 \text{ kg ha}^{-1} \text{ yr}^{-1}$) < F + C plot ($3.4 \text{ kg ha}^{-1} \text{ yr}^{-1}$) < NF plot ($5.7 \text{ kg ha}^{-1} \text{ yr}^{-1}$).

12.4.6 Nitrogen and Phosphorus Input via Litter

The amount of litterfall distributed as follows: F + C plot ($2.1 \text{ kg ha}^{-1} \text{ yr}^{-1}$) < F plot ($4.3 \text{ kg ha}^{-1} \text{ yr}^{-1}$) < NF plot ($4.7 \text{ kg ha}^{-1} \text{ yr}^{-1}$). Total amount of nitrogen and phosphorus input annually in the litter are shown in Table 12.4. The amount of nitrogen differed among the experimental plots as follows: F + C plot ($22.3 \text{ kg ha}^{-1} \text{ yr}^{-1}$) < NF plot ($46.1 \text{ kg ha}^{-1} \text{ yr}^{-1}$) \approx F plot ($46.6 \text{ kg ha}^{-1} \text{ yr}^{-1}$). The amount of phosphorus differed among the experimental plots as follows: F + C plot ($0.6 \text{ kg ha}^{-1} \text{ yr}^{-1}$) < NF plot ($1.5 \text{ kg ha}^{-1} \text{ yr}^{-1}$) \approx F plot ($1.6 \text{ kg ha}^{-1} \text{ yr}^{-1}$). The amount of litterfall corresponded to the content of nutrients.

Table 12.4 The amount of nitrogen and phosphorus in litterfall

	Amount in litterfall ($\text{kg ha}^{-1} \text{ yr}^{-1}$)		
	F	NF	F + C
Nitrogen	46.6	46.1	22.3
Phosphorus	1.6	1.5	0.6

12.4.7 Change of Understory Vegetation for 2 years

The change of numbers of understory vegetation between 2016 and 2018 is shown in Fig. 12.8. In April 2016, about six months after starting the enclosure experiments, the number of understory vegetation was equally low in the three studied plots. *Ilex pedunculosa*, which is known as one of the unpalatable deer plant in Japan, was the dominant species as a result of deer browsing before setting the enclosures. In August 2018, however, three plots showed distinctive difference in the number and type of understory vegetation. The F plot showed a twofold increase in the number of understory vegetation, while the NF plot didn't change. The F + C plot showed a sharp increase not only in total number, but also in species diversity.

12.5 Discussion

12.5.1 The Effects of Deer Browsing and Clear-Cutting on the Pattern of Soil Erosion

The amount and intensity of precipitation are among the most important factors in soil erosion (Piacentini et al. 2018). An associative increase in the amount and intensity of rainfall, as evidenced by a positive correlation between them ($r = 0.64$, $p < 0.001$) in this study, has a greater impact on runoff and erosion than just an increase the increase in rainfall (Nearing et al. 2005). Both the amount of precipitation and the intensity positively correlated with the amount of eroded soil in all experimental plots ($p < 0.001$).

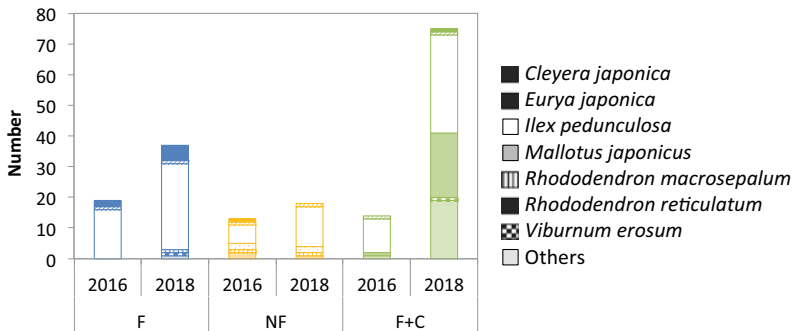


Fig. 12.8 Changes in the number of understory vegetation of each experimental plot. The vegetation data in 2016 was cited from Nagashima et al. (2019)

Although the amount of precipitation and intensity showed similar correlation coefficients with the amount of eroded soil for the F plot ($r = 0.80$ vs $r = 0.75$) and the NF plot ($r = 0.82$ vs $r = 0.75$), the intensity of precipitation showed higher correlation coefficient with the amount of eroded soils ($r = 0.92$) than did the rainfall amount ($r = 0.69$) for the F + C plot. This suggests that precipitation intensity may have a greater effect on soil erosion in the F + C plot, possibly due to the canopy loss after clear-cutting. Canopy intercepts rainfall before the water hits the soil surface. If the height of canopy is less than 5 m, as is the case at this study site, the kinetic energy of the through fall becomes not only lower than that of precipitation (Tsukamoto 1976), but also almost constant, regardless of the difference in rainfall intensity (Mizugaki et al. 2010). Thus, the canopy interception of rainfall decreased the soil losses (Li et al. 2019). In contrast, an open canopy or loss of a canopy exposes the soil surface directly to the energy of a raindrop, which increases with the intensity of rainfall in this site. In addition, aggregates of the 200–2000 μm fraction were broken and ground by a high kinetic energy of raindrop (Table 12.2). Thus, a higher intensity of rainfall promoted soil erosion (Li et al. 2019), especially in the F + C plot. However, the response to intense rainfall in this plot will be less sensitive as time increases because vegetation recovery is progressive after clear-cutting (Nakamori et al. 2012).

Despite the presence of a canopy, the NF plot showed the greatest soil erosion at a given amount of precipitation in each sampling period, as shown by the largest slope in the single linear regression analysis among the three experimental plots (Fig. 12.9). The slope values increased in the following order: F plot (1.1) < F + C plot (3.4) < NF plot (5.1), suggesting the increasing erodibility of soil surface in this order. We considered that the highest erodibility at the plot NF would be an indirect effect of deer overpopulation. One of the potential effects of deer on soil erosion is heavy browsing of understory vegetation or plant litter. Previous studies have reported that a decrease in the forest floor coverage by

heavy browsing can increase soil erosion (Miyashita et al. 2008). The F plot doubled the number of understory vegetation during the sampling period, which can be attributed to the enclosure to prevent from deer browsing (Fig. 12.8). In contrast, the NF plot showed only a slight increase in the number of understory vegetation. Thus, the regeneration of the understory vegetation enhanced by the enclosure for deer may contribute to decrease soil erosion in the F plot. In addition, we considered that deer trampling may put a greater impact on soil surface condition, which can drastically increase land surface compaction even within a year (Sukemori et al. 1995). Soil compaction reduces the infiltration rate of water (Sukemori et al. 1995), thereby increasing runoff and soil erosion. Although we did not record the degree of deer trampling in our site, a lower permeability coefficient at a higher bulk density (Fig. 12.4) than the value of the forest surface soil in Japan, as well as a larger volume of runoff (Table 12.1) and a weaker water drainage efficiency (Fig. 12.5) at the NF plot strongly indicates that the progress of soil compaction is one of the driving forces of soil erosion. The bulk density ranges were 0.13–1.52 g cm^{-3} , the average was 0.48 g cm^{-3} (Nanko et al. 2014), and the permeability was commonly greater than the 10^{-2} in forest surface soils in Japan (Komatsu et al. 2014; Miyata et al. 2009). Besides, the F + C plot showed a remarkably increased in the number and species of understory vegetation during sampling period (Fig. 12.8). This was due to the influx of sunlight from the cutting of trees, which contributed to the regeneration of trees, seedlings, and seeds buried in the soil. Thus, even though soil erosion has increased considerably, the regeneration of trees, i.e., the purpose of the experiment at the F + C plot has been successful.

A relatively low level of soil erosion than was expected from the regression line was obtained for a few sampling period (Fig. 12.9). These samples were collected mainly from winter to spring, when there was a rich litter layer. The litter layer acts as a buffer material that mitigates the flow speed of surface runoff and weakens the transport of earth and sand (Kitahara 1998). Therefore, forest floor coverage by litter layers is

Fig. 12.9 The relationship between the rainfall and the amount of eroded soil

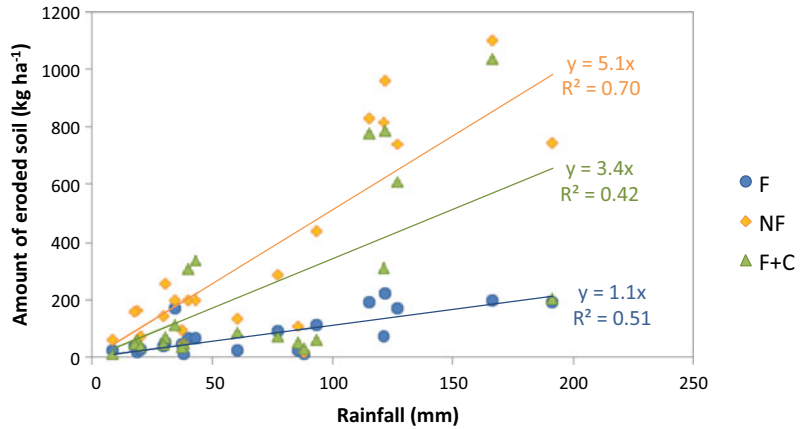
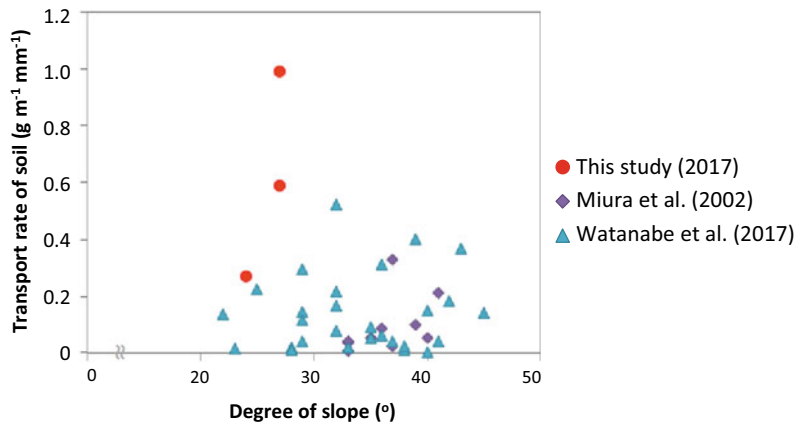


Fig. 12.10 Comparison of the relationship between the degree of slope and soil transport rate in this study with that calculated by Miura et al. (2002) and Watanabe et al. (2017) for representative forest slopes in Japan



highly effective to suppress soil erosion, regardless of the surface condition of mineral soils.

The transport rates of soil in Japanese forest were $0.0075\text{--}0.40\text{ g m}^{-1}\text{ mm}^{-1}$ (Miura et al. 2002; Watanabe et al. 2017). This rate ranges between 0.01 and 0.22 for forest soils with gentle slope $<35^\circ$, whereas at steep forest slopes it can reach $0.40\text{ g m}^{-1}\text{ mm}^{-1}$ (Fig. 12.10). The soil transport rates in this study site with $24^\circ\text{--}27^\circ$ degree slope were $0.27\text{--}0.99\text{ g m}^{-1}\text{ mm}^{-1}$. These values of the NF and F + C plots were clearly higher than those previously observed in Japanese forest with similar slope angles. This comparison also emphasizes that deer browsing and trampling due to overpopulation at the NF plot and the loss of canopy due to clear-cutting in the F + C plot enhanced soil erosion.

12.5.2 The Adverse Effects of Surface Soil Loss on Forest Ecosystem

Firstly, soil erosion has led to the loss of nutrients; the loss of carbon, nitrogen, and phosphorus increased as the amount of eroded soil increased. Carbon, nitrogen, phosphorus were the richest in the surface soil of a profile, and declined with depth (Spycher et al. 1983; Yang et al. 2010; Jobbágy and Jackson 2001). So, this result indicated that the subsurface soils were prone to soil erosion at the NF and F + C plots. Attiwill and Adams (1993) reported that the litterfall input of nitrogen and phosphorus were 60 and $2\text{ kg ha}^{-1}\text{ yr}^{-1}$, respectively, in a typical eucalypt forest. The input of nitrogen and

phosphorus with litterfall in this study (i.e., N: 22.3–46.6 kg ha⁻¹ yr⁻¹, P: 0.6–1.6 kg ha⁻¹ yr⁻¹) was similar to or smaller than in the previous study. Losses of nitrogen and phosphorus due to soil erosion were larger than the litterfall input at the NF and F + C plots. Although all nitrogen and phosphorus in the eroded soil were not phytoavailable, these results suggested that soil erosion severely deprived soil nutrients and then led to the prevention of vegetation growth, the disturbance of the forest ecosystem.

Secondly, the loss of surface soil due to soil erosion exposed root (Giambelluca et al. 2010; Tilahun 2015). Root exposure can lead to a decrease in nutrient uptake due to a decrease in water absorption with drought (Manning 1979). Root exposure reduced soil stability (Stofeel et al. 2013) such as holding soil particles by the root and then can reduce the resistance of trees to lodging by wind (Manning, 1979).

Thirdly, an increase in the influx of sediments into a lake or reservoir due to soil erosion promotes an eutrophication of phosphorus in the water (Michioku 2007). Anoxic conditions in deep waters due to eutrophication caused dramatic killing of fish and a large flowering of blue-green algae (Duncan et al. 2012) and affected aquatic ecosystems. Thus, soil erosion is a serious problem not only for forest soil, but also for the ecosystem. Strategies to prevent soil erosion are greatly important, such as mulching the soil surface, reducing the number of deer, preventing their access or clear-cutting trees with their stems and branches left on the soil surface.

12.6 Conclusion

Deer intensity and clear-cutting of trees increased soil erosion and led to greater loss of nutrients (i.e., carbon, nitrogen, and phosphorus) from the forest ecosystem. Under the canopy, soil erosion corresponded to the amount of precipitation, while on the canopy openings, soil erosion corresponded to the rainfall intensity. The effect of deer increased soil erosion by more than 4 times. Not only the deer browsing, but soil compaction

due to deer trampling was also one of the main reasons for accelerated soil erosion. Although clear-cutting is effective for regeneration of trees, it can potentially lead to depletion of nutrients in the forest ecosystem due to accelerated soil erosion. Judging by the fact that it is rather difficult to prevent an increase of precipitation intensity in accordance with global warming, rational strategies such as mulching the soil surface, reducing deer access or clear-cutting trees with their stems and branches left on the soil surface would be necessary to conserve the forest ecosystem.

Acknowledgements We thank M. Shibata of Laboratory of Terrestrial Ecosystems Management, Kyoto University, T. Nishikiori of National Agriculture and Food Research Organization, and K. Noda and M. Ogawa of Kyoto City Greenery Association for their help in conducting this study. We also thank S. Ogasawara, R. Ito, S. Kataoka, Y. Matsuyama, M. Terashima, M. Tomita, M. Hirose, R. Kitayama, Y. Tanaka, S. Ito, K. Kurokawa, Y. Nishii, F. Masai, M. Aitani, S. Kariya, H. Saito, and R. Naohara of Laboratory of Soil Chemistry, Kyoto Prefectural University for setting experimental devices and collecting samples. This study was partly supported by the JSPS KAKENHI grants (No. 26450202 and No. 17H06171).

References

- Attiwill MP, Adams AM (1993) Tansley review No. 50 Nutrient cycling in forests. *New Phytol.* 124 (4):561–582. <https://doi.org/10.1111/j.1469-8137.1993.tb03847.x>
- Choi IC, Kim NH, Shin HJ, Tenhunen J, Nguyen TT (2017) Economic valuation of the aquatic biodiversity conservation in South Korea: correcting for the endogeneity bias in contingent valuation. *Sustainability* 9(6):1–20. <https://doi.org/10.3390/su9060930>
- Duncan E, Kleinman PJA, Sharpley AN (2012) Eutrophication of lakes and rivers. In: *Encyclopedia of life science*. Wiley, Chichester, UK
- Ehhalt D, Prather M, Dentener F, Derwent R, Dlugokencky E, Holland E, Isaksen I, Katima K, Kirchhoff V, Matson P, Midgley P, Wang M (2001) Atmospheric chemistry and greenhouse gases. In: Joos F, McFarland M (eds) *Climate change 2001: the scientific basis*. Cambridge University Press, Cambridge, pp 245–287
- Fujibe F, Yamazaki N, Kobayashi K (2006) Long-term changes of heavy precipitation and dry weather in Japan (1901–2004). *J Meteorol Soc Jpn* 84(6):1033–1046. <https://doi.org/10.2151/jmsj.84.1033>

- Furusawa H, Hino T, Kaneko S, Araki M (2005) Effects of dwarf bamboo (*Sasa nipponica*) and deer (*Cervus Nippon centralis*) on the chemical properties of soil and microbial biomass in a forest at Ohdaigahara, central Japan. *Bull For Pro Res Inst* 4(2):157–165. <http://www.ffpri.affrc.go.jp/labs/kanko/395-2.pdf>
- Giambelluca TW, Sutherland RA, Nanko K, Mudd R, Ziegler AD (2010) Effects of miconia on hydrology: a first approximation. In: Loope LL, Mayer JY, Hardesty BD, Smith SW (eds) *Proceeding of the international Miconia conference*, Keanae, Maui, Hawaii, USA, May 4–7 2009, Maui Invasive Species Committee and Pacific Cooperative Studies Unit, University of Hawaii at Manoa, 7p
- Holz DJ, Williard KWJ, Edwards PJ, Schoonover JE (2015) Soil erosion in humid regions: a review. *J Contemp Water Res Educ* 154:48–59. <https://doi.org/10.1111/j.1936-704X.2015.03187.x>
- Horsley SB, Stout SL, deCalesta DS (2003) White-tailed deer impact on the vegetation dynamics of anorthern hardwood forest. *Ecol Appl* 13(1):98–118
- Japan Meteorological Agency (2017) Search for the past meteorological data. <https://www.data.jma.go.jp/obd/stats/etrn/>. Accessed Dec 2019
- Jobbágy EG, Jackson RB (2001) The distribution of soil nutrients with depth: global patterns and the imprint of plants. *Biogeochemistry* 53(1):51–77. <https://doi.org/10.1023/A:1010760720215>
- Kimoto M, Yasutomi N, Yokoyama C, Emori S (2005) Projected changes in precipitation characteristics around Japan under the global warming. *SOLA* 1:85–88. <https://doi.org/10.2151/sola.2005-023>
- Kitahara H (1998) Prevention of surface erosion by forests (in Japanese). *Jpn For Soc* 22:16–22
- Komatsu Y, Onda Y, Ogura A (2014) Relation between infiltration rate, cover material and hydraulic conductivity of forest soils in Japanese Cedar and Hiba *Arborvitae* Plantation Forests (in Japanese). *J Jpn Soc Hydrol Water Resour* 27(3):125–134. <https://doi.org/10.3178/jjshwr.27.125>
- Kubono T, Ito S (2002) *Raffaëlea quercivora* sp. nov. associated with mass mortality of Japanese oak, and the ambrosia beetle (*Platypus quercivorus*). *Mycoscience* 43:255–260. <https://doi.org/10.1007/S102670200037>
- Kuroda K, Osumi K, Oku H (2012) Reestablishing the health of secondary forests ‘*Satoyama*’ endangered by Japanese oak wilt: a preliminary report. *J Agric Ext Rural Dev* 4(9):192–198. <https://doi.org/10.5897/JAERD12.047>
- Kyoto City Greening Association (2015) The park of Takaragaike: the Heaven of Children Play Park (in Japanese) 4p. (Brochure).
- Lal R (2014) Soil conservation and ecosystem services. *Int Soil Water Conserv Res* 2(3):36–47. [https://doi.org/10.1016/S2095-6339\(15\)30021-6](https://doi.org/10.1016/S2095-6339(15)30021-6)
- Li G, Wan L, Cui M, Wu B, Zhou J (2019) Influence of canopy interception and rainfall kinetic energy on soil erosion under forests. *Forests* 10(6):509. <https://doi.org/10.3390/f10060509>
- Lv X, Yu X, Fan D, Li Q (2012) Estimation of non-point source pollution loads caused by soil erosion in China. *J Food Agric Environ* 10(2):1045–1050
- Manning RE (1979) Impacts of recreation on riparian soils and vegetation. *Water Res Bull* 15(1):30–43. <https://doi.org/10.1111/j.1752-1688.1979.tb00287.x>
- Michioku K (2007) Nutrient-sediment loads from forest catchments and their influence on lake and reservoir eutrophication. *Annal J Hydraul Eng JSCE* 51:K3–K6
- Miura S, Hirai K, Yamada T (2002) Transport rates of surface materials on steep forested slopes induced by raindrop splash erosion. *J For Res* 7:201–211. <https://doi.org/10.1007/BF02763133>
- Miyashita T, Suzuki M, Ando D, Fujita G, Ochiai K, Asada M (2008) Forest edge creates small-scale variation in reproductive rate of sika deer. *Popul Ecol* 50:111–120. <https://doi.org/10.1007/s10144-007-0068-y>
- Miyata S, Kosugi K, Gomi T, Mizuyama T (2009) Effect of forest floor coverage on overland flow and soil erosion on hillslopes in Japanese cypress plantation forests. *Water Res Res* 45:W06402. <https://doi.org/10.1029/2008WR007270>
- Mizugaki S, Nanko K, Onda Y (2010) The effect of slope angle on splash detachment in an unmanaged Japanese cypress plantation forest. *Hydrol Process* 24:576–587. <https://doi.org/10.1002/hyp.7552>
- Nagashima K (2017) Seedling establishment and its factors in forests damaged by oak-wilt disease and deer browsing (in Japanese with an English summary). *J Jpn Soc Reveg Technol* 43(1):83–85
- Nagashima K, Shimomura T, Tanaka K (2019) Early-stage vegetation recovery in forests damaged by oak wilt disease and deer browsing: effects of deer-proof fencing and clear-cutting. *Landsc Ecol Eng* 15:155–166
- Nagashima K (2015) Takaragaike symposium: relationship diagram of issues surrounding forests of Takaragaike (in Japanese). Kyoto City Greening Association (ed) 4p. (Brochure)
- Nakamori Y, Takii T, Miura S (2012) Variation in fine earth, sediment, and litter movement with different forest management practices on a steep slope in a *Chamaecyparis obtusa* plantation (in Japanese with English summary). *J Jpn For Soc* 94:120–126
- Nanko K, Ugawa S, Hashimoto S, Imaya A, Kobayashi M, Sakai H, Ishizuka S, Miura S, Tanaka N, Takahashi M, Kaneko S (2014) A pedo-transfer function for estimating bulk density of forest soil in Japan affected by volcanic ash. *Geoderma* 213:36–45. <https://doi.org/10.1016/j.geoderma.2013.07.025>
- Nearing MA, Jetten V, Baffaut C, Cerdan O, Couturier A, Hernandez M, Bissonnais YL, Nichols MH, Nunes JP, Renschler CS, Souchere V, Oost KV (2005) Modeling response of soil erosion and runoff to changes in precipitation and cover. *CATENA* 61:131–154. <https://doi.org/10.1016/j.catena.2005.03.007>
- Nishigaki T, Sugihara S, Kilasara M, Funakawa S (2016) Surface runoff generation and soil loss under different

- soil and rainfall properties in the Uluguru Mountains, Tanzania. *Land Degrad Develop*. Wiley, Chichester, UK
- Nishizawa K, Tatsumi S, Kitagawa R, Mori AS (2016) Deer herbivore affects the functional diversity of forest floor plants via changes in competition-mediated assembly rules. *Ecol Res* 31:569–578. <https://doi.org/10.1007/s11284-016-1367-6>
- Nomiya H, Suzuki W, Kanazashi T, Shibata M, Tanaka H, Nakashizuka T (2002) The response of forest floor vegetation and tree regeneration to deer exclusion and disturbance in riparian deciduous forest, Central Japan. *Plant Ecol* 164:263–276. <http://www.springerlink.com/content/v778g5k265657671/fulltext.pdf>
- Niwa S, Mariani L, Kaneko N, Okada H, Sakamoto K (2011) Early-stage impacts of sika deer on structure and function of the soil microbial food webs in a temperate forest: a large-scale experiment. *For Ecol Manag* 261(3):391–399
- Piacentini T, Galli A, Marsala V, Miccadei E (2018) Analysis of soil erosion induced by heavy rainfall: a case study from the NE Abruzzo Hills Area in Central Italy. *Water* 10(10):1314. <https://doi.org/10.3390/w10101314>
- Soil Survey Staff (2014) *Keys to soil taxonomy*, 12th edn. U. S. Department of Agriculture and Natural Resources Conservation Service, Washington
- Spycher G, Sollins P, Rose S (1983) Carbon and Nitrogen in the light fraction of a forest soil: vertical distribution and seasonal patterns. *Soil Sci* 135(2):79–87
- Stofeel M, Corona C, Ballesteros-Cánovas JA, Bodoque JM (2013) Dating and quantification of erosion processes based on exposed roots. *Earth Sci Rev* 123:18–34. <https://doi.org/10.1016/j.earscirev.2013.04.002>
- Sukemori S, Komatsu M, Takami K, Arai K (1995) The effects of treading by reindeer and yeso sika deer hooves on the compaction of land surface in grazing areas. *Jpn J Livest Manag* 30(3):81–85
- Takatsuki S (2009) Effects of sika deer on vegetation in Japan: a review. *Bio Conserv* 142:1922–1929. <https://doi.org/10.1016/j.biocon.2009.02.011>
- Tilahun A (2015) Perception of the farmers' on the existence of soil erosion in the case of Sekela District, Amhara State, Ethiopia. *J Poverty Invest Dev* 12:23–31
- Tsujino R, Noma N, Yumoto T (2004) Growth of sika deer (*Cervus nippon yakushimae*) population in the western lowland forests of Yakushima Island, Japan. *Mammal Study* 29:105–111. <https://doi.org/10.3106/mammalstudy.29.105>
- Tsukamoto Y (1976) Forest canopy and rain drop erosion (in Japanese). *Jpn Soc For Environ* 17(2):5–9
- Watanabe Y, Suzuki Y, Sakai H (2017) Variation of surface soil movements in plantation forests subject to potential future tree management practice: observations of surface organic matter, vegetation cover and sediment discharge over a three year period. *J Jpn For Soc* 99:24–33
- Yang YH, Fang JY, Guo DL, Ji CJ, Ma WH (2010) Vertical patterns of soil carbon, nitrogen and carbon: nitrogen stoichiometry in Tibetan grasslands. *Biogeosci Dis* 7(1):1–24. <https://doi.org/10.5194/bg-7-1-2010>



Soil Compaction Due to Agricultural Field Traffic: An Overview of Current Knowledge and Techniques for Compaction Quantification and Mapping

Thomas Keller, Mathieu Lamandé,
Mojtaba Naderi-Boldaji, and Renato
Paiva de Lima

Abstract

Soil compaction caused by agricultural vehicles is a global problem affecting a considerable proportion of all arable land and causing tremendous costs to farmers and society. Soil

compaction reduces soil porosity and modifies pore geometry, thereby adversely affecting key soil ecological, hydrological and agronomic functions. This chapter provides an overview of current knowledge on stress propagation, soil compressive behaviour, impacts of soil compaction on soil properties and functions and recovery of soil structure after compaction, and discusses the costs of soil compaction. We provide an overview of non-destructive measurement techniques and approaches for improving description and quantification of soil compaction at spatial scales from the soil pore to the field. Finally, we discuss sensor systems for on-the-go mapping of soil compaction and provide a perspective for future development of sensor fusions for soil compaction identification and mapping.

T. Keller (✉)
Department of Soil and Environment, Swedish
University of Agricultural Sciences, Box 7014,
75007 Uppsala, Sweden
e-mail: thomas.keller@slu.se

T. Keller
Department of Agroecology and Environment,
Agroscope, Reckenholzstrasse 191, 8046 Zürich,
Switzerland

M. Lamandé
Department of Agroecology, Research Centre
Foulum, Aarhus University, Box 50, 8830 Tjele,
Denmark
e-mail: mathieu.lamande@agro.au.dk

M. Lamandé
Faculty of Environmental Sciences and Natural
Resource Management, Norwegian University of
Life Sciences, NMBU, Box 5003, 1432 Ås, Norway

M. Naderi-Boldaji
Department of Mechanical Engineering of
Biosystems, Shahrekord University, Box 115,
88186-34141 Shahrekord, Iran
e-mail: naderi.mojtaba@sku.ac.ir

R. P. de Lima
Department of Agricultural Engineering, Federal
Rural University of Pernambuco, Rua Dom Manoel
de Medeiros, s/n, DoisIrmãos, Recife, PE
52171-900, Brazil

Keywords

Soil stress · Stress–strain relationship · Soil
functions · X-ray computed tomography ·
Acoustic emissions · Geophysics · Horizontal
penetrometer · Sensor fusion

13.1 Introduction

Soil compaction due to agricultural field traffic has been a subject of concern for decades. While initial studies were mainly addressing the agronomic consequences of soil compaction and in particular the loss of soil productivity

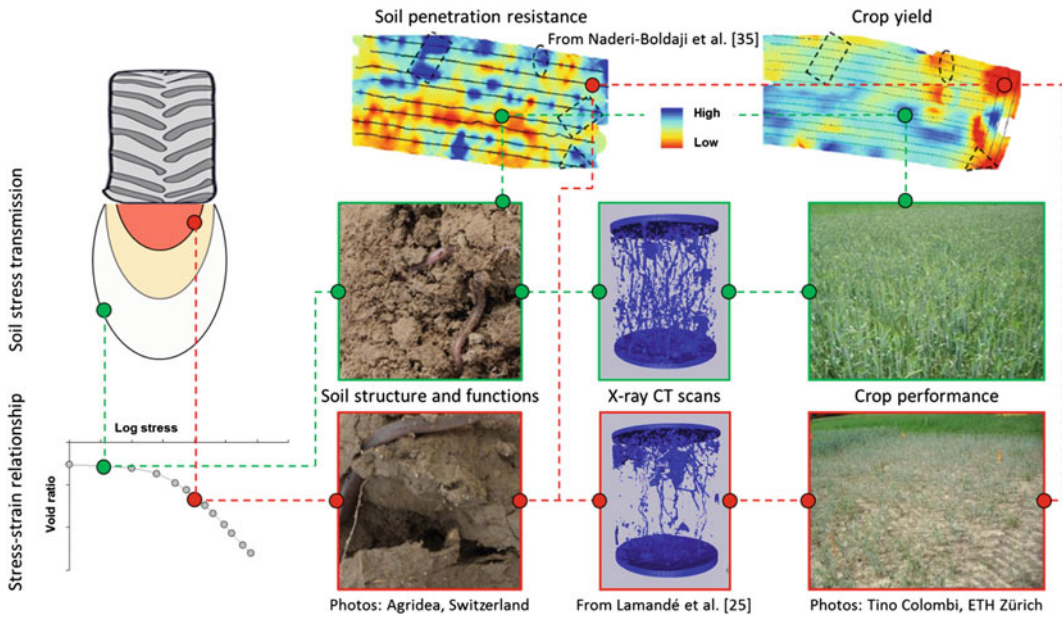


Fig. 13.1 Schematic illustration of the soil compaction process (from Keller et al. 2018)

(Håkansson et al. 1987), the negative impact of compaction on soil ecological functions and services has received growing attention during more recent decades (Gregory et al. 2015; Alaoui et al. 2018). Nevertheless, productivity is still a major concern, not least driven by the predicted increase in the demand for food, forages and fibre (Tilman et al. 2001) and the projected worsened growing conditions as a consequence of climate change (Wheeler and von Braun 2013). This chapter focuses on soil compaction of arable soil. However, compaction is of concern also in the context of forest management, military operations on agricultural, forest or natural land, and recreational off-road traffic.

Soil compaction not only leads to a reduction in soil pores space (and associated increase in bulk density), but also changes pore size distribution towards smaller pores, and reduces pore continuity and pore connectivity. Adverse modification in the spatial arrangement and stability of solids and pore spaces (voids), i.e. soil structure, affects many physical, chemical and biological processes in soil, with mostly negative consequences for soil functions and ecosystem

services, and negative impacts on living conditions for plants and soil organisms (Fig. 13.1).

Soil compaction is a problem of global importance, especially in mechanized modern agriculture. The extent of soil degradation by compaction is not well quantified, but recent estimates suggest a quarter of all European soils are compacted (Schjønning et al. 2015a, b). Soil degradation caused by compaction creates significant costs to farmers and society. For example, annual direct (e.g. yield loss) and indirect costs (e.g. increased flood risk) due to compaction were estimated by Graves et al. (2015) to 470 M€ yr⁻¹ for England and Wales. Trends of steadily increasing weight and power of agricultural machinery (Schjønning et al. 2015a, b; Keller et al. 2019), driven by economical pressure and efficiency considerations, suggest that the already acute problem of soil compaction will aggravate. Similar trends of increasing weights are reported for forestry machinery (Nordfjell et al. 2019). Moreover, the ecological and economical damage caused by soil compaction is expected to escalate in future climate with more frequent high intensity rainfalls as well as more frequent dry spells (Keller et al. 2019).

This chapter gives an overview of the current state of soil compaction research (limited to soil compaction due to agricultural field traffic) and identifies some knowledge gaps and opportunities for future research. Sections 13.2, 13.3 and 13.4 are organized along the “chain of cause” of soil compaction (Fig. 13.1): we review and discuss measurements and modelling of soil stress propagation, soil compressive behaviour (stress–strain relationships), and compaction impacts on soil properties and functions. Although we discuss these aspects in a sequential way, we acknowledge that they may be interrelated: for example, soil mechanical properties and deformation may affect the soil stress propagation. The next two sections discuss the costs of soil compaction, and the mechanisms and rates of compaction recovery. This is followed by a section on quantifying compaction state and processes using non-destructive techniques, and a section on soil compaction mapping using on-the-go sensor systems. The conclusions and outlook summarize our chapter and offer some ideas for future research directions.

13.2 Stress Propagation in Soil: Measurements and Modelling

Knowledge of stress propagation in soil and of stress state at a particular soil depth are important for quantifying soil deformation and associated changes in soil properties caused by vehicle traffic (Berisso et al. 2012). Neither measuring nor modelling soil stress is simple, though.

In situ measurements of soil stress are challenging because it is problematic to install sensor probes without disturbing the soil structure and because it is difficult to obtain good probe-soil contact especially for load cell type probes (Kirby 1999a, b). Probe dimensions (e.g. surface to height ratio) and probe material properties (e.g. ratio of probe to soil stiffness) are known to affect the probe reading (Weiler and Kulhawy 1982; Kirby 1999a, b; Lamandé et al. 2015). However, as long as the ratio of “true stress” (i.e. the stress in the soil without probe) to stress obtained from the sensor probe is known, this

can be corrected for (Lamandé et al. 2015). Although some work to quantify the ratio of “true” stress to probe-obtained stress has been done (Weiler and Kulhawy 1982; Kirby 1999a, b; Berli et al. 2006; Lamandé et al. 2015), further research to analyse stress fields around sensor probes and to establish relationships between true stress and measured stress as a function of sensor geometry, soil and probe material properties are needed.

Different probe types are used for measurements of soil stress (Keller et al. 2016): fluid inclusion type sensors and load cell type sensors. Installation of fluid inclusion type sensors, such as the “Bolling probe” (Bolling 1985), is relatively quick and only involves drilling a small hole (e.g. 0.01 m diameter; Keller et al. 2016) from the surface to the desired depth, hence minimally disturbing soil structure, and probe-soil contact can be assured by inflating the probe to a pre-stress. The pressure measured with a fluid-filled flexible pressure probe is directly related to the mean normal stress, but the ratio of probe pressure to mean normal stress is a function of Poisson’s ratio of soil (Berli et al. 2006). Hence, correct interpretation of the measured pressure requires knowledge of the soil Poisson’s ratio. Moreover, Poisson’s ratio of soil could change during loading; however, little is known about that. Poisson’s ratio of soil can be measured in triaxial tests or from a combination of confined and unconfined uniaxial compression tests as shown by Eggers et al. (2006).

Load cell type sensors measure a stress in a certain direction (most often vertical normal stress). Sensors could have either one sensing phase or multiple transducers, e.g. for measurements of the complete stress state. The latter is known as stress-state transducer and such sensors contain six differently oriented load cells. However, uncertainties of computed stress components (e.g. octahedral normal stress and octahedral shear stress) from the six measured stresses may not be negligible (Gräsle 1999). Disturbance of soil structure is typically larger for load cell type sensors than for fluid pressure sensors because of their larger size, and probe-soil contact is difficult to assure, as the load cell

sensors are stiff. Lamandé et al. (2007) implemented a wedging mechanism to ensure probe-soil contact for cylindrical load cell transducers. Ensuring a good probe-soil contact may be especially difficult for stress-state transducers because of the complex probe geometry.

Three principally different approaches are used for modelling stress propagation in soil beneath a tyre or track. These are the analytical approach based on the work of Boussinesq (1885), Fröhlich (1934) and Söhne (1953), the finite element framework (e.g. Raper et al. 1995; Richards et al. 1997; Horn et al. 1998; Gysi et al. 2000; Peth et al. 2006; Gonzales Cueto et al. 2016; Keller et al. 2016), and the discrete element method (e.g. Smith and Peng 2013; Johnson et al. 2015; Du et al. 2017; Jiang et al. 2018; De Pue and Cornelis 2019). For an overview and more detailed explanation of the different approaches, we refer the reader to Défossez and Richard (2003), Richards and Peth (2009), Keller et al. (2013a) and Nawaz et al. (2013). Modelling soil stress is challenging due to several reasons (see e.g. Keller and Lamandé 2010). Knowledge of the stresses at the soil surface, where the vehicle is in contact with the soil, referred to as the upper model boundary condition or upper stress boundary condition, are crucial for simulation of soil stress. However, the distribution of stresses at the tyre-soil or track-soil interface is typically uneven and not precisely known. Models have been developed for estimation of the distribution of vertical stress below tyres from tyre characteristics and wheel load (Keller 2005; Schjønning et al. 2008, 2015a, b), and a similar model has been presented for rubber tracks by Keller and Arvidsson (2016). The estimated stress distribution from these models can then be used as input of the upper stress boundary condition in models for prediction of stress propagation. Another approach is to simulate the tyre/track-soil interaction, e.g. using finite element modelling as demonstrated by (Gonzales Cueto et al. 2016).

As for modelling any soil process, the representation of soil heterogeneity, anisotropy and layering is challenging in models. Typically,

these features are strongly simplified in models. For example, the soil profile is represented with one homogeneous isotropic layer in the widely used models based on the Boussinesq (1885) solution. The impact of soil conditions (e.g. soil moisture, affecting soil strength) and structure on stress distribution is not well understood. It is generally accepted that vertical stress is more concentrated under the load the drier and harder the soil (Söhne 1953; Hartge and Horn 2016). However, Lamandé and Schjønning (2011a) measured higher vertical stresses in dry soil than in wet soil. Keller et al. (2014, 2016) showed that the vertical stress is little affected by soil layering unless unrealistic material (i.e. soil) properties are used; however, other stress components (e.g. horizontal stresses) are influenced by soil properties. Lamandé and Schjønning (2011b) measured differences in stress transmission in recently tilled and undisturbed soil. Naveed et al. (2016) showed that the stress distribution in soil is more heterogeneous when deformations are small (Fig. 13.2). Forces are known to propagate along “load chains” in granular material (e.g. Voivret et al. 2009), implying that some particles may be heavily loaded while other particles are isolated from the load chains and not loaded. With increasing deformation, the load chains become less discrete and the load is more uniformly spread among the particles (Davis and Selvadurai 2002). Simulating load chains requires a granular matter physics approach (discrete element methods). We note that recently tilled soil resembles a granular material. However, consolidation and coalescence of soil fragments created by tillage (Or and Ghezzehei 2002) will transform the soil with time towards a material that might be well approximated by a continuum. How we model stress propagation in soil may also be a question of the scale of consideration: at the microscale, we need to account for load chains, while in a large-scale description we can describe the average stresses by continuum theory. In summary, the impacts of soil properties and conditions (soil strength, soil moisture, soil structure) on stress transmission are still not well understood.

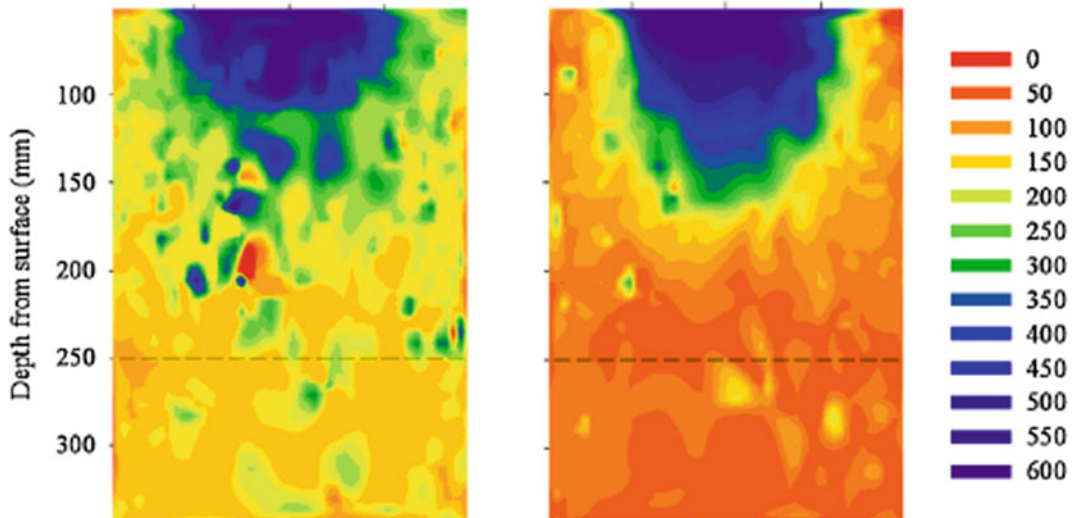


Fig. 13.2 Distribution of vertical stress in structured soil (19% clay) when loaded with 275 kPa (left) and 620 kPa (right). (Slightly modified from Naveed et al. (2016))

13.3 Soil Compressive Behaviour

Soil is a three-phase system consisting of solids (individual particles) and voids, where the voids are occupied by air (when soil is completely dry), water (when soil is fully saturated) or both (unsaturated soils) (Hillel 2004). Both the volume and connectivity of voids (i.e. soil structure) as well as the proportion of air and water in the voids (i.e. the degree of saturation) affect the mechanical behaviour of soils. Soil may deform under external or internal stresses that could be caused by natural processes (e.g. wetting–drying cycles, bioturbation by plant roots and fauna) or anthropogenic activity (e.g. agricultural field traffic). The focus of this section is on soil behaviour during compression under external loads.

Mechanical behaviour of soil during compression implies a decrease in soil volume under the application of a load (e.g. an agricultural vehicle), and is characterized by the soil compressive properties (Horn et al. 2003). The compressive properties of soil are obtained from the relationship between (the logarithm of) applied stress and a measure of the compaction

state (strain, void ratio, specific volume or bulk density) measured in uniaxial compression tests or triaxial tests (O’Sullivan and Robertson 1996). Although triaxial tests could more realistically mimic stress conditions in the field, uniaxial tests are commonly used because they are simpler and cheaper, and therefore more accessible. A limitation of the uniaxial compression test is that mean normal stress, σ_m , is not measured. Volumetric deformation (e.g. decrease in void ratio) is therefore often related to vertical stress (σ_v), which is the known applied stress in uniaxial compression tests. However, volumetric deformation is related to σ_m (and not σ_v) (e.g. Davis and Selvadurai 1996). The mean normal stress could be calculated if the ratio of radial stress (σ_r) to σ_v (known as the coefficient of earth pressure, K_0) was known, as $\sigma_m = \frac{1}{3}[\sigma_v + 2\sigma_r]$ and $\sigma_r = K_0 \sigma_v$ in a cylindrical sample. For uniaxial confined compression tests, Koolen and Kuipers (1983) suggested a value for K_0 of 0.5. However, the stress field within a sample and therefore K_0 are affected by friction at the soil-cylinder wall interface and the soil Poisson ratio, and vary as a function of sample size (Koolen 1974; Rosine and Sabbagh 2015; Lima and Keller 2019).

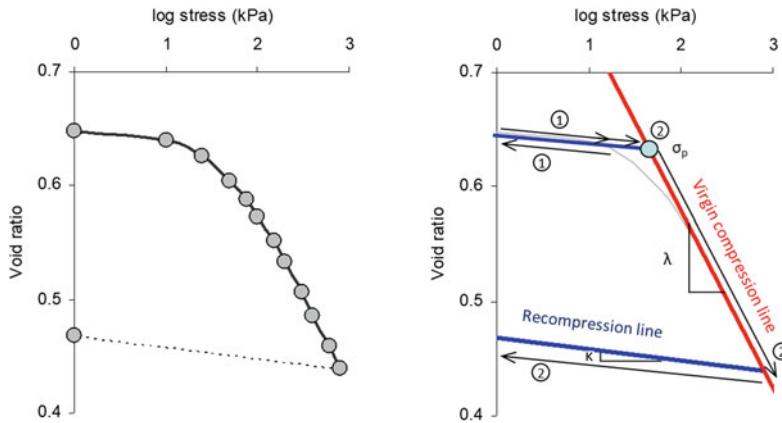


Fig. 13.3 Example of a measured compression curve (left), and idealized model of compression and rebound (right) with two potential stress paths: 1—only elastic deformation, applied stress < precompression stress; 2—

plastic deformation, applied stress > precompression stress. λ : compression index; κ : recompression index; σ_p : precompression stress

According to Lima and Keller (2019), effects of soil-wall friction can be neglected for large sample diameter (D) to height (h) ratios (e.g. $D/h > 8$); in such a case, K_0 becomes a function of the soil Poisson's ratio. The authors suggested that Poisson's ratio should always be measured for improved interpretation of data from uniaxial compression tests.

The compression curve can be divided into an elastic and a plastic part. The point of transition from elastic to plastic deformation is called recompression stress (σ_p). Deformation is expected to be elastic and reversible if the applied stress is smaller than σ_p . If the applied stress exceeds σ_p , soil deformation is irreversible, causing permanent deformation (i.e. compaction). Consequently, soil compaction due to vehicular traffic could be avoided by ensuring that the applied stress does not exceed σ_p . However, it has been shown that soil deformation is not completely elastic even when the applied stress does not exceed the precompression stress, and evidence of this has been presented from uniaxial compression tests and in situ measurements Atkinson 1993, Kirby 1994; O'Sullivan and Robertson 1996; Keller et al. 2012).

The compression curve in log stress space has a sigmoidal shape, but is often approximated (or

idealized) by two lines: the virgin compression line and the recompression (or swelling) line (Fig. 13.3). The virgin compression line is defined by the specific volume at stress = 1 kPa (corresponding to log stress = 0), N , and the slope of the virgin compression line, termed compression index, λ . The recompression line is given by the initial void ratio (or initial specific volume) and the slope of the recompression line, called recompression (or swelling) index, κ . The recompression line describes elastic behaviour, and κ yields information on the elasticity of soil and the magnitude of rebound upon stress release. The virgin compression line characterizes plastic behaviour, and λ is a measure of soil compressibility. A higher value of κ indicates greater soil elasticity, whereas a higher value of λ is associated with higher susceptibility to compaction. A higher value of σ_p indicates a higher soil (compressive) strength, and therefore lower risk of soil compaction (Schjønning and Lamandé 2018).

Compressive properties vary with soil texture and are affected by soil state variables such as soil compactness and soil moisture. However, only few studies (e.g. O'Sullivan et al. 1996; Défossez and Richard 2003; Keller and Arvidsson 2007; Lima et al. 2018) have characterized all the three compressive parameters necessary to

describe the compression curve (i.e. N , λ and κ ; cf. Fig. 13.3). Studies show that N , λ and κ increase with decreasing initial bulk density (e.g. Imhoff et al. 2004; Saffih-Hdadi et al. 2009; Lima et al. 2018). The effect of texture on compressive properties is not clear, and seems to depend on soil moisture, bulk density and organic matter content (Reichert et al. 2018). Recent studies show that σ_p generally increases with increasing bulk density and decreases with increases in soil organic matter content, clay content and soil moisture (Reichert et al. 2018).

The effect of soil moisture on compressive properties is complex, partly because the soil degree of saturation and the matric potential change during loading. Adding to the complexity, these changes depend on the initial soil moisture conditions (initial matric potential, initial degree of saturation), soil hydraulic properties (e.g. hydraulic conductivity) as well as the deformation during loading (Larson and Gupta 1980; Cui et al. 2010; Peth et al. 2010). It was found that λ is highest at intermediate initial water contents or matric suctions, and lower at either lower or higher initial water contents (e.g. Estabragh et al. 2004; Pereira et al. 2007; Lima et al. 2018). Because λ represents the rate of volumetric deformation during loading when stresses exceed σ_p (cf. Fig. 13.3), this implies that there is an optimal (critical) water content for the occurrence of maximum compaction, which is consistent with results from Proctor compaction tests indicating an optimum water content for maximum compaction.

Different methods exist to determine the σ_p from soil compression data, resulting in different values for the σ_p (see Dias Junior and Pierce 1995; Cavalieri et al. 2008; Gregory et al. 2006; Lamandé et al. 2007). This together with the use of different sample sizes, loading conditions, different stress components (σ_m or σ_v), different logarithms (natural logarithm or logarithm to the base 10) and different measures of compactness (bulk density or void ratio) makes comparisons of data from different laboratories challenging, and hinders the development of generally applicable pedo-transfer functions for soil compressive properties based on large datasets. Existing

pedo-transfer functions for soil compressive properties are therefore typically based on relatively limited data and/or do not include all properties needed to describe the full compression curve (e.g. Lebert and Horn 1991; Défossez and Richard 2003; Saffih-Hdadi et al. 2009; Severiano et al. 2013; Schjønning and Lamandé 2018; Reichert et al. 2018). We see an urgent need for more generally applicable pedo-transfer functions for compressive properties of arable soil that are based on large data sets (e.g. across countries). Such functions could be incorporated in existing decision support tools (e.g. Terranimo[®]; Stettler et al. 2014) for improved predictions of compaction risks due to agricultural field traffic.

13.4 Impacts of Soil Compaction on Soil Properties and Functions

Impacts of soil compaction on soil properties and soil functions were reviewed for forestry (Green and Sands 1980; O’Ruark et al. 1982; Day and Bassuk 1994), pastoral systems (Drewry et al. 2008), and arable systems (Wolkowski 1990; Batey 2009; Alaoui et al. 2011; Nawaz et al. 2013)—we refer the reader to these for a general overview. Taylor and Brar (1991), Unger and Kaspar (1994), Kozolwski (1999) and Lipiec et al. (2003) presented reviews focusing on the impacts of soil compaction on root growth, for crop or trees. Therefore, this section will only provide a brief overview of soil compaction impacts on soil properties and functions, present examples of selected results and highlight some specific aspects that have thus far received little attention.

Compaction is defined as a reduction in total porosity for a given soil volume. However, not only the volume, but also the pore size distribution, and the shape of the pore system will be affected, as structural deformation during compaction is a combination of shear and compression (e.g. Alaoui et al., 2011). Berisso et al. (2013a) reported an effect of long-term subsoil compaction on the anisotropy of macropores.

Mossadeghi-Björklund et al. (2019) observed a reduction of volume of pores with a diameter between 0.06 and 0.3 mm in diameter, but not for pores with a larger diameter. A range of studies reported a reduction of primarily the volume of larger pores in the topsoil (e.g. Bullock et al. 1985; Schäffer et al. 2007; Dörner et al. 2010) as well as in the subsoil (e.g. Berisso et al. 2012; Schjønning et al. 2013; Pulido-Moncada et al. 2019). Hence, compaction will have consequences on a range of physical, chemical and biological processes taking place in the macroporosity (rapid transport of water, soil aeration, and root growth). For example, long-term subsoil compaction reduced saturated hydraulic conductivity (Horn et al. 1995), the relative gas diffusion coefficient and air permeability (Simojoki et al. 2008; Berisso et al. 2012; Pulido-Moncada et al. 2019). Reduction of macroporosity due to compaction increases the risk of preferential flow in the few macropores still connected to the soil surface (Kulli et al. 2003; Etana et al. 2013), and thereby facilitate colloids transport of nutrients (e.g. phosphorus) and pollutants (pesticides) (Jarvis 2007). A reduction of aeration has been shown to increase emissions of the greenhouse gas N_2O through denitrification at anaerobic sites (Bakken et al. 1987; Hansen et al. 1993; Simojoki et al. 1991; Sitaula et al. 2000). The effect of compaction on root growth can be due to an increase of soil penetration resistance (Taylor and Gardner 1963; Bengough et al. 2011; Valentine et al. 2012; Colombi et al. 2018), a reduction of aeration (Czyz 2004) or a reduction of available water (Tarawally et al. 2004). Often, compaction results in a resource accessibility problem, meaning that roots are not able to grow to where the resources are, e.g. because root growth is decreased due to increased soil penetration resistance (Hettiaratchi 1990; Colombi and Keller 2019). A soil quality index, the least limiting water range (LLWR), combines these three aspects (soil strength, soil aeration and soil water holding capacity) into one factor to evaluate soil suitability for plant growth (Lety 1985; da Silva et al. 1994). Soil structure deformation due to compaction has been shown to reduce the LLWR

(Chen et al. 2014; Pulido-Moncada and Munckholm 2019). Groenevelt et al. (2001) introduced the integral water capacity (IWC) concept, which has some advantages over the LLWR concept, but essentially uses the same limiting soil physical properties as the LLWR. However, instead of using one cut-off value for each limiting soil physical property, IWC uses smooth continuous weighting functions for the various limiting soil physical properties that are bounded by two transition points: one where crop development starts being limited and one where the limitation becomes total. New criteria at the wet and dry ends of the IWC, based on soil physical and plant physiological considerations, were recently proposed by Meskini-Vishkaee et al. (2018). Similar to the LLWR, the IWC is sensitive to soil compaction.

Poor root growth due to dense and poorly aerated soil reduces crop yield (Håkansson and Reeder 1994; Alakukku 1999). Early studies indicate that a single compaction event caused by field traffic with wheel loads of only 5 Mg resulted in a permanent yield loss of approximately 2.5% due to compaction of the subsoil (Håkansson and Reeder 1994). However, today's machinery includes wheel loads of up to 12 Mg; consequently, yield losses are expected to be much higher than of reported by Håkansson and Reeder (1994). Recent Danish field trials with modern machinery (tractor + 3-axles slurry tanker) with wheel loads of 6–8 Mg have shown yield losses of 8–40% (average 19%) in spring barley primarily caused by compaction of the topsoil (Schjønning et al. 2016).

Most of these findings come from “track-by-track” compaction field experiments, meaning that the whole surface is compacted, which simulate random traffic patterns. Berisso et al. (2013b) investigated the consequences of soil compaction on air-filled porosity and air permeability in a vertical plan in the field across (i.e. perpendicular to) the wheel rut (Fig. 13.4). Their results showed that compression was highest beneath the centre of the wheel rut, but that shear deformation was largest close to the edge of the wheel rut resulting in significant reduction of air permeability. Most studies compare the structural

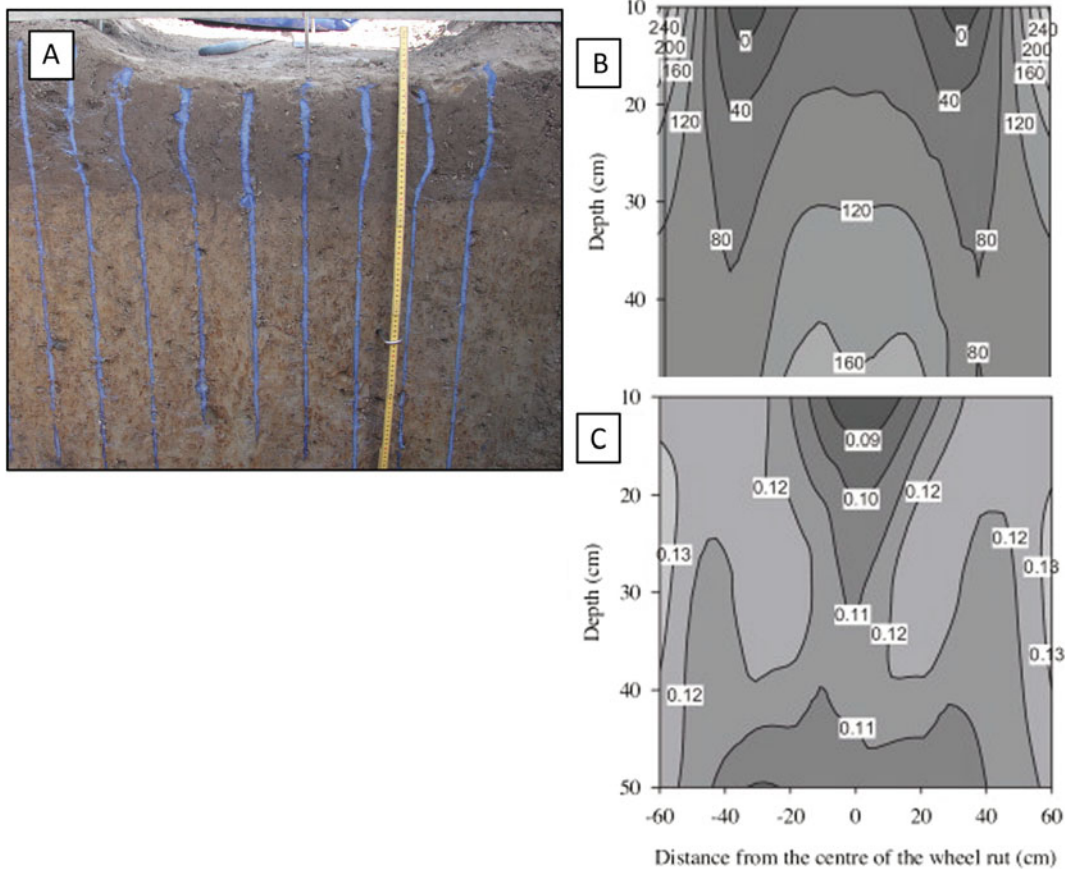


Fig. 13.4 **a** Visualization of soil distortion close to the edge of the wheel rut after the passage of an agricultural vehicle (from Berisso 2013). Before the wheeling experiment, vertical holes were drilled and filled with a dyed

sand. **b** Air-filled porosity (in $\text{m}^3 \text{m}^{-3}$) and **c** air permeability (in μm^2) measured at three depths and interpolated across the wheel rut after a wheeling experiment (from Berisso et al. (2013b))

state of soil before and after traffic, but not deformation paths during compaction, as real-time visualization of deformation is difficult, especially in situ. Horn and Baumgartl (1999), Arvidsson et al. (2002) and Keller et al. (2002) measured soil stress and soil displacement in situ during traffic, but conversion of soil displacement to structural deformation and consequences for soil functional properties (e.g. fluid transport properties) is not straightforward. Stress-strain relationships that are needed for prediction of the impact of load application on soil properties and functions are typically obtained from laboratory tests (e.g. uniaxial compression tests, cf. Sect. 13.3), but the loading conditions and stress fields in such tests may significantly differ from

those in situ (e.g. Keller et al. 2012). Lamandé et al. (2018) observed a similar increase in sub-soil bulk density below a tyre and a track that were equally loaded. However, a larger decrease of air permeability was measured below the track than below the tyre, indicating different deformation of the air-filled pore system between the two undercarriage systems. This could be explained by a longer loading time beneath the track, or by the uneven contact stress distribution beneath the wheels and rollers of the track undercarriage acting similar to multiple wheel passes, but the exact reason is not known. In spite of decades of research on the topic, there is a need for a better understanding of deformation processes during compaction. A better

quantitative knowledge of soil deformation would also facilitate better predictions of how soil properties and functions are modified by vehicular traffic. Assouline (2006) proposed a model to estimate changes in the hydraulic conductivity function caused by changes in bulk density. The model was based on data from uniaxial compression characteristics (Assouline 2002). Ghezzehei and Or (2003) proposed a modelling framework to quantify the densification of soil aggregate packings subjected to external loads, and the consequences of this mechanical deformation on hydraulic functioning. These two modelling approaches are promising, but are so far only developed for simple geometrical considerations and loading conditions. Future research would need to expand on these frameworks to account for more complex stress fields as found under tyres and tracks of agricultural vehicles.

13.5 Economical and Ecological Costs of Soil Compaction

Soil compaction causes economical and ecological damage to land users and society. The costs evolve because compaction adversely affects the capacity of soils to support a range of ecosystem functions and services, as discussed in the previous section. The damage and associated costs of soil compaction include the following:

- Loss of productivity (Håkansson et al. 1987; Håkansson and Reeder 1994);
- Increase in the incidence and severity of flooding and erosion, caused by modification of surface water partitioning towards less infiltration (and hence less groundwater recharge) and more surface run-off (Horn et al. 1995; Rogger et al. 2017; Alaoui et al. 2018);
- Decline in water quality because of increased risk of preferential flow increasing the risk of nutrient and pesticide leaching (Jarvis 2007);
- Increase in greenhouse gas emissions, either via impeded soil aeration (Lipiec and Stepniewski 1995; Horn et al. 1995; Ball 2013), or via increased fuel consumption during tillage and decreased fertilizer use efficiency (Chamen et al. 2015; Graves et al. 2015).
- Decrease in carbon input from roots due to higher soil mechanical resistance and impeded soil aeration (Bengough et al. 2011; Kätterer et al. 2011), and therefore decline of soil organic carbon in the long-term (Colombi et al. 2019)

The costs include both on-site effects (e.g. loss of productivity) and off-site effects (e.g. flooding, erosion, greenhouse gas emissions). Although the annual costs of soil compaction are tremendous—Graves et al. (2015) estimated total annual costs of soil compaction to 470 M£ yr⁻¹ for England and Wales—there is limited information in concrete terms at the national and continental scale. There could be several reasons for that. First, the amount (acreage) and severity of soil compaction at relevant scales is largely unknown. Several sources mention that 25–45% of all agricultural land in Europe is compacted (Oldeman et al. 1991; Graves et al. 2015; Schjøning et al. 2015a, b; Brus and van den Akker 2018). Second, compaction results in significant off-site damage (e.g. flooding, greenhouse gas emissions, water quality), which might be difficult to associate to the source (Graves et al. 2015). Third, certain costs, particularly off-site costs, may be difficult to value in monetary terms.

Graves et al. (2015) ascribed ca. 40% of the total compaction costs to on-site costs, and about 60% to off-site costs. Loss of crop productivity accounted to ca. 80% of the on-site costs. The off-site costs were largely caused by flooding damage (ca. 65% of off-site costs) and increased greenhouse gas emissions (ca. 35% of off-site costs). The total annual costs of 470 M£ yr⁻¹ for England and Wales, corresponding to 540 M€ yr⁻¹, amount to approximate costs of 56.4 € yr⁻¹ per hectare agricultural area (Fig. 13.5). Although conditions vary across Europe, this number may be indicative for other European countries too. Keller et al. (2019), using different assumptions, estimated the costs of productivity loss due to subsoil compaction in Sweden to



Fig. 13.5 On-site and off-site costs of soil compaction according to Graves et al. (2015). Numbers are based on estimated cost of soil compaction in England and Wales by Graves et al. (2015). Here, we expressed the costs in €

per hectare arable land, for which we considered the total costs and the total area of arable land (i.e. not only the compaction-affected area) as given by Graves et al. (2015). GHG: green house gas; N: nitrogen

between 33 and 145 M€ yr⁻¹, and showed that this is a significant fraction (between ca. 4 and 18%) of the total agricultural income in Sweden.

Although there is little doubt that the annual costs to society caused by soil compaction are significant, we lack reliable estimates of the economical and ecological damage of soil compaction. Therefore, there is a need for better estimates of the extent and severity of soil compaction at national scales, and a need for data to quantify the cost of compaction. The latter requires a need to link knowledge on compaction processes at small scales (pore to plot scale; *cf.* Sect. 13.4) to processes at the catchment and regional scales, as also advocated by Rogger et al. (2017) and Alaoui et al. (2018).

13.6 Mechanisms and Rates of Recovery of Soil Structure and Functions After Compaction

The magnitude of the economical and ecological costs of soil compaction (see Sect. 13.5) are largely dependent on the rate of recovery of soil structure and function after a compaction event,

because the costs can be seen as the cumulative loss of functionality integrated over the time period until soil has effectively recovered to its pre-compaction functionality (Keller et al. 2017). Therefore, quantitative knowledge of recovery rates is crucial for proper quantification of compaction costs. Moreover, knowledge of the relative impact of different mechanisms (natural abiotic and biotic processes, as well as soil management impacts such as tillage) on recovery rates are needed to potentially accelerate recovery, thereby reducing compaction costs. More generally, since the same mechanisms are involved in recovery of soil structure after disturbance by compaction and in soil structure evolution, quantitative knowledge of compaction recovery should also be useful to improve soil structure by soil management.

Although knowledge of recovery from compaction is as important as knowledge of the compaction processes itself, the former is much less studied. One reason for this is the vastly different time scales involved in compaction (seconds) and recovery from compaction (decades) (Fig. 13.6). Experimental evidence suggests that subsoil compaction is persistent for decades (Håkansson and Reeder 1994; Peng and

Horn 2008; Berisso et al. 2012) or even centuries (Webb 2002). Another reason may be that the complex interplay of different recovery mechanisms makes quantifications difficult. The key natural mechanisms that contribute to compaction recovery are abiotic processes (driven by climatic forces: wetting–drying and freezing–thawing processes) and biotic processes (bioturbation by plant roots, root water uptake, bioturbation by earthworms and other soil fauna, and microbiological activity). Moreover, soil management may play an important role, e.g. via soil fragmentation and loosening by tillage. However, what we are largely lacking is quantitative information and modelling frameworks that would allow predictions of recovery rates of different soil properties and functions as a function of compaction severity, soil type, soil depth, climate and soil use and management. We advocate for more research on compaction recovery (and soil structure improvement in general). Apart from mechanistic experiments aiming at improved quantification of key mechanisms, there is a need for experimental-observational studies, which requires long-term (years to decades) monitoring (e.g. Keller et al. 2017; Lucas et al. 2019), as well as for developing modelling concepts and approaches (Verbecken et al. 2016; Vogel et al. 2018).

13.7 Non-invasive Methods to Quantify Compaction State and Processes

Non-invasive (non-destructive) techniques provide possibilities to quantify soil deformation and changes in soil structure due to natural processes, mechanical loading or during stress application, and thereby allow for better understanding of soil deformation processes and characterizing the soil structure. The current non-invasive techniques (Fig. 13.7) are applied either for laboratory (e.g. X-ray computed tomography) or for in situ (i.e. geophysical techniques) measurements. Laboratory measurements such as X-ray computed tomography imaging are performed on soil core samples, which allow detailed characterization of soil structure but involves removing soil from its natural in situ conditions (Romero-Ruiz et al. 2018). Moreover, extrapolating findings from laboratory measurements to in situ conditions may be problematic. Geophysical techniques enable soil structure characterization at field scale as well as long-term monitoring. Geophysical techniques can be used in laboratory settings (e.g. Flammer et al. 2001; Koestel et al. 2008). Here, we discuss their potential for in situ characterization of soil structure at scales of the experimental plot and

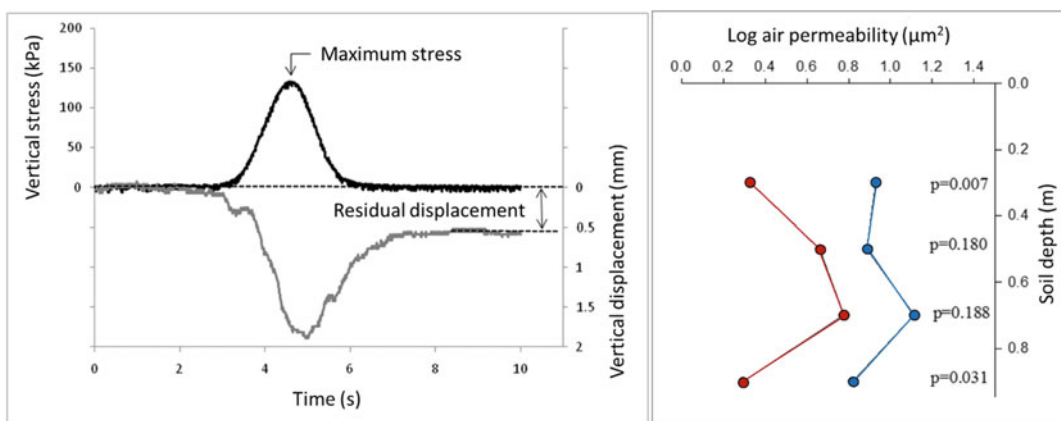


Fig. 13.6 (Left) Dynamics of vertical soil stress and vertical displacement during the passage of a tyre from an agricultural vehicle (from Keller et al. 2012), and (right) air permeability in plots that were compacted with

agricultural machinery 14 years prior to sampling (red) and in plots that did not receive experimental compaction (blue) (from Berisso et al. 2012)

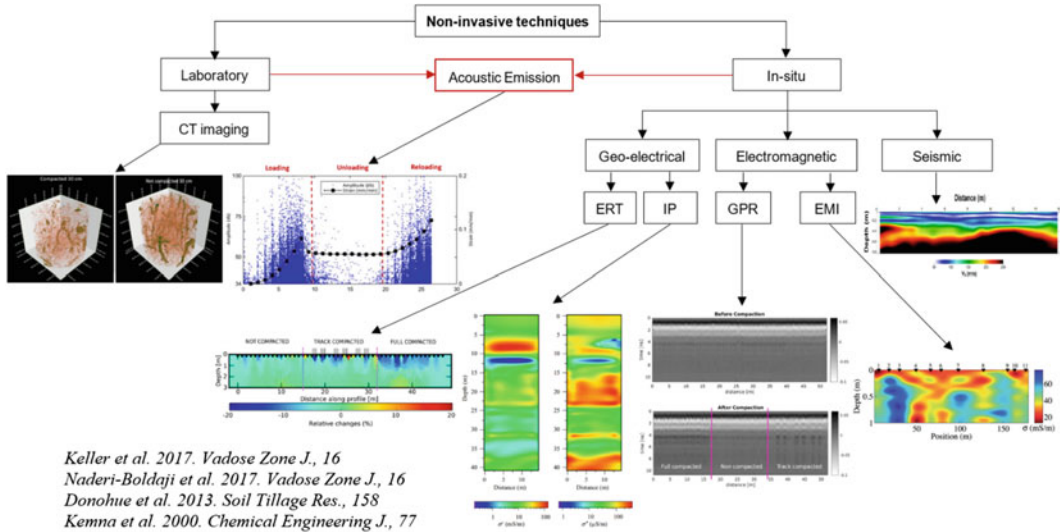


Fig. 13.7 Non-invasive techniques to quantify soil structural change and compaction process (modified from Romero-Ruiz et al. 2018)

larger. Geophysical properties (e.g. electrical resistivity, dielectric permittivity or seismic velocity) can be used to quantify changes in soil bulk properties (e.g. porosity, clay content and saturation) and structural form properties. However, we have limited knowledge about the links between geophysical properties and soil structural properties (e.g. macroporosity and its connectivity). Additional to the geophysical techniques, acoustic emission (AE) offers a potential technique that can be deployed for both laboratory and in-field evaluations of soil deformation regimes at a particle-scale under stress application, which may help to better understand the soil compaction process when combined with other techniques.

13.7.1 X-ray Computed Tomography

During the last decade, the development and use of X-ray computed tomography (CT) imaging technique and analysis method in soil research has been tremendous. CT imaging consists of directing X-rays at an object from multiple orientations and measuring the decrease in intensity along a series of linear paths. This decrease is characterized by Beer's law (Beer 1852), which

describes intensity reduction as a function of X-ray energy, path length and material linear attenuation coefficient. A specialized algorithm is then used to reconstruct the distribution of X-ray attenuation in the volume being imaged. X-ray attenuation is primarily a function of X-ray energy and the density and composition of the exposed material. Analysis of CT images of soil samples allows for direct quantification of soil structural features, in particular pore system characteristics (Fig. 13.1). Various properties of soil pores and pore networks have been estimated using X-ray CT imaging. The X-ray image resolution is limited by the size of the scanner detector and the size of the scanned soil sample. Due to these limitations, most work considers macropores. Quantification typically includes macroporosity, macropore diameter, perimeter and area, circularity, equivalent cylindrical diameter, tortuosity, hydraulic radius in three-dimensions (pore volume/wall area), numerical density of networks and connectivity (Taina et al. 2008). In soil compaction research, X-ray CT offers considerable advantages, because it is non-invasive and further allows for mapping of both the soil matrix and the macropores under different stress states by repeatedly scanning the same soil sample. This is desirably preferred over

physical methods that indirectly measure bulk soil pore structure from different physical measurements (e.g. saturated hydraulic conductivity, soil water retention) while disturbing the sample (Naveed et al. 2016). However, the technique is not yet developed to be applied for in situ field evaluations (i.e. its application is still limited to laboratory evaluations of soil samples). CT has been used to quantify changes in the soil pore structure due to compaction (e.g. Schäffer et al. 2007) and to provide experimental evidence of long-term compaction effects (Lamandé et al. 2013). However, there are only few studies that use CT to quantify soil deformation under mechanical stress. Schäffer et al. (2008) quantified the deformation and stability of artificial macropores as a function of applied stress. They concluded decreases in both the porosity and connectivity of the macropores with increased trafficking. Peth et al. (2010) could show that soil deformation under hydraulic and mechanical stresses is spatially highly heterogeneous. Kim et al. (2010) reported a large decrease in various X-ray CT-derived macropore characteristics under compaction of soil from 0 to 30 cm depth. Strain due to uniaxial compression was calculated from CT images by following the displacement of stones (Naveed et al. 2016) and by the displacement of garnet particles mixed into soil (Schlüter and Vogel 2016). In a long-term soil structure observatory for monitoring post-compaction evolution of soil structure, Keller et al. (2017) showed the decrease in pore connectivity and in porosity using CT images of compacted and non-compacted soil samples confirmed by measurements of air-filled porosity and gas transport properties.

13.7.2 Geophysical Methods

Geophysical techniques may be used especially for in situ measurement of soil structural traits and structure dynamics at large (e.g. field) scale. As reviewed by Romero-Ruiz et al. (2018), geoelectrical and electromagnetic (EM) techniques are sensitive to soil hydrological states and could therefore be used to assess the

influence of pore space and pore distribution on soil hydrology. EM techniques include the DC-resistivity (Binley and Kemna 2005) and electromagnetic induction (EMI) methods probing electrical resistivity (or inversely, electrical conductivity), which depends strongly on pore connectivity; the induced polarization (IP) method (Kemna et al. 2012) that senses soil chargeability that depends on the pore size distribution and the ground penetrating radar (GPR) method (Annan 2005) that is sensitive to soil permittivity and therefore to soil moisture, interfaces, and cavities.

Soil electrical resistivity is obtained from spatially distributed voltages resulting from current injections via an array of electrodes that are installed on the soil surface or in boreholes (so-called Wenner array). It can be also measured by EMI, which induces a magnetic field into the soil and senses some selected components of the field from which the subsurface electrical resistivity can be calculated. Physical models have been developed to relate the bulk soil electrical resistivity to soil properties (e.g. porosity and clay content) and state variables (e.g. soil salinity, water content and water saturation), their interactions, and spatial arrangement (e.g. Archie 1942; Linde et al. 2006). However, petrophysical models of DC-resistivity do typically not consider pore network heterogeneity, and do not differentiate between pore sizes (e.g. microporosity and macroporosity) (Romero-Ruiz et al. 2018). The effect of soil density (compaction) on DC-resistivity is relatively well studied. In general, at a given partial saturation and salinity, the overall effect of soil compaction is a decrease in soil electrical resistivity. This offers electrical resistivity (tomography) as a valuable property (technique) for studying soil structure changes due to compaction (e.g. Rossi et al. 2013; Keller et al. 2017).

Induced polarization (IP) is a complementary measurement to electrical resistivity. They are usually measured at the same time by inserting two electrodes into the earth surface and passing a current through them. After the resistivity measurement is made, the current is shut off and the IP is measured. The IP is caused by the

current placed into the earth “charging” specific mineral phases similar to a capacitor. Chargeability is the result of build-up of ionic charges due to accumulation of ions at impermeable boundaries (e.g. pore throat). The polarization measures the slow decay of voltage from this stored charge after the flow of electric current ceases. The IP survey can be made in time-domain and frequency-domain modes. In time-domain IP, chargeability is the main geophysical property targeted. In frequency-domain IP, complex electrical conductivity is measured over the frequency range of injected alternative current. IP properties are sensitive to the specific surface area of soil, and hence to clay content and clay type. The frequency dependent complex electrical conductivity is dependent on grain size distribution (Friedman 2005). It was argued that frequency-domain IP parameters could be used to monitor soil water dynamics in macropores (Ghorbani et al. 2008; Breede 2013). This suggests that IP has a great potential in characterizing the soil structural form.

Ground penetrating radar (GPR) uses electromagnetic radiation in the microwave band (10 MHz to 2.6 GHz) of the radio spectrum, and detects the reflected signals from subsurface. A GPR consists of transmitter and receiver antennas, the transmitter emits EM energy into the ground. The energy is reflected, refracted or scattered back to the surface when encounters boundaries between materials with different permittivity (e.g. in soil, the GPR signal is affected by the interaction of EM waves at the soil surface, its propagation through the soil and scattering at interfaces). A receiving antenna can then record the variations in the return signal. One important aspect of GPR functioning is the penetration depth, which is highly affected by the electrical conductivity of the medium in which the EM energy penetrates, and the frequency of the EM wave. Increasing the electrical conductivity and frequency both decreases the penetration depth, e.g. from several thousand metres in ice, up to 15 m in dry sand and a few centimetres in moist clay soils (i.e. materials with high electrical conductivity). GPR propagation velocity is highly influenced by soil water

content. Any effect on soil that causes heterogeneities in water content (i.e. in dielectric constant), e.g. compaction, will change the GPR responses. This is the reason of attention to this technique in numerous soil compaction studies. André et al. (2012) measured GPR reflections to identify compaction in a vineyard. Zones with strong reflections presented a compacted soil profile and a poor development of the vine in comparison to a weak reflection in an uncompacted zone where the vine presented a higher development. Similarly, Petersen et al. (2005) used observed strong reflections in GPR signals for compacted soil. Keller et al. (2017) performed GPR measurements in a compaction experiment found that the radargram after compaction showed an enhancement of signal amplitudes compared with non-compacted soil.

Geoelectrical and EM methods provide limited information about soil mechanical status. Soil mechanical properties (e.g. strength and elastic moduli) are better characterized using shallow seismic methods (Socco et al. 2010; Foti et al. 2011; Donohue et al. 2013; Keller et al. 2013a). The sensitivity of seismic measurements to soil mechanical properties could be capitalized for detection of compacted layers. There are many studies in the field of geotechnical engineering that link seismic signatures to soil mechanical states such as liquefaction resistance, penetrometer mechanical impedance, shear and bulk moduli and soil density (e.g. Yunmin et al. 2005; Mandal et al. 2016; Bhowmick 2017; Sabba and Uyanik 2017). Keller et al. (2013b) used compression waves (P-waves) to illustrate the dynamic soil behaviour during repeated wheeling. Mapping of compacted zones and distinguishing between compacted and uncompacted areas has been shown using shear waves (S-waves) (Donohue et al. 2013) and electrical resistivity tomography (ERT) (Besson et al. 2013).

A crucial step to advance the use of geophysical methods in soil research is to characterize and quantify relationships between geophysical properties and soil properties and states. Geophysical properties of soil depend on two aspects (Romero-Ruiz et al. 2018): (i) a

constitutive aspect—geophysical properties depend on the relative volumetric proportions of the constituents with their individual physical properties; and (ii) a structural aspect—geophysical properties depend on spatial distribution and connectivity of different constituents. The sensitivity of geophysical methods to soil physical properties varies. Some methods are primarily sensitive to interfaces (wave-based physics: seismic and GPR reflection methods), while others respond to bulk properties (diffusion-based physics: DC-resistivity, and EMI). Therefore, the combination of different geophysical methods could potentially offer new ways for characterization of soil structure (Romero-Ruiz et al. 2018).

13.7.3 Acoustic Methods

The macroscopic mechanical response of soil under loading is shaped by microscopic grain scale interactions and intrinsic mechanical properties. Application of mechanical stresses to soil results in deformation, micro-fracturing, particle motion and liquid reconfiguration, which release measurable amounts of stored elastic energy in the form of acoustic emissions (AEs). AEs are relatively high frequency (10–1000 kHz), i.e. beyond the range audible to human ear, rapid (few milliseconds), small magnitude body waves generated by the abrupt release of stored strain energy from a delimited source region. AE monitoring provides a window into grain scale processes not attainable with traditional monitoring techniques. Sources of AE in soils are mechanical interactions between moving particles, the formation of cracks, a sudden release of force chains due to failure, particle crushing, sliding, and friction, grain cementation fracturing, liquid bridge rupture, and the rupture of roots and other fibres (Michlmayr et al. 2012). These micro-mechanical events may generate elastic waves with distinguishable frequency and energy content (Michlmayr and Or 2014), thus offers new (and non-invasive) means for indirect

inference of the nature of particle interactions and soil deformation regimes. For instance, characterizing AE from soil during stress application can provide insights on the onset of yielding, i.e. elastic versus plastic soil deformation. This was the subject of the early applications of AE technology in soil mechanics, backing to a series of studies for in situ determination of pre-stress (i.e. precompression stress, σ_p) in granular and cohesive soils (Koerner et al. 1984a, b; Deutsch et al. 1989), and detection of soil shear failure for early warning of slope movements (Koerner et al. 1977). Determining a safe threshold for imminence of soil permanent deformation (i.e. compaction) under mechanical stress applied by machinery traffic is of great importance in agricultural soil compaction (Keller et al. 2012). This is conventionally estimated by mechanical compression tests and analysing the resulting stress-void ratio relationship (*cf.* Sect. 13.3). The macroscopic stress-void ratio relationships for a soil provide only limited information about soil structural changes during deformation and how various functions related to structure are modified due to mechanical loading. The identification and characterization of micro-mechanical processes may improve understanding of how macroscopic soil deformation is governed and how soil functions vary under mechanical loading. The use of passive AEs offers a useful and promising tool for analysing the stress-deformation regimes of soil during compression. Acoustic emission monitoring can complement mechanical measurements of stress-deformation by providing a measure of discrete mechanical interactions as singular events (Brzesowsky et al. 2014; Naderi-Boldaji et al. 2017). Acoustic emission technology has been coupled with laboratory mechanical tests on soil samples in numerous studies, but no effort can be found yet that applies AE for characterizing the soil deformation process under field vehicular traffic. Deployment of acoustic wave guides as part of monitoring networks can facilitate AE monitoring at a given depth under traffic.

13.8 In Situ Measurements for Mapping the State of Soil Compaction

Mapping the state of soil compaction across agricultural fields and landscapes would help to (i) better estimate the extent of land degradation by compaction (severity of compaction and area affected), (ii) obtain information on soil traffic management and land use impacts on soil compaction, which in turn would help in the development and refinement of sustainable management guidelines (Alaoui and Diserens 2018), (iii) explain within-field crop yield variability (Fig. 13.1) (Lipiec and Usowicz 2017) and (iv) apply site-specific soil management (e.g. site-specific/variable depth tillage) (Raper 1999; Raper et al. 2005) and achieve better timeliness in field operations.

Mapping of the compaction state within a field at a useful spatial resolution requires on-the-go sensors. Moreover, a suitable sensor for on-the-go measurement of soil compaction must permit measurements in a soil profile to enable site-specific delineation of the thickness and depth of compacted layers, e.g. for precision (variable depth) tillage. This may be achieved by geophysical methods (see previous section) or more feasibly by soil strength sensors in the form of horizontal penetrometers and soil cutting tools. Geophysical techniques are non-destructive, but the interpretation of the signal may be difficult because they provide bulk information, i.e. a relatively large soil volume is involved and many factors affect geophysical properties. Soil penetration resistance provides a direct measure of soil mechanical resistance but only considers a small soil volume and is influenced by several soil properties (e.g. soil moisture, density, texture and structure). A quantitative measure for the state of soil compaction to be captured by (on-the-go) sensors and to suitably explain crop yield variability is yet ambiguous. Naderi-Boldaji and Keller (2016) found strong correlation between the soil degree of compactness (i.e. relative density) and the soil physical quality index S (Dexter 2004). Moreover, the degree of compactness has

been shown to be a useful indicator of soil compaction state in relation with crop yield variability (Håkansson and Lipiec 2000). This motivated to evaluate the prediction of soil relative density by horizontal penetrometer to see if a unique model could be obtained to estimate the relative density from horizontal penetrometer resistance across soil textures (Naderi-Boldaji et al. 2016).

A standardized measure of soil compaction state should account for soil mechanical resistance, soil texture and structure, soil density and water content. Hence, combination of different sensors (i.e. sensor fusion) is needed (Fig. 13.8). There has been significant progress in the development of sensor fusions on horizontal penetrometers or cutting tools for simultaneous measurement of soil water content and soil texture additional to soil mechanical strength. Sensor fusion systems include (i) mechanical-optical fusion (Mouazen and Ramon 2006), (ii) mechanical-dielectric-Gamma ray fusion (Naderi-Boldaji et al. 2013), (iii) optical-dielectric fusion (Al-Asadi and Mouazen 2014) and (iv) mechanical-dielectric-acoustic fusion (Naderi-Boldaji et al. 2019). Where optical visible-near-infrared (Vis-NIR) spectroscopy sensors are available, they can be fused with soil strength sensors to simultaneously measure the strength affecting soil physical properties, i.e. soil moisture (Mouazen et al. 2005), soil texture and organic matter (Christy 2008; Brickleymer and Brown 2010). Commercial devices can be found that integrate Vis-NIR and electrical conductivity (EC) sensors on a vertical penetrometer (see P4000, Veris Tech. Virginia, USA), however, the technology is not yet economical to be implemented on a multi-tip horizontal penetrometer for discrete-depth characterizing the state of soil compaction. As a simple and low-cost sensor, dielectric sensors are often used for soil moisture on sensor fusions of soil compaction (Sun et al. 2006; Naderi-Boldaji et al. 2012). The natural Gamma radiation from the earth was related to soil mineral composition and thus suggested an instrument for soil texture mapping (e.g. the Mole, Soil Company, The Netherlands).

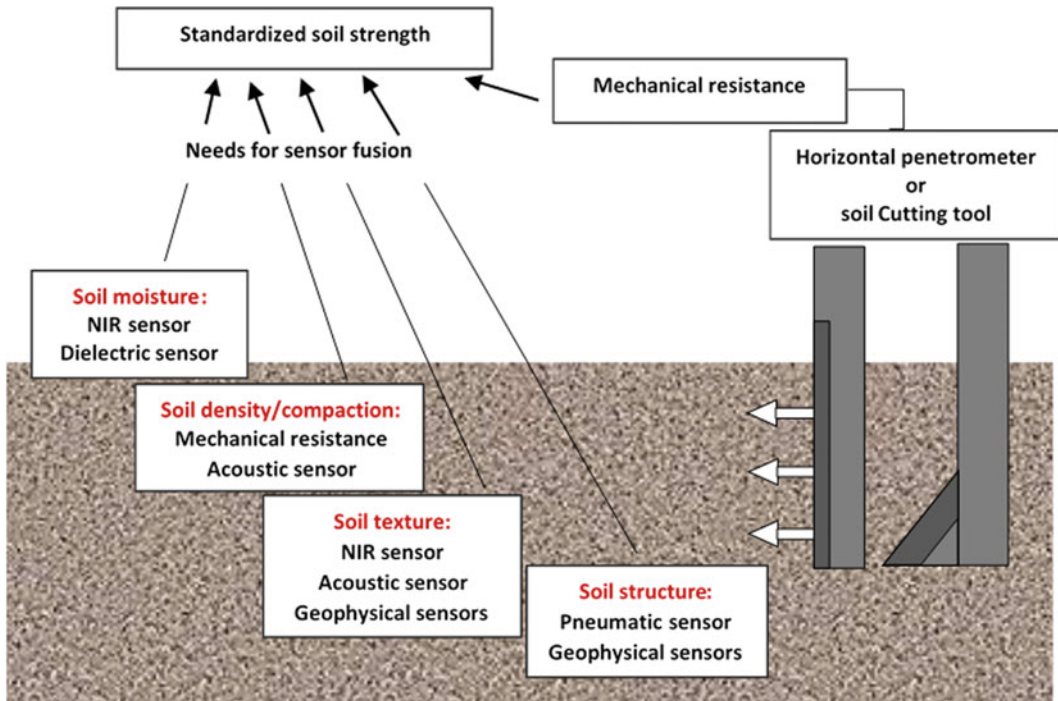


Fig. 13.8 Sensor fusion for on-the-go mapping of soil compaction (modified from Srinivasan 2006)

However, the Gamma ray sensor measures an average soil texture within a 1–1.5 m soil profile, which may not be suitable for soil compaction profile sensors. Acoustic sensors (either in low frequency 0–20 kHz or in high frequency >20 kHz) have been recently under evaluation for quantifying soil texture (Tate 2016; Naderi-Boldaji et al. 2019). They can be simply integrated on the tips of horizontal penetrometers or the soil cutting instruments. The premise on application of acoustic sensors is that the passive acoustics generated at the soil-probe interface and between the soil particles (within the zone of soil failure around the moving probe) carry information on soil particle size distribution (i.e. soil texture). As the soil strength is strongly affected by soil structure, a proper sensor for soil structure needs to be fused with others for soil compaction characterization. Limited attempts were made to develop a pneumatic sensor for on-the-go measurement of soil air permeability, but results were not satisfactory (Koostra and Stombaugh 2003). Combination of geophysical

methods with other sensors may provide opportunities for measurements of ancillary soil properties (e.g. soil structure) for soil compaction mapping but has not received much attention yet.

13.9 Summary, Conclusions and Outlook

The ecological and economic costs of soil compaction caused by agricultural field traffic are tremendous. However, the estimates of these costs are uncertain because there is limited knowledge on the extent and severity of soil compaction at field, region, country and continent scale. The already acute problem of soil compaction is likely to aggravate in the future. First, due to the continuing trend towards heavier and more powerful machinery. And second, due to the projected increase in extreme weather events that is expected to aggravate problems of reduced crop growth due to increased soil mechanical resistance of compacted soil, as well

as aggravate flooding caused by decreased infiltration and water storage capability of compacted soil.

Models and decision support systems can help minimize or avoid soil compaction due to agricultural field traffic. However, several aspects of the soil compaction process are still not fully understood—better knowledge could help refine models, yielding better predictions of compaction risks. The influence of soil conditions and soil structure (e.g. soil moisture, soil compactness, soil layering) on stress propagation remains unclear. Interactions between soil texture, soil structure and matric suction and their impact on soil compressive properties and behaviour deserve further attention. Our ability to predict changes in soil properties and functions due to soil deformation during compaction is still limited. Quantitative knowledge of soil structure recovery rates and times after compaction under different soil management, in different climates and for different soils is relatively poor. Non-destructive techniques offer possibilities to quantify soil deformation and to acquire new insights in soil deformation processes, in particular at small scales (e.g. pore scale). Geophysical methods can be applied in situ at larger scales (field plot, and potentially beyond) and could help to better understand soil structure dynamics (e.g. compaction, recovery) at field scale, to better quantify the extent and severity of soil compaction, and to link knowledge of soil deformation and compaction effects on soil properties at small scales to processes at landscape scales (e.g. hydrological functioning).

References

- Alakukku L (1999) Subsoil compaction due to wheel traffic. *Agric Food Sci Fin* 8:331–351. <https://doi.org/10.23986/afsci.5634>
- Alaoui A, Diserens E (2018) Mapping soil compaction—a review. *Curr Opin Environ Sci Health* 5:60–66. <https://doi.org/10.1016/j.coesh.2018.05.003>
- Alaoui A, Lipiec J, Gerke HH (2011) A review of the changes in the soil pore system due to soil deformation: a hydrodynamic perspective. *Soil Tillage Res* 115–116:1–15. <https://doi.org/10.1016/j.still.2011.06.002>
- Alaoui A, Rogger M, Peth S, Blöschl G (2018) Does soil compaction increase floods? A review. *J Hydrol* 557:631–642. <https://doi.org/10.1016/j.jhydrol.2017.12.052>
- Al- RA, Mouazen AM (2014) Combining frequency domain reflectometry and visible and near infrared spectroscopy for assessment of soil bulk density. *Soil Tillage Res* 135:60–70. <https://doi.org/10.1016/j.still.2013.09.002>
- André F, van Leeuwen C, Saussez S, Van Durmen R, Bogaert P, Moghadas D et al (2012) High-resolution imaging of a vineyard in south of France using ground-penetrating radar, electromagnetic induction and electrical resistivity tomography. *J Appl Geophys* 78:113–122. <https://doi.org/10.1016/j.jappgeo.2011.08.002>
- Annan AP (2005) GPR methods for hydrogeological studies. In: Rubin Y, Hubbard SS (eds) *Hydrogeophysics*. Springer, Dordrecht, The Netherlands, pp 185–213. https://doi.org/10.1007/1-4020-3102-5_7
- Archie GE (1942) The electrical resistivity log as an aid in determining some reservoir characteristics. *Trans AIME* 146:54–62. <https://doi.org/10.2118/942054-G>
- Arvidsson J, Trautner A, Keller T (2002) Influence of tyre inflation pressure on stress and displacement in the subsoil. *Adv Geocol* 35:331–338
- Assouline S (2002) Modeling soil compaction under uniaxial compression. *Soil Sci Soc Am J* 66:1784–1787. <https://doi.org/10.2136/sssaj2002.1784>
- Assouline S (2006) Modeling the relationship between soil bulk density and the hydraulic conductivity function. *Vadose Zone J* 5:697–705. <https://doi.org/10.2136/vzj2005.0084>
- Atkinson J (1993) *An introduction to the mechanics of soils and foundations through critical state soil mechanics*. McGraw-Hill international series in civil engineering, London
- Bakken LR, Børresen T, Njøs A (1987) Effect of soil compaction by tractor traffic on soil structure, denitrification, and yield of wheat (*Triticum aestivum* L.). *Eur J Soil Sci* 38:541–552. <https://doi.org/10.1111/j.1365-2389.1987.tb02289.x>
- Ball BC (2013) Soil structure and greenhouse gas emissions: a synthesis of 20 years of experimentation. *Eur J Soil Sci* 64:357–373. <https://doi.org/10.1111/ejss.12013>
- Batey T (2009) Soil compaction and soil management: a review. *Soil Use Manag* 25:335–345. <https://doi.org/10.1111/j.1475-2743.2009.00236.x>
- Beer A (1852) Bestimmung der Absorption des rothen-Lichts in farbigen Flüssigkeiten [Determination of the absorption of red light in colored liquids]. *Ann Phys Chem* 86:78–88. <https://doi.org/10.1002/andp.18521620505>
- Bengough AG, McKenzie BM, Hallett PD, Valentine T (2011) Root elongation, water stress, and mechanical impedance: a review of limiting stresses and beneficial

- root tip traits. *J Exp Bot* 62:59–68. <https://doi.org/10.1093/jxb/erq350>
- Berisso FE (2013) Traffic induced compaction and distortion effects on soil pore characteristics and functions. PhD thesis, Aarhus University. ISBN: 978-87-92869-61-6
- Berisso FE, Schjønning P, Keller T, Lamandé M, Etana A, de Jonge LW, Iversen BV, Arvidsson J, Forkman J (2012) Persistent effects of subsoil compaction on pore characteristics and functions in a loamy soil. *Soil Tillage Res* 122:42–51. <https://doi.org/10.1016/j.still.2012.02.005>
- Berisso FE, Schjønning P, Keller T, Lamandé M, Simojoki A, Iversen BV, Alakukku L, Forkman J (2013a) Gas transport and subsoil pore characteristics: anisotropy and long-term effects of compaction. *Geoderma* 195–196:184–191. <https://doi.org/10.1016/j.geoderma.2012.12.002>
- Berisso FE, Schjønning P, Lamandé M, Weisskopf P, Stettler M, Keller T (2013b) Effects of the stress field induced by a running tyre on the soil pore system. *Soil Tillage Res* 131:36–46. <https://doi.org/10.1016/j.still.2013.03.005>
- Berli M, Eggers CG, Accorsi ML, Or D (2006) Theoretical analysis of fluid inclusion for in situ soil stress and deformation measurements. *Soil Sci Soc Am J* 70:1441–1452. <https://doi.org/10.2136/sssaj2005.0171>
- Besson A, Séger M, Giot G, Cousin I (2013) Identifying the characteristic scales of soil structural recovery after compaction from three in-field methods of monitoring. *Geoderma* 204–205:130–139. <https://doi.org/10.1016/j.geoderma.2013.04.010>
- Bhowmick S (2017) Role of Vp/Vs and Poisson's ratio in the assessment of foundation(s) for important civil structure(s). *Geotech Geol Eng* 35:527–534. <https://doi.org/10.1007/s10706-016-0106-7>
- Binley A, Kemna A (2005) DC resistivity and induced polarization methods. In: Rubin Y, Hubbard SS (eds) *Hydrogeophysics*. Springer, Dordrecht, The Netherlands, pp 129–156
- Bolling I (1985) How to predict soil compaction from agricultural tires. *J Terramech* 22:205–223
- Boussinesq J (1885) Application des potentiels à l'étude de l'équilibre et des mouvements des solides élastiques. Gauthier-Villars, Paris, p 30p
- Breede K (2013) Characterization of effective hydraulic properties of unsaturated porous media using spectral induced polarization (SIP). PhD thesis, Forschungszentrum Jülich, Germany
- Bricklemeyer RS, Brown DJ (2010) On-the-go VisNIR: potential and limitations for mapping soil clay and organic carbon. *Comput Electron Agric* 70:209–216. <https://doi.org/10.1016/j.compag.2009.10.006>
- Brus DJ, van den Akker JJH (2018) How serious a problem is subsoil compaction in the Netherlands? A survey based on probability sampling. *Soil* 4:37–45. <https://doi.org/10.5194/soil-4-37-2018>
- Bzesowsky RH, Spiers CJ, Peach CJ, Hangx SJT (2014) Time independent compaction behavior of quartz sands. *J Geophys Res Solid Earth* 119:936–956. <https://doi.org/10.1002/2013JB010444>
- Bullock P, Fedoroff N, Jongerius A, Stoops G, Tursina T (1985) Handbook for soil thin section description. Waine Research Publ, Wolverhampton, UK, 152p
- Cavaliere KMV, Arvidsson J, da Silva AP, Keller T (2008) Determination of precompression stress from uniaxial compression tests. *Soil Tillage Res* 98:17–26
- Chamen WCT, Moxey AP, Towers W, Balana B, Hallatt PD (2015) Mitigating arable soil compaction: a review and analysis of available cost and benefit data. *Soil Tillage Res* 146:10–25. <https://doi.org/10.1016/j.still.2014.09.011>
- Chen G, Weil RR, Hill RL (2014) Effects of compaction and cover crops on soil least limiting water range and air permeability. *Soil Tillage Res* 136:61–69. <https://doi.org/10.1016/j.still.2013.09.004>
- Christy CD (2008) Real-time measurement of soil attributes using on-the-go near infrared reflectance spectroscopy. *Comput Electron Agric* 61:10–19. <https://doi.org/10.1016/j.compag.2007.02.010>
- Colombi T, Keller T (2019) Developing strategies to recover crop productivity after soil compaction—a plant eco-physiological perspective. *Soil Tillage Res* 191:156–161. <https://doi.org/10.1016/j.still.2019.04.008>
- Colombi T, Torres LC, Walter A, Keller T (2018) Feedbacks between soil penetration resistance, root architecture and water uptake limit water accessibility and crop growth—a vicious circle. *Sci Tot Environ* 626:1026–1035. <https://doi.org/10.1016/j.scitotenv.2018.01.129>
- Colombi T, Walder F, Büchi L, Sommer M, Liu K, Six J, van der Heijden MGA, Charles R, Keller T (2019) On-farm study reveals positive relationship between gas transport capacity and organic carbon content in arable soil. *Soil* 5:91–105. <https://doi.org/10.5194/soil-5-91-2019>
- Cui K, Defossez P, Cui YJ, Richard G (2010) Soil compaction by wheeling: changes in soil suction caused by compression. *Eur J Soil Sci* 61:599–608
- Czyz EA (2004) Effects of traffic on soil aeration, bulk density and growth of spring barley. *Soil Tillage Res* 79:153–166. <https://doi.org/10.1016/j.still.2004.07.004>
- Da Silva AP, Kay BD, Perfect E (1994) Characterisation of the least limiting water range of soils. *Soil Sci Soc Am J* 58:1775–1781. <https://doi.org/10.2136/sssaj1994.03615995005800060028x>
- Davis RO, Selvadurai APS (1996) *Elasticity and geomechanics*. Cambridge University Press, Cambridge
- Davis RO, Selvadurai APS (2002) *Plasticity and geomechanics*. Cambridge University Press, Cambridge
- Day SD, Bassuk NL (1994) A review of the effects of soil compaction and amelioration techniques on landscape trees. *J Arboricult* 20:9–17. <https://www.urbanforestry.frec.vt.edu/documents/articles/1994Arboriculture.pdf>
- De Pue J, Cornelis W (2019) DEM simulation of stress transmission under agricultural traffic Part 1:

- comparison with continuum model and parametric study. *Soil Tillage Res* 195:104408. <https://doi.org/10.1016/j.still.2019.104408>
- Défossez P, Richard G (2003) Models of soil compaction due to traffic and their evaluation. *Soil Tillage Res* 67:41–64. [https://doi.org/10.1016/S0167-1987\(02\)00030-2](https://doi.org/10.1016/S0167-1987(02)00030-2)
- Deutsch WL, Koerner RM, Lord AE (1989) Determination of prestress of in situ soils using acoustic emissions. *J Geotech Eng Div ASCE* 115:228–245
- Dexter AR (2004) Soil physical quality. Part I: theory, effects of soil texture, density and organic matter and effects on root growth. *Geoderma* 120:201–214. <https://doi.org/10.1016/j.geoderma.2003.09.004>
- Dias Junior MS, Pierce FJ (1995) A simple procedure for estimating preconsolidation pressure from soil compression curves. *Soil Technol* 8:139–151
- Donohue S, Forristal D, Donohue LA (2013) Detection of soil compaction using seismic surface waves. *Soil Tillage Res* 128:54–60. <https://doi.org/10.1016/j.still.2012.11.001>
- Dörner J, Dec D, Peng X, Horn R (2010) Effect of land use change on the dynamic behaviour of structural properties of an Andisol in southern Chile under saturated and unsaturated hydraulic conditions. *Geoderma* 159:189–197. <https://doi.org/10.1016/j.geoderma.2010.07.011>
- Drewry JJ, Cameron KC, Buchan GD (2008) Pasture yield and soil physical property responses to soil compaction from treading and grazing—a review. *Aust J Soil Res* 46:237–256
- Du Y, Gao J, Jiang L, Zhang Y (2017) Numerical analysis on tractive performance of off-road wheel steering on sand using discrete element method. *J Terramech* 71:25–43. <https://doi.org/10.1016/j.jterra.2017.02.001>
- Eggers CG, Berli M, Accorsi ML, Or D (2006) Deformation and permeability of aggregated soft earth materials. *J Geophys Res* 111:B10204. <https://doi.org/10.1029/2005JB004123>
- Etana A, Larsbo M, Keller T, Arvidsson J, Schjønning P, Forkman J, Jarvis N (2013) Persistent subsoil compaction and its effects on preferential flow patterns in a loamy till soil. *Geoderma* 192:430–436. <https://doi.org/10.1016/j.geoderma.2012.08.015>
- Estabragh AR, Javadi AA, Boot JC (2004) Effect of compaction pressure on consolidation behaviour of unsaturated silty soil. *Can. Geotech J* 41:540–550
- Flammer I, Blum A, Leiser A, Germann P (2001) Acoustic assessment of flow patterns in unsaturated soil. *J Appl Geophys* 46:115–128. [https://doi.org/10.1016/S0926-9851\(01\)00032-5](https://doi.org/10.1016/S0926-9851(01)00032-5)
- Foti S, Parolai S, Albarello D, Picozzi M (2011) Application of surface-wave methods for seismic site characterization. *Surv Geophys* 32:777–825. <https://doi.org/10.1007/s10712-011-9134-2>
- Friedman SP (2005) Soil properties influencing apparent electrical conductivity: a review. *Comput Electron Agric* 46:45–70. <https://doi.org/10.1016/j.compag.2004.11.001>
- Fröhlich OK (1934) *Druckverteilung im Baugrunde*. Springer, Vienna
- Ghezzehei TA, Or D (2003) Pore-space dynamics in a soil aggregate bed under a static external load. *Soil Sci Soc Am J* 67:12–19. <https://doi.org/10.2136/sssaj2003.1200>
- Ghorbani A, Cosenza P, Ruy S, Doussan C, Florsch N (2008) Non-invasive monitoring of water infiltration in a silty clay loam soil using spectral induced polarization. *Water Resour Res* 44:W08402. <https://doi.org/10.1029/2007WR006114>
- González O, Iglesias Coronel CE, López Bravo E, Recarey Morfa CA, Herrera Suárez M (2016) Modelling in FEM the soil pressures distribution caused by a tyre on a Rhodic Ferrasol soil. *J Terramech* 63:61–67. <https://doi.org/10.1016/j.jterra.2015.09.003>
- Gräsele W (1999) *Numerische Simulation mechanischer, hydraulischer und gekoppelter Prozesse in Böden unter Verwendung der Finite Elemente Methode*. Schriftenreihe Institut für Pflanzenernährung und Bodenkunde der Universität Kiel, Band 48, 400 pp
- Graves AR, Morris J, Deeks LK, Rickson RJ, Kibblewhite MG, Harris JA, Farewell TS, Truckle I (2015) The total costs of soil degradation in England and Wales. *Ecol Econ* 119:399–413. <https://doi.org/10.1016/j.ecolecon.2015.07.026>
- Greacen EL, Sands R (1980) Compaction of forest soils. A review. *Aust J Soil Res* 18:163–189. <https://doi.org/10.1071/SR9800163>
- Gregory AS, Whalley WR, Watts CW, Bird NRA, Hallett PD, Whitmore AP (2006) Calculation of the compression index and precompression stress from soil compression test data. *Soil & Tillage Res* 89:45–55
- Gregory AS, Ritz K, McGrath SP, Quinton JN, Goulding KWT, Jones RJA, Harris JA, Bol R, Wallace P, Pilgrim ES, Whitmore AP (2015) A review of the impacts of degradation threats on soil properties in the UK. *Soil Use Manag* 31:1–15. <https://doi.org/10.1111/sum.12212>
- Groenevelt PH, Grant CD, Semetsa S (2001) A new procedure to determine soil water availability. *Austr J Soil Res* 39:577–598. <https://doi.org/10.1071/SR99084>
- Gysi M, Klubertanz G, Vulliet L (2000) Compaction of an Eutric Cambisol under heavy wheel traffic in Switzerland: Field data and modelling. *Soil Tillage Res* 56:117–129. [https://doi.org/10.1016/S0167-1987\(00\)00132-X](https://doi.org/10.1016/S0167-1987(00)00132-X)
- Håkansson I, Lipiec J (2000) A review of the usefulness of relative bulk density values in studies of soil structure and compaction. *Soil Tillage Res* 53:71–85. [https://doi.org/10.1016/S0167-1987\(99\)00095-1](https://doi.org/10.1016/S0167-1987(99)00095-1)
- Håkansson I, Reeder RC (1994) Subsoil compaction by vehicles with high axle load extent, persistence and crop response. *Soil Tillage Res* 29:277–304. [https://doi.org/10.1016/0167-1987\(94\)90065-5](https://doi.org/10.1016/0167-1987(94)90065-5)
- Håkansson I, Voorhees WB, Elonen P, Raghavan GSV, Lowery B, van Wijk ALM, Rasmussen K, Riley H (1987) Effect of high axle-load traffic on subsoil

- compaction and crop yield in humid regions with annual freezing. *Soil Tillage Res* 10:259–268. [https://doi.org/10.1016/0167-1987\(87\)90032-8](https://doi.org/10.1016/0167-1987(87)90032-8)
- Hansen S, Mæhlum JE, Bakken LR (1993) N₂O and CH₄ fluxes in soil influenced by fertilization and tractor traffic. *Soil Biol Biochem* 5:621–630. [https://doi.org/10.1016/0038-0717\(93\)90202-M](https://doi.org/10.1016/0038-0717(93)90202-M)
- Hartge KH, Horn R (2016) *Essential soil physics*. Schweizerbart Science Publisher, Stuttgart, p 391
- Hettiaratchi DRP (1990) Soil compaction and plant root growth. *Philos Trans R Soc B* 329:343–355. <https://doi.org/10.1098/rstb.1990.0175>
- Hillel D (2004) *Introduction to environmental soil physics*. Elsevier Academic Press, Amsterdam, 2004. xvi + 494. ISBN 0-12-348655-6
- Horn R, Baumgartl T (1999) Dynamic properties of soils. In: Sumner ME (ed) *Handbook of soil science*. CRC Press, Boca Raton, pp A19–A51
- Horn R, Domżzał H, Słowińska-Jurkiewicz A, van Owerkerk C (1995) Soil compaction processes and their effects on the structure of arable soils and the environment. *Soil Tillage Res* 35:23–36. [https://doi.org/10.1016/0167-1987\(95\)00479-C](https://doi.org/10.1016/0167-1987(95)00479-C)
- Horn R, Richards BG, Gräse W, Baumgartl T, Wiermann C (1998) Theoretical principles for modelling soil strength and wheeling effects: a review. *Z Pflanzenernaehr Bodenkd* 161:333–346
- Horn R, Way T, Rostek J (2003) Effect of repeated tractor wheeling on stress/strain properties and consequences on physical properties in structured arable soils. *Soil Tillage Res* 73:101–106
- Imhoff S, Da Silva, AP, Fallow D (2004) Susceptibility to compaction, load support capacity, and soil compressibility of Hapludox. *Soil Sci Soc Am J* 68:17–24
- Jarvis NJ (2007) A review of non-equilibrium water flow and solute transport in soil macropores: principles, controlling factors and consequences for water quality. *Eur J Soil Sci* 58:523–546. <https://doi.org/10.1111/j.1365-2389.2007.00915.x>
- Jiang M, Dai Y, Cui L, Xi B (2018) Experimental and DEM analyses on wheel-soil interaction. *J Terramech* 76:15–28. <https://doi.org/10.1016/j.jterra.2017.12.001>
- Johnson JB, Kulchitsky AV, Duvoy P, Iagnemma K, Senatore C, Arvidson RE, Moore J (2015) Discrete element method simulations of Mars exploration rover wheel performance. *J Terramech* 62:31–40. <https://doi.org/10.1016/j.jterra.2015.02.004>
- Kätterer T, Bolinder MA, Andrén O, Kirchmann H, Menichetti L (2011) Roots contribute more to refractory soil organic matter than above-ground crop residues, as revealed by a longterm field experiment. *Agric Ecosyst Environ* 141:184–192. <https://doi.org/10.1016/j.agee.2011.02.029>
- Keller T, Carizzoni M, Berisso FE, Stettler M, Lamandé M (2013a) Measuring the dynamic soil response during repeated wheeling using seismic methods. *Vadose Zone J* 12. <https://doi.org/10.2136/vzj2013.01.0033>
- Keller T, Colombi T, Ruiz S, Manalili MP, Rek J, Stadelmann V, Wunderli H, Breitenstein D, Reiser R, Oberholzer H, Schymanski S, Romero-Ruiz A, Linde N, Weisskopf P, Walter A, Or D (2017) Long-term soil structure observatory for monitoring post-compaction evolution of soil structure. *Vadose Zone J* 16. <https://doi.org/10.2136/vzj2016.11.0118>
- Keller T, Lamandé M, Naderi-Boldaji M, Lima RP (2018) Approaches towards understanding soil compaction processes. In: Sychev VG, Mueller R L (eds) *Novel methods and results of landscape research in Europe, Central Asia and Siberia, vol II*. Publishing House FSBSI «Pryanishnikov Institute of Agrochemistry», pp 274–279
- Keller T (2005) A model for prediction of the contact area and the distribution of vertical stress below agricultural tyres from readily-available tyre parameters. *Biosyst Eng* 92:85–96. <https://doi.org/10.1016/j.biosystemseng.2005.05.012>
- Keller T, Arvidsson J (2016) A model for prediction of vertical stress distribution near the soil surface below rubber-tracked undercarriage systems fitted on agricultural vehicles. *Soil Tillage Res* 155:116–123. <https://doi.org/10.1016/j.still.2015.07.014>
- Keller T, Arvidsson J, Schjønning P, Lamandé M, Stettler M, Weisskopf P (2012) In situ subsoil stress-strain behavior in relation to soil precompression stress. *Soil Sci* 177:490–497. <https://doi.org/10.1097/SS.0b013e318262554e>
- Keller T, Berli M, Ruiz S, Lamandé M, Arvidsson SP, Selvadurai APS (2014) Transmission of vertical soil stress under agricultural tyres: comparing measurements with simulations. *Soil Tillage Res* 140:106–117. <https://doi.org/10.1016/j.still.2014.03.001>
- Keller T, Lamandé M (2010) Challenges in the development of analytical soil compaction models. *Soil Tillage Res* 111:54–64. <https://doi.org/10.1016/j.still.2010.08.004>
- Keller T, Lamandé M, Peth S, Berli M, Delenne J-Y, Baumgarten W, Rabbel W, Radjāi F, Rajchenbach J, Selvadurai APS, Or D (2013b) An interdisciplinary approach towards improved understanding of soil deformation during compaction. *Soil Tillage Res* 128:61–80. <https://doi.org/10.1016/j.still.2012.10.004>
- Keller T, Ruiz S, Stettler M, Berli M (2016) Determining soil stress beneath a tire: measurements and simulations. *Soil Sci Soc Am J* 80:541–553. <https://doi.org/10.2136/sssaj2015.07.0252>
- Keller T, Sandin M, Colombi T, Horn R, Or D (2019) Historical increase in agricultural machinery weights enhanced soil stress levels and adversely affected soil functioning. *Soil Tillage Res* 194:104293. <https://doi.org/10.1016/j.still.2019.104293>
- Keller T, Trautner A, Arvidsson J (2002) Stress distribution and soil displacement under a rubber-tracked and a wheeled tractor during ploughing, both on-land and within furrows. *Soil Tillage Res* 68:39–47. [https://doi.org/10.1016/S0167-1987\(02\)00082-X](https://doi.org/10.1016/S0167-1987(02)00082-X)
- Keller T, Arvidsson J (2007) Compressive properties of some Swedish and Danish structured agricultural soils measured in uniaxial compression tests. *Eur J Soil Sci* 58:1373–1381

- Kemna A, Binley A, Cassiani G, Niederleithinger E, Revil A, Slater L et al (2012) An overview of the spectral induced polarization method for near-surface applications. *Near Surf Geophys* 10:456–468. <https://doi.org/10.3997/1873-0604.2012027>
- Kemna A, Binley A, Ramirez A, Daily W (2000) Complex resistivity tomography for environmental applications. *Chem Eng J* 77:11–18. [https://doi.org/10.1016/S1385-8947\(99\)00135-7](https://doi.org/10.1016/S1385-8947(99)00135-7)
- Kim H, Anderson SH, Motavalli PP, Gantzer CJ (2010) Compaction effects on soil macropore geometry and related parameters for an arable field. *Geoderma* 160:244–251. <https://doi.org/10.1016/j.geoderma.2010.09.030>
- Kirby JM (1994) Simulating soil deformation using a critical state model: I. Laboratory tests. *Eur J Soil Sci* 45:239–248
- Kirby JM (1999a) Soil stress measurements: part I: transducer in a uniform stress field. *J Agric Eng Res* 72:151–160. <https://doi.org/10.1006/jaer.1998.0357>
- Kirby JM (1999b) Soil stress measurements: part II: transducer under a plate. *J Agric Eng Res* 72:151–160
- Koerner RM, Lord AE, McCabe WM (1977) Acoustic-emission behavior of cohesive soils. *J Geotech Eng Div ASCE* 103:837–850
- Koerner RM, Lord AE, Deutsch WL (1984a) Determination of prestress in granular soils using AE. *J Geotech Eng Div ASCE* 110:346–358
- Koerner RM, Lord AE, Deutsch WL (1984b) Determination of prestress in cohesive soils using AE. *J Geotech Eng Div ASCE* 110:1537–1548
- Koestel J, Kemna A, Javaux M, Binley A, Vereecken H (2008) Quantitative imaging of solute transport in an unsaturated and undisturbed soil monolith with 3-D ERT and TDR. *Water Resour Res* 44:W12411. <https://doi.org/10.1029/2007WR006755>
- Koolen (1974) A method for soil compactibility determination. *J Agric Eng Res* 19:271–278
- Koolen AJ, Kuipers H (1983) *Agricultural soil mechanics*. Adv Ser Agric Sci 13. Springer, Heidelberg, Germany
- Koostra BK, Stombaugh TS (2003) Development and evaluation of a sensor to continuously measure air permeability of soil. ASAE Meeting Paper No. 031072. St. Joseph, Mich.: ASAE.
- Kozolwski TT (1999) Soil compaction and growth of woody plants. *Scan J Forest Res* 14:596–619. <https://doi.org/10.1080/02827589908540825>
- Kulli B, Gysi M, Flühler H (2003) Visualizing soil compaction based on flow pattern analysis. *Soil Tillage Res* 70:29–40. [https://doi.org/10.1016/S0167-1987\(02\)00121-6](https://doi.org/10.1016/S0167-1987(02)00121-6)
- Lamandé M, Greve MH, Schjønning P (2018) Risk assessment of soil compaction in Europe—rubber tracks or wheels on machinery. *Catena* 167:353–362. <https://doi.org/10.1016/j.catena.2018.05.015>
- Lamandé M, Keller T, Berisso FE, Stettler M, Schjønning P (2015) Accuracy of soil stress measurements as affected by transducers dimensions and shape. *Soil Tillage Res* 145:72–77. <https://doi.org/10.1016/j.still.2014.08.011>
- Lamandé M, Schjønning P (2011a) Transmission of vertical stress in a real soil profile. Part I: site description, evaluation of the Söhne model, and the effect of topsoil tillage. *Soil Tillage Res* 114:57–70. <https://doi.org/10.1016/j.still.2011.05.004>
- Lamandé M, Schjønning P (2011b) Transmission of vertical stress in a real soil profile. Part III: effect of soil water content. *Soil Tillage Res* 114:78–85. <https://doi.org/10.1016/j.still.2010.10.001>
- Lamandé M, Schjønning P, Tøgersen FA (2007) Mechanical behaviour of an undisturbed soil subjected to loadings: effects of load and contact area. *Soil Tillage Res* 97:91–106. <https://doi.org/10.1016/j.still.2007.09.002>
- Lamandé M, Wildenschild D, Berisso FE, Garbout A, Marsh M, Moldrup P, Keller T, Hansen SB, de Jonge LW, Schjønning P (2013) X-ray CT and laboratory measurements on glacial till subsoil cores—assessment of inherent and compaction-affected soil structure characteristics. *Soil Sci* 178:359–368. <https://doi.org/10.1097/SS.0b013e3182a79e1a>
- Larson WE, Gupta SC, Useche RA (1980) Compression of agricultural soils from eight soil orders. *Soil Sci Soc Am J* 44:450–457
- Lebert M, Horn R (1991) A method to predict the mechanical strength of agricultural soils. *Soil Tillage Res* 19:275–286
- Letey J (1985) Relationship between soil physical properties and crop production. In: Stewart BA (ed), *Advances in soil science*. Springer, New York, NY, pp 277–294
- Lima RP, Silva AP, Giarola NFB, Silva A, Rolim M, Keller T (2018) Impact of initial bulk density and matric suction on compressive properties of two Oxisols under no-till. *Soil Tillage Res* 175:168–177
- Lima RP, Keller T (2019) Impact of sample dimensions, soil-cylinder wall friction and elastic properties of soil on stress field and bulk density under uniaxial compression test. *Soil Tillage Res* 189:15–24
- Linde N, Binley A, Tryggvason A, Pedersen LB, Revil A (2006) Improved hydrogeophysical characterization using joint inversion of cross-hole electrical resistance and ground-penetrating radar travel time data. *Water Resour Res* 42:W04410. <https://doi.org/10.1029/2006WR005131>
- Lipiec J, Medvedev VV, Birkas M, Dumitru E, Lyndina TE, Rousseva S, Fulajtár E (2003) Effect of soil compaction on root growth and crop yield in Central and Eastern Europe. *Int Agrophys* 17:61–69. https://www.researchgate.net/publication/26551807_Effect_of_soil_compaction_on_root_growth_and_crop_yield_in_Central_and_Eastern_Europe
- Lipiec J, Stepniewski W (1995) Effects of soil compaction and tillage systems on uptake and losses of nutrients. *Soil Tillage Res* 35:37–52. [https://doi.org/10.1016/0167-1987\(95\)00474-7](https://doi.org/10.1016/0167-1987(95)00474-7)
- Lipiec J, Usowicz B (2017) Spatial variability of soil properties and cereal yield in a cultivated field on sandy soil. *Soil Tillage Res* 174:241–250. <https://doi.org/10.1016/j.still.2017.07.015>

- Lucas M, Schlüter S, Vogel H-J, Vetterlein D (2019) Soil structure formation along an agricultural chronosequence. *Geoderma* 350:61–72. <https://doi.org/10.1016/j.geoderma.2019.04.041>
- Mandal T, Tinjum JM, Edil TB (2016) Non-destructive testing of cementitiously stabilized materials using ultrasonic pulse velocity test. *Transport Geotech* 6:97–107
- Meskini-Vishkaee F, Mohammadi MH, Neyshabouri MR (2018) Revisiting the wet and dry ends of soil integral water capacity using soil and plant properties. *Soil Res* 56:331–345
- Michlmayr G, Cohen D, Or D (2012) Sources and characteristics of acoustic emissions from mechanically stressed geologic media: a review. *Earth Sci Rev* 112:97–114
- Michlmayr G, Or D (2014) Mechanisms for acoustic emissions generation during granular shearing. *Granul Matter* 16:627–640
- Mossadeghi-Björklund M, Jarvis N, Larsbo M, Forkman J, Keller T (2019) Effects of compaction on soil hydraulic properties, penetration resistance and water flow patterns at the soil profile scale. *Soil Use Manag* 35:367–377
- Mouazen AM, Baerdemaeker JD, Ramon H (2005) Towards development of on-line soil moisture content sensor using a fibre-type NIR spectrophotometer. *Soil Tillage Res* 80:171–183
- Mouazen AM, Ramon H (2006) Development of on-line measurement system of bulk density based on on-line measured draught, depth and soil moisture. *Soil Tillage Res* 86:218–229
- Nader-Boldaji M, Keller T (2016) Degree of soil compactness is highly correlated with the soil physical quality index S. *Soil Tillage Res* 159:41–46
- Nader-Boldaji M, Alimardani R, Hemmat A, Sharifi A, Keyhani A, Dolatsha N, Keller T (2012) Improvement and field-testing of a combined horizontal penetrometer for on-the-go measurement of soil water content and mechanical resistance. *Soil Tillage Res* 123:1–10
- Nader-Boldaji M, Bahrami M, Keller T, Or D (2017) Characteristics of acoustic emissions from soil subjected to confined uniaxial compression. *Vadose Zone J* 16. <https://doi.org/10.2136/vzj2017.02.0049>
- Nader-Boldaji M, Sharifi A, Alimardani R, Hemmat A, Keyhani A, Loonstra EH, Weisskopf P, Stettler M, Keller T (2013) Use of a triple-sensor fusion system for on-the-go measurement of soil compaction. *Soil Tillage Res* 128:44–53
- Nader-Boldaji M, Tekeste MZ, Nordstorm RA, Barnard DJ, Birrel SJ (2019) A mechanical-dielectric-high frequency acoustic sensor fusion for soil physical characterization. *Comput Electron Agric* 156:10–23
- Nader-Boldaji M, Weisskopf P, Stettler M, Keller T (2016) Predicting the relative density from on-the-go horizontal penetrometer measurements at some arable top soils in Northern Switzerland. *Soil Tillage Res* 159:23–32
- Naveed M, Schjøning P, Keller T, de Jonge LW, Moldrup P, Lamandé M (2016) Quantifying vertical stress transmission and compaction-induced soil structure using sensor mat and X-ray computed tomography. *Soil Tillage Res* 158:110–122
- Nawaz MF, Bourrie G, Trolard F (2013) Soil compaction impact and modelling. A review. *Agron Sustain Dev* 33:291–309
- Nichols TA, Bailey AC, Johnson CE, Grisso RD (1987) A stress-state transducer for soil. *Trans ASAE* 30:1237–1241
- Nordfjell T, Öhman E, Lindroos O, Ager B (2019) The technical development of forwarders in Sweden between 1962 and 2012 and of sales between 1975 and 2017. *Int J Forest Eng* 30:1–13
- O’Ruark GA, Mader DL, Tattar TA (1982) The influence of soil compaction and aeration on the root growth and vigour of trees—a literature review. Part 1. *Arboricult J* 6:251–265
- Oldeman LR, Hakkeling RTA, Sombroek WG (1991) World map of the status of human-induced soil degradation. An explanatory note. ISRIC Wageningen, Netherlands/UNEP, Nairobi, Kenya, 34 pp
- Or D, Ghezzehei TA (2002) Modeling post-tillage soil structural dynamics: a review. *Soil Tillage Res* 64:41–59
- O’Sullivan MF, Robertson EAG (1996) Critical state parameters from intact samples of two agricultural soils. *Soil Tillage Res* 39:161–173
- Peng X, Horn R (2008) Time-dependent, anisotropic pore structure and soil strength in a 10-year period after intensive tractor wheeling under conservation and conventional tillage. *J Plant Nutr Soil Sci* 171:936–944
- Pereira JO, Defossez P, Richard G (2007) Soil susceptibility to compaction by wheeling as a function of some properties of a silty soil as affected by the tillage system. *Eur J Soil Sci* 58:34–44
- Petersen H, Fleige H, Rabbel W, Horn R (2005) Applicability of geophysical prospecting methods for mapping soil compaction variability of soil texture on farm land. *J Plant Nutr Soil Sci* 168:68–79
- Peth S, Horn R, Fazekas O, Richards BG (2006) Heavy soil loading its consequence for soil structure, strength, deformation of arable soils. *J Plant Nutr Soil Sci* 169:775–783
- Peth S, Nellesen J, Fischer G, Horn R (2010) Non-invasive 3D analysis of local soil deformation under mechanical and hydraulic stresses by μ CT and digital image correlation. *Soil Tillage Res* 111:3–18
- Pulido-Moncada M, Munkholm LJ (2019) Limiting water range: a case study for compacted subsoils. *Soil Sci Soc Am J* 84:982–992
- Pulido-Moncada M, Munkholm LJ, Schjøning P (2019) Wheel load, repeated wheeling, and traction effects on subsoil compaction in northern Europe. *Soil Tillage Res* 186:300–309
- Raper RL (1999) Site-specific tillage for site-specific compaction: is there a need? In: *Proceedings of the*

- international conference on dryland conservation/zone Tillage, China Agriculture University, Beijing, China, pp 66–68
- Raper RL, Johnson CE, Bailey AC, Burt EC, Block WA (1995) Prediction of soil stress beneath a rigid wheel. *J Agric Eng Res* 61:57–62
- Raper RL, Schwab EB, Dabney SM (2005) Measurement and variation of site-specific hardpans for silty upland soils in the Southeastern United States. *Soil Tillage Res* 84:7–17
- Reichert JM, Mentges MI, Rodrigues MF, Cavalli JP, Awe GO, Mentges LR (2018) Compressibility and elasticity of subtropical no-till soils varying in granulometry organic matter, bulk density and moisture. *Catena* 165:13–357
- Richards BG, Baumgartl T, Horn R, Gräse W (1997) Modelling the effects of repeated wheel loads on soil profiles. *Int Agrophys* 11:177–187
- Richards BG, Peth S (2009) Modelling soil physical behaviour with particular reference to soil science. *Soil Tillage Res* 102:216–224
- Rogger M, Agnoletti M, Alaoui A, Bathurst JC, Bodner G, Borga M, Chaplot V, Gallart F, Glatzel G, Hall J, Holden J, Holko L, Horn R, Kiss A, Kohnová S, Leitingner G, Lennartz B, Parajka J, Perdigão R PS, Plavcová L, Quinton JN RM, Salinas JL, Santoro A, Szolgay J, Tron S, van den Akker JH, Viglione A, Blöschl G (2017) Land use change impacts on floods at the catchment scale: challenges and opportunities for future research. *Water Resour Res* 53:5209–5219. <https://doi.org/10.1002/2017WR020723>
- Romero-Ruiz A, Linde N, Keller T, Or D (2018) A review of geophysical methods for soil structure characterization. *Rev Geophys* 56:672–697
- Rosine TN, Sabbagh TT (2015) The impact of the diameter to height ratio on the compressibility parameters of saturated fine-grained soils. *IJERT* 4:8–19
- Rossi R, Amato M, Pollice A, Bitella G, Gomes JJ, Bochicchio R, Baronti S (2013) Electrical resistivity tomography to detect the effects of tillage in a soil with a variable rock fragment content. *Eur J Soil Sci* 64:239–248
- Sabba N, Uyanik O (2017) Prediction of reinforced concrete strength by ultrasonic velocities. *J Appl Geophys* 141:13–23
- Saffih-Hdadi K, Defossez P, Richard G, Cui YJ, Tang AM, Chaplain VA (2009) Method for predicting soil susceptibility to the compaction of surface layers as a function of water content and bulk density. *Soil Tillage Res* 105:96–103
- Schäffer B, Stauber M, Mueller TL, Müller R, Schulin R (2008) Soil and macro-pores under uniaxial compression. I. Mechanical stability of repacked soil and deformation of different types of macro-pores. *Geoderma* 146:183–191
- Schäffer B, Stauber M, Müller R, Schulin R (2007) Changes in the macro-pore structure of restored soil caused by compaction beneath heavy agricultural machinery: a morphometric study. *Eur J Soil Sci* 58:1062–1073
- Schjønning P, Lamandé M (2018) Models for prediction of soil precompression stress from readily available soil properties. *Geoderma* 320:115–125
- Schjønning P, Lamandé M, Berisso FE, Simojoki A, Alakukku L, Andreasen RR (2013) Gas diffusion, non-Darcy air permeability and CT images of a clay subsoil affected by compaction. *Soil Sci Soc Am J* 77:1977–1990
- Schjønning P, Lamandé M, Munkholm LJ, Lyngvig HS, Nielsen JA (2016) Soil precompression stress, penetration resistance and crop yields in relation to differently-trafficked, temperate-region sandy loam soils. *Soil Tillage Res* 163:298–308
- Schjønning P, Lamandé M, Tøgersen FA, Arvidsson J, Keller T (2008) Modelling effects of tyre inflation pressure on the stress distribution near the soil-tyre interface. *Biosyst Eng* 99:119–133
- Schjønning P, Stettler M, Keller T, Lassen P, Lamandé M (2015a) Predicted tyre-soil interface area and vertical stress distribution based on loading characteristics. *Soil Tillage Res* 152:52–66
- Schjønning P, van den Akker JH, Keller T, Greve MH, Lamandé M, Simojoki A, Stettler M, Arvidsson J, Breuning-Madsen H (2015b) Driver-Pressure-State-Impact-Response (DPSIR) analysis and risk assessment for soil compaction—a European perspective. *Adv Agron* 133:183–237
- Schlüter S, Vogel HJ (2016) Analysis of soil structure turnover with garnet particles and X-ray microtomography. *PLoS One* 11:e0159948
- Severiano EC, Oliveira GC, Dias Junior MS, Curi N, Costa KAP, Carducci CE (2013) Preconsolidation pressure, soil water retention characteristics, and texture of Latosols in the Brazilian Cerrado. *Soil Res* 51:193–202
- Simojoki A, Fazekas-Becker O, Horn R (2008) Macro- and microscale gaseous diffusion in a Stagnic Luvisol as affected by compaction and reduced tillage. *Agric Food Sci* 17:252–264
- Simojoki A, Jaakola A, Alakukku L (1991) Effect of compaction on soil air in a pot experiment and in the field. *Soil Tillage Res* 19:175–186
- Sitaula BK, Hansen S, Sitaula JIB, Bakken LR (2000) Effect of soil compaction on N₂O emission in agricultural soil. *Chemosphere Glob Change Sci* 2:367–371
- Smith W, Peng H (2013) Modeling of wheel-soil interaction over rough terrain using the discrete element method. *J Terramech* 50:277–287
- Socco LV, Foti S, Boiero D (2010) Surface-wave analysis for building near-surface velocity models—established approaches and new perspectives. *Geophysics* 75:75A83–75A102
- Söhne W (1953) Druckverteilung im Boden und Bodenformung unter Schlepperreifen (Pressure distribution in the soil and soil deformation under tractor tyres). *Grundl Land Technik* 5:49–63

- Srinivasan A (2006) Handbook of precision agriculture: principles and applications. Food products press®. An imprint of the Haworth press, Inc., 10 Alice Street, Binghamton, NY, 13904-1580
- Stettler M, Keller T, Schjønning P, Lamandé M, Lassen P, Pedersen J, Weisskopf P (2014) Terranimo®—a web-based tool for evaluating soil compaction. *Landtechnik* 69:132–138
- Sun Y, Ma D, Schulze Lammers P, Schmittmann O, Rose M (2006) On-the-go measurement of soil water content and mechanical resistance by a combined horizontal penetrometer. *Soil Tillage Res* 86:209–217
- Taina IA, Heck RJ, Elliot TR (2008) Application of X-ray computed tomography to soil science: a literature review. *Can J Soil Sci* 88:1–20
- Tarawally MA, Medina H, Frometa ME, Itza CA (2004) Field compaction at different soil-water status: effects on pore size distribution and soil water characteristics of a Rhodic Ferralsol in western Cuba. *Soil Tillage Res* 76:95–103
- Tate BL (2016) Soil texture determination by an acoustic cone penetrometer method. Master thesis, University of Illinois at Urbana-Champaign, USA
- Taylor HM, Brar GS (1991) Effect of compaction on root development. *Soil Tillage Res* 19:111–119
- Taylor HM, Gardner HR (1963) Penetration of cotton seedlings taproots as influenced by bulk density, moisture content and strength of soil. *Soil Sci* 96:153–156
- Tilman D, Fargione J, Wolff B, D'Antonio C, Dobson A, Howarth R, Schindler D, Schlesinger WH, Simmerloff D, Swackhamer D (2001) Forecasting agriculturally driven global environmental change. *Science* 292:281–284
- Unger PW, Kaspar TC (1994) Soil compaction and root growth: a review. *Agron J* 86:759–766
- Valentine TA, Hallett PA, Binnie K, Young MW, Squire GR, Hawes C, Bengough AG (2012) Soil strength and macropore volume limit root elongation rates in many UK agricultural soils. *Ann Bot* 110:259–270
- Vereecken H, Schnepf A, Hopmans JW, Javaux M, Or D, Roose T, Vanderborght T, Young MH, Amelung W, Aitkenhead M, Allison SD, Assouline S, Baveye P, Berli M, Brüggmann N, Finke P, Flury M, Gaiser T, Govers G, Ghezzehei T, Hallett P, Hendricks Franssen HJ, Heppell J, Horn R, Huisman JA, Jacques D, Jonard F, Kollet S, Lafolie F, Lamorski K, Leitner D, McBratney A, Minasny B, Montzka C, Nowak W, Pachepsky Y, Padarian J, Romano N, Roth K, Rothfuss Y, Rowe EC, Schwen A, Šimůnek J, Tiktak A, Van Dam J, van der Zee SEATM, Vogel HJ, Vrugt JA, Wöhling T, Young IM (2016) Modeling soil processes: review, key challenges, and new perspectives. *Vadose Zone J* 15:1–57
- Vogel H-J, Bartke S, Daedlow K, Helming K, Kögel-Knabner I, Lang B, Rabot E, Russell D, Stössel B, Weller U, Miesmeier M, Wollschläger U (2018) A systemic approach for modelling soil functions. *SOIL* 4:83–92
- Voivret C, Radjai F, Delenne J-Y, El Yousoufi MS (2009) Multiscale force networks in highly polydisperse granular media. *Phys Rev Lett* 102:178001
- Webb RH (2002) Recovery of severely compacted soils in the Mojave Desert, California, USA. *Arid Land Res Manag* 16:291–305
- Weiler WA, Kulhawy FH (1982) Factors affecting stress cell measurements in soil. *J Geotech Eng Div* 108:1529–1584
- Wheeler T, von Braun J (2013) Climate change impacts on global food security. *Science* 341:508–513
- Wolkowski RP (1990) Relationship between wheel-traffic-induced soil compaction, nutrient availability, and crop growth: a review. *J Prod Agric* 3:460–469
- Yunmin C, Han K, Ren-Peng C (2005) Correlation of shear wave velocity with liquefaction resistance based on laboratory tests. *Soil Dyn Earthq Eng* 25:461–469



Modeling of Field Traffic Intensity and Soil Compaction Risks in Agricultural Landscapes

14

Rainer Duttmann, Katja Augustin,
Joachim Brunotte, and Michael Kuhwald

Abstract

To mitigate the harmful effects of heavy vehicle traffic and high wheeling frequency knowledge about the susceptibility of a soil against soil compaction is indispensable. Given the highly variable nature of the load bearing capacity of a soil throughout a year, this paper presents a multidimensional approach to assess soil compaction risk at the field scale, considering the spatio-temporal

changes in soil strengths on the one hand side and the machinery-induced load and stress inputs on the other. At the example of two newly developed models, the field traffic model FiTraM and the spatially explicit soil compaction risk assessment model SaSCiA, this study assesses the actual soil compaction risk resulting from real field traffic activities during a complete season of silage maize cropping. For this purpose, we used GPS data recorded by all farm vehicles involved in tillage, spraying, and harvesting processes. GPS signal data served for the mapping of wheeling intensity and the calculation of the spatially distributed inputs of changing wheel load and contact area stress. These data were subsequently used for soil compaction risk modeling based upon readily available soil and weather data. Our model results indicate that nearly 95% of a field has been wheeled throughout the season, where harvest traffic at higher load contributes to more than the half of the totally wheeled area. Coupling the two models FiTraM and SaSCiA allows for estimating the spatially distributed soil compaction risk in the topsoil and the subsoil considering the single field operations. The results show that soil compaction risk varies greatly within individual fields. Thus, the need for analyzing and monitoring the effects of farm traffic on soil compaction at high spatial and temporal becomes obvious in order to sustain the diverse functions of soils.

R. Duttmann (✉) · K. Augustin · M. Kuhwald
Division of Physical Geography: Landscape Ecology
and Geoinformation Science, Department of
Geography, University of Kiel (CAU),
Ludewig-Meyn-Str. 8, 24098 Kiel, Germany
e-mail: duttmann@geographie.uni-kiel.de

K. Augustin
e-mail: augustin@geographie.uni-kiel.de

M. Kuhwald
e-mail: kuhwald@geographie.uni-kiel.de

R. Duttmann
Center for Geoinformation, University of Kiel
(CAU), Neufeldtstr. 10, Laurispark - Geb. 32, 24118
Kiel, Germany

J. Brunotte
Institute of Agricultural Technology, Johann
Heinrich von Thünen Institute, Bundesallee 50,
38116 Braunschweig, Germany
e-mail: joachim.brunotte@thuenen.de

Keywords

Spatial and temporal compaction · Field traffic models · Maize · Wheel load mapping

14.1 Introduction

Soil compaction is known as one of the main threats to soil fertility of farmland soils (FAO 2015). It negatively affects soil structure and the related physical, chemical and biological soil functions, resulting in a decline of natural soil productivity and an increase in soil erosion, surface run-off and greenhouse gas emission (Horn 1985; Alaoui et al. 2018). Moreover, soil compaction increases the operational costs including remediation and alleviation measures, and the environmental costs as well (Hamza and Andersson 2005; Chamen et al. 2015; Keller et al. 2017).

Jones et al. (2003) estimate that 36% of the European subsoils are highly susceptible to compaction, while other studies suggest 32% of the European soils to be prone to severe soil compaction (EC 2012). Recent work of Schjønning et al. (2015) assumes that a quarter of all European soils have been compacted. The main causes for the ongoing expansion of soil compaction on cropland are the increasing sizes and weights of farm machinery over the last decades on the one hand side and a non-site-adapted field traffic, which disregards the spatially and temporally varying changes in the load bearing capacity of the soil on the other. Assuming that the trend in machinery growth will continue unless technological innovation or a paradigm change take hold (Keller et al. 2017), a further increase of cropland soils affected by soil compactions may be suspected.

Already today certain farm operations, such as slurry spreading or harvesting, are outsourced to agricultural contracting companies. In many cases, their machinery is employed along pre-assigned operating plans, regardless the prevailing soil moisture conditions at the scheduled operation time. Extending this practice could

contribute to a further incline in soil compaction, independent of the predicted future changes in the amount and distribution of precipitation, which above all will shorten the time slots for heavy farm vehicle traffic in spring (slurry spreading) and fall (e.g., harvest of sugar beets and silage maize). This holds especially for temperate humid regions. As exemplarily shown by Rulfová et al. (2017) calculations for the area of the Czech Republic point to an increase in the mean amount of precipitation and in the rain intensity index (= mean precipitation amount of wet days) in spring and fall, while the number of wet days is supposed to decline in these seasons. However, it remains open, to what extent the reduced number of wet days will be overcompensated by a higher amount of precipitation and rainfall intensity and thus leading to longer lasting higher soil water content due to a reduced evapotranspiration in spring and fall.

Under moist soil conditions that typically occur at times of liquid manure application and the harvest of sugar beets and silage maize as well, the risk of topsoil and subsoil compaction increases strongly, because the external mechanical stresses applied by heavy farm vehicles exceed the internal strength of the soil (cf. Nevens and Reheul 2003; Peth et al. 2006). High wheel or axle load of farm machinery and wheeling intensity (e.g., wheeled area percentage and repeated wheel-to-wheel passages) substantially increase the risk of soils to irreversible soil deformation and subsoil compaction (Soane et al. 1982; Håkansson and Reeder 1994; Hamza and Andersson 2005). While the first pass of a farm vehicle mainly contributes to topsoil compaction (e.g., Botta et al. 2009), repeated wheeling at the same or even lower axles loads can affect the subsoil and finally result in persistent subsoil compaction (Berisso et al. 2012; Etana et al. 2013). The effects of multiple wheeling on stress propagation inside the soil and on the behavior of soil structure and soil physical functions have been intensely described by Horn (2003), Alakukku et al. (2003), Botta et al. (2009), Tolon-Becerra et al. (2010), Lamandé and Schjønning (2011) and Schjønning et al. (2016).

Modern farm vehicles like bunker harvesters for sugar beets and implements like slurry spreaders can reach load weights of 60 Mg and wheel loads exceeding 10 Mg (Schjønning et al. 2015, 2016). With respect to subsoil compaction wheel loads >50 kN (~5 Mg) are classified as 'high' by the International Working Group on subsoil compaction (van den Akker et al. 2003). Diserens (2009) stated that axle loads >10 Mg result in severe soil compaction.

In order to calculate the machinery-induced stress input and stress propagation inside the soil, a number of models has been developed (e.g., Horn and Fleige 2003; Keller et al. 2007, 2015; Schjønning et al. 2008, 2015; Diserens 2009; Rücknagel et al. 2015). However, the application of these models does not consider the spatial distribution of wheel tracks and wheel track patterns and the variation of loads and stresses exerted to soil during the individual field management operations. To precisely map the machinery-related driving forces of soil compaction inside of a field, positional data collected by vehicle-mounted Global Navigation Satellite System (GNSS) technology, such as dGPS or RTK-(real time kinematic) GPS receivers can be applied and used as input data for field traffic modeling and soil compaction risk assessment.

To-date, only a limited number of studies focus on the spatially distributed modeling of field traffic activities and intensities by using this geo-data source. Based on differential GPS data, Grisso et al. (2004) estimated field efficiency from traffic patterns for planting and harvesting operations of soybean and corn production systems. Yule et al. (1999), Richards (2000), and Kroulík et al. (2009) applied GPS data to map vehicle movement and traffic intensity. To assess on-road and in-field transportation effort during silage maize harvest and to map the vehicle-specific loads and ground contact stresses exerted to soil through harvest traffic, Duttman et al. (2013a, b) developed a modeling approach, which considers the tracked GPS positions of the operating machinery and its construction characteristics (e.g., masses, axle widths, tire sizes) as

well. Based on this model, Duttman et al. (2014) simulated the spatially varying soil stress and compaction risk beneath the individual tyre tracks using the pre-compression stress approach developed by Horn and Fleige (2003). This finally enabled to construct a three-dimensional soil model that displays the compaction risk at different soil depths. In a more recent work, Augustin et al. (2019) developed the field traffic model FiTraM, which automatically calculates the spatial distribution of wheel tracks and field traffic intensities from GPS signal and machinery data. This model also calculates the dynamic changes in wheel load and contact area stress during individual field management operations (e.g., ploughing, spraying, harvesting). Because of these capabilities it can form the basis to further evaluate the compaction risk inside of a field at a given field traffic event, by coupling the FiTraM with the soil compaction risk assessment model (SaSCiA) developed by Kuhwald et al. (2018). The latter model calculates soil compaction risks for different soil depths considering the moisture-dependent variation of soil strengths at daily resolution. The combination of both models enables to estimate the trafficability of a field and thus can support to decision-making due to a more sustainable traffic management of cropland soils.

This study gives an example of the combined use of the FiTraM and the SaSCiA model in order to predict the spatially and temporally varying soil compaction risk under real land use. It aims at

- (I.) quantifying and mapping of field traffic intensity during silage maize cropping cycle by using (i.) the wheel track area, (ii.) the area percentage of the summarized inputs of wheel load and contact area stress, and (iii.) the area percentage of repeatedly wheeled ground area as indicators, and
- (II.) calculating and assessing the trafficability of a field against the background of the actual soil compaction risk, considering the moisture-dependent changes in soil strength in the top soil and the subsoil.

14.2 Materials and Methods

The modeling of field traffic intensity and the field's trafficability has been performed for the study site 'Adenstedt' of the SOILAssist-Project (www.soilassist.de). This project is part of the German research program 'BonaRes—soil as a sustainable resource for the bioeconomy' (www.bonares.de) funded by the Federal Ministry of Education and Research (BMBF).

The study site 'Adenstedt' (52°00'30" N, 9° 56'15" E) is located 25 km south of the city of Hildesheim and situated in the central part of the Lower Saxon Hill Country (Germany). Mean annual temperature in this region is about 9.4 °C (DWD 2017, weather station Hildesheim), the annual precipitation sum amount to 741 mm. Soils in this area are mainly derived from deeply weathered loess and dominated by Luvisols and stagnic Luvisols (FAO 2014). They consist of medium to strong clayey silt and organic matter contents of about 2% in the A-horizon. While these soils provide high fertility and productivity, they are highly prone to soil compaction under wet conditions, especially when trafficked with high vehicle load. Common crop rotations in this area comprise sugar beet (*Beta vulgaris* L.), winter wheat (*Triticum aestivum* L.), and winter barley (*Hordeum vulgare* L.). Currently, the cropping of silage maize (*Zea mays* L.) for bio-gas production has become of increasing importance, substituting for crops such as winter barley and sugar beets at a progressive rate. On the average, silage maize realizes a yield of about 55 Mg (fresh mass) per hectare between 2011 and 2016 (LSN 2017) in this area.

14.2.1 Experimental Approach of This Study

As shown by Duttmann et al. (2013a; b), a single silage maize harvest can affect up to 63% of a field through wheeling. This applies especially for field traffic activities optimized under the constraints of operating time, labor time and machine efficiency only, regardless the negative

effects of multiple wheeling and high wheel loads. In order to analyze to what extent these effects might be reduced not only for harvest traffic, but all typical traffic operations conducted during a silage maize growing season, our research design is founded on the following advisements:

1. field traffic activities at the various farm operations (primary and secondary tillage, spraying, harvest, mulching of maize stubbles) aim at minimizing the area percentage affected by wheeling,
2. field traffic should be directed along previously formed wheel ruts, although the different axle width, working width and sizes of the vehicles hinder a fully overlap of all the wheel tracks, and thus an application of a true controlled traffic farming (CTF) system (e.g., Taylor, 1983; Tullberg et al. 2018),
3. field traffic at harvest is limited to only one harvester and one transport vehicle operating in the field at one time. Empty transport vehicles remain at the field border until loading and follow the paths of the previous vehicles or the harvester, respectively.

Using these specifications, we expect to portray a more optimized arrangement of field traffic adapted to silage maize cropping under a typical regional setting of machinery, tillage conditions, and farm traffic operations. The study has been conducted in 2016 on a 5.5 ha field with rectangular field borders (Fig. 14.3). A detailed description of this site is given by Kuhwald et al. (2016, 2017). Silage maize was drilled with a 6-row seeder at a distance of 75 cm between the single seed rows.

All traffic activities and vehicle movements inside the field were recorded by on-board RTK-GPS- (Trimble) or vehicle-mounted dGPS-receivers (Leica Viva CS10) located on the towing vehicles and on the silage maize harvester. The registered GPS signal data provide a high positional accuracy with an error less than 2.5 cm in horizontal direction under optimal use (Augustin et al. 2019). GPS data were registered continuously at a time interval of 1 s. The

technical characteristics of the machinery employed during the silage maize growing season are shown in Table 14.1. Table 14.2 gives a brief overview of the tillage, maintenance, and harvest operations applied within this study.

14.2.2 Modeling of Field Traffic and Traffic Operations

To spatially represent traffic intensity of agricultural machinery inside a field, the modeling system FiTraM (Augustin et al. 2019) has been applied. Based on RTK-GPS- or dGPS data and a machinery data base that contains the technical properties of common machinery used in the study region so far, this model enables the (re)-construction of the courses and sizes of the wheel tracks put on soil during the individual farm operations.

Moreover it allows to compute the changes in vehicle mass (e.g., during loading or deloading processes) including the changes in wheel load and ground contact stress separated for every single wheel moving along a path. In detail, the modeling routines established in FiTraM comprise the representation of several work processes such as ploughing, mulching, sowing, spraying, and harvesting, including

- forward movements of tractors with lifted implements (e.g., plough, sowing machine, sprayer),
- backward movements of a tractor (reversing) with lifted implements, and
- forward movements of tractors with lowered implements.

The field traffic model (FiTraM) is programmed in Python and uses various packages (e.g., fiona, shapely and gdal) to reconstruct the wheel tracks. The application is connected to a PostgreSQL database, which stores the technical data of the machinery.

Figure 14.1 shows the principle set up of FiTraM and the major steps in data processing. A detailed documentation of FiTraM is given by Augustin et al. (2019).

14.2.3 Modeling the Actual Soil Compaction Risk Due to Real Field Traffic Activities

Calculation of the spatially and temporally varying soil compaction risk considering the real technical settings and labor days of the machinery, the actual states of soil moisture and dependent soil strengths at different soil depths has been performed by using the spatially explicit soil compaction risk assessment model SaSCiA (Kuhwald et al. 2018). This model generates maps of the daily varying soil compaction risk at different depths of the soil up to 2 m, separated into intervals of 10 cm. Along with the spatial representation it provides look-up tables that summarize the soil compaction risk in forms of area statistics.

The SaSCiA model is technically realized in ‘R’ (version 3.3.1, R Core Team 2017) using the packages ‘plyr’ (Wickham 2011), ‘sp’ (Pebesma and Bivand 2005; Bivand et al. 2013), ‘raster’ (Hijmans 2016), and ‘rgdal’ (Bivand et al. 2016). Its schematic structure is illustrated in Fig. 14.2. The model consists of three core components to calculate the dynamic changes in the load bearing capacity of the soil, the soil strength, respectively,

1. modeling of the soil water content at daily intervals and different soil depths using the MONICA model (Nendel et al. 2011),
2. calculation of the actual soil strength based on the pre-compression stress approach according to Horn and Fleige (2003), implemented in SaSCiA in the modified and enhanced approach of Rücknagel et al. (2012, 2013) in order to consider the changes in soil strength at various soil water contents, and
3. estimation of soil stress at different soil depths following the approaches from Koolen et al. (1992) and Rücknagel et al. (2015).

In this study, soil moisture was continuously measured over the growing season at 24 sites and two depths (20 and 40 cm) with PlantCare-soil-sensors. These moisture data were used as input

Table 14.1 Technical data of the vehicles operated during the maize growing season

Work process	Vehicle	Axle	Mass ^a (unloaded) [Mg]	Mass ^b (loaded) [Mg]	Axle width [m]	Tyre dimension	Inflation pressure [kPa]	Working width [m]
Primary tillage	New Holland (NH) T7.270 + Lemken Opal 160	Front	4.56	3.08	2.02	600/70R30	90	2.9
		Rear	5.02	8.32	2.05	710/70R42	90	
Fertilizing	NH M160 + Amazone ZAM 1200	Front	2.64	1.66	1.95	540/65R28	120	27
		Rear	4.24	6.72	1.95	650/65R38	110	
Secondary tillage	NH T7.270 + Kongskilde Germinator	Front	3.86	3.3	2.02	600/70R30	70	5.4
		Rear	5.12	6.92	2.05	710/70R42	70	
Sowing	Deutz-Fahr Agrotion M625 + Gaspardo MTE-R	Implement	4.12	2.46	2.60	380/55-17	130	4.5
		Front	2.76	2.76	1.94	540/65R28	170	
		Rear	4.70	5.38	1.84	650/65R38	170	
		Implement	1.80	2.78	1.6	7.50-16	70	
Spraying (pesticides)	Lamborghini R6.150 + Rau 2500	Front	1.25	1.18	1.94	AC65 540/65R28	250	27
		Rear	1.94	2.24	1.83	AC85 520/85R38	180	
Harvest (cutting)	NH Forage Cruiser FR550	Implement	0.98	1.95	1.91	9.-42	300	6
		Front	14.22	-	2.50	800/70R38	170	
		Rear	5.38	-	2.66	600/65R28 IMP AC65	140	
		Implement	14.22	-	2.50	800/70R38	170	
Harvest (transport)	NH T7.270 + Joskin Drakkar 7600	Front	4.33	4.16	2.02	600/70R30	110	-
		Rear	5.78	7.63	2.05	710/70R42	110	
		Trailer front	3.95	10.13	2.26	750/45R26.5	220	
		Trailer rear	4.08	10.21	2.26			
Mulching	NH M160 + Agrimaster RV 2800 + Muething MU-M/S 220	Front	2.72	3.45	1.95	540/65R28	120	2.8
		Rear	4.80	5.68	1.95	650/65R38	110	

^a Axle mass of tractors with lowered implements as used for primary tillage, ^b axle mass of tractors with lifted implements

Table 14.2 Actual dates of work processes due to silage maize growing in 2016

Day	Month	Year	Work process	Machine
22	April	2016	Primary tillage	NH T7.270 + Lemken Opal 160
22		2016	Fertilizing ^a	NH M160 + Amazone ZAM 1200 ^a
22		2016	Secondary tillage	NH T7.270 + Kongskilde Germinator
23		2016	Sowing	Deutz-Fahr Agrottron M625 + Gaspardo MTE-R
21	May	2016	Spraying	Lamborghini R6.150 + Rau 2500
27	September	2016	Harvest (cutting)	NH Forage Cruiser FR550
27		2016	Harvest (transport)	NH T7.270 + Joskin Drakkar 7600
27		2016	Mulching	NH M160 + Agrimaster RV 2800 + Muething MU-M/S 220

^a This work process has not been recorded because of a technical failure

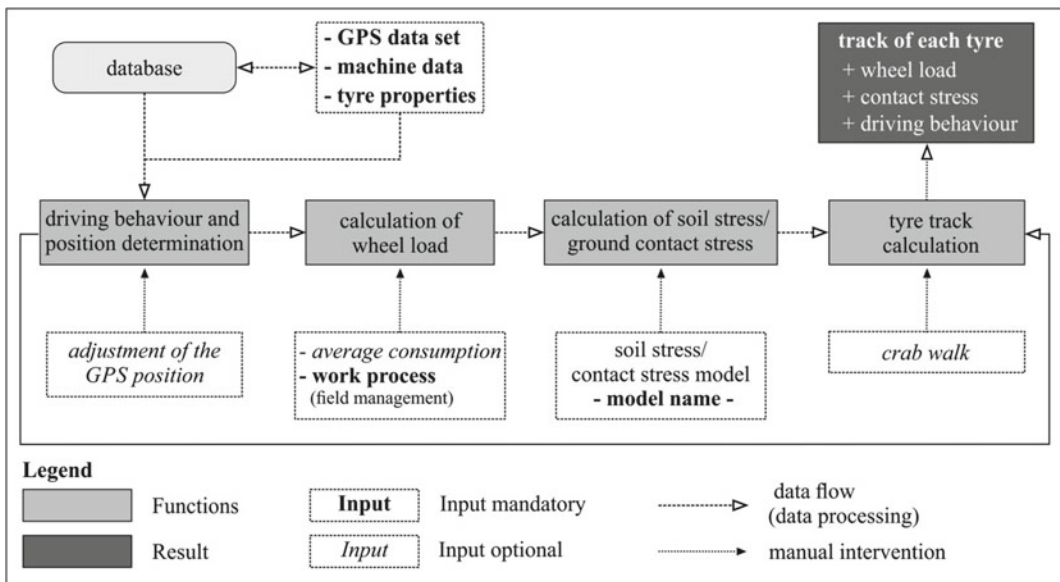


Fig. 14.1 Schematic structure and general work processes of the field traffic model FiTraM (according to Augustin et al. 2019, simplified)

data for SaSCiA, so that the MONICA model has not been applied here.

As the major result, SaSCiA calculates the ‘Soil Compaction Index’ (SCI)-numbers according to Rücknagel et al. (2015). The SCI expresses the difference between the logarithm of soil stress (log kPa) and the logarithm of soil strength (log kPa) at the individual soil depths. Table 14.3 shows the ranking of the SCI numbers in forms of classes of different soil compaction risks (cf. Rücknagel et al. 2015; Götze et al. 2016). A full

model description and documentation of SaSCiA is given by Kuhwald et al. 2018.

14.2.4 Data

Soil data used for compaction risk modeling were taken from a field scale soil map, constructed by Kuhwald (2019). Soil data include a quantitative description of the following soil properties in horizontal and vertical

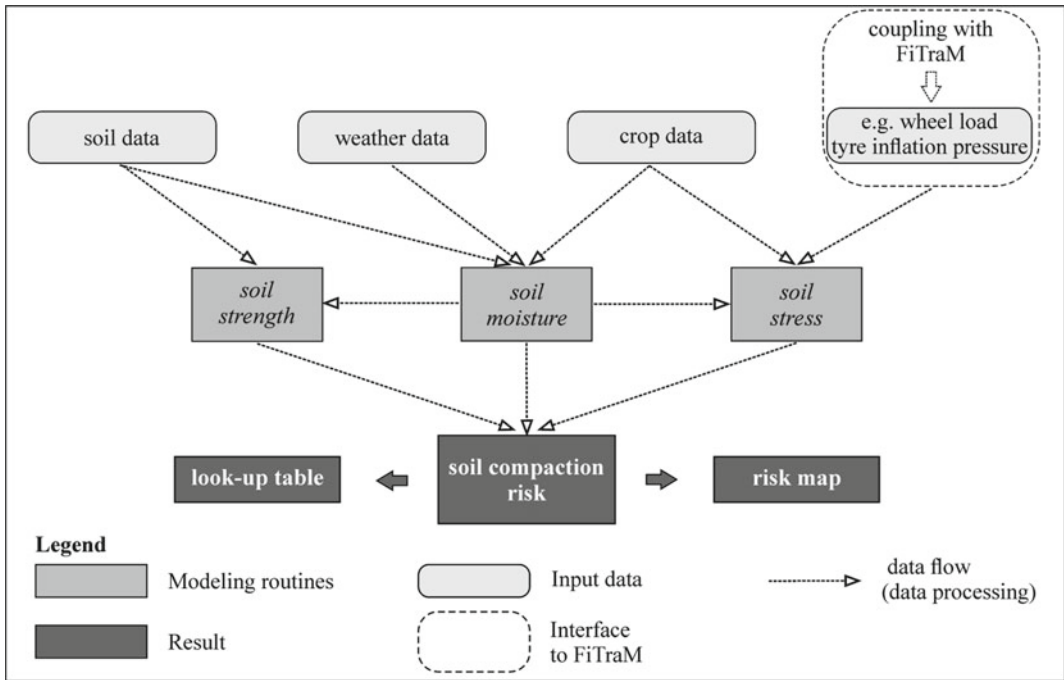


Fig. 14.2 Principle structure of the spatially explicit soil compaction risk assessment model SaSCiA (according to Kuhwald et al. 2018, simplified)

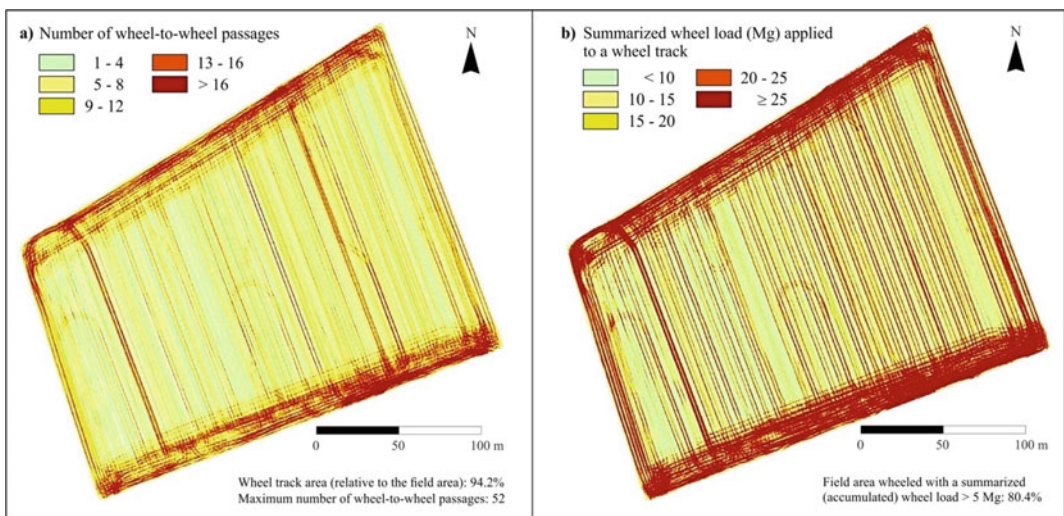


Fig. 14.3 Modeled patterns of wheel-to-wheel passages (a) and spatial distribution of accumulated wheel load (b) applied to soil throughout a complete silage maize growing season (without fertilizing)

differentiation: soil texture class, organic carbon content, air-dry bulk density, aggregate structure, water capacity, and available water capacity (cf. Kuhwald et al. 2018). Information about crop

cultivation and the dates of the single farm operations like tillage, sowing, spraying, and harvest were extracted from the field register of the collaborating farmer (Table 14.2). The same

Table 14.3 Classification of the soil compaction index (SCI) (Rücknagel et al 2015; Götze et al. 2016)

SCI (log kPa)	Soil compaction risk
≤ 0	No risk
0–0.1	Low
0.1–0.2	Medium
0.2–0.3	High
0.3–0.4	Very high
>0.4	Extremely high

holds for the machinery data (cf. Table 14.1). Weather data at a daily basis (amount of precipitation, air temperature, relative humidity, and sunshine duration) were received from the German Weather Service (DWD) (Climate Data Center, DWD 2019) for the next neighbored weather Station ‘Alfeld’.

14.3 Results and Discussion

14.3.1 Spatial Modeling of Wheel Track Patterns and Field Traffic Intensity

Recent development in on-board navigation technology and in geo-spatial modeling as well offers powerful instruments to design strategies to optimize field traffic and to mitigate the effects of harmful soil compaction. An example of the combined use of GNSS data and spatial modeling to calculate field traffic intensity and to quantify the stress input into soil is shown in Fig. 14.3. Based on the FiTraM results, this figure presents the spatial patterns of field traffic resulting from all vehicle movements inside the field throughout the complete maize growing season. To assess field traffic intensity, we used the percentage of wheeled area related to the field size, the number of wheel-to-wheel passages and the summarized wheel loads along a wheel path as indicators. Although field traffic in this study followed an area saving strategy with driving in previously formed ruts as much as possible, it shows that nearly all the field area has been affected by wheeling. On average 94.2% of the field has been wheeled in the minimum once

(Table 14.4). Highest wheeling density and number of repeatedly trafficked wheel paths were detected in the headland sections and in an area close the field gate (cf. Fig. 14.3), lower right corner). In detail, more than 98% of the headland sections have been ‘consumed’ through repeated traffic activities, like turning maneuvers during tillage operations and transportation traffic during harvest wheeling (cf. Duttmann et al. 2013a, b, 2014). But even in the inner field the percentage of the wheeled area amount to more than 92% related to the complete field. The contribution of the single work processes to the overall wheel track area is specified in Table 14.4. For primary tillage (cultivator) it shows that 59% of the field area is subject to wheeling, while maize harvest and the transportation of maize take up to 54.9% of the field area (Figs. 14.4 and 14.5).

Compared to primary tillage, harvest and transport operations reveal a noticeably higher area percentage of repeatedly trafficked wheel paths and a significantly larger share and number of multiple wheel passages of highest load inputs (Table 14.4).

As demonstrated in Fig. 3b, the patterns of summarized wheel load give a clear indication of those field sections that are mainly affected by multiple wheel-to-wheel passages at high load. Among the aforementioned headland and field gate sections, the paths directed from the field entrance to the opposite field border were found to be the hot spots of highest wheeling intensity, because the empty transporters were directed along that route to approach to the harvester’s position. Calculations show that ca. 34% of the complete field has been wheeled more than four times only through harvest traffic (Table 14.4; cf.

Table 14.4 Wheel track area and number of wheel passages during a silage maize growing season including all field work processes

Work process	Wheel track area (%)			Area affected by >4 wheel passages (%)	Max. number of wheel-to-wheel passages
	Inner field	Headlands	Complete field		
Primary tillage	54.5	71.8	59.0	5.5	21
Secondary tillage	29.0	54.0	46.1	4.6	22
Sowing	31.2	49.0	35.8	0.9	13
Spraying	5.0	8.8	6.0	0.4	8
Harvest (forage harvester)	29.0	54.0	35.4	0.8	14
Harvest (transport of harvest goods)	34.1	74.6	44.6	14.4	42
<i>Complete harvest (cutting and transport)</i>	<i>44.2</i>	<i>85.9</i>	<i>54.9</i>	<i>34.2</i>	<i>44</i>
Mulching (maize stubbles)	29.5	49.7	34.7	1.4	13
All work processes	92.6	98.4	94.2	76.3	52

Figs. 14.4 and 14.5). In total, approximately 80% of the field area got an accumulated load input >5 Mg throughout the season, where more than 28% of the field received summarized wheel loads >25 Mg. During harvest 51.5% of the field got an accumulated wheel load input of >5 Mg (Fig. 14.5). In contrast to many other farms in this region, a slurry tanker has not been employed for fertilizing because of farm management decisions. Considering the widespread use of modern slurry tankers as it is common today, a further increase in wheel area percentage and wheel-to-wheel passages at high load could be expected.

Repeated wheeling at the same or a higher load increases the risk of soil compaction. According to van den Akker et al. (2003), wheel loads >50 kN (~5 Mg) are assumed to have high impact on subsoil compaction. Calculations in this study prove that the wheel load accumulated over the growing season is far beyond this threshold value, covering more than three fourths of the entire field area (Fig. 4b; Table 14.4). However, these numbers represent the sum of load input of all wheeling actions and do not account for a potential recovery of soil structure between the single dates of load input. On the

other side, it is known that multiple wheeling even with low axle load can lead to subsoil compaction under corresponding conditions (Hamza and Andersson 2005). Botta et al. (1999, 2009) reported that repeated traffic >5 passes of a tractor with axle loads <30 kN induces subsoil compaction, while up to the fifth wheel passage ground contact stress mainly contributes to topsoil compaction. For a Luvisol comparable to the soil of our study site, Zink et al. (2011) demonstrated that 10 passes at wheel loads of about 6.3 Mg (tire inflation pressure 250 kPa) and 7.5 Mg (tire inflation pressure 350 kPa) resulted in a strong decline in air capacity up to a depth of 60 cm and in a decline in the topsoil's saturated hydraulic conductivity. Following these findings, we suggest that the summarized (accumulated) wheel loads calculated by FiTraM support to identifying areas of an increased susceptibility to subsoil compaction.

However, our model results also indicate that even when following the rules of good agricultural practice in field management (e.g., Brunotte and Fröba 2007) as in this study, a further reduction of traffic intensity during maize is limited by the given machinery outfit.

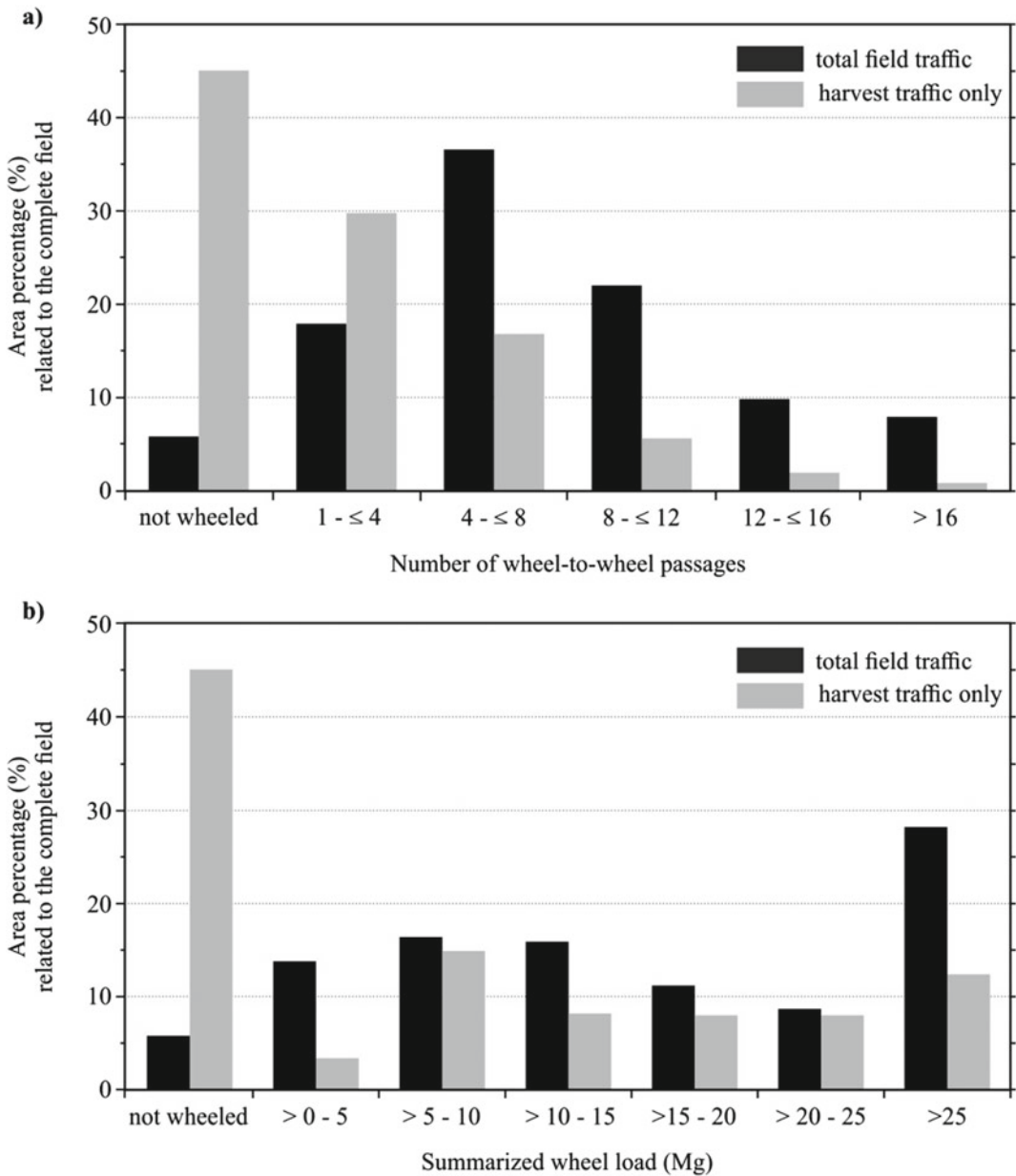


Fig. 14.4 Area percentage of the number of wheel-to-wheel-passages (a) and summarized wheel load inputs (b) throughout a complete silage maize growing season (without fertilizing), separated into total field traffic (dark grey) and harvest traffic (cutting and transportation) only (light grey)

Compared to other studies on silage maize harvest traffic from Duttmann et al. (2013b, c), who observed the effects of a field traffic strategy that splits the tracks of the transport vehicles from those of the forage harvester (driving on parallel routes) the reduction of the

wheeled area seems small, but verifiable. Following an area saving traffic strategy, we found a decrease in the wheeled area percentage between 1 and 9%, depending on the size and shape of a field and the vehicle properties.

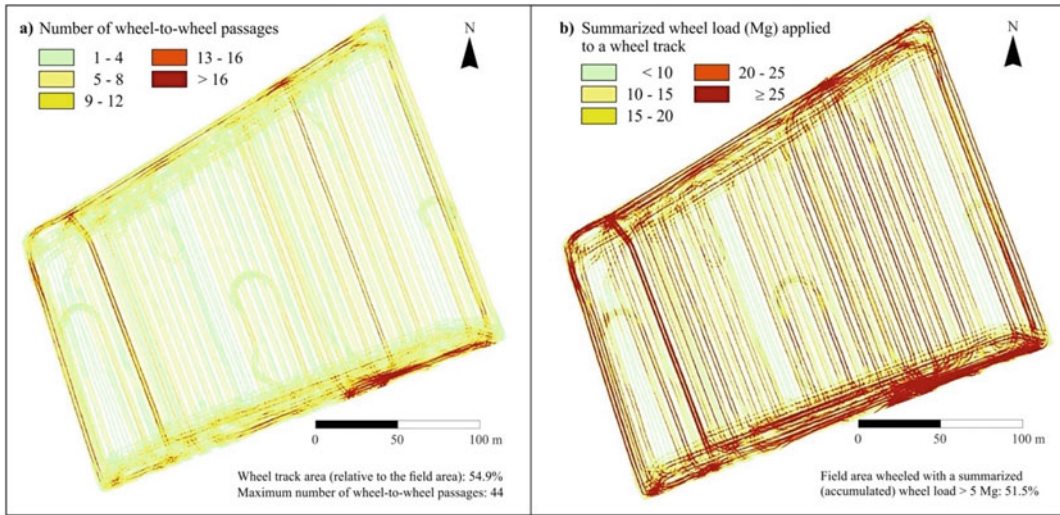


Fig. 14.5 Modeled patterns of wheel-to-wheel passages (a) and spatial distribution of accumulated wheel load (b) applied to soil during silage maize harvest (cutting and transportation)

Because the machinery composition cannot be changed in the short term, future farm investment should focus on machinery settings that enable a stronger application of a controlled traffic farming (CTF) system as supposed by Tullberg (2010) and Tullberg et al. (2018) in order to avoid soil compaction by reducing the area affected by traffic.

14.3.2 Spatial Modeling of the Spatially and Temporally Varying Soil Compaction Risk Due to Real Machinery Operations

As long as the recent settings of farm machinery disenable a stronger reduction in field traffic intensity, the more the timing of field management operations with regard to the actual state of soil moisture and related soil strength becomes the decisive factor to minimize soil compaction. The moisture-dependent actual soil compaction risk can be predicted with the SaSCiA model (Kuhwald et al. 2018) at daily time steps. Thus, combining both models FiTraM and SaSCiA offers potential to a foresighted planning of field

traffic operations (if the vehicle paths are known prior to field work). The next paragraph demonstrates the interplay of these models to assessing the actual soil compaction risks due to the field traffic activities described above.

Soil compaction risk at a given date depends on the actual state of soil strength and the stresses applied to soil by farm machinery. Both parameters, soil strength and soil stress, are highly variable in their temporal and spatial distribution resulting in a day by day change of soil compaction risk. As demonstrated by Kuhwald et al. (2018) for larger regions, soil compaction risk dynamics and the spatial patterns of soil compaction risk can also be predicted for individual fields, if a model takes into account

- (i.) the wheel load changes during single field operations, which lead to continuously varying stress inputs by the machinery employed (cf. Fig. 5b) and
- (ii.) the daily varying state in soil strength, which depends on the spatial distribution of the physical soil characteristics, such as texture, structure, and actual moisture (Fig. 14.6).

Figure 14.7 exemplarily demonstrates the spatial and temporal variation of soil compaction

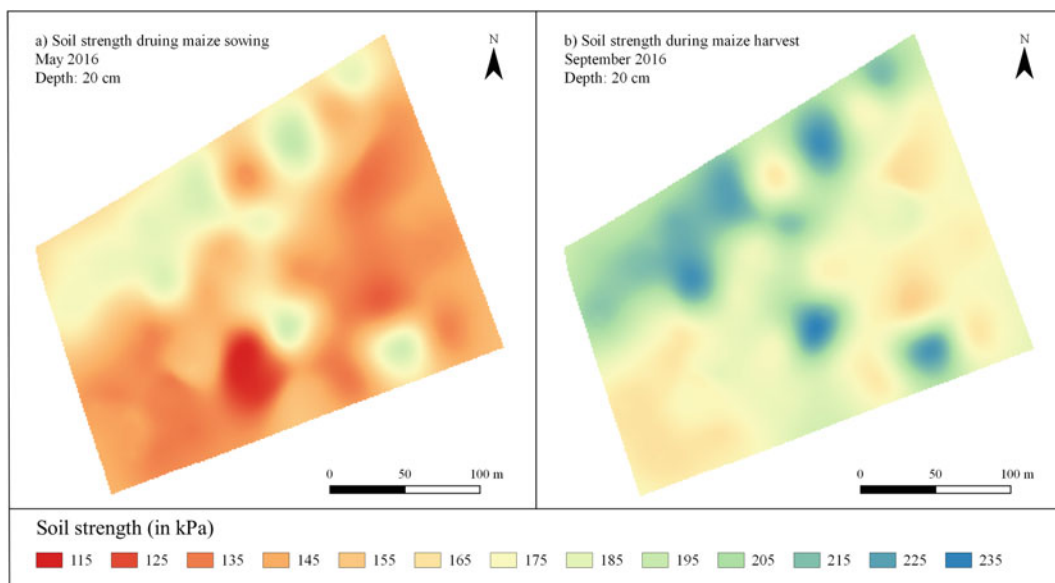


Fig. 14.6 Spatio-temporal variation of soil strength at a depth of 20 cm demonstrated for moist soil conditions (May, **a**) and for dryer soil conditions (September, **b**)

risk patterns modeled for two different states of soil moisture and two work processes (sowing and harvest of silage maize). While sowing in April 2016 was performed on relatively moist soils (water content: 25–29 vol%; cf. Table 14.5), silage maize harvest in September 2016 took place under comparatively dry soil conditions because of an untypical draught situation this summer. During maize sowing (Fig. 7a; Table 14.5) soil compaction risk of the topsoil (20 cm) varies between ‘no risk’ and ‘very high risk’, whereupon the ‘medium’ risk class covers about 23% of the trafficked field. Regarding the subsoil (depth 40 cm) less than 1.5% of the field area reveal ‘low’ to ‘medium’ risk, while the remaining part of the trafficked field does not show any compaction risk (Table 14.5).

As demonstrated in Fig. 7a, ‘high’ top soil compaction risks occur in the (southern) headlands, especially in the ruts of the turning vehicle. As soon as a turning maneuver is completed, compaction risk declines to a lower risk class because of the load changes of the rear axle. Lifting the sowing implement during the turning maneuver increases the wheel load of the rear axle (cf. Augustin et al. 2019), resulting in a

higher soil compaction risk in the headlands. The same process can be observed in the northern headlands, but at a smaller compaction risk class due to increased soil strength in this field section. In the inner field, no significant changes in wheel load occur. This suggests that the modeled patterns of soil compaction risk only result from varying soil strengths. Compared to harvest (Fig. 7b) the smaller area percentage of medium and high compaction risk explains through the lower mass of the machinery (Table 14.1) used for sowing, although the soil moisture was higher in spring.

The effects of decreasing soil moisture on the increase in load bearing capacity, especially in the subsoil, are summarized in Table 14.5. It reveals that the forage harvester and the transport vehicles that were operated at a soil moisture equal to 50% of the field capacity affect a larger area of increased compaction risk in the upper 20 cm, compared to sowing (cf. Table 14.5), while the subsoil (≥ 40 cm) was not affected through machinery stress inputs at all (Fig. 7b; Table 14.5).

Harvest of silage maize is assumed to be one of the major reasons for (sub)soil compaction

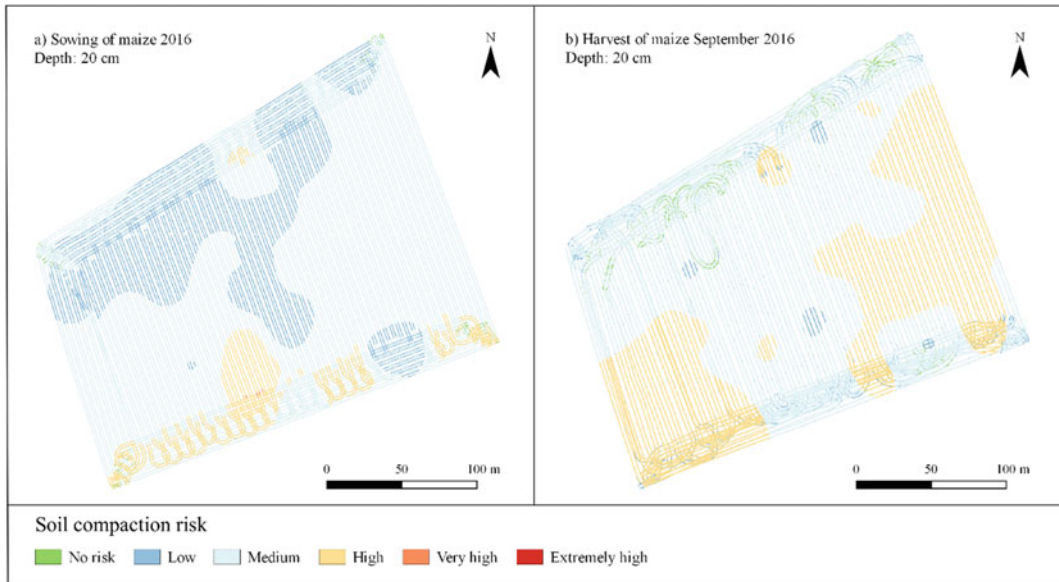


Fig. 14.7 Actual soil compaction risk modeled with SaSCiA for silage maize seeding (a) and harvest (b) in 2016

(Nevens and Reheul 2003; Peth et al. 2006). The present study, however, reveals relatively low soil compaction risk in the topsoil and no soil compaction risk in the subsoil during silage maize harvest. The apparent contradiction explains through the untypical meteorological conditions in 2016. While the amount of precipitation until June was in the same range as the long-term mean, the period from July to September was the driest since the last 10 years (DWD, weather station Alfeld). At harvest time, soil moisture was at 20.1 vol% in the top soil and at 19.3 vol% in the subsoil ($\sim pF$ 3.5). The desiccated soil provided high soil stability and strength (Fig. 6b), which finally better protected against the negative effects of heavy vehicle traffic as they are typical for silage maize harvest traffic in this region under average climate conditions (Duttmann et al. 2013a, 2014). This makes clear that a reliable assessment of soil compaction risk due to silage maize harvest needs to consider the actual state of soil moisture and related soil strength, while assessments using long-term averaged data on soil moisture and soil strength hide the considerable temporal and spatial variability of soil compaction risk and can lead to misinterpretation.

14.4 Synthesis

Coupling of both models FiTraM and SaSCiA supports to identifying and assessing soil compaction risks inside a field at high spatial resolution. The modeling results make clear that soil compaction risk varies noticeably across a single field, depending on the given soil conditions, especially on the distribution of soil texture and soil moisture, and on the work processes and machinery as well. Thus, disregarding the spatio-temporal changes of these variables can lead to misinterpretation of soil compaction risk when assigning a uniform risk class to the entire field. The heterogeneous distribution of soil stress and soil compaction risk inside of a field require new modeling approaches to enable a more realistic representation of field traffic activities and related compaction risks, changing from a two-dimensional perspective to a three-/four-dimensional view (e.g., Duttmann et al. 2014). A first modeling attempt based on readily available data and on empirical model approaches is presented in this study.

However, spatially differentiated modeling of machinery-induced load and stress inputs and the

Table 14.5 Area percentage of compaction risk in the topsoil (depth 20 cm) and in the subsoil (depth 40 cm) calculated for real dates of field management operations and machinery employed during a silage maize cropping season

Trafficked area (%) and soil compaction risk class (SCI) (%)	Soil depth (cm)	Field operations in 2016						
		Primary tillage	Secondary tillage	Sowing	Spraying	Harvester	Transportation	Mulching (maize stubbles)
Area not trafficked ^a		41.0	53.9	64.2	94.0	64.6	55.4	65.3
Area trafficked ^a		59.0	46.1	35.8	6.0	35.4	44.6	34.7
No risk	20	44.2	44.6	0.1	5.8	0.6	0.4	34.4
	40	56.7	44.9	34.1	5.8	36.4	44.3	34.3
Low risk	20	13.1	0.3	8.3	0.1	1.3	8.1	0.0
	40	0.7	0.0	1.2	0.1	0.0	0.0	0.0
Medium risk	20	<0.1	0.0	23.5	0.1	22.3	24.7	0.0
	40	0.0	0.0	<0.1	0.1	0.0	0.0	0.0
High risk	20	0.0	0.0	3.5	0.1	12.2	11.1	0.0
	40	0.0	0.0	0.0	0.1	0.0	0.0	0.0
Very high risk	20	0.0	0.0	<0.1	0.0	0.0	0.0	0.0
	40	0.0	0.0	0.0	0.0	0.0	0.0	0.0
Extremely high risk	20	0.0	0.0	0.0	0.0	0.0	0.0	0.0
	40	0.0	0.0	0.0	0.0	0.0	0.0	0.0
Summarized area of modeled SCI ^b	20	57.4	44.9	35.5	6.1	36.4	44.3	34.4
	40	57.4	44.9	35.5	6.1	36.4	44.3	34.4
Soil moisture	20	25.1 (±1.4)			24.2 (±1.4)	20.1 (±0.9)		
	40	26.9 (±2.3)			25.6 (±1.4)	19.3 (±1.0)		

^a Calculated with FiTraM (cf. Table 14.4)

^b Deviations in the area percentage of the trafficked area (according to FiTraM) and the summed area of the single soil compaction risk classes result from converting the line data (vector data) of calculated tyre tracks into raster data (cell size 5*5 cm) as used for deriving the SCI with SaSCiA

calculation of soil compaction risks at the scale of a field remain challenging. Limitations in applying the FiTraM have been intensely discussed by Augustin et al. (2019). Among others, restrictions refer to calculating the uneven distribution of wheel load, when driving cross or perpendicular to a slope, or when running in a furrow (cf. Alakukku et al. 2003; Nolting et al. 2011). Moreover, the recent version of FiTraM does not consider real biomass yield for calculating the wheel load changes during load processes at harvesting campaigns, but assumes a linear increase in wheel load between the start and end points of loading. Future studies will

have to test to what extent the use of ultra sonic sound sensors (e.g., Nolting et al. 2011) plugged to the tyres of self-propelled vehicles and wheeled implements as well may improve our modeling results. Besides, calculating soil compactions risk with SaSCiA is subjected to two major limitations. The first concerns the number of repeated wheel passages, because the current version of SaSCiA can only consider one wheel path. Negative effects of repeated wheeling which may result in harmful (sub) soil compaction (e.g., Canillas and Salokhe 2002; Botta et al. 2009) are not taken into account yet. The second limitation refers to the calculation of soil

stress. For modeling the soil stress SaSCiA actually uses an approach developed by Koolen et al. (1992), supplemented by a routine for concentration-factor calculation according to Rücknagel et al. (2015), requiring wheel loads and tyre inflation pressure as mandatory input data (cf. Kuhwald et al. 2018). In addition to wheel load and tire inflation pressure, soil stress depends on the contact area and the related contact area stress (e.g., Arvidsson and Keller 2007; Schjønning et al. 2012). Due to an optimized assessment of soil compaction risks, the integration of tyre sizes, contact area, and contact area stress into soil stress calculation routines will be subject of further studies.

14.5 Conclusions

Spatial modeling of field traffic intensity using positional data collected from vehicle-mounted GPS receivers connected with the design description data of the machinery enables a precise mapping of machinery load and stress inputs into soil. As shown at the example of the FiTraM it is possible not only to represent the vehicle paths and to identify the hot spots of load and stress inputs, but also to predict the changes in load and stress input beneath the single tyre tracks at a high spatial resolution. In this way, the main driving forces for soil compaction in arable soils can be quantitatively estimated in their spatially varying distribution. Transferring the calculated ground contact stress data into a soil compaction risk assessment model, like SaSCiA finally facilitates the prediction of compaction effects of individual traffic operations at given dates and different soil depths. Comparing the externally induced stresses against the load bearing capacity enables to deduce recommendations of the allowable load inputs under the actual soil conditions. Moreover, our models assist to sampling strategies for soil compaction monitoring at the field and landscape scales. They allow to exactly quantify the mechanical impact of farm machinery at every position inside

a trafficked field, which helps to select relevant measurement sites to observe the effects of field traffic on soil functions and on yield response over time. At the moment our compaction risk assessment model works upon (pre)registered GPS track data and thus, only gives information about past situations. In order to move from an 'ex post' to an 'ex ante' assessment of soil compaction risk and to use the aforementioned models as tools for field traffic planning prior to field operation, next steps will be to automatically predict the optimal courses for farm machinery. This includes the integration of existing algorithms to automated field traffic planning (e.g., Stock et al. 2016) based on given machinery properties and the involvement of actual weather forecast data.

Acknowledgements Funding of the project by the Federal Ministry of Education and Research (BMBF) within the BonaRes research initiative (Grant No. 031B0684C) is greatly acknowledged. The authors thank all members of the SOILAssist project team and the external partners for support.

References

- Alakukku L, Weisskopf P, Chamen WCT, Tijink FGJ, van der Linden JP, Pires S, Sommer C, Spoor G (2003) Prevention strategies for field traffic-induced subsoil compaction: a review: part 1 Machine/soil Interactions. *Soil Tillage Res* 73(1–2):14–160. [https://doi.org/10.1016/S0167-1987\(03\)00107-7](https://doi.org/10.1016/S0167-1987(03)00107-7)
- Alaoui A, Rogger M, Peth S, Blöschl G (2018) Does soil compaction increase floods? A review. *J Hydrol* 557:631–642. <https://doi.org/10.1016/j.jhydrol.2017.12.052>
- Arvidsson J, Keller T (2007) Soil stress as affected by wheel load and tyre inflation pressure. *Soil Tillage Res* 96(1–2):284–291. <https://doi.org/10.1016/j.still.2007.06.012>
- Augustin K, Kuhwald M, Brunotte J, Duttmann R (2019) FiTraM: A model for automated spatial analyses of wheel load, soil stress and wheel pass frequency at field scale. *Biosyst Eng* 180:108–120. <https://doi.org/10.1016/j.biosystemseng.2019.01.019>
- Berisso FE, Schjønning P, Keller T, Lamandé M, Etana A, de Jonge LW, Iversen BV, Arvidsson J, Forkman J (2012) Persistent effects of subsoil compaction on pore size distribution and gas transport in a

- loamy soil. *Soil Tillage Res* 122:42–51. <https://doi.org/10.1016/j.still.2012.02.005>
- Bivand RS, Pebesma EJ, Gomez-Rubio V (2013) *Applied spatial data analysis with r*, 2nd edn. Springer, New York. ISBN 978-1-4614-7618-4
- Bivand RS, Keitt T, Rowlingson B (2016) *rgdal: bindings for the geospatial data abstraction library*. R package version 1.1-10
- Botta GF, Jorajuria CD, Draghi TL (1999) Soil compaction during secondary tillage traffic. *Agro-Sciencia* 15:139–144
- Botta GF, Tolon-Beccerra A, Tourn FB (2009) Effect of the number of tractor passes on soil rut depth and compaction in two tillage regimes. *Soil Tillage Res* 103:381–386. <https://doi.org/10.1016/j.still.2008.12.002>
- Brunotte J, Fröba N (2007) Schlaggestaltung - kostensenkend und bodenschonend. KTBL-Schrift 460, Darmstadt, Germany
- Canillas EC, Salokhe VM (2002) Modeling compaction in agricultural soils. *Soil Tillage Res* 65(2):221–230. [https://doi.org/10.1016/S0167-1987\(02\)00002-8](https://doi.org/10.1016/S0167-1987(02)00002-8)
- Chamen WCT, Moxey AP, Towers W, Balana B, Hallett PD (2015) Mitigating arable soil compaction: a review and analysis of available cost and benefit data. *Soil Tillage Res* 146(Part A):10–25. <https://doi.org/10.1016/j.still.2014.09.011>
- Diserens E (2009) Calculating the contact area of trailer tyres in the field. *Soil Tillage Res* 103(2):302–309. <https://doi.org/10.1016/j.still.2008.10.020>
- Duttmann R, Brunotte J, Bach M (2013a) Spatial analyses of field traffic intensity and modeling of changes in wheel load and ground contact pressure in individual fields during a silage maize harvest. *Soil Tillage Res* 126:100–111. <https://doi.org/10.1016/j.still.2012.09.001>
- Duttmann R, Schwanebeck M, Nolde M, Horn R (2014) Predicting soil compaction risks related to field traffic during silage maize harvest. *Soil Sci Soc Am J* 78(2):408–421. <https://doi.org/10.2136/sssaj2013.05.0198>
- Duttmann R, Brunotte J, Bach M (2013b) Evaluierung der schlaginternen Bodenbelastung durch Befahrung und Ableitung von Optimierungshilfen für den Praktiker. *Landbauforschung* 63(2):171–190. https://literatur.thuenen.de/digbib_extern/bitv/dn052244.pdf
- Duttmann R, Bach M, Brunotte J (2013c) Befahrungskaktivität bei der Silomaisernte. In: *Kuratorium für Technik und Bauwesen in der Landwirtschaft - KTBL (ed) Logistik rund um die Biogasanlage*. KTBL-Schrift 498, Darmstadt, pp 63–73
- DWD (Deutscher Wetterdienst) (2019) Klimadaten Deutschland. https://werdis.dwd.de/werdis/start_js_jsp.do. Accessed 01 May 2019
- EC (European Commission - Joint Research Centre) (2012) *The state of soil in Europe. A contribution of the JRC to the European Environment Agency's environment—state and outlook*. Publications Office of the European Union, Luxembourg. <https://doi.org/10.2788/77361>
- Etana A, Larsbo M, Keller T, Arvidsson J, Schjøning P, Forkman J, Jarvis N (2013) Persistent subsoil compaction and its effects on preferential flow patterns in a loamy till soil. *Geoderma* 192:430–436. <https://doi.org/10.1016/j.geoderma.2012.08.015>
- FAO (2014) *World reference base for soil resources. International soil classification system for naming soils and creating legends for soil maps*. World soil resources report 106, Food and Agriculture Organization of the United Nations, Rome
- FAO (2015) *Status of the world's soil resources. Main report*. Food and Agriculture Organization of the United Nations and Intergovernmental Panel on soils, Rome, Italy. <http://www.fao.org/3/a-i5199e.pdf>. Accessed 01 May 2019
- Götze P, Rücknagel J, Jacobs A, Märlander B, Koch HJ, Christen O (2016) Environmental impacts of different crop rotations in terms of soil compaction. *J Environ Manag* 181:54–63. <https://doi.org/10.1016/j.jenvman.2016.05.048>
- Grisso RD, Kocher MF, Adamchuk VI, Jasa PJ, Schroeder MA (2004) Field efficiency determination using traffic pattern indices. *Appl Eng Agric* 20(5):563–572. <https://digitalcommons.unl.edu/biosysengfacpub/167>
- Håkansson I, Reeder RC (1994) Subsoil compaction by vehicles with high axle load—extent, persistence and crop response. *Soil Tillage Res* 29:277–304
- Hamza MA, Andersson WK (2005) Soil compaction in cropping systems. A review of the nature, causes and possible solutions. *Soil Tillage Res* 82:121–145. <https://doi.org/10.1016/j.still.2004.08.009>
- Hijmans RJ (2016) raster: geographic data analysis and modeling. r package version 2.5-8
- Horn R (1985) Model experiments about the interaction between mechanical stress application and changes in redox potential values (in German, with English summary and captions). *Z Pflanz Bodenkunde* 148:47–53
- Horn R (2003) Stress-strain effects in structured unsaturated soils on coupled mechanical and hydraulic processes. *Geoderma* 116(1–2):77–88. [https://doi.org/10.1016/S0016-7061\(03\)00095-8](https://doi.org/10.1016/S0016-7061(03)00095-8)
- Horn R, Fleige H (2003) A method for assessing the impact of load on mechanical stability and on physical properties of soils. *Soil Tillage Res* 73(1–2):89–99. [https://doi.org/10.1016/S0167-1987\(03\)00102-8](https://doi.org/10.1016/S0167-1987(03)00102-8)
- Jones RJA, Spoor G, Thomasson AJ (2003) Vulnerability of subsoils in Europe to compaction: a preliminary analysis. *Soil Tillage Res* 73(1–2):131–143. [https://doi.org/10.1016/S0167-1987\(03\)00106-5](https://doi.org/10.1016/S0167-1987(03)00106-5)
- Keller T, Défossez P, Weisskopf P, Arvidsson J, Richard G (2007) SoilFlex: a model for prediction of soil stresses and soil compaction due to agricultural field traffic including a synthesis of analytical approaches. *Soil Tillage Res* 93(2):391–411. <https://doi.org/10.1016/j.still.2006.05.012>
- Keller T, Silva AP, Tormena CA, Giarola NFB, Cavalieri KMV, Stettler M, Arvidsson J (2015) Soilflexllwr: linking a soil compaction model with the least

- limiting water range concept. *Soil Use Manag* 31 (2):321–329. <https://doi.org/10.1111/sum.12175>
- Keller T, Colombi T, Ruiz S, Manalili MP, Rek J, Stadelmann V, Wunderli H, Breitenstein D, Reiser R, Oberholzer H, Schymanski S, Romero-Ruiz A, Linde N, Weisskopf P, Walter A, Or D (2017) Long-term soil structure observatory for monitoring post-compaction evolution of soil structure. *Vadose Zone J*. <https://doi.org/10.2136/vzj2016.11.0118>
- Koolen AJ, Lerink P, Kurstjens DAG, van den Akker JJH, Arts WBM (1992) Prediction of aspects of soil-wheel systems. *Soil Tillage Res* 24(4):381–396. [https://doi.org/10.1016/0167-1987\(92\)90120-Z](https://doi.org/10.1016/0167-1987(92)90120-Z)
- Kroulík M, Kumbhára F, Hůla J, Honzík I (2009) The evaluation of agricultural machines field trafficking intensity for different soil tillage technologies. *Soil Tillage Res* 105(1):171–175. <https://doi.org/10.1016/j.still.2009.07.004>
- Kuhwald M, Blaschek M, Minkler R, Nazemtseva Y, Schwanebeck M, Winter J, Duttmann R (2016) Spatial analysis of long-term effects of different tillage practices based on penetration resistance. *Soil Use Manag* 32(2):240–249. <https://doi.org/10.1111/sum.12254>
- Kuhwald M, Blaschek M, Brunotte J, Duttmann R (2017) Comparing soil physical properties from continuous conventional tillage with long-term reduced tillage affected by one-time inversion. *Soil Use Manag* 33 (4):611–619. <https://doi.org/10.1111/sum.12372>
- Kuhwald M, Dörnhöfer K, Oppelt N, Duttmann R (2018) Spatially explicit soil compaction risk assessment of arable soils at regional scale: the SaSCiA-model. *Sustainability* 10(1618):1–29. <https://doi.org/10.3390/su10051618>
- Kuhwald M (2019) Detection and modelling of soil compaction of arable soils: from field survey to regional risk assessment. Dissertation, Christian-Albrechts-Universität zu Kiel, Kiel
- Lamandé M, Schjønning P (2011) Transmission of vertical stress in a real soil profile. Part II: effect of tyre size, inflation pressure and wheel load. *Soil Tillage Res* 114(2):71–77. <https://doi.org/10.1016/j.still.2010.08.011>
- LSN (Landesamt für Statistik Niedersachsen) (2017) Bodennutzung und Ernte 2017. Die Bodennutzung der landwirtschaftlichen Betriebe in Niedersachsen. Anbau und Erntemengen auf den landwirtschaftlich genutzten Flächen. Statistische Berichte CI 1, CII 1, C II 2, C II 3 -j/2017. <https://www.statistik.niedersachsen.de/themenbereiche/landwirtschaft/themenbereich-land-und-forstwirtschaft-fischerei—statistische-berichte-173829.html>. Accessed 31 Mar 2019
- Nendel C, Berg M, Kersebaum KC, Mirschel W, Specka X, Wegehenkel M, Wenkel KO, Wieland R (2011) The Monica model: Testing predictability for crop growth, soil moisture and nitrogen dynamics. *Ecol Model* 222(9):1614–1625. <https://doi.org/10.1016/j.ecolmodel.2011.02.018>
- Nevens F, Reheul D (2003) The consequences of wheel-induced soil compaction and subsoiling for silage maize on a sandy loam soil in Belgium. *Soil Tillage Res* 70:175–184. [https://doi.org/10.1016/S0167-1987\(02\)00140-X](https://doi.org/10.1016/S0167-1987(02)00140-X)
- Nolting K, Brunotte J, Sommer C, Ortmeier B (2011) Reifeneinfederung Kontra Radlast. *Die Landtechnik* 66(3):194–197
- Pebesma EJ, Bivand RS (2005) Classes and methods for spatial data in r. *R News* 5(2):9–13. <https://CRAN.R-project.org/doc/Rnews/>
- Peth S, Horn R, Fazekas O, Richards BG (2006) Heavy loading and its consequences for soil structure, strength, and deformation of arable soils. *J Plant Nutr Soil Sci* 169(6):775–783. <https://doi.org/10.1002/jpln.200620112>
- Richards T (2000) Development of a system for mapping the performance of agricultural field operations. EngD Thesis, Cranfield University, Silsoe, UK
- Rücknagel J, Christen O, Hofmann B, Ulrich S (2012) A simple model to estimate change in precompression stress as a function of water content on the basis of precompression stress at field capacity. *Geoderma* 177–178:1–7. <https://doi.org/10.1016/j.geoderma.2012.01.035>
- Rücknagel J, Götze P, Hofmann B, Christen O, Marshall K (2013) The influence of soil gravel content on compaction behaviour and pre-compression stress. *Geoderma* 209–210:226–232. <https://doi.org/10.1016/j.geoderma.2013.05.030>
- Rücknagel J, Hofmann B, Deumelandt P, Reinicke F, Bauhardt J, Hülsbergen KJ, Christen O (2015) Indicator based assessment of the soil compaction risk at arable sites using the model REPRO. *Ecol Indic* 52:341–352. <https://doi.org/10.1016/j.ecolind.2014.12.022>
- Rulfová Z, Beranová R, Kyselý J (2017) Climate change scenarios of convective and large-scale precipitation in the Czech Republic based on EURO-CORDEX data. *Int J Climatol* 37:2451–2465. <https://doi.org/10.1002/joc.4857>
- Schjønning P, Lamandé M, Tøgersen FA, Arvidsson J, Keller T (2008) Modelling effects of tyre inflation pressure on the stress distribution near the soil-tyre interface. *Biosyst Eng* 99(1):119–133. <https://doi.org/10.1016/j.biosystemseng.2007.08.005>
- Schjønning P, Lamandé M, Keller T, Pedersen J, Stettler M (2012) Rule of thumb for minimizing subsoil compaction. *Soil Use Manag* 28(3):378–393. <https://doi.org/10.1111/j.1475-2743.2012.00411.x>
- Schjønning P, Stettler M, Keller T, Lassen P, Lamandé M (2015) Predicted tyre-soil interface area and vertical stress distribution based on loading characteristics. *Soil Tillage Res* 152:52–66. <https://doi.org/10.1016/j.still.2015.03.002>
- Schjønning P, Lamandé M, Munkholm LJ, Lyngvig HS, Nielsen JA (2016) Soil precompression stress, penetration resistance and crop yields in relation to differently trafficked, temperate-region sandy loam

- soils. *Soil Tillage Res* 163:298–308. <https://doi.org/10.1016/j.still.2016.07.003>
- Soane BD, Dickson JW, Campbell DJ (1982) Compaction by agricultural vehicles: a review. III. Incidence and control of compaction in crop production. *Soil Tillage Res* 2:3–36. [https://doi.org/10.1016/0167-1987\(82\)90030-7](https://doi.org/10.1016/0167-1987(82)90030-7)
- Stock S, Lingemann K, Stiene S, Hertzberg J (2016) Towards a flexible hybrid planner for machine coordination in arable farming. In: Ruckelshausen A, Meyer-Aurich A, Rath T, Recke G, Theuvsen B (eds) *Informatik in der Land-, Forst- und Ernährungswirtschaft - Fokus Intelligente Systeme - Stand der Technik und neue Möglichkeiten*. Proceedings 36. GIL-Jahrestagung, 22.-23 Februar, Osnabrück, pp 205–208
- Taylor JH (1983) Benefits of permanent traffic lanes in a controlled traffic crop production system. *Soil Tillage Res* 3(4):385–395
- Tolón-Becerra A, Botta GF, Lastra-Bravo X, Tourn M, Melcon FB, Vazquez J, Rivero D, Linares P, Nardon G (2010) Soil compaction distribution under tractor traffic in almond (*Prunus amygdalus* L.) orchard in Almería España. *Soil Tillage Res* 107(1):49–56. <https://doi.org/10.1016/j.still.2010.02.001>
- Tullberg J (2010) Tillage, traffic and sustainability—a challenge for ISTRO. *Soil Tillage Res* 111:26–32. <https://doi.org/10.1016/j.still.2010.08.008>
- Tullberg J, Antille DL, Bluett C, Eberhard J, Scheer C (2018) Controlled traffic farming effects on soil emissions of nitrous oxide and methane. *Soil Tillage Res* 176:18–25. <https://doi.org/10.1016/j.still.2017.09.014>
- Van den Akker JJH, Arvidsson J, Horn R (2003) Introduction to the special issue on experiences with the impact and prevention of subsoil compaction in the European Union. *Soil Tillage Res* 73:1–8. [https://doi.org/10.1016/S0167-1987\(03\)00094-1](https://doi.org/10.1016/S0167-1987(03)00094-1)
- Wickham H (2011) The split-apply-combine strategy for data analysis. *J Statistic Softw* 40(1):1–29. <https://www.jstatsoft.org/v040/i01>
- Yule IJ, Kohnen G, Nowak M (1999) A tractor performance monitor with DGPS capability. *Comput Electron Agric (Special Edition: Spatial yield recording of non-grain crops)* 23(2):155–174
- Zink A, Fleige H, Horn R (2011) Verification of harmful subsoil compaction in loess soils. *Soil Tillage Res* 114:127–134. <https://doi.org/10.1016/j.still.2011.04.004>



Ecotoxicological Assessment of Brownfield Soil by Bioassay

15

Tamara V. Bardina, Marina V. Chugunova,
Valery V. Kulibaba,
and Victoria I. Bardina

Abstract

The study provides a comparative assessment of the ecotoxicity of brownfield soil contaminated due to past environmental damage in the Northwestern region of the Russian Federation using different laboratory bioassay methods. The bioassay was carried out using *Avena sativa* (L.) seeds as a test plant. The contact bioassay was carried out using a natural complex of microorganisms directly present in the samples of brownfield soil, as well as in the seeds of higher plants (*Triticum aestivum* L.). The level of toxicity of the examined soils for microorganisms was determined based on statistically significant differences in respiratory activity between contaminated and control samples. Test parameters such as germination, root length and plant biomass were determined for phytotoxicity. The technology developed and patented by the St. Petersburg Research Center for Ecological Safety at the Russian Academy of Sciences was used as a contact bioassay in conjunction with generally accepted methods for determining acute and chronic phytotoxicity. A study of physical and

chemical parameters (pH, specific conductivity, content of heavy metals and organic eco-toxicants) was carried out to assess the ecological status of the soils. The combination of the methods of bioassay and chemical analysis provided a reliable assessment of the ecological status of contaminated and brownfield soils. The proposed contact bioassay laboratory method showed high sensitivity for the soils studied. The results of two biotest systems applied in the contact bioassay (soil microorganisms and higher plants) complemented and confirmed one another. If the final ecological status cannot be detected by contact phytotoxicity for the soils containing unknown contaminants, then the chronic phytotoxicity assay should be carried out. For the reliable ecotoxicological assessment of the soil in industrial zones, it is necessary to use both eluate and contact methods in laboratory bioassays. These methods are affordable, fast and accurate and can be used at the preparatory stage of the environmental monitoring of soils from similar sites located in different zones with a temperate climate.

Keywords

Environmental damage · Landscape · Brownfield soil · Bioassay · Phytotoxicity · Microorganisms

T. V. Bardina (✉) · M. V. Chugunova · V. V. Kulibaba · V. I. Bardina
Scientific Research Centre for Ecological Safety,
Russian Academy of Sciences (SRCES RAS),
19711018, Korpurnaya str, St. Petersburg, Russia

Abbreviations

ANOVA	Analysis of variance
GC	Gas chromatography
GOST	Acronym for Russian governmental standard
HM	Heavy metal
ISO	International organization for standardization
MPC	Maximum permissible concentration
MR	2.1.7.2297-07 2007
PAHs	Polycyclic aromatic hydrocarbons
PCBs	Polychlorinated biphenyls
WRB	World reference base for soil resources

15.1 Introduction

Areas of land with past environmental damage from industrial waste are associated with similar environmental problems in every country (Antić-Mladenović et al. 2015; Čakmak et al. 2018; Rodríguez-Eugenio et al. 2018; Olsson et al. 2019; Saljnikov et al. 2019; Bech 2020; EEA 2020; SOER 2020), including the Russian Federation (Pitulko 2013; Timofeev et al. 2019; Konstantinova et al. 2020). These areas are extremely specific in their genesis and typology. They include decommissioned industrial waste disposal sites, landfills, refuse sites and dumps. Long-term industrial waste disposal without appropriate protective measures in these areas has led to the accumulation of various toxic substances in the soil. However, it is not always possible to assess the real risk to brownfield soil (Keys to Soil Taxonomy 2014) based on chemical and physical tests only. This situation has arisen due to the limited list of pollutants and methods for detecting them regulated by legislation documents. In addition, the presence of pollutants of unknown composition with cumulative toxic effects narrows the scope of studies (Bardina et al. 2017; Alvarenga et al. 2012; Niss et al. 2018). Studying only soil organisms (Materu and Heise

2019) or analysing only chemical and physical soil properties can provide information on the amount of individual or specific pollutants, but does not detect all the hazardous substances present in the samples (Wadhia and Thompson 2007) and does not provide information on the cumulative effects of pollutants on organisms (Materu and Heise 2019).

Currently, many researchers agree that toxicological studies using bioassay tests are necessary to evaluate the environmental risks associated with soil contamination, as they have great potential to test for the bioavailability of pollutants and associated risks to the environment (Bucheli and Fent 2009). Various biotests exploit the ability of specific organisms to respond to exposure to pollutants or contaminated field samples under standard conditions by altering their vital functions. Therefore, bioassays can be used for a variety of purposes, such as bio-monitoring (Rakshith et al. 2016), early warning systems, for regulatory purposes (Power and Boumphrey 2004; Tonkes et al. 2016) and effect screening (Carbajo et al. 2015). Though the interpretation of the biotest outputs might be limited by the complexity of multispecies interactions (Fent 2004), their results successfully complement others soil pollution risk assessments (e.g. Brown et al. 2016) by registering the total toxic impact of multiple pollutants on a test organism. A number of researchers have proposed that these methods should be included in environmental monitoring systems (Ribe et al. 2012; Terekhova 2012; Płaza et al. 2010; Terekhova et al. 2014; Domínguez-Rodríguez et al. 2020; Huera-Lucero et al. 2020), since the contemporary ecological evaluation of soil quality should target the development of a wider array of methodologies, including applicative methods that ensure the test culture comes into contact with solid soil particles. In addition, it is vitally important to identify sensitive organisms of ecological value that can be used in toxicity testing, and to complement ecotoxicological data on the impact of industrial waste contamination (Materu and Heise 2019). The accumulated knowledge in the field of the soil–organism–toxicant relationship needs updating before any confident

conclusions can be made about the ecotoxicological status of the soil, and to develop effective practical measures for restoring the soil and its biota on a global scale. Many researchers agree that there is an urgent need to develop new bioassay methods and approaches and to identify whether these methods can be used for the environmental monitoring of specific sites (Matejczyk et al. 2011; Ekelund and Häder 2018; Domínguez-Rodríguez et al. 2020). New methods are needed to detect the effects of specific pollutants on target organisms (Escher et al. 2017; Ankley et al. 2016), as well as to develop approaches for successfully transferring effective bioassays from laboratory to field scale (Hansen 2018).

The functional characteristics of soil microflora are the most important and reliable indicators in the evaluation of solid multicomponent substrates, as soil organisms are a vital component of soil ecosystem and a major link in the cycle of biogenic elements and energy flows in the biosphere (Dobrovolskaya et al. 2015; Schlöter et al. 2018; Thiele-Bruhn et al. 2020; Wang et al. 2018; Erktan et al. 2020). Microbial communities determine the speed and direction of substances' transformation into multicomponent solid substrates (Finn et al. 2017), such as brownfield soils and natural soil substrate, while supporting the environmental balance (homeostasis) in the soil (Odum and Barrett 2004). In addition, microorganisms are the most sensitive bioindicators of all soil biota, since they react more quickly to changes in the environment; therefore, they are successfully used as test cultures in bioassays (Terekhova 2011; Ezeokoli et al. 2020).

An integral indicator of soil biological activity or intensity, the rate of the metabolic activities of heterotrophic soil microorganisms ultimately results in CO₂ being released via soil respiration (Pantani et al. 2020). Soil respiration is considered one of the most important indicators of soil microbial status, and of the whole soil ecosystem (Ryan and Law 2005; Luo and Xuhui 2006; Saljnikov et al. 2017a, b; Liu et al. 2018; Warner et al. 2019; Zhao et al. 2020). The laboratory bioassay of plants (phytotest) is a necessary link in a number of toxicological studies. This method has certain advantages: it is economical,

fast and sensitive, while providing reliable results; therefore, it is widely used in environmental studies of soils (Terekhova et al. 2016), employing the seeds of higher plants as a test culture. Currently, eluate and contact (substrate) methods are often used contemporaneously in biotests. The toxic effect of pollutants dissolved in aqueous extracts of plants is investigated using eluate analysis methods. However, in our opinion, in order to adequately assess the toxicity of brownfield soils which have been subject to environmental damage from industrial waste for a long time, not only eluate methods, but also contact methods should be used in laboratory biotests (Bardina et al. 2014, 2016). In addition, the question of whether and when to carry out chronic test experiments, which are more expensive and time-consuming, has not yet been resolved (Solomon et al. 2008). Contact microbiological tests in Russia are based on the assessment of how a contaminated substrate affects an artificially introduced test organism. However, since brownfield soils contain a significant amount of viable microflora, it is possible to use a complex of soil microorganisms as a test culture for ecological diagnostics. Our research studied whether various methods of laboratory bioassay can be used to assess the ecotoxicity of brownfield soil on territories with a long-term history of solid industrial waste landfills, and how successful they are.

15.2 Materials and Methods

15.2.1 Study Sites

The study was conducted on five sites with past environmental damage, located in different landscapes of northwest Russia (Fig. 15.1).

Site 1 covers an area of six hectares located in the coastal zone of Lake Ladoga, within the boundaries of the South Priladozhsky fluvial terrace (59°43'44" N 31°36'59" E). The long-term disposal (over thirty-eight years) of mixed types of construction waste and industrial waste has led to a diffuse pollution of the Podzolic surface-gleyic soil (*Luvic Stagnosol*, WRB 2015) (Fig. 15.2).



Fig. 15.1 Map of the study sites (S1, S2, S3, S4, S5). Scale 1:1.500000



Fig. 15.2 Site I: Mixed types of construction waste and industrial waste, *Luvic Stagnosols*

Site II covers an area of eight hectares located in the Primorsky landscape, an area beneath a mainly flat landscape with some low hills on former industrial lands ($60^{\circ}20'11''$ N $29^{\circ}53'59''$ E). As Hazard Class 4 construction waste and household waste has been deposited in this area (Fig. 15.3), the toxic elements have accumulated chronically, leading to the background pollution of the *Podzolic surface-gleyic* soil.

Site III is a significant area around 150 hectares located within the boundaries of the Ordovik Plateau ($59^{\circ}43'12''$ N $29^{\circ}18'23''$ E). The territory was under a significant load of multi-component pollution for more than thirty years

(Fig. 15.4), suffering diffuse, varied pollution in the upper soil horizons of *Sod-calcareous (Rendzic Leptosols)* loam soil.

Site IV is located in the coastal zone of Lake Ladoga and is an open dump with long-term storage of industrial waste ($59^{\circ}40'22''$ N $31^{\circ}01'04''$ E). Dumps with a height of 8 m occupy an area of 6.7 hectares; they are composed of weakly packed brownfield soil consisting of toxic waste from the production of sulphuric acid. Waste storage was discontinued in 1978. These brownfield soils have a complex component composition with a predominance of iron and heavy metals (Fig. 15.5).



Fig. 15.3 Site II: Former industrial lands, presently used for construction waste and household waste, *Luvic Stagnosols*



Fig. 15.4 Site III: Multicomponent pollution for more than 30 years, *Rendzic Leptosols*



Fig. 15.5 Site IV: Coast of Ladoga Lake—open dump with long-term storage of industrial waste

Site V (Fig. 15.6) is a 53-hectare area used for the disposal of slag and ash. Industrial operations here ended in 2008 (59°50'20" N 30°58'35" E).

The dump is composed of fine ash, slag and contaminated fine-grained sand (primitive brownfield soil).



Fig. 15.6 Site V: Ash disposal area on primitive brownfield soil

15.2.2 Soil Sampling

For ecotoxicological assessment, mixed brownfield soil from dumps was sampled from a plot of 10 m² in accordance with the national standard, taken from the upper horizons at depths of 0–5 and 5–20 cm using a titanium soil drill (GOST 17.4.4.02-201 2018). At Sites I, II and V, one composite sample was taken from each plot. At Site III, the soil was sampled from three plots with different rates of anthropogenic impact (industrial waste, waste of uncertain composition and low-volume mixed waste). At Site IV, the soil was sampled from two plots (top and bottom of dump).

15.2.3 Analytical Methods

15.2.3.1 Physical and Chemical Analyses

Due to various anthropogenic impacts, it was assumed that the brownfield soils studied differed in terms of their physical and chemical characteristics. In the selected soil samples, the pH was tested using the potentiometric method and specific electrical conductivity methods. The total content of all the forms of heavy metals was determined using inductively coupled plasma mass spectrometry (PND F16.1:2.3:3.11-98 2005) after extraction by digesting the soil samples with nitric acid (1:1) (Mineev 2001). The content of organic pollutants—polychlorinated biphenyls (PCB), organochlorine pesticides and oil products—was analysed using gas

chromatography GC-2010 (GC-2010, Shimadzu, Japan) with an electron capture detector; 3,4benzo(a)pyrene was identified with a highly efficient liquid chromatography analyser (Flyuorat-02, Russia) (MUK 4.1.1061-01 2013).

To estimate the integrative level of chemical contamination, we calculated the total index of pollution Z_c : $Z_c = \sum C_s/C_b - (n - 1)$, where C_s is the concentration of a chemical substance in the sample (mg kg⁻¹), C_b is the regional background concentration (mg kg⁻¹) and n is the number of substances. Z_c values below 16 indicate permissible contamination levels, values from 16 to 32 are moderately hazardous, values from 32 to 128 are hazardous and Z_c values above 128 indicate extremely hazardous contamination (SANPIN 2003).

15.2.3.2 Microbiological Analysis

Microbial activity was determined by soil respiration, trapping the carbon dioxide (CO₂) in sodium hydroxide (NaOH) which was released from the soil during incubation in a closed system. The trapped CO₂ was determined by measuring electrical conductivity (Alef 1995). Soil samples were pre-moistened with distilled water to 60% of their water holding capacity and composted at room temperature prior to the incubation of the samples. The detailed procedure is described in Alef (1995). The level of toxicity was determined based on statistically significant differences between the respiratory activity of the contaminated samples and the control substrate.

15.2.3.3 The Laboratory Bioassay

In accordance with the regulations of the Russian Federation for Environmental Protection, the ecotoxicity of the contaminated soils was determined based on certified eluate and direct contact (solid-phase) bioassays (Nikolaeva and Terkhova 2017). First, the acute phytotoxicity of the soil samples was evaluated by testing the effect of soil–water extract on the *Avena sativa* test culture using the bioassay methods adopted in the Russian Federation (MR 2.1.7.2297-07 2007). The biotest of the soil–water extract on oat seeds was based on the seeds' ability to adequately respond to the chemical effect by changing their germination (test function is the length of the roots). The phytotoxicity threshold was a more than 20% decrease in root length in the test sample in comparison with the control (Et). Distilled water was used for the control.

As the result of the water-soil extraction method can be underestimated due to the presence of insoluble contaminants in the substrate, the biotest was also carried out on a solid sample using the contact biotest method (Terkhova et al. 2016; Bardina et al. 2016). This bioassay method was carried out according to the international standard (ISO 11269-2, ISO 22030: 2005, US EPA, OCSPP 850.4230, OECD Test No. 208). Since the exposure time of the experiment was 14–21 days, it can be described as a chronic phytotoxicity biotest. For the first time in Russia, a laboratory contact bioassay was developed at the St. Petersburg Research Center for Environmental Safety, at the Russian Academy of Sciences (Kapelkina et al. 2009). The test cultures were wheat (*Triticum aestivum* L.) and barley (*Hordeum vulgare* L.), which were measured for two test parameters (germination and root length): N1 is the change in the seed germination of the test soil relative to the control sample (%); N2 is the change in the length of the seedling root in the test soil compared with the control sample (%). From our point of view, the lack of a toxicity rating scale for bioassay methods makes it difficult to use them in monitoring studies. Therefore, a scale for acute toxicity in contaminated brownfield soils was developed based on the measured test parameters:

- V—practically non-toxic ($0 < N1 \leq 20$; $0 < N2 \leq 20$);
- IV—low toxicity ($0 < N1 \leq 20$; $20 < N2 \leq 50$);
- III—moderately toxic ($20 < N1 \leq 70$; $50 < N2 \leq 70$);
- II—dangerously toxic ($70 < N1 < 100$; $70 < N2 < 100$);
- I—highly hazardously toxic ($N1 = N2 = 100$).

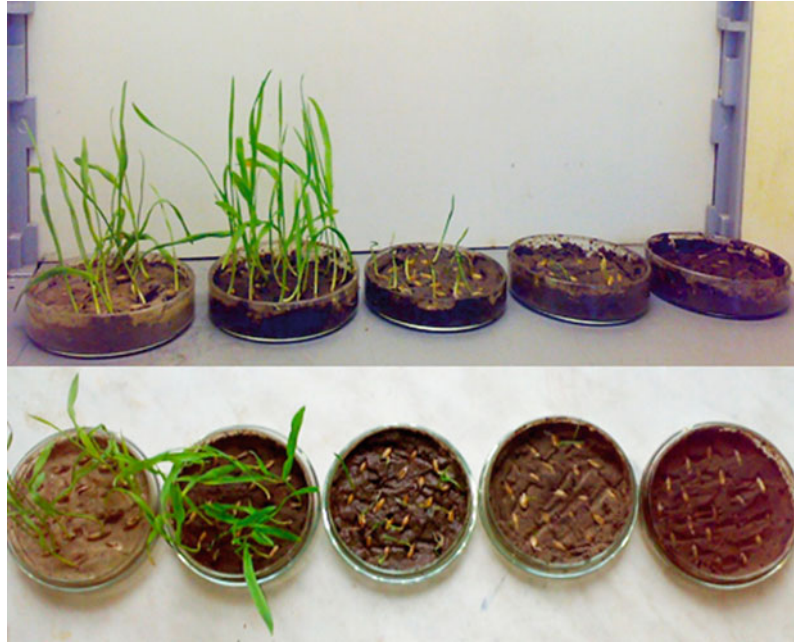
We used a control soil sample which has not been subjected to anthropogenic impact and has a particle size distribution and humus content similar to the sample studied. The exposure period was seven days and was carried out in Petri dishes (Fig. 15.7).

One of the most important tasks when determining phytotoxicity is to decide when it is necessary to conduct a chronic bioassay experiment after using the acute bioassay method. This is important because chronic laboratory bioassays are more expensive and time-consuming (Terkhova et al. 2016; Solomon et al. 2008). We tested most samples for the chronic presence of phytotoxicity. The chronic bioassay method was carried out on oat (*Avena sativa* L.) (GOST R ISO 22030-2009 2010). This standard is identical to the international standard ISO 22030:2005 “Soil quality. Biological methods. Chronic toxicity in higher plants” and is used to assess the quality of soils containing unknown contaminants. The tested parameter was the biomass of plants. A series of dilutions of the test sample with control samples were used to establish chronic toxicity. For the standard soil, a mixture of fertile soil and sand was used with a pH, mechanical composition and organic carbon content close to the sample.

15.2.4 Statistics

To identify the dominant tendencies and a range of measured biological characteristics, the arithmetic means and standard errors were calculated (sample size n always equalled four). A one-way analysis of variance (ANOVA) and Tukey's post-hoc test were used to compare the means. Differences were considered significant at

Fig. 15.7 Wheat germination stages during the bioassay



$p < 0.05$. Data analysis was performed with Statistica 10.0.

15.3 Results and Discussion

15.3.1 Physical and Chemical Characteristics of Brownfield Soil

All the samples studied had a near-neutral and neutral reaction (pH 5.9–6.9), except samples from Site IV, which was acidic (pH 2.9–5.4). Salinisation was not identified at any of the sites. Chemical analyses showed that the main pollutants of the soil were heavy metals. According to the national standard (SANPIN 2.1.7.1287-03 2003), the total indicator of soil contamination by Zc in the soil of Site I was classified in the dangerous category of pollution ($Zc = 65.5$ units), while the soil of Sites II and III was classified in background pollution categories ($Zc = 7.3$ – 7.4 units). The soil at Site IV was

classified in an “extremely dangerous” pollution class ($Zc = 607$ units), and the contamination in the soil at Site V was low ($Zc = 17.7$).

Organic pollutants were found in the soil of Site I (PCB = 0.160 mg kg^{-1}) and in insignificant quantities in the soil of Site II (PCB = 0.072 mg kg^{-1}). Among the organic pollutants, the concentration of polychlorinated biphenyls was above MPC (0.16 mg kg^{-1} against 0.06 mg kg^{-1}). The greatest amount of organic toxicants was found in the soil of Site III. The main pollutants were 3,4-benzo(a)pyrene (0.085 mg kg^{-1} against MPC 0.02 mg kg^{-1}) and polychlorinated biphenyls (0.20 mg kg^{-1} against MPC 0.06 mg kg^{-1}). These substances are extremely toxic even in small concentrations and cause cell death. According to accepted standards, the content of organic toxicants in the soil samples did not exceed the allowed concentrations. However, the 3-ring polycyclic aromatic hydrocarbons (PAHs) may be particularly toxic at the bimolecular level, as proved by the studies of Incardona et al. (2005) and Lors et al. (2010)

15.3.2 Microbiological Status of Soils Studied

The results of the microbiological studies are presented in Table 15.1. The brownfield soil from Site II was characterised by the lowest respiratory activity. The decrease in the respiration rate compared with the control averaged 62%, which indicates a significant distortion of microbiocenosis functioning. Apparently, the very low respiratory activity in this soil is explained by strong pollution of this soil (more

than 60%). At Site I, the inhibition of soil respiration was recorded only at a depth of 5–20 cm in comparison with the control sample (25%). This level of biological degradation is considered ecologically acceptable, since it does not exceed the critical threshold for the loss of soil ecosystem stability by more than 30% of its bio-organic potential (Yakovlev and Evdokimova 2011).

All soil samples from Site III were toxic to the microbial biota to some degree, where their biological activity was two times lower than in the control. The microbial community in this area

Table 15.1 Respiration rate of soil microbial communities

Plot	Sampling depth, cm	Soil respiration rate, mg CO ₂ /100 g/day	Soil respiration (sample vs. control), %
Site I			
Control	0–5	29.4 ± 0.7 ^a	–
	5–20	22.6 ± 0.4 ^b	–
1	0–5	30.2 ± 1.9 ^a	+2.7
	5–20	17.0 ± 0.3 ^c	–24.8
Site II			
Control	0–5	31.0 ± 1.6 ^d	–
	5–20	21.1 ± 1.0 ^f	–
1	0–5	10.7 ± 0.6 ^g	–65.5
	5–20	9.0 ± 0.6 ^g	–57.4
Site III			
Control	0–5	10.1 ± 1.0 ^h	–
	5–20	8.0 ± 0.4 ^j	–
1	0–5	6.3 ± 0.4 ^k	–37.6
	5–20	5.5 ± 0.1 ^k	–31.3
2	0–5	7.5 ± 0 ^l	–25.7
	5–20	6.0 ± 0.2 ^k	–25.0
3	0–5	4.8 ± 0.04 ^k	–52.4
	5–20	3.7 ± 0.1 ^z	–53.8
Site IV			
Control	0–20	32.0 ± 1.8 ^x	–
1	0–20	17.2 ± 1.2 ^c	–46.3
2	0–20	17.4 ± 0.4 ^c	–45.7
Site V			
Control	0–20	32.0 ± 1.8 ^y	–
1	0–20	36.5 ± 2.5 ^b	+14.0

Data are given as average ± standard error. Different letters represent significant differences between the samples (LSD test, $p \leq 0.05$)

showed the least resistance to the inhibitory effects of pollutants. This level of degradation of the microbiocenosis is considered very high and difficult to reverse (Yakovlev and Evdokimova 2011; Anderson 1982; Gorobtsova et al. 2016). We assume that the toxicity of this soil to microorganisms was associated with the disposal of waste containing a number of highly toxic and potentially mutagenic components. The respiratory activity of the soil microbiota from Site III (plots 1 and 2) was 25–37% less than in the control. However, in practice, the degree of this decrease was at the permissible level of disturbance in soil quality, i.e. a loss of bio-organic potential of less than 30% for the sustainable functioning of the soil ecosystem (Yakovlev and Evdokimova 2011). Therefore, due to its low significance, the processes of microbiocenosis degradation in these soils are considered reversible.

Table 15.1 shows that brownfield soils formed at another dump with by-products from sulphuric acid production (Site IV) were characterised by almost the same biological activity, at a level two times lower than in the control. The toxicity of these soils to microbiota was probably due to the very high content of heavy metals. The soil of the brownfield slag-ash dump (Site V) did not differ significantly from the control in terms of respiratory activity, which indicates that it was not toxic for the natural complex of microorganisms. The absence of toxicity seems to be associated with the specific chemical composition of the soil, which had a high content of biophilic elements, in particular phosphorus.

Our microbiological studies allowed us to conclude that the pollution of brownfield soil from Sites I and V, which contained industrial and construction waste, did not lead to a significant disturbance in the content of soil microorganisms, indicating that the ecosystem as a whole functions normally. A significant decrease was found in the functional activity of the soil microbiota at Sites II and III (Plot 3) under the influence of industrial wastes, indicating the violation of the soils' ecology and a decrease in their stability and self-restoring capacity. Brownfield soils formed on waste dumps from

the production of sulphuric acid (Site IV) were characterised by significantly lower respiratory activity compared with the control, indicating their toxicity to microbiocenoses.

Chemical analyses showed that the main pollutants of the brownfield soil were heavy metals. Soil microorganisms are first exposed to the direct and indirect impacts of heavy metals (Nannipieri et al. 2012; Lenart-Boroń and Boroń 2014; Chu 2018). Although some metals (e.g. Fe, Zn, Cu, Ni, Co) are of vital importance for many microbial activities at low concentrations, high concentrations of heavy metals may have inhibitory or even toxic effects on living organisms (Abdu et al. 2017; Bruins et al. 2000). Working in situ, Fazekašová and Fazekaš (2020) showed that the activity of soil enzymes showed considerable differences in the impact zone of mining activities in Slovakia.

On the other hand, in a number of studies, heavy metals were not found to have any effect on the soil biota. This is because, in some cases, heavy metal contamination can reduce the diversity of the soil microbial community, but not reduce the number of microbes (Doelman 1986). Also, for example, long-term exposure to heavy metals can lead to the selection of resistant species or strains (Piotrowska-Seget and Cycoń 2005; Abdu et al. 2017). Some microorganisms have the ability to adapt to an environment contaminated with heavy metals, exhibiting processes of biosorption, bioprecipitation, extracellular sequestration, transport mechanisms and/or chelation (Haferburg and Kothe 2007), which is used for the bioremediation of soils contaminated with heavy metals.

15.3.3 Ecotoxicity of Brownfield Soils in a Laboratory Bioassay

15.3.3.1 Acute Phytotoxicity

The results of the bioassay of extracted water (eluate) on oats showed that the effect of inhibition was observed in the soils of Site III and in the brownfield soil of Site IV (40.1–42.1%). Phytotoxicity was not detected in the remaining soil–water extracts (Table 15.2). On the contrary,

the toxicological analysis performed on wheat seeds using the contact bioassay method revealed the presence of toxicity at four sites: Site I—moderate toxicity, Site II—low toxicity, Site IV—dangerous degree of toxicity and Site V—small degree of toxicity (Table 15.3). The soils from Site IV were extremely contaminated with heavy metals.

The contact bioassay results were well aligned with the results of the heavy metal content test. A correlation analysis showed a fairly close,

direct relationship between the response of the tested wheat (germination index N1) and the Zc index (+0.97). The laboratory eluate and contact bioassays contributed to the detection of toxicity in varying rates at all sites (Table 15.4).

On the one hand, acute biotests offer the advantage of a shorter period being required to get a result; however, they may not be representative of the toxicity of the soil itself (e.g. Domínguez-Rodríguez et al. 2020). Our results showed that the close positive correlation

Table 15.2 Bioassay with the seeds of *Avena sativa* L.

Plot	Sampling depth, cm	Root length, mm	Toxic effect, E _t %	Reaction of the test organisms
Site I				
Control	0–20	50.1 ± 2.7 ^a	0	No reaction
1	0–5	58.5 ± 2.3 ^b	+16.9	No reaction
	5–20	59.6 ± 2.7 ^b	+18.9	No reaction
Site II				
Control	0–20	50.1 ± 2.7 ^a	0	No reaction
1	0–5	50.8 ± 2.7 ^a	+1.4	No reaction
	5–20	53.4 ± 6.0 ^a	+6.6	No reaction
Site III				
Control	0–20	72.8 ± 0.6 ^f	0	No reaction
1	0–5	51.8 ± 5.9 ^d	–28.8	Growth supression
	5–20	64.4 ± 5.4 ^g	–11.5	No reaction
2	0–5	67.1 ± 0.3 ^g	–7.8	No reaction
	5–20	67.9 ± 5.6 ^g	–6.8	No reaction
3	0–5	74.4 ± 2.6 ^f	+2.6	No reaction
	5–20	52.5 ± 10.1 ^d	–27.9	Growth supression
Site IV				
Control	0–20	46.1 ± 3.7 ^h	0	No reaction
1	0–5	27.6 ± 0.8 ^j	–40.1	Growth supression
	5–20	26.7 ± 0.1 ^j	–42.1	Growth supression
2	0–5	40.4 ± 3.7 ^h	+12.4	No reaction
	5–20	49.4 ± 3.7 ^k	+7.2	No reaction
Site V				
Control	0–20	46.1 ± 3.7 ^h	0	No reaction
1	0–5	39.1 ± 3.1 ^h	–15.1	No reaction
	5–20	40.9 ± 3.7 ^h	–11.4	No reaction

Data are given as mean value ± standard error. Different letters represent significant differences between samples on plots (LSD test, $p \leq 0.05$)

Table 15.3 Contact bioassay with seeds of *Triticum aestivum* L.

Plot	Sampling depth, cm	Germination rate, %	Germination rate (N1)	Root length, mm	Root length (N2)	Degree of toxicity
Site I						
Control	0–20	83.3 ± 3.3 ^a	0	25.4 ± 1.5 ^a	0	V
1	0–5	60.0 ± 2.1 ^b	–27.9	27.5 ± 1.8 ^a	+8.3	III
	5–20	64.0 ± 2.5 ^b	–23.2	28.6 ± 1.7 ^a	12.6	III
Site II						
Control	0–20	83.3 ± 3.3 ^a	–	25.4 ± 1.5 ^a	–	–
1	0–5	81.7 ± 3.0 ^a	–1.9	18.1 ± 0.8 ^b	–28.7	IV
	5–20	80.3 ± 2.1 ^a	–3.6	19.1 ± 2.1 ^b	–24.8	IV
Site III						
Control	0–20	95.5 ± 3.5 ^c	0	26.5 ± 1.0 ^c	0	V
1	0–5	90.0 ± 3.5 ^c	–5.3	32.2 ± 4.6 ^v	+21.4	V
	5–20	95.0 ± 0 ^c	0	46.3 ± 3.1 ⁿ	+74.4	V
2	0–5	95.5 ± 3.5 ^c	0	25.3 ± 1.0 ^c	–4.4	V
	5–20	95.5 ± 3.5 ^c	0	21.3 ± 1.0 ^c	–19.8	V
3	0–5	87.5 ± 3.3 ^d	–7.9	40.8 ± 3.4 ⁿ	+53.6	V
	5–20	87.5 ± 1.8 ^d	–7.9	43.0 ± 3.2 ⁿ	+62.1	V
Site IV						
Control	0–20	87.5 ± 1.8 ^d	0	19.7 ± 0.5 ^e	0	V
1	0–5	32.5 ± 5.3 ^e	–62.9	1.9 ± 0.4 ^f	–90.4	II
	5–20	0.5 ± 0.4 ^f	–99.4	0.5 ± 0.4 ^g	–97.5	II
2	0–5	30.0 ± 3.5 ^e	–65.7	2.3 ± 0.9 ^f	–88.3	II
	5–20	67.5 ± 8.8 ^g	–22.9	3.0 ± 0.5 ^f	–84.8	II
Site V						
Control	0–20	87.5 ± 1.8 ^d	0	19.7 ± 0.5 ^e	0	V
1	0–5	81.7 ^f	–6.6	17.3 ^z	–31.9	IV
	5–20	90.0 ^f	–2.8	16.4 ^z	–35.4	IV

Data are given as mean value ± standard error; degrees of sample toxicity are: II—highly toxic, III—moderately toxic, IV—slightly toxic and V—almost non-toxic. Different letters represent significant differences between the samples on the plots (LSD test, $p \leq 0.05$)

between the biotest and the pollution index indicates that the results of acute biotests may serve as a reliable concomitant indicator of soil ecotoxicity for microorganisms at a specific site.

15.3.3.2 Chronic Phytotoxicity

Samples from Sites I, II, IV and V from a depth of 0–20 cm were investigated for chronic phytotoxicity. In all the samples where acute toxicity was detected using the contact method, the presence of chronic toxicity was recorded in

differing rates. In the sample from Site II, slight chronic phytotoxicity was recorded, which disappeared upon dilution by 50%. In the latter, acute toxicity was found to a smaller extent (Table 15.5).

Chemical analysis showed that the main pollutants of the soil cover at Sites I, IV and V were heavy metals. Chronic toxicity was found in these samples, with the toxic effect disappearing only in mixtures already containing 25% of the sample. We found that the dry weight of plants in

Table 15.4 Integrated estimates of the soil toxicity (eluate bioassay)

Plot	Sampling depth, cm	<i>Avena sativa</i>	<i>Triticum aestivum</i>
		Reaction of the test organisms	Degree of toxicity
Site I			
1	0–5	Non-toxic	Moderately toxic
	5–20	Non-toxic	Moderately toxic
Site II			
1		Non-toxic	Slightly toxic
		Non-toxic	Slightly toxic
Site III			
1	0–5	Non-toxic	Almost non-toxic
	5–20	Toxic	Almost non-toxic
2	0–5	Non-toxic	Almost non-toxic
	5–20	Toxic	Almost non-toxic
3	0–5	Toxic	Almost non-toxic
	5–20	Non-toxic	Almost non-toxic
Site IV			
1	0–5	Toxic	Highly toxic
	5–20	Toxic	Highly toxic
2	0–5	Non-toxic	Highly toxic
	5–20	Non-toxic	Highly toxic
Site V			
1	0–5	Non-toxic	Slightly toxic
	5–20	Non-toxic	Slightly toxic

these samples, determined on the 30th day, correlated significantly with the total index of sample metal contamination Z_c ($r = -0.82$). Thus, a relationship was revealed between chronic toxicity and the main pollutants of the test sample and heavy metals.

The toxic effect of heavy metals on soil microbial communities may have various manifestations associated with the close affinity of heavy metals and microorganisms (Haferburg and Kothe 2007), resulting in the inactivation of certain biological macromolecules and the deterioration of the diversity of sensitive microbial communities. This increases the number of communities which can adapt to the heavy metal load, or if the concentration of heavy metals is higher than the organisms can handle, in their

death (Giller et al. 1998; Chu 2018). On the other hand, some biological compounds such as metallothionein ligands and smaller molecules such as glycine and taurine cannot be degraded due to heavy metals since they are quickly assimilated into the food chain, thus jeopardising the health of animals and humans (Chu 2018).

Both acute and chronic bioassays using the contact method showed similar trends in the assessment of ecotoxicity and correlated well with the index of heavy metal contamination. However, the test cultures exhibited different levels of sensitivity to the investigated array of pollutants, which suggests that the choice of a set of biotests should be made taking into account the specificity of the soil and the sensitivity of an individual culture to a specific pollutant.

Table 15.5 Chronic phytotoxicity of brownfield soil

Plot, sample content in the mixture, %	Dry weight on day 15, g		Dry weight on day 30, g	
	Average weight	% of control	Average weight	% of control
Site I				
Control	0.118 ^e	–	0.140 ^e	–
1. 100	0.036 ^f	30.5 ^c	0.055 ^f	39.6 ^c
50	0.073 ^g	61.9 ^g	0.126 ^g	89.8 ^j
25	0.110 ^e	93.2 ^d	0.140 ^e	100 ^e
Site II				
Control	0.118 ^e	–	0.140 ^e	–
1. 100	0.053 ^j	44.9 ^k	0.105 ^j	74.8 ^f
50	0.065 ^q	55.1 ^l	0.148 ^e	105.6 ^k
Site IV				
Control	0.048 ^a	–	0.129 ^a	–
4. 100	0	0	0	0
50	0.032 ^b	66.7 ^a	0.110 ^b	85.3 ^a
25	0.050 ^a	104.2 ^b	0.119 ^b	92.2 ^b
Site V				
Control	0.048 ^a	–	0.129 ^a	–
5. 100	0.015 ^c	31.2 ^c	0.046 ^d	31.0 ^c
50	0.044 ^a	91.7 ^d	0.090 ^e	69.8 ^d
25	0.049 ^a	102.1 ^b	0.130 ^a	100.8 ^e

Different letters represent significant differences between samples on plots (LSD test, $p \leq 0.05$)

15.4 Conclusion

Biotest systems using a natural complex of microorganisms as test organisms and seeds of higher plants were tested on brownfield soil with long-term past environmental damage and different rates of chemical pollution. Different test cultures were found to have different levels of sensitivity to the spectrum of toxicants in the sites studied. The results showed that when determining the acute phytotoxicity of brownfield soils, the proposed approach of contact bioassays on wheat was relatively sensitive. The results proved that when the contact method does not enable acute phytotoxicity to be detected in brownfield soils, then a test for chronic phytotoxicity is recommended to reliably assess the

ecological state of abandoned soils in industrial zones containing unknown pollutants.

The study showed that the behaviour and response of test organisms to heavy metals and organic pollutants vary with the pollution load, type of pollutant and pedoclimatic factors. An interdisciplinary approach should be taken to better understand the geological and biological interactions between soil microorganisms, plants and various pollutants and thus develop a reliable, efficient, resource-saving bioassay suite for ecotoxicological assessment. We suggest that eluate and contact methods should be used together in laboratory bioassays for a reliable ecotoxicological assessment of the soil cover in industrial zones. These methods are easy, fast and accurate, and can therefore be used on similar landfill sites in other temperate zones and

serve as a primary stage in assessing the ecological status of these sites.

References

- Abdu N, Abdullahi AA, Abdulkadir A (2017) Heavy metals and soil microbes. *Environ Chem Lett* 15:65–84. <https://doi.org/10.1007/s10311-016-0587-x>
- Alef K (1995) Soil respiration. In: Alef K, Nannipieri P (eds) *Methods in soil microbiology and biochemistry*. Academic Press Inc., San Diego, pp 214–215
- Alvarenga P, Palma P, de Varennes A, Cunha-Queda AC (2012) A contribution towards the risk assessment of soils from the São Domingos Mine (Portugal): chemical, microbial and ecotoxicological indicators. *Environ Pollut* 161:50–56. <https://doi.org/10.1016/j.envpol.2011.09.044>
- Anderson JP (1982) Soil respiration. In: Page AL, Millar RH, Keeney DH (eds) *Methods of soil analysis, Part 2. Agronomy 9, 2nd edn*. American Society of Agronomy, Madison, Wisc. pp 831–871
- Ankley G, Escher BI, Hartung T, Shah I (2016) Pathway-based approaches for environmental monitoring and risk assessment. *Environ Sci Technol* 50(19):10295–10296
- Antić-Mladenović S, Kresović M, Rinklebe J, Frohne T, Stárk HJ, Ličina V (2015) Impact of different redox conditions on thallium (im)mobilisation in soil (Serbia). *Zemljiste i Biljka* 64(2):27–41. http://www.sdpz.rs/images/casopis/2015/ZIB_vol64_no2_2015_pp27-41.pdf
- Bardina TV, Kulibaba VV, Chugunova MV, Bardina VI (2016) Ecotoxicity diagnostics of soils of the past environmental damage industrial facilities with the help of the biotesting systems (Диагностика экотоксичности промышленных объектов прошлого экологического ущерба с помощью биотест систем). *Reg Environ Issues* 2:20–25
- Bardina TV, Chugunova MV, Kulibaba VV, Bardina VI (2014) Evaluation of the ecological state of the past environmental damage objects soils with bio-testing methods (Оценка экологического состояния почвогрунтов объектов прошлого экологического ущерба методами биотестирования). *Reg Environ Issues* 5:37–42
- Bardina TV, Chugunova MV, Kulibaba VV, Polyak YM, Bardina V, Kapelkina LP (2017) Applying bioassay methods for ecological assessment of the soils from the brownfield sites. *Water Air Soil Pollut*. 228–351. <https://doi.org/10.1007/s11270-017-3521-3>
- Bech J (2020) Soil contamination and human health: part 1—preface. *Environ Geochem Health* 42:1–6. <https://doi.org/10.1007/s10653-019-00513-1>
- Brown AR, Whale G, Jackson M, Marshall S, Hamer M, Solga A, Kabouw P et al (2016) Toward the definition of specific protection goals for the environmental risk assessment of chemicals: a perspective on environmental regulation in Europe. *Integr Environ Assess Manag* 13(1):17–37. <https://doi.org/10.1002/ieam.1797>
- Bruins MR, Kapil S, Oehme FW (2000) Microbial resistance to metals in the environment. *Ecotoxicol Environ Saf* 45:198–207. <https://doi.org/10.1006/eesa.1999.1860>
- Bucheli TD, Fent K (2009) Induction of cytochrome P450 as a biomarker for environmental contamination in aquatic ecosystems. *Criti Rev Environ Sci Technol* 25(3):201–268. <https://doi.org/10.1080/10643389509388479>
- Čakmak D, Perović V, Kresović M, Jaramaz D, Mrvić V, Belanović Simić S, Saljnikov E, Trivan G (2018) Spatial distribution of soil pollutants in urban green areas (a case study in Belgrade). *J Geochem Explor* 188:308–317. <https://doi.org/10.1016/j.gexplo.2018.02.001>
- Carbajo JB, Perdígón-Melón JA, Petre AL, Rosal R, Letón P, García-Calvo E (2015) Personal care product preservatives: risk assessment and mixture toxicities with an industrial wastewater. *Water Res* 72:174–185. <https://doi.org/10.1016/j.watres.2014.12.040>
- Chu D (2018) Effects of heavy metals on soil microbial community. *IOP Conf Ser Earth Environ Sci* 113:8–10, 012009. <https://iopscience.iop.org/article/10.1088/1755-1315/113/1/012009/pdf>
- Dobrovolskaya TG, Zvyagintsev DG, Chernov IY, Golovchenko AV, Zenova GM, Lysak LV, Manucharova NA, Marfenina OE, Polyanskaya LM, Stepanov AL, Umarov MM (2015) The role of microorganisms in the ecological functions of soils. *Eurasian Soil Sci* 48(9):959–967. <https://doi.org/10.1134/S1064229315090033>
- Doelman P (1986) Resistance of soil microbial communities to heavy metals. In: Jensen V, Kioller A, Sorensen CH (eds) *Microbial communities in soil*. Elsevier Applied Science Publishers, London, pp 369–384
- Domínguez-Rodríguez VI, Adams RH, Sánchez-Madrigal F, Pascual-Chablé JLS, Gómez-Cruz R (2020) Soil contact bioassay for rapid determination of acute toxicity with *Eisenia foetida*. *Heliyon* 6(1):e03131. <https://doi.org/10.1016/j.heliyon.2019.e03131>
- EEA Report (2020) Land and soil pollution—widespread, harmful and growing. The European environment—state and outlook 2020. <https://www.eea.europa.eu/signals/signals-2020/articles/land-and-soil-pollution>. Accessed 7 Mar 2021
- Ekellund NGA, Häder D-P (2018) Environmental monitoring using bioassays. In: *Bioassays*, pp 419–437. <https://doi.org/10.1016/B978-0-12-811861-0.00021-8>
- Erktan A, Or D, Scheu S (2020) The physical structure of soil: determinant and consequence of trophic interactions. *Soil Biol Biochem* 148:107876. <https://doi.org/10.1016/j.soilbio.2020.107876>
- Escher BI, Hacker Müller J, Polte T et al (2017) From the exposome to mechanistic understanding of chemical-induced adverse effects. *Environ Int* 99:97–106. <https://doi.org/10.1016/j.envint.2016.11.029>

- Ezeokoli OT, Bezuidenhout CC, Maboeta MS, Khasa DP, Adeleke RA (2020) Structural and functional differentiation of bacterial communities in post-coal mining reclamation soils of South Africa: bioindicators of soil ecosystem restoration. *Sci Rep* 10(1):1759. <https://doi.org/10.1038/s41598-020-58576-5>
- Fazekašová D, Fazekaš J (2020) Soil Quality and heavy metal pollution assessment of iron ore mines in Nizna Slana (Slovakia). *Sustainability* 12(6):2549. <https://doi.org/10.3390/su12062549>
- Fent K (2004) Ecotoxicological effects at contaminated sites. *Toxicology* 205(3):223–240. <https://doi.org/10.1016/j.tox.2004.06.060>
- Finn D, Kopittke PM, Dennis PG, Dalal RC (2017) Microbial energy and matter transformation in agricultural soils. *Soil Biol Biochem* 111:176–192. <https://doi.org/10.1016/j.soilbio.2017.04.010>
- Giller KE, Witter E, Mcgrath SP (1998) Toxicity of heavy metals to microorganisms and microbial processes in agricultural soils: a review. *Soil Biol Biochem* 30(10–11):1389–1414. [https://doi.org/10.1016/S0038-0717\(97\)00270-8](https://doi.org/10.1016/S0038-0717(97)00270-8)
- Gorobtsova ON, Gedgafova FV, Uligova TS, Tembotov RK (2016) A comparative assessment of the biological properties of soils in the cultural and native cenoses of the Central Caucasus (using the example of the Terskii variant of altitudinal zonation in Kabardino-Balkaria). *Eurasian Soil Sci* 49(1):89–94. <https://doi.org/10.1134/S1064229316010063>
- GOST 17.4.4.02-2017 (2018) Nature protection. Soils. Methods for sampling and preparation of soil for chemical, bacteriological, helminthological analysis (Методы отбора и подготовка проб для химического, бактериологического и гельминтологического анализа). Moscow, 12 p
- GOST R ISO 22030-2009 (2010) Biological methods. Chronic phytotoxicity against higher plants (Хроническая фитотоксичность в отношении высших растений) Moscow, Standard Inform, p 20
- Haferburg G, Kothe E (2007) Microbes and metals: interactions in the environment. *J Basic Microbiol* 47:453–467. <https://doi.org/10.1002/jobm.200700275>
- Hansen P-D (2018) Applications for the real environment. In: Häder D-P, Erzinger GS (eds) *Bioassays*, pp 403–418. <https://doi.org/10.1016/B978-0-12-811861-0.00020-6>
- Huera-Lucero T, Labrador-Moreno J, Blanco-Salas J, Ruiz-Téllez T (2020) A framework to incorporate biological soil quality indicators into assessing the sustainability of territories in the Ecuadorian Amazon. *Sustainability* 12(7):3007. <https://doi.org/10.3390/su12073007>
- Incardona JP, Carls MG, Teraoka H, Sloan CA, Collier TK, Scholz NL (2005) Aryl hydrocarbon receptor-independent toxicity of weathered crude oil during fish development. *Environ Health Perspect* 113:1755–1762. <https://doi.org/10.1289/ehp.8230>
- Kapelkina LP, Bardina TV, Bakin LG, Chugunova MV, Gerasimov AO (2009) Methods for measuring seed germination and root length of seedlings of higher plants to determine the toxicity of technogenically polluted soils (Методика выполнения измерений всхожести семян и длины корней проростков высших растений для определения токсичности техногенно загрязненных почв) FR 1.39.2006.02264, p 19
- Konstantinova E, Minkina T, Sushkova S, Antonenko E, Konstantinov A (2020) Levels, sources, and toxicity assessment of polycyclic aromatic hydrocarbons in urban topsoils of an intensively developing Western Siberian city. *Environ Geochem Health* 42:325–341. <https://doi.org/10.1007/s10653-019-00357-9>
- Lenart-Boroń A, Boroń P (2014) The effect of industrial heavy metal pollution on microbial abundance and diversity in soils—a review. *Environ Risk Assess Soil Contam. Maria C. Hernandez-Soriano*, IntechOpen. <https://doi.org/10.5772/57406>
- Liu X, Chen S, Yang Z et al (2018) Will heterotrophic soil respiration be more sensitive to warming than autotrophic respiration in subtropical forests? *Eur J Soil Sci* 70(3):655–663. <https://doi.org/10.1111/ejss.12758>
- Lors C, Ponge J-F, Aldaya MM (2010) Comparison of solid-phase bioassays and ecoscores to evaluate the toxicity of contaminated soils. *Environ Pollut* 158(8):2640–2647. <https://doi.org/10.1016/j.envpol.2010.05.005>
- Luo Y, Zhou X (2006) *Soil respiration and the environment*. Academic Press, pp 328
- Matejczyk M, Grazyna AP, Nalecz-Jawecki G, Ulfig K, Markowska-Szczupak A (2011) Estimation of the environmental risk posed by landfills using chemical, microbiological and ecotoxicological testing of leachates. *Chemosphere* 82:1017–1023. <https://doi.org/10.1016/j.chemosphere.2010.10.066>
- Materu SF, Heise S (2019) Eco-toxicity of water, soil, and sediment from agricultural areas of Kilombero Valley Ramsar wetlands, Tanzania. *Ecosyst Health Sustain* 5(1):256–269. <https://doi.org/10.1080/20964129.2019.1695545>
- Mineev VG (2001) *Workshop on agricultural chemistry: textbook*. Moscow State University Publ., pp 689 (Практикум по агрохимии: Учеб. Пособие, с. 689)
- MR 2.1.7.2297-07 (2007) Justification of the hazard class of production and consumption waste by phytotoxicity. Methodical recommendations, Federal Service for Supervision of Consumer Rights Protection and Human Welfare, 30 p. (MP 2.1.7.2297–07, Методические рекомендации. 2.1.7. Почва. Очистка населенных мест. Бытовые и промышленные отходы. Санитарная охрана почвы. Обоснование класса опасности отходов производства и потребления по фитотоксичности). <https://docs.cntd.ru/document/1200061157>
- MUK 4.1.1061-01 (2013) Chromatographic-mass spectrophotometric determination of volatile substances in soil and in industrial and consumption wastes (МУК 4.1.1061–01. Хромато-масс-спектрометрическое определение летучих органических веществ в почве и отходах производства и потребления. 4.1.

- Методы контроля. Химические факторы). <https://files.stroyinf.ru/Data2/1/4294814/4294814993.htm>
- Nannipieri P, Giagnoni L, Renella G et al (2012) Soil enzymology: classical and molecular approaches. *Biol Fertil Soils*. 48:743–762. <https://doi.org/10.1007/s00374-012-0723-0>
- Nikolaeva OV, Terekhova VA (2017) Improvement of laboratory phytotesting for ecotoxicological assessment of soil. *Eurasian Soil Sci* 50:1105–1114. <https://doi.org/10.1134/S1064229317090058>
- Niss F, Rosenmai AK, Mandava G et al (2018) Toxicity bioassays with concentrated cell culture media—a methodology to overcome the chemical loss by conventional preparation of water samples. *Environ Sci Pollut Res* 25:12183–12188. <https://doi.org/10.1007/s11356-018-1656-4>
- Odum EP, Barrett GW (2004) *Fundamentals of ecology*, 5th edn. Brooks Cole, Belmont, CA, pp 624
- Olsson L, Barbosa H, Bhadwal S, Cowie A, Deluska K, Flores-Renteria D, Hermans K, Jobbagy E, Kurz W, Li D, Sonwa DJ, Stringer L (2019) Land degradation. In: Shukla PR, Skea J, Calvo Buendia E, Masson-Delmotte V, Pörtner H-O, Roberts DC, Zhai P, Slade R, Connors S, van Diemen R, Ferrat M, Haughey E, Luz S, Neogi S, Pathak M, Petzold J, Portugal Pereira J, Vyas P, Huntley E, Kissick K, Belkacemi M, Malley J (eds) *Climate change and land: an IPCC special report on climate change, desertification, land degradation, sustainable land management, food security, and greenhouse gas fluxes in terrestrial ecosystems*. In press. https://www.ipcc.ch/site/assets/uploads/sites/4/2019/11/07_Chapter-4.pdf. Accessed 7 Mar 2021
- Pantani O, Fioravanti F, Stefanini FM et al (2020) Accounting for soil respiration variability—case study in a Mediterranean pine-dominated forest. *Sci Rep* 10:1787. <https://doi.org/10.1038/s41598-020-58664-6>
- Piotrowska-Seget Z, Cyoń M (2005) Kozdrój J (2005) Metal-tolerant bacteria occurring in heavily polluted soil and mine spoil. *Appl Soil Ecol* 28:237–246. <https://doi.org/10.1016/j.apsoil.2004.08.001>
- Pitulko VM (2013) Man-made systems and environmental risk. (Техногенные системы и экологический риск). “Academy” Publishing House, 357 p
- Plaza G, Nałęcz-Jawecki G, Pinyakong O, Illmer P (2010) Ecotoxicological and microbiological characterisation of soils from heavy metal and hydrocarbon contaminated sites. *Environ Monit Assess* 163:477–488. <https://doi.org/10.1007/s10661-009-0851-7>
- PND F16.1:2.3:3.11-98 (2005). Method of measuring the content of metals in solid objects by the method of spectrometry with inductive-binded plasma (ПНД Ф 16.1:2.3:3.11-98 Методика выполнения измерений содержания металлов в твердых объектах методом спектрометрии с индуктивно-связанной плазмой). <https://meganorm.ru/Data2/1/4293777/4293777593.pdf>
- Power EA, Boumphrey RS (2004) International trends in bioassay use for effluent management. *Ecotoxicology* 13(5):377–398. <https://doi.org/10.1023/B:ECTX.0000035290.89590.03>
- Rakshith D, Santosh P, Pradeep TP, Gurudatt DM, Baker S, Rao HY, Pasha A, Satish S (2016) Application of bioassay-guided fractionation coupled with a molecular approach for the dereplication of antimicrobial metabolites. *Chromatographia* 79(23–24):1625–1642. <https://doi.org/10.1007/s10337-016-3188-8>
- Ribe V, Auleniusa E, Nehrenheima M, Martellb U, Odlarea M (2012) Applying the Triad method in a risk assessment and metal industry site. *J Hazard Mater* 207–208(15):15–20. <https://doi.org/10.1016/j.jhazmat.2011.07.120>
- Rodríguez-Eugenio N, McLaughlin M, Pennock D (2018) Soil pollution: a hidden reality. Rome, FAO, 142 pp. <http://www.fao.org/3/i9183en/i9183en.pdf>
- Ryan MG, Law BE (2005) Interpreting, measuring, and modeling soil respiration. *Biogeochemistry* 73:3–27. https://www.fs.fed.us/rm/pubs_other/rmrs_2005_ryan_m001.pdf. Accessed 7 Mar 2021
- Saljnikov E, Mrvić V, Čakmak D, Jaramaz D, Perović V, Antić-Mladenović S, Pavlović P (2019) Pollution indices and sources apportionment of heavy metal pollution of agricultural soils near the thermal power plant. *Environ Geochem Health*. <https://doi.org/10.1007/s10653-019-00281-y> Online ISSN 1573-2983pp. 5-15
- Saljnikov E, Čakmak D, Koković N, Stajković-Srbinić O, Mrvić V, Perović V, Sikirić B (2017a) Soil respiration and main soil characteristics on different types of soils in west Serbia. *Zemljiste I Biljka* 63(2):1–10. http://www.sdpz.rs/images/casopis/2014/ZIB_vol63_no2_2014_pp1-10.pdf
- Saljnikov E, Čakmak D, Muhanbet A, Kresović M (2017b) Biological indices of soil organic matter in long term fertilisation experiment. *Zemljiste I Biljka* 63(2):11–20. http://www.sdpz.rs/images/casopis/2014/ZIB_vol63_no2_2014_pp11-20.pdf
- SANPIN 2.1.7.1287-03 (2003) Sanitary and epidemiological requirements for soil quality (Санитарно-эпидемиологические требования к качеству почвы). Moscow, p 12
- Schlöter M, Nannipieri P, Sørensen SJ, van Elsas JD (2018) Microbial indicators for soil quality. *Biol Fertil Soils* 54(29). <https://doi.org/10.1007/s00374-017-1248-3>
- SOER (2020) Land and soil. The European Environment State and Outlook 2020. <https://www.eea.europa.eu/publications/soer-2020>. Accessed 7 Mar 2021
- Soil Survey Staff. 2014. Soil Survey Staff (2014) Keys to soil taxonomy, 12th edn. USDA-Natural Resources Conservation Service, Washington, DC
- Solomon KR, Brock TCM, De Zwart D et al (2008) Extrapolation in the context of criteria setting and risk assessment. Extrapolation practice for ecotoxicological effect characterization of chemicals. SETAC Press & CRC Press, Boca Raton, FL, USA, pp 1–32

- Terekhova VA (2011) Soil bioassay: problems and approaches. *Eurasian Soil Sci* 44(2):173–179. <https://doi.org/10.1134/S1064229311020141>
- Terekhova VA, Pukalchik MA, Yakovlev AS (2014) The triad approach to ecological assessment of urban soils. *Eurasian Soil Sci* 47(9):952–958. <https://doi.org/10.1134/S1064229314090129>
- Terekhova VA, Voronina LP, Nikolaeva OV, Bardina TV, Kalmatskaya OA, Kiryushina AP, Uchanov PV, Kreslavsky VD, Vasilieva GK (2016) The use of phytotesting for solving problems of ecological soil science. *Bulletin “The use and protection of natural resources in Russia”* 3:37–41 (Терехова В.А., Воронина Л.П., Николаева О.В., Бардина Т.В., Калмацкая О.А., Кирюшина А.П., Учанов П.В., Креславский В.Д., Васильева Г.К. Применение фитотестирования для решения задач экологического почвоведения // Использование и охрана природных ресурсов в России. 2016. № 3. с. 37–41)
- Terekhova VA (2012) Realisation of the biotic concept of environmental control in soil-ecological regulation (Реализация биотической концепции экологического контроля в почвенно-экологическом нормировании) *Use and protection of natural resources in Russia* 4:31–34
- Thiele-Bruhn S, Schlöter M, Wilke B-M, Beaudette LA, Martin-Laurent F, Cheviron N, Mougin Ch, Römbke J (2020) Identification of new microbial functional standards for soil quality assessment. *Soil* 6:17–34. <https://doi.org/10.5194/soil-6-17-2020>
- Timofeev IV, Shartova N, Kosheleva N, Kasimov N (2019) Potential toxic elements in topsoils and health risk assessment for the mining W–Mo centre in the Baikal region. In: EGU2018 “Soil contamination and human health: advances and problems of risk assessment”, the European Geosciences Union (EGU) Conference held in Vienna, April 2018
- Tonkes M, den Besten PJ, Leverett D (2016) Bioassays and tiered approaches for monitoring surface water quality and effluents. In: den Besten PJ, Munawar M (eds) *Ecotoxicological testing of marine and freshwater ecosystems: emerging techniques, trends and strategies*. CRC Press, Boca Raton, pp 57–100. <https://doi.org/10.1201/9781420037500>
- Wadhia K, Thompson KC (2007) Low-cost ecotoxicity testing of environmental samples using microbiotests for potential implementation of the water framework directive. *TrAC Trends Anal Chem* 26(4):300–307. <https://doi.org/10.1016/j.trac.2007.01.011>
- Wang Ch, Liu D, Bai E (2018) Decreasing soil microbial diversity is associated with decreasing microbial biomass under nitrogen addition. *Soil Biol Biochem* 120:126–133. <https://doi.org/10.1016/j.soilbio.2018.02.003>
- Warner DL, Bond-Lamberty B, Jian J, Stell E, Vargas R (2019) Spatial predictions and associated uncertainty of annual soil respiration at the global scale. *Glob Biogeochem Cycles* 33(12):1733–1745. <https://doi.org/10.1029/2019GB006264>
- WRB (2015) IUSS Working Group WRB. 2015. World reference base for soil resources 2014, update 2015 international soil classification system for naming soils and creating legends for soil maps. *World Soil Resources Reports No. 106*. FAO, Rome, p 192
- Yakovlev AS, Evdokimova MV (2011) Ecological standardisation of soil and soil quality control. *Eur Soil Sci* 44(5):534–546. <https://doi.org/10.1134/S1064229311050152>
- Zhao P, Pumpanen J, Kang Sh (2020) Spatio-temporal variability and controls of soil respiration in a furrow-irrigated vineyard. *Soil Tillage Res* 196:104424. <https://doi.org/10.1016/j.still.2019.104424>



Methodology for the Preparation and Study of Multicomponent Certified Reference Materials for Soils Contaminated with Heavy Metals

Galina A. Stupakova, Elena E. Ignateva,
Tatyana I. Shchiplitsova,
and Dmitrii K. Mitrofanov

Abstract

A procedure was developed for preparing certified reference materials (CRMs) for the composition of the matrix of natural soils containing mobile heavy metals in concentrations exceeding their background levels. The procedure for preparing soil CRMs includes sampling soil under natural conditions, drying, grinding and sieving it, mixing it thoroughly for homogenisation, preparing a water solution with pre-set concentrations of heavy metal salts, mixing the soil with a solution of heavy metal salts, and evaporating water at 105 °C. The metrological characteristics of CRMs—homogeneity and stability over time—were determined, and factors affecting the homogeneity of CRMs were revealed: the soil type and texture, the nature of the pollutant, and the pH of the metal solution. An estimate was made of how the heterogeneous distribution of different elements contributed to the error in the CRM values. The contents of copper, zinc, lead, cadmium, nickel, cobalt, and mercury in CRMs were certified in an

intra-laboratory study with the participation of 57 accredited Russian laboratories.

Keywords

Reference material · Metrological supply · Heavy metals · Homogeneity · Stability

16.1 Introduction

The acquisition of reliable information and new knowledge on the soil requires the metrological support of analytical measurements, including the use of certified reference materials (CRMs) for soil composition. The provision of CRMs should be considered depending on the specific analytical needs (method and object) and their application range (calibration, procedure validation, intra-laboratory control, qualification assessment). Each method has a specific measuring range. In a number of methods used to determine mobile and acid-soluble metals in the soil (Stupakova et al. 2018), the lower determination limits for some metals (copper, lead, zinc) are based on their maximum permissible concentrations (MPCs) rather than the actual contents of elements in the soil.

Although a wide range of CRMs have been developed for metals in the soil, some methods require CRMs in which the analytical ranges of heavy metals exceed their contents in natural

G. A. Stupakova (✉) · E. E. Ignateva ·
T. I. Shchiplitsova · D. K. Mitrofanov
Pryanishnikov All-Russian Research Institute
of Agrochemistry, Pryanishnikova str. 31, 127550
Moscow, Russia
e-mail: vniiia@list.ru

soils and sometimes their MPCs, but these cannot be provided. In these cases, the matrix of CRMs is unsuitable for inter-laboratory testing of procedures used to measure the mass fractions of mobile and acid-soluble metals. No soil CRMs with the certified concentrations of metals are available for the following metal ranges (ppm): mobile metal forms: copper, from 2.0 to 30.0; zinc, from 3.0 to 30.0; lead, from 5.0 to 25.0; and cadmium, from 1.0 to 7.0; acid-soluble metal forms: copper and zinc, from 20 to 1000; lead, from 10.0 to 3000; and cadmium, from 1.0 to 100 ppm (Stupakova et al. 2017).

Different mechanisms and forms of binding heavy metals exist in soils because of the diversity of soil types, their redox and acid–base properties, and their sorption capacities. Heavy metal compounds coming into the soil are decomposed by soil organic acids, sorbed by soil exchange complex (SEC) components, or precipitated in the form of insoluble salts, depending on the soil conditions. For example, some heavy metals form insoluble or low-soluble sulphides under acid reduction conditions; however, lead, nickel, cobalt, copper, zinc, cadmium and mercury form relatively mobile forms under these conditions (Glazovskaya and Bogdanova, <https://soilatlas.ru>). The fixation of metals in the soil is mainly due to organic matter, clay minerals, and iron and manganese hydroxides. Humus-enriched soils (Chernozems) have the maximum sorption capacity for pollutants, and soils with a light texture and a thin humus horizon, e.g., podzolic soils, have the minimum sorption capacity. Soddy-podzolic soils are characterised by a medium sorption capacity (Krechetov and Alyabina, <https://soilatlas.ru>).

The metrological support of agroindustrial-complex laboratories involves their provision with CRMs, including the development of new types of multicomponent CRMs, the matrix of which is as close as possible to the matrix of the test object (soil) and which contain pollutants (heavy metals) in concentrations exceeding the ranges found in natural soils.

The diversity of soil types and textures causes problems when selecting the most suitable matrix to prepare multicomponent CRMs, i.e., soil for

simultaneous enrichment with several heavy metals. Additional soil CRMs are required with a homogeneous composition and containing mobile heavy metals in concentrations exceeding the background level. Such multicomponent CRMs are suitable for testing the measurement procedures used to determine toxicants in the soil.

16.2 Materials and Methods

The following soil types from the register of CRMs composed by the Pryanishnikov All-Russian Research Institute of Agrochemistry were used as natural matrices for the preparation of CRMs: podzolic soil (Podzol); loamy sandy, loamy, and silty loamy soddy-podzolic soil (Umbric Albeluvisol); silty loamy light-grey forest soil (Albic Phaeozem); sandy loamy, loamy, and silty loamy leached Chernozem (Luvic Chernozem); sandy loamy, loamy, and silty loamy calcareous Chernozem (Calcic Chernozem); sandy loamy podzolised Chernozem (Luvic Phaeozem); and loamy and silty loamy ordinary Chernozem (Haplic Chernozem).

The soils were dried in the air and milled on a soil mill to a particle size of no more than 1 mm; samples of 2 kg were then collected. The following procedure was used. A water solution was prepared containing the following salts: $\text{Cu}(\text{NO}_3)_2$, $\text{Zn}(\text{NO}_3)_2$, $\text{Pb}(\text{NO}_3)_2$, $\text{Cd}(\text{NO}_3)_2$, $\text{Ni}(\text{NO}_3)_2$, $\text{Co}(\text{NO}_3)_2$ and $\text{Hg}(\text{NO}_3)_2$. For this purpose, the calculated concentrations of heavy metal nitrates in 0.1–1 N nitric acid were prepared; the calculated volumes of these solutions were mixed and diluted with distilled water to obtain a total volume sufficient to completely wet the soil, but without a water layer forming over the soil surface. The solution pH was adjusted to ~ 2.5 by adding water or nitric acid, if necessary. This pH was used because basic metal salts can begin to precipitate at a $\text{pH} > 3$; in addition, a $\text{pH} \sim 2.5$ is the “natural” limit for acid rain, especially in regions of high anthropogenic pollution. The soil was mixed with the prepared solution under permanent stirring for ~ 20 min. to avoid the formation of dry-soil

or solution zones. The wet soil was thoroughly mixed again and dried in an oven at 105 °C until it reached a constant weight (~ 30 h). The dried soil was milled on a laboratory mill, passed through a 1-mm sieve, and thoroughly mixed to prevent possible stratification.

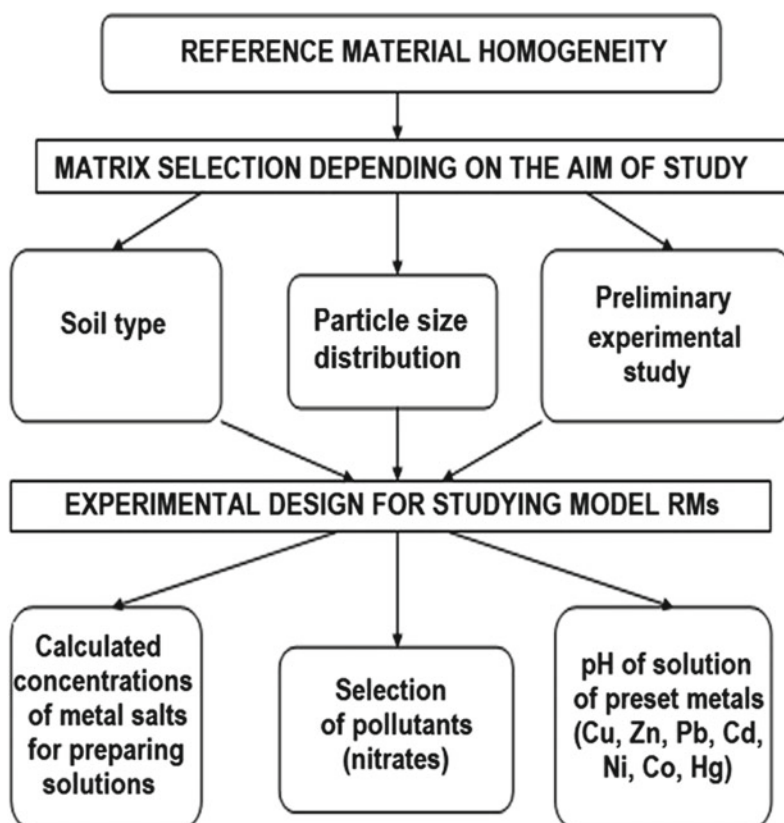
The metrological characteristics of reference materials (RMs) (homogeneity, stability, certified value, standard uncertainty of the certified value) were determined according to the corresponding standards: GOST ISO Guide 35-2015 (2017) and RMG 93-2015 (2016). The homogeneity of RMs was studied before the beginning of certification tests. The homogeneity of CRMs TM-04-18 and TM-05-18 was estimated for each certified parameter. The contents of mobile heavy metals in soil RMs were determined in an inter-laboratory study (GOST 2003) with the participation of 57 accredited test laboratories. Mobile

heavy metals were determined by atomic absorption analysis (RD 1990; M-MVI-80-2008 (2008)).

16.3 Results

Homogeneity, i.e., the uniformity of properties in all parts, is an essential quality parameter of CRMs. Determining RM homogeneity allows a component of the certified value uncertainty (error) to be estimated. This uncertainty component can vary significantly depending on the nature of the RM. During experimental studies, a set of factors affecting the homogeneity of soil RMs was revealed (Scheme 16.1). These are the type and texture of soil, the occurrence form of pollutant, and the pH of the metal solution.

Scheme 16.1 Factors affecting the homogeneity of RMs



It was found that light- and medium-textured soddy-podzolic soils are suitable matrices for model RMs contaminated with heavy metals. Chernozemic soils sorb mercury, lead, and cadmium well, but they are heterogeneous in composition, because heavy metals form poorly soluble compounds (sulphides, phosphates, etc.) under neutral and alkaline conditions, which are difficult to homogenise in the soil. Heavy soils with a high content of clay minerals sorb zinc well, but these soils are heterogeneous because of their high coherence.

A set of CRMs for loamy soddy-podzolic soil with high contents of heavy metals (TM-04-18 and TM-05-18) was prepared according to Patent RU No. 2660861 of 10 July 2018 (Method for preparing certified reference materials for soil contaminated with heavy metals) (Patent RU No. 2660861 2018). The volumes of experimental studies on the estimation of RM homogeneity and stability are given in Table 16.1.

To characterise the homogeneity of prepared RMs, the distribution heterogeneity was estimated for seven certified elements from the experimental data. The homogeneity parameter was calculated using the contents of heavy metals in a set of 13 samples analysed in six replicates by an accredited test laboratory. The standard uncertainty (error) of RM due to material heterogeneity and the total standard

uncertainty of the certified RM value were calculated (Table 16.2).

To estimate how the distribution heterogeneity of each element (copper, zinc, lead, cadmium, nickel, cobalt, and mercury) affects the total standard uncertainty (error) of the certified value, the contribution of heterogeneity uncertainty to the total standard uncertainty of the certified value was calculated (Table 16.3). The contribution of heterogeneity to the error in the certified value for copper, cobalt, and nickel in CRM TM-04-18 was found to be insignificant: 2.1–5.3%. The distributions of cadmium, lead, and zinc in the RMs studied are the least homogeneous (their contributions vary from 21.1 to 25.6%). In CRM TM-05-18, the contribution of the distribution heterogeneity of cobalt, nickel, copper, zinc, and lead to an error in the certified value varying from 36 to 24.4%. The distribution heterogeneity of mercury is similar in both CRMs (from 11.8 to 13.8%).

When the results of the experimental estimation of homogeneity for the studied CRMs was statistically processed, this showed that the CRM error, taking into account the inhomogeneity error, does not exceed the permissible error of the certified value for all certified parameters of TM-04-18 and TM-05-18. Thus, material of RMs is homogeneous with respect to all parameters studied (Table 16.2).

Table 16.1 Study and estimation of metrological parameters used to test the procedure for preparing, studying and certifying RMs for soil composition

Certified parameters: mobile copper, zinc, lead, cadmium, nickel, cobalt, mercury ^a	Extractant: ammonium acetate buffer with pH 4.8	
	CRM TM-04-18 ^b	CRM TM-05-18 ^b
Number of homogeneity tests ^c	546	546
Number of stability tests ^d	120 (Cd, Ni, Co)	90 (Cd, Co)
Total number of tests for all parameters in the inter-laboratory study	399	399
Number of interlaboratory study participants	57	57

^aCold vapour atomic absorption spectrometry was used for mercury

^bMatrix: loamy soddy-podzolic soil

^cMultiple measurements of 7 certified parameters (13 samples in 6 replicates per parameter)

^dStudy of the most unstable certified parameters (30 samples for each unstable parameter over a period of 2.5 years)

Note CRM TM-04-18, CRM TM-05-18 soil CO indices; CO-certified object

Table 16.2 Estimation of heterogeneity error (S_h) in the certification of RM

Parameter	Certified value \hat{A}	Certification error $\Delta_{\hat{A}}$	Standard uncertainty due to heterogeneity of certified value, S_h	Total standard uncertainty of certified value D_{cert}	Permissible error of certified value, Δ_p
<i>CRM TM-04-18</i>					
Copper, ppm	2.81	0.09	0.004	0.090	0.28
Zinc, ppm	10.2	0.43	0.128	0.500	1.02
Lead, ppm	12.2	0.71	0.172	0.789	1.22
Cadmium, ppm	5.38	0.18	0.042	0.199	0.54
Nickel, ppm	2.93	0.13	0.007	0.131	0.29
Cobalt, ppm	2.29	0.14	0.003	0.140	0.23
Mercury, ppm	0.84	0.084	0.012	0.087	0.11
<i>CRM TM-05-18</i>					
Copper, ppm	10.40	0.32	0.123	0.404	1.04
Zinc, ppm	2.48	0.07	0.026	0.087	0.25
Lead, ppm	16.3	0.54	0.151	0.619	1.63
Cadmium, ppm	2.38	0.12	0.028	0.132	0.24
Nickel, ppm	8.40	0.36	0.150	0.469	0.84
Cobalt, ppm	7.34	0.20	0.104	0.289	0.73
Mercury, ppm ⁻¹	0.61	0.050	0.006	0.051	0.08

Table 16.3 Contribution of the heterogeneity of metal distribution to the total CRM error

Metrological parameter	Metrological parameter values, ppm, for parameters						
	Copper	Zinc	Lead	Cadmium	Nickel	Cobalt	Mercury
<i>CRM TM-04-18</i>							
S_h	0.004	0.128	0.172	0.042	0.007	0.003	0.012
D_{cert}	0.090	0.500	0.789	0.199	0.131	0.140	0.087
Contribution of heterogeneity uncertainty (error) to the total error of the CRM value, %	4.4	25.6	21.8	21.1	5.3	2.1	13.8
<i>CRM TM-05-18</i>							
S_h	0.123	0.026	0.151	0.028	0.150	0.104	0.006
D_{cert}	0.404	0.087	0.619	0.132	0.469	0.289	0.051
Contribution of heterogeneity uncertainty (error) to the total error of the CRM value, %	30.4	29.9	24.4	21.2	32.0	36.0	11.8

Table 16.4 Results of analysis for estimating the stability of mobile cobalt, ppm

CRM TM-04-18		Permissible value range		α	Δ_T	U_n	R_n	$n * U_n + 1$
X_{cert}	X_1	X_2	α	Δ_T	$(1 - \varphi)U_n - 1$	U_n	R_n	$n * U_n + 1$
2.29	1.60	2.98	0.2	0.15				
Measurement no., n	Measurement result, X_n	Difference, d_n	$\alpha * d_n$					
1	2.29	0.00	0	0	0	0		0.002
2	2.30	0.01	0.002	0.000	0.000	0.002	0.002	-0.021
3	2.23	-0.06	-0.012	0.002	0.002	-0.010	0.012	-0.013
4	2.31	0.02	0.004	-0.008	-0.008	-0.004	0.006	0.074
5	2.40	0.11	0.022	-0.003	-0.003	0.019	0.023	0.154
6	2.37	0.08	0.016	0.015	0.015	0.031	0.012	-0.224
7	1.98	-0.31	-0.062	0.025	0.025	-0.037	0.068	-0.335
8	2.20	-0.09	-0.018	-0.030	-0.030	-0.048	0.011	-0.290
9	2.30	0.01	0.002	-0.038	-0.038	-0.036	0.012	-0.009
10	2.43	0.14	0.028	-0.029	-0.029	-0.001	0.035	0.012
11	2.30	0.01	0.002	-0.001	-0.001	0.001	0.002	0.450
12	2.49	0.20	0.040	0.001	0.001	0.041	0.040	0.513
13	2.34	0.05	0.010	0.033	0.033	0.043	0.002	0.913
14	2.47	0.18	0.036	0.034	0.034	0.070	0.027	0.842
15	2.31	0.02	0.004	0.056	0.056	0.060	0.010	0.332
16	2.16	-0.13	-0.026	0.048	0.048	0.022	0.038	-0.645
17	2.00	-0.29	-0.058	0.018	0.018	-0.040	0.062	-0.786
18	2.22	-0.07	-0.014	-0.032	-0.032	-0.046	0.006	0.000
	Raw	a	Su	Sa		Quantile $t_{0.95; a}$	t_{cert}	0.969
			0.019	0.0012		1.73	0.30	T(years)
	0.022	0.0003						6.2
CRM TM-05-18		Permissible value range		α	Δ_T	U_n	R_n	$n * U_n + 1$
X_{cert}	X_1	X_2	α	Δ_T	$(1 - \varphi)U_n - 1$	U_n	R_n	$n * U_n + 1$
7.34	5.14	9.54	0.2	0.49				
Measurement no., n	Measurement result, X_n	Difference, d_n	$\alpha * d_n$					
1	7.34	0.00	0	0	0	0		0.118
2	7.93	0.59	0.118	0.000	0.000	0.118	0.118	0.001

(continued)

Table 16.4 (continued)

CRM TM-04-18																	
3	6.87	-0.47	-0.094	0.094	0.000	0.118	0.157										
4	7.60	0.26	0.052	0.000	0.052	0.052	0.119										
5	7.28	-0.06	-0.012	0.042	0.030	0.022	0.409										
6	7.63	0.29	0.058	0.024	0.082	0.052	-0.255										
7	6.80	-0.54	-0.108	0.066	-0.042	0.124	-0.224										
8	7.35	0.01	0.002	-0.034	-0.032	0.010	-1.453										
9	6.56	-0.78	-0.156	-0.026	-0.182	0.150	-1.325										
10	7.33	-0.01	-0.002	-0.145	-0.147	0.034	-0.458										
11	7.70	0.36	0.072	-0.118	-0.046	0.101	-0.447										
12	7.32	-0.02	-0.004	-0.037	-0.041	0.005	-0.654										
13	7.23	-0.11	-0.022	-0.033	-0.055	0.014	-0.723										
14	7.28	-0.06	-0.012	-0.044	-0.056	0.001	0.805										
15	7.85	0.51	0.102	-0.044	0.058	0.113	2.430										
16	7.92	0.58	0.116	0.046	0.162	0.104	-0.742										
17	6.46	-0.88	-0.176	0.130	-0.046	0.208	-3.317										
18	6.55	-0.79	-0.158	-0.037	-0.195	0.149	-0.000										
	Rav	a	Su	Sa	Quantile $t_{(n-1)}$: 0.95 a	t_{last}	T(years)										
	0.081	-0.0020	0.072	0.0043	1.73	0.46	5.4										

Note: dh—time instability error d
 X—the result of measuring the attested characteristic of CO at the n-th moment of time
 Xj—the first result obtained when studying CO stability
 σ —coefficient selected depending on the standard deviation of the random error of the measurement procedure (value from the table)
 Δ —permissible error from instability to determine the expiry date of a CO specimen
 Un—smoothed value of the difference in measurement results at a time n (n = 18)
 Rn—sliding span
 R—average span
 a—coefficient of linear dependence of the error on instability
 Su—standard deviation of smoothed estimates calculated from the mean span R
 Sa—standard deviation of the coefficient a

Table 16.5 Values of CRMs of soil contaminated with heavy metal salts

Certified parameter	Certified value and absolute expanded uncertainty (error) of the certified value	
	loamy soddy-podzolic soil	
	CRM TM-04-18	CRM TM-05-18
	Mass fractions of mobile metals and mercury	
Copper, ppm	2.81 ± 0.09	10.4 ± 0.4
Zinc, ppm	10.2 ± 0.5	2.48 ± 0.09
Lead, ppm	12.2 ± 0.8	16.3 ± 0.6
Cadmium, ppm	5.38 ± 0.20	2.38 ± 0.13
Nickel, ppm	2.93 ± 0.16	8.40 ± 0.47
Cobalt, ppm	2.29 ± 0.14	7.34 ± 0.29
Mercury, ppm	0.84 ± 0.09	0.61 ± 0.05

The stability of RMs was estimated from the results of periodical testing of the certified values over a period of 2.5 years for the most unstable component: the content of mobile cobalt. Experimental studies were performed, and the results processed to estimate the uncertainty due to instability according to State regulations (R 50.2.031-2003 2003) (Table 16.4).

The lifetimes of CRMs were determined: 62 months for TM-04-18 and 54 months for TM-05-18. For the certification of RMs, their material was sent out to 57 accredited laboratories of Russia. The values of CRMs and the uncertainties of the certified values are given in Table 16.5.

The traceability of the results of an intra-laboratory study on SI units is achieved using calibrated instruments by competent test laboratories, including those accredited for conformance to the requirements of GOST ISO/IEC 17025 and strictly following measurement procedures according to RD 52.18.289 and M-MVI-80-2008 (M-MVI-80-2008 2008; RD 52.18.289-90 2009).

16.4 Conclusions

1. A procedure was developed for preparing reference materials for soils contaminated with heavy metals, and a patent was filed.
2. A set of multicomponent soil RMs (TM-04-18 and TM-05-18) certified for toxicological

parameters (copper, zinc, lead, cadmium, nickel, cobalt, and mercury) was developed.

3. In the developed certified reference materials (CRMs), the contribution of the distribution heterogeneity of different elements to the error of the certified value was estimated.
4. These CRMs were developed based on the matrix of natural soil and containing mobile heavy metals typical of contaminated agricultural lands, in concentrations exceeding the background level, with homogeneous RM properties and stable RMs over time. They are designed for laboratories of agroindustrial complexes and other sectors of the economy to test the quality of measurements of heavy metals in soils.

References

- Glazovskaya MA, Bogdanova MD. Soil horizons as geochemical barriers. Electronic version of the National Atlas of Soils of Russian Federation, pp 248–249. (Почвенные горизонты как геохимические барьеры. Электронная версия Национального атласа почв Российской Федерации. С. 248–249; Информационная система Почвенно-географическая база данных России). <https://soilatlas.ru>. Accessed 7 Mar 2021
- GOST 8.532-2002 (2003) State system for ensuring the uniformity of measurements. Certified reference materials of composition of substances and materials (Государственная система обеспечения единства

- измерений. Сертифицированные стандартные образцы состава веществ и материалов) Interlaboratory metrological certification. Content and order of works. Moscow
- GOST ISO Guide 35-2015 (2017) Reference materials. General and statistical principles for certification. Moscow (Стандартные образцы. Общие и статистические принципы сертификации). <http://docs.cntd.ru/document/1200127745>. Accessed 7 Mar 2021
- Krechetov PP, Alyabina IO. Sorption functions of soils. Electronic version of the National Atlas of Soils of Russian Federation, pp 246–247. (Сорбционные функции почв. Информационная система Почвенно-географическая база данных России). <https://soilatlas.ru>. Accessed 7 Mar 2021
- M-MVI-80-2008 (2008) Procedure for measuring the mass fractions of elements in soils, grounds, and bottom sediments by atomic-emission and atomic-absorption spectrometry. St. Petersburg (Методика выполнения измерений массовой доли элементов в пробах почв, грунтов и донных отложениях методами атомно-эмиссионной и атомно-абсорбционной спектрометрии). <https://files.stroyinf.ru/Data2/1/4293824/4293824289.htm>. Accessed 7 Mar 2021
- Patent RU No. 2660861 of 10 July 2018. Method of preparing reference materials of soil contaminated with heavy metals [Electronic resource]. http://www1.fips.ru/fips_servl/fips_servlet. Accessed 7 Mar 2021
- R 50.2.031-2003 (2003) National measurement standards. Standard specimens of composition and properties of substances and materials. Method for assessment of stability characteristics. Moscow (Стандартные образцы состава и свойств веществ и материалов. Методика оценивания характеристики стабильности). <http://docs.cntd.ru/document/1200034453>. Accessed 7 Mar 2021
- RD 52.18.289-90 (1990) Methodological guidelines. Procedure for measuring the mass fractions of mobile metal forms (copper, lead, zinc, nickel, cadmium, cobalt, chromium, manganese) in soil samples by atomic absorption analysis. Moscow (Методика выполнения измерений массовой доли подвижных форм металлов (меди, свинца, цинка, никеля, кадмия, кобальта, хрома, марганца) в пробах почвы атомно-абсорбционным анализом). <http://docs.cntd.ru/document/1200048596>. Accessed 7 Mar 2021
- RD 52.18.289-90 (2009) General requirements for the competence of testing and calibration laboratories (IDT). Minsk (Общие требования к компетентности испытательных и калибровочных лабораторий) <http://docs.cntd.ru/document/1200048596>. Accessed 7 Mar 2021
- RMG 93-2015 (2016) State system for ensuring the uniformity of measurements. Estimation of metrological characteristics of reference materials. Moscow (Оценивание метрологических характеристик стандартных образцов). <http://docs.cntd.ru/document/1200138923>. Accessed 7 Mar 2021
- Stupakova GA, Ignat'eva EE, Pankratova KG, Shchiplitsova TI, Mitrofanov DK (2018) Current problems in the metrological supply of technogenically contaminated soil tests. In: Proceedings of the international scientific and practical conference on the current problems of soil science, ecology and agriculture, Kursk, Russia (Актуальные проблемы метрологического обеспечения проб техногенно загрязненных грунтов. В материалах международной конференции по актуальным проблемам почвоведения, экологии и сельского хозяйства, Курск), pp 433–437
- Stupakova GA, Pankratova KG, Ignat'eva EE, Shchelokov VI, Shchiplitsova TI, Mitrofanov DK (2017) Problems in the development and application of certified reference materials of soils contaminated with heavy metals, *Plodorodie*, no 2, p 6. (Проблемы разработки и применения стандартных образцов почв, загрязненных тяжелыми металлами, *Плодородие*, № 2, с. 6)



Bioaugmentation and Biostimulation: Comparison of Their Long-Term Effects on Ecotoxicity and Biological Activity of Oil-Contaminated Soil

Yulia Polyak, Lyudmila Bakina,
Marina V. Chugunova, Natalya Mayachkina,
Alexander Gerasimov, and Vladimir M. Bure

Abstract

The long-term effects of biostimulation and bioaugmentation on the ecotoxicity and biological properties of oil-contaminated soil were studied. The dynamics of the soil chemical characteristics, petroleum hydrocarbon biodegradation, toxicity to plants and crustaceans, microbial respiration and enzymatic activity were evaluated in a long-term field experiment. The highest toxicity of soils exposed to both biostimulation and bioaugmentation was found during the first year after contamination. Toxicity to plants had decreased gradually in remediated soils three years into the experiment, while the enzymatic activity of soil was strongly affected even after nine years. Both biostimulation and bioaugmentation had a positive effect on the ecotoxicity and biological activity of soil. However, much of the decontamination can be related to degradation activities of indigenous microbiota. Bioaugmentation demonstrated higher efficiency compared to activity of native

microorganisms at the initial stages of remediation, while no difference between biostimulation and bioaugmentation were found later. Our results indicate that stimulating the indigenous soil microbiota by nutrients is sufficient to achieve successful bioremediation of podzolic soil.

Keywords

Hydrocarbons · Pollution · Remediation · Podzolic soil · Toxicity · Bioassay · Enzymatic activity · Basal respiration

17.1 Introduction

Today, oil pollution can be considered a global problem for the environment. Oil spills have affected large areas of land, rivers, lakes and seas. Each year, from 0.10 to 0.25% of petroleum products penetrate soil and water ecosystems (Garcia-Lor et al. 2012). Oil-contaminated soils are unsuitable for agricultural and recreational uses and have become a major environmental issue in many countries. This problem is of great importance in Russia since Russian oil production exceeds 10 million barrels per day. The huge quantities of crude and refined oils that are transported over long distances and consumed in large amounts are associated with increases in environmental contamination with oil and its derivatives (Wolińska et al. 2016).

Y. Polyak (✉) · L. Bakina · M. V. Chugunova ·
N. Mayachkina · A. Gerasimov
Scientific Research Centre for Ecological Safety of
Russian Academy of Sciences, Korpunaya str. 18,
Saint Petersburg 197110, Russia

Y. Polyak · V. M. Bure
St. Petersburg State University, Universitetskaya
emb. 7–9, Saint Petersburg 199034, Russia

Contaminants have a harmful effect on the ecosystems due to their environmental toxicity. When the soil is contaminated with oil, this changes the soil characteristics, affecting plants, soil animals, soil microbiota and overall soil health (Leitgib et al. 2007; Bakina et al. 2021b). The toxicity of oil towards soil organisms has been widely studied at different levels (Tang et al. 2011; Domínguez-Rodríguez et al. 2020). Soil quality after contamination and remediation efforts may be assessed using earthworms, springtail testing and plant growth experiments (Hentati et al. 2013; Huera-Lucero et al. 2020). Soil animals and plants offer a sensitive mechanism to evaluate the toxic effects generated by petroleum hydrocarbons. One indicator of toxic potential in contaminated soil is the soil organisms' desire to avoid contamination (Hünd-Rinke et al. 2005). Plant assays are applied to evaluate the efficiency of bioremediation processes in petroleum-contaminated soils (Shen et al. 2016). Oil contamination reduces plant growth due to a lack of viable seeds, reduced germination, and unsatisfactory soil conditions.

The environmental impact oil has on the soil's functions can clearly be seen from the alterations in soil microbial community (Silva-Castro et al. 2015). Oil contamination changes the composition and diversity of the microbial community, influencing the activity of microorganisms and soil enzymes. Stress conditions may increase the release of biologically active microbial metabolites (Barazani and Friedman 2001; Polyak and Sukharevich 2019). Microbiological indicators such as predominant microorganisms and enzymatic activities have been widely analysed in order to determine the level of microbial activity and biodegradation potential in contaminated soils (Liu et al. 2011; Huera-Lucero et al. 2020). The succession of microorganisms is a necessary condition for effective soil purification from petroleum hydrocarbons. Soil microorganisms that are able to degrade hydrocarbons are usually stimulated in polluted soils. Their ability to metabolise petroleum hydrocarbons has successfully been used to date as one of the most versatile and environmentally friendly methods for decontaminating oil-polluted land (Silva-

Castro et al. 2013; Li et al. 2020). Various studies have demonstrated how efficient bioremediation is in the rehabilitation of oil-polluted soils (Dias et al. 2012; Souza et al. 2014; Ławniczak et al. 2020).

The complexity of oil ingredients and the formation of intermediate products cause problems in reducing the ecotoxicity of oil-contaminated soils. Autochthonous microorganisms' ability to degrade hydrocarbons is usually affected by toxic pollutants (Xu and Lu 2010). A slow rate of biodegradation can be increased by inoculating the contaminated environment with hydrocarbon-utilising bacteria (bioaugmentation) and introducing nutrients (biostimulation). Nutrient supplementation may speed up the biodegradation process because oil contamination results in a high C:N ratio that is unfavourable to microbial activity (Choi et al. 2002; Kim et al. 2005).

To evaluate the effectiveness of bioremediation and the strength of soil ecotoxicity, the response of living organisms in bioassays can be compared with the results of bioindication. The data obtained by bioassay are consistent with results of bioindication using soil enzymatic activity (Polyak et al. 2018a, b). Due to the fact that remediation methods affect not just the oil content, but the enzymatic response of soil microbiota, soil microbial activity is a sensitive biological and biochemical indicator of soil quality (Gong 2012; Kaczyńska et al. 2015).

Data from microbial activities related to contaminated soils are important for evaluating whether there are grounds to use bioremediation, selecting remediation strategies, and monitoring the bioremediation process (Margesin et al. 2000; Medvedeva et al. 2010; Wu et al. 2016). Dehydrogenases, catalase and urease are considered to be informative in monitoring the removal of hydrocarbons from the soil (Dawson et al. 2007; Polyak and Bakina 2015). The rate of hydrocarbon biodegradation and the suitability of bioremediation treatments are strongly influenced by the initial physico-chemical and biological characteristics of the soil (Calvo et al. 2019). Furthermore, the efficiency of bioremediation depends on environmental factors that influence

oil biodegradation: the soil type, oil concentration, temperature, pH, humidity, the availability of oxygen, nutrients and the microbial activity (Bento et al. 2005; Varjani and Upasani 2017). Any variation in environmental factors could affect the activity of soil microbiota and the oil biodegradation process.

The data on the effects of different remediation strategies mostly come from laboratory studies performed under controlled conditions; long-term field bioremediation experiments are rare (Polyak et al. 2018a, b). Laboratory studies cannot reflect all changes that occur under natural conditions with time. To develop effective bioremediation methods, it is necessary to achieve the same good results in the field as in the laboratory: a challenging task.

In the present study, a field experiment was carried out to reveal the effect of oil on soil ecotoxicity and biological activity over nine years and to assess the effectiveness of biostimulation and bioaugmentation rehabilitation methods. The aims were to assess the soil quality and determine the optimal bioremediation strategy by evaluating the effects achieved with nutrients and oil-degrading microorganisms. In

this study, the effect of oil contamination on plants, animals and soil biological properties was analysed to evaluate the response of the soil biota and the effectiveness of different methods of remediation.

17.2 Materials and Methods

The field study was performed in North-West Russia on an experimental field near St. Petersburg (59°44'34" N, 30°22'49" E) (Fig. 17.1). The soil itself was a loamy podzol (*Albeluvisols*, WRB 2006) with 30.3% clay, 21.6% silt, and 48.1% sand. The experiment duration was nine years.

Square plots were separately set in an aligned part of the study area. Experimental design included uncontaminated control, treatment with 10 L m⁻² of crude oil (natural attenuation), treatment with 10 L m⁻² of crude oil and nutrients (biostimulation), and treatment with 10 L m⁻² of crude oil, a commercial bacterial product and nutrients (bioaugmentation) (Fig. 17.2). Soil samples were collected one week and three months after the contamination,

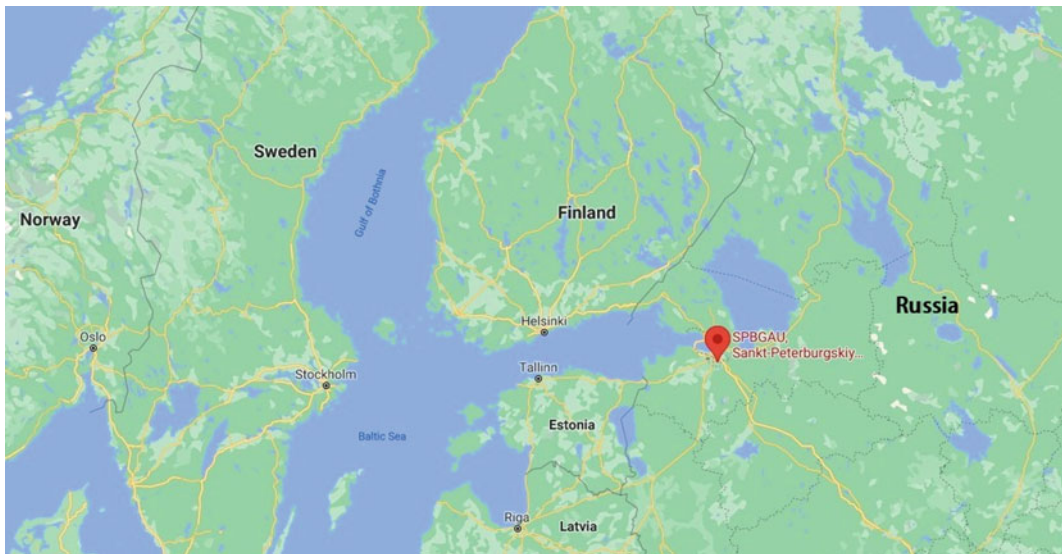


Fig. 17.1 Location of the experimental field

Fig. 17.2 Treatment of the experimental plots



and thereafter annually, in September. Each plot was divided into four replications, and ten sampling sites were selected for every subplot using a randomised repetition technique. Ten soil samples were collected from each sub-plot using an auger with a diameter of 20 cm and sieved through <math><2\text{ mm}</math> mesh. The composite sample from the four sub-plots weighed 900 g.

The soil pH was determined by potentiometry, using a glass electrode. The hydrolytic acidity was determined as follows: the samples were treated with 0.5 M dm^{-3} Ca-acetate solution adjusted to pH 8.2 in the ratio of 1:2.5. The suspensions were shaken at room temperature for one hour then filtrated. The filtrates were titrated with a 0.1 M dm^{-3} NaOH solution in the presence of phenolphthalein indicator, and the hydrolytic acidity values were calculated from the amount of alkali consumed. The content of soil organic matter was determined using the Tyurin wet-combustion method based on the oxidation of a small portion of the soil with potassium dichromate, followed by titration of the excess potassium dichromate with Mohr's salt (Arinushkina 1970). Ammonium was extracted from the soil with a 2% KCl solution, and its presence was determined using the Nessler method. This method is based on the

interaction of an ammonium ion with an alkaline solution of potassium mercury iodide $\text{K}_2(\text{HgI}_4) + \text{KOH}$, with the formation of insoluble mercurammonium iodide. The Ca^{2+} and Mg^{2+} ions present were precipitated using Nessler's reagent, causing the solution to opalesce. Nitrates were extracted from the soil with 0.05% K_2SO_4 in a soil-to-solution ratio of 1:5 and shaken for three minutes, then their level was determined by colorimetric analysis with phenoldisulphonic acid. The available phosphorus was determined via photolorimetry, based on the ability of phosphorus to form a complex phosphorus-molybdenum heteropoly acid $\text{H}_3[\text{P}(\text{Mo}_3\text{O}_{10})_4]$ with molybdate in an acidic medium. Upon the further addition of tin to the solution as a reducing agent, molybdenum from phosphoric-molybdic acid is partially reduced to pentavalent Mo with the formation of a complex compound, molybdenum blue (Arinushkina 1970). The available potassium was determined using the flame photometry method (Arinushkina 1970). Total petroleum hydrocarbons (TPHs) were measured according to PND F 16.1:2.21-98 (2012).

Ecotoxicological assessment was performed at the contaminated soil plots to monitor the effectiveness of the bioremediation process. The

ecotoxicity of the contaminated soils was determined by eluate and direct contact (solid-phase) bioassays. For soil extraction, 50 g of the soil sample was suspended in 200 mL deionised water. The mixture was shaken at 220 rpm for 4 h and filtered with a 0.45 µm filter. The eluates were stored at 4 °C until their ecotoxicological analysis. The test species selected for this study were the higher plants and invertebrates. The soil eluates were tested in acute toxicity bioassays using the cladoceran crustacean *Daphnia magna* Straus. *Daphnia magna* bioassay is based on crustaceans' mortality when exposed to toxic substances. The duration of the experiment was 96 h. Solid-phase bioassays were based on the germination and growth of the common wheat *Triticum aestivum* L. Soil samples were placed in 100 mm diameter Petri dishes with the moisture adjusted to 60% of the maximum water holding capacity. 20 seeds with >90% germination rate were arranged on the soil surface. The test dishes were incubated at 20 °C for 72 h. The measurement endpoints used were seed germination and seedling growth (roots and shoots). To measure the above-ground biomass of grass, we weighted plants from each plot. Plants were cut at their base. Mowing was carried out at the end of the growing season.

Soil basal respiration (BR) was analysed using the alkali absorption method (Alef 1995). We determined soil dehydrogenase activity (DA) using triphenyltetrazolium chloride assay (Haziev 2005). Activity of catalase (CA) was determined by the potassium permanganate titration (Johnson and Temple 1964). Urease activity (UA) was analysed using colorimetric determination of ammonium (Haziev 2005).

All the data were the means of three triplicates, and results are reported as the mean ± standard deviation (SD). Statistical analyses were performed using the StatSoft Statistica 10 software.

17.3 Results and Discussion

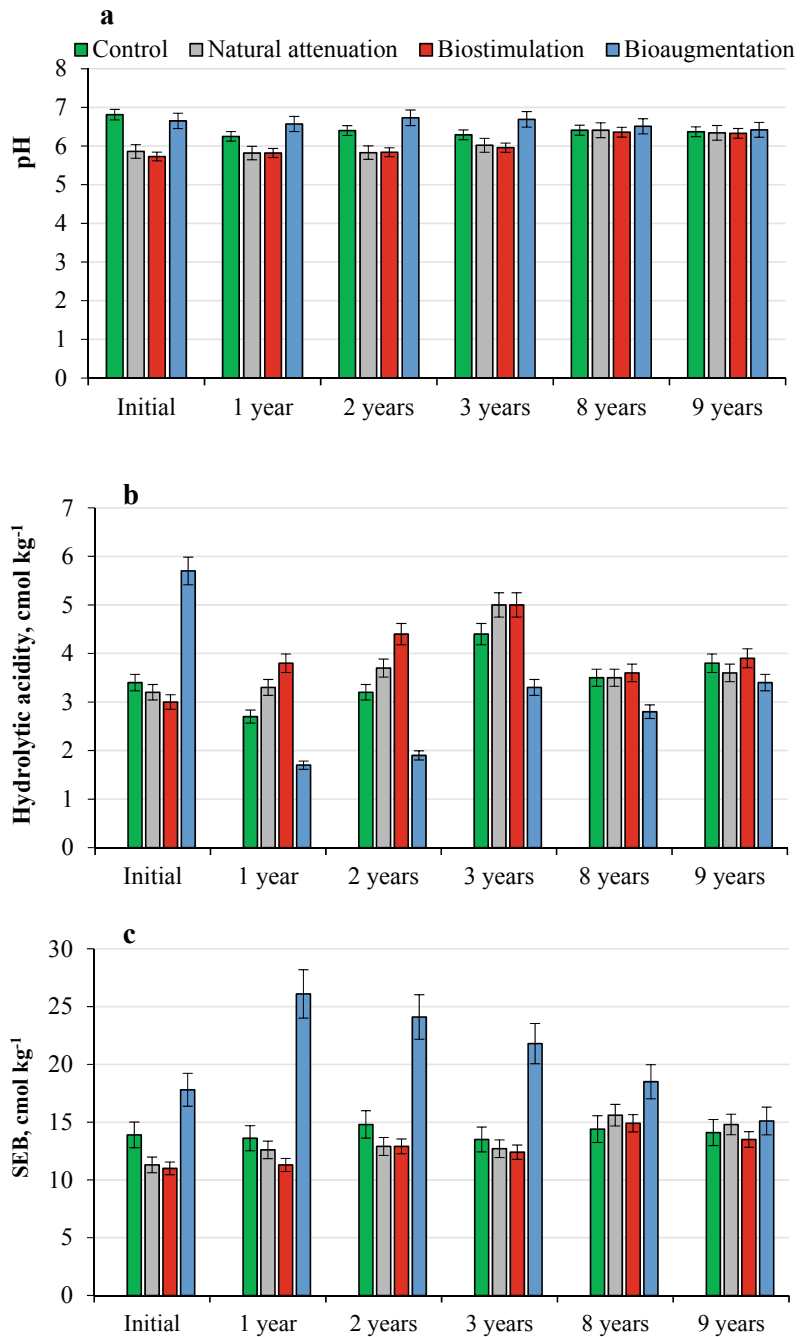
17.3.1 Dynamics of Soil Chemical Properties

The main factors limiting remediation of oil contaminated soils include soil chemical characteristics, the proportion of mineral fraction of the soil, and nutrient content (Das and Chandran 2010). An optimal temperature, pH, water, oxygen, and inorganic nutrients are essential to support microorganism growth and biodegradation processes. The dynamics of soil characteristics are shown in Fig. 17.3. We observed a continuous decrease in pH caused by the low mobility of exchangeable bases and increased hydrolytic acidity of oil-contaminated soils. The initial pH values of control and oil-contaminated soils were 6.8 and 5.8, respectively (Fig. 17.3a). The pH value was similar in the soils under natural attenuation and biostimulation, while the pH was significantly higher in the soils undergoing bioaugmentation (6.65, $p < 0.05$). In the soils under natural attenuation and biostimulation, the pH remained at the level 5.8 for three years after contamination.

The increase in the sum of exchangeable bases one year into the experiment can be attributed to the gradual dissolution of carbonates (Fig. 17.3c). Later on, a gradual desalination of carbonates and the recovery of initial soil acidity due to TPH biodegradation was observed. By the end of the experiment, there was no significant difference in the acid–base ratio between the different treatments.

One limiting factor in biodegradation is phosphorus and nitrogen availability. Our results showed that the total organic carbon was significantly higher in contaminated soils ($p < 0.05$). Moreover, the addition of oil significantly reduced the available potassium, phosphorous and nitrate nitrogen ($p < 0.05$) (Figs. 17.4 and 17.5).

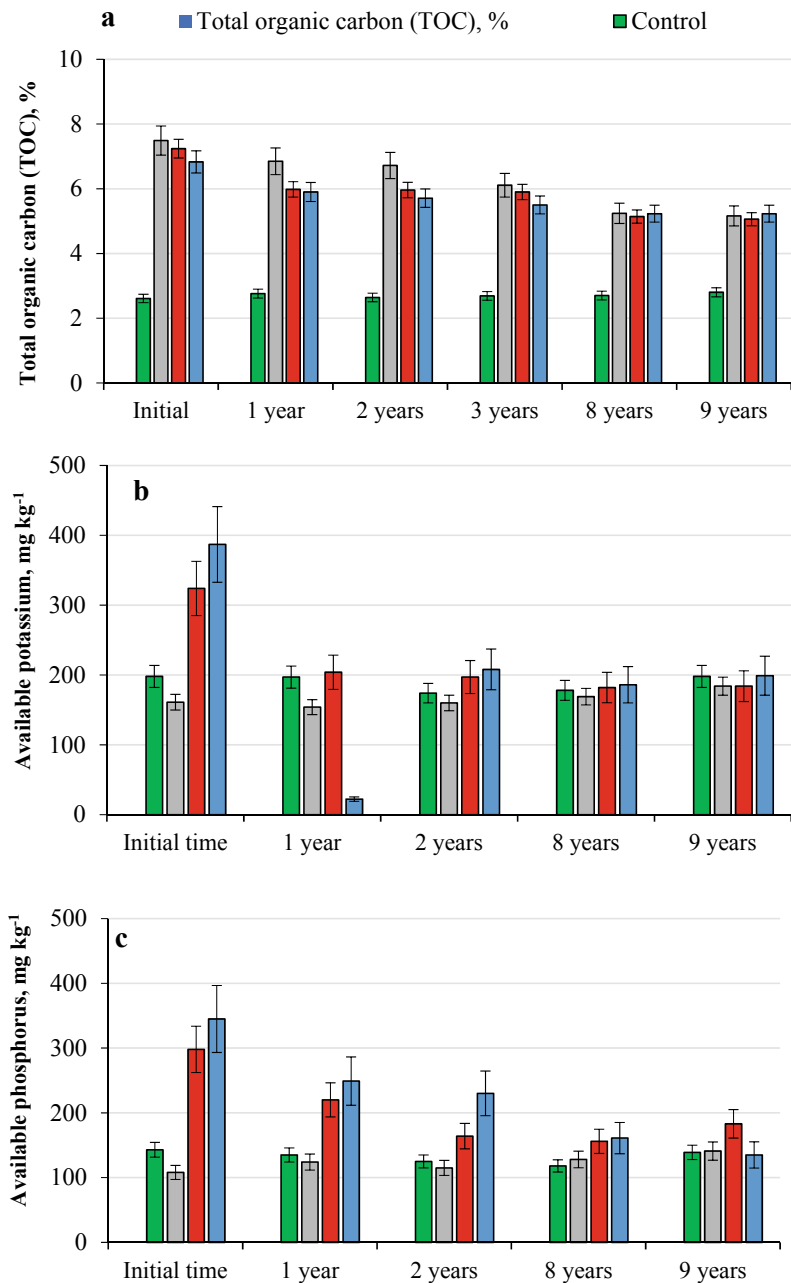
Fig. 17.3 Chemical characteristics of oil-contaminated soil exposed to different remediation strategies: **a**—pH; **b**—hydrolytic acidity (HA); **c**—sum of exchangeable bases (SEB)



The concentration of available phosphorus (AP) decreased in contaminated soil and increased when bioremediation methods were used (Fig. 17.4). The N-NH₄ content increased by 50% in contaminated soil undergoing

bioaugmentation and biostimulation treatments (Fig. 17.5a). However, this increased N-NH₄ concentration persisted only for the first few months, after which it decreased to the control values. The content of N-NO₃ increased by

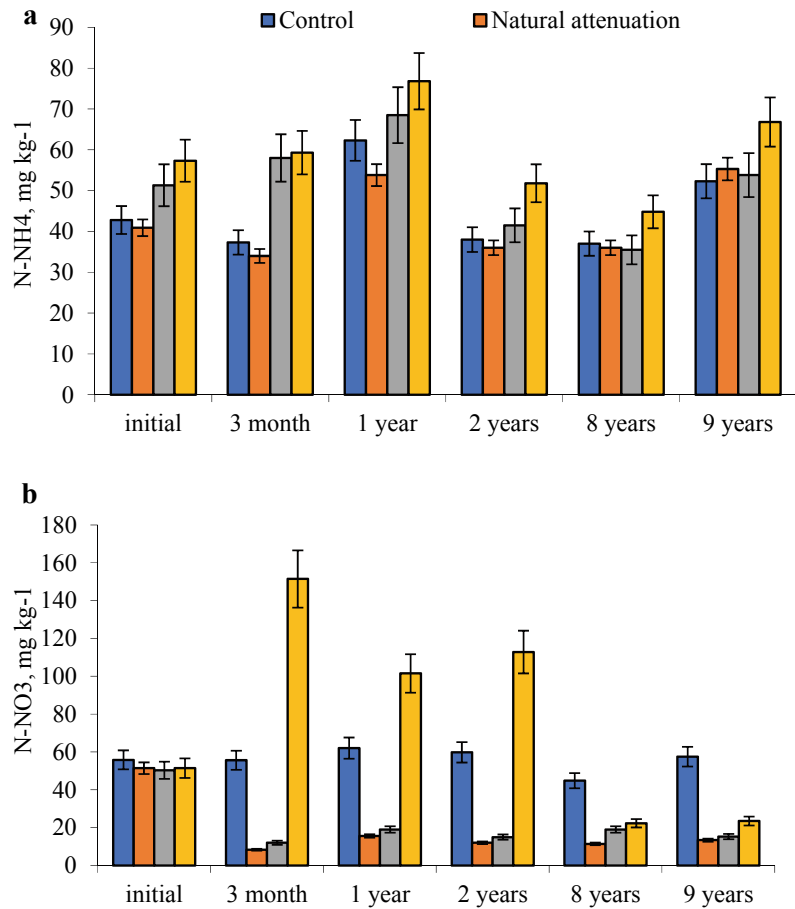
Fig. 17.4 Total organic carbon (a); available phosphorus (b); and available potassium (c) concentrations in oil-contaminated soil exposed to different remediation strategies



250% in contaminated soil undergoing bioaugmentation (Fig. 17.5b). In the soils subject to natural attenuation and biostimulation, the nitrate nitrogen content decreased by 80–85%. The decrease can be explained as a result of microbial utilisation and changes in the composition of soil

microbiota (John et al. 2011; Marchand et al. 2017). Nine years into the experiment, the N-NO_3 content remained the same in unpolluted soil, while in oil-contaminated soils, it was still low. Nutrient depletion in the polluted soil over time can be attributed to the microbial

Fig. 17.5 Nitrogen concentrations of oil-contaminated soil exposed to different remediation strategies: **a** N-NH₄; **b** N-NO₃



metabolism, immobilisation into biomass, immobilisation onto soil colloids, and washing out (Margesin and Schinner 2001).

17.3.2 Hydrocarbon Biodegradation Under Different Bioremediation Strategies

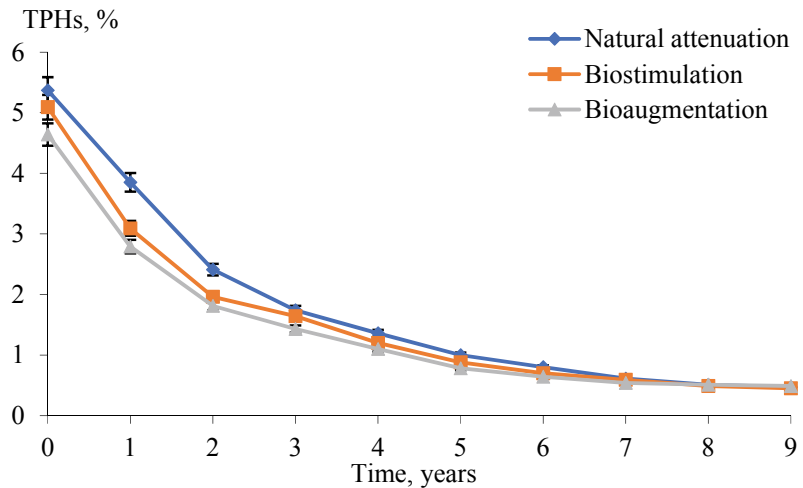
The removal of hydrocarbons from the soil is due to various processes including chemical evaporation, photo-oxidation, oxidation, and biodegradation. One or more of these processes may play a key role in hydrocarbon degradation, but in general, microbial degradation (mineralisation) is the most important element in decontamination. This process is the basis of all

biological methods for remediating contaminated soils.

The effect of remediation strategies on the biodegradation of total petroleum hydrocarbons (TPHs) is presented in Fig. 17.6. The rate of biodegradation processes was the fastest in the first year. It decreased later, though a short-term increase in the rate of biodegradation was provided by biostimulation and bioaugmentation treatments. After the first year, 39.3% of TPH were degraded in the soil exposed to biostimulation. In the soil exposed to bioaugmentation, the degradation of TPHs was similar reaching 39.9%. The TPH degradation rate was lower under natural attenuation, corresponding 28.3% of degradation.

In soils exposed to biostimulation and bioaugmentation, the biodegradation of TPHs reached 61.0% after the second year. In the soil

Fig. 17.6 Biodegradation of total petroleum hydrocarbons in oil-contaminated soil exposed to biostimulation and bioaugmentation



exposed to natural attenuation, the level of biodegradation was only 55.1%. After the third year, the level of oil degradation was similar with all treatments. About 90% of initial hydrocarbons were degraded in all three conditions at the end of the study. The decrease in the degradation rate after the third year is presumably related to the removal of most available hydrocarbons, while only persistent compounds with higher molecular weights remained (Riveroll-Larios et al. 2015). Moreover, toxic intermediates of higher molecular weight hydrocarbon degradation can inhibit the activity of degrading microorganisms.

These data have shown that bioaugmentation and simpler nutrient addition have a comparable influence on oil biodegradation processes. Bioaugmentation can accelerate the initial phase of biodegradation, but stimulating the indigenous soil microorganisms with nutrients is also sufficient. Thus, biostimulation is an effective tool to enhance the removal of petroleum hydrocarbons in contaminated soil.

17.3.3 Ecotoxicity Evaluation

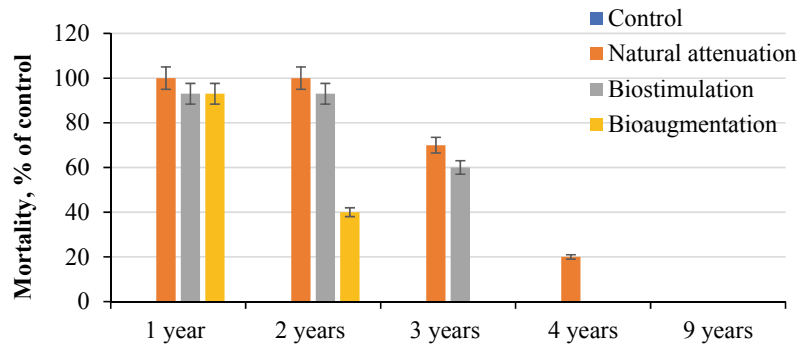
The liquid-phase bioassays showed a decrease in the toxicity of soil undergoing bioaugmentation three years after contamination, while soil exposed to biostimulation remained toxic for

four years. In the direct contact tests, soils exposed to biostimulation and bioaugmentation became non-toxic in three years. The longest toxicity period was found for soil under natural attenuation. This soil's toxicity to test organisms had disappeared five years after contamination.

Different toxicity dynamics were detected in the contaminated soils using acute toxicity bioassay (Fig. 17.7). The results revealed a strong toxic effect on soils undergoing both biostimulation and bioaugmentation during the first year after contamination. We found that the mortality of *Daphnia* in all water extracts was 90–100% compared to the control, indicating a very high degree of soil toxicity.

Later on, the level of toxicity depended on the remediation strategy. After two years, the toxicity of water extracts from the soil undergoing bioaugmentation had decreased (mortality was 40% of that for the control). However, the toxicity of the soil undergoing biostimulation and natural attenuation remained high (mortality was 90–100% of that for the control). After three years of bioaugmentation treatment, the water extracts had become non-toxic and the survival rate of *Daphnia* was similar to the control, reaching 100%. *Daphnia* mortalities in water extracted from the soils undergoing biostimulation and natural attenuation were 60 and 70% of the control values, respectively.

Fig. 17.7 Acute toxicity to *Daphnia magna* of oil-contaminated soil exposed to different remediation strategies



We found that the soil exposed to biostimulation had lost its toxicity after four years. The survival rate of *Daphnia* was 100%. After five years, oil-contaminated soil under natural attenuation became non-toxic. The survival rate of crustaceans reached 90% compared to the control. Thus, bioaugmentation contributes to a more rapid decrease in soil toxicity as compared with biostimulation, while the longest period of toxicity was found for the soil under natural attenuation. Direct-contact ecotoxicity tests were used to evaluate soil toxicity during the bioremediation. Contact tests performed directly on soil samples are known to be a more sensitive tool to evaluate the ecotoxicity of hydrocarbon-contaminated soil than the tests using soil extracts (Hubálek et al. 2007). We applied contact bioassay to determine soil toxicity for wheat. The results of measuring the root length, expressed as a percentage relative to the control (unpolluted soil), are presented in Fig. 17.8. The root length of wheat was strongly inhibited in contaminated soil. The growth was most severely

affected during the natural attenuation treatment. We observed strong inhibition of plant growth in the first year after soil contamination. An 80% decrease in root length compared to the control was observed in the natural attenuation and bioaugmentation treatments. Plant growth was 60% inhibited relative to the control in the biostimulation treatment.

Soils exposed to both biostimulation and bioaugmentation became non-toxic in three years. A different response pattern was found for the soil under natural attenuation. This soil showed a longer period of phytotoxicity becoming non-toxic for plants in four years. After four years of contamination, no significant differences in the length of plant roots were found between the soils under natural attenuation and the control ($p > 0.05$). These results are in line with the dynamics of grass growing in the experimental plots. The above-ground grass biomass was annually recorded in the field at the end of the growing season. The dynamics of plant growth differentiated between natural

Fig. 17.8 Phytotoxicity of oil-contaminated soil exposed to different remediation strategies

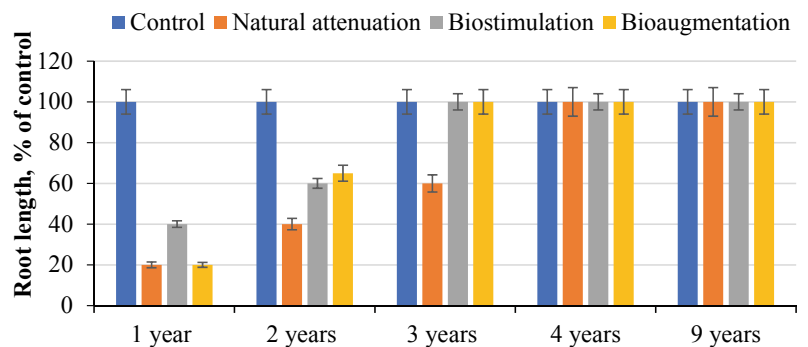
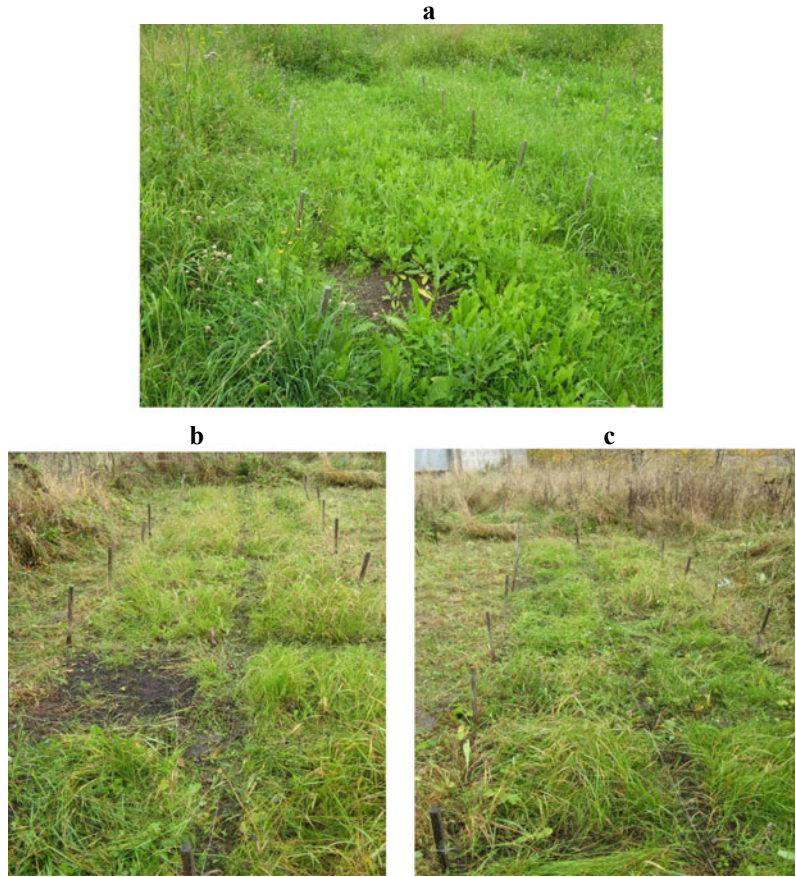


Fig. 17.9 Plant growth in the experimental plots at the trial field: **a**—3 months (dominants are dandelion, clover, cereals, sow thistle, chickweed, etc.; a plot without vegetation is natural attenuation); **b**—two years (dominants are cereals; more diverse plant composition; a plot without vegetation is natural attenuation); **c**—three years (the same overgrowth of all plots, including natural attenuation, is clearly visible)

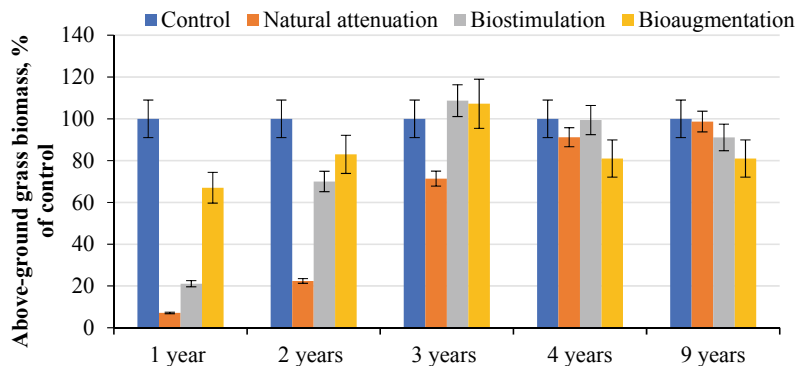


attenuation and bioremediation treatments (Fig. 17.9).

One year after contamination, an almost complete inhibition of plant growth was observed in the plots undergoing biostimulation and natural attenuation treatments. The differences in plant biomass in these plots and control

were 79 and 93%, respectively (Fig. 17.10). Other studies have shown that high rates of plant mortality and a decrease in plant biomass are a typical response to oil contamination (Gallegos Martinez et al. 2000; Basumatary et al. 2012; Polyak et al. 2020). The highest biomass was recorded in the soil undergoing bioaugmentation

Fig. 17.10 The dynamics of grass growing in oil-contaminated soil exposed to different remediation strategies



(67% of the biomass in the control). Grass growth was still inhibited in the contaminated soil two years into the experiment. Nevertheless, in the plots undergoing biostimulation and bioaugmentation, the biomass increased to 70 and 83% of that in the control, respectively.

After three years, only naturally attenuated soil was still toxic to plants (biomass decreased by 29% of the control value). Four years after the start of the experiment and later, there were no significant differences between the control soil and the soils exposed to natural attenuation, biostimulation and bioaugmentation. Successful plant growth in oil-contaminated soils may be explained by the decrease in TPH concentration over time. The remaining petroleum compounds might be bound or unavailable, preventing them from being further biodegraded and meaning they are not toxic to plants (Salanitro et al. 1997). Additionally, plants' ability to adapt to the presence of petroleum hydrocarbons increases their survival and growth rates.

17.3.4 Dynamics of Soil Biological Activity

Microbial respiration rate is an integral indicator of soil biological activity (Anan'eva et al. 2005; Chumchalová and Kubal 2020). This indicator is very important when we examine oil-contaminated soils since the oxidation of

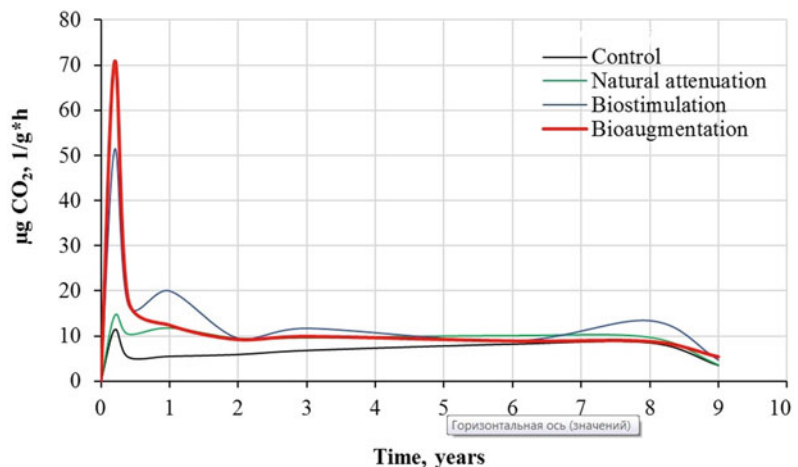
petroleum hydrocarbons by microorganisms is always accompanied by the release of carbon dioxide. The amount of CO₂ determines whether the mineralisation process is complete and the highest possible amount of hydrocarbon energy is used (Mariano et al. 2010). Even though production of carbon dioxide is not a direct measure of the oil carbon biotransformation, changes in basal respiration (BR) are known to indirectly reflect the biodegradation of oil by microorganisms (Bakina et al. 2021a).

The highest level of basal respiration was recorded one week after the start of the experiment (Fig. 17.11). Within the first week after the addition of oil, BR increased, and exceeded control values by several times in the soil from the biostimulation and bioaugmentation treatments. At the same time, hydrocarbon concentrations were at their highest in this period of measurement.

After three months, the amount of TPHs decreased by 26–28%. Respiratory activity also decreased sharply, at twice the rate of the control values, in the soils exposed to biostimulation and bioaugmentation. Over the subsequent two years, a further decrease in the biological activity of these soils was observed. BR recovered from the stimulative effect and reached the level of unpolluted soil after two years. No further significant differences in BR were found between the treatments and unpolluted soil ($p > 0.05$).

In the soils exposed to natural attenuation, initial stimulation of BR was less significant than

Fig. 17.11 Basal respiration in oil-contaminated soil exposed to different remediation strategies



in the soils exposed to biostimulation and bioaugmentation (1.3 times higher relative to the control) and reached the control level after two years.

Biostimulation significantly increased BR (by five times), indicating that nutrients intensified the degrading activity of the indigenous microbiota. The use of both NPK and a biopreparation (bioaugmentation) further enhances the efficiency of biodegradation: BR increased by seven times. However, the stimulating effect of bioaugmentation on BR declined over time in the same way as the effect of biostimulation. This phenomenon may be explained by the reduction of inoculum concentration in the soil after three months. The elimination of introduced bacterial cultures by native microorganisms is often observed in the first 2–3 months after preparations are added to contaminated soils (Kozlova et al. 2014; Masy et al. 2016).

We found that one year after the start of the experiment, BR was 1.3 times higher in the samples exposed to biostimulation compared to the samples where degrading microorganisms were added. Natural attenuation showed the

lowest change in the respiration rate. Other researchers also point to the higher efficiency of biostimulation compared to other treatment types (Tumaikina et al. 2008).

In addition to the respiration rates, soil enzyme activity might be an informative indicator of the intensity of microbiological processes in contaminated soil (Lee et al. 2020). Dehydrogenase activity (DA) was sensitive to the soil contamination and remediation strategies (Table 17.1). The highest level of dehydrogenase activity was found under conditions of bioaugmentation.

At the beginning of the experiment, the activity of dehydrogenase reduced dramatically in the soils exposed to natural attenuation and biostimulation. After the first week, the value of DA fell to 68 and 43% compared to the control, respectively. Three months after contamination, DA was just 5–20% of the control values in all contaminated soils, and it increased only slightly after one year. Two years after contamination, bioaugmentation supported the highest DA (77% of that in uncontaminated soil), while natural attenuation and biostimulation demonstrated

Table 17.1 Activity of urease, catalase and dehydrogenase in petroleum-hydrocarbon-contaminated soil exposed to different remediation strategies

Remediation strategy	Initial time	3 months	1 year	2 years	3 years	9 years
Urease (% compared to unpolluted soil)						
Unpolluted soil	100 ^a	100 ^a	100 ^a	100 ^a	100 ^a	100 ^a
Natural attenuation	144 ^b	63 ^b	134 ^b	74 ^a	103 ^a	73 ^a
Biostimulation	214 ^c	101 ^a	103 ^a	45 ^b	65 ^b	91 ^a
Bioaugmentation	500 ^d	194 ^c	114 ^{ab}	51 ^b	65 ^b	89 ^a
Catalase (% compared to unpolluted soil)						
Unpolluted soil	100 ^a	100 ^a	100 ^a	100 ^a	100 ^a	100 ^a
Natural attenuation	36 ^b	49 ^b	44 ^b	35 ^c	47 ^b	74 ^{ab}
Biostimulation	93 ^a	96 ^a	100 ^a	61 ^b	61 ^b	64 ^b
Bioaugmentation	125 ^a	100 ^a	108 ^a	74 ^{ab}	56 ^b	74 ^{ab}
Dehydrogenase (% compared to unpolluted soil)						
Unpolluted soil	100 ^a	100 ^a	100 ^a	100 ^a	100 ^a	100 ^a
Natural attenuation	68 ^c	17 ^b	33 ^b	48 ^c	54 ^b	56 ^b
Biostimulation	43 ^d	5 ^c	20 ^c	33 ^c	39 ^c	55 ^b
Bioaugmentation	122 ^b	20 ^b	26 ^{bc}	72 ^b	60 ^b	67 ^b

Different lowercase letters in the same column represent a significant difference at $p \leq 0.05$

lower DA levels (33–48%). DA was still low (55–67% compared to the control) nine years after contamination. There were no differences between treatments at that time. These results indicate reduced soil quality, and potentially unsafe conditions for soil microbiota, even though no toxic effects were found on higher organisms.

As well as dehydrogenase activity, the activity of catalase (CA) was strongly inhibited by soil contamination with oil. There was significant difference in how CA responded to various methods of remediation. Natural attenuation produced the least catalase activity (35–47% of that in uncontaminated soil) for the three years period. After nine years, CA was still below the values of control soil. Biostimulation demonstrated no changes in CA during the first year and a decrease to 61–64% in subsequent years. Under conditions of bioaugmentation, the stimulation of CA was observed during the first week, but it returned to the control value after three months and reduced to 56–74% of the control value later. By the end of the experiment, catalase activity had somewhat improved but remained significantly lower than pre-contamination levels with all three treatments ($p < 0.05$).

Even more complex response to soil contamination was evaluated for urease activity (UA). Right after the contamination, UA increased by 1.5 times in polluted soil (natural attenuation). In soil exposed to biostimulation UA increased by two times, while the highest stimulation effect (by five times compared to the control) was found in the soil exposed to bioaugmentation. Within three months, the activity of urease decreased, and stimulation effect was found only in soil under bioaugmentation.

After one year, UA in the soils exposed to natural attenuation increased to the control level, where it remained unchanged in the years that followed. In soils exposed to biostimulation and bioaugmentation treatments, UA was below control values for the second and third year, while after nine years UA was similar to unpolluted soil in all treatments.

These results indicate that microbial parameters respond differently to oil contamination

during the first year and over the next eight years related to hydrocarbon biodegradation. Dehydrogenase and catalase activities decreased initially due to contamination, while soil respiration rates were high in oil-contaminated soil. At a later stage, enzymatic activities increased, while the soil basal respiration decreased to control level. Although the negative effect of oil contamination reduced after the first year, the rates of dehydrogenase and catalase activities detected in unpolluted soil were never reached. Even by the ninth year of the experiment, when a 90% decontamination level was reached, the activity of microbial communities still continued to be suppressed. Of the studied biological parameters, soil dehydrogenase activity appears to be the most sensitive indicator that was relevant to all remediation strategies.

Nutritional deficiencies may limit the degradation potential of native microorganisms able to degrade hydrocarbons despite the fact that their abundance is increasing in the presence of oil and oil products (Silva-Castro et al. 2015). Strong response to the addition of nutrients and raising rate of oil degradation suggest close relationships between soil microbiota and these parameters. The positive correlations of the available nutrient content with the enzymatic activities, basal respiration and hydrocarbon concentration in the polluted soil indicate the importance of nutrients for bioremediation processes.

17.4 Conclusions

In this study, biostimulation and bioaugmentation remediation strategies were compared over a nine-year period. Ecotoxicity testing was carried out on oil-contaminated podzolic soils to determine when the treated soil became safe for biota and for the disposal of remediated soils. Ecotoxicity bioassays revealed a high toxicity of soils exposed to both biostimulation and bioaugmentation during the first year after contamination. The soil toxicity persisted for 3–4 years.

Our results showed that bioaugmentation only works more efficiently than local microorganisms

in the initial stages of decontamination. With increasing incubation time, no differences were found between the recovery strategies. Thus, biostimulation may be a better bioremediation strategy for the podzolic soil examined here. A better understanding of the differences in soil environments of microbial activity and of the relationships between these two aspects may be of assistance for forecasting ecosystem attributes and processes in the case of oil contamination.

Acknowledgements This study was supported by SRCES RAS state research topic no. AAAA-A19-119020190122-6. The authors would like to thank Valentina Murygina at Moscow State University for providing the preparation for bioaugmentation treatment.

References

- Alef K (1995) Soil respiration. In: Alef K, Nannipieri P (eds) *Methods in applied soil microbiology and biochemistry*. Academic Press, Harcourt Brace & Company, London, pp 214–219
- Anan'eva ND, Sus'yan EA, Khakimov FI, Deeva NF (2005) The influence of polychlorinated biphenyls on the microbial biomass and respiration in gray forest soil. *Eurasian Soil Sci* 38(7):770–775
- Arinushkina EV (1970) *Manual on chemical analysis of soils*. (Пособие по химическому анализу почв) Publishing House of Moscow State University, Moscow, p 488 (in Russian)
- Bakina LG, Chugunova MV, Polyak YM, Mayachkina NV, Gerasimov AO (2021a) Bioaugmentation: possible scenarios due to application of bacterial preparations for remediation of oil contaminated soil. *Environ Geochem Health* 43(6):2347–2356. <https://doi.org/10.1007/s10653-020-00755-4>
- Bakina LG, Polyak YM, Gerasimov AO, Mayachkina NV, Chugunova MV, Khomyakov YV, Vertebny VA (2021b) Mutual effects of crude oil and plants in contaminated soil: a field study. *Environ Geochem Health*. <https://doi.org/10.1007/s10653-021-00973-4>
- Barazani O, Friedman J (2001) Allelopathic bacteria and their impact on higher plants. *Crit Rev Microbiol* 27:41–55. <https://doi.org/10.1080/20014091096693>
- Basumatary B, Saikia R, Bordoloi S (2012) Phytoremediation of crude oil contaminated soil using nut grass, *Cyperus rotundus*. *J Environ Biol* 33(5):891–896. PMID: 23734455. <https://www.altmetric.com/details/2057177>
- Bento FM, Camargo FAO, Okeke BC, Frankenberger WT (2005) Comparative bioremediation of soils contaminated with diesel oil by natural attenuation, biostimulation and bioaugmentation. *Bioresour Technol* 96(9):1049–1055. <https://doi.org/10.1016/j.biortech.2004.09.008>
- Calvo C, Rodríguez-Calvo A, Robledo-Mahón T, Manzanera M, González-López J, Aranda E, Silva-Castro GA (2019) Biostimulation of crude oil-polluted soils: influence of initial physicochemical and biological characteristics of soil. *Int J Environ Sci Technol* 16:4925–4934. <https://doi.org/10.1007/s13762-019-02269-8>
- Choi SC, Kwon KK, Sohn JH, Kim SJ (2002) Evaluation of fertilizer additions to stimulate oil biodegradation in sand seashore mesocosms. *J Microbiol Biotechnol* 12:431–436
- Chumchalová J, Kubal M (2020) Laboratory tests for aerobic bioremediation of the contaminated sites in the Czech Republic. *Plant Soil Environ* 66:191–199. <https://doi.org/10.17221/673/2019-PSE>
- Das N, Chandran P (2010) Microbial degradation of petroleum hydrocarbon contaminants: an overview. *Biotechnol Res Int* T2011(941810):1–13. <https://doi.org/10.4061/2011/941810>
- Dawson JJC, Godsiffé EJ, Thompson IP, Ralebitso-Sr TK, Killham KS, Paton GI (2007) Application of biological indicators to assess recovery of hydrocarbon impacted soils. *Soil Biol Biochem* 39:164–177. <https://doi.org/10.1016/j.soilbio.2006.06.020>
- Dias RL, Ruberto L, Hernández E, Vázquez SC, Balbo AL, Del Panno MT, MacCormack WP (2012) Bioremediation of an aged diesel oil-contaminated Antarctic soil: evaluation of the “on site” biostimulation strategy using different nutrient sources. *Int Biodeterior Biodegrad* 75:96–103. <https://doi.org/10.1016/j.ibiod.2012.07.020>
- Domínguez-Rodríguez VI, Adams RH, Sánchez-Madrigal F, Pascual-Chablé JLS, Gómez-Cruz R (2020) Soil contact bioassay for rapid determination of acute toxicity with *Eisenia foetida*. *Heliyon* 6(1):e03131. <https://doi.org/10.1016/j.heliyon.2019.e03131>
- Gallegos Martínez M, Gomez Santos A, Gonzalez Cruz L, de Oca M, Garcia MA, Yanez Trujillo L, Zermeno Eguia Liz JA, Gutierrez-Rojas M (2000) Diagnostic and resulting approaches to restore petroleum-contaminated soil in a Mexican tropical swamp. *Water Sci Technol* 42:377–384. <https://doi.org/10.2166/wst.2000.0538>
- García-Lor E, Sancho JV, Serrano R, Hernandez F (2012) Occurrence and removal of pharmaceuticals in wastewater treatment plants at the Spanish Mediterranean area of Valencia. *Chemosphere* 87:453–462. <https://doi.org/10.1016/j.chemosphere.2011.12.025>
- Gong XB (2012) Remediation of weathered petroleum oil-contaminated soil using a combination of biostimulation and modified Fenton oxidation. *Int Biodeterior Biodegrad* 70:89–95. <https://doi.org/10.1016/j.ibiod.2012.02.004>

- Haziev FH (2005) Methods of soil enzymology (Методы энзимологии почвы). Nauka, Moscow, p 252 (in Russian)
- Hentati O, Lachhab R, Ayadi M, Ksibi M (2013) Toxicity assessment for petroleum-contaminated soil using terrestrial invertebrates and plant bioassays. *Environ Monit Assess* 185:2989–2998. <https://doi.org/10.1007/s10661-012-2766-y>
- Hubálek T, Vosáňlová S, Matějů V, Matějů V, Kováčová N, Novotný Č (2007) Ecotoxicity monitoring of hydrocarbon-contaminated soil during bioremediation: a case study. *Arch Environ Contam Toxicol* 52:1–7. <https://doi.org/10.1007/s00244-006-0030-6>
- Huera-Lucero T, Labrador-Moreno J, Blanco-Salas J, Ruiz-Téllez T (2020) A framework to incorporate biological soil quality indicators into assessing the sustainability of territories in the Ecuadorian Amazon. *Sustainability* 12:3007. <https://doi.org/10.3390/su12073007>. doi:10.3390/su12073007
- Hünd-Rinke K, Lindemann M, Simon M (2005) Experiences with novel approaches in earthworm testing alternatives. *J Soils Sediments* 5:233–239. <https://doi.org/10.1065/jss2005.06.142>
- John RC, Akpan MM, Essien JP, Ikpe DI (2011) Fate of nitrogen-fixing bacteria in crude oil contaminated wetland ultisol. *Bull Environ Contam Toxicol* 87:343–353. <https://doi.org/10.1007/s00128-011-0320-1>
- Johnson JL, Temple KL (1964) Some variables affecting measurement of catalase activity in soil. *Soil Sci Soc Am J* 28:207–216
- Kaczyńska G, Borowik A, Wyszowska J (2015) Soil dehydrogenases as an indicator of contamination of the environment with petroleum products. *Water Air Soil Pollut* 226:372. <https://doi.org/10.1007/s11270-015-2642-9>
- Kim SJ, Choi DH, Sim DS, Oh Y-S (2005) Evaluation of bioremediation effectiveness on crude oil-contaminated sand. *Chemosphere* 59(6):845–852. <https://doi.org/10.1016/j.chemosphere.2004.10.058>
- Kozlova EN, Stepanov AL, Lysak LV (2014) Application of bacterial-humus preparations in the remediation of soils contaminated with diesel fuel. *Eurasian Soil Sci* 47(5):449–452. <https://doi.org/10.1134/S106422931405010X>
- Ławniczak Ł, Woźniak-Karczewska M, Loibner AP, Heipieper HJ, Chrzanowski Ł (2020) Microbial degradation of hydrocarbons—basic principles for bioremediation: a review. *Molecules* 25(4):856. <https://doi.org/10.3390/molecules25040856>
- Lee SH, Kim MS, Kim JG, Kim SO (2020) Use of soil enzymes as indicators for contaminated soil monitoring and sustainable management. *Sustainability* 12(19):1–14. <https://doi.org/10.3390/su12198209>
- Leitgib L, Kálmán J, Gruiz K (2007) Comparison of bioassays by testing whole soil and their water extract from contaminated sites. *Chemosphere* 66(3):428–434. <https://doi.org/10.1016/j.chemosphere.2006.06.024>
- Li Q, Huang Y, Wen D, Fu R, Feng L (2020) Application of alkyl polyglycosides for enhanced bioremediation of petroleum hydrocarbon-contaminated soil using *Sphingomonas changbaiensis* and *Pseudomonas stutzeri*. *Sci Total Environ* 719:137456. <https://doi.org/10.1016/j.scitotenv.2020.137456>
- Liu P-WG, Chang TC, Whang L-M, Kao C-H, Pan P-T, Cheng S-S (2011) Bioremediation of petroleum hydrocarbon contaminated soil: effects of strategies and microbial community shift. *Int Biodeterior Biodegrad* 65(8):1119–1127. <https://doi.org/10.1016/j.ibiod.2011.09.002>
- Marchand C, St-Arnaud M, Hogland W, Bell TH, Hijri M (2017) Petroleum biodegradation capacity of bacteria and fungi isolated from petroleum-contaminated soil. *Int Biodeterior Biodegrad* 116:48–57. <https://doi.org/10.1016/j.ibiod.2016.09.030>
- Margesin R, Schinner F (2001) Bioremediation (natural attenuation and biostimulation) of diesel-oil-contaminated soil in an alpine glacier skiing area. *Appl Environ Microbiol* 67:3127–3133. <https://doi.org/10.1128/AEM.67.7.3127-3133.2001>
- Margesin R, Zimmerbauer A, Schinner F (2000) Monitoring of bioremediation by soil biological activities. *Chemosphere* 40(4):339–346. [https://doi.org/10.1016/S0045-6535\(99\)00218-0](https://doi.org/10.1016/S0045-6535(99)00218-0)
- Mariano AP, Tomasella RC, Di Martino C (2010) Aerobic biodegradation of butanol and diesel oil blends. *Afr J Biotechnol* 9(42):7094–7101. <https://doi.org/10.5897/AJB10.110>
- Masy T, Demaneche S, Tromme O, Thonart P, Jacques P, Hilgsmann S, Vogel TM (2016) Hydrocarbon biostimulation and bioaugmentation in organic carbon and clay-rich soils. *Soil Biol Biochem* 99:66–74. <https://doi.org/10.1016/j.soilbio.2016.04.016>
- Medvedeva N, Polyak Y, Zaytseva T, Zharikov G (2010) Biodegradation of mustard gas hydrolysis products in contaminated soils. In: Steinberg RV (ed) Contaminated soils: environmental impact disposal and treatment. Nova Science Publishers, NY, pp 289–314
- PND F 16.1:2.21-98 (2012) Quantitative chemical analyses of soils. (Количественный химический анализ почв). Moscow (in Russian)
- Polyak YM, Sukharevich VI (2019) Allelopathic interactions between plants and microorganisms in soil ecosystems. *Biol Bull Rev* 9(6):562–574. <https://doi.org/10.1134/S2079086419060033>
- Polyak YM, Bakina LG, Chugunova MV, Mayachkina NV, Gerasimov AO, Bure VM (2018) Effect of remediation strategies on biological activity of oil-contaminated soil—a field study. *Int Biodeterior Biodegrad* 126:57–68. <https://doi.org/10.1016/j.ibiod.2017.10.004>
- Polyak Y, Bakina L, Mayachkina N, Polyak M (2020) The possible role of toxigenic fungi in ecotoxicity of two contrasting oil-contaminated soils—a field study. *Ecotoxicol Environ Saf* 202:110959. <https://doi.org/10.1016/j.ecoenv.2020.110959>
- Polyak YM, Bakina LG (2015) Enzymatic diagnostics of oil contaminated soil in the North-Eastern Russia. In: Shoba SA, Kovaleva NO (eds) Proceedings of the international scientific conference “The role of soil in

- the biosphere and human life” (Ферментативная диагностика нефтезагрязненных почв Северо-Востока России. В кн .: Шоба С.А., Ковалева Н. О. (ред.) Материалы Международной научной конференции «Роль почвы в биосфере и жизни человека»). MAKS Press, Moscow, pp 223–224 (in Russian)
- Polyak YM, Bakina LG, Mayachkina NV, Drozdova IV, Kaplan AV, Golod DL (2018) Biodiagnostics of the cultivated urban soil polluted by metals: bioindication and bioassay. *J Soils Environ* 1(4):231–242 (in Russian). <https://doi.org/10.31251/pos.v1i4.34>
- Riveroll-Larios J, Escalante-Espinosa E, Fócil-Monterrubio RL, Díaz-Ramírez IJ (2015) Biological activity assessment in Mexican tropical soils with different hydrocarbon contamination histories. *Water Air Soil Pollut* 226(10):353. <https://doi.org/10.1007/s11270-015-2621-1>
- Salanitro JP, Dorn PB, Huesemann MH, Moore KO, Rhodes IA, Rice Jackson LM, Vipond TE, Western MM, Wisniewski HL (1997) Crude oil hydrocarbon bioremediation and soil ecotoxicity assessment. *Environ Sci Technol* 31:1769–1776. <https://doi.org/10.1021/es960793i>
- Shen W, Zhu N, Cui J, Wang H, Dang Z, Wu P, Luo Y, Shi C (2016) Ecotoxicity monitoring and bioindicator screening of oil-contaminated soil during bioremediation. *Ecotoxicol Environ Saf* 124:120–128. <https://doi.org/10.1016/j.ecoenv.2015.10.005>
- Silva-Castro GA, Rodelas B, Perucha C, Laguna J, González-López J, Calvo C (2013) Bioremediation of diesel-polluted soil using biostimulation as post-treatment after oxidation with Fenton-like reagents: assays in a pilot plant. *Sci Total Environ* 445–446:347–355. <https://doi.org/10.1016/j.scitotenv.2012.12.081>
- Silva-Castro GA, Uad I, Rodríguez-Calvo A, González-López J, Calvo C (2015) Response of autochthonous microbiota of diesel polluted soils to landfarming treatments. *Environ Res* 137:49–58. <https://doi.org/10.1016/j.envres.2014.11.009>
- Souza EC, Vessoni-Penna TC, de Souza Oliveira RP (2014) Biosurfactant enhanced hydrocarbon bioremediation: an overview. *Int Biodeterior Biodegrad* 89:88–94. <https://doi.org/10.1016/j.ibiod.2014.01.007>
- Tang JC, Wang M, Wang F, Sun Q, Zhou QX (2011) Eco-toxicity of petroleum hydrocarbon contaminated soil. *J Environ Sci* 23(5):845–851. [https://doi.org/10.1016/S1001-0742\(10\)60517-7](https://doi.org/10.1016/S1001-0742(10)60517-7)
- Tumaikina YA, Turkovskaya OV, Ignatov VV (2008) Degradation of hydrocarbons and their derivatives by a microbial association on the base of Canadian pondweed. *Appl Biochem Microbiol* 44(4):382–388. <https://doi.org/10.1134/S000368380804008X>
- Varjani SJ, Upasani VN (2017) A new look on factors affecting microbial degradation of petroleum hydrocarbon pollutants. *Int Biodeterior Biodegrad* 120:71–83. <https://doi.org/10.1016/j.ibiod.2017.02.006>
- Wolińska A, Kuźniar A, Szafranek-Nakonieczna A, Jastrzębska N, Roguska E, Stepniewska Z (2016) Biological activity of autochthonic bacterial community in oil-contaminated soil. *Water Air Soil Pollut* 227:130. <https://doi.org/10.1007/s11270-016-2825-z>
- WRB (2006) World reference base for soil resources 2006. Food and Agriculture Organization of the United Nations, Rome, p 2015
- Wu M, Dick WA, Li W, Wang X, Yang Q, Wang T, Xu L, Zhang M, Chen L (2016) Bioaugmentation and biostimulation of hydrocarbon degradation and the microbial community in a petroleum-contaminated soil. *Int Biodeterior Biodegrad* 107:158–164. <https://doi.org/10.1016/j.ibiod.2015.11.019>
- Xu Y, Lu M (2010) Bioremediation of crude oil-contaminated soil: comparison of different biostimulation and bioaugmentation treatments. *J Hazard Mater* 183:395–401. <https://doi.org/10.1016/j.jhazmat.2010.07.038>



Environmental Pollution in the Vicinity of an Aluminium Smelter in Siberia

18

Irina A. Belozertseva, Marija Milić,
Sonja Tošić, and Elmira Saljnikov

Abstract

Detailed studies of snow and soil contamination within the influence zone of the Irkutsk Aluminium Metallurgical Plant were carried out for the period of 1996–2015. The main types of atmospheric and soil pollution and the amounts and distribution area of the pollutants were described. The study revealed that within 1 km of the aluminium smelter, the maximum fluoride concentration in the snow meltwater reached 66 mg dm^{-3} . The relationship between technogenic soil and snowpack pollution was assessed, and their effect on some soil parameters was revealed. A standard

determination of technogenic loads was carried out in relation to the significant and sensitive soil parameters. The maximum level of technogenic load was obtained by determining critical points on the “load vs. effect” curve. The values of the “dose–effect” relationship can be used to determine the maximum permissible concentration (MPC) and maximum impermissible concentration (MIC) of the potentially toxic elements in the soil. The amounts of the total forms of fluoride, aluminium and sodium were, respectively, 0.66 and 0.84 g kg^{-1} , 82 and 93 g kg^{-1} , and 24 and 26 g kg^{-1} for the upper (MPC) and lower (MIC) limits. This highlights how the soil environment is polluted with these substances emitted from the Irkutsk aluminium smelter.

I. A. Belozertseva
V.B. Sochava Institute of Geography SB RAS,
Ulan-Batorskaya Street 1, 664033 Irkutsk, Russia

I. A. Belozertseva
Irkutsk State University, Sukhe-Bator street 5,
664011 Irkutsk, Russia

M. Milić
Faculty of Technology and Metallurgy, University of
Belgrade, Karnegijeva 4, Belgrade, Serbia
e-mail: marija.pavlovic@tmf.bg.ac.rs

S. Tošić · E. Saljnikov (✉)
Institute of Soil Science, Teodora Drajzera 7, 11000
Belgrade, Serbia

E. Saljnikov
Mitscherlich Academy for Soil Fertility (MITAK),
GmbH, Prof.-Mitscherlich-Allee 1, 14641
Paulinenaue, Germany

Keywords

Aluminium smelter · Pollution · Atmosphere ·
Snow · Soil

18.1 Introduction

The soil surface represents a direct sink for pollutants emitted into the atmosphere by metallurgical plants. Heavy metals enter plants from the soil and are transmitted through food chains, thus posing a toxic risk to plants, animals and

humans. They have a general toxic, carcinogenic, mutagenic effect, causing many health disorders. Solid particulates containing contaminants are emitted from the operations of metallurgical plants as fine fractions ($<2\ \mu\text{m}$) and as fractions less than $0.5\ \mu\text{m}$ (Csavina et al. 2012; Csavina et al. 2014; Sorooshian et al. 2012). There are many studies devoted to studying the health effects of integrated effect of airborne particulates (Heinrich et al. 2013; Jimenez et al. 2011; Bhattacharya and Samal 2018). Martin and Larivière (2014) summarised the literature published on how aluminium smelters affect human health, concluding that exposure to airborne particulate matter $<10\ \mu\text{m}$ causes respiratory disorders in adults and children, while particulate matter $<2.5\ \mu\text{m}$ is strongly associated with adverse cardiovascular disorders.

Primary aluminium production is a necessary industrial segment. Global aluminium production grew by 52% between 2010 and 2018 (Saevarsdottir et al. 2019). However, the process of aluminium smelting poses health risks to both the workers who manage it and to residents of neighbouring territories (Martin and Larivière 2014). This is because smelting plants are large emitters of PAHs and mutagens (Martin and Larivière 2014; Alfheim and Wikström 1984; Zhang et al. 2020), as well as other potentially toxic pollutants, such as beryllium, particulate matter, sulphur dioxide, and fluorides (Martin and Larivière 2014; Davydova and Znamenskaya 2016; Abdul-Wahab and Alsubhi 2019; Zhang et al. 2020; Jafari et al. 2020). Gibbs and Sévigny (2007), Deger et al. (2012) and others found a correlation between morbidity and mortality from chronic diseases not only among electrolysis workers but also among residents living nearby. Studying the Irkutsk aluminium smelter's environmental impact, Khavina (2007) revealed that the aggregate influence of unfavourable factors of physical and chemical origin can lead not only to diseases of individual systems of the human body but also to disorders of the natural ageing processes and to a reduction in human life expectancy. Thus, for example, death in residents of the town studied near the Shelekhov smelter is primarily associated with

circulatory system disorders, and the average life expectancy of men and women there is less than the global average: 54 and 69 years, respectively (Matorova 2005).

Another serious environmental impact from the operation of the primary aluminium smelter is the high amount of carbon dioxide and other greenhouse gases emitted (Pandey and Prakash 2020). In 2009, the average world level of GWP was 23.96 tonnes of CO_2 per tonne of aluminium production (Steen-Olsen 2009). Aluminium smelting makes up 72% of overall GWP, followed by alumina refining and ingot casting (Sanchez and Stern 2016). Further, aluminium production leads to the release of greenhouse gases such as CF_4 and C_2F_6 , which pose a very high global warming threat as they have long lifetimes in the atmosphere (50,000 and 100,000 years, respectively) (Sanchez and Stern 2016).

Following the industrial load, the effects of transport-related air pollution on environmental quality are also among the leading concerns related to sustainable environmental management. Research in recent decades has consistently indicated the adverse effects of atmospheric pollution on human and animal health (Sanchez et al. 2020). The highest contributors from urban transport to the overall level of urban pollution are nitrogen oxides, hydrocarbons and carbon monoxide, and particulate matter (WHO 2005), which also may pose a detrimental effect to organisms. Many studies have proved that organic substances such as phenols, formaldehyde, methyl mercaptan and others are especially toxic to living organisms (e.g., Honda and Suzuki 2020; Sanchez et al. 2020), including specific studies on the Irkutsk region, which has intense aluminium smelting industries (Pomazkina et al. 1999; Koval et al. 1993; Naprasnikova and Makarova 2005).

Though the carcinogenic, allergic and mutagenic effects of many of the polluting substances are known, their hazard class has not yet been established (Matorova 2005). Szostek et al. (2015) found that concentrations of fluoride between 100 and 200 mg per kg of soil have a positive effect on microbial diversity and soil activity. The primary toxic pollutant due to the

operation of Al smelters is fluorine compounds, in both gaseous and particulate forms. These forms of fluoride in the aluminium smelter regions are difficult to identify since they are associated with solid particles and sulphur oxide. Despite the fact that fluoride is not readily available to plants, it can be absorbed by plants at much higher concentrations in contaminated soils (Senkondo et al. 2018), having a toxic effect on plant growth and development (Kumar et al. 2017). The solubility of fluoride is closely associated with inherent soil characteristics such as the clay fraction, content of carbonates and acidity (Choudhary et al. 2019), where a pH value around 5.5–6 is considered as a threshold for the maximum sorption of F (Saxena and Rani 2012; Choudhary et al. 2019).

Endowed with a large forested area, Irkutsk city boasts a significant positive balance contributing to the stability of landscapes and impressive clean-air resources (Fig. 18.1). However, Siberia's intense industrial development has resulted in the emergence of manufacturing complexes clustering within the bounds of a particular limited territory and thus subjecting it to significant technogenic pollution. As a result, the quality of the air in most residential areas of the Irkutsk region has worsened (Belozertseva et al. 2017a, b). The production capacity of the aluminium smelters in southern Siberia varies from 450 (Irkutsk Aluminium Smelter (IrAZ)) to more than 1,000,000 tonnes per year (Bratsk Aluminium Smelter (BrAZ)). The IrAZ uses an electrolysis method to produce primary aluminium, which pollutes the environment with fluorine compounds, carbon and sulphur oxides, as well as Hazard Class I substances: vanadium, chromium and nickel compounds, and polycyclic aromatic hydrocarbons, such as benzo(a)pyrene, some of which are characterised by mutagenic and carcinogenic activity. According to the Ministry of Natural Resources and Environmental Protection of the Russian Federation (2013), JSC RUSAL-IrkAZ, which is located in the town of Shelekhov, causes 77% of general emissions of these polluting substances, and JSC Irkutsk TEP-5 produces 19% of general emissions.

These enterprises are leaders in the amount of pollutants emitted into the atmosphere, exceeding maximum permissible concentrations.

The city of Shelekhov is situated within the lowland broad valley of the Irkut River and its right tributary, the Olkha River. The accumulation and stagnation of pollutants in the urban atmosphere in this area are aided by the unfavourable meteorological conditions, which are characterised by a high frequency of ground air temperature inversions and weak winds. The residential neighbourhoods of the city are located within about 1.5 km of the aluminium smelter which is the source of the pollution, i.e., in close proximity. Sirina (2009) reported that emissions of pollutants into the atmosphere from the Irkutsk Metallurgical Plant resulted in the average daily threshold of particulate matter in the air exceeding 254–744 h per month in both industrial and residential areas. In addition to the unfavourable location of the town, increased urban air pollution is also associated with a decrease in the ability of the natural environment to self-purify from pollutants that have accumulated since the metallurgical plant was put into production 50 years ago. In the area studied, industrial emissions of pollutants are largely responsible for the substances of Hazard Class I–III: nonferrous metallurgy—F, HF, Al, Mn, Co, Ni, Na, Ba, Cu, Pb, Fe, Zn, Mo, Be, V, Hg, Cd, benzo(α)pyrene, Cr, NO₂, dust, and SO₂ from nonferrous metallurgy; solids (ash and dust), SO₂, CO₂, Ca, S, Sr, Fe, Mn, Mg, Ba, Co, Cu, Ni, and Cd from the heat and power industries.

In the Irkutsk Aluminium Smelter (IrAZ), a new electrolysis technology was implemented to make the plant's operation and environmentally friendly. The concern, however, is the doubling in the production volume of aluminium in the last few decades. Therefore, the main purpose of the study was to establish how technogenic emissions from the Irkutsk aluminium smelter affect the properties of the soil adjacent to the plant. The objectives were to study the chemical composition of snow as an indicator of technogenic soil pollution, to identify the transformation of the composition and properties of soils under the



Fig. 18.1 Location of the study site

influence of technogenic pollutants, and to standardise the measurement of technogenic pollution according to various soil parameters.

18.2 Materials and Methods

18.2.1 Soil and Snow Sampling

Soil samples were collected in accordance with certified techniques included on the list of State Standards. The source of fluorine pollution was studied according to the “Procedural Recommendations on Identification of Degraded and Polluted Lands” (1995), approved by the Russian Committee on Land, the Ministry of Agriculture and the Ministry of Natural Resources. The system of environmental observations of the soils and earth materials was designed based on landscape-geochemical differentiation with regard to the geochemical barriers and the most

likely routes of superficial and ground (subsoil) pollutant migration, at 0.5, 1, 2, 6, 20 and 70 km from a factory. A total of 64 main soil profiles were opened, with more than 192 samples taken for physico-chemical analysis. An “envelope” system of soil sampling was used, taking five individual samples at the centre and corners of a square with 10 m sides. The sampling depth corresponded to the thickness of the horizons. In addition, samples for the content of fluoride were collected from the following sites and substrates: the water of Lake Baikal, snowpack from the Lake Baikal basin, Angara river waters, the coast of the Baikal and from the settlements located near the source of pollution (Table 18.4). A total of 64 snow samples were collected in late February to March with weighing-type snow sampler VC-43 (NPO Taifun, Russia) to determine the snow depth and density. At the sampling time, the period of accumulation was from 131 to 140 days.

18.2.2 Analytical Methods

The snowpack was analysed for the content of the following elements: F, Al, Si, Mn, Ba, Pb, Ca, Na, K, Cu, Sr, Cr, Mg, V, Ni, Fe, Ti, Co, S and Cl. The elements studied were categorised into classes according to their concentration and distribution pattern. The dynamics of particulate matter in snow meltwater within the zone of up to 0.5 km from IrkAZ were studied within the period from 1994 to 2014. The zonal distribution of particulate matter in the snowpack was determined depending on the proximity of the smelter for the winter periods of two years. The content of fluoride in the snow meltwater was determined at different distances and locations in the vicinity of the pollution source and Lake Baikal. A maximum permissible environmental load was calculated by Vorobeychik et al. (1994). The maximum load levels were obtained by determining critical points on the “load vs. effect” curve using appropriate equations (calculation is shown in the results section). The concentration coefficient (C_c) was calculated as the ratio of the content of chemical elements in the contaminated area to their concentration in the background “conditionally uncontaminated” area. The suspended material (particulate matter) in snowpack and dry residue was determined using the weight method (Semenov 1977).

All analytical work was performed at the laboratory of V.B. Sochava Institute of Geography SB RAS (IG SB RAS) using standardised techniques. Concentrations of basic anions and cations in snowmelt were determined by standard chemical methods by capillary electrophoresis (Shpeyzer and Mineeva 2006; GOST 1982). Cations were determined based on the separation of cations due to differences in their electrophoretic mobility during migration through a quartz capillary in an electrolyte under the action of an electric field. This was followed by recording the difference in optical absorption by the electrolyte and cations in the ultraviolet region of the spectrum. When determining anions in aqueous extracts, a substance that is opaque in the UV region (chromium oxide) was introduced into the background electrolyte for indirect

photometric detection. The range of measured values of the mass fraction of anions and cations is 1–20,000 mg/kg (million).

The soil pH was determined by potentiometry using combined electrodes, with a soil: solution ratio of 1:2.5. The fluoride concentration was measured on ionomer N-120 with a fluorine-selective electrode. The total contents of metals were determined using the quantitative spectral technique with a DFS-8 spectrograph (distributed file system), atomic emission spectroscopy was carried out using the Optima 2000DV (optical emission spectrometer), and standard chemical methods according to the Russian state standards (Mazurak 1975; Arinushkina 1970; Semenov 1977). The humus content was determined with a modified Tyurin method (Arinushkina 1970). The group and fractional composition of humus was determined using Tyurin’s pyrophosphate method as modified by Ponomareva and Plotnikova (1975). This method includes the following operations: a direct extraction with 0.1 N NaOH is obtained from the first soil sample (the rest of the soil is discarded), while the second portion of the same soil undergoes decalcification with 0.1 N H₂SO₄ → 0.1 N NaOH extraction → 0.02 N NaOH extraction with 6-h heating in a water bath → insoluble humus residue. This scheme makes it possible to subdivide humus into three fractions of humic acids and four fractions of fulvic acids.

The rate of cellulose degradation was determined using a cotton cloth placed on a 15 cm wide area, reinforced from the outside with a plastic wrap, and set to the entire depth of the soil cut. After the expiry of the exposure period, the canvases were carefully removed, cleaned of soil and sequentially treated with 1% hydrochloric acid, 1% soda solution and distilled water, dried, and then weighed. Cellulose activity was calculated based on the change in the mass of tissue samples from the initial mass in %. The intensity of the fibre destruction process was determined according to a scale: very weak <10, weak 10–30, medium 30–50, strong 50–80, and very strong >80% (Haziyevev 2005). Biochemical activity was determined using the express method developed by Aristovskaya and

Chugunova (1989). This method is based on recording the rate (in hours) of decomposition of a nitrogen-containing organic compound (carbamide). This method is considered very sensitive and not only enables the differences between the objects studied to be revealed but also allows the soils to be differentiated according to their biopotential. This method facilitates the task of assessing the current state of soil activity to a certain extent due to its efficiency and, at the same time, information content. The toxicity of soils was determined based on the viability and seedling length of the tested plants (Schubert 1988). Biotesting is the registration of changes in selected test objects' biological parameters (test functions) under the influence of toxic substances in laboratory and/or field conditions. Plants that respond well to environmental pollution by changing their growth and development have noticeable visual signs. At the same time, bioindicators integrate biologically significant effects of pollution.

18.3 Findings

On the territory of 1 km from IrkAZ, the maximum F concentration in the snowmelt water reached 66 mg dm^{-3} , which comprises 2.6 t km^{-2} . In the snowpack, concentration coefficients (C_c) of 40–60 were observed for Sr, V, Mg, Cr, Ni, Fe, and Co; C_c , 60–100 for Pb, Ca, Cu; and C_c , > 100 for F, Al, Na, Mn, and Ba (Table 18.1).

The area of the most severe pollution occupies about 14 km^2 , including the southern part of Shelekhov and the northern half of the Olkha towns. The accumulation of particulate matter (PM) in the snowpack in the industrial district exceeded $20 \text{ } \mu\text{g m}^{-2}$, reaching $18 \text{ } \mu\text{g m}^{-2}$ in the sanitary protection zone around IrkAZ, $1\text{--}13 \text{ } \mu\text{g m}^{-2}$ in the residential districts, and $2\text{--}5 \text{ } \mu\text{g m}^{-2}$ in the horticultural and agricultural suburban areas.

Emissions from the smelter fell dramatically by the year 2004, involving a significant decrease in PM (suspended material) and dissolved matter (dry residue) in the snowpack (Table 18.2).

However, in 2008, pollution of the snowpack increased and reached the levels of 2000–2002. The data in Table 18.2 also indicate that wind direction plays a major role in pollution of the snow cover. Pollutants from IrkAZ were transported aurally, predominantly in a northwest direction (Fig. 18.2). The fluoride content in the snowpack of the Lake Baikal is given in Table 18.3 (Belozertseva et al. 2017a, b).

Near the Listvyanka settlement on the coast of Lake Baikal (70 km from Irkutsk Aluminium Smelter), an increased fluoride content was observed in the snowpack, characteristic of the technogenic emissions of the aluminium industry. Close to the aluminium smelter, the concentration of fluoride in snow was tens and hundreds of times higher than in the Listvyanka settlement (Table 18.4).

Soil urease activity at distances of 0.5, 1, 2 and 6 km from the metallurgical plant decreases 11, 6, 7 and threefold (Fig. 18.3), respectively. The content of mobile P_2O_5 and NO_3 (basic plant nutrients that are correlated with contaminants) decreases from 0.16 mg g^{-1} to zero and from 0.08 mg g^{-1} to 0.01 mg g^{-1} , respectively (Figs. 18.4, 18.5 and 18.6, Table 18.5).

In the zone to 0.5 km, soil toxicity, determined by seed germination and the length of seedlings of the tested plants (pine and lettuce), was 30% lower than the control, due to the high content of the polluting substances (Fig. 18.7).

The soil humus composition revealed a two-fold decrease in its mobile fraction, i.e., fulvic acids, and an increase by 2–3 times in the fractions bound to calcium and iron oxides (Table 18.6, Fig. 18.7). The organic matter decomposition indicators were correlated to a greater extent with F and Pb (Fig. 18.8), while the contents of mineral nutrients were more closely correlated with Al, Na, Ba, Pb and Cu (Fig. 18.5) (Belozertseva 2000).

18.4 Discussion

The bulk of technogenic emissions was deposited on the soil surface, which is an important component of the urban environment. Soils have the

Table 18.1 Concentration of the elements in snow meltwater and how this exceeds the maximum background content near the Irkutsk Aluminium Smelter (IrKAZ) (0.5 km northeast of the plant) (Belozertseva 2018)

Element	1996		2002		2010	
	Content, mg/L ⁻¹	Extent this exceeds background, times	Content, mg L ⁻¹	Extent this exceeds background, times	Content, mg L ⁻¹	Extent this exceeds background, times
F	55.0	208	50.0	189	43.0	159
Al	7.60	54	10.8	77	11.1	79
Si	6.27	31	3.81	19	1.51	8
Mn	0.80	52	0.18	12	0.11	7
Ba	0.50	49	0.10	10	0.01	1
Pb	0.07	27	0.02	8	0.01	4
Ca	7.00	23	2.32	7	9.30	28
Na	67.5	123	18.0	33	35.3	64
K	5.10	15	0.98	3	2.36	7
Cu	0.06	32	0.02	11	0.01	6
Sr	0.12	17	0.03	4	0.06	2
Cr	0.04	16	0.01	4	0.00	1
Mg	5.90	26	1.62	7	1.61	7
V	0.04	20	0.01	5	0.02	10
Ni	0.09	45	0.02	10	0.01	5
Fe	27.1	27	5.67	6	0.04	1
Ti	1.10	13	0.23	3	0.00	1
Co	0.01	20	0.00	16	0.00	15
S	7.10	10	1.70	2	10.0	12
Cl	0.31	3	0.28	3	3.55	30

ability to neutralise hazardous substances by limiting the amounts that enter the animal and human diet to a certain limit. This mechanism is enabled due to the system of geochemical barriers such as sorption by soil organic substances and clay particles (Glazovskaya 2012; Uddin 2017; Kuźniar et al. 2018; Lasota et al. 2020). Kabata-Pendias and Mukherjee (2007) found that in calcium-rich soils, fluoride reacts with calcium and forms the poorly soluble compound CaF₂ (fluorite); therefore, the calcium geochemical barrier is important for the intra- and inter-soil migration of fluoride (Rezaei et al. 2017). There are many studies highlighting that the main source of anthropogenic pollution with fluoride is the use of F-bearing fertilisers and chemicals

(Litvinovich and Pavlova 2002; Brindha et al. 2011; Bhattacharya and Samal 2018; Choudhary et al. 2019; Singh et al. 2020). However, in industrial metallurgical regions, the main sources of environmental contamination with technogenic pollutants are aluminium and steel plants (Arshad and Eid 2018; Davydova and Znamenskaya 2016; Jafari et al. 2020; Kousehlar and Widom 2020). This was supported by the findings of our research.

The sharp decrease in emissions of particulate matter in 2004 was a result of the modernisation of the production process by introducing the anode baking technique and advanced equipment for the purification of gaseous emissions, accompanied by a decrease in the output of

Table 18.2 Concentration of particulate matter in snow meltwater within the zone up to 0.5 km from IrkAZ for the period from 1996 to 2014, g dm⁻¹ (Belozertseva 2013)

Year	Suspended material (solid residue)	Dry residue	Suspended material (solid residue)	Dry residue
	Northeast wind direction		Southeast wind direction	
1996	7.90	1.18	2.56	0.08
1998	4.60	0.12	2.15	0.09
2000	4.50	0.30	1.87	0.10
2002	1.92	0.02	1.17	0.01
2004	0.62	0.01	0.38	0.01
2006	1.07	0.02	0.34	0.01
2008	2.52	0.30	1.32	0.06
2010	2.78	0.18	1.05	0.11
2012	2.31	0.20	2.03	0.10
2014	2.40	0.16	1.97	0.09

primary aluminium. However, due to the commissioning of the fifth series of electrolysis production and an increase in the production of primary aluminium, pollution of the snowpack increased by 2008, returning to the levels of 2000–2002.

The results of the studies on the territory of the IrkAZ aluminium smelter allowed the chemical elements found in the snow–soil system to be categorised into three groups according to their distribution. **The first group** included F, Al, Na, Mn and Ba and was characterised by concentrations in the snow-soil system that were 50 times higher and more compared to the background value, while those in the soil were five times higher and more (Table 18.1). The **second group** included Ca and Cu, with concentrations that were 25–50 and 3–5 times higher in the snowpack and soil, respectively, compared to the background values. In the **third group**, which included Co, Ni, Sr, Mg, Fe, Ti, V and Cr, the concentration of the elements exceeded the background level by 25 and 3 times in the snow and soil, respectively. In the topsoil, the concentration coefficient C_c for Al, Na, Mn, Ba was 5–7; for F it was 20, and for the remaining elements it was less than 5.

The aluminium production process played a major role in environmental pollution with active and toxic fluoride, which is in Hazard Class I.

The gaseous form of fluoride (HF) is especially toxic because it enters bodily skin and tissues easily and quickly, causing poisoning and severe burns, while breathing hydrogen fluoride damages lung tissues (Bajraktarova-Valjakova et al. 2018). Polomski et al. (1982) and Haidouti (1991) suggested that industrial pollution significantly increases the amount of labile and water-soluble concentrations of F, which is associated with changes in the pH of the soil (Choudhary et al. 2019) due to the fact that fluoride forms labile F compounds with soil components, such as clay minerals, Ca, Mg, Fe and Al compounds due to the formation of stable bonds (Omueti and Jones 1977).

In the soil samples from the town of Shelekhov, the maximum accumulation of fluoride, at 10–14 MPC (maximum permissible concentration), was found in the zone of IrkAZ, while in the sanitary protection zone around the smelter and in its residential districts, it was 3–6 MPC (GN 2.1.7.2041-06 2006) and 1–2 MPC, respectively, exceeding the background level of the region. Though there was a decrease in the amount of solid pollutants at a distance from the smelter, the amount of water-soluble fluoride remained at a relatively high level (Table 18.4). At a distance of 6 km from the source, it decreases only to the MPC level in the upper soil layer. By the end of the growing season, a

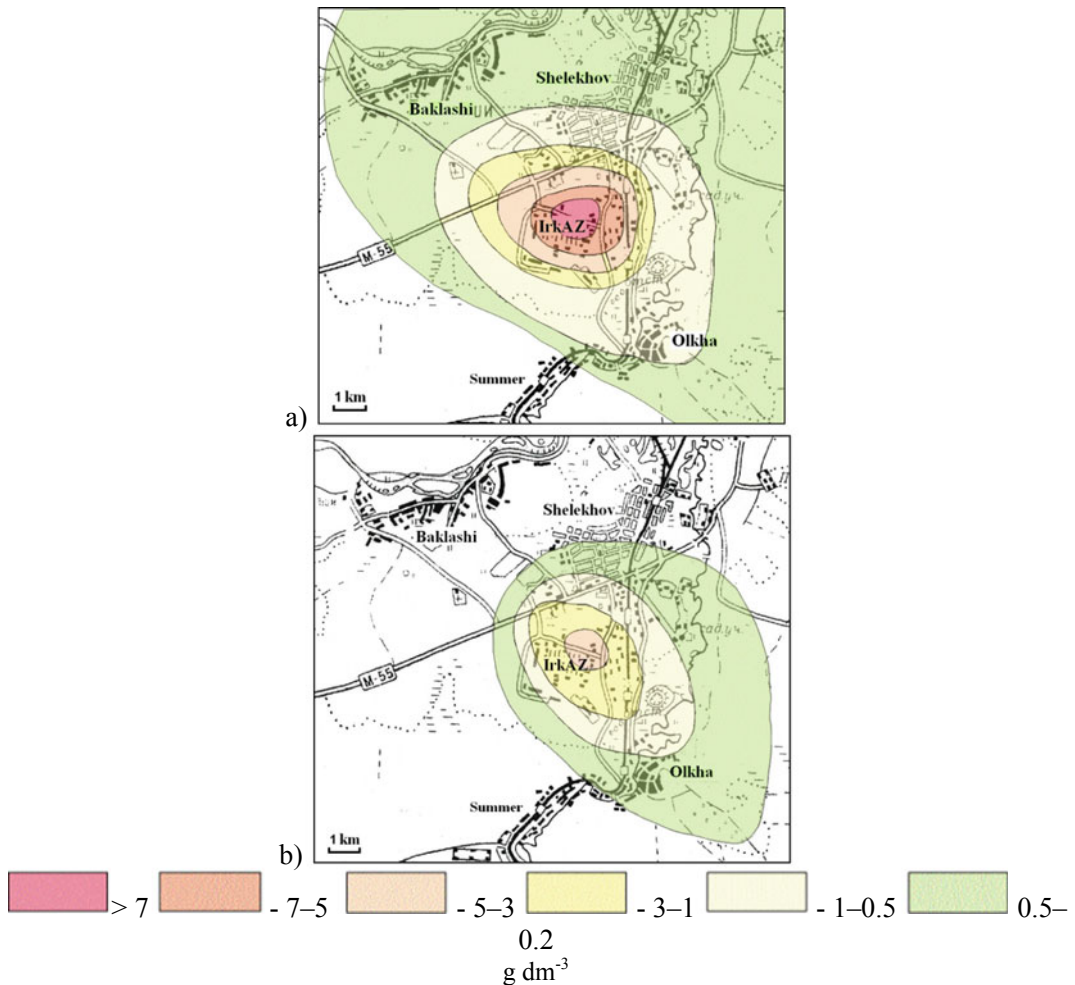


Fig. 18.2 Content of particulate matter in snow for the winter period in 1996 (a) and 2010 (b) in the IrkAZ impact zone, g dm^{-3}

decrease in the content of various forms of fluoride was observed, which is associated with the process of soil self-cleaning and the involvement of fluoride in the bioproduction process (Table 18.7). Kvande and Drabløs (2014) reported that even a short-term exposure to the extremely high dust and fluorides during the prebake phase of the aluminium production is considered to be a risk factor in causing occupational asthma.

The highest concentrations of the pollutants from Group I are explained by the chemical reactions during the aluminium smelting process involving AlF_3 and NaOH . When the aluminium

fluoride undergoes hydrolysis, an extremely toxic gaseous hydrogen fluoride (HF) forms (Kvande and Drabløs 2014). The surface area of the nanoparticles emitted into the atmosphere is large, and compounds on their surface, such as HF and SO_2 , pose a high health risk (Thomassen et al. 2006). The concentrations of macro- and micro elements in the snowpack near the smelter were influenced by the technology and quality of the raw materials used in the production of aluminium. The raw material for aluminium production, in the form of alumina brought from Ural, Kazakhstan and the Achinsky alumina mill in the Krasnoyarsk Region, contains Be—

Table 18.3 Content of fluoride in the snow of Lake Baikal and adjacent territory, 2015 (Belozertseva et al. 2017a, b)

Lake Baikal basin	Contents	F ⁻ , mg dm ⁻³
Southern	Mean	0.127
	Max	0.950
	Min	0.020
Middle	Mean	0.075
	Max	0.155
	Min	0.015
Northern	Mean	0.064
	Max	0.125
	Min	0.016
Total for Baikal	Mean	0.089
		0.7–1.5

Sources ASIL (2015), GN 2.1.5.1315-03 (2015), GOST 2874-82 (1999)

Table 18.4 Concentration of fluoride in the snow meltwater from the sampling sites, 2015 (Belozertseva et al. 2015)

Location	F ⁻ , mg dm ⁻³
The water area of Lake Baikal, 2 km to the southeast of the Listvyanka settlement	0.105
The coast of Lake Baikal, 1 km to the southeast of Listvyanka	0.156
The water area of Lake Baikal, opposite Listvyanka	0.025
Angara River source	0.291
The water area of Lake Baikal, opposite Listvyanka	0.110
On the road between Irkutsk and Listvyanka, Nikola settlement	0.141
The water area of Lake Baikal, 1 km to the northwest of Listvyanka	0.200
The water area of Lake Baikal, opposite Listvyanka	0.029
Coast of Lake Baikal, Listvyanka	0.165
Settlement of Listvyanka	0.102
Coast of Lake Baikal, Semenikh basin, Big Goloustnoye settlement	0.093
Water area of Lake Baikal, Big Gotoustnoye settlement	0.074
Water area of Lake Baikal, 2 km to the southwest of Big Goloustnoye	0.022
Coast of Lake Baikal, Big Goloustnoye	0.216
On the road between Irkutsk and Big Goloustnoye	0.033
Water area of Lake Baikal, 0.3 km from the Big Gotoustnoye settlement	0.032
Water area of Lake Baikal, 0.5 km from the Big Gotoustnoye settlement	0.029
Coast of Lake Baikal, 2 km to the southeast of Big Goloustnoye	0.094
0.5 km to the southeast of the Irkutsk Aluminium Smelter (IrAZ)	60.050
1 km to the southeast of the IrAZ	52.005
2 km to the southeast of the IrAZ	18.020
6 km to the southeast of the IrAZ	2.400
20 km to the southeast of the IrAZ	2.120

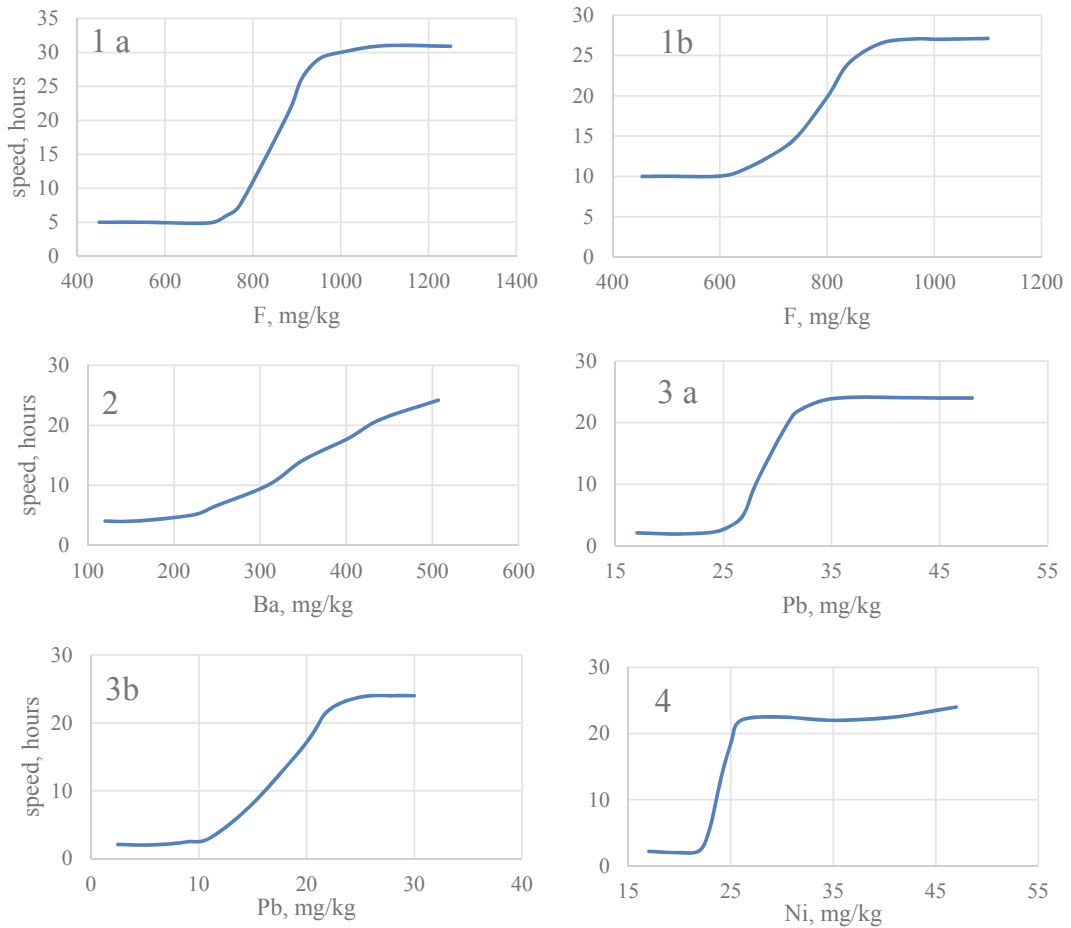


Fig. 18.3 Biochemical activity of soils (urea destruction rate to pH = 8, h) depending on the content of F total (1a), F acid soluble (1b), Ba acid soluble (2), Pb total (3a), Pb acid soluble (3b), Ni acid soluble (4)

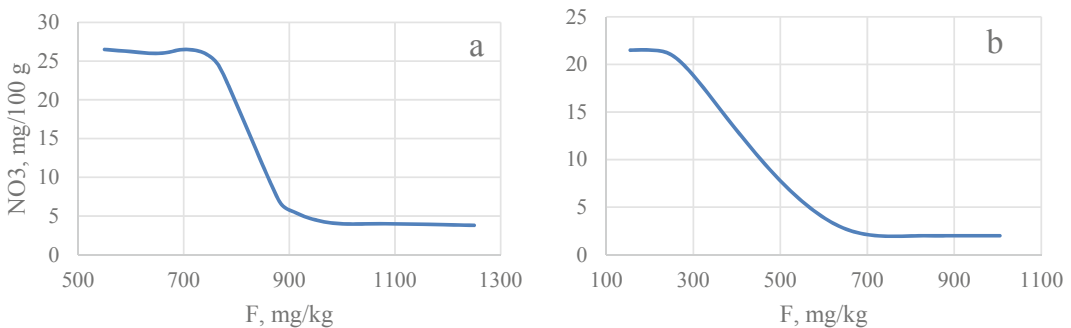


Fig. 18.4 Content of NO₃⁻ depending on the concentration of F total (a) and F acid soluble (b)

0.08 mg kg⁻¹; Pb—20–100; Li—0.5; Mn—8–10–30; Ba—20–30; U—0.12–0.14; Cu—0.1–50; Bi—1–5; Cr—1–6; Sc—0.1; Co—0.4–0.5; 0.5; As—0.6–1; Ag—20–80; Zn—4–4000 mg kg⁻¹ and a group of rare elements.

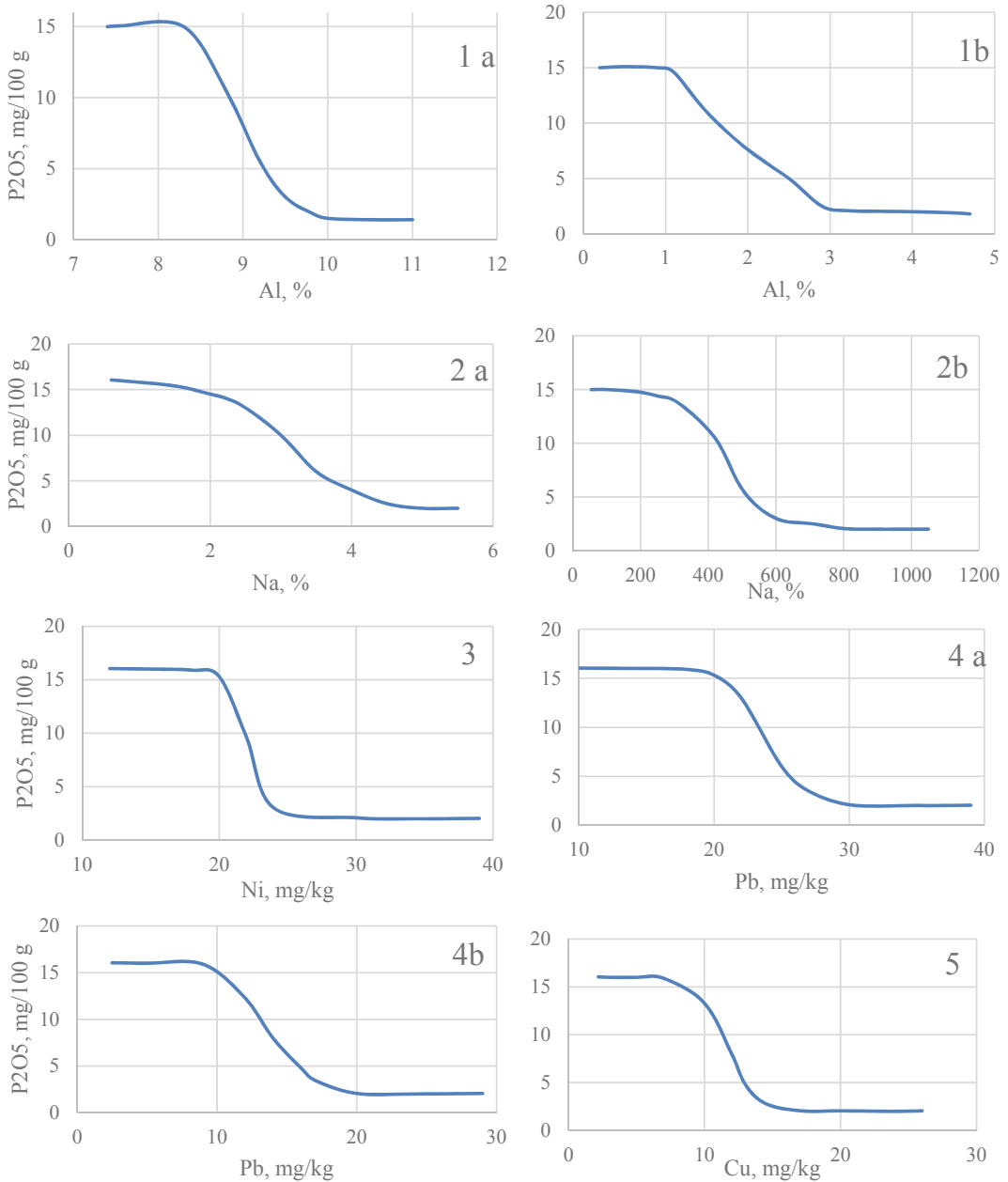


Fig. 18.5 Content of P_2O_5 depending on the concentrations of Al total (1a), Al acid soluble (1b), Na total (2a), Na acid soluble (2b), Ni acid soluble (3), Pb total (4a), Pb acid soluble (4b), Cu acid soluble (5)

An examination of the soil environment's susceptibility to the loads from IrkAZ operation revealed a number of properties that are very sensitive to pollution, such as the decomposition rate of cellulose and urease activity, characterising the decomposition of organic nitrogenous

compounds, soil toxicity and the presence of mobile forms of nitrogen, phosphorus, potassium, and organic matter in soil (Table 18.8). The amount of these properties at a distance of up to 0.5 km from the metallurgical plant was more than one order of magnitude lower than the

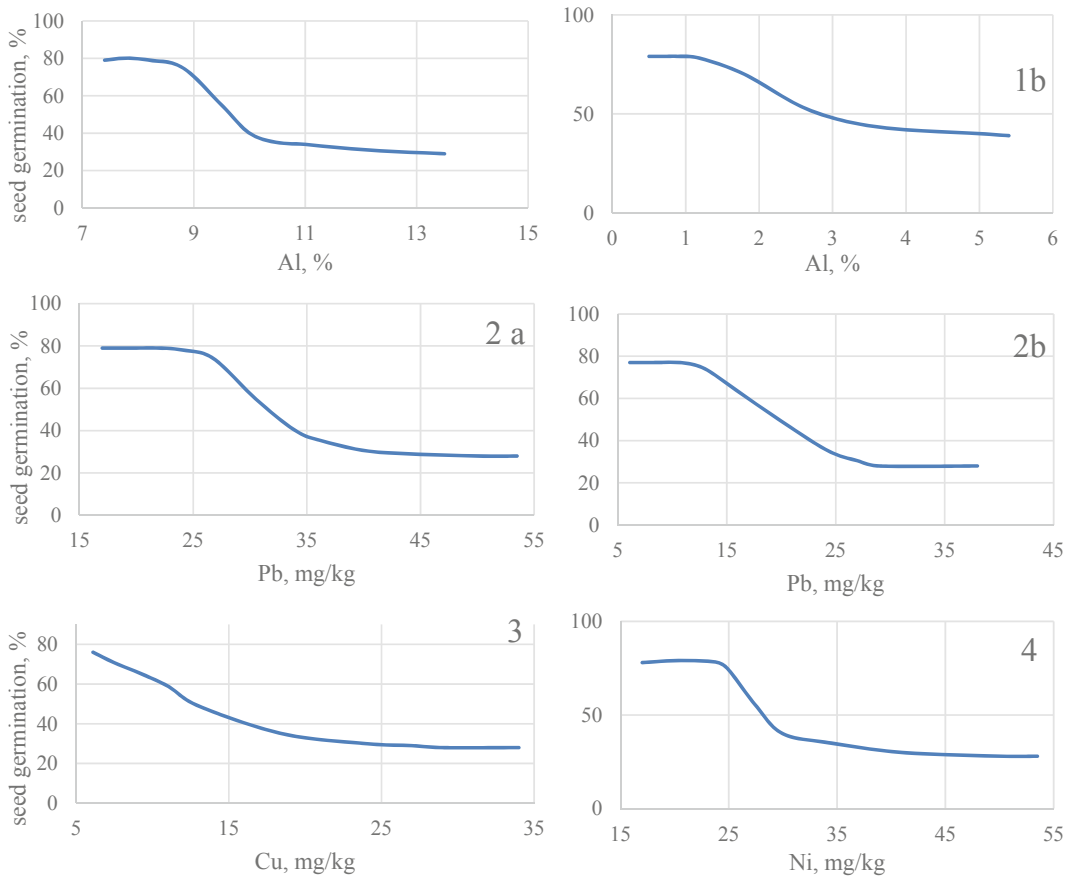


Fig. 18.6 Average seed germination versus Al total (1a), Al acid soluble (0.1 HCl) (1b), %, Pb total (2a), Pb acid soluble (2b), Cu acid soluble (3), Ni acid soluble

(4) (Belozertseva 2018) MPC—maximum permissible concentration (lower critical point); MIC—maximum impermissible concentrations (upper critical point)

background values, and approached those values the further the distance from the pollution source. This suggests that the nutritional and biological properties of these soils are highly affected by the technogenic load. Decreased urease activity is associated with a toxic effect of pollutants on soil microflora (Wang et al. 2007; Silva-Castro et al. 2015). Wang et al. (2007) also found a good correlation between the soil enzymatic activity and distance from the smelter. Due to their sensitivity, on the one hand soil microorganisms are good indicators of the pollution level of soil environment, while on the other hand they can serve as a good soil remediation agent (Calvo et al. 2019; Domínguez-Rodríguez et al. 2020).

Higher concentrations of contaminants usually accumulate in the uppermost organic horizons of the soil (Vaněk et al. 2013; Ettlér 2016), associated with a higher capture of emissions from smelters by wood canopies, which leads to higher levels of pollution in the litter and thus in the humus layer. However, the downward movement of contaminants can occur via leaching (Fernandez et al. 2007; Gruszecka and Wdowin 2013), mechanical disturbance such as soil tillage (Ettlér et al. 2005), and biological activity of soil fauna (Sterckeman et al. 2000; Fernandez et al. 2010).

The results of our study revealed that, under different degrees of pollution, the response of soil

Table 18.5 Content of basic plant nutrients (NO_3 , NH_4 , K_2O , P_2O_5) in the soil depending on distance and direction from aluminium plant

Content, mg 100 g^{-1}	Distance from the smelter			
	0.5 km	1 km	2 km	6 km
<i>Southwest</i>				
NO_3	1	4	4	8
NH_4	70	70	65	74
K_2O	8	11	11	17
P_2O_5	1	2	13	15
<i>Northwest</i>				
NO_3	4	7	7	8
NH_4	71	29	34	47
K_2O	7	11	8	12
P_2O_5	0	6	13	13
<i>Northeast</i>				
NO_3	4	6	8	8
NH_4	40	87	119	120
K_2O	10	12	21	24
P_2O_5	5	10	13	16
<i>Southeast</i>				
NO_3	–	14	14	–
NH_4	–	43	44	–
K_2O	–	26	49	–
P_2O_5	–	16	1	–

properties to the increase in concentration of F, Al, Na, Ba, Pb, Cu, and Ni in soils was clearly pronounced in terms of the “dose–effect” feedback. The response of an ecological parameter such as seed germination to pollution was characterised by a stepped trend, in which a strong bend in the curve is quite noticeable between the upper and lower levels of values (Fig. 18.6) (Belozertseva 2000). This implies that seed germination responds quickly to a certain amount of an individual pollutant. The point of the fastest change in a parameter is called a critical point. The fact that the affected area has not undergone significant changes is a manifestation of the stability and functioning of self-regulation mechanisms in the soil, as shown by the smooth transition of seed germination for Cu (Fig. 18.6, 3). With an increase in the load, the stability of the soil decreases with concomitant degradation of individual properties. The maximum load

levels were obtained after determining the critical points on the load–effect curve (Fig. 18.6, 1a, b, 2a, b, 3a, b, 4), which was built on the basis of sensitive parameters which changed regularly depending on the amount of pollutants. We suggest that the observed critical point is the beginning of the fastest change in the parameter.

The lower critical point is considered the maximum permissible concentration (MPC) of a chemical element at which changes in soil parameters are still reversible. The permissible concentrations of chemical elements are indicated by the upper critical point, at which the changes in soil parameters are no longer reversible. The critical points of the function that approximates the “load–effect” relationship were calculated using the method proposed by Vorobeychik et al. (1994). The most appropriate approximating regression equation is a logistic curve as follows (18.1):

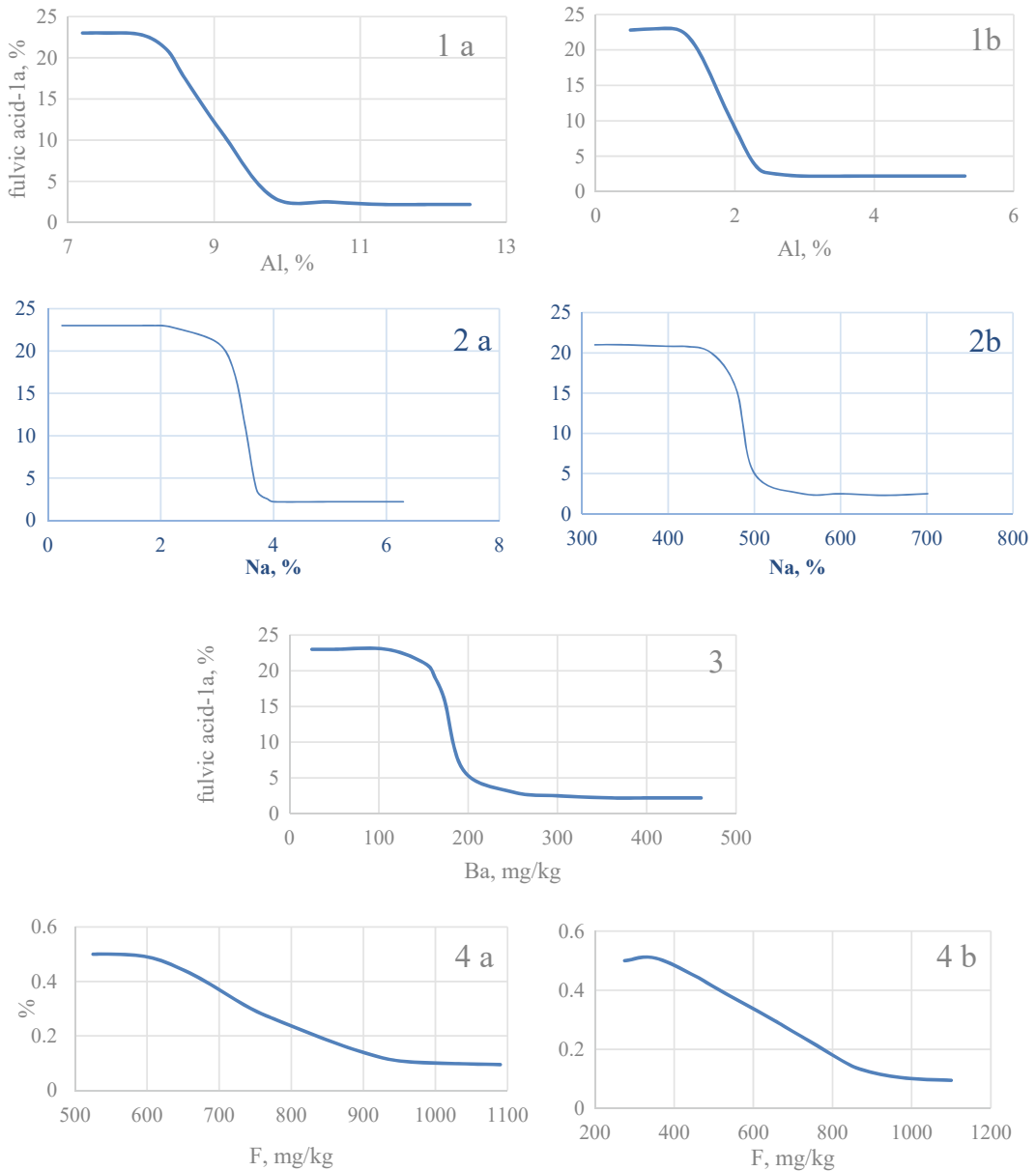


Fig. 18.7 Content of fulvic acid-Ia depending on the concentration of Al total (1a), Al acid soluble (1b), Na total (2a), Na acid soluble (2b), Ba acid soluble (3) и F total (4a), Fa acid soluble (4b)

$$y = \frac{A - a_0 + a_0}{1 + \exp(\alpha + \beta x)} \quad (18.1)$$

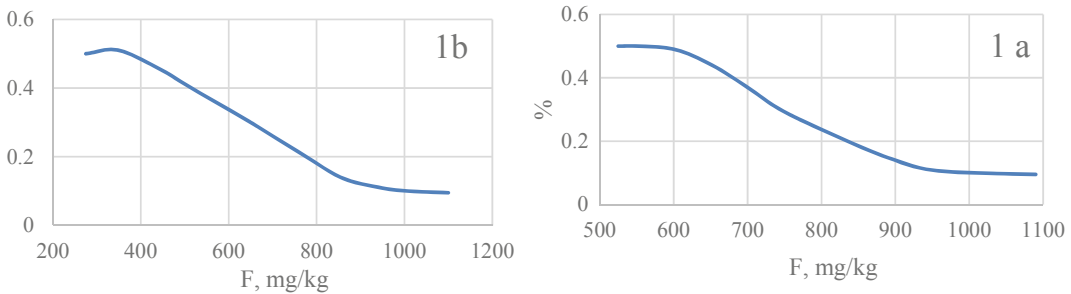
where y is an estimation of parameter; x is an estimation of loading; α, β, γ are factors; a_0 is the minimum level; A is the maximum level.

Critical points on the graph are the maximum permissible concentration (MPC) and impermissible concentration (MIC), calculated according to the following factors:

Top of the equation: *maximum impermissible concentration (MIC) (at which irreversible processes occur)* (Eqs. 18.2 and 18.3):

Table 18.6 Composition of humus in the surface horizon of soils at different distances southeast of the smelter, % to the total C soil

Distance, km	Total C	Fulvic acids (FA)				Humic acids (HA)					FA/HA	Non-hydrolysable residue
		1	2	3	Σ	1a	1	2	3	Σ		
0.5	4.13	5.6	6.7	3.9	16.2	2.4	4.3	9.1	7.0	18.8	0.86	70.0
1	8.9	7.1	2.8	0.9	10.8	4.6	4.2	8.8	6.2	19.8	0.55	69.4
2	10.0	11.4	1.7	14.4	27.5	6.8	4.3	4.4	4.2	20.7	1.33	45.8
6	1.69	15.9	1.3	14.2	31.4	23.7	6.6	4.3	4.2	38.8	0.81	30.0
20	5.0	17.2	1.2	7.8	32.2	21.8	8.2	4.1	5.4	39.5	0.82	28.3
70	2.1	17.9	1.2	11.4	30.5	23.8	8.3	1.4	4.4	37.9	0.80	34.2

**Fig. 18.8** Cellulose degradation rate (% per day) depending on the content of F total (1a) and F acid soluble (1b)

$$x_t = \frac{-\alpha + \ln(2 - \sqrt{3})}{\beta} \quad (18.2)$$

$$y_t = \frac{A - a_0 + a_0}{3 - \sqrt{3}} \quad (18.3)$$

Bottom of the equation: *maximum permissible concentration (MPC)*, Eqs. 18.4 and 18.5:

$$x_b = \frac{-\alpha + \ln(2 + \sqrt{3})}{\beta} \quad (18.4)$$

$$y_b = \frac{A - a_0 + a_0}{3 + \sqrt{3}} \quad (18.5)$$

From the aspect of sanitary and hygienic standards, a concentration at the maximum permissible level causes serious health disorders in human beings (e.g., Bajraktarova-Valjakova et al. 2018; Abdeldayem 2020), while concentrations at the maximum impermissible level are lethal for humans. In the first case, the processes

are reversible (that is, the system can return to its original state). In the second case, they are irreversible. The maximum permissible environmental load implies the lowest of the high loads on the various natural components. The values of the “dose–effect” relationship can be used to determine the maximum permissible and impermissible concentrations of elements in soils (the upper and lower critical points on plots) (Fig. 18.3). Based on the total form, they were, respectively, 0.66 and 0.84 g kg⁻¹ for fluoride; 82 and 93 g kg⁻¹ for aluminium; and 24 and 26 g kg⁻¹ for sodium. Based on the acid-soluble form, they were 220 and 580 mg kg⁻¹ for fluoride; 9 and 24 mg kg⁻¹ for aluminium; and 250 and 480 mg kg⁻¹ for sodium for the upper (MPC) and lower (MIC) limits, respectively. This underlines the extent to which the soil environment is polluted with these substances emitted from the Irkutsk aluminium smelter (Table 18.6).

Table 18.7 Gross and acid-soluble content of macro-elements and trace elements in the soils depending on distance and direction from the smelter and season

Direction	Distance, km	Horizon, Depth, cm	Mg/kg																													
			%		Na		Mn		F		Ba		Sr		Cu		Ni		Co		Pb											
			Al	G*	G	A	S	A	G	A	S	A	G	A	S	A	G	A	S	A	G	A	S	A								
North-east	0.5	O 0-1	3.2	5.6	4.5	9.2	1	0.5	0.8	0.1	0.05	760	720	365	1939	536	22	685	178	80	102	44	25	121	24	15	33	12	8	68	56	6
		AEL/BEL 1-28	15	4.3	4.9	6.4	1.2	0.3	0.4	0.09	0.03	775	428	311	1238	350	148	595	133	33	81	37	10	70	43	22	15	9	8	76	32	6
		BT28-50	12	3.4	3.4	7.2	0.4	0.1	0.2	0.04	0.02	684	472	205	519	230	33	244	58	16	61	21	25	62	12	10	10	5	3	34	17	4
	1	O 0-0.05	14	5	4.6	5.6	1.2	0.06	0.2	0.04	0.05	5200	5018	2565	1401	344	182	511	70	23	74	13	11	77	17	29	18	5	5	45	18	6
		AEL/BEL 0.05-22	9.4	3.2	3.2	3.1	1.1	0.07	0.2	0.04	0.03	750	395	252	1237	360	51	322	82	4	61	10	12	68	21	15	10	7	5	25	7	2
		BT 22-50	19	2.6	2.8	2	0.2	0.02	0.2	0.02	0.01	680	502	368	638	255	44	247	18	13	48	5	7	47	14	1	10	4	0.4	22	7	2
	2	AY 0-7	11	3.6	3.2	3.6	0.14	0.03	0.2	0.07	0.04	900	762	608	1097	464	260	337	230	22	47	28	20	90	58	27	18	16	14	46	23	0.8
		AEL/BEL 7-10	8.5	2.8	2.6	2.1	0.09	0.02	0.2	0.03	0.03	680	662	548	934	354	93	272	57	10	60	10	10	70	20	22	13	7	8	25	9	0.5
		BT 10-50	8.6	2	2	2.1	0.04	0.01	0.2	0.06	0.01	428	403	408	644	133	74	398	19	15	40	18	8	71	66	4	17	6	1	21	9	4.5
	6	O 0-0.5	7.4	1.9	1.5	1	0.02	0.02	0.2	0.1	0.03	565	558	548	597	391	235	449	269	74	59	49	15	81	19	24	17	16	14	23	17	19
AY 0.5-6		7.8	1.2	1	0.8	0.03	0.01	0.2	0.03	0.03	573	474	328	598	279	185	238	56	71	61	8	10	59	20	18	16	11	11	23	10	9	
AEL/BEL 6-11		7.9	0.8	0.8	1.1	0.03	0.01	0.2	0.02	0.02	402	368	365	508	154	89	254	23	28	48	6	8	62	22	15	13	8	1	18	8	5	
South-east	0.5	BT 11-50	8.1	1.8	1	1	0.04	0.01	0.2	0.02	0.02	423	402	248	537	129	81	246	19	19	47	13	16	49	18	12	11	10	11	20	9	8
		O 0-3	25	5.2	3.2	7.2	0.01	0.07	0.3	0.08	0.08	4516	4390	3658	1069	574	274	309	97	12	62	33	38	101	89	69	14	10	32	20	29	
		AEL/BEL 3-12	33	1.2	1.2	6.8	0.6	0.05	0.2	0.07	0.03	7954	7700	7658	914	511	34	311	135	113	54	18	13	59	51	17	14	12	4	34	22	5
	1	BT 12-50	10	1.6	1.4	7	0.5	0.02	0.2	0.05	0.02	902	856	342	562	137	23	222	17	17	35	21	12	54	15	16	13	7	4	19	5	7
		O 0-0.5	7.7	2.9	2	4.5	0.08	0.05	0.2	0.06	0.05	873	732	638	907	785	183	232	209	107	53	10	17	71	22	25	9	8	8	32	17	1
		AY/AEL 0.5-23	8	2.2	2.1	3.2	0.06	0.03	0.2	0.05	0.05	919	714	614	727	187	119	238	46	47	48	10	14	55	21	24	8	3	7	34	7	0.7
	2	BEL/BT 23-60	8.1	1.1	1.2	2.1	0.04	0.01	0.2	0.05	0.05	618	546	548	535	177	111	233	51	46	47	15	16	65	28	25	15	8	8	19	6	6
		O 0-0.2	7.5	1	0.9	3.2	0.01	0.05	0.2	0.1	0.05	700	408	328	592	518	534	256	98	12	52	36	19	66	25	23	17	15	8	31	8	15
		AY 0.2-26	7.4	1	0.8	3.1	0.06	0.02	0.2	0.03	0.04	720	518	352	456	164	77	267	36	15	47	11	21	58	21	28	9	8	9	26	10	16
	6	AEL 26-60	8	0.9	1	2.1	0.04	0.1	0.2	0.05	0.04	543	133	68	472	174	64	277	27	37	46	17	16	63	25	16	13	12	6	20	12	1
O 0-0.2		8	1.8	1.5	1.1	0.04	0.02	0.2	0.11	0.02	473	378	355	476	181	117	275	123	24	59	8	8	59	33	5	10	8	2	26	8	2	
AEL/BEL 0.2-23		7.9	0.9	0.9	0.9	0.04	0.01	0.2	0.04	0.02	411	402	248	493	166	105	265	121	64	48	10	8	56	20	10	15	4	4	20	6	2.3	
BT 23-60	8	1	1	1	0.02	0.01	0.2	0.09	0.02	445	382	198	496	164	105	279	229	59	46	16	4	49	22	7	9	8	3	19	7	0.4		

(continued)

Table 18.7 (continued)

Direction	Distance, km	Horizon, Depth, cm	Mg/kg																								
			%												Mg/kg												
			Al	Na		Mn		F		Ba		Sr		Cu		Ni		Co		Pb							
			G	A	S	A	G	A	S	A	G	A	S	A	G	A	S	A	G	A	S	A	G	A	S	A	
			A**	A***																							
	70	O 0-5	1.5	1	0.01	0.2	0.06	0.01	380	98	56	511	24	70	14	45	8	44	3	8	1						1.7
		AY/EL 5-10	7.9	0.9	0.03	0.02	0.05	0.02	428	109	62	511	163	45	30	10	40	8	50	20	18	12	8	5	20	6	3
		BEL/BT 10-60	8.1	1	0.8	0.03	0.03	0.02	402	68	36	535	166	68	56	4	42	9	56	20	13	10	9	4	21	8	3.3

* Gross and ** Acid soluble; *** Spring and autumn

Table 18.8 Maximum permissible concentration (MPC, lower critical point) and maximum unacceptable concentrations (MUC, upper critical point) of elements in soils (gross (G) and acid-soluble (A) content), mg kg⁻¹ (Al, Na gross content, %)

Soil parameter	Critical point																					
	Lower		Upper		Lower		Upper		Lower		Upper		Lower		Upper							
	Upper	lower	Upper	lower	Upper	Lower	Upper	Lower	Upper	Lower	Upper	Lower	Upper	Lower	Upper							
F	Al		Na		Ba		Pb		Cu		Ni											
G	A	G	A	G	A	G	A	G	A	G	A	G	A	G	A	G	A					
G	A																					
Average thickness of litter (O horizon)	880	700	700	-*	-	-	X**	-	6.0	-	X	-	-	-	-	-	X	X				
65																						
Urease activity	910	840	740	650	-	-	-	-	-	X	-	-	32	22	26	11	-	26				
-	22																					
Mobile forms of N (NO ₃)	840	580	750	220	-	-	-	-	-	-	-	-	-	-	-	-	-	-				
-																						
Phosphorus P ₂ O ₅	-	-	-	9.8	3.2	8.2	1.1	4.1	550	2.2	250	-	26	16	24	10	13	7	22			
-	20																					
Rate of cellulose decomposition	950	860	660	380	-	-	-	-	-	-	-	-	-	-	-	-	-	-	-			
-																						
Fulvic acid – Ia “an active humus”	930	720	X	X	9.3	2.4	8.3	1.5	3.4	480	3.1	470	170	160	-	-	-	-	-			
-																						
Toxicity	-	-	-	-	9.5	3.0	8.2	1.1	-	-	-	-	-	-	34	22	27	11	X	19	-	24
-	X																					
In the most sensitive parameter	840	580	660	220	9.3	2.4	8.2	1.1	3.4	480	2.2	250	170	160	26	16	24	10	13	7	X	22
65	20																					

* No “dose-effect” dependence observed; X** Values do not reach the upper critical point

The parameters of this relationship were converted to determine the maximum permissible and impermissible loads of pollutants, respectively: 2.2 and 10.2 t km⁻² year⁻¹ for PM, 2.4 and 5.2 t km⁻² year⁻¹ for fluoride, 19.0 and 42.0 t km⁻² year⁻¹ for aluminium, 0.8 and 4.0 t km⁻² year⁻¹ for sodium, and 0.04 and 0.84 t km⁻² year⁻¹ for barium; 7 and 26 kg km² year⁻¹ for lead, 5 and 20 kg km² year⁻¹ for copper, and 2 and 17 kg km² year⁻¹ for nickel. Taking into account the existing emissions, their concentrations need to be reduced by 2 and 13 times to comply with the maximum permissible and impermissible levels, respectively.

18.5 Conclusions

Our studies have identified soil and snow cover contamination at MPC and MIC levels by elements such as F, Al, Na, Ba, Pb, Cu and Ni. Based on the existing amount of technogenic emissions from the Irkutsk aluminium smelter, it is necessary to reduce emissions of the pollutants studied by 0–3.7 times to reach the level of maximum permissible concentrations (MPC) of various elements (F, Al, Na, Ba, Pb, Cu, Ni) and by 1.2–26.2 times to reach the level of the maximum impermissible concentrations of various elements (F, Na, Cu, Ni).

Introducing the new fifth series of electrolysis production to improve the safety of technology for baking anodes at the Irkutsk Aluminium Smelter greatly reduced emissions of pollutants. However, as aluminium production has doubled, the amount of pollutants emitted remains high. Therefore, during the commissioning of new facilities and during the technical re-equipment of existing facilities, it is recommended to take additional measures to minimise emissions of pollutants. The main environmental measures should include a change in technology, an increase in the efficiency of treatment facilities, and strict monitoring of compliance with approved standards. At the same time, the standards must correspond to the technological level of production and the characteristics of climatic

conditions, i.e., environmental regulations must be taken into account.

References

- Abdeldayem R (2020) A preliminary study of heavy metals pollution risk in water. *Appl Water Sci* 10(1). <https://doi.org/10.1007/s13201-019-1058-x>
- Abdul-Wahab S, Alsubhi Z (2019) Modeling and analysis of hydrogen fluoride pollution from an aluminum smelter located in Oman. *Sustain Urban Areas* 51:101802. <https://doi.org/10.1016/j.scs.2019.101802>
- Alfheim I, Wikström L (1984) Air pollution from aluminum smelting plants I. The emission of polycyclic aromatic hydrocarbons and of mutagens from an aluminum smelting plant using the söderberg process. *Toxicol Environ Chem* 8(1):55–72. <https://doi.org/10.1080/02772248409357041>
- Arinushkina EV (1970) Manual on chemical analysis of soils. Moscow University, Moscow, 489 pp (Аринушкина Е.В. Руководство по химическому анализу почв. Московский университет, Москва)
- Aristovskaya MA, Chugunova MV (1989) Express method of determination of biological activity of soils. *Pochvovedenie* 11:142–148 (Аристовская М. А., Чугунова М.В. Экспресс-метод определения биологической активности почв. Почвоведение)
- Arshad M, Eid EM (2018) The environmental impact of fluoride emissions from aluminum smelter at Jazan Economic City (JEC), Baish, Saudi Arabia on the surrounding ecosystem. In: Conference: 13th annual scientific research day at: King Khalid University, Abha, Saudi Arabia. https://www.researchgate.net/publication/325120454_The_Environmental_Impact_of_Fluoride_Emissions_from_Aluminum_smelter_at_Jazan_Economic_City_JEC_Baish_Saudi_Arabia_on_the_surrounding_Ecosystem. Accessed 18 Mar 2021
- Bajraktarova-Valjakova E, Korunoska-Stevkovska V, Georgieva S et al (2018) Hydrofluoric acid: burns and systemic toxicity, protective measures, immediate and hospital medical treatment. *Macedonian J Medi Sci* 6(11):2257–2269 <https://www.ncbi.nlm.nih.gov/pmc/articles/PMC6290397>
- Belozertseva IA (2000) Impact of technogenic emissions on a soil cover of the Top Angarski Krai (on the example of a zone of influence of Irkutsk aluminum plant). Doctoral thesis, Irkutsk, 161 pp (19.02.2016: <http://elibrary.ru/download/23677651.pdf>). (Белозерцева И.А. Влияние техногенных выбросов на почвенный покров Верхнего Ангарского края (на примере зоны влияния Иркутского алюминиевого завода). Докторская диссертация, Иркутск)
- Belozertseva IA (2013) Monitoring of environmental pollution in the influence zone of the Irkutsk Aluminium smelter. Voda: Khimiya i Ekologiya 10

- (64):33–38 (Белозерцева И.А. Мониторинг загрязнения окружающей среды в зоне влияния Иркутского алюминиевого завода//Вода: Химия и экология). <http://cs1.isc.irk.ru/BD/Журналы/Вода-химия%20и%20экология%202013/№10/стр%2033-38.pdf>
- Belozertseva IA (2018) Ecological rationing of technogenic loads of soils in the influence area of an aluminum smelter in Siberia. In: Sychev VG, Mueller L (eds) Novel methods and results of landscape research in Europe, Central Asia and Siberia (in five volumes). Vol. 2. Understanding and monitoring processes in soils and water bodies. Publishing House FSBSI “Pryanishnikov Institute of Agrochemistry”, Moscow, pp 206–211 (02.12.2019: <http://vniia-pr.ru/mosografi/pdf/tom2-44.pdf>)
- Belozertseva IA, Vorobyeva IB, Vlasova NV, Lopatin DN, Yanchuk MS (2015) Pollution of the atmosphere and fluorine content in the snow of the water area of Baikal. *Modern Prob Sci Educat* 2(2). <http://www.science-education.ru/ru/article/view?id=22004>
- Belozertseva IA, Vorobyeva IB, Vlasova NV et al (2017a) Chemical composition of snow in the water area of Lake Baikal and on the adjacent territory. *Geogr Nat Resour* 38:68–77. <https://doi.org/10.1134/S1875372817010097>
- Belozertseva IA, Vorobjeva IB, Vlasova NV, Lopatina DN, Janchuk MS (2017b) Pollution of a snow on water area of lake Baikal and adjoining territory. *Vodnye resursy* 44(3):471–484 (Загрязнение снега на акватории озера Байкал и прилегающей территории. Водные Ресурсы). https://www.researchgate.net/publication/318360718_ZAGRAZNIENIE_SNEGA_NA_AKVATORII_OZ_BAJKAL_I_PRILEGAUSEJ_TERRITORII. Accessed 18 Mar 2021
- Bhattacharya P, Samal AC (2018) Fluoride contamination in groundwater, soil and cultivated foodstuffs of India and its associated health risks: a review. *Res J Recent Sci* 7(4):36–47. <http://www.isca.in/rjrs/archive/v7/i4/6.ISCA-RJRS-2018-028.php>
- Brindha K, Rajesh R, Murugan R, Elango L (2011) Fluoride contamination in groundwater in parts of Nalgonda District, Andhra Pradesh, India. *Environ Monit Assess* 172:481–492. <https://doi.org/10.1007/s10661-010-1348-0>
- Calvo C, Rodríguez-Calvo A, Robledo-Mahón T, Manzanera M, González-López J, Aranda E, Silva-Castro GA (2019). Biostimulation of crude oil-polluted soils: influence of initial physicochemical and biological characteristics of soil. *Int J Environ Sci Technol* 1–10. <https://doi.org/10.1007/s13762-019-02269-8>
- Choudhary S, Rani M, Devika OS et al (2019) Impact of fluoride on agriculture: a review on its sources, toxicity in plants and mitigation strategies. *Int J Chem Stud* 7(2):1675–1680. <https://www.chemijournal.com/archives/2019/vol7issue2/PartAB/7-2-263-789.pdf>
- Csavina J, Field J, Taylor MP, Gao S, Landázuli A, Betterton EA, Sáez AE (2012) A review on the importance of metals and metalloids in atmospheric dust and aerosol from mining operations. *Sci Total Environ* 433:58–73. <https://doi.org/10.1016/j.scitotenv.2012.06.013>
- Csavina J, Taylor MP, Félix O, Rine KP, Sáez AE, Betterton EA (2014) Size-resolved dust and aerosol contaminants associated with copper and lead smelting emissions: implications for emission management and human health. *Sci Total Environ* 493:750–756. <https://doi.org/10.1016/j.scitotenv.2014.06.031>
- Davydova ND, Znamenskaya TI (2016) Geological problems of Siberia associated with the development of nonferrous metallurgy. *Geogr Nat Resour* 37(4):313–318. <https://doi.org/10.1134/S1875372816040053>
- Deger L, Plante C, Jacques L et al (2012) Active and uncontrolled asthma among children exposed to air stack emissions of sulphur dioxide from petroleum refineries in Montreal, Quebec: a cross-sectional study. *Can Respir J* 19:97–102. <https://www.ncbi.nlm.nih.gov/pmc/articles/PMC3373279/>
- Domínguez-Rodríguez VI, Adams RH, Sánchez-Madrigal F, Pascual-Chablé JLS, Gómez-Cruz R (2020) Soil contact bioassay for rapid determination of acute toxicity with *Eisenia foetida*. *Heliyon* 6(1):e03131. <https://doi.org/10.1016/j.heliyon.2019.e03131>, <https://europepmc.org/article/med/31909284>
- Ettler V (2016) Soil contamination near non-ferrous metal smelters: a review. *Appl Geochem* 64:56–74. <https://doi.org/10.1016/j.apgeochem.2015.09.020>
- Ettler V, Vaněk A, Mihaljevič M, Bezdička P (2005) Contrasting lead speciation in forest and tilled soils heavily polluted by lead metallurgy. *Chemosphere* 58(2005):1449–1459. <https://doi.org/10.1016/j.chemosphere.2004.09.084>
- Fernandez C, Labanowski J, Cambier P, Jongmans AG, van Oort F (2007) Fate of airborne metal pollution in soils as related to agricultural management. 1. Zn and Pb distributions in soil profiles. *Eur J Soil Sci* 58:547–559. <https://doi.org/10.1111/j.1365-2389.2006.00827.x>
- Fernandez C, Labanowski J, Jongmans T, Bermond A, Cambier P, Lamy I (2010) Fate of airborne metal pollution in soils as related to agricultural management. 2. Assessing the role of biological activity in micro-scale Zn and Pb distributions in A, B and C horizons. *Eur J Soil Sci* 61:514–524. <https://doi.org/10.1111/j.1365-2389.2010.01256.x>
- Gibbs GW, Sévigny M (2007) Mortality and cancer experience of Quebec aluminum reduction plant workers. Part 3: monitoring the mortality of workers first employed after January 1st, 1950. *J Occup Environ Med* 49:1269–1287. <https://doi.org/10.1097/JOM.0b013e3181593da8>
- Glazovskaya MA (2012) Geochemical barriers in soils: typology, functional features, and ecological significance. Landscape geochemistry and soil geography. Centenary of M.A. Glazkovskaya, Moscow, April, pp 26–44 (Глазовская М.А. (2012) Геохимические барьеры в почвах: типология, функциональные

- особенности, экологическое значение. Ландшафтная геохимия и география почв. 100-летие М.А.Глазковской. Москва, апрель 26–44.)
- GN 2.1.7.2041-06 (2006) The threshold limit values (TLV) of chemicals in the soil: hygienic standards. Federal Centre of Hygiene and Epidemiology of Rospotrebnadzor, Moscow, 15 pp. <https://ohranatruda.ru/upload/iblock/c0a/4293850511.pdf>. Accessed 18 Mar 2021
- GOST (State Standard) (1982) 7.1.3.07-82: Regulations on water quality control in water bodies and streams, 1982, renewed by the Order of RF Ministry of Natural Resources. http://ohranatruda.ru/ot_biblio/normativ/data_normativ/9/9212. Accessed 18 Mar 2021
- GOST (1982) 2874-82. Drinking water. Hygienic requirements and quality control. <http://gostvoda.ru/d/677526/d14-gost-2874-82> (in Russian)
- Gruszecka AM, Wdowin M (2013) Characteristics and distribution of analysed metals in soil profiles in the vicinity of a postflotation waste site in the Bukowno region, Poland. *Environ Monitor Assess* 185 (10):8157–8168. <https://doi.org/10.1007/s10661-013-3164-9>. <https://europemc.org/article/med/23519844>
- Haidouti C (1991) Fluoride distribution in soils in the vicinity of a point emission source in Greece. *Geoderma* 49:129–138. [https://doi.org/10.1016/0016-7061\(91\)90096-C](https://doi.org/10.1016/0016-7061(91)90096-C)
- Haziyevev FH (2005) Methods of a soil enzymology (Методы почвенной энзимологии). Moscow, Nauka 73–74 pp (05.12.2019: <https://search.rsl.ru/ru/record/01002807734>)
- Heinrich J, Thiering E, Rzehak P et al (2013) Long-term exposure to NO₂ and PM₁₀ and all-cause and cause-specific mortality in a prospective cohort of women. *Occup Environ Med* 70:179–186. <https://oem.bmj.com/content/oemed/70/3/179.full.pdf>
- Honda M, Suzuki N (2020) Toxicities of polycyclic aromatic hydrocarbons for aquatic animals. *Int J Environ Res Public Health* 17:1363. <https://www.ncbi.nlm.nih.gov/pmc/articles/PMC7068426/>
- Jafari Y, Jones BG, Pacheco JC et al (2020) Trace element soil contamination from smelters in the Illawarra region, New South Wales, Australia. *Environ Earth Sci* 79:372. <https://doi.org/10.1007/s12665-020-09115-y>
- Jimenez E, Linares C, Martinez D, Díaz J (2011) Particulate air pollution and short-term mortality due to specific causes among the elderly in Madrid (Spain): seasonal differences. *Int J Environ Health Res* 21:372–390. <https://doi.org/10.1080/09603123.2011.560251>
- Kabata-Pendias A, Mukherjee AB (2007) Trace elements from soil to human. Springer, Berlin Heidelberg
- Khavina LA (2007) Economical and geographical features a sorazvitiya of the monostructural city and aluminum production (on the example of Shelekhov and Irkutsk aluminum plant). Doctoral thesis, Irkutsk, 20 pp (05.12.2019: <https://elibrary.ru/item.asp?id=16127475>). Accessed 18 Mar 2021
- Koval PV, Belogolova GA, Burenkov EK, Pampura VD (1993) Baikal polygon: international and national projects of geochemical mapping and monitoring of the environment. *Geol Geophys* 34(10–11):238–252 (Коваль П.В., Белоголова Г.А., Буренков Э.К., Пампура В.Д. Геохимическое картирование и мониторинг природной среды на Байкальском полигоне//Геология и геофизика, т. 34 (10/11), с. 238–252)
- Kousehlar M, Widom E (2020) Identifying the sources of air pollution in an urban-industrial setting by lichen biomonitoring—a multi-tracer approach. *Appl Geochem* 121:104695. <https://doi.org/10.1016/j.apgeochem.2020.104695>
- Kumar K, Giri A, Vivek P, Kalaiyaran T, Kumar B (2017) Effects of fluoride on respiration and photosynthesis in plants: an overview peertechz. *J Environ Sci Toxic* 2(2):043–047. <https://doi.org/10.17352/pjest.000011>
- Kuźniar A, Banach A, Stepniowska Z, Frąc M, Oszust K, Gryta A, Klos M, Wolińska A (2018) Community-level physiological profiles of microorganisms inhabiting soil contaminated with heavy metals. *Int Agrophys* 32:101–109
- Kvande H, Drabløs PA (2014) The aluminum smelting process and innovative alternative technologies. *J Occup Environ Med* 56(5 Suppl):23–32. https://www.researchgate.net/publication/262148554_The_Aluminum_Smelting_Process_and_Innovative_Alternative_Technologies. Accessed 18 Mar 2021
- Lasota J, Błońska E, Łyszczarz S et al (2020) Forest humus type governs heavy metal accumulation in specific organic matter fractions. *Water Air Soil Pollut* 231(80). <https://doi.org/10.1007/s11270-020-4450-0>
- Litvinovich AV, Pavlova OYu (2002) Fluoride in the soil-plant system under use of chemical reclamation and contamination of environment with technogenic emissions. *Agrochimia* 2:66–76 (А.В. Литвинович, О.Ю.Павлова. Фтор в системе почва-растение при применении в сельском хозяйстве средств химизации и загрязнении объектов природной среды техногенными выбросами//Агрохимия. 2002.№2. С.66–76.)
- Martin SC, Larivière C (2014) Community health risk assessment of primary aluminum smelter emissions. *J Occup Environ Med* 56(5 Suppl):33–39. <https://europemc.org/article/pmc/pmc4131939>
- Matorova NI (2005) Formation of health of children's population in industrial centres. PhD in biological sciences. Moscow, 338 pp (05.12.2019: <https://www.disserscat.com/content/formirovanie-zdorovya-detskogo-naseleniya-v-promyshlennykh-tsentrakh>). Accessed 18 Mar 2021
- Mazurak AP (1975) Agrochemical methods of investigating soils. Nauka, Moscow, 656 pp (Мазурак А.П. (1975) Агрохимические методы исследования почв. Наука, Москва, 656 с.)
- Ministry of Natural Resources and Environmental Protection of the Russian Federation (2013) The state

- report: about a state and about environmental protection of the Russian Federation in 2012, 455 pp (05.12.2019: http://www.mnr.gov.ru/docs/gosudarstvennye_doklady/o_sostoyanii_i_ob_okhrane_okruzhayushchey_sredy_rossiyskoy_federatsii/132221/). Accessed 18 Mar 2021
- Naprasnikova EV, Makarova AP (2005) Sanitary-microbiological and biochemical features of soil cover in Pre-Baikal cities and towns. (Санитарно-микробиологические и биохимические особенности почвенного покрова городов прибайкалья). *Sibirskii Meditsinskii Zhurnal* 4:67–71 (05.12.2019: <https://elibrary.ru/item.asp?id=11482225>). Accessed on 18 Mar 2021
- Omueti JAI, Jones RL (1977) Fluoride adsorption by Illinois soils. *J Soil Sci* 28:564–572. <https://doi.org/10.1111/j.1365-2389.1977.tb02264.x>
- Pandey AK, Prakash R (2020) Opportunities for sustainability improvement in aluminium industry. *Eng Rep* 2(5):e12160. <https://doi.org/10.1002/eng2.12160>
- Polomski J, Flöhler H, Blaser P (1982) Accumulation of air-borne fluoride in soils. *J Environ Qual* 11:457–461. <https://doi.org/10.2134/jeq1982.00472425001100030028x>
- Pomazkina LV, Kotova LG, Radnaev AB (1999) Biogeochemical cycles of nitrogen in agro ecosystems on polluted soils in the forest-steppe of the Baikal region. *Eurasian Soil Sci* 32(6):705–709 (05.12.2019: <https://elibrary.ru/item.asp?id=13319754>). Accessed 18 Mar 2021
- Ponomareva VV, Plotnikova TA (1975) Agrochemical methods of soil research. Moscow “Nauka”, pp 47–55. <https://findpatent.ru/patent/265/2659939.html>. Accessed 18 Mar 2021
- Procedural Recommendations on Identification of Degraded and Polluted Soils (1995) Russian Committee on Land Use, Ministry of Agriculture, Ministry of Natural Resources, Moscow, 21 pp. (05.12.2019: <http://docs.cntd.ru/document/902101153>). Accessed 18 Mar 2021
- Rezaei M, Nikbakht M, Shakeri A (2017) Geochemistry and sources of fluoride and nitrate contamination of ground water in Lar area, south Iran. *Environ Sci Pollut Res* 24(18):15471–15487. <https://doi.org/10.1007/s11356-017-9108-0>
- Saevarsdottir G, Kvande H, Welch B (2019) Aluminum production in the times of climate change: the global challenge to reduce the carbon footprint and prevent carbon leakage. *JOM: J Min Metals Mater Soc*. <https://doi.org/10.1007/s11837-019-03918-6>
- Sanchez M, Milà C, Sreekanth V et al (2020) Personal exposure to particulate matter in peri-urban India: predictors and association with ambient concentration at residence. *J Expo Sci Environ Epidemiol* 30:596–605. <https://doi.org/10.1038/s41370-019-0150-5>
- Sanchez L-F, Stern D-I (2016) Drivers of industrial and non-industrial greenhouse gas emissions. *Ecol Econ* 124:17–24. https://openresearch-repository.anu.edu.au/bitstream/1885/99872/3/01_Sanchez_Drivers_of_Industrial_2016.pdf. Accessed 18 Mar 2021
- Saxena S, Rani A (2012) Fluoride ion leaching kinetics for alkaline soils of Indian origin. *J Sci Res Replica* 1:29–40. <https://doi.org/10.9734/JSRR/2012/2101>
- Schubert R (ed) (1988) Bioindication of pollution of terrestrial ecosystems. Moscow: translated from German, Mir. 348 pp
- Semenov AD (1977) Manual on chemical analysis of land waters. Gidrometeoizdat, Leningrad, 486 pp (Семенов А.Д. Руководство по химическому анализу поверхностных вод суши. Гидрометеоздат, Ленинград, 486 стр.)
- Senkondo Y, Mkumbo S, Sospeter P (2018) Fluorine and copper accumulation in lettuce grown on fluoride and copper contaminated soils. *Comm Soil Sci Plant Anal* 49(21):2638–2652. <https://doi.org/10.1080/00103624.2018.1526950>
- Shpeyzer GM, Mineeva LA (2006) Guide to the chemical analysis of waters: a methodical grant. Irkutsk state university, 55 pp (Шпейзер Г.М., Минеева Л.А. (2006) Руководство по химическому анализу вод: методическое пособие. Иркутский государственный университет) http://window.edu.ru/catalog/pdf2txt/170/37170/14182?p_page=1
- Silva-Castro G, Uad I, Rodríguez-Calvo A, González-López J, Calvo C (2015) Response of autochthonous microbiota of diesel polluted soils to land-farming treatments. *Environ Res* 137:49–58. <https://doi.org/10.1016/j.envres.2014.11.009>
- Singh G, Sinam G, Kriti K et al. (2020) Soil pollution by fluoride in India: distribution, chemistry and analytical methods. In: Shukla V, Kumar N (eds) Environmental concerns and sustainable development. Springer Nature Singapore Pte Ltd. https://www.researchgate.net/publication/332795863_Soil_Pollution_by_Fluoride_in_India_Distribution_Chemistry_and_Analytical_Methods. Accessed 18 Mar 2021
- Sirina NV (2009) An extended abstract of the PhD thesis with the title “Air pollution assessment caused by primary aluminum smelters in Irkutsk region” Khabarovsk, Russia (Сирина Н.В. Расширенный автореферат кандидатской диссертации на тему «Оценка загрязнения атмосферного воздуха предприятиями первичного алюминия в Иркутской области» Хабаровск, Россия)
- Sorooshian A, Csavina J, Shingler T, Dey S, Brechtel FJ, Sáez AE, Betterton EA (2012) Hygroscopic and chemical properties of aerosols collected near a copper smelter: implications for public and environmental health. *Environ Sci Technol* 46(2012):9473–9480. <https://doi.org/10.1021/es302275k>
- Steen-Olsen K (2009) Environmental assessment of aluminium production in Europe: Current situation and future scenarios. Norwegian University of Science and Technology, Trondheim, Norway, <https://ntnuopen.ntnu.no/ntnu-xmlui/handle/11250/233622>. Accessed 18 Mar 2021
- Sterckeman T, Douay F, Proix N, Fourrier H (2000) Vertical distribution of Cd, Pb and Zn in soils near smelters in the North of France. *Environ Pollut* 107

- (2000):377–389. [https://doi.org/10.1016/S0269-7491\(99\)00165-7](https://doi.org/10.1016/S0269-7491(99)00165-7)
- Szostek R, Ciećko Z, Walczak M, Swiontek-Brzezinska M (2015) Microbiological and enzymatic activity of soil after pollution with fluorine. *Polish J Environ Studies* 24(6):2641–2646. <https://doi.org/10.15244/pjoes/59491>
- Thomassen Y, Koch W, Dunkhorst W, Ellingsen DG, Skaugset NP, Jordbekken L, Arne Drabløs P, Weinbruch S (2006) Ultrafine particles at workplaces of a primary aluminium smelter. *J Environ Monit* 8 (1):127–133. <https://doi.org/10.1039/B514939H>
- Uddin MK (2017) A review on the adsorption of heavy metals by clay minerals, with special focus on the past decade. *Chem Eng J* 308:438–462. <https://doi.org/10.1016/j.cej.2016.09.029>
- Vorobeychik EL, Sadykov OF, Farafontov MG (1994) Calculation of the limiting values of load, in ecological standardisation of technogenic pollutions of terrestrial ecosystems (Regional Level), Yekaterinburg. Nauka, 280 pp (05.12.2019: https://www.studmed.ru/vorobeychik-el-sadykov-of-farafontov-mg-ekologicheskoe-normirovanie-tehnogennyh-zagryazneniy-nazemnyh-ekosistem-lokalnyy-uroven_cad70247f80.html). Accessed 18 Mar 2021
- Vaněk A, Chrastrný V, Komárek M (2013) Geochemical position of thallium in soils from a smelter-impacted area. *J Geochem Explor* 124:176–182. <https://doi.org/10.1016/j.gexplo.2012.09.002>
- Wang Y, Shi J, Wang H et al (2007) The influence of soil heavy metals pollution on soil microbial biomass, enzyme activity, and community composition near a copper smelter. *Ecotoxicol Environ Saf* 67(1):75–81. <https://doi.org/10.1016/j.ecoenv.2006.03.007>
- WHO (2005) Health effects of transport-related air pollution. In: Krzyzanowski M, Kuna-Dibbert B, Schneider J (eds) WHO library cataloguing in publication data, https://www.euro.who.int/__data/assets/pdf_file/0006/74715/E86650.pdf?ua=1. Accessed 18 Mar 2021
- Zhang Y, Yan Q, Wang J, Han S, He R, Zhao Q, Jin M, Zhang R (2020) Emission characteristics and potential toxicity of polycyclic aromatic hydrocarbons in particulate matter from the prebaked anode industry. *Sci Total Environ* 722:137546. <https://doi.org/10.1016/j.scitotenv.2020.137546>



Technogenic Fluorine in the Siberian Steppe Soils Due to a Metallurgical Plant Operation

19

Nina D. Davydova

Abstract

This paper presents the results of long-term landscape and geochemical research on the distribution of gas and dust emissions produced by aluminium plants located in the South Minusinsk basin (Khakassia, Russia). The chemical composition of solid and liquid constituents and the content of pollutants was determined in every component of the landscape. It was revealed that the main polluting elements with an anomaly index above 10 in the solid and liquid aerosol phases were F, Al, Na and Ni, compared to the solid soil phase and snow meltwater of the background. The accompanying elements were Zn, Cu, Sr, Ba, Ca, Mg, Mn, Fe and V, whose content exceeded the background levels by 2–10 times. The technogenic load of the main pollutants and their distribution in the atmosphere (snow)–soil solution–soil system were determined. The mechanisms of their primary and secondary differentiation in landscape soils were studied, and their accumulation and distribution levels in soil profile were calculated. The analysed indicators, including toxicity, showed that the main pollutant was

fluorine (F). The nature of its migration and accumulation was determined to a large extent by biogeochemical, physico-chemical and geochemical barriers. The fluorine load was calculated on the basis of the maximum permissible concentrations (MPCs) of 10 mg kg⁻¹ (load—soil content) and using cartographic maps of their surface distribution.

Keywords

Landscape · Soil · Pollutants · Migration · Fluorine · Load · Rating

19.1 Introduction

Technogenesis, which became the main geochemical factor on the Earth's surface in the twentieth century, led to the threat of increasing geochemical barriers (Perelman 1986) at the global, regional, and local levels. The problem of environmental pollution remains an urgent issue today (Volkova and Davydova 1987). Large airborne emissions in urban areas of Russia increased by 60–150% from 1998 to 2008, reaching maximum values of 2,000,000 tonnes per year in industrial centres (Kasimov 2013). In that regard, one of the main challenges of our time is to monitor each source of environmental pollution in order to minimise its negative consequences.

N. D. Davydova (✉)

V.B. Sochava Institute of Geography of the Siberian Branch of the Russian Academy of Sciences, Ulan-Batorskaya Street 1, Irkutsk 664033, Russia
e-mail: davydova@irigs.irk.ru

Over the past decades, non-ferrous industries have been developing rapidly, including the production of aluminium, which ranks first in terms of its manufacturability. Aluminium production is highly energy-intensive, has a significant environmental impact and releases a large proportion of energy as waste heat (Saevarsdottir et al. 2020; Brough and Jouhara 2020). However, as a source of pollutants, aluminium production plants are the largest producers of fluoride worldwide. They release this toxic compound in gaseous and solid forms (Divan et al. 2008; Choudhary et al. 2019). Fluoride is an essential element necessary for the normal development of living organisms at concentrations below 1.5 µg/ml, but at higher doses it can pose a lethal risk to plants and animals (Khairnar et al. 2015). The consumption of fluoride-polluted food and water causes fluorosis, which affects the bones. Very high concentrations may cause bone deformation and birth defects (ATSDR 2003; Weinstein and Davison 2004; Adimalla et al. 2019). There are several major sources of environmental fluoride contamination, both from natural sources (natural rocks, volcanic eruptions) and anthropogenic sources (phosphate fertilisers, metallurgical plant emissions, etc.) (Zhang et al. 2007; Zhang et al. 2013; Rezaei et al. 2017; Choudhary et al. 2019; Bombik et al. 2020; Vithanage and Bhattacharya 2015; Bhat et al. 2015; Singh et al. 2020). Industrial pollution sources release gaseous fluorides (e.g., HF, SiF₄) and particulate fluorides (e.g., AlF₃, Na₃AlF₆, CaF₂), and can raise soil F concentrations by between 2 and 20 times (e.g., Polomski et al. 1982; Gritsan et al. 1995). However, the effect of these F pollution sources is generally restricted to within 10–20 km downwind (e.g., Haidouti 1991) and becomes most serious where the density of F emitters is high (e.g., Gritsan et al. 1995). Today, there are technologies to remove fluoride from factories' smoke; however, after usage, the cleaning system is also disposed of in landfills. This waste contains soluble F, which can enter the soil, while emissions of fluoride compounds into the atmosphere remain, thus polluting the environment (IPCS 2002; Franzaring et al. 2006).

The available literature presents a wide range of health risks and ways in which fluoride pollutes the environment, mainly associated with mining activities, air deposition and the use of fertilisers containing fluorine (e.g., Bharti et al. 2017; Bhattacharya and Samal 2018; Adimalla et al. 2019; Artiola et al. 2019; Bombik et al. 2020; Singh et al. 2020). However, there have been only few studies on fluoride pollution of the soil environment from aluminium smelters (e.g., Davydova and Znamenskaya 2016; Choudhary et al. 2019). Russian Siberia accounts for about half of the total output of the country's nonferrous metallurgy and produces more than 70% of Russian aluminium (Davydova and Znamenskaya 2016), thus representing a serious source of fluoride emissions. Moreover, the aluminium industry in Russia continues to develop with the strategic goals of shifting the metal production centres from the western regions of Russia to Siberia. At the same time, there are plans to replace small aluminium smelters with large high-performance plants (from 0.5 to 1 million tonnes per year). However, the equipment and technologies required to increase labour productivity and improve the production process have not been fully developed and implemented. The intention to increase industrial production in modern technological conditions leads to a higher load of pollutants in the environment (precipitation, soil, plant, and groundwater) due to the inefficient purification systems in factories which are still being modernised. All these activities, acting in synergetically, threaten environmental safety over large areas, a threat which is especially acute in the Siberian steppes of Russia, where the long-term operation of aluminium plants has resulted in a considerable accumulation of pollutants, including fluoride compounds, which are present in every environmental component (Davydova and Znamenskaya 2016). In the Siberian steppes, soils' capacity for self-cleaning is insufficient due to the lack of precipitation, although damage to steppe vegetation is not observed visually, since it is more resistant than coniferous forests (Davydova and Znamenskaya 2016). Similar conditions can be observed in the steppe

landscapes of Khakassia with its fertile Chernozems. Here, since 1985, the state-owned “RUSAL Sayanogorsk” has been operating its two aluminium plants. From the very beginning of the operation of aluminium smelters, fluorides are constantly found in meltwater, soil and vegetation around the plants (Saraev and Kharakhinova 1992; Savkova et al. 2003; Egunova 2009). Although the “RUSAL Sayanogorsk” claims that the smelter is equipped with relatively modern filtering technologies and is environmentally safe (Nikitin 2020), the situation requires specific complex landscape/geochemical research into the environmental components to identify the territories which are exposed to the gas and dust emissions produced by the plants.

A concentration of pollutants in snow meltwater can serve as an indicator of a site’s environmental condition. Snowpack is widely used in atmospheric pollution zones (Engelhard et al. 2007; Davydova 2015; Talovskaya et al. 2015; Shevchenko et al. 2020) as an absorbent because its chemical composition not only reflects the state of the atmosphere but also makes it possible to quantify the flows of pollutants into the landscapes and assess their value for each landscape component or element. After the snow melts, the substances coming from the atmosphere are mainly deposited on the soil surface and, in this case, it is important to know their solubility properties, which determine their migration ability. For this purpose, in our study, the chemical composition of both solid suspensions and soluble compounds was also determined in snow meltwater samples. Davydova and Znamenskaya (2016) found that during 30 years of the operation of Al smelters in Khakassia, the primary pollutants of the soil and snow cover were F, Al, and Na.

The general goal of this research was to study the level of soil environmental pollution due to the operation of the large aluminium plants in the Siberian steppes. The hypothesis was that the technologies used in giant aluminium plants are not environmentally friendly and pollute adjacent landscapes, primarily with fluoride. The following tasks were set and performed:

- study of the chemical composition of technogenic substances (in a solid, slightly soluble or soluble state) in the snowpack
- identification of pollutant associations and detection of main pollutants
- establishment of the load and levels of main pollutants in the main landscape components (soil and vegetation) with their spatial distribution in cartographic maps
- study of their primary distribution in the landscapes and secondary distribution in the soils
- study of the secondary distribution of fluorine in soil in order to determine the role of geochemical barriers in its radial migration
- assessment of fluorine loads
- ascertainment of technogenic geochemical anomalies.

19.2 Materials and Methods

19.2.1 Site Description

Steppe landscapes were studied in the South Minusinsk basin, located in the West Sayan Mountains and the Kuznetsk Alatau range. At present, an energy-intensive industrial complex is being developed here on the basis of the Sayano-Shushenskaya hydroelectric power station (HPP). The largest industrial enterprise in the region is “RUSAL Sayanogorsk”, which owns the Sayanogorsk and Khakas aluminium plants. Both plants are located between the Abakan and Yenisei rivers, on the second terrace above the floodplain of the left bank of the Yenisei River, 15 km north of the West Sayan Mountains foothills. Aluminium production at the Sayanogorsk plant, with an estimated capacity of 510,000 tonnes per year, started in 1985. Construction of the Khakas aluminium plant began in 2006 at the same industrial site. By 2014, the combined capacity of the plants had reached 839,000 tonnes of aluminium per year and was thus the main source of pollution in the study area.

19.2.2 Pedological Description

The agriculture of the study territory is well developed due to the predominance of fertile Chernozem soils. Chernozem calcic soils and their subtypes, Chernozem salic and Sodic Chernozem soils, are widespread in the basin. They vary in their depth, humus content, grain size distribution and parent material. The soils are mainly of heavy loam and clay texture and occupy high terraces as well as the summits and slopes of ridges. The soils studied were mainly formed under xerophytic vegetation (*Stipa krylovii*, *Leymus chinensis*, *Helictotrichon schellianum*, *Koeleria cristata*, *Astragalus multicaulis*, *Artemisia glauca*, *Artemisia frigida* L., and others). Large massifs of dispersed calcareous and cryogenic-mycelial Chernozem subtypes with meadow grass and mixed steppe herbs are found in elevated hilly terrains along the northern and north-eastern slopes and in the river valleys.

All Chernozemic soils have the following common features: a relatively friable soil profile, a gradual colour change in the humus horizon, and elevated carbonate bedding. The effervescence in a 10% HCl solution is usually observed in the upper part of the carbonate horizon, except for the soils formed on red and variegated colluvium of Ordovician carbonate rocks, whose effervescence is observed in the lower part of the umbric horizon. Alkaline soil reactions and the nature of the absorbing complex have a significant effect on the weak structure of these soils. Water-stable aggregates (>1 mm) constitute more than 10% (Tanzybaev and Bulatova 2001).

Depending on their specific features, all the Chernozems which were studied can be divided into four groups: shallow low-humus, medium low-humus, shallow medium-humus, and medium-humus. The humus content in the AU horizon varied greatly (from 5 to 12%) depending on the particle size distribution. Particularly important was that in Chernozemic soils formed on red rocks, the humus content is lower than in their analogues formed on different rocks. The adsorption capacity in heavy loam and clay soils was 45 mmol 100 g⁻¹. Calcium dominated in the

compositions of absorbed cations. Soil formation in Khakassia is characterised by the development of Solonchak and Solonetz soil types.

19.2.3 Climatic Conditions

The climate and orography of the study area play a decisive role in dispersing dust and gas emissions. However, a typically low wind speed (up to 5 ms⁻¹) in this area has a weak scattering ability. Low wind speeds and high inversion create a high pollution potential. In the industrial hub which was studied, southwestern (51%) and westerly winds (18%) prevail. The frequency of northeast winds is 17%; easterly and southerly winds make up 3–5%. The wind regime in the layer from the land surface to 500 m above is characterised by the prevalence of a southwest direction with a shift in a western direction in the upper layers (USSR Climate Guide 1969).

19.2.4 Sampling of Soil and Snow Materials

Field data was collected and the impact of dust and gas emissions on landscape components was assessed as part of an extensive, comprehensive programme based on the principles and methods of landscape geochemistry (Perelman and Kasimov 1999; Glazovskaya 2002; Davydova 2017).

Snow cover pollution monitoring was mainly carried out using a radial beam system from the emission source. This method enables approximate quantitative parameters to be obtained on cartographic maps. Next, the flow of technogenic substances entering the soil from the plants is assessed, and their chemical composition and distribution are determined. Snow samples were taken from a specific research area in 3–5 replications along the entire depth of the snow layer and placed in plastic bags (Davydova 2017).

To map the spatial distribution of the pollutants, the upper soil layer (0–10 cm) was sampled in the same area using the “envelope method” (GOST 17.4.4.02-84) with monolith sampling. Key areas (catenae) were selected for

more detailed research in the pollution zone and 40 km west of the plants. The soil cross sections were described in line with Ostrikova (2008) and diagnosed as described by Shishov et al. (2004).

19.2.5 Analytical Methods

A quantitative chemical analysis of the snow water, partially soluble suspensions (solid aerosols), soil solutions, and solid soil phases was carried out in a certified chemical analysis centre run by the Sochava Institute of Geography of the Siberian Branch of the Russian Academy of Sciences. The analytical methods used were those approved by GOST (All-Union State Standard), PNDP (Reference Documents for Environmental Protection) and RD (Regulatory Documents). The samples were analysed for the anionic and cationic composition and the content of 20 chemical elements: Si, Al, Fe, Ca, Mg, K, Na, Ti, Mn, P, F, Sr, Ba, Zn, Cu, Ni, Cr, Co, Pb and V. Spectrometers used in the analysis were Optima 2000 DV, an atomic emission spectrometer with inductively coupled plasma and Analyst 400 by Perkin Elmer (USA), an atomic absorption spectrometer with direct electrothermal atomisation.

The solid material was prepared for the analysis in two ways: (1) by melting suspension subsamples, soil, and rock with lithium metaborate 1:5 at a temperature of 850 °C and dissolving the melted mass in hot 5% HNO₃ using a magnetic mixer and (2) by acid combustion of the samples (with the mixture of HNO₃, HCl, and HF) using the microwave decomposition system *MW 3000 Anton Paar GmbH* with a subsequent solution neutralisation by H₃BO₃.

The content of the elements in the snow water and soil water extracts was determined directly in the solutions by injecting the liquid into the combustion chamber with a capillary.

The fluorine content in the samples was determined by direct potentiometry using an *Ekspert-001* ion meter and a fluorine-selective electrode *ELIS 131F* after melting the samples in a 1:5 mixture with carbonic anhydrous K–Na at a

temperature of 850 °C and dissolving the melted mass in distilled water.

The basic physico-chemical and chemical soil properties which were studied were as follows. The particle size distribution was determined using the pipette method (GOST 12536-2008). The humus content was determined using the modified Tyurin method (Mineev 2001), and the total N was determined titrimetrically following the Kjeldal method (GOST 26107-84). Exchangeable Ca and Mg were determined using the atomic adsorption method. The method is based on the extraction of exchangeable calcium and exchangeable magnesium from the soil with a solution of potassium chloride and the subsequent measurement of light absorption by free atoms of the elements. Exchangeable Na was determined photometrically using a method based on the extraction of exchangeable and soluble sodium with a solution of ammonium acetate with a concentration of 1 mol/dm³ (GOST 26950-86) at a soil/solution ratio of 1:20 and subsequently determining the amount of sodium in the extract with a flame photometer. At the same time, the soluble sodium in the aqueous extract is determined and the exchange rate is calculated based on the difference (GOST 1986). Exchangeable Al was determined by the extraction of exchangeable (mobile) aluminium from the soil with a solution of potassium chloride, obtaining a coloured complex of aluminium with chromazurol or xylenol orange in a weakly acidic medium, followed by photometry of the coloured solution. The influence of iron is prevented by restoring it to a bivalent state with ascorbic acid (GOST 26485-85).

The cation exchange capacity was determined according to GOST 17.4.4.01-84 (1984): the soil sample was mixed with a buffer solution of barium chloride and filtered by thoroughly washing off the remaining soil from the glass onto the filters with a buffer solution of barium chloride in several stages to completely displace the cations until the pH of the filtrate becomes equal to the initial pH value of 6.5. After saturation with barium, the soil sample on the filter was washed once with distilled water and left in

the air overnight. The dried filter with soil was transferred into a flask with a capacity of 200 ml and was dosed with 100 ml of sulphuric acid solution. Then the contents were shaken for five minutes and filtered. The filtrate was titrated with a sodium hydroxide solution to a pH value of 8.3 and took on slightly pink colour in the presence of phenolphthalein.

The soil organic matter was fractionated using the Tyurin method with the modification by Ponomareva and Plotnikova (1980: the soil sample was directly extracted with 0.1 N NaOH (the rest of the soil was discarded)). Then the second portion of the same soil sample was decalcified with 0.1 N H₂SO₄ followed by extraction with 0.1 N NaOH and 0.02 N NaOH. Finally, after six hours of heating in a water bath, an insoluble humus residue was obtained.

19.2.6 Calculations

Concentration coefficients were used to determine changes in the content of pollutants in the area studied. The Concentration Coefficient (CC) = the Pollution Area Coefficient (PAC)/ Background Coefficient (BC), where BC and PAC refer to the element concentration in the samples of the background landscape components and the pollution area components, respectively. Concentration coefficients were then used to calculate the total pollution index $Z_c = \sum K_c - (n - 1)$, where n is the number of chemical elements with $CC > 1.0$ (Saet and Smirnova 1983). A new geochemical transformation coefficient (TC) was implemented $TC = CCE_1/CCE_2$, where CCE_1 and CCE_2 denote the concentration of chemical elements in the original technogenic substance and in the objects of the pollution zone (soils, soil solutions, plants, etc.) at a certain period of time. A sanitary and hygiene assessment of the pollutants' toxicity was carried out based on the maximum permissible concentrations (MPCs) of chemical substances for soil (GN 2.1.7.2041-06) and water (Sanitary Norms and Regulations 2010). The chemical composition of the water samples was calculated using the Kurlov formula in mmol%,

where 100% is equal to the amount of substance equivalents for cations and anions separately (Nikanorov and Posokhov 1985). Statistical data processing and correlation analysis were carried out as described by Gubin and Ostashkov (2007).

19.3 Findings

19.3.1 The Solid Substance

The solid substance found in dust and gas emissions is particles of various sizes and chemical composition (Manisalidis et al. 2020). The major element emitted into the atmosphere due to the operation of the aluminium smelters was Al, constituting 34.50–40.70%, which significantly distinguishes it from the background and lithosphere soils that have a silicon base. The silicon content does not exceed 10%, the iron content is 2.12–3.22%, and the sodium content is 1.17–1.54%. Increased concentrations were observed for fluorine (0.90–1.54%) and nickel (200–700 mg kg⁻¹) and for Cu, Zn, V, Co and Sr. As the distance from the source of emissions increased, the content of the most potentially toxic elements, Al, F, and Ni, in the solid substance gradually decreased, which indicates their source. A comparative analysis of the mass fraction of chemical elements in the background soils and in the solid substance deposited near the industrial plant showed an elevated concentration of eight elements in the aerosols (CC is the lower index): F₂₃ Ni_{15.9} Al_{5.6} V_{2.5} Cu_{2.5} Zn₂ Co_{1.9} Sr_{1.5}. The potential total soil pollution index (Z_c) was 47, which is high and hazardous.

19.3.2 The Soluble Substance

The soluble substance in the snow meltwater made up 10% of the total substance in a sample. Fluorides and sodium salts showed the highest solubility levels, at 88.6% and 85.9%, respectively. The substances associated with Fe, Si and Al were poorly soluble in snow meltwater (0.2%, 0.5% and 8.1%, respectively). Mineralisation of the meltwater near industrial plants in different

years varied from 146 to 45 mg dm⁻³, decreasing at an increasing distance from the source of pollution (Table 19.1). The water was more mineralised compared to the background meltwater: it was 13 times higher on the territory of the plant and 4.5 times higher at a distance of five kilometres from the plant. Its chemical composition is well represented by Kurlov's formulas (Table 19.1). The background meltwater has a chloride-hydrocarbonate and sodium-calcium composition, while the meltwater in the zone of dust and gas deposition was very different, with a sulphate-fluoride and sodium-aluminium composition. The salinity of snow meltwater decreased with the distance from the pollution source up to 6 km, but the chemical composition remained practically unchanged in terms of the ratio of ions.

Depending on the content of the chemical elements in the meltwater, their concentration coefficients and total pollution indices varied both in space and time, which was reflected in the maximum value of $CC-F_{524,3}Al_{434,9}Na_{76,3}-Ni_{59,8}Mn_{13,4}Sr_{13,3}Ca_{12,1}Mg_{11,4}Si_{6,9}Zn_{6,1}Ba_{4,5}K_{3,3}Fe_{2,9}V_{2,5}Pb_{1,8}Co_{1,8}$, where $Zc = 1159$ near the plants where the total pollution level is very high and extremely hazardous. However, at a distance of five or six kilometres from the sanitary protection zone, the pollution level decreased significantly, especially that of the main pollutants, which was reflected in the decrease in $CC-F_{141,2}Al_{120,6}Na_{13,5}-Ni_{7,2}Sr_{4,8}Ca_{4,6}Ba_{4,1}Fe_{4,0}Mg_{3,9}Mn_{3,8}Zn_{3,2}V_{2,8}Si_{2,5}K_{1,6}$. Although the total pollution index decreased by five times ($Zc = 304$), the content of F^- , Na^+ , Al^{3+} was still quite high.

Table 19.1 Anion and cation composition of the snow meltwater (mg dm⁻³) at different distances from the aluminium plants

Sample number	pH	Anions				Cations					\sum of salts, mg dm ⁻³
		HCO ₃ ⁻	Cl ⁻	SO ₄ ²⁻	F ⁻	Ca ²⁺	Mg ²⁺	K ⁺	Na ⁺	Al ³⁺	
<i>0.5 km southeast of the plants</i>											
7	6.55	28.67	3.02	32.00	35.18	7.06	1.43	2.00	18.38	15.84	143.58
14	6.13	23.18	1.60	24.48	39.00	5.42	1.28	0.98	21.92	14.66	132.52
64	5.91	16.10	0.85	42.00	40.50	10.75	3.28	0.43	18.81	13.41	146.13
97	5.94	21.11	2.48	26.90	23.35	5.08	1.12	0.63	11.65	12.42	104.72
Average	6.13	22.27	1.99	31.35	34.51	7.07	1.78	1.01	17.69	14.08	131.75
*M ₁₃₂ F63SO ₄ 22HCO ₃ 12Cl2/Al54Na27K14Ca12Mg5											
<i>2 km southeast of the plants</i>											
28	6.31	11.59	2.66	16.00	13.5	3.11	0.49	0.49	11.71	5.3	64.85
63	6.17	10.98	0.85	11.34	20.00	3.60	0.87	0.25	12.50	6.32	66.71
96	5.96	17.08	2.49	18.24	16.00	2.20	0.84	2.34	10.81	8.19	78.19
Average	6.15	13.22	2.00	15.19	16.50	2.97	0.73	1.03	11.67	6.60	69.91
*M ₇₀ F59SO ₄ 22HCO ₃ 15Cl4/Al54Na27K14Ca12Mg5											
<i>5–6 km southeast of the plants</i>											
15	5.60	3.05	2.70	11.21	10.53	2.25	0.61	0.37	9.11	3.10	42.93
29	6.13	7.93	2.66	11.60	9.00	3.04	0.61	0.40	8.51	3.02	46.77
62	5.80	9.76	2.18	10.08	13.00	3.78	0.92	0.17	3.99	6.05	49.92
95	6.07	5.49	3.48	11.60	7.00	3.60	0.65	0.58	3.36	3.63	39.41
Average	5.90	6.56	2.76	11.12	9.88	3.17	0.70	0.38	6.24	3/95	44.76
*M ₄₅ F55SO ₄ 25HCO ₃ 12Cl8/Al46Na29Ca18Mg6K1											

Note * = Kurlov formula, % of total substance equivalents, M = mineralisation, mg dm⁻³

In terms of the migration speed and environmental impact, soluble substances emitted into the atmosphere were much more active than the solid substances: fluoride reached 55–63%, sodium was 27–30, aluminium was 46–54, calcium was 12–18 and magnesium was 5–6%.

19.3.3 Technogenic Load

As the distance from the pollution source increased, the technogenic load significantly decreased in a northerly direction. The mass decreased by five times at a distance of 1 km and by 10 times at a distance of 10 km from the plants. The decrease was less significant in the northeast and southeast directions (Fig. 19.1). On the periphery of the pollution area (20–30 km), the technogenic load approximated the usual background values. In the winter period (120 days), most of the pollutants were deposited in the sanitary protection zone and beyond at a distance of 5–6 km. During the downward movement of the pollutants, the main soluble and partially soluble pollutants were similar in mass, except Al from the solid emissions, the amount of which was much higher and ranged from 78 to 0.6 t km⁻² per year (Table 19.2).

19.3.4 Soil

The Na⁺ content in the soil solutions of upper soil horizons in the polluted area was similar to the F⁻ content. However, in the lower horizons it exceeded the F⁻ content several times, but its load was less severe (Table 19.3). It is practically impossible to determine the amount of Na remaining in the soil since steppe soils initially contain an increased amount of water-soluble Na salts as a result of natural enrichment, which does not allow us to calculate the technogenic component of this element. The level of Al in technogenically polluted soils is also difficult to determine due to its abundance in the lithosphere. The partially soluble forms found in the soil were quite high (Table 19.2).

19.3.5 Fluoride Vertical Migration

In addition, F penetration into the depth of the soil profile with significant differentiation along genetic horizons was detected. At a depth of 30–40 cm, the sub-humus horizon usually contains the smallest amount of pollutant. Its elevated accumulation was observed at a depth of 40–50 cm in the carbonate-rich horizon. On the summit plains, a layer enriched with water-soluble F⁻ up to 2 MPC was observed at a depth of 130–150 cm. Less fluorine accumulated in the lower horizons of the alluvial dark-humus saline soils of the lake depressions. At a distance of 10.5 km from the plants, the solonchic carbonate-rich Chernozems on the southern steep slopes, which face the plants and are only slightly water permeable, showed a significant level of pollution. The solonchic horizon can contain more than 1MPC of water-soluble F⁻. Peaty and salic soil horizons also showed a high ability to accumulate fluorine.

19.4 Discussion

19.4.1 The Solid Substance

When a technogenic substance precipitates onto the soil, it diffuses and undergoes a transformation. Unlike Na⁺ and Al³⁺, the presence of technogenic fluoride ion in soils is quite easily detected. It correlated well with its loads at $r = 0.94$ (water-soluble form) and $r = 0.75$ (total), while for Al and Na no correlation was observed ($r = 0.20$ and 0.26 , respectively). The correlations between the active forms of the elements with their total amount were on the same level (high for fluorine and low for aluminium and sodium). Similarly to our results, Davydova and Znamenskaya (2016) found that during 30 years of operation of Al smelters in Khakassia, the annual input of water-soluble fluorine in the composition of solid matter (250–300 mg/m²) and that of fluorine (150–250 mg/m²) led to an increase in the F content in water extracts of the soil to the MPC

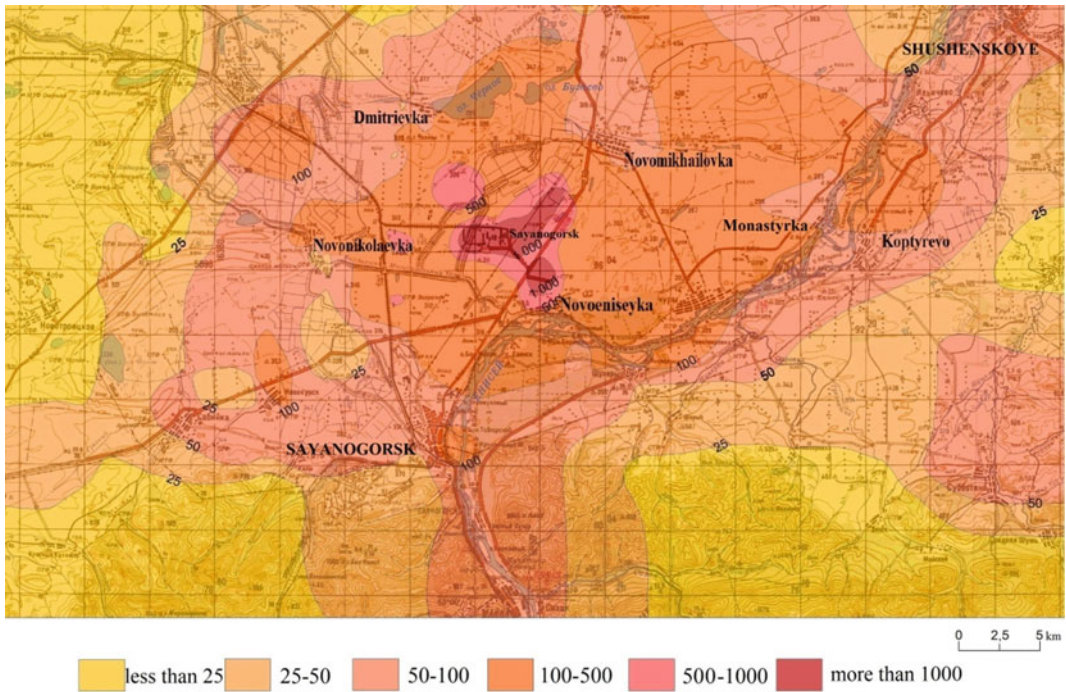


Fig. 19.1 Annual fluoride-ion load on the soil in the area studied (kg km^{-2})

Table 19.2 Pollutant load on the landscape (kg km^{-2} per year) at different distances from the plants, km

Distance	0.5	1	2	5	7	Distance	0.5	1	2	5	7
Element	Soluble substance					Element	Partially soluble substance				
F^-	4490	3329	2612	1095	454	F	4223	3026	2375	912	378
Na^+	3225	2150	1342	575	240	Na	2932	2580	1610	523	218
Al^{3+}	2576	1715	1187	358	189	Al	78,176	52,500	20,574	9384	5197

(10 mg/kg) and higher, and from 0.05 to 0.2% in the solid phase of the soil.

19.4.2 The Soluble Substance

The results from the soluble substrate confirm previous reports that the concentration of pollutants in snow meltwater can serve as an indicator of a site’s environmental condition (Talovskaya et al. 2015). Generally, the results on the fluoride concentration in the snowmelt water in the first impact zone of the Al smelter were within the range of the data reported in other parts of the

world (Ouellet 1987; Rogovenko et al. 2010; Yanchenko et al. 2013). Talovskaya et al. (2015) reported that within a distance of 1–3 km from the pollution source, the concentration of fluoride in filtrated meltwater was 3–7 times higher than within 5–10 km. In our study, the average fluoride concentration in samples at the first distance (0.5 km) was 3.49 times that at the third distance (5–6 km) (Table 19.1). These differences can be explained by differences in the atmospheric system, as well as the wind regime of a particular site (Talovskaya et al. 2015). In addition, the form and amount of water-soluble fluoride depends on the air environment during

Table 19.3 Anion and cation composition of the water extracts from the soil in the polluted area

Horizon, depth, cm	pH	Anions				Cations					∑ of salts, mg/dm ³
		HCO ₃ ⁻	Cl ⁻	SO ₄ ⁻	F ⁻	Ca ²⁺	Mg ²⁺	K ⁺	Na ⁺	Al ³⁺	
Dispersed carbonated Chernozem (s.c.s. 450) at a distance of 2 km north of the plants (valley of the Yenisei River)											
U ^a 0–14	7.22	$\frac{0.13^b}{76.25}$	$\frac{0.10}{35.45}$	$\frac{0.20}{96.00}$	$\frac{0.18}{34.80}$	$\frac{0.32}{64.40}$	$\frac{0.13}{15.80}$	$\frac{0.14}{54.00}$	$\frac{0.07}{16.00}$	$\frac{0.01}{0.95}$	78.61
U/CA 14–35	7.31	$\frac{0.15}{91.50}$	$\frac{0.09}{31.90}$	$\frac{0.20}{96.00}$	$\frac{0.02}{4.50}$	$\frac{0.26}{52.00}$	$\frac{0.12}{14.60}$	$\frac{0.01}{4.40}$	$\frac{0.07}{16.15}$	$\frac{0.03}{2.35}$	62.16
BCA 35–61	7.72	$\frac{0.15}{91.50}$	$\frac{0.09}{31.90}$	$\frac{0.25}{120.00}$	$\frac{0.05}{8.75}$	$\frac{0.19}{38.00}$	$\frac{0.13}{15.80}$	$\frac{0.02}{7.80}$	$\frac{0.19}{43.35}$	$\frac{0.01}{0.90}$	71.37
Cca 61–80	7.30	$\frac{0.10}{61.00}$	$\frac{0.11}{39.90}$	$\frac{0.25}{120.0}$	$\frac{0.03}{5.50}$	$\frac{0.18}{35.40}$	$\frac{0.16}{19.75}$	$\frac{0.04}{14.30}$	$\frac{0.12}{26.65}$	$\frac{0.01}{0.95}$	6.54
Chemical composition of the mountain soil solution. AU: fluoride-sulphate/calcium											
Chernozem rich in carbonate (s.c.s. 456) at a distance of 7 km northwest of the plants (summit of the southern slope)											
U 0–20	7.35	$\frac{0.15}{91.50}$	$\frac{0.22}{78.00}$	$\frac{0.50}{240.0}$	$\frac{0.07}{12.75}$	$\frac{0.74}{160.6}$	$\frac{0.07}{9.00}$	$\frac{0.08}{31.65}$	$\frac{0.04}{9.25}$	$\frac{0.01}{0.50}$	126.85
U/CA 20–50	7.44	$\frac{0.16}{97.60}$	$\frac{0.16}{57.60}$	$\frac{0.20}{96.00}$	$\frac{0.03}{6.60}$	$\frac{0.47}{93.55}$	$\frac{0.05}{5.90}$	$\frac{0.01}{2.95}$	$\frac{0.04}{10.15}$	$\frac{0.003}{0.30}$	58.65
CA 50–74	7.73	$\frac{0.06}{36.60}$	$\frac{0.20}{70.90}$	$\frac{0.10}{48.00}$	$\frac{0.03}{5.50}$	$\frac{0.17}{34.30}$	$\frac{0.09}{10.95}$	$\frac{0.01}{4.10}$	$\frac{0.15}{34.45}$	$\frac{0.01}{0.80}$	50.33
Cca 74–90	8.35	$\frac{0.15}{88.45}$	$\frac{0.16}{57.60}$	$\frac{0.10}{48.00}$	$\frac{0.13}{30.00}$	$\frac{0.26}{51.35}$	$\frac{0.08}{10.30}$	$\frac{0.02}{7.30}$	$\frac{0.25}{58.40}$	$\frac{0.10}{9.30}$	70.76

Note: chemical properties of the aqueous soil solution. The umbric (U) horizon is of a sulphate-calcium composition; the colluvic/calcaric horizon (Cca) is of a fluoride-hydrocarbonate chloride/sodium-calcium composition

^a U—umbric horizon; U/BCA—umbric/B horizon calcaric; U/CA—umbric/calcaric horizon; Cca—colluvic/calcaric horizon

^b Numerator—mmol 100 g⁻¹, denominator—mg kg⁻¹

transportation. Thus, atmospheric gaseous hydrogen fluoride is absorbed by air moisture to form an aerosol or smog of a hydrofluoric acid solution (Arnesen et al. 1995). Similarly, Semenov et al. (2020), studying the snowpack in Lake Baikal, reported that the elemental composition of snow meltwater varied significantly from place to place.

Gradually accumulating in the soil, solid aluminates mostly remain poorly soluble. The level of Al³⁺ content in the soil solutions from the upper layer of the polluted area (Table 19.3) and the background level were equally low. This is caused by Al's low migration ability in the neutral and weakly alkaline conditions of steppes and deserts. Its concentrations in aqueous extracts were also low compared to F⁻ and Na⁺, and its spatial distribution was limited. However, it tends to accumulate in the lower horizons,

increasing the pH level (up to 8.4–9.5) (Table 19.3, soil cross section (s.c.s.) 456).

The potential pollution of the initial soil solution with meltwater pollutants is characterised by the association of seven chemical elements (in CC ratio): F_{159,6} Ni_{49,8} Al_{29,3} Na_{23,6} Zn_{4,9} Mn_{3,5} Sr_{1,6}. The total pollution index was 265, which is high and hazardous. The actual pollution of the upper soil layer (0–10 cm) with F in the area adjacent to the plants was 39 times lower compared to the background soil solutions (F_{39,2}Na_{4,3} Ni_{3,8} K_{2,5} Cu_{2,0} Cr_{2,0} Mg_{1,6}) and 159.6 times lower than the MPC. Aluminate pollution was not observed at all. This ratio made it possible to identify fluorine as a primary element polluting the soil, as a result of technogenic impact.

To determine temporary changes in fluorine concentration, a database of ten-year interval was

developed based on various studies conducted on the territory of the South-Minusinsk basin, particularly in the area of dust and gas emissions coming from the “RUSAL Sayanogorsk” aluminium plants. The analysis is based on the research materials of the author of the current paper, covering the data obtained in 2005–2016. The results of the field data revealed a positive trend in soil pollution with fluorine. During the period from 1985 to 1990, after the launch of the aluminium smelter, an elevated fluorine content in the soil was mostly observed in the top layer (2.5 cm) within the sanitary protection zone and in the northeast at a distance of 3–4 km (Saraev 1993). Twenty-five years later, the area of pollution had expanded and the fluorine concentrations had increased, exceeding the background level by 2–5 times (Fig. 19.2). Thus, the upper 0–10 cm of the dispersed calcareous Chernozem of the Yenisei Valley is enriched with water-soluble F^- up to 3.5 and 1 MPC (10 mg kg^{-1}) at 2 and 5–7 km from the plant, respectively (Table 19.3). Calcareous Chernozems on steep slopes surrounding the Yenisei Valley (except for the areas located in the wind shadow) are polluted with increased intensity (especially in the summit plains and upwind slopes). This is caused not only by the difference in loads but also by the fact that the slopes are of a loamy texture and a dense structure, unlike the well-drained sandy and gravelly soils of the valley. Along with the active form, the total form of the fluorine also increased, reaching 1000–2000 mg kg^{-1} in different areas. The depth of the polluted upper layer of the soil increased to 10–15 cm.

Some authors reported that fluoride can form labile F compounds with soil components, such as clay minerals, Ca, Mg, and especially with Fe and Al through the formation of stable bonds (Omueti and Jones 1977; Elrashidi et al. 1998). Fluoride binds to clay by displacing hydroxide from the surface of the clay (Bower and Hatcher 1967; Meeussen et al. 1996). Later, it was established that solubility and sorption of F compounds is also highly dependent on the soil pH. A pH value from 5.5 (Ruan et al. 2004) to 6 (Gilpin and Johnson 1980) is the point of

maximum F sorption. This was also proved by the fact that the greatest F adsorption occurred in non-calcareous soils, which generally contain higher Al levels (Omueti and Jones 1977; Barrow and Ellis 1986). The negatively charged F^- replaces $-OH/H_2O$ groups bound to surface Al atoms as a ligand exchange by breaking the Al–OH bonds (Harrington et al. 2003). Subsequently, the release of the OH ions can raise the pH, which enables more F in to be released in the soil solution (Stevens et al. 2000).

The transformation of the chemical composition of the solutions occurred, while the snow meltwater (Table 19.2) was transported to the soil solutions (Table 19.3). The following sequence of meltwater transformation was obtained in areas located at a distance of 2 and 7 km from the source of pollution (where the transformation coefficient (TC) is the lower index) $-Al^{3+}_{35-40}Na^+_{3-4}F^-_{2-4}HCO_3^-_{0.4-0.9}SO_4^{2-}_{0.2-0.8}Cl^-_{0.2-0.3}Mg^{2+}_{0.1-0.4}Ca^{2+}_{0.1-0.2,1}K^+_{0.1}$. The toxicity coefficient > 1.0 indicates that pollutants were absorbed by the upper soil layer through the meltwater, while the coefficient < 1.0 indicates their transition from the solid soil phase to the soil solution in addition to the meltwater. This leads to the neutralisation of the slightly acidic snow meltwater. Of the total number of anions entering the migration process, the quantitative indicators for the elements were (%) F^- —26–40, Na^+ —27–30, Al^{3+} —2–3. The content of Na^+ in the soil solutions may be overestimated due to the natural enrichment.

The upper soil horizons with a high sorption ability act not only as physico-chemical barriers but also as mechanical barriers, since they are characterised by different speeds of substance movement due to their location in the solid–liquid interface. Correlation analysis showed a positive relationship between fluorine and humus ($r = 0.84$). Furthermore, the higher the total fluorine contents in the upper horizons, the closer the relationship. It is important to determine how close this relationship is quantitatively, in other words, how the fluorine is distributed in humus fractions. It was revealed that a significant amount of this element (12–25%) is found in the extracts of humic acids after their decomposition

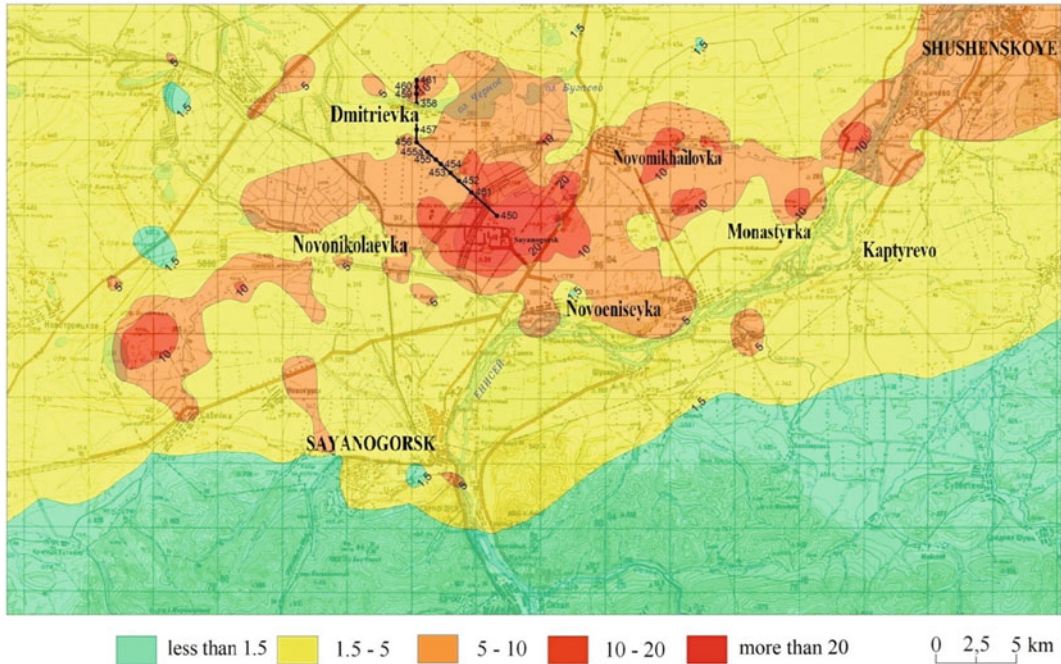


Fig. 19.2 Accumulation of fluoride ion (mg kg^{-1}) over a 30-year period in the soils (0–10 cm) in the vicinity of aluminium plants in Khakassia. 450–461 are the numbers of the soil profiles

with calcium 0.1 *N* solution of H_2SO_4 . Presumably, fluorine in a humic substance exists in the form of organofluorine calcareous complexes, which are slightly soluble in water. Therefore, the accumulation of fluorine in the upper soil layers occurs not only due to the mechanical deposition of solid particles from the atmosphere but also due to their solution in and interaction with organic substances in soils.

The sub-humus horizon of the carbonate-rich Chernozems was low in fluorine (Fig. 19.3) due to their periodic wetting to a depth of 30–50 cm. Partial immobilisation of the element occurred below a depth of 50 cm in the evaporation barrier in combination with the calcium (sedimentary) barrier. Among the fluorine-binding elements found in the soil, calcium is of great importance, or, less often, magnesium. Therefore, the presence of a calcareous carbonate horizon is considered crucial against the migration of water-soluble fluorine, when the fluoride ion passes from an active state to a slightly soluble fluorite (CaF_2) as a result of subsurface evaporation and

sedimentation (Fig. 19.3b). As a rule, the maximum amount of F is found in the carbonate horizons which have the highest content of Ca. But if any soluble salts are present in the soil, part of the fluorine remains in their composition (Fig. 19.3a). The highest amount of acid-soluble fluorine (12–88%) was accumulated in calcium-rich (9–12%) carbonate horizons located at a depth of 50–100 cm. Elevated concentrations of F (different concentrations) were also observed at a depth of 100–150 cm, including the sediments on boulders and gravel in the form of whitish deposits and microcrystalline friable formations. Presumably, this corresponds to the depth the precipitation most often reaches. This distribution of the element is facilitated by the fractures from the soil drying in summer and freezing in winter. Morphologically, they appear on the sides of the fractures in the form of humus tongues. In addition to fluorite, salts of varying degrees of solubility also accumulate in the evaporation barrier: calcium sulphate, sodium sulphate, soda, fluorides and aluminates. Thus,

the detoxification of the upper soil horizons occurs through the gradual leaching of elements. In the case of fluorine, this pattern is mostly typical for valley soils (Fig. 19.3) with a high solution filtration rate (up to 9 m per day). Similar findings were reported earlier showing that soils with a relatively high Ca content are very effective in fluoride fixing. However, at a high pH, adsorbed F is displaced by the increased concentration of OH in the soil solution (Larsen and Widdowson 1971). This causes an increasingly unfavourable electrostatic potential, which decreases the retention of F in the soil and increases the F concentration in the soil solution (Saxena and Rani 2012; Choudhary et al. 2019).

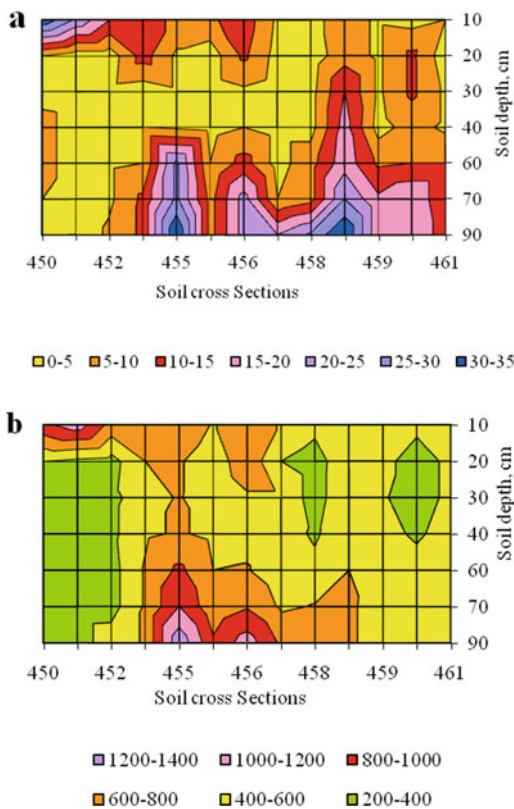


Fig. 19.3 Distribution of fluorine (mg kg^{-1}) in the steppe soils of the landscape geochemical profile of the area surrounding the aluminium plants of Khakassia: *a*—ionic form, *b*—total form. Locations of soil cross sections: the Yenisei River valley (s.c.s. 450–452), upwind southeastern slope (s.c.s. 454–456), downwind northeastern slope (s.c.s. 457, 458), saline lake depression (s.c.s. 358), upwind southern slope (s.c.s. 459–461)

The solonetzic Chernozem that was rich in carbonate showed a distinct subsoil differentiation of fluorine due to the presence of a thick solonetz horizon: soil profile no. 460 (medium-Solonetzic Chernozem rich in carbonate), although it is located at a considerable distance from the pollution source (11.5 km). The Solonetzic horizon combines the functions of several barriers, which were determined using the values of the correlation coefficients between fluorine and a set of indicators determining its migration ability. The humus horizon located above the Solonetzic layer contains an elevated amount of total fluorine and a reduced amount of water-soluble fluorine due to its migration into the underlying Solonetzic horizon. Saxena and Rani (2012) found that increased concentrations of F, resulting in an alkaline pH, enabled a higher amount of fluoride to be released from the soil surface and, subsequently, plant availability increased. Here, fluoride accumulates in an active form and hardly enters the solid soil phase, which is confirmed by its small content compared with the total amount (Fig. 19.2). Alkaline conditions contribute to its retention in the active state (Perelman 1989; Davydova 2017). An alkaline barrier does not quite correspond to the common definition of the main barrier function (i.e., the transformation of an element into a non-active form), in this case serving as an active barrier, also known as a starter barrier. There are many such examples under the conditions of technogenesis. For instance, the mobilisation of heavy metals was observed in the acid barrier, which was formed as a result of the input of strong acid ions through the atmosphere. That is why it is called a “reaction barrier” (Shabanov and Marichev 2018). A case has also been observed in which Cd is transformed into various active forms, comprising up to 88% of its total content (Elspe 1988).

The significant enrichment of urban soils with active forms of these elements is also reported by Kosheleva et al. (2015). The fact that the Solonetzic layer commonly swells during soaksage puts it among the mechanical barriers that facilitate the accumulation of soluble substances. The functions of an evaporation barrier serve the

same purpose, which can be concluded from the positive relationship of the pollutant with the total mineralisation of the soil solutions ($r = 0.90$) and its constituent components of Na^+ , Ca^{2+} , HCO_3^- , SO_4^{2-} . The sorption capacities of the horizon were determined by the presence of the direct positive relationship ($r = 0.93$) of active fluorine with the fine earth fraction (particles <0.01 mm). It can be assumed that this connection is not very strong since there was no increase in the total form of the element. The absorbed Ca^{2+} , Mg^{2+} and Na^+ cations may serve as an obstacle, as evidenced by their highly negative correlation ($r = -0.99$) with the content of total fluorine. To some extent, fluorine migrates to deeper layers of the soil profile, where it gradually accumulates, including within the content of the soluble salts of other geochemical barriers. As a result, the accumulation of fluorides (up to 2 MPC) in the Solonetzic soils can be observed in the area located at a considerable distance from the source of pollution.

19.4.3 Technogenic Load on Soil

The specificity and area of pollution were reflected well in the mass fraction of chemical elements of the liquid phase and particulate matter in the meltwater, which mainly depended on the landscape conditions (Table 19.2). An important role in the primary distribution is played by factors such as the direction and speed of wind, relief (peaks, surface slope ratio, upwind or downwind slopes), and vegetation (forest, grass or the absence thereof). This pattern is more visible in water-soluble fluorides.

The impact of technogenic loads on the soil was studied focusing on MPC ($10 \text{ mg kg}^{-1}\text{F}$) and comparing the cartographic maps (Figs. 19.1 and 19.2), which reflect the load and content of water-soluble fluorine in the soil, respectively. In addition, there are data showing the content of all the forms of F accumulated in the soil over the

past 30 years of the plant's operation (Table 19.4).

19.4.4 Fluoride Vertical Migration

Fluorine penetrated into the depths of the soil by convection. Almost the entire soil profile was involved in the immobilisation of F while the soil solutions moved in the radial direction (Fig. 19.3). However, their highest concentrations were found in genetic horizons that have specific features (sorption, sedimentation, acidity, alkalinity, etc.). Therefore, the soil can be considered as a system of geochemical barriers (Davydova and Snytko 2005; Glazovskaya 2012). In the conditions of atmospheric pollution, the upper organogenic and humic layers gain essential importance, acting as sorption and biogeochemical barriers. They are divided into organic layers (peat, forest litter and steppe mat, peat and humus-accumulative horizons) and an organomineral layer (humus horizon). Their barrier ability is assessed based on their depth, peat type, depth and quality of humus, and particle size distribution (Gerasimova and Bogdanova 2013).

19.4.5 Fluoride Geochemical Anomaly

The landscapes of the technogenic anomalies which formed exhibited a significant increase in the migration flow capacity of the chemical elements in comparison with the background (10 times higher). In terms of quantity, they are distributed using an anomaly coefficient (AC). The threshold value adopted for fluorine is 10. In the research area, a tenfold increase in the fluorine content (150–200 times higher in snow) was observed in the main landscape components at a distance of 5–6 km from the “RUSAL Sayanogorsk” aluminium plants, indicating the presence of a technogenic fluoride geochemical anomaly (Fig. 19.4).

Table 19.4 Criteria for assessing the soil cover pollution with fluorides (based on fluorine)

Criteria	Load, tkm ⁻² per year		Content in soil, mgkg ⁻¹	
	Form of occurrence			
	Water-soluble	Slightly soluble	Water-soluble	Total
Permissible	0.10	0.12	10	500
Critical	0.30	0.20	15	800
Inadmissible	0.50	0.80	30	1000
Background	0.005	0.02	1.5	400

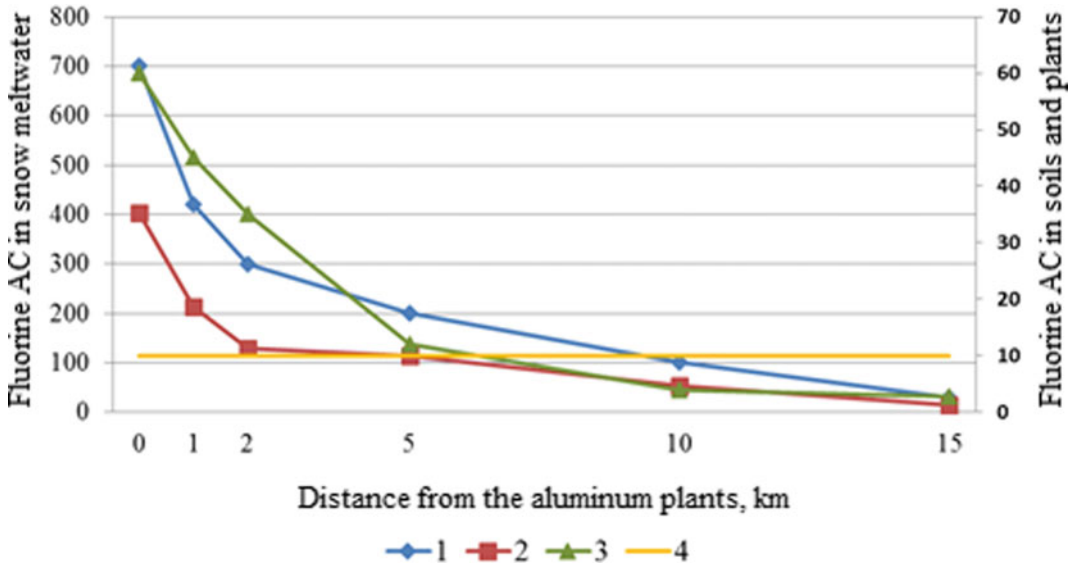


Fig. 19.4 The distribution of the fluorine technogenic anomaly coefficient (AC) in the landscape components: 1—snowpack, 2—soil solutions, 3—green phytomass, 4—threshold anomaly index = 10

19.5 Conclusion

Unlike previous studies, the presented work covers all components of the landscape (soils, plants, sediments, water bodies) and all the results obtained were analysed in a complex, interrelated manner. In addition, the analysis of the results obtained was based on extensive studies, including field, laboratory and office work. Our objectives and goals were achieved, and the following conclusions were drawn:

- The main pollutants which accumulated in the snowpack during the winter season were F, Al, Na and Ni, while the accompanying

elements were Mn, Sr, Ca and Mg. The secondary polluting elements were represented by Cu, Zn, Ba, Fe and V. Fluorine was the main pollutant in terms of its input, its migration intensity in soils, and its environmental toxicity.

- Toxic elements were present in all components of the landscape in the vicinity of the plants: the atmosphere, snowpack, rainwater, plants, solid soil phase, soil solutions and groundwater of the depressions.
- The transport distance for most of the pollutants was 25–30 km to the north, northeast and east, shifting to the Yenisei River valley. The main flow of the pollutants contained in the technogenic substances was mostly

deposited on the summits, upwind slopes and forest areas. The smallest amounts of the substances deposited on the open arable lands were found in wind shadows. Wetlands with salty depressions were the most enriched with pollutants, especially in the upper peat layers, as a result of secondary lateral redistribution.

- The radial migration of pollutants in soils is a complex process which depends on the individual physical and chemical properties of an element, the soil characteristics and environmental factors. The presence of soil and geochemical barriers (such as organogenic, sorption, sediment, and evaporation barriers) is an important condition for the migration and accumulation of fluorine.
- In the conditions of technogenesis, elements can accumulate in the barriers in their active forms. This does not fully correspond to the common definition of a barrier's main function, i.e., to transform an element into an inactive and slightly mobile form. In this particular case, they acquire a new role as active barriers or starter barriers.
- Depending on the indices of the total pollution of the snowpack, soil solution and solid phase potential, the geoecological situation was estimated as hazardous. An estimation of the fluorine load on the soil showed that an input of 5 kg/ha^{-1} of total fluorine per year should be adopted as a critical value for the region which was studied. Nickel exhibited low mobility. Only small amounts accumulated in the upper soil layers and in the carbonate horizons, but mainly near the aluminium plants.
- The results obtained underline the need to reduce gas and dust emissions at the RUSAL Sayanorsk aluminium smelters and monitor their work. This will contribute to a comprehensive assessment of environmental and geochemical hazards at aluminium production sites at different times, help identify areas with different degrees of danger and encourage the adoption of environmentally friendly decisions on the development of technologies for filtering exhaust gases and dust emissions or ways to reduce aluminium production.

References

- Adimalla N, Venkatayogi S, Das SVG (2019) Assessment of fluoride contamination and distribution: a case study from a rural part of Andhra Pradesh, India. *Appl Water Sci* 9:94. <https://doi.org/10.1007/s13201-019-0968-y>
- Arnesen AKM, Abrahamsen G, Sandvik G, Krogstad T (1995) Aluminium-smelters and fluoride pollution of soil and soil solution in Norway. *Sci Total Environ* 163:39–53. [https://doi.org/10.1016/0048-9697\(95\)04479-K](https://doi.org/10.1016/0048-9697(95)04479-K)
- Artiola JF, Walworth JL, Musil SA, Crimmins MA (2019) Chapter 14—Soil and land pollution. In: *Environmental and pollution science*, 3rd edn, pp 219–235. Academic Press. <https://doi.org/10.1016/B978-0-12-814719-1.00014-8>
- ATSDR (2003) Toxicological profile for fluorides, hydrogen fluoride, and fluorine. US Department of Health and Human Services, Public Health Service Agency for Toxic Substances and Disease Registry; Atlanta, GA. <http://www.atsdr.cdc.gov/ToxProfiles/tp.asp?id=212&tid=38>. Accessed 7 Mar 2021
- Barrow NJ, Ellis AS (1986) Testing a mechanistic model. III. The effects of pH on fluoride retention by a soil. *J Soil Sci* 37:287–293. <https://doi.org/10.1111/j.1365-2389.1986.tb00030.x>
- Bharti VK, Giri A, Kumar K (2017) Fluoride sources, toxicity and its amelioration: a review. *Ann Environ Sci Toxicol* 2(1):021–032. <https://doi.org/10.17352/aest.000009>
- Bhat N, Jain S, Asawa K, Tak M, Shinde K, Singh A, Gandhi N, Gupta VV (2015) Assessment of fluoride concentration of soil and vegetables in vicinity of zinc smelter, Debari, Udaipur, Rajasthan. *J Clin Diagn Res* 9(10):ZC63–ZC66. <https://pubmed.ncbi.nlm.nih.gov/26557620/>
- Bhattacharya P, Samal AC (2018) Fluoride contamination in groundwater, soil and cultivated foodstuffs of India and its associated health risks: a review. *Res J Recent Sci* 7(4):36–47
- Bombik E, Bombik A, Rymuza K (2020) The influence of environmental pollution with fluorine compounds on the level of fluoride in soil, feed and eggs of laying hens in Central Pomerania Poland. *Environ Monit Assess* 192:178. <https://doi.org/10.1007/s10661-020-8143-3>
- Bower CA, Hatcher JT (1967) Adsorption of fluoride by soils and minerals. *Soil Sci* 103:151–154. <https://doi.org/10.1097/00010694-196703000-00001>
- Brough D, Jouhara H (2020) The aluminium industry: a review on state-of-the-art technologies, environmental impacts and possibilities for waste heat recovery. *Int J Thermofluids* 1–2:100007. <https://doi.org/10.1016/j.ijft.2019.100007>
- Choudhary S, Rani M, Devika OS et al (2019) Impact of fluoride on agriculture: a review on its sources, toxicity in plants and mitigation strategies. *Int J Chem Studies* 7(2):1675–1680. <https://www.chemijournal.com>

- com/archives/2019/vol7issue2/PartAB/7-2-263-789.pdf. Accessed 7 Mar 2021
- Davydova ND (2015) Monitoring of the natural environment of the regions of Siberia based on the snowpack pollution. *Fundamental Res* 8(3):469–475 (Давыдова Н.Д. Мониторинг природной среды регионов Сибири по загрязнению снежного покрова. *Фундаментальные исследования* 8 (3):469–475). <https://www.elibrary.ru/item.asp?id=24083001>. Accessed 7 Mar 2021
- Davydova ND (2017) Transformation of aerotechnogenic substance flows in steppe landscapes. *Landscape Geochemistry. Centenary of A.I. Perelman*. Moscow, April 2017, pp 297–328 (Давыдова Н.Д. Трансформация аэротехногенных потоков веществ в степных ландшафтах. *Ландшафтная геохимия. 100-летие А.И. Перельман*. Москва, апрель 2017 г., с. 297–328)
- Davydova ND, Snytko VA (2005) Landscape and geochemical barriers and their classification. *Geogr Nat Res* 4:24–30 (Давыдова Н.Д., Снытко В.А. Ландшафтные и геохимические барьеры и их классификация. *География и природные ресурсы* 4: 24–30)
- Davydova ND, Znamenskaya TI (2016) Geological problems of Siberia associated with the development of nonferrous metallurgy. *Geogr Nat Res* 37(4):313–318 (Давыдова Н.Д., Знаменская Т.И. Геологические проблемы Сибири, связанные с развитием цветной металлургии. *География и природные ресурсы* 37 (4):313–318). <https://www.elibrary.ru/item.asp?id=27523300>. Accessed 7 Mar 2021
- Divan AMD Jr, Oliva MA, Ferreira FA (2008) Dispersal pattern of airborne emissions from an aluminum smelter in Ouro Preto, Brazil, as expressed by foliar fluoride accumulation in eight plant species. *Ecol Ind* 8:454–461. <https://doi.org/10.1016/j.ecolind.2007.04.008>
- Egunova NA (2009) Monitoring of the ecological condition of the soils in the area of the technogenic impact of the Sayanogorsk aluminum plant. N.F. Katanov University of Khakassia, Abakan, p 116 (Егунова Н.А. Мониторинг экологического состояния почв в зоне техногенного воздействия Саяногорского алюминиевого завода. Абакан: Н.Ф. Катуновский университет Хакасии, с. 116), <https://www.dissertac.com/content/monitoring-ekologicheskogo-sostoyaniya-pochv-v-zone-tekhnogennogo-vozdeystviya-sayanogorskog>. Accessed 7 Mar 2021
- Elrashidi MA, Persaud N, Baligar VC (1998) Effect of fluoride and phosphate on yield and mineral composition of barley grown on three soils. *Comm Soil Sci Plant Anal* 29:3–4. <https://doi.org/10.1080/00103629809369945>
- Elspe BR (1988) Mobile und mobilisierbare Schwermetallfraktionen in Boden und im Bodenwasser: dargestellt für die Elemente Blei, Cadmium, Eisen, Mangan, Nickel und Zink unter landwirtschaftlichen Nutzflächen. Selbstverlag Der Marburger Geographischen Gesellschaft 109:176
- Engelhard C, De Toffol S, Lek I, Rauch W, Dallinger R (2007) Environmental impacts of urban snow management The alpine case study of Innsbruck. *Sci Tot Environ* 382:286–294. <https://doi.org/10.1016/j.scitotenv.2007.04.008>
- Franzaring J, Hrenn H, Schumm C, Klumpp A, Fangmeier A (2006) Environmental monitoring of fluoride emissions using precipitation, dust, plant and soil samples. *Environ Pollut* 144:158–165. <https://doi.org/10.1016/j.envpol.2005.12.033>, <https://europepmc.org/article/med/16504357>
- Gerasimova MI, Bogdanova MD (2013) Small-scale maps of geochemical barriers. *Geogr Nat Res* 3:9–17 (Герасимова М.И., Богданова М.Д. Мелкомасштабные карты геохимических барьеров. *География и природные ресурсы* 3: 9–17), <http://www.izdatgeo.ru/pdf/gipr/2013-3/9.pdf>. Accessed 7 Mar 2021
- Gilpin L, Johnson AH (1980) Fluorine in agriculture in soils of southeastern Pennsylvania. *Soil Sci Soc Am J* 44:255–258. <https://doi.org/10.2136/sssaj1980.03615995004400020010x>
- Glazovskaya MA (2002) Geochemical basis of the typology and methods of natural landscape research, 2nd edn. Smolensk, Moscow, Oikumena, p 288 (Глазовская М.А. Геохимические основы типологии и методов исследования природных ландшафтов. 2 издание. Смоленск, Москва, Ойкумена, с. 288), <https://www.geokniga.org/bookfiles/geokniga-glazovskayaghosnovytipologiiilandshaftov2002.pdf>. Accessed 7 Mar 2021
- Glazovskaya MA (2012) Geochemical barriers in soils: typology, functional features, and ecological significance. *Landscape geochemistry and soil geography. Centenary of M.A. Glazovskaya*. Moscow, April, pp 26–44. (Глазовская М.А. Геохимические барьеры в почвах: типология, функциональные особенности, экологическое значение. *Ландшафтная геохимия и география почв. 100-летие М.А. Глазовской*. Москва, апрель 26–44). http://media.geogr.msu.ru/sbornik_dokladov_Glazovskaya_konf_apr_2012.pdf. Accessed 7 Mar 2021
- GN 2.1.7.2041-06 (2006) Maximum permissible concentrations of chemical substances in soil: hygienic regulations. Federal Centre for Hygiene and Epidemiology of the Federal Service for Supervision of Natural Resources Usage, Moscow, p 15
- GOST 26107-84 (1984) Soils. Methods for determination of total nitrogen. Moscow, Standard Publishing, p 9
- GOST 26485-85 (1985) Soils. Determination of exchangeable aluminum using methods of the Central Scientific Research Institute of Agrochemical Services. Standards Publishing, Moscow, p 5
- GOST 26487-85 (1985) Soils. Determination of exchangeable calcium and exchange (mobile) magnesium using methods of the Central Scientific Research

- Institute of Agrochemical Services. Standards Publishing, Moscow, p 13
- GOST 26950-86 (1986) Soils. Methods for determination of exchangeable sodium. Standards Publishing, Moscow, p 6
- GOST 26213-91. (1991). Soils. Methods for determination of organic substance. Moscow, Standards Publishing, p 6
- GOST 17.4.4.01-84-2008 (2008) Nature conservation. Soils. Methods for determination of cation exchange capacity. Moscow, Standartinform, p 7. <http://docs.cntd.ru/document/1200012802>. Accessed 7 Mar 2021
- GOST 17.4.4.02-84-2008 (2008) Environmental protection. Soils. Methods of sampling and sample preparation for chemical, bacteriological and helminthological analysis. Moscow, p. 11
- GOST 12536-2008 (2014) Grounds. Methods for laboratory determination of granulometric (grain) and microaggregate composition. Moscow, Standartinform p 16
- Gritsan NP, Miller GW, Schumatkov GG (1995) Correlation among heavy metals and fluoride in soil, air and plants in relation to environmental damage. *Fluoride* 28:180–188
- Gubin VI, Ostashkov VN (2007) Statistical methods of experimental data processing. Tumen State Oil and Gas University, p 202. ISBN 978-5-88465-844-3 (Губин В.И., Осташков В.Н. Статистические методы обработки экспериментальных данных. Учебное пособие для студентов технических вузов. Тюмень: Тюменский государственный нефтегазовый университет, с. 202)
- Haidouti C (1991) Fluoride distribution in soils in the vicinity of a point emission source in Greece. *Geoderma* 49:129–138. [https://doi.org/10.1016/0016-7061\(91\)90096-C](https://doi.org/10.1016/0016-7061(91)90096-C)
- Harrington LF, Cooper EM, Vasudevan D, (2003) Fluoride sorption and associated aluminum release in variable charge soils. *J Coll Interface Sci* 267:302–313. [https://doi.org/10.1016/S0021-9797\(03\)00609-X](https://doi.org/10.1016/S0021-9797(03)00609-X). <https://pubmed.ncbi.nlm.nih.gov/14583205/>
- IPCS (2002) Fluorides. Geneva, World Health Organisation, International Program on Chemical Safety (Environmental Health Criteria 227)
- Kasimov NS (2013) In: Filimonov MV (ed) *Ecogeochemistry of landscapes*. IP, Moscow (Касимов НС, Экогеохимия ландшафтов. Москва, Ред. Филимонов И.П)
- Khairnar MR, Dodamani AS, Jadhav HC, Naik RG, Deshmukh MA (2015) Mitigation of fluorosis—a review. *J Clin Diagn Res* 9(6):ZE05–ZE09. <https://doi.org/10.7860/JCDR/2015/13261.6085>
- Kosheleva NS, Kasimov NS, Vlasov DV (2015) Factors of the accumulation of heavy metals and metalloids in the geochemical barriers of urban soils. *Eurasian Soil Sci* 48(5):476–492. <https://doi.org/10.1134/S1064229315050038>
- Larsen S, Widdowson AE (1971) Soil fluorine. *J Soil Sci* 22:210–222. <https://doi.org/10.1111/j.1365-2389.1971.tb01608.x>
- Manisalidis I, Stavropoulou E, Stavropoulos A, Bezirtzoglou E (2020) Environmental and health impacts of air pollution: a review. *Front Public Health* 20(8):14. <https://doi.org/10.3389/fpubh.2020.00014>
- Meeussen JCL, Scheidegger A, Hiemstra T, Van Riemsdijk WH, Borkovec M (1996) Predicting multicomponent adsorption and transport of fluoride at variable pH in a goethite-silica sand system. *Environ Sci Technol* 30:481–488. <https://doi.org/10.1021/es950178z>
- Mineev VG (2001) Textbook, 2nd edn. Moscow State University, Moscow, p 689
- Nikanorov AM, Posokhov EV (1985) *Hydrochemistry*. Gidrometeoizdat, Leningrad, p 232
- Nikitin E (2020) Rusal plans US\$190 million refit to Sayanogorsk electrode production equipment. *Aluminium Insider*. <https://aluminiuminsider.com/rusal-plans-us190-million-refit-to-sayanogorsk-electrode-production-equipment/>. Accessed 7 Mar 2021
- Omueti JAI, Jones RL (1977) Fluoride adsorption by Illinois soils. *J Soil Sci* 28:564–572. <https://doi.org/10.1111/j.1365-2389.1977.tb02264.x>
- Ostrikova KT (2008) Field identifier of Russian soils. V. V. Dokuchaev Soil Institute, Moscow, p 282 (Острикова К.Т. Полевой определитель почв России. Москва: В.В. Докучаева, с. 282). http://www.esoil.ru/images/stories/pdf/Field_guide.pdf. Accessed 7 Mar 2021
- Ouellet M (1987) Reduction of airborne fluoride emissions from Canadian aluminium smelters as revealed by snow chemistry. *Sci Total Environ* 66:65–72. [https://doi.org/10.1016/0048-9697\(87\)90078-7](https://doi.org/10.1016/0048-9697(87)90078-7)
- Perelman AI (1986) *Geochemical barriers: theory and practical applications*. *Appl Geochem* 1(6):669–680, November–December 1986. [https://doi.org/10.1016/0883-2927\(86\)90088-0](https://doi.org/10.1016/0883-2927(86)90088-0)
- Perelman AI (1989) *Geochemistry*. Moscow, High School, p 528 (Перельман А.И. Геохимия. Москва, Высшая школа, с. 528)
- Perelman AI, Kasimov NS (1999) *Landscape Geochemistry*. Moscow, Astreya, 2000, p 763 (Перельман А.И., Касимов Н.С. Геохимия ландшафтов. Москва, Астрей, 763 стр) <http://media.geogr.msu.ru/Library/Perelmann100.pdf>. Accessed 7 Mar 2021
- Polomski J, Flüher H, Blaser P (1982) Accumulation of air-borne fluoride in soils. *J Environ Qual* 11:457–461. <https://doi.org/10.2134/jeq1982.00472425001100030028x>
- Ponomareva VV, Plotnikova TA (1980) Humus and soil formation. Leningrad, Nauka, p 223 (Пономарева ВВ, Плотникова ТА (1980) Гумус и Почвообразование. Ленинград, Наука, 223 стр)
- Rezaei M, Nikbakht M, Shakeri A (2017) Geochemistry and sources of fluoride and nitrate contamination of ground water in Lar area, south Iran. *Environ Sci Pollut Res* 24(18):15471–15487. <https://doi.org/10.1007/s11356-017-9108-0>
- Rogovenko ES, Blinnikova NV, Shubin AA, Bondarev LG (2010) Environmental monitoring of anthropogenic pollution of snow cover of one of the

- industrial districts of Krasnoyarsk Journal of Siberian Federal University. Chemistry 4(3):387–394 (Пороженко Е.С., Блиникова Н.В., Шубин А.А., Бондарев Л.Г. Экологический мониторинг антропогенного загрязнения снежного покрова одного из промышленных районов Красноярска. Вестник Сибирского федерального университета. Химия 4(3):387–394). <https://cyberleninka.ru/article/n/ekologicheskij-kontrol-antropogennogo-zagryazneniya-snegovogo-pokrova-odnogo-iz-promyshlennyh-rayonov-g-krasnoyarska/viewer>. Accessed 7 Mar 2021
- Ruan J, Ma L, Shi Y, Han W (2004) The impact of pH and calcium on the uptake of fluoride by tea plants (*Camellia sinensis* L.). Ann Botany 93(1):97–105. <https://doi.org/10.1093/aob/mch010>
- Saet UE, Smirnova RS (1983) Geochemical principles of the identification of zones affected by industrial emissions in urban agglomerations. Geography Issues, Moscow, Mysl, Collection 120:45–55 (Саэт Ю.Е., Смирнова Р.С. Геохимические принципы выявления зон воздействия промышленных выбросов в городских агломерациях. Вопросы географии, 120:45–55.)
- Saevarsdottir G, Kvande H, Welch BJ (2020) Aluminum production in the times of climate change: the global challenge to reduce the carbon footprint and prevent carbon leakage. JOM 72:296–308. <https://doi.org/10.1007/s11837-019-03918-6>
- Sanitary Norms and Regulations 2.1.4.1074-01 (2010) Hygienic requirements for water quality of the centralized systems of drinking water supply. Quality Control. Russian Ministry of Healthcare. Moscow [Electronic Resource] docs.cntd.ru/document/901798042. Accessed 7 Dec 2018
- Saraev VG (1993) Fluorine content in the soil of Minusinsky basin in the area affected by the aluminum plant. Soil Sci 2:94–97 (Сараев В.Г. Содержание фтора в почвах Минусинской котловины в зоне действия Алюминиевого завода. Почвоведение 2: 94–97)
- Saraev VG, Kharakhinova SI (1992) Fluorine content levels in the soils and biological objects of the South Minusinsk Basin under the impact of the aluminum plant. Novosibirsk, p 52, Published in All-Russian Institute for Scientific and Technical Information, 03.08.1992, No. 2548-B92 (Сараев В.Г., Харахинова С.И. Уровни содержания фтора в почвах и биологических объектах Южно-Минусинского бассейна под воздействием алюминиевого завода. Новосибирск, с. 52, опубликовано во ВИНТИ, 03.08.1992, № 2548-B92)
- Savkova VP, Novozhilova LP, Mursalimov MM (2003) Assessment of the impact of the Sayanogorsk aluminum plant on the soil cover. Scientific technical report of 2002, Abakan, p 79 (Савкова В.П., Новожилова Л.П., Мурсалимов М.М. Оценка воздействия Саяногорского алюминиевого завода на почвенный покров. Научно-технический отчет 2002, Абакан, с. 79)
- Saxena S, Rani A (2012) Fluoride ion leaching kinetics for alkaline soils of Indian origin. J Sci Res Replica 1:29–40. <https://doi.org/10.9734/JSRR/2012/2101>
- Semenov MY, Silaev AV, Semenov YM, Begunova LA (2020) Using Si, Al and Fe as tracers for source apportionment of air pollutants in lake Baikal snowpack. Sustainability 12(8):3392. <https://doi.org/10.3390/su12083392>
- Shabanov MV, Marichev MS (2018) Change patterns in acid-base properties of soils in the area of technogenesis (the case of Krasnoyarsk industrial hub). J Ural State Mineral Res Univ 1(49):55–61 (Шабанов М.В., Маричев М.С. Закономерности изменения кислотно-основных свойств почв в зоне техногенеза (на примере Красноуральского промышленного узла). Вестник Уральского государственного минерально-сырьевого университета)
- Shevchenko VP, Vorobyev SN, Krichkov IV et al (2020) Insoluble particles in the snowpack of the Ob River basin (Western Siberia) a 2800 km submeridional profile. Atmosphere 11(11):1184. <https://doi.org/10.3390/atmos11111184>
- Shishov LL, Tonkonogov VD, Lebedeva II, Gerasimova MI (2004) Classification and diagnostics of the Russian soils. Oikumena, Smolensk, p 342 (Шишов Л.Л., Тонконогов В.Д., Лебедева И.И., Герасимова М.И. (2004) Классификация и диагностика почв России. Смоленск: Ойкумена, с. 342)
- Singh G, Sinam G, Kriti K et al (2020) Soil pollution by fluoride in India: distribution, chemistry and analytical methods. In: Shukla V, Kumar N (eds) Environmental concerns and sustainable development. Springer Nature Singapore Pte Ltd
- Stevens DP, McLaughlin MJ, Randall PJ et al (2000) Effect of fluoride supply on fluoride concentrations in five pasture species: levels required to reach phytotoxic or potentially zootoxic concentrations in plant tissue. Plant Soil 227:223–233. <https://doi.org/10.1023/A:1026523031815>
- Talovskaya AV, Osipova NA, Filimonenko EA et al (2015) Fluorine concentration in snow cover within the impact area of aluminium production plant (Krasnoyarsk city) and coal and gas-fired power plant (Tomsk city). IOP Conf Ser Earth Environ Sci 27:012043. <https://iopscience.iop.org/article/10.1088/1755-1315/27/1/012043>
- Tanzybaev MG, Bulatova NU (2001) Specific Features of the Chernozems of Khakassia Formed on the Calcareous Rocks. OOO Ivan Fedorov, Tomsk, p 160 (Танзыбаев М.Г., Булатова Н.У. Особенности чернозёмов Хакасии, сложенных на известняковых породах. Томск: ООО Иван Федоров, 160 с.)
- USSR Climate Guide (1969) Leningrad: Gidrometeoizdat, Edition 21, part IV, p. 402 (Климатический справочник СССР. Ленинград: Гидрометеоздат, издание 21, часть IV, с. 402)
- Vithanage M, Bhattacharya P (2015) Fluoride in drinking water: health effects and remediation. In: Lichtfouse E, Schwarzbauer J, Robert D (eds) CO₂ sequestration,

- biofuels and depollution, environmental chemistry for a sustainable world. Springer, Cham, pp 105–151. <https://doi.org/10.1007/978-3-319-11906-94>
- Volkova VG, Davydova ND (1987) Technogenesis and landscape transformation. Nauka Publishing House. Novosibirsk, Siberian branch, 189 p. (Волкова В.Г., Давыдова Н.Д. Техногенез и трансформация ландшафта. Наука, Новосибирск, Сибирский филиал, 189 с.)
- Weinstein LH, Davison A (2004) Fluorides in the environment: effects on plants and animals. CABI Publishing, Oxon
- Yanchenko NI, Baranov AN, Chebykin EP (2013) Peculiarities and factors influencing distribution of metal, rare-earth elements, hydrogen and fluoride in snow filtrate and solid deposits of Bratsk city. Vestnik of ISTU 10(81):141–149 (Янченко Н.И., Баранов А.Н., Чебыкин Е.П. Особенности и факторы, влияющие на распределение металлов, редкоземельных элементов, водорода и фторида в фильтрате снега и твердых отложениях г. Братска Вестник ИрГТУ 10 (81):141–149)
- Zhang B, Hong M, Zhang B, Zhang X, Zhao Y (2007) Fluorine distribution in aquatic environment and its health effect in the Western Region of the Songnen Plain, Northeast China. Environ Monit Assess 133:379–386. <https://doi.org/10.1007/s10661-006-9592-z>
- Zhang L, LiQ, Ma L, Ruan J (2013) Characterisation of fluoride uptake by roots of tea plants (*Camellia sinensis* L. O. Kuntze). Plant Soil 366:659–669. <https://doi.org/10.1007/s11104-012-1466-2>



Contamination of the Agroecosystem with Stable Strontium Due to Liming: An Overview and Experimental Data

Anton Lavrishchev, Andrey V. Litvinovich,
Olga Yu Pavlova, Vladimir M. Bure,
Uwe Schindler, and Elmira Saljnikov

Abstract

This chapter presents the results of a long-term study on the dynamics of calcium and strontium in soil and plants when liming with chalk-containing strontium. The ameliorant used was a conversion chalk obtained as a by-product of the production of complex fertilisers and contained 1.5% stable strontium. Four experiments were conducted to study the behaviour of Ca and Sr in the soil–plant system on acid sod-podzolic soils (*Umbric Albeluvisol Abruptic*). The specific goal was to trace the entire pathway of Sr from the dissolution of the ameliorant, fixation of Sr

in the soil-absorbing complex, migration along the profile and finally accumulation in plants of various biological families and in various plant organs. The results showed that the 1.5% Sr contained in the conversion chalk has a high chemical activity. The complete dissolution of high doses of the chalk was achieved in 3–4 years. The migratory mobility of strontium was determined in a series of column experiments. The amount of leached Sr was found to depend on its initial content in the soils, the humus content (HA1 fraction) and the volume of washing water. It was found that the first fraction of humic acids plays a leading role in the fixation of Sr in non-limed soil, which contained about 50% of the total soil strontium. The addition of the Sr-containing chalk increased the leaching of strontium, but Sr was not completely removed from soil after multiple washings. The results showed that the accumulation of Sr in the generative and vegetative organs of plant was controlled by the barrier and barrier-free mechanisms. Strontium-free conversion chalk can be a highly effective ameliorant for reducing waste dumps generated when processing raw phosphate rocks.

A. Lavrishchev
St. Petersburg State Agrarian University,
Peterburgsoye Ave. 2, 196601 St. Petersburg,
Pushkin, Russia

A. V. Litvinovich · O. Yu. Pavlova
Agrophysical Research Institute, Grazhdanskiy Ave.
14, 195220 St. Petersburg, Russia

V. M. Bure
St. Petersburg State University, Universitetskaya
Emb. 7/9, 199034 St. Petersburg, Russia

U. Schindler · E. Saljnikov (✉)
Mitscherlich Akademie Für Bodenfruchtbarkeit
(MITAK) GmbH, Prof.-Mitscherlich-Allee 1, 14641
Paulinenaue, Germany
e-mail: schindler@mitak.org

E. Saljnikov
Institute of Soil Science, Teodora Drajzera 7, 11000
Belgrade, Serbia

Keywords

Stable strontium · Liming · Contamination ·
Sod-podzolic soil · Humic acids

Abbreviations

CC	Conversion chalk
CEC	Cation exchange capacity
DC	Discrimination coefficient
GOST	Acronym for Russian governmental standard
HA	Humic acid
HA1	Humic acid fraction 1
HA2	Humic acid fraction 2
HA3	Humic acid fraction 3
Hy	Hydrolytic acidity
MAC	Maximum allowed concentration
NPK	Nitrogen, phosphorus, potassium
PAC-1	Portable Carbonate Analyzer
TA	Total acidity
WRB	World Reference Base for Soil Resources

20.1 Introduction

20.1.1 Strontium in Soil

In nature, strontium is found in the form of a mixture of four stable isotopes: Sr^{84} , Sr^{86} , Sr^{87} and Sr^{88} , the proportion of which is, respectively, 0.56, 9.86, 7.02 and 82.56% (Dubchak 2018; Gupta et al. 2018a). The content of strontium in rocks is determined by the presence of strontium-containing minerals, the most common being strontianite SrCO_3 and celestine SrSO_4 (Höllriegl and München 2011). To date, extensive information has been collected in the literature on the content of strontium in soils (Vinogradov 1952; Toikka et al. 1981; Sheudzhen 2003; Kashparov et al. 2003, 2005; Kabata-Pendias 2011; Sahoo et al. 2016; Dubchak 2018; Bataille et al. 2020; Pathak and Gupta 2020) and organisms (Myrvang et al. 2016; Dresler et al. 2018; Hanaka et al. 2019; Sasmaz et al. 2020). The stable and radioactive isotopes of an element act identically in most physical, chemical and biological processes (Nedobukh and Semenishchev 2020). Burger and Lichtscheidl-Schultz (2018) have summarised an extended range of literature

sources on the wide scope of strontium behaviour issues in the soil–plant system. Kowalski and Andrianova (1970) summarised the data on the strontium content in various biogeochemical zones on the territory of the former Soviet Union: soils of the taiga-forest non-Chernozemic zone contain $3.2 \times 10^{-2}\%$; forest-steppe and steppe soils contain $0.9\text{--}1.0 \times 10^{-2}\%$; dry-steppe semi-desert and desert soils contain $8.2 \times 10^{-2}\%$; mountain soils contain $2.6 \times 10^{-2}\%$ and alluvial soils contain $6.8 \times 10^{-2}\%$. Significant fluctuations in Sr content can be observed depending on the soil's genetic characteristics. For example, in the brown mountain forest soil of the Krasnodar (Russia), the concentration of strontium is 111 mg kg^{-1} , and in the humus-calcareous soil, it is 544 mg kg^{-1} (Sheudzhen 2003). A detailed study of Sr content in the soils of Karelia showed that the concentration of Sr fluctuated from 40 to 900 mg kg^{-1} of the soil mass (Toikka et al. 1981).

The upper horizon of podzolic soils worldwide contains on average 87 mg kg^{-1} of Sr (Kabata-Pendias 2011). In the sod-podzolic soils of Russia, the concentration of this element, depending on the particle size distribution, ranges from 50 to 500 mg kg^{-1} (Tyuryukanova 1976): in sandy and sandy loam soils, the smallest amount being from 50 to 300 mg kg^{-1} , and in loamy soils from 200 to 500 mg kg^{-1} . The proposed background strontium concentration for the soils of the northwest of the Non-Chernozemic Zone of Russia is 156 mg kg^{-1} (Muravyov et al. 2000).

The relationship between water-soluble, exchangeable and acid-soluble forms of strontium compounds in soils is determined by their genesis, the nature of their use, the agrochemical and physico-chemical properties of individual horizons and other factors. In long-term irrigated Serozem-oasis soils, the share of acid-soluble Sr accounts for 52–100% of its total content (Litvinovich and Pavlova 1999). Burger and Lichtscheidl-Schultz (2018) summarised that a low soil pH, low content of organic matter and CEC increase the mobility, vertical distribution and bioavailability of strontium. Yuditseva and

Mamontova (1979), studying the effect of various ratios of exchangeable and non-exchangeable forms of Sr in soil, found that the addition of lime, monosubstituted calcium and potassium phosphates, peat and its ash promoted the transition of Sr⁹⁰ from exchangeable forms to non-exchangeable forms in the soil. Their results showed that monosubstituted calcium and potassium phosphates had the greatest effect on increasing the content of non-exchangeable strontium.

Stable strontium refers to the elements of the third class of danger (GOST 26213-91) and is thus present in most soils in most plants (Iserman 1981; Annenkov and Yudintseva 2002), posing an environmental risk. Labunska et al. (2021) revealed that the dramatic explosion of the Chernobyl nuclear power plant in 1980s has a continuing legacy and that local residents may be exposed to radionuclides due to the consumption of contaminated cereals.

Strontium and calcium are satellite elements from a geochemical point of view and are similar in their physical and chemical characteristics (Kabata-Pendias 2011; Dubchak 2018) since they both have a similar ionic radius and the same valence. Strontium is released into the soil from rocks containing a heterogeneous mix of Sr-containing minerals (Chadwick et al. 2009; Lavrishchev et al. 2018) as well as via routine and accidental discharge (Fukushima Daiichi accident: Report 2015; Sahoo et al. 2016).

Strontium mobility and plant uptake from the soil are influenced, among other things, by the soil's chemical composition, acidity and cultivation (Burger and Lichtscheidl-Schultz 2018), its physic-chemical and mineralogical characteristics (Dubchak 2018) and its biological characteristics (Sudhakaran et al. 2018). Strontium enters plant cells through mechanisms transporting the plasma membrane for calcium and potassium (Burger and Lichtscheidl-Schultz 2018). Previous studies have shown that strontium plays a role similar to calcium in many metabolic processes in plant

cells (Mengel and Kirkby 1987; Moyen and Roblin 2010; Lin et al. 2015) as well as having a complex dependency on Ca in the soil (Solecki and Chibowski 2002; Kashparov et al. 2005).

20.1.2 Strontium Toxicity to Animals and Humans

In the bone tissues of animals and humans, strontium replaces calcium, leading to various bone diseases often confined to local geochemical provinces with excess Sr in soils (Dubchak 2018). An example is the Chita and Amur regions (Urovskaia endemic areas) (Kowalski et al. 1964), where there was found to be a risk of contamination of agricultural soils and crops by stable Sr as a result of extensive use of fertilisers and ameliorants containing Sr. Moreover, in the Baikal region, Urov's disease, which was first described 150 years ago (Yurenski 1849), is associated with a loss of Ca in human bones. The negative consequences of the excessive deposition of Sr in animals' skeleton (replacing calcium with strontium) were most likely due to the different radii of the nucleus of these elements (Ca—1.9 Å, and Sr—2.1 Å). This means that the excess amount of Sr in bone tissue might lead to bone deformation. According to Hamilton and Minski (1972), a high content of Sr in human bone in the southeast and northwest of England was associated with a distribution of calcareous rocks, particularly apatite containing 7.3% of Sr²⁺.

20.1.3 Strontium in Agricultural Chemicals (Fertilisers and Ameliorants)

The use of strontium-containing fertilisers and ameliorants in agricultural production leads to an increase in both the total content and exchangeable forms of this element in soils (Ermokhin and Ivanov 1990; Lavrishchev 2000; Litvinovich

et al. 1999a, 2000, 2001; Karpova et al. 2004; Karpova and Gomonoova 2006; Thomsen and Andreased 2019; Frei et al. 2020; Labunska et al. 2021). According to Kabata-Pendias (1979), the amount of stable strontium in phosphate fertilisers can range from 25 to 500 mg kg⁻¹. According to Litvinovich et al. (2011), in a 50-year field experiment on the addition of phosphate fertilisers and ameliorants, the soil received from 53 to 70.9 kg ha⁻¹ of stable strontium, depending on the treatment. Strontium-containing chemicals applied at rates of a few tonnes per hectare are particularly dangerous, unlike mineral fertilisers (Thomsen and Andreased 2019). The latter authors established that about 85–90% of agricultural strontium comes from the early application of agricultural lime in the Vallerbæk catchment of Denmark, while up to 10% comes from fertiliser, and up to 10% from manure. The application of mineral fertilisers and ameliorants may also significantly alter the amount of mobile Sr in the soil.

In traditional ameliorants, the content of stable strontium is low. According to Nebolsin and Nebolsina (1997), dolomite powder contains 0.1–0.15% Sr, which is practically negligible in the soil. Litvinovich et al. (2016) reported the content of stable strontium in the screening of crushed stone production in the Leningrad Region as 160 mg kg⁻¹ (0.016%). Nevertheless, these authors proposed to monitor changes in the strontium content in soils. Bataille et al. (2020) suggest that the extent of agricultural contamination in baseline samples remains unknown but could seriously complicate the development of bioavailable ⁸⁷Sr/⁸⁶Sr baselines in regions with active or historical agriculture.

The use of strontium-containing industrial wastes (conversion chalk, phosphogypsum, ash) as chemical ameliorants poses a significantly greater risk of soil pollution with strontium. One such ameliorant is conversion chalk (CC), containing 1.5% strontium. A single use of such chalk on acid sod-podzolic light-textured soil led

to 90 kg ha of Sr entering the soil (Litvinovich et al. 1998).

20.1.4 Soil Organic Matter and Strontium

No studies on the relationship between the level of humus in soil and the content of stable strontium have yet been conducted; there is only a small amount of indirect data. Thus, Lykov et al. (2006) showed that the use of organic fertilisers enhances Sr sorption by soil. Van Bergeijk et al. (1992) found that Sr transfer decreased with an increasing soil organic matter content, while Fedorkova et al. (2012) found that the mobility and distribution of Sr⁹⁰ were mostly absorbed by fulvic acids. On the other hand, Stekolnikov et al. (2011), Oufqir et al. (2014) and Dubchak (2018) established that humic substances control the mobility and plant availability of alkaline-earth metals in the soil. Soluble strontium is easily bound to organic matter, specifically adsorbed in colloidal humic and fulvic acids (Burger and Lichtscheidl-Schultz 2018). Guillen et al. (2015) established that mobilisation of Sr by fulvic acids resulted in the formation of soluble colloids and was especially pronounced in soils with a low pH. By contrast, Sr bound to humic acids resulted in the formation of stable complexes. This is supported by the higher vertical migration of Sr in soil where the humic horizon was removed (Kazachonok 2017). Generally, it is accepted that soil with a low content of humus and a low pH results in a high uptake of Sr by the soil (e.g. Vidal et al. 2001; Sysoeva et al. 2005). Since the upper soil layer is most humified, the arable soil layer is expected to contain the highest amount of Sr. Jeske (2013) found that the fraction of Sr bound to soil organic matter was highest in the humified soil horizons of podzolic soil. In this chapter, we discuss the role of fractions of soil humic acids (HA1 and HA2) in the binding and migration of Sr.

20.1.5 Solubility and Migration Ability of Calcium (Ca) and Strontium (Sr) in Soil

Although a large number of papers have been published on the losses of Ca from soil (Bélanger et al. 2008; Youngil et al. 2009; Pousada-Ferradás et al. 2012; Adomaitis et al. 2013; Pavlova et al. 2019), and specifically from podzolic soils (Nebolsin and Nebolsina 2005), there is a lack of published data on studies of Ca and Sr leaching from limed soil (Kabrick et al. 2011) and the interaction of calcium and strontium in plant uptake (Rowley et al. 2018; Bataille et al. 2020).

Agricultural production leads to increased weathering (destruction) of primary and secondary minerals (Litvinovich 1985). This is because they are affected by plant root secretions. It is considered to have been established that plants secrete from 20 to 40% of photosynthetic organic substances into the rhizosphere through the root system. Organic acids such as fumaric, succinic, malonic, malic, citric, tartaric, oxalic, glucuronic, gluconic acids and others were revealed in the composition of the root secretions of cereals (Ivanov 1973). Obviously, these compounds are able to actively affect minerals, including carbonates, increasing their solubility in soil. Kabata-Pendias and Mukherjee (2007) found that the solubility of strontium bicarbonate is higher than that of calcium bicarbonate, suggesting that strontium is more mobile in soil than calcium. Over time, strontium is fixed in clay minerals (Rafferty et al. 1981), increasing the content of water-soluble and exchangeable forms of Sr (Lazarevich and Chernukha 2007). Moreover, it can be transported with a dust flow to neighbouring territories (Carling et al. 2020).

20.1.5.1 Dissolution and Migration of Ca in Soil

According to modern concepts (Nebolsin and Nebolsina 2005), the interaction of calcareous materials with soil occurs with the participation of two mechanisms: (1) the gradual transition of the bases into the soil solution with subsequent reaction with the soil absorbing complex and

(2) contact exchange of surface particles of lime and soil. The exchange process does not affect the inner layers of the granules.

Of all the cations that can migrate in soils, calcium has the highest mobility (Litvinovich and Nebolsina 2012). In humid climates, the main source of calcium loss is vertical migration with precipitation (Kopáček et al. 2017). According to Gorbunov et al. (1981), the high mobility of Ca in soils of the percolation and periodical percolation water regime is associated with a large ionic radius of Ca (1.06 Å) (Sekine et al. 2017), which does not allow it to participate in the construction of the crystal lattice of minerals and to firmly (irreplaceably) become fixed in the soils. Although exchangeable Ca is resistant to migration with percolation water, it is in equilibrium with the Ca of the soil solution (Shilnikov et al. 2004; Fernández-Sanjurjo et al. 2014). Bakina (2012) explains that the high mobility of Ca in podzolic soils is due to the specificity of humus in their profile: this has a weak ability to retain Ca, leading it to be rapidly removed beyond the soil profile. This assumes that Ca leaching from podzolic soils is associated with the climatic conditions of the region, and with the physicochemical properties of the soils.

20.1.5.2 Dissolution and Migration of Sr in Soil

Strontium remains mobile in a wide range of soil conditions—oxidising, acidic, neutral and reducing media—since Sr⁹⁰ is not involved in the ion exchange reactions (Dubchak 2018). However, specific data on the extent of migration of this element are rare and contradictory. In a model experiment on the horizontal migration of Sr, Zubareva et al. (1989) showed that the total discharge of Sr increased with an increase in gradient under rain irrigation, where the solid discharge made up 70% and the filtrate discharge 30% of the total losses. The possibility of the horizontal migration of Sr added with conversion chalk on the surface of soils was also established by Makovsky et al. (2008). Their study of the 12 profiles of Sierozem-oasis soils showed that under long-term irrigation, Sr accumulates in the lower part of the soil. In most soils, Sr

accumulates by eluvial-illuvial means, with a maximum content at a depth of 60–70 cm (Litvinovich and Pavlova 1999). On the other hand, Makovsky et al. (2008) did not find any Sr present in the drainage waters at 1 m depth 2 years after liming of sod-podzolic soil with conversion chalk at a dose of 9.9 t ha^{-1} .

Currently, several mechanisms of Sr transport in soil are recognised (Pavlotskaya 1974): convective transport in the form of soluble salts and complex compounds with organic ligands or solid particles transported mechanically with the infiltration of rainfall; and due to diffusion in the soil solution. However, the experimental material on Sr transport in the soil–plant system in the literature is controversial and, therefore, difficult to compare. In this regard, studies with a sufficiently large number of measurements have the most informative value, allowing us to study patterns of accumulation and distribution, and build appropriate models. Thus, one of the aims of our study was to establish the rate of leaching of Ca and Sr from the root zone.

20.1.6 Plant Uptake of Calcium and Strontium: Ca/Sr Ratio and Barrier Height

There is not much information in the literature on the mechanisms behind the bioavailability of strontium (Bataille et al. 2020). There are also many gaps in our knowledge of how liming affects the content and behaviour of Sr in the soil (Thomsen and Andreased 2019). During plant uptake, the alkaline earth metals (Ca and Sr) have a competitive nature. As a rule, soil liming reduces the transfer of Sr to plants (Lavrishchev 1997, 1999, 2000; Litvinovich et al. 2000, 2002). Soil cultivation leads to strengthened sorption bonds between the exchangeable Sr and the soil-absorbing complex, which prevents it from penetrating into plants (Lykov 1986). However, even a high content of organic matter in sod-podzolic sandy loam soil (4.6%) did not prevent strontium contamination of carrots when using conversion chalk at a dose of 7 t ha^{-1} (Litvinovich et al. 2005).

The change in the ratio of $^{90}\text{Sr}/\text{Ca}$ during plant uptake from the soil is a discrimination coefficient, which usually depends on the content of Ca in the soil, plant species and plant growth phase. Sr is usually more strongly fixed in the soil compared to Ca, causing a Sr discrimination effect (Dubchak 2018).

Different plants have an unequal ability to accumulate Sr in their tissues (Litvinovich et al. 1999b, 2008). Marakushin and Fyodorov (1977), proposed the following order of cultures according to their ability to accumulate Sr: clover > corn > timothy grass > vetch > potato > oats > barley > rye. Ermokhin and Ivanov (1990) ranked individual crops according to the intensity of assimilation of Sr from fertilisers: onions > beets > beets > pumpkins > potatoes. The existing standards for the content of stable strontium in soils and plants were evaluated and compared based on the experimental data gathered by Lavrishchev et al. (2019).

According to Titov et al. (2007), several physiological barriers prevent toxicants from entering the above-ground plant organs: the soil–root, root–stem and stem–inflorescence borders. The entry of toxic elements into plants through the roots can be regulated by mechanisms that reduce their concentration on the outer surface of the root cell membrane, resulting in fewer metals entering the cell (Morel et al. 1986). The latter studies on the barrier heights were done on heavy metals; however, few studies were found on strontium assimilation barriers. Handley and Overstreet (1962) and Pinkas and Smith (1966) confirmed the existence of barriers close to the cell surface that limit the non-metabolic uptake of Sr.

20.1.7 Hypotheses and Goals of the Study

Because the strontium route from soil to plant depends on the degree of soil pollution, the soil type and the soil's physical and chemical properties and fertility, and since these parameters are prone to short- and long-term changes, the Sr transfer factor should be regularly re-checked

and corrected. On the other hand, there are studies showing that liming acid soils prevent Sr from becoming bioavailable to plants due to a sharp increase in their Ca and Mg content (Yudintseva and Gulyakin 1998). A decreased content of hydrogen ions and an increased content of calcium ions strengthen the binding of Sr in the soil, limiting plant uptake of Sr (Aleksakhin and Korneev 2001). Kultakhmetov et al. (2003) found that liming at a dose corresponding to full hydrolytic acidity reduces the content of Sr in crops by 1.5–3 times depending on the soil type and initial acidity.

This study presents calcium and strontium dynamics in soil and assimilation by plants during the dissolution of conversion chalk (Lavrishchev et al. 2018) as well as the impact of the conversion chalk on the transformation of humic acids in *Umbric Albeluvisol Abruptic* soils (WRB 2007). The general objective of this research was to study the behaviour of Ca and Sr in the soil–plant system using conversion chalk to lime acid sod-podzolic soils. The specific objective was to trace the entire path of Sr from the dissolution of the ameliorant, the fixation of Sr in the soil absorbing complex, its migration along with the profile and finally its accumulation in plants of various biological families and in various plant organs. The tasks were:

- Studying the dissolution rate of conversion chalk in the soil and identifying the distribution pattern of mobile and soluble forms of Ca and Sr in the soil

- Comparing the migration rate of Ca and Sr in the sod-podzolic soil
- Defining the role of humic acids in the binding of Sr in the soil
- Determining individual plant species' ability to accumulate Sr
- Identifying differences in the accumulation of Ca and Sr in grain and barley straw.

20.2 Materials and Methods

20.2.1 Soil and Lime Characteristics

Acidic sod-podzolic soils (*Umbric Albeluvisol Abruptic*, WRB 2007) from natural grassland with a higher humus content and absorption capacity (Soil No. 1) and from forest soil (Soil No. 2) were used in the series of field and pot experiments (Table 20.1). The conversion chalk (CC) used as an ameliorant in this study was a byproduct of the industrial production of nitrogen fertilisers by the joint-stock company “Akron” (Veliky Novgorod, Russia). It contained 90% CaCO₃ and 1.5% Sr. From 1985 to 1994, this industrial waste was intensively used as a liming material in the Novgorod and Leningrad regions of Russia. Such long-term application of an ameliorant containing stable strontium may pose a risk of crop contamination by translocation into vegetative organs and groundwater via leaching (e.g. Gupta et al. 2018b).

Table 20.1 Physical–chemical characteristic of sod-podzolic soils

Humus, %	pH _{KCl}	Total acidity, TA	Exch. acidity	CEC	Ca	Sr	Ca: Sr	Fractions < 0.01 mm, %
		mmol(eq) 100 g ⁻¹			Mg kg ⁻¹			
<i>Soil No. 1</i>								
3.02	4.1	5.4	2.5	22	7358	135	54.5	18.6
<i>Soil No. 2</i>								
1.76	4.2	5.6	0.75	14	5396	112	48.2	21.6

TA—total acidity; Exch. acidity—exchangeable acidity; CEC—cation exchange capacity

20.2.2 Design of Experiment No. 1: Chalk Dissolution Rate

Experiment No. 1 was conducted on the two soils studied in pots containing 5 kg soil as follows: (1) NPK (background); (2) Background + CC (0.1TA); (3) Background + CC (0.2TA); (4) Background + CC (0.5TA); (5) Background + CC (1TA), where the dose 1TA (tonnes per hectare) = $1.5 \times \text{TA}$ (total acidity). The experiment was performed in four replications for 3 years. Rape, vetch and wheat were grown successively on grassland and forest soils (Soil 1 and Soil 2, respectively).

20.2.3 Design of Experiment No. 2: Precision Experiment (Sr Translocation in Tissues)

In Experiment No. 2, we designed the maximum possible number of situations to obtain data sufficient to reveal that the accumulation of Sr in the

tissues of selected crops clearly depended on a wide range of lime doses over a period of 5 years (Photograph 20.1). Pots containing five kilograms of grassland soil (No. 1) were arranged according to the scheme (1) NPK; (2) NPK + CC (0.1TA); (3) NPK + CC (0.2TA); (4) NPK + CC (0.3TA); (5) NPK + CC (0.4TA); (6) NPK + CC (0.5TA); (7) NPK + CC (0.6TA); (8) NPK + CC (0.7TA); (9) NPK + CC (0.8TA); (10) NPK + CC (0.9TA); (11) NPK + CC (1.0TA); (12) NPK + CC (1.1TA); (13) NPK + CC (1.2TA); (14) NPK + CC (1.3TA); (15) NPK + CC (1.4TA); (16) NPK + CC (1.5TA); (17) NPK + CC (1.6TA); (18) NPK + CC (1.7TA); (19) NPK + CC (1.8TA); (20) NPK + CC (1.9TA); (21) NPK + CC (2.0TA); (22) NPK + CC (2.2TA); (23) NPK + CC (2.5TA); (24) NPK + CC (3.0TA), where the dose 1TA (tons per hectare) = $1.5 \times \text{TA}$ (total acidity). The crops grown successively were rape, vetch, barley, rape and rape. A precise experiment enabled the number of treatments to be significantly increased by eliminating repetitions.

Photograph 20.1 Precise pot experiment studying the behaviour of stable Sr in the soil–plant system. St Petersburg State Agrarian University, Russia (photograph by A. Lavrishchev)



20.2.4 Design of Experiment No. 3: Pot Experiment (Sr Uptake by Varieties of Wheat)

Experiment No. 3 is a pot experiment carried out to study the pattern of accumulation of stable Sr by various crop varieties within the same species on forest soil (No. 2). This experiment was laid out on the soils of Experiment No. 2. Seven varieties of spring wheat were selected in the following design: (1) Leningradka variety—no liming; (2) Leningradka—liming with CC (1.5 Hy); (3) Velikovskaya variety—no liming; (4) Velikovskaya—liming with CC (1.5 Hy); (5) Gorkovskaya variety—no liming; (6) Gorkovskaya variety—liming with CC (1.5 Hy); (7) Leningradskaya-89—no liming (8) Leningradskaya-89—liming with CC (1.5 Hy); (9) Zhak-24 variety—non-liming; (10) Zhak-24—liming with CC (1.5 Hy); (11) Vladimirskaya variety—no liming; (12) Vladimirskaya—liming with CC (1.5 Hy); (13) Opochetskaya variety—no liming; (14) Opochetskaya—liming with CC (1.5 Hy). The soil weight in each pot was five kilograms; each treatment was carried out in four replications.

20.2.5 Design of Experiment No. 4: Column Experiment (Migration of Ca and Sr)

Experiment No. 4 was performed in columns to study the migration ability of Ca and Sr in forest soil (No. 2), limed by chalk and composted for 30 days in a thermostat at 28 °C (Photograph 20.2). During composting, humidity was kept at 60%. After composting, the soil was dried, ground and sieved through a 1 mm sieve and placed in a polyvinyl chloride column with a diameter of seven cm. The packing density was 1–1.1 gcm⁻³. The height of the soil in the column was 17 cm. In total, eight washings were carried out with a strictly calculated amount of distilled water, corresponding to the average annual amount of precipitation simulating the annual rate of water percolation. 400 ml of distilled water was used per wash.

After the eighth wash, the soil was removed from the column, limed again and composted for 30 days. The experiment lasted 9 months, excluding two periods of 1–2 days of composting. Each of 16 washings was performed in five replications.

Photograph

20.2 Laboratory experiment to study the migration ability of stable strontium in the soil (photograph by A. Lavrishchev)



20.2.6 Analytical Methods

The total content of Sr in washing waters was determined by X-ray fluorescence spectral analyser ORTEC-6111-TEFA (ORTEC Incorporated USA). The water-soluble Ca and Sr (WSCa and WSSr) were extracted from the soil with an ammonium acetate buffer (pH 4.8) and distilled water and analysed on an atomic absorption spectrophotometer (Shimadzu, Japan). The content of unreacted carbonates was analysed with a Portable Carbonate Analyzer (PAC-1).

The content of humus was determined with the Tyurin wet-digestion method (1937). The fractional composition of humus was determined with the Ponomareva method as modified by Plotnikova and Orlova (1984). A 0.1 N NaOH solution was used not to extract metals from soils, but to extract most of the humus substances without disturbing their chemical nature (Tyurin 1937; Aleksandrova 1970). The Ca and Sr in an individual fraction of humus acids (HAs) were extracted by digestion in the HCl + HNO₃ mixture followed by the dissolution of the residue in distilled water. The fractions of soil humus determined were: Fraction 1 (HA1) extracted by 0.1 N NaOH, Fraction 2 (HA2) extracted by 0.1 N NaOH after decalcification of soil, Fraction 3 (HA3) extracted after 6 h heating of soil in a water bath. Statistical analysis was performed using Microsoft Excel and Statistica (SPSS Inc).

20.3 Results and Discussion

20.3.1 Conversion Chalk (CC) Dissolution Rate

The rate of the conversion chalk (CC) dissolution was determined from the content of unreacted carbonates (Table 20.2). The complete dissolution of chalk in the soil limed with 0.2TA (total acidity) was achieved in the year of application CC; the soil limed with 0.5TA in the third year, while, in the soil limed with 1TA, the amount of residual carbonates was only 7.5%, which indicates an almost complete dissolution of the ameliorant in the third year of the experiment.

20.3.2 Calcium and Strontium Accumulation in Limed Soils

Liming with CC with a dose of 1TA increased the total content of Ca in both soils by 27–32% from the initial value (Table 20.3). The soils with different humus content showed significant differences in the accumulation of mobile Ca. After the first year of the experiment, depending on the doses of CC, the content of mobile Ca compounds in Soil No. 1 ranged between 1390 and 3356 mg kg⁻¹ (20.4–36.4% of the total content), and that in Soil No. 2 between 171 and 1118 mg kg⁻¹ (3.2–15.8% of the total content).

Table 20.2 Dynamics of unreacted carbonate content in the soils, %

Treatment	First year	Second year	Third year
1. NPK (background)	0	0	0
2. Background + CC (0.1TA)	Traces	0	0
3. Background + CC (0.2TA)	Traces	0	0
4. Background + CC (0.5TA)	15.1 ± 4.2	9.0 ± 1.5	0
5. Background + CC (1.0TA)	26.0 ± 8.2	20.0 ± 5.4	7.5 ± 1.9

Note NPK (background)—nitrogen, phosphorus and potassium fertiliser; CC—conversion chalk; TA—total acidity

Table 20.3 Content of different forms of Ca and Sr compounds in the soil, mg kg⁻¹

Treatment	First year			Second year			Third year											
	Total		Water soluble	Total		Water soluble	Total		Water soluble									
	Ca	Sr	Ca	Sr	Ca	Sr	Ca	Sr	Ca	Sr								
<i>Soil No. 1</i>																		
1. NPK (background)	7245	119	1366	8.5	16.7	0	7003	121	1200	11.1	180	1.2	6767	110	555	16.1	220	2.9
2. Background + CC (0.1TA)	7351	125	1390	12.0	9.4	0.5	7185	149	1675	23.5	225	2.3	7475	134	1620	35.3	236	4.2
3. Background + CC (0.2TA)	8144	181	1665	17.9	10.6	0.4	6889	129	1725	20.5	220	1.9	7300	139	1644	34.4	267	4.9
4. Background + CC (0.5TA)	8386	198	2270	33.7	6.6	0.1	7891	178	2250	35.2	222	3.5	7891	160	1930	49.8	365	9.0
5. Background + CC (1.0TA)	9213	221	3356	66.2	26.6	0.6	8944	213	4025	67.2	585	16.3	8677	210	3730	86.1	660	19.5
<i>Soil No. 2</i>																		
1. NPK (background)	5370	116	113	5.1	50	0.9	5122	82	98	5.2	-	-	No data					
2. Background + CC (0.1TA)	5411	120	171	9.2	50	1.2	5361	120	1313	13.8	216	7.8						
3. Background + CC (0.2TA)	5759	123	286	13.6	89	2.3	5691	107	815	18.8	274	10.0						
4. Background + CC (0.5TA)	6117	130	592	28.5	140	4.4	6008	114	528	31.5	421	17.0						
5. Background + CC (1.0TA)	7066	180	1118	51.8	205	7.5	7000	137	267	63.8	687	32.0						

Note NPK (background)—nitrogen, phosphorus and potassium fertiliser; CC—conversion chalk; TA—total acidity

Obviously, the replenishment of the content of mobile Ca compounds in Soil No. 1 was associated with the mineralisation of grass-root residues. This assumption is supported by the findings of Zhang and Wang (2015), who found that both coarse and fine roots contribute to the release of nutrients into soil, particularly at lower latitudes. In addition, low-molecular weight organic acids formed in this process contributed to the enhanced decomposition of chalk carbonate. Higher absorption capacity of Soil No. 1 contributed that part of the mobile Ca was fixed in the soil. During the experiment, the content of mobile Ca continued to increase, which was associated with the continued dissolution of CC.

The content of water-soluble Ca (WSCa) also depended on the dose of chalk applied. After the first year, its concentration ranged between 9.4 and 26.6 mg kg⁻¹ in Soil No. 1, and between 50 and 205 mg kg⁻¹ in Soil No. 2. The differences in the content of WSCa were probably due to the dissolution of chalk in Soil No. 1, which was accompanied by saturation of the soil absorption complex. Meanwhile, in Soil No. 2, the capacity of the absorption complex was low, and a large amount of available Ca remained in the soil solution. During the experiment, the content of WSCa is increased. The use of lime dose in 1TA increased the total Sr content in soils by 60–63% of its initial content. The content of mobile Sr compounds, depending on the doses of CC, was from 2.6 to 29.9% (12.0–66.2 mg kg⁻¹) of the total content in Soil No. 1 and 9.2–28.8% (9.2–51.8 mg kg⁻¹) in Soil No. 2. During the experiment, the share of mobile Sr (WSSr) in its total content in the soil is increased. The regularities of the dynamics of WSSr were very similar to the dynamics of WSCa.

Strontium-contaminated soils were classified according to Popov and Soloviev (1991): slightly hazardous—<10 mg kg⁻¹, medium hazardous—10–15 mg kg⁻¹, moderately hazardous—15–25 mg kg⁻¹, highly hazardous—25–50 mg kg⁻¹ and non-agricultural soil >50 mg kg⁻¹. Classification of the data showed that after the complete dissolution of the lime at the dose of 0.1–0.2TA, the soil passes into the moderately hazardous and highly hazardous classes.

20.3.3 Calcium and Strontium Migration from the Limed Soil

Higher content of mobile Ca and Sr in the soil promotes both their penetration into plants and migration down the soil profile (Pavlova et al. 2019). The effect of liming on the migration ability of Ca, as presented in previous works (Litvinovich et al. 2018), showed that regardless of the type of liming material, soil loses basic cations, but the rate of the losses depends on the chemical composition of the amendment. Another work by Litvinovich et al. (2008) studying how liming affected the migration of Sr showed that the amount of leached strontium depended on its initial content in the soil, the content of humus and the volume of percolating water. Dubchak (2018) found that the migration rate of Sr increases with an increase in the exchangeable Ca content both in a pot and in field experiments.

In the control treatment, the first washing collected the maximum amount of Ca (Table 20.4). The total loss of Ca and Sr after eight washings was very significant and amounted to 70.2 mg. Liming increased Ca loss by leaching due to the washes. The total volume of leached Ca from limed soil for all eight washes was 266.3 mg, which is 3.8 times more than in the control treatment. The share of Ca losses from CC was 67.25%. The high migratory ability of Ca in natural soil was due to the large reserve of its water-soluble compounds formed after the mineralisation of grass-root residues, and the weak ability of podzolic loam-sandy soils to retain bases (Bakina 2012; Litvinovich et al. 2018) and other plant nutrients (Burakova and Bakšiene 2021). The complete removal of mobile Sr from the natural soil (control) was achieved in the third wash (Table 20.4). This was obviously due to the low content of mobile Sr in natural soil (0.12% of the total).

The addition of Sr with the conversion chalk resulted in increased metal migration. Strontium was found in the leachate of each washing with the maximum concentration being in the first wash. In contrast to Ca, the eluvial loss of Sr

Table 20.4 Amount of leaching Ca and Sr in 16 washes and two liming applications, mg

Treatment	Ca		Sr	
	Control	Liming	Control	Liming
First liming before washes (Ca—291.6 mg per column; Sr—12.15 mg per column)				
1	40.00	79.80	0.12	1.2
2	2.20	39.00	0	0.4
3	1.40	38.00	0.04	0.5
4	8.00	28.50	0	0.4
5	4.00	26.40	0	0.4
6	7.60	21.00	0	0.4
7	4.80	19.80	0	0.3
8	2.20	13.80	0	0.2
Σ	70.2	266.3	0.16	3.8
% of added (1–8 washes)		67.25%		29.95
Second liming after 8th wash: Ca—291.6 mg per column; Sr—12.15 mg per column				
For the two liming applications (before the 1st wash + after the 8th wash): Ca—583.2 mg per column; Sr—24.30 mg per column				
9	1.98	33.20	0	0.70
10	1.80	15.40	0	0.42
11	1.30	17.40	0	0.41
12	1.17	12.90	0	0.48
13	0.98	11.80	0	0.36
14	0.71	11.60	0	0.34
15	0.59	11.40	0	0.35
16	0.40	10.00	0	0.32
Σ	8.93	123.7	0	3.38
% of added (9–16 washes)	–	39.35%	–	27.8
For 16	79.13	390	0.16	7.18
% of added for 16 washes	–	53.3%	–	28.9%

from the chalk for all eight washes was only 29.95% of the added Sr amount. The migration ability of Sr is most affected by the presence of other cations in the solution (Sanzharova 2005), while the mobility functions of ^{90}Sr in soil–plant system are mainly determined by stable Sr as its isotopic carrier, and by the non-isotopic carrier, stable Ca^{2+} (Dubchak 2018).

Kuke et al. (2016) suggested that, apart from the soil and plant characteristics, the direction of Sr–Ca interaction also depends on other element's function. Strontium isomorphically replaces Ca and Mg from calcite and limestone,

gypsum and dolomite (Sanzharova 2005). Then, stable Sr and Ca are absorbed by the soil solid phase, predominantly via ion exchange. In our study, repeated composting of the control soil did not increase Ca migration. The filtrates of the second observation period contained less Ca than the first experiment (Table 20.4). The second application of CC accelerated eluvial losses of Ca. Since most of the Ca leached with the first washing (79.8%), and continued to leach with each next wash, after the eighth wash, the filtrate contained 13.8% Ca. However, after the second liming, the Ca losses again increased compared

with the control (in the filtrate of the ninth wash, it was 33.2%). Over the 16 washings, the total Ca leached from the CC was 53.3% of the added, and for Sr, 28.9% of the added, indicating that the Ca migration rate was almost double that of Sr. This was obviously due to the different bond strengths of these alkaline-earth metals with an absorbing complex of the soil. Particularly, the increased concentrations of Ca⁺⁺ in the soil solution strengthened the binding of Sr in soil (Aleksakhin and Korneev 2001). Given the competitive nature of the translocation of Ca and Sr in plants, a narrowing of the Ca/Sr ratio should be expected due to the addition of chalk, and, as a consequence, a deterioration in crop quality.

20.3.4 Soil Organic Matter and Accumulation of Calcium and Strontium in Soil

Over the 33 years of the experiment, 53–70.9 kg of Sr per hectare was added with fertilisers and ameliorants, which is 5.1–6.1 times more than in native soil. This invites a question: Which soil components contribute to Sr retention, preventing its leaching? In this regard, the concentration

of alkaline earth metals in an individual humic fraction may be of interest.

Mineral elements directly associated with humic acids (HAs) entering soil solution are widely used in humus research carried out by studying the ash composition of humic substances, extracted by 0.1 N NaOH. Earlier studies showed that the migration of Sr increases with increased acidity and organic matter content (Lazarevich and Chernukha 2007). However, the ability of individual fractions of HA to retain Sr has not yet been clarified.

The content of Ca in the HA1 fraction from the control soil was low (Table 20.5), only 0.6% of the total Ca content in the soil. The not significant tendency of higher Ca in limed soils was found. The results are consistent with findings by Ponomareva and Plotnikova (1980) and Bakina (1987), who reported that brown humic acids have a low ability to fix calcium. The fact that the HA1 fraction accumulated 50% of the total Sr in the soil (Table 20.5) indicates the important role of this fraction in the accumulation of this metal. This is confirmed by the content of the absolute amount of Sr in the HA1, which was almost six times higher than the amount of adsorbed Ca.

The column Experiment No. 4 showed that 79.1 mg Ca and 0.16 mg Sr leached from the

Table 20.5 Content of alkaline-earth metals in different fractions of humic acids

Treatment	Ca		Sr	
	% of the fraction weight	% of the total Ca content in the soil	% of the fraction weight	% of the total Sr content in the soil
<i>HA1</i>				
Control	0.25	0.60	1.48	49.9
Liming	0.51	0.46	1.33	21.2
LSD ₀₅	–	–	0.168	–
<i>HA2</i>				
Control	0.061	0.008	0.073	0.60
Liming	0.119	0.015	0.073	0.39
<i>HA3</i>				
Control	0.022	0.003	0.089	0.72
Liming	0.019	0.002	0.066	0.63
LSD ₀₅	0.0116		0.0465	

HA1—humic fraction by 0.1 N NaOH; HA2—humic fraction extracted by 0.1 N NaOH after decalcification of soil; HA3—humic fraction extracted after 6 h heating of soil in a water bath

non-limed soil. Leaching of Sr ceased after the third wash, while Ca was found in high concentrations after the 16 washes. These results imply that despite the similar geochemical properties, Ca and Sr differ in their accumulation in different fractions of soil organic matter and strength of their bonds with soil adsorbing complex.

The share of calcium in the non-limed soil was 17%, and that of Sr made up 9% of the total reserve. Probably, the HA1 fraction absorbs Sr over a longer period and under certain soil conditions. Other components of soil humus were obviously also involved in the fixing of the Sr added with lime. In their study on strontium binding with humic acid, Paulenová et al. (2000) found that in neutral and basic solutions, increased ionisation of carboxylate groups leads to a complete repulsion of humic acid and an increase in the binding of Sr with this polyelectrolyte.

20.3.5 Accumulation of Ca and Sr in Plants

20.3.5.1 Accumulation of Ca and Sr by Different Varieties of Spring Wheat in Vegetative and Generative Parts of the Plants

Litvinovich et al. (2013) found that the soil with a lack of mobile Ca and low CEC accumulated Sr more intensively. In addition, an antagonistic effect of Ca and Sr may result that strontium affects plants' absorption of calcium (Kuke et al. 2016; Zhang et al. 2020). A significant difference in the Sr content in different species, varieties and cultivars can be observed even within the same crop (Dubchak 2018; Sasmaz et al. 2020). In the pot experiments carried out by Korneeva (1970), the accumulation of radioactive strontium in nine species and varieties of spring wheat was 2–3 times greater. In the field experiments with 54 varieties of spring wheat, the accumulation of radioactive strontium was 2–4 times greater.

To study the varietal features in accumulation of stable Sr and Ca, we selected seven varieties

of spring wheat in Experiment No. 3 (Table 20.6). The results indicate that different varieties of spring wheat differed in their ability to accumulate Ca in their organs. The highest level of Ca accumulated in the straw of the domestic Vladimirskaya and Leningradskaya varieties, as well as the Brazilian variety Zhak-24: 0.68; 0.57 and 0.62% of Ca in the air-dry mass of straw, respectively. The lowest Ca content in the straw was found in the Opochetskaya variety (0.42%). The content in varieties with the highest levels of accumulation was 1.6 times that in those with the lowest levels. Identified differences were significant at a level of $p < 0.05$. The concentration of Ca in the grain of plants was lower than in straw. The lowest concentration was in the Opochetskaya variety (0.018%). All other wheat varieties accumulated significantly more calcium. The amount of calcium found in the grain of the Vladimirskaya variety (highest content) exceeded the concentration of this element in the grain of the Opochetskaya variety by 2.8 times.

Enrichment of the soil with Ca during liming enhanced the transition of this element to both the vegetative and generative organs of wheat. The exception was the Vladimirskaya and Leningradka varieties, where liming did not lead to the accumulation of Ca in the grain. In other liming treatments, the concentration of Ca in the straw was 1.75–2.7 times higher than without liming. The differences were statistically significant. In wheat grain, the increase in calcium content from the liming treatment was 1.1–2.6 times higher than from non-liming.

Table 20.6 shows that the concentration of Sr in the straw of the studied wheat varieties ranged from 35.7 to 58.9 mg kg⁻¹ dry weight of plants (1.6 times). The lowest content was found in Gorkovskaya (38 mg kg⁻¹), Opochetskaya (35.7 mg kg⁻¹) and Leningradskaya-97 (44.6 mg kg⁻¹), the highest content in Vladimirskaya (58.9 mg kg⁻¹) and Leningradka (47.1 mg kg⁻¹). The Ca/Sr ratio in the straw of various varieties of spring wheat ranged from 94 to 132, i.e. it was relatively favourable, except for the Leningradskaya-97 variety, where the Ca/Sr ratio was unfavourable (76) in the case of

Table 20.6 Content of Ca and Sr in straw and grain of various varieties of spring wheat, mg kg⁻¹ dry plant mass

Variety	Ca, mg kg ⁻¹		Sr, mg kg ⁻¹		Ca/Sr	
	Grain	Straw	Grain	Straw	Grain	Straw
<i>Without liming</i>						
Leningradsкая-89	380	5700	0.44	44.6	863	128
Opochetskaya	180	4200	0.89	35.7	202	93.5
Vladimirsкая	500	6770	0.58	58.9	862	114
Velikovskaya	420	5600	0.34	44.9	1235	125
Gorkovskaya	400	4850	0.39	38.0	1025	128
Leningradka	300	5600	0.10	47.1	3000	119
Jak-24	400	6200	0.49	47.1	816	132
<i>With liming</i>						
Leningradsкая-89	450	11,950	2.04	157.7	220	76
Opochetskaya	470	11,100	2.32	124.7	202	89
Vladimirsкая	350	11,900	0.86	143.6	407	83
Velikovskaya	470	12,270	4.22	140.4	111	88
Gorkovskaya	500	10,620	0.18	117.4	2777	91
Leningradka	270	10,280	0.89	123.3	303	84
Jak-24	550	13,600	5.88	155.9	94	87
LSD ₀₅	34.5	150.4	–	17.6		

the liming treatment. The concentration of Sr in the grain of various varieties of wheat in the treatment without liming did not exceed 1 mg kg⁻¹ of air-dry mass and ranged from 0.1 to 0.89 mg kg⁻¹.

Liming led to an increase in the content of Sr in wheat grain. Its concentration increased from 0.1 mg kg⁻¹ (Leningradka variety) to 5.88 mg kg⁻¹ (Brazilian variety Zhak-24). Comparison with the results gained by Ilyin (1991) on the strontium concentration in the storage organs of cereals (6 mg kg⁻¹) grown on uncontaminated soils showed that the content of this element in spring wheat grain did not exceed average values, i.e. it fitted into the range characteristic for uncontaminated plants. The Ca/Sr ratio ranged from 94 (relatively favourable) to 2777 (favourable).

The wheat varieties selected for the study were obviously able to withstand the flow of strontium into the generative organs, preserving the hygienic purity of the grain. The Ca/Sr ratio was favourable. The correlation coefficient between the concentration of Sr in the grain and

straw was $r = 0.6$. A low value for the correlation coefficient may indicate the existence of barriers in wheat plants on the path of strontium entering the generative organs. Otherwise, the correlation coefficient should be higher. The results showed that if wheat varieties are selected which can limit the intake of Sr in the commodity part of the production, this makes it possible to grow crops with a favourable Ca/Sr ratio on soils contaminated with strontium.

20.3.5.2 Accumulation of Sr and Ca in Generative and Vegetative Organs of the Spring Wheat

The theoretical premise was the well-known fact that the generative organs of plants accumulate significantly fewer toxicants than vegetative organs (Iserman 1981; Ilyin 1991; Dubchak 2018). According to Ilyin (1991), the lowest content of toxicants in the reproductive organs of plants compared with their vegetative organs is associated with the protective mechanisms that prevent toxicants from penetrating into these

organs to maintain their reproductive ability. From the roots, metals are transported to higher organs through xylem vessels with the transpiration stream (Sarret et al. 2002; Dinu et al. 2020; Yaseen et al. 2020). According to Titov et al. (2007), plants are capable of preventing heavy metals from accumulating in their cells thanks to the mechanisms of immobilising metal ions in the cell wall, inhibiting ion transport across the plasma membrane and releasing them from the cells into the environment.

At the same time, with an increase in Ca and Sr in the external environment, their concentrations increase in the above-ground organs—stems and leaves—and then in the grain. This suggests that the protective mechanisms that function at the level of cells and tissues are not able to completely prevent toxicants from penetrating from the roots into the shoots of plants, or from the stem into the grain.

It was found that the vegetative and generative organs of plants accumulate alkaline earth metals in different ways (Fig. 20.1). The assimilation of calcium in the straw occurred in a barrier-free type. In the treatments with liming up to 1.8 TA (5400 mg kg⁻¹), some differences in Ca content were found, but no differences were observed at the higher doses. In the barley grain, Ca assimilation also depended on the dose of chalk added, where the increase continued up to the 2TA (6000 mg kg⁻¹ soil) dose of lime.

The accumulation of Ca and Sr by barley straw was similar and occurred in a barrier-free type. Strontium accumulation coefficients ranged from 3.0 to 11.7. The Ca/Sr ratio for the plants from all treatments in the experiment was unfavourable (<80), according to Mineev (1989), who suggested that the Ca/Sr ratio in plants is optimal at 160:1 or more, relatively favourable at 80:1 and unfavourable <80:1. The nature of the movement of these elements in the soil–plant system implies that Ca passed into the straw relatively more intensively than Sr. The change in the ratio of ⁹⁰Sr/Ca during plant uptake from the soil is a discrimination coefficient, which usually depends on the content of Ca in the soil, the plant species and the plant growth phase. In our study, the discrimination coefficient

(DC) was >1 indicating that Sr is fixed stronger in soil compared with Ca, causing a Sr discrimination effect (Dubchak 2018).

The accumulation Ca and Sr in the straw (Fig. 20.1a, c) and Ca in the grain of barley (Fig. 20.1b) confirmed that they were significantly similar. Plant uptake of these elements in straw occurred in a barrier-free type and depended on the dose of CC applied. The maximum level of their accumulation in the above-ground parts of the plants was obtained using the chalk doses from 1.8 to 2.5 TA. By contrast, the accumulation of Sr in the grain was a barrier type. Up to the dose of 1.5 TA (4500 mg kg⁻¹ soil), the accumulation of Sr in the grain changed slightly (from 13.6 to 16–20 mg kg⁻¹). An increase in the Sr content in the grain (40 mg kg⁻¹) was recorded at a dose of 1.6 TA (4800 mg kg⁻¹ soil), and the highest content (115 mg kg⁻¹) was found in the treatment with the chalk dose of 1.9 TA (5700 mg kg⁻¹ soil). The higher CC doses led to a slight decrease in the content of Sr in the grain. The different accumulation pattern of Sr by the different plant organs was previously reported (Sowa et al. 2014; Dresler et al. 2018). Although strontium exhibits a high physical and chemical similarity to calcium, our study showed that the mechanism by which Ca and Sr passed into the generative organs of barley was different. This confirms the existence of a biochemical mechanism in plants for the selective passage of these two elements into generative organs.

20.3.5.3 Barrier Height Indicator

The *barrier height* indicator (Minkina et al. 2011), calculated as the ratio of the metal concentration in the adjacent parts of the plant (stem/grain), indicates that the protective mechanisms of the grain have a high ability to resist the toxicant intake. In our study, the barrier height increased steadily in the treatments with lime doses up to 1.5Hy, reaching maximum values of 29 units, i.e. the concentration of strontium in the straw exceeded the concentration in the grain by 29 times (Fig. 20.2).

With a further increase in the dose of lime and an increase in the concentration of Sr in the stem,

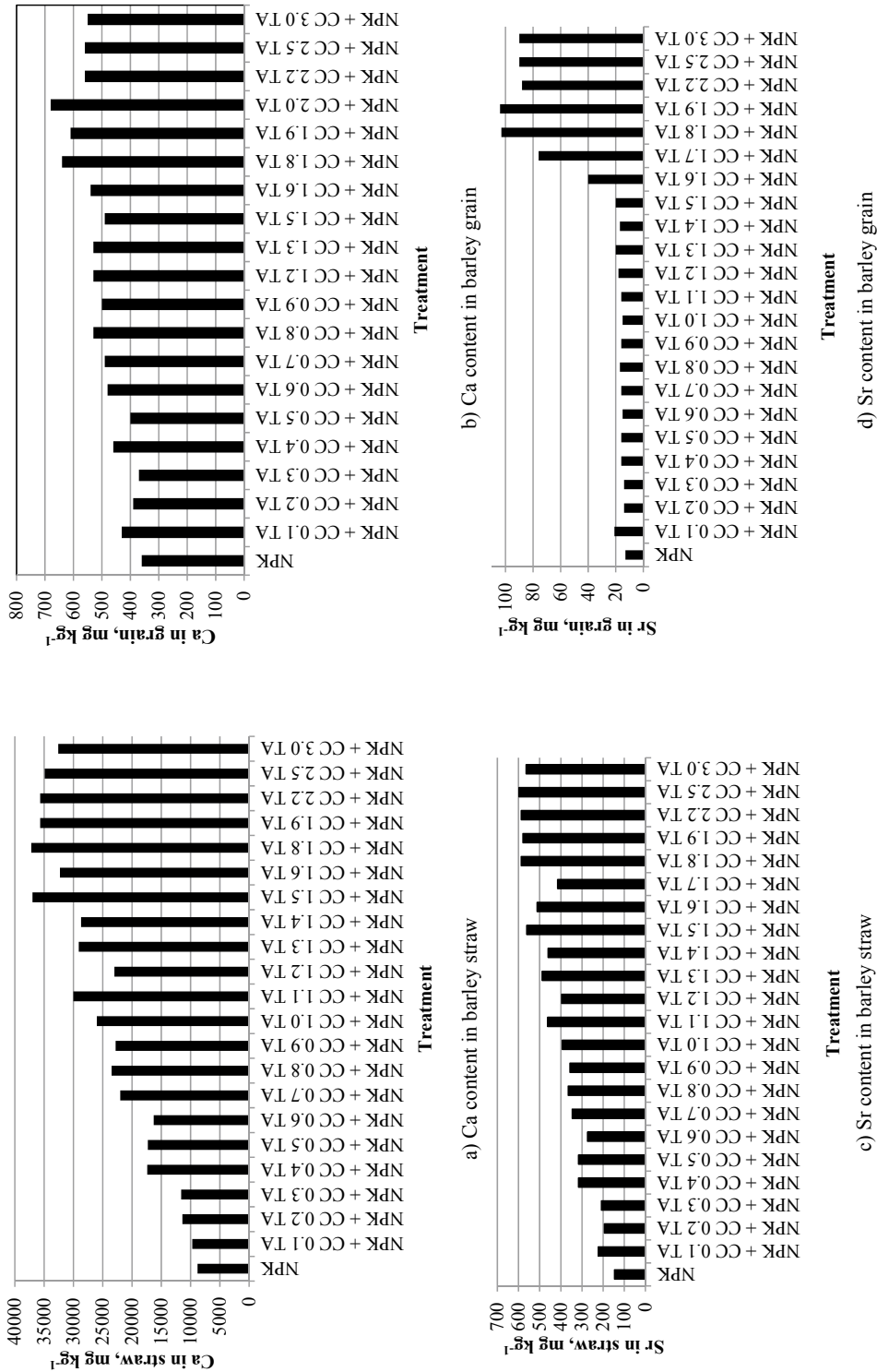


Fig. 20.1 Calcium and strontium in barley straw and grain

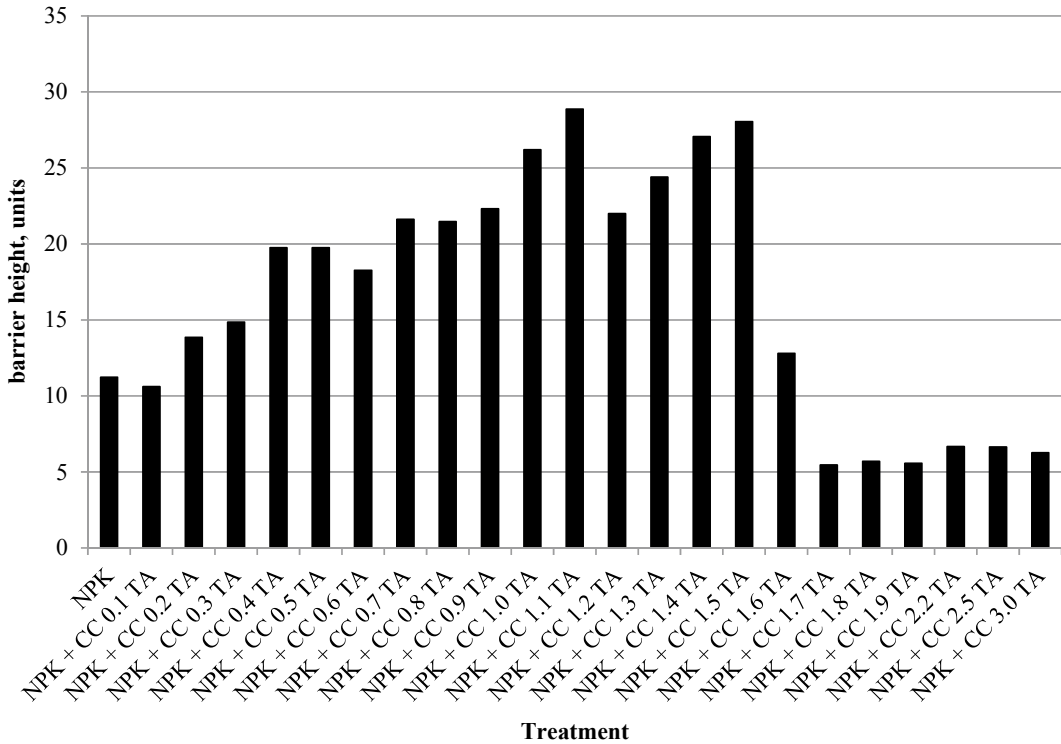


Fig. 20.2 Variation in the barrier height depending on the dose of lime

the protective mechanisms cease to cope, and the system tends to equalise the concentrations. At a dose of 1.6 Hy, the barrier height already decreased to 12.8 units, and from a dose of 1.7 Hy dropped to the 5.5–6.7 unit interval, which is even lower than in the control treatment.

It is important to note that both the barrier height and the threshold concentration of the pollutant in the soil, at which the protective mechanisms stop blocking the flow of metal into the generative organs, are individual indicators for a particular species and even a plant variety within the same species. This is clearly illustrated in Fig. 20.3, where the barrier heights of seven varieties of spring wheat are presented (Lavrishchev and Litvinovich 2019). Figure 20.3 demonstrates that the barrier height for various wheat varieties grown without liming varied in a wide range, from 40 units for the “Opochetskaya” variety up to 471 units for the “Leningradka” variety. After liming with CC at a dose of 1.5 Hy, the barrier height in the varieties

studied changed, ranging from 27 to 652 units. In a number of varieties, the barrier height increased (Opochetskaya, Vladimirskaya and Gorkovskaya). This suggests that these plants have not yet crossed the critical dose of the ameliorant and the associated threshold concentration of the toxicant in the soil. In other varieties (Leningradskaya-89, Velikovskaya, Leningradka and Jak-24), the barrier height decreased. This probably indicates that for these varieties the dose of 1.5 Hy CC was higher than the critical dose and the associated threshold concentration of stable Sr in the soil, at which the protective mechanisms of the plant are not able to prevent an increase in the concentration of toxicant in the grain.

The difference in the uptake of Ca and Sr by plants was due to their different role for plants. In experimental and empirical studies, Kuke et al. (2016) confirmed that strontium accumulation in different organs of the plant differs depending on many factors, including not only soil and plant

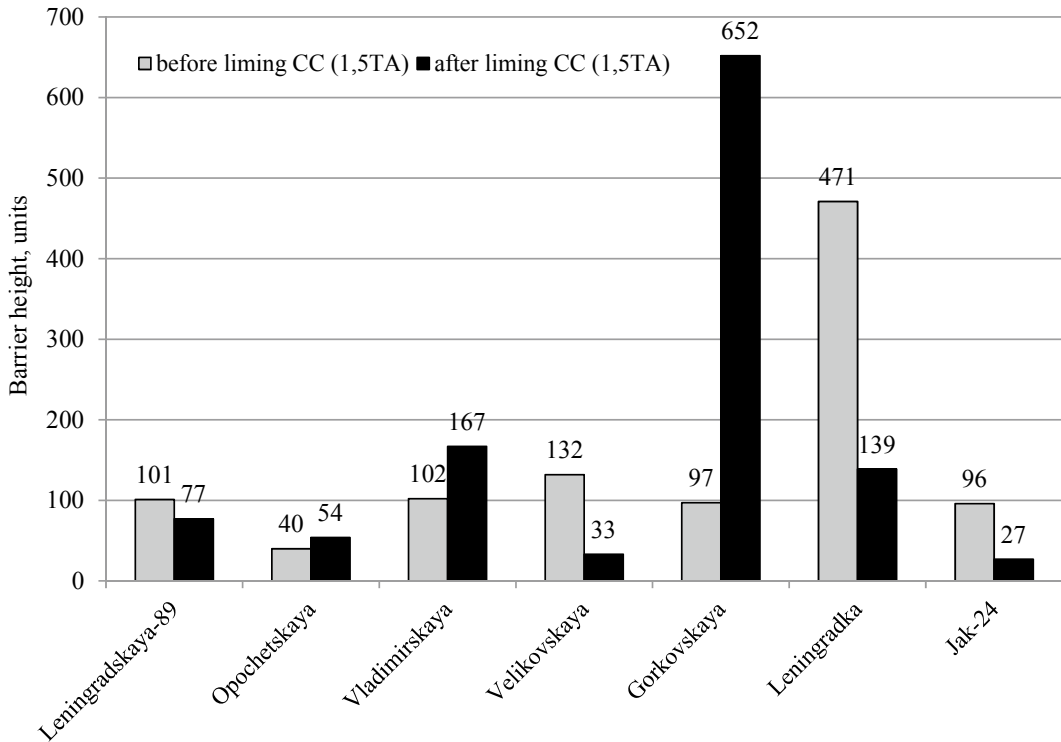


Fig. 20.3 Barrier height in different varieties of spring wheat

characteristics but also their concentrations in soil as well as the function of other elements in the soil. In the latter study, the highest correlation between Sr and Ca was observed in the root of cabbage and spinach. Zhang et al. (2020) found that high concentrations of Sr did not inversely affect the photosynthetic capacity of Chinese cabbage, but inhibited the growth of plants as strontium affected the absorption of calcium.

The physiological function of Ca in plants is associated with photosynthesis (Thor et al. 2020), as it is a part of the cell nucleus. Plants use a lot of calcium to neutralise acids in their cells as salts of pectic acid, carbonate, sulfate, oxalate. Calcium is involved in the movement of carbohydrates, regulates the acid–base balance in plants (Nebolsin and Nebolsina 2005) and helps plants adapt to biotic and abiotic stresses (Yoshioka and Moeder 2020). The physiological role of Sr in plants has not been studied extensively and there are many controversial or inconsistent data. Byhun et al. (1980) report that

the amylase in which calcium is replaced by strontium had retained its activity but differed in terms of some physical properties. Conversely, Walsh (1945) believes that strontium carbonate can replace calcium carbonate only to neutralise the acidic environment but cannot replace it biochemically. Summarising the data published on the availability of strontium to plants, Burger and Lichtscheidl-Schultz (2018) suggested that the form of the anion of strontium salts influences its absorption by plants.

In our study, the content of Sr in barley grain was lower than in straw in all treatments because the reproductive phase begins relatively late and the generative organs are less sensitive to excess pollutants than the vegetative organs (Austenfeld 1979). The results of this study showed that, in the soil–grain system, when chalk is used at a dose of 1.6 TA, calcium passes into the grain more intensively than strontium. In the precision experiment with a gradual increase in the dose (dose steps of 0.1 TA), we managed to identify

the “drop point” of the barrier height; that is, the concentration at which the protective mechanisms of the grain stop working and the toxicant immediately accumulates in large quantities in the grain.

20.4 Conclusion

1. No differences in the content of exchangeable Sr were observed between the grassland and forest soils. The humus fraction HA1 was the main strontium-fixing component in non-limed soil, retaining about 50% of the total Sr in the soil. A particularly high degree of Sr accumulation by plants was observed in soils with a low CEC and a lack of mobile calcium.
2. Our results showed that plants clearly distinguish between Ca and Sr during assimilation and transfer calcium into the cell, blocking the penetration of strontium. Ca was delivered to straw and grain and Sr was delivered to straw of barley by the barrier-free mechanism. By contrast, Sr was transported to the grain by the barrier mechanism. The plants studied manifested a function protecting them against the delivery of toxic elements into reproductive organs.
3. Many issues remain to be clarified regarding the mechanisms by which Sr accumulates in various parts of plants. In particular, the problems of strontium contamination are very relevant in the Russian Federation, since there are no regulatory acts defining the maximum allowable concentrations (MACs) for soil and plants for this element.
4. On agricultural soils using strontium-containing fertilisers and ameliorants, it is necessary to monitor the content of stable strontium in soils and plants. This requires comprehensive studies involving soil scientists, agronomists, physiologists and medical hygienists.
5. Finally, our results showed that if strontium was removed from the conversion chalk, it would become a highly effective ameliorant that is not inferior to traditional liming materials. On one hand, this could reduce the accumulation of dumps formed during the

processing of raw phosphates, and on the other hand, it could provide a highly efficient liming material without the toxic effect of strontium.

Acknowledgements The preparation of this chapter was partially supported by the Ministry of Education, Science and Technological Development of the Republic of Serbia, contract no. 451-03-68/2020-14.

References

- Adomaitis T, Staugaitis G, Mažvila J, Vaišvila Z, Arbačiauskas J, Lubyte J, Šumskis D, Švėgžda A (2013) Leaching of base cations as affected by a forty-year use of mineral fertilization. *Zemdirbyste-Agri* 100(2):119–126. <https://doi.org/10.13080/z-a.2013.100.015>. http://www.zemdirbyste-agriculture.lt/wp-content/uploads/2013/06/100_2_str15.pdf. Accessed 18 Mar 2021
- Aleksakhin RM, Korneev NM (2001) *Agricultural radioecology*, Moscow, p 243 (Алексахин Р.М., Корнеев Н.М. Сельскохозяйственная радиэкология, Москва, с. 243)
- Aleksandrova LN (1970) Soil humic substances: their formation, composition, properties, and value for pedogenesis and fertility. Leningrad, Agricultural Institute, pp 142–232 (Александрова Л.Н. Гуминовые вещества почвы: их образование, состав, свойства, значение для почвообразования и плодородия. Ленинград, Сельскохозяйственный институт, с.142: 232.)
- Annenkov BN, Yudinseva EV (2002) *Fundamentals of agricultural radiology*. Moscow, p 297 (Анненков Б. Н., Юдинцева Е.В. Основы сельскохозяйственной радиологии, Москва, с. 297.)
- Austenfeld FA (1979) Zur Phytotoxizität von Nickel- und Kobaltsalzen in Hydrokultur bei *Phaseolus vulgaris* L. *Z. Pflanzenernähr und Bodenkunde* Bd 142(6):769–777
- Bakina LG (1987) The effect of liming on the content, composition and properties of humus from clayey Soddy-Podzolic soils. Dissertation for the Candidate of Doctor of Sciences, Leningrad (Бакина Л.Г. Влияние известкования на содержание, состав и свойства гумуса глинистых дерново-подзолистых почв. Диссертация на звание кандидата сельскохозяйственных наук, Ленинград)
- Bakina LG (2012) Role of fractions of humic substances in soil-ecological processes. Doctoral thesis, Archives of Agrophysical Institute, St. Petersburg, Russia (Бакина Л.Г. Роль фракций гуминовых веществ в почвенно-экологических процессах. Докторская диссертация, Архив Агрофизического института, Санкт-Петербург, Россия)

- Bataille C, Crowley BE, Wooller MJ, Bowen GJ (2020) Advances in global bioavailable strontium isoscapes. *Palaeogeogr Palaeoclimatol Palaeoecol* 555:109849. <https://doi.org/10.1016/j.palaeo.2020.109849>
- Bélanger, Paré D, Hendershot WHCh (2008) Determining nutrient availability in forest soils. In: Carter MR, Gregorich EG (eds) *Soil sampling and methods of analysis*. Canadian Society of Soil Science. Taylor & Francis Group for CRC Press
- Burakova A, Bakšienė E (2021) Leaching losses of main nutrients by incorporating organic fertilisers into light texture soils Haplic Luvisol. *Environ Eng Res* 26 (4):200190. <https://doi.org/10.4491/eer.2020.190>
- Burger A, Lichtscheidl-Schultz I (2018) Strontium in the environment: review about reactions of plants towards stable and radioactive strontium isotopes. *Sci Total Environ* 653:1458–1512. <https://doi.org/10.1016/j.scitotenv.2018.10.312>
- Byhun V, Kraschenko G, Kouchnirenko L, Verkhovod L (1980) Strontium in the diet of corn. In: ‘Trace elements in the environment’ Kiev. Naukova Dumka, pp 35–38 (Быхун В., и др. Стронций в рационе кукурузы. В «Микроэлементы в окружающей среде» Киев. Наукова думка стр. 35–38)
- Carling GT, Fernandez DP, Rey KA, Hale CA, Goodman MM, Nelson ST (2020) Using strontium isotope to trace dust from a drying Great Salt lake to adjacent urban areas and mountain snowpack. *Environ Res Lett* 15:114035. <https://doi.org/10.1088/1748-9326/abbfc4>
- Chadwick OA, Derry LA, Bern CR, Vitousek PM (2009) Changing sources of strontium to soil and ecosystems across the Hawaiian Islands. *Chem Geol* 267:64–76. <https://doi.org/10.1016/j.chemgeo.2009.01.009>
- Dinu C, Vasile GG, Buleandra M et al (2020) Translocation and accumulation of heavy metals in *Ocimum basilicum* L. plants grown in a mining-contaminated soil. *J Soils Sediments* 20:2141–2154. <https://doi.org/10.1007/s11368-019-02550-w>
- Dresler S, Wójcicki-Kosior M, Sowa I, Strzemski M, Sawicki J, Kováčik J, Blicharski T (2018) Effect of long-term strontium exposure on the content of phytoestrogens and allantoin in soybean. *Int J Mol Sci* 4;19(12):3864. <https://doi.org/10.3390/ijms19123864>
- Dubchak S (2018) Distribution of strontium in soil: interception, weathering, speciation, and translocation to plants 2018. In: Gupta DK, Walther C (eds) *Behaviour of strontium in plants and the environment*. Springer International Publishing AG. https://doi.org/10.1007/978-3-319-66574-0_3
- Ermokhin YuI, Ivanov AF (1990) On the accumulation of strontium in soils and plants when using mineral fertilizers and phosphogypsum in Western Siberia. In: Proceedings conference ‘microelements in biology and their application in agriculture and medicine’, Samarkand, p 152 (Ермохин Ю.И., Иванов А.Ф. О накоплении стронция в почвах и растениях при применении минеральных удобрений и фосфогипса в Западной Сибири. Тезисы II Всесоюзной конференции «Микроэлементы в биологии и их применение в сельском хозяйстве и медицине», Самарканд, с. 152.)
- Fedorokova EP, Pakhnenko EP, Sanzharova NI (2012) Chemical forms of radioactive strontium interaction with organic matter of different soil types. *Moscow Univ Soil Sci Bull* 67(3):133–136. Allerton Press, Inc. (Федоркова Е.П., и др. Химические формы взаимодействия радиоактивного стронция с органическими веществами различных типов почв. Вестник Московского университета по почвоведению 67 (3): 133–136.)
- Fernández-Sanjurjo MJ, Alvarez-Rodríguez E, Núñez-Delgado A, Fernández-Marcos ML, Romar-Gasalla A (2014) Nitrogen, phosphorus, potassium, calcium and magnesium release from two compressed fertilizers: column experiments. *Solid Earth* 5:1351–1360. <https://doi.org/10.5194/se-5-1351-2014>
- Frei R, Frei KM, Jessen S (2020) Shallow retardation of the strontium isotope signal of agricultural liming—implications for isoscapes used in provenance studies. *Sci Total Environ* 706:135710. <https://doi.org/10.1016/J.SCITOTENV.2019.135710>
- Fukushima Daiichi accident (2015) Technical volume 4/5. Radiological consequences. International Atomic Energy Agency, Vienna, p 262
- Gorbunov NI, Yudina LN, Zarubina TG (1981) Rate of acid neutralization by lime. *Pochvovedenie* 1:150–156 (Горбунов Н.И. Скорость нейтрализации кислот известью. Почвоведение)
- GOST 26213-91 Soils. Methods of determination of soil organic matter (Почвы. Методы определения органического вещества). <http://docs.cntd.ru/document/1200023481>
- Guillen J, Baeza A, Corbacho J, Munoz-Munoz J (2015) Migration of ¹³⁷Cs, ⁹⁰Sr, and ²³⁹⁺²⁴⁰Pu in Mediterranean forests: influence of bioavailability and association with organic acids in soil. *J Environ Radioact* 144:96–102. <https://doi.org/10.1016/j.jenvrad.2015.03.011>
- Gupta D, Deb U, Walther C, Chatterjee S (2018a) Strontium in the ecosystem: transfer in plants via root system. In: Gupta D, Walther C (eds) *Behaviour of strontium in plants and the environment*. Springer, Switzerland, Cham, pp 1–18
- Gupta DK, Schulz W, Steinhäuser G, Walther C (2018b) Radiostromium transport in plants and phytoremediation. *Environ Sci Pollut Res* 25:29996–30008. <https://doi.org/10.1007/s11356-018-3088-6>
- Hamilton EJ, Minski MJ (1972) Abundance of the chemical elements in man’s diet and possible relations with environmental factors. *Sci Total Environ* 1:375–394. [https://doi.org/10.1016/0048-9697\(73\)90025-9](https://doi.org/10.1016/0048-9697(73)90025-9)
- Hanaka A, Dresler S et al (2019) The impact of long-term and short-term strontium treatment on metabolites and minerals in *Glycine max*. *Molecules* 24(21):3825. <https://doi.org/10.3390/molecules24213825>

- Handley R, Overstreet R (1962) Uptake of strontium by roots of *Zea mays*. *Plant Physiol* 38:180–184. <https://www.atsdr.cdc.gov/toxprofiles/tp159-c6.pdf>
- Höllriegel V, München HZ (2011) Strontium in the environment and possible human health effects. In: Nriagu JO (ed) *Encyclopaedia of environmental health*. Elsevier, pp 797–802. <https://doi.org/10.1016/B978-0-444-52272-6.00638-3>
- Ilyin VB (1991) Heavy metals in the soil-plant system. Novosibirsk, Science, Siberian Branch, p 150 (Тяжёлые металлы в системе почва-растение. Наука. Сибирское отделение)
- Iserman K (1981) Uptake of stable strontium by plants and effects on plant growth. In: Skornaya SC (ed) *Handbook of stable strontium*. Plenum Press, New York
- Ivanov VP (1973) Plant secretions and their importance in the life of phytocenoses. Moscow, Nauka 295 pp (Иванов В.П. Растительные выделения и их значение в жизни фитоценозов. Москва, Наука, с. 295).
- Jeske A (2013) Mobility and distribution of barium and strontium in profiles of podzolic soils. *Soil Sci Ann* 64 (1):2–7. Verista. <https://doi.org/10.2478/ssa-2013-0001>
- Kabata-Pendias A (2011) *Trace elements in soils and plants*, 4 edn. CRC Press, Taylor & Francis Group, Boca Raton, London, New York, 548 pp
- Kabata-Pendias A, Mukherjee A (2007) *Trace elements from soil to human*. Springer, Berlin, p 550
- Kabata-Pendias A, Pendias H (1979) *Trace elements in the biological environment*. *Wid. Geol.*, Warsaw, 300 pp
- Kabrick JM, Goyné KW, Fan Zh, Mainert D (2011) Landscape determinants of exchangeable calcium and magnesium in Ozrak Highland forest soils. *Soil Sci Soc Am J* 75(1):164–180. <https://doi.org/10.2136/sssaj2009.0382>
- Karpova EA, Gomonova NF (2006) Strontium in agrocenosis on sod-podzolic soil under conditions of long-term action and aftereffect of fertilizers. *Soil Sci* 7:870–875 (Стронций в агроценозе на дерново-подзолистой почве в условиях длительного действия и последствия удобрения. Почвоведение)
- Karpova EA, Karpova EA, Potatueva YuA (2004) Consequences of the use of various forms of phosphate fertilizers: strontium in the system of sod-podzolic soil—plants. *Agrochemistry* 1:91–96 (Последствия применения различных форм фосфорных удобрений: стронций в системе дерново-подзолистая почва – растения. Агрохимия)
- Kashparov V, Lundin S, Zvarych S, Yoshchenko V, Levchuk S, Khomutinin Y, Maloshtan IM, Protsak V (2003) Territory contamination with the radionuclides representing the fuel component of Chernobyl fallout. *Sci Total Environ* 317:105–119. [https://doi.org/10.1016/S0048-9697\(03\)00336-X](https://doi.org/10.1016/S0048-9697(03)00336-X)
- Kashparov VA, Lazarev NM, Polischuk SV (2005) Problems of agricultural radiology in Ukraine at the present stage. *Agroecol J* 3:31–41 (ВА Кашпаров, НМ Лазарев, СВ Полищук; Проблемы сельскохозяйственной радиологии в Украине на современном этапе. Агроэкологический журнал, 31–41)
- Kazachonok N (2017) Assessment of entry of ^{90}Sr into plants in case of a heterogeneous radiation contamination of ecosystems. In: Gupta D, Walther C (eds) *Behaviour of strontium in plants and the environment*. Springer, Cham, Switzerland, pp 45–60
- Kopáček J, Kaňa J, Bičárová S, Fernandez JJ, Hejzlar J, Kahounová M, Norton SA, Stuchlík E (2017) Climate change increasing calcium and magnesium leaching from granitic alpine catchment. *Environ Sci Technol* 51(1):159–166. <https://doi.org/10.1021/acs.est.6b03575>
- Korneeva NV (1970) The influence of species characteristics of spring wheat on the transition of strontium-90 from soil to plants. *Reports of the All-Union Academy of Agricultural Sciences* 1:5–7 (Влияние видовых особенностей яровой пшеницы на переход стронция-90 из почвы в растения. Докл. ВАСХНИЛ)
- Kowalski VV, Andrianova GA (1970) Trace elements in the soils of the USSR. Moscow, Nauka, p 180 (Ковальски ВВ, Андрианова ГА. Микроэлементы в почвах СССР)
- Kowalski VV, Blokhin RI, Zazorina EF, Nikitina II (1964) The biogeochemical strontium province. In: *The proceedings of the meeting on the geochemistry of hypergenesis*, Minsk pp 84–93 (Ковальский В.В., и др. Биогеохимическая стронциевая провинция. Минск с. 84–93)
- Kuke D, Shujuan L, Yingxue H, Dong Y, Fengshou Z, Shuifeng W, Jinghua G, Wei Z, Xin W, Xiaoyan J (2016) Simulating the transfer of strontium-90 from soil to leafy vegetables by using strontium-88. *Water Air Soil Pollut* 227(11):414. <https://doi.org/10.1007/s11270-016-3098-2>
- Labunska I, Levchuk S, Kashparov V, Holiaka D, Yoschenko L, Santillo D, Johnston P (2021) Current radiological situation in areas of Ukraine contaminated by the Chernobyl accident: Part 2. Strontium-90 transfer to culinary grains and forest woods from soils of Ivankiv district. *Environ Int* 146:106282. <https://doi.org/10.1016/j.envint.2020.106282>
- Lavrishchev AV (1997) The effect of conversion chalks on the intake of calcium and strontium in rape plants. In: *The abstracts of the international student conference 'Crisis of soil resources: causes and effects'*. St. Petersburg, pp 82–83 (Лаврищев А. Влияние конверсионного мела на поступление кальция и стронция в растения. Тезисы докладов международной студенческой конференции «Кризис почвенных ресурсов: причины и следствия». Санкт-Петербург)
- Lavrishchev AV (1999) The dynamics of the content of calcium and strontium compounds available for plants when using conversion chalk for liming acidic soils. In: *XXI century—youth, education, ecology, noosphere*, pp 65–66 (Динамика содержания доступных для растений соединений кальция и стронция при

- использовании конверсионного мела для известкования кислых почв)
- Lavrishchev AV (2000) Calcium and strontium in the soil-plant system when liming soils with conversion chalk (case study, Acron Novgorod). Doctoral thesis, St. Petersburg, 123 pp (А. Лаврищев. Кальций и стронций в системе почва-растение при известковании почв конверсионным мелом. Докторская диссертация)
- Lavrishchev A, Litvinovich A (2019) Stable strontium in aroecosystems. St. Petersburg, Lan, p 192. ISBN 978-5-8114-3926-3 (Лаврищев А., Литвинович А. Стабильный стронций в агроэкосистемах, СПб., Лань)
- Lavrishchev A, Litvinovich A, Bure V, Pavlova O, Saljnikov E (2018) Strontium dynamics in soil and assimilation by plants during dissolution of conversion chalk. *Biol Commun* 63(3):163–173 <https://doi.org/10.21638/spbu03.2018.302>
- Lazarevich NV, Chernukha GA (2007) Behavior of technogenic radionuclides in soil-plant system. Gorki, BGSKhA, 43 pp (Лазаревич Н.В., Чернуха Г.А. Поведение техногенных радионуклидов в системе почва-растение. Горки, БГСХА, стр.43.43)
- Lin Q, Qin X, Li F-M, Siddique KHM, Brandl H, Xu J (2015) Uptake and distribution of stable strontium in 26 cultivars of three crop species: oats, wheat, and barley for their potential use in phytoremediation. *Int J Phytorem* 17(3):264–271. <https://doi.org/10.1080/15226514.2014.898016>
- Litvinovich AV (1985) Changes in composition and properties of sod-podzolic soils and their fine-dispersed fractions after drying and in long-term agricultural use. Doctoral thesis. Leningrad (Литвинович А.В. Изменение состава и свойств дерново-подзолистых глееватых почв и их тонкодисперсных фракций при осушении и длительном сельскохозяйственном использовании)
- Litvinovich AV, Nebolsina ZP (2012) Duration of action of lime and liming efficiency. *Agrochemistry* 10:79–94 (Литвинович А.В., Небольсина З.П. Продолжительность действия мелиорантов в почвах и эффективность известкования. *Агрохимия*, 10:79–94)
- Litvinovich AV, Pavlova OYu (1999) Content and distribution pattern of total and acid-soluble forms of compounds of heavy metals in the profile of gray-earth-oasis soils in the zone of the chemical plant. *Agrochemistry* 8:68–78 (Литвинович А.В., Павлова Ю.О. Содержание и особенности распределения валовых и кислорастворимых форм соединений тяжёлых металлов в профиле серозёмно-оазисных почв в зоне действия химического завода. *Агрохимия*)
- Litvinovich AV, Pavlova OYu, Lavrishchev AV (1998) Effect of various doses of conversion chalk on pass of Sr into plants. In: Humus and soil formation, St. Petersburg, Pushkin, pp 154–159 (Литвинович А.В., Павлова О.Ю., Лаврищев А.В. Влияние различных доз конверсионного мела на переход Sr в растения)
- Litvinovich AV, Pavlova OYu, Lavrishchev AV (1999a) Leaching of calcium and strontium from soil limed with conversion chalk. *Agrochemistry* 9:64–67 (Литвинович А.В., Павлова О.Ю., Лаврищев А.В. О вымывании кальция и стронция из почвы, произвесткованной конверсионным мелом. *Агрохимия* 9:64–67)
- Litvinovich AV, Pavlova OYu, Lavrishchev AV (1999b) Accumulation of calcium and strontium by plants of various biological families grown on soils with different absorption capacities after reclamation by conversion chalk. In: Field experiments—for sustainable land use. Proceedings of the third international colloquium. International Organization for the Mechanization of Field Experiments and Research (IAMFE). Agrophysical Research Institute, St. Petersburg, pp 153–154 (Накопление кальция и стронция растениями различных биологических семейств, выращенных на почвах с различной ёмкостью поглощения после мелиорации конверсионным мелом)
- Litvinovich AV, Drichko OYu, Pavlova OYu (2000) Evaluation of the parameters of the function of calcium and strontium retention by sod-podzolic sandy loam soil during reclamation by conversion chalk (model experiments). In: Materials of the international scientific-practical conference—modern problems of experimental work, pp 204–210 (Литвинович А.В. Дричко О.Ю., Павлова О.Ю. Оценка параметров функции удержания кальция и стронция дерново-подзолистой супесчаной почвой при мелиорации конверсионным мелом)
- Litvinovich AV, Pavlova OYu, Lavrishchev AV, Bikyukov VA (2001) Decomposition of conversion chalk in sod-podzolic soil due to the threat of contamination with stable strontium. *Agrochemistry* 11:64–68 (Литвинович А.В., Павлова О.Ю., Лаврищев А.В., Бикюков В.А. Разложение конверсионного мела в дерново-подзолистой почве в связи с угрозой её загрязнения стабильным стронцием. *Агрохимия*)
- Litvinovich AV, Pavlova OYu, Lavrishchev AV (2002) Finding ways to use conversion chalk safely. In: Humus and soil formation. St. Petersburg, pp 112–125 (Литвинович А.В., Павлова О.Ю., Лаврищев А.В. Поиск путей безопасного использования конверсионного мела)
- Litvinovich AV, Pavlova OYu, Lavrishchev AV, Vitkovskaya SE (2005) Ecological aspects of liming of soils with conversion chalk. *Plodorodie* 1:23–26 (Литвинович А.В., Павлова О.Ю., Лаврищев А.В., Витковская С.Е. Экологические аспекты известкования почв конверсионным мелом. *Плородордие*)
- Litvinovich AV, Pavlova OYu, Yuzmukhametov DN, Lavrishchev AV (2008) The migration capacity of stable strontium in soddy-podzolic soils of the Russian northwest (data of simulation experiments). *Eurasian Soil Sci* 41(5):502–508. <https://doi.org/10.1134/S1064229308050050>

- Litvinovich AV, Nebolsina ZP, Vitkovskaja SE, Yakovleva LV (2011) Effect of long-term use of phosphate fertilizers and ameliorants on the accumulation in soils and plants of stable strontium. *Agrohimiya*, 11:35–41 (Литвинович А.В., Небольсина З.П., Витковская С.Е., Яковлева Л.В. Влияние длительного применения фосфорных удобрений и мелиорантов на накопление в почвах и растениях стабильного стронция. *Агрохимия* 11:35–41)
- Litvinovich AV, Lavrishchev AV, Pavlova OYu (2013) The behavior of Ca and Sr in the soil-plant system from liming with a strontium-containing ameliorant. In: *Proceedings the 1st international Congress on Soil Science, XIII National Congress in Soil Science: "Soil-Water-Plant"* 23–26, September, Belgrade, Serbia, pp 17–34. http://data.sfb.bg.ac.rs/sftp/olivera.kosanin/book_of_proceedings.pdf
- Litvinovich AV, Pavlova OYu, Lavrishchev AV, Bure VM, Kovleva AO (2016) Reclamation properties, fertilizer value and dissolution rate in soils of various sizes of dolomite screenings used for road construction. *Agrochemistry* 2:31–41 (Литвинович А.В., Павлова О.Ю., Лаврищев А.В., Буре В.М., Ковлева А.О. Мелиоративные свойства, удобрительная ценность и скорость растворения в почвах различных по размеру фракций отсева доломита, используемого для дорожного строительства. *Агрохимия*)
- Litvinovich AV, Lavrishchev AV, Bure V, Pavlova O, Kovleva A, Salnikov E (2018) Influence of limestone and dolomite on the duration of liming effect and Ca losses in *Umbric Albelvisols Abruptic*. *Agrochimica-Pisa* 62(2):143–155. <https://doi.org/10.12871/00021857201824>
- Lykov AM (1986) The influence of permanent crops, crop rotation and fertilizers on the fertility of light loamy sod-podzolic soil. *Bull Timiryazev Agri Acad* 2:2–13 (Лыков А.М. Влияние бессменных культур, севооборота и удобрений на плодородие легкосуглинистой дерново-подзолистой почвы)
- Lykov AM, Prudnikova AG, Prudnikov AD (2006) To the problem of ecologization of tillage in modern farming systems. *Plodorodie* 6:1–5 (Лыков А.М., Прудникова А.Г., Прудников А.Д. К проблеме экологизации обработки почвы в современных системах земледелия. *Плодородие*)
- Makovsky RD, Prudnikov AD, Dragunov OG (2008) Migration of strontium added with ameliorant. *Agrochem Bull* 3:10–12 (Маковский Р.Д., Прудников А.Д., Драгунов О.Г. Миграция стронция, внесенного с мелиорантами. *Агрохимический вестник*)
- Marakushin AV, Fyodorov EA (1977) Sizes of strontium-90 accumulation by field crops during long-term cultivation in crop rotation. *Agrochemistry* 9:102–107 (Маракушин А.В., Федоров Е.А. Величина накопления стронция-90 полевыми культурами при многолетнем выращивании в севообороте *Агрохимия* 9:102)
- Mengel K, Kirkby EA (1987) *Principles of plant nutrition*. International Potash Institute, Bern (Switzerland), pp 461–474
- Mineev VG (1989) Ecological problems of agricultural chemistry. *Agro-Indus Complex Russia* 4:37–39 (Минеев В.Г. Экологические проблемы агрохимии. *Агропромышленный комплекс России*, 4: 37–39)
- Minkina TM, Burachevskaya MV, Chaplygin VA, Bakoev SYu, Antonenko EM, Belogorskaya SS (2011) The accumulation of heavy metals in the soil-plant system under pollution. *Sci J Russian Res Inst Ameliorat* 4 (Минкина Т.М. и др. Накопление тяжелых металлов в системе почва-растение в условиях загрязнения)
- Morel JL, Mench M, Guckert A (1986) Measurement of Pb²⁺, Cu²⁺ and Cd²⁺ binding with mucilage exudates from maize (*Zea mays* L.) roots. *Biol Fertil Soils* 2:29–34. <https://doi.org/10.1007/BF00638958>
- Moyen C, Roblin G (2010) Uptake and translocation of strontium in hydroponically grown maize plants, and subsequent effects on tissue ion content, growth and chlorophyll a/b ratio: comparison with Ca effects. *Environ Exp Bot* 68:247–257. <https://doi.org/10.1016/j.envexpbot.2009.12.004>
- Muravyov AG, Karryev BB, Lyandzberg AR (2000) Assessment of soil ecological state. St. Petersburg, Krismos Publ., 160 pp (Муравьев А.Г. Оценка экологического состояния почвы)
- Murvang MB, Hillersøy MH, Heim M, Bleken MA, Gjengedal E (2016) Uptake of macro nutrients, barium, and strontium by vegetation from mineral soils on carbonate and pyroxenite bedrock at the Lillebukt Alkaline Complex on Stjernøy, Northern Norway. *J Plant Nutr Soil Sci* 179(6). <https://doi.org/10.1002/jpln.201600328>
- Nebolsin AN, Nebolsina ZP (1997) Change in some properties of the soil absorbing complex of sod-podzolic light loamy soil under the influence of liming. *Agrochemistry* 10:5–11 (Небольсин А.Н., Небольсина З.П. Изменение некоторых свойств почвенного поглощающего комплекса дерново-подзолистой легкосуглинистой почвы под влиянием известкования. *Агрохимия*)
- Nebolsin AN, Nebolsina ZP (2005) *Theoretical foundations of liming*. St. Petersburg, 252 pp (Небольсин А.Н., Небольсина З.П. Теоретические основы известкования. Санкт-Петербург, 252 с.)
- Nedobukh and Semenishchev (2020) Strontium: source, occurrence, properties, and detection. In: Pathak P, Gupta DJ (eds) *Strontium contamination in the environment*. Springer
- Oufqir S, Bloom PR, Torner BM (2014) The retention of calcium, barium, and strontium ions by a mollisol humic acid: spectroscopic investigation. In: *Geophysical research abstracts*, vol 16, EGU201 (4-16985), EGU General Assembly. <https://meetingorganizer.copernicus.org/EGU2014/EGU2014-16985.pdf>. Accessed 18 Mar 2021

- Pathak P, Gupta DK (2020) Strontium contamination in the environment. Springer. ISBN: 978-3-030-15313-7
- Paulenová A, Rajec P, Žemberyová M, Sasköiová G, Višský V (2000) Strontium and calcium complexation by humic acid. *J Radioanal Nucl Chem* 246 (3):623–628. <https://doi.org/10.1023/A:1006727409230>
- Pavlotskaya FI (1974) Migration of radioactive products of global fallout in soils. Moscow, Atomizdat, 215 pp (Павловская Ф.И. Миграция радиоактивных продуктов глобальных выпадений в почвах)
- Pavlova O, Litvinovich A, Lavrishchev A, Bure V, Saljnikov E (2019) Eluvial losses of Ca from Umbric Albeluvisols Abruptic produced by different doses of lime: column experiment. *Zemljište I Biljka* 68(2):1–12. <https://doi.org/10.5937/ZemBilj1901001P>. http://www.sdpz.rs/images/casopis/2019/zib_68_1_47_pavlova.pdfv. Accessed 18 Mar 2021
- Pinkas L, Smith L (1966) Physiological bases of differential strontium accumulation in two barley genotypes. *Plant Physiol* 41(9):1471–1475. <http://www.plantphysiol.org/content/plantphysiol/41/9/1471.full.pdf>
- Plotnikova TA, Orlova NE (1984) Application of the modified Ponomareva-Plotnikova procedure for the determination of the composition, nature and properties of soil humus. *Pochvovedenie* 8:120 (Плотникова Т.А., Орлова Н.Е. Применение модифицированной методики Пономаревой-Плотниковой для определения состава, природы и свойств почвенного гумуса. Почвоведение)
- Ponomareva VV, Plotnikova TA (1980) Humus and pedogenesis: methods and results of study. Leningrad. (Пonomareva В.В., Плотникова Т.А. Гумус и почвообразование: методы и результаты изучения. Ленинград.)
- Popov VV, Soloviev GA (1991) Monitoring of soil contamination with heavy metals. *Chimizatsia sel'skogo hozyaistva* 11:80–82 (Попов В.В., Соловьев Г. А. Мониторинг загрязнения почв тяжелыми металлами. Химизация Сельского Хозяйства)
- Pousada-Ferradás Y, Seoane-Labandeira S, Mora-Gutiérrez A, Núñez-Delgado A (2012) Risk of water pollution due to ash-sludge mixtures: column trials. *Int J Environ Sci Technol* 9:1–29. <https://doi.org/10.1007/s13762-011-0014-6>
- Rafferty P, Shiao S-Y, Binz CM, Meyer RE (1981) Adsorption of Sr(II) on clay minerals: effects of salt concentration, loading, and pH. *J Inorg Nuclear Chem* 43(4):797–805. [https://doi.org/10.1016/0022-1902\(81\)80224-2](https://doi.org/10.1016/0022-1902(81)80224-2)
- Rowley MC, Grand S, Verrecchia EP (2018) Calcium-mediated stabilization of soil organic carbon. *Biogeochemistry* 137(1–2):27–49. <https://doi.org/10.1007/s10533-017-0410-1>
- Sahoo SK, Kavasi N, Sorimachi A, Arae H, Tokonami Sh, Mietelski JW, Lokas E, Yoshida S (2016) Strontium-90 activity concentration in soil samples from the exclusion zone of the Fukushima daiichi nuclear power plant. *Sci Rep* 6(23925). <https://www.nature.com/articles/srep23925>
- Sanzharova NI (2005) Role of chemistry in the rehabilitation of agricultural lands exposed to radioactive contamination. *Russian Chem J* 3:22–34. (PDF) Distribution of strontium in soil: interception, weathering, speciation, and translocation to plants. https://doi.org/10.1007/978-3-319-66574-0_3. <https://www.researchgate.net/publication/320692180>. Accessed 18 Mar 2021
- Sarret G, Saumitow-Laprade P, Bert V, Proax O, Hazemam JL, Traverse AS, Marcus MA, Manceau A (2002) Forms of zinc accumulated in the hyper accumulator *Arabidopsis halleri*. *Plant Physiol* 130:1815–1826. <https://doi.org/10.1104/pp.007799>
- Sasmaz M, Uslu Senel G, Obek E (2020) Strontium accumulation by the terrestrial and aquatic plants affected by mining and municipal wastewaters (Elazig, Turkey). *Environ Geochem Health*. <https://doi.org/10.1007/s10653-020-00629-9>
- Sekine Yu, Motokawa R, Kozai N, Ohnuki T, Matsumura D, Tsuji T, Kawasaki R, Akiyoshi K (2017) Calcium-deficient hydroxyapatite as a potential sorbent for strontium. *Sci Rep* 7:2064. <https://doi.org/10.1038/s41598-017-02269-z>
- Sheudzhen AKh (2003) Biogeochemistry. Майкоп: GURIPP “Adygea”, 1028 pp (Шеуджен А.Х. Биогеохимия. Майкоп: ГУРИПП «Адыгея», 2003, стр 1028)
- Shilnikov IA, Akanova NI, Fedotova LS (2004) Determination of calcium losses from arable soils in the field experiments. *Plodородие* 2:21–23 (Шильников И.А., Аканова Н.И., Федотова Л.С. Определение потерь кальция с пахотных почв в полевых опытах. Плодородие 2: 21–23)
- Solecki J, Chibowski S (2002) Studies on Horizontal and vertical migration of ⁹⁰Sr in soil systems. *Polish J Environ Stud* 11(2):157–163
- Sowa I, Wójciak-Kosior M, Strzemski M, Dresler S, Szwerc W, Blicharski T, Szymczak G, Kocjan R (2014) Biofortification of soy (*Glycine max* (L.) Merr.) with strontium ions. *J Agric Food Chem* 62 (23):5248–5252. <https://doi.org/10.1021/jf501257r>
- Stekolnikov KE, Kotov VV, Sokolova SA, Tsyplakov SE (2011) Modeling the process of interaction of heavy metal cations with humic acids. In: Collection of papers: innovative fundamental and applied research in the field of chemistry in agricultural production, pp 56–62 (Стекольников К.Е. и др. Моделирование процесса взаимодействия катионов тяжелых металлов с гумусовыми кислотами)
- Sudhakaran M, Ramamoorthy D, Savitha V, Balamurugan S (2018) Assessment of trace elements and its influence on physico-chemical and biological properties in coastal agroecosystem soil, Puducherry region. *Geol Ecol Landscapes* 2(3):169–176. <https://doi.org/10.1080/24749508.2018.1452475>
- Sysoeva A, Konopleva I, Sanzharova N (2005) Bioavailability of radiostrontium in soil: experimental study

- and modelling. *J Environ Radioact* 81:269–282. <https://doi.org/10.1016/j.jenvrad.2004.01.040>
- Thomsen E, Andreasson R (2019) Agricultural lime disturbs natural strontium isotope variations: implications for provenance and migration studies. *Sci Adv* 5(3):eaav8083. <https://doi.org/10.1126/sciadv.aav8083>
- Thor K, Jiang S, Michard E et al (2020) The calcium-permeable channel OSCA1.3 regulates plant stomatal immunity. *Nature* 585:569–573. <https://doi.org/10.1038/s41586-020-2702-1>
- Titov AF, Talanova VV, Kaznina NM, Laidinen GF (2007) Plant resistance to heavy metals. Petrozavodsk, Russia, p 172 (Титов А.Ф. и др. Устойчивость растений к тяжелым металлам. Петрозаводск, Россия, с. 172)
- Toikka MA, Perevozchikova EM, Levkina TI (1981) Strontium in soils and cities of Karelia. In: Trace elements in the environment. Kiev, Naukova Dumka Publisher, pp 28–30 (Тойкка М.А. и др. Стронций в почвах и городах Карелии. Микроэлементы в окружающей среде)
- Tyurin IV (1937) Soil organic matter. Sel'hozgiz, Moscow-Leningrad, p 270 (Тюрин И.В. Органическое вещество почвы М.-Л. Сельхозгиз)
- Tyuryukanova EB (1976) Ecology of strontium-90 in soils. Moscow, Atomizdat, 128 pp (Тюрюканова Е.В. Экология стронция-90 в почвах)
- Van Bergeijk KE, Noordijk H, Lembrechts J, Frissel MJ (1992) Influence of pH, soil type and soil organic matter content on soil-to-plant transfer of radiocesium and strontium as analysed by a nonparametric method. *J Environ Radioact* 15(3):265–276. [https://doi.org/10.1016/0265-931X\(92\)90062-X](https://doi.org/10.1016/0265-931X(92)90062-X)
- Vidal M, Camps M, Grebenshikova N et al (2001) Soil- and plant-based countermeasures to reduce ^{137}Cs and ^{90}Sr uptake by grasses in natural meadows. *J Environ Radioact* 56:139–156. [https://doi.org/10.1016/S0265-931X\(01\)00051-0](https://doi.org/10.1016/S0265-931X(01)00051-0)
- Vinogradov AP (1952) Patterns of the distribution of trace elements. In: Trace elements in the life of plants and animals. Moscow (Виноградов А.П. Закономерности распределения микроэлементов)
- Walsh T (1945) The effect on plant growth of substituted strontium for calcium in acid soils. *Proc Roy Irish Acad B* 50:287
- WRB (2007) IUSS Working Group WRB. World Reference Base for Soil Resources 2006, first update 2007. World Soil Resources Reports No. 103. FAO, Rome
- Yaseen W Sajjad B, Azam I, Ajaz H (2020) Effects of Heavy Metals on Plant Growth and Metal Accumulation in Moringa Plant. *Int Res J Sci Tech* 1(2):126–137. <https://irjst.com/wp-content/uploads/March2020-v1-i2/IRJST122008.pdf>. Accessed 18 Mar 2021
- Yoshioka K, Moeder W (2020) Calcium channel in plants helps shut the door on intruders. *Nature* 585:507–508. <https://doi.org/10.1038/d41586-020-02504-0>
- Youngil C, Driscoll CT, Johnson CE, Siccama TG (2009) Chemical changes in soil and soil solution after calcium silicate addition to a Northern Hardwood Forest. *Biogeochemistry* 100(1–3):3–20. <https://doi.org/10.1007/s10533-009-9397-6>. <https://www.jstor.org/stable/40800606>
- Yudintseva EV, Gulyakin IV (1998) Agrochemistry of radioactive isotopes of caesium and strontium. Atomizdat, Moscow, p 415. (Юдинцева Е.В., Гулякин И.В. Агрохимия радиоактивных изотопов цезия и стронция. Атомиздат, Москва, стр.415.)
- Yudintseva EV, Mamontova LA (1979) Behavior of ^{90}Sr in soils upon application of phosphate, lime and peat. *Soil Sci* 12:51–61 (Юдинцева Е.В., Мамонтова Л.А. Поведение ^{90}Sr в почвах при внесении фосфатов, извести и торфа. Почвоведение)
- Yurenki IM (1849) On the ugliness of the inhabitants of the banks of the river Urov in Eastern Siberia. *Proc Imp Free Econ Soc* (Юренский И.М. Об уродливости жителей берегов речки Уров в Восточной Сибири)
- Zhang X, Wang W (2015) The decomposition of fine and coarse roots: global patterns and their controlling factors. *Sci Rep* 5:9440. <https://doi.org/10.1038/srep09940>
- Zhang W, Kang Z, Wang Q, Qiu N, Chen M, Zhou F (2020) The biological effects of strontium (^{88}Sr) on Chinese cabbage. *Plant Soil Environ* 66:149–154. <https://doi.org/10.17221/108/2020-PSE>
- Zubareva IF, Moskevich LP, Kovenya SV (1989) Strontium-90 removal from drained soil during water erosion. *Agrochemistry* 4:144–147 (Зубарева и др. Вынос стронция-90 из дренированной почвы в процессе водной эрозии. Агрохимия)



Concentration, Background Values and Limits of Potential Toxic Elements in Soils of Central Serbia

21

Vesna V. Mrvić, Elmira Saljnikov,
Biljana Sikirić, and Darko Jaramaz

Abstract

This paper presents the results of a large-scale investigation into the content and distribution of potentially toxic elements in the soil throughout Central Serbia, focusing on soil types and the background limits for the most important trace elements. Pseudo-total forms of arsenic, chromium, copper, cadmium, nickel, lead and zinc were determined in 5022 surface soil samples taken using a grid system (3.3 × 3.3 km) in agricultural soil and forest throughout Central Serbia (as part of the Republic of Serbia's national pedogeochemical research). It has been established that most of the studied territory is unpolluted. Ni, Cr and As have been found to be the largest contaminants (4.2%, 1.8%, 1.9% of samples, respectively, were above the remediation value) with predominant geochemical con-

tamination. The background limits of trace elements in the soils of Central Serbia, calculated by the [Median + 2MAD] method, had the lowest values, between 87 and 90%. With the other two methods, TIF and in particular [Mean + 2Sdev], more approximate values were obtained, commonly between 95 and 98%. The results show that it is necessary to revise the limit values of trace elements in the legislation of the Republic of Serbia, especially for Ni and Cr, which are mainly of natural origin. In areas with a heterogeneous geological composition and with different anthropogenic impacts, a greater number of background limits should be determined for pedochemical units or for homogeneous administrative units.

Keywords

Background limits · Potential toxic elements · Soil type · Pedogeochemical composition

V. V. Mrvić (✉) · E. Saljnikov · B. Sikirić ·
D. Jaramaz
Institute of Soil Science, Teodora Dradžera 17, 11000
Belgrade, Serbia

E. Saljnikov
Mitscherlich Academy for Soil Fertility (MITAK),
GmbH, Prof.-Mitscherlich-Allee 1, 14641
Paulinenaue, Germany

21.1 Introduction

Industrial development, the use of chemicals in agriculture and urbanisation has caused an increase in the content of heavy metals in the soil and other parts of the environmental ecosystem, which can have a harmful effect on crop quality and human and animal health. The content and

distribution of potential toxic elements (PTEs) in soils and the assessment of environmental risk have been studied in many countries (Kabata-Pendias and Pendias 2001; Adriano 2001; Dregulo and Bobylev 2021; Truchet et al. 2021; Qin et al. 2021). The excessive accumulation of chemical pollutants degrades the physical and biological characteristics of soil and adversely affects plant growth (Gupta and Sandallo 2011; Capparelli et al. 2020; Guo et al. 2020; Makuleke and Ngole-Jeme 2020). Moreover, they enter the food chain, causing serious diseases in animals and humans (Nagaijyoti et al. 2010; Yang et al. 2019; Rutigliano et al. 2019), and negatively affect the soil biome when accumulated in toxic concentrations (e.g. Khan et al. 2010; Zhen et al. 2019). Among the anthropogenic sources, the sources considered most polluting are mining and the combustion of fossil fuels, industrial by-products, traffic-generated PTE flows, power plants, domestic and urban waste disposal and the use of agrochemicals, organic fertilisers and plastic materials (e.g. Raheem et al. 2018; Jaramaz 2018; Saljnikov et al. 2019; Leed and Smithson 2019; Stewart 2020; Gruszecka-Kosowska et al. 2020; Prathumratana et al. 2020; Qaswar et al. 2020). Rapidly expanding urban and industrial areas (Khan et al. 2018; Huang et al. 2019a, b; Leed and Smithson 2019) and the operation of greenhouses (Wang et al. 2020; Sun et al. 2020) pose additional threats to soil quality due to the increased loads of PTEs, micro- and nano-plastics and urban waste.

Soil pollution is defined as chemical soil degradation associated with the presence of a chemical or substance which is out of place and/or presents at a higher than normal concentration and has adverse biological or toxic effects on any non-targeted organism. This may include pollution from local sources (such as landfills, spills and factory sites; the application of chemicals such as fertilisers, pesticides, ameliorants, etc.) and diffuse or air-borne pollution (atmospheric deposition). Soil contamination with trace elements is one of the most actively investigated areas since it jeopardises the proper functioning of the soil's productive and ecological functions. When assessing soil

contamination with trace elements due to anthropogenic activities, it is crucial to determine the natural background limits (Mrvić et al. 2014; Jaramaz 2018). Background limits (or geochemical limits) of potentially toxic elements in environmental geochemistry are often defined as the difference between the natural and anthropogenic concentration of an element, or as values of the level of action in environmental regulations—the concentrations above which further research is required or where remediation is required (Reimann and Caritat 2017). Background limits are also the basis for calculating individual indices offering a better qualitative interpretation of pollution risk, such as enrichment factors, risk factors and potential environmental risk (Qingjia et al. 2008; Hu et al. 2013; Čakmak et al. 2018; Saljnikov et al. 2019; Wang et al. 2021).

Due to anthropogenic activities, it is difficult to determine the natural background concentrations of trace elements in the soil. Therefore, various statistical methods are used to determine the possible limits of geochemical content. There are a large number of studies on background limits for different continents, countries or narrower areas. They use different statistical methods, the most important being the identification of interruptions on CDF graphics, the upper threshold in the box plot (Tukey's inner fence, TIF) and 98% (Reimann and Caritat 2017), TIF (International Organization for Standardization, ISO 2005, Annex B), median, geometric mean or geometric standard deviation method (Santos-Francés et al. 2017; Beygi and Jalali 2018), CDF charts and percentages (most commonly 95%) (e.g. Ander et al. 2013). Different methods produce different geochemical boundaries, and their choice depends on the purpose and established criteria. Previous studies have shown that the background limit of trace elements depends on the method applied, as well as on the parent material, soil type, soil weathering processes, content of organic matter and texture. Therefore, the background limit of trace elements should be determined locally.

This chapter presents data from large-scale, long-term investigations into soil quality

throughout Central Serbia with the aim of studying the content and distribution of potentially toxic elements (PTEs), focusing on their concentrations in various soil types. The study included the background limits determined for the most important PTEs in Central Serbia as a whole and in a small number of selected areas with a heterogeneous pedochemical composition. The study was part of the project “Studies on the influence of soil quality and irrigation water to efficient crop production and environmental protection” (2011–2019), including the main results of the prior study “Fertility control and determination of the content of harmful and hazardous elements in the soil of the Republic of Serbia” (1993–2007).

21.2 Sampling and Analytical Methods

Soil samples were taken throughout Central Serbia in a 3.3×3.3 km grid system covering agricultural landscapes and forests, in the period from 1993 to 2007. At each location, a composite soil sample was taken from a depth of 0–30 cm (Fig. 21.1). A total of 5022 soil samples were taken. Laboratory analyses included the determination of the concentration of potential pollutants from air-dry soil samples sieved through a mesh with a diameter of 2 mm. Pseudo total forms of chromium, copper, cadmium, nickel, lead and zinc were determined by HNO_3 and H_2O_2 digestion according to the following protocol: 2 g of soil sample were transferred into a 150 ml Erlenmeyer flask, then 20 ml of concentrated HNO_3 was added and a glass funnel put on the flask. The Erlenmeyer flask was placed on an electric stove heated to 150 °C and heated with gentle stirring for 2 h. It was left to cool for 5 min, then 3 ml of 30% H_2O_2 was added. The mixture was slightly heated to react with the peroxide, followed by gentle boiling for 15 min. Then, the mixture was cooled in an Erlenmeyer flask and transferred quantitatively into a normal 100 ml vessel, rinsing with deionised water. The solution was then filtered through Whatman No. 41 and stored in PVC bottles before an AAS

reading (GBC SensAA Dual, HG 260–060, Australia). Mercury and arsenic were determined after digestion with HNO_3 and H_2O_2 , and an AAS reading, using a hydride system. To ensure quality control, blank samples were used, and a referent soil sample was determined for all the elements studied (NCS ZC 73,005 soil, CNAC for Iron and Steel). The MERCK standards were used for the calibration of SensAA Dual.

21.3 Statistical Data Processing

The software SPSS version 16 was used for statistical analysis. The background limits were determined using the calculations described by Reimann et al. (2005): classical [$\text{Mean} \pm 2\text{Sd}$], [$\text{Median} \pm 2\text{MAD}$], box plot—Tukey’s upper inner fence (TIF). The values were based on percentages: 90, 95 and 98% of the data set that can also define threshold values were also obtained (Ander et al. 2013). For some regions, the geochemical limits using graph methods were also determined: box plot (Tukey 1977) and cumulative probability plot—CDF. The [$\text{Mean} \pm 2\text{Sd}$] (Sd represents standard deviation) is a classic method in which extreme values have a strong influence. Since geochemical data are asymmetrical, non-independent and do not have an identical distribution, the advantage is given to other methods that do not strongly build on statistical assumptions (Reimann et al. 2005). In the [$\text{Median} \pm 2\text{MAD}$] method, the median is defined for a sample $\times 1, \dots, x_n$ as the median (x_i), and the median absolute deviations ($\text{MAD} = \text{Median } i (|X_i - \text{Median } j (X_j)|)$). In the box plot method, the upper inner fence (Tukey’s Inner Fence, TIF) is calculated, the limit above which individual isolated points (outliers) appear, according to the formula: $\text{TIF} = \text{third quarter } (x) + 1.5 * \text{HB } (x)$, where HB represents the box length, i.e. the difference between the third and the first quarter (75th to 25th percentiles).

Since geochemical data usually have a right-skewed distribution, logarithmic data transformation was performed to translate it into a symmetric distribution, in order to determine the

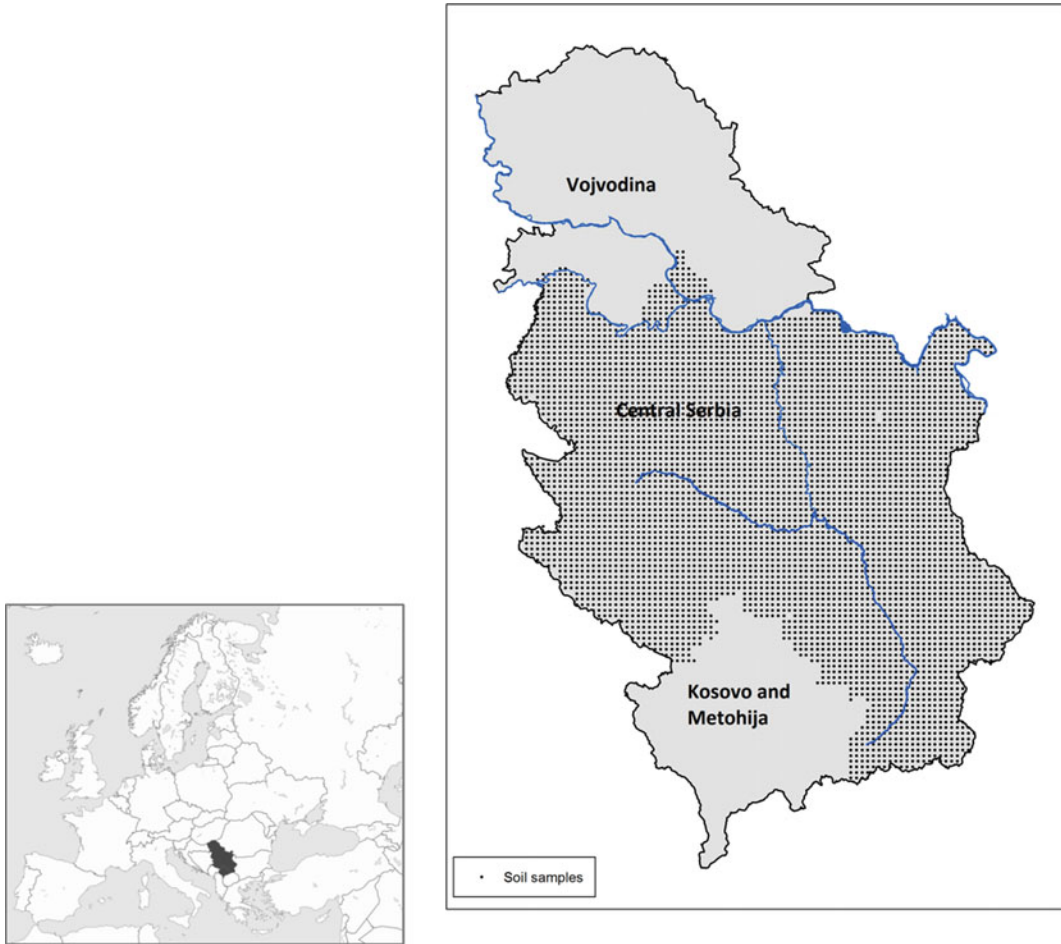


Fig. 21.1 Location of the Republic of Serbia and sampled points in Central Serbia

statistical parameters (and then calculate antilogarithm limit values). According to Reimann et al. (2005), if the coefficient of variation $CV > 100\%$, the logarithmic transformation of the data is necessary, and if the CV value is between 70 and 100%, the logarithmic scale will be informative.

21.4 Description of the Study Area

The area of the Republic of Serbia is 8,836,100 ha, including Central Serbia (5,596,800 ha) and two Autonomous Provinces: Vojvodina (2,150,600 ha) and Kosovo and Metohija (1,088,700 ha). The natural

characteristics (relief, geological composition, climate, vegetation and hydrography) in Serbia are very heterogeneous, including about 35 types of soil, with varying properties and production values (according to the current soil classification, Škorić et al. 1985). There are three pedogeographical regions in Serbia, which differ in terms of both their topography and pedological diversity.

The lowland region includes plains (Pannonia Plain, Mačva, Stig) and wide alluvial river valleys with an altitude of less than 200 m (Fig. 21.2). This part is characterised by a Quaternary geological matrix, loess deposited on loess terraces and loess plateaus, and alluvial deposits along river flows (Fig. 21.3). The

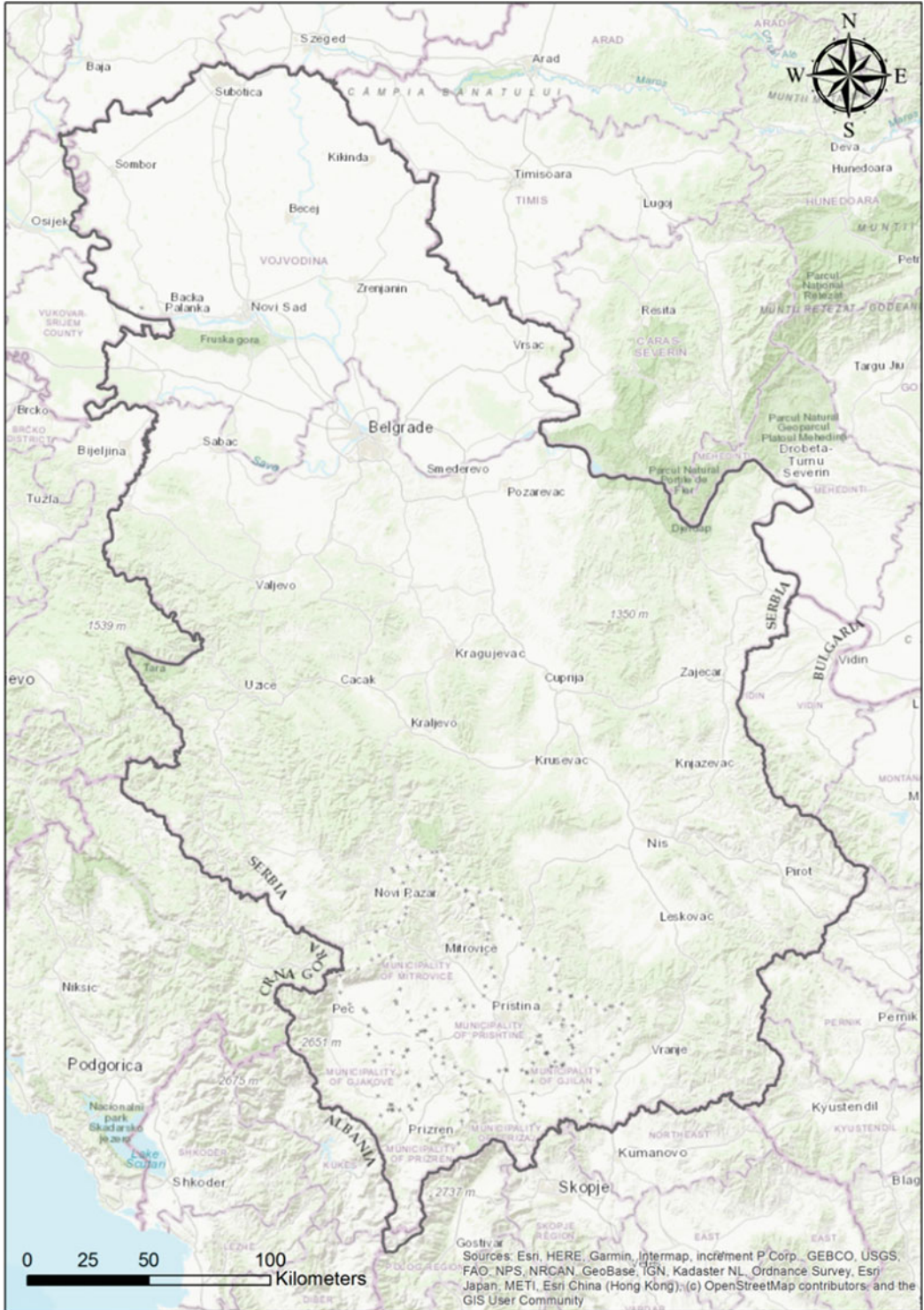


Fig. 21.2 Topographical map of the Republic of Serbia

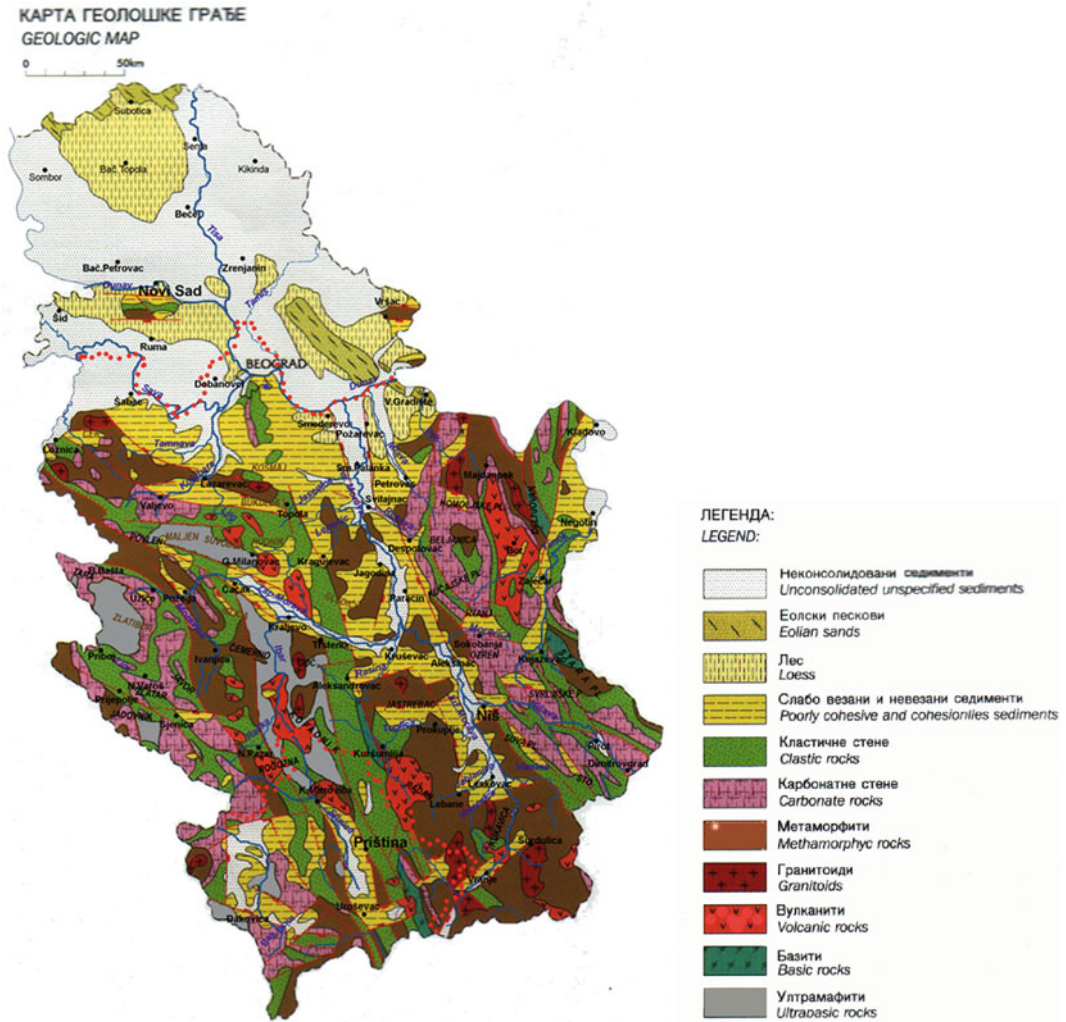


Fig. 21.3 Geological map of Serbia (Geozavod—Gemini Belgrade and “Magic Map” Smederevska Palanka, 2003). Unconsolidated sediments include alluvial areas,

terraces and swamp loess. Clastic rocks: flysch, diabase-chert formations, sandstone, marl

climate is temperate continental, and deep and very fertile soils with high productive capabilities have formed: Chernozem, Gelysol and Fluvisol (Fig. 21.4). Smaller areas feature less productive soils—Solonetz and Solonchak, as well as Arenosol (WRB 2014).

The relief is represented by valleys and low hills at an altitude of 200–500 m, predominantly with Neogenic sediments (clay, loam, sand, marl, flysch, etc.). The soils formed on these substrates are usually of medium depth, with a heavier texture and/or acidic, and are classified as

Vertisols, Eutric Cambisols, Luvisols and Stagnosols (WRB 2014). The hilly/mountainous region occupies about half of the territory of Serbia (western and southeastern parts) and includes an area with altitudes above 500 m. The climate is mountainous, with long, harsh winters, especially on high elevations above 1000 m. The low mountains are dominated by Dystric and Eutric Cambisols formed on magmatic, metamorphic and silicate sedimentary rocks, and by high mountain Rankers. Easily weathered carbonate rocks have formed Rendzinas, while hard

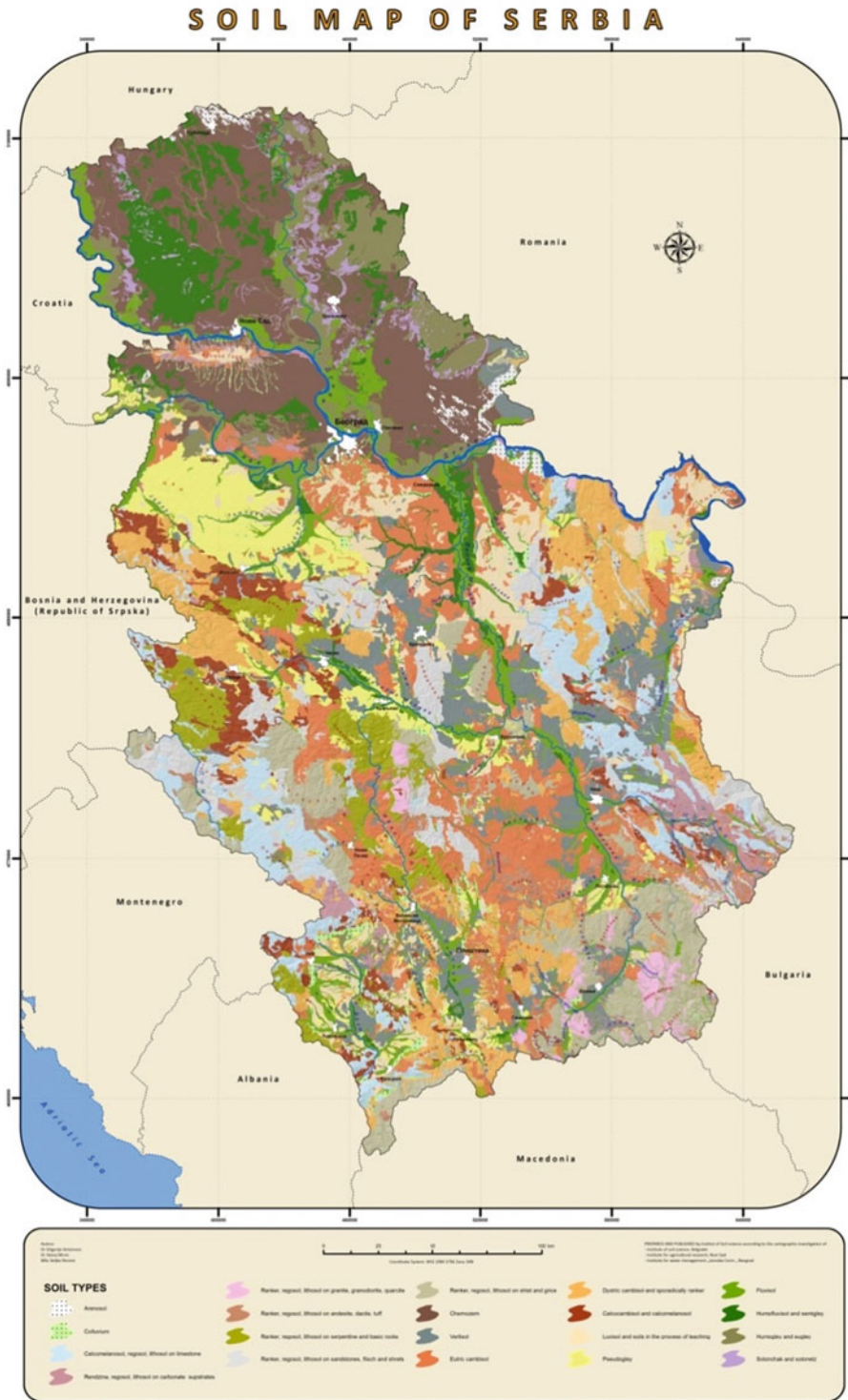


Fig. 21.4 Pedological map of Serbia (Published by the Institute for Soil Sciences; authors: Antonović, Mrvić and Perović 2013)

limestone has formed Calcomelanosols and Calcocambisols. These mountain soils are often found in complexes with underdeveloped soils—Lithosols and Regosols (WRB 2014).

21.5 Anthropogenic Soil Contamination

In Serbia, the main sources of anthropogenic soil pollution are agrochemical measures (fertilisers, crop protection chemicals, etc.), vehicle emissions, industrial enterprises, power plants, mining and metallurgical enterprises (Fig. 21.5).

21.6 Content and Distribution of Potentially Toxic Elements in Soils of Central Serbia

Various pedogenetic factors, especially the geological composition of Central Serbia and anthropogenic sources of pollution, have resulted in a significant variation in the concentration and distribution of the potentially toxic elements (PTEs) studied here: As, Cr, Cu, Ni, Pb and Zn (Table 21.1). The coefficient of variation (CV) for all elements (except Zn) was above 100%, which indicates high data dispersion.

The results showed that the data have a right-skewed and elongated distribution compared to normal, which is typical for geochemical data. The PTE content varied, and the average values were in the range reported for global soils (Adriano 2001).

Based on the remediation values (RVs) in the legislative acts of the Republic of Serbia (Regulation SG 30/2018), the results showed that most soils were not contaminated with heavy metals. Above-RV Ni was often present (4.2% samples $>210 \text{ mg kg}^{-1}$), followed by Cr (1.8% samples $>380 \text{ mg kg}^{-1}$) and As (1.9% samples $>55 \text{ mg kg}^{-1}$), and other elements $<0.8\%$. Figure 21.6 shows the locations where the heavy

metal content was higher than the remediation value.

The increased content of elements was mainly observed in hilly and mountainous regions, under forest and grass vegetation. The heavy metal content varied with the soil type, parent material and distance from the pollutant. In western and central Serbia, high concentrations of Ni and Cr in the soil were observed on serpentine rocks, which occupy about 300,000 ha and are naturally rich in Ni and Cr (as well as Mg, Fe, Co), often exceeding 1000 mg/kg (Kadović et al. 2002; Jakovljević and Stevanović 2004; Đorđević et al. 2005). High values of these elements (above RVs) were recorded on the mountains of Zlatibor, Ozren, Maljen and Suvobor, and the mountains around the river Ibar: Goč, Čemerno and Kopaonik (Mrvić et al. 2009). To the south of Ivanica, at the foot of the Čemerno and Golija Mountains, samples with high arsenic (As) content were found in the area of mineral deposits, most often in contact with igneous rocks and shales, with occurrences of lead–zinc, tungsten and antimony (Brković et al. 1968).

In northeastern Serbia, elevated concentrations of As and Cu were due to the operation of the mining and smelting plant in Bor, which processes copper ore (Čakmak et al. 2014). O'Neill (1995) states that mine and smelter pollution accounts for 40% of the world's total anthropogenic arsenic pollution.

In southeastern Serbia, a considerable number of sites were found with elevated As concentrations. Around the town of Vranje, the soil was formed on Eocene sediments and pyroclastic rocks, and around the town of Bosilegrad, it was formed on schist. These areas have deposits of Pb and Zn and several mines (Grot, Kriva Feja). Also, around Bosilegrad, some small areas were found with phosphorites, which, together with clay, is the biggest natural source of arsenic (Meharg et al. 1998). The results of large-scale studies showed that the origin of heavy metals in the area studied was mainly geochemical.

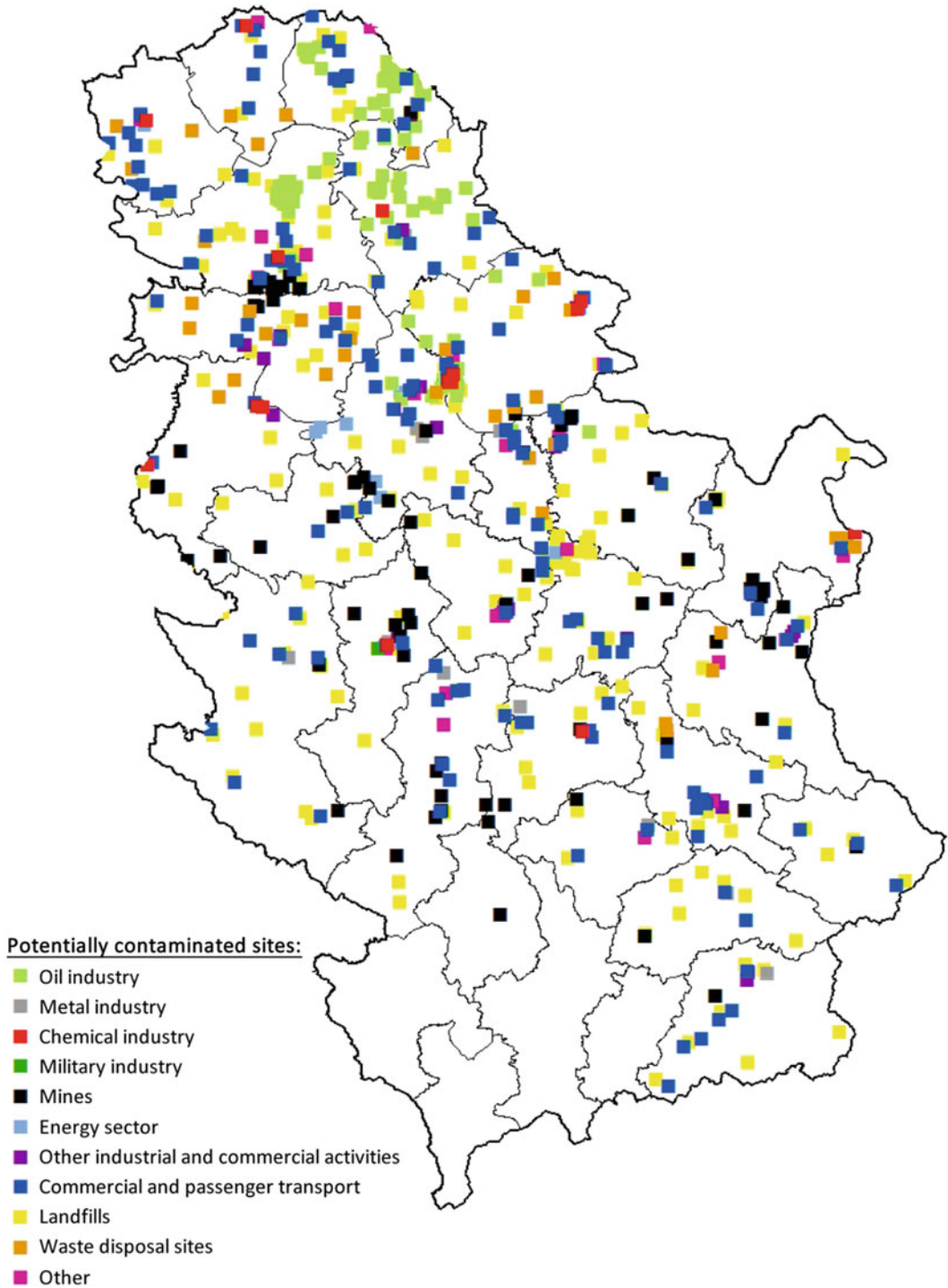


Fig. 21.5 Map of potentially contaminated locations in the Republic of Serbia (Serbian Environmental Protection Agency, SEPA (2018): Towards soil decontamination in

the Republic of Serbia. ISBN: 978-86-87159-20-4). Available online: <http://www.sepa.gov.rs/download/zemljiste/KaDekontaminacijiZemljista.pdf>

Table 21.1 Statistical parameters of the concentration of potentially toxic elements in the soils of Central Serbia (Mrvić et al. 2019)

Statistical parameters	As	Cr	Cu	Ni	Pb	Zn
Average	10.15	47.97	26.92	57.80	39.67	47.67
Standard deviation	15.90	85.41	41.42	143.34	40.40	33.65
Skewness	9.35	5.81	13.94	6.30	9.92	6.30
Kurtosis	136.93	45.06	304.82	49.05	183.81	89.89
Minimum	0.10	0.10	0.10	0.10	0.10	0.10
Maximum	382.00	1218.80	1285.80	1900.00	1031.30	740.00
CV%	156.55	178.04	153.86	247.98	101.84	70.58
Percentage 25	4.70	16.37	13.80	11.72	21.00	30.51
Percentage 50	6.80	27.00	19.00	24.00	31.00	41.90
Percentage 75	10.00	44.00	28.00	41.97	47.45	58.00

21.7 Content of Potentially Toxic Elements as Related to Soil Types

The median values of the concentration of heavy metals by soil types or groups of soil types are shown in Table 21.2 (Mrvić et al. 2013). The Rankers formed on granite had a lower content of most elements, which is typical for silica and quartz-rich rocks (Kabata-Pendias and Pendias 2001; Aubert and Pinta 1977). The Rankers on andesite and calcomelanosol showed a higher As and Cu content because these soils dominate on the territory of the copper mine and the smelter in Bor. As mentioned earlier, the Ranker formed on serpentine is distinguished by significantly higher concentrations of Ni and Cr compared with other types, which is typical for the soil on this substrate (Adriano 2001). In addition, the soils of the river valleys contain somewhat higher concentrations of Ni and Cr, because the alluvial deposits of some rivers (especially the Velika Morava) consist of a material originating

in serpentine. This was also confirmed by studies by Jakovljević et al. (1997), Čakmak et al. (2017), and Antić-Mladenović et al. (2018). In addition to differences between soil types, the content of heavy metals varied within the same soil type, most often in those that occupy large areas: Dystric Cambisols, Eutric Cambisols and Rankers on schist.

21.8 Background Values and Limits of PTEs for the Territory of Central Serbia

This section presents the variations of background values and the background limits of PTEs for the entire territory of Central Serbia, calculated based on the content of elements in the surface soil layer in 5022 samples (Mrvić et al. 2019). The following calculation methods were used: classical [Mean \pm 2Sd], [Median \pm 2MAD], box plot—upper inner fence (TIF) (Table 21.3). According to the results (Table 21.1), the coefficient of variation for all elements studied (except Zn) was

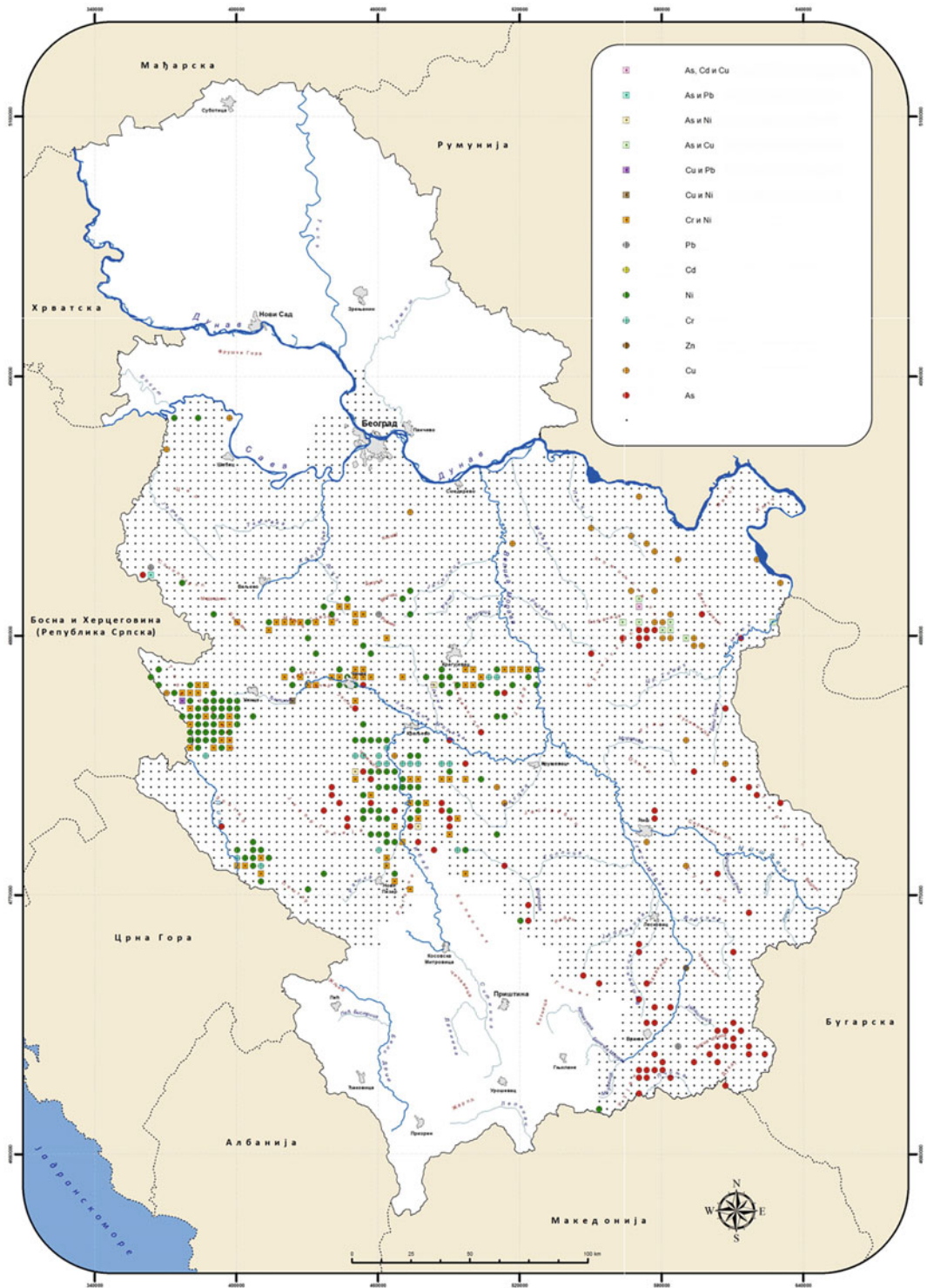


Fig. 21.6 Locations where the content of potential toxic elements (PTEs) is above remediation values (RVs) (Mrvić et al. 2013)

Table 21.2 The content of potential toxic elements in the soil types in Central Serbia—median values (mg kg^{-1}) (Mrvić et al. 2013)

Soil type, national classification ^a (WRB 2014) ^b	As	Cd	Cr	Cu	Hg	Ni	Pb	Zn
Arenosol and Regosol on sand (Arenosol and Leptic Regosol (Arenic))	4.60	1.11	11.95	21.29	0.09	22.41	24.44	36.61
Colluvium (Colluvic Regosol)	6.10	0.43	23.30	19.10	0.05	22.71	27.73	36.00
Calcomelasol (Mollic Leptosol)	8.40	1.20	24.95	20.66	0.10	20.45	33.80	40.55
Rendzina (Rendzic Leptosol, Leptic Calcisol)	7.50	1.10	24.40	17.00	0.09	18.00	25.20	35.00
Ranker on granite, granodiorite, quarclatite (Umbric Leptosol)	5.30	0.30	12.00	13.00	0.08	11.00	23.00	35.80
Ranker on andesite, dacite, tuff (Mollic Umbrisol, Umbric Leptosol)	8.00	0.35	19.75	21.00	0.07	13.63	46.15	38.50
Ranker on serpentine and basic rocks (Eutric Leptosol)	4.20	0.70	194.5	20.56	0.08	164.0	44.70	38.25
Ranker on sandstones and flysch (Leptosols)	7.70	0.65	29.30	19.00	0.08	25.80	38.50	42.40
Ranker on schist and gneiss (Umbric Leptosol)	7.70	0.35	21.00	19.00	0.08	18.00	32.50	41.00
Chernozem	4.70	0.20	29.95	20.35	0.04	32.00	23.00	43.02
Vertisol	6.80	0.70	32.05	21.90	0.06	22.21	29.53	37.00
Eutric Cambisol	6.20	0.40	30.05	18.40	0.07	22.94	27.50	40.00
Dystric Cambisol	6.40	0.65	15.10	19.48	0.08	14.64	26.66	42.58
Calcocambisol (Leptic Cambisol (Clayic))	7.80	0.78	29.05	19.65	0.12	29.18	37.58	47.88
Luvisol	5.50	0.71	25.00	17.50	0.05	26.77	26.10	42.63
Pseudogley (Planosol, Stagnosol)	7.40	0.65	22.65	15.40	0.07	30.83	36.08	47.50
Fluvisol	8.00	0.50	30.05	20.90	0.08	32.00	30.00	44.55
Humofluvisol (Gleyic Phaeozem (Pachic))	7.15	0.30	47.50	21.86	0.05	58.22	33.72	44.84
Humogley and Eugley (Mollic Gleysol (Clayic) and Gleysol)	6.10	0.20	33.40	22.23	0.07	30.79	28.71	42.00

^aNational classification (Škorić et al. 1985)^bWorld Reference Base for Soil Resources (2014)

above 100%, so the logarithmic transformation was applied for them.

The results showed that the values calculated with the [Median + 2MAD] method are significantly lower than using the other two methods, as shown in other studies (Reimann and Garrett 2005; Ander et al. 2013; Reimann and Caritat 2017; Mrvić et al. 2011). The number of locations with values above the background limit, for detailed observation, is 10.9–16.0% (Table 21.3).

The other two methods resulted in higher and more approximate values, so the number of points with unusual values is 1.2–4.7%.

In relation to the geochemical limits for European agricultural soils using the TIF method (Reimann et al. 2018), the geochemical limits obtained in Central Serbia were lower for As, Cu and Zn (42–70% of the listed values), and higher for Pb, Ni and Cr (123–185%).

Table 21.3 Background limits of the PTEs calculated by different methods and their boundary values according to the legislation of the Republic of Serbia (Mrvić et al. 2019)

Statistic	As	Cr	Cu	Ni	Pb	Zn
Mean + 2Sdev	31.26	235.50	82.41	261.22	127.35	114.96
Median + 2MAD	14.69	72.28	38.37	84.72	69.34	68.14
TIF	30.90	193.64	82.22	284.45	161.16	99.24
90%	16.30	80.92	45.60	95.47	71.10	78.88
95%	25.00	151.47	65.25	167.50	88.51	96.17
98%	53.05	364.22	100.64	567.08	122.35	124.78
MDK	25	100	100	50	100	300
RV	55	380	190	210	530	720

MDK—maximum allowed concentrations (Regulation, SG RS 23/1994)

RV—remediation value (Regulation SG 30/2018, uncorrected values)

Geochemical limits determined by [Mean + 2Sdev] and TIF methods are closer to the levels of legislation, and for some elements, they are even higher, so there is a need to revise the limit values of hazardous and harmful elements in the legislation of the Republic of Serbia, especially regarding Ni and Cr, which are primarily of natural origin.

Different methods produce different geochemical boundaries, and the choice depends to a large extent on sociological and economic possibilities (Reimann and Caritat 2017; Stajković-Srbinić et al. 2017, 2018). The locations with element concentrations above higher limits (TIF and [Mean + 2Sdev] method), with intensive agriculture production, may take priority in environmental protection activities. For the geologically and pedologically homogeneous territories that are subject to severe anthropogenic pollution, a more rigorous method, such as [Median + 2MAD], should be given priority.

21.9 Background Concentration and Limits of PTEs in Specific Regions

When determining a unique background limit over large areas, for example, for an entire country or region, spatial variations in soil

properties and types are usually ignored, leading to the overestimation or underestimation of PTE contamination (Diez et al. 2009). Therefore, it is important to determine geochemical boundaries at the local level. The pedogeochemical composition in Serbia is complex, even in a very small space. The background limits of some heavy metals were determined in two regions: Braničevski, in Eastern Serbia and Moravički, in Western Serbia (Fig. 21.7).

21.9.1 Braničevski Region

The Braničevski region is located in Eastern Serbia and covers an area of 3865 km² (Fig. 21.1). The geological composition is very diverse, but there are fewer serpentine rocks compared with Western Serbia (Krstić et al. 1974). Although there is little industrial activity in the study area, some potential pollutants are found in nearby regions, such as the copper industry in Bor, ferrous metallurgy in Smederevo and the Belgrade-Niš highway. The background boundaries determined by different methods are shown in Table 21.4.

The background limits for Cu and Zn in the Braničevski region were closer to the limit values of Central Serbia, while for Ni, Cr and Pb they



Fig. 21.7 Braničevski and Moravički regions, Serbia

Table 21.4 Background limits of trace elements determined with different methods (mg kg⁻¹) in Braničevski region (Mrvić et al. 2011)

Elements	[Mean + 2Sdev]		[Median + 2MAD]		Upper whisker		98th percentile	Outer limit CDF
	Natural	Anti-log	Natural	Anti-log	Natural	Anti-log		
Cd	3.52	7.23	2.55	3.03	3.92	4.07	2.95	3.10
Cr	52.8	85.1	34.3	39.1	46.47	49.50	62.9	50.0
Cu	180	105	33.2	38.7	49.0	53.6	238	125
Hg	0.364	0.331	0.13	0.173	0.21	0.25	0.54	0.25
Ni	78.9	118	43.8	54.8	64.0	83.0	130.0	65.0
Pb	75.5	77.1	34.8	38.11	46.67	51.11	110	60.0
Zn	115	122	61.0	67.9	85.1	92.5	150	90.0

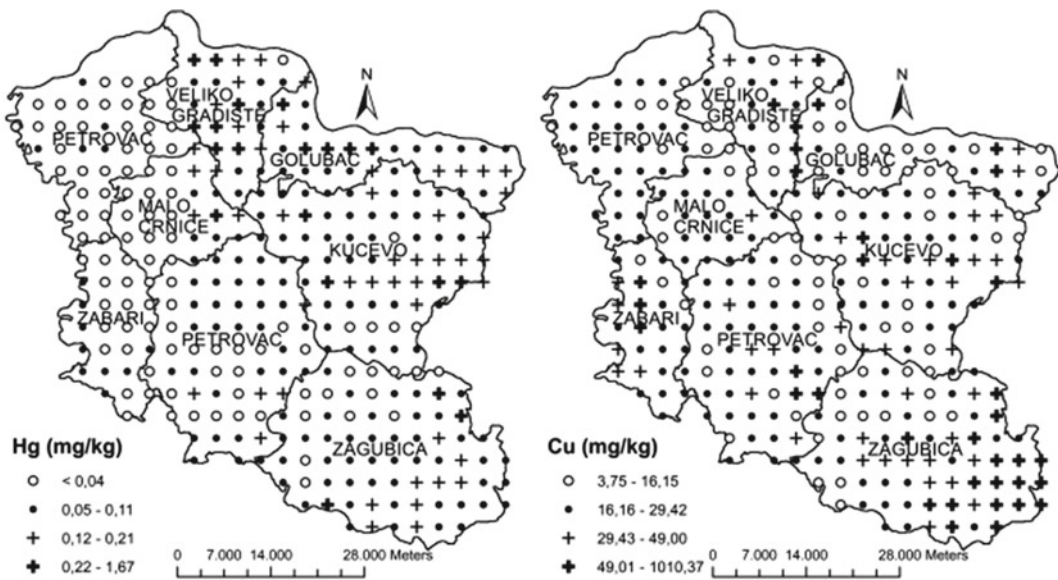


Fig. 21.8 Distribution of Hg and Cu in the topsoil of Braničevski region

were significantly lower (about 1.5–1.8 times with Median + 2MAD method).

The distribution of Hg and Cu is displayed in Fig. 21.8. The first set of maps was compiled from the natural values of a box plot for the whole area. Several high-content groups (values >75%) were found for each element. To confirm the differences, the Kruskal–Wallis test was additionally performed. In the absence of accurate geological maps, the easiest way to verify in practice is to organise the data by municipalities according to administrative

boundaries. This test showed that there are indeed significant differences ($p = 0.000$) between the concentrations of trace elements in each municipality.

There are groups with apparently higher values of Cu (and Zn, Pb and Cd) in the part of southeastern municipalities (Zagubica, Kucevo and Petrovac), due to geological formations that are rich in these metals (green schists, metavolcanites, carbonate rocks with magmatism) (Kalenić et al. 1976). Spearman’s correlation analysis confirmed that in the Zagubica region,

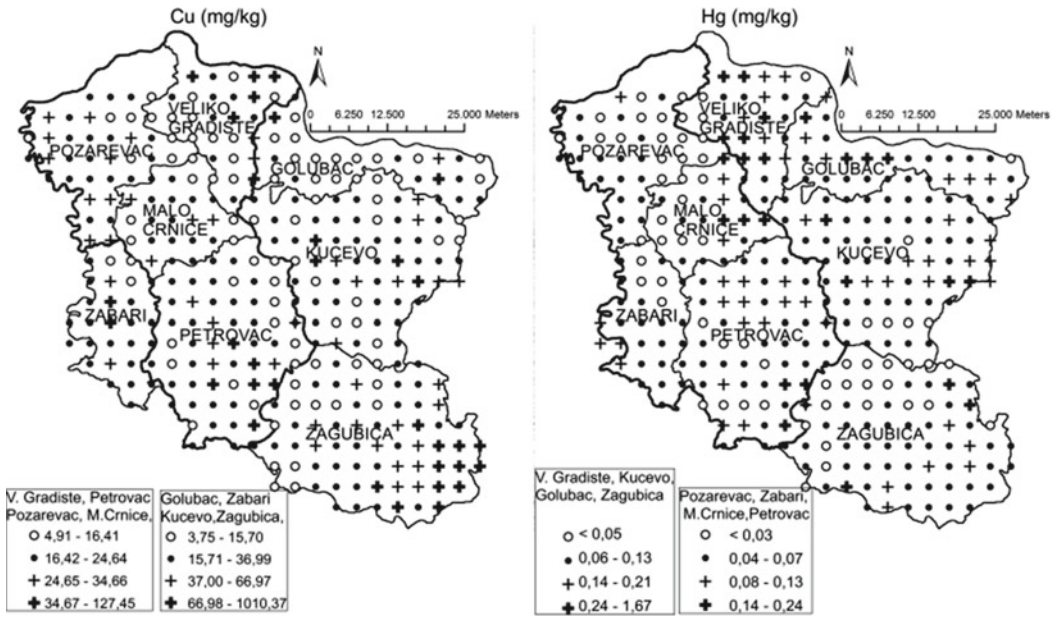


Fig. 21.9 Distribution of Cu and Hg in topsoil of Branicevski region with modified background limits

there is a high and medium correlation between these elements.

Higher values of Cu and Hg are found in the western Kucevo, Veliko Gradiste and Golubac, in the alluvial sediments of the Pek River, which flows through ore-bearing regions in the upper reaches. In addition, in Veliko Gradiste and Golubac, in the Ramsko-Golubacka sands, there is elevated Hg content, significantly higher than in others municipalities (Mann-Whitman test, p 0.039; 0.041). The distribution of elements is under the dominant effect of the geochemical factor.

Based on these maps, the municipalities were grouped in to homogeneous units and calculate the new, more realistic background limits. The new maps for Cu and Hg are presented in Fig. 21.9.

The data on Cu were grouped in two units: one with low content (Požarevac, Malo Crnice, Veliko Gradiste, Petrovac) and the other with a high content (compiled from all other municipalities). In the first group, the new background limit was lower by about 30% than the previous background, and in the rest of the territory, it was higher by about 20%. The new background limits

for Hg for the eastern part were slightly higher and in the western part, they were about half the original limit.

The maps showed that in those parts of the territory where background limits were significantly increased, despite the relatively high concentration of elements, the number of potentially polluted sites where a negative impact can be expected decreases, given the fact that geochemical sources of pollutants are dominant, and vice versa. The results showed that this grouping of data gives a much more realistic background limit, which allows for a better assessment of environmental risks.

21.9.2 Moravički Region

The Moravički region is located in Western Serbia, covering an area of 3016 km². In the northern part of the region, there are the cities of Cacak, Pozega, Lučani and Gornji Milanovac, with more developed industry and more intensive agriculture than in the southern part. The geological composition of the area is uneven. The

Table 21.5 Background limits of Cd and Cr determined with different methods (mg kg^{-1}) in the Moravički region (Mrvić et al. 2014)

Element	[Mean + 2Sdev]		[Median + 2MAD]		Box plot Upper whiskers	
	Natural	Antilog	Natural	Antilog	Natural	Antilog
Cd	1.58	1.99	0.86	1.135	1.387	3.20
Cr	489	717.8	112.6	245.5	222.1	924

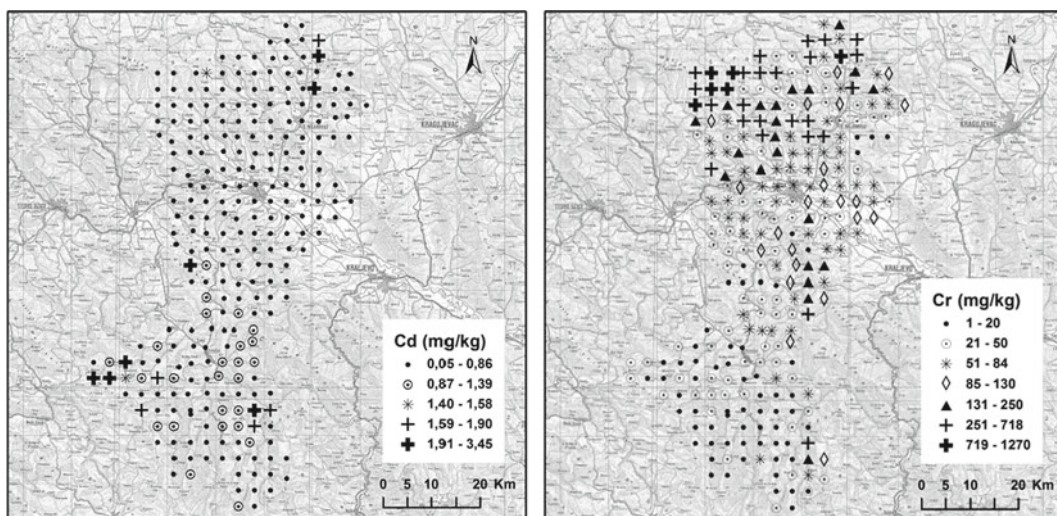


Fig. 21.10 Spatial distribution of Cd and Cr in soils of Moravički region (mg kg^{-1})

geochemical limits of the content of Cd and Cr in the soil are shown in Table 21.5.

The calculated geochemical limits for Cd in this region were significantly lower than in the Braničevski region, and the boundaries for Cr were higher than in Central Serbia (by more than three times), and especially in the Braničevski region. The coefficients of variation for Cd and Cr were 87% and 173%, respectively.

The spatial distribution maps of Cr and Cd in the Moravički region have been compiled based on geochemical limits calculated using various methods (Fig. 21.10). The spatial distribution of Cd confirms that most of the area has low concentrations, below 0.86 mg kg^{-1} , which was the limit determined by [Median + 2MAD] method. The higher values obtained by the [Mean + 2 Sdev] and box plot method corresponded to the soils on quartz latites and flysch on Mount Rudnik and around Pridvorica (ore area), as well

as several samples on carbonate rocks. According to Alloway (1995), igneous and metamorphic rocks contain up to 1.6 mg kg^{-1} of Cd, and clay cherts and clays up to 11 mg kg^{-1} , and some carbonates up to 12 mg kg^{-1} , with the highest content in the sulphide ore.

The spatial distribution of Cr varied due to different soil types and geological substrates. In the southern part, the limit values would be $20\text{--}50 \text{ mg kg}^{-1}$ (quarterly values), for soils on shales, phyllites and quartz latites. Cr concentrations obtained by the [Median + 2MAD] method were about 250 mg kg^{-1} , which corresponds to the soil on the basic rocks, gabbro and diabase. The background limits obtained by the logarithmic function by the [Mean + 2Sdev] and the box plot methods were very high ($700\text{--}900 \text{ mg kg}^{-1}$) and corresponded only to the soil on the ultrabase rocks (on the Suvobor, Čemerno and Maljen mountains). The results showed that

in areas with a heterogeneous geological composition, it is necessary to identify a larger number of background boundaries within homogeneous pedogeochemical units.

21.10 Conclusions

The monitoring of the content and distribution of potential toxic elements (PTEs) in the surface soil layer in Central Serbia and the background limits of selected elements established that most of the territory is not polluted. Within the polluted areas, Ni, Cr and As were found to be the main pollutants (4.2%, 1.8% and 1.9% of samples showed values above the remediation value, respectively). Their higher concentrations were mostly of geochemical origin.

Comparing the median values for PTEs according to the soil types, it was found that Rankers on serpentine and basic rocks have a very high content of Ni and Cr. Elevated concentrations of these elements were also found in Fluvisols, and especially Humofluvisols of the rivers, where sediments mainly originate in the area with serpentine rocks. The lowest concentrations of all elements were found in Rankers on acidic magmatic and metamorphic rocks. The content of heavy metals varied within the same type, most of all in those that cover large areas: Dystric Cambisols, Eutric Cambisols, and Rankers on schist.

The background limits were determined for As, Cr, Cu, Ni, Pb and Zn in soils for the entire territory of Central Serbia. The background limits calculated by the [Median + 2MAD] method had the lowest values, from 87 to 90%. Using two other methods, TIF and, in particular, [Mean + 2Sdev], more approximate values were obtained, usually between 95 and 98%, which are similar to those for agricultural soils in Europe. The results showed that it is necessary to revise the limit values of hazardous and harmful elements in the legislation of the Republic of Serbia, especially with regard to Ni and Cr, which are primarily of natural origin.

The results gained by determining the background limits in the Braničevski and Moravički regions showed that in territories with a heterogeneous geological composition and various anthropogenic impacts, more background limits should be determined depending on pedogeochemical units or on homogeneous administrative units. The study made it possible to identify areas with increased concentrations of PTEs, which need to be further studied for their harmful or toxic effects and, if necessary, to develop recommendations for remediation measures.

Acknowledgements This work was supported by the Ministry of Education, Science and Technological Development of the Republic of Serbia, (reference number 451-03-9/2021-14/200007 and 451-03-09/2021-14/200011), and by the Ministry of Agriculture, Forestry and Water Management of the Republic of Serbia.

References

- Ander L, Jonson C, Cave M, Palumbo-Roe B, Nathanai P, Murray L (2013) Methodology for the determination of normal background concentrations of contaminants in English soil. *Sci Total Environ* 454–455:604–618. <https://doi.org/10.1016/j.scitotenv.2013.03.005>
- Adriano DC (2001) Trace elements in terrestrial environment: biogeochemistry, bioavailability, and risk of metals, 2nd edn
- Alloway BJ (1995) Cadmium. In: Alloway BJ (ed) Heavy metals in soils. Blackie Academic and Professional, Glasgow, UK, pp 122–152
- Antić-Mladenović S, Kresović M, Čakmak D, Perović V, Saljnikov E, Ličina V, Rinklebe J (2018) Impact of a severe flood on large-scale contamination of arable soils by potentially toxic elements (Serbia). *Environ Geochem Health*. <https://doi.org/10.1007/s10653-018-0138-4>
- Aubert H, Pinta M (1977) Trace elements in Soil. Development in Soil Science 7. Elsevier Scientific Publishing Co., Amsterdam, 395 pp
- Beygi M, Jalali M (2018) Background levels of some trace elements in calcareous soils of the Hamedan Province, Iran. *CATENA* 162:303–316. <https://doi.org/10.1016/j.catena.2017.11.001>
- Brković T, Malešević M, Urošević M, Trifunović S, Radovanović Z (1968) Tumač za list Ivanjica K 34–7. Osnovna geološka karta 1:100 000. Zavod za geološka i geofizička istraživanja. Belgrade
- Capparelli MV, McNamara JC, Grosell MG (2020) Tissue accumulation and the effects of long-term dietary

- copper contamination on osmoregulation in the mudflat fiddler crab *MinUca rapax* (Crustacea, Ocypodidae). *Bull Environ Contam Toxicol* 104:755–762. <https://doi.org/10.1007/s00128-020-02872-3>
- Čakmak D, Perović V, Saljnikov E, Jaramaz D, Sikirić B (2014) Spatial modeling of ecological areas by fitting the limiting factors for As in the vicinity of mine, Serbia. *Environ Sci Poll Res* 21(5):3764–3773. <https://doi.org/10.1007/s11356-013-2320-7>
- Čakmak D, Perović V, Antić-Mladenović S, Kresović M, Saljnikov E, Mitrović M, Pavlović P (2017) Contamination, risk, and source apportionment of potentially toxic microelements in river sediments and soil after extreme flooding in the Kolubara River catchment in Western Serbia. *J Soils Sediments* 18(5):1–13. <https://doi.org/10.1007/s11368-017-1904-0>
- Čakmak D, Perović V, Kresović M, Jaramaz D, Mrvić V, Belanović-Simić S, Saljnikov E, Trivan G (2018) Spatial distribution of soil pollutants in urban green areas (a case study in Belgrade). *J Geochem Explor* 188:308–317. <https://doi.org/10.1016/j.gexplo.2018.02.001>
- Diez M, Simón M, Martín F, Dorronsoro C, García I, Van Gestel CAM (2009) Ambient trace element background concentrations in soils and their use in risk assessment. *Sci Total Environ* 407:4622–4632. <https://doi.org/10.1016/j.scitotenv.2009.05.012>
- Đorđević A, Jakovljević M, Maksimović S, Cupać S (2005) Sadržaj mobilnog nikla u serpentinskim rankerima Srbije. *Zemljište i Biljka* 54(3):193–199
- Dregulo AM, Bobylev NG (2021) Heavy metals and arsenic soil contamination resulting from wastewater sludge urban landfill disposal. *Pol J Environ Stud* 30(1):81–89. <https://doi.org/10.15244/pjoes/121989>
- Gruszecka-Kosowska A, Baran A, Wdowin M et al (2020) The contents of the potentially harmful elements in the arable soils of southern Poland, with the assessment of ecological and health risks: a case study. *Environ Geochem Health* 42:419–442. <https://doi.org/10.1007/s10653-019-00372-w>
- Guo B, Hong C, Tong W et al (2020) Health risk assessment of heavy metal pollution in a soil-rice system: a case study in the Jin-Qu Basin of China. *Sci Rep* 10:11490. <https://doi.org/10.1038/s41598-020-68295-6>
- Gupta DK, Sandallo LM (eds) (2011) *Metal toxicity in plants: perception, signalling and remediation*. Springer, London
- Hu Y, Liu X, Bai J, Shih K, Zeng EY, Cheng H (2013) Assessing heavy metal pollution in the surface soils of a region that had undergone three decades of intense industrialization and urbanization. *Environ Sci Pollut Res* 20(9):6150–6159. <https://doi.org/10.1007/s11356-013-1668-z>
- Huang J, Peng S, Mao X, Li F, Guo S, Shi L et al (2019a) Source apportionment and spatial and quantitative ecological risk assessment of heavy metals in soils from a typical Chinese agricultural county. *Process Saf Environ Prot* 126:339–347
- Huang L, Riggins CW, Villamil MB, Rodríguez-Zas S, Zabaloy MC (2019b) Long-term N fertilization imbalances potential N acquisition and transformations by soil microbes. *The Science of the total environment*, ISSN: 1879-1026, vol 691, pp 562–571. <https://doi.org/10.1016/j.scitotenv.2019.07.154>
- ISO (International Organization for Standardization) (2005) *Soil quality—guidance on the determination of background values*. International Standard ISO 19258: 2005, 24 pp
- Jakovljević M, Kostić N, Stevanović D, Blagojević S, Wilson M, Lj M (1997) Factors influencing the distribution of heavy metals in the alluvial soils of the Velika Morava River Valley, Serbia. *Appl Geochem* 12:637–642. [https://doi.org/10.1016/S0883-2927\(97\)00019-X](https://doi.org/10.1016/S0883-2927(97)00019-X)
- Jakovljević M, Stevanović D (2004) Sadržaj i oblici korisnih i štetnih mikroelemenata u zemljištu prirodnih livada Zlatibora. *Acta Agriculturae Serbica IX* (17):179–184
- Jaramaz D (2018) *The impact of anthropogenic pollution on soil degradation at wide area of Bor City*. Doctoral thesis, Faculty of Forestry, University of Belgrade, Serbia
- Kabata-Pendias A, Pendias H (2001) *Trace elements in soils and plants*. CRC Press, 3rd edn, p 331
- Kadović R, Knežević M, Belanović S (2002) *Procena kvaliteta zemljišta, monografija “Teški metali u šumskim ekosistemima Srbije”* (Kadović R, Knežević M (ed)), Šumarski fakultet Univerziteta u Beogradu i Ministarstvo za zaštitu prirodnih bogastava i životne sredine Republike Srbije. Belgrade, pp 187–200
- Kalenić M, Đorđević M, Krstić B, Bogdanović P, Milošaković R, Divljan M, Čičulić M, Džodžo R, Rudolf Lj, Jovanović Lj (1976) *Tumač za list Bor L 34–141*. Osnovna geološka karta 1:100 000. Zavod za geološka i geofizička istraživanja. Belgrade
- Khan S, Hesham EA, Min Q, Štafiquir R, He J (2010) Effects of Cd and Pb on soil microbial community structure and activities. *Environ Sci Pollut Res* 17:288–296. <https://doi.org/10.1007/s11356-009-0134-4>
- Khan MN, Mobin M, Abbas ZK, Alamri SA (2018) Fertilizers and their contaminants in soils, surface and groundwater. In: DellaSala DA, Goldstein MI (eds) *The encyclopedia of the anthropocene*, vol 5, pp 225–240. Elsevier, Oxford
- Krstić B, Rakić B, Veselinović M, Dolić D, Rakić M, Anđelković J, Banković V (1974) *Tumač za list Aleksinac K 34–20*. Osnovna geološka karta 1:100 000. Zavod za geološka i geofizička istraživanja. Belgrade
- Leed R, Smithson M (2019) Ecological effects of soil microplastic pollution. *Sci Insight* 30(3):70–84. <https://doi.org/10.15354/si.19.re102>; <https://ssrn.com/abstract=3484641>
- Makuleke P, Ngole-Jeme VM (2020) Soil heavy metal distribution with depth around a closed landfill and their uptake by *Datura Stramonium*. *Appl Environ*

- Soil Sci 8872475. <https://doi.org/10.1155/2020/8872475>
- Meharg A, Shore RF, Broadgate K (1998) Edaphic factors affecting the toxicity and accumulation of arsenate in the earthworm *Lumbricus terrestris*. *Environ Toxicol Chem* 17(6):1124–1131
- Mrvić V, Zdravković M, Sikirić B, Čakmak D, Kostić-Kravljanac Lj (2009) Sadržaj štetnih i opasnih elemenata. In: Mrvić V, Antonović G, Martinović Lj (eds) Plodnost i sadržaj opasnih i štetnih materija u zemljištima centralne Srbije, Institut za zemljište, Beograd, pp 75–145
- Mrvić V, Kostić-Kravljanac Lj, Čakmak D, Sikirić B, Brebanović B, Perović V, Nikoloski M (2011) Pedo-geochemical mapping and background limit of trace elements in soils of Branicevo Province (Serbia). *J Geochem Explorat* 109(1–3):18–25. <https://doi.org/10.1016/j.gexplo.2010.09.005>
- Mrvić V, Antonović G, Čakmak D, Perović V, Maksimović S, Saljnikov E, Nikoloski M (2013) Pedological and Pedo-geochemical map of Serbia. In: Proceedings the 1st international Congress on Soil Science, XIII National Congress in Soil Science: “Soil-Water-Plant”, 23–26, September, Belgrade, Serbia, pp 93–105
- Mrvić V, Kostić-Kravljanac Lj, Sikirić B, Delić D, Jaramaz D (2014) Metode za ocenu granica prirodnog sadržaja Cr i Cd u zemljištu Moravičkog okruga. *Glasnik Šumarskog Fakulteta, Beograd* 109:137–148. <https://doi.org/10.2298/GSF1409137M>
- Mrvić V, Sikirić B, Jaramaz D, Koković N, Nikoloski M (2019) Background and threshold values of potentially toxic elements in soil at Central part of Republic of Serbia. *Ratarstvo i povrtarstvo* 56(1):1–6. <https://scindeks.ceon.rs/article.aspx?artid=1821-39441901001M>
- Nagaijyoti PC, Lee KD, Sreekanth VM (2010) Heavy metals, occurrence and toxicity for plants: a review. *Environ Chem Lett* 8:199–216. <https://doi.org/10.1007/s10311-010-0297-8>
- O'Neill P (1995) Arsenic. In: Alloway BJ (ed) *Heavy metals in soils*, 2nd edn. UK
- Prathumratana L, Kim R, Kim K (2020) Lead contamination of the mining and smelting district in Mitrovica, Kosovo. *Environ Geochem Health* 42:1033–1044 (2020). <https://doi.org/10.1007/s10653-018-0186-9>
- Qaswar M, Yiren L, Jing H et al (2020) Soil nutrients and heavy metal availability under long-term combined application of swine manure and synthetic fertilizers in acidic paddy soil. *J Soils Sediments* 20:2093–2106. <https://doi.org/10.1007/s11368-020-02576-5>
- Qin G, Niu Zh, Yu J, Li Zh, Ma J, Xiang P (2021) Soil heavy metal pollution and food safety in China: effects, sources and removing technology. *Chemosphere* 267:129205. <https://doi.org/10.1016/j.chemosphere.2020.129205>
- Qingjia G, Juna D, Yunchuanb X, Qingfeib W, Liqiangb Y (2008) Calculating pollution indices by heavy metals in ecological geochemistry assessment and a case study in parks of Beijing. *J China Univ Geosci* 19(3):230–241
- Raheem A, Sikarwar VS, He J, Dastyar W, Dionysiou DD, Wang W, Zhao M (2018) Opportunities and challenges in sustainable treatment and resource reuse of sewage sludge: a review. *Chem Engineer J* 337:616–641. <https://doi.org/10.1016/j.cej.2017.12.149>
- Regulation SG RS 23/1994 (1994) Pravilnik o dozvoljenim količinama opasnih i štetnih materija u zemljištu i vodi za navodnjavanje i metodama njihovog ispitivanja. <https://www.pravno-informacioni-sistem.rs/SIGlasnikPortal/eli/rep/sgrs/ministarstva/pravilnik/1994/23/1/reg>. Accessed 1 Apr 2021
- Regulation SG 30/2018 (2018) Uredba o programu sistemskog praćenja kvaliteta zemljišta, indikatorima za ocenu rizika od degradacije zemljišta i metodologiji za izradu remedijacionih programa. <https://www.pravno-informacioni-sistem.rs/SIGlasnikPortal/eli/rep/sgrs/vlada/uredba/2018/30/2/reg>
- Reimann C, Caritat P (2017) Establishing geochemical background variation and threshold values for 59 elements in Australian surface soil. *Sci Total Environ* 578:633–648. <https://doi.org/10.1016/j.scitotenv.2016.11.010>
- Reimann C, Garrett RG (2005) Geochemical background concept and reality. *Sci Total Environ* 350:12–27. <https://doi.org/10.1016/j.scitotenv.2005.01.047>
- Reimann C, Filzmoser P, Garrett RG (2005) Background and threshold: critical comparison of methods of determination. *Sci Total Environ* 346:1–16. <https://doi.org/10.1016/j.scitotenv.2004.11.023> Accessed on April 1, 2021
- Reimann C, Fabian K, Birke M, Filzmoser P, Demetriades A, Négrel P, Orts K, Matschullat J, Caritat P (2018) GEMAS: Establishing geochemical background and threshold for 53 chemical elements in European agricultural soil. *Appl Geochem* 88:302–318. <https://doi.org/10.1016/j.apgeochem.2017.01.021>
- Rutigliano FA, Marzaioli R, De Crescenzo S, Trifuoggi M (2019) Human health risk from consumption of two common crops grown in polluted soils. *Sci Total Environ* 691:195–204. <https://doi.org/10.1016/j.scitotenv.2019.07.037>
- Saljnikov E, Mrvić V, Čakmak D, Jaramaz D, Perović V, Antic-Mladenović S, Pavlović P (2019) Pollution indices and sources appointment of heavy metal pollution of agricultural soils near the thermal power plant. *Environ Geochem Health* 41(5):2265–2279. <https://doi.org/10.1007/s10653-019-00281-y>
- Santos-Francés F, Martínez-Graña A, Alonso Rojo P, García Sánchez A (2017) Geochemical background and baseline values determination and spatial distribution of heavy metal pollution in soils of the Andes Mountain Range (Cajamarca-Huancavelica, Peru). *Int J Environ Res Public Health* 14(8):859–865. <https://doi.org/10.3390/ijerph14080859>
- Stajković-Srbinić O, Delić D, Rasulić N, Kuzmanović D, Houskova B, Sikirić B, Mrvić V (2017) Microorganisms in soils with high nickel and chromium concentrations in Western Serbia. *Polish J Environ*

- Stud 26(4):1663–1671. <https://doi.org/10.15244/pjoes/68566>
- Stajković-Srbinić O, Buntić A, Rasulić N, Kuzmanović Dj, Dinić Z, Delić D, Mrvić V (2018) Microorganisms in soils with elevated heavy metal concentrations in southern Serbia. *Arch Biol Sci* 70(4):707–716. <https://doi.org/10.2298/ABS180504034S>
- Stewart AG (2020) Mining is bad for health: a voyage of discovery. *Environ Geochem Health* 42:1153–1165. <https://doi.org/10.1007/s10653-019-00367-7>
- Sun Y, Ren X, Pan J et al (2020) Effect of microplastics on greenhouse gas and ammonia emissions during aerobic composting. *Sci Total Environ* 737:139856. <https://doi.org/10.1016/j.scitotenv.2020.139856>
- Škorić A, Čirić M, Filipovski G (1985) Klasifikacija zemljišta Jugoslavije. Sarajevo
- Truchet DM, Buzzi NS, Negro CL, Mora MC, Marcovecchio JE (2021) Integrative assessment of the ecological risk of heavy metals in a South American estuary under human pressures. *Ecotoxicol Environ Safety* 208:111498. <https://doi.org/10.1016/j.ecoenv.2020.111498>
- Tukey JW (1977) *Exploratory data analysis*. Addison-Wesley, Reading.
- Wang Z, Gong D, Zhang Y (2020) Investigating the effects of greenhouse vegetable cultivation on soil fertility in Lhasa, Tibetan Plateau. *Chin Geogr Sci* 30:456–465. <https://doi.org/10.1007/s11769-020-1118-z>
- Wang Xi, Li Xi, Yan Xi, Tu Ch, Yu Zh (2021) Environmental risks for application of iron and steel slags in soils in China: a review. *Pedosphere* 31(1):28–42. [https://doi.org/10.1016/S1002-0160\(20\)60058-3](https://doi.org/10.1016/S1002-0160(20)60058-3)
- WRB (2014) IUSS Working Group WRB. 2015. World Reference Base for Soil Resources 2014, update 2015 International soil classification system for naming soils and creating legends for soil maps. *World Soil Resources Reports No. 106*. FAO, Rome, p 192
- Yang Sh, He M, Zhi Yu, Chang SX, Gu B, Liu X, Xu J (2019) An integrated analysis on source-exposure risk of heavy metals in agricultural soils near intense electronic waste recycling activities. *Environ Int* 133, part B, 105239 <https://doi.org/10.1016/j.envint.2019.105239>
- Zhen Z, Wang S, Luo S, Ren L, Liang Y, Yang R, Li Y, Zhang Y, Deng S, Zou L, Lin Z, Zhang D (2019) Significant impacts of both total amount and availability of heavy metals on the functions and assembly of soil microbial communities in different land use patterns. *Front Microbiol* 10:2293. <https://doi.org/10.3389/fmicb.2019.02293>



Impact of Weathering and Revegetation on Pedological Characteristics and Pollutant Dispersion Control at Coal Fly Ash Disposal Sites

Olga Kostić, Miroslava Mitrović,
and Pavle Pavlović

Abstract

Fly ash (FA) as a product of coal combustion in thermal power plants is a hazardous material that is deposited in the immediate vicinity of power plants due to its low rate of utilisation. As a result, fertile agricultural land turns into fly-ash dumps, which disperse fine ash particles around the environment, and toxic materials and salts are leached into groundwater. Revegetating fly ash dumps has proven to be the best way to stabilise the ash both physically and chemically. However, the establishment of vegetation cover at such sites is severely hampered by the unfavourable physical and chemical properties of the unweathered ash, which contains high amounts of potentially toxic elements (PTEs). This chapter provides an overview and discusses the most important issues related to the establishment of vegetation cover at FA

disposal sites and the role of plants in stabilising pollutants and mitigating their negative effects as well as their role in soil formation processes. Natural vegetation plays an essential role due to its tolerance to numerous stress conditions caused by pollution and its ability to accumulate PTEs. It has been established that the use of natural plants by means of auxiliary restoration of vegetation cover with the support of appropriate agronomic practices (integrated biotechnological approach) can effectively help control the spread of PTEs and support the phytoremediation of this type of environment. The overview has revealed that ash weathering and the development of vegetation have positive effects on the physical and chemical characteristics of wet FAs. Positive changes were manifested in the morphology and texture of ash, a decrease in alkalinity and salinity, the development of horizon A due to the accumulation of organic matter and an increase in organic carbon, nitrogen, phosphorus and adsorption capacity. These changes were most pronounced in the upper layer of the FA and are important indicators of the onset of soil formation processes. It is concluded that these processes and the time elapsed after the revegetation are the main driving factors. They are extremely important for the successful ecological reclamation of fly ash disposal sites and long-term environmental protection.

O. Kostić (✉) · M. Mitrović · P. Pavlović
Department of Ecology, Institute for Biological
Research ‘Siniša Stanković’ – National Institute of
the Republic of Serbia, University of Belgrade,
Bulevar despota Stefana 142, 11060 Belgrade,
Serbia
e-mail: olgak@ibiss.bg.ac.rs

Keywords

Coal fly ash · Disposal sites · Bare/unweathered · Revegetated/weathered · Physico-chemical properties · Initial soil formation

22.1 Introduction

Environmental pollution caused by coal combustion in thermal power plants is a complex and serious phenomenon. Its negative effects on the living world have been studied intensively over the last few decades (Carlson and Adriano 1993; Sushil and Batra 2006; Pavlović and Mitrović 2013; Pandey and Singh 2010, 2012; Pandey et al. 2015; Sarwar et al. 2017; Buha-Marković et al. 2020). The widespread use of fossil fuels contributes to emissions of hazardous substances into the air, and the deposition of the fly ash produced in the combustion process results in a deterioration in the quality of soil and groundwater, which serve as a sink for dumping solid and liquid wastes (Sawidis et al. 2011; Kostić et al. 2015). In addition to the direct deposition of contaminants in soil as point-source pollution, these activities, due to complex environmental processes, can result in their dispersion across the surrounding areas and also much further afield, i.e. leading to indirect air, soil and water contamination through soil, water or atmospheric deposition (Tarazona 2014; Pavlović et al. 2019). Different pollutants, particularly potentially toxic elements (PTEs), affect human health and the environment in different ways depending on their properties, such as their potential for dispersion, solubility, bioavailability and carcinogenicity (Tchounwou et al. 2012; Panagos et al. 2013; Pavlović et al. 2018). Among them, heavy metals stand out as extremely hazardous because they can accumulate in extremely high concentrations due to their poor biodegradability and, as a result, can pollute drinking water, soil, feed and food and threaten the life of people, plants, animals and microorganisms (Rajaganapathy et al. 2011; Minnikova et al. 2017; Zwolak et al. 2019; Hong

et al. 2020; Kinuthia et al. 2020). Disposal sites of coal fly ash, a by-product from thermal power plants, are a constant source of pollution due to the ash's light texture and high PTE content. For this reason, they are considered one of the biggest causes of environmental degradation and pollution (Carlson and Adriano 1993; Pavlović et al. 2004; Kostić et al. 2015; Bhatia 2020). The growing scale of this worldwide problem is highlighted by recent estimates suggesting that there will be a 53% increase in electricity consumption by 2035 with fossil fuel combustion, mainly coal, making up approximately 90% of its production (Yao et al. 2015). This will result in an exponential growth in global FA levels, which amounted to 777.1×10^9 kg in 2010, and it is predicted that they will reach 2000×10^9 kg by 2020 (ACAA 2001; Heidrich et al. 2013). At present, the largest FA-producing countries in the world are China (395×10^9 kg), the USA (118×10^9 kg) and India (105×10^9 kg), while somewhat less is produced in Europe (EU-15; 52.6×10^9 kg), Africa and the Middle Eastern (32.2×10^9 kg), Russia (26.6×10^9 kg), the rest of Asia (16.7×10^9 kg), Australia (13.1×10^9 kg), Japan (11.1×10^9 kg) and Canada (6.8×10^9 kg) (Heidrich et al. 2013). In developed countries, the average utilisation rate of FA in the construction material industry and in soil amelioration, with the aim of improving its physical and chemical properties, has increased over the last decades from 30 to 53%, ranging from 10.6% in Africa and the Middle East, 13.8% in India, 18.8% in Russia, 33.8% in Canada, 42.1% in the USA, 45.8% in Australia, 67.1% in China, 66.5% in the rest of Asia, 90.9% in the EU-15, to as high as 96.4% in Japan (Asokan et al. 2005; Heidrich et al. 2013; Yao et al. 2015). However, FA utilisation only amounts to 25% globally, meaning the remainder must be treated as waste. It is dumped in open areas near thermal power plants, and, unfortunately, the area of such sites is constantly increasing (Pavlović and Mitrović 2013; Yao et al. 2015). According to some estimates, FA disposal sites cover approximately 3235 km^2 of fertile, potentially agricultural land across the

world (Pandey and Singh 2012). By way of illustration, there is the example of China, where every tonne of fly ash occupies 0.27–0.33 ha of soil (He et al. 2012).

In general, FA is deposited in landfill wet or dry in accordance with national standards that impose specific requirements in terms of site selection and measures to be implemented to prevent wind dispersal, leakage and runoff. Dry ash deposition includes filling pits, mine shafts or strip-mine areas, or creating dry ash dumps for this purpose. Meanwhile, wet ash deposition involves transporting a mixture of ash and water (in a suitable ratio, 1:10 or less) as slurry through pipes and depositing it in lagoons or wet ash ponds (US EPA 1988, Fig. 22.1). The spread of small FA particles in the environment and the leaching of toxic elements and salts into the groundwater confirm that these dumps pose a serious global and environmental threat to the entire living world (Adriano et al. 2002; Georgakopoulos et al. 2002; Pandey and Singh 2010; Pandey et al. 2010, 2011; Weber et al. 2017; Tsiptsias et al. 2020). In a number of countries, high concentrations of heavy metals in the water (Ruhl et al. 2010) and soil (Petaloti et al. 2006; Keegan et al. 2006; Papaefthymiou 2008; Zhai et al. 2009) near thermal power plants have often been noted, correlated with the prevailing wind direction (Sawidis et al. 2011; Dragović et al. 2013; Raja et al. 2015; Čujić et al. 2017; Dalton et al. 2018). This can be a cause of health problems for the residents of nearby settlements (US EPA 2007). While the whole point of creating ash dumps is to protect the environment, the measures taken cannot completely prevent the ash spreading by wind, leakage and runoff at many such sites, and it still covers a significant area (Haynes 2009).

In this sense, revegetation is a useful, plant-based decontamination technology, which has been favoured over the last few decades for the mitigation of these negative effects and for the ecological reclamation of degraded areas arising

from FA deposition (Pavlović et al. 2004; Mitrović et al. 2008; Haynes 2009; Pandey et al. 2016; Gajić et al. 2018; Roy et al. 2018). The creation of vegetation cover in landfills of residential complexes, i.e. restoring the vegetation cover, leads to the physical and chemical stabilisations of this mobile substrate. Plants absorb and bind toxic chemical elements by their root system, preventing them from spreading and leaching, which helps improve the overall quality of such habitats (Carlson and Adriano 1993; Vajpayee et al. 2000; Balatincez and Kretschmann 2001; Haynes 2009; Pandey et al. 2009, 2012; Técher et al. 2012). Even so, unfavourable physical and chemical conditions (tendency to compaction, poor water/air ratios, high alkaline reaction and salinity, lack of nitrogen and available phosphorus) and a high content of PTEs often inhibit natural rooting and plant survival on bare ash (Gupta et al. 2002; Pavlović et al. 2004; Mitrović et al. 2008; Haynes 2009; Pandey and Singh 2010; Ram et al. 2015; Kostić et al. 2018). For this reason, the natural colonisation of plant species on FA dumps occurs extremely slowly without human intervention and can be measured for decades. Even then, the pollution problem is not completely solved (Cheung et al. 2000; Juwarkar and Jambhulkar 2008; Ram et al. 2008; Krzaklewski et al. 2012). Hence, assisted revegetation using naturally growing plant species from the surrounding areas, which have already adapted to local ecological conditions, is the best method for shortening the natural process of colonisation of FA dumps (landfills). In addition, it facilitates the creation of dense and relatively species-rich vegetation to reduce the mobility of contaminants (Pandey and Singh 2012; Pandey 2015; Żołnierz et al. 2016; Panda et al. 2020a).

This chapter presents the most important issues related to the role of fly ash landfill plants in stabilising pollutants (PTEs) and mitigating the hazardous environmental impacts of fly ash deposition. In addition, it defines the most important physical and chemical properties of

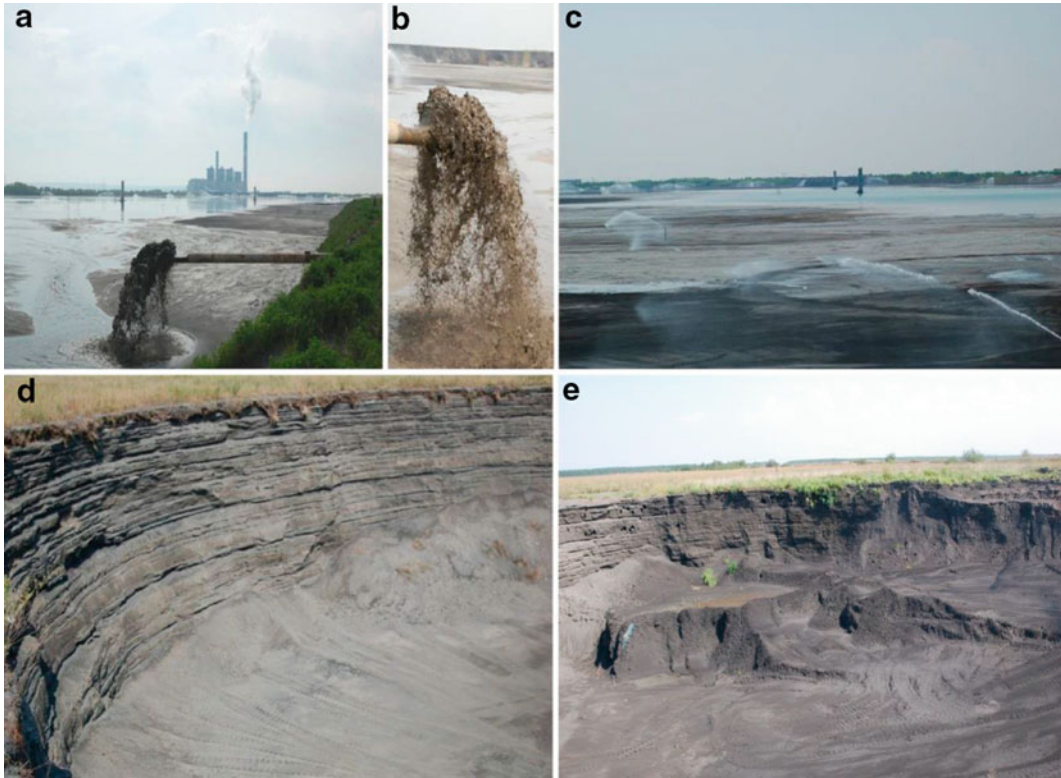


Fig. 22.1 Discharge of fly ash into a wet ash pond using a wet disposal system (**a**, **b** and **c**), and fly ash deposits after water have drained away (**d** and **e**), at the ash

disposal site of the “Nikola Tesla A” thermal power plant in Obrenovac, Serbia (*photographs by Olga Kostić*)

ash and the content of PTEs, which have negative effects on the growth and development of plants at FA dumps (landfills) and, therefore, directly affect the potential for the phytoremediation of ash deposits. Furthermore, some ecophysiological characteristics of the plants that spontaneously colonise FA disposal sites are discussed. These plants are candidates for the revegetation and phytoremediation of such sites due to their tolerance of pollution and their ability to accumulate PTEs. Particular attention is paid to how the development and succession of vegetation improves the physical and chemical characteristics of ash. These attributes are important indicators of the success of both revegetation and processes initiating soil formation. They are also of exceptional importance for the successful ecological reclamation of ash disposal sites.

22.2 How the Physical and Chemical Characteristics of Fly Ash Affect the Revegetation of Fly Ash Disposal Sites

Unweathered and unvegetated ash is characterised by extremely diverse physical and chemical characteristics and toxicity. Its characteristics depend not only on the type of coal, geological origin and chemical and mineral composition but also on the technological process of coal combustion, including the temperature, content of unburned residues, characteristics of emission control devices, methods of ash transportation and deposition (Adriano et al. 1980; Haynes 2009; Izquierdo and Querol 2012). These characteristics of FA are also key factors

determining the creation of plantations on the ash disposal sites (Pandey et al. 2009; Haynes 2009; Yao et al. 2015).

The major components of FA are metallic oxides with different levels of unburned carbon (Yao et al. 2015). Ash typically has an aluminosilicate matrix, as evidenced by levels of basic oxides—in descending order: $\text{SiO}_2 > \text{Al}_2\text{O}_3 > \text{Fe}_2\text{O}_3 > \text{CaO} > \text{MgO} > \text{K}_2\text{O}$, as presented in Table 22.1. There are two classes of fly ash, defined according to their chemical composition or minimum content of the sum of $\text{SiO}_2 + \text{Al}_2\text{O}_3 + \text{Fe}_2\text{O}_3$ in the ash—Class F (>70%) and Class C (>50%) (American Society for Testing and Materials, ASTM C618-05). Class F fly ash is characterised by a low CaO content (<10%); in Class C fly ash, it is somewhat higher (>15%). Class C fly ash is produced from the combustion of sub-bituminous coal or lignite and is characterised by high pozzolanic activity, i.e. the ability to harden and strengthen in the presence of water (Kalinski and Yerra 2006). The deposition of this type of ash at disposal sites that are exposed to weathering results in the formation of solid cemented layers. This layer is usually found at a depth of around 10–20 cm, which can hinder precipitation runoff and significantly hamper plant root penetration and growth and the

establishment of plant cover (Carlson and Adriano 1993; Haynes 2009).

Unweathered ash has a sandy texture with a dominant sand fraction (82–97%) and a much lower clay fraction (1–2%) (Table 22.2). This texture, as well as the absence of clay minerals and humus, results in a weak binding of ash particles, high porosity (>70%) and low to medium bulk density (Weber et al. 2015). For this reason, unweathered FA is characterised by a low adsorption capacity (Kostić et al. 2018; Uzarowicz et al. 2018a; Table 22.3) and relatively low water-holding and nutrient retention capacity (Pavlović et al. 2004; Técher et al. 2012; Weber et al. 2015).

The pH value of the ash/water system mainly depends on the Ca/S molar ratio in the ash, although other minor alkalis or alkaline earth cations may also contribute to the balance (Ward et al. 2009; Izquierdo and Querol 2012; Yao et al. 2015). Based on the Ca/S ratio, the pH of raw fly ash can vary from 4.5 to 12, with most ashes being alkaline (Carlson and Adriano 1993; Bilski et al. 1995; Kolbe et al. 2011; Table 22.3). The high alkalinity of FA leads to a deficit of essential macronutrients (P) and micronutrients (Fe, Mn, Zn and Cu), as these elements form insoluble compounds in alkaline conditions,

Table 22.1 Silicate analysis of different types of FA

Silicate analysis of FA (%)							
	Lignite FA ^a	Bituminous FA ^a	Sub to bituminous FA ^a	Serbia ^b	Australia ^c	India ^c	Denmark ^c
SiO_2	15–45	20–60	40–60	60–70	31.4–68.55	38.5–63.2	39.4–40.3
Al_2O_3	10–25	5–35	20–30	11–27	21.58–32.96	20.6–26.2	25.7–27.7
Fe_2O_3	4–15	10–40	4–10	8.87	0.95–27.06	4.9–11.0	8.8–11.4
CaO	15–40	1–12	5–30	4–8	0.05–3.88	1.3–3.6	2.2–2.5
MgO	3–10	0–5	1–6	1.6–2.8	0.02–1.55	1.3–25.9	15.1–18.6
SO_3	0–15	0–4	0–2	0.7–1.8	ND–0.16	–	–
P_2O_5	–	–	–	0.05–0.2	0.03–2.02	–	–
Na_2O	0–6	0–4	0–2	0.2–0.7	ND–0.15	0.4–2.6	1.3–2.3
K_2O	0–4	0–3	0–4	0.5–0.7	0.12–0.73	0.2–2.9	–
TiO_2	–	–	0–3	0.3–1.0	1.24–2.31	0.3–1.3	0.1–0.3
LOI	0–5	0–15	0–3	–	–	–	–

^aHeidrich et al. (2013); ^bSimonović (2003); ^cPathan et al. (2003); LOI—loss on ignition; ND—not detected

Table 22.2 Physical properties of FA

Physical properties	Bare/unweathered ash	Revegetated/weathered ash	Period (years)	Country	References
Sand (%)	82	76–87	11	Poland	Weber et al. (2015)
	97.11	95.26	3	Serbia	Kostić et al. (2018)
	97.11	54.18	11	Serbia	Kostić et al. (2018)
	93	79	20	Poland	Uzarowicz et al. (2018a)
	93	63	30	Poland	Uzarowicz et al. (2018a)
Silt (%)	17	11–13	11	Poland	Weber et al. (2015)
	1.11	3.86	3	Serbia	Kostić et al. (2018)
	1.11	42.76	11	Serbia	Kostić et al. (2018)
	6	19	20	Poland	Uzarowicz et al. (2018a)
	6	33	30	Poland	Uzarowicz et al. (2018a)
Clay (%)	1	2–11	11	Poland	Weber et al. (2015)
	1.78	0.87	3	Serbia	Kostić et al. (2018)
	1.78	3.06	11	Serbia	Kostić et al. (2018)
	1	2	20	Poland	Uzarowicz et al. (2018a)
	1	4	30	Poland	Uzarowicz et al. (2018a)

which are less available to plants (Carlson and Adriano 1991; Adriano et al. 2002). At the same time, in alkaline conditions, the solubility of As, B, Cr, Mo, Se, Sb, V and W increases, which can lead to them having an increased level in plant tissues, while the solubility of Cd, Co, Hg, Ni, Pb and Sn decreases (Page et al. 1979; Adriano et al. 1980; Izquierdo and Querol 2012). In addition, the high pH of ash can have a harmful effect on the microorganisms that participate in N fixing, by decreasing their number (Gupta et al. 2002).

Unweathered ash is characterised by a large amount of soluble salts, particularly potentially

toxic boron salts, since no leaching by precipitation has taken place (Table 22.3). Specifically, for some types of fly ash, EC values can be extremely high, even $>13 \text{ dS m}^{-1}$, which is another limiting factor for the establishment of vegetation (Page et al. 1979; Carlson and Adriano 1993), since the EC threshold for sensitive plants is 1.5 dS m^{-1} (Maas 1990). Salinity stress slows down plant growth by affecting the normal functioning of physiological processes such as photosynthesis, respiration, nitrogen fixation and carbohydrate metabolism (Chen et al. 2008; Stavridou et al. 2020). Moreover, increased

Table 22.3 Chemical properties of FA

Chemical properties	Bare/unweathered ash	Revegetated/weathered ash	Revegetation/Weathering period (years)	Country	References
pH	8.54	8.41	2	India	Chu (2008)
	8.5	7.3–7.7	11	Poland	Weber et al. (2015)
	9.5	8.53–9.08	14	India	Pandey et al. (2015)
	9.5	8.35–8.88	24	India	Pandey et al. (2015)
	11.3–14.9 _{KCl}	7.1	60	Poland	Uzarowicz et al. (2017)
	8.03	7.78	3	Serbia	Kostić et al. (2018)
	8.03	7.72	11	Serbia	Kostić et al. (2018)
	8.7–11	8.5–8.7	20	Poland	Uzarowicz et al. (2018a)
	8.7–11	7.9–9.0	30	Poland	Uzarowicz et al. (2018a)
EC (dS/m) μS/cm	4.8	2.18	2	India	Chu (2008)
	1.02	0.158–0.612	11	Poland	Weber et al. (2015)
	0.15	0.073–0.112	14	India	Pandey et al. (2015)
	0.15	0.052–0.091	24	India	Pandey et al. (2015)
	0.353	0.203	3	Serbia	Kostić et al. (2018)
	0.353	0.184	11	Serbia	Kostić et al. (2018)
	2.09–2.56	1.32–1.48	20	Poland	Uzarowicz et al. (2018a)
	2.09–2.56	1.07–1.46	30	Poland	Uzarowicz et al. (2018a)
CEC (cmol kg ⁻¹)	36.78	41.85	3	Serbia	Kostić et al. (2018)
	36.78	68.72	11	Serbia	Kostić et al. (2018)
	34.7	55.6–66.8	20	Poland	Uzarowicz et al. (2018a)
	34.7	51.7–72.3	30	Poland	Uzarowicz et al. (2018a)
BS (%)	100	88	3	Serbia	Kostić et al. (2018)
	100	82	11	Serbia	Kostić et al. (2018)
	99.4–100	98.9–99.1	20	Poland	Uzarowicz et al. (2018a)
	99.4–100	98.2–99.2	30	Poland	Uzarowicz et al. (2018a)

(continued)

Table 22.3 (continued)

Chemical properties	Bare/unweathered ash	Revegetated/weathered ash	Revegetation/Weathering period (years)	Country	References
C (%)	0.21	0.61	2	India	Chu (2008)
	0.41–1.12	2.9–3.2	3	India	Juwarkar and Jambhulkar (2008)
	2.1	0.5–1.3	11	Poland	Weber et al. (2015)
	0.00	0.17–0.78	14	India	Pandey et al. (2015)
	0.00	0.31–1.11	24	India	Pandey et al. (2015)
	0–1.7	9.9–19.9	60	Poland	Uzarowicz et al. (2017)
	3.19	2.03	3	Serbia	Kostić et al. (2018)
	3.19	1.46	11	Serbia	Kostić et al. (2018)
	1.2–6.9	1.9–38.8	20	Poland	Uzarowicz et al. (2018a)
	1.2–6.9	1.3–37.1	30	Poland	Uzarowicz et al. (2018a)
N (%)	0.0214	0.404	2	India	Chu (2008)
	0.031–0.182	0.38–0.82	3	India	Juwarkar and Jambhulkar (2008)
	0.00	0.02–0.14	11	Poland	Weber et al. (2015)
	0.02	0.04–0.06	14	India	Pandey et al. (2015)
	0.02	0.05–0.08	24	India	Pandey et al. (2015)
	0–0.01	0.29–0.74	60	Poland	Uzarowicz et al. (2017)
	0.02	0.09	3	Serbia	Kostić et al. (2018)
	0.02	0.19	11	Serbia	Kostić et al. (2018)
	0.03	0.09–0.9	20	Poland	Uzarowicz et al. (2018a)
	0.03	0.02–0.88	30	Poland	Uzarowicz et al. (2018a)

(continued)

Table 22.3 (continued)

Chemical properties	Bare/unweathered ash	Revegetated/weathered ash	Revegetation/Weathering period (years)	Country	References
C/N	-	9.6–27	11	Poland	Weber et al. (2015)
	190.4	27.0–34.5	60	Poland	Uzarowicz et al. (2017)
	159.5	22.56	3	Serbia	Kostić et al. (2018)
	159.5	7.68	11	Serbia	Kostić et al. (2018)
	33–197	20–42	20	Poland	Uzarowicz et al. (2018a)
	33–197	15–42	30	Poland	Uzarowicz et al. (2018a)
K ₂ O (mg/100 g)	3–12	170–200	3	India	Juwarkar and Jambhulkar (2008)
	21.1	10.4–17.5	11	Poland	Weber et al. (2015)
	15.00	38.20	3	Serbia	Kostić et al. (2018)
	15.00	59.50	11	Serbia	Kostić et al. (2018)
P ₂ O ₅ (mg/100 g)	12–26	170–190	3	India	Juwarkar and Jambhulkar (2008)
	0.8	0.8–26.2	11	Poland	Weber et al. (2015)
	0.136	1.021–2.023	14	India	Pandey et al. (2015)
	0.136	1.406–2.514	24	India	Pandey et al. (2015)
	7.49	25.32	3	Serbia	Kostić et al. (2018)
	7.49	12.81	11	Serbia	Kostić et al. (2018)

salinity reduces the osmotic potential and impairs the uptake of ions, which leads to their imbalance or even toxicity. This disturbs metabolic and enzyme activity and membrane functioning (Hasegawa et al. 2000; Arif et al. 2020; Gupta et al. 2021). This is why, in the initial stages of the colonisation of bare ash, plants that are naturally adapted to high salt levels (halophytes) can appear, or even plants that can be categorised as invasive based on their characteristics.

For example, at the TENT-A disposal site in Obrenovac (Serbia), species were found that they naturally grow in salt deserts and on the seashores as well as in other semiarid habitats of the Mediterranean region, such as the halophytes *Salsola sp.* (through natural colonisation) and *Tamarix tentandra* (planted with the aim of stabilisation/preventing ash dispersal). Tamarisk was planted at this disposal site due to its high tolerance to salt-induced stress (Newete et al.

2019). It can tolerate salt concentrations of up to 15,000 ppm (Carman and Brotherson 1982). At the same time, in addition to these halophytes, unweathered ash is also colonised by invasive ruderal plant species such as *Conyza canadensis*, *Xanthium strumarium*, *Asclepias syriaca* and *Oenothera biennis*.

An extremely low N and C content (resulting from the oxidation of organic C and N during coal combustion) is another main limiting factor for plant growth (Carlson and Adriano 1993; Haynes 2009) (Table 22.3). Carbon in unweathered ash is formed exclusively from particles of unburned coal, and not from organic matter, which plays a significant role in providing plants with water, nutrients and energy, particularly due to the sandy texture of FA. However, at the initial stages of revegetation in ash dumps, even this kind of carbon can partially compensate for the lack of organic matter in FA (Fettweis et al. 2005). Bare ash is also characterised by a low

content of available P and K (Table 22.3). The deficit of these essential nutrients in plants growing on FA results from their precipitation with large amounts of soluble Ca and the creation of insoluble compounds of P with Fe and Al at the high pH of unweathered ash (Adriano et al. 1980; Cheung et al. 2000; Chu 2008; Kostić et al. 2018).

Unweathered FA is also characterised by a frequently excessive level of total PTE content, which is a significant indicator of the total level of contamination (Table 22.4). Even so, the leaching and bioavailability of elements are affected not only by their total content but also by their volatility during coal combustion conditions, operating parameters, the transport system, their different chemical forms, their binding state, metal properties, environmental factors, organic matter content and the physical and chemical properties of the ash (Bódog et al. 1996; Popović et al. 2001; Jankowski et al. 2006; Haynes 2009;

Table 22.4 Concentrations of major elements including PTEs in FA

Element (mg kg ⁻¹)	Typical concentration in FA ^a	India ^b	Greece ^c	Serbia ^d	Normal range in soil ^e	*Critical total concentration in soil ^f
As	2.0–70	5–68	20.8	158–172	0.1–30	20–50
B	2.0–5000	100–1000	0.3	410–980	1–134	–
Ba	0.01–1.0	26–1275	229.4	890	–	–
Cd	0.1–100	1–26	1.49	<3		3–8
Co	1.0–100	7–128	18.7	12		25–50
Cr	3.0–900	10–353	148.9	310–385	1.4–1100	75–100
Cu	10.0–2000	39–1000	74.9	132–225	1–100	60–125
Hg	0.01–12	0–0.005	–	0.21		0.3–5
Mn	30.0–3000	–	218.3	380–812	7–9200	1500–3000
Mo	1.0–250	8–100	7.25	16	0.1–7.2	2–10
Ni	10.0–3000	29–265	217.4	122–205	1–110	100
Pb	3.0–500	10–144	62.4	126		100–400
Sb	0.8–25	–	0.82	–		–
Se	0.2–50	1–10	9.97	<2	0.005–1.9	5–10
V	–	40–190	116.2	254		–
Zn	10.0–1000	10–250	130.0	107–125	3.5–362	70–400

^aHaynes (2009); ^bAsokan et al. (2005); ^cGeorgakopoulos et al. (2002); ^dPavlović et al. (2004); Kostić et al. (2018); ^eKabata-Pendias and Pendias (2001); ^fAlloway (1990); *The critical total concentration in soil is the level above which toxicity to plants is possible

Izquierdo and Querol 2012; Krgović et al. 2014; Kostić et al. 2018).

Specifically, during combustion, the mineral fraction of coal undergoes various transformations, such as decomposition, volatilisation, fusion, agglomeration and condensation. As a result, chemical elements in the original coal matrix become susceptible to leaching, particularly when in contact with water, or during transport and deposition in landfills (Jones 1995). During coal combustion, susceptible elements (B, As, Cr, Hg, Cl, Se, S, Cd, Cu, Mo, Sb, V and Zn) are leached from the surface layer of FA particles, which is few microns thick. Meanwhile, in the inner layer, the elements not directly exposed to leaching accumulate (Mn, Ni, Ba, Co and Pb), meaning that their release depends on the dissolution of elements in the surface layer (Jones 1995; Iyer 2002; Kukier et al. 2003). The release of elements in the silicate matrix of ash requires a long period of exposure to the effects of weathering (Theis and Wirth 1977). Leach tests carried out on FA samples classified B as a highly mobile element (>70% extractable fraction) and as a mobile element (30–70% extractable fraction), while Cr, Zn, Cu, Ni and Mn were categorised as less mobile elements (<30% extractable fraction) (Querol et al. 1996). Ash has been found to leach most of its soluble B in just 15 min of contact with water, making it one of the most significant environmental pollutants (Weber et al. 2015; Cox et al. 1978). The solubility of As in water ranges from 0.001–25 to 52%: more is released from acidic fly ash as the pH increases, while this tendency is reversed in alkaline fly ash (Querol et al. 2001; Moreno et al. 2005). The water-leachable amount of Zn in alkaline fly ash varies widely, from 0.02 to 0.2 mg/kg (Moreno et al. 2005; Izquierdo and Querol 2012). The mobility progressively increases with decreasing pH, attaining extractable proportions of 3–9% (Kim and Hesbach 2009). The amount of mobile Cu has been estimated at 2.6% (Sočo and Kalemekiewicz 2007); the mobility progressively increases with decreasing pH, attaining extractable proportions of 8%. The continuous release of B, Zn, Cr, Ni and As during the hydraulic transport and

dumping of ash means that these elements are highly significant pollutants (Popović et al. 2001; Kostić et al. 2018). As the liquid/solid ratio and the time spent in contact with water increases, the risk that FA poses to the environment increases proportionally (Ibrahim 2015; Jankowski et al. 2006). However, numerous studies have shown that the total content of PTEs in FA decreases even after its deposition, although to a lesser extent (Maiti and Jaiswal 2008; Mitrović et al. 2008; Pandey 2012; Kostić et al. 2018). This may be caused by an improvement in the physico-chemical properties of FA and an increase in the content of organic matter. This has a positive effect on the sorption characteristics of ash after the formation of vegetative cover as well as the precipitation of elements for the formation of secondary solids, which are more stable when ash interacts with water (Kabata-Pendias and Pendias 2001; Jankowski et al. 2006; Kostić et al. 2018; Tables 22.2, 22.3 and 22.4).

22.3 The Importance of Revegetation at Ash Disposal Sites

The unfavourable physical and chemical properties of bare FA as well as the fact that it is completely devoid of any life form, i.e. it does not act as a “seed bank”, which lead to the formation of biologically empty areas where the FA is deposited. These are initially devoid of any vegetation or have only sparse plant cover (Shaw 1996). However, the weathering of ash leads to the leaching of some phytotoxic elements from the root zone, creating conditions for colonisation by tolerant plants, most of the early colonisers being herbaceous in nature (Chu 2008; Maiti and Jaiswal 2008; Pandey et al. 2015; Pandey 2012; Kostić et al. 2018). Studies on the colonisation of plants in ash dumps have shown that this is a long process, with the formation of woody vegetation taking many years. For example, it took approximately 20 years for willow and poplar woodland (autochthonous plant communities along large rivers) to form at

the ash dump of the Kostolac thermal power plant (Serbia), while beech/willow and oak woodland in England took 25 and 50 years, respectively (Hall 1957; Shaw 1992; Djordjević-Miloradović et al. 2012).

On unweathered ash, in the first few years following deposition, isolated populations of plants most commonly form on the edges of the ash pond. This means that the majority of its surface has no plant cover and is exposed to aeolian erosion and leaching. Hence, the protective function of the vegetation, i.e. the containment of pollutant dispersion, is not fully ensured (Shaw 1992; Pandey 2015). In terms of plant diversity, the number of species naturally found at fly ash landfills varies, from 11 found in China (Chu 2008), 58 in India (Pandey et al. 2015), 84 in Poland (Jasionkowski et al. 2016), to 91 in central Serbia (Kostić et al. 2018) and 125 in southern Serbia (Mustafa et al. 2012). In the initial stages of the colonisation of ash deposits, the dominant group of colonisers comprises herbaceous annuals from the families *Asteraceae* (*Conyza canadensis*) and *Amaranthaceae* (*Chenopodium album* and *Chenopodium botrys*), which are characterised by a short lifecycle, rapid growth and high seed production (Gajić et al. 2018, 2019). *Conyza canadensis* forms a dense vegetative cover on the ash and produces a large amount of organic material both below and above ground, which means it is very important in the formation of humus (Djordjević et al. 2006). The presence of *C.canadensis*, a co-dominant species, in the initial stages of vegetation succession was also found at the fly ash disposal sites in Tennessee (Gonsoulin 1975). During the first stage of colonisation, under conditions of increased salinity, halophyte species such as *Salsola sp.* can be found as well as other species from the *Amaranthaceae* family, which at later stages, with boron leaching, are replaced by species characteristic of grassy/legume/ruderal communities (Shaw 2009). This was the case at the ash disposal site at the Drax thermal power plant in Yorkshire, where there was a succession from halophyte to ruderal species, with a predominance of legumes and grasses (Shaw 1996). The presence of plants

in the *Poaceae* family as another element of original vegetation at ash disposal sites is a result of their resistance to drought and their ability to grow in low nutrient conditions. Their fibrous roots help slow down erosion, increase soil shear strength and preserve soil moisture, while the drying of vegetative parts (roots and shoots) after they die provides nutrients and organic carbon (Maiti and Maiti 2015). This creates more favourable conditions for further colonisation with other plant species. In the early and middle stages of succession, before the invasion of polycarpic perennials, perennial monocarpic herbaceous species appear, which accumulate assimilates in their leaf rosettes (*Oenothera biennis*) or roots (*Daucus carota*) in the autumn and, thus, gain an advantage in terms of colonisation the year after (Djordjević-Miloradović 1998). The perennial species *Calamagrostis epigejos*, *Phragmites communis* and *Festuca rubra* (*Poaceae*), as well as *Tussilago farfara* and *Cirsium arvense* (*Asteraceae*), proliferate in the ash dumps not only by seed spread but also due to the growth of stolons, bulbs, tubers and rhizomes, from which they extract nutrients to survive during unfavourable periods, especially during drought in summer or during cold winters. *C. epigejos*, a common species in various ruderal habitats, vigorously colonises various types of landfill, where it exhibits a competitive advantage over species planted to revegetate them, forming dense, long-lasting and almost monospecific stands (Rebele and Lehmann 2002; Żolnierz et al. 2016; Mitrović et al. 2008; Šourková et al. 2005). The benefit of its presence in such landscapes is manifested in the physical stability of the fly ash, an increased availability of certain nutrients and increased microbial activity (Stefanowicz et al. 2015). Meadow species such as *Festuca arundinacea*, *Festuca rubra*, *Lolium perenne*, *Poa trivialis* and *Poa annua* (*Poaceae*), *Rumex acetosa* (*Polygonaceae*), *Taraxacum officinale* (*Asteraceae*) and *Vicia cracca* (*Fabaceae*) can also be helpful for the restoration of fly ash landfills (Jasionkowski et al. 2016). Legumes are a key plant species that, due to their ability to fix atmospheric nitrogen, are well adapted to growing on fly ash

disposal sites. There, they grow rapidly and enhance substrate characteristics by increasing the organic carbon and total nitrogen content through readily decomposable litter (Jambhulkar and Juwarkar 2009; Maiti and Prasad 2016).

Although a study by Mulhern et al. (1989) showed that herbaceous species grow better on fly ash than woody ones, species from the genera *Acacia*, *Alnus*, *Amorpha*, *Ceanothus*, *Colutea*, *Eleagnus*, *Gleditsia*, *Hippophae*, *Leucaena* and *Robinia* have been found to tolerate unfavourable physico-chemical conditions of fly ash due to their ability to absorb atmospheric N (Hodgson and Townsend 1973; Cheung et al. 2000; Kostić et al. 2018; Woś et al. 2020). Native Central European trees such as species from the genera *Salix*, *Populus* and *Pinus* are also suitable for fly ash reclamation, especially in the early stages of primary succession (Čermák 2008). As already mentioned, colonisation by woody plant species is facilitated by the initial colonisation of herbaceous species as this mitigates the unfavourable physico-chemical properties of bare ash (Kullu and Behera 2011). In the last few decades, numerous studies have focused on trees' ability to adapt to such polluted habitats and, possibly, be used for phytoremediation purposes (Hodgson and Townsend 1973; Duggan and Scanlon 1974; Hodgson and Buckley 1975; Mulhern et al. 1989; Carlson and Adriano 1991, 1993; Rai et al. 2004; Gupta and Sinha 2008; Maiti and Jaiswal 2008; Jamil et al. 2009; Cheung et al. 2000; Agarwal et al. 2011; Bisht et al. 2011; Kostić et al. 2012; Krzaklewski et al. 2012; Mitrović et al. 2012; Pietrzykowski et al. 2015, 2018; Kalashnikova et al. 2020; Woś et al. 2020).

Although they are affected by numerous stress factors, it has been shown that sustainable plant communities can still form on ash if species are chosen that can grow under multiple stress conditions that are critical in this process (Cheung et al. 2000; Rai et al. 2004; Gajić et al. 2016, 2019). It was also found that species differ in terms of their tolerance to stress conditions prevailing in the ash dumps and exhibit different adaptive strategies for survival (Pavlović et al. 2004; Pierzynski et al. 2004; Rai et al. 2004; Gupta and Sinha 2008; Maiti and Jaiswal 2008;

Mitrović et al. 2012; Kostić et al. 2012; Gajić et al. 2013, 2018, 2016). Ecological studies have shown that species must meet the following suitability criteria for the re-vegetation of such habitats:

- must grow naturally in the region and tolerate local climatic and edaphic conditions and pests,
- must be perennials,
- must have high biomass, an extensive root system and the capacity for vegetative multiplication and N-fixation (N-fixers),
- must tolerate unfavourable pH levels, increased salinity and the toxicity of FA,
- must be adapted to nutrient deficits and tolerate extremely high temperatures and drought (Pandey et al. 2009; Pandey and Singh 2011; Pavlović and Mitrović 2013; Pietrzykowski et al. 2018).

Hence, in recent decades, emphasis has been placed on the importance of using plant species that have spontaneously infiltrated this kind of anthropogenically degraded habitat from the immediate surroundings (Shaw 1996; Djurdjević-Miloradović 1998; Pavlović et al. 2004; Djurdjević et al. 2006; Chu 2008; Mitrović et al. 2008; Gupta and Sinha 2008; Kostić et al. 2012; Mitrović et al. 2012; Mustafa et al. 2012; Pandey 2012; Pandey et al. 2012; Gajić et al. 2013; Morariu et al. 2013; Pandey et al. 2015; Żołnierz et al. 2016; Gajić et al. 2018; Panda et al. 2020a). The analysis of different species in different ash dumps has shown that most of those that spontaneously colonise these anthropogenically formed habitats and can be used for revegetation and, potentially, for phytoremediation due to their resistance to adverse conditions, come from the families *Asteraceae*, *Amaranthaceae*, *Poaceae* and *Fabaceae* (Table 22.5).

Sowing and planting tolerant plant species reduces the time required for revegetation through the natural ecological succession of vegetation (Pandey 2015; Żołnierz et al. 2016; Kostić et al. 2018). In addition, ash dumps can be successfully revegetated by increasing plant resilience through the use of ecological

Table 22.5 Overview of plants that spontaneously colonise fly ash disposal sites or that are successfully used for revegetation

Family	Species	References
<i>Aizoaceae</i>	<i>Mesembryanthemum aionis</i> , <i>Mesembryanthemum nodiflorum</i>	Jusaitis and Pillman (1997)
<i>Altingiaceae</i>	<i>Liquidambar styraciflua</i>	Carlson and Adriano (1991)
<i>Amaranthaceae</i>	<i>Amaranthus deflexus</i> , <i>Amaranthus hybridus</i> , <i>Atriplex holocarpa</i> , <i>Atriplex lindleyi</i> , <i>Atriplex vesicaria</i> , <i>Chenopodium acuminatum</i> , <i>Chenopodium album</i> , <i>Enchylaena tomentosa</i> , <i>Halosarcia halocnemoides</i> , <i>Halosarcia pergranulata</i>	Jusaitis and Pillman (1997), Morgenthal et al. (2001), Chu (2008), Gupta and Sinha (2008), Maiti and Jaiswal (2008)
<i>Apiaceae</i>	<i>Daucus carota</i>	Djordjević-Miloradović (1998)
<i>Apocynaceae</i>	<i>Calotropis procera</i>	Gupta and Sinha (2008), Mukhopadhyay et al. (2017)
<i>Asteraceae</i>	<i>Achillea millefolium</i> , <i>Artemisia vulgaris</i> , <i>Blumea lacera</i> , <i>Carduus acanthoides</i> , <i>Cirsium arvense</i> , <i>Crepis setosa</i> , <i>Eclipta alba</i> , <i>Eclipta prostrata</i> , <i>Conyza canadensis</i> , <i>Hieracium spp.</i> , <i>Matricaria indora</i> , <i>Parthenium hysterophorus</i> , <i>Senecio vulgaris</i> , <i>Solidago serotina</i> , <i>Sonchus arvensis</i> , <i>Sonchus oleraceus</i> , <i>Taraxacum officinale</i> , <i>Tussilago farfara</i> , <i>Vernonia cinerea</i> , <i>Xanthium strumarium</i>	Shaw (1992), Djordjević-Miloradović (1998), Pavlović et al. (2004), Gupta and Sinha (2008), Dwivedi et al. (2008), Maksimović et al. (2008), Mustafa et al. (2012), Jasionkowski et al. (2016), Mukhopadhyay et al. (2017), Gajić et al. (2018)
<i>Betulaceae</i>	<i>Alnus incana</i> , <i>Alnus glutinosa</i> , <i>Alnus viridis</i> , <i>Betula pubescens</i> , <i>Betula pendula</i>	Krzaklewski et al. (2012), Pietrzykowski et al. (2015), Pietrzykowski et al. (2018), Kalashnikova et al. (2020)
<i>Boraginaceae</i>	<i>Echium vulgare</i>	Mustafa et al. (2012)
<i>Brassicaceae</i>	<i>Diplotaxis tenuifolia</i> , <i>Lepidium bonariensis</i> , <i>Sinapis nigra</i> , <i>Sisymbrium loeselii</i> , <i>Sisymbrium orientale</i>	Djordjević-Miloradović (1998), Morgenthal et al. (2001), Mustafa et al. (2012)
<i>Caryophyllaceae</i>	<i>Silene vulgaris</i>	Djordjević-Miloradović (1998)
<i>Combretaceae</i>	<i>Terminalia arjuna</i>	Agarwal et al. (2011)
<i>Convolvulaceae</i>	<i>Ipomea carnea</i>	Pandey (2012), Pandey et al. (2015)
<i>Cyperaceae</i>	<i>Cyperus esculentus</i> , <i>Cyperus rotundus</i> , <i>Fimbristylis polytrichoides</i> , <i>Pycneus glomeratus</i>	Djordjević-Miloradović (1998), Chu (2008), Mukhopadhyay et al. (2017)
<i>Dennstaedtiaceae</i>	<i>Pteridium aquilinum</i>	Chu 2008
<i>Elaeagnaceae</i>	<i>Elaeagnus angustifolia</i>	Djordjević et al. (2006)
<i>Equisetaceae</i>	<i>Equisetum ramosissimum</i>	Dwivedi et al. (2008)
<i>Euphorbiaceae</i>	<i>Croton bonplandianum</i> , <i>Ricinus communis</i>	Pandey (2013), Mukhopadhyay et al. (2017), Panda et al. (2020b)
<i>Fabaceae</i>	<i>Acacia auriculiformis</i> , <i>Acacia lebeck</i> , <i>Acacia nilotica</i> , <i>Amorpha fruticosa</i> , <i>Bauhinia variegata</i> , <i>Cassia siamea</i> , <i>Cassia surattensis</i> , <i>Cassia tora</i> , <i>Chamaecrista bienis</i> , <i>Cicer arietinum</i> , <i>Dalbergia sissoo</i> , <i>Genista ovata</i> , <i>Lespedeza cuneata</i> , <i>Leucaena leucocephala</i> , <i>Lotus corniculatus</i> , <i>Medicago</i>	Gutenmann et al. (1976), Mulhern et al. (1989), Shaw (1992), Dželetović and Filipović (1995), Shaw (1996), Cheung et al. (2000), Vajpayee et al. (2000), Morgenthal et al. (2001), Gupta et al. (2004), Pavlović et al. (2004), Rai et al. (2004), Tripathi et al. (2004), Sinha and Gupta (2005), Djurdjević

(continued)

Table 22.5 (continued)

Family	Species	References
	<i>lupulina, Medicago sativa, Melilotus officinalis, Ononis spinosa, Pithecellobium dulce, Pongamia pinnata, Prosopis juliflora, Robinia pseudoacacia, Sesbania cannabina, Trifolium pretense, Trifolium repens, Vicia sativa, Vicia cracca</i>	et al. (2006), Jambhulkar and Juwarkar (2009), Gupta and Sinha (2008), Maksimović et al. (2008), Pandey et al. (2009), Agarwal et al. (2011), Djordjević-Miloradović et al. (2012), Kostić et al. (2012), Mustafa et al. (2012), Pandey et al. (2015), Jasionkowski et al. (2016), Pandey et al. (2016), Woś et al. (2020)
Hypericaceae	<i>Hypericum perforatum</i>	Mustafa et al. (2012), Djordjević-Miloradović (1998)
Limnanthaceae	<i>Limnanthes spp.</i>	Dwivedi et al. (2008)
Malvaceae	<i>Sida cordifolia</i>	Gupta and Sinha (2008)
Myrtaceae	<i>Syzygium cumini</i>	Agarwal et al. (2011)
Moraceae	<i>Morus alba,</i>	Agarwal et al. (2011)
Nitrariaceae	<i>Nitraria billardieri</i>	Jusaitis and Pillman (1997)
Onagraceae	<i>Epilobium collinum, Oenothera biennis,</i>	Pavlović et al. (2004), Gajić et al. (2013)
Plantaginaceae	<i>Plantago lanceolata</i>	Mustafa et al. (2012)
Platanaceae	<i>Platanus occidentalis</i>	Carlson and Adriano (1991)
Poaceae	<i>Agropyron elongatum, Agrostis capillaries, Alopecurus myosuroides, Arrhenatherum elatius, Brachiaria serrata, Bromus arvensis, Bromus sterilis, Calamagrostis epigejos, Chloris gayana, Cynodon dactylon, Dactylis glomerata, Dendrocalamus strictus, Digitaria eriantha, Eleusine indica, Eragrostis sp., Festuca arundinacea, Festuca rubra, Heteropogon contortus, Holcus lanatus, Hyparrhenia hirta, Lolium perenne, Miscanthus × giganteus, Neyraudia reynaudiana, Panicum repens, Phragmites communis, Poa annua, Poa trivialis, Puccinellia maritime, Saccharum bengalense, Saccharum munja, Saccharum spontaneum, Setaria sphacelate, Sorghum halepense, Sorghum vulgare var. sudanense, Tristachya leucothrix, Vulpia myuros,</i>	Mulhern et al. (1989), Shaw (1996), Morgenthal et al. (2001), Van Rensburg et al. (2003), Djurdjević et al. (2006), Maiti and Nandhini (2006), Chu (2008), Dwivedi et al. (2008), Maksimović et al. (2008), Mitrović et al. (2008), Pandey et al. (2009), Djordjević-Miloradović et al. (2012), Mustafa et al. (2012), Pandey et al. (2012), Técher et al. (2012), Gajić et al. (2013, 2016), Pandey et al. (2015), Jasionkowski et al. (2016), Żołniercz et al. (2016)
Polygonaceae	<i>Rumex acetosella, Rumex crispus</i>	Mustafa et al. (2012), Jasionkowski et al. (2016)
Salicaceae	<i>Populus alba, P. nigra, Salix alba</i>	Shaw (1992), Pavlović et al. (2004), Djordjević-Miloradović et al. (2012), Kostić et al. (2012)
Scrophulariaceae	<i>Verbascum phlomoides</i>	Pavlović et al. (2004)
Solanaceae	<i>Solanum nigrum, Solanum surattense</i>	Dwivedi et al. (2008), Pandey et al. (2016)
Tamaricaceae	<i>Tamarix chinensis, Tamarix galica, Tamarix tetrandra</i>	Chu (2008), Pavlović et al. (2004), Kostić et al. (2012)
Thelypteridaceae	<i>Thelypteris dentate</i>	Kumari et al. (2013)
Typhaceae	<i>Typha latifolia</i>	Maiti and Jaiswal (2008), Pandey et al. (2014, 2015)

engineering and an integrated biotechnological approach (Pandey and Singh 2012). In particular, apart from using suitable plant species such as legumes, grasses and other tolerant species, assisted revegetation includes biological intervention involving various low-cost, readily available fertilisers and organic amendments (i.e. press mud, paper factory sludge, boulder clay, farmyard manure, compost, sewage sludge, etc.), site-specific native microbes and mycorrhizal inoculation (Cheung et al. 2000; Rai et al. 2004; Juwarkar and Jambhulkar 2008; Ram et al. 2008; Hryniewicz et al. 2009; Jambhulkar and Juwarkar 2009; Babu and Reddy 2011; Krzaklewski et al. 2012; Pandey 2015; Kostić et al. 2018).

Successful revegetation and the establishment of a sustainable plant cover through human intervention begin with the use of grasses and legumes (genera: *Agropyron*, *Arrhenatherum*, *Cynodon*, *Dactylis*, *Festuca*, *Lolium*, *Phleum*, *Phragmites*, *Poa*, *Saccharum*, *Lotus*, *Medicago*, *Vicia*, etc.). Besides stabilising the ash physically, this also improves its physico-chemical properties and enables colonisation by subsequent species (Mitrović et al. 2008; Gajić et al. 2016; Pandey 2015; Kostić et al. 2018; Gajić et al. 2020) (Fig. 22.2).

The natural succession of invasive native species should be accompanied by plantations of tolerant, ecologically and socioeconomically suitable shrub and tree species from the genera *Acacia* (*A. nilotica*, *A. auriculiformis*, *A. catechu*, *A. lebbek*), *Albizia* (*A. lebbek*, *A. procera*), *Acer*, *Alnus*, *Betula*, *Casuarina* (*C. equisetifolia*), *Cassia* (*C. siamea*), *Dalbergia* (*D. sissoo*), *Dendrocalamus* (*D. strictus*), *Eucalyptus* (*E. globulus*, *E. hybrid*, *E. tereticornis*), *Leucaena* (*L. leucocephala*), *Liquidambar* (*L. styraciflua*), *Pinus*, *Platanus* (*P. occidentalis*) *Populus* (*P. deltoids*, *P. euphratica*, *P. alba*), *Prosopis* (*P. juliflora*, *P. cineraria*), *Ricinus*, *Robinia* (*R. pseudoacacia*), *Salix*, *Sesbania*, *Tamarix* (*T. tetrandra*) and *Tectona* (*T. grandis*). This would not only lead to the development of a productive, richly diverse ecosystem, but would also ensure bioenergy conservation, carbon sequestration, biogeochemical and hydrological cycling as well

as phytoremediation (Carlson and Adriano 1991; Shaw 1992; Cheung et al. 2000; Isebrands and Karnosky 2001; Pavlović et al. 2004; Čermák 2008; Juwarkar and Jambhulkar 2008; Pandey et al. 2009; Kostić et al. 2012; Pandey 2015; Pietrzykowski et al. 2018; Roy et al. 2018; Kalashnikova et al. 2020; Panda et al. 2020b; Woś et al. 2020).

Phyto-stabilising plants are of great importance for the revegetation of ash dumps since, by immobilising PTEs in their roots and rhizosphere, they reduce their mobility, leaching and ecotoxicity. By covering the substrate effectively, they also prevent the dispersion of particles and erosion caused by wind and surface runoff, i.e. they provide physical and chemical phytostabilisations of the FA (Barton et al. 2005; Vangronsveld et al. 2009). By increasing the content of organic matter in the ash, these plants improve the unfavourable physico-chemical properties of ash and, through their decomposition and mineralisation, the nutritive and biological characteristics of this substrate are significantly improved over time. All these contribute to the successful revegetation of the fly ash dumps, on the one hand, and the initiation of soil formation processes on the other (Juwarkar and Jambhulkar 2008; Pandey et al. 2015; Kostić et al. 2018).

22.4 Changes in the Physical and Chemical Properties of Fly Ash During Weathering and Revegetation—Indicators of Early Paedogenesis

So far, most studies on the revegetation of fly ash deposits have focused on species selection and vegetation establishment techniques (Mitrović et al. 2008; Kostić et al. 2012; Pandey 2015; Żolnierz et al. 2016), while changes in the physical and chemical properties of the FA during deposition and revegetation, the impact of these changes on the behaviour of contaminants and the developing ash-derived soil have not been given enough attention (Haynes 2009). However, people also play an important role in soil formation: there is an anthropogenic impact

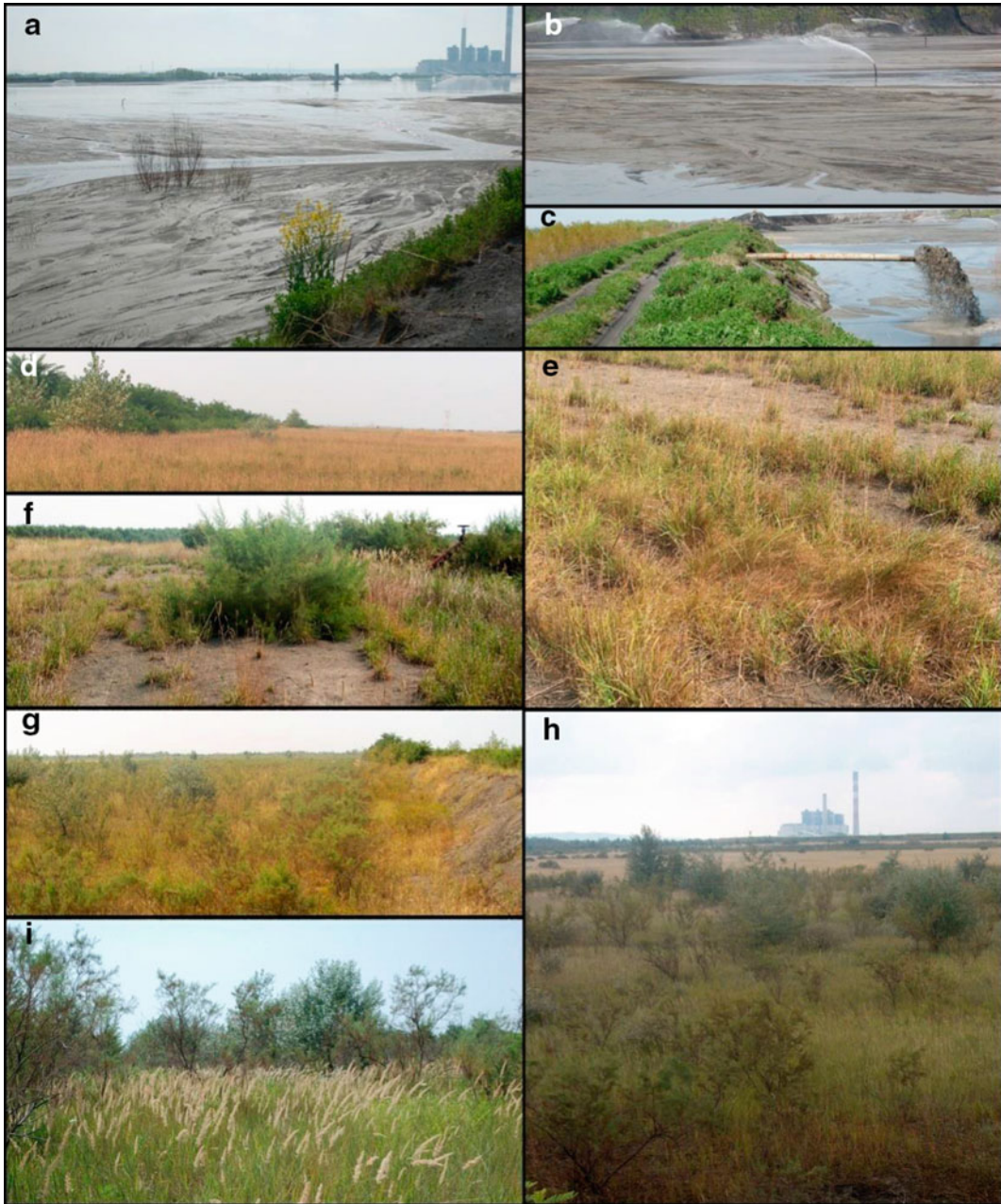


Fig. 22.2 Assisted revegetation at the ash disposal site of the “Nikola Tesla A” thermal power plant, Obrenovac, Serbia: discharge of fly ash into an active ash pond (**a–c**); revegetation of an inactive ash pond using a grass/legume

mix—age of vegetation: 3-year old (**d–f**); spontaneous colonisation of a passive ash pond—age of vegetation: 11-year old (**g–i**) (photographs by *O. Kostić*)

due to the formation of technogenic parent materials and the alteration of paedogenesis conditions (De Kimpe and Morel 2000; Richter 2007; Hout et al. 2015). Therefore, the World Reference Base for Soil Resources now recognises a specific reference soil group, technogenic soils (Technosols)—soils containing more than 20% materials created or modified by industrial activities (WRB 2006). Similarly to natural substrates, technogenic parent materials evolve under the influence of soil-forming factors such as climate, plant development, animals and microorganisms (Shaw 1992; Zevenbergen et al. 1999; Filcheva et al. 2000; Zikeli et al. 2002, 2004; Chu 2008; Arocena et al. 2010; Alday et al. 2012; Zhao et al. 2013; Hout et al. 2015; Kostić et al. 2018). In terms of the climate's impact on Technosols, the development of organic horizons in soils formed in coal quarry tailing dumps was found to be less pronounced in arid environments (Sokolov et al. 2015).

The success of the revegetation of ash dumps is conditioned by many factors, the most important being the initial processes of soil formation. The importance of initiating these processes is high, particularly when the revegetation occurs directly on ash, bearing in mind the extremely unfavourable physico-chemical properties of the raw FA (Tables 22.3 and 22.4). The best way to study the soil formation process on ash is to recognise and investigate the sequence of soils developed on the same parent material (Zikeli et al. 2002, 2004; Kostić et al. 2018; Uzarowicz et al. 2018a, b). This is due to the fact that this chronosequence includes soils that differ from each other in certain physico-chemical characteristics due to the passage of time as a soil-forming factor (Stevens and Walker 1970).

Soil formation on ash deposits is a very slow and lengthy process, lasting several decades (Shaw 1992; Weber et al. 2015), with the time elapsed since restoration being the main driving agent (Shaw 1992; Alday et al. 2012). The management and long-term disposal of FA in open areas expose it to the constant influence of natural factors (weathering and vegetation cover). This leads to changes in its physico-chemical and mineralogical characteristics,

which are a crucial precondition for the formation of a sustainable vegetative cover and the successful long-term phytoremediation of FA wastelands. The most important indicators of this process are a decrease in ash alkalinity, salinity and toxicity, a change in the morphology, texture and physical properties of the ash, the development of an A soil horizon due to the accumulation of soil organic matter and an increase in organic carbon (C), nitrogen (N), various phosphorus fractions and its adsorptive capacity. These transformations are most pronounced in the upper layer of FA, from several centimetres to several dozen centimetres in thickness (Shaw 1992; Zevenbergen et al. 1999; Cheung et al. 2000; Zikeli et al. 2002, 2004; Chu 2008; Juwarkar and Jambhulkar 2008; Weber et al. 2015; Uzarowicz and Zagórski 2015; Pandey et al. 2015; Uzarowicz et al. 2017; Tomaszewicz et al. 2018; Kostić et al. 2018; Uzarowicz et al. 2018a, 2018b; Konstantinov et al. 2020) (Table 22.6).

The rapid and intense weathering that was often reported during the early paedogenesis of Technosols can be explained by the disequilibrium between technogenic materials and environmental conditions (Séré et al. 2010). For instance, substantial mineral weathering may occur when materials are subjected to the transition from a reducing environment to an oxidising one at the surface when materials containing soluble salts are subjected to rainfall-driven leaching (Page et al. 1979; Carlson and Adriano 1993; Grünwald et al. 2007; Séré et al. 2010; Scholtus et al. 2014). Likewise, the properties of the materials, such as a reduction in particle size and low crystallinity, together with extreme physical and chemical conditions promoting material alterations (high or low pH, high temperature, high humidity), may also favour mineral weathering (Hout et al. 2015). In the initial stages of alkaline ash weathering, crystalline aluminosilicate particles of FA decompose relatively quickly, affected by external environmental factors and high pH. They form particles of aluminosilicate clay, which provide a physical and chemical barrier (coating, encapsulating and incorporating) restricting the leaching of the

Table 22.6 Case studies of the impact of FA management on its physical, chemical and mineralogical properties and early paedogenesis

Study site	Objectives	Age (years)	Observations	References
Rye House power station, Lee Valley, southern England	Vegetative cover and soil development on abandoned pulverised fuel ash	7–24	Vegetation succession is typical of disturbed habitats. Shrubs from the genera <i>Salix</i> and <i>Betula</i> appear after 10–15 years, <i>Salix/Betula</i> woodland after 25 years. Decline in pH and increase in litter depth and mass with site age. Vertical gradient of all examined soil variables. Soil development is more closely correlated with site age than with plant community composition	Shaw (1992)
Ramagundam, India and Hørsholm, Denmark	Chemical properties of two types of ash in tropical and cool oceanic climates	10	Weathering affects the chemical properties of ash (e.g. an increase in CEC and oxalate-extractable Al and Si and a decrease in pH). Neofomed clay composition is independent of coal source and weathering climate. Rapid clay formation provides physical and chemical immobilisation of toxic HMs. In the long term, fly ash can be converted into fertile soil capable of supporting agriculture	Zevenbergen et al. (1999)
Tsang-Tsui Lagoon, Castle Peak Power Station, China	Evaluation of <i>Acacia auriculiformis</i> and <i>Leucaena leucocephala</i> for growth on lagoon ash ameliorated with amendments (30% vermiculate or sewage sludge) both with and without N ₂ -fixing bacteria inoculation		Both ameliorants improved the physical properties of the lagoon ash by increasing porosity and aeration for root development. Sewage sludge compost increased the nutrient levels of the infertile lagoon. <i>Acacia auriculiformis</i> had better growth performance than <i>Leucaena leucocephala</i>	Cheung et al. (2000)
Lignite ash landfills in Saxony-Anhalt, Germany	Changes in the physical and chemical properties of naturally weathered lignite ashes, differing in age and methods of disposal (landfills and sluicing to settling ponds)	5–30	Soil development was established at all sites as well as the downward movement of gypsum and decarbonisation in the topsoils of the profiles. pH 7–8 indicated a rapid initial release of substances and the transformation of non-	Zikeli et al. (2002)

(continued)

Table 22.6 (continued)

Study site	Objectives	Age (years)	Observations	References
			weathered compounds to more stable ones. Paedogenic organic carbon enriched by ruderal vegetation. An increased C:N ratio with profile depth, indicating the input of organic matter into topsoils	
Lignite ash landfills in Saxony-Anhalt, Germany	Evaluation of cation exchange properties of natural weathered lignite-ash substrates, differing in terms of age and methods of disposal (landfills and sluicing to settling ponds)	5–32	At pH 8.1, lignite-ash-derived soils had a higher CEC (25.1–88.8 cmol _c kg ⁻¹) in ash at dumped landfills than in ash at lagoons. The influence of the parent material was more important than the degree of weathering. The content of total organic C (consisting of paedogenic organic matter and coked lignite particles), together with the content of silt and clay, played a statistically significant role in determining the CEC	Zikeli et al. (2004)
West lagoon, Deep Bay, Hong Kong	Relationship of naturally colonising vegetation and chemical properties of the fly ash	2	Vegetated ash has significantly reduced salinity and extractable Na, Al, Mn, K and Pb, and an increased organic C content compared with bare ash	Chu (2008)
Khaperkheda thermal power station, Khaperkheda, Maharashtra State, India	Impact of biological intervention (organic amendments and nitrogen-fixing strains) on the restoration and revegetation of fly ash	1–3	Biological amendments enhance biomass production and improve the physical characteristics of FA (infiltration rate, bulk density, water holding capacity, porosity), its chemical characteristics (N, P, K, and organic matter content) and its microbiological characteristics. Increased organic matter content complexes metals such as Cd, Cu, Ni and Pb and decreases their toxicity properties	Juwarkar and Jambhulkar (2008)
FA landfill of the Adamów Power Plant, Turek, Poland	Impact of revegetation, fertilisation and the addition of different materials (sewage sludge	11	An improvement in several substrate properties in the topsoil (structure, neutralisation of the	Weber et al. (2015)

(continued)

Table 22.6 (continued)

Study site	Objectives	Age (years)	Observations	References
	and boulder clay) on the physical and chemical properties of fly ash		reaction, leaching of salts and CaCO ₃ and an increase in P and N content) was established. Even so, the period of 11 years was too short for the development of genetic soil horizons, i.e. the development of Regosols or Technosols	
Thermal power stations and landfills in Poland: “Łaziska” (bituminous coal) in Łaziska Górne and “Patnów” and “Konin” (lignite) in Konin, Poland	Establishing the mineral and chemical composition of technogenic soils (Technosols) developed from fly ash		Soils developed from waste derived from the combustion of bituminous coal consisted mainly of mineral phases inherited from the “fresh” ash, while soils developed from waste derived from the combustion of lignite were more complex	Uzarowicz and Zagórski (2015)
FA deposits at the Feroze Gandhi Unchahar Thermal Power Plant, Raebareli, Uttar Pradesh, India	Identification of potential plant species for the restoration of FA deposits	10–24	Fly ash from the rhizosphere of the dominant species (<i>Saccharum spontaneum</i> , <i>Saccharum bengalense</i> , <i>Typha latifolia</i> and <i>Cynodon dactylon</i>) is characterised by lower pH, EC, average porosity and water holding capacity, and higher total organic carbon, available P and N, total N and microbial biomass carbon than bare fly ash	Pandey et al. (2015)
Abandoned ash disposal sites of thermal power stations: “Łaziska” in Łaziska Górne, southern Poland (bituminous coal), and “Patnów” and “Konin” in Konin, central Poland (Miocene lignite)	Analysis of the properties of technogenic soils (Technosols), derived from the ash resulting from the combustion of bituminous coal and lignite, classification, the establishment of indicators of early paedogenesis	<5–60	Technosol properties are primarily influenced by the type of ash (fly ash vs. bottom ash), the fuel type (bituminous coal vs. lignite), the mode of ash deposition and the type of disposal site (settling pond vs. dry landfill), the accumulation of soil organic matter and climatic/weather conditions (leaching of soluble compounds by water from precipitation). The development of soil structure in the A horizon related to the accumulation of soil organic matter was observed, as were a	Uzarowicz et al. (2017)

(continued)

Table 22.6 (continued)

Study site	Objectives	Age (years)	Observations	References
			decrease in pH (from strongly alkaline towards less alkaline or acidic), the formation of paedogenic carbonates and their subsequent leaching from topsoil and the release of oxalate-extractable Al and Si during paedogenesis. The soils studied were classified according to the WRB as Spolic Technosols (or Leptic Spolic Technosols) with various supplementary qualifiers (Alcalic or Eutric, Arenic and/or Loamic, Calcic or Protocalcic, Fluvic, Hyperartefactic, Loxic, Relocatic, Tephric or Vitric)	
“Dolna Odra” power plant, Nowe Czarnowo (West Pomeranian Province), Poland	Analysis of the properties of soils developed on the basis of black coal ash		Reclamation of black coal ash landfill sites, involving the imposition of a layer of material enriched in organic matter, resulting in the formation of anthropogenic soils suitable for afforestation	Tomaszewicz et al. (2018)
“Nikola Tesla” thermal power plant, Obrenovac, Serbia	Influence of weathering and vegetation development on changes in the physical and chemical properties of FA	3–11	Weathering and revegetation processes caused an increase in the clay and silt fractions, a reduction in alkalinity and salinity, and an increase in CEC, total N and available P and K content, particularly in the surface layer (0–10 cm) over time. The initiation of soil formation processes allowed the spontaneous colonisation of new plants and, in later stages, an increase in diversity (55 species after 3 years and 80 species after 11 years). A reduction in the total content of As, B, Cr, Cu, Mn, Ni and Zn and their mobility were also established	Kostić et al. (2018)

(continued)

Table 22.6 (continued)

Study site	Objectives	Age (years)	Observations	References
Bełchatów thermal power station, Poland	Characterisation of morphological, physical and chemical indicators of the paedogenesis of technogenic soils (Technosols) developed on fly ash and bottom ash settling ponds	Several months to 30 years	Indicators of early paedogenesis were determined: changes in the consistency of ash material due to root action, the accumulation of soil organic matter in topsoil and the formation of O and A horizons, a decrease in pH and salinity, an increase in total N and the formation of paedogenic carbonates	Uzarowicz et al. (2018a)
Abandoned ash disposal sites of thermal power stations: “Łaziska”, Łaziska Górne, southern Poland (bituminous coal), and “Patnów” and “Konin”, Konin, central Poland (Miocene lignite)	Determining mineral transformation in technosols derived from FA resulting from the combustion of bituminous and lignite coals	<5–60	Technosols developed from bituminous coal ash contained mineral phases inherited from the ash (aluminosilicate glass, mullite, quartz, magnetite, hematite and traces of maghemite and barite) as the predominant constituents. Technosols developed from lignite ash contained aluminosilicate glass, quartz and hematite inherited from fly ash as well as a variety of secondary minerals (vaterite, calcite, bassanite, gypsum, ettringite, hydrotalcite and brucite), which were formed as an effect of rapid mineral transformations after ash deposition	Uzarowicz et al. (2018b)
Ash dumps of Tyumen combined heat and power (CHP-1) plant, Russia	Soil formation and properties of soils formed in areas of self-overgrown ash disposal sites formed due to peat combustion	30	The main indicators of paedogenic processes are the formation of humus horizons, the decrease in alkalinity in the upper part of the profile, the disturbance of the primary stratification of the parent material and the formation of paedogenic carbonates	Konstantinov et al. (2020)

PTEs that are mobilised during the dissolution of crystalline particles. In the long term, under conditions of free drainage, this can initiate the conversion of fly ash into fertile soil that may even be capable of supporting agriculture (Zevenbergen et al. 1999). Unlike soils that are developed from FA derived from bituminous coal combustion, which consist mainly of mineral phases inherited from the raw FA, soils developed on FA derived from lignite combustion are more complex, with a variety of secondary minerals, such as vaterite, calcite, bassanite, gypsum, ettringite, hydrotalcite and brucite (Uzarowicz and Zagórski 2015; Uzarowicz et al. 2018b). The fine roots of initial vegetation can retain clay particles from FA and contribute to the granulation of the substrate, which can also be achieved through the addition of different amendments (Cheung et al. 2000; Juwarkar and Jambhulkar 2008; Weber et al. 2015; Tomaszewicz et al. 2018; Uzarowicz et al. 2018a). Field capacity, porosity and aggregation are most favourable in the root zone (5–10 cm) and at disposal sites where the revegetation process has been established longest and the vegetative cover is the densest (Zhao et al. 2013). In addition, higher clay content can lead to a more favourable water regime, the development of capillarity and a higher amount of water available to plants (Weber et al. 2015).

Ash deposition in wet ash ponds and weathering reduce the amount of carbonates and soluble salts, which are significant limiting factors for the initial establishment of plant cover at FA disposal sites (Zevenbergen et al. 1999; Zikeli et al. 2002; Chu 2008; Haynes 2009; Weber et al. 2015; Pandey et al. 2015; Uzarowicz et al. 2017; Uzarowicz et al. 2018a). As a result of leaching, soluble compounds can precipitate into deeper layers (secondary calcite in cracks) and lead to the formation of calcic, gypsic or sodic horizons (Zikeli et al. 2002, 2005; Howard et al. 2013; Huot et al. 2014; Santini and Fey 2015). Cracks formed by the plant roots also contribute to the leaching of salts by initiating a preferential downward water flow (Kostić et al. 2018).

The development of vegetation at ash disposal sites is the only source of organic matter in the

substrate through the input of litter and fine roots, i.e. the accumulation of carbon, nitrogen and other essential macro- and micro-elements in the surface layer of FA ponds (Shaw 1992; Zikeli et al. 2002, 2004; Chu 2008; Weber et al. 2015; Pandey et al. 2015; Uzarowicz et al. 2018a; Kostić et al. 2018). The accumulation of organic matter depends on the nature and the density of the vegetative cover. Moreover, as vegetation ages, there is an increase in the content of C originating from decomposed organic material (Néel et al. 2003; Pandey et al. 2015). The accumulation of organic matter and humic acids as products of fly ash transformation causes a decrease in the ash pH levels (Djurđević et al. 2006; Weber et al. 2015; Kostić et al. 2018). This may have a negative effect on the adsorptive complex and the behaviour of contaminants (Zikeli et al. 2004). Even so, an increase in the clay and silt fraction, along with the accumulation of organic material in the surface layer of the fly ash, has a positive impact by increasing the cation exchange capacity (CEC) (Zevenbergen et al. 1999; Zikeli et al. 2004; Kostić et al. 2018). The clay material can react with the organic matter produced during revegetation of the site. Thus, the developing soil will effectively sequester C, leading to the rapid accumulation of organic matter and the formation of a large soil microbial community (Zikeli et al. 2004; Machulla et al. 2004). Sometimes, organic C derived from unburned coal can hide the true extent of the plant phytoremediation potential (Djurđević et al. 2006). However, according to Fettweis et al. (2005), it can partially compensate for the lack of C originating from decomposed organic material in the first few decades. Hence, determining the C:N ratio is a much better indicator of soil organic matter formation (Zikeli et al. 2002; Kostić et al. 2018). The duration of the revegetation process also has a favourable impact on N content, which is one of the main limiting factors for the establishment of plant cover in the early stages of revegetation (Juwarkar and Jambhulkar 2008; Haynes 2009; Weber et al. 2015; Pandey et al. 2015; Kostić et al. 2018; Uzarowicz et al. 2018a). Although N accumulation at the beginning of the process can result from the use of fertilisers,

organic amendments and amelioration measures, the decomposition of the N-fixing plant litter, which is desirable in the early stages of revegetation, contributes to a significant increase (Cheung et al. 2000; Gupta et al. 2002; Juwarkar and Jambhulkar 2008; Kostić et al. 2015; Tomaszewicz et al. 2018; Pietrzykowski et al. 2018). The increase in nutrient levels (N, P and K) in the surface layers of the ash is a result of both the accumulation of dead plant parts and an increase in the CEC, thanks to the accumulation of humus (Pandey et al. 2015; Kostić et al. 2018).

It has been established that organic matter from the initial vegetation improves both the physical properties of the ash (bulk density, water holding capacity, aeration, temperature and structure) and its chemical properties (cation exchange capacity and nutrient content), and the matter's decomposition and mineralisation regulate the nutrient content and flow. This confirms that the nutritive, biological and microbiological characteristics of fly ash can improve significantly over time (Djurdjević et al. 2006; Walker and del Moral 2009; Pandey and Singh 2012; Pandey et al. 2015). Thus, conditions are created for colonisation by subsequent species, which means that plant succession and soil chronosequences develop concomitantly, increasing the success of re-vegetation (Shaw 1992; Chu 2008; Kostić et al. 2018). The appearance of tree species and an increase in their number and cover projection shows that planted and naturally colonising herbaceous species help improve the initially extremely unfavourable conditions. This accelerates the colonisation of less resistant and tolerant tree species, increasing the diversity and functionality of plant communities on ash dumps (Kullu and Behera 2011; Kostić et al. 2012; Pavlović et al. 2004). Due to their high growth rate, constant biomass productivity, deep root system and better soil aggregation, tree species make a significant contribution to the improvement of physical and chemical characteristics and play a very important role in the phytostabilisation of FA disposal sites, reducing pollution in the long term (Zhao et al. 2013).

22.5 Conclusion

Fly ash, a product of coal combustion in thermal power plants, is a hazardous material that, if not utilised, is treated as industrial waste and is deposited on land in the immediate vicinity of the power plant. From there, fine ash particles are dispersed throughout the environment, and toxic materials and salts are leached into groundwater, which means these areas become a permanent source of pollution and pose an environmental risk to the environment.

The creation of vegetation cover (revegetation) at the FA disposal sites ensures the physical and chemical stabilisation of this mobile and toxic substrate, since plants absorb and bind toxic chemical elements through their root system or accumulate them in the above-ground parts, preventing their spread and leaching. This improves the overall quality of such landscapes. In addition to the phyto-stabilisation of PTEs, this type of vegetation cover has other beneficial properties, including an improvement in the physical and chemical properties of fly ash, which differs greatly from the unweathered/bare ash. Specifically, the mineral weathering of ash and deposition of organic matter due to revegetation induces the process of soil formation, which will ensure the long-term, sustainable management of ash disposal sites. The best indicators of this process are a change in the morphology, texture and physical properties of ash, a decrease in ash alkalinity and salinity, the development of horizon A due to the accumulation of soil organic matter and an increase in the content of organic matter, carbon (C), nitrogen (N), various fractions of phosphorus and the ash's adsorptive capacity. These transformations are most noticeable in the upper layer.

Soil formation on ash deposits is a long and very slow process, in which the time elapsed after the revegetation is the main driving factor. It influences the effect of the landfill on the environment by binding PTEs and other contaminants, stabilising the FA landfill in the long term, and protecting the surrounding environment.

Acknowledgements This work was supported by the Ministry of Education, Science and Technological Development of Serbia, grant no. 451-03-9/2021-14/ 200007.

References

- ACAA (American Coal Ash Association) (2001) Proceedings of the 14th international symposium on management and use of Coal Combustion Products (CCPs). Alexandria, VA
- Adriano DC, Page AL, Elsewi AA, Chang AC, Straughan I (1980) Utilization and disposal of fly ash and other coal residues in terrestrial ecosystems: a review. *J Environ Qual* 9(3):333–344. <https://doi.org/10.2134/jeq1980.00472425000900030001x>
- Adriano DC, Weber J, Bolan NS, Paramasivan S, Koo BJ, Sajwan KS (2002) Effects of high rates of coal fly ash on soil, turfgrass, and groundwater quality. *Water Air Soil Poll* 139:365–385. <https://doi.org/10.1023/A:1015895922471>
- Agarwal D, Agarwal MK, Yunus M, Gautam SK (2011) Phytoremediation of fly ash by assessing growth responses of the local tree species. *J Pure App Sci Technol* 1(2):123–134
- Alday JG, Marrs RH, Martinez-Ruiz C (2012) Soil and vegetation development during early succession on restored coal wastes: a six-year permanent plot study. *Plant Soil* 353(1):305–320. <https://doi.org/10.1007/s11104-011-1033-2>
- Alloway BJ (1990) Heavy metals in soil. Blackie and Son Ltd., London, p 339
- Arif Y, Singh P, Siddiqui H, Bajguz A, Hayat Sh (2020) Salinity induced physiological and biochemical changes in plants: an omic approach towards salt stress tolerance. *Plant Phys Biochem* 156:64–77. <https://doi.org/10.1016/j.plaphy.2020.08.042>
- Arocena JM, van Mourik JM, Schilder MLM, Faz Cano A (2010) Initial soil development under pioneer plant species in metal mine waste deposits. *Restor Ecol* 18 (S2):244–252. <https://doi.org/10.1111/j.1526-100X.2009.00582.x>
- Asokan P, Mohini Saxena S, Asolekar R (2005) Coal combustion residues—environmental implications and recycling potentials. *Resour Conserv Recycl* 43:239–262. <https://doi.org/10.1016/j.resconrec.2004.06.003>
- ASTM C618-05 (2005) Standard specification for fly ash and raw or calcined natural pozzolan for use as mineral admixture in Portland cement concrete. In: Annual book of ASTM standards. ASTM; West Conshohocken, Pennsylvania. <https://www.astm.org/DATABASE.CART/HISTORICAL/C618-05.htm>. Accessed 18 Mar 18 2021
- Babu AG, Reddy MS (2011) Dual inoculation of arbuscular mycorrhizal and phosphate solubilizing fungi contributes in sustainable maintenance of plant health in fly ash ponds. *Water Air Soil Poll* 219:3–10. <https://doi.org/10.1007/s11270-010-0679-3>
- Balatinecz JJ, Kretschmann DE (2001) Properties and utilization of poplar wood. In: Dickmann DI, Isebrands JG, Eckenwalder JE, Richardson J (eds) *Poplar culture in North America*. NRC Research Press, Ottawa, Ontario, Canada, pp 277–291
- Barton C, Marx D, Adriano D, Koo BJ, Newman L, Czapka S, Blake J (2005) Phytostabilization of a landfill containing coal combustion waste. *Environ Geosci* 12 (4):251–265. <https://doi.org/10.1306/eg.06210404021>
- Bhatia A (2020) Coal fly ash from thermal power plants—waste management: a green approach. *Int J Innovative Res Sci Eng Technol (IJIRSET)* 9(5):2634–2640
- Bilski JJ, Alva AK, Sajwan KS (1995) Fly ash. In: Rehcigl JE (ed) *Soil amendments and environmental quality*. Lewis, Boca Raton, pp 237–363
- Bisht SS, Mishra R, Praveen B, Panda AK, Panda KK, Routray A (2011) Phytoremediation studies on coal mine waste and coal fly ash by *Leucaena leucocephala*. *Int J Biosci Biochem Bioinform* 1(4):252–255. <https://doi.org/10.7763/IJBBB.2011.V1.47>
- Bódog I, Polyák K, Csikós-Hartyányi Z, Hlavay J (1996) Sequential extraction procedure for the speciation of elements in fly ash samples. *Microchem J* 54:320–3302
- Buha-Marković JZ, Marinković AD, Nemoda SD, Savić JZ (2020) Distribution of PAHs in coal ashes from the thermal power plant and fluidized bed combustion system; estimation of environmental risk of ash disposal. *Environ Pollut* 266(3):115282. <https://doi.org/10.1016/j.envpol.2020.115282>
- Carlson CL, Adriano DC (1991) Growth and elemental content of two tree species growing on abandoned coal fly ash basins. *J Environ Qual* 20:58–587. <https://doi.org/10.2134/jeq1991.00472425002000030013x>
- Carlson CL, Adriano DC (1993) Environmental impacts of coal combustion residues. *J Environ Qual* 22:227–247. <https://doi.org/10.2134/jeq1993.00472425002200020002x>
- Carman JG, Brotherson JD (1982) Comparisons of sites infested and not infested with Saltcedar (*Tamarix pentandra*) and Russian Olive (*Elaeagnus angustifolia*). *Weed Sci* 30(4):360–364. <http://www.jstor.org/stable/4043625>
- Čermák P (2008) Forest reclamation of dumpsites of coal combustion by-products (CCB). *J For Sci* 54:273–280. <https://doi.org/10.17221/6/2008-JFS>
- Chen HJ, Chen JY, Wang SJ (2008) Molecular regulation of starch accumulation in rice seedling leaves in response to salt stress. *Acta Physiol Plant* 30(2):135–142. <https://doi.org/10.1007/s11738-007-0101-y>
- Cheung KC, Wong JPK, Zhang ZQ, Wong JWC Wong MH (2000) Revegetation of lagoon ash using the legume species *Acacia auriculiformis* and *Leucaena leucocephala*. *Environ Pollut* 109:75–82. [https://doi.org/10.1016/s0269-7491\(99\)00235-3](https://doi.org/10.1016/s0269-7491(99)00235-3)
- Chu LM (2008) Natural revegetation of coal fly ash in a highly saline disposal lagoon in Hong Kong. *Appl Veg Sci* 11:297–306. <https://doi.org/10.3170/2008-7-18427>
- Cox JA, Lundquist GL, Prtyjazny A, Schmulbach CD (1978) Leaching of boron from coal ash. *Environ Sci*

- Technol 12:722–723. <https://doi.org/10.1021/es60142a010>
- Čujić M, Dragović S, Đorđević M, Dragović R, Gajić B (2017) Environmental assessment of heavy metals around the largest coal fired power plant in Serbia. CATENA 148:26–34. <https://doi.org/10.1016/j.catena.2015.12.001>
- Dalton A, Feig GT, Barber K (2018) Trace metal enrichment observed in soils around a coal fired power plant in South Africa. Clean Air J 28(2):1–9. <https://doi.org/10.17159/2410-972x/2018/v28n2a1>
- De Kimpe CR, Morel JL (2000) Urban soil management: a growing concern. Soil Sci 165(1):31–40
- Djordjević L, Mitrović M, Pavlović P, Gajić G, Kostić O (2006) Phenolic acids as bioindicators of fly ash deposit revegetation. Arch Environ Contam Toxicol 50:488–495. <https://doi.org/10.1007/s00244-005-0071-2>
- Đorđević-Miloradović J (1998) Population dynamics of plants in the primary succession of the vegetation on the waste ash deposits of the thermoelectric power station Kostolac. Dissertation/Doctoral thesis, Faculty of Biology, University of Belgrade, Belgrade 459 pp (in Serbian)
- Đorđević-Miloradović J, Miloradović M, Savić M (2012) Recultivation and land planting of deposits of fly ash and tailings in Kostolac, Company for Recultivation and land planting, RIO Kostolac, 136 pp (in Serbian)
- Dragović S, Čujić M, Slavković-Bešković L, Gajić B, Bajat B, Kilibarda M, Onjia A (2013) Trace element distribution in surface soils from a coal burning power production area: a case study from the largest power plant site in Serbia. CATENA 104:288–296. <https://doi.org/10.1016/j.catena.2012.12.004>
- Duggan JC, Scanlon DH (1974) Evaluation of municipal refuse compost for ash pond stabilization. Compost Sci Util 15(1):26–30
- Dwivedi S, Srivastava S, Mishra S, Dixit B, Kumar A, Tripathi KRD (2008) Screening of native plants and algae growing on fly-ash affected areas near National Thermal Power Corporation, Tanda, Uttar Pradesh, India for accumulation of toxic heavy metals. J Hazard Mater 158:359–365. <https://doi.org/10.1016/j.jhazmat.2008.01.081>
- Dželetović Ž, Filipović R (1995) Grain characteristics of crops grown on power plant ash and bottom slag deposit. Resour Conserv Recycl 13:105–113. [https://doi.org/10.1016/0921-3449\(94\)00040-C](https://doi.org/10.1016/0921-3449(94)00040-C)
- Fettweis U, Bens O, Huüttl FR (2005) Accumulation and properties of soil organic carbon at reclaimed sites in the Lusatian lignite mining district afforested with *Pinus* sp. Geoderma 129:81–91. <https://doi.org/10.1016/j.geoderma.2004.12.034>
- Filcheva E, Noustorova M, Gentcheva-Konstadiniva VS, Haigh JM (2000) Organic accumulation and microbial action in surface coal-mine spoils, Pernik, Bulgaria. Ecol Eng 15:1–15. [https://doi.org/10.1016/S0925-8574\(99\)00008-7](https://doi.org/10.1016/S0925-8574(99)00008-7)
- Gajić GM, Djurdjević LA, Kostić OA, Jarić SV, Mitrović MM, Stevanović BM, Pavlović PŽ (2016) Assessment of the phytoremediation potential and an adaptive response of *Festuca rubra* L. sown on fly ash deposits: native grass has a pivotal role in ecorestoration management. Ecol Eng 93:250–261. <https://doi.org/10.1016/j.ecoleng.2016.05.021>
- Gajić G, Djurdjević L, Kostić O, Jarić S, Mitrović M, Pavlović P (2018) Ecological potential of plants for phytoremediation and ecorestoration of fly ash deposits and mine wastes. Front Environ Sci 6. Article 124. <https://doi.org/10.3389/fenvs.2018.00124>
- Gajić G, Djurdjević L, Kostić O, Jarić S, Stevanović B, Mitrović M, Pavlović P (2020) Phytoremediation potential, photosynthetic and antioxidant response to arsenic-induced stress of *Dactylis glomerata* L. Sown on Fly Ash Deposits. Plants 9:657. <https://doi.org/10.3390/plants9050657>
- Gajić G, Mitrović M, Pavlović P (2019) Ecorestoration of fly ash deposits by native plant species at thermal power stations in Serbia. In: Pandey V, Baudh K (eds) Phytomanagement of polluted sites. Elsevier, pp 113–177. <https://doi.org/10.3389/fenvs.2018.00124>
- Gajić G, Pavlović P, Kostić O, Jarić S, Djurdjević L, Pavlović D, Mitrović M (2013) Ecophysiological and biochemical traits of three herbaceous plants growing on the disposed coal combustion fly ash of different weathering stage. Arch Biol Sci 65(4):1651–1667. <https://doi.org/10.2298/ABS1304651G>
- Georgakopoulos A, Filippidis A, Kassoli-Fourmaraki A, Fernández-Turiel HL, Llorens JF, Mousty F (2002) Leachability of major and trace elements of fly ash from Ptolemais power station, Northern Greece. Energy Source 24:103–113. <https://doi.org/10.1080/00908310252774426>
- Gonsoulin JG (1975) A study of plant succession on three TVA fly ash pits in Middle Tennessee. Castanea 40 (1):44–56
- Grünewald G, Kaiser K, Jahn R (2007) Alteration of secondary minerals along a time series in young alkaline soils derived from carbonatic wastes of soda production. CATENA 1(3):487–496. <https://doi.org/10.1016/j.catena.2007.03.022>
- Gupta AK, Rai UN, Tripathi RM, Inouhe M (2002) Impacts of fly ash on soil and plant responses. J Plant Res 115:401–409. <https://doi.org/10.1007/s10265-002-0057-3>
- Gupta, D. K., Rai, U. N., Sinha, S., Tripathi, R. D., Nautiyal, B. D., Rai, P., & Inouhe, M. (2004). Role of Rhizobium (CA-1) inoculation in increasing growth and metal accumulation in *Cicer arietinum* L. growing under fly-ash stress condition. Bull Environ Contam Toxicol 73(2). <https://doi.org/10.1007/s00128-004-0446-5>
- Gupta AK, Sinha S (2008) Decontamination and/or revegetation of fly ash dykes through naturally growing plants. J Hazard Mater 153(3):1078–1087. <https://doi.org/10.1016/j.jhazmat.2007.09.062>
- Gupta S, Schillaci M, Walker R et al (2021) Alleviation of salinity stress in plants by endophytic plant-fungal symbiosis: current knowledge, perspectives and future

- directions. *Plant Soil* 461:219–244. <https://doi.org/10.1007/s11104-020-04618-w>
- Gutenmann WH, Bache CA, Youngs WD, Lisk DJ (1976) Selenium in fly ash. *Science* 191(4230):966–967. <https://doi.org/10.1126/science.1251212>
- Hall IG (1957) The ecology of disused pit heaps in England. *J Ecol* 45:689–720
- Hasegawa PM, Bressan RA, Zhu JK, Bhonert HJ (2000) Plant cellular and molecular responses to high salinity. *Annu Rev Plant Phys* 51:463–499. <https://doi.org/10.1146/annurev.arplant.51.1.463>
- Haynes RJ (2009) Reclamation and revegetation of fly ash disposal sites—challenges and research needs. *J Environ Manage* 90:43–53. <https://doi.org/10.1016/j.jenvman.2008.07.003>
- He Y, Luo Q, Hu H (2012) Situation analysis and countermeasures of China's fly ash pollution prevention and control. *Procedia Environ Sci* 16:690–696. <https://doi.org/10.1016/j.proenv.2012.10.095>
- Heidrich C, Feuerborn HJ, Weir A (2013) Coal combustion products—a global perspective. *VGB Powertech* 12:46–52
- Hodgson DR, Buckley GP (1975) A practical approach towards the establishment of trees and shrubs on pulverized fuel ash. In: Chadwick MJ, Goodman GT (eds) *The ecology of resource degradation and renewal*. Blackwell, Oxford, pp 305–329
- Hodgson DR, Townsend WN (1973) The amelioration and revegetation of pulverized fuel ash. In: Hutnik RJ, Davis G (eds) *Ecology and reclamation of devastated land, vol 2*. Gordon and Breach, London, pp 247–270
- Hong Ya, Liao W, Yan ZhF, Bai YCh, Feng ChL, Xu ZX, Xu DY (2020) Progress in the research of the toxicity effect mechanisms of heavy metals on freshwater organisms and their water quality criteria in China. *J Chem, Hindawi ID* 9010348, pp 12. <https://doi.org/10.1155/2020/9010348>
- Howard JL, Dubay BR, Daniels WL (2013) Artifact weathering, anthropogenic microparticles and lead contamination in urban soils at former demolition sites, Detroit, Michigan. *Environ Pollut* 179:1–12. <https://doi.org/10.1016/j.envpol.2013.03.053>
- Hryniewicz K, Baum C, Niedojadło J, Dahm H (2009) Promotion of mycorrhiza formation and growth of willows by the bacterial strain *Sphingomonas* sp. 23L on fly ash. *Biol Fert Soils* 45:385–394. <https://doi.org/10.1016/j.envpol.2013.03.053>
- Huot H, Simonnot MO, Watteau F, Marion P, Yvon J, De Donato P, Morel JL (2014) Early transformation and transfer processes in a Technosol developing on iron industry deposits. *Eur J Soil Sci* 65:470–484. <https://doi.org/10.1111/ejss.12106>
- Huot H, Simonnot MO, Morel JL (2015) Pedogenetic trends in soils formed in technogenic parent materials. *Soil Sci* 180(4/5):182–192. <https://doi.org/10.1097/SS.0000000000000135>
- Ibrahim LAA (2015) Chemical characterization and mobility of metal species in fly ash–water system. *Water Sci* 29(2):109–122. <https://doi.org/10.1016/wsj.2015.10.001>
- Isebrands JG, Karnosky DF (2001) Environmental benefits of poplar culture. In: Dickmann DI, Isebrands JG, Eckenwalder JG, Richardson J (eds) *Poplar culture in North America, Part A, ch. 6*. Ottawa, ON, NRC Research Press, National Research Council of Canada, pp 207–218
- Iyer R (2002) The surface chemistry of leaching coal fly ash. *J Hazard Mater* 93:321–329. [https://doi.org/10.1016/S0304-3894\(02\)00049-3](https://doi.org/10.1016/S0304-3894(02)00049-3)
- Izquierdo M, Querol X (2012) Leaching behavior of elements from coal combustion fly ash: an overview. *Int J Coal Geol* 94:54–66. <https://doi.org/10.1016/j.coal.2011.10.006>
- Jambhulkar HP, Juwarkar AA (2009) Assessment of bioaccumulation of heavy metals by different plant species grown on fly ash dump. *Ecotox Environ Safe* 72(4):1122–1128. <https://doi.org/10.1016/j.ecoenv.2008.11.002>
- Jamil S, Abhilash PC, Singh N, Sharma PN (2009) *Jatropha curcas*: a potential crop for phytoremediation of coal fly ash. *J Hazard Mater* 172:269–275. <https://doi.org/10.1016/j.jhazmat.2009.07.004>
- Jankowski J, Ward CR, French D, Groves S (2006) Mobility of trace elements from selected Australian fly ashes and its potential impact on aquatic ecosystems. *Fuel* 85:243–256. <https://doi.org/10.1016/j.fuel.2005.05.028>
- Jasionkowski R, Wojciechowska A, Kamiński D, Piernik A (2016) Meadow species in the early stages of succession on the ash settler of power plant EDF Toruń SA in Toruń, Poland. *Ecol Quest* 23:79–86. <https://doi.org/10.12775/EQ.2016.008>
- Jones DR (1995) The leaching of major and trace elements from coal ash. In: Swaine DJ, Goodarzi F (eds) *Environmental aspects of trace elements in coal*. Springer, pp 221–262
- Jusaitis M, Pillman A (1997) Revegetation of waste fly ash lagoons. I. Plant selection and surface amelioration. *Waste Manage Res* 15:307–321. <https://doi.org/10.1006/wmre.1996.0086>
- Juwarkar AA, Jambhulkar HP (2008) Restoration of fly ash dump through biological interventions. *Environ Monit Assess* 139(1–3):355–365. <https://doi.org/10.1007/s10661-007-9842-8>
- Kabata-Pendias A, Pendias H (2001) *Trace elements in soils and plants*. CRC Press LLC, Boca Raton, London, New York, Washington
- Kalashnikova IV, Migalina SV, Ronzhina DA, Ivanov LA, Ivanova LA (2020) Functional response of *Betula* species to edaphic and nutrient stress during restoration of fly ash deposits in the Middle Urals (Russia). *Environ Sci Pollut Res* 28:12714–12724. <https://doi.org/10.1007/s11356-020-11200-5>
- Kalinski ME, Yerra PK (2006) Hydraulic conductivity of compacted cement–stabilized fly ash. *Fuel* 85(16):2330–2336. <https://doi.org/10.1016/j.fuel.2006.04.030>
- Keegan TJ, Farago ME, Thornton I, Hong B, Colville RN, Pesch B, Jakubis P, Nieuwenhuijsen MJ (2006) Dispersion of As and selected heavy metals around a

- coal-burning power station in central Slovakia. *Sci Total Environ* 358(1):61–71. <https://doi.org/10.1016/j.scitotenv.2005.03.020>
- Kim AG, Hesbach P (2009) Comparison of fly ash leaching methods. *Fuel* 88:926–937. <https://doi.org/10.1016/j.fuel.2008.11.013>
- Kinuthia GK, Ngure V, Beti D et al (2020) Levels of heavy metals in wastewater and soil samples from open drainage channels in Nairobi, Kenya: community health implication. *Sci Rep* 10:8434. <https://doi.org/10.1038/s41598-020-65359-5>
- Kolbe JL, Lee LS, Jafvert CT, Murarka IP (2011) Use of alkaline coal ash for reclamation of a former strip mine. In: *Proceedings of 2011 World of Coal Ash (WOCA) Conference*, May 9–12, 2011, Denver, CO, USA
- Konstantinov A, Novoselov A, Konstantinova E, Loiko S, Kurasova A, Minkina T (2020) Composition and properties of soils developed within the ash disposal areas originated from peat combustion (Tyumen, Russia). *Soil Sci Ann* 71(1):3–14. <https://doi.org/10.37501/soilsa/121487>
- Kostić O, Jarić S, Gajić G, Pavlović D, Pavlović M, Mitrović M, Pavlović P (2018) Pedological properties and ecological implications of substrates derived 3 and 11 years after the revegetation of lignite fly ash disposal sites in Serbia. *CATENA* 163:78–88. <https://doi.org/10.1016/j.catena.2017.12.010>
- Kostić O, Mitrović M, Knežević M, Jarić S, Gajić G, Djurdjević L, Pavlović P (2012) The potential of four woody species for the revegetation of fly ash deposits from the ‘Nikola Tesla-A’ thermoelectric plant (Obrenovac, Serbia). *Arch Biol Sci* 64(1):145–158. <https://doi.org/10.2298/ABS1201145K>
- Kostić O, Mitrović M, Vitorović G, Jarić S, Pavlović D, Pavlović M, Gajić G, Pavlović P (2015) Effects of industrial facilities on potential soil contamination in rural settlements of the Belgrade area. In: “Sustainable land use” Scientific Conference, 10 September 2015, Rimski Šančevi, Novi Sad. *Proceedings*, pp 139–146 (In Serbian)
- Krgović R, Trifković J, Milojković-Opsenica D, Manojlović D, Mutić J (2014) Leaching of major and minor elements during the transport and storage of coal ash obtained in power plant. *Sci World J* 212506. <https://doi.org/10.1155/2014/212506> (8 pages)
- Krzaklewski W, Pietrzykowski M, Woś B (2012) Survival and growth of alders (*Alnus glutinosa* (L.) Gaertn. and *Alnus incana* (L.) Moench) on fly ash technosols at different substrate improvement. *Ecol Eng* 49:35–40. <https://doi.org/10.1016/j.ecoleng.2012.08.026>
- Kukier U, Ishak CF, Sumner ME, Miller WP (2003) Composition and element solubility of magnetic and non-magnetic fly ash fractions. *Environ Pollut* 123:255–266. [https://doi.org/10.1016/S0269-7491\(02\)00376-7](https://doi.org/10.1016/S0269-7491(02)00376-7)
- Kullu B, Behera N (2011) Vegetational succession on different age series sponge iron solid waste dumps with respect to top soil application. *Res J Environ Earth Sci* 3(1):38–45
- Kumari A, Pandey VC, Rai UN (2013) Feasibility of fern *Thelypteris dentata* for revegetation of coal fly ash landfills. *J Geochem Explor* 128:147–152. <https://doi.org/10.1016/j.gexplo.2013.02.005>
- Maas EV (1990) Crop salt tolerance. In: Tanji KK (ed) *Agricultural salinity assessment and management*. ASCE Manuals and Reports on Engineering Practice No. 71. American Society of Civil Engineering, New York, pp 262–304
- Machulla G, Zikeli S, Kastler M, Jahn R (2004) Microbial biomass and respiration in soils derived from lignite ashes: a profile study. *J Plant Nutr Soil Sci* 167:449–456. <https://doi.org/10.1002/jpln.200421392>
- Maiti SK, Jaiswal S (2008) Bioaccumulation and translocation of metals in the natural vegetation growing on fly ash lagoons: a field study from Santaldih thermal power plant, West Bengal, India. *Environ Monit Assess* 136:355–370. <https://doi.org/10.1007/s10661-007-9691-5>
- Maiti SK, Maiti D (2015) Ecological restoration of waste dumps by topsoil blanketing, coir-matting and seeding with grass–legume mixture. *Ecol Eng* 77:74–84. <https://doi.org/10.1016/j.ecoleng.2015.01.003>
- Maiti SK, Nandhini S (2006) Bioavailability of metals in fly ash and their bioaccumulation in naturally occurring vegetation: a pilot scale study. *Environ Monit Assess* 116:263–273. <https://doi.org/10.1007/s10661-006-7355-5>
- Maiti D, Prasad B (2016) Revegetation of fly ash—a review with emphasis on grass-legume plantation and bioaccumulation of metals. *Appl Ecol Env Res* 14:185–212. https://doi.org/10.15666/aer/1402_185212
- Maksimović S, Blagojević S, Pivić R, Stanojković A (2008) Quality characteristics of some grass species cultivated on fly-ash deposits of a thermal power station. *Fresen Environ Bull* 17(5):584–588
- Minnikova TV, Denisova TV, Mandzhieva SS, Kolesnikov SI, Minkina TM, Chaplygin VA, Burachevskaya MV, Sushkova SN, Bauer TV (2017) Assessing the effect of heavy metals from the Novocherkassk power station emissions on the biological activity of soils in the adjacent areas. *J Geochem Explor* 174:70–78. <https://doi.org/10.1016/j.gexplo.2016.06.007>
- Mitrović M, Jarić S, Kostić O, Gajić G, Karadžić B, Djurdjević L, Lj O, Pavlović D, Pavlović M, Pavlović P (2012) Photosynthetic efficiency of four woody species growing on fly ash deposits of a Serbian “Nikola Tesla—A” thermoelectric plant. *Pol J Environ Stud* 21(5):1339–1347
- Morariu F, Măsu S, Lixandru B, Popescu D (2013) Restoration of ecosystems destroyed by the fly ash dump using different plant species. *J Anim Sci Technol* 46(2):180–184
- Mitrović M, Pavlović P, Lakušić D, Djurdjević L, Stevanović B, Kostić O, Gajić G (2008) The potential

- of *Festuca rubra* and *Calamagrostis epigejos* for the revegetation of fly ash deposits. *Sci Total Environ* 407:338–347. <https://doi.org/10.1016/j.scitotenv.2008.09.001>
- Moreno N, Querol X, Andrés JM, Stanton K, Towler M, Nugteren H, Janssen-Jurkovicová M, Jones R (2005) Physico-chemical characteristics of European pulverized coal combustion fly ashes. *Fuel* 84:1351–1363. <https://doi.org/10.1016/j.fuel.2004.06.038>
- Morgenthal TL, Cilliers SS, Kellner K, van Hamburg H, Michael MD (2001) The vegetation of fly ash disposal sites at Hendrina Power Station II: floristic composition. *S Afr J Bot* 67:520–532. [https://doi.org/10.1016/S0254-6299\(15\)31184-4](https://doi.org/10.1016/S0254-6299(15)31184-4)
- Mukhopadhyay S, Rana V, Kumar A, Maiti SK (2017) Biodiversity variability and metal accumulation strategies in plants spontaneously inhibiting fly ash lagoon, India. *Environ Sci Pollut Res* 24:22990–23005. <https://doi.org/10.1007/s11356-017-9930-4>
- Mulhern DW, Robel RJ, Furness JC, Hensley DL (1989) Vegetation of waste disposal areas at a coal-fired power plant in Kansas. *J Environ Qual* 18:285–292. <https://doi.org/10.2134/jeq1989.00472425001800030007x>
- Mustafa B, Hajdari A, Krasniqi F, Morina I, Riesbeck F, Sokoli A (2012) Vegetation of the ash dump of the ‘Kosova A’ power plant and the slag dump of the ‘Ferronikeli’ smelter in Kosovo. *Res J Environ Earth Sci* 4(9):823–834
- Néel C, Bril H, Courtin-Nomade A, Dutreuil JP (2003) Factors affecting natural development of soil on 35-year-old sulphide-rich mine tailings. *Geoderma* 111(1):1–20. [https://doi.org/10.1016/S0016-7061\(02\)00237-9](https://doi.org/10.1016/S0016-7061(02)00237-9)
- Newete SW, Allem SM, Venter N, Byrne MJ (2019) Tamarix efficiency in salt excretion and physiological tolerance to salt-induced stress in South Africa. *Int J Phytorem* 22(1):3–9. <https://doi.org/10.1080/15226514.2019.1633997>
- Page AL, Elseewi AA, Straughan IR (1979) Physical and chemical properties of fly ash from coal-fired power plants with reference to environmental impacts. *Residue Rev* 71:83–120. https://doi.org/10.1007/978-1-4612-6185-8_2
- Panagos P, Liedekerke MV, Yigini Y, Montanarella L (2013) Contaminated sites in Europe: review of the current situation based on data collected through a European network. *J Environ Public Health*, vol 2013. Article ID 158764, pp 11. <https://doi.org/10.1155/2013/158764>
- Panda D, Mandal L, Barik J (2020a) Phytoremediation potential of naturally growing weed plants grown on fly ash-amended soil for restoration of fly ash deposit. *Int J Phytoremediat* 22(11):1195–1203. <https://doi.org/10.1080/15226514.2020.1754757>
- Panda D, Mandal L, Barik J, Padhan B, Bisoi SS (2020b) Physiological response of metal tolerance and detoxification in castor (*Ricinus communis* L.) under fly ash-amended soil. *Heliyon* 6(8):e04567. <https://doi.org/10.1016/j.heliyon.2020.e04567>
- Pandey VC (2012) Invasive species based efficient green technology for phytoremediation of fly ash deposits. *J Geochem Explor* 123:13–18. <https://doi.org/10.1016/j.gexplo.2012.05.008>
- Pandey, V. C. (2013). Suitability of *Ricinus communis* L. cultivation for phytoremediation of fly ash disposal sites. *Ecol Eng* 57, 336–341. <https://doi.org/10.1016/j.ecoleng.2013.04.054>
- Pandey VC (2015) Assisted phytoremediation of fly ash dumps through naturally colonized plants. *Ecol Eng* 82:1–5. <https://doi.org/10.1016/j.ecoleng.2015.04.002>
- Pandey VC, Abhilash PC, Singh N (2009) The Indian perspective of utilizing fly ash in phytoremediation, phytomanagement and biomass production. *J Environ Manage* 90:2943–2958. <https://doi.org/10.1016/j.jenvman.2009.05.001>
- Pandey SK, Bhattacharya T, Chakraborty S (2016) Metal phytoremediation potential of naturally growing plants on fly ash dumpsite of Patratu thermal power station, Jharkhand, India. *Int J Phytoremediat* 18(1):87–93. <https://doi.org/10.1080/15226514.2015.1064353>
- Pandey VC, Prakash P, Bajpai O, Kumar A, Singh N (2015) Phytodiversity on fly ash deposits: evaluation of naturally colonized species for sustainable phytoremediation. *Environ Sci Pollut Res* 22(4):2776–2787. <https://doi.org/10.1007/s11356-014-3517-0>
- Pandey VC, Singh N (2010) Impact of fly ash incorporation in soil systems. *Agric Ecosyst Environ* 136:16–27. <https://doi.org/10.1016/j.agee.2009.11.013>
- Pandey VC, Singh K (2011) Is *Vigna radiata* suitable for the revegetation of fly ash landfills? *Ecol Eng* 37:2105–2106. <https://doi.org/10.1016/j.ecoleng.2011.07.003>
- Pandey VC, Singh B (2012) Rehabilitation of coal fly ash basins: current need to use ecological engineering. *Ecol Eng* 49:190–192. <https://doi.org/10.1016/j.ecoleng.2012.08.037>
- Pandey VC, Singh JS, Kumar A, Tewari DD (2010) Accumulation of heavy metals by Chickpea grown in fly ash treated soil: effect on antioxidants. *Clean—Soil Air Water* 38(12):1116–1123. <https://doi.org/10.1002/clen.201000178>
- Pandey VC, Singh JS, Singh RP, Singh N, Yunus M (2011) Arsenic hazards in coal fly ash and its fate in Indian scenario. *Resour Conser Recycl* 55:819–835. <https://doi.org/10.1016/j.resconrec.2011.04.005>
- Pandey VC, Singh K, Singh RP, Singh B (2012) Naturally growing *Saccharum munja* L. on the fly ash lagoons: a potential ecological engineer for the revegetation and stabilization. *Ecol Eng* 40:95–99. <https://doi.org/10.1016/j.ecoleng.2011.12.019>
- Pandey VC, Singh N, Singh RP, Singh DP (2014) Rhizomediation potential of spontaneous grown *Typha latifolia* on fly ash basins: study from the field. *Ecol Eng* 71:722–727. <https://doi.org/10.1016/j.ecoleng.2014.08.002>
- Papaefthymiou H (2008) Elemental deposition in the vicinity of a lignite power plant in Southern Greece. *J Radioanal Nucl Chem* 275(2):433–439. <https://doi.org/10.1007/s10967-007-7046-x>

- Pathan SM, Aylmore LAG, Colmer TD (2003) Properties of several fly ash materials in relation to use as soil amendments. *J Environ Qual* 32:687–693. <https://doi.org/10.2134/jeq2003.6870>
- Pavlović P, Mitrović M (2013) Thermal power plants in Serbia—the impact of ash on soil and plants. In: Anđelković M (ed) *Energy and the environment, scientific gatherings, book 4*, Serbian Academy of Art and Science (SANU). Belgrade, pp 429–433
- Pavlović P, Marković M, Kostić O, Sakan S, Đorđević D, Perović V, Pavlović D, Pavlović M, Čakmak D, Jarić S, Paunović M, Mitrović M (2019) Evaluation of potentially toxic element contamination in the riparian zone of the River Sava. *CATENA* 174:399–412. <https://doi.org/10.1016/j.catena.2018.11.034>
- Pavlović P, Mitrović M, Djurdjević L (2004) An ecophysiological study of plants growing on the fly ash deposits from the “Nikola Tesla-A” thermal power station in Serbia. *Environ Manag* 33(5):654–663. <https://doi.org/10.1007/s00267-004-2928-y>
- Pavlović D, Pavlović M, Čakmak D, Kostić O, Jarić S, Sakan S, Đorđević D, Mitrović M, Gržetić I, Pavlović P (2018) Fractionation, mobility, and contamination assessment of potentially toxic metals in urban soils in four industrial Serbian cities. *Arch Environ Contam Toxicol* 75:335–350. <https://doi.org/10.1007/s00244-018-0518-x>
- Popovic, A., Djordjevic, D., & Polic, P. (2001). Trace and major element pollution originating from coal ash suspension and transport processes. *Environ Int* 26(4), 251–255. [https://doi.org/10.1016/S0160-4120\(00\)00114-8](https://doi.org/10.1016/S0160-4120(00)00114-8)
- Petaloti C, Triantafyllou A, Kouimtzis T, Samara C (2006) Trace elements in atmospheric particulate matter over a coal burning power production area of western Macedonia, Greece. *Chemosphere* 65(11):2233–2243. <https://doi.org/10.1016/j.chemosphere.2006.05.053>
- Pierzynski GM, Heitman JL, Kulakov PA, Kluitenberg GJ, Carlson J (2004) Revegetation of waste fly ash landfills in a semiarid environment. *J Range Manage* 57:312–319. [https://doi.org/10.2111/1551-5028\(2004\)057\[0312:ROWFAL\]2.0.CO;2](https://doi.org/10.2111/1551-5028(2004)057[0312:ROWFAL]2.0.CO;2)
- Pietrzykowski M, Krzaklewski W, Woś B (2015) Preliminary assessment of growth and survival of green alder (*Alnus viridis*), a potential biological stabilizer on fly ash disposal. *J Forest Res* 26(1):131–136. <https://doi.org/10.1007/s11676-015-0016-1>
- Pietrzykowski M, Woś B, Pająk M, Wanic T, Krzaklewski W, Chodak M (2018) Reclamation of a lignite combustion waste disposal site with alders (*Alnus* sp.): assessment of tree growth and nutrient status within 10 years of the experiment. *Environ Sci Pollut Res* 25:17091–17099. <https://doi.org/10.1007/s11356-018-1892-7>
- Querol X, Juan R, Lopez-Soler A, Fernandez-Turiel JL, Ruiz CR (1996) Mobility of trace elements from coal and combustion wastes. *Fuel* 75:821–838. [https://doi.org/10.1016/0016-2361\(96\)00027-0](https://doi.org/10.1016/0016-2361(96)00027-0)
- Querol X, Umana JC, Alastuey A, Ayora C, Lopez-Soler A, Plana F (2001) Extraction of soluble major and trace elements from fly ash in open and closed leaching systems. *Fuel* 80:801–813. [https://doi.org/10.1016/S0016-2361\(00\)00155-1](https://doi.org/10.1016/S0016-2361(00)00155-1)
- Rai UN, Pandey K, Sinha S, Singh A, Saxena R, Gupta DK (2004) Revegetation fly ash landfills with *Prosopis juliflora* L.: impact of different amendments and Rhizobium Inoculation. *Environ Int* 30:293–300. [https://doi.org/10.1016/S0160-4120\(03\)00179-X](https://doi.org/10.1016/S0160-4120(03)00179-X)
- Raja R, Nayak AK, Shukla AK, Rao KS, Gautam P, Lal B, Tripathi R, Shahid M, Panda BB, Kumar A, Bhattacharyya P, Bardhan G, Gupta S, Patra DK (2015) Impairment of soil health due to fly ash-fugitive dust deposition from coal-fired thermal power plants. *Environ Monit Assess* 187(11):679. <https://doi.org/10.1007/s10661-015-4902-y>
- Rajaganapathy V, Xavier F, Sreekumar D, Mandal PK (2011) Heavy metal contamination in soil, water and fodder and their presence in livestock and products: a review. *J Environ Sci Technol* 4(3):234–249. <https://doi.org/10.3923/jest.2011.234.249>
- Ram LC, Jha SK, Tripathi RC, Mesto RE, Selvi VA (2008) Remediation of fly ash landfills through plantation. *Remed J* 18(4):71–90. <https://doi.org/10.1002/rem.20184>
- Ram LC, Masto RE, Srivastava NK, George J, Selvi VA, Das TB, Pal SK, Maity S, Mohanty D (2015) Potentially toxic elements in lignite and its combustion residues from a power plant. *Environ Monit Assess* 187:4148. <https://doi.org/10.1007/s10661-014-4148-0>
- Rebele F, Lehmann C (2002) Restoration of a landfill site in Berlin, Germany by spontaneous succession. *Restor Ecol* 10:340–347. <https://doi.org/10.1046/j.1526-100X.2002.01026.x>
- Richter DD (2007) Humanity’s transformation of Earth’s soil: pedology’s new frontier. *Soil Sci* 172(12):957–967. <https://doi.org/10.1097/ss.0b013e3181586bb7>
- Roy M, Roychowdhury R, Mukherjee P (2018) Remediation of fly ash dumpsites through bioenergy crop plantation and generation: a review. *Pedosphere* 28(4):561–580. [https://doi.org/10.1016/S1002-0160\(18\)60033-5](https://doi.org/10.1016/S1002-0160(18)60033-5)
- Ruhl L, Vengosh A, Dwyer GS, Hsu-Kim H, Deonarine A (2010) Environmental impacts of the coal ash spill in Kingston, Tennessee: an 18-month survey. *Environ Sci Tech* 44:9272–9278. <https://doi.org/10.1021/es1026739>
- Santini TC, Fey MF (2015) Fly ash as a permeable cap for tailings management: pedogenesis in bauxite residue tailings. *J Soils Sediments* 15(3):552–564. <https://doi.org/10.1007/s11368-014-1038-6>
- Sarwar N, Imran M, Shaheen MR, Ishaque W, Kamran MA, Matloob A, Rehman A, Hussain S (2017) Phytoremediation strategies for soils contaminated with heavy metals: modifications and future perspectives. *Chemosphere* 141:710–721. <https://doi.org/10.1016/j.chemosphere.2016.12.116>

- Sawidis T, Metentzoglou E, Mitrakas M, Vasara E (2011) A study of chromium, copper, and lead distribution from lignite fuels using cultivated and non-cultivated plants as biological monitors. *Water Air Soil Poll* 220:339–352. <https://doi.org/10.1007/s11270-011-0758-0>
- Scholtus N, Echevarria G, Florentin L, Bonis ML, De Donato P, Simonnot MO, Morel JL (2014) Expected evolution of a Technosol derived from excavated Callovo-Oxfordian clay material. *J Soils Sediments* 15 (2):332–346. <https://doi.org/10.1007/s11368-014-1020-3>
- Séré G, Schwartz C, Ouvrard S, Renat JC, Watteau F, Villemin G, Morel JL (2010) Early pedogenetic evolution of constructed Technosols. *J Soils Sediments* 10(7):1246–1254. <https://doi.org/10.1007/s11368-010-0206-6>
- Shaw PJA (1996) Role of seedbank substrates in the revegetation of fly ash and gypsum in the United Kingdom. *Restor Ecol* 4:61–70. <https://doi.org/10.1111/j.1526-100X.1996.tb00108.x>
- Shaw PJA (1992) A preliminary study of successional changes in vegetation and soil development on unamended fly ash (PFA) in southern England. *J Appl Ecol* 29:728–736. <https://doi.org/10.2307/2404482>
- Shaw PJA (2009) Soil and fertilizer amendments and edge effects on the floral succession of pulverized fuel ash. *Restor Ecol* 17(1):68–77. <https://doi.org/10.1111/j.1526-100X.2007.00345.x>
- Simonović B (2003) Report on waste, surface and ground waters monitoring in the “Nikola Tesla–A” thermal power station at Obrenovac. Holding Institute of General and Physical Chemistry, Belgrade, 36 pp
- Sinha S, Gupta AK (2005) Translocation of metals from fly ash amended soil in the plant of *Sesbania cannabina* L. Ritz.: effect on antioxidants. *Chemosphere* 61:1204–1214. <https://doi.org/10.1016/j.chemosphere.2005.02.063>
- Sočo E, Kalemekiewicz J (2007) Investigations of sequential leaching behaviour of Cu and Zn from coal fly ash and their mobility in environmental conditions. *J Hazard Mater* 145:482–487. <https://doi.org/10.1016/j.jhazmat.2006.11.046>
- Sokolov DA, Androkhonov VA, Kulizhskii SP, Domozhakova EA, Loiko SV (2015) Morphogenetic diagnostics of soil formation on tailing dumps of coal quarries in Siberia. *Eurasian Soil Sci* 48(1):95–105. <https://doi.org/10.1134/S1064229315010159>
- Šourková M, Frouz J, Šantrůčková H (2005) Accumulation of carbon, nitrogen and phosphorus during soil formation on alder spoil heaps after brown-coal mining, near Sokolov (Czech Republic). *Geoderma* 124:203–214. <https://doi.org/10.1016/j.geoderma.2004.05.001>
- Stavridou E, Webster RJ, Robson PRH (2020) The effects of moderate and severe salinity on composition and physiology in the biomass crop *Miscanthus × giganteus*. *Plants* 9(10):1266. <https://doi.org/10.3390/plants9101266>
- Stefanowicz AM, Kapusta P, Błonska A, Kompała-Bąba A, Woźniak G (2015) Effects of *Calamagrostis epigejos*, *Chamaenerion palustre* and *Tussilago farfara* on nutrient availability and microbial activity in the surface layer of spoil heaps after hard coal mining. *Ecol Eng* 83:328–337. <https://doi.org/10.1016/j.ecoleng.2015.06.034>
- Stevens PR, Walker TW (1970) The chronosequence concept and soil formation. *Q Rev Biol* 45:333–350. <https://www.jstor.org/stable/2821008>
- Sushil S, Batra VS (2006) Analysis of fly ash heavy metal content and disposal in three thermal power plants in India. *Fuel* 85:2676–2679. <https://doi.org/10.1016/j.fuel.2006.04.031>
- Tarazona JV (2014) Pollution, soil. In: Wexler P (ed) *Encyclopedia of toxicology*, 3rd edn. Elsevier, pp 1019–1023
- Tchounwou PB, Yedjou CG, Patlolla AK, Sutton DJ (2012) Heavy metal toxicity and the environment. In: Luch A (ed) *Molecular, clinical and environmental toxicology*, vol 3. Environmental toxicology. Springer, Basel, pp 133–164
- Técher D, Laval-Gilly P, Bennisroune A, Henry S, Martinez-Chois C, D’Innocenzo M, Falla J (2012) An appraisal of *Miscanthus x giganteus* cultivation for fly ash revegetation and soil restoration. *Ind Crop Prod* 36:427–433. <https://doi.org/10.1016/j.indcrop.2011.10.009>
- Theis TL, Wirth JL (1977) Sorptive behavior of trace metals on fly ash in aqueous systems. *Environ Sci Technol* 11:1096–1100. <https://doi.org/10.1021/es60135a006>
- Tomaszewicz T, Chudecka J, Gamrat R, Stankowski S (2018) Suitability of soils developed on the basis of black coal ash as a forest habitat. *Polish J Soil Sci L/2*:131–140. <https://doi.org/10.17951/pjss/2017.50.2.131>
- Tripathi RD, Vajpayee P, Singh N, Rai UN, Kumar A, Ali MB, Kumar B, Yunis M (2004) Efficiency of various amendments for amelioration of fly-ash toxicity: growth performance and metal composition of *Casia siamea* Lamk. *Chemosphere* 54:1581–1588. <https://doi.org/10.1016/j.chemosphere.2003.09.043>
- Tsioptsias C, Samiotis G, Lefteri L, Amanatidou E (2020) Cr(VI) leached from lignite fly ash—assessment of groundwater contamination risk. *Water Air Soil Pollut* 231:373. <https://doi.org/10.1007/s11270-020-04750-4>
- US EPA (United States Environmental Protection Agency) (1988) Rep. 530-SW-88-002. Wastes from combustion of coal by electric utility power plants, U. S. Government Print Office, Washington, DC
- US EPA (United States Environmental Protection Agency) (2007) Human and ecological risk assessment of coal combustion wastes. U.S. Environmental Protection Agency, Office of Solid Waste, Research Triangle Park, NC 27709
- Uzarowicz Ł, Kwasowski W, Śpiewak O, Świtoniak M (2018a) Indicators of pedogenesis of Technosols developed in an ash settling pond at the Belchatów

- thermal power station (central Poland). *Soil Sci Ann* 69(1):49–59. <https://doi.org/10.2478/ssa-2018-0006>
- Uzarowicz Ł, Skiba M, Leue M, Zagórski Z, Gąsiński A, Trzcziński J (2018b) Technogenic soils (Technosols) developed from fly ash and bottom ash from thermal power stations combusting bituminous coal and lignite. Part II. Mineral transformations and soil evolution. *CATENA* 162:255–269. <https://doi.org/10.1016/j.catena.2017.11.005>
- Uzarowicz Ł, Zagórski Z (2015) Mineralogy and chemical composition of technogenic soils (Technosols) developed from fly ash and bottom ash from selected thermal power stations in Poland. *Soil Sci Ann* 66(2):82–91. <https://doi.org/10.1515/ssa-2015-0023>
- Uzarowicz Ł, Zagórski Z, Mendak E, Bartmiński P, Szara E, Kondras M, Oktaba L, Turek A, Rogoziński R (2017) Technogenic soils (Technosols) developed from fly ash and bottom ash from thermal power stations combusting bituminous coal and lignite. Part I. Properties, classification, and indicators of early pedogenesis. *CATENA* 157:75–89. <https://doi.org/10.1016/j.catena.2017.05.010>
- Vajpayee P, Rai UN, Choudhary SK, Tripathi RD, Singh SN (2000) Management of fly ash landfills with *Cassia surattensis* Burm: a case study. *B Environ Contam Toxicol* 65:675–682. <https://doi.org/10.1007/s0012800176>
- Van Rensburg L, Morgenthal TL, Van Hamburg H, Michael MD (2003) A comparative analysis of the vegetation and topsoil cover nutrient status between two similarly rehabilitated ash disposal sites. *Environmentalist* 23:285–295. <https://doi.org/10.1023/B:ENVR.0000031359.70523.4a>
- Vangronsveld J, Herzig R, Weyens N, Boulet J, Adriaenssens K, Ruttens A, Thewys T, Vassilev A, Meers E, Nehnevajova E, van der Lelie D, Mench M (2009) Phytoremediation of contaminated soils and groundwater: lessons from the field. *Environ Sci Pollut R* 16:765–794. <https://doi.org/10.1007/s11356-009-0213-6>
- Walker LR, del Moral R (2009) Lessons from primary succession for restoration of severely damaged habitats. *Appl Veg Sci* 12:55–67. <https://doi.org/10.1111/j.1654-109X.2009.01002.x>
- Ward CR, French D, Jankowski J, Dubikova M, Li Z, Riley KW (2009) Element mobility from fresh and long-stored acidic fly ashes associated with an Australian power station. *Int J Coal Geol* 80:224–236. <https://doi.org/10.1016/j.coal.2009.09.001>
- Weber J, Kocowicz A, Debicka M, Jamroz E (2017) Changes in soil morphology of Podzols affected by alkaline fly ash blown out from the dumping site of an electric power plant. *J Soil Sediment* 17:1852–1861. <https://doi.org/10.1007/s11368-016-1599-7>
- Weber J, Strączyńska S, Kocowicz A, Gilewska M, Bogacz A, Gwizdź M, Debicka M (2015) Properties of soil materials derived from fly ash 11 years after revegetation of post-mining excavation. *CATENA* 133:250–254. <https://doi.org/10.1016/j.catena.2015.05.016>
- World Reference Base for Soil Resources (2006) FAO, ISRIC and ISSS, Rome
- Woś B, Pająk M, Krzaklewski W, Pietrzykowski M (2020) Verifying the utility of black Locust (*Robinia pseudoacacia* L.) in the reclamation of a lignite combustion waste disposal site in Central European Conditions. *Forests* 11(8): 877. <https://doi.org/10.3390/f11080877>
- Yao ZT, Ji XS, Sarker PK, Tang JH, Ge LQ, Xia MS, Xi YQ (2015) A comprehensive review on the applications of coal fly ash. *Earth-Sci Rev* 141:105–121. <https://doi.org/10.1016/j.earscirev.2014.11.016>
- Zevenbergen C, Bradley JP, Van Reeuwijk LP, Shyam AK, Hjelmar O, Comans RNJ (1999) Clay formation and metal fixation during weathering of coal fly ash. *Environ Sci Technol* 33:3405–3409. <https://doi.org/10.1021/es9900151>
- Zhai M, Totolo O, Modisi MP, Finkelmann RB, Kelesitse SM, Menyatso M (2009) Heavy metal distribution in soils near Palapye, Botswana: an evaluation of the environmental impact of coal mining and combustion on soils in a semi-arid region. *Environ Geochem Hlth* 31(6):759. <https://doi.org/10.1007/s10653-009-9260-7>
- Zhao Z, Shahrour I, Bai Z, Fan W, Feng L, Li H (2013) Soils development in opencast coal mine spoils reclaimed for 1–13 years in the West-Northern Loess Plateau of China. *Eur J Soil Biol* 55:40–46. <https://doi.org/10.1016/j.ejsobi.2012.08.006>
- Zikeli S, Jahn R, Kastler M (2002) Initial soil development in lignite ash landfills and settling ponds in Saxony-Anhalt, Germany. *J Plant Nutr Soil Sc* 165:530–536. [https://doi.org/10.1002/1522-2624\(200208\)165:4%3c530::AID-JPLN530%3e3.0.CO;2-J](https://doi.org/10.1002/1522-2624(200208)165:4%3c530::AID-JPLN530%3e3.0.CO;2-J)
- Zikeli S, Kastler M, Jahn R (2004) Cation exchange properties of soils derived from lignite ashes. *J Plant Nutr Soil Sc* 167(4):439–448. <https://doi.org/10.1002/jpln.200421361>
- Zikeli S, Kastler M, Jahn R (2005) Classification of anthrosols with vitric/andic properties derived from lignite ash. *Geoderma* 124(3–4):253–265. <https://doi.org/10.1016/j.geoderma.2004.05.004>
- Żołnierz L, Weber J, Gilewska M, Strączyńska S, Pruchniewicz D (2016) The spontaneous development of understory vegetation on reclaimed and afforested post-mine excavation filled with fly ash. *CATENA* 136:84–90. <https://doi.org/10.1016/j.catena.2015.07.013>
- Zwolak A, Sarzyńska M, Szyrka E et al (2019) Sources of soil pollution by heavy metals and their accumulation in vegetables: a review. *Water Air Soil Pollut* 230:164. <https://doi.org/10.1007/s11270-019-4221-y>



Impact of Flood Disaster on Agricultural Land and Crop Contamination at the Confluence of the Bosna River

Tihomir Predić, Petra Nikić Nauth,
Bojana Tanasić, Tatjana Docić-Kojadinović,
Tatjana Cvijanović, and Duška Bjelobrč

Abstract

The Western Balkans Region (Croatia, Bosnia and Herzegovina and Serbia) was affected by disastrous floods on a large scale in May 2014. The total flooded area occupied approximately 10,000–13,000 km². Research results on soil and crop contamination in a flooded area of 2845 ha of agricultural land located at the confluence of the Bosna and Sava Rivers are presented in this paper. The duration of the flood was up to 22 days. The maximum height of the water in the flooded areas was three metres. In total, 62 soil samples were collected, comprising 31 soil samples from arable land, 13 samples of flood sediment and 18 samples of plant material. The soil and plant samples were analysed for the concentrations of Pb, Cd, Cr, Ni, Zn and Cu using an atomic absorption spectrophotometer. The pH of the flood sediment was alkaline. The soil pH was in the range of slightly acidic (pH H₂O > 6.03) to alkaline (pH H₂O 8.25). In the flood sediment and soil samples, elevated Zn concentrations (flood sediment: 102–171 mg kg⁻¹, soil: 59.7–276 mg kg⁻¹) and Cu concentrations (flood sediment: 41.5–

58.2 mg kg⁻¹, soil: 25.7–85.3 mg kg⁻¹) were determined. The Ni concentration in the flood sediment was 240–295 mg kg⁻¹, and that in the soil was 129–452 mg kg⁻¹, which classified these soils as contaminated with Ni. The content of Cu in plant material (green fruits of peppers and tomatoes, onions, potatoes) was below the MAC (<5 mg kg⁻¹ fresh weight) at all sites. In all the analysed vegetables and corn grown in the alkaline soil (pH in H₂O 8.88–8.13), the Ni content was <5 mg kg⁻¹ of dry matter. At all sites with slightly acidic soil (pH in H₂O 6.03–6.72), the Ni content in the corn, soybean and alfalfa was >5 mg kg⁻¹ of dry matter. Analyses of soybean, alfalfa and corn showed that in slightly acidic soils with a high concentration of Ni, and due to the changes in the redox potential of the soil, some heavy metals can dissolve and become available for absorption by plants. The results obtained showed that the floods that occurred in May 2014 have not polluted the agricultural land with the tested heavy metals. However, they slightly increased concentrations of Ni, Zn and Cu in the places where the flood sediment depth was more than 5 cm. The Ni content in the arable layer of agricultural land depended to a large extent on long-term previous floods, since it accumulated along with flood deposits and mixed with soil during agricultural work.

T. Predić (✉) · P. Nikić Nauth · B. Tanasić ·
T. Docić-Kojadinović · T. Cvijanović · D. Bjelobrč
Agro-Ecology Department, Agricultural Institute of
the Republic of Srpska, Knjaza Miloša 17, 78000
Banja Luka, Bosnia and Herzegovina

Keywords

Flood disaster · Arable land · Bosna River · Soil contamination · Plant contamination

23.1 Introduction

All climatic models suggest that extreme climatic events will occur more frequently in the near future (Kisić et al. 2015). In April 2014, seven cyclones (RHMZ RS 2014) passed through the territory of Bosnia and Herzegovina (B&H), during which more than twice the average rainfall (1961–1990) was recorded (Banja Luka 214 mm, 177.4 mm Doboje and Prijedor 163.8 mm). In addition, a large cyclone reached its peak and hit Bosnia and Herzegovina on 14–16 May. These events resulted in long-lasting floods on the territories in Bosnia and Herzegovina, Croatia and Serbia, with catastrophic consequences. The flood killed 86 people and damaged property worth more than one billion euros. In Croatia, Bosnia and Herzegovina and Serbia, the floods hit the areas of the Sava River basin, as well as its tributaries (ARSO, 2014).

Bosnia and Herzegovina suffered hardest from these floods. The rainfall exceeded the record of the previous 120 years. In some areas of B&H,

about 150 l m^{-2} of precipitation fell in a period of 48 h (13–14 May 2014) (EC, UN, WBG 2014). Along most of the Bosna River, the probability of such precipitation was once every 100–200 years and in some places even once in 500 years (ARSO 2014). According to the ECHO Joint Assessment Report (2014), 60 towns and cities were severely affected on an approximate total area of $10,000 \text{ km}^2$ – $13,000 \text{ km}^2$, and over 43,000 houses were damaged or destroyed. The number of landslides exceeded 3,000, which, in addition to all the other damage, moved land mines and warning signs to unidentified sites. Large areas of fertile land were flooded and crops destroyed (Fig. 23.1). The most heavily affected areas were at the mouths of the rivers flowing into the Sava River (Vrba, Bosna, Drina and Tinja River). The Sava River broke through the embankment and flooded 10,000 hectares of agricultural land in the Semberija region. The maximum height of the water in the flooded areas was three metres (Fig. 23.2).

The water remained in place for between 2 and 30 days and left behind, among other things, layers of sedimentation which were 0.5 to 20 cm thick (Fig. 23.3) (Predić et al. 2016).

The Ministry of Agriculture, Forestry and Water Management of the Republic of Srpska developed a set of short- and long-term flood

Fig. 23.1 The state of destroyed wheat cropping (photo by Predić)



Fig. 23.2 Water heights in flooded areas (photo by Predić)



Fig. 23.3 Layer of flood sediment (photo by Predić)



mitigation measures, launching a new production cycle and restoring facilities affected by the flood. The urgent short-term measures included testing agricultural land in the flooded area for the presence of contaminants as the basis for developing measures or recommendations for the remediation of contaminated land.

All areas subjected to the floods on the territory of the Republic of Srpska were investigated. In this chapter, we present the results of the

research on soil pollution in the flooded zone located at the mouth of the Bosna and Sava Rivers (an area at a high risk of pollution) (Fig. 23.4). The Bosna River (271 km long) and its tributaries flow through the industrial zone in B&H (which houses the metallurgical plant in Zenica, the coal mines and power plants in Kakanj, the cellulose and paper factory in Maglaj, the oil refinery in Modriča, the power plants in Tuzla, etc.). Before the war in 1992, it was the most developed



Fig. 23.4 The studied flooded area in the Bosna River Basin

industrial zone in Yugoslavia. The total catchment area is 10,810 km² (21.5% of total B&H territory) and there are approximately 1.5 million residents. Almost 40% of the population of B&H lives in the catchments of the Bosna River (NATO SPS 2014). The flood resulted in soil and sludge deposition from the upper Bosna River over an area of 2,845 hectares.

The Sava River destroyed the embankment on 17 May and flooded 9,709 hectares of the most fertile agricultural land in Bosnia and Herzegovina, in Semberija. The water remained for 30 days and left behind sediments between 0.5 and 20 cm thick, depending on the duration of water retention.

In the beginning, at the confluence of the Bosnia and Sava Rivers, an estimation of the danger of heavy metal contamination was prevented. Because the Sava River had no dam construction to reduce sediment transport by keeping the material in the reservoirs, the water from the Sava burst the left bank and flooded 7,854 ha of agricultural land (satellite images dated 21 May 2014). In those areas, after the water receded, the sludge deposition was between 0.5 and 20 cm thick, and in some places even up to 1 m (Kisić et al. 2015).

River sediments, an integral and dynamic part of rivers, form as a result of weathering of minerals and soils upstream and are prone to downstream transport. The sediment particles consist mainly of silt and fine-grained sand composed of calcite, quartz, feldspars, illite and kaolinite (Vuković et al. 2014).

Toxic heavy metals in river systems have been a subject of many studies due to their abundance and persistence in the environment, as well as their subsequent accumulation in aquatic habitats (Sakan et al. 2009; Amoatey and Baawain 2019; Hong et al. 2020; Khursheed et al. 2020; Yunus 2020). McGrath (1984) reported that heavy metals from waste sludge remain for 10³–10⁴ years in the soil. Later, the same authors showed that 45 years after the introduction of waste sludge, 80% of added Ni and Cr were found in the soil of cultivation experiments.

Heavy metals in river sludge can be of geochemical (natural) and anthropogenic origin.

Under natural conditions, without human influence, the content of heavy metals depends on the soil-forming parent material. Rivers constantly receive traces of heavy metals from terrestrial sources such as rock weathering. Relatively higher levels of heavy metals entering rivers and streams continuously or intermittently are associated with anthropogenic sources such as urban and industrial wastewater, fossil fuel combustion and atmospheric deposition (Sekabira et al. 2010; Pandey et al. 2010; Malsiu et al. 2020; Qian et al. 2020). Heavy metals of anthropogenic origin are usually introduced into river systems in the form of inorganic complexes or hydrated ions. These ions are easily adsorbed on the surfaces of sediment particles due to the relatively weak physical or chemical bonds. Thus, heavy metals of anthropogenic origin are predominantly found in the labile extractable sediment fractions (Singh et al. 2007). As a rule, the levels of trace metal in sediments show noticeable seasonal and regional variations, which are explained by both anthropogenic influences and natural processes (Tuna et al. 2007).

Heavy metals can be immobilised in the river sediments and involved in the processes of absorption, co-precipitation and complexation or co-adsorbed with other elements such as oxides or hydroxides of Fe and Mn. For example, Cd in the sediment remains bound to the adsorbed, exchangeable and carbonate (AEC) fraction. Thus, being weakly bound, it exhibits intermittent remobilisation (Laxen 1985). The latest study by Qian et al. (2020) showed that Cd headed the descending order of predominant pollutants in Dongting Lake sediments in China. Algül and Beyhan (2020), studying the sediments in Lake Bafa (Turkey), found that in the case of the heavy metals they studied, Cd was from an anthropogenic source. On the other hand, Fe, Mn, Cr and Ni remain in the residual phase, while Cu comes in the form of amorphous Fe oxyhydroxide phases (Sharmin et al. 2010).

Speciation of Cd, Cu, Zn and Pb in the sediments revealed that they were more bioavailable than the other metals studied, and therefore, posed a greater ecological hazard (Vuković et al. 2014; Qian et al. 2020). Studies by the Federal

Institute for Agriculture in Sarajevo carried out in the territory of Zavidovići (middle reaches of the Bosna River) showed that the silts fraction of the soil contained up to 700 mg kg^{-1} of total Ni (FIAS 2014). This study did not establish whether the Ni was of geochemical or anthropogenic origin. Increased nickel content was established by Novković et al. (2008) in studies on the Ni content in agricultural land in the lower valley of the Vrbas River, which flows parallel to the Bosna River (about 50–70 km further west). In the samples analysed, a homogeneous vertical and horizontal distribution of Ni was found. The geochemical map of the Vrbas River basin (Mojičević et al. 1976) shows that the geochemical origin of Ni is predominantly magmatic rocks (igneous rocks, peridotite and serpentine), brought by the river from natural sites in the upper courses (Ure and Berrow, 1982, Massoura et al. 2006). Recently, of the various environmental pollutants, considerable attention has been paid to nickel (Ni^{2+}) due to its rapidly growing concentrations in soil, air and water (Pavlovkin et al. 2016; Khair et al. 2020). Most agricultural soils contain an average of $25 \text{ mg Ni}^{2+} \text{ kg}^{-1}$ dry weight soil, but its content often substantially increases to $26,000 \text{ mg kg}^{-1}$ due to human activities such as mining, emissions from smelters, coal and oil burning, wastewater, phosphate fertilisers and pesticides (Holmgren et al. 1993; Pavlovkin et al. 2016). Nickel is commonly used in household products such as stainless steel, nonferrous alloys, plating, Ni–Cd batteries and coins, so there is a high likelihood of an increase in Ni content from urban areas. Usually, concentrations of heavy metals in the river sediments are used to identify the history and intensity of Ni accumulation (Pandey and Singh, 2017).

Regional studies showed that in the agricultural land of the river valleys of right tributaries of the Sava River in B&H (Vrbas, Bosna-Sava) and the Morava River in Serbia, Ni concentrations increased to 500 mg/kg and Cr to 250 mg/kg , but their origin was geochemical (Novaković et al. 2008; Anitić-Mladenović et al. 2011 and 2017; Vuković et al. 2014; Babajić et al. 2017).

This study was designed to determine how the remaining flood deposits affected concentrations of heavy metals (HMs) and whether they might pose a risk of pollution to agricultural land and crops. In this study, we did not aim to determine the origin of heavy metals (geological or anthropogenic). The Republic of Srpska in B&H has not yet established a permanent monitoring system for agricultural land pollution, although most of the preliminary studies have been completed. Thus, the results of this study cannot be compared with the previous situation (before the floods), but offer a starting point for further monitoring programmes.

23.2 Materials and Methods

23.2.1 Area Studied

The area studied covered the territories at the confluence of the Bosna and Sava Rivers (Fig. 23.4). The Bosna and its tributaries ($10,457 \text{ km}^2$ catchment area) flow through what were once the most industrially developed areas. The flooding in this area exposed people and animals to the risk of contamination with toxic and hazardous trace elements (Predić et al. 2016).

In May 2014, the Bosna River flooded an area of $2,845 \text{ ha}$ at the confluence with the Sava River (Fig. 23.5), including $1,942 \text{ ha}$ (68%) of agricultural land (arable, meadows and abandoned) and 903 ha (32%) of non-agricultural land (urban and forests). The population in this area is about 7,000.

23.2.2 Sampling of Soil, Flood Sediment and Plant Materials

Due to the urgency of the situation and the scale of the flood, the sampling was designed as a grid net system. The ETRS89 Cartesian reference frame with a cell size of $500 \text{ m} \times 500 \text{ m}$ was used.

The density of sampling points depended on the estimated risk of contamination, the area and

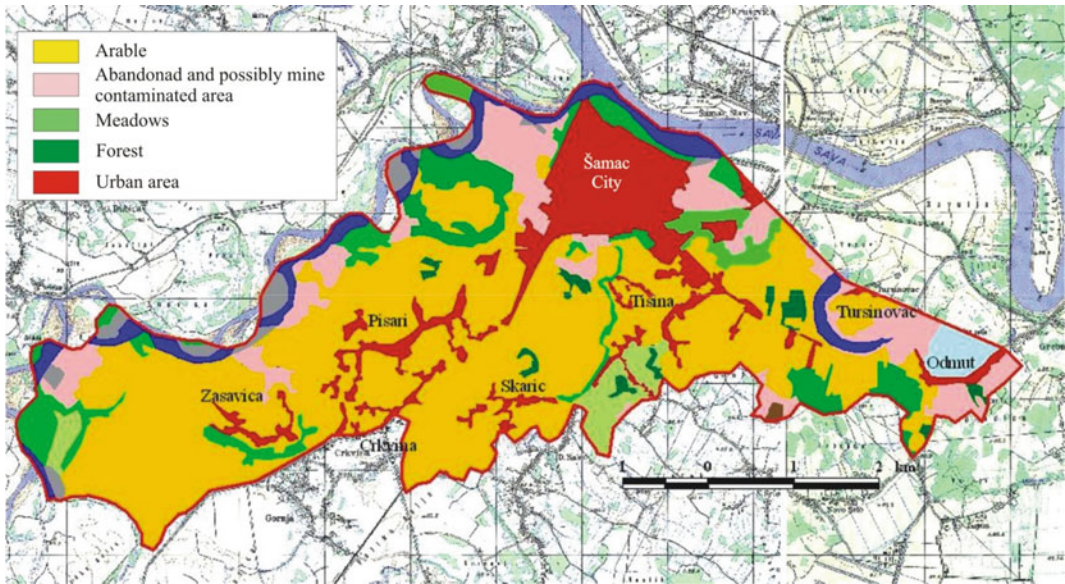


Fig. 23.5 Land cover/land use on the flooded area

the duration of the flood (water retention). In the area with a high estimated risk of contamination (confluence of the Bosna River), the sampling density was 2×2 km in the areas with shorter periods of flooding (up to 4 days), 1×1 km in the areas with longer periods of flooding (4–15 days) and 500×500 m in the areas with a long period of flooding > 15 days.

When the concentration of the heavy metal was higher than the MAC value (maximum allowed concentration), then additional samples were taken around the point at a smaller scale.

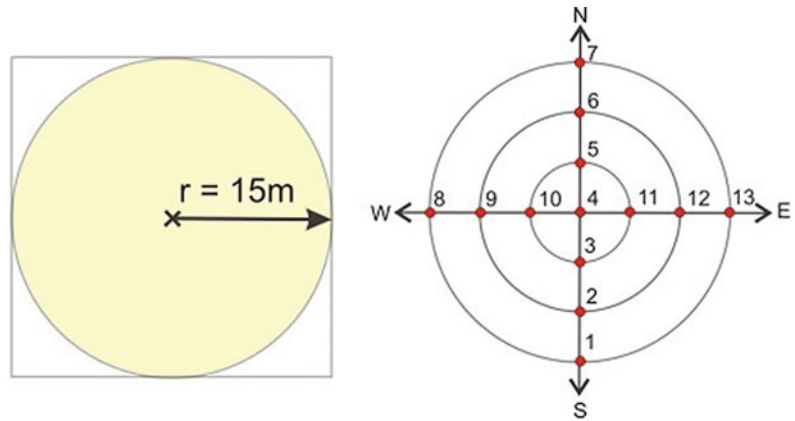
Sampling sites were located using the Global Positioning System (GPS Oregon 550–Garmin). The samples were taken from the flood sediment (thickness greater than 0.5 cm) and from the arable soil layer (0–25 cm) (Fig. 23.6).

Samples of the soil and flood sediments were taken in a 15 m radius (area of 706.5 m^2). On average, one sample consists of 13 individual samples (Fig. 23.7). Twelve individual samples were taken from the intersections of the main directions (N, S, E and W) along three concentric circles with radii of 5, 10 and 15 m, while the



Fig. 23.6 Soil and flood sediment sampling, Site No. 16 (photo by Predić)

Fig. 23.7 Scheme for taking an average soil sample (area of 706.5m²)



thirteenth sample was taken from the centre of the circle (Predić et al. 2013) (Fig. 23.7).

The sampled points were geo-positioned and photographed, and basic information was collected about the site (the length and type of flooding, crop conditions and damage caused). No samples were taken from areas without crops prior to the flood due to the danger of land mines that could have been moved from the designated places.

The sampling was carried out when the soil was dry enough to clearly distinguish the flood sediment from the soil. After discharge of the flood waters, due to the high groundwater level and/or due to the inaccessibility of the point, the samples were taken in two periods: the first 20 days after the flood (water stagnated from 2 to 14 days) and the second 40 days after the flood (water stagnated from 15 to 22 days). During the second sampling, flood sediment samples were not taken because the area had already been cultivated and new crops were planted.

The plant material was sampled according to the same principle as for the soil and from the same sites (Fig. 23.7). The plant material collected consisted of the fruits of peppers and tomatoes, beans without pods, the whole onion plant, potato tubers, the above-ground part of alfalfa, corn and soybean (middle leaf).

In total, 31 soil samples, 13 sediment samples and 18 samples of plant material were collected for analysis (Fig. 23.8).

23.2.3 Analytical Methods

The following parameters in the soil and flood sediment samples were analysed: pH in H₂O and in 1 M KCl (ratio 1:2.5; PHM 240 radiometer); humus (by wet oxidation using potassium dichromate as the oxidising agent, YSSS 1966); available phosphorus and potassium (by AL method, Egner-Riehm; YSSS1966) and pseudo-total contents of Pb, Cd, Cr, Ni, Zn and Cu were determined by atomic absorption spectrophotometry, the flame technique (AAS Thermo Electron Corporation – SOLAR S4), after digestion with nitric acid (HNO₃, 65%) + hydrogen peroxide (H₂O₂, 30%), (US EPA Method 3050B, US EPA 1996). The content of total heavy metals in soil was interpreted in accordance with the Dutch Soil Remediation Circular (2013) and the Serbian Regulation on the Systematic Monitoring of Land Quality, Indicators for Assessing the Risk of Land Degradation and the Methodology for Developing Remediation Programmes (Official Gazette of Serbia 2010). The contents of Pb, Cd, Cr, Ni, Zn and Cu in dry

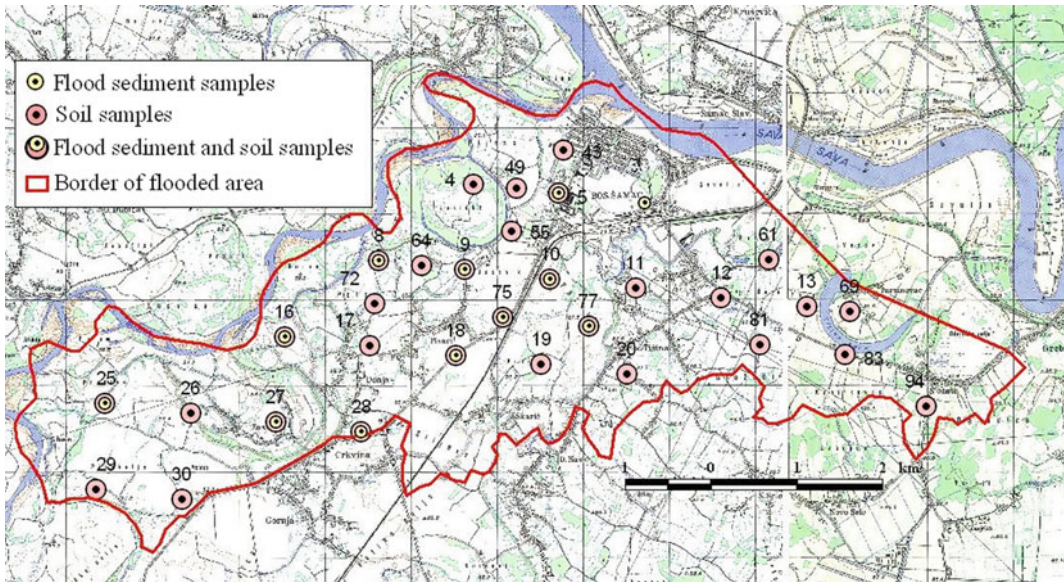


Fig. 23.8 Distribution of the sampling sites

plant material were determined with AAS after acid digestion (HNO_3 , HClO_4 , H_2SO_4 , ratio of 20:2:1). ArcMap 10.0 was used to spatially display and interpolate data.

23.3 Results

23.3.1 Soil and Flood Sediment

The examined soils have different levels of fertility, which is related to their different soil types,

land uses and fertilisation. The flood sediment has more uniform basic fertility parameters (Table 23.1). The content of humus and available phosphorus varied from low to medium, and that of available potassium from low to good.

The pH of flood sediments was alkaline (pH H_2O 7.83–8.34), while the soils were from slightly acidic (pH H_2O 6.03) to alkaline (pH H_2O 8.25) (Table 23.1, Fig. 23.9). The Bosna and Sava River banks are represented by Calcaric Fluvisols (WRB 2015), while central parts of the flood plains are dominated by Eutric Fluvisols

Table 23.1 The basic soil and flood sediment parameters

	pH		Humus	mg/100 g	
	H_2O	KCl	%	P_2O_5	K_2O
Sediment					
Interval of variation	7.80–8.34	7.00–7.50	1.30–4.00	4.50–12.7	12.0–39.4
Average	8.11	7.27	2.41	7.53	23.18
STD	0.15	0.12	0.81	2.35	7.84
Soil					
Interval of variation	6.03–8.25	4.60–7.49	1.10–11.2	1.20–43.1	10.9–62.9
Average	7.76	6.86	2.17	14.42	21.47
STD	0.56	0.66	0.58	11.41	10.27

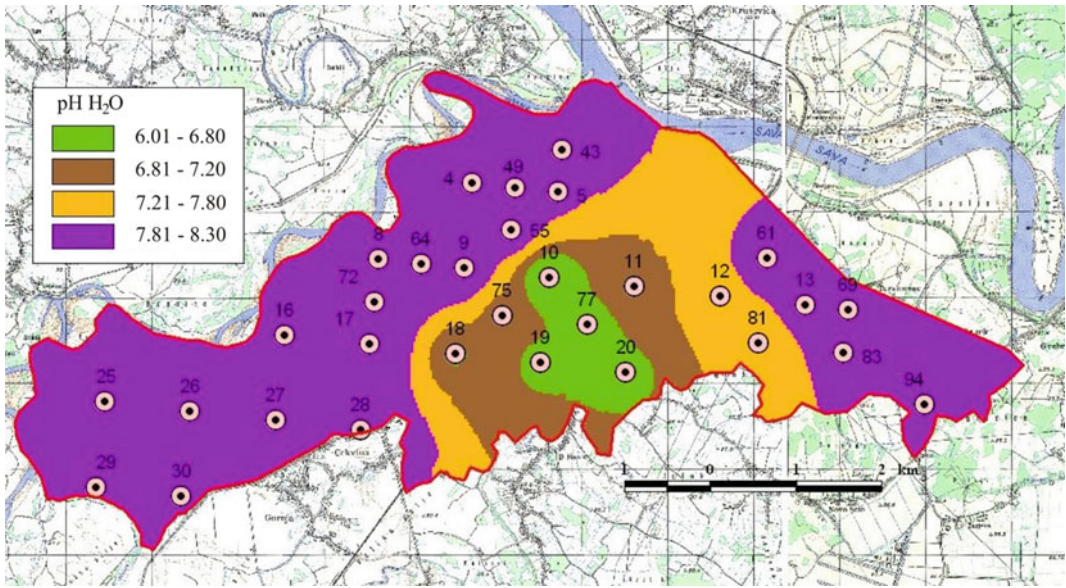


Fig. 23.9 Active acidity (pH in H₂O) of arable soil layer (0–25 cm)

with smaller areas of Mollic Gleysols (Pedological map of Bosnia and Herzegovina (1973)).

According to the classification in Table 23.3 and the Dutch Soil Remediation Circular (2013), the pseudo-total contents of lead (Pb), cadmium (Cd) and chromium (Cr) in the flood sediment and soil were within expected concentrations (Table 23.2). An increased content of Zn (150 to 171 mg Zn kg⁻¹) was found in 11 out of 13 flood sediment samples (84%, Table 23.4). The Zn content of the topsoil varied widely, from 59.7 to 276 mg Zn kg⁻¹ (Table 23.3). An increased

content was found only in three samples, along the Bosna River (Site No. 8, Fig. 23.8) and along the Sava River (Site Nos. 13 and 94, Fig. 23.8). The spatial distribution of Zn obtained by interpolation in the flooded areas (Fig. 23.10) revealed an increased content of Zn along the Bosna and Sava Rivers where floods are common and frequent.

The pseudo-total content of Cu in the flood sediment was increased in all samples and varied in the range of 41.5–58.2 mg Cu kg⁻¹ (Table 23.2). In the arable soil layer, it varied in a

Table 23.2 Pseudo-total content of heavy metals in the flood sediment and soil

	mg kg ⁻¹					
	Pb	Cd	Cr	Ni	Zn	Cu
Sediment						
Interval of variation	18.5–34.0	0.05–0.3	18.3–57.4	240–295	102–171	41.5–58.2
Average	26.9	0.10	36.6	271	151	49.6
STDEV	4.80	0.10	13.7	15.6	21.1	5.9
Soil						
Interval of variation	10.8–70.0	0.05–1.30	7.50–76.3	129–452	59.7–276	25.7–85.3
average	32.2	0.1	48.2	281	117	44.4
STDEV	14.9	0.2	16.6	53.5	40.0	13.5

Table 23.3 Limit values for concentrations of heavy metals in soil*

Classification	mg kg ⁻¹					
	Pb	Cd	Cr	Ni	Zn	Cu
Expected content	<85	<0.8	<130	<35	<140	<36
Increased content	85–150	0.8–5.0	130–250	35–100	140–500	36–100
Contaminated	150–600	5–20	250–800	100–500	500–3000	100–500
Remediation	>600	>20	>800	>500	>3000	>500

*Regulation on the systematic monitoring of land quality, indicators for assessing the risk of land degradation and the methodology for developing remediation programmes (Official Gazette of Serbia 88/201)

Table 23.4 Pseudo-total content of Ni, Zn and Cu in the flood sediment and soils from the same sites

Site	Ni mg kg ⁻¹		Zn mg kg ⁻¹		Cu mg kg ⁻¹	
	Flood sediment	Soil	Flood sediment	Soil	Flood sediment	Soil
5	275	252	154	107	50.7	46.3
8	294	452	155	183	43.2	85.3
9	276	237	164	91.9	57.9	41.4
10	241	129	102	73.7	41.5	29.7
16	281	238	157	80.2	51.7	36.5
18	281	243	170	84.9	57.3	39.4
25	276	270	144	94.1	42.0	33.3
27	272	249	150	73.6	46.4	37.7
28	267	248	101	79.3	45.7	38.2
75	284	249	171	85.9	58.2	42.0
77	262	253	156	92.5	51.7	42.4
Interval of variation	241–295	129–452	101–171	73.6–183	41.5–58.2	29.7–85.3
Average	274	256	148	95.1	49.7	42.9

wider range of 25.7–62.3 mg Cu kg⁻¹ except for one sample with 85.3 mg Cu kg⁻¹ (Site No. 8, the Bosna River, Fig. 23.8). The average content of Cu in the soil (117 mg kg⁻¹) was lower than in the flood sediment (151 mg kg⁻¹, Table 23.2).

The content of pseudo-total Ni in all soil and flood sediment samples was above 100 mg kg⁻¹, which classifies these soils as contaminated with Ni (Dutch Soil Remediation Circular 2013 and Official Gazette of Serbia 2010). In the samples of flood sediment, the concentrations of Ni were similar, ranging between 241 mg kg⁻¹ and 295 mg Ni kg⁻¹. In arable soil, the Ni

concentration ranged between 29 mg kg⁻¹ and 298 mg kg⁻¹, except for one sample with 452 mg kg⁻¹ (Site No. 8, Fig. 23.8). To find out if this was the only case, two more samples were taken around Site No. 8 (samples 64 and 72, Fig. 23.8). The results of the analysis showed that this was a single case of contamination since the total Ni content in the topsoil at Site No. 64 was 295 mg Ni kg⁻¹ and that at Site No. 72 was 269 mg Ni kg⁻¹, which is within the range of most of the soil samples.

In addition, it was noted that at Site No. 8 the thicker layer of sediments (1–2 m) that was

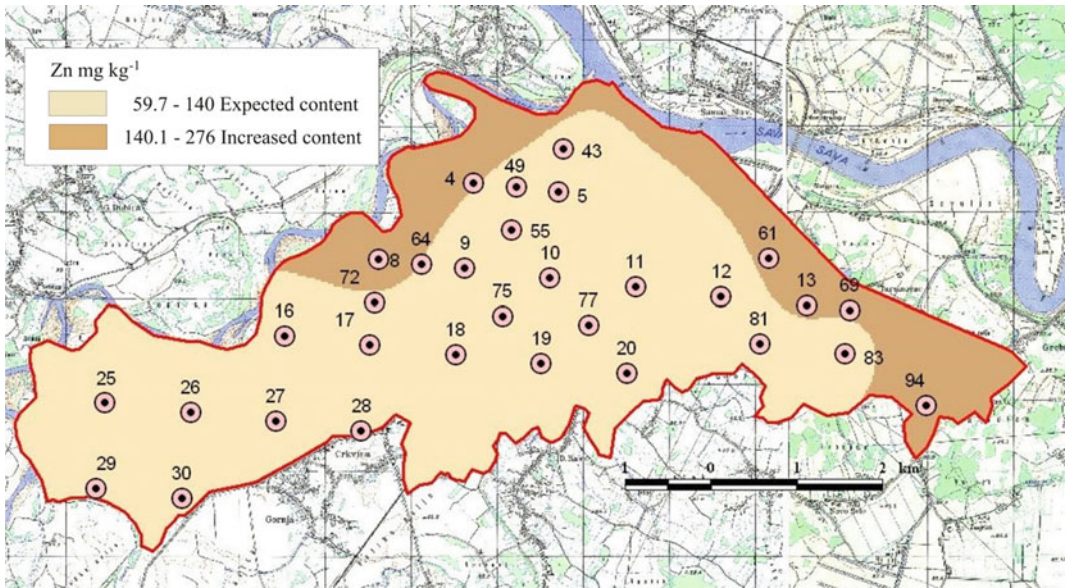


Fig. 23.10 Content of pseudo-total Zn in arable soil in flooded areas

deposited due to the earlier flooding events was incorporated into the soil due to the cultivation of agricultural production. For this reason, the arable topsoil (0–25 cm), which was a mixture of old floods deposits and soil material, was taken again. The situation with Site No. 8 explains the

results that are in comparison with the results from other sites, i.e. the concentrations of Ni, Zn and Cu were higher in the soil than in the flood sediment (Predić et al. 2016).

Figure 23.11 shows the spatial distribution of Ni concentration in the arable soil (n = 31).

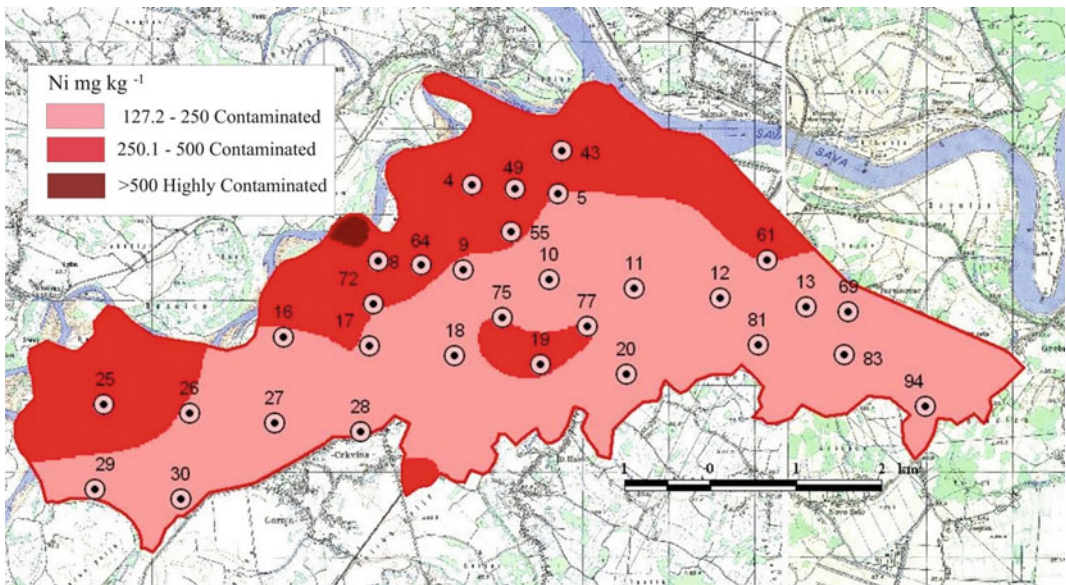


Fig. 23.11 Content of pseudo-total Ni in arable/topsoil in the flooded area

Although the content of Ni determined over the entire flooded area exceeded $100 \text{ mg Ni kg}^{-1}$, the soils along the Bosna River contained higher Ni concentrations than soils from the rest of the flooded area.

Table 23.4 presents the results for the pseudo-total content of Ni, Zn and Cu from 13 sites. With the exception of Site No. 8, which was explained above, the content of Ni, Zn, and Cu in the flood sediment was greater than in the upper layers of the soil (Fig. 23.12).

The content of Ni in the samples where the flood sediment was mixed with the soil is shown in Table 23.5. The samples were taken from the sown area 40 days after the last flood. In these areas, the water stagnated for 15 to 22 days, and the thickness of the flood sediment before ploughing was 8–10 cm.

These areas are located closest to the confluence of the Bosna River, where the greatest accumulation of water occurs because of frequent floods. Therefore, the higher concentrations of

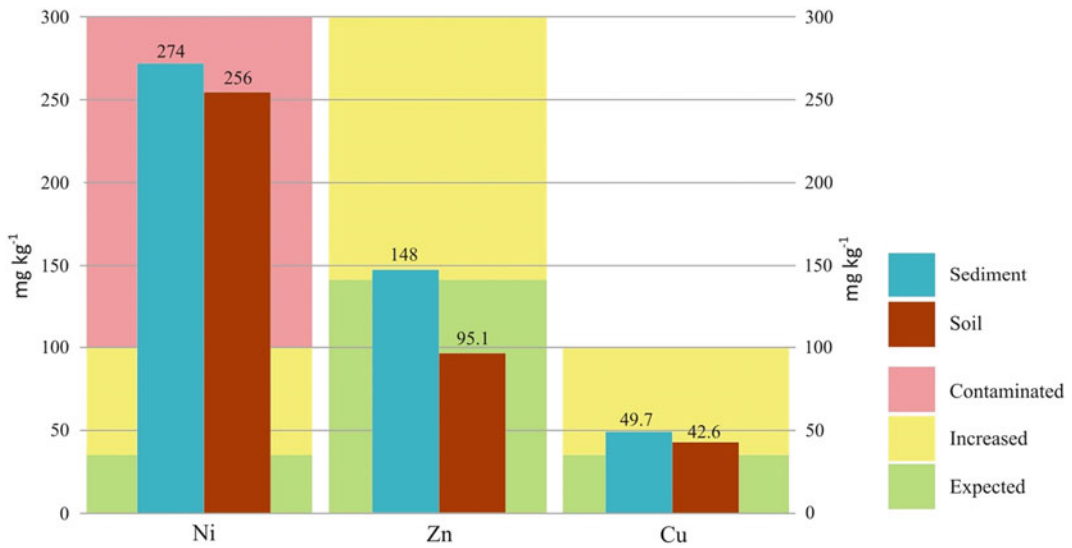
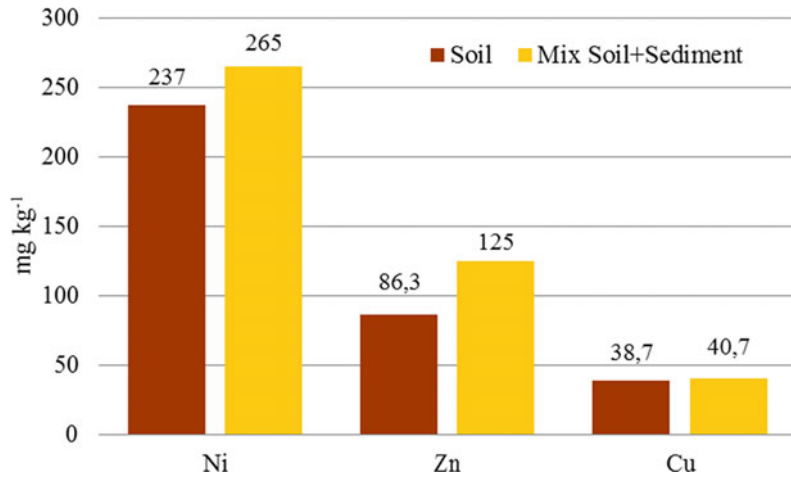


Fig. 23.12 Content of pseudo-total Ni, Zn and Cu in the flood sediment and topsoil layer (0–25 cm)

Table 23.5 Content of pseudo-total Ni, Zn and Cu in samples where the flood sediment was mixed with the soil

Site	mg kg ⁻¹		
	Ni	Zn	Cu
4	270	214	46.7
43	292	109	30.2
49	261	148	37.0
55	275	113	49.0
61	254	103	43.1
64	295	103	46.5
69	201	93.3	35.7
72	269	115	37.0
Interval of variation	201–292	93.3–214	30.2–49.0
Average	265	125	40.7

Fig. 23.13 Content of pseudo-total Ni, Zn and Cu in topsoil and the mixture of flood sediment and topsoil



pseudo-total Ni (254–295 mg kg⁻¹) and Zn (103–214 mg kg⁻¹) were determined in these samples (Nos. 4, 43, 49, 55, 61, 64 and 72, Fig. 23.8). This was confirmed by the results of soil analysis from Site No. 69, which was located 5 km from the confluence and was flooded less frequently. Thus, these soils contain less flood sediment and lower concentrations of Ni (201 mg kg⁻¹) and Zn (93 mg kg⁻¹). Comparing the data in Table 23.4 (excluding Site No. 8) and Table 23.5, the conclusion can be drawn that flood sediment mixing with soil led to an increase in the pseudo-total amount of Ni, Zn and Cu in the topsoil (Fig. 23.13).

Of all the analysed elements (Pb, Cd, Cr, Ni, Zn and Cu), only the Ni content was above the limit value (100 mg Ni kg⁻¹) in all soil and flood sediment samples. This classifies these soils as contaminated with Ni (Dutch Soil Remediation Circular (2013) and Official Gazette of Serbia 2010) (Table 23.3). Thus, a significant concentration of Ni in agricultural soil was of natural origin, due to the long-term accumulation of old flood sediments containing serpentine minerals brought from the upper course of the Bosna River. This fact is confirmed by Babajić et al. (2017), who showed that potentially toxic Cr and Ni are genetically related to the most widespread ultramafic rocks in the wider Maglaj area, including the middle basin of the Bosna River. Chromium and nickel were genetically associated with ferromagnesium minerals (olivine and

pyroxene), which are the main petrogenic minerals in ultramafic rocks and are subjected to alteration processes under exogenous conditions. A detailed study showed that the origin of chromium and nickel in the soil of the wider Maglaj area is geogenic.

In the flood sediments from the middle course of the Bosna River (Zavidovići), high concentrations of total Ni were found, up to 752 mg Ni kg⁻¹ (FIAS 2014). This study did not establish whether the Ni content was of geochemical or anthropogenic origin. However, according to Mojičević et al. (1976), serpentinite and peridotite rocks were found in the middle reaches of the Bosna River and its tributaries. These rocks are the main carriers of Ni and Cr in nature (Massoura et al. 2006; Reimann et al. 2014).

NATO SPS (2014) tested the content of heavy metal in the sediments of the Bosna River at 20 km before the confluence. Seven sampled sites were located near the potential contaminants. In their study, of all the heavy metals (Pb, Cd, As, Hg, Ni, Cr, Zn and Cu), only the content of Ni continuously increased from 15 to 170 mg kg⁻¹.

The studies conducted in all flooded areas in B&H (in 2014) showed that the Ni content in the Bosna River basin (129–452 mg kg⁻¹) was significantly higher than in the areas flooded by other rivers: the Sava (80–112 mg kg⁻¹), the Drina (80–107 mg kg⁻¹) and the Vrbas (47–151 mg kg⁻¹) (JU PIRS 2014). In the flooded

area of the Sava basin in Serbia, the content of Ni was lower and ranged between 50 and 100 mg Ni kg⁻¹. However, in the West Morava basin, it was up to 438 mg kg⁻¹ (Ministry of Agriculture of the Republic of Serbia (2014)). Research carried out by Antić-Mladenović et al. (2017) showed a prevailing geological origin for Ni, Cr, As and Pb; a mixed origin for Cd and Zn and a prevailing anthropogenic origin for Cu in the soils and sediments in the West Morava River basin.

The results of the pseudo-total content of Ni, Zn and Cu in the soil and flood sediments, as well as their horizontal and vertical distribution in the flood zone of the Bosna River, showed that their content in arable land was largely due to long-term old floods, i.e. the continuous deposition of flood sediment and its mixing with soil due to agricultural practices.

23.3.2 Plant Material Analyses

The 18 plant materials were collected 40 days after the flood began. At the sampled sites, the flood water remained between 15 and 22 days. The plant material was also collected from Site No. 8 (with the highest concentration of Ni in the soil) and from the other three sites (Nos. 10, 20 and 77; Fig. 23.8) with a slightly acidic reaction. Corn was a dominant crop at the studied sites

when sown after the withdrawal of water and was sampled at a phase of 4, 5 and 6 leaves (Table 23.7). At Site No. 8, the corn was sampled at a phase of 10–11 leaves as the flood lasted 3–4 days. The soybean (Site Nos. 10 and 20) and alfalfa (Site No. 77) were at the beginning of flowering. The vegetables planted after the flood (peppers, tomato, bean, onion and potato) were sampled from the two sites (Nos. 43 and 55). The content of heavy metals in plants is shown in Tables 23.6 (vegetables) and 7 (corn, soybean and alfalfa samples).

In the European regulations (EC REGULATION No 1881/2006), the maximum levels for certain contaminants in foods are provided only for Pb and Cd. In vegetables and potatoes, the maximum Pb concentration is 0.10 mg kg⁻¹ and that of Cd is 0.05 mg kg⁻¹; in potato tubers, it is 0.10 mg kg⁻¹ (fresh weight). According to Regulation (EC) No 396/2005 (PESTICIDES EU MRLs), the maximum level of Cu in beans without pods is 20.0 mg kg⁻¹ and that in peppers, tomatoes, onions and potatoes is 5.0 mg kg⁻¹ (fresh weight). In all tested vegetables, the Pb and Cd were found in traces, while the content of Cu (Table 23.6) was below the MAC. In the above EC Regulations, maximum levels for Ni, Cr and Zn are not provided. According to published data, the typical level of Zn in vegetative parts of plants is 10–150 mg kg⁻¹ (Chaney 1989). In our study, the content of Zn was within this range at both sites.

Table 23.6 Content of heavy metal in the vegetables

Site No	Type of sample	Vegetable/sampled part	pH		mg kg ⁻¹ dry mater					
			H ₂ O	KCl	Pb*	Cd*	Cr*	Ni	Zn	Cu
43	Soil	–	8.05	7.49	38.2	0.53	55.3	292	109	30.2
	Plant	Bean/whole plant	–		n.d	n.d	n.d	4.85	28.2	9.64
		Peppers/green fruit	–		n.d	n.d	n.d	0.73	1.36	0.44
		Tomato/green fruit	–		n.d	n.d	n.d	0.12	1.41	0.48
		Onion/bulb and pen	–		n.d	n.d	n.d	0.45	3.66	0.33
55	Soil	–	8.09	7.12	37.9	0.51	64.6	275	113	49.0
	Plant	Bean/whole plant	–		n.d	n.d	n.d	3.84	15.04	6.42
		Peppers/green fruit	–		n.d	n.d	n.d	0.26	1.54	0.54
		Tomato/green fruit	–		n.d	n.d	n.d	0.17	1.57	0.38
		Potato tubers	–		n.d	n.d	n.d	0.23	2.36	1.01

* Pb, Cd and Cr in plant material were not detected (n.d.) using AAS flame techniques

Regardless of the higher Ni content in the soil (292 and 275 mg kg⁻¹) in the vegetables, the concentration of Ni was from 0.07 to 0.73 mg Ni kg⁻¹ dry matter. This concentration is in line with the results published earlier. According to Kabata-Pendias (2010), a Ni concentration of up to 5 mg Ni kg⁻¹ of dry matter is considered an acceptable content in plants. In the legumes (flowering phase), the Ni content in the vegetative part contained a higher concentration of Ni (3.84 and 4.85 mg kg⁻¹) compared to the fruit. This is explained by the fact that Ni is an essential micronutrient and an integral part of the enzymes urease, methyl-coenzyme M reductase, hydrogenase and carbon monoxide dehydrogenase (Adriano 2001).

Based on the foregoing, it can be concluded that the Ni content in the plants studied was not associated with an increased content in the alkaline soil which was classified as contaminated (Dutch Soil Remediation Circular (2013) and Official Gazette of Serbia 2010, Table 23.3). However, in alkaline, slightly alkaline and neutral soils, heavy metals were present in insoluble and almost insoluble forms. We can, therefore, assume that the potential risk of uptake of increased concentrations of Ni, Zn and Cu by crops is low regardless of their content in the soil. This assumption was proved by the results on the tested vegetables from the sites studied. However, the content of Ni in green parts of the crops (3.84–4.85 mg kg⁻¹) showed the need for further research into heavy metals in leafy vegetables (lettuce, spinach, cabbage, etc.) in flooded alkaline soil.

Different types of plants have different abilities to assimilate certain elements due to the different behaviour of their rhizospheres, which passively and actively release root exudates, including organic compounds, protons and CO₂. Plants can significantly change the chemical composition of the soil near their roots, such as the pH, redox potential and the presence of inorganic and organic ligands (Hinsinger and Courchesne 2008; Hinsinger et al. 2005).

In slightly acidic soil with a longer retention of surface water or high groundwater levels, undesirable redox conditions might lead to the dissolution of some heavy metals and their uptake by plants. Antić-Mladenović et al. (2017) stated in their work that considerable amounts of Ni can be mobilised during low redox potential despite a high Ni retention capacity of the soil. This observation was confirmed in our study with the crops grown in slightly acidic soil (Table 23.7). In our study, a Ni content exceeding 5 mg/kg was found only in the crops (corn, soybeans and alfalfa) growing in slightly acidic soil (Site Nos. 10, 20 and 77).

Unfortunately, in this study, there were no samples of soy and alfalfa grown on alkaline soils. However, the result for Ni in corn leaves from Site No. 10 can be compared with the results for Ni in corn leaves from another ten sites with alkaline soil.

In the slightly acidic soil (Site No. 10), the content of Ni in the corn leaf (7.89 mg kg⁻¹) was six times higher than in the alkaline soil (Site No. 4—1.3 mg Ni kg⁻¹), while the Ni concentration in Site No. 4 (270 mg kg⁻¹) was two times higher than at Site No. 10 (129 mg kg⁻¹). Similar trends were observed in other sites with alkaline soil (Table 23.7, Fig. 23.14).

Analyses of the soybean and alfalfa showed an increased accumulation of Ni in slightly acidic soils (Fig. 23.14). As mentioned earlier, prolonged water stagnation and/or a high groundwater table can lead to the dissolution of some of the heavy metals and their absorption by plants due to the shift in soil redox conditions.

Analyses of corn leaves and vegetables showed that the increased concentration of Ni in the alkaline soils (above MAC: > 50 mg kg⁻¹) did not result in an increase in Ni in plant material. Other authors also reported low concentrations of Ni (<5 mg Ni kg⁻¹) in plant material from alkaline soils (Jakšić et al. 2013; Šefket et al. 2011).

Given the above and because, the most reported concentration of Ni as limit values for

Table 23.7 The content of heavy metals in the plant material of corn, soybean and alfalfa samples

Site No	Type of sample	Plant species/plant sample	pH		mg kg ⁻¹ dry matter					
			H ₂ O	KCl	Pb	Cd	Cr	Ni	Zn	Cu
10	Soil	–	6.03	4.60	13.7	0.71	9.92	129	73.7	29.7
	Plant	Corn/middle leaf			n.d	0.92	n.d	7.89	26.0	9.36
		Soybeans/middle leaf			n.d	1.21	n.d	8.41	25.5	8.06
20	Soil	–	6.72	5.62	20.9	0.32	50.2	156	96.8	37.5
	Plant	Soybeans/middle leaf			n.d	1.11	n.d	10.5	39.3	10.1
77	Soil	–	6.66	5.56	18.5	n.d	24.1	253	92.5	42.4
		Alfalfa/whole plant			n.d	1.32	n.d	5.87	20.7	8.6
4	Soil	–	8.00	n.d	70.0	0.41	51.2	270	214	46.7
	Plant	Corn/middle leaf			n.d	0.71	n.d	1.29	47.1	11.4
8	Soil	–	8.20	7.10	25.7	0.75	38.5	452	183	85.3
	Plant	Corn/middle leaf			n.d	0.39	n.d	2.36	12.7	6.9
49	Soil	–	8.13	7.43	52.2		47.6	261	148	37.0
	Plant	Corn/middle leaf			n.d	0.95	n.d	0.98	23.9	10.4
61	Soil	–	7.88	7.09	27.4	0.51	76.3	254	103	43.1
	Plant	Corn/middle leaf			n.d	0.98	n.d	2.49	23.0	15.2
64	Soil	–	7.99	7.14	34.1	0.35	56.7	295	103	46.5
	Plant	Corn/middle leaf			n.d	0.99	n.d	1.00	24.8	9.71
69	Soil	–	8.13	7.08	26.7	0.41	39.0	201	93.3	35.7
	Plant	Corn/middle leaf			n.d	1.22	n.d	1.97	29.9	5.44
72	Soil	–	8.13	7.16	26.5	0.47	54.9	269	88.6	37.0
	Plant	Corn/middle leaf			n.d	0.53	n.d	1.81	23.6	11.7

contaminated soils in the territory of the former Yugoslavia was 50–100 mg kg⁻¹ (Official Gazette of Montenegro 1997; Official Gazette of FBiH 2009; Official Gazette of Serbia 2010; Official Gazette of Croatia 2014), there is a need to harmonise the limit values of the total Ni content in alkaline soils.

The results obtained for plant material can be considered as preliminary studies based on a small number of samples that cannot be statistically processed, and contribute to reliable conclusions. However, certain observations and directions can be given for further research into crop contamination due to flooding. Permanent soil monitoring obviously needs to be established for a more comprehensive investigation of Ni

concentrations in various plants used in human and animal nutrition in the area studied.

23.4 Conclusions

A large amount of flood water resulted in flood sediment from a few millimetres to 10 cm thick being deposited over a large agricultural area as a potential source of pollution.

- The flood sediments had an alkaline pH, while the acidity of soil samples ranged from slightly acidic to alkaline. In the flood sediment and the soil samples, the expected concentrations of pseudo-total Pb, Cd and Cr and

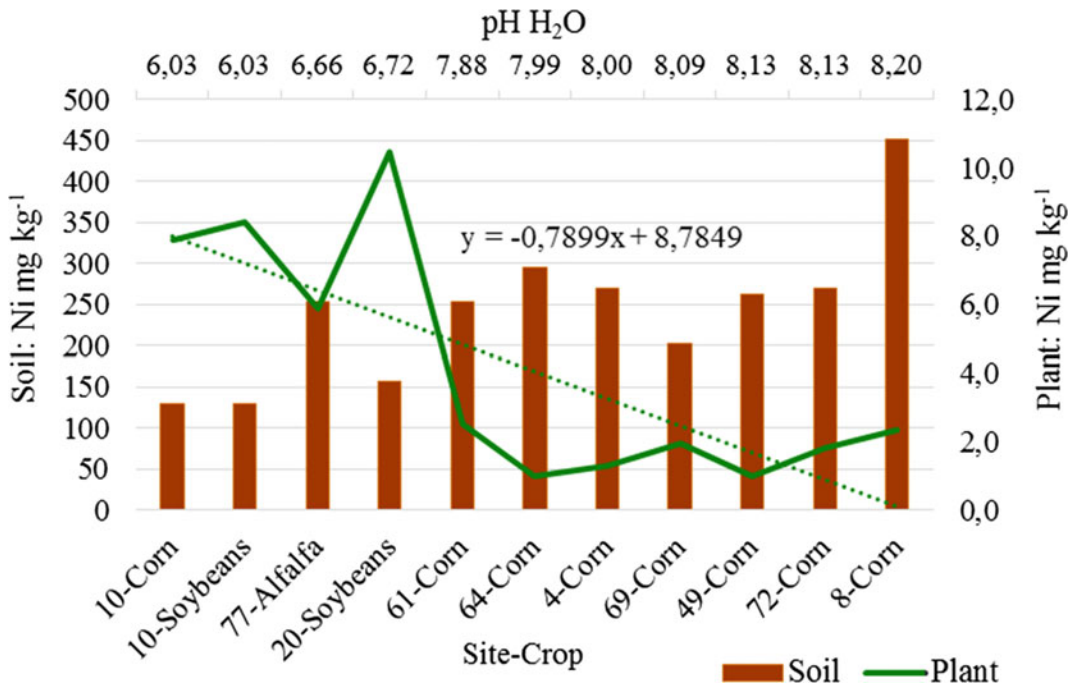


Fig. 23.14 Concentrations of Ni in plants depending on soil acidity and concentration of Ni in soil

the elevated concentrations of pseudo-total Zn and Cu were determined.

- The content of pseudo-total Ni in the flood sediment and in the soil classified these soils as contaminated.
- The concentrations of Ni, Zn and Cu in the soil and flood sediment, along with their horizontal and vertical distribution, indicated that these elements were mainly accumulated in the arable layer of agricultural land due to many years of regular flooding. In addition, regularly repeated deposits of flood sediment were mixed with soil material during agricultural production activities.
- In alkaline soils, the heavy metals were in insoluble forms, so the potential risk of their uptake in higher concentrations was very low, as confirmed by the analyses of plant materials for the content of Ni, Zn and Cu.
- In slightly acidic soils at elevated concentrations of Ni and under the reduced conditions due to the longer retention of surface water and a higher level of groundwater, some

metals may dissolve. This can cause plant uptake of potentially toxic elements and hence contaminate the food chain.

- In the flood zone on slightly acidic soil, it is necessary to monitor the content of heavy metals in leafy vegetables.
- Since the content of analysed heavy metals in the flood sediments was slightly different from their content in the topsoil, we can conclude that the flood in May 2014 did not pollute agricultural land, but caused a slight increase in the content of Ni, Zn and Cu in places where the flood sediment depth was >5 cm.
- This research showed the need to establish a permanent monitoring system for agricultural land in areas with a high flood risk by establishing permanent monitoring stations.

Acknowledgements These studies were funded by the Ministry of Agriculture, Forestry and Water Management of the Republic of Srpska, Bosnia and Herzegovina, under the Short-Term and Long-Term Millennium Development Programme.

References

- Adriano DC (2001) Trace elements in terrestrial environments, biogeochemistry, bioavailability, and risk of metals, 2nd edn. Springer, New York
- Algül F, Beyhan M (2020) Concentrations and sources of heavy metals in shallow sediments in Lake Bafa, Turkey. *Sci Rep* 10:11782. <https://doi.org/10.1038/s41598-020-68833-2>
- Amoatey P, Baawain MS (2019) Effects of pollution on freshwater aquatic organisms. *Water Environ Res* 91(10):1272–1287. <https://doi.org/10.1002/wer.1221>
- Antić-Mladenović S, Rinklebe J, Frohne T, Stark H-J, Wennrich R, Tomić Z et al (2011) Impact of controlled redox conditions on nickel in a serpentine soil. *J Soils Sediments* 11:406–415. <https://doi.org/10.1007/s10653-018-0138-4>
- Antić-Mladenović S, Frohne T, Kresović M, Stark HJ, Tomić Z, Ličina V et al (2017) Biogeochemistry of Ni and Pb in a periodically flooded arable soil: fractionation and redox-induced (im)mobilization. *J Environ Manag* 186(2):141–150. <https://doi.org/10.1016/j.jenvman.2016.06.005>
- ARSO (2014) Agency for the environment of the republic of Slovenia. Agencija Republika Slovenija za okolje in prostor: Analiza poplavnog događaja u maju 2014. U Bosni i Hercegovini za rijeku Bosnu u okviru pomoći Republike Slovenije. https://www.arso.gov.si/vode/poro%c4%8dila%20in%20publikacije/Koncno%20porocilo_Analiza%20poplave%20maja%202014%20za%20porecje%20reke%20Bosne.pdf. Accessed 20 Nov 2020
- Babajić E, Babajić A, Stjepić Srkalović Ž, Srkalović D, Ustalić S, Akmađić H (2017) Chromium and nickel in soil in the wider Maglaj area—concentration and genesis. *Arch Techn Sci* 17(1):13–20. <http://srpskiarhiv.rs/global/pdf/onlinefirst/002-18OIF-v2.pdf>
- Chaney RL (1989) Toxic element accumulation in soils and crops: protecting soil fertility and agricultural food-chains. In: Bar-Yozef B, Barrow NI, Goldshmid J (eds) *Inorganic contaminants in the Vadose Zone*. Springer, Berlin, pp 140–158
- Dutch Soil Remediation Circular (2013) Groundwater target values, soil remediation intervention values. <http://eca-suelo.com.pe/wp-content/uploads/2018/08/15.-Soil-Remediation-Circular-2013-version-of-1-July-2013.pdf>. Accessed 20 Nov 2020
- EC REGULATION No. 1881/2006 of 19 December 2006 setting maximum levels for certain contaminants in foodstuffs (2006). <https://eur-lex.europa.eu/legal-content/EN/TXT/PDF/?uri=CELEX:02006R1881-20150731&from=EN>. Accessed 20 Nov 2020
- EC, UN i WBG (2014) Assessment of needs and renewal in Bosnia and Herzegovina (Procjena potreba za oporavkom I obnovom u Bosni I Hercegovini). <http://www.mvp.gov.ba/Baneri-Linkovi/4juli2014ProcjenapotrebazaoporavakiobnovuBiH-Sazetak.pdf>. Accessed 20 Nov 2020
- Echo Joint Assessment Report (2014) Floods in Bosnia and Herzegovina, vol 10. http://ec.europa.eu/echo/files/news/bosnia_herzegovina_floods_joint_report_en.pdf. Accessed 20 Nov 2020
- FIAS (2014) Izvještaj o analizi tla sa poplavnih područja u Federaciji BiH (Report on Analysis of Soils from Floods in the Federation of BiH), unpublished results, Federal Institute of Aagropedology, Sarajevo
- Hinsinger P, Courchesne F (2008) Biogeochemistry of metals and metalloids at the soil–root interface. In: Violante A, Huang PM, Gadd GM (eds) *Biophysicochemical processes of heavymetals and metalloids in soil environments*. Wiley, New York, pp 267–310
- Hinsinger P, Gobran GR, Gregory PJ et al (2005) Rhizosphere geometry and heterogeneity arising from root-mediated physical and chemical processes. *New Phytol* 168:293–303. <https://doi.org/10.1111/j.1469-8137.2005.01512.x>
- Holmgren GGS, Meyer MW, Chaney RL, Daniels RB (1993) Cadmium, lead, zinc, copper, and nickel in agricultural soils of the United States of America. *J Environ Qual* 22(2):335–348. <https://doi.org/10.2134/jeq1993.00472425002200020015x>
- Hong Y-j, Liao W, Yan Z-f, Bai Y-c, Feng C-l, Xu Z-x, Xu D-y (2020) Progress in the research of the toxicity effect mechanisms of heavy metals on freshwater organisms and their water quality criteria in China. *J Chemistry* 9010348:12. <https://doi.org/10.1155/2020/9010348>
- Jakšić SP, Vučković SM, Vasiljević S, Grahovac N, Popović V, Šunjka DB, Dozet GK (2013) Accumulation of heavy metals in *Medicago sativa* L. and *Trifolium pratense* L. at the contaminated fluvisol, Hemijska industrija, 67(1):95–101
- JU PIRS (2014) Utvrđivanje stanja zagađenja poljoprivrednog zemljišta poplavljenih površina u maju 2014. god., JU Poljoprivredni institute Republike Srpske, Izvještaj broj 838-1/2014, pp 1–27
- Kabata-Pendias A (2010) Trace elements in soils and plants, 4th edn, p 548
- Khair KU, Farid M, Ashraf U et al (2020) Citric acid enhanced phytoextraction of nickel (Ni) and alleviate *Mentha piperita* (L.) from Ni-induced physiological and biochemical damages. *Environ Sci Pollut Res* 27:27010–27022. <https://doi.org/10.1007/s11356-020-08978-9>
- Khursheed W, Manzoor J, Dar A, Shuab R (2020) Heavy metal intrusion and accumulation in aquatic ecosystems. In: Fresh water pollution dynamics and remediation, pp 83–104. https://doi.org/10.1007/978-981-13-8277-2_6
- Kisić I, Komesarović B, Birkas M, Gajić-Čapka M (2015) Sanacija tala zahvaćenih poplavama. In: 50th Croatian and 10th international symposium on agriculture, Opatija, Croatia, proceedings, pp 28–36
- Laxen DPH (1985) Trace metal adsorption/co-precipitation of hydrous ferric oxide under realistic conditions. *Water Res* 19:1229–1236
- Malsiu A, Shehu I, Stafilov T, Faiku F (2020) Assessment of heavy metal concentrations with fractionation

- method in sediments and waters of the Badovci Lake (Kosovo). *J Environ Public Health* 3098594:14. <https://doi.org/10.1155/2020/3098594>
- Massoura ST, Echevarria G, Becquer T, Ghanbaja J, Leclerc-Cessac E, Morel J (2006) Control of nickel availability by nickel bearing minerals in natural and antropogenic soils. *Geoderma* 136:28–37. <https://doi.org/10.1016/j.geoderma.2006.01.008>
- McGrath SP (1984) Metal concentrations in sludges and soils from a long-term field trail. *J Agric Sci* 103 (1):25–35. <https://doi.org/10.1017/S002185960004329X>
- McGrath SP (1995) Chromium and nickel. In: Alloway BJ (ed) *Heavy metals in soils*. Blackie Academic & Professional, Glasgow, UK, pp 152–178
- Ministry of Agriculture of the Republic of Serbia (2014) (Ministarstvo poljoprivrede I zaštite životne sredine Republike Srbije): Uprava za zaštitu bilja, Fitosanitarna inspekcija, Izveštaj o sadržaju teških metala I opštim agrohemijskim svojstvima zemljišta sa poplavljenog područja Republike Srbije, Beograd, pp 1–68
- Mojičević M, Vilovski S, Tomić B. (1976) Institut za geološka istraživanja Sarajevo, 1964–1969. god. Osnovna geološka karta SFRJ, Banja Luka 1:100000, pp 33–119
- NATO SPS (2014) Development of a decision support system for reducing risk from environmental pollution in the Bosna river, NATO ESP.EAP.SFP 984073, Final Report, Bratislava & Sarajevo, pp 1–80. Accessed 20 Nov 2020
- Novaković D, Antić-Mladenović S, Predić T, Lukić R (2008) Distribution of nickel in the soils of the Vrbas river valley. *Agroknowledge J* 9(2):69–77
- Official Gazette of Serbia (Službeni glasnik RS) (2010) Uredba o program sistematskog praćenja kvaliteta zemljišta, indikatorima za ocenu rizika od degradacije zemljišta I metodologiji za izradu remedijacionih programa, broj 88/2010
- Official Gazette of Croatia (2014) (Narodne novine) Pravilnik o zaštiti poljoprivrednog zemljišta od onečišćenja, broj 09/2014
- Official Gazette of Montenegro (1997) (Službeni list RCG) Pravilnik o dozvoljenim količinama opasnih I štetnih materija u zemljištu I metodama za njihovo ispitivanje, broj 18/1997
- Official Gazette of Federation of Bosnia and Herzegovina (2009) (Službene novine Federacije BiH), Pravilnik o utvrđivanju dozvoljenih količina štetnih I opasnih materija u zemljištu I metode njihovog ispitivanja, broj 72/2009
- Pandey J, Shubhashish K, Pandey R (2010) Heavy metal contamination of Ganga river at Varanasi in relation to atmospheric deposition. *Trop Ecol* 51(2):365–373. https://www.researchgate.net/publication/288469832_Heavy_metal_contamination_of_Ganga_river_at_Varanasi_in_relation_to_atmospheric_deposition
- Pandey J, Singh R (2017) Heavy metals in sediments of Ganga River: up- and downstream urban influences. *Appl Water Sci* 7(4):1669–1678. <https://doi.org/10.1007/s13201-015-0334-7>, Accessed 20 Nov 2020
- Pavlovkin J, Fiala R, Čiamporová M, Martinka M, Repka V (2016) Impact of nickel on grapevine (*Vitisvinifera* L.) root plasma membrane, ROS generation, and cell viability. *Acta Bot Croat* 75(1):25–30. <https://doi.org/10.1515/botcro-2016-0017>,
- Pedological map of Bosnia and Herzegovina (1973) sekcija Brod 4, 1: 50000, Zavod za agropedologiju, Sarajevo
- Predić T, Nikić Nauth P, Radanović B, Predić A (2016) State of heavy metals pollution of flooded agricultural land in the North Part of Republic of Srpska. *Agro-Knowl J* 17(1):19–27. <https://doi.org/10.7251/AGREN1601019P>
- Predić T, Lukić R, Nikić Nauth P, Cvijanović T, Docić Kojadinović T, Malčić T, Jokić D, Radanović B (2013) Introduction of continuous monitoring of agricultural land of Republic of Srpska. In: *Proceeding, of the 1st international congress on soil science XIII national congress in soil science*, Belgrade, pp 1–16
- Reimann C, Birke M, Demetriades A, Filzmoser P, O'Connor P (2014) *Chemistry of Europe's agricultural soils*. Data DVDPart A; Geol Jb, B 102, BGR, Hannover, Germany
- Qian B, Tang C, Yang Y, Xiao X (2020) Pollution characteristics and risk assessment of heavy metals in the surface sediments of Dongting Lake water system during normal water period. *Eur J Remote Sens*. <https://doi.org/10.1080/22797254.2020.1763207>
- RHMZRS (2014) Meteorološki I hidrološki aspekti poplava u Republici Srpskoj, maj 2014 (Метеоролошки и хидролошки аспекти поплава у Републици Српској, мај 2014) Republički hidrometeorološki zavod RS, Banja Luka, pp 1–39, <http://www.RHMZRS.com/assets/images/meteorologija/>. Accessed 25 May 2019
- Sakan MS, Đorđević SD, Manojlović DD, Polić SP (2009) Assessment of heavy metal pollutants accumulation in the Tisza river sediments. *J Environ Manag* 90(11):3382–3390. <https://doi.org/10.1016/j.jenvman.2009.05.013>
- Sekabira K, Oryem Origa H, Basamba TA, Mutumba G, Kakudidi E (2010) Assessment of heavy metal pollution in the urban stream sediments and its tributaries. *Int J Environ Sci Tech* 7(3):435–446. <https://doi.org/10.1007/BF03326153>
- Singh PK, Malik A, Basant N, Singh KV, Basant A (2007) Multi-way data modeling of heavy metal fractionation in sediments from Gomti River (India). *Chemom Intell Lab Syst* 87(2):185–193
- Sharmin S, Zakir HM, Shikazono N (2010) Fractionation profile and mobility pattern of trace metals in sediments of Nomi River, Tokyo Japan. *J Soil Sci Environ Manag* 1(1):001–014
- Šefket G, Bukalo E, Trako E (2011) Monitoring the content of heavy metals in soil and plants in environment Iron works in Zenica, *Kvalitet* 2011, 7. Scientific

- conference with international participation, Neum, pp 1–6
- Tuna AL, Yilmaz F, Demirak A, Ozdemir N (2007) Sources and distribution of trace metals in the Saricay stream basin of southwestern Turkey. *Environ Monit Assess* 125(1–3):47–57. <https://doi.org/10.1007/s10661-006-9238-1>
- Vuković D, Stanković JS, Vuković Ž, Janković K (2014) Transport and storage of heavy metals in the Sava River Basin in Serbia. *J Serbian Chem Soc* 79(3):379–387. <https://doi.org/10.2298/JSC130128085V>
- US EPA (1996) Method 3050B. Acid digestion of sediments, sludges, and soils revision 2
- Ure AM, Berrow ML (1982) The elemental constituents of soils. In: Bowen HYM (ed) *Environmental chemistry*, vol 2. Royal Society of Chemistry, London, pp 94–204
- WRB, IUSS Working Group (2015) World reference base for soil resources 2014, update 2015 International soil classification system for naming soils and creating legends for soil maps. World soil resources reports No. 106. FAO, Rome
- YSSS (1966) *Manual for Soil chemical analysis—Book 1*, Yugoslav society of soil science, pp 1–270, Belgrade
- Yunus K (2020) A review on the accumulation of heavy metals in coastal sediment of Peninsular Malaysia. *Environ Clim Chang* 1(1):21–35. <https://doi.org/10.1108/EFCC-03-2020-0003>, <https://www.emerald.com/insight/2633-4070.htm>



Poorly Soluble and Mobile Forms of Heavy Metals in the Soils of the Volga Steppes

Victor V. Pronko, Dmitry Yu. Zhuravlev,
Tatyana M. Yaroshenko, Nadezhda
F. Klimova, and Sonja Tošić

Abstract

To this day, scientists argue about the extent and rate of accumulation of heavy metals and potentially toxic substances in the soil. Questions regarding the forms of heavy metals, their spatial distribution, solubility, plant availability, etc., are still relevant. It is known that the content of heavy metals is considerably influenced by the content and composition of soil organic matter, particle size distribution, soil pH and parent rocks, as well as redox conditions. Since 2007, the steppe soils of the Volga region have been monitored for the content of heavy metals in virgin and arable landscapes. In this work, the content of poorly soluble and mobile forms of Zn, Cu, Pb, Cd, Ni, Hg and As in 0–20 cm topsoil was determined in two types and eight subtypes of Chernozem and chestnut soils. Some differ-

ences were found in the accumulation of heavy metals between the soil types and subtypes which were studied. No changes were found in the content of poorly soluble heavy metals between the virgin and corresponding arable soil in the Volga steppes. The content of heavy metals in all the soils which were studied was below the maximum allowed concentrations. The relative content of the mobile forms of heavy metals as a percentage of the total varied from 7–25% for Cd and 0.5–2.2% for Zn and Cu. The accumulation of Pb, Cd, Ni and As in soils located near the large industrial zone showed an increasing trend. The maximum allowed concentrations of heavy metals were not exceeded in the soils studied. Also, agricultural soil management did not significantly increase the heavy metal concentrations.

Keywords

Heavy metals · Volga region · Chernozem · Chestnut soils · Virgin land · Arable land

V. V. Pronko (✉)
Scientific Production Association “Power of Life”,
St. Bolshaya Sadovaya 239, Saratov, Russia
e-mail: victor-pronko@mail.ru

D. Yu. Zhuravlev · T. M. Yaroshenko · N. F. Klimova
Research Institute of Agriculture of the South-East,
St. Tulaykova 7, Saratov, Russia

S. Tošić
Institute of Soil Science, St. TeodoraDrajzera 7,
Belgrade, Serbia
e-mail: sonja.tosic@soilinst.rs

24.1 Introduction

The world’s population is expected to increase by 2 billion in the next 30 years, from 7.7 billion currently to 9.7 billion in 2050 (UN 2019). This inevitably calls for a tremendous amount of

resources and energy from the earth and an enormous amount of food, fibre and other vital services for living. Moreover, the trend towards an increase in the world's population is promoting accelerated industrialisation and urbanisation, ultimately leading to various environmental problems associated with the depletion of non-renewable resources such as soil, and to the excessive accumulation of potentially toxic and hazardous elements in every niche of our environment (Gupta and Sandallo 2011; Tošić et al. 2019; Zhen et al. 2019; Guo et al. 2020), including the animal and human food chain (e.g. Yang et al. 2019; Rutigliano et al. 2019).

Anthropogenic impacts on soil are the most diverse, leading to various changes in soil formation processes and soil properties, which sometimes cause irreparable damage, especially to agricultural production. Kabata-Pendias and Szeke (2015) reported that anthropogenic metals are usually likely to be very mobile and easily available to plants. Forms of the metals of both origins may be transformed due to pedogenic processes and they become “pedogenic” metals, greatly controlled by soil properties. The contamination of arable lands mainly occurs due to the overuse of pesticides, ameliorants, airborne toxic elements and industrial and urban landfills (Huang et al. 2019; Gruszecka-Kosowska et al. 2020; Orlova et al. 2017). It is important to define the background limit values in areas of intense human activity, to know the level of potentially toxic elements (PTEs) which must be restored after the end of the land exploitation (Tošić et al. 2020). The excess accumulation of chemical pollutants leads to a degradation of the soil's physical, chemical and biological characteristics and adversely affects plant growth (Gupta and Sandallo 2011; Hashem et al. 2017; Guo et al. 2020; Qaswar et al. 2020) and loss of biodiversity (Guerra et al. 2020), posing risks to human and animal health (Tchounwou et al. 2012; Steffan et al. 2018; Bakshi and Banik, 2018; Zwolak et al. 2019; Cambier et al. 2019).

At the end of the last century, there was a surge in the number of studies on the accumulation of microelements in concentrations toxic to organisms in the soil and agricultural crops (e.g.

Alloway 1995; Nannipieri et al., 1997; Giller et al. 1998; Kabata-Pendias and Pendias 2001). Modern agricultural practices, the excessive use of fertilisers and pesticides and inappropriate irrigation systems have adversely affected the natural quality and fertility of cultivated land. A significant increase in crop production is based on an increase in the use of chemicals and fertilisers, including insecticides and pesticides. Both the use of mineral fertilisers and the production of industrial fertilisers are potential sources of contamination of the soil–plant food chain system with heavy metals, such as Hg, Cd, As, Pb, Cu, Ni and Cu (Adriano 2001; Lavrishchev et al. 2018).

Regardless of the source, all anthropogenically produced heavy metals ultimately accumulate in soil either by point-source or diffuse contamination (Rodríguez-Eugenio et al., 2018). The scale and speed of their accumulation, as well as their further transformation (solubility, mobility and stability), substantially depend on the properties of the soil, parent rock, organic matter and clay content and soil acidity or alkalinity (Alekseev 1992; Dobrovolsky 1999; Karpova and Mineev 2015; Cambier et al. 2019; Król et al. 2020). In an alkaline environment, the mobility and availability of some heavy metals for plants are typically sharply reduced (Sheudzhen 2010; Król et al. 2020). Most researchers report that the low soil pH substantially enhances the phytotoxicity of heavy metals (Karpova and Mineev 2015; Kabata-Pendias and Pendias 2001). Wang et al. (2006) found that plant availability of Cd and Zn increased with an increase in the soil pH. Giro-Paloma et al. (2020) reported that when the mean pH was between 9.0 and 11.0, the concentration of pH-dependent metals/metalloids decreases significantly. In contrast, organic matter (Kim et al. 2015; Hou et al. 2020) and clay particles (Marques et al. 2009; Kim et al. 2015; Kome et al. 2019) can reduce the availability of heavy metals to plants through immobilisation, acting as a sorbent and neutraliser for many pollutants entering the soil (Shafronov 2007).

Humic substances form various complex organo-mineral compounds (fulvates and

humates) with heavy metals, which significantly reduce heavy metals' migratory ability and plant accessibility. The relative surface area of soil and the ability of soil colloids to complex with ligands also regulate heavy metal availability to plant roots (e.g. Magnuson et al. 2001; Marques et al. 2009). However, an excess accumulation of heavy metal in soil can degrade the soil humus through the greater accumulation of fulvic acids (Ladonin and Margolina 1997) and negatively affect the soil's biological properties (Friedlová 2010; Tang et al. 2019). In addition, the prolonged technogenic impact of heavy metal salts generally leads to noticeable changes in the number of major groups of microorganisms. Research by Evdokimova et al. (1984) showed that soil contamination with copper (2–3 times higher than the background level) significantly altered the microbial community. The most sensitive groups were saprophytic microorganisms and actinomycetes, which play an important role in the mineralisation of plant residues, while the number of oligotrophic microorganisms and fungi in HM-contaminated soils increased. The effect of the total and mobile forms of individual heavy metal is not yet clearly understood (Cambier et al. 2019; Ogunlaja et al. 2019). Zhen et al. (2019) found that both the total amount and availability of heavy metals had a significant influence on soil ecological functions and microbial community across land use patterns.

Previous studies reported that one of the most toxic elements for organisms is lead (Pb) (Nikitin 2014; Medvedev and Derevyagin 2017). The study by Saljnikov et al. (2019) examining how PTE emissions from a thermal power plant (Kostolac) affected the contamination of cropland showed that 73% of the variance of the sources of As, Cu and Pb was of anthropogenic origin for most of their content in Serbia. Similarly, Tošić et al. (2020) found that concentrations of As and Cu in the copper mining area of Serbia's Bor municipality were 18.8% and 30.4% above the maximum allowed concentrations (MACs). Tóth et al. (2016) reported that, in Europe, the soils under agricultural use have a higher percentage of samples with a concentration of heavy metals above the threshold value

for ecological or health risk (MEF 2007), than other land uses. Studies on the effect of Pb on the agroecosystem were conducted at the "Belgorod" Centre for Agrochemical Services from 1998–2003, based on 20 reference objects (typical and leached Chernozems). The results showed that the average total content of Pb in topsoil was $13 \pm 0.8 \text{ mg kg}^{-1}$. Earlier, the results of the full testing and monitoring of regional soils showed that concentrations of Pb did not exceed the maximum allowed concentrations (MACs) and were 65 mg kg^{-1} on loamy and clay soils with a $\text{pH} < 5.5$, and 130 mg kg^{-1} on soils with a $\text{pH} > 5.5$ (Lukin and Avramenko 2006). However, the results of field experiments on arable ordinary carbonate-heavy loamy Chernozem in the fields of the soil faculty of Moscow State University and the Agroecological Faculty of Rostov-on-Don Agrarian University showed that the Chernozem soils of the Volga steppes are negatively affected by heavy metals (HMs) (Minkina et al. 2006). They found that heavy metal contamination of soil has a direct toxicological biochemical effect that leads to soil degradation. In their study, a single soil contamination with relatively low doses of Pb, Zn and Cu (2–3 times lower than the MPC) led to the partial mobilisation of humus 2 years later. This was manifested in an increase in the relative content of mobile organo-mineral compounds and an increase in the proportion of fulvic acids. The fact that this happened in Chernozem soil, the humus of which is considered a relatively stable system, indicates that the fertile agricultural lands of the Volga steppes are in ecological danger (Minkina et al. 2006).

The limit toxicity values of PTEs depend greatly on climatic and pedoclimatic factors, which determine the degree to which the toxic compounds are released (Król et al. 2020). Different countries or regions have adopted their own limits on the level of heavy metals in food. A number of studies have categorised the heavy metals according to their toxicity for living organisms in the following order: $\text{Hg} > \text{Cu} > \text{Zn} > \text{Ni} > \text{Pb} > \text{Cd} > \text{Cr} > \text{Sn} > \text{Fe} > \text{Mn} > \text{Al}$ (e.g. Wang et al. 2003; Filipiak-Szok et al. 2015). According to the legislation of the Russian

Federation (GOST 17.4.1.02-83, 1985), the chemical elements are divided into three classes according to their toxicity and hazardousness, with regulated maximum allowed concentrations for each element (Guidelines 1992):

Hazard Class I: arsenic, cadmium, mercury, selenium, lead, zinc, fluorine, benz(a)pyrene.

Hazard Class II: boron, cobalt, nickel, molybdenum, copper, antimony, chromium.

Hazard Class III: barium, vanadium, tungsten, manganese, strontium, acetophenone.

The aim of this research was to study and compare the content of the most abundant potentially toxic elements (Zn, Cu, Pb, Cd, Ni, Hg, As) in their poorly soluble and mobile forms both in virgin and arable agricultural landscapes on the eight subtypes of Chernozem and chestnut soils of the Volga steppes.

24.2 Materials and Methods

The following objects were studied: three subtypes of Chernozem soils (Typical, Ordinary and Southern) (Egorov et al. 1977) on the right bank of the Volga River and five subtypes of chestnut soil (Kastanozem, WRB 2014): Dark chestnut on the terraces of the left bank of the Volga, and dark chestnut, chestnut, light chestnut and meadow chestnut on the high plain of the Saratov Trans-Volga region. Each soil studied was sampled from arable and virgin sites. Soil subtypes differed in terms of their humus reserves, particle size distribution, vegetation and moisture and temperature regimes. For each soil subtype, 16 samples were taken (eight from virgin soil and eight from arable land). In agricultural landscapes, the effect of the application of various fertilisers containing heavy metals was studied and compared with their virgin analogues. In total, 128 samples were analysed for the content of organic carbon and total nitrogen, pH, particle size distribution, carbonates and concentrations of zinc (Zn), copper (Cu), lead (Pb), cadmium (Cd), nickel (Ni), arsenic (As) and mercury (Hg).

The soil acidity (pH) was determined by potentiometry, using a glass electrode. The content of soil humus was determined using the wet

combustion Tyurin method, by oxidising a small portion of the soil with potassium dichromate, then titrating the excess potassium dichromate with Mohr's salt (Mineev 2001); the total nitrogen was determined by titration using the Kjeldahl method (GOST 26107-84 1984); and the content of carbonates was determined in an aqueous extract by titration with a solution of sulphuric acid to pH 8.3 and bicarbonate to pH 4.4. The end point of the titration was set using a pH meter or by changing the colour of phenolphthalein (pH 8.3) and methyl orange (pH 4.4) (GOST 26424-85 1986); the particle size distribution was determined with the pipette method (GOST 12536-2014 2014).

Poorly soluble and mobile forms of heavy metals were determined according to the Guidelines for the Determination of Heavy Metals in Farmland Soils and Crop Production (Guidelines 1992). First, air-dried soil samples ground to <2 mm were analysed for their moisture content. Then, to determine the poorly soluble forms, 10 g of soil was placed in conical flasks with a volume of 200–250 cm³ and 50 cm³ of 1 N HCl was added. The suspension was then shaken for 1 h and left covered overnight. The next day, the suspension was filtered and analysed on an atomic adsorption spectrophotometer. The mobile forms (plant form) of the elements studied were extracted with a solution of ammonium acetate with a pH of 4.8 at a ratio of 1:10 after 1 h of shaking and left overnight. The extracts of soil samples were then analysed for the poorly and mobile forms using the quantitative spectral technique on a spectrograph DFS-8 (distributed file system) and atomic emission spectroscopy on the Optima 2000DV (optical emission spectrometer). The toxicity level of heavy metals in the soil was determined according to the legislation of the Russian Federation for the maximum permissible concentrations (MPCs) of chemical substances in soil (GN 2.1.7.2041-06, 2006).

The functional groups of soil humus were characterised (fractionation) using a NaOH 1 N extract solution (extraction of humic acid fraction) and water (fulvic acid fraction). Insoluble humic compounds were found as the difference

between the total humus content and the isolated fractions of humic and fulvic acids.

The dry bulk density (BD) of the soil (g/cm^3) was determined using the Kachinsky method with a 100 cm^3 volumetric cylinder. Steel cylinders of a known mass and 100 cm^3 volume with a sharpened edge were used to take the intact samples in 4–6 repetitions. In the laboratory, the cylinders were oven dried at a temperature of $105 \text{ }^\circ\text{C}$ to a constant weight. After drying, the mass of the absolutely dry soil was determined and the bulk density of the dry soil was calculated. The granulometric composition was determined following wet dispersion with the pipette method (GOST 12536–2014 2014). The amount of absorbed substances (Ca, Mg and Na) was determined with the Kappen-Gilkovits method (GOST 27821–88 1988). The method is based on the reaction of absorbed soil bases with hydrochloric acid and the subsequent titration of non-reacted acid with sodium hydroxide. The reduction–oxidation potential (ROP) was determined on an electric potentiometer using a special electrode. The data obtained were analysed using ANOVA, the means were compared with an LSD test to find significant differences and the significant differences were analysed using the multiple t-test method.

24.3 Results and Discussion

24.3.1 Basic Soil Parameters

Chernozem soils were formed under a steppe climate with rich grassy vegetation. Therefore, the humus content was quite high: from 3.6% (southern Chernozem) to 7.7% (typical Chernozem). Humic acid predominated in the composition of soil humus: it was 2–4 times greater than the content of available fulvic acids. The ploughing of virgin Chernozem soils (250–300 years ago in the Volga region) led to a decrease in the humus content and the proportion of humic acids, and the reserves of nitrogen also decreased. Cultivated soils did not differ from virgin soils in terms of the total content of phosphorus and potassium compounds

(Table 24.1). The soil solution's reaction to Chernozem soils was predominantly neutral. On southern Chernozems, it proved to be slightly alkaline.

The mass ploughing of chestnut soils in the Volga region began in the middle of the twentieth century. These soils were formed under severe hydrothermal conditions. Therefore, they contain much less humus than Chernozems. The only exceptions are meadow chestnut soils, which formed along the lower valleys of steppe rivers.

The predominance of mineralisation processes over humification in these soils contributed to the fact that during ploughing, the humus content and total nitrogen decreased. In terms of the content of phosphorus and potassium, the only tendency noted was a decrease in their amount (Table 24.1). The reaction of soil solution to chestnut soils ranged from neutral to alkaline. The ploughing of Chernozem and chestnut soils led to their compaction (Table 24.2). In the Volga region, more than 80% of zonal soils have a heavy loamy and light clayey granulometric composition. It should also be noted that, although the values for the content of clay particles are similar, the soils studied differ significantly in the amount of the smallest particles (dust + silt). Their content ranges from 20% for typical Chernozems to 58% for light chestnut soil. Calcium predominates in the composition of the absorbed bases of Chernozems, while magnesium content was 5–10 times less. In chestnut soils, the proportion of magnesium sharply increases, and sodium is present in the soil absorption complex. Determination of the ROP potential showed that in all the soils studied, oxidative processes prevail over reductive ones (Table 24.2).

24.3.2 Zinc

Zinc is an essential trace element for living organisms, since it is part of the enzymes that are involved in the processes of respiration and metabolism of carbohydrates, proteins and phosphates (Kabata-Pendias and Pendias 2001; Medvedev and Derevyagin 2017). Its deficiency in human and animal diets has a wide range of

Table 24.1 Agrochemical properties of the studied soil types and subtypes of the Volga steppes (layer 0–20 cm)

Subtypes of soils	Agro background	Humus, %				Total reserves, %			pH _{water}
		1	2	3	4	N	P ₂ O ₅	K ₂ O	
Subtypes of Chernozem									
Typical	virgin*	7.7	39	9	52	0.46	0.17	1.50	6.7
	arable land	7.1	33	9	58	0.40	0.15	1.50	6.8
Ordinary	virgin	8.1	38	12	50	0.31	0.13	1.70	6.4
	arable land	6.0	34	14	52	0.29	0.13	1.75	6.6
South	virgin	5.4	30	10	60	0.24	0.12	2.15	6.8
	arable land	3.6	28	14	58	0.20	0.11	2.00	7.3
LSD _{0.5}		0.51	–	–	–	0.04	0.02	0.34	0.4
Chestnut soils									
Dark chestnut river terraces	virgin	3.1	39	17	44	0.21	0.18	1.81	7.4
	arable land	2.8	24	16	60	0.13	0.16	1.75	7.9
Dark chestnut high plain	virgin	4.0	38	19	43	0.20	0.18	1.96	7.8
	arable land	2.8	37	20	43	0.13	0.17	1.86	8.2
Chestnut high plain	virgin	3.0	35	20	45	0.20	0.16	1.84	8.0
	arable land	2.2	31	22	47	0.12	0.15	1.80	8.5
Light chestnut high plain	virgin	2.6	31	22	47	0.15	0.14	2.07	8.5
	arable land	1.8	29	20	51	0.11	0.15	2.01	8.6
Meadow chestnut river valleys	virgin	6.0	36	21	33	0.22	0.13	1.29	7.3
	arable land	3.3	31	21	48	0.17	0.13	1.21	6.7
LSD _{0.5}		0.62	–	–	–	0.05	0.02	0.26	0.5

Notes *virgin land—no evidence of cultivation history was found in a search of the literature and maps; LSD—least square difference at $p < 0.05$; 1—total humus; 2—humic acids, % of total humus; 3—fulvic acids, % from total humus; 4—insoluble humic compounds, % of total humus

health impacts (Chasapis et al. 2020). Moreover, its excess accumulation in soil causes negative changes in its physical and physico-chemical properties, as well as the inhibition of biological activity (Chernykh 2001; Singh et al. 2011) and plant growth (Greany 2005). In calcareous soil, such as steppe Chernozem and chestnut soils, the content of Zn in the Fe oxides, both amorphous and crystalline, is much higher than in acidic and neutral soils (Xiang et al. 1995).

Our research has established that the Zn content in Chernozems at a depth of 0–20 cm ranged from 103 kg/ha⁻¹ (ordinary Chernozem) to 83 kg/ha⁻¹ (southern Chernozem). Ordinary Chernozems had the highest concentrations of Zn and southern Chernozems the lowest (Fig. 24.1a, b). These results indirectly supported earlier studies indicating that a decrease in humus

content and an increase in the clay fraction complicate the extraction of Zn with concentrated hydrochloric acid. Zinc ions become immobile when bound in the interlayers of the crystal lattice of clay minerals. Also, Zn forms stable complexes with organic matter and thus usually accumulates in soil horizons with a high humus content (Ivanov 1996). However, at the same time, the content of mobile Zn was highest in the typical Chernozem (2.5–2.8% of total); 5–5.6 times higher than in the southern Chernozem (Table 24.3).

Generally, concentrations of poorly soluble Zn in the monchestnut soils were at almost the same level as in the Chernozem (Fig. 24.1). The exception was the dark chestnut soils, where the Zn concentration was 20–37% higher than in Chernozems at a depth of 0–20 cm. The

Table 24.2 Physical and physico-chemical properties of the studied soil types and subtypes of the Volga steppes (0–20 cm layer)

Subtypes of soils	Agro background	Dry bulk density, g/cm ³	Soil particles, %		Absorbed bases, mg-equivalent/100 g				ROP, mV
			<0.01 mm	>0.01 mm	Sum	Ca ⁺	Mg ⁺	Na ⁺	
Subtypes of Chernozem									
Typical	virgin*	1.05	45	55	48	40	8	0	437
	arable land	1.15	42	58	44	40	4	0	482
Ordinary	virgin	1.09	53	47	40	32	8	0	434
	arable land	1.19	55	45	50	46	4	0	393
South	virgin	1.15	54	46	38	28	10	0	388
	arable land	1.21	60	40	36	30	6	0	407
LSD _{0.5}		0.07	–	–	2.2	1.8	0.9	0	20.0
Chestnut soils									
Dark chestnut river terraces	virgin	1.19	40	60	37.8	20.5	17.0	0.3	407
	arable land	1.22	42	58	30.2	15.9	14.0	0.3	426
Dark chestnut high plain	virgin	1.22	52	48	39.3	23.5	15.5	0.3	426
	arable land	1.24	55	45	36.8	19.3	17.0	0.5	445
Chestnut high plain	virgin	1.23	54	46	33.9	27.2	5.0	1.7	400
	arable land	1.26	58	42	36.4	26.0	8.5	1.9	426
Light Chestnut high plain	virgin	1.24	62	38	30.6	15.8	12.4	2.4	424
	arable land	1.28	66	34	28.6	16.0	10.4	2.2	474
Meadow chestnut river valleys	virgin	1.21	45	55	27.8	15.7	10.2	1.9	403
	arable land	1.22	48	52	26.7	15.0	9.7	2.0	418
LSD _{0.5}		0.05	–	–	1.9	0.7	0.5	–	15.4

Notes *virgin land—no evidence of cultivation history was found in a search of the literature and maps; LSD—least square difference; ROP—redox potential

possibility of an increased accumulation of Zn in chestnut soils was mentioned previously (Sheudzhen 2010), and is associated with higher pH values in those soils (Table 24.1). The range of Zn concentrations in our study was relatively evenly distributed among the Chernozem soils studied, but was in a narrower range (35–53 mg kg⁻¹) than in the grasslands of the Orenburg region, where they were 10.2–35.8 mg kg⁻¹ as reported by Groshev et al. (2007)—or in the light chestnut soils of Volga River valley, which ranged from 29.4 to 195.0 mg kg⁻¹ (Okolelova et al. 2014; Zaikina et al. 2016).

The content of Zn extracted by ammonium acetate was low in all subtypes of chestnut soils (Table 24.1). This is associated with a generally low solubility of Zn (Alloway 2008), due to the high pH values and high concentrations of calcium carbonates and phosphates. The inverse effect of the low solubility of Zn in this soil is manifested in the inhibition of Zn availability to plants (Alloway 2008; Lu et al. 2011). In addition, the amount of Zn in virgin and arable soils of the same type was almost at the same level. The concentrations of Zn did not exceed the MAC values in all analysed samples (the MAC

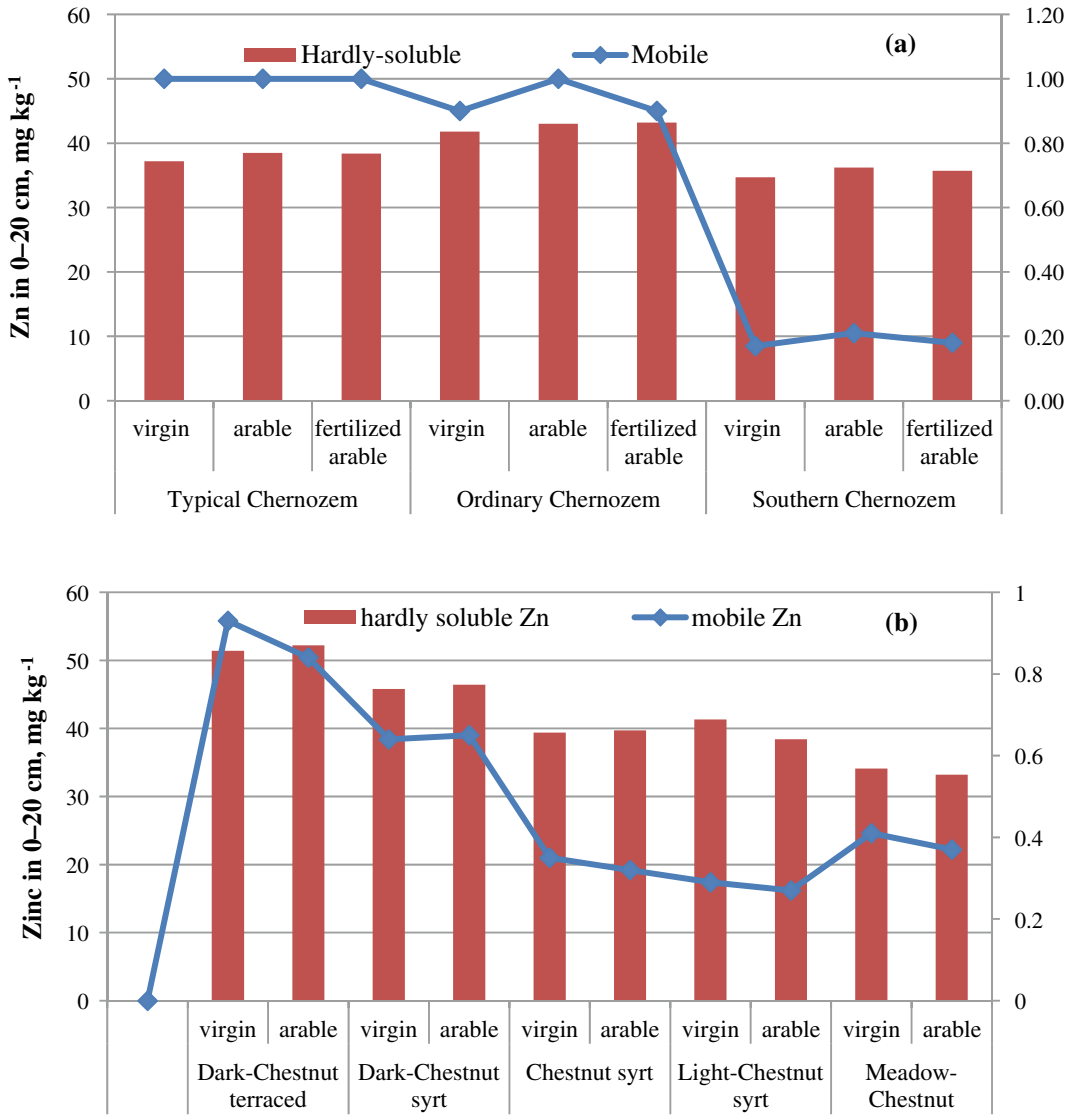


Fig. 24.1 Content of poorly soluble and mobile Zn in (a) Chernozem and (b) chestnut soils in 0–20 cm topsoil

value for Zn in the Russian Federation is 58 mg kg⁻¹).

24.3.3 Copper (Cu)

Copper plays a very important role in many physiological processes (photosynthesis, respiration, redistribution of carbohydrates, restoration and fixation of atmospheric nitrogen). At high concentrations, Cu compounds become

toxic for plants: they can cause chlorosis, inhibit root system growth and increase the amount of mobile fulvic acids in the soil (Dobrovolsky 1997). They also become toxic for humans, causing anaemia, liver and kidney damage and stomach and intestinal irritation (Wuana and Okieimen 2011). The adsorption of divalent copper to organic and inorganic soil particles determines its concentrations in the soil solution. In highly humified soils, the Cu⁺⁺ is strongly bound by various organic and organo-mineral

Table 24.3 Content of mobile heavy metals (% from total content) at a soil depth of 0–20 cm

Soil subtype	Land use	Zn	Cu	Pb	Cd	Ni	As	Hg
Chernozems soil								
Typical Chernozem	Virgin	2.8	1.9	5.0	7.7	4.1	5.4	3.6
	Arable	2.7	1.6	5.1	7.6	4.0	5.5	3.7
	Fertilised arable	2.5	1.7	5.1	7.5	4.4	5.4	3.5
Ordinary Chernozem	Virgin	2.2	1.4	6.5	5.0	5.6	4.4	3.0
	Arable	2.2	1.4	6.6	5.0	5.8	4.2	3.2
	Fertilised arable	2.0	1.3	6.8	5.2	5.9	4.2	3.0
Southern Chernozem	Virgin	0.5	0.7	15.0	24.4	6.2	7.2	2.4
	Arable	0.6	0.5	15.3	25.9	6.9	7.4	2.6
	Fertilised arable	0.5	0.6	15.4	26.2	6.8	7.9	2.5
Chestnut soils								
Dark chestnut terraced	Virgin	1.8	1.1	4.1	6.1	2.6	3.8	2.4
	Arable	1.6	1.2	4.0	6.0	2.5	3.4	2.5
Dark chestnut syrt	Virgin	1.4	0.9	3.9	5.6	2.4	3.2	2.7
	Arable	1.4	0.8	3.7	5.5	2.4	3.5	2.6
Chestnut syrt	Virgin	0.9	0.7	3.0	6.0	2.0	3.0	2.2
	Arable	0.8	0.7	3.2	5.8	1.9	3.0	2.2
Light chestnut syrt	Virgin	0.7	0.6	2.6	5.2	1.8	2.9	2.1
	Arable	0.7	0.6	2.4	5.0	1.7	2.8	2.0
Meadow chestnut	Virgin	1.2	1.3	1.9	2,12.1	2,42.4	3,33.3	2,62.6
	Arable	1.1	1.4	1.8	2,22.2	2,32.3	3,43.4	2,72.7

compounds (Mengel et al. 2001), therefore only a small fraction of copper is found in solution as ionic copper, Cu(II). Moreover, the solubility of Cu sharply increases at pH 5.5 (Martínez and Motto 2000), but in calcareous soils its availability greatly decreases.

The obtained concentrations of Cu were within global average values (Ballabio et al. 2018). В черноземных почвах Поволжья в слое 0–20 см содержится трудно растворимых соединений меди неуклонно снижалось от черноземов типичных и обыкновенных к черноземам южным (рис. 2). In the Chernozem soils, the content of poorly soluble Cu steadily declined from typical and ordinary Chernozem to southern Chernozem at a depth of 0–20 cm (Fig. 24.2). Наши расчеты показали, что максимум соединений меди обнаружен на черноземе обыкновенном – 49 кг/га. The

highest Cu content was found in ordinary Chernozem (49 kg/ha⁻¹) and the smallest на черноземе южном находилось 30 кг/га или в 1,6 раз ниже. In southern Chernozem (30 kg/ha⁻¹). These results confirm earlier reports that the high amount of carbonates reduces the mobility of Cu, as is the case for southern Chernozems (Sheudzhen 2010; Al-Mur 2020; Piri et al. 2020). In their study on heavy metal solubility, Piri et al. (2020) found that applying diatomite to soil caused the metals to convert from labile to non-labile forms, hence potentially decreasing the toxicity of metals in multi-metal-contaminated soil.

From Table 24.3, we can see that the content of mobile Cu extracted by the acetate-ammonium buffer solution in the southern Chernozem was 3.8–3.0 times lower than in the typical Chernozem. In chestnut soils on the dry Volga

steppes, an increased accumulation of poorly soluble Cu was found in the subtypes containing a higher amount of organic matter, such as dark chestnut on the left bank terraces and meadow chestnut (Fig. 24.2a, b). In line with this, the most humified dark chestnut soil had 73 kg/ha⁻¹

of Cu, meadow chestnut had 59 kg/ha⁻¹ and the arable light chestnut soil with lowest humus and very high clay content had 36 kg/ha⁻¹ of Cu at 0–20 cm. Our results also confirm earlier studies indicating that carbonates, which greatly control the soil CEC in southern Chernozem, reduce the

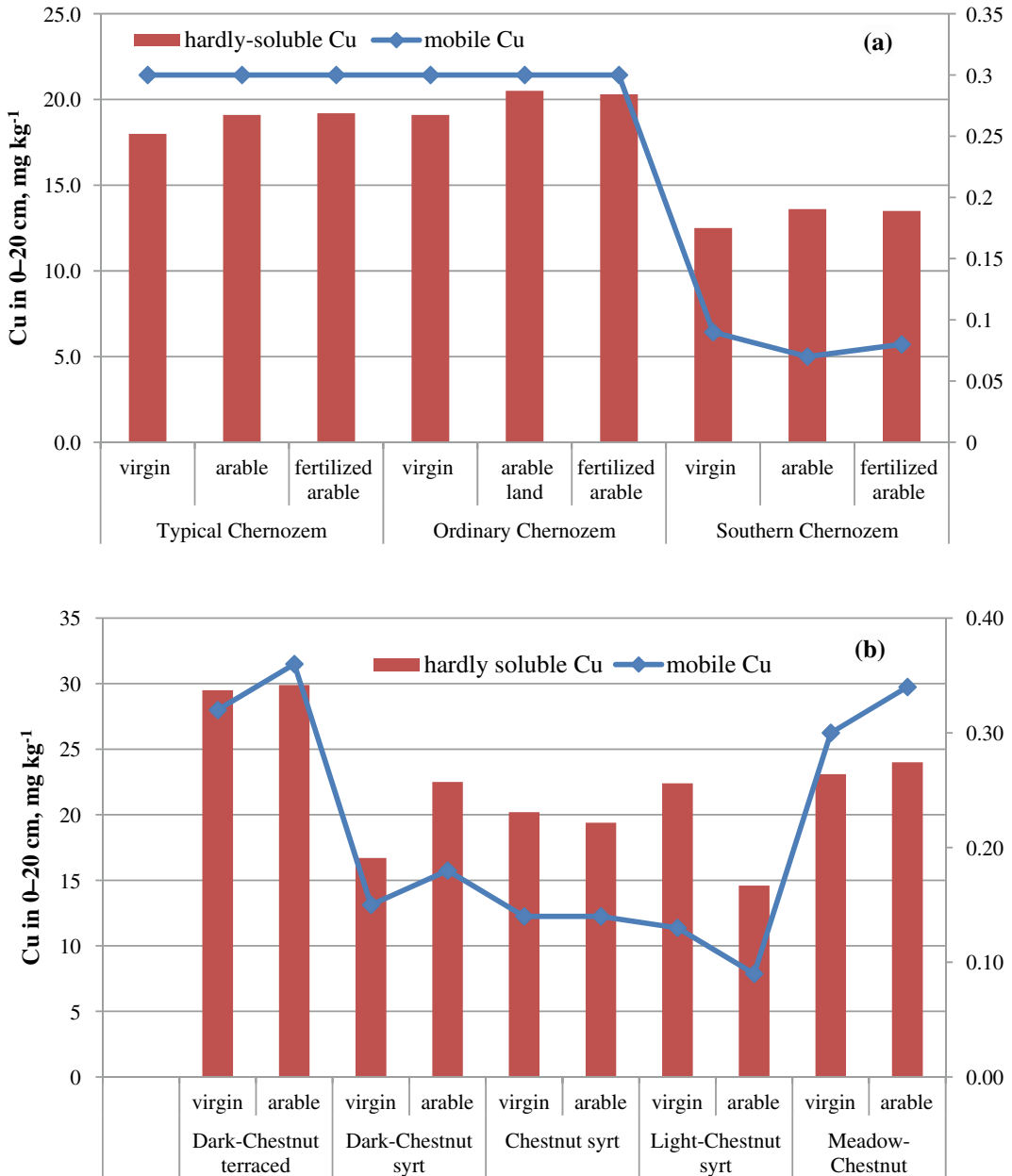


Fig. 24.2 Content of poorly soluble and mobile Cu in (a) Chernozem and (b) chestnut soils in 0–20 cm topsoil

mobility of Cu. Similarly, Małeckı et al. (2016) found a close relationship between the level of soil CEC and the migration behaviour of Zn and Cu.

The content of mobile forms of Cu extracted with hydrochloric acid in chestnut soils ranged from 0.7 to 1.2% of the total amount. No soils were found with Cu concentrations exceeding the MAC limits for the Russian Federation (55 mg kg⁻¹ Cu extracted with 1 N HCl). Mengel et al. (2001) found less plant-available Cu on more humified soils due to immobilisation by organic compounds. However, in our study, it is likely that the presence of carbonates in the Southern Chernozem was more influential than the humus content. This is confirmed by Al-Mur (2020), who, when studying the distribution and behaviour of heavy metals in the sediments of the Red Sea, found that when organic matter decomposes, Cu is released, which could be adsorbed on the surface of clay minerals.

24.3.4 Lead (Pb)

Lead is highly toxic in soil, in that it adversely affects the biological activity of a number of bacteria and their enzymes in the soil (Khan et al. 2010; Martín et al. 2014; Zhen et al. 2019). When ingested, it causes various diseases in animals and humans (Aleksseev 1992; Karpova and Mineev 2015; WHO 2020). In the soils of the Russian Federation, the MAC for poorly soluble Pb is 32 mg kg⁻¹, and that for the mobile form is 6 mg kg⁻¹ (GN 2.1.7.2041-06 2006). Lead is considered an inactive trace element; therefore, during anthropogenic pollution, it mainly accumulates in the upper soil layer. In natural conditions, its mobility is mainly controlled by the soil properties and weathering of minerals. Martín et al. (2014) found that the concentrations of soluble Pb were much higher in calcareous than in acid soils. In addition, Pb is easily absorbed by soil organic compounds. For example, in a sequential fractionation of Pb contained in calcareous sediment, Al-Mur et al. (2020) found that high concentrations of Pb were

recorded in the fraction bound to organic extract'.

In the typical and ordinary Chernozem soils studied, the Pb content was nearly the same (Fig. 24.3a, b), ranging from 30 to 34 kg/ha⁻¹ at a depth of 0–20 cm. In the southern Chernozem, the content of poorly soluble Pb was from 42 to 44 kg/ha⁻¹; that is, 29–40% higher than in other Chernozem subtypes. The systematic input of Pb with dust, precipitation and combustion products from nearby industrial enterprises also led to its mobile forms accumulating in the topsoil. In all the Southern Chernozem soils studied, the concentrations of mobile Pb were 2.3–3.0 times higher than in other Chernozem subtypes (Table 24.3). This can be attributed to the higher content of bases in southern Chernozem and their close proximity to the major industrial and transport centre, which explains the accumulation of Pb not only in arable lands, but also in the virgin lands.

The content of Pb in the chestnut soils studied was relatively stable. In the dark chestnut and chestnut subtypes, it ranged from 30 to 32 kg/ha⁻¹ at a soil depth of 0–20 cm. In the light chestnut and meadow chestnut soils, it was 36–40 kg/ha⁻¹. This accumulation of Pb is largely determined by the amount and ratio of the salts of Fe and Ca (Sheudzhen 2010), which differed in the soils studied.

Mobile forms of Pb ranged between 4.1% (in dark chestnut) and 1.8% (in meadow chestnut), indicating that the amount of mobile Pb steadily decreased as the content of clay and Ca in the soil increased. Similarly, Piri et al. (2020) found that the addition of calcareous material to soil was significantly correlated with the immobilisation of Pb: the timing and the rate of diatomite addition impacted various fractions of Pb in soil.

24.3.5 Cadmium (Cd)

Cadmium, like lead, is a non-essential element that belongs to the most toxic metals. Cadmium is characterised by a fairly uniform distribution in the parent rocks. The geochemistry of Cd is

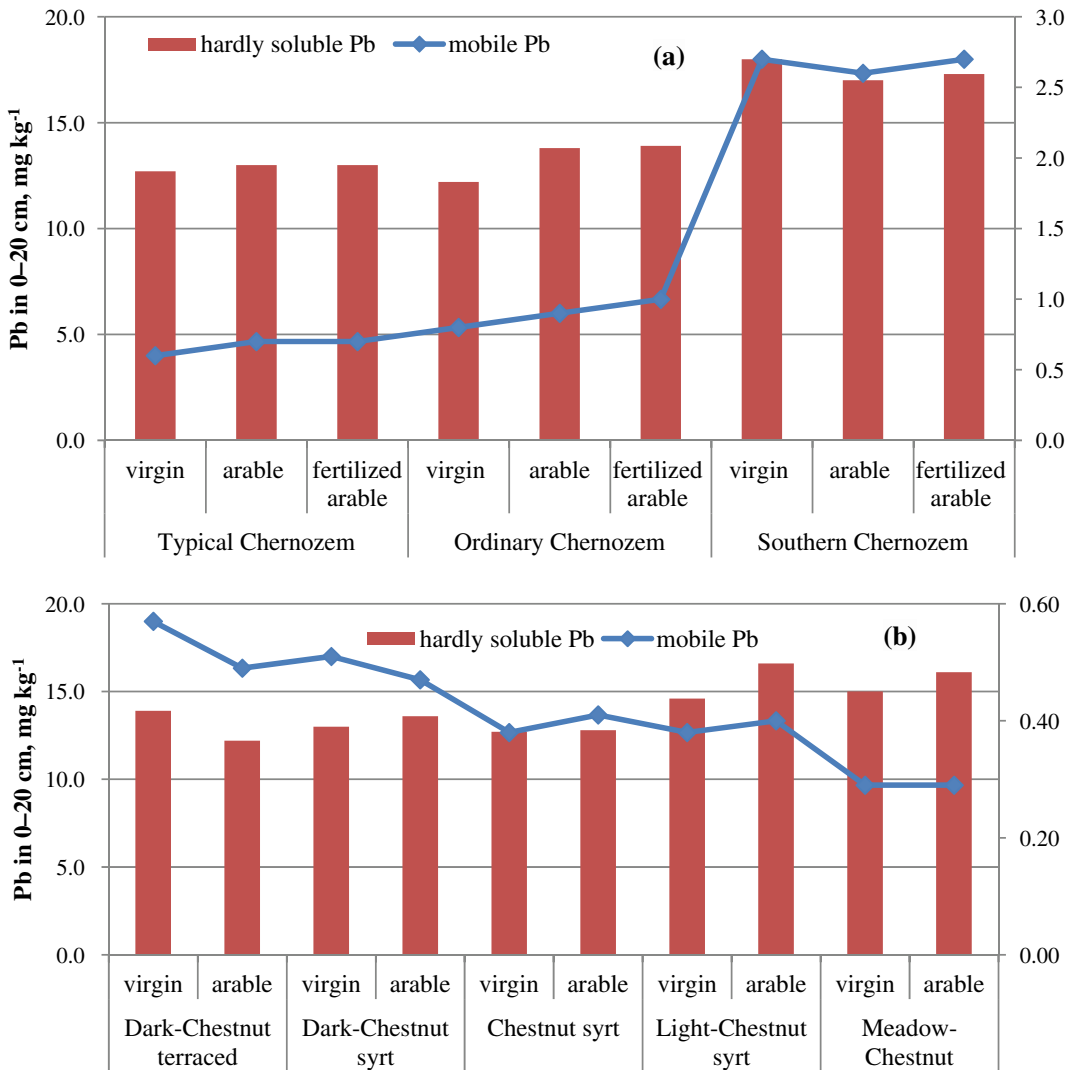


Fig. 24.3 Content of poorly soluble and mobile Pb in (a) Chernozem and (b) chestnut soils in 0–20 cm topsoil

closely related to the geochemistry of Zn, but unlike Zn it is highly mobile in an acidic environment (Kabata-Pendias and Pendias, 2001; Podar and Ramsey 2005). Mouni et al. (2017) and Zemanová et al. (2014) studied a series of heavy metals (Pb, Cu, Zn and Cd) and found that Cd had the lowest sorption ability. As Cd is highly toxic for plants, soil microorganisms and living organisms, in the Russian Federation the MAC limit for poorly soluble Cd is $<2 \text{ mg kg}^{-1}$ and that for mobile Cd is $<0.5 \text{ mg kg}^{-1}$ (GN

2.1.7.2041-06, 2006). By comparison, in Germany, the MAC limit for soil Cd is 3 mg kg^{-1} .

In typical and ordinary Chernozems, the Cd content was 0.7 to 0.8 kg/ha-1 at a soil depth of 0–20 cm (Fig. 24.4a, b), while in the southern Chernozem it was 1.5–1.6 kg/ha⁻¹, i.e. twice as high. This had the same cause as for Pb, i.e. the sample sites were near an industrial centre. The relative content of mobile Cd in typical and ordinary Chernozems ranged between 5.0 and 7.6% of the total content (Table 24.3). Due to its low sorption ability, the amount of Cd in the

southern Chernozem accounted for a quarter of its total reserves (24.4–26.2%) Относительная доля подвижных соединений кадмия в черноземах типично и обыкновенно была в пределах 5,0–7,6% от общего содержания труднорастворимых соединений данного элемента (табл. 1).

In the dark chestnut, chestnut and light chestnut soils, the content of poorly soluble Cd

was 0.6–0.9 kg/ha-1 at a soil depth of 0–20 cm (Fig. 24.4). These levels of Cd are similar to the levels in Chernozem soils. In the meadow chestnut soil, its content was 17–22% less. These differences are associated with the content of soil organic matter: the meadow chestnut soil was the most humified, which affected the Cd accumulation in that soil (Alekseev 1992; Medvedev and Derevyagin 2017).

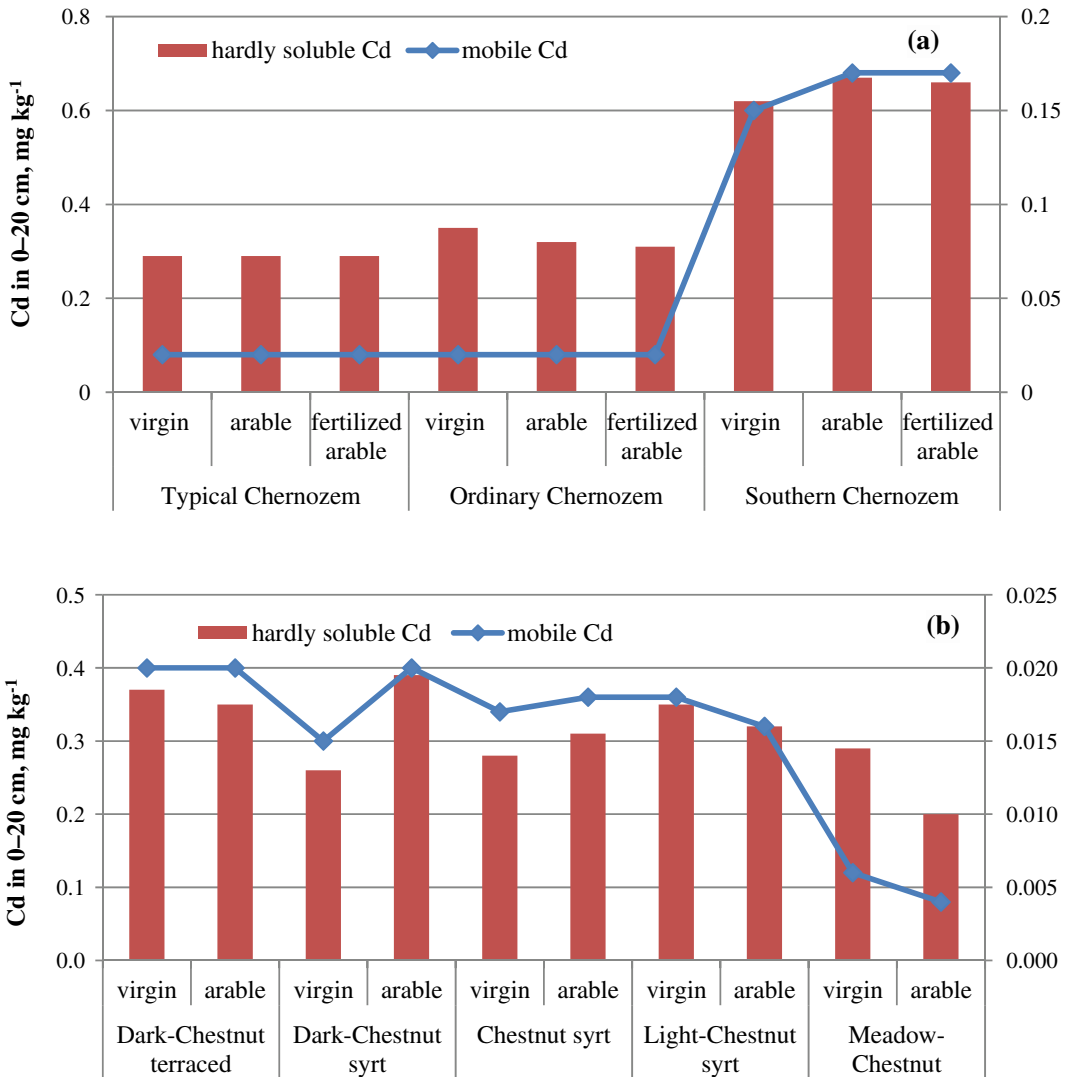


Fig. 24.4 Content of poorly soluble and mobile Cd in (a) Chernozem and (b) chestnut soils in 0–20 cm topsoil

24.3.6 Nickel (Ni)

A small concentration of Ni is necessary for normal plant growth and soil enzymes that are actively involved in the transformations of N compounds (Kabata-Pendias and Pendias 2001). In soil, the Ni content is determined by the properties of parent rocks, the amount of SOM and the degree of anthropogenic load (Karpova and Mineev 2015; Medvedev and Derevyagin 2017). Our studies confirmed these statements. Among the Chernozem soils, the maximum amount of Ni was found in the arable ordinary Chernozem (83 kg/ha^{-1}) (Fig. 24.5a, b), while its virgin analogue had 14% less (71 kg/ha^{-1}). Typical and southern Chernozems had 71 and 76 kg/ha^{-1} of Ni, respectively. No anthropogenic impact on the accumulation of Ni in the Chernozem was observed.

The content of mobile Ni increased by one-third from the typical to the southern Chernozem (Table 24.1). In the dry steppe chestnut soils, the Ni content ranged from 98 to 67 kg/ha^{-1} at a soil depth of 0–20 cm. Figure 24.5 shows that dark chestnut terrace soil contained a higher amount of Ni than Chernozem. This is due to the different composition of the parent rock, and primarily the different amounts of Fe and Mn oxides in the soil minerals (Chernykh 2001). In the dark chestnut, chestnut and meadow chestnut soils of the Syrt plain, a clear accumulation of Ni was observed in the fertilised arable lands. This can probably be explained by the emissions of diesel combustion engines, containing Ni (Chernykh 2001; Medvedev et al. 2009). The content of mobile Ni was 2–3 times less in chestnut than in Chernozem soils (Table 24.1). In spite of soil contamination with Ni from fertilisation activities on the studied Chernozem and chestnut soils of Volga steppes, the accumulation of Ni did not lead to toxic concentrations, which were below the MACs. In the Russian Federation, these are 56 and 4 mg kg^{-1} for poorly soluble and mobile Ni, respectively.

24.3.7 Arsenic (As)

Arsenic falls into the group of highly toxic elements. It can be released into the soil both through natural processes (e.g. rock weathering) and anthropogenically (mining, agrochemicals, pesticides, fuel combustion, etc.) (Čakmak et al. 2015; Saljnikov et al. 2019). Agricultural practices may pose a great risk of soil contamination with As (Pejović et al. 2017; Antić-Mladenović et al., 2019). In Chernozem soil of the Volga steppes, As content in the upper soil layer varied from 5 to 10 kg/ha^{-1} (Fig. 24.6a, b). Arsenic is strongly associated with oxides of Fe, Al and Ca (Adriano 2001). Its mobile form is involved in the organo-mineral complexes (Čakmak et al. 2015). The hydrolysis of these oxides (including the hydrolysis by soil microbes) promotes the transformation of As into mobile forms.

In Chernozem soils, the amount of As ranged between 4.2 and 7.9% of its total content (Table 24.3), which, as for Pb and Cd, is a good indicator of proximity to urban and industrial zones. In chestnut soil, the amount of poorly soluble As was from 6 to 8 kg/ha^{-1} . Moreover, its content in the arable land was lower compared to the virgin analogue. For the chestnut and light chestnut soils, these differences were 4–8%, while for the dark chestnut soils the differences were 20–26%. In the arable dark chestnut soil, an increased content of mobile As was found compared to the other chestnut soils. Since the dark chestnut soil has a higher humus content than other subtypes of chestnut soils, higher solubilisation of As presumably occurred in the vegetated 0–20 cm soil depth due to the intensive biological and microbiological activities (Simmer et al. 2017). Microorganisms mostly exist in the topsoil and actively participate in the hydrolysis of oxides associated with soil As (in this case mostly Ca oxides), thus increasing the concentrations of mobile As in the top layer of arable dark chestnut soil. The content of mobile As in all chestnut soils was considerably less than in

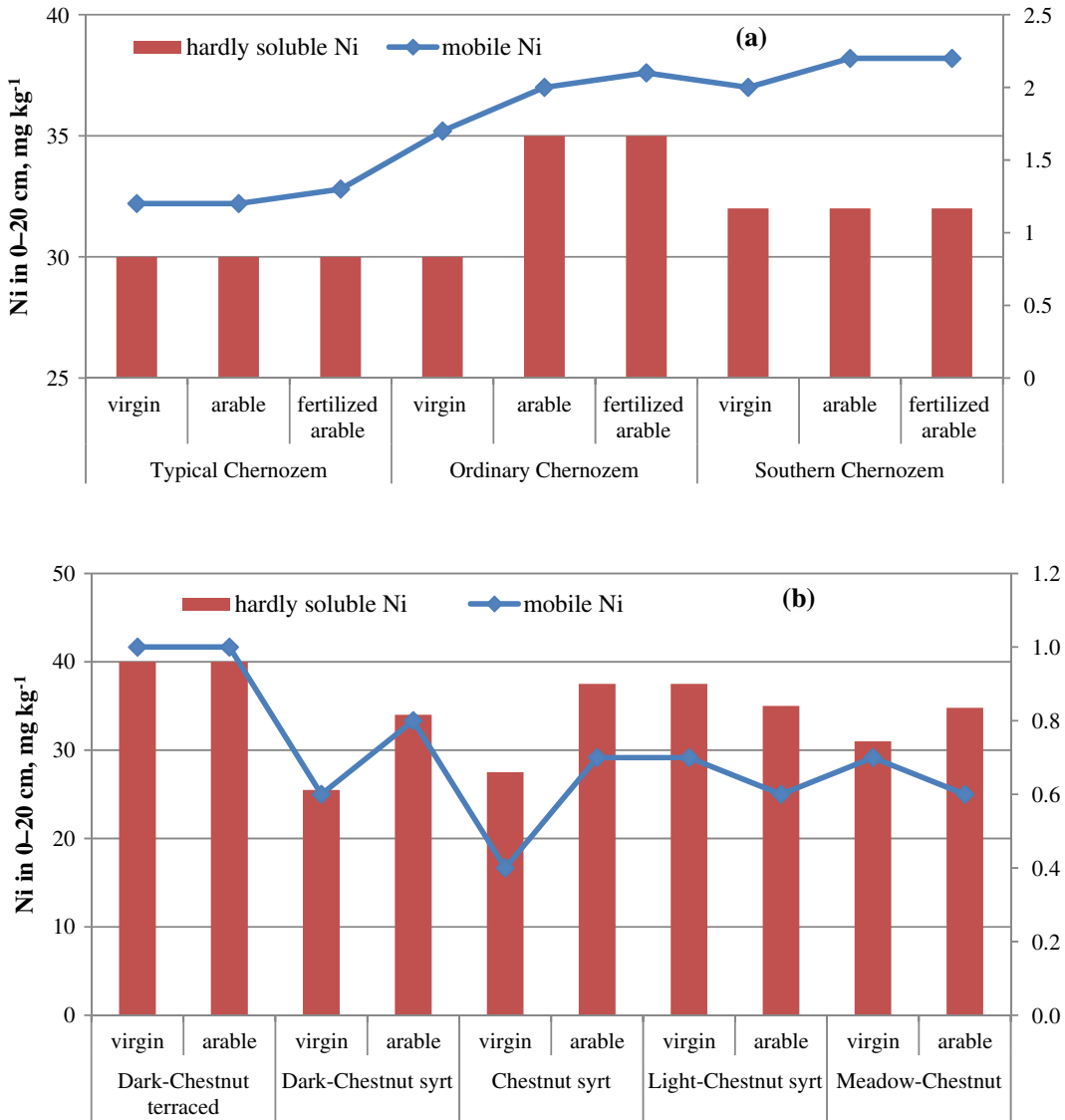


Fig. 24.5 Content of poorly soluble and mobile Ni in (a) Chernozem and (b) chestnut soils in 0–20 cm topsoil

the Chernozem (2.8–3.8% of the total). In all the soils studied, the concentration of As was below the MAC (in the Russian Federation, the MAC for As is 20 mg kg⁻¹ for poorly soluble forms).

24.3.8 Mercury (Hg)

Mercury contamination is of significant concern worldwide owing to its toxic effect on human health (Beckers and Rinklebe 2017). Mercury is

a highly mobile element. In neutral and weakly alkaline soils, it mainly accumulates in the form of weakly mobile organic complexes. This implies that highly humified soils accumulate a higher amount of Hg (Sheudzhen 2010; García-Sánchez et al. 2014). However, our results did not support this hypothesis, because the Hg content was the same on both Chernozem and chestnut soils, despite the fact that the humus content in these soils differed by 3–4 times (7.7 and 1.78% in Typical Chernozem and light

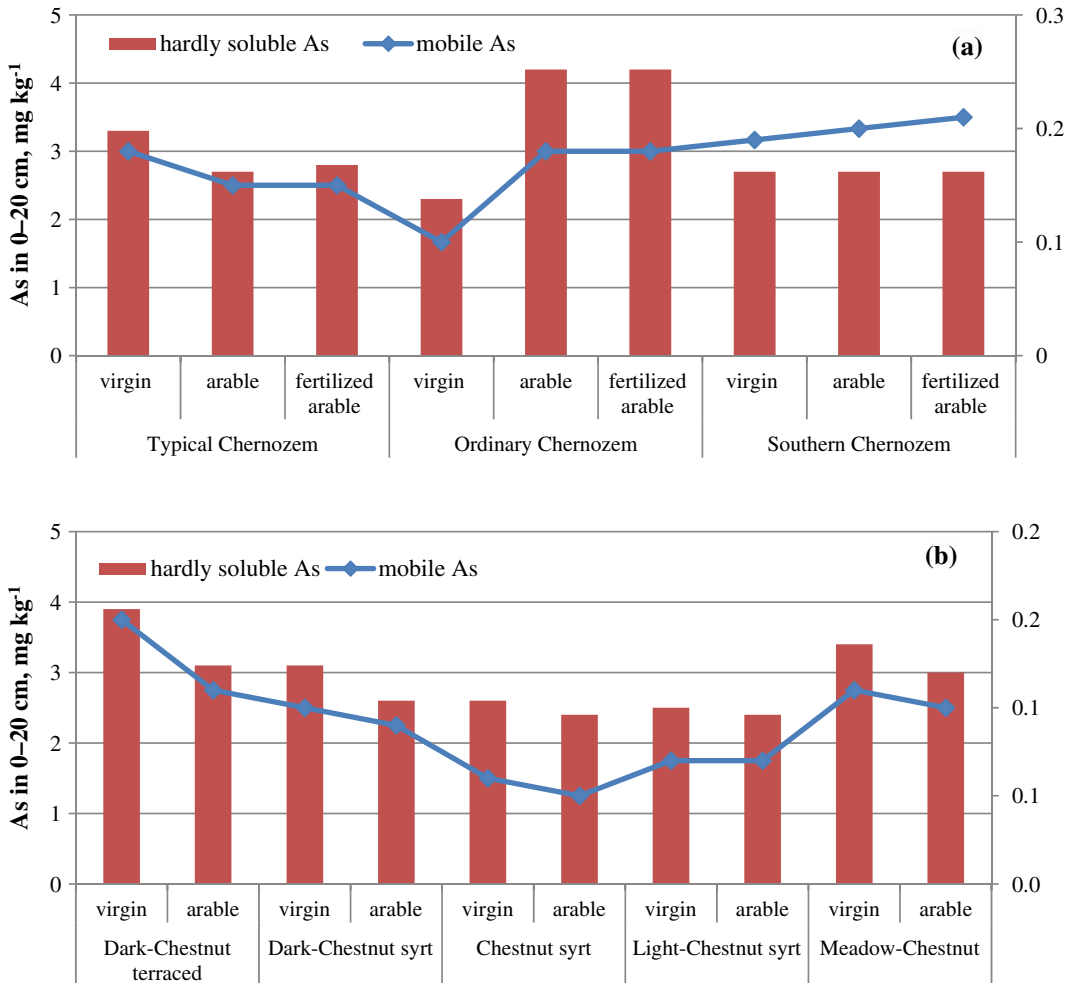


Fig. 24.6 Content of poorly soluble and mobile As in (a) Chernozem and (b) chestnut soils in 0–20 cm topsoil

chestnut, respectively) (Fig. 24.7a, b). The content of poorly soluble Hg ranged from 0.07 to 0.04 kg/ha⁻¹ in the 0–20 cm soil layer. This is 105–80 times lower than the MAC (2.1 mg kg⁻¹). The content of mobile Hg was within 2.1–3.7% of the total, or 3–4 g ha⁻¹. Results of this kind were expected since Hg generally has relatively low plant availability (Li et al. 2010) due to its easy adsorption and complexation in solid media (Luo et al. 2009). Some studies showed that using activated carbon (Gilmour et al. 2018) and activated clay (Yin et al. 2016) facilitated the immobilisation of methylmercury, one of the most toxic forms of Hg.

Testing five types of vegetables, Yu et al. (2018) found that when the soil pH was <6.5, the Hg content was higher in vegetables, while at soil pH > 7.5, the Hg content was lower. The same research established that the level of SOMs in soil greatly influences the accumulation of Hg in various parts of the plants and in different tissues of the plants. Our results showed that the soils studied had no risk of contamination with Hg; however, due to its potential for biomagnification in the food chain (O'Connor et al. 2019), particular concern should be paid to its further accumulation in agricultural landscapes.

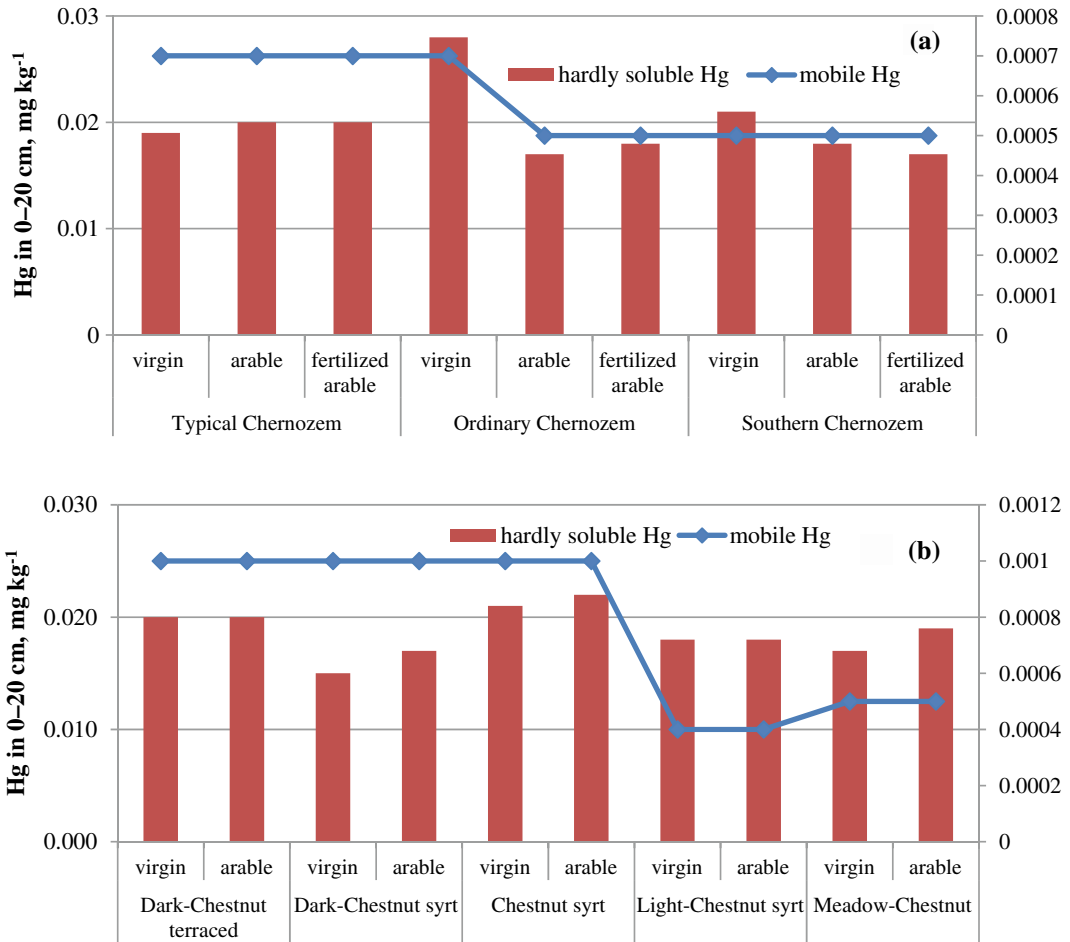


Fig. 24.7 Content of poorly soluble and mobile Hg in (a) Chernozem and (b) chestnut soils in 0–20 cm topsoil

24.3.9 Discussion

Chernozems and chestnut soils usually have a neutral or slightly alkaline reaction. Under these conditions, the mobility of heavy metals is much lower than in the soils with an acidic reaction (Karpova and Mineev 2015; Chernykh 2001). Hu et al. (2013) and Piri et al. (2020) found that in calcareous soils, the low availability of metals was due to sorption by CaCO₃ and also due to the low desorption influenced by the high pH compared with acidic soils. Therefore, we did not expect any significant movement of heavy metals in the soil profile or their noticeable accumulation.

Simultaneous determination of the contents of heavy metals on virgin soil and on its arable

analogues showed that agricultural activities such as fertilisation did not lead to the accumulation of the studied trace elements in these soils. This statement is supported by the data presented in Table 24.4 and Table 24.5. The tables show the content of heavy metals in the fertilisers and the amount of heavy metals entering the soil.

The mechanisms by which heavy metals are immobilised in soil are still under discussion by scientists. Since the organic matter of the soil consists of various fractions with different biochemical compositions and turnover times, the specifics of the relationship of each link in the soil system with heavy metals entering the soil are very complex and depend on the chemical composition of the soil environment, the

Table 24.4 Heavy metal content in various types of fertilisers, g t⁻¹, (Karpova and Mineev 2015)

Fertiliser	Zn	Cu	Pb	Cd	Ni	As
Potassium nitrate	0–12	2–24	8–20	00	12–30	0–5
Potassium chloride	11–57	4–23	2–12	1–5	7–30	1–3
Urea	2–29	2–52	0	0	5–34	0–2
Ammonium nitrate	6–30	2–18	0–1	0–1	4–17	0
Double superphosphate from apatite	10–15	45–51	18–43	3–5	10–23	3–5
Amorphous phosphate	19–40	30–50	38–56	3–10	23–36	8–18

Table 24.5 Input of trace elements with agrochemicals containing the maximum content of pollutants (Karpova and Mineev 2015; Derevyagin 2017)

Mineral fertilisers (60 kg/ha ⁻¹ of active substances annually)	Manure 50 t/ha ⁻¹ (once per rotation)
Zn—0.05–0.3 kg ha ⁻¹	Zn—1.4–5.0 kg ha ⁻¹
Cu—0–0.1 kg ha ⁻¹	Cu—0.05–1.0 kg ha ⁻¹
Pb—0.04–0.2 kg ha ⁻¹	Pb—0.04–0.2 kg ha ⁻¹
Cd—0.3–5.0 g ha ⁻¹	Cd—2.0–100.0 g ha ⁻¹
Ni—0.03–0.2	Ni—8.0–350.0 g ha ⁻¹
Hg—0–3.0 g ha ⁻¹	Hg—0–0.1 g ha ⁻¹
As—1–10 g ha ⁻¹	As—0.3–1.4

structure and composition of organic soil molecules and the mineral part of the soil. This may include synergistic and antagonistic effects between all the soil constituents, which can control the processes of adsorption and desorption of elements and substances, including nutrients. For example, Lasota et al. (2020) found that of the metals they studied (Cd, Cr, Cu, Ni, Pb and Zn), all of them, especially Cd, positively correlated with the carbon in the light fraction of SOM in organic horizons, while Cr, Cu, Ni and Pb content correlated with the carbon in the light fraction of soil organic matter in mineral horizons. Meanwhile, the carbon in the occluded light fraction of soil organic matter strongly correlated with Cr, Cu, Ni, Pb and Zn in organic horizons and with all metals in mineral horizons. The carbon in the heavy fraction of soil organic matter strongly correlated with the Cr, Cu and Pb

content in organic horizons and with Cd, Cr, Mn and Zn in mineral horizons. Al-Mur (2020) found that the total organic carbon content was significantly positively correlated with the total Fe, total Zn, total Cu, total Ni, but only weakly with Mn, Pb and Cd. In the dry steppes of the Volga River, future monitoring of soil pollution with heavy metals should pay more attention to soil parameters such as the acidity, clay content, physical and chemical characteristics of soil colloids and the composition and structure of soil organic matter.

24.4 Conclusions

Studies on Chernozem and chestnut soils in the Volga steppes showed that the content of Zn, Cu, Pb, Cd, Ni, As and Hg in the upper 0–20 cm of

all the soils studied is lower than the maximum allowed concentrations. A trend toward an increase in the accumulation of mobile forms of Pb, Cd, Ni and As was observed only in the Southern Chernozem, which was located in the immediate vicinity of the industrial zone. Simultaneous studies on arable and virgin soils showed no contamination due to agricultural practices.

Taking into account the favourable agrochemical and physical properties of the studied steppe soils, as well as the concentrations of the microelements studied—that were less than the MAC values—it can be concluded that the soils of this region are not polluted with heavy metals, which implies that agricultural products in this region are safe in this respect. However, the cumulative sum of the emissions from large industrial and urban cities may potentially cause soil contamination with toxic trace elements. Therefore, further monitoring of soil contamination with PTEs should be included in environmental policy plans, with an emphasis on mobile forms of Pb, Cd, Ni and As in areas with a higher risk of contamination.

References

- Adriano DC (2001) Trace elements in terrestrial environments. Springer, New York, pp XIX, 533. <https://doi.org/10.1007/978-1-4757-1907-9>
- Alekseev YuV (1992) Heavy metals in soils and plants. Moscow, p 200 (Тяжелые металлы в почвах и растениях. Москва, с. 200)
- Alloway BJ (1995) Heavy metal in soils. Springer Netherlands, ISBN 978-94-010-4586-5, pp XIV, 368
- Alloway BJ (2008) Zinc in soils and crop nutrition, 2nd edn. International Zinc Association and International Fertilizer Industry Association, Brussels Google Scholar
- Al-Mur BA (2020) Geochemical fractionation of heavy metals in sediments of the Red Sea Saudi Arabia. *Oceanologia* 62(1):31–44. <https://doi.org/10.1016/j.oceano.2019.07.001>
- Antić-Mladenović S, Kresović M, Čakmak D, Perović V, Saljnikov E, Ličina V, Rinklebe J (2019) Impact of a severe flood on large-scale contamination of arable soils by potentially toxic elements (Serbia). *Environ Geochem Health* 41:249–266. <https://doi.org/10.1007/s10653-018-0138-4>
- Bakshi S, Banik Ch (2018) The impact of heavy metal contamination on soil health. In: Recosky D (ed) *Managing soil health for sustainable agriculture*. Vol 2: monitoring and management. Burleigh Dodds Science Publishing, Cambridge, UK. <https://doi.org/10.19103/AS2017.0033.20>
- Ballabio C, Panagos P, Lugato E, Huang J-H, Orgiazzi A, Jones A, Fernández-Ugalde O, Borrelli P, Montanarella L (2018) Copper distribution in European topsoils: an assessment based on LUCAS soil survey. *Sci Tot Environ* 636:282–298. <https://doi.org/10.1016/j.scitotenv.2018.04.268>
- Beckers F, Rinklebe J (2017) Cycling of mercury in the environment: sources, fate, and human health implications: a review. *Crit Rev Environ Sci Technol* 47:693–794. <https://doi.org/10.1080/10643389.2017.1326277>
- Čakmak D, Saljnikov E, Skrivanj S, Roglić G, Bakrac S, Sikirić B, Manojlić D (2015) Identification of different sources and forms of arsenic in the vicinity of ore mining in Serbia. *Fresenius Environ Bull* 24 (12b):4635–4643. <http://cherry.chem.bg.ac.rs/handle/123456789/2027>
- Cambier Ph, Michaud A, Paradelo R et al (2019) Trace metal availability in soil horizons amended with various urban waste composts during 17 years—Monitoring and modelling. *Sci Tot Environ* 651 (2):2961–2974. <https://doi.org/10.1016/j.scitotenv.2018.10.013>
- Chasapis CT, Ntoupa PA, Spiliopoulou CA et al (2020) Recent aspects of the effects of zinc on human health. *Arch Toxicol* 94:1443–1460. <https://doi.org/10.1007/s00204-020-02702-9>
- Chernykh NA (2001) Ecotoxicological aspects of soil contamination with heavy metals. Moscow, Pushchino, p 148 (Экотоксикологические аспекты загрязнения почв тяжелыми металлами. Москва, Пушкино, стр.148)
- Dobrovolsky VV (1997) Biospheric cycles of heavy metals and the regulatory role of the soil. *Pochvovedenie* 4:433–441. (Биосферные циклы тяжелых металлов и регулирующая роль почвы. Почвоведение)
- Dobrovolsky VV (1999) Highly dispersed soil particles as a factor of mass transfer of heavy metals in the biosphere. *Pochvovedenie* 11:1309–1317. (Высокодисперсные частицы почвы как фактор массопереноса ТМ в биосфере)
- Egorov VV, Ivanova EN, Fridland VM (1977) Classification and soil diagnostics of the USSR. *Kolos* p 225 (Классификация и диагностика почв СССР. Колос с. 225) <http://www.geokniga.org/books/3460>
- Evdokimova GA, Kislykh EE, Mozgov NP (1984) Biological activity of soils under conditions of airborne industrial pollution in the Far North. *Leningrad*, p 120. (Биологическая активность почв в условиях промышленного загрязнения воздуха на Крайнем Севере. Ленинград, с.120)

- Filipiak-Szok A, Kurzawa M, Szlyk E (2015) Determination of toxic metals by ICP-MS in Asiatic and European medicinal plants and dietary supplements. *J Trace Elem Med Biol* 30:54–58. <https://doi.org/10.1016/j.jtemb.2014.10.008>
- Friedlová M (2010) The influence of heavy metals on soil biological and chemical properties. *Soil and Water Research* 5(1):21–27. <https://doi.org/10.17221/11/2009-SWR>
- García-Sánchez M, Sípková A, Száková J, Kaplan L, Ohecová P, Tlustoš P (2014) Applications of organic and inorganic amendments induce changes in the mobility of mercury and macro- and micronutrients of soils. *Sci World J* 2014:407049. <https://doi.org/10.1155/2014/407049>
- Giller KE, Witter E, Mcgrath SP (1998) Toxicity of heavy metals to microorganisms and microbial processes in agricultural soils. *Soil Biol Biochem* 30(10–11):1389–1414. [https://doi.org/10.1016/S0038-0717\(97\)00270-8](https://doi.org/10.1016/S0038-0717(97)00270-8)
- Gilmour C, Bell T, Soren A, Riedel G, Kopec D, Bodaly D, Ghosh U (2018) Activated carbon thin-layer placement as an in situ mercury remediation tool in a Penobscot River salt marsh. *Sci Total Environ* 621:839–848. <https://doi.org/10.1016/j.scitotenv.2017.11.050>
- Giro-Paloma J, Formosa J, Chimenos JM (2020) Stabilization study of a contaminated soil with metal(loid)s adding different low-grade MgO degrees. *Sustainability* 12:7340. <https://doi.org/10.3390/su12187340>
- GN 2.1.7.2041-06 (2006) The maximum allowed concentration (MAC) of chemicals in the soil. Moscow, p 8 (ГН 2.1.7.2041–06. Предельно допустимая концентрация (ПДК) химических веществ в почве. Москва с. 8), <https://files.stroyinf.ru/Data2/1/4293850/4293850511.pdf>
- GOST 26107-84 (1984) Soils. Methods for determination of total nitrogen, p 9. Standard Publ., Moscow. (ГОСТ 26107–84. Почвы. Методы определения общего азота. Москва, Стандарт. стр.9), <https://files.stroyinf.ru/Data2/1/4294828/4294828346.pdf> Accessed on 7 March 2021
- GOST 12536-2014. (2014). Grounds. Methods for laboratory determination of granulometric (Grain) and microaggregate composition, p 16. Standartinform, Moscow. (ГОСТ 12536-2008. Основания. Методы лабораторного определения гранулометрического (зернового) и микроагрегатного состава. Москва, Стандартинформ стр.16), <http://docs.cntd.ru/document/1200116022>
- GOST 26424-85 (1986) Soils. Methods for determination of carbonate and bicarbonate ions in water extract (Почвы. Методы определения ионов карбоната и бикарбоната в водной вытяжке), <http://docs.cntd.ru/document/gost-26424-85>. Accessed on 7 March 2021
- GOST 27821-88 (1988) Soils. Determination of base absorption sum by Karpen method (Почвы. Определение суммы поглощенных оснований по методу Каппена), http://snipov.net/c_4702_snip_104831.html. Accessed on 7 March 2021
- Greany KM (2005) An assessment of heavy metal contamination in the marine sediments of Las Perlas Archipelago, Gulf of Panama. M.S. thesis, School of Life Sciences Heriot-Watt University, Edinburgh, Scotland
- Groshev IV, Grogorieva IV, Shakhmatova TN (2007) The ecological role of heavy metals in the formation of the biogeo-resource potential of steppe ecosystems. *Bulletin of Orenburg State Agrarian University, Russia*. (Экологическая роль тяжелых металлов в формировании биогеоресурсного потенциала степных экосистем. Вестник Оренбургского государственного аграрного университета, Россия)
- Gruszecka-Kosowska A, Baran A, Wdowin M et al (2020) The contents of the potentially harmful elements in the arable soils of southern Poland, with the assessment of ecological and health risks: a case study. *Environ Geochem Health* 42:419–442. <https://doi.org/10.1007/s10653-019-00372-w>
- Guerra CA, Rosa IMD, Valentini E et al (2020) Global vulnerability of soil ecosystems to erosion. *Landscape Ecol*. <https://doi.org/10.1007/s10980-020-00984-z>
- Guidelines for the determination of heavy metals in farmland soils and crop production (1992) CINA0, Moscow, p. 61. <https://files.stroyinf.ru/Index2/1/4293771/4293771886.htm>
- Guo B, Hong C, Tong W et al (2020) Health risk assessment of heavy metal pollution in a soil-rice system: a case study in the Jin-Qu Basin of China. *Sci Rep* 10:11490. <https://doi.org/10.1038/s41598-020-68295-6>
- Gupta DK, Sandallo LM (eds) (2011) Metal toxicity in plants: perception, signalling and remediation. ISBN 978-3-642-22081-4. Springer, London
- Hashem T, Abbas H, Farid IM et al (2017) Accumulation of some heavy metals in plants and soils adjacent to Cairo—Alexandria agricultural highway. *Egyptian J Soil Sci* 57(2):215–232. <https://doi.org/10.21608/ejss.2016.281.1047>
- Hou R, Wang L, O'Connor D, Tsang DCW, Rinklebe J, Hou D (2020) Effect of immobilizing reagents on soil Cd and Pb lability under freeze-thaw cycles: implications for sustainable agricultural management in seasonally frozen land. *Environ Int* 144:106040. <https://doi.org/10.1016/j.envint.2020.106040>
- Hu Y, Nan Z, Su J, Wang N (2013) Heavy metal accumulation by poplar in calcareous soil with various degrees of multi-metal contamination: implications for phytoextraction and phytostabilization. *Environ Sci Pollut Res Int* 20:7194–7203. <https://doi.org/10.1007/s11356-013-1711-0>
- Huang J, Peng S, Mao X, Li F, Guo S, Shi L et al (2019) Source apportionment and spatial and quantitative ecological risk assessment of heavy metals in soils from a typical Chinese agricultural county. *Process Safety Environ Prot* 126:339–347. <https://doi.org/10.1016/j.psep.2019.04.023>

- Ivanov VV (1996) Ecological geochemistry of elements, p 356. Ecology, Moscow (Экологическая геохимия элементов. Москва, Экология стр.356)
- Kabata-Pendias A, Pendias H (2001) Trace elements in soils and plants, 3rd edn, p 403. CRC Press, Boca Raton. <http://base.dnsgb.com.ua/files/book/Agriculture/Soil/Trace-Elements-in-Soils-and-Plants.pdf>. Accessed on 7 March 2021
- Kabata-Pendias A, Szeke B (2015) Trace elements in abiotic and biotic environments. CRS Press, Francis&Taylor Group, Boca Raton, FL, p 440. <https://doi.org/10.1201/b18198>
- Karpova OS, Mineev VG (2015) Heavy metals in the agroecosystem. Moscow State University Publ., p 252 (Тяжелые металлы в агроэкосистеме. Издательство МГУ, с. 252)
- Khan S, AelL H, Qiao M, Rehman S, He JZ (2010) Effects of Cd and Pb on soil microbial community structure and activities. *Environ Sci Pollut Res Int* 17 (2):288–296. <https://doi.org/10.1007/s11356-009-0134-4>
- Kim RY, Yoon JK, Kim TS, Yang JE, Owens G, Kim KR (2015) Bioavailability of heavy metals in soils: definitions and practical implementation—a critical review. *Environ Geochem Health* 37:1041–1061. <https://doi.org/10.1007/s10653-015-9695-y>
- Kome GK, Enang RK, Tabi FO, Yerima BPK (2019) Influence of clay minerals on some soil fertility attributes: a review *Open. J Soil Sci* 9:155–188
- Król A, Mizerna K, Bożym M (2020) An assessment of pH-dependent release and mobility of heavy metals from metallurgical slag. *J Hazard Mater* 384:121502. <https://doi.org/10.1016/j.jhazmat.2019.121502>
- Ladonin DL, Margolina SE (1997) The interaction of humic acids with heavy metals. *Pochvovedenie* 7:806–811. (Взаимодействие гуминовых кислот с тяжелыми металлами. Почвоведение 7: 806–811)
- Lasota J, Błońska E, Lyszczarz S et al (2020) Forest humus type governs heavy metal accumulation in specific organic matter fractions. *Water Air Soil Pollut* 231:80. <https://doi.org/10.1007/s11270-020-4450-0>
- Lavrishchev A, Litvinovich A, Bure V, Pavlova O, Saljnikov E (2018) Strontium dynamics in soil and assimilation by plants during dissolution of conversion chalk. *Biol Comm* 63(3):163–173. <https://doi.org/10.21638/spbu03.2018.302>
- Li J, Lu Y, Shim H, Deng X, Lian J, Jia Z, Li J (2010) Use of the BCR sequential extraction procedure for the study of metal availability to plants. *J Environ Monit* 12(2):466–471. <https://doi.org/10.1039/B916389A>
- Lu XC, Tian XH, Cui J, Zhao AQ, Yang XW, Mai W (2011) Effects of combined phosphorus-zinc fertilization on grain zinc nutritional quality of wheat grown on potentially zinc-deficient calcareous soil. *Soil Sci* 176:684–690. <https://doi.org/10.1097/SS.0b013e3182331635>
- Luksin SV, Avramenko PM (2006) Lead content in agroecosystems of the Belgorod region. *Agrochem Bull* 5:10–11 (Содержание свинца в агроэкосистемах Белгородской области. Агрохимический вестник, 5: 10–11)
- Luo W, Lu Y, Wang B, Tong X, Wang G, Shi Y, Wang T, Giesy JP (2009) Distribution and sources of mercury in soils from former industrialized urban areas of Beijing China. *Environ Monit* 158(1–4):507–517. <https://doi.org/10.1007/s10661-008-0600-3>
- Magnuson ML, Kelty CA, Kelty KC (2001) Trace metal loading on water-borne soil and dust particles characterized through the use of Split-flow thin-cell fractionation. *Anal Chem* 73(14):3492–3496. <https://doi.org/10.1021/ac0015321>
- Matecki JJ, Kadzikiewicz-Schoeneich M, Szostakiewicz-Hołownia M (2016) Concentration and mobility of copper and zinc in the hypergenic zone of a highly urbanized area. *Environ Earth Sci* 75:24. <https://doi.org/10.1007/s12665-015-4789-5>
- Marques APGC, Rangel AOSS, Castro PML (2009) Remediation of heavy metal contaminated soils: phytoremediation as a potentially promising clean-up technology. *Crit Rev Environ Sci Technol* 39(8):622–654. <https://doi.org/10.1080/10643380701798272>
- Martin F, Simón M, García I, Romero A, González V (2014) Pollution of Pb in soils affected by pyrite tailings: influence of soil properties, environmental risk assessment of soil contamination, Maria C. Hernandez-Soriano. *IntechOpen*. <https://doi.org/10.5772/57270>, <https://www.intechopen.com/books/environmental-risk-assessment-of-soil-contamination/pollution-of-pb-in-soils-affected-by-pyrite-tailings-influence-of-soil-properties>. Accessed on 7 March 2021
- Martinez CE, Motto HL (2000) Solubility of lead, zinc and copper added to mineral soils. *Environ Pollut* 107 (1):153–158. [https://doi.org/10.1016/S0269-7491\(99\)00111-6](https://doi.org/10.1016/S0269-7491(99)00111-6)
- Medvedev IF, Derevyagin SS (2017) Heavy metals in ecosystems. Publishing House “Rakurs”, Saratov, p178 (Тяжелые металлы в экосистемах. Саратов: издательство «Ракурс» с178.). <https://www.arisersar.ru/Litera/107.12.17.pdf>
- Medvedev IF, Derevyagin SS, Gubarev DI (2009) Distribution of heavy metals in the Volga chernozem by the main azonal landscapes and elements of the agrolandscapes. *Plodorodie* 3:52–53. (Распределение тяжелых металлов в черноземе Волги по основным азональным ландшафтам и элементам агроландшафтов. Плодородие 3: 52–53), <https://www.arisersar.ru/Litera/107.12.17.pdf>. Accessed on 7 March 2021
- MEF (2007) Ministry of the Environment, Finland Government Decree on the Assessment of Soil Contamination and Remediation Needs, 214/2007, <https://www.finlex.fi/en/laki/kaannokset/2007/en20070214.pdf>. Accessed on 7 March 2021
- Mengel K, Kirkby EA, Kosegarten H, Appel T (2001) Soil copper. In: Mengel K, Kirkby EA, Kosegarten H, Appel T (eds) Principles of plant nutrition. Springer, Dordrecht, pp 599–611. https://doi.org/10.1007/978-94-010-1009-2_16

- Mineev VG (2001) Workshop on agrochemistry. Moscow State University Publishing House, p 689 (Минеев В.Г. Практикум по агрохимии, МГУ) <http://bookshare.net/index.php?id1=4&category=chem&author=mineevvg&book=2001>. Accessed on 7 March 2021
- Minkina TM, Motuzova GV, Nazarenko OG (2006) Interaction of heavy metals with organic matter of Chernozem ordinary. *Pochvovedenie* 7:804–811 (Взаимодействие тяжелых металлов с органическим веществом чернозема обыкновенного. *Почвоведение* 7: 804–811)
- Mouni L, Belkhir L, Bouzaza A et al (2017) Interactions between Cd, Cu, Pb, and Zn and four different mine soils. *Arab J Geosci* 10:77. <https://doi.org/10.1007/s12517-017-2864-9>
- Nannipieri P, Badalucco L, Landi L, Pietramellara G (1997) Measurement in assessing the risk of chemicals to the soil ecosystem. In: Zelikoff JT (ed) *Ecotoxicology: responses, biomarkers and risk assessment*. OECD Workshop, SOS Publ., Fair Haven, NY, USA, pp 507–534
- Nikitin SN (2014) The influence of chemicals and biologization on the content of lead and cadmium in grain crops. *Zemledelye* 8:35–37 (Влияние химии и биологизации на содержание свинца и кадмия в зерновых культурах. *Земледелие*, 8: 35–37)
- O'Connor D, Hou D, Ok YS et al (2019) Mercury speciation, transformation, and transportation in soils, atmospheric flux, and implications for risk management: a critical review. *Environ Int'l* 126:747–761. <https://doi.org/10.1016/j.envint.2019.03.019>
- Ogunlaja A, Ogunlaja OO, Okewole DM, Morenikeji OA (2019) Risk assessment and source identification of heavy metal contamination by multivariate and hazard index analyses of a pipeline vandalised area in Lagos State Nigeria. *Sci. Total Environ.* 651:2943–2952. <https://doi.org/10.1016/j.scitotenv.2018.09.386>
- Okolelova AA, Zheltobryukhov VF, Egorova GS et al. (2014) Content and regulation of heavy metals in soils of Volgograd. Volgograd State University, p. 144 (Содержание и регуляция тяжелых металлов в почвах Волгограда. Волгоградский государственный университет)
- Orlova T, Melnichuk A, Klimenko K et al. (2017) Reclamation of landfills and dumps of municipal solid waste in a waste management system: methodology and practice. In: IOP Conf. Series: Earth and Environ Sci 90(1):13, 012110. <https://doi.org/10.1088/1755-1315/90/1/012110>
- Pejović M, Bajat B, Gospavić Z, Saljnikov E, Kilibarda M, Čakmak D (2017) Layer-specific spatial prediction of as concentration in copper smelter vicinity considering the terrain exposure. *J Geochem Explor* 179:25–35. <https://doi.org/10.1016/j.gexplo.2017.05.004>
- Piri M, Sepehr E, Samadi A et al. (2020) Contaminated soil amendment by diatomite: chemical fractions of zinc, lead, copper and cadmium. *Int J Environ Sci Technol.* <https://doi.org/10.1007/s13762-020-02872-0>
- Podar D, Ramsey MH (2005) Effect of alkaline pH and associated Zn on the concentration and total uptake of Cd by lettuce: comparison with predictions from the CLEA model. *Sci Total Environ* 347(1–3):53–63. <https://doi.org/10.1016/j.scitotenv.2004.11.024>
- Qaswar M, Yiren L, Jing H et al (2020) Soil nutrients and heavy metal availability under long-term combined application of swine manure and synthetic fertilizers in acidic paddy soil. *J Soils Sediments* 20:2093–2106. <https://doi.org/10.1007/s11368-020-02576-5>
- Rodríguez-Eugenio N, McLaughlin M, Pennock D (2018) Soil Pollution: a hidden reality. Rome, FAO, p 142. <http://www.fao.org/3/i9183en/i9183en.pdf>
- Rutigliano FA, Marzaioli R, De Crescenzo S, Trifuoggi M (2019) Human health risk from consumption of two common crops grown in polluted soils. *Sci Total Environ* 691:195–204. <https://doi.org/10.1016/j.scitotenv.2019.07.037>
- Saljnikov E, Mrvić V, Čakmak D, Jaramaz D, Perović V, Antić-Mladenović S, Pavlović P (2019) Pollution indices and sources apportionment of heavy metal pollution of agricultural soils near the thermal power plant. *Environ Geochem Health* 41:2265–2279. <https://doi.org/10.1007/s10653-019-00281-ypp.5-15>
- Shafronov OD (2007) Heavy metals in soils of reference areas of the Nizhny Novgorod region. *Plodorodie*, pp 7–9. (Тяжелые металлы в почвах эталонных участков Нижегородской области)
- Sheudzhen AKh (2010) *Agrobiogeochemistry*, 2nd edn. KubGAU, Krasnodar, p 877 (Агробιοгеохимия, 2-е изд., Краснодар, КубГАУ, с. 877)
- Simmer M, Bommer J, Frischknecht S, Christl I, Kotsev T, Kretzschmar R (2017) Reductive solubilization of arsenic in a mining-impacted river floodplain: influence of soil properties and temperature. *Environ Pollut* 231(Pt1):722–731. <https://doi.org/10.1016/j.envpol.2017.08.054>
- Singh R, Gautam N, Mishra A, Gupta R (2011) Heavy metals and living systems: an overview. *Indian J Pharmacol* 43(3):246–253. <https://doi.org/10.4103/0253-7613.81505>, <https://www.ijp-online.com/text.asp?2011/43/3/246/81505>
- Steffan JJ, Brevik EC, Burgess LC, Cerdà A (2018) The effect of soil on human health: an overview. *Eur J Soil Sci* 69(1):159–171. <https://doi.org/10.1111/ejss.12451>
- Tang J, Zhang J, Ren L, Zhou Y, Gao J, Luo L, Yang Y, Peng Q, Huang H, Chen A (2019) Diagnosis of soil contamination using microbiological indices: a review on heavy metal pollution. *J Environ Manag* 242:121–130. <https://doi.org/10.1016/j.jenvman.2019.04.061>
- Tchounwou PB, Yedjou CG, Patlolla AK, Sutton DJ (2012) Heavy metal toxicity and the environment. *Exp Suppl* 101:133–164. https://doi.org/10.1007/978-3-7643-8340-4_6
- Tóth G, Hermann T, Da Silva MR, Montanarella L (2016) Heavy metals in agricultural soils of the European

- Union with implications for food safety. *Environ Int* 88:299–309. <https://doi.org/10.1016/j.envint.2015.12.017>
- Tošić S, Mrvić V, Jaramaz D, Saljnikov E (2020) Soil contamination with potentially toxic elements in the municipality of Bor. *Bull Fac For* 122:107–124. <https://doi.org/10.2298/GSF2022107T>
- Tošić S, Mrvić V, Jaramaz D (2019). Basic characteristics of soil fertility of Bor municipality. In: Proceedings of the XIII Environmental protection of urban and suburban settlements. Serbia, pp 115–122
- UN (2019) World population prospects. <https://population.un.org/wpp/>. Accessed on 7 March 2021
- Wang AS, Angle JS, Chaney RL, Delorme TA, Reeves RD (2006) Soil pH effects on uptake of Cd and Zn by *Thlaspi caerulescens*. *Plant Soil* 281(1–2):325–337. <https://doi.org/10.1007/s11104-005-4642-9>
- Wang Q, Cui Y, Liu X, Dong Y, Christie P (2003) Soil contamination and plant uptake of heavy metals at polluted sites in China. *J Environ Sci Health, Part A* 38:823–838. <https://doi.org/10.1081/ESE-120018594>
- WHO (2020) World health organisation, <https://www.who.int/news-room/fact-sheets/detail/lead-poisoning-and-health>. Accessed on 7 March 2021
- WRB (2014) World reference base for soil resources. Food and agriculture organization of the United Nations Rome, 2015; access <http://www.fao.org/3/i3794en/i3794en.pdf>. Accessed on 7 March 2021
- Wuana RA, Okieimen FE (2011) Heavy metals in contaminated soils: a review of sources, chemistry, risks and best available strategies for remediation. *Int'l Scholarly Res Not* 2011:20. <https://doi.org/10.5402/2011/402647>
- Xiang HF, Tang HA, Ying QH (1995) Transformation and distribution of forms of zinc in acid, neutral and calcareous soils of China. *Geoderma* 66(1–2):121–135. [https://doi.org/10.1016/0016-7061\(94\)00067-K](https://doi.org/10.1016/0016-7061(94)00067-K)
- Yang Sh, He M, Zhi Yu, Chang SX, Gu B, Liu X, Xu J (2019) An ointegrated analysis on source-exposure risk of heavy metals in agricultural soils near intense electronic waste recycling activities. *Environ Int*, part B 133:105239. <https://doi.org/10.1016/j.envint.2019.105239>
- Yin D, He T, Zeng L, Chen J (2016) Exploration of amendments and agronomic measures on the remediation of methylmercury-polluted rice in a mercury mining area. *Water Air Soil Pollut* 227:333. <https://doi.org/10.1007/s11270-016-3014-9>
- Yu H, Li J, Luan Y (2018) Meta-analysis of soil mercury accumulation by vegetables. *Sci Rep* 8:1261. <https://doi.org/10.1038/s41598-018-19519-3>
- Zaikina VN, Okolelova AA, Kesterina NG, Sviridova YuA (2016) Accumulation of heavy metals in Light-Chestnut and alluvial soils of Volgograd-Volzhski agglomeration. *Bull Samara Sci Cent Russ Acad Sci* 18(2):2 (Накопление тяжелых металлов в каштановых и аллювиальных почвах Волгоград-Волжской агломерации. Вестник Самарского научного центра РАН), <https://cyberleninka.ru/article/n/akkumuljatsiya-tyazhelyh-metallov-v-svetlo-kashtanovyh-i-allyuvialnyh-pochvah-aglomeratsii-volgograd-volzhskiy/viewer>. Accessed on 7 March 2021
- Zemanová V, Trakal L, Ochečová P, Száková J, Pavlíková D (2014) A model experiment: competitive sorption of Cd, Cu, Pb and Zn by three different soils. *Soil Water Res.* 9:97–103. <https://www.agriculturejournals.cz/publicFiles/128690.pdf>
- Zhen Z, Wang S, Luo S, Ren L, Liang Y, Yang R, Li Y, Zhang Y, Deng S, Zou L, Lin Z, Zhang D (2019) Significant impacts of both total amount and availability of heavy metals on the functions and assembly of soil microbial communities in different land use patterns. *Front Microbiol* 10:2293. <https://doi.org/10.3389/fmicb.2019.02293>
- Zwolak A, Sarzyńska M, Szpyrka E et al (2019) Sources of soil pollution by heavy metals and their accumulation in vegetables: a review. *Water Air Soil Pollut* 230:164. <https://doi.org/10.1007/s11270-019-4221-y>



Impact of Tailing Outflow on Soil Quality Around the Former Stolice Mine (Serbia)

25

Snežana Belanović Simić, Dušica Delić,
Predrag Miljković, Jelena Beloica,
Sara Lukić, Olivera Stajković-Srbljinović,
Milan Knežević, and Ratko Kadović

Abstract

The accumulation of harmful microelements in the soil can cause long-term adverse effects, while their deposition can be toxic both for people and the environment. The study of agricultural land flooded in 2014 with tailing outflow due to an accident at the tailing dump of the Stolice mine in Kostajnik (western Serbia) is focused on the contents of heavy metals (Pb, Cd, Zn, Cu, Ni, Cr and Mn) in the soils and the biological activity of these soils. The Stolice-Kostajnik mine belongs to the Zajača mining site in the Boranje area, and its mining operations ceased in 1990. Soil samples were taken from open soil profiles in the flooded and unflooded areas at fixed depths of 0–10 cm, 10–20 cm and 20–40 cm to analyse their physical and chemical properties, the content of heavy metals and the soil's microbiological properties. The potential environmental risk and the source of heavy metals in the soils studied were determined using the enrichment factor (EF), the potential environ-

mental risk index (RI) and statistical methods such as the principal component analysis (PCA) and the Pearson correlation matrix. Significantly higher concentrations of Pb, Zn and Cd were found in the soil that was flooded with the tailing outflow, than in the unflooded soils. Statistically significant differences were found between the total number of microflora, fungi and *Azotobacter* in the flooded and unflooded soils. In the flooded soil, the mean values of the enrichment factor (EF) declined in the following order: Zn > Cd > Pb > Cu > Cr > Ni. On the basis of the average value of the potential environmental risk, it was concluded that the flooded soils are classified as at high ecological risk, while the unflooded areas are classified as at low ecological risk.

Keywords

Potentially toxic elements/heavy metals · Soil · Tailing outflow · Enrichment factor · Potential environmental risk

S. Belanović Simić (✉) · P. Miljković · J. Beloica · S. Lukić · M. Knežević · R. Kadović
Faculty of Forestry, University of Belgrade, Kneza Višeslava 1, 11030 Belgrade, Serbia
e-mail: snezana.belanovic@sfb.bg.ac.rs

D. Delić · O. Stajković-Srbljinović
Institute of Soil Science, Teodora Drajzera 7, 11000 Belgrade, Serbia

25.1 Introduction

The deposition of potentially toxic elements (PTEs) in soils and terrestrial ecosystems arouses particular interest in both theoretical and practical terms, because their accumulation can cause long-term adverse effects, and the underlying risks can be toxic for humans and the

environment. After a mine is closed, the mining process and accompanying industrial activities and tailing landfills continue to have a long-lasting impact on the degradation of land and socio-cultural and economic aspects (Kossoff et al. 2014; Blengini et al. 2019; Kan et al. 2020). All over the world, as a result of these activities, a large amount of heavy metals (HMs) associated with mineral particles are released into the environment, primarily in rivers and river sediments (Hudson-Edwards et al., 2003).

Flotation tailings are mainly inert solid material generated in industrial production, which are primarily harmful because the ore contains potentially toxic elements, and some substances are added during the industrial processing of the ore (Dožić et al. 2010; Sahu and Dash, 2011). In mining areas, erosion processes (water and aeolian erosion) are highly intense, and the impact of chemical degradation of the soil caused by local pollutants is also high (Đorović 2005). In addition, tailings change both physically and chemically after sedimentation (Kossoff et al. 2014).

Potentially toxic elements (such as heavy metals) are present in the soil naturally (Adriano 2001). However, in all soils, and especially in agricultural soils, contamination by some PTEs is caused by various anthropogenic activities, and occurs as a result of diffuse pollution, which is a significant form of pollution due to its partially irreversible nature (Belanović Simić 2017). There is a wide variety of airborne pollutants of natural origin, and of their anthropogenic sources, which include numerous combustion methods, thermal power plants and industrial activities (Pavlović and Mitrović 2016). Industrial activities, which are an integral part of mining, make a considerable contribution to the deposition of PTEs (heavy metals) in soils. Huber et al. (2008) set out the basic pathways of soil contamination: atmospheric deposition, agricultural activities, local sources (including floods), waste disposal and accidents. Wuana and Okieimen (2011) show the simple balance of heavy metals (PTEs) with the equation: $M_{total} = (M_p + M_a + M_f + M_{ag} + M_{ow} + M_{ip}) - (M_{cr} + M_l)$, where “M” is heavy metal, p

originates in the geological substrate, a is from atmospheric deposition, f is from fertilisers, ag is of agrochemical origin, ow is organic waste, ip is other inorganic pollutants, cr is losses due to crop removal and l is losses by rinsing, evaporation, etc.

In the biochemical cycles of heavy metals in the soil, the participation of microorganisms is an important factor in maintaining soil functions (Panikov 1999). The number and activity of microorganisms, their interactions and their relationships with other elements of soil ecosystems significantly affect the physical, chemical and biological processes in the pedosphere (Lombard et al. 2011). In addition, the physico-chemical properties of the soil and anthropogenic activity as a result of industrial and agricultural production affect the number and activity of microorganisms (García-Orenes et al. 2013; Zhou et al. 2014; Gagnon et al. 2020). The toxic effects of heavy metals in the soil are also explained by the reduction in enzymatic activity, a reduction in soil respiration by 3 to 45% and a decrease in microbial biomass by 21–53% (Zhou et al. 2014; Li et al. 2018; Fazekášová and Fazekáš 2020).

Additional problems in maintaining soil functions occur after floods, when the soil which is contaminated with heavy metals becomes a source of contamination for other components of the environment, and since they are persistent, their presence in the soil is long-lasting (Demeková et al. 2016). Globally, alluvial soils represent an area for agricultural production. Due to the flotation of tailings, these soils could be contaminated with PTEs (metals and metalloids), which are potentially toxic (Hudson-Edwards et al. 2003; Wang et al. 2010; Kossoff et al. 2014). Various studies around the world have studied the presence of heavy metals in soils near mines and their impact on biological, chemical and physical processes in the soil (Escarré et al. 2011; Bech et al., 2012; Bajkić et al. 2013; Ma et al. 2015; Demeková et al. 2016; Teixeira et al. 2018; Hirwa et al. 2019; Daldoul et al. 2019; Kabala et al. 2020), as well as in water and sediment (Hudson-Edwards et al. 2003; Macklin et al. 1999; Kossoff et al. 2014).

The literature lists examples of soil contamination due to the outflow of tailing dumps (Paya and Rodriguez 2018; Ferronato and Torretta 2019; Sliti et al. 2019; Okereafor et al. 2019; Agboola et al. 2020; Palansooriya et al. 2020; WISE Uranium project 2020), although many accidents are believed not to be reported due to poor publicity and legal consequences (Kossoff et al. 2014). The last major accident occurred at the Córrego de Feijão mine in Brazil in January 2019, when 12 million m³ of materials were released with consequences for the environment and human health. In 2018, four separate major accidents occurred in Mexico, Peru, Australia and Brazil. From 2014 to 2017, 12 major accidents occurred in the world (in the USA, Israel, China, etc.). In Europe, cases have been reported with serious consequences for soil and water ecosystems. These cases occurred in Spain in 1998, in Romania in 2000, and in Hungary in 2010. In Serbia, soil erosion by water is one of the most important types of soil degradation (Đorović 2005; Belanović et al. 2013a, b).

In May 2014, a serious accident occurred with about 1.2 million tonnes of ore in Serbia at the tailing landfill of the Stolice mine in Kostajnik, which was closed in 1987 (Vidojević et al. 2015). In this natural accident, more than 100,000 m³ of tailing sludge poured into the Kostajnik creek, from which the Korenita River is formed as a seasonal tributary of the Jadar River. Downstream of the tailing, a flood wave covered a strip of land 50–75 m wide on the left and right banks with a sedimentary layer that was 5–10 cm thick (Vidojević et al. 2015).

In May 2014, the total precipitation recorded in the Krupanj area was from 288.2 mm (the Krupanj station) to 647 mm (the Planina station), of which 174.4 mm or 60.5% (the Krupanj station), and 428 mm or 66.15% (the Planina station) were from 14 to 16 May (Nišavić et al. 2014). Since the soil was already saturated, the precipitation from 14 to 16 May caused surface runoff and flooding.

The accident occurred on the territory of the Serbian-Macedonian province, where the most important zones of antimony, lead and zinc are located (Đokić 2012). Within the territory,

several tailings were formed by mining activity, including Bobija (mining and separation tailing), Zajača (smelter), Stolice (flotation), Brasina (mining and separation), Kostajnik (mining) (Đokić and Jovanović 2009). The same authors reported significant concentrations of potentially toxic elements found in the tailings: in addition to the expected contents, others such as Sb and As, Pb, Cd, Zn and Cu were found in the tailing in Stolice, Kostajnik. There are several tailing landfills in Zajača and the wider area, including Bobija, which are a permanent source of pollution, primarily of groundwater, and a lead smelter is located nearby. The area is characterised by the major ore minerals, composed of pyrite and stibnite. The later is oxidised to form valentinite (Sb₂O₃) and senarmontite (Sb₂O₃), which are also found in the area. These ores are located along the boundaries between the limestone and schist of the Carboniferous period. The parent rock of the soils formed in the Stolice area are dacites and schist (EDD Master plan 2008).

In the area adjacent to the former Stolice mine, the tailing outflow from the Kostajnik landfill contributed to the contamination of agricultural land due to high waters in 2014, as well as air pollution and inputs from agricultural activities (fertilisers, pesticides and insecticides).

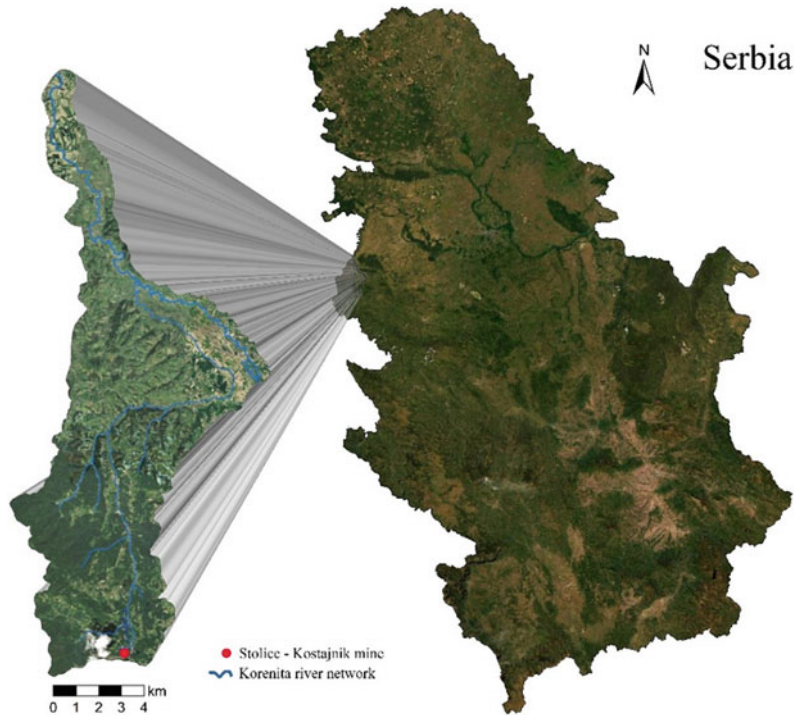
The present study aimed to (1) determine the status of soil quality after a tailing outflow, focusing on the content of potentially toxic elements (heavy metals—Pb, Cd, Zn, Cu, Ni, Cr and Mn) and the biological activity of these soils; (2) evaluate the ecological risk of heavy metals in the soil.

25.2 Materials and Methods

25.2.1 Area Studied

The Stolice-Kostajnik mine is part of the Zajača mining site in the Boranja area of western Serbia. The area studied covers the territory downstream from the flotation tailing to the mouth of the Korenita River into Jadar and part of the Jadar Valley, with a total area of 120.18 km² (Fig. 25.1). The area is located between 44°

Fig. 25.1 Location of area studied: Stolice-Kostajnik mine in western Serbia



23.830' and 44°38.100' N and 19°15.350' and 19°23.750' E.

In 2014, soil samples were collected after the reconnaissance of the terrain in the unflooded and flooded areas in the watershed of the Kostajnik creek and the Korenita River to the Jadar (Fig. 25.2). The sampling was conducted from 1 to 30 June 2018.

25.2.2 Sample Collection

Soil samples were taken from the open soil profiles (Fig. 25.2) at fixed depths of 0–10 cm, 10–20 cm and 20–40 cm to analyse the physical and chemical properties, content of heavy metals (Pb, Zn, Cd, Cu, Ni, Cr, Mn) and microbiological properties (total number of microflora, fungi, actinomycetes and bacteria from the genus *Azotobacter*) in the surface soil layer (0–10 cm). Additionally, a composite of five sub-samples from 0–10 cm was taken with an auger (Fig. 25.2). The samples were air-dried for two weeks, crushed using a mortar and pestle then

sieved to 2 mm and thoroughly homogenised before further treatment. Finally, the soil samples were stored in tightly sealed polyethylene bags until further analysis (YSSR 1966a). The samples for testing the soil's microbiological properties were taken from the composite samples of the surface layer (0–10 cm). To prevent cross-contamination between the samples, the auger was cleaned with 5% ethanol before every new sampling.

25.2.3 Soil Analysis

The mechanical composition was analysed using the pyrophosphate B-pipette method (ISO 11277: 1998).

The soil reaction (pH) was measured in water using a 1: 5 soil solution ratio (ISO 10390: 2005). The total cation exchange capacity (CEC in $\text{cmol}_c\text{kg}^{-1}$) was determined using the Kappen method (YSSR 1997) and the level of soil saturation with bases (%) calculated by Hissink (YSSR 1997). The soil organic carbon

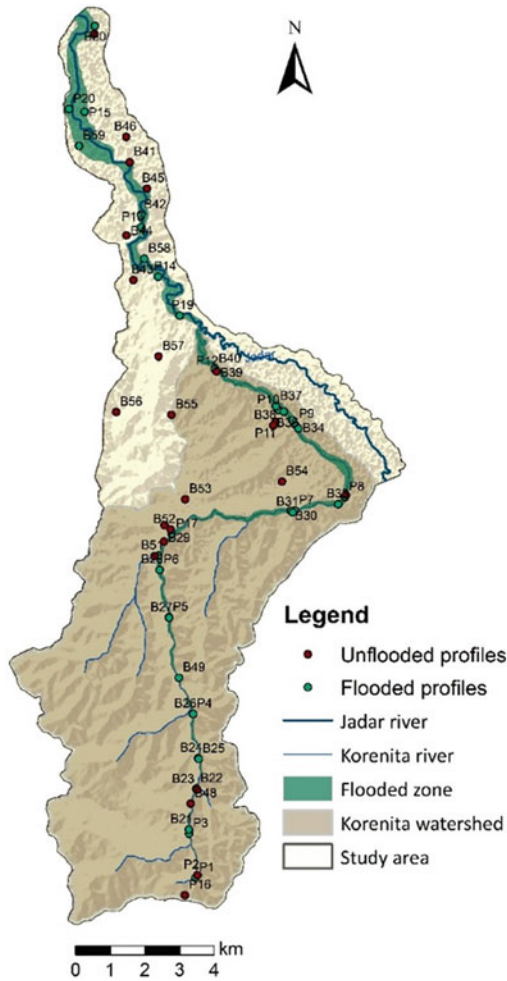


Fig. 25.2 The position of flooded and unflooded profiles at the Korenita River basin

(SOC) was measured using the Tyurin method (SRPS ISO 14235:2005 2005) and the total nitrogen using the Kjeldahl method (ISO 11261:2005 2005). Plant-available P and K were determined with the Egner-Riehm method (YSSR 1997). The carbonates, in the form of CaCO_3 , were measured with the volumetric method (ISO 10693: 1994 1994). To determine the total content of heavy metals (Pb, Zn, Cd, Cu, Ni, Cr, Mn), the soil was digested using the Aqua Regia (HCl-HNO_3 , 3:1) extraction method, and the HM concentrations were analysed using the AAS method. (ISO 11466: 1995 Soil quality 1995).

The total number of microflora, fungi and actinomycetes, and the number of bacteria from the genus *Azotobacter*, were determined using the agar plate method, based on the principle of inoculating culture media that are selective for those microorganisms, with a decimal dilution of the examined soil suspension (plate count on selective nutrient medium). The total microflora was determined with the agarised soil extraction method; the number of fungi on the Czapek medium and actinomycetes on a synthetic sucrose agar were determined as described by Krasilnikov, while the number of *Azotobacter* spp. was determined using the Tchanov method in a liquid-N-free medium with mannitol, using the most probable number (MPN) method (Govedarica and Jarak 1996; YSSR 1966b; Sarić 1989).

25.2.4 Statistical and Mathematical Methods

A t-test was used to determine statistically significant differences between the properties of unflooded and flooded soils. The significance of the correlations between the content of heavy metals in the flooded soils and some chemical properties of these soils was analysed using the Pearson correlation matrix and principal component analysis (PCA) with Varimax rotation (SPSS 2007). The Kaiser–Meyer–Olkin (KMO) measure of sampling adequacy and Bartlett’s test for sphericity were used to determine the factorability.

The geospatial representation of the pollution indices was obtained using appropriate GIS software. The geospatial distribution of the enrichment factor (EF) and potential environmental risk index (RI) were obtained by interpolation using the complex geostatistic empirical Bayesian kriging (EBK) method.

To assess the potential impact of anthropogenic activity on the concentration of heavy metals in the soil, the *enrichment factor* (EF) is calculated using the following equation (Acosta et al. 2011; Sakan et al. 2015; Marković et al. 2018):

$$EF = \frac{\left[\frac{C_n}{C_r}\right]_{\text{sample}}}{\left[\frac{C_n}{C_r}\right]_{\text{background}}} \quad (25.1)$$

where C_n represents the metal, and C_r is the reference metal. Manganese was used as the reference background element. Mn is mainly of lithogenic origin, and its anthropogenic sources are minimal (Loska et al. 1997; Marković et al. 2018). According to the EF value, the following five classes of soil enrichment are described: minimal enrichment ($EF < 2$), moderate enrichment ($2 < EF < 5$), significant enrichment ($5 < EF < 20$), very high enrichment ($20 < EF < 40$) and extremely high enrichment levels ($EF > 40$).

The potential Ecological risk index (RI) is calculated according to the following equation (Håkanson 1980):

$$RI = \sum_{i=1}^n E_r^i \quad (25.2)$$

where n is the total number of metals and E_r is an individual ecological risk index calculated using the equation:

$$E_r^i = T_r^i * PI \quad (25.3)$$

where T_r is the coefficient of toxicity of a particular metal (Zn—1, Cu—5, Pb—5, Ni—5, Cr—2, Cd—30), and PI is the calculated individual pollution factor.

The potential ecological risk index is defined into four classes as described by Luo et al. (2007): $RI < 65$ —low; $65 \leq RI < 130$ —medium; $130 \leq RI < 260$ —significant and $RI \geq 260$ —very high.

25.3 Results and Discussion

25.3.1 Basic Properties of the Soils Studied

Five soil types were identified in the area studied, according to the IUSS WG WRB classification

(2015): Fluvisol, Calcic Cambisol, Stagnosol, Dystric Cambisol and Luvisol. Only one soil type—alluvial soil (Fluvisol)—was identified in the areas flooded in 2014 during the tailing outflow. Other types of soil were found outside the flooded zone.

Tables 25.1 and 25.2 show the basic physical and chemical properties of the unflooded and flooded soils. Statistical differences have not been tested for a set with a small number of variables.

A statistically significant difference ($p < 0.05$) was found in terms of the particle size distribution of the flooded and unflooded soils, the sand and clay content in all the layers studied to a depth of 40 cm, and the silt content at 0–10 cm. The variability in the textural composition at 0–40 cm of the alluvial floodplain soil reflects the hydrological conditions of the floodwater sedimentation. According to the established ratio of particle size fractions, the soil textures are loamy sand, sandy loam, silty loam, loam and silty clay loam. The unflooded soils were silty loam and silty clay and clay in a single profile of brown soil on limestone. The textural composition of the floodplain soil provides good aeration and water permeability.

The soils' acidity correlated with the content of calcium carbonate. Statistically significant differences were found in the pH values ($p < 0.05$) comparing the flooded and unflooded soils. The soils studied were poorly provided with humus. The content of organic carbon in the flooded and unflooded soils exhibited significant differences in the surface layer ($p < 0.05$). Despite the fact that the total nitrogen in the soil, especially in agricultural soil, depends on land use and on mineral and organic fertilisers, there was no statistically significant difference between the flooded and unflooded soils in the total N content.

All the profiles of alluvial soil in the flooded zone to a depth of 40 cm contained free calcium carbonate. All the soils were saturated with bases. Fertilisation and the tailing outflow presumably have a high impact on the content of readily available phosphorus in the soil. Depending on the content of readily available

Table 25.1 Average values of the basic soil properties

Layer	Sand %	Silt %	Clay %	pH (H ₂ O)	SOC %	Total N% ^{ns}
Flooded						
0–10 cm (n = 31)	45.6 ± 24.9*	40.8 ± 18.0	12.2 ± 7.9	7.72 ± 0.4*	0.98 ± 0.4	0.18 ± 0.06
10–20 cm (n = 12)	40.5 ± 21.3*	44.8 ± 14.8	14.8 ± 7.7	7.51 ± 0.5*	1.26 ± 0.5 ^{ns}	0.18 ± 0.06
20–40 cm (n = 12)	31.6 ± 16.9*	49.9 ± 9.5	18.4 ± 8.8	7.51 ± 0.7*	0.96 ± 0.3 ^{ns}	0.17 ± 0.02
Unflooded						
0–10 cm (n = 27)	15.6 ± 9.4	58.4 ± 6.7*	24.13 ± 9.5*	6.77 ± 0.7	1.38 ± 0.25*	0.18 ± 0.03
10–20 cm (n = 7)	17.0 ± 9.8	54.3 ± 11.1 ^{ns}	28.8 ± 11.4*	6.72 ± 0.8	1.11 ± 0.2	0.2 ± 0.02
20–40 cm (n = 7)	11.9 ± 9.3	50.1 ± 15.5 ^{ns}	37.9 ± 18.6*	6.7 ± 0.7	0.79 ± 0.3	0.19 ± 0.01

t-test *p < 0.05; **p < 0.01; ns—not significant.

Table 25.2 Average values of the CaCO₃ content, CEC, base saturation, readily available phosphorus and potassium

Layer, cm	CaCO ₃ , % ^{ns}	CEC, cmol _c ·kg ⁻¹ ^{ns}	V, % ^{ns}	Available P ₂ O ₅ , mg·100 g ⁻¹ soil	Available K ₂ O, mg·100 g ⁻¹ soil
Flooded					
0–10	6.9 ± 4.8(n = 26)	24.6 ± 10.7(n = 5)	78.7 ± 19.8 ns	22.7 ± 18.2** (n = 31)	10.8 ± 4.6
10–20	9.3 ± 5.5(n = 7)	25.4 ± 10.1(n = 4)	85.2 ± 15.7 ns	23.9 ± 21.7 (n = 7) *	12.0 ± 7.2
20–40	10.3 ± 5.7(n = 7)	31.4 ± 12.6(n = 6)	86.6 ± 15.7 ns	13.6 ± 19.9(n = 7)	8.7 ± 3.1
Unflooded					
0–10	–	21.4 ± 5.8(n = 21)	66.8 ± 21.6	5.68 ± 4.3(n = 27)	16.6 ± 12.7*
10–20	–	25.4 ± 10.5(n = 7)	71.9 ± 23.3	3.0 ± 2.3(n = 7)	23.04 ± 19.5 ns
20–40	–	23.5 ± 7.3(n = 7)	70.4 ± 24	1.79 ± 1.2 (n = 7)	18.3 ± 12.9 ns

t-test *p < 0.05; **p < 0.01; ns—not significant

potassium, the samples belong to the poorly to well supplied classes.

25.3.2 Microbiological Characteristics of the Soils Studied

Significant differences in the total number of microflora, fungi and bacteria of the genus *Azotobacter* were found between the flooded and unflooded soils, while there were no significant differences in the number of actinomycetes (Table 25.3). In the soils of the flooded area, a significantly smaller total number of microflora and fungi was found compared to the unflooded soils, which indicated their sensitivity to changes in the soil caused by flooding and the negative

impact exerted on them by heavy metals from the tailing.

The low number of bacteria of the *Azotobacter* genus in the entire area studied indicates poor soil fertility, since the genus *Azotobacter* prefers fertile and well-aerated soils. It can be assumed that the presence of heavy metals added with the tailing caused a decrease in the total number of microflora, fungi and *Azotobacter* in the flooded area. For the whole area studied, the total number of microorganisms was negatively correlated with Cr, Cu, Ni, Cd and Mn. These results are in agreement with other studies showing the negative effect of heavy metals on microbial communities in the soil, which can directly affect soil fertility (Ahmad et al. 2005; Prasad et al. 2012; Lenart and Wolny-Koładka 2013). The number

Table 25.3 Total number of microorganisms, fungi, actinomycetes and *Azotobacter* spp. in the soils studied

	Total microflora ($\times 10^6$ CFU g ⁻¹)	Fungi ($\times 10^4$ CFU g ⁻¹)	Actinomycetes ($\times 10^4$ CFU g ⁻¹)	<i>Azotobacter</i> spp. (MPN g ⁻¹)
Flooded				
Average \pm Sd	11.97 \pm 13.8	8.85 \pm 7.9	5.91 \pm 4.03 ^{ns}	131.8 \pm 135.02*
Unflooded				
Average \pm Sd	17.84 \pm 13.2*	14.5 \pm 9.9**	4.95 \pm 3.1	64.04 \pm 56.34

t-test * $p < 0.05$; ** $p < 0.01$; ns—not significant

of actinomycetes did not differ significantly between the flooded and unflooded areas, which was expected for this group of microorganisms, because they have a low sensitivity to environmental stress factors and even heavy metals. Some results indicated resistance to metals and an ability to consume metals, which can be widespread amongst actinomycetes growing in contaminated environments (Amoroso et al. 1998). Due to their mycelial form and variety of metabolism and growth characteristics, actinomycetes can use the mechanisms of tolerance to and detoxification of heavy metals, producing chelating agents that bind metals and reduce their toxicity (Kavamura and Esposito 2010; El Baz et al. 2015).

The presence of Cd and Pb is harmful to microorganisms. Higher concentrations of both harmful and essential elements reduce the number of populations of microorganisms and biochemical activity (Čakmak et al. 2016).

An analysis of the total number of microflora, fungi, actinomycetes and the *Azotobacter* in the soil indicated that more than 50% of the area studied does not exhibit optimal soil fertility and biogenicity. Therefore, it is necessary to undertake certain agrotechnical measures to improve the physico-chemical and microbiological properties of these soils.

25.3.3 Contents of Heavy Metals in the Soils Studied

The content of Pb and Cd in all layers of the flooded soil to a depth of 40 cm was significantly higher ($p < 0.01$) than in the unflooded soil (Table 25.4). Their average values were greater

than the permissible limit values (Official Gazette of the Republic of Serbia 30/2018). Similarly, the Zn content was significantly higher ($p < 0.01$) in the 0–20 cm layer of the flooded soil: the average values were greater than the permissible limits (Official Gazette of the Republic of Serbia 30/2018).

The content of Pb, Cd and Zn was lower in the flooded soil compared to the published data (Rafiei et al. 2010; Wang et al. 2010; Macklin et al. 1999). In the unflooded soils, the content of Pb, Cd and Zn was below the permissible limit values (Official Gazette of the Republic of Serbia 30/2018). The content of Cu, Cr and Ni in all soils was below the limit values, except for Cu, which differed significantly in the 0–10 cm layer of the flooded soils. The contents of Cr and Ni were significantly higher in the 0–40 cm layer of the unflooded soils, while the content of Mn did not change.

25.3.4 Air Deposition of Pb and Cd in the Area Studied

The data on the airborne input of heavy metals (Cd and Pb) was retrieved from the EMEP/MSCE database. Changes in the total annual atmospheric deposition of Cd and Pb over the period 1990–2015 were observed in the “Stolice” study area, with a substantially decreasing trend for both heavy metals (Figs. 25.3 and 25.4). The box-and-whisker plot shows the total amounts (cumulative value for the respective period) of Cd and Pb for Serbia for the 1990–2015 period. The red “x” signs denote the cumulative value for the Stolice area. As the graph shows, the localities studied belong to an area with a higher level of atmospheric pollution (third quartile).

Table 25.4 Average contents and range of Pb, Cd, Zn, Cu, Cr, Ni and Mn (mg·kg⁻¹) in the soils studied

cm	Pb (mg·kg ⁻¹)	Cd (mg·kg ⁻¹)	Zn (mg·kg ⁻¹)	Cu (mg·kg ⁻¹)	Cr (mg·kg ⁻¹)	Ni (mg·kg ⁻¹)	Mn (mg·kg ⁻¹)
	Flooded						
0-10	147.12 ± 122.81**	3.14 ± 3.54**	516.11 ± 575.3**	18.39 ± 5.39*	17.67 ± 9.55	20.09 ± 8.99	920 ± 145.98
Range (n = 31)	15.26-378.56	0.10-11.26	50.33-1999.9	11.40-30.56	7.92-46.58	12.09-60.26	557.4-1265.2
10-20	150.2 ± 154.06**	2.84 ± 3.71**	475.69 ± 600.57**	20.10 ± 7.83 ^{ns}	17.09 ± 6.1	19.11 ± 3.72	941.9 ± 140.2
Range (n = 12)	34.33-502.62	0.10-11.58	61.09-1931.01	12.95-43.49	8.40-27.97	13.88-26.07	761.4-1130.1
20-40	118.41 ± 181.26**	1.54 ± 2.43**	248.98 ± 410.23 ^{ns}	20.46 ± 11.26	18.14 ± 5.52	20.88 ± 5.25	952.5 ± 149.5
Range (n = 12)	22.73-674.71	0.10-8.49	54.52-1519.54	11.43-54.10	7.59-23.63	11.94-29.89	
	Unflooded						
0-10	23.45 ± 7.42	0.14 ± 0.11	65.55 ± 14.96	15.78 ± 4.64	28.12 ± 4.36**	23.32 ± 7.51 ^{ns}	1013.9 ± 282.9 ^{ns}
Range (n = 27)	11.19-43.21	< d.l. -0.39	44.35-98.75	7.82-30.21	19.93-35.90	12.65-52.67	649.3-1836.9
10-20	24.16 ± 7.72	0.12 ± 0.06	77.84 ± 18.79	19.05 ± 4.12	28.71 ± 3.58**	27.98 ± 5.52**	1097.6 ± 563.6 ^{ns}
Range (n = 7)	12.8-37.8	0.01-0.21	53.31-112.82	12.45-25.49	22.97-33.93	19.33-35.88	515.1-2351.6
20-40	25.19 ± 8.29	0.11 ± 0.1	89.45 ± 34.17	21.50 ± 6.09 ^{ns}	28.39 ± 4.40**	31.87 ± 8.79**	1246.7 ± 783.8 ^{ns}
Range (n = 7)	13.3-39.98	0.003-0.34	56.09-163.49	14.71-32.68	22.69-36.35	22.06-48.27	264.7-3011.7

*p < 0.01; **p < 0.05; ns—not significant

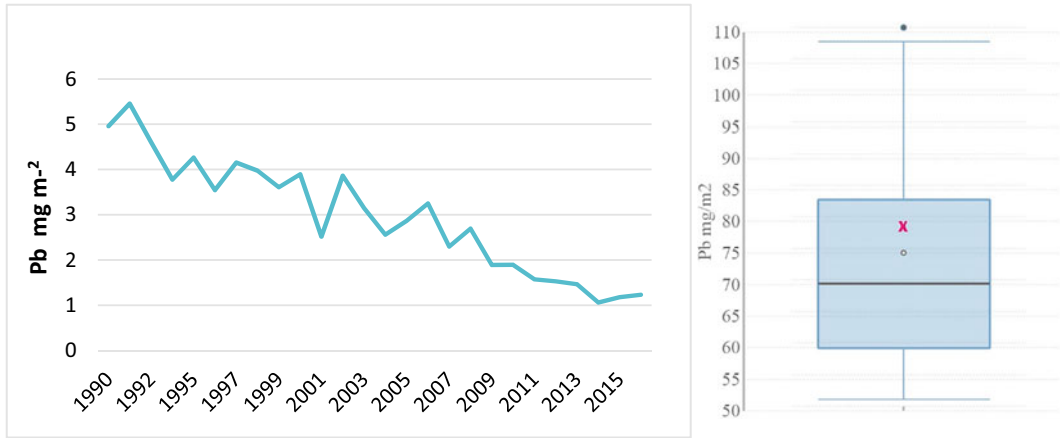


Fig. 25.3 Time series data of Pb deposition for the area studied (left); cumulative values of Pb for the Republic of Serbia for the 1990–2015 period (right)

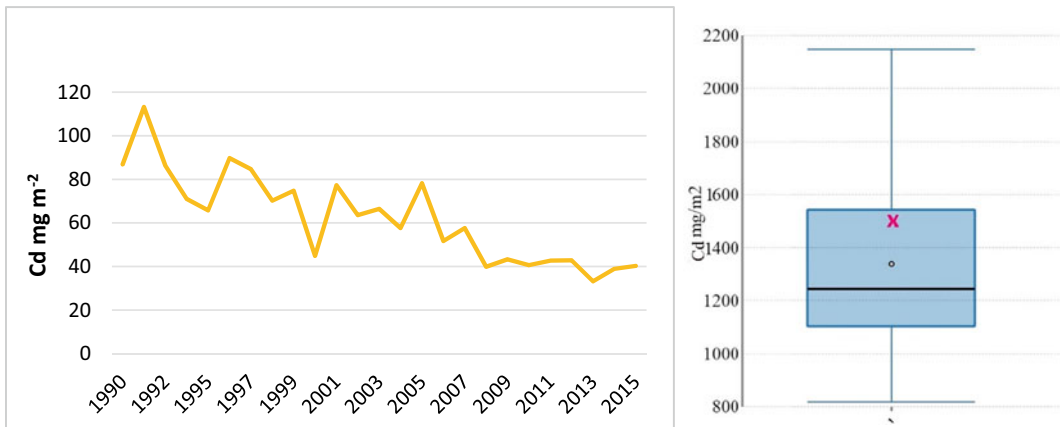


Fig. 25.4 Time series data of Cd deposition for the area studied (left); cumulative values of Cd for the Republic of Serbia for the 1990–2015 period (right)

The higher deposition of heavy metals can also be explained by active mining in this area. The reduction in the atmospheric input of Cd and Pb is the result of various activities, including measures to reduce emissions, as well as the economic downturn and industrial restructuring which have taken place in HELCOM (Helsinki Commission) and other EMEP (European Monitoring and Evaluation Programme) countries

(Bartnicki et al. 2017). The Stolice mine ceased operations in 1990, which led to a reduction in emissions. Although the Zajača metallurgical plant continued production, its main activity has been redirected to the production of Pb from secondary raw materials (Project 2012). Depositions of nitrogenous and sulphuric acids did not exceed the critical values (Čakmak et al. 2014) in the wider area studied, which means that all soils

studied underwent a recovery phase. High air depositions of Pb and Cd affected soil conditions in this area.

25.3.5 Impact of Tailings on Contamination of Soil in the Flooded Area

In addition to the impacts of agricultural activities and air deposition, the introduction of tailings additionally loaded the soil with heavy metals, which led to a decrease in biochemical activity. The content of primarily Zn, Cd and Pb in the flooded soils has a clear tendency to decrease with an increasing distance from the tailing dam, which is in the function of the particulate contaminant (Figs. 25.5 and 25.6). Vandenberg et al. (2011) explain that the distance from the source of pollution significantly affects the metal content in alluvium, and that some elements such as Zn, Mn and Cu are carried further downstream compared to Cd and Pb. Oprea et al. (2010) reported that soils are

contaminated with high concentrations of metals at a distance of 25–30 km from the source of pollution (smelters and mines). Molnárová et al. (2018) found that trees (*Salix* sp, *A. glutinosa*) on coastal streams in mining areas absorb a large amount of heavy metals. According to published data, the metal content in alluvial soils increases and their accumulation increases as the diameter of sediment particles decreases.

Earlier studies in the Zajača region (Čakmak et al. 2016) revealed that Cu, Ni, Cr and Zn, and in most cases also Cd, were subject to geological origin, since Cu, Ni and Cr do not originate from the tailings. The correlations (Pearson coefficient) between the total content of HMs and some chemical properties of the soils in the flooded zone support this finding (Table 25.5).

Significant correlation was found between Zn and Pb (0.95**), Zn and Cd (0.99**) and Pb and Cd (0.97**) in the flooded zone, where the tailing outflow occurred. This indicates their common origin from the tailings, because the concentrations in the flooded soils were significantly higher than in the unflooded soils. On the other hand, there was a statistically significant

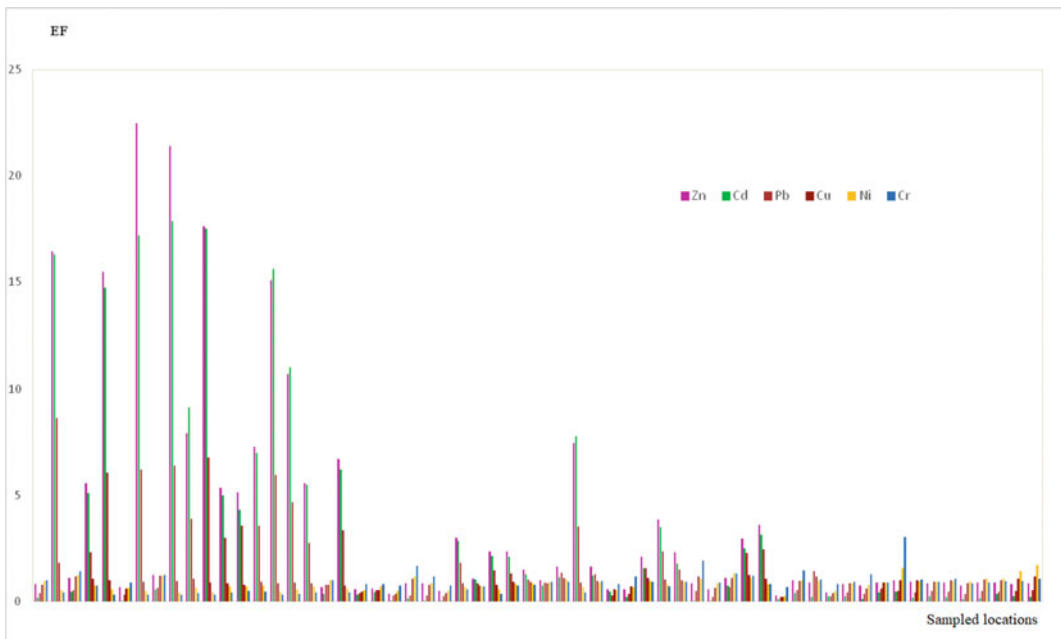


Fig. 25.5 Enrichment factor of heavy elements for flooded soils

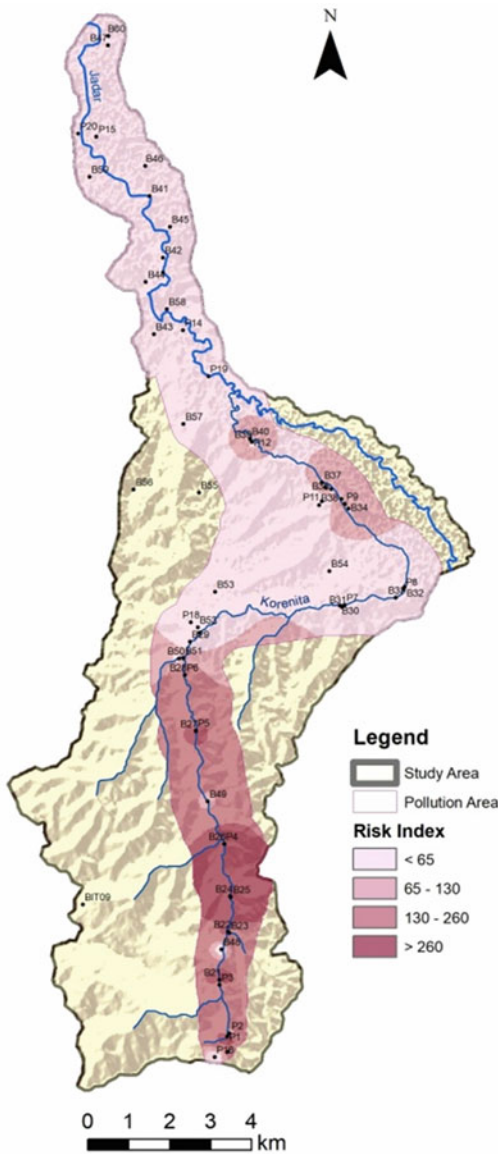


Fig. 25.6 Pollution zones according to the total potential environmental risk

correlation between Ni and Cr (0.77**), but the correlation between Cr and other elements was significantly negative, while the correlation of Ni with Cu (0.46**) and of Ni with Mn (0.37*) was positive.

The correlation between Mn and Cu was also significant (0.55**), indicating their common origin, which is also associated with the content of Ni. The humus was positively correlated with

Ni and Cr, and negatively correlated with Zn, Pb and Cd.

The available phosphorus correlated well with Zn, Pb, Cd, and negatively with Ni and Cr. Cao et al. (2003) suggested that phosphates effectively immobilise Pb, while having a slightly lower effect on Zn and Cu in contaminated soils. The pH of the soils studied ranged from 7.36 to 8.24, which is essential for the immobilisation of microelements (Adriano 2001). In addition, at higher pH values the availability of HMs is reduced, so no statistically significant correlation between the elements and pH was found in the soils studied.

Based on factor analysis of the variables (HMs and available phosphorus and potassium), they were grouped around three factors that determine 87.1% of the cumulative variance (Table 25.6). Factors were selected by the characteristic value criterion (eigenvalue of about 1) and combined with the criterion of the percentage of explained total variance. The KMO test result was 0.671, and the Bartlett sphericity test was significant (0.0001, $p < 0.05$).

The first factor (F1) explains 54.3% of the total variability, and includes the Cd, Zn, Pb, and readily available phosphorus variables (Table 25.7). It is significantly higher in the flooded than in the unflooded soils. This indicates that the deposited tailings have a significant impact on phosphorus (Table 25.2). A high negative factor load was found for the Ni (-0.66) and Cr (-0.804), which indicates that these elements have a different origin. This factor can be explained by the anthropogenic impact and the impact of flotation tailings, as well as the impact of long-term mining activities. The second factor (F2) explains 23.7% of the total variability and includes the Cu, Ni and Mn. This factor partially explains the geological impacts and partially the influence of other anthropogenic activities. The third factor (F3) explains 9.1% of the total variability and includes readily available potassium from agricultural activities.

25.3.5.1 Pollution Indices

Assessment of contamination in the surface soil layer of the soils studied was based on the

Table 25.5 Correlation matrix between the total content of heavy metals in the soil and some chemical and biological properties of the soils in the flooded area

	Zn	Cu	Pb	Ni	Cr	Cd	Mn	pH	Humus	Readily avail. P ₂ O ₅	Readily avail. K ₂ O
Zn	1	0.24	0.95**	-0.46*	-0.58**	0.99**	0.21	0.06	-0.65**	0.89**	-0.42*
Cu		1	0.35	0.46**	0.21	0.24	0.55**	0.04	0.14	0.27	0.12
Pb			1	-0.48**	-0.62**	0.97**	0.21	0.13	-0.63**	0.092**	-0.41*
Ni				1	0.77**	-0.49**	0.37*	-0.01	0.51**	-0.50**	0.35
Cr					1	-0.62**	-0.06	-0.18	0.65**	-0.62**	0.33
Cd						1	0.19	0.09	-0.67**	0.93**	-0.40*
Mn							1	0.03	0.08	0.16	0.12
pH								1	-0.06	0.14	0.07
humus									1	-0.59**	0.42*
Read. avail. P ₂ O ₅										1	-0.24
Read. avail. K ₂ O											1

**Correlation is significant at the 0.01 level (2-tailed). *Correlation is significant at the 0.05 level (2-tailed)

Table 25.6 Parameters of the factor analysis

Factor	(Eigenvalue)	Variance, %	Cumulative variance, %
1	4.889	54.322	54.322
2	2.134	23.713	78.035
3	0.815	9.051	87.086
4	0.644	7.153	94.240
5	0.281	3.124	97.364
6	0.125	1.384	98.748
7	0.085	0.940	99.688
8	0.024	0.272	99.960
9	0.004	0.040	100.000

Table 25.7 Results of the factor analysis and factor load distribution after varimax rotation

	Component		
	1	2	3
Cd	0.938	0.151	-0.243
Readily available phosphorus	0.935	0.139	-0.065
Pb	0.927	0.208	-0.252
Zn	0.910	0.173	-0.273
Cr	-0.804	0.361	-0.065
Cu	0.138	0.902	-0.028
Mn	0.190	0.744	0.214
Ni	-0.660	0.685	0.041
Readily available potassium	-0.267	0.174	0.905

Extraction method: principal component analysis. Rotation method: Varimax with Kaiser normalisation. Rotation converged in 5 iterations

Table 25.8 Average values of the enrichment factor (EF)

	EFPb	EFCd	EFZn	EFCu	EFCr	EFNi
	Flooded					
Average ± Sd	2.71 ± 2.10**	5.24 ± 5.58**	5.84 ± 6.15**	0.96 ± 0.21 ^{ns}	0.72 ± 0.50	0.79 ± 0.27
	Unflooded					
Average ± Sd	0.43 ± 0.17	0.25 ± 0.21	0.77 ± 0.24	0.80 ± 0.28	1.07 ± 0.29**	0.88 ± 0.29 ^{ns}

**p < 0.01; * p < 0.05; ns—not significant

Table 25.9 Average values of the individual pollution index (Er) and total potential environmental risk (RI)

	ErPb	ErCd	ErZn	ErCu	ErCr	ErNi	RI
	Flooded						
Average ± Sd	10.53 ± 8.7**	123.58 ± 139.7**	4.61 ± 5.2**	3.75 ± 1.1 ^{ns}	1.10 ± 0.6	3.11 ± 1.4	146.7 ± 153.6**
	Unflooded						
Average ± Sd	1.77 ± 0.6	6.07 ± 4.7	0.63 ± 0.1	3.24 ± 0.9	1.75 ± 0.3**	3.59 ± 1.2**	17.1 ± 6.1

**p < 0.01; * p < 0.05; ns—not significant

following calculated indices: enrichment factor (ER) and the individual pollution index (Er), i.e. the total environmental risk potential (RI). Tables 25.8 and 25.9 show that both the enrichment factor and the individual pollution index for Pb, Cd and Zn in the soils flooded with tailings are several times higher than in the unflooded soils, while the opposite was found for Cr and Ni. In addition, the PCA analysis confirmed that Pb, Zn and Cd originated from the tailings, while Cr and Ni partially come from the parent rock.

In the flooded area, the mean values of the enrichment factor (EF) decline in the following order: Zn > Cd > Pb > Cu > Cr > Ni. The anthropogenic factor had the greatest impact on Zn and Cd, so the EF values decreased with increasing distance from the tailing dump (Fig. 25.5). Significant differences in the spatial distribution of tailings and soil pollution can also be seen in the distribution of the EF. Based on the average value of the total environmental risk potential, it can be concluded that the flooded soils are classified as at significant environmental risk, while the unflooded soils are classified as at low environmental risk. Figure 25.6 shows the pollution zones with the highest pollution determined, approximately 4 km from the tailing outflow.

25.4 Conclusions

The study have shown that the content of HMs in the flooded soils—primarily Zn, Cd and Pb—was significantly higher in the flooded soils compared to the unflooded ones. The contents of Cr and Ni were significantly higher in the unflooded soils, while the contents of Mn did not differ. In addition to the outflow tailing, the area studied has been affected by mining activities for a long time.

According to the EMEP/MSC-E database, the atmospheric deposition of Cd and Pb decreased significantly in the 1990–2015 period, but the total amounts for this period relate to the area with a higher level of atmospheric pollution. Significant differences in the total number of microflora, fungi and *Azotobacter* were found when comparing the flooded and unflooded soils. The low number of *Azotobacter* in the entire area studied indicates poor soil fertility. The presence of Cd and Pb is harmful to microorganisms. The total number of microflora, fungi, actinomycetes and the *Azotobacter* in the soil indicates that the soil in more than 50% of the area studied does not have optimal fertility and biogenicity. Therefore, appropriate agrotechnical measures

must be undertaken to improve the physico-chemical and microbiological soil characteristics.

Based on the average value of the total environmental risk potential, it can be concluded that the flooded soils are at significant environmental risk, while the unflooded soils are classified as at low environmental risk. In addition, PCA analysis confirmed that Pb, Zn and Cd originated from the tailings, while Cr and Ni partially came from the parent rock. In the flooded area, the mean values of the enrichment factor (EF) decreased in the following order: Zn > Cd > Pb > Cu > Cr > Ni. Thus, the greatest pollution was found in the flooded soils, where pollution decreases as the distance from the tailing dump increases.

Given the high pollution of flooded soils with heavy metals, further studies are necessary, primarily because of the possible human health risk. Further studies should focus on the analysis of available soil elements and the content of elements in the water and vegetation. It is also recommended to use organic fertilisers on all soils and to use polymers and/or zeolites to bind harmful microelements in flooded soils with a high level of pollution.

Acknowledgements This article was written as part of the projects “Environmental pollution testing services due to tailings outflow from flotation Stolice”, reference no. 451-03-9/2021-14/200169, financially supported by the Ministry of Environmental Protection of the Republic of Serbia, and “Studying Climate Change and its Influence on the Environment: Impacts, Adaptation and Mitigation” (III43007), financed by the Ministry of Education and Science of the Republic of Serbia, 2011–2019.

References

- Acosta JA, Martínez-Martínez S, Faz A, Arocena J (2011) Accumulations of major and trace elements in particle size fractions of soils on eight different parent materials. *Geoderma* 161(1–2):30–42. <https://doi.org/10.1016/j.geoderma.2010.12.001>
- Adriano DC (2001) Trace elements in terrestrial environments: biogeochemistry, bioavailability, and risks of metals. Springer, New York, pp 1–866
- Agboola O, Babatunde DE, Fayomi OSI, Sadiku ER, Popoola P, Moropeng L, Yahaya A, Mamudu OA (2020) A Review on the impact of mining operation: monitoring, assessment and management. *Results Eng* 100181 (in press). <https://doi.org/10.1016/j.rineng.2020.100181>
- Ahmad I, Hayat S, Ahmad A, Inam A, Samiullah I (2005) Effect of heavy metal on survival of certain groups of indigenous soil microbial population. *J Appl Sci Environ Manag* 9:115–121. <https://tspace.library.utoronto.ca/bitstream/1807/6430/1/ja05021.pdf>
- Amoroso JM, Castro GR, Carlino FJ, Romero NC, Hill RT (1998) Screening of heavy metal-tolerant actinomycetes isolated from the Salí River. *J Gen Appl Microbiol* 44:129–132. <https://doi.org/10.2323/jgam.44.129>
- Bajkić S, Naračić T, Đolić L, Đorđević D, Nikodinović-Runčić J, Morić I, Vasiljević B (2013) Microbial diversity and isolation of multiple metal-tolerant bacteria from surface and underground pits within the copper mining and smelting complex Bor. *Arch. Biol. Sci., Belgrade*, 65 (1): 375–386. <http://cherry.chem.bg.ac.rs/handle/123456789/1559>
- Bartnicki J, Gusev A, Aas W, Gauss M, Jonson JE (2017) Atmospheric supply of nitrogen, cadmium, mercury, lead, and PCDD/Fs to the Baltic Sea in 2015. EMEP Centres Joint Report for HELCOM. EMEP/MS-CW Technical Report 1/2017. Norwegian Meteorological Institute. Oslo, Norway. <http://www.emep.int/pub/helcom/2017/index.html>
- Bech J, Corrales I, Tume P, Barcelo J, Duran P, Roca N, Poschenrieder C (2012) Accumulation of antimony and other potentially toxic elements in plants around a former antimony mine. *J Geochem Explor* 113:100–105. <https://doi.org/10.1016/j.gexplo.2011.06.006>
- Belanović S, Perović V, Vidojević D, Kostadinov S, Knežević M, Kadović R, Košanin O (2013a) Assessment of soil erosion intensity in Kolubara district, Serbia. *Fresenius Environ Bull.* [Print ed.], 22 (5A):1556–1563. ISSN 1018–4619. <http://www.psp-parlar.de/>
- Belanović S, Bjedov I, Čakmak D, Obratov-Petković D, Kadović R, Beloica J (2013b) Influence of Zn on the availability of Cd and Cu to *Vaccinium* species in unpolluted areas—A Case study of Stara planina Mt. (Serbia). *Carpathian J Earth Environ Sci* 8(3):5–14
- Belanović Simić S (2017) Soil quality—challenges of land use (Kvalitet zemljišta—izazovi sistema korišćenja). The University of Belgrade. Faculty of Forestry, CD CD-ROM, ISBN 978-86-7299-258-8, pp. 1–214 (in Serbian)
- Blengini GA, Mathieux F, Mancini L, Nyberg M, Viegas HM (Editors), Salminen J, Garbarino E, Orveillon G, Saveyn H, Mateos Aquilino V, Llorens González T, García Polonio F, Horckmans L, D'Hugues P, Balomenos E, Dino G, de la Feld M, Mádaí F, Földessy J, Mucsi G, Gombkötő I, Calleja I (2019) Recovery of critical and other raw materials from mining waste and landfills: State of play on existing practices, EUR 29744 EN, Publications Office of the European Union, Luxembourg. ISBN 978-92-76-08568-3. <https://doi.org/10.2760/600775>, JRC116131
- Čakmak D et al (2016) State of non-agricultural land of industrial zones of bigger cities in the Republic of

- Serbia in aspect of biological and chemical quality (Stanje nepoljoprivrednog zemljišta industrijskih zona većih gradova u Republici Srbiji sa aspekta biološkog i hemijskog kvaliteta). Report, Institute of Soil Science, Belgrade, pp 1–158 (in Serbian)
- Čakmak D, Beloica J, Perovic V, Kadovic R, Mrvic V, Knezevic J, Belanovic S (2014) Atmospheric deposition effects on agricultural soil acidification state key study: Krupanj municipality. *Arch Environ Protec* 40 (2):137–148. <https://doi.org/10.2478/aep-2014-0022>, <http://archive.sciendo.com/AEP/aep.2014.40.issue-2/aep-2014-0022/aep-2014-0022.pdf>
- Cao RX, Ma LQ, Chen M, Singh SP, Harris WG (2003) Phosphate-induced metal immobilization in a contaminated site. *Environ Pollut* 122:19–28. [https://doi.org/10.1016/S0269-7491\(02\)00283-X](https://doi.org/10.1016/S0269-7491(02)00283-X)
- Demeková L, Jezný T, Bobul'ská L (2016) Assessment of soil heavy metal pollution in a former mining area—before and after the end of mining activities. *Soil Water Res* 12:1–8, <https://doi.org/10.17221/107/2016-SWR>
- Đokić B (2012) Geo-chemical characteristics of the flotation tailing Grot (South-eastern Serbia) (Geo-hemijske karakteristike flotacijskog jalovišta rudnika Grot (Jugoistočna Srbija)). PhD, University of Belgrade—Faculty of Mining and Geology, Belgrade, pp 1–214 (in Serbian)
- Đokić BV, Jovanović M (2009) Technogenic waste dumps of metal mines in Serbia. Workshop: applied environmental geochemistry-anthropogenic impact on the human environment in the SE Europe. RESTCA, Geological Survey of Slovenia, Ljubljana, pp 36–38
- Dorović M (2005) Water and Eolic erosion (Vodna i eolska erozija). *Acta Biologica Yugoslavica, YSSR* (in Serbian)
- Dožić S, Đukić M, Bogdanović G, Stanojvlović R, Lukić S, Đunišijević-Bojović D, Bjedov I (2010): New approach to the reclamation of the old flotation tailings in Bor. *Bull Fac For* 101:35–47. <http://scindeks.ceon.rs/article.aspx?artid=0353-45371001035D>
- Daldoul G, Souissi R, Tilil H, Elbahri D, El Hamiani O, Chebbi N, Boularbah A, Souissi F (2019) Assessment of heavy metal toxicity in soils contaminated by a former Pb–Zn mine and tailings management using flotation process, Jebel Ghazlane, Northern Tunisia. *Environ Earth Sci* 78:703. <https://doi.org/10.1007/s12665-019-8720-3>
- EDD Master Plan (2008) Study for promoting the Mining Industry of Serbia, final report (summary). Japan International Cooperation Agency, Economic Development Department, Belgrade, pp 1–64
- El Baz S, Baz M, Barakate M, Hassani L, El Gharmali A, Imzilen B (2015) Resistance to and accumulation of heavy metals by actinobacteria isolated from abandoned mining areas. *Sci World J*. <https://doi.org/10.1155/2015/761834>
- Escarre J, Lefèbvre C, Raboyeau S, Dossantos A, Gruber W, Cleyet Marel JC, Frérot H, Noret N, Mahieu S, Collin C, van Oort F (2011) Heavy metal concentration survey in soils and plants of the les malines mining district (Southern France). Implications for Soil Restoration, *Water Air Soil Pollution*, 216:485–504. https://www2.ulb.ac.be/sciences/lagev/fichiers/Escarre_et_al_2011.pdf
- Fazekášová D, Fazekáš J (2020) Soil quality and heavy metal pollution assessment of iron ore mines in Nizna Slana (Slovakia). *Sustainability* 12(6):2549. <https://doi.org/10.3390/su12062549>
- Ferronato N, Torretta V (2019) Waste mismanagement in developing countries: a review of global issues. *Int J Environ Res Public Health* 16(6):1060. <https://doi.org/10.3390/ijerph16061060>
- Gagnon V, Rodrigue-Morin M, Tremblay J, Wasserscheid J, Champagne J, Bellenger JP, Greer CW, Roy S (2020) Life in mine tailings: microbial population structure across the bulk soil, rhizosphere, and roots of boreal species colonizing mine tailings in northwestern Québec. *Ann Microbiol* 70:41. <https://doi.org/10.1186/s13213-020-01582-9>
- García-Orenes F, Morugán-Coronado A, Zornoza R, Scow K (2013) Changes in soil microbial community structure influenced by agricultural management practices in a Mediterranean agro-ecosystem. *PLoS One* 8 (11):e80522. <https://doi.org/10.1371/journal.pone.0080522>
- Govedarica M, Jarak M (1996): Practicum in microbiology (Praktikum iz mikrobiologije), 2nd ed. Faculty of Agriculture, Novi Sad, Serbia (in Serbian)
- Håkanson L (1980) An ecological risk index for aquatic pollution control: a sedimentological approach. *Water Res* 14:975–1001. [https://doi.org/10.1016/0043-1354\(80\)90143-8](https://doi.org/10.1016/0043-1354(80)90143-8)
- Hirwa H, Nshimiyimana FX, Ngendahayo E, Akimpaye B, Nahayo L, Ngamata OM, de Dieu Bazimenyera J (2019) Evaluation of soil contamination in mining areas of Rwanda. *Am J Water Sci Eng* 5(1):9–15. <https://doi.org/10.11648/j.ajwse.20190501.12>
- Huber S, Prokop G, Arrouays D, Banko G, Bispo A, Jones RJA, Kibblewhite MG, Lexer W, Möller A, Rickson RJ, Shishkov T, Stephens M, Toth G, Van den Akker JJH, Varallyay G, Verheijen FGA, Jones AR (eds) (2008) Environmental Assessment of Soil for Monitoring: volume I Indicators & Criteria. EUR 23490 EN/1, Office for the Official Publications of the European Communities, Luxembourg, pp 1–339
- Hudson-Edwards KA, Macklin MG, Jamieson HE, Brewer P, Coulthard TJ, Howard AJ, Turner J (2003) The impact of tailings dam spills and clean-up operations on sediment and water quality in river systems: the Rios Agrio-Guadiamar, Aznalcollar Spain. *Appl Geochem* 18:21–239. [https://doi.org/10.1016/S0883-2927\(02\)00122-1](https://doi.org/10.1016/S0883-2927(02)00122-1)
- ISO 10390 (2005) Soil quality—Determination of pH, International Organization for Standardization, Switzerland
- ISO 10693 (1994) Soil Quality—Determination of carbonate content, Volumetric method, International Organization for Standardization, Switzerland

- ISO 11261(2005) Soil quality—determination of total nitrogen, modified Kjeldahl method, International Organization for Standardization, Switzerland
- ISO 11277 (1998) Soil quality—determination of particle size distribution in mineral soil material, method by sieving and sedimentation, International Organization for Standardization, Switzerland
- ISO 11466 (1995) Soil quality—extraction of trace elements soluble in aqua regia, International Organization for Standardization, Switzerland
- ISO 14235 (2005) (SRPS ISO 14235:2005) Soil quality—Determination of organic carbon by sulfochromic oxidation, Institute for Standardization of Serbia
- IUSS Working Group WRB (2015) World Reference Base for Soil Resources 2014, update 2015 International soil classification system for naming soils and creating legends for soil maps. World Soil Resources Reports No. 106. FAO, Rome
- Kabala C, Galka B, Jezierski P (2020) Assessment and monitoring of soil and plant contamination with trace elements around Europe's largest copper ore tailings impoundment. *Sci Tot Environ* 738:139918. <https://doi.org/10.1016/j.scitotenv.2020.139918>
- Kan X, Dong Y, Feng L, Zhou M, Hou H (2020) Contamination and health risk assessment of heavy metals in China's lead-zinc mine tailings: a meta-analysis. *Chemosphere* 2020:128909. <https://doi.org/10.1016/j.chemosphere.2020.128909>
- Kavamura VN, Esposito E (2010) Biotechnological strategies applied to the decontamination of soils polluted with heavy metals. *Biotechnol Adv* 28(1):61–69. <https://doi.org/10.1016/j.biotechadv.2009.09.002>
- Kossoff D, Dubbin WE, Alfredsson M, Edwards SJ, Macklin MG, Hudson-Edwards KA (2014) Mine tailings dams: Characteristics, failure, environmental impacts, and remediation. *Appl Geochem* 51:229–245. <https://doi.org/10.1016/j.apgeochem.2014.09.010>
- Lenart A, Wolny-Koładka K (2013) The effect of heavy metal concentration and soil pH on the abundance of selected microbial groups within arcelor mittal poland steelworks in Cracow. *Bull Environ Contam Toxicol* 90(1):85–90. <https://doi.org/10.1007/s00128-012-0869-3>
- Li Q, Hu Q, Zhang C, Jin Z (2018) Effects of Pb, Cd, Zn, and Cu on soil enzyme activity and soil properties related to agricultural land-use practices in karst area contaminated by Pb-Zn tailings. *Pol J Environ Stud* 27(6):2623–2632. <https://doi.org/10.15244/pjoes/81213>
- Lombard N, Prestat E, van Elsas JD, Simonet P (2011) Soil-specific limitations for access and analysis of soil microbial communities by metagenomics. *FEMS Microbiol Ecol* 78:31–49. <https://doi.org/10.1111/j.1574-6941.2011.01140.x>
- Loska K, Cebula J, Pelczar J, Wiechuła D, Kwapuliński J (1997) Use of enrichment, and contamination factors together with geoaccumulation indexes to evaluate the content of Cd, Cu, and Ni in the Rybnik water reservoir in Poland. *Water Air Soil Pollut* 93:347–365. <https://doi.org/10.1023/A:1022121615949>
- Luo W, Lu Y, Giesy JP, Wang T, Shi Y, Wang G, Xing Y (2007) Effects of land use on concentrations of metals in surface soils and ecological risk around Guanting Reservoir, China. *Environ Geochem Health* 29:459–471. <https://doi.org/10.1007/s10653-007-9115-z>
- Ma L, Sun J, Yang Z, Wang L (2015) Heavy metal contamination of agricultural soils affected by mining activities around the Guanxi River in Chenhou Southern China. *Environ Monit Assess* 187(12):731–740. <https://doi.org/10.1007/s10661-015-4966-8>
- Macklin MG, Hudson-Edwards KA, Jamieson HE, Brewer P, Coulthard TJ, Howard AJ, Remenda VH (1999) Physical stability and rehabilitation of sustainable aquatic and riparian ecosystems in the Rio Guadiamar, Spain. Following the Aznalcóllar Mine Tailings Dam Failure, IMWA Proceedings 1999, International Mine Water Association 2012, 1999 IMWA Congress, Sevilla, Spain, pp 271–278
- Marković M, Zuliani T, Belanović Simić S, Mataruga Z, Kostić O, Jarić S, Vidmar J, Milačić R, Janez Ščančar J, Mitrović M, Pavlović P (2018) Potentially toxic elements in the riparian soils of the Sava River. *J Soils Sediments* 18:3404–3414. <https://doi.org/10.1007/s11368-018-2071-7>
- Molnárová M, Ružičková J, Lehotská B, Takáčová A, Fargašová A (2018) Determining As, Cd, Cu, Pb, Sb, and Zn in Leaves of Trees Collected near Mining Locations of Malé Karpaty Mts. in the Slovak Republic. *Pol J Environ Stud* 27(5):2179–2191. <https://doi.org/10.15244/pjoes/78889>
- Nišavić A, Zarić M, Gulan M, Dekić LJ (2014) Meteorological conditions in May 2014 and the possibility of forecasting heavy precipitation (Meteorološki uslovi u maju 2014. godine i mogućnost prognoziranja obilnih padavina). Expert Meeting Floods in Serbia in May 2014, RHMZ, Belgrade (in Serbian)
- Official Gazette of the Republic of Serbia (30/2018) Decree on limit values for polluting, harmful and hazardous substances in soil (Uredba o graničnim vrednostima zagađujućih, štetnih i opasnih materija u zemljištu) (in Serbian), <https://www.pravno-informacioni-sistem.rs/SIGlasnikPortal/eli/rep/sgrs/vlada/uredba/2018/30/2/reg>. Accessed on 18 March 2021
- Okereafor G, Makhatha M, Mekuto L, Mavumengwana V (2019) Evaluation of trace elemental levels as pollution indicators in an abandoned gold mine dump in ekuhuleni area, South Africa [Online First]. *IntechOpen*. <https://doi.org/10.5772/intechopen.89582>, <https://www.intechopen.com/online-first/evaluation-of-trace-elemental-levels-as-pollution-indicators-in-an-abandoned-gold-mine-dump-in-ekurh>
- Oprea G, Michnea A, Mihali C, Senilă M, Roman C, Jelea S, Butean C, Barz M (2010) Arsenic and antimony content in soil and plants from Baia Mare

- area Romania. *Am J Environ Sci* 6(1):33–40. <https://doi.org/10.3844/ajessp.2010.33.40>
- Palansooriya KN, Shaheen SM, Chen SS, Tsang D, Hashimoto Y, Hou D, Bolan N, Rinklebe J, Ok Y (2020) Soil amendments for immobilization of potentially toxic elements in contaminated soils: a critical review. *Environ Int* 134:105046. <https://doi.org/10.1016/j.envint.2019.105046>
- Panikov NS (1999) Understanding and prediction of soil microbial community dynamics under global change. *Appl Soil Ecol* 11(2–3):161–176. [https://doi.org/10.1016/S0929-1393\(98\)00143-7](https://doi.org/10.1016/S0929-1393(98)00143-7)
- Pavlović P, Mitrović M (2016) Soil Contamination (Kontaminacija zemljišta). In: Belanović Simić S (Ed) Degradation and protection of soil thematic proceedings (u Zborniku radova “Degradacija i zaštita zemljišta”), University of Belgrade—Faculty of Forestry, pp 107–136 (in Serbian)
- Paya PA, Rodriguez EN (2018) Status of local soil contamination in Europe: revision of the indicator “Progress in the management contaminated sites in Europe”. JRC Publications Office of the European Union, https://publications.jrc.ec.europa.eu/repository/bitstream/JRC107508/jrc107508_2018.1264_src_final_progress_in_the_management_contaminated_sites_in_europe_eur_29124_en_online-final_1.pdf. Accessed on 18 March 2021
- Prasad D, Gangavarapu S, Krishna B (2012) Effect of cadmium on abundance and diversity of free living nitrogen fixing *Azotobacter* spp. *J Environ Sci Technol* 5(3):184–191. <https://scialert.net/abstract/?doi=jest.2012.184.191>
- Project (2012) Excerpt from the Project for Remediation, Closure and Recultivation of Tailing Dump (Slag) from the Smeltery in Zajača (Izvod iz Projekta sanacije, zatvaranja i rekultivacije deponije jalovine (šljake) iz topionice u Zajači). Institute “Kirilo Savić”, Belgrade, pp 1–30 (in Serbian). www.iks.rs
- Rafiei B, Khodaet AS, Khodabakhsh S, Hashemi M, Nejad MB (2010) Contamination assessment of lead, zinc, copper, cadmium, arsenic and antimony in Ahangan mine soils, Malayer, west of Iran. *Soil Sedim Contam* 19:573–586. <https://doi.org/10.1080/15320383.2010.499921>
- Teixeira RA, Fernandes AR, Ferreira JR, Vasconcelos SS, Braz AMS (2018) Contamination and soil biological properties in the Serra Pelada mine—Amazonia Brazil. *Rev Bras Cienc Solo* 42:e0160354. <https://doi.org/10.1590/18069657rbcs20160354>
- Sahu HB, Dash S (2011) Land Degradation due to mining in India and its mitigation measures. In: Proceedings of second international conference on environmental science and technology, February 26–28, Singapore
- Sakan S, Dević G, Relić D, Anđelković I, Sakan N, Đorđević D (2015) Risk assessment of trace element contamination in river sediments in Serbia using pollution indices and statistical methods: a pilot study. *Environ Earth Sci* 73:6625–6638. <https://doi.org/10.1007/s12665-014-3886-1>
- Sarić Z (1989) Laboratory exercises in microbiology (Praktikum iz mikrobiologije). Naučna knjiga, Belgrade, pp 1–199 (in Serbian)
- Sliti N, Abdelkrim C, Ayed L (2019) Assessment of tailings stability and soil contamination of Kef Ettout (NW Tunisia) abandoned mine. *Arab J Geosci* 12:73. <https://doi.org/10.1007/s12517-018-4204-0>
- SPSS (2007) SYSTAT version 16, Statistics. Chicago
- Vandeberg GS, Martin CW, Pierzynski GM (2011) Spatial distribution of trace elements in floodplain alluvium of the upper Blackfoot River Montana. *Environ Earth Sci* 62(7):1521–1534. <https://doi.org/10.1007/s12665-010-0637-9>
- Vidojević D, Jovičić M, Dimi, B, Baćanović N (2015) Environmental degradation due to damage to the mine tailings “Stololice” Kostajnik in 2014 (Degradacija životne sredine usled oštećenja jalovišta rudnika “Stololice” u Kostajniku 2014. godine). Agency for Environmental Protection, Belgrade, ppt., www.sepa.gov.rs (in Serbian)
- Wang X, He M, Xie J, Xi J, Lu X (2010) Heavy metal pollution of the world largest antimony mine-affected agricultural soils in Hunan province (China). *J Soils Sediments* 10:827–837. <https://doi.org/10.1007/s11368-010-0196-4>
- WISE Uranium Project (2020) Chronology of major tailings dam failures (from 1960, last updated 25 Sept. 2020) <http://www.wise-uranium.org/mdaf.html>. Accessed on 18 March 2021
- Wuana RA, Okeimen FE (2011) Heavy metals in contaminated soils. a review of sources, chemistry, risks and best available strategies for remediation. *Int’l Sch Res Network ISRN Ecol* 2011:1–20. <https://doi.org/10.5402/2011/402647>
- YSSR (1966a) Chemical Methods of soil testing (Hemijske metode ispitivanja zemljišta). Book I Bogdanović and Racz (ed) Yugoslav Society for Soil Research, Belgrade, pp 1–270 (in Serbian)
- YSSR (1966b) Microbiological methods of soil and water testing (Mikrobiološke metode ispitivanja zemljišta i voda). Book II Bogdanović and Racz (ed) Yugoslav Society for Soil Research, Belgrade, pp 1–124 (in Serbian)
- YSSR (1997) Study methods for soil physical properties (Metode istraživanja i određivanja fizičkih svojstava zemljišta). In: Bošnjak et al (ed) Yugoslav Society for Soil Research, Novi Sad, pp 1–278 (in Serbian)
- Zhou L, Yang B, Xue N, Li F, Seip HM, Cong X, Yan Y, Liu B, Han B, Li H (2014) Ecological risks and potential sources of heavy metals in agricultural soils from Huanghuai Plain China. *Environ Sci Pollut Res Int.* 21(2):1360–1369. <https://doi.org/10.1007/s11356-013-2023-0>



Dušica Delić, Olivera Stajković-Srbinović,
and Aneta Buntić

Abstract

Coal fly ash, a by-product of coal combustion in thermal power plants, is a fine powder made up of small, spherical, glass-like particles, the major matrix of which is ferro-alumino-silicate minerals. This review presents the detrimental and beneficial physical, chemical and biological properties of fly ash. These are a consequence of its particular chemical composition and can cause an environmental hazard, but also, under some conditions, enable it to be used in some branches of industry. Fly ash generally contains potentially dangerous and harmful heavy metals, organic pollutants and some radionuclides. Toxic concentrations of these in water, soil and air, as a consequence of ash scattering, can cause ecological problems (land degradation in the vicinity of the power plant), health problems (for human and animal respiration) and agricultural problems (harmful influence on soil, soil microorganisms and crops) in the ash dump surroundings and by leaching into watercourses and moving further into the food chain. The millions of

tonnes of fly ash produced annually worldwide (about 800 Mt per year) are a major problem in many countries. Phytoremediation has been used to prevent the detrimental influences of fly ash on the environment. Grasses are suitable for cultivation on fly ash dumps as an initial, quick way to cover the ash dump and prevent ash from scattering. However, the best plant application is a mixture of grasses and legumes, due to the legumes' ability to fix N_2 . When legumes are supplied with N_2 -fixing bacteria (fam. *Rhizobiaceae*), a highly effective bioinoculant, the net effect is the replacement of the mineral N fertiliser that would otherwise be required. The process of phytoremediation needs an enormous N_2 content as fly ash contains little or no N. Symbiotic N_2 fixation is discussed as an environmentally friendly, cost-effective method to supply crops with nitrogen. The root nodulation of the legumes can be used for an eco-toxicological evaluation of soils contaminated with fly ash heavy metals. Amendments for the effective establishment of remediation plants on ash dumps are reported in this review. Among them, the application of microorganisms (plant growth promoting rhizobacteria), alone or with the plants in this process, constitutes a more sustainable and cost-effective approach for removing heavy metals from fly ash dumps. However, nanotechnology could also help to remove heavy metals from fly ash dumps. Due to some desirable fly ash properties, primarily

D. Delić (✉) · O. Stajković-Srbinović · A. Buntić
Department of Microbiology, Institute of Soil
Science, Teodora Drajzera 7, 11000 Belgrade, Serbia
e-mail: dusica.delic@soilinst.rs

A. Buntić
e-mail: aneta.buntic@soilinst.rs

its alkaline pH, and some macro- and microelements, some of which are very rare, as well as the ash's ability to transition into nanoparticles, fly ash has been used in many branches of industry, especially the construction industry and agriculture. However, around 40% of fly ash worldwide is not utilised, so the dumps this produces still require constant monitoring of their surrounding land, water and agricultural crops. Greater use of fly ash would improve the circular economy.

Keywords

Ash dump · Heavy metals · Microorganisms · *Rhizobium* · Bioremediation · Circular economy

26.1 Introduction

Coal fly ash (hereafter termed fly ash) is a by-product of the combustion of bituminous, sub-bituminous or lignite coals which are burnt in coal-fired thermal power plants to generate electricity (Gupta et al. 2004; Jala and Goyal 2006). Coal is still the most widely used source of energy for electricity generation in the world, making up around 40% of the power mix for the past 20 years (World Economic Forum, 2019). Eight hundred million tonnes (800 Mt) of fly ash are produced by global coal combustion alone, primarily in China, India, the USA and countries in the EU (Uliasz-Bocheńczyk and Bąk 2018). Other countries that stand out globally for their coal fly ash production are Australia, Canada, South Africa, Japan, Indonesia, Russia, Italy, Greece, Poland, Germany and Turkey (Jambhulkar et al. 2018; Sebi 2019) (Table 26.1). In China, around 600 Mt of fly ash is estimated to be produced in thermal power plants, with about 200 Mt needing to be stored due to the ash's incomplete exploitation (Ma et al. 2017). In India, about 196.44 Mt of fly ash were produced in 2017/2018 in thermal power plants (Yadav and Fulekar, 2018a; Sharma and Akhai 2019), and the predicted increase is more than 442 Mt year⁻¹ by the end of 2035 (Jambhulkar et al.

2018). In Serbia, more than 70–75% of electricity is generated using lignite combustion (Pivić et al. 2008), producing 6–7 Mt year⁻¹ of fly ash (Terzić et al. 2012; Vukićević et al. 2018). One branch (TENT A) (Fig. 26.1) of the “Nikola Tesla” thermal power plant (TENT), in Obrenovac, Serbia, produced 3.92 Mt of fly ash from lignite coal combustion in 2013 (Kisić et al. 2016). The second branch of TENT is TENT B.

A complete description of fly ash production is that “fly ash is produced by burning coal in pulverised coal combustion boilers where it ignites, generating heat and producing a molten mineral residue that is carried off in the flue gas and usually collected from flue gas by means of collection device such as cyclones and electrostatic precipitators” (Jambhulkar et al. 2018). Approximately 80% of all coal ash produced worldwide is in the form of fly ash (Mahvash et al. 2017). Fly ash collected by electrostatic precipitators constitutes 70% of all coal combustion by-products (Gupta et al. 2004; Jala and Goyal 2006; Haynes 2009). The adjective “fly” resulted from the ash being transported from the combustion chamber by the exhaust gases (Yadav and Fulekar 2018a).

A residue of coal combustion, fly ash is classified as solid waste that is collected in ash dumps (landfill) if it is not utilised in agriculture and industry. The use of fly ash is continuously rising in middle income developing countries (India-lower middle income country, China-upper middle income country) (Country classifications 2020; The World Bank 2020), and remains at a high level in developed countries (Denmark, Germany) (Kishor et al. 2010; Uliasz-Bocheńczyk and Bąk 2018; Yousuf et al. 2020). In China, 14% to 20% of fly ash was used from 1980–1999, but from 1999 to 2015, the amount used increased by five times (to about 67% according to Yao et al. 2015). Recent data shows that India increased fly ash utilisation by about 6.3 times from 1998 (10% of ash was utilised) to 2017 (63%) (Yadav and Fulekar 2018a). In 2018, utilisation was 67% (Sharma and Akhai 2019) (Table 26.2). While only about 50% of fly ash is utilised in the USA, in the EU, the use of fly ash currently runs at more than 90%. In Germany,

Table 26.1 Fly ash production and utilisation in the world

Continent	Country/Region	Production (Mt year ⁻¹)	Utilisation (%)	References
Asia	China	600	70	Ma et al. 2017
	India	196	67	Sharma and Akhai 2019
	Korea	10.3	85.4	“2016 World-Wide CCP Network (WWCCPN): member information 2018/2019” (Harris et al. 2019)
	Japan	12.3	99.3	
	Other Asia	12.3	67.6	
America	USA	107.4	56	
Canada	4.8	54.2		
Australia	Australia	12.3	43.5	
Europe	European Union	140	94.3	
Africa and Middle East		32.2		
Russia		21.3	27.2	
Serbia		6–7	Low	Terzić et al. 2012; Vukićević 2018; Kisić et al. 2016

**Fig. 26.1** “Nikola Tesla A” thermal power plant (TENT A), Obrenovac, Serbia (photo by L. Maričić)

Table 26.2 Fly ash production and utilisation in India from 1998–99 to 2017–18 (CEA, 2018; Yadav and Fulekar 2018a; Sharma and Akhai 2019)*

	2009	2010–11	2011–12	2012–13	2013–14	2014–15	2015–16	2016–17	2017–18
	Mt								
Fly ash production	112.00	131.09	145.42	163.56	172.87	184.14	176.84	169.25	196.44
Fly ash utilisation	/	73.13	85.05	100.37	99.62	102.54	107.77	107.10	131.87
% used	38.00	55.79	58.48	61.37	57.37	55.69	60.97	63.28	67.13

*CEA reports 2018

Italy and Denmark, 100% of fly ash is recovered. The lowest utilisation of fly ash occurs in Russia (10%), which does not correlate with its huge fly ash production (Uliasz-Bocheńczyk and Bąk 2018).

26.2 Physico-Chemical and Biological Properties of Fly Ash

Fly ash mainly consists of amorphous glass and a few crystalline phases, i.e. mineral constituents of the coal which are not fully burnt. These minerals consist of quartz (SiO_2), *aluminosilicate* glasses, mullite ($3\text{Al}_2\text{O}_3 \cdot 2\text{SiO}_2$), hematite (Fe_2O_3), magnetite (Fe_3O_4), calcite (CaCO_3), borax ($\text{Na}_2\text{B}_4\text{O}_7 \cdot 10\text{H}_2\text{O}$ or $\text{Na}_2[\text{B}_4\text{O}_5(\text{OH})_4] \cdot 8\text{H}_2\text{O}$) and gypsum ($\text{CaSO}_4 \cdot 2\text{H}_2\text{O}$) (Basu et al. 2009; Pandey and Singh, 2010). Small, spherical, fine glass-like particles of fly ash, which are heterogeneous in nature, have a mixture of ferro-alumino-silicate minerals as their major matrix (Jala and Goyal 2006).

The chemical composition of fly ash has been analysed by various techniques: X-ray diffraction (XRD), Fourier transform infrared (FTIR), magic angle spinning nuclear magnetic resonance (MAS-NMR) and X-ray photoelectron spectroscopy (XPS). The structure of aluminosilicates of pure fly ash is characterised well using these instrumentation techniques, which can also be used in geopolymer or element extraction (Liu et al. 2019). Other techniques used to determine

the chemical and physical properties of fly ash include CHN elemental analyses, X-ray fluorescence (XRF), scanning electron microscopy and inductively coupled plasma atomic emission spectroscopy (Al-Mayman 2017).

The chemical composition and mineralogy of fly ash vary according to the different feed coal traits and the source of the coal, as well as the type, design and operation of the combustion boiler used (Yadav and Fulekar 2018a; Liu et al. 2019). Data on the chemical composition of fly ash oxides originating in China, Serbia and India are presented in Table 26.3. Two types of ash originate from the Chinese Gujiao Power Plant and Xishan Thermal Power Plant (in a major region for coal-fired power generation in China). The first ash type (FA-1) was from a pulverised coal boiler, while the second one (FA-2) was from a circulating fluidised-bed boiler. FA-1 and FA-2 have very different contents of silicon dioxide (SiO_2) (70.30% and 42.19%, respectively) and aluminium oxide (Al_2O_3 , 17.04% and 25.41%, respectively) (Liu et al. 2019). In comparison, in Serbia, fly ash produced from electrostatic precipitation (siliceous fly ash from lignite coal combustion) at TENT and other power plants had higher percentages of CaO and MgO (Kisić et al. 2012; Kostić et al. 2012; Liu et al. 2019), comparable with the oxide composition of fly ash from India (Kishor et al. 2010) (Table 26.3).

Concerning the biological properties of fly ash, pure ash—i.e. fresh ash placed as active surface dump (Fig. 26.2) in the form of a specific

Table 26.3 Chemical composition of fly ash from China FA-1 and FA-2 (Liu et al. 2019), in Serbian lignite fly ash (Kostić et al. 2012) and Indian fly ash (Kishor et al. 2010)

Chemical Composition of FA* (%)	SiO ₂	Al ₂ O ₃	Na ₂ O	K ₂ O	CaO	MgO	P ₂ O ₅	TiO ₂	MnO	Fe ₂ O ₃	SO ₃
Chinese FA											
FA-1 Chinese	70.30	17.04	0.17	0.93	1.79	0.32	0.19	1.39	0.03	3.23	
FA-2 Chinese	42.19	25.41	0.25	1.08	1.84	0.49	0.14	1.06	0.03	6.50	
FA from Serbian lignite coal	64.44	18.20	0.30	0.72	5.18	2.98	0.09	0.72		5.52	1.70
Indian FA	52.5	22.8	1.0	1.3	4.9	1.3				7.5	
Class F	36.9	17.6	1.7	0.6	25.2	5.1				6.2	
Class C											

*FA – Fly ash; average values for major-element oxides for Chinese FA, Indian FA and Serbian FA

commixture of ash and water—does not contain microorganisms (it is sterile), while ash biore-mediated in a passive ash dump has a very small number of microorganisms (Bogdanović 1990; Juwarkar and Jambhulkar 2008; Rasulić et al. 2007; Haynes 2009) (Fig. 26.3).

26.2.1 Physical Properties of Fly Ash

The size of fly ash particles usually varies from 0.01 to 100 µm (Pandey and Singh 2010) but, according to some authors, can range up to 150 µm (Yadav and Fulekar 2018a). The ash consists of silt (8–85%), sand (7–90%), clay (0–10%) and gravel-sized (0–10%) particles (Basu et al. 2009; Yadav and Fulekar 2018a). The ash has a low bulk density, high surface area and light texture, with a consistency similar to talcum powder. This particle size is responsible for the ash's poor hydrophysical characteristics: weak water retention and rapid water filtration. The colour of fly ash depends on the parent coal and carbon content and can vary from tan to grey or black (Pandey and Singh 2010; Yadav and Fulekar 2018a).

26.2.2 Chemical Properties of Fly Ash

Chemically, fly ash is made up of oxides, primarily Si, Al and Fe along with Ca, Mg, Na and K (these two groups comprise 90 and 99% of the

oxides in fly ash, respectively), followed by a low content of biogenic elements (N and P) and some microelements. In fact, fly ash is deficient in N and P, as N is volatilised in the form of oxides during coal combustion and P is lost due to its high solubility and the production of insoluble P compounds by reactions between soluble P and excessive Fe and Al in the coal (Gupta et al. 2004; Pandey and Singh 2010). In general, fly ash is free of N (Gupta et al. 2004; Jala and Goyal 2006; Basu et al. 2009; Pandey and Singh 2010; Kostić et al. 2012). The low total nitrogen content in fly ash (average 0.043%) from TENT, Obrenovac, Serbia, is notable (Pivić et al. 2007c). The C/N ratio in ash is very high, which means there is greater immobilisation of N than mobilisation, while the organic matter is inert despite being present in significant amounts, since it is largely derived from partly-combusted coal (Pivić et al. 2007c). Some results show that certain microelements generally enrich fly ash particles: As, B, Co, Mo, S, Se (Adriano et al. 2001). Macro- and microelements present in coal generally become concentrated in fly ash.

Overall, it can be concluded that fly ash consists of macroelements (essential macronutrients such as Ca, Mg, Na, K and S) (Antonkiewicz et al. 2020; Tauanov et al. 2020) and microelements including heavy metals (in alphabetical order): As, B, Ba, Br, Cd, Cl, Co, Cu, Cr, Fe, Ga, Hg, I, In, Mo, Ni, Pb, Po, Rb, Sb, Sc, Se, Sr, Ti, W, V and Zn (Miricioiu and Niculescu 2020; Tauanov et al. 2020). Biogenic

Fig. 26.2 Active surface fly ash dump at the “Nikola Tesla A” thermal power plant (TENT A), Obrenovac, Serbia (Photo by L. Maričić)



or essential heavy metals for living organisms are Fe, Mn, Co, Mo, Se, Zn, Cu and B, while abiogenic or non-essential heavy metals are Ni, Cd, Cr, Co, Pb, As, Hg, V and Ba (Gupta et al. 2002; Basu et al. 2009; Tiwari et al. 2008; Yadav and Fulekar 2018a). Whether Ni should be declared a biogenic or abiogenic microelement remains a moot point (Dinić et al. 2019). Although some authors (Kabata-Pendias and Szeke 2015) believe that there is no evidence that Ni plays an essential role in plant metabolism, recent studies have indicated that Ni is an

essential microelement for plants (Wenzel et al. 2018). Moreover, research showed long ago that Ni is a microelement required for the hydrogen-dependent growth of *Rhizobium japonicum* and for the expression of urease activity in soybean leaves (Klucas et al. 1983). The concentrations of microelements in fly ash are extremely variable depending upon the composition of the parent coal, combustion conditions and production methods (Yadav and Fulekar 2018a). Fly ash also contains radionuclides (e.g. Ra, Th, U, 40 K), although these have negligible or low



Fig. 26.3 Passive fly ash dump at the “Nikola Tesla A” thermal power plant (TENT A), Obrenovac, Serbia (Photo by L. Maričić)

impacts on the surrounding environment. The results of ten-year fly ash radioactivity measurements at TENT-B in Serbia indicate that the 266 Ra, 232 Th and 40 K content is below the allowable concentration, meaning that fly ash from TENT-B is safe (Kisić et al. 2012, 2013). Fly ash also contains hazardous organic pollutants (methyl sulphates, polychlorinated biphenyls, chlorinated benzofurans, dioxins and polycyclic aromatic hydrocarbons) (Malhotra et al. 2017; Jambhulkar et al. 2018).

The pH of fly ash is an important characteristic. Fly ash pH ranges from acid to alkaline, i.e. pH 4.5 to pH 12. Depending on their pH value and calcium/sulphur ratio, fly ashes are classified as acidic (pH 1.2 up to 7), mildly alkaline (pH 8–9), or strongly alkaline (pH 11–13) (Gupta et al. 2002; Bhatt et al. 2019). The pH mostly depends on the sulphur content of the parent coal, and thus on the type of coal (Adriano et al. 1980; Chaudhary et al. 2011). This means that the content of sulphurous compounds in fly ash

applied to soil influences the soil pH (Basu et al. 2009). Taking this into account, together with the lime (CaO) content, there are two main types of fly ash classified according to the content of Ca, Si, Al and Fe: a low lime type (Class F—less alkaline with lower sulphate content) and a high lime type (Class C—more alkaline with higher sulphate content) (Kishor et al. 2010; Yadav and Fulekar 2018a) (Table 26.4). Fly ash from Serbian power plants is in class F, with pozzolanic properties, and consists of siliceous ash with a low concentration of calcium compounds (less than 10% CaO) (Vukićević et al. 2018). Fly ash with a Ca/S ratio of less than about 2.5 generates acidic extracts, whereas fly ash with a Ca/S ratio higher than 2.5 produces alkaline extracts (Pandey and Singh, 2010). According to the American Society for Testing and Materials, ash with > 70% of $\text{SiO}_2 + \text{Al}_2\text{O}_3 + \text{Fe}_2\text{O}_2$ can be classified as Class F (derived from anthracite or bituminous coal combustion), while ash with 50–70% of $\text{SiO}_2 + \text{Al}_2\text{O}_3 + \text{Fe}_2\text{O}_2$ can be classified

as Class C (derived from sub-bituminous lignite coal combustion) (Franus et al. 2015). There is no unique international classification of fly ash (Bhatt et al. 2019).

In conclusion, fly ash's physico-chemical and mineralogical properties vary widely depending on the nature of the parent coal, combustion conditions, type of emission control devices, storage and handling methods (Jala and Goyal 2006; Pandey and Singh 2010).

26.2.3 Heavy Metals in Fly Ash

In comparison with a typically healthy soil, fly ash can contain higher contents of various heavy metals (atomic density above $3.5\text{--}5\text{ g cm}^{-3}$) and metalloids (microelements at the boundary between metal and non-metal), which can have toxic effects when they are in their soluble forms,

especially on microorganisms and microbiological processes in the soil (Giller et al. 1989, 1998; Onjia et al. 2004; Haynes, 2009; Stan et al. 2011; Dinić et al. 2019).

Fly ash usually contains the metalloids Si, As, B and Sb. Oxides of Fe and Al and phosphates in fly ash are insoluble aluminosilicate structures which attract and bind toxic microelements (Sb, As, Be, Cd, Pb, Hg, Se and V), limiting their biological toxicity (Basu et al. 2009). The element Al in fly ash is predominantly bound in insoluble aluminosilicate forms, which limits its biological toxicity. However, the content of heavy metals such as Pb, Ni, Cd, Cr, Cu and Zn, etc. can be high in fly ash (Kishor et al. 2010). In the fly ash produced by TENT, the content of Ni can be slightly above the threshold content and is equal to the natural geochemical Ni content in Serbian soils formed from serpentine and alkaline magmatic rock. Moreover, the content of

Table 26.4 Properties of Class F and Class C fly ash (2018a adapted from Kishor et al. 2010; Yadav and Fulekar; *Bhatt et al. 2019)

Properties	Class F	Class C
Produced from burning	harder, older anthracite and bituminous coal	younger lignite and sub-bituminous coal
Al ₂ O ₃ content	22.8%, higher	17.6%, less
Fe ₂ O ₃ content	7.5%, higher	6.2%, less
MgO content	1.3%, higher	5.1%, less
Na ₂ O	1%, less	1.7, higher
K ₂ O	1.3%, higher	0.6%, less
Lime content (CaO)	<(5%*) 20%	>(15%*) 20%
Calcium content (calcium hydroxide, calcium sulphate and glassy components)	1–12%	30–40%
Alkali and sulphate content	Low amount	High amount
	Requires cementing agent such as PC, quicklime, hydrated lime	Self-cementing properties
Air entrainer needed	Needed	Not required
Sulphate exposure conditions	Used in high sulfate exposure conditions	Cannot be used in high sulfate exposure conditions
Fly ash content concrete mixes	Used in high fly ash content	Limited to low fly ash content
	Used for structural concretes, HP concretes, high sulphate exposure concretes	Primarily residential construction

metalloid B can be high, and due to its great solubility, B can then pollute groundwater and, through the food chain, affect living organisms (Pivić et al. 2007d).

Decreasing the solubility of heavy metals reduces or even prevents the detrimental effects of heavy metals on plants. Heavy metals are not very soluble at neutral to mid-alkaline pHs or in the presence of carbonate. In addition, phosphorus fertilisers reduce the solubility of heavy metals due to the creation of poorly soluble phosphates. Fly ash from TENT, Obrenovac, Serbia, has a neutral to alkaline pH, values which allow the process of heavy metal immobilisation in the ash (Pivić et al. 2007c; Maksimović et al. 2008).

One method for treating fly ash uses thermal plasma in a plasma reactor. In a pyrolysis/combustion plasma system to produce fly ash, the fraction of carbon is reduced. In the next step, the product obtained by the combustion of fly ash is vitrified in a plasma furnace. Therefore, the fly ash is detoxified by plasma vitrification, producing amorphous and glassy slag that can be placed in an ash dump. Heavy metals are confined in the silicon matrix, generating a very low risk of leaching (Al-Mayman et al. 2017).

26.3 Detrimental Influence of Fly Ash Dumping on the Environment

Ash dumps, sources of fine airborne particles of ash, are surface sources of air, water and soil pollution. This causes ecological problems (land degradation in the vicinity of the power plant), health problems (for human and animal respiration) and agricultural problems (harmful influence on soil and crops). The detrimental effect of an ash dump on the nearby environment (terrestrial and aquatic ecosystems) happens under the influence of wind erosion of fly ash and due to water filtration through the slurry form of the ash, i.e. through the commixture of ash and water. Airborne particles (<100 µm size) of ash uplifted from the material deposited in the ash

dump can be suspended in the air for long periods and are often invisible (Maiti and Prasad 2016). One of the extremely hazardous ingredients of fly ash is crystalline silica, which can cause pulmonary damage and silicosis—lung fibrosis caused by the inhalation of dust containing silica (Aranyl and Bradof 1981; IARC, 1987).

Due to its fine texture, fly ash is capable of covering the terrain, and its constituent toxic metals and metalloids can have negative effects on the nearby environment (Basu et al. 2009; Parab et al. 2015; Maiti and Prasad 2016). The effects of fly ash on soil microorganisms depend on the amount of fly ash in the soil (Kishor et al. 2010), but not always on how long microorganisms are exposed to fly ash (Ullah et al. 2015).

The number and activity of microorganisms are important biological properties of soil because microorganisms provide and sustain the fertility of the soil. Microbial activity in the soil can be limited by the poor characteristics of fly ash: excess concentrations of microelements and soluble salts, salinity, extreme pHs, a lack of substrate C and poor N supply. Microorganisms have diverse responses to different concentrations of heavy metals (Pandey and Singh, 2010; Nayak et al. 2015). For example, extremely alkaline fly ash can have negative effects on the biological traits of soil (Kishor et al. 2010). In this sense, the incorporation of fly ash into different soil types influences the soil's physical and chemical characteristics, which then has a stressful effect on plants and the microbiota, including rhizobial bacteria (Karla et al. 2000; Rebah et al. 2002; Delić et al. 2010). Under some circumstances, fly ash deposited on soil can reduce microbial numbers, soil respiration or soil enzyme activity, or can negatively influence the soil N-cycling processes of nitrification and N mineralisation (Kishor et al. 2010; Pandey and Singh 2010; Parab et al. 2015). There are significant negative correlations between the content of alkali/alkaline earth metals, heavy metals and macronutrients with soil enzymatic activity and/or microbial biomass (Woch et al. 2018). Early indicators of soil degradation include changes in the numbers of some groups of

microorganisms and their metabolic activities; these can be detected even before changes appear in the soil's physico-chemical parameters (Pankhurst et al. 1995).

The processes of preparing a commixture of ash and water to deposit fly ash in the ash dump (active dump) and of bioremediation (passive dump) are carried out to protect the environment against the scattering of fly ash. On the other hand, water filtered through these dumps can pollute groundwater and watercourses (Maiti and Prasad 2016).

We can conclude that, overall, it is of great importance to improve our control of soil, water and air pollution by suppressing the movement of heavy metals into the groundwater and thereafter into the food chain (Maiti and Prasad 2016). One important measure for reducing the pollution caused by fly ash is the process of phytoremediation with specific tolerant/resistant microorganisms. This kind of phytomanagement is the most cost-effective and eco-friendly approach to reduce the detrimental influence of fly ash dumps on the environment.

26.3.1 Direction and Distance of Fly Ash Scattering

The effect of ash scattering from an ash dump towards the surroundings depends on the direction and power of the wind and can occur even in the presence of very weak airflow (Simić et al. 2015). Cicek and Koparal (2004) concluded that very high quantities of sulphur and heavy metals from fly ash effectively occurred within a 10 km radius of a thermal power plant, particularly in the prevailing wind direction, but they gradually reduced in density and effect (measured in the soil and tree leaves) beyond that distance. The prevailing wind direction is also an important factor affecting whether surrounding soils are affected by fly ash dump at TENT B, Obrenovac, Serbia (prevailing winds are westerlies and north-westerlies) (Cokić et al. 2002).

The effect of distance from an ash dump on the presence of the symbiotic N₂-fixing bacterium, *Sinorhizobium (Ensifer) meliloti* in soil

was shown when the soil samples were taken from the immediate vicinity of TENT B (100 m–4900 m) (Delić et al. 2010) (Fig. 26.4). At that site, the impact zone of the fly ash dump extends up to 5 km from the ash dump (Kisić et al. 2016). *S. meliloti* was not detected at all in any soil up to 670 m from the ash dump, but *S. meliloti* (at levels ranging from 8 g⁻¹ soil to 2.8 × 10⁴ g⁻¹ soil) was present only in alfalfa field soils starting from distances of 670 m to 2450 m from the ash dump (Table 26.5). This strongly indicates the harmful influence of fly ash on *S. meliloti*, but also the protective role of the alfalfa host plant rhizosphere (Vojinović et al. 1989; Delić-Vukmir et al. 1994) in combating the influence of fly ash (Table 26.5). The numbers of *S. meliloti* detected in all soil samples at greater distances from the fly ash dump (2600–4900 m) (40 to 9 × 10⁴ g⁻¹ soil) and taken from the fields with different crops indicate that fly ash does not have a harmful influence on this bacterium over the whole impact zone of TENT B (Delić et al. 2010).

26.3.2 Effects of Heavy Metals From Fly Ash Dumps on Surrounding Soils

One of the most common factors that have a detrimental influence on the physico-chemical traits and biogenicity of soils is an excessive content of microelements; especially heavy metals, which are constituents of fly ash. In healthy soil, microelements are usually present only in small amounts. However, microelements include heavy metals, many of which are potentially toxic elements with the prescribed maximum allowed concentrations (MACs) in soil (SG RS 23/1994 1994) (Table 26.6) or maximum permissible concentrations of mobile metal forms (MPC_{mob}), since they can be detrimental for living organisms above this amount. High levels of potentially toxic microelements can be of natural origin, e.g. from geological sources, but in recent decades, their increased level in the soil, air and water cycle has been of anthropogenic origin (industry, road transport and intensive



Fig. 26.4 Impact zone of the fly ash dump at the “Nikola Tesla B” thermal power plant (TENT B), Obrenovac, Serbia (Photo by L. Maričić)

agriculture). Investigations into the heavy metals present in the impact zone (coal basin) of the “Kostolac” thermal power plant, Serbia, have shown that increased concentrations in the soil of three heavy metals (As, Pb and Cu) were of anthropogenic origin (fly ash), while other heavy metals (Ni, Co, Cd, Cr and Zn) were of geological origin (Cokić et al. 2002; Saljnikov et al. 2019).

The availability of data on the heavy metal content in soils varies widely between countries. In addition, the classification of heavy metals according to their hazard degree in soils differs between countries due to differing standards and norms as well as the ecological and toxicological data available in each country (Vodyanitskii 2016).

Heavy metal activity mostly occurs in those layers of the substrate/soil that are rich in organic matter and microbial biomass and have a high cation exchange capacity. However, the metal activity depends on the physico-chemical

properties of the substrate spatially, pH, levels of inorganic and organic anions and environmental factors.

In low concentrations, some heavy metals (Cu, Zn, Mn, Fe, Mo and metalloid B) are necessary for the growth and development of living organisms (plants, microorganisms and animals) and are considered to be biogenic (Ahemad 2019), whereas high concentrations can be toxic to those organisms (Klucas et al. 1983; Jakšić et al. 2013; Simić et al. 2015; Mailti and Prasad 2016). However, abiogenic heavy metals such as Ni, Cd, Cr, Pb, As, Hg, V and Ba are particularly toxic for the living world. According to Russian researchers, Pb, Cd, Hg, Zn, Mo, Ni, Co, Sn, Cu and V are the most typical heavy metals contaminating the soil (Orlov et al. 2005; Vodyanitskii 2016).

Some heavy metals in fly ash mostly pollute the environment in the form of gases, smoke, and soot particulates (Cr, Ni, Mn, Hg, As and Cd), while others (such as metalloid B, Fe, Mn and

Table 26.5 Number and activity of *Sinorhizobium (Ensifer) meliloti* isolates from 19 locations at different distances from the fly ash dump (Delić et al. 2010)

Distance (m)	Land use system	pH (H ₂ O)	Number (MPN)	Isolation and activity
100	Maize field	6.70	0	/
300	Corn field	4.29	0	/
400	Maize field	5.55	0	/
670	Maize field	4.52	0	/
1000	Alfalfa field	4.55	5×10^4	+ , + , -
1200	Wheat field	6.90	0	/
1250	Alfalfa field	4.65	2×10^4	+ + , +
1450	Maize field	4.00	8	/
1700	Meadow	3.95	0	/
1700	Alfalfa field	4.55	2.8×10^4	+ + + , + , +
2100	Red clover field	4.70	0	/
2100	Alfalfa field	4.40	3×10^3	+ , - , +
2100	Soybean field	4.00	0	/
2450	Meadow	4.95	0	/
2600	Corn field	7.15	1.8×10^5	+ , + +
2650	Alfalfa field	5.98	50	+ + + , + + , -
4350	Wheat field	7.00	9×10^4	+ + + , + , + , -
4500	Corn field	6.90	40	-
4900	Corn field	7.06	1.5×10^2	+ +

Table 26.6 Serbian regulatory limits for microelements in soils and irrigation waters (SG RS 23/1994 1994)

Microelements	MAC* in soil mg kg ⁻¹	MAC in water mg l ⁻¹
Cadmium	up to 3	up to 0.01
Lead	up to 100	up to 0.1
Mercury	up to 2	up to 0.001
Arsenic	up to 25	up to 0.05
Chromium	up to 100	up to 0.5
Nickel	up to 50	up to 0.1
Fluorine	up to 300	up to 1.5
Copper	up to 100	up to 0.1
Zinc	up to 300	up to 1.0
Boron	up to 50	up to 1.0

*MAC—maximum allowed concentration

As) are more soluble and are transported by groundwater or other hydrological means. B is a metalloid and microelement necessary for plant growth, but in some concentrations, it can be phytotoxic. In fly ash from TENT B, the content of B is around the threshold value that can be toxic for the soil ecosystem and plants, because in alkaline reactions, B is solubilised in groundwater (borate and tetraborate react with K and Na) (Adriano et al. 1980; Filipović et al. 1997; Mrvić et al. 2004; Pivić et al. 2008; Kostić et al. 2012; Alloway 2013).

While low concentrations of heavy metals can promote the activity of some microorganisms, elevated heavy metal levels in soils can have detrimental or even hazardous effects on living organisms and ecosystems (Ghani 2010; Wuana and Okieimen 2011; Shi and Ma 2017). High microelement concentrations also have negative effects on the most important biological processes such as photosynthesis and respiration in plants, and on symbiotic N₂ fixation (Hix 1994; Zahran 1999; Pavlović et al. 2007; Mitrović et al. 2012; Kostić et al. 2012).

In soil, however, the expression of a heavy metal's negative effect depends on the soil type, the level of heavy metal, the presence of other heavy metals in the soil, the toxicity threshold of the heavy metal for animals, plants and microorganisms and animal, and plant and microbial sensitivity (classified as sensitive, tolerant or resistant) to the heavy metal. In terms of fly ash, heavy metal expression also depends on the ash-weathering processes. All of these factors indicate the complexity of heavy metals' on the ecosystems (Khalil et al. 1996; Wyszowska et al. 2007; Ghani 2010; Kostić et al. 2012; Simić et al. 2015; Stajković-Srbinović et al. 2017, 2018). In one study, there were no significant differences detected in microbiological characteristics between soils without increased heavy metal concentrations and soils with slightly elevated levels of heavy metals (Stajković-Srbinović et al. 2018). Significant negative correlations were detected only between some groups of microorganisms and available Ni and Cr in serpentine soils (Stajković-Srbinović et al. 2017). In both studies (Stajković-Srbinović et al.

2017, 2018), stepwise multiple regression analyses indicate that the chemical properties of the soil (pH, P, etc.) are what most affect the number of microorganisms.

26.3.3 Influence of Fly Ash on Rhizobial Bacteria and the Process of Symbiotic N₂-fixation

Symbiotic N₂ fixation between rhizobial bacteria (fam. *Rhizobiaceae*) and legumes (fam. *Fabaceae*) is one of the most important natural processes for supplying soils and plants with nitrogen from the air (N₂). The process of symbiotic N₂ fixation is particularly useful in poor and degraded soils (de la Peña and Pueyo 2012).

Soil contamination with heavy metals over longer periods can have a negative influence on root nodulation, and can also influence the absence of N₂ fixation such that only ineffective variants of the normal rhizobial species survive (Giller et al. 1989; Manier et al. 2009; Stan et al. 2011). At TENT B, in surrounding soils in the fly ash impact zone (up to 4 900 m distant), 78% of *S. meliloti* isolates are able to fix nitrogen from the air (N₂) but only a small percentage of isolates (30%) are highly efficient nitrogen fixers. This nitrogen-fixing efficiency of *S. meliloti* isolates based on the shoot dry weight and total N content of alfalfa (host plant) was tested in laboratory conditions (Table 26.7) (Delić et al. 2010). However, Broos et al. (2004) concluded that the metal toxicity (Zn, Cd and Cu) which is detrimental for symbiotic N₂ fixation cannot be generalised. For example, the effectiveness of symbiotic N₂ fixation in the host plant white clover (*Trifolium repens* L.) was influenced by the number of microsymbiont rhizobial bacteria seeded into the metal-contaminated soils (Broos et al. 2004).

Research has shown that heavy metals have a negative effect on the survival of effective rhizobial bacteria and on the degree of nodulation (even causing the absence of nodulation) in legumes (clover and chickpea) in contaminated soils (Zahran 1999; Stan et al. 2011; Kostić et al.

Table 26.7 Nitrogen-fixing efficiency of *Sinorhizobium (Ensifer) meliloti* isolates originating from soils in the impact zone of a fly ash dump (Delić et al. 2010)

Soil type/land use system	Shoot dry weight (mg plant ⁻¹)	Total N content (mg plant ⁻¹)	Activity
Pseudo-gley/alfalfa field	43.80 ^a	1.708	+ + +
Humo-gley/wheat field	42.50 ^{ab}	1.700	+ + +
Pseudo-gley/alfalfa field	39.77 ^c	1.471	+ + +
Pseudo-gley/alfalfa field	36.07 ^c	1.371	+ +
Pseudo-gley/alfalfa field	35.83 ^c	1.254	+ +
Fluvisol/corn field	33.73 ^c	1.417	+ +
Fluvisol/corn field	32.27 ^c	1.033	+ +

^a, ^{ab}, ^c Means in a column followed by the same subscript letters are not significantly different according to Duncan multiple range test ($P \leq 0.05$)

2012). These results confirmed the conclusion by Wetzel and Werner (1995) that nodulation can be used for ecotoxicological evaluation of contaminated soils, because some heavy metals (and some other detrimental substances) can reduce nodulation before the host plant is visibly damaged. Research on N₂ fixation by *Acacia auriculiformis* showed that heavy metals have a more detrimental influence on nodulation than on the effectiveness of symbiotic N₂ fixation, but the most detrimental effect is on the growth of rhizobial bacteria (Zhang et al. 1998). The inhibitory effects of toxic levels of heavy metals on nodule number correlate with decreases in rhizobial bacteria in soil (Stan et al. 2011). However, the number of rhizobial bacteria in soil depends on the concentration and type of heavy metal and the bacterial species.

One study showed that *Bradyrhizobium* was more resistant to heavy metals than other rhizobial bacteria (Tong and Sadowsky, 1994; Ahammad, 2019). However, other research showed that rhizobial species such as *S. meliloti*, *Rhizobium fredii*, *Rhizobium leguminosarum* (Kinkle et al. 1994) and *Agrobacter tumefaciens* (Alexander et al. 1999) were more resistant than *Bradyrhizobium*.

Miličić et al. (2006) revealed that particular isolates of seven rhizobial species (*Bradyrhizobium japonicum*, *S. meliloti*, *Rhizobium trifoli*, *R. leguminosarum* vs. *phaseoli*, *R. leguminosarum* vs. *viciae* *Rhizobium loti*, *Rhizobium galega*) had different levels of intrinsic tolerance to the applied concentrations of heavy metals. All the

bacteria examined showed the lowest intrinsic tolerance to Ni and Cu, while most bacteria had the highest intrinsic tolerance to Pb, Zn and Hg. Cd and Cr concentrations of 50–75 µg ml⁻¹ had inhibitory effects on the growth of most rhizobial bacteria examined. Differences in growth with different concentrations of heavy metals were found not only among different rhizobial species, but also among isolates of one species, which shows that the intrinsic tolerance of rhizobial strains depends on each rhizobial bacterium's genetic structure.

26.3.3.1 Genetic Acquisition of Rhizobial Resistance

Microbial resistance to the effects of heavy metal stressors has a genetic basis. The development of microbial resistance in response to chronic high/toxic heavy metal concentrations can occur in natural habitats (Stajković-Srbinović et al. 2018). Chronic high heavy metal concentrations exert selection pressure on rhizobial bacteria, leading the bacteria to adapt to these pollutants via the expression of certain genes, often plasmid-borne, which can influence bacterial behaviour and survival. This explains why the acquisition of new genetic traits by rhizobial bacteria, enabling them to adapt to heavy metal pollutants, results in a simultaneous decrease in the expression of nodulation genes. Many soil microorganisms, particularly gram-negative bacteria, can acquire plasmids to develop resistance to high levels of heavy metals (Silver 1992; Silver and Misra 1988). Stan et al. (2011)

suggested the price for the survival of *Rhizobium* in a heavy metal-polluted area is the alteration of some genes, including those involved in symbiosis and, probably, in N_2 fixation.

The acquisition of genes resistant to high levels of heavy metals can cause decreased genetic diversity within one species. Zahran (1999) reported high similarity among plasmid profiles of rhizobial isolates in soils containing heavy metals—indicating that there was a lack of genetic diversity in the population surviving at high concentrations of heavy metals—and those isolates, specifically for clover, were ineffective N_2 fixers (concentrations of heavy metals were close to MACs according to current guidelines).

26.4 Bioremediation of Fly Ash Dumps

26.4.1 The Main Goal

Fly ash can be very toxic to the surroundings due to its constituent heavy metal content. The fact that most electricity is generated in coal-fired power plants raises the question of how to best preserve the environment against fly ash pollution provoked by wind erosion (Gupta et al. 2004; Pivić et al. 2007b; Al-Mayman et al. 2017). Moreover, ash disposal in slurry form requires extra consumption of water resources, provoking water erosion and pollution of groundwater. It is important to implement continuous monitoring of surrounding land and analyse the soil and groundwater, not only to understand the total heavy metal content, but also to track accessible forms of heavy metals that directly influence plants and the food chain (Kisić et al. 2016; Saljnikov et al. 2019). The disposal and utilisation of fly ash need careful assessment to prevent arable land from being converted into landfills and toxic metals accumulating in the soil and water.

The Law on Environmental Protection (Official Gazette of the Republic of Serbia No. 135/2004, 36/2009, 36 2009—other law, 72/2009—other law, 43/2011—Declaration of Constitutional Court, 14/2016, 76 / 2018,

95/2018) defined remediation as “the process of undertaking measures in order to halt the pollution and further degradation of the environment to a safe level for future use of the location, including the arrangement of the area, revitalisation, and recultivation thereof.” The use of particular plants for this purpose is the process of phytoremediation. Systematic monitoring of the soil quality, indicators for the evaluation of soil degradation and the methodology used to create remediation programmes (Official Gazette of the Republic of Serbia No. 135/2004) prescribes limit values determining the concentration of hazardous and harmful substances that could indicate significant contamination and remediation values in soil and groundwater (Vidojević et al. 2014).

The cultivation of particular crops on ash dumps in the process of phytoremediation is used to prevent ash scattering and render the ash free from toxic substances and microelements applying the experience gained from cover crop technology (Ugrenović and Filipović 2017) (Fig. 26.5). The aim of this process is to reduce soil, air and water pollution by curbing the movement of heavy metals into the groundwater and through the food chain (Jala and Goyal 2006; Kishor et al. 2010).

The phytoremediation process is completed with remediation techniques: 1. Rhizodegradation: rhizospheric microorganisms help in the degradation of organic xenobiotic pollutants (Tangahu et al. 2011); 2. Phytovolatilisation: pollutants are converted to a volatile form and are subsequently liberated into the atmosphere (Marques et al. 2009); 3. Phytoextraction: pollutants accumulate in harvestable biomass, i.e. shoots (Bhargava et al. 2012); 4. Phytotransformation: highly toxic contaminants transform into less toxic forms, i.e. Cr(VI) to Cr(III) (Tangahu et al. 2011); 5. Phytodegradation: degradation of organic xenobiotics by plant enzymes within plant tissues (Khan 2005); 6. Phytostabilisation: mobility of pollutants becomes limited by the plant roots in their rhizosphere (Yang et al. 2014); 7. Phytofiltration: sequestration of pollutants by plants from contaminated water (Ghosh and Singh 2005).

Fig. 26.5 Phytoremediation of fly ash dump in the passive fly ash dump of “Nikola Tesla B” thermal power plant, Obrenovac, Serbia (TENT B) (Photo by L. Maričić)



Moreover, phytoremediation can stabilise ash dumps, controlling wind and water erosion, which positively influences the gradual restoration of the site by reducing substrate leaching, the bioaccumulation of metals and the sequestration of carbon in soil–plant systems. Consecutive phytoremediation processes can enhance the fertility of the area, curtail erosion and air pollution and also remediate the metal-contaminated substrate. It must be underlined that for both agriculture and ecology, phytomanagement is the most cost-effective and eco-friendly approach for managing fly ash dumps. The ultimate goal of good phytomanagement is its positive influence by creating shelter for wildlife and bio-resources for local inhabitants in proper rehabilitation programmes (Jala and Goyal 2006; Maksimović et al. 2008; Kishor et al. 2010; Maiti and Prasad 2016).

The very low fertility and possibly the toxic properties of fly ash means the dumps themselves are not suitable environments for the colonisation and survival of microorganisms. At the beginning of remediation, the fly ash dump is characterised by a low number of microorganisms with low activity, particularly the free-living and symbiotic N_2 -fixing bacteria which are important for supplying the ash substrate with nitrogen compounds (Kostić et al. 2012). They must be brought from the neighbouring soils, although

only tolerant isolates of bacteria and fungi can survive and proliferate according to their different genetic potentials for survival in the severe conditions of the fly ash substrate (Gupta et al. 2004; Juwarkar and Jambhulkar 2008; Maiti and Prasad 2016). Colonised fly ash usually contains a heterotrophic microbiota, in general, N_2 -fixing bacteria (most often rhizobial species) and mycorrhizal fungi. Tolerant microorganisms are likely to undergo advantageous selection according to the specific abiotic and biotic factors of fly ash, creating symbiotic associations with plants established on the dump.

26.4.2 Plants Used for Ash Dump Phytoremediation

Plants chosen for phytoremediation (re-cultivated plants) must be stress-tolerant to withstand the agro-ecological conditions in ash dumps. The plants are mostly highly tolerant to drought conditions and toxic levels of heavy metals. Re-cultivated plants include specific species of grasses, legumes, some trees, cereals and oilseed crops. Mixes of particular grasses can be used alone or with specific legumes (Maiti and Prasad 2016). In particular, biochemical analysis can be used to indicate the plant species that are suitable for recultivating and revegetating an ash

dump. The accumulation of heavy metals in plants depends not only on the total heavy metal content in the soil, but also on the available metal content, the affinity of the plant species to the heavy metals, and the individual or interactive effects of different soil properties. In addition, some heavy metal mixtures (two metals) in the ash can inhibit or stimulate physiological processes in the plants, changing the detrimental effects of the heavy metals in particular plants (Simić et al. 2014, 2015; Maiti and Prasad 2016).

Grasses are suitable for initial vegetation cover because they can grow in spite of the ash dump's nutrient-poor conditions, and they are generally stress-tolerant (mostly drought-tolerant) crops which are capable of surviving the adverse ash dump conditions (Maiti and Prasad 2016). Specific perennial grasses are the most suitable for this purpose. The particular morphological and physiological traits of specific grasses enable the reduction of water erosion, preserve the ash substratum moisture and structure, thanks to their massive fibrous roots, and enhance the nutrient supply of the ash dump via the grass shoots produced—the biomass. Hardy tuft grasses can thereafter find application as mulches. One of the most profitable types of grasses is the group of aromatic grasses (*Saccharum munja*, *Saccharum spontaneum*, *Cymbopogon martinii*, *Vetiveria zizanioides*, *Cymbopogon flexuosus* and *Cymbopogon winterianus*). *S. munja* is one of the most highly regarded grasses for phytoremediation due to its propensity to stabilise the ash-soil binding capability and correct physical traits of the ash substrate. Additionally, this grass is a species which naturally colonises fly ash dumps (Maiti and Prasad 2016).

Forage legumes are suitable and very effective for ash dump remediation and recultivation because of their huge above-ground biomass, ability to symbiotically fix nitrogen and very deep, massive roots (Jambhulkar and Juwarkar 2009). Leguminous plants fix atmospheric nitrogen in association with *Rhizobium* bacteria to increase soil N (Juwarkar and Jambhulkar 2008). The symbiotic association of alfalfa-*S. meliloti* fixes 250–300 kg N ha⁻¹, forming one

of the most efficient associations for natural N₂ fixation (Delić et al. 2013; Delić 2014). This is an effective way to increase organic C and total N content in the ash dump substrate and to absorb heavy metals from the substrate. To create an initial vegetation cover, fast-growing and drought-tolerant species of forage legumes with a role as green manure are best. However, alfalfa, a perennial legume, is also suitable for initial vegetation cover due to its high potential for symbiotic N₂ fixation. *Alnus* spp. should also be mentioned: this is a non-leguminous tree that can form a symbiotic association with N₂-fixing organisms (usually bacteria of the genus *Frankia*) and can be used as a cover crop which can fix nitrogen from the air (N₂) (Maiti and Prasad 2016).

A grass-legume mixture is the most efficient way to cover an ash dump because the mixture can readily colonise the surface, developing a thick vegetation mat in a short time (Simić et al. 2015; Maiti and Prasad, 2016). In Serbia, the grass species commonly used in ash dump remediation or land recultivation are red fescue (*Festuca rubra* L.), Italian ryegrass (*Lolium multiflorum* Lam.), tall fescue (*Festuca arundinacea* Schreb.), common oat (*Avena sativa*), tall oat grass, (*Arrhenatherum elatius* (L.) P. Beauv. ex J. Presl & C. Presl.) and orchard grass (*Dactylis glomerata* L.). The legumes often used for ash dump remediation are forage crops: alfalfa (*Medicago sativa* L.), lupine (*Lupinus* sp. L.), winter pea (*Pisum sativum* L.), bird's-foot trefoil (*Lotus corniculatus* L.), soybean (*Glicine max* L.) or the perennial leguminous shrub, false indigo (*Amorpha fruticosa* L.) (Pivić et al. 2008, Pivić et al. 2007c; Mitrović et al. 2008; Simić et al. 2015; Bilski et al. 2012).

On an ash dump, the seeding process requires the introduction of large quantities of seed and fertiliser boosted with higher levels of nitrogen, P and K than is used in classical agriculture.

Tripathi et al. (2004) suggested three methods of applying leguminous species with grasses: pasture legumes with grasses (for initial colonisation of the ash dump and with minimum application of mineral N due to symbiotic N₂ fixation), legumes with non-legumes (high rate of

N fertiliser), and sequential cropping of grasses followed by legumes (for fast surface cover of the dump and the use of leguminous trees, forb and shrubs) (Maiti and Maiti 2015).

Tree species selected on the basis of their economic importance (for the construction, wood and paper industries, fuelwood and plywood) can be used for revegetating and remediating fly ash dumps. They have a useful trait of accumulating heavy metals in their underground root parts and are unpalatable as foods in nature so there is no risk of heavy metals entering the food chain (Maiti and Pradas 2016). Tamarix (*Tamarix tetrandra* Pallas), which are deciduous shrubs or small trees, white poplar (*Populus alba* L.) and black locust (*Robinia pseudoacacia* L.) can also be utilised (Mitrović et al. 2012). However, tree species are difficult and slow to establish in the harsh and poor conditions of ash dumps, so grasses and legumes are more often applied for remediation and recultivation processes. Besides the plant species already mentioned, the following species have been used for ash dump remediation: wheat (*Triticum aestivum* L.), sunflower (*Helianthus annuus* L.), black pine (*Pinus nigra*), European larch (*Larix decidua*), orchard apple (*Malus domestica*) and alder (*Alnus* spp). For example, by means of its root exudates, the sunflower rhizosphere can influence the ability of soil microbiota (some genera of Proteobacteria) to reduce organic pollutant levels (polycyclic aromatic hydrocarbons) in the process of rhizoremediation (Tejeda-Agredano et al. 2013) (Fig. 26.6).

Apart from revegetation with plants deliberately cultivated in the process of remediation, ash dumps can be remediated by naturally occurring revegetation via naturally growing species (Kostić et al. 2012; Pandey et al. 2015; Žolnierz et al. 2016). One of the best is *S. munja* (Pandey et al. 2012), but ferns (*Pteris vittata* L.), *Ampeopteris prolifera* (Retz.) Copel., *Azolla caroliniana* L., *Diplazium esculentum* (Retz.) Sw. and *Thelypteris dentata* (Forsk.) and woody plants can also play a part (Srivastava et al. 2005; Haynes 2009; Kumari et al. 2013). Ferns have a very good ability to remediate the ash substrate due to their ability to sequester carbon and

acquire heavy metals without toxic effects. These traits are difficult to find in crop plants. Some of the most effective ferns for revegetation are *T. dentata* and naturally growing *A. caroliniana*, due to their high tolerance for heavy metals in fly ash (Haynes, 2009; Pandey, 2012; Kumari et al. 2013).

Moreover, the non-nodulated cassod tree (*Cassia siamea* Lamk), a nodulated species of chickpea (*Cicer arietinum*) (Pandey et al. 2010) and castor bean (*Ricinus communis* L.), which naturally grow on fly ash dumps, are suitable plant species for revegetation in tropical and subtropical regions. The leguminous shrub false indigo (*A. fruticosa* L.) can also naturally colonise ash dumps. This shrub has the adaptive capacity to survive and develop tolerance to stress in fly ash dumps at TENT A, even 11 (Kostić et al. 2012) and 13 years after planting (Mitrović et al. 2012). Studying the ash deposited at TENT A, Kostić et al. (2012), found that the shrub *A. fruticosa* has great potential to be a successful early coloniser on ash dumps as it tolerates some heavy metals (B, As and Mo), high salinity, high temperatures and drought, and can fix N₂. In other research, some species used as pioneer plants for remediation (bioaccumulation of some heavy metals) of ash dump can naturally recolonise ash dump: legumes, alfalfa (*M. sativa* L.) and sweet clover (*Melilotus officinalis* (L.) Pall.) and crop weeds such as gallant soldier (*Galisoga parviflora*), creeping thistle (*Cirsium arvense* (L.) Scop.), reed canary grass (*Phalaris arundinacea* L.) and sheep's sorrel (*Rumex acetosella*) (Dželetović et al. 2013; Simic et al. 2014). These plants were used in the research carried out by Simic et al. (2014). The results showed that these plants did not accumulate high amounts of heavy metals in spite of their different taxonomy and morphology depending on pH, plant species and interactions between heavy metals which can create an antagonistic relationship. These results indicate that plant species that are natural colonisers of ash dumps can be used for the bioremediation and biorecultivation of fly ash dumps.

The vitality of plants growing in the stress conditions of fly ash dumps depends on the plant

Fig. 26.6 Sunflower plants (*Helianthus annuus* L.) used for ash dump remediation (“Nikola Tesla” thermal plant, Obrenovac, Serbia) (Photo by L. Maričić)



species, its adaptive capacity, its tolerance to some stress factors and the weathering time after planting.

With the aim of improving the plants' remediation traits, a genetic approach to phytoremediation involves the use of genetic engineering to amend plants' metal uptake, transport and sequestration. This results in novel transgenic plants with improved remediation traits (Eapen and D'souza 2005).

26.4.3 Cost-effectiveness of Fly Ash Dump Bioremediation

The process of bioremediation receives more support from industry and agriculture if it has some economic value (Pandey and Singh 2010). As stated above, the plants used for remediation are often used in industry or agriculture for useful purposes (e.g. construction, wood and paper industries). Biomass production should be the modern approach to controlling the problem of fly ash dumps and landfill management (Maiti and Prasad 2016) and should be initiated at later stages of restoration. Aromatic grasses (*C. martinii*, *C. flexuosus*, *V. zizanioides* and *C. winterianus*) are used in perfumery, pharmaceuticals and cosmetics. Heavy metal toxicity in the oil extracted from different parts of these grasses can

be avoided by specific, industrial processing methods (Khajanchi et al. 2013). Gupta et al. (2013) underline that aromatic grasses are suitable for use in the process of ash dump recultivation due to the porous nature of fly ash, which leads to excellent root growth, and due to the aromatic grasses' unpalatability, minimal water requirement and perennial nature.

26.4.4 Symbiotic N₂ Fixation in Bioremediation

A major strategy for restoring soil fertility after depletion is the conservation and sustainable use of rhizobia which are tolerant to heavy metals and able to fix N₂ in association with legumes. The complexity of the process of symbiotic N₂ fixation requires both symbionts to be tolerant to environmental stress conditions (Chaudhary et al. 2011) and means that compatibility between symbionts, which has a highly significant effect on the N₂ fixation process, must be taken into account (Delić et al. 2013). Gupta et al. (2004) showed that tolerant rhizobial bacteria species in fly ash yield tolerant plants, which already grow on landfills and can accumulate heavy metals. Inoculation of the legume *Cicer arietanum* L. with tolerant isolates of specific rhizobial species in an ash dump with optimal oxygen content and

without capping increased host plant tolerance, biomass and photosynthesis pigmentation. This makes *C. arietanum* ideal for the bioremediation of N-deficient fly ash dumps. Similar results were obtained using other legumes (genera *Vigna angularis*, *V. radiata*, *C. arietanum* and *Prosopis juliflora* L. (Gupta et al. 2004; Rai et al. 2004; Chaudharya et al. 2011).

It is important to underline that the proper number of rhizobial bacteria in the proper quantity of rhizobial inoculum must be used to inoculate the legumes in the remediation process, otherwise nodulation will be reduced, or bacteria will not grow sufficiently (Gupta et al. 2004; Chaudhary et al. 2011; Buntić et al. 2019). *Rhizobium* has been reported to be a key element for plant establishment under xeric and imbalanced nutrient conditions (Chaudhary et al. 2011).

The transfer of heavy metals from soil to plant is a very complex process which depends on natural and anthropogenic factors, but primarily, uptake, translocation and bioaccumulation depend on the heavy metal and plant species (Maiti and Prasad 2016). In general, phytoremediation depends on the plant growth rate. The accumulation of heavy metals from the soil in the roots of Norway spruce (*Picea abies*) and poplar (*Populus tremula*) was about 10–20 times more than in the controls and the root accumulation capacity was highest after the first vegetation period (Brunner et al. 2008). Physico-chemical and biological factors such as the pH, soil mineralogy, texture, salinity, amount of humic acids and presence of organic chelators are responsible for heavy metal availability and bioaccumulation in the plants (Pandey et al. 2010). Pandey (2013) studied the ability of castor bean (*R. communis* L.) used as a vegetation cover on a heavy-metal-enriched fly ash dump. *T. dentata* is a fern species that accumulates more metals in its roots/rhizome than in its fronds (Kumari et al. 2011). Pandey et al. (2010) also found higher heavy metal concentrations in the root parts of chickpea growing on fly ash. The tendency of plants to accumulate metals in their above-ground and below-ground parts is directly proportional to the amount and duration of exposure to the fly ash. Heavy metals are generally

sequestered in the root cell vacuoles to diminish metal toxicity. Roots often act as a barrier against heavy metal translocation and are more tolerant to toxic metal concentrations, thus explaining their higher accumulation of these minerals compared to shoots (Shanker et al. 2005).

26.4.5 Amendments for Efficient Establishment of Plants Suitable for Bioremediation of Ash Dumps

The chemical characteristics of fly ash are poor in general, and thus not available for crop growing. Besides the toxic concentration of heavy metals, the plant growth on fly ash dumps is limited due to the high pH of fly ash, its high concentration of soluble salts and its nutrient deficiency due to the low contents of N and P or absence of N (Chaudhary et al. 2011). In addition, the physical traits of fly ash can restrict root growth due to the fine particle size of the ash (Kostić et al. 2012).

Only rarely does an ash dump have fly ash with the characteristics of fertile soil (Pivić et al. 2008; Mrvić et al. 2004; Kostić et al. 2012). This situation did, however, occur in the TENT ash dump in Obrenovac, because the contents of potentially toxic elements were under the MACs, with the exception of the B metalloid, while the lack of P was solved by applying mineral P fertiliser (Mrvić et al. 2004; Pivić et al. 2008).

It is necessary to determine and add the particular amendments needed to establish the plants which are suitable for bioremediation of each ash dump. The aim is to create an ash dump with high fertility and good physical properties, which involves the spatial ash texture. Amendments might include topsoil, mineral fertilisers, natural or waste organic substrates, chemical substances and microbial amendments.

Moreover, irrigation of the ash dump is a very important process to prevent wind erosion and to supply the remediation crops with water. The irrigation must be carefully planned because fly ash has a high capacity for water infiltration and thus does not retain moisture. In fact, the poor

quality of fly ash's physical traits means there can be a need for particular methods for irrigating fly ash dumps. In the ash dumps at TENT, the irrigation regime varies depending on the substrate traits and water inflow regime (Mrvić et al. 2004; Pivić et al. 2002, 2007a).

26.4.5.1 Mineral Fertiliser as an Amendment

Mineral fertiliser is an important modification that is applied to improve the initial establishment of the green cover remediation plants. According to current practices, high rates of mineral fertilisers have to be applied. It was suggested that NPK should be applied in the absence of topsoil, and the N:P:K ratio has been defined for the initial fertiliser application (15:15:15 or 19:19:19) (Dželetović and Filipović, 1995; Punshon et al. 2002).

26.4.5.2 Topsoil as an Amendment

Topsoil is the most suitable amendment applied to fly ash to allow plants that are suitable for bioremediation to become established (Maiti and Prasad 2016). Topsoil can be used to improve the physico-chemical conditions of fly ash in order to supply the ash with nutrients and to reduce toxic microelements in the ash. At TENT, 10 cm of topsoil followed by the same volume of clay is the usual amendment added to each ash dump in preparation for remediation. This mixture provides the required physical conditions and available nutrients to the plants used in phytoremediation.

26.4.5.3 Organic Amendments

Besides topsoil, mulch, dewatered biosolids, composted chicken manure and other animal wastes, farmyard manure, green waste, mill mud, compost, biosolids, sewage sludge and other organic amendments (Maiti and Prasad 2016) can be used to amend fly ash dumps. Mulch helps to decrease wind and water erosion and the surface temperature, and curtails water loss through evaporation, improving infiltration and the water holding capacity of the fly ash. In these suitable conditions, the accumulation of soil organic matter is increased, providing a slow

release of nutrients. These organic amendments are perhaps the best material to generate substrate with good physico-chemical properties and a desirable microbial community (Haynes 2009).

26.4.5.4 Chemical Amendments

Chemical amendments such as EDTA, limestone and biochar (residual charcoal) can play their part as amendments for fly ash dumps (Evangelou et al. 2007; Belyaeva and Haynes 2012). Field and pot studies also show that other substances, e.g. inorganic sewage sludge and vermiculite, improve the growth of bioremediation plants (Juwarkar and Jambhulkar 2008; Schwab et al. 1989; Cheung et al. 2000).

26.4.5.5 Nanotechnology and Heavy Metal Removal From Fly Ash

A somewhat different approach for the remediation of fly ash uses the biogenic synthesis of nanoparticles. The application of biogenic maghemite ($\gamma\text{-Fe}_2\text{O}_3$) nanoparticles was studied for its ability to selectively remove toxic heavy metals from a 20% aqueous solution of fly ash (Yadav and Fulekar 2018b). Maghemite was synthesised using Tridax leaf extract. Using this method, up to 85% of the Pb was removed in 2 h and up to 96% removed in 24 h (Yadav and Fulekar 2018b).

26.4.5.6 Microorganisms as Amendments in Phytoremediation and Bioremediation

Applications of microorganisms, alone or with the plants in the process of bioremediation, are a more sustainable and cost-effective approach for removing heavy metals from fly ash dumps or contaminated soils in comparison with most remediation techniques, which are expensive and can have detrimental effects on the soil structure (Kumar and Verma 2018). Indigenous microorganisms and microbial inoculants can be applied as fly ash amendments in the processes of bioremediation and phytoremediation with the following aims:

- (1) To assist plants by sequestering heavy metals during the phytoremediation process (Kumar and Verna, 2018). They help the plants to absorb detrimental levels of microelements in their tissues. Recently, microorganism-mediated processes of heavy metal uptake by plants have been studied (Ma et al. 2011). Microbial metabolites in the rhizosphere reduce metal mobility and bioavailability, meaning the minerals can become biodegradable and less toxic. These metal-containing metabolites can easily be produced in situ in rhizospheric soils.
- (2) To encourage the growth of plant-growth-promoting rhizobacteria (PGPR), which, in turn, encourages the growth of the bioremediation plants and supplies the ash substrate with N, P, Fe or hormone substances. The interface between the remediated plant and rhizobacteria hosts the complex root activities that occur in the rhizosphere, such as the uptake and release of microelements. In Ni-contaminated soil, Wenzel et al. (2018) carried out research into phytostabilisation using excluders and phytoextraction by hyperaccumulator plant species, and underlined that managing the rhizosphere by inoculation with PGPR isolates holds promise for the further enhancement of phytoremediation (Table 26.8):
- (3) Bacteria in the rhizosphere and plant-associated microorganisms (epiphytic and endophytic bacteria as well as rhizobial bacteria) also produce some growth-promoting substances such as siderophores and growth hormones including indole acetic acid (IAA) and 1-amino cyclopropane-1-carboxylic acid (ACC) deaminase, which further improve vegetation growth (Babu and Reddy 2011; Ullah et al. 2015; Malhotra et al. 2017; Knežević et al. 2021).
- (4) N₂-fixing cyanobacteria or rhizobial bacteria which are tolerant to heavy metals have been used to enhance N and P content and reduce metal toxicity in fly ash. Rhizobial bacteria that are heavy-metal-tolerant can help in the translocation and bioaccumulation of heavy metals in plant tissues (root and/or shoot part of the plant) (Gupta et al. 2004). In contaminated land, Jing et al. (2019) isolated a Cu-Pb-Cd-tolerant strain of *S. meliloti* (designated D10) from root nodules of alfalfa (*M. sativa* L.) and the strain successfully established symbiosis with the host plant (Fig. 26.7). In this way, alfalfa mixed with perennial ryegrass and *Sorghum bicolor* plants can be used in combination with this tolerant *S. meliloti* strain to remediate soils contaminated with Cu, Pb and Cd heavy metals.
- (3) To remediate the substrate and reduce leaching of harmful heavy metals from the substrate via the bioaccumulation and biosorption of metals (immobilisation of metals), making the ash substrate less toxic (Ma et al. 2011; Babu and Reddy 2011; Zhou et al. 2014; Maiti and Prasad 2016). Bacteria with the trait of immobilising harmful heavy metals can be used to stop these metals from leaching into waters or can enhance the bioavailability of some metals (e.g. Cu) during fly ash bioremediation. Bioavailable heavy metal is the fraction of total metal pollutant in a substrate which can be involved in the metabolism of microorganisms or plant cells in the process of bioaccumulation, or can be sequestered in the process of biosorption (when the metal becomes attached to surface elements of dead microorganisms) (Kukić 2016). The pH of soil significantly affects the bioavailability of Cu, Ni, Mn and Pb, but the impacts of the organic matter content and clay depend on the particular microelements present (Dinić et al. 2019).
- (4) To promote long-term carbon sequestration in soil, mediated through the priming effect of fungi (Fontaine et al. 2011). In a study carried out in the south-eastern USA, fungal endophyte infection increased the carbon sequestration potential of tall fescue stands (Iqbal et al. 2012).

Table 26.8 Plants and plant growth-promoting rhizobacteria used for bioremediation (Ullah et al. 2015; Kumar and Verma 2018)

PGP bacteria	Associated plant(s)	Heavy metal(s)	Beneficial features/bacterial characteristic	References
<i>Achromobacter</i> sp. E4L5	<i>Sedum plumbizincicola</i>	Cd, Zn, Cu	ACC, IAA, siderophore, P solubilisation	Ma et al. (2015)
<i>Achromobacter xylooxidans</i> Ax10	<i>Brassica juncea</i>	Cu	ACC, IAA, P solubilisation	Ma et al. (2009a)
<i>Azotobacter chroococcum</i> HKN-5	<i>Brassica juncea</i>	Pb, Zn, Cu, Cd	IAA, gibberellins	Wu et al. (2006)
<i>Azotobacter chroococum</i>	<i>Zea mays</i> L	Pb	IAA, decrease in soil pH	Hadi and Bano (2010)
<i>Bacillus cereus</i>	<i>Orychophragmus violaceus</i>	Zn; Cd	ACC, IAA, siderophores; improve plant growth and root elongation	He et al. (2010); Liang et al. (2014)
<i>Bacillus cereus</i> SRA10	<i>Brassica juncea</i>	Ni	ACC, IAA, P solubilisation, Ni mobilisation	Ma et al. (2009b)
<i>Bacillus endophyticus</i> NBRFT4	<i>Brassica juncea</i>	Cd, Cu, Ni	Siderophores, organic acids, protons and other unspecified enzymes	Tiwari et al. (2012)
<i>Bacillus megaterium</i> HKP-1	<i>Brassica juncea</i>	Pb, Zn, Cu, Cd	IAA, gibberellins	Wu et al. (2006)
<i>Bacillus mucilaginosus</i> HKK-1	<i>Brassica juncea</i>	Pb, Zn, Cu, Cd	IAA, gibberellins	Wu et al. (2006)
<i>Bacillus pumilus</i> E2S2	<i>Sedum plumbizincicola</i>	Cd, Zn, Cu	ACC, IAA, siderophore, P solubilisation	Kumar and Verma (2018), Ma et al. (2015)
<i>Bacillus pumilus</i> NBRFT9	<i>Brassica juncea</i>	Cd, Cu, Ni	Siderophores, organic acids, protons and other unspecified enzymes	Tiwari et al. (2012)
<i>Bacillus</i> sp. E2S2	<i>Sedum plumbizincicola</i>	Cd, Zn	ACC, IAA, siderophore, P solubilisation	Ma et al. (2015)
<i>Bacillus</i> sp. SN9	<i>Brassica juncea</i> ; <i>Brassica oxyrrhina</i>	Ni	ACC, IAA, P solubilisation, Ni mobilisation	Ma et al. (2009c); Ma et al. (2011)
<i>Bacillus subtilis</i>	<i>Orychophragmus violaceus</i>	Cd; Zn	Improve plant growth and root elongation; ACC, IAA, siderophores	Liang et al. (2014); He et al. (2010)
<i>Bacillus thuringiensis</i> GDB-1	<i>Alnus firma</i>	Cd, Ni, As, Cu, Pb, Zn	ACC, IAA, siderophore, P solubilisation	Babu et al. (2013), Kumar and Verma (2018)
<i>Bradyrhizobium japonicum</i>	Lettuce	Cd, Pb	IAA	Seneviratne et al. (2016)
<i>Claroideoglomus claroideum</i>	<i>Calendula officinalis</i> L	Cd, Pb	Accumulation of secondary metabolites and enhanced antioxidant capacity	Hristozkova et al. (2016)

(continued)

Table 26.8 (continued)

PGP bacteria	Associated plant(s)	Heavy metal(s)	Beneficial features/bacterial characteristic	References
<i>Cupriavidus taiwanensis</i>	<i>Mimosa pudica</i>	Pb, Cu, Cd	Biodegradation, biosorption, release of extracellular products	Chen et al. (2008)
<i>Enterobacter</i> sp. JYX7	<i>Polygonum pubescens</i>	Cd, Pd, Zn	ACC, IAA, siderophore, P solubilisation	Jing et al. (2014)
<i>Enterobacter cloacae</i> CAL2	<i>Brassica napus</i>	As	IAA, ACC, siderophores, antibiotics	Nie et al. (2002)
<i>Flavobacterium</i> sp.	<i>Orycophragmus violaceus</i>	Zn	ACC, IAA, siderophores	He et al. (2010)
<i>Funneliformis mosseae</i>	<i>Calendula officinalis</i> L	Cd, Pb	Accumulates secondary metabolites and enhances antioxidant capacity	Hristozkova et al. (2016)
<i>Glomus etunicatum</i>	<i>Calopogonium mucunoides</i>	Pb	Promotes acquisition of plant nutrients (P, S and F)	De Souza et al. (2012), Kumar and Verma (2018)
<i>Glomus fasciculatum</i>	<i>Helianthus annuus</i> L	Cd, Zn	Promotes the dry biomass of the plant, accumulation (Zn, Cd) in root and shoot	Mani et al. (2016)
<i>Klebsiella</i> sp. BAM1	<i>Helianthus annuus</i>	Cd	IAA, ACC	Prapagdee et al. (2013)
<i>Klebsiella</i> sp. JYX10	<i>Polygonum pubescens</i>	Cd, Pd, Zn	ACC, IAA, siderophore, P solubilisation	Jing et al. (2014)
<i>Microbacterium</i> sp. G16	<i>Brassica napus</i>	Pb	IAA, ACC, siderophore	Sheng et al. (2008)
<i>Micrococcus</i> sp. MU1	<i>Helianthus annuus</i>	Cd	IAA, ACC	Prapagdee et al. (2013)
<i>Paenibacillus macerans</i> NBRFT5	<i>Brassica juncea</i>	Cd, Cu, Ni	Siderophores, organic acids, protons and other unspecified enzymes	Tiwari et al. (2012)
<i>Pantoea agglomerans</i> Jp3-3	<i>Brassica napus</i>	Cu	IAA, siderophores, ACC, P solubilisation	Zhang et al. (2011a, b)
<i>Pseudomonas fluorescens</i> ACC9	<i>Brassica napus</i>	Cd	IAA, ACC, siderophores	Dell'Amico et al. (2008)
<i>Pseudomonas putida</i>	<i>Gladiolus grandiflorus</i> L	Cd, Pb	Improves plant growth and root elongation and enhanced accumulation (Cd, Pb)	Mani et al. (2016)
<i>Pseudomonas aeruginosa</i>	<i>Orycophragmus violaceus</i>	Zn; Cd	ACC, IAA, siderophores; improves plant growth and root elongation	He et al. (2010); Liang et al. (2014)
<i>Pseudomonas brassicacearum</i>	<i>Brassica juncea</i>	Zn	Metal chelation	Adediran et al. (2015)
<i>Pseudomonas fluorescens</i> G10	<i>Brassica napus</i>	Pb	IAA, ACC, siderophore	Sheng et al. (2008)

(continued)

Table 26.8 (continued)

PGP bacteria	Associated plant(s)	Heavy metal(s)	Beneficial features/bacterial characteristic	References
<i>Pseudomonas jessenii</i> PjM15	<i>Ricinus communis</i>	Zn	Biosorption, mobilisation, ACC, IAA, siderophores	Rajkumar and Freitas, (2008)
<i>Pseudomonas putida</i>	<i>Helianthus annuus</i> L	Cd, Zn	Promotes the dry biomass of the plant, accumulation (Zn, Cd) in root and shoot	Mani et al. (2016)
<i>Pseudomonas</i> sp. PsM6	<i>Ricinus communis</i>	Zn	Biosorption, mobilisation, ACC, IAA, siderophores	Rajkumar and Freitas, (2008)
<i>Pseudomonas</i> sp. SRI2	<i>Brassica juncea</i>	Ni	ACC, IAA, P solubilisation Ni mobilisation	Ma et al. (2009c)
<i>Pseudomonas</i> spp. Lk9	<i>Solanum nigrum</i> L	Cd, Zn, Cu	Biosurfactants, siderophore, organic acid	Chen et al. (2014)
<i>Pseudomonas thivervalensis</i> Y1-3-9	<i>Brassica napus</i>	Cu	IAA, siderophores, ACC, P solubilisation	Zhang et al. (2011a, b)
<i>Pseudomonas tolaasii</i> ACC23	<i>Brassica napus</i>	Cd	ACC, siderophores, IAA	Dell'Amico et al. (2008)
<i>Pseudomonas veronii</i>	<i>Sedum alfredii</i>	Zn	IAA, decreases soil pH, supply of P and Fe	Long et al. (2013)
<i>Psychrobacter</i> sp. SRS8, SRA1 and SRA2	<i>Brassica juncea</i>	Ni	ACC, IAA, P solubilisation, Ni mobilisation	Ma et al. (2009c, b)
<i>Rahnella</i> sp.	<i>Amaranthus hypochondriacus</i> , <i>A. mangostanus</i> , <i>Solanum nigrum</i>	Cd	IAA, siderophores, ACC, P solubilisation	Yuan et al. (2013)
<i>Rahnella</i> sp. JN6	<i>Brassica napus</i>	Cd, Pb, Zn	IAA, ACC, siderophores, P solubilisation	He et al. (2013a, b)
<i>Rhizobium leguminosarum</i>	<i>Brassica juncea</i> ; <i>Zea mays</i> L	Zn; Pb	Metal chelation; IAA, decrease soil pH	Adediran et al. (2015); Hadi and Bano (2010)
<i>Staphylococcus arlettae</i> NBRIEAG-6	<i>Brassica juncea</i>	As	IAA, siderophores, ACC	Srivastava et al. (2013)
<i>Stenotrophomonas</i> sp. E1L	<i>Sedum plumbizincicola</i>	Cd, Zn, Cu	ACC, IAA, siderophore, P solubilisation	Ma et al. (2015)
<i>Thiobacillus thiooxidans</i>	<i>Gladiolus grandiflorus</i> L	Cd, Pb	Improves plant growth and root elongation and enhanced accumulation (Cd, Pb)	Mani et al. (2016)

(5) To enhance the root mass by a significant amount (it can be almost doubled), which protects plants from stress conditions and increases the carbon sequestration potential

of some grasses. Mycorrhizal fungi have particular potential for use as root mass enhancers (Iqbal et al. 2012; Maiti and Prasad 2016).

Fig. 26.7 The heavy-metal-tolerant *Sinorhizobium meliloti* strain successfully establishes symbiosis with host plant (alfalfa) nodules on the plant root (Institute of Soil Science, Belgrade, Serbia)



26.5 Useful Traits of Fly Ash

Fly ash is classified as a waste material according to the Green Waste List published by the Organisation for Economic Cooperation and Development (OECD), but under the Basel Convention, fly ash is not considered a waste material (Basu et al. 2009). This emerging opposite opinion of fly ash's qualities is ascribable to its possible useful traits, which, nonetheless, must be determined by proper analyses, and the fly ash must then be utilised in suitably controlled processes. However, in many countries, fly ash is not utilised at all (Basu et al. 2009), since only its harmful traits are taken into account, and not its useful characteristics. In spite of that, when large amounts of fly ash started to become an environmental problem, some feasible solutions to this issue were introduced. Fly ash has now found general application in building and road construction, embankments, reclamation of low-lying areas and mine filling, brick and tile production, the cement and concrete industry and zeolite synthesis. Fly ash can also be utilised in agriculture with the aim of correcting the physico-chemical properties of arable land. In addition, fly ash has been applied as a sorbent to clean waste gases and as an agent for

removing toxic compounds from waste (Uliasz-Bocheńczyk and Bak 2018; Yadav and Fulekar 2018a; González-Martínez et al. 2019).

It has to be underlined that, in spite of these useful applications for fly ash, its proper disposal and judicious use are extremely important in the contexts of environmental and biological health (Liu et al. 2019).

26.5.1 Use of Fly Ash in Agriculture

Fly ash has great potential in agriculture to improve soil fertility due to some of its alkaline characteristics and high mineral content, particularly the biogenic macroelements (Sharma and Kalra, 2006; Jala and Goyal 2006; Kishor et al. 2010). Therefore, it can be used as a fertiliser or amendment to improve the physico-chemical and biological characteristics of soil. Soil amelioration with fly ash has been advocated for the last three decades in different soil types (Parab et al. 2015).

Applying Fly ash to agricultural soils can improve their physical properties such as conductivity, water-holding capacity, density and porosity (Adriano and Weber 2001; Pathan et al. 2003; Jala and Goyal 2006; Kishor et al. 2010; Kohli and Goyal 2010). The fine particle size of

fly ash positively affects the water-holding capacity and removes the compaction of clay soils. In fly-ash-ameliorated soil, these physical properties provide soil characteristics that are desirable for plant growth: increased water-holding capacity and reduced bulk density (Kohli and Goyal 2010).

Fly ash can have positive effects on the chemical properties of soil too, increasing the contents of essential macro- and micronutrients and organic carbon, while shifting the soil pH to neutral due to fly ash's lime content. However, the extent to which problematic soils can be corrected and recovered depends on the content of fly ash used and soil type. These effects improve soil fertility by neutralising acid in the soil, thus decreasing the toxic effects of Al and Mn anions in acidic soils and increasing Ca^{2+} and Mg^{2+} availability (Sharma and Kalra 2006; Kishor et al. 2010; Sheoran et al. 2014; Maiti and Prasad 2016). Moreover, in alkaline soil, when the pH is shifted to near neutral using fly ash, conditions are also improved, as Al^{3+} is soluble and toxic above soil pH 8.0 and under pH 5. Meanwhile, in neutral soil, Al toxicity is prevented by the formation of the insoluble form of Al, $\text{Al}(\text{OH})_3$ (Pandey and Singh 2010). The majority of plant nutrients are available for the plants between pH 6.5 to 7, so in this regard, fly ash can be extremely useful. Sheoran et al. (2014) used fly ash to improve the soil's physico-chemical characteristics and crop production. As an ameliorating agent for acid soils, alkaline fly ash can increase the pH of arable land, reducing the use of lime, which can be cost-effective (Kishor et al. 2010; Basu et al. 2009; Parab et al. 2015). In acidic soil, the lime in fly ash can release B, S and Mo in forms which are useful for crops (Pandey and Singh 2010). Moreover, the application of alkaline fly ash is an ecologically profitable process due to the reduced lime production, causing lower emissions of gas pollutants including greenhouse gases (sulphur oxides (SO_x), carbon dioxide (CO_2), carbon monoxide (CO), methane (CH_4), nitrous oxide (N_2O) and nitrogen oxides (NO_x)), which are responsible for global warming (Basu et al. 2009).

However, suitable doses of ameliorating fly ash must be used to amend acidic soils. Fly ash must be applied carefully in agriculture as heavy metals can have toxic effects in the higher trophic levels through the food chain. As a result, plant materials and soil samples from these fly-ash-ameliorated areas must be subject to regular analyses.

26.5.2 Use of Fly Ash to Correct the Soil's Biological Properties

The biological properties of soil can be corrected with increases in microbial activity. When fly ash is used to amend soil, increases in soil microbiota, microbial activity and microbial enzyme activity depend on the quantity of fly ash used. Surridge et al. (2009) found that fly ash amendment has a limited effect on soil due to fly ash's high content of heavy metals, which can obstruct microbial activities in the soil. Therefore, it is important to apply optimal doses of fly ash for any ameliorating processes. Optimal doses of fly ash stimulate soil respiration, enzyme activity (dehydrogenase activity, protease, amylase, invertase), microbial proliferation, microbial biomass and activity of plant growth-promoting microorganisms, such as *Azotobacter chroococcum*, rhizobial bacteria, *Actinomyces*, fungi, arbuscular mycorrhizal fungi and phosphorus-solubilising bacteria (Klucas et al. 1983; Kishor et al. 2010; Kohli and Goyal 2010; Parab et al. 2015). Amending Class F, bituminous fly ash to soil at a rate of 505 mg ha^{-1} did not have any negative effect on the soil microorganisms (Schutter and Fuhrmann 2001), content of microelements, microbial activity or crop yield (Nayak et al. 2015). Low concentrations of Cd, which can occur in fly ash, can promote the activity of some microorganisms (Shi and Ma 2017).

The increased mobility of Ca^{2+} and OH^- by fly ash amendment increases the diversity of bacterial species in soil (Surridge et al. 2009). Moreover, the proliferation and activity of microorganisms in the soil increased, as did the

microbial diversity, after fly ash was applied in combination with the organic manure, sewage sludge (Wong and Wong 1986; Sims et al. 1995; Jala and Goyal 2006; Parab et al. 2015). Organic matter and fly ash amendments together in soil act synergetically and have an additive effect because, in this mixture, organic matter reduces the concentration of toxic metals through sorption, lowers the C/N ratio and provides organic compounds to stimulate microbial proliferation and diversity (Wong and Wong 1986; Kohli and Goyal 2010). An increased, more active microbial biomass then stimulates nutrient cycling (N and P cycling), and the result of this is the release into the soil of plant nutrients that are favourable for plant growth and soil recovery (Kohli and Goyal 2010).

Fly ash can be also applied in agriculture to improve or boost crop growth and yield and nutrient uptake because of the significant contents of its nutrient elements (Ca, K, Mg and S) (Antonkiewicz et al. 2020; Yousuf et al. 2020; Mishra and Dash 2020). Mixed amendment with fly ash, paper factory sludge and farmyard manure increases crop yield and the soil pH and improves the soil's physico-chemical properties (Basu et al. 2009). For this purpose, fly ash can be mixed with other materials such as brick kiln dust. The influence of fly ash can be more effective when earthworms, wheat straw or phosphate are added simultaneously. Fly ash amendment can also stimulate root growth and excretion in the soil. The results of fly ash amendment were longer root length (lettuce), higher amino acid content (soybean), better seed germination and higher yield of clover (*T. repens* L.), soybean (*G. max* L.), chickpea (*C. arietanum*), common bean (*Phaseolus vulgaris*), some grasses including barley (*Hordeum vulgare* L.) and wheat (*T. aestivum*), triticale, maize (*Zea mays* L.), tomato (*Solanum lycopersicum* L.), onion (*Allium cepa* L.) (Rizvi and Khan 2009; Parab et al. 2015; Lau and Wong 2001), different brassicas (*Brassica parachinensis*, *B. chinensis*, *B. oleracea*, *B. campestris*) (Wong and Wong, 1990; Jayasinghe and Tokashiki 2012), alfalfa (*M. sativa*) (Wong and Wong 1989) and rice (*Oryza sativa*) (Lee et al. 2006) (Maiti and

Prasad 2016). However, it is important to understand that edible leafy vegetables must never be grown in soils amended with fly ash due to the risk of heavy metals moving into the human food chain. Fly ash amendment of soils to increase biomass production in the soil can be useful in forestry and wasteland reclamation (Rizvi and Khan 2009).

26.5.3 Use of Fly Ash as a Raw Material for Construction and Industry

In the last decade, fly ash has taken up a position as the world's fifth largest raw material resource (Liu et al. 2019). Fly ash can be a suitable material for constructing embankments in geotechnical engineering projects (Miricioiu and Niculescu 2020; Rastogi and Paul 2020), which decreases the amount of soil used for landfill and reduces CO₂ emissions (Mahvash et al. 2017). In addition, it can be used as an alternative to conventional materials in the construction of geotechnical and geoenvironmental infrastructure (Terzić et al. 2012; Maiti and Prasad 2016; Mahvash et al. 2017; Vukićević et al. 2018). Due to its inherent traits, fly ash can be used in concrete manufacturing to produce concrete admixed products (such as pozzolans), in cement production to construct buildings and roads, and in the cement industry to produce synthetic zeolites, bricks and blocks, as an aggregate material in Portland cement, to manufacture glass and ceramic, and to synthesise geopolymers (Terzić et al. 2012; Vukićević et al. 2018). As a consequence, cement production and its CO₂ emissions are reduced. Fly ash with a high carbon content is widely used as an insulator and adsorbent (Liu et al. 2019). Fly ash's adsorbent quality has a positive effect on soil's potential for carbon sequestering (Kishor et al. 2010; Mahvash et al. 2017; Liu et al. 2019). According to a CEA report, fly ash is used in the greatest quantities in the cement sector (Ghosh and Kumar 2019). Type F fly ash dominates the fly ash market due to its resistance to sulphate attack, low cost and

high workability, all factors that make it popular in this market (Ghosh and Kumar 2019). The Serbian fly ash market is active, but in general, this product is purchased by cement producers (Kisić et al. 2012). In lignite coal combustion, the herbaceous biomass of energy crops (e.g. *Cynara cardunculus*) is suitable for firing with lignite. The aim is to ameliorate the ash quality produced during the combustion process when the coal is of average quality. This co-firing approach could be a good option for the beneficial use, *inter alia*, of low-quality coal in construction materials (Fuller et al. 2018).

Moreover, fly ash can also be used as a potential source of rare earth elements (Ga, Al, U, Se, niobium (Nb) and zirconium (Zr)) (Liu et al. 2019). Rare earth elements have been recognised as critical raw materials which are crucial for many modern technological applications (Franus et al. 2015). Some of the rare earth elements have a role in high technology equipment (lanthanum, europium, erbium and neodymium being the most important), renewable energy or military applications (Franus et al. 2015; Liu et al. 2019).

Attempts have been made to find an effective method for using fly ash in the nanotechnology area, with the aim of modifying the fly ash by transforming micron-sized fly ash into nanostructured fly ash (Babu Rao et al. 2010). Raghavendra et al. (2014, 2016) modified fly ash micron particles to create smooth and glassy fly ash nanoparticles. The nano fly ash can modify the physical properties of a polymer matrix, imparting new features to the polymer. This nano-fly-ash-modified polymer could be used as a construction material in some industries (for example, the aerospace and automobile industries). Planetary ball milling was used by Raghavendra et al. (2014) to vastly increase the surface area of fly ash from $0.31 \text{ m}^2 \text{ g}^{-1}$ to $24.65 \text{ m}^2 \text{ g}^{-1}$, reduce the crystallite size from 59 to 26%, decrease the average particle size from 11 μm to 148 nm, and produce a unique particle shape and texture. Two years later, Raghavendra et al. (2016) carried out research on fly ash nanoparticle usage in the textile industry. The flexural and tensile properties of micron-sized

and nano-sized fly ash particles that were combined with jute/glass hybrid epoxy composites were compared with conventional fibres/glass composites. The fly ash nano-filler hybrid composites had better flexural strength than did the glass fibre composites. However, the application of fly ash nanoparticles has not yet been developed enough to allow their full application in different branches of industry, so their positive impact on the circular economy and the environment remains to be scientifically proven.

26.6 Conclusion

In spite of the successful process of ash dump phytoremediation and the rising usage of fly ash in some branches of industry and agriculture, coal fly ash is still a threat to the environment and human health. There is a concern at the global level because about 40% of the fly ash produced is still unused, while global energy demand is growing along with the attitude that coal is a reliable and secure energy source. Many countries are increasing coal consumption in spite of the importance of renewable energy sources (e.g., geothermal, hydro, wind and solar). Coal's share of the global energy mix continues to rise and there is an assumption that it will come close to surpassing oil as the world's biggest energy source.

Currently, a global trend is to circulate resources to potentially achieve the Sustainable Development Goals. The concept in India and China, which many countries are emulating, is to manage and use fly ash as part of implementing a circular economy and the 5R concepts: reduce, reuse, recycle, remanufacture and repair.

Serbia should implement the European Commission's approach proposed for new coal combustion, so that greenhouse gas emissions are reduced by 2050 by 80 to 95% compared with 1990 levels. The question is what kind of effect (positive or negative) will occur during the permanent exposure of valuable agricultural land to fly ash. For that reason, remediated plant materials, soils ameliorated by fly ash, and industrial products and creations containing fly ash as an

additive must be the subjects of permanent, strategic scientific monitoring, with regular analyses showing what changes need to be implemented for safe coal fly ash use and disposal.

Acknowledgements Financial support for this investigation was provided by the Ministry of Education, Science and Technological Development of the Republic of Serbia, (contract No. 451-03-09/2021-14/200011).

References

- Adediran GA, Ngwenya BT, Mosselmans JFW, Heal KV, Harvie BA (2015) Mechanisms behind bacteria induced plant growth promotion and Zn accumulation in *Brassica juncea*. *J Hazard Mater* 283:490–499, <https://www.sciencedirect.com/science/article/abs/pii/S0304389414008139>
- Adriano CD, Page AL, Elseewi AA, Chang AC, Straughan I (1980) Utilization and disposal of fly-ash and other coal residues in terrestrial ecosystems: a review. *J Environ Qual* 9(3):333–344
- Adriano DC, Weber JT (2001) Influence of fly ash on soil physical properties and turf grass establishment. *J Environ Qual* 30(2):596–601
- Ahemad M (2019) Remediation of metalliferous soils through the heavy metal resistant plant growth promoting bacteria: paradigms and prospects. *Arab J Chem* 12(7):1365–1377, <https://www.sciencedirect.com/science/article/pii/S1878535214002688>
- Alexander E, Pham D, Steck TR (1999) The viable-but-nonculturable condition is induced by copper in *Agrobacterium tumefaciens* and *Rhizobium leguminosarum*. *Appl Environ Microbiol* 65(8):3754–3756, <https://aem.asm.org/content/65/8/3754>
- Alloway BJ (2013) Sources of heavy metals and metalloids in soils. In: Heavy metals in soils. Springer, Dordrecht, pp 11–50. https://doi.org/10.1007/978-94-007-4470-7_2
- Al-Mayman S, Al-Shunaifi I, Albeladi A, Ghiloufi I, Binjuwair S (2017) Treatment of fly ash from power plants using thermal plasma. *Beilstein J Nanotechnol* 11(8):1043–1048. <https://www.ncbi.nlm.nih.gov/pubmed/28546898>
- Antonkiewicz J, Popławska A, Kołodziej B, Ciarkowska K, Gambuś F, Bryk M, Babula J (2020) Application of ash and municipal sewage sludge as macronutrient sources in sustainable plant biomass production. *J Environ Manag* 264:110450. <https://doi.org/10.1016/j.jenvman.2020.110450>
- Babu AG, Kim JD, Oh BT (2013) Enhancement of heavy metal phytoremediation by *Alnus firma* with endophytic *Bacillus thuringiensis* GDB-1. *J Hazard Mater* 250:477–483, <https://www.sciencedirect.com/science/article/pii/S0304389413001234>
- Babu AG, Reddy S (2011) Dual inoculation of arbuscular mycorrhizal and phosphate solubilizing fungi contributes in sustainable maintenance of plant health in fly ash ponds. *Water Air Soil Poll* 219:3–10. <https://doi.org/10.1007/s11270-010-0679-3>
- Babu Rao J, Narayanaswami P, Siva Prasad K (2010) Thermal stability of nano structured fly ash synthesized by high energy ball milling. *Int J Eng Sci Technol* 2(5):284–299, <https://www.ajol.info/index.php/ijest/article/viewFile/62577/50511>
- Basu M, Pande M, Bhadoria PBS, Mahapatra SC (2009) Potential fly ash utilization in agriculture: a global review. *Prog Nat Sci* 19(10):1173–1186, <https://www.sciencedirect.com/science/article/pii/S1002007109001579>
- Belyaeva NO, Haynes JR (2012) Comparison of the effects of conventional organic amendments and biochar on the chemical, physical and microbial properties of coal fly ash as a plant growth medium. *Environ Earth S* 66:1987–1997
- Bhargava A, Carmona FF, Bhargava M, Srivastava S (2012) Approaches for enhanced phytoextraction of heavy metals. *J Environ Manag* 105:103–120, <https://www.sciencedirect.com/science/article/pii/S0301479712001831>
- Bhatt A, Priyadarshini S, Mohanakrishnan AA, Abri A, Sattler M, Techapaphawit S (2019) Physical, chemical, and geotechnical properties of coal fly ash: a global review. *Case Stud Construct Mater* e00263. <https://www.sciencedirect.com/science/article/pii/S2214509518303735>
- Bilski J, Jacob D, McLean K, McLean E, Lander M (2012) Preliminary study of coal fly ash (FA) phytoremediation by selected cereal crops. *Adv Biores* 3(4):176–180, <https://www.ncbi.nlm.nih.gov/pmc/articles/PMC5891152/>
- Bogdanović V (1990) Presence of some microorganisms groups in ash deposit under acacia (*Robinia pseudoacacia*) TE Lazarevac. *Zemljiste i Biljka* 39(2):139–145
- Broos K, Uyttendaele M, Mertens J, Smolders E (2004) A survey of symbiotic nitrogen fixation by white clover grown on metal contaminated soils. *Soil Biol Biochem* 36(4):633–640, <https://www.sciencedirect.com/science/article/abs/pii/S0038071704000264>
- Brunner I, Luster J, Günthardt-Goerg MS, Frey B (2008) Heavy metal accumulation and phytostabilisation potential of tree fine roots in a contaminated soil. *Environ Pollut* 152(3):559–68, <https://www.ncbi.nlm.nih.gov/pubmed/17707113>
- Buntić AV, Stajković-Srbinić OS, Knežević MM, Kuzmanović ĐŽ, Rasulić NV, Delić DI (2019) Development of liquid rhizobial inoculants and preinoculation of alfalfa seeds. *Arch Biol Sci* 71(2):379–387, http://www.serbiosoc.org.rs/arch/index.php/abs/article/viewFile/3503/pdf_239
- Sebi C (2019) Explaining the increase in coal consumption worldwide. *The Conversation*, Academic rigour, journalistic flair

- CEA (Central electricity authority New Delhi) (2018) Report on flyash generation at coal/lignite based power station. Its utilization in the country for the year 2017–2018, https://cea.nic.in/old/reports/others/thermal/tcd/flyash_201718.pdf. Accessed 31 March 2021
- Chaudhary K, Inouhe M, Rai UN, Mishra K, Gupta DK (2011) Inoculation of Rhizobium (VR-1 and VA-1) induces an increasing growth and metal accumulation potential in *Vigna radiata* and *Vigna angularis* L. growing under fly-ash. *Ecol Eng* 37:1254–1257
- Chen L, Luo S, Li X, Wan Y, Chen J, Liu C (2014) Interaction of Cd hyperaccumulator *Solanum nigrum* L. and functional endophyte *Pseudomonas* sp. Lk9 on soil heavy metals uptake. *Soil Biol Biochem* 68:300–308, <https://www.sciencedirect.com/science/article/abs/pii/S0038071713003659>
- Chen WM, Wu CH, James EK, Chang JS (2008) Metal biosorption capability of *Cupriavidus taiwanensis* and its effects on heavy metal removal by nodulated *Mimosa pudica*. *J Hazard Mater* 151(2–3):364–371, <https://www.sciencedirect.com/science/article/pii/S0304389407008345>
- Cheung KC, Wong JPK, Zhang ZQ, Wong JWC, Wong MH (2000) Revegetation of lagoon ash using the legumes species *Acacia auriculiformis* and *Leucaena leucocephala*. *Environ Pollut* 109:75–82, <https://www.sciencedirect.com/science/article/pii/S0269749199002353>
- Cieek A, Koparal AS (2004) Accumulation of sulfur and heavy metals in soil and tree leaves sampled from the surroundings of Tunçbilek Thermal Power Plant. *Chemosphere* 57(8):1031–1036, <https://www.sciencedirect.com/science/article/pii/S0045653504006253>
- Cokić Z, Pivić R, Mrvić V, Brebanović B (2002) Osobine pepela na deponiji TE Kostolac i tehnologija biološke rekultivacije. ELEKTRA II-ISO14000:398–400
- Country classifications (2020) World Economic Situation Prospects. Statistical annex, United Nations, New York, 2020. https://www.un.org/development/desa/dpad/wp-content/uploads/sites/45/WESP2020_Annex.pdf. Accessed on 31 March 2021
- de la Peña C, Pueyo J (2012) Legumes in the reclamation of marginal soils, from cultivar and inoculant selection to transgenic approaches. *Agron Sustain Dev* 32:65–91, <https://hal.archives-ouvertes.fr/hal-00930493/document>
- De Souza LA, de Andrade SAL, de Souza SCR, Schiavinato MA (2012) Arbuscular mycorrhiza confers Pb tolerance in *Calopogonium mucunoides*. *Acta Physiol Plant* 34:523–531
- Delić D, Stajković O, Rasulić N, Jošić D, Kuzmanović Đ, Maksimović S, Miličić B (2010) Presence and activity of *Sinorhizobium meliloti* as the indicator of potential N₂ fixation ability of TP “Nikola Tesla” Obrenovac surrounding soils. *Zemljiste i Biljka* 59(2):117–128, <https://scindeks.ceon.rs/article.aspx?artid=0514-66581002117D>
- Delić D, Stajković-Srbinić O, Radović, J Kuzmanović Dj, Rasulić N, Simić A, Knežević-Vukčević J (2013) Differences in symbiotic N₂ fixation of alfalfa, *Medicago sativa* L. cultivars and *Sinorhizobium* spp. strains in field conditions. *Roum Biotechnol Lett* 18(6):8743–8750, <https://www.rombio.eu/vol118nr6/2%20Dusica%20Delic.pdf>
- Delić D (2014) Rizobijalne bakterije u poljoprivrednoj proizvodnji leguminoza (Rhizobial bacteria in agricultural production of legumes). Zadužbina Andrejević, Belgrade, p 100
- Delić-Vukmir D, Lugić Z, Radin D, Knežević-Vukčević J, Simić D (1994) Presence and density of root nodulation *Rhizobium meliloti* bacteria in different soil types of the Krusevac region. *Mikrobiologija* 31:117–122
- Dell’Amico E, Cavalca L, Andreoni V (2008) Improvement of Brassica napus growth under cadmium stress by cadmium-resistant rhizobacteria. *Soil Biol Biochem* 40:74–84
- Dinić Z, Maksimović J, Stanojković-Sebić A, Pivić R (2019) Prediction models for bioavailability of Mn, Cu, Zn, Ni and Pb in soils of republic of Serbia. *Agronomy* 9(12):856. <https://doi.org/10.3390/agronomy9120856>
- Dželetović Ž, Živanović I, Pivić R, Simić A, Lazić G, Maksimović J (2013) Mogućnosti korišćenja višegodišnjih rizomatoznih trava za melioracije oštećenih zemljišnih površina. Melioracije 13, January 24, Novi Sad, Proceedings, 130–137
- Dželetović ŽS, Filipović R (1995) Grain characteristics of crops grown on power plant ash and bottom slag deposit. *Resour Conserv Recycl* 13(2):105–113
- Eapen S, D’souza SF (2005) Prospects of genetic engineering of plants for phytoremediation of toxic metals. *Biotechnol Adv* 23(2):97–114, <https://www.sciencedirect.com/science/article/abs/pii/S0734975004000941>
- Evangelou MWH, Bauer U, Ebel M, Schaeffer A (2007) The influence of EDDS and EDTA on the uptake of heavy metals of Cd and Cu from soil with tobacco *Nicotiana tabacum*. *Chemosphere* 68:345–53, <https://www.sciencedirect.com/science/article/pii/S0045653506018042>
- Filipović R, Protić N, Cokić Z, Torehi T (1997) Biološke mere na deponijama pepela i šljake sa aspekta zaštite vazduha od zagađenja. Naučno–stručno savetovanje EKO 97, Obrenovac, 1997, Zbornik radova
- Fontaine S, Henault C, Aamor A, Bdioui N, Bloor JMG, Maire V, Mary B, Revailot S, Maron PA (2011) Fungi mediate long term sequestration of carbon and nitrogen in soil through their priming effect. *Soil Biol Biochem* 43:86–96, <https://www.sciencedirect.com/science/article/abs/pii/S0038071710003500>
- Franus W, Wiatros-Motyka MM, Wdowin M (2015) Coal fly ash as a resource for rare earth elements. *Environ Sci Pollut Res Int* 22(12):9464–9474. <https://doi.org/10.1007/s11356-015-4111-9>

- Fuller A, Maier J, Karampinis E, Kalivodova J, Grammelis P, Kakaras E, Scheffknecht G (2018) Fly ash formation and characteristics from (co-) combustion of an herbaceous biomass and a Greek lignite (low-rank coal) in a pulverized fuel pilot-scale test facility. *Energies* 11(6):1581. <https://doi.org/10.1007/s11356-015-4111-9>
- Ghani A (2010) Toxic effects of heavy metals on plant growth and metal accumulation in Maize (*Zea mays* L.). *Iranian J Toxycol* 3(3):326–334
- Ghosh M, Singh S (2005) A review on phytoremediation of heavy metals and utilization of it's by products. *Asian J Energy Environ* 3:214–231
- Ghosh SK, Kumar V (2019) Circular economy and fly ash management. Editor Springer, ISBN 978-981-15-0014-5
- Giller KE, Witter E, Mcgrath SP (1998) Toxicity of heavy metals to microorganisms and microbial processes in agricultural soils: a review. *Soil Biol Biochem* 30:1389–1414
- Giller KE, Mcgrath SP, Hirsch PR (1989) Absence of nitrogen fixation in clover grown on soil subject to long-term contamination with heavy metals is due to survival of only ineffective *Rhizobium*. *Soil Biol Biochem* 21:841–848
- González-Martínez A, de Simón-Martín M, López R, Táboas-Fernández R, Bernardo-Sánchez A (2019) Remediation of potential toxic elements from wastes and soils: analysis and energy prospects. *Sustainability* 11(12):3307. <https://www.mdpi.com/2071-1050/11/12/3307/htm>
- Gupta DK, Rai UN, Sinha S, Tripathi RD, Nautiyal BD, Rai P, Inouhe M (2004) Role of *Rhizobium* (CA-1) inoculation in increasing growth and metal accumulation in *Cicer arietinum* L. growing under fly-ash stress condition. *Bull Environ Contam Toxicol* 73(2):424–431. <https://link.springer.com/article/10.1007%2Fs00128-004-0446-5?LI=true>
- Gupta DK, Rai UN, Tripathi RD, Inouhe M (2002) Impacts of fly-ash on soil and plant responses. *J Plant Res* 115(6):401–409
- Gupta AK, Verma SK, Khan K, Verma RK (2013) Phytoremediation using aromatic plants: a sustainable approach for remediation of heavy metals polluted sites. *Environ Sci Technol* 47:10115–10116
- Hadi F, Bano A (2010) Effect of diazotrophs (*Rhizobium* and *Azobactor*) on growth of maize (*Zea mays* L.) and accumulation of Lead (Pb) in different plant parts. *Pak J Bot* 42(6):4363–4370. [http://www.pakbs.org/pjbot/PDFs/42\(6\)/PJB42\(6\)4363.pdf](http://www.pakbs.org/pjbot/PDFs/42(6)/PJB42(6)4363.pdf)
- Harris D, Heidrich C, Feuerborn J (2019) Global aspects on coal combustion products. <https://www.coaltrans.com/insights/article/global-aspects-on-coal-combustion-products>. Accessed on 31 March 2021
- Haynes JR (2009) Reclamation and revegetation of fly ash disposal sites challenges and research needs. *J Environ Manag* 90:43–53. <https://www.sciencedirect.com/science/article/pii/S0301479708001631>
- He CQ, Tan GE, Liang X, Du W, Chen YL, Zhi GY, Zhu Y (2010) Effect of Zn tolerant bacterial strains on growth and Zn accumulation in *Orychophragmus violaceus*. *Appl Soil Ecol* 44(1):1–5
- He H, Ye Z, Yang D, Yan J, Xiao L, Zhong T, Yuan M, Cai X, Fang Z, Jing Y (2013a) Characterization of endophytic *Rahnella* sp. JN6 from *Polygonum pubescens* and its potential in promoting growth and Cd Pb, Zn uptake by *Brassica napus*. *Chemosphere* 90:1960–1965. <https://www.sciencedirect.com/science/article/pii/S0045653512012969>
- He J, Ma C, Ma Y, Li H, Kang J, Liu T, Polle A, Peng C, Luo Z (2013) Cadmium tolerance in six poplar species. *Environ Sci Pollut Res* 20:163–174
- Hix R. (1994) Determining the status of microbes in polluted sediments using thin layer chromatography-flame ionization detection lipid analysis. *Bios* 60–68. <https://www.jstor.org/stable/4608254?seq=1>
- Hristozkova M, Geneva M, Stancheva I, Boychinova M, Djonova E (2016) The contribution of arbuscular mycorrhizal fungi in attenuation of heavy metal impact on *Calendula officinalis* development. *Appl Soil Ecol* 101:57–63. <https://www.sciencedirect.com/science/article/pii/S0929139316300087>
- IARC (1987) International Agency for Research on Cancer (IARC) World Health Organization—monographs on the evaluation of the carcinogenic risk of chemicals to humans. international agency for research on cancer, vol. 42. Lyon, France. ISSN 1450-801X, ISBN 978-86-525-019-7
- Iqbal J, Siegrist JA, Nelson JA, McCulley RL (2012) Fungal endophyte infection increases carbon sequestration potential of southeastern USA tall fescue stands. *Soil Biol Biochem* 44:81–92. <https://www.sciencedirect.com/science/article/abs/pii/S0038071711003439>
- Jakšić SP, Vučković SM, Vasiljević SL, Grahovac NL, Popović VM, Šunjka DB, Dozet GK (2013) Akumulacija teških metala u Medicago sativa L. i Trifolium pratense L. na kontaminiranom fluvisolu (Accumulation of heavy metals in Medicago sativa L. and Trifolium pratense L. at the contaminated fluvisol). *Hem Ind* 67(1):95–101. http://www.ache.org.rs/HI/2013/No1/HEMIND_Vol67_%20No1_p95-101_Jan-Mar_2013.pdf. Accessed on 31 March 2021
- Jala S, Goyal D (2006) Fly ash as a soil ameliorant for improving crop production—a review. *Bioresour Technol* 97(9):1136–1147. <https://www.sciencedirect.com/science/article/pii/S0960852404003244>
- Jambhulkar HP, Juwarkar AA (2009) Assessment of bioaccumulation of heavy metals by different plant species grown on fly ash dump. *Ecotoxicol Environ Saf* 72(4):1122–1128
- Jambhulkar HP, Shaikh SMS, Kumar MS (2018) Fly ash toxicity, emerging issues and possible implications for its exploitation in agriculture; Indian scenario: a review. *Chemosphere* 213:333–344. <https://www.ncbi.nlm.nih.gov/pubmed/30241077>
- Jing YX, Yan JL, He HD, Yang DJ, Xiao L, Zhong T, Yuan M, Cai XD, Li SB (2014) Characterization of

- bacteria in the rhizosphere soils of *Polygonum pubescens* and their potential in promoting growth and Cd, Pb, Zn uptake by *Brassica napus*. *Int J Phytoremed* 16:321–333. <https://doi.org/10.1080/15226514.2013.773283>
- Jing YAN, Li X, Xia-Fang S, Lin-Yan H (2019) Isolation of heavy metal-tolerant *Sinorhizobium meliloti* and the effect on copper uptake of alfalfa, perennial ryegrass and Sorghum bicolor plants grown on copper-contaminated soil[J]. *Acta Prataculturae Sinica* 28(2):102–111. <http://cyxb.magtech.com.cn/EN/abstract/abstract5036.shtml>
- Juwarkar AA, Jambhulkar HP (2008) Restoration of fly ash dump through biological interventions. *Environ Monit Assess* 139(1–3):355–365. <https://doi.org/10.1007/s10661-007-9842-8>
- Kabata-Pendias A, Szteke B (2015) Trace elements in abiotic and biotic environments. CRC Press, Boca Raton, FL, USA. ISBN 9781482212792
- Kalra N, Harit RC, Sharma SK (2000) Effect of flyash incorporation on soil properties of texturally variant soils. *Bioresour Technol* 75(1):91–93
- Khajanchi L, Yadav RK, Kaur R, Bundela DS, Khan MI, Chaudhar M, Meena RL, Dar SR, Singh G (2013) Productivity essential oil yield, and heavy metal accumulation in lemon grass (*Cymbopogon flexuosus*) under varied wastewater—groundwater irrigation regimes. *Ind Crop Prod* 45:270–278
- Khalil MA, Abdel-Lateif HM, Bayoumi BM, van Straalenb NM (1996) Analysis of separate and combined effects of heavy metals on the growth of *Aporrectodea caliginosa* (Oligochaeta; Annelida), using the toxic unit approach. *Appl Soil Ecol* 4(3):213–219. <https://www.sciencedirect.com/science/article/pii/S0929139396001151>
- Khan AG (2005) Role of soil microbes in the rhizospheres of plants growing on trace metal contaminated soils in phytoremediation. *J Trace Elem Med Biol* 18(4):355–364. <https://www.sciencedirect.com/science/article/pii/S0946672X05000349>
- Kinkle BK, Sadowsky MJ, Johnstone K, Koskinen WC (1994) Tellurium and selenium resistance in rhizobia and its potential use for direct isolation of *Rhizobium meliloti* from soil. *Appl Environ Microbiol* 60(5):1674–1677. <https://aem.asm.org/content/aem/60/5/1674.full.pdf>
- Kishor P, Ghosh AK, Kumar D (2010) Use of flyash in agriculture: a way to improve soil fertility and its productivity. *Asian J Agric Res* 4(1):1–14. <http://docsdrive.com/pdfs/knowledge/ajar/0000/17422-17422.pdf>
- Kisić D, Miletić S, Gržetić I (2012) Fly ash radioactivity measurements in electric power industry of Serbia thermal power Plants. *Engineering 1*, <https://pdfs.semanticscholar.org/426f/ed7c558d4ac8d347ec3c3cdc37651c03d5eb.pdf>
- Kisić DM, Miletić SR, Radonjić VD, Radanović SB, Filipovic JZ, Gržetić IA (2013) Prirodna radioaktivnost uglja i letećeg pepela u termoelektrani “Nikola Tesla B”. *Hem Ind* 67(5):729–738. <http://vinar.vin.bg.ac.rs/bitstream/handle/123456789/5803/article5799.pdf?sequence=1>. Accessed on 31 March 2021
- Kisić D, Marinković J, Jovanović G, Vukotić Lj, Đakonović M, Stanimirović B, Cvijanović P, Glišić I (2016) Monitoring zemljišta u okolini deponija pepela i šljake termoelektrana javnog preduzeća “Elektroprivreda Srbije”, Integrisani skup “Zemljište 2016”, May 10, Vršac, Proceedings, pp 30–39
- Klucas RV, Hans FJ, Russell SA, Evans HJ (1983) Nickel: a micronutrient element for hydrogen-dependent growth of *Rhizobium japonicum* and for expression of urease activity in soybean leaves. *Proc Natl Acad Sci* 80(8):2253–2257. <https://www.pnas.org/content/pnas/80/8/2253.full.pdf>
- Knežević MM, Stajković-Srbinić OS, Assel M, Milić MD, Mihajlovski KR, Delić DI, Buntić AV (2021) The ability of a new strain of *Bacillus pseudomycoloides* to improve the germination of alfalfa seeds in the presence of fungal infection or chromium. *Rhizosphere-Neth* 18:100353. <https://doi.org/10.1016/j.rhisph.2021.100353>
- Kohli SJ, Goyal D (2010) Effect of fly ash application on some soil physical properties and microbial activities. *Acta Agrophys* 16(2):327–335. http://www.old.acta-agrophysica.org/artikuly/acta_agrophysica/ActaAgr_182_2010_16_2_327.pdf. Accessed on 31 March 2021
- Kostić O, Mitrović M, Knežević M, Jarić S, Gajić GM, Djurdjević L, Pavlović P (2012) The potential of four woody species for the revegetation of fly ash deposits from the “Nikola Tesla-a” thermoelectric plant (Obrenovac, Serbia). *Arch Biol Sci* 64(1):145–158. <http://ibiss-r.rcub.bg.ac.rs/handle/123456789/299>
- Kukić D (2016) Biosorpcija jona teških metala iz vode izluženim rezancima šećerne repe (Biosorption of heavy metal ions from water by leached sugar beet noodles). Dissertation, University of Novi Sad p 192. <https://nardus.mpn.gov.rs/handle/123456789/7104?locale-attribute=en>. Accessed on 31 March 2021
- Kumar A, Verma JP (2018) Does plant–microbe interaction confer stress tolerance in plants: a review? *Microbiol Res* 207:41–52. <https://www.sciencedirect.com/science/article/pii/S0944501317307954>
- Kumari A, Pandey CV, Rai NU (2013) Feasibility of fern *Thelypteris dentata* for revegetation of coal fly ash landfills. *J Geochem Explor* 128:147–152. <https://www.sciencedirect.com/science/article/pii/S037567421300040X>
- Kumari A, Lal B, Pakade YB, Chand P (2011) Assessment of bioaccumulation of heavy metal by *Pteris Vittata* L. growing in the vicinity of fly ash. *Int J Phytoremediat* 13(8):779–787. <https://doi.org/10.1080/15226514.2010.525561>
- Lau SSS, Wong JWC (2001) Toxicity evaluation of weathered coal fly ash amended manure compost. *Water Air Soil Poll* 128(3–4):243–254. <https://doi.org/10.1023/A:1010332618627>
- Lee H, Ho SH, Lee CH, Lee YB, Kim PJ (2006) Fly ash effect on improving soil properties and rice productivity in Korean paddy soils. *Bioresour Technol*

- 97:1490–1497, <https://www.sciencedirect.com/science/article/pii/S0960852405003470>
- Liang X, He CQ, Ni G, Tang GE, Chen XP, Lei YR (2014) Growth and Cd accumulation of *Orychophragmus violaceus* as affected by inoculation of Cd tolerant bacterial strains. *Pedosphere* 24(3):322–329, <https://www.sciencedirect.com/science/article/abs/pii/S1002016014600187>
- Liu Y, Zeng F, Sun B, Jia P, Graham IT (2019) Structural characterizations of aluminosilicates in two types of fly ash samples from Shanxi Province, North China. *Minerals* 9(6):358, <https://www.mdpi.com/2075-163X/9/6/358>
- Long XX, Chen XM, Wong JWC, Wei ZB, Wu QT (2013) Feasibility of enhanced phytoextraction of Zn contaminated soil with Zn mobilizing and plant growth promoting endophytic bacteria. *T Nonferr Metal Soc* 23(8):2389–2396, <https://www.sciencedirect.com/science/article/abs/pii/S1003632613627466>
- Ma S-H, Xu M-D, Qiqige, Wang X-H, Zhou X (2017) Challenges and developments in the utilization of fly ash in China. *Int J Environ Sci Dev* 8(11):781–785, <http://www.ijesd.org/vol8/1057-C3001.pdf>
- Ma Y, Oliveira RS, Nai F, Rajkumar M, Luo Y, Rocha I, Freitas H (2015) The hyper accumulator *Sedum plumbizincicola* harbors metal-resistant endophytic bacteria that improve its phytoextraction capacity in multi-metal contaminated soil. *J Environ Manag* 156:62–69
- Ma Y, Rajkumar M, Freitas H (2009a) Inoculation of plant growth promoting bacterium *Achromobacter xylosoxidans* strain Ax10 for the improvement of copper phytoextraction by *Brassica juncea*. *J Environ Manag* 90(2):831–837, <https://estudogeral.sib.uc.pt/bitstream/10316/39151/file40a340c35e1c40bb9a8714a61ef58e24.pdf>. Accessed on 31 March 2021
- Ma Y, Rajkumar M, Freitas H (2009b) Improvement of plant growth and nickel uptake by nickel resistant-plant growth promoting bacteria. *J Hazard Mater* 166(2–3):1154–1161, <https://estudogeral.sib.uc.pt/bitstream/10316/9984/1/ficheiro.pdf>
- Ma Y, Rajkumar M, Freitas H (2009c) Isolation and characterization of Ni mobilizing PGPB from serpentine soils and their potential in promoting plant growth and Ni accumulation by *Brassica* spp. *Chemosphere* 75(6):719–725, <https://estudogeral.sib.uc.pt/bitstream/10316/9980/1/ficheiro.pdf>. Accessed on 31 March 2021
- Ma Y, Rajkumar M, Luo Y, Freitas H (2011) Inoculation of endophytic bacteria on host and non-host plants—effects on plant growth and Ni uptake. *J Hazard Mater* 195:230–237
- Mahvash S, López-Querol S, Bahadori-Jahromi A (2017) Effect of class F fly ash on fine sand compaction through soil stabilization. *Heliyon* 3(3):e00274 <https://www.sciencedirect.com/science/article/pii/S2405844016319910>
- Maiti D, Prasad B (2016) Revegetation of fly ash—a review with emphasis on grass-legume plantation and bioaccumulation of metals. *Appl Ecol Environ Res* 14(2):185–212
- Maiti SK, Maiti D (2015) Ecological restoration of waste dumps by topsoil blanketing, coir-matting and seeding with grass–legume mixture. *Ecological Eng* 77:74–84, <https://www.sciencedirect.com/science/article/abs/pii/S092585741500004X>
- Maksimović S, Blagojević S, Pivić R, Stanojković A (2008) Quality characteristics of some grass species cultivated on fly-ash desposits of a thermal power station. *Fresenius Environ Bull* 17(5):584–588
- Malhotra S, Mishra V, Karmakar S, Sharma RS (2017) Environmental predictors of indole acetic acid producing rhizobacteria at fly ash dumps: nature-based solution for sustainable restoration. *Front Environ Sci* 5. <https://doi.org/10.3389/fenvs.2017.00059>, <https://platform.think-nature.eu/content/environmental-predictors-indole-acetic-acid-producing-rhizobacteria-fly-ash-dumps-nature>. Accessed on 31 March 2021
- Mani D, Kumar C, Patel NK (2016) Integrated micro-biochemical approach for phytoremediation of cadmium and lead contaminated soils using *Gladiolus grandiflorus* L. cut flower. *Ecotoxicol Environ Saf* 124:435–446, <https://www.sciencedirect.com/science/article/abs/pii/S0147651315301639>
- Manier N, Deram A, Broos K, Denayer FO, Wan Haluwyn C (2009) White clover nodulation index in heavy metal contaminated soils – A potential bioindicator. *J Environ Qual* 38:685–692, <https://www.ncbi.nlm.nih.gov/pubmed/19244489>
- Marques AP, Rangel AO, Castro PM (2009) Remediation of heavy metal contaminated soils: phytoremediation as a potentially promising clean-up technology. *Crit Rev Enl Sci Tec* 39(8):622–654. <https://doi.org/10.1080/10643380701798272>
- Miličić B, Delić D, Stajković O, Rasulić N, Kuzmanović Đ, Jošić D (2006) Effects of heavy metals on rhizobial growth. *Roum Biotechnol Lett* 11(6):2995–3003, <https://e-repository.org/rbl/vol.11/iss.6/7.pdf>. Accessed on 31 March 2021
- Miricioiu MG, Niculescu V-C (2020) Fly ash, from recycling to potential raw material for mesoporous silica synthesis. *Nanomaterials* 10(3):474
- Mishra SS, Dash MR (2020) Utilization of fly ash in agriculture: a better way to manage industrial solid waste. *Agric Food: E-Newsl* 2(7):389–391
- Mitrović M, Jarić S, Kostić O, Gajić G, Karadžić B, Djurdjević L, Lj O, Pavlović D, Pavlović M, Pavlović P (2012) Photosynthetic efficiency of four woody species growing on fly ash deposits of a Serbian “Nikola Tesla – A” thermoelectric plant. *Pol J Environ Stud* 21(5):1339–1347
- Mitrović M, Pavlović P, Lakušić D, Djurdjević L, Stevanović B, Kostić O, Gajić G (2008) The potential of *Festuca rubra* and *Calamagrostis epigejos* for the revegetation of fly ash deposits. *Sci Total Environ* 407(1):338–347, <https://www.sciencedirect.com/science/article/pii/S0048969708008966>
- Mrvić V, Pivić R, Cokić Z, Čakmak D, Smiljančić Ž, Kisić D (2004) Osobine pepela na eksperimentalnoj

- deponiji TENT B (hidrotransport u suspenziji 1:1) u odnosu na klasični sistem, Treća međunarodna konferencija o upravljanju zaštitom okoline energetska efikasnost u energetici, Electra III, Herceg Novi, 341–346
- Nayak AK, Raja R, Rao KS, Shukla AK, Mohanty S, Shahid M, Tripathi R, Panda BB, Bhattacharyya P, Kumar A, Lal B, Sethi SK, Puri C, Nayak D, Swain CK (2015) Effect of fly ash application on soil microbial response and heavy metal accumulation in soil and rice plant. *Ecotoxicol Environ Saf* 114:257–62. <https://www.sciencedirect.com/science/article/pii/S0147651314001389>
- Nie L, Shah S, Burd GI, Dixon DG, Glick BR (2002) Phytoremediation of arsenate contaminated soil by transgenic canola and the plant growth promoting bacterium *Enterobacter cloacae* CAL2. *Plant Physiol Biochem* 40(4):355–361
- Onija A, Marković J, Slavković L, Andrić V (2004) Analitičke tehnike za određivanje tragova metala u uglju i letećem pepelu. Treća međunarodna naučno-stručna konferencija o upravljanju zaštitom okoline (energetska efikasnost u energetici). 7–11 juni, Herceg Novi, 348–351
- Orlov SD, Sadovnikova LK, Sukhanova NI (2005) *Khimiya pochv* (Soil Chemistry). Vysshaya Shkola, Moscow [in Russian]
- Pandey VC (2013) Suitability of *Ricinus communis* L. cultivation for phytoremediation of fly ash disposal sites. *Ecology Eng* 57:336–34. <https://www.sciencedirect.com/science/article/abs/pii/S0925857413001729?via%3Dihub>
- Pandey VC, Prakash P, Bajpai O, Kumar A, Singh N (2015) Phytodiversity on fly ash deposits: Evaluation of naturally colonized species for sustainable phytoremediation. *Environ Sci Pollut Res* 22(4):2776–2787. <https://doi.org/10.1007/s11356-014-3517-0>
- Pandey VC, Singh JS, Kumar A, Tewari DD (2010) Accumulation of Heavy Metals by Chickpea Grown in Fly Ash Treated Soil: Effect on Antioxidants. *Clean-Soil Air Water* 38(12):1116–1123. <https://doi.org/10.1002/clen.201000178>
- Pandey VC, Singh K, Singh RP, Singh B (2012) Naturally growing *Saccharum munja* L. on the fly ash lagoons: a potential ecological engineer for the revegetation and stabilization. *Ecol Eng* 40:95–99
- Pandey VC, Singh N (2010) Impact of fly ash incorporation in soil systems. *Agr Ecosyst Environ* 136(1–2):16–27. <https://www.sciencedirect.com/science/article/abs/pii/S0167880909003442>
- Pankhurst CE, Hawke BG, McDonald HJ, Kirkby CA, Buckerfield JC, Michelsen P, Doube BM (1995) Evaluation of soil biological properties as potential bioindicators of soil health. *Anim Prod Sci* 35:1015–1028. <http://www.publish.csiro.au/an/EA9951015>. Accessed on 31 March 2021
- Parab N, Sinha S, Mishra S (2015) Coal fly ash amendment in acidic field: effect on soil microbial activity and onion yield. *Appl Soil Ecol* 96:211–216, <https://www.sciencedirect.com/science/article/pii/S0929139315300603>
- Pathan SM, Aylmore LAG, Colmer TD (2003) Soil properties and turf growth on a sandy soil amended with fly ash. *Plant Soil* 256(1):103–114. <https://doi.org/10.1023/A:1026203113588>
- Pavlović P, Mitrović M, Đurđević L, Gajić G, Kostić O, Bojović S (2007) Ecological potential of *Spirea vanhouttei* (Briot) Zabel for urban (Belgrade city) and fly ash deposit (Obrenovac) landscaping in Serbia. *Pol J Environ Stud* 16(3):427–431
- Pivić R, Mrvić V, Brebanović B, Cokić Z (2002) Neophodnost navodnjavanja u cilju zasnivanja biljnog pokrivača na odlagalištima pepela termoelektrana Kostolac i Obrenovac. International conference: "Upravljanje zaštitom životne sredine u Elektroprivredi"—Electra II, Tara, Proceedings, pp 411–414
- Pivić R, Cokić Z, Mrvić V, Brebanović B (2007a) Infiltracione karakteristike pepela i izbor najbolje prilagođenog načina navodnjavanja na deponijama pepela i šljake, International conference: "Otpadne vode, komunalni čvrsti otpad i opasan otpad", 02–05. April 2007, Kruševac, Proceedings, pp 199–203
- Pivić R, Cokić Z, Maksimović S, Stanojković A (2007b) Faze biološke rekultivacije na deponiji pepela i šljake u cilju zaštite okoline od eolske erozije, Međunarodna konferencija Otpadne vode, komunalni čvrsti otpad i opasan otpad, 02–05. April 2007, Kruševac, pp 194–198
- Pivić R, Maksimović S, Cokić Z, Stanojković A (2007c) Kvalitativna svojstva travnih vrsta *Lotus corniculatus* i *Festuca rubra* gajenih na deponiji pepela i šljake, Prva regionalna naučno-stručna konferencija o upravljanju industrijskim otpadom: Ispitivanje industrijskog otpada/karakterizacija i kategorizacija, Kopaonik, 22–25. Oktobar 2007, pp 1–6
- Pivić R, Maksimović S, Cokić Z, Stanojković A (2007d) Kvalitativna svojstva travnih vrsta *Lotus corniculatus* i *Festuca rubra* gajenih na deponiji pepela i šljake, Industrijski otpad. Prva regionalna naučno-stručna konferencija o upravljanju industrijskim otpadom: Ispitivanje industrijskog otpada / karakterizacija i kategorizacija, Kopaonik, 22–25. oktobar 2007, pp 1–6. ISBN 85013-04-1
- Pivić R, Maksimović S, Cokić Z (2008) Mogućnost gajenja odredenih travnih vrsta na deponijama pepela i šljake termoelektrana (Possibility of cultivation of specific grass species on ash and slag disposal of thearmoelectric power plants). *POP* 1(1):87–93. Tehnološki fakultet u Boru, Reciklaža i održivi razvoj
- Prapagdee B, Chanprasert M, Mongkolsuk S (2013) Bioaugmentation with cadmium-resistant plant growth-promoting rhizobacteria to assist cadmium phytoextraction by *Helianthus annuus*. *Chemosphere* 92(6):659–666. <https://www.sciencedirect.com/science/article/pii/S0045653513002117>
- Punshon T, Adriano DC, Weber JT (2002) Restoration of drastically eroded land using coal fly ash and poultry biosolid. *Sci Total Environ* 296(1–3):209–225. <https://www.sciencedirect.com/science/article/pii/S0048969702001286>

- Raghavendra G, Ojha S, Acharya SK, Pal SK, Ramu I (2016) Evaluation of mechanical behaviour of nanometer and micrometer fly ash particle-filled woven bidirectional jute/glass hybrid nanocomposites. *J Ind Text* 45(6):1268–1287
- Raghavendra G, Ojha S, Acharya SK, Pal SK (2014) Fabrication and characterization of nano Fly ash by planetary ball Milling. *Int J Mater Sci Innovat* 2(3):59–68
- Rai UN, Pandey K, Sinha S, Singh A, Saxena R, Gupta DK (2004) Revegetating fly ash landfills with *Prosopis juliflora* L.: impact of different amendments and Rhizobium inoculation. *Environ Int* 30(3):293–300,
- Rajkumar M, Freitas H (2008) Influence of metal resistant-plant growth promoting bacteria on the growth of *Ricinus communis* in soil contaminated with heavy metals. *Chemosphere* 71(5):834–842
- Rastogi A, Paul VK (2020) A critical review of the potential for fly ash utilization in construction-specific applications in India. *Environ Res Eng Manag* 76(2):65–75. <https://doi.org/10.5755/j01.arem.76.2.25166>
- Rasulić N, Stajković O, Delić D, Cokić Z, Karbozova E, Kuzmanović Đ, Miličić B (2007) Effect of TE "Nikola Tesla" aerosol on the microflora of ash heaps and the surrounding soils. In: "Otpadne vode, komunalni čvrst otpad i opasan otpad", Proceedings, Kruševac, Serbia. April 2–5, 2007, pp 190–193
- Rebah FB, Prevost D, Tyagi RD (2002) Growth of alfalfa in sludge-amended soils and inoculated with rhizobia produced in sludge. *J Environ Qual* 31(4):1339–1348
- Rizvi R, Khan AA (2009) Response of eggplant (*Solanum melongena* L.) to fly ash and brick kiln dust amended soil. *Biol Med* 1(2):20–24, http://biomedonline.com/Articles/vol1_2_20-24.pdf
- Sajtnikov E, Mrvić V, Cakmak D, Jaramaz D, Perović V, Antić Mladenović S, Pavlović P (2019) Pollution indices and sources apportionment of heavy metal pollution of agricultural soils near the thermal power plant. *Environ Geochem Heal* 41(5):2265–2279. <https://doi.org/10.1007/s10653-019-00281-y>
- Shutter EM, Fuhrmann JJ (2001) Soil microbial community responses to fly ash amendment as revealed by analyses of whole soils and bacterial isolates. *Soil Biol Biochem* 33(14):1947–1958
- Schwab AP, Ohlenbusch PD, Tomecek MB (1989) Revegetation of coal ash wastes without soil. An Interim Report. Agronomy Department, Throckmorton Hall, Kansas State University, Kansas
- Seneviratne M, Gunaratne S, Bandara T, Weerasundara L, Rajakaruna N, Seneviratne G, Vithanage M (2016) Plant growth promotion by *Bradyrhizobium japonicum* under heavy metal stress. *South Afr J Bot* 105:19–24, <https://www.sciencedirect.com/science/article/pii/S0254629916002490>
- SG RS 23/1994 (1994) Pravilnik o dozvoljenim količinama opasnih i štetnih materija u zemljištu i vodi za navodnjavanje i metodama njihovog ispitivanja, "Službeni Glasnik RS", broj 23/1994 ("Official Gazette Rep Serb.", 1994; 23: Regulation of allowed quantities dangerous and harmful substances in soil and water for irrigation and methods of their testing). <http://www.pravno-informacionisistem.rs/SIGlasnikPortal/eli/rep/sgrs/ministarstva/pravilnik/1994/23/1/reg>
- Shanker AK, Cervantes C, Loza-Tavera H, Avudainayagam S (2005) Chromium toxicity in plants. *Environ Int* 31(5):739–753
- Sharma V, Akhai S (2019) Trends in utilization of coal fly ash in India: a review. *J Eng Des Anal* 12(1):12–16
- Sharma SK, Kalra N (2006) Effect of fly ash incorporation on soil properties and productivity of crops—a review. *J Sci Indus Res* 65:383–390, <http://nopr.niscair.res.in/bitstream/123456789/4839/1/JSIR%2065%285%29%20383-390.pdf>. Accessed on 31 March 2021
- Sheng XF, Xia JJ, Jiang CY, He LY, Qian M (2008) Characterization of heavy metal-resistant endophytic bacteria from rape Brassica napus roots and their potential in promoting the growth and lead accumulation of rape. *Environ Pollut* 156(3):1164–1170
- Sheoran HS, Duhan BS, Kumar A (2014) Effect of fly ash application on soil properties: a review. *J Agroecol Nat Resour Manag* 1:98–103
- Shi W, Ma X (2017) Effects of heavy metal Cd pollution on microbial activities in soil. *Ann Agric Environ Med* 24(4):722–725, <https://pdfs.semanticscholar.org/e65d/5d70c5e0be91f0a1c93638dc9a7f4124164a.pdf>
- Silver S (1992) Plasmid-determined metal resistance mechanisms: range overview. *Plasmid* 27(1):1–3, <https://www.sciencedirect.com/science/article/pii/0147619X9290001Q>
- Silver S, Misra TK (1988) Plasmid-mediated heavy metal resistance. *Annu Rev Microbiol* 42:717–743. <https://www.annualreviews.org/doi/10.1146/annurev.mi.42.100188.003441>
- Simić A, Dželetović ŽS, Vučković S, Sokolović DR, Delić DI, Mandić V, Anđelković BS (2015) Usability value and heavy metals accumulation in forage grasses grown on power station ash deposit. *Hem Ind* 69(5):459–467, <http://r.istocar.bg.ac.rs/bitstream/handle/123456789/456/454.pdf?sequence=1>. Accessed on 31 March 2021.
- Simić A, Dželetović Ž, Vučković S, Čupina B, Mandić V, Krstić Đ (2014) Trace elements concentrations in Herbaceous plants from ash deposit of thermal power station. Integrated meeting "Planning and land use and landfills in terms of sustainable development and new remediation technologies", Zrenjanin, Proceedings: 167–174.
- Sims JT, Vasilas BL, Ghodrati M (1995) Development and evaluation of management strategies for the use of coal fly ash as a soil amendments. In: Proceedings of the 11th international symposium of the Am Coal Ash Assoc., Orlando, Florida, pp 8.1–18
- Srivastava M, Ma LQ, Singh N, Singh S (2005) Antioxidant responses of hyperaccumulators and

- sensitive species to arsenic. *J Exp Bot* 56:1335–1342, <https://academic.oup.com/jxb/article/56/415/1335/493769>
- Srivastava S, Verma PC, Chaudhary V, Singh N, Abhilash PC, Kumar KV, Sharma N, Singh N (2013) Inoculation of arsenic-resistant *Staphylococcus arlettae* on growth and arsenic uptake in *Brassica juncea* (L.) Czern. Var. R-46. *J Hazard Mater* 262:1039–1047, <https://www.sciencedirect.com/science/article/abs/pii/S0304389412008254>
- Stajković-Srbinović O, Buntić A, Rasulić N, Kuzmanović Đ, Dinić Z, Delić D, Mrvić V (2018) Microorganisms in soils with elevated heavy metal concentrations in southern Serbia. *Arch Biol Sci* 70(4):707–716, <http://www.serbiosoc.org.rs/arch/index.php/abs/article/view/2913>. Accessed on 31 March 2021
- Stajković-Srbinović O, Delić D, Rasulić N, Dj K, Houšková B, Sikirić B, Mrvić V (2017) Microorganisms in soils with high nickel and chromium concentrations in Western Serbia. *Pol J Environ Stud* 26 (4):1663–1671
- Stan V, Gament E, Cornea CP, Voaideş C, Mirela D, Plopeanu G (2011) Effects of heavy metal from polluted soils on the rhizobium diversity. *Not Bot Hort Agrobot Cluj* 39(1):88–95, <https://www.notulaeobotanicae.ro/index.php/nbha/article/view/6081>
- Surridge AKJ, Merwe A, Kruger R (2009) Preliminary microbial studies on the impact of plants and South African fly ash on amelioration of crude oil polluted soils. In: World of Coal Ash (WOCA) conference, proceedings (Lexington 4–7 May, 2009), Kentucky USA 2009, pp 4–7, <http://www.flyash.info/2009/008-surridge2009.pdf>. Accessed on 31 March 2021
- Tangahu BV, Abdullah S, Rozaimah S, Basri H, Idris M, Anuar N, Mukhlisin M (2011) A review on heavy metals (As, Pb, and Hg) uptake by plants through phytoremediation. *Int J Chem Eng* 2011:e939161, <https://www.hindawi.com/journals/ijce/2011/939161/>
- Tauanov Zh, Azat S, Baibatyrova A (2020) A mini-review on coal fly ash properties, utilization and synthesis of zeolites. *Int J Coal Prep Util*. <https://doi.org/10.1080/19392699.2020.1788545>
- The World Bank (2020) At glance. The World Bank in India. <https://www.worldbank.org/en/india/overview>. Accessed on 31 March 2021
- Tejeda-Agredano MC, Gallego S, Vila J, Grifol M, Ortega-Calvo JJ, Cantos M (2013) Influence of the sunflower rhizosphere on the biodegradation of PAHs in soil. *Soil Biol Biochem* 57:830–840
- Terzić A, Radojević Z, Miličić L, Pavlović L, Aćimović Z (2012) Leaching of the potentially toxic pollutants from composites based on waste raw material. *Chem Ind Chem Eng Q* 18(3):373–383, <http://www.doiserbia.nb.rs/img/doi/1451-9372/2012/1451-93721200013T.pdf>. Accessed on 31 March 2021
- Tiwari S, Kumari B, Singh SN (2008) Evaluation of metal mobility/immobility in fly ash induced by bacterial strains isolated from the rhizospheric zone of *Typha latifolia* growing on fly ash dump. *Bioresour Technol* 99(5):1305–1310, <https://www.sciencedirect.com/science/article/pii/S0960852407001459>
- Tiwari S, Singh SN, Garg SK (2012) Stimulated phytoextraction of metals from fly ash by microbial interventions. *Environ Technol* 33(21):2405–2413. <https://doi.org/10.1080/09593330.2012.670269>
- Tong Z, Sadowsky MJ (1994) A selective medium for the isolation and quantification of *Bradyrhizobium japonicum* and *Bradyrhizobium elkanii* strains from soils and inoculants. *Appl Environ Microbiol* 60(2):581–586, <https://pubmed.ncbi.nlm.nih.gov/16349188/>. Accessed on 31 March 2021
- Tripathi RD, Vajpayee P, Singh N, Rai UN, Kumar A, Ali MB, Kumar B, Yunus M (2004) Efficacy of various amendments for amelioration of fly-ash toxicity: growth performance and metal composition of *Cassia siamea* Lamk. *Chemosphere* 54:1581–1588, <https://www.sciencedirect.com/science/article/pii/S0045653503009639>
- Ugrenović V, Filipović V (2017) Cover crops: achievement of sustainability in the ecological systems of agriculture. In: Jean-Vasile A, Nicolò D (eds) Sustainable entrepreneurship and investments in the green economy, IGI Global, USA, 255–278. ISSN/ISBN 978-1-53610-255-0 (e-book). <https://doi.org/10.4018/978-1-5225-2075-7.ch009>, <https://www.igi-global.com/chapter/cover-crops/174476>
- Uliasz-Bocheńczyk A, Bąk P (2018) Management of waste from energy production—waste combustion in Poland. In: IOP conference series: materials science and engineering 427(1):012019, IOP Publishing
- Ullah A, Heng S, Munis MFH, Fahad S, Yang X (2015) Phytoremediation of heavy metals assisted by plant growth promoting (PGP) bacteria. *Environ Exp Bot* 117:28–40
- Vidojević D, Bacanović N, Dimić B (2014) Contaminated sites management in the Republic of Serbia. Integrated meeting “Planning and land use and landfills in terms of sustainable development and new remediation technologies”, Zrenjanin, Proceedings, pp 25–34
- Vodyanitskii YN (2016) Standards for the contents of heavy metals in soils of some states. *Ann Agrar Sci* 14 (3):257–263, <https://www.sciencedirect.com/science/article/pii/S1512188716300665>
- Vojinović Ž, Miličić B, Radin D, Dj K (1989) Prisustvo i aktivnost *R. meliloti* i *R. trifolii* u nekim zemljištima Srbije. *Mikrobiologija* 26:69–81
- Vukićević M, Popović Z, Despotović J, Lazarević L (2018) Fly ash and slag utilization for the serbian railway substructure. *Transport* 33(2):389–398. <https://doi.org/10.3846/16484142.2016.1252427>
- Wenzel WW, Kidd PS, Puschenreiter M, Rosenkranz T (2018) Nickel biogeochemistry at the Soil–Plant Interface. In: Tsadilas C, Rinklebe J, Selim M (eds) Nickel in soils and plants. CRC Press, Boca Raton, FL, UAS, 21–50. ISBN 9781498774604, <https://doi.org/10.1201/9781315154664-2>. Accessed on 31 March 2021
- Wetzel A, Werner D (1995) Ecotoxicological evaluation of contaminated soil using the legume root nodule

- symbiosis as effect parameter. *Environ Toxicol Water Qual* 10(2):127–134. <https://doi.org/10.1002/tox.2530100207>
- Woch MW, Radwańska M, Stanek M, Łopata B, Stefanowicz AM (2018) Relationships between waste physicochemical properties, microbial activity and vegetation at coal ash and sludge disposal sites. *Sci Total Environ* 642:264–275
- Wong MH, Wong JWC (1986) Effects of fly ash on soil microbial activity. *Environ Pollut Series A, Ecol Biol* 40(2):127–144. <https://www.sciencedirect.com/science/article/abs/pii/0143147186900802>
- World Economic Forum (2019) These countries are driving global demand for coal. <https://www.weforum.org/agenda/2019/02/these-countries-are-driving-global-demand-for-coal/>. Accessed on 31 March 2021
- Wu S, Cheung K, Luo Y, Wong M, (2006) Effects of inoculation of plant growthpromoting rhizobacteria on metal uptake by *Brassica juncea*. *Environ Pollut* 140(1):124–135. <https://www.sciencedirect.com/science/article/pii/S0269749105003611>
- Wuana RA, Okieimen FE (2011) Heavy metals in contaminated soils: a review of sources, chemistry, risk and best available strategies for remediation, *Isrn Ecol* 2011:ID402647
- Wyszkowska J, Boros E, Kucharski J (2007) Effect of interactions between nickel and other heavy metals on the soil microbiological properties. *Plant Soil Environ* 53(12):544–552. <https://81.0.228.28/publicFiles/00480.pdf>
- Yadav VK, Fulekar MH (2018a) The current scenario of thermal power plants and fly ash: production and utilization with a focus in India. *Int J Adv Eng Res Dev* 5(4):768–777
- Yadav VK, Fulekar MH (2018b) Biogenic synthesis of maghemite nanoparticles (γ -Fe₂O₃) using *Tridax* leaf extract and its application for removal of fly ash heavy metals (Pb, Cd). *Mater Today: Process* 5(9):20704–20710
- Yang S, Liang S, Yi L, Xu B, Cao J, Guo Y, Zhou Y (2014) Heavy metal accumulation and phytostabilization potential of dominant plant species growing on manganese mine tailings. *Front Environ Sci Eng* 8(3):394–404. <https://link.springer.com/article/10.1007%2Fs11783-013-0602-4>
- Yao ZT, Ji XS, Sarker PK, Tang JH, Ge LQ, Xia MS, Xi YQ (2015) A comprehensive review on the applications of coal fly ash. *Earth-Sci Rev* 141:105–121
- Yuan M, He H, Xiao L, Zhong T, Liu H, Li S, Deng P, Ye Z, Jing Y (2013) Enhancement of Cd phytoextraction by two *Amaranthus* species with endophytic *Rahnella* sp. JN27. *Chemosphere* 103:99–104. <https://www.sciencedirect.com/science/article/pii/S0045653513016305>
- Yousuf A, Manzoor ShO, Youssouf M, Malik ZA, Khawaja S (2020) Fly ash: production and utilization in India—an overview. *J Mater Environ Sci* 11(6):911–921. https://www.jmaterenvironsci.com/Document/vol11/vol11_N6/JMES-2020-1182-Yousuf.pdf. Accessed on 31 March 2021
- Zahran HH (1999) Rhizobium-legume symbiosis and nitrogen fixation under severe conditions and in an arid climate. *Microbiol Mol Biol Rev* 63(4):968–989. <https://mmbr.asm.org/content/membr/63/4/968.full.pdf>
- Zhang X, Xia H, Li ZA, Zhuang P, Gao B (2011) Identification of a new potential Cd-hyperaccumulator *Solanum photeinocarpum* by soil seed bank-metal concentration gradient method. *J Hazard Mater* 189(1–2):414–419
- Zhang Y, He L, Chen Z, Wang Q, Qian M, Sheng X (2011b) Characterization of ACC deaminase-producing endophytic bacteria isolated from copper-tolerant plants and their potential in promoting the growth and copper accumulation of *Brassica napus*. *Chemosphere* 83(1):57–62. <https://www.sciencedirect.com/science/article/pii/S0045653511000695>
- Zhang ZQ, Wong MH, Nie XP, Lan CY (1998) Effects of zinc (zinc sulfate) on Rhizobia-earleaf acacia (*Acacia auriculaeformis*) symbiotic association. *Bioresour Technol* 64(2):97–104. <https://www.sciencedirect.com/science/article/pii/S0960852497001831>
- Zhou H, Zhou X, Zeng M, Liao BH, Liu L, Yang WT, Wu YM, Qiu QY, Wang YJ (2014) Effects of combined amendments on heavy metal accumulation in rice (*Oryza sativa* L.) planted on contaminated paddy soil. *Ecotoxicol Environ Saf* 101:226–232
- Żołniercz L, Weber J, Gilewska M, Strączyńska S, Pruchniewicz D (2016) The spontaneous development of understory vegetation on reclaimed and afforested post-mine excavation filled with fly ash. *Catena* 136:84–90. <https://www.sciencedirect.com/science/article/abs/pii/S0341816215300679>



Crop Yield Limitation by Soil Organic Matter Decline: A Case Study from the US Pacific Northwest

27

Rajan Ghimire, Prakriti Bista,
and Stephen Machado

Abstract

Soil degradation has become a significant challenge for agricultural and environmental sustainability. Continuous depletion in soil organic carbon (SOC) and nitrogen (N) in the past century has considerably affected agricultural productivity and sustainability in semiarid drylands of the inland Pacific Northwest (IPNW) of the USA. This chapter discusses linkages between soil organic matter depletion and yield decline in a winter wheat-summer fallow (WW-SF) system in the IPNW based on data obtained from a long-term study (>80 y). Studies conducted in dryland winter wheat-summer fallow (WW-SF) systems revealed a decrease in SOC and N storage in the profile. Specifically, SOC content decreased by $280 \text{ kg ha}^{-1} \text{ yr}^{-1}$ in the top 30 cm soil depth with fall burning of crop residue (FB), while it was decreased by $226 \text{ kg ha}^{-1} \text{ yr}^{-1}$ in no burning of crop residue (NB). The decline in yield was

observed with a decrease in SOC and N stocks over the years, mainly due to long fallow periods between wheat crops, crop residue burning, insufficient residue returns, and intensive tillage practices. The only treatment that maintained SOC in the top 30 cm depth was manure (MN) treatment, indicating that SOC and N, added in larger amounts under this treatment, play a crucial role in SOC maintenance, crop production, and sustainability of WW-SF systems. Results of the long-term studies show a continued declining trend in SOC and nutrients under the WW-SF system, thus negatively impacting soil health, further reducing crop yield in dryland cropping in the IPNW. A decrease in SOC and N in the soil profile leads to soil degradation, affecting the sustainability of dryland WW-SF systems in the IPNW and similar agroecosystems worldwide. Cropping system intensification, residue addition, or organic amendment additions can maintain SOC and support sustainable crop production.

Keywords

Drylands · Soil degradation · Soil organic carbon · Sustainability · Wheat-fallow system

R. Ghimire (✉)
Agricultural Science Center, New Mexico State
University, 2346 State Road 288, Clovis, NM 88101,
USA
e-mail: rghimire@nmsu.edu

P. Bista · S. Machado
Oregon State University, Columbia Basin
Agricultural Research Center, Pendleton, OR, USA
e-mail: Stephen.Machado@oregonstate.edu

27.1 Introduction

Feeding 9.1 billion people by 2050 while minimizing environmental degradation is the greatest challenge currently facing humankind. The soil is a foundational resource for sustainable agriculture and environmental quality. Therefore, soil degradation, a decline in soil health with associated reductions in ecosystem functioning and services, significantly impact global food production and human nutrition. Semiarid drylands in the IPNW region of the USA face challenges in sustainably increasing crop yields due to a decrease in soil health, specifically, the continuous decline in soil organic matter (SOM) and nutrients in soil profiles (Machado et al. 2006; Brown and Huggins 2012). Farmers in this region typically burn or remove residues after crop harvest in the fall, till soils, and fallow land for 13–14 months after harvest (Schillinger et al. 2003; Schillinger and Papendick 2008). Long-fallow periods, repeated tillage, and crop residue removal lead to a rapid depletion in SOM and nutrients, ultimately reducing soil health and crop yields.

Soil organic matter is a key component for improving soil health because SOM controls many soil properties and processes important for sustainable crop production. Long-term studies have consistently demonstrated the value of increasing carbon (C) inputs to maintain soil fertility and combat land degradation. Studies at the Pendleton Long-term Experiments (PLTES) revealed that dryland cropping systems that include long fallow periods and intensive tillage had lost 50–70% of the SOC, a proxy of SOM, storage in the last 80 years (Ghimire et al. 2015). In the same period, about 37–70 kg N ha⁻¹ was lost in grain harvest each crop year, leading to continuous depletion in soil N reservoir and decline in crop production. Management systems that increase SOC and N, proxies of SOM accrual, are pertinent to sustainable crop production and environmental quality improvement. For example, green manuring, compost and biosolids application, and crop residue recycling increase SOC compared to farming practices that

do not add organic matter (Rasmussen and Parton 1994; Wuest and Gollany 2013; Chatterjee et al. 2017; Kumar et al. 2020; Li et al. 2020). Dryland producers in the IPNW still rely on soil management strategies that do not produce enough C inputs or add external inputs to support crop production, leading to the downward spiral of soil health degradation over the years.

Long-term studies that evaluate SOC and nutrients for several decades have significantly contributed to our understanding of how management systems affect SOC sequestration, nutrient cycling, and associated ecosystem services. Long-term studies are specifically important in semiarid regions where soil responses to management practices on SOC and nutrient accumulation are very slow (Rasmussen and Parton 1994; Machado 2011). Pendleton long-term experiments (PLTEs), the oldest long-term experiments in the western US with more than 80 years of cropping history, provide valuable information on how changes in SOC and nutrient dynamics over time have affected agroecosystems services in the semiarid drylands. Here, we present the case study that compares the long-term trend of SOC and N and their relationship with winter wheat yield in a WW-SF system.

27.2 Experimental Site and Treatments

Assessment of yield decline as a function of SOM depletion was studied in the Crop Residue Long-term experiment (CR-LTE), one of the WW-SF studies conducted at the Columbia Basin Agricultural Research Center (CBARC) at Pendleton, OR (45°42'N, 118°36'W, 438 m elev.). The soil at the study site had a silt loam texture with low to medium fertility status. The site had a Mediterranean climate. Detail of the treatments and experimental design was presented in Ghimire et al. (2015, 2018). In brief, this case study evaluated SOC, N, and crop yield under FB, NB, MN, and pea vine (PV) treatments in the CR-LTE (Table 27.1). Winter wheat residues were removed by burning in FB

Table 27.1 Soil carbon (C) and nitrogen (N) inputs and rate of change during 1931–2010 in 0–30 cm depth of selected treatments in the crop residue long-term experiment

Trt†	Annualized C input			dC/dt	Annualized N input			dN/dt
	Crop residue	Other sources	Total		Crop residue	Other amendments	Total	
	Mg ha ⁻¹ yr ⁻¹				Kg ha ⁻¹ yr ⁻¹			
FB	0.46	–	0.46	–0.26	5.64	–	5.64	–0.015
NB	1.51	–	1.51	–0.21	18.5	–	18.29	–0.016
PV	2.13	0.41	2.54	–0.10	26.0	18.5	44.5	–0.004
MN	2.83	0.85	3.68	+0.02	35.0	70.0	105.0	+0.003

†FB and NB indicate fall burning and no burning of crop residues, PV is pea vine incorporation, and MN is manure application.

treatment throughout the study period (1931–2010), while residues were retained in the NB treatment. Additional residue/amendment was supplied through the cattle manure and pea vines in MN and PV treatments. The study was established in 1931, and a medium-tall variety (Rex M-1) of winter wheat was grown until 1966. Multiple semi-dwarf varieties have been grown since then across the treatments compared in this case study (Ghimire et al., 2015).

Fall burning of wheat residue in FB treatment was conducted in late September after wheat harvest (Fig. 27.1), followed by the rod weeding of the field in the spring to control weeds. Primary tillage in late spring of the fallow year incorporated crop residues to a depth of 20 cm in PV, MN, and NB treatments. Pea vine residues from a nearby farm-field added 0.41 Mg C ha⁻¹ yr⁻¹ and 18.5 kg N ha⁻¹ yr⁻¹. Similarly, steer manure from a nearby cattle operation added 0.85 Mg C ha⁻¹ yr⁻¹ and 70 kg N ha⁻¹ yr⁻¹ in addition to above- and belowground biomass C and nutrients from wheat residues. Wheat residues added annual C input equivalent to 2.13 Mg ha⁻¹ and 2.83 Mg ha⁻¹ in PV and MN treatments. Wheat residue added 1.51 Mg ha⁻¹ yr⁻¹ and 18.5 kg ha⁻¹ yr⁻¹ C and N inputs in NB, and 0.46 Mg ha⁻¹ yr⁻¹ and 5.64 kg ha⁻¹ yr⁻¹ C and N inputs in FB.

Winter wheat was planted in mid-October and harvested in mid-July of the following year. The

field was left fallow for the 14 months after wheat harvest and before planting the next wheat crop in the following year. Tillage practices included cultivation with moldboard plow in the fall and using cultivator and harrow in the spring. Until 2002, wheat was planted at 90 kg ha⁻¹ in rows 17.3 cm apart using a John Deere no-till drill and after that at 92 kg ha⁻¹ in rows 16.5 cm apart using Great Plains International Disc Drill. Wheat yield was estimated at approximately 9–12% grain moisture by harvesting a center portion of a plot.

Giddings hydraulic probe was used to collect soil samples from 0–30 cm and 30–60 cm depths after wheat harvest (Fig. 27.2). Hand probes was used for collecting soil samples in earlier years. After all visible crop residues, including roots, stems, and leaves, were removed, soil samples were sieved to pass through a 2-mm screen. Then, approximately 10-g subsamples were oven-dried at 60 °C for 72 h, finely ground (0.05 mm) on a Shatter Box 8530 ball mill, and SOC and N were analyzed in a dry combustion CN analyzer. This method of soil sampling and analysis was used in 1995, 2005, and 2010 samplings. The SOC analysis method for samples collected during 1931–1986 varied based on the analyzers available (Rasmussen and Parton, 1994). The SOC and N content (kg ha⁻¹) were calculated by using SOC and N concentrations (g kg⁻¹) and soil bulk density (BD) data collected at



Fig. 27.1 Winter wheat-summer fallow system typical to the inland Pacific Northwest of USA (a) and fallow field after fall burning of wheat residues (b) at Pendleton, OR, USA

different periods of the experiment (Ghimire et al. 2015).

Treatment averages were used for long-term trend analysis of wheat yield (1931–2010), SOC, and N. After 1967, semi-dwarf varieties replaced the medium-tall variety (Rex M-1) planted from

1931 to 1967. Hence, for the time-periods 1931–1966 and 1967–2010, wheat yield trends under different treatments were analyzed separately using a linear or quadratic autoregression procedure (PROC AUTOREG) in SAS. Furthermore, suitable (linear or quadratic)



Fig. 27.2 Soil sample collection from long-term experiments at Pendleton OR, USA

autoregression models were used for the trend analysis of SOC and TN (1931–2010). The yield trend from 1931 to 2010 was also analyzed using an autoregressive integrated moving average (ARIMA) model (Brocklebank and Dickey, 2003), a time-series forecasting approach to understand long-term trends.

$$[(1 - B)Y]_t = \mu + \left(\frac{\theta(B)}{\phi(B)} \right) \times a_t \quad (27.1)$$

where, Y is the response variable, B is the backshift operator, t is time (year), and the backshift operation $BX_t = X_{t-1}$, μ is a mean term; $\theta(B)$ is the moving-average operator, $\phi(B)$ is the autoregressive operator, and $a_t =$ random error. Pearson correlation quantified the relationship between SOC, TN, and wheat yield. Results from

statistical analyses were deemed significant when $p < 0.05$.

27.3 Results and Discussion

27.3.1 Changes in Soil Organic Carbon and Nitrogen

The SOC and TN in the drylands of IPNW have significantly depleted due to the continuous use of WW-SF system. The long-term trend of SOC from 1931–2010 showed a linear decrease over time. The SOC declined at the rate of $116 \text{ kg ha}^{-1} \text{ yr}^{-1}$ in PV, $280 \text{ kg ha}^{-1} \text{ yr}^{-1}$ in FB, and $226 \text{ kg ha}^{-1} \text{ yr}^{-1}$ in NB treatments in 0–30 cm depth (Fig. 27.3). The rapid decrease in SOC was associated with low biomass C input and

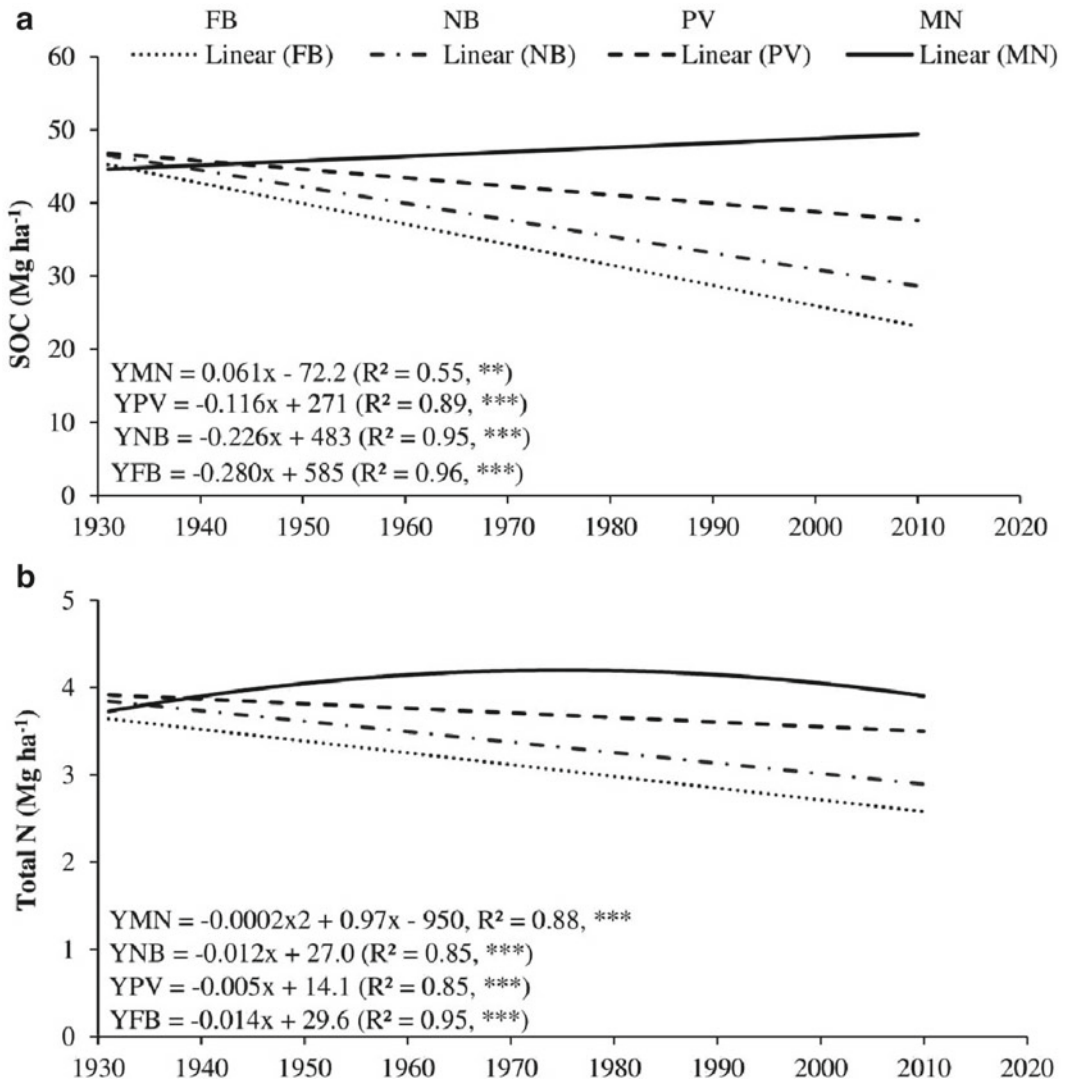


Fig. 27.3 The trend of soil organic carbon (a) and total N (b) in 0–30 cm depth of crop residue long-term experiment (1931–2010). FB, fall burning of wheat residue; MN, manure application (22.4 Mg ha⁻¹ crop⁻¹); PV, pea vine incorporation (2.24 Mg ha⁻¹ crop⁻¹); and

NB, no burning of wheat residue. Stars ** and *** indicate that trends are statistically significant at $p < 0.01$ and $p < 0.001$, respectively. Recent unpublished data for 2010–2020 show a continued declining trend in SOC and N

SOC loss during soil microbial respiration. Our unpublished data show that trend of SOC has not been changed during 2010–2020 as well. The SOC maintenance in agroecosystems depends on C input from crop residues, amendments, and soil microbial biomass and loss through decay or erosion (Huggins et al. 1998; Smith 2008; He et al. 2020; Wiesmeier et al. 2020). A previous study in the CR-LTE revealed

that a minimum biomass C input of about 3.27 Mg ha⁻¹ yr⁻¹ is required to maintain SOC in a WW-SF system in the IPNW drylands (Machado 2011). Considering root biomass C as 45% of aboveground biomass C, the annual return of above- and belowground residue C was insufficient in PV, NB, and FB treatments. In addition, more than half of the residue C was lost due to burning in the FB treatment of this

experiment. Biomass C input was up to 72% and 33% lower in FB and NB, respectively, than the required C input to maintain the SOC in these systems. Insufficient organic inputs likely caused the continuous depletion in SOC content. The average SOC content increased in MN treatment at $61 \text{ kg ha}^{-1} \text{ yr}^{-1}$ in 0–30 cm soil depth. In this case, C input was enough to maintain the SOC level suggesting that manure addition could be one of the ways to revert soil degradation in semiarid drylands where crop residue C is not enough to maintain SOC.

Variation in decay rates of organic residues affects SOC equilibrium in agroecosystems (Huggins et al. 1998). A higher decay rate (dC/dT ; dN/dT) would be expected with the larger input of organic residues, but studies at CBARC showed a lower SOC decay rate in PV and FB treatments (Table 27.1). It appears pea vine and fall burning lowered SOC decay rate while manure application did not affect SOC decay. Therefore, manure-derived C was accumulated in surface soil. In contrast, residue burning removed the labile fraction of biomass C, leaving more recalcitrant materials in the soil with a low decay rate (Neff et al. 2005).

We speculated high-quality pea residue, as indicated by its low C:N ratio helped in reducing SOC decay by reducing priming of existing organic matter in the soil. The C:N ratio for different treatments was as follows: manure (12.1), pea vines (22.2), and wheat residue (81.8). Huggins et al. (1998) showed that low C:N ratio residues minimizes SOC depletion and contribute to SOM building. On the other hand, a lower decay rate in FB compared to NB

treatment is probably attributed to the loss of readily decomposable organic compounds during residue burning. The limited amount of recalcitrant SOC was not enough for maintaining SOC. The labile SOC also has a high decay rate making it more susceptible to loss. More research toward understanding the biochemical composition of residues and the SOC decay rate will help our understanding of how a change in residue quality after burning influences SOC and N dynamics in agroecosystems.

The trend of TN in 0–30 cm depth of MN treatment followed a polynomial curve indicating that soil N increased slightly during the 1931–1995 period and decreased afterward (Fig. 27.3). In PV, NB, and FB treatments, soil TN decreased linearly from 1931–2010. The rate of TN loss was $5 \text{ kg ha}^{-1} \text{ yr}^{-1}$, $12 \text{ kg ha}^{-1} \text{ yr}^{-1}$, and $14 \text{ kg ha}^{-1} \text{ yr}^{-1}$ and in PV, NB, and FB treatments, respectively. It appears soil N content also has a threshold to maintain soil profile N and support sustainable crop production. Similarly, a related PLTEs study by Ghimire et al. (2017) showed that to maintain crop yield in a WW-SF system in the IPNW, the addition of $90 \text{ kg N ha}^{-1} \text{ crop}^{-1}$ ($45 \text{ kg N ha}^{-1} \text{ yr}^{-1}$) is required.

27.3.2 Wheat Yield Trends

We observed a linear decrease in the yield of medium-tall variety (Rex M-1) in all treatments during 1931–1966, with a significant loss in wheat production in NB and FB treatments. The rate of yield decline was 9 kg ha^{-1} in MN, 18 kg ha^{-1} in PV, 30 kg ha^{-1} in NB, and

Table 27.2 Summary statistics of a long-term trend in crop yield in medium-tall (1931–1966) and short wheat varieties (1967–2010) using the best fitting Autoregressive models

Trt	1931–1966		1967–2010	
	Model	Significance	Model	Significance
FB	$CY_{(FB)t} = -0.036t + 73.3$	***	$CY_{(FB)t} = -0.02t + 43.9$	***
NB	$CY_{(NB)t} = -0.030t + 60.8$	***	$CY_{(NB)t} = -0.02t + 42.4$	**
PV	$CY_{(PV)t} = -0.018t + 37.0$	ns	$CY_{(PV)t} = -0.002t^2 + 6.61t - 6552$	*
MN	$CY_{(MN)t} = -0.009t + 21.1$	ns	$CY_{(MN)t} = -0.004t^2 + 14.0t - 13921$	**

† $CY_{(x)t}$ = Crop yield in treatment X, where X include FB, NB, PV, MN; FB = fall burning of crop residue; NB = no burning of crop residue; PV = pea vine incorporation; MN = manure addition; t = time (year).

36 kg ha⁻¹ in FB treatments per year during this period (Table 27.2). However, the yield trend of semi-dwarf varieties (1967–2010) followed a polynomial trend in MN and PV treatments and a linear trend in yield in FB and NB treatments with the loss of 20 kg ha⁻¹ yr⁻¹. Moreover, wheat yields were not significantly different between FB and NB treatments despite some differences in SOC and N loss. Throughout the study period, both treatments did not receive any organic amendments or fertilizers.

The overall trend of wheat yield from 1931–2010 was analyzed using ARIMA models (Fig. 27.4). The ARIMA models use a combination of autoregressive (AR), integration (I), and moving average (MA) functions. An ARIMA model represents the autoregressive components (p), the number of differencing operators (d), and the moving average term to generate outcomes. Since we had a difference in wheat varieties over time, this was the best approach to evaluate the overall trend. Wheat yield increased across all treatments after introducing semi-dwarf wheat varieties in 1967, but within a few years, it started to decrease again,

specifically in FB and NB treatments. The high yield of semi-dwarf wheat varieties sustained for several years in PV and MN before the decreasing trend started in the 1990s. Our recent unpublished data show that the declining trend has continued even during 2010–2020.

27.3.3 Soil Organic Carbon and Nitrogen Loss Affect Wheat Yield

High SOC and N content are often associated with good soil aggregation (Six et al. 2002; Zhou et al 2020), high microbial biomass, activity, and diversity (Ghimire et al. 2014), high root biomass (Qin et al. 2004), and improved water storage (Sherrod et al. 2005). These improvements in soil quality indicators are often associated with high crop yields and quality. In contrast, insufficient organic inputs, repeated tillage, erosion, or other forms of soil degradation (Fig. 27.5) negatively impact crop production. For example, low organic C and N input likely caused continuous depletion in SOC and N contents and reduced

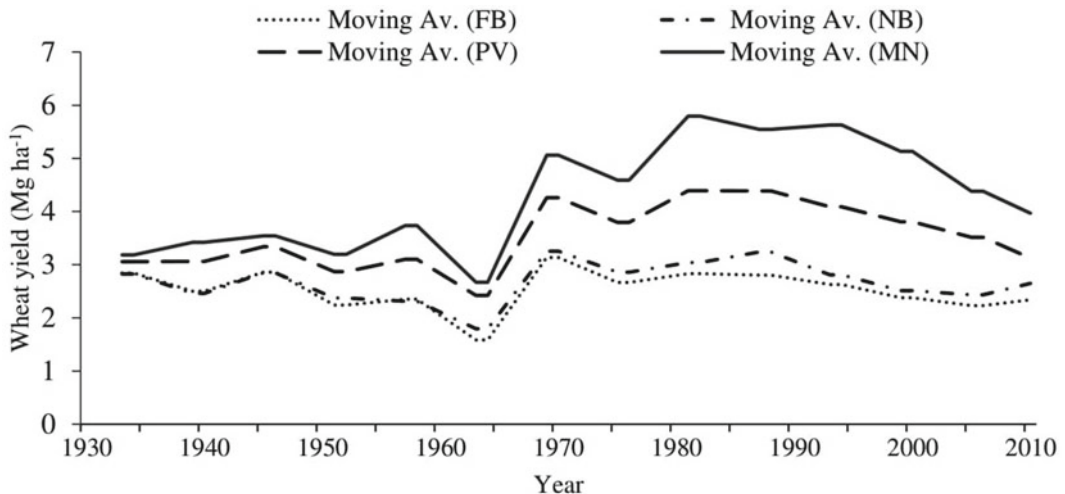


Fig. 27.4 Crop yield trend during 1931–2010 in the selected treatment of crop residue long-term experiment using autoregressive integrated moving average (ARIMA) model. FB, fall burning of wheat residue; MN, manure

application (22.4 Mg ha⁻¹ crop⁻¹); PV, pea vine incorporation (2.24 Mg ha⁻¹ crop⁻¹); and NB, no burning of wheat residue



Fig. 27.5 Wind erosion in the conventionally tilled wheat field in eastern Oregon, USA

Table 27.3 Soil carbon and nitrogen at 0–30 cm soil depth was highly correlated with crop yield in selected treatments of the crop residue long-term experiment

Period	SOC†		TN	
	Correlation	Significant	Correlation	Significance
1931–1966	0.79	***	0.86	***
1967–2010	0.87	***	0.92	***
1931–2010	0.56	***	0.65	***

†Correlation analysis between annual winter wheat yield, soil organic carbon (SOC), and total nitrogen (TN) data for the given period of time.

wheat yield in the WW-SF systems (Table 27.3). Specifically, no external input of N was supplied through mineral fertilizer or legumes to the FB and NB treatments for > 80 years. These treatments were highly N limited for much of the study period, while 37–70 kg N ha⁻¹ was lost in grain harvest each year (Rasmussen and Parton 1994).

Grain N data from 1986–2004 showed MN treatment was the only treatment that maintained a positive N balance (Ghimire et al., 2018). Insufficient N from residues and continuous depletion of N stock from the soil profile caused all other treatments to have a net negative N balance. The MN and PV treatments appeared to have maintained a positive N balance for several years, at least in the surface soil. This positive N

balance helped in maintaining crop yields in MN treatments, but ultimately yield decline was observed starting 1990s. Since TN mineralization was the only source of available N for the crop in FB and NB treatments, irrespective of the crop variety changes over time, the continuous depletion of TN was observed in these treatments, leading to greater decline in crop yields.

It is often argued that N addition can minimize crop yield decline in the WW-SF system. The previous study on these plots demonstrated the addition of 90 kg N ha⁻¹ crop⁻¹ is needed to maintain crop yield in a WW-SF system (Ghimire et al., 2017). However, further increase in N input did not increase wheat yield, rather decreased SOC and TN stock and increased soil acidity (Fig. 27.6). Similarly, the addition of

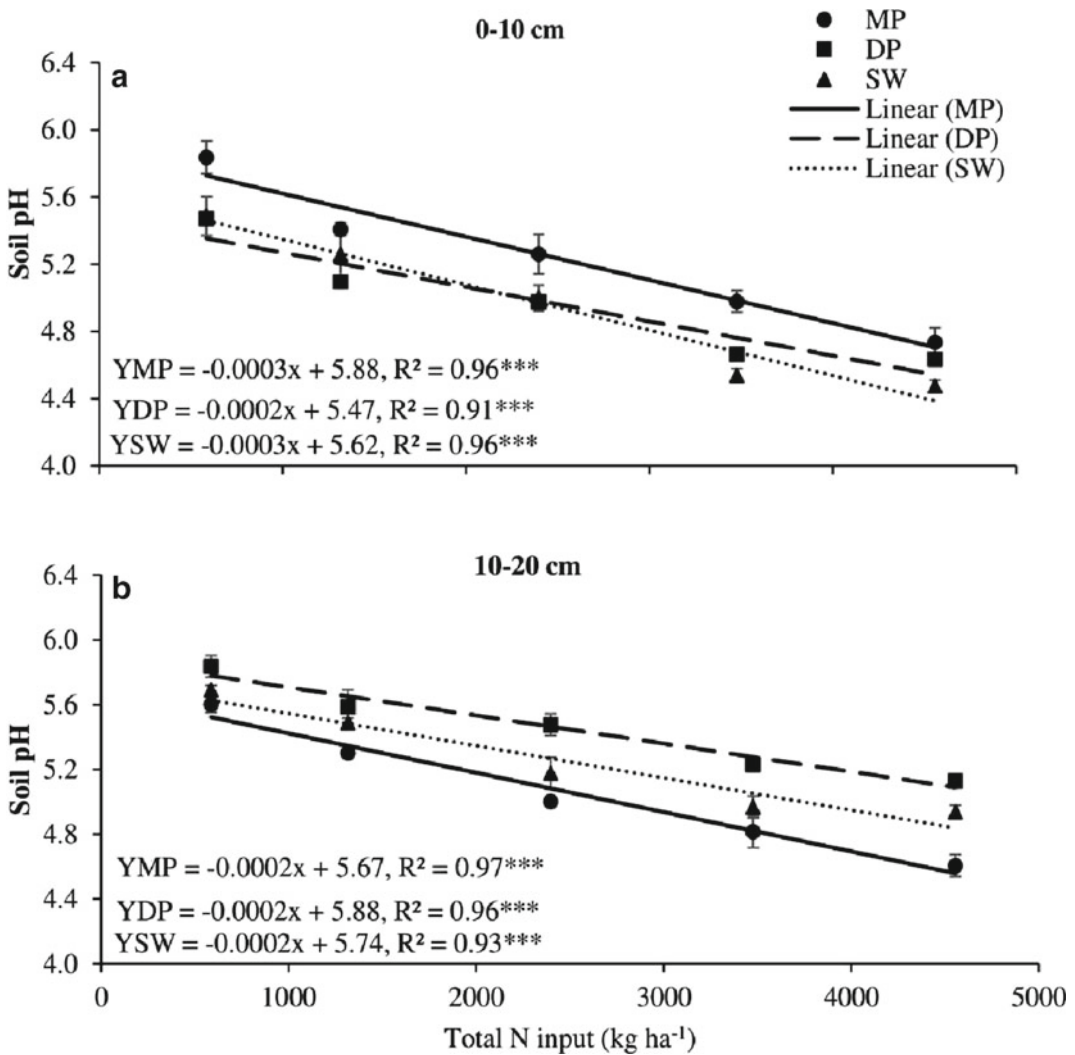


Fig. 27.6 The relationship between total fertilizer N input (1941–2010) and soil pH in 2010 in (a) 0–10 and (b) 10–20 cm depths of a winter wheat–summer fallow

system under moldboard plow (MP), disc plow (DP), and sweep (SW) tillage management

180 kg N ha^{-1} every other year (annual rate of 90 $\text{kg N ha}^{-1} \text{yr}^{-1}$) in a long-term WW-SF experiment did not stop the depletion of SOC and N. The N input on manure treatment was 105 $\text{kg N ha}^{-1} \text{yr}^{-1}$, which was sufficient to maintain positive N balance in 0–30 cm depth, but did not offset yield loss during 1995–2010 and beyond, potentially due to loss of SOC and N reservoir from below 30 cm soil depth (Ghimire et al. 2018). Furthermore, the decline rate in SOC was more rapid after 1986, possibly due to

a change in wheat from tall to semi-dwarf varieties (Ghimire et al. 2015). The biomass C supply controls SOC levels in agroecosystems. Semi-dwarf varieties produce smaller biomass compared to tall varieties, reducing biomass C and N inputs.

27.3.4 Importance of Subsoil Fertility to Maintain Wheat Yield

The nutrients and SOC in the top 20–30 cm soil depth from the surface have been extensively studied. However, very few studies report changes in subsoil fertility and their potential impacts on soil processes because the response of deeper soil to management changes usually takes several

decades. Long-term experiments, such as CR-LTE, can be an excellent resource for understanding the role of subsoil C and nutrients on crop yield and sustainability. Although SOC was maintained in surface 0–30 cm depth in MN treatment of the CR-LTE, its level in 30–60 cm decreased consistently across all treatments (Fig. 27.7) at a rate of 175–200 kg ha⁻¹ yr⁻¹. Loss of the soil functions associated with

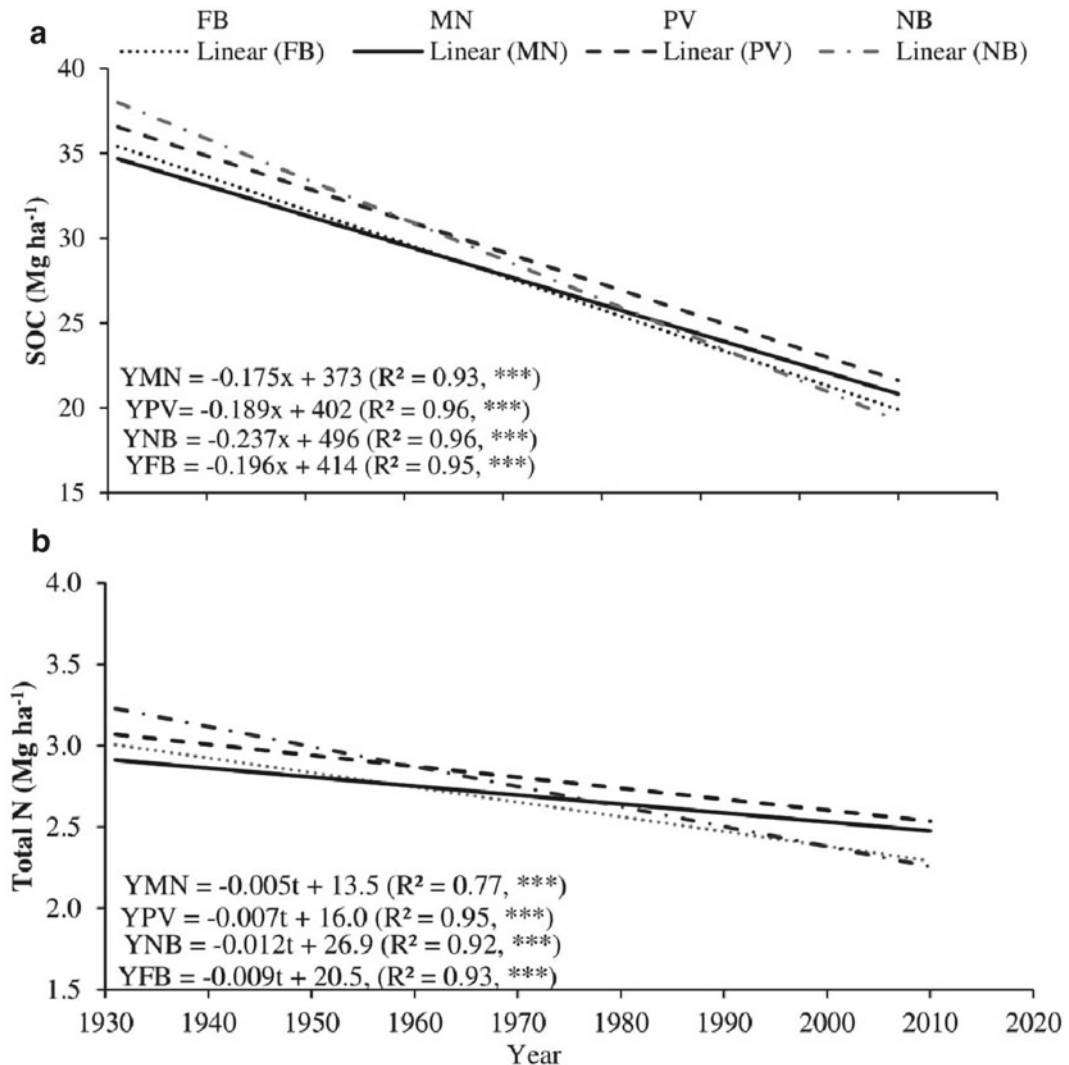


Fig. 27.7 The trend of soil organic carbon (a) and total N (b) in subsoil (30–60 cm) depths of crop residue long-term experiment (1931–2010). FB, fall burning of wheat residue; MN, manure application @22.4 Mg ha⁻¹ crop⁻¹;

PV, pea vine incorporation (2.24 Mg ha⁻¹ crop⁻¹); and NB, no burning of wheat residue (Modified from Ghimire et al. 2018)

depletion in SOC and N has significantly reduced crop yield and SOM turnover (Huggins et al. 1998; Sherrod et al. 2005). The SOC loss from the lower depth may have contributed substantially to low soil nutrient and water storage, thereby decreasing wheat yields.

27.4 Conclusion

The study of SOC, N, and winter wheat yield trends over >80 demonstrated the crucial role of long-term field experiments for understanding management impacts on soil health and possible site degradation risks. Our study shows the adverse effects of current soil management practices on soil health, resulting in SOM depletion and crop yield decline. The only treatment that maintained SOC in the top 30 cm soil was manured (MN) treatment. Larger amounts of organic matter input under this treatment played a pivotal role in maintaining SOC and sustaining crop production in the WW-SF system. Nevertheless, decrease in SOM under the WW-SF system will continue to negatively impact soil health and reduce crop yields in the drylands of the IPNW. Imbedding long-term analytical data into Agroecosystem Models and other innovative experiments could help in finding sustainable management practices for cropping systems in the IPNW region of the US and semiarid agroecosystems facing soil degradation. The SOC and N in soil profiles play a crucial role in improving the sustainability of dryland farming in semiarid environments.

References

- Brocklebank JC, Dickey DA (2003) SAS for forecasting time series. SAS Institute Inc., Cary, NC, USA
- Brown TT, Huggins DR (2012) Soil carbon sequestration in the dryland cropping region of the Pacific Northwest. *J Soil Water Conserv* 67:406–415
- Chatterjee R, Gajjela S, Thirumdasu RK (2017) Recycling of organic wastes for sustainable soil health and crop growth. *Int J Waste Resour* 7:296. <https://doi.org/10.4172/2252-5211.1000296>
- Ghimire R, Machado S, Bista P (2018) Decline in soil organic carbon and nitrogen limits yield in wheat-fallow systems. *Plant Soil* 422:423–435
- Ghimire R, Machado S, Bista P (2017) Soil pH, soil organic matter, and crop yields in winter wheat-summer fallow systems. *Agron J* 109:706–717
- Ghimire R, Machado S, Rhinhart K (2015) Long-term crop residue and nitrogen management effects on soil profile carbon and nitrogen in wheat-fallow systems. *Agron J* 107:2230–2240
- Ghimire R, Norton JB, Stahl PD, Norton U (2014). Soil microbial substrate properties and microbial community responses under irrigated organic and reduced-tillage crop and forage production systems. *PLoS One* 9(8):e103901
- He G, Zhang Zh, Zhang J, Huang X (2020) Soil organic carbon dynamics and driving factors in typical cultivated land on the karst Plateau. *Int J Environ Res Public Health*, 17:5697. <https://doi.org/10.3390/ijerph17165697>
- Huggins DR, Buyanovsky GA, Wagner GH, Brown JR, Darmody RG, Peck TR, Lesoing GW, Vanotti MB, Bundy LG (1998) Soil organic C in the tallgrass prairie-derived region of the corn belt: effects of long-term crop management. *Soil till Res* 47:219–234
- Kumar S, Samiksha, Sukul P (2020) Green manuring and its role in soil health management. In: Giri AV (ed) Chapter 13: Springer Nature Switzerland AG 2020B. *Soil Health, Soil Biology*, vol 59. https://doi.org/10.1007/978-3-030-44364-1_13219
- Li Z, Zhang X, Xu J. et al. (2020) Green manure incorporation with reductions in chemical fertilizer inputs improves rice yield and soil organic matter accumulation. *J Soils Sediments* 20:2784–2793 (2020). <https://doi.org/10.1007/s11368-020-02622-2>
- Machado S (2011) Soil organic carbon dynamics in the Pendleton long-term experiments: implications for biofuel production in Pacific Northwest. *Agron J* 103:253–260
- Machado S, Reinhart K, Petrie S (2006) Long-term cropping system effects on carbon sequestration in eastern Oregon. *J Environ Qual* 35:1548–1553
- Neff JC, Harden JW, Gleixner G (2005) Fire effects on soil organic matter content, composition, and nutrients in boreal interior Alaska. *Can J for Res* 35:2178–2187
- Qin RJ, Stamp P, Richner W (2004) Impact of tillage on root systems of winter wheat. *Agron J* 96:1523–1530
- Rasmussen PE, Parton WJ (1994) Long-term effects of residue management in wheat-fallow. I. Inputs, yield, and soil organic matter. *Soil Sci Soc Am J* 58:523–530
- Schillinger WF, Papendick RI (2008) Then and now: 125 years of dryland wheat farming in the Inland Pacific Northwest. *Agron J* 100:S166–S182

- Schillinger WF, Papendick RI, Guy SO, Rasmussen PE, van Kessel C (2003) Dryland cropping in the Western United States. Pacific northwest conservation tillage handbook series No 28, Chapter 2—Conservation tillage systems and equipment
- Sherrod LA, Peterson GA, Westfall DG, Ahuja LR (2005) Soil organic carbon pools after 12 years in no-till dryland agroecosystems. *Soil Sci Soc Am J* 69:1600–1608
- Six J, Feller C, Deneff K, Ogle SM, Sa JCD, Albrecht A (2002) Soil organic matter, biota and aggregation in temperate and tropical soils—effects of no-tillage. *Agronomie* 22:755–775
- Smith P (2008) Land use change and soil organic carbon dynamics. *Nutr Cycl Agroecosyst* 81:169–178
- Wiesmeier M, Mayer S, Burmeister F, Hübner R, Kögel-Knabner I (2020) Feasibility of the 4 per 1000 initiative in Bavaria: a reality check of agricultural soil management and carbon sequestration scenarios. *Geoderma* 369:114333. <https://doi.org/10.1016/j.geoderma.2020.114333>
- Wuest SB, Gollany HT (2013) Soil organic carbon and nitrogen after application of nine organic amendments. *Soil Sci Soc Am J* 77:237–245
- Zhou M, Liu C, Wang J et al (2020) Soil aggregates stability and storage of soil organic carbon respond to cropping systems on Black Soils of Northeast China. *Sci Rep* 10:265. <https://doi.org/10.1038/s41598-019-57193-1>



Changes in the Composition and Dynamics of Soil Humus and Physical Properties in Dark Chestnut Soils of Trans-Volga Dry Steppes After 75 and 35 years of Irrigation Agriculture

Nina A. Pronko, Viktor V. Korsak,
Lubov G. Romanova,
and Alexandr S. Falkovich

Abstract

Soil organic matter transformations and changes were studied in hydrophysical and physical properties of Dark Chestnut soils (Kastanozems) in the dry steppes of the Trans-Volga region after 35 and 75 years of irrigation. The parameters studied included fractional groups of humic acids; balance and reserves of humus; particle size distribution; composition and distribution of soil micro- and macroaggregates; mineralogical composition; and changes in soil structural properties (aggregate stability). At the site with 75 years of irrigation, the soils with different water regimes (automorphic and hydromorphic Dark Chestnut) and different levels of groundwater were studied and compared with a non-irrigated automorphic analogue. Humus losses in the irrigated soils were found to be greater than in non-irrigated soils. The decrease in the content and reserves of humus

due to irrigation was accompanied by negative changes in its qualitative composition. The results showed that long-term irrigation, especially in the hydromorphic hydrological regime, leads to an increase in the soil density, blockiness and clay content, and the degree of clay dispersion. This, in turn, led to an increase in the specific soil surface and a decrease in the total porosity. The observed soil dehumification and the compaction and destruction of the soil structure were the most dangerous degradation processes affecting the Kastanozems in the region, which reduced the efficiency of irrigated agriculture. Our results showed that even soils with a high content of stable humus, such as Kastanozems, lose their fertility and are prone to degradation with extensive, long-term, continuous irrigation. The results obtained should convince decision-makers to rethink the existing system of growing crops under irrigation in order to prevent losses of humus and the deterioration of soil physical properties, and to develop or adapt an ecologically sustainable irrigation system.

N. A. Pronko (✉) · V. V. Korsak · L. G. Romanova
Nikolai Vavilov State Agrarian University,
Sovetskaya Street, 60, Saratov 410056, Russia

A. S. Falkovich
Nikolai Chernyshevsky National Research State
University, Astrakhanskaya street, 83, Saratov
410012, Russia

Keywords

Irrigation · Dark chestnut soils · Dry steppe · Volga region · Humus · Soil density · Soil structure · Microporosity · Macroporosity

28.1 Introduction

According to the UN (2015), about half of global agricultural land is moderately or severely degraded. The most dangerous manifestations of agrolandscape degradation are dehumification, compaction and the destruction of the soil structure (Blum 2011; Zhou et al. 2020), which reduce the effectiveness of agriculture around the world. The man-made factors initiating or contributing to the degradation of soil include improper irrigation and excess mechanical disturbance of the soil (Montgomery 2007; Olsson et al. 2019; Gupta et al. 2019), which lead to the loss of the top soil layer, accelerating the loss of fertility due to nutrient mining and leaching (Gupta et al. 2019; Zhang et al. 2020) and accelerating the mineralisation of soil organic matter (SOM) (Lal 2004; UNDP 2019; Franko and Witing 2020), the loss of biodiversity (Borelli et al. 2017; Guerra et al. 2020) and the loss of soil aggregate stability (Murray and Grant 2007; Zhou et al. 2020).

The most common anthropogenic soil compaction occurs due to excess mechanical impact in terms of the weight load and the intensity of tillage (Keller et al. 2019; Parkhomenko et al. 2019; Bondi et al. 2020). Soil compaction can induce or accelerate other soil degradation processes, such as erosion or landslides due to the reduced infiltration rate, and increased runoff in sloping areas. On plains, compaction can cause waterlogging, resulting in the destruction of aggregates and causing crust formation (Ayuso et al. 2019). Soil compaction leads to a decrease in total porosity due to a decrease in the pore volume of large inter-aggregates and aggregates. These pores provide aeration, absorption and water filtration. There is also an increase in the volume of pores containing inaccessible and poorly accessible moisture for plants (Murray and Grant 2007; Gajić et al. 2020). As a result, on highly compacted soils the crop yield can be reduced by 50–60% (Czyż et al. 2001; Pronko et al. 2014) due to increased surface runoff resulting in soil erosion and the limited spatial growth and development of plant roots (Unger and Kaspar 1994; Correa et al. 2019). Soil factors

associated with compaction include weak soil texture, soil moisture and low levels of organic matter (Bondi et al. 2020).

Soil dehumification is an extremely negative process, since soil humus plays a huge, multi-functional role in soil fertility. Humus is a universal system that determines and regulates the level of almost all elements of the soil; this, in turn, affects the level of soil fertility (Tuyev 1989). The content of organic matter is one of the most important indicators of soil quality and health (e.g. see Franzluebbers 2002; Obalum et al. 2017; Jensen et al. 2020; Zhao et al. 2021). It significantly determines the soil's biological functions (existence and functioning of soil fauna and flora), chemical functions (e.g. nutrient cycling) and physical functions (soil structure, aggregation, runoff, water and air regimes, etc.) (Gregorich et al. 1994; Franzluebbers 2002; Bünemann et al. 2018; Wiesmeier et al. 2019; Zhou et al. 2020). In agricultural landscapes under the same climatic conditions, the processes leading to losses of humus and soil structure, as well as compaction, are largely controlled by the genetic properties of the soil and by land use (Pronko and Korsak 2001; Kalinichenko et al. 2012; Agneessens et al. 2014).

The aggregate stability of a soil is generally strongly correlated with its organic matter content (Chenu et al. 2000; Zhou et al. 2020): soils with a high organic matter content are less susceptible to the compressive and destructive effects of irrigation (Currie 2006). However, different-sized aggregates protect and bind organic molecules in different ways. Organic carbon in microaggregates is less susceptible to change than that in macroaggregates (Zhou et al. 2020). On the other hand, different fractions of SOMs (both stable and labile) differently influence micro- and macroaggregates (Zhou et al. 2020; Xu et al. 2020). Organic matter increases the cohesion of aggregates by binding mineral particles with organic polymers, or through the physical entrapment of particles by fine roots or fungi mycelia (Tisdall and Oades 1982; Chenu and Guérif 1991). However, the direct relationship between the SOC level and the level of

changes in related ecosystem attributes has not yet been established (Obalum et al. 2017; Lorenz et al. 2019). Similarly, the lack of understanding of how different organic carbon pools function makes it hard to predict SOC responses to climate and land use changes (Poeplau et al. 2020; Lal 2020). Soil organic matter consists of different fractions and organo-mineral complexes that vary in terms of biochemical properties such as the turnover rate and in terms of physico-chemical properties such as adsorption and desorption capacities.

It is especially important to understand the nature of SOM transformations and the development of soil compaction under irrigation. Irrigation may have positive and negative effects on soil quality and crop harvest (Isweiri and Qian 2017; Li et al. 2018) depending on the suitability of the selected irrigation technique and water quality. However, increasing population growth demands the production of more food, fibre and energy. Irrigated agriculture produces about 40% of food worldwide. Considering that irrigated lands comprise only 17% of all arable lands, the intensive exploitation of these lands may inevitably initiate processes potentially resulting in the degradation of soil quality (Tuninetti et al. 2019).

The deterioration of physical soil properties via altered water and air regimes, such as soil compaction, increased bulk density (e.g. Nunes et al. 2020) and a decline in soil fertility under heavy, long-lasting irrigation (Nikolskii et al. 2019), are some of the effects of improper irrigation techniques and regimes. The adverse effect of irrigation with saline waters has achieved widespread attention due to the huge soil salinisation problems it has caused. However, freshwater irrigation may also have negative consequences such as the degradation of soil quality due to the loss of SOM (Nikolskii et al. 2019). For example, arable Chernozem soils in Russia lost 1–2% of their organic matter after 20 years of irrigation with freshwater (Nikolskii-Gavrilov et al. 2014). Long-term irrigation may cause the destruction of soil aggregates and compaction due to the reduction of soils' infiltration capacity (Keller et al. 2019; Negev et al.

2020). Apart from restricting root growth and development (Tebebu et al. 2020), compacted soil also increases runoff and the risk of accelerated erosion (O'Sullivan and Simota 1995).

In Russia, the average loss of humus in the soils not affected by water erosion over the past 15 years was 9.5%, and the average annual loss was 0.62 t/ha⁻¹. The humus loss in the different natural and agro-zones of the Saratov region was 6–16% over the past 20 years, while the average annual deficit in the humus balance was 0.59–0.91 t/ha⁻¹ (Pronko et al. 2018). For the Russian Federation, the share of improved land is 38% and the share of degraded land is 12%. Using the Lund–Potsdam–Jena managed land model, Guggenberger et al. (2020) found that the Kulunda steppes in Russian Siberia have lost about 20–35% of their organic carbon since their cultivation. In general, the Degradation Neutral Balance Index (DNBI) for the Russian Federation over the period of 2000–2015 is 26% (Andreeva and Kust 2020).

In Russia, there are 1,003,000 hectares of irrigated arable lands (Edelgeriev 2019). In the Privolzhsky Federal Municipality, the total area of irrigated land in 2017 was 4,658,700 hectares, 2,172,700 ha of which (46.6%) is in a good state, 1,340,800 ha (28.8%) in a satisfactory state and 1,145,200 ha (24.6%) in a non-satisfactory state (Edelgeriev 2019). The dry steppes of the Saratov region are a vast area of arable lands located on the left bank of the Volga River, with a long history of irrigated agriculture, and the major cropland area. The main hypothesis of the study was that these lands, which have been under the influence of anthropogenic loads for a long time, could undergo serious changes in their productive parameters and inherent properties. The aim of this research was to study the level and nature of dehumification, compaction and loss of structure in irrigated Dark Chestnut soils in the Volga steppes to reveal the degree of degradation of selected soil parameters. The tasks were to determine the changes in the soil humus content and composition, and in the soil's physical properties such as microaggregate stability and particle size distribution. Within the soil type

studied, irrigated soils with hydromorphic and automorphic water regimes were compared with non-irrigated analogues.

28.2 Materials and Methods

28.2.1 Site Description

The Saratov region is located in the southeast of the European part of Russia, in the northern part of the Lower Volga region (Fig. 28.1). The area of the region is 101,200 square kilometres. The climate is moderately continental with average monthly air temperatures in summer from 20 °C in the north of the Right Bank to 24 °C in the southeast of the Trans-Volga region. Average monthly temperatures in January range from −11 °C in the southwest of the Right Bank to −14 °C in the northeast of the Trans-Volga region. The annual amount of precipitation ranges 500–580 mm in the meadow steppes in the northwest of the Right Bank and from 375 to 425 mm in the semi-desert of the Trans-Volga region. The main river—the Volga—divides the

region into two. The eastern part (the Trans-Volga) consists of the Syrtovaya plain and the northern part of the Caspian lowland. The western part (on the right bank) is occupied by the Volga Upland and the Oka-Don Plain. The Volga River valley in the Saratov region is represented by floodplains and terraces above the floodplain with fertile lands, which are especially significant in size in the Trans-Volga region. Chernozem and Chestnut soils prevail on the territory of the Saratov region, with Chernozems making up 50.4% and Chestnut soils 30.0%.

The Chestnut soil (Egorov et al. 1977) (Kastanozem, WRB 2014) which was studied is a typical soil type for the irrigated landscapes of the Volga dry steppes. The two studied sites have been irrigated with water from the Volga River, with bicarbonate-calcium mineralisation (0.2–0.3‰), for 75- and 35-year periods, respectively (Falkovich et al. 2017).

Site No. 1 is located at the Yershov Experimental Station of Irrigated Agriculture of The South-East Research Institute of Agriculture 51° 22'16"N, 48°13'54"E is on Dark Chestnut soil and has been irrigated since 1934. At this site, the



Fig. 28.1 Location of the Saratov region (free maps source: <http://www.maphill.com/russia/volga/saratov-oblast/location-maps/physical-map/>)

composition and structure of soil humic substances as affected by 75 years of irrigation agriculture were first studied using fractionation analysis. Second, the soil's physical and hydrophysical parameters were studied, such as its macro- and microaggregate composition and particle size distribution. The soil was sampled at the end of September after harvesting.

Site No. 2 is located at the "Agrofirma Volga" agricultural company located at 51°36'24" N, 46°3'26"E in the Saratov region and has been irrigated since 1974. At this site, changes in the humus balance as affected by 35 years of irrigation were studied on Dark Chestnut soil. The soil was sampled at the end of September after harvesting.

28.2.2 Laboratory Analyses

The soil was sampled according to the integrated monitoring system for soil fertility in agricultural territories (Guidelines for the integrated monitoring of soil fertility 2003). The amount of total carbon was determined by dry combustion using a CNS analyser. Carbonate and bicarbonate ions were determined in an aqueous extract by titration with a solution of sulphuric acid to pH 8.3 and bicarbonate to pH 4.4. The end point of the titration is set using a pH meter or by changing the colour of phenolphthalein (pH 8.3) and methyl orange (pH 4.4) (GOST 26424-85). The content of organic carbon was calculated by the difference between the total carbon and carbonate carbon. The humus content was determined using the Tyurin wet-combustion method based on the oxidation of a small portion of the soil with potassium dichromate, followed by titration of the excess potassium dichromate with Mohr's salt (Mineev 2001). The fractional-group composition of the humus was determined using the Ponomareva-Plotnikova method, as modified by Plotnikova and Orlova (1984). Three fractions of humic acids and four fractions of fulvic acids were isolated and analysed. This division is based primarily on the reactivity of the fractions, namely the isolation conditions (Pavlova et al.

2018). Humic acids are subdivided into Fraction 1 (HA-1)—soluble directly in 0.1 N NaOH. This fraction is "free" and associated with non-silicate (mobile) sesquioxides. Fraction 2 (HA-2)—soluble in 0.1 N NaOH after soil decalcification and associated with calcium. Fraction 3 (HA-3)—soluble in 0.02 N NaOH at 6 h heating for water bath and associated with stable forms of sesquioxides and clay minerals. The fractions of fulvic acids FA1a, FA-1, FA-2 and FA-3 are linked by ester bonds with HA and are subdivided as humic acids. Additionally, Fraction FA-1a, the so-called "aggressive" fraction, is isolated as soluble in 0.1 N H₂SO₄, which is "free" and associated with mobile sesquioxides. This fraction is the most aggressive free fraction. Non-hydrolysable residue (humins) is strongly associated with mineral components of the soil HA and FA, as well as partially decomposed plant remains (Mineev 2001).

The particle size distribution (PSD) was determined by the densimeter method, based on sedimentation governed by Stokes' law, which relates the size of the particle to the sedimentation velocity in a liquid (Vadyunina and Korchagina 1986).

The solid phase density was determined by the pycnometric method as described by Shein (2005). The pycnometer with distilled water and soil suspension was boiled to remove air, adding distilled water as it evaporated to half the volume. After boiling, the pycnometer and its contents were cooled to a temperature of 20 °C, and the boiled and cooled water was added to the volume; the pycnometer was then weighed. The density of the solid phase D was calculated by the formula: $D = \frac{A}{(B+A)-C}$; $A = \frac{100 \cdot a}{100 + W}$, where p is the density of the soil solid phase, g/cm³; A is the mass of dry soil; a is the mass of air-dried soil, g; W is the hygroscopic moisture content, %; B is the mass of the pycnometer with water, g; C is the mass of the pycnometer with water and soil, g.

The soil density was determined in undisturbed samples collected by drilling. A soil sample was taken using a steel cylinder of known

volume (typically about 100 cm³, ring diameter 5.6 and height 4 cm). In a laboratory, the soil sample was removed from the cylinder and weighed, the soil moisture was determined and the soil density, ρ_b , was calculated as $\rho_b = \frac{m_1 * 100}{(100 + W)V_b}$, where m_1 is the soil weight (g) from the cylinder, at natural moisture W (%), and V_b is the volume of the cylinder, cm³.

A mineralogical analysis of the silt fractions was performed by X-ray diffraction (Whittig 1965): to remove carbonates and organic matter, the soil samples were treated with 1 N NaOAc (pH 5) and H2O2. Then, 1 N NaOAc (pH 7) was separately added to the samples along with Na-dithionite to remove divalent cations and free iron oxides, respectively. After the complete dispersion of the samples in distilled water, the soils were separated by sedimentation by centrifugation into three fractions of different sizes: <0.2 μ m, 0.2–1 μ m and 2–20 μ m. The particle size fractions were saturated with Mg²⁺ and K⁺ from 1 N chloride solutions and then rinsed to remove the salt. Oriented aggregates for X-ray diffraction analysis were prepared by drying dispersed samples in water on glass slides and silicon dioxide. Then, the samples saturated with Mg were subjected to X-ray irradiation in the air-dried and glycerol-solvated states. Samples saturated with potassium were subjected to X-ray irradiation after drying in air and heating to 300 and 550 °C for 2 h.

The structural composition and aggregate stability were analysed using the dry and wet sieve methods as follows as described by Savvinov (1931).

– *The dry sieve* method determines the number of aggregates of different sizes. An average sample of 0.5–2.5 kg is taken from a sample of undisturbed air-dry soil. Stones, gravel, roots and other inclusions, if any, are selected from the sample. The sample is sieved through a set of sieves with hole diameters of 10, 7, 5, 3, 2, 1, 0.5 and 0.25 mm. Each fraction of the aggregates is separately collected, weighed and calculated as a percentage. The fraction size <0.25 mm is calculated

from the difference between the mass of the soil taken for analysis and the sum of the fraction >0.25 mm. The sample taken for analysis minus the mass of inclusions (stones, gravel, etc.) is taken as 100%. According to the data from the dry sieving, the structure coefficient is determined: $C_{str} = A/B$, where C_{str} is the structure coefficient; A is the sum of aggregates ranging from 0.25 to 10 mm (%) and B is the sum of aggregates <0.25 mm and lumps >10 mm (%).

– *Wet sieving* determines the water resistance of aggregates analysed from 50 g of an average sample of all fractions of aggregates obtained by dry sieving, in proportion to their percentage. The sample was poured into a 1-L glass cylinder and water was added up to 2/3 of the cylinder volume to displace air. To accelerate the expulsion of air, the cylinder was closed with a stopper, tilted twice to a horizontal position and returned to a vertical position. The soil was left for 10 min at rest, after which the cylinder was filled up to the top with water and turned upside down, waiting until all soil particles settled down. Then, the cylinder was returned to its original position and left until the soil reached the bottom. After 10 such revolutions, the closed cylinder was overturned above a set of the sieves standing in water (6 sieves with hole diameters of 5, 3, 2, 1, 0.5 and 0.25 mm). The transferred soil was sieved under water. Then the sieve with a hole diameter of <1 mm was removed without removing the entire set of sieves from the water, and the rest were shaken 5 more times and removed from the water. The aggregates remaining on the sieves were rinsed into porcelain cups with a stream of water from a wash bottle. The excess water was drained, and the soil was dried and weighed. The percentage of each fraction was determined. The content of fractions is calculated as $x = m_1 100/m$, where X is the content of aggregates of a certain size (%); 1 is the mass of the units (without large inclusions), g; and m is the soil sample taken for analysis (50 g) minus large mechanical inclusions.

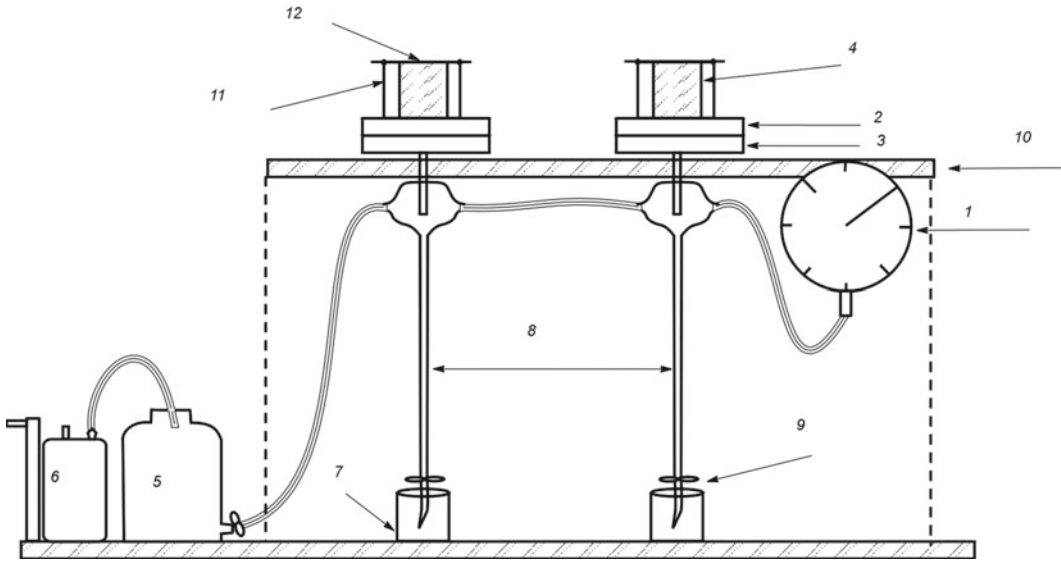


Fig. 28.2 Scheme of the vacuum-capillary meter device: 1—pressure gauge; 2—filter; 3—funnel; 4—soil monoliths; 5—receiver to maintain the vacuum; 6—vacuum

pump; 7—water collecting glass; 8—burettes; 9—valve shutter; 10—tripod; 11—studs for fixing the sample; 12—cap

Hydrophysical parameters of Dark Chestnut soils at Site No. 1 (Yershov Experimental Station) were determined on a vacuum-capillary-metric device (Fig. 28.2) designed by Shapovalova with a modification by Platonova and Shmyglya (Platonova and Shmyglya 1986). The intact soil samples (10 × 10 cm) were placed in an air-impermeable porous membrane after a capillary saturation. Negative air pressure under the membrane was created in successive steps from −5 kPa (−0.05 air pressure) to −90 kPa (−0.9 air pressure). Data was processed for the correlation and regression analysis using the Statistica 5.5 program and MS Excel (Dospikhov 1985). Geoinformation and geostatistical methods implemented in the ArcGIS Desktop software package were used for the data processing (Seiler 1999; Delfiner and Chilès 2000).

Negative pressure was maintained at each stage until the outflow of water from the sample stopped, followed by the next stage of vacuuming. The volume of water flowing from the sample and the corresponding time intervals were measured at each stage of the pressure discharge. Before and after the experiment, the moisture of the sample was measured. The completeness of

the outflow of moisture was checked at the end of the experiment based on the residual soil moisture from the upper and lower parts of the sample (Pronko et al. 2005).

28.3 Results and Discussion

28.3.1 Changes in the Humus Content of a Dark Chestnut Soil Irrigated for 75 years (Yershov, Site no. 1)

28.3.1.1 Humus Content in Dark Chestnut Soil Irrigated for 75 years

The loss of soil humus means not only a decrease in its content and reserves but also the deterioration in its composition (Hoffland et al. 2020; Wiesmeier et al. 2019; Kleber and Lehmann 2019; Kögel-Knabner and Rumpel 2018; Ndzelu et al. 2020). Studies of the amount and composition of humus in the Dark Chestnut soils irrigated for 75 years at Site No. 1 (Yershov Experimental Station) showed the following.

Table 28.1 Content of organic carbon and humus in Dark Chestnut soil irrigated for 75 years (Yershov, Site No. 1)

Layer, cm	Content, %		Non-hydrolysable residue	Ratio of humic to fulvic acids
	Organic carbon	Humus		
Hydromorphic irrigated soil (GWL < 2 m)				
0–22	1.60	2.66	49.0	2.0
22–40	1.46	2.52	47.5	2.2
40–60	0.77	1.33	43.6	1.1
60–100	0.44	0.76	35.5	0.8
Automorphic irrigated soil (GWL > 10 m)				
0–22	1.46	2.52	54.6	1.8
22–40	1.47	2.53	54.5	1.7
40–60	1.15	2.16	47.2	1.4
60–100	0.47	0.81	39.5	1.1
Automorphic non-irrigated soil				
0–22	1.51	2.60	51.2	1.7
22–40	1.51	2.55	52.3	1.6
40–60	0.93	1.60	43.8	1.3
60–100	0.52	0.90	47.4	0.9

GWL—groundwater level

After 75 years of irrigation, the humus content in the 0–40 cm soil layer was 2.52–2.76%, regardless of land use (irrigated or non-irrigated) (Tables 28.1 and 28.2). This value corresponds to a low level of humus for heavy loamy Dark Chestnut soils and indicates a high degree of exploitation of both irrigated and nearby non-irrigated soils in this region (Table 28.1). Below the arable layer, a gradual decrease in humus content was observed. Moreover, in the irrigated soil with a deep groundwater level (GWL) the humus profile was most extended. The humus content in the 40–60 cm layer of the automorphic soil with low GWL was 2.16% versus 1.33% in soil with a high GWL and 1.60% in a rainfed analogue. In our opinion, this was due to the movement of mobile forms of humic substances from the upper to the lower horizons during the irrigation of automorphic soil. This is supported by numerous humus drips observed in the 40–60 cm soil layer, which were more strongly manifested in the irrigated automorphic soil. The humus content in the soils of this site was less than 1% (0.76–0.90%) in all soils studied at a depth of 60–100 cm. The observed leaching of

humus substances was greatly influenced by the soil hydrophysical properties, as well as the composition and biochemistry of the soil humus fractions, such as different fractions of humic acids (HAs): free HA1, calcium-bound HAs, strongly bound HA and fulvic acids (FAs)—FAs bound to HA1, FAs bound with HA2 and strongly bound FAs.

In non-irrigated soil, the share of humic acids (HAs) in the upper 0.6 m layer was 29–32% of the total carbon, whereas calcium humates made up 20% (Table 28.1). The amount of HAs in the 0.5–1.0 m layer decreased to 25.4%, 13.5% of which was Ca-associated HAs. The content of HA in the first metre of automorphic irrigated soil ranged from 28.5 to 31.8%, with a tendency to increase down the profile.

The ability of humic substances to form water-insoluble complexes (humic acids and humates) with metal ions and hydroxides, and to interact with minerals and a wide variety of organic compounds, including alkanes, fatty acids, pesticides and other potentially toxic compounds, is an important characteristic. This ability reduces the adverse effects of toxic

Table 28.2 Fractional composition of humus in Dark Chestnut soils irrigated for 75 years (Yershov, Site No. 1)

Layer, cm	Humic acid				Fulvic acids				Total	
	Free (HA1)	Calcium bound (HA2)	Strongly bound (HA3)	Total	Aggressive (FA1a)	Bound to HA1 (FA1)	Bound to HA2 (FA2)	Strongly bound (FA3)		
Hydromorphic irrigated soil (GWL < 2 m)										
0-22	6.6	18.1	9.4	34.1	3.1	1.3	8.1	4.4	16.9	
22-40	6.6	19.2	10.3	36.1	3.4	0.7	8.9	3.4	16.4	
40-60	6.5	16.2	6.5	29.2	6.5	0	14.2	6.5	27.2	
60-100	7.7	15.9	4.6	28.2	11.4	0	13.6	11.3	36.3	
Automorphic irrigated soil (GWL > 10 m)										
0-22	5.5	15.7	8.2	29.4	3.4	1.4	7.5	3.9	16.2	
22-40	5.4	14.3	8.8	28.5	3.4	1.0	8.5	4.1	17.0	
40-60	5.9	17.4	7.8	31.1	2.6	1.7	11.3	6.1	21.7	
60-100	8.5	12.7	10.6	31.8	4.3	1.0	16.0	7.4	28.7	
Automorphic non-irrigated soil										
0-22	1.9	20.5	8.6	31.0	3.3	1.3	9.3	3.9	17.8	
22-40	1.4	19.9	7.9	29.2	3.3	2.0	8.6	4.6	18.5	
40-60	2.6	20.4	8.6	31.6	3.2	2.2	12.8	6.4	24.6	
60-100	2.3	13.5	9.6	25.4	3.8	1.0	14.8	7.6	27.2	

HA—humic acid; FA—fulvic acid; FA1a—GWL—groundwater level

elements and compounds on soil microorganisms and plants (Popov 2004).

The ratio of HAs to FAs is an indicator of the quality of soil humus: the larger the ratio, the stabler the soil humus (Kononova 1963). As a result of the changes in the humus composition of Dark Chestnut soils at Site No. 1, the ratio of humic acid carbon (HAC) to fulvic acid carbon (FAC) increased slightly in the upper half-metre to 2.0–2.2 in the hydromorphic irrigated soil against 1.6–1.7 in the non-irrigated soil (Table 28.1).

In the second half-metre, no changes were observed. In the irrigated automorphic soils, no increase in humus content was found. The amount of C in aromatic functional groups is a key feature in humic heteropolymers (Semenov et al. 2013). Laird et al. (2008) found that the majority of aromatic carbon (60%) was in charred particles of clay of 0.2–5 µm in size, implying that the biogenic part of humic acids in these soils was very low in aromatic carbon (Semenov et al. 2013). Olk et al. (2000), comparing labile fractions of HA with stabler calcium humates, found that mobile fractions contain fewer carboxyl groups.

Orlov (1998) believes that FAs appear only after the acidic or basic hydrolysis of SOM, and that different ratios between HAs and FAs reflect the specific structural features of HAs associated with their origin, and not with the actual proportions of two separate groups of compounds. He suggested that the highest biological activity on the surface soil layer probably contributes to the formation of condensed alkali-soluble humic substances with greater stability. This implies that the less recalcitrant and the more hydrolysable HAs are, the higher the portion of FAs seems to be (Semenov et al. 2013). Likewise, in our study a larger HA/FA ratio was found on the first top soil layers.

28.3.1.2 Fractional Composition of Humus in Dark Chestnut Soil Irrigated for 75 years

Continuous irrigation changed the distribution of fractional groups of humus along the depth of Dark Chestnut soils (Table 28.2): the number of

mobile organic substances increased as they separated out significantly along the soil profile (they were leached to a second half-metre). The content of Ca-associated HAs decreased (especially in automorphic irrigated soils), indicating an increase in the migration ability of the humus in the soils. The content of humic acids (HAs) in the irrigated hydromorphic soil was 34.1–36.1% and 28.2–29.2% in the first and second half-metres, respectively, which is higher than in the other soils (Table 28.2). The content of the HAs associated with Ca in the irrigated soils, especially in automorphic soils, was slightly lower than in the non-irrigated analogue, indirectly indicating the leaching of Ca from the upper soil horizons during the irrigation. The content of fulvic acids (FAs) tended to increase down the profile. Moreover, this trend was more strongly manifested in the irrigated hydromorphic soil, where it is increased from 16.9% in the upper 22 cm to 36.3% in the lower 60–100 cm. In comparison, in the irrigated automorphic soil it was 16.2% in the upper soil layer and increased to 28.7% in the lower part. In the non-irrigated soil, it increased from 17.8–27.2%, respectively.

The amount of free humic acids and those associated with mobile sesquioxides (HA1; FA1; FA1a) in the irrigated soils was 2–3 times higher than in the non-irrigated soils. The greatest amount of HA1—7.7–6.5% (of total C)—was found in the hydromorphic soil.

A significant increase was also found in the content of aggressive fulvic acids (FA1a) up to 6.5–11.4% in the second half-metre of irrigated soils, against 3.2–3.8% in the non-irrigated soil. An increase in the content of mobile humic substances in irrigated soils can probably be explained by the more intensive cultivation system introduced. According to our study, the direction of the humification of plant residues contributed primarily to the formation of FAs (FA1a, FA1 bound to HA1). Later, part of these fractions was leached, which was supported by a higher accumulation of FAs in the second half-metre of the irrigated soils, while some of them were converted into humic acids (mostly HA1).

Although humic acids are tightly bound to soil particles and colloids and therefore more resistant

to microbial attack, they can be removed from soil by water movements (Susic 2016), especially in hydromorphic or irrigated soils. Chukov (1998) suggests that FAs predominantly consist of carbohydrates, amino acids, alcohols and other aliphatic structures, while HAs are more likely to feature an aromatic fragment. Cook and Langford (1998) used NMR spectroscopy to show that the fulvic acid from forest soil had mostly fixed, non-functionalised alkyl structures followed by more mobile non-functional aromatic units, and even more mobile carbohydrate groups. In contrast, humic acids from the same soil consisted of immobile and slightly more mobile aromatic structures. Other studies also confirm that aromatic groups were more mobile than alkyl groups (e.g. Ghabbour et al. 2001).

Khalaf et al. (2003) suggested that the alkyl-rich HA fractions contain heterogeneous, dynamically limited sorption media, while the aromatic-rich fractions contain many mobile sorption domains. Semenov et al. (2013) confirmed earlier studies indicating that oxygen-rich materials (e.g. cellulose and hemicelluloses) are more easily degraded in moist conditions, resulting in the enrichment of carbon-rich lignin and humic acids. According to Orlov (1998), the presence of FAs in the aquatic environment is also associated with both the dissolution of unstable HAs and the association of non-humic substances with FAs. Sutton and Sposito (2006), summarising related publications using modern spectroscopic X-ray and pyrolysis studies of humic substance composition and structure, concluded that humic substances are collections of diverse components of relatively low molecular mass, forming dynamic associations stabilised by hydrophobic interactions and hydrogen bonds. These associations are capable of organising themselves into micellar structures in suitable aqueous environments.

Thus, as a consequence of the migration of humic substances, the humus content in the Dark Chestnut soils was at the same low level, regardless of irrigation and hydromorphism. The irrigation of automorphic soils led to the erosion of the soil profile: the humus content decreased in the arable layer and increased in the sub-arable layer.

28.3.1.3 Micro- and Macroaggregate Composition of Dark Chestnut Soils Irrigated for 75 years (Site no. 1)

Studies on changes in the physical properties of Dark Chestnut soils irrigated for 75 years (Yershov, Site No. 1) showed an increase in soil density, blockiness and clay content, while the total porosity decreased. Depending on the particle size distribution (PSD), the Dark Chestnut soil which was studied has a heavy loam clay and coarse-silty texture (Tables 28.3 and 28.4). The total content of silt and clay (particles <0.01 mm) in all the soils studied was more than 55%. The soils also had a high content of particles <0.001 mm, which means they have insufficiently favourable physical properties for cropping. Under the influence of irrigation, the formation of an additional amount of silt particles was observed. Thus, at a depth of 0–40 cm, the non-irrigated soil clay content was 29.8%, and in the irrigated soils the content of clay increased to 32.6–35.0%. In the second half-metre, this trend was less pronounced. The increase in the clay fraction in irrigated soil compared to non-irrigated soil was due to a decrease in the content of fine and very fine sand particles (0.25–0.05 mm) from 8 to 6% in non-irrigated soils to 6.0–3.5% in irrigated soils.

The same trend was observed for a coarse silt fraction (0.05–0.01 mm). According to this data, the process of the physical destruction of coarse silt particles increases in irrigated soils. This can be explained by the fact that the physical destruction of illites and strong aggregates containing illites and smectites (minerals with a labile lattice) intensifies, leading to clay sizes. This statement is confirmed by the results of the mineralogical analysis of clay fractions of the soils which were studied (Table 28.5). The Dark Chestnut soils which were studied are represented by an illite–smectite mixture, and by chlorite and kaolinite. All of the soils studied, regardless of land use and the moisture regime, had the following distribution of clay minerals: a decrease in chlorites in the upper horizons due to their destruction and transformation into labile structures, and an increase in the content of illites

Table 28.3 Particle size distribution of Dark Chestnut soils irrigated for 75 years (Yershov, Site No. 1)

Layer, cm	Fractions of particle size distribution in mm, % by weight				
	0.25–0.05	0.05–0.01	0.01–0.005	0.005–0.001	< 0.001
Hydromorphic irrigated soil (GWL < 2 m)					
0–22	7.92	34.72	9.25	15.51	32.58
22–40	5.08	36.25	8.76	15.08	34.81
40–59	5.74	32.36	9.83	15.32	36.75
59–100	5.22	32.88	8.07	16.87	36.96
Automorphic irrigated soil (GWL > 10 m)					
0–22	5.46	34.02	10.85	15.79	33.87
22–40	3.61	34.14	11.79	15.49	34.96
40–59	3.92	33.27	10.47	15.79	36.54
59–100	3.98	32.01	10.37	16.19	37.44
Automorphic non-irrigated soil					
0–22	7.16	36.08	10.74	16.51	29.68
22–40	6.11	35.67	10.86	17.56	29.80
40–59	7.92	32.87	7.54	17.08	34.59
59–100	6.94	33.92	7.40	17.53	34.21

Table 28.4 Microaggregate composition of Dark Chestnut soils irrigated for 75 years (Yershov, Site No. 1)

Layer, cm	Microaggregate composition, % by weight					
	mm					
	1–0.25	0.25–0.05	0.05–0.01	0.01–0.005	0.005–0.001	< 0.001
Hydromorphic irrigated soil (GWL < 2 m)						
0–22	2.10	14.40	55.64	11.97	12.16	4.84
22–40	5.99	14.68	51.42	9.83	11.79	6.26
40–59	8.60	10.87	45.13	11.01	15.99	8.41
59–100	5.72	15.10	44.52	9.67	19.15	5.83
Automorphic irrigated soil (GWL > 10 m)						
0–22	6.06	21.66	46.25	9.00	12.62	4.41
22–40	5.59	20.66	50.46	7.32	11.69	4.28
40–59	11.46	14.45	41.91	9.53	15.90	6.74
59–100	7.32	16.34	55.34	7.90	22.11	4.78
Automorphic non-irrigated soil						
0–22	5.77	17.54	54.75	8.79	9.37	3.78
22–40	5.41	17.50	54.49	9.53	9.30	3.75
40–59	8.71	12.45	44.64	9.91	16.52	8.91
59–100	6.33	17.05	42.63	9.59	15.38	9.02

Table 28.5 Mineralogical analysis of silt fractions of Dark Chestnut soils irrigated for 75 years (Yershov, Site No. 1)

Soils	Layer, cm	Mineral content, % of total components			
		Illites	Smectites	Kaolinite	Chlorite
Hydromorphic irrigated soil (GWL < 2 m)	0–22	66	20	4	10
	22–40	54	36	2	8
	40–59	37	48	1	14
	59–100	42	37	1	20
Automorphic irrigated soil (GWL > 10 m)	0–22	66	28	0	6
	22–39	62	25	0	13
	39–60	44	40	1	15
	60–100	34	46	0	20
Automorphic non-irrigated soil	0–24	58	28	0	14
	24–42	53	32	2	13
	42–64	32	47	0	21
	64–100	40	34	1	25

in the upper horizons, associated with the process of illitisation.

These processes were more pronounced under irrigation. The content of chlorites in the clay fraction was 6–20% in irrigated and 13–25% in non-irrigated soils due to the intensification of their physical destruction and their transformation into mixed-layer structures (illites). The intensification of illitisation was also observed in irrigated soils, which is reflected in an increase in the content of mica by 66% in the arable layer compared to 58% in non-irrigated soil. There were no differences in the content of swelling minerals (smectites) in soils with different moisture regimes.

In experiments with different technologies for arable land management, Kuvaeva (2012) found that changes in the group composition of humus in the fractions of microaggregates were due to the nature of the components of their mineral phase and humus. In all microaggregates finer than 5 µm which were enriched with clay minerals (silty and fine dust), depending on the conditions of the soil environment, the extent to which the components of the fulvate group are fixed in the form of clay-organic complexes changes; therefore, the content of the fulvate group and the residue was subject to significant fluctuations.

In our study, a comparison of the results of PSD and microaggregate composition analyses showed that the clay fraction was redistributed due to the coarse silt (particles with a diameter of 0.05–0.01 mm) and fine and very fine sand (0.25–0.05 mm) fractions. However, this also manifested for the sand fraction (>0.25 mm), since the PSD analysis showed that this fraction was absent in all three soils, while the microaggregate analysis revealed content from 6 to 11%. This was probably due to the high content and activity of clay, which directly starts the macroaggregation process, skipping the microaggregation phase, since there was apparently an active bonding of microaggregates to form water-resistant aggregates. Our findings are supported by those of Totsche et al. (2018), who reported that microaggregates resist strong mechanical and physico-chemical stresses and survive slaking in water due to their strong bonds. In irrigated hydromorphic soils, the Kachinsky dispersion coefficient (the ratio of the clay content in the microaggregate to the clay content in PSD) was higher than in non-irrigated soils (13–18 and 12, respectively) at 0–40 cm. This indicates a decrease in the water resistance of the irrigated soils' microstructure. The soil disaggregation index determined by microaggregate analysis (the

ratio of clay content in irrigated soils to clay content on non-irrigated soils) also confirms the occurrence of dispersion in the upper 0–40 cm layer of soils irrigated in the long term. This process was especially evident in a 22–40 cm layer (“plough sole”) of irrigated hydromorphic soil.

Clay charges are responsible for the substitution of ions. Rengasamy (2019) reported that the charge in the clay mineral layer contributed by isomorphous substitution may be large, but the charge available for hydration may be quite different. In our study, the proportion of illite increased during irrigation, since illite K is associated with the layer being charged by intraspheric complexation, leading to the intraspheric complexation of cations (Slade et al. 1991; Sposito et al. 1999). The intraspheric complexation of cations or molecules involves covalent bonding by clays resulting in hydrophobicity, whereas the extraspheric complexation of cations involves ionic bonding (electrostatic attraction), facilitating hydration (Rengasamy 2019). Similar to our findings, Basga et al. (2018) found that heavy tillage and irrigation induce clay dispersion. In their study, despite the lower difference in clay mineralogy, the Vertisols studied revealed variable clay dispersion behaviour with respect to land use and farming practices (tillage and irrigation). According to our findings, the long-term irrigation of arable lands can lead not just to clay dispersion but also to clay eluviation as clay is translocated from the upper to lower horizon (Warrington et al. 2007).

According to Travnikova et al. (1992), humic substances of clay fractions are formed on the surface of clay minerals from low-molecular products of the transformation of organic residues by polycondensation, possibly with the participation of bacteria, and are fixed by chemical bonds in clay-organic complexes. Fractions which are 1–50 μm in size are a favourable habitat for soil microorganisms and microfauna, since the sizes of their micropores and niches (about 0.8–3 μm) create optimal conditions for the supply of moisture and air and protection from predators (Titova et al. 1989). In these microaggregates, well-formed high-molecular-weight

humic substances with increased aromaticity are formed from the high-molecular decomposition products of organic residues, metabolites and lysis products of microbes, fungi and actinomycetes (Alexandrova 1980). These mainly take the form of metal humates.

28.3.1.4 Soil Structure of the Dark-Chestnut Soils Irrigated for 75 years (Yershov, Site no. 1)

An important agrophysical characteristic of the soil is its structure, which is determined by the nature of the relative arrangement of particles and structural units, as well as by the size and design of the pore spaces (Ganzhara et al. 2002; Gajić et al. 2020). The main factor determining the soil structure and its stability over time and after a process of agricultural use is a mechanically strong, water-resistant structure. Visual observations showed that the structure of the arable layer of the soils which were studied is lumpy and lumpy-powdery. Irrigated soils were characterised by increased density and high clumpiness of the structure and adhesion of the upper soil layers.

The results of structural-aggregate analysis using the sieve method (Savvinov 1931) also showed increased clumpiness of the irrigated soils compared to the non-irrigated analogue (Fig. 28.3). The content of aggregates >10 mm was 83–63% in irrigated soil with a high groundwater level, and 62–54% in irrigated soil with a low groundwater level, compared with 52–44% in non-irrigated soil. In non-irrigated soil, clumpiness increased with depth, while in irrigated soil it was mainly found in the upper 0–22 cm layer. This is explained by the higher humidity and increased dispersion of the upper layers of irrigated soils, where they adhere and are compacted due to agricultural machinery. This leads to the irreversible destruction of the macrostructure and the formation of adhered soils. In addition, the highest content of agronomically valuable water-resistant aggregates (>0.25 mm) was found in hydromorphic soil (49–50% in the upper half-metre) compared to 33–31% in automorphic irrigated soil and 32–

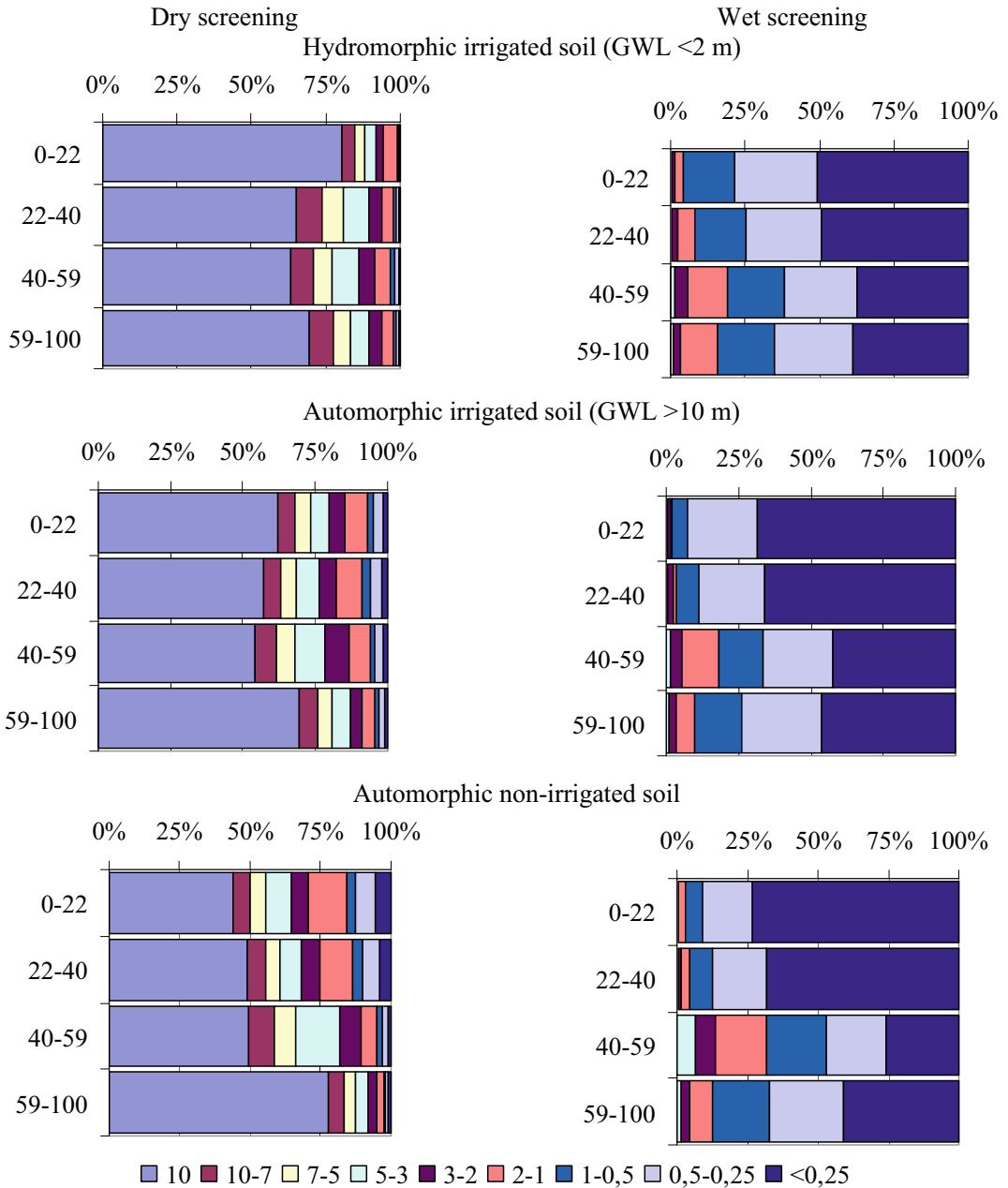


Fig. 28.3 Structural composition of particle size distribution in Dark Chestnut soils irrigated for 75 years (Yershov, Site No. 1)

27% in non-irrigated soil. This is due to a large number of active clay particles in irrigated soils and changes in the hydrothermal conditions during irrigation (especially at a high GWL), as well as the lack of severe drying in these soils

compared to non-irrigated soils. It should also be noted that over the 30 years of agricultural operation, the water resistance of both irrigated and non-irrigated soils at Site No. 1 has deteriorated. During this period, the number of water-

resistant aggregates in the arable layer of non-irrigated soils decreased by three times and that in irrigated soils by 1.5 times. Together with an unfavourable structure, this confirms the high level of soil degradation at Site No. 1 (the Yershov station). Rengasamy (2019) reported that soil moistening typically leads to the slaking of the clods, with macroaggregates breaking down into microaggregates. This does not always result in the destruction of the soil structure, but reorganises the relative ratio of existing structural forms of the soil. However, in our study, 75 years of irrigation obviously resulted not only in the simple disaggregation of soil particles but also in the destruction of structure, leading to soil degradation.

The most agronomically valuable (optimal) structures for cultivated plants are meso-aggregates of 0.25–10 mm in size, with high porosity (more than 45%), mechanical strength and water resistance (Ganzhara et al. 2002; Gajić et al. 2020). The agrophysical state of the soil is also characterised by its density and total and differential porosity. In both sites, despite ploughing, the density of the top 0–40 cm layer in irrigated soils was higher (1.10–1.28 g cm⁻³ in automorphic soil with GWL > 10 m, and 1.17–1.39 g cm⁻³ in hydromorphic soil with GWL < 2 m) than in non-irrigated soils (1.03–1.07 g cm⁻³). No clear change in density was detected down the profile. The maximum density was observed in the carbonaceous horizons at a depth of 60–100 cm (1.48–1.57 g cm⁻³). In irrigated automorphic soil, the density of this horizon was much lower (1.35 g cm⁻³), which is explained by the leaching of carbonates to the lower depth. Porosity in the upper half-metre of irrigated soil decreased to 48–56% and 52–59% in hydromorphic conditions and automorphic conditions, respectively, compared with 60% in non-irrigated soil. In the 60–100 cm layer, the lowest porosity (41.6%) was observed in non-irrigated soil, which is due to a high content of carbonates. In irrigated soils, the porosity was slightly higher (45.8% and 50.4% in hydromorphic and automorphic soils, respectively).

Extreme soil compaction in the arable and sub-arable layers was observed during the growing season (from spring to autumn). This indicates a high degree of destructure and physical degradation of the Dark Chestnut soils at site No 1, which is most intense during irrigation under hydromorphic conditions. Changes in the differential porosity were most pronounced in irrigated soils during the formation of hydromorphic conditions: the moisture-saving micropores increased, while capillary pores and aeration pores, which provide a favourable air regime, decreased. The micropores with a diameter of less than 3.5 microns prevailed in the upper soil layer (0–55 cm) (Fig. 28.4).

However, if they made up 24.1–27.3% of the volume in non-irrigated soil, then the number of micropores increased to 32.5–48.0% as a result of prolonged irrigation at a high GWL. At the same time, there was a decrease in the number of capillary pores with a diameter of 30–3.5 μm (from 1.9–13.1% to 0.7–3.2%) and also a decrease in the number of aeration pores with a diameter of more than 30 μm (from 3.9–10.0% to 1.1–2.8%). The observed changes in the pore ratio caused a deterioration in the air regime of irrigated-hydromorphic soils. The calculated ratio of the pores <3.5 microns and the pores >30 microns (water-holding and aeration pores) sharply increased under irrigation at high GWL and reached 11.5–42.7 against 2.9–6.9% in a non-irrigated analogue. In our opinion, this ratio can be used to assess the water–air regime of soils. At low GWLs there were no large changes in the differential porosity of soils irrigated in the long term compared with non-irrigated soil.

Calculation of the moisture content in pores of different diameters and a comparison of the obtained values with soil-hydrological constants showed that in all three soil profiles, the predominant amount of capillary-suspended moisture was in the micropores with a diameter <3.5 microns. This prevents water from being available to plants. The increase in micropores of <3.5 microns in diameter in hydromorphic

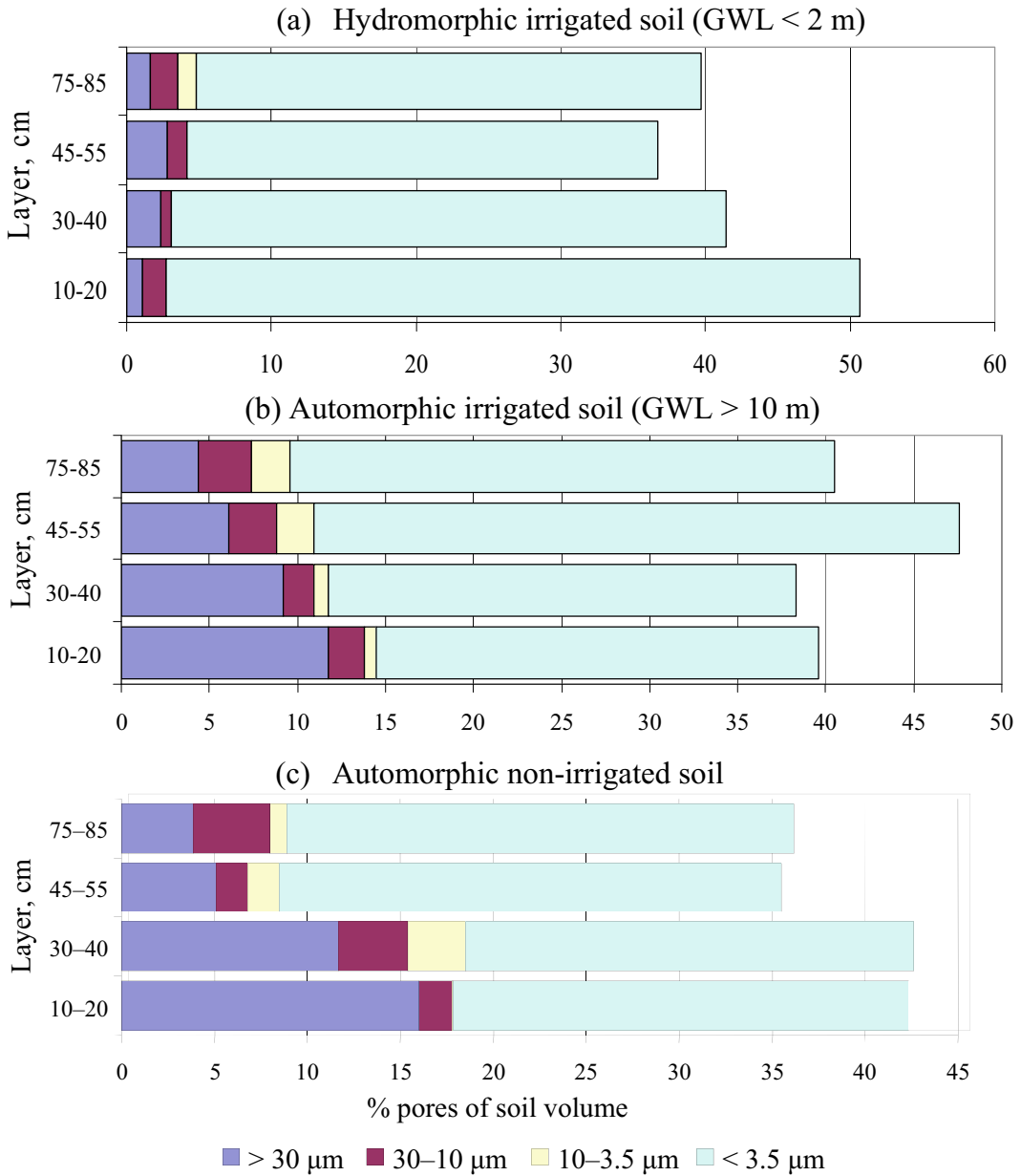


Fig. 28.4 Differential porosity of Dark Chestnut soil irrigated for 75 years (Yershov, Site No. 1)

irrigated soil was apparently due to its compaction as a result of constant over-moistening and due to an increase in clay particles. The observed changes indicate the appearance of soil

adhesion and the deterioration of the water-air regime. In general, a tendency to degradation was observed in soils irrigated in the long term, especially with a high groundwater level.

28.3.2 A Retrospective Analysis of the Dynamics of Humus Content Changes in Dark Chestnut Soils Irrigated for a Period of 35 years, Site no. 2

A retrospective analysis of the dynamics of humus content changes in Dark Chestnut soils irrigated for 35 years at Site No. 2 (“Agrofirma Volga” Saratov region) revealed a number of tendencies. Current studies covered a total area of 2,353 hectares at this site. The potential soil fertility was characterised by great territorial diversity, with 42.3% of the surveyed lands characterised by low and very low humus contents, 45.2% having a medium humus content and 12.5% having a high humus content (Fig. 28.5).

Monitoring of the humus content in the soils of Site No. 2 showed that a dehumification process has been taking place (6a). In 1990, the

average humus content in the soil of the surveyed fields was 3.05%, whereas by 2007 it had decreased to 2.90%. A comparative assessment of changes in the humus content in individual irrigated fields in the period from 1990 to 2007 was carried out using GIS monitoring. Over a period of 17 years, an increase in the humus content was observed on 16% of the fields, no changes were seen on 34% and dehumification was observed on 50% of the irrigated fields (Fig. 6b). A linear regression dependence of the humus content (%G) on time (T) was $G = 22.6 - 0.0098 \times T$; $r = 0.57$, which shows that, over the observed period, the humus content decreased annually by 0.01% in absolute terms, that is, in the first 20 years of irrigation.

The calculated humus balance for the 17 years across all the fields almost fully confirms the actual changes in the humus content (Fig. 28.7). On average, a decrease in humus was observed in all fields examined, of 6.4 t/ha⁻¹ according to the calculated data and 5.0 t/ha⁻¹ according to the actual data. The difference between the



Fig. 28.5 Humus content (left) and humus supply (right) of Dark Chestnut soil irrigated for 35 years (Agrocompany “Volga”, Site No. 2)

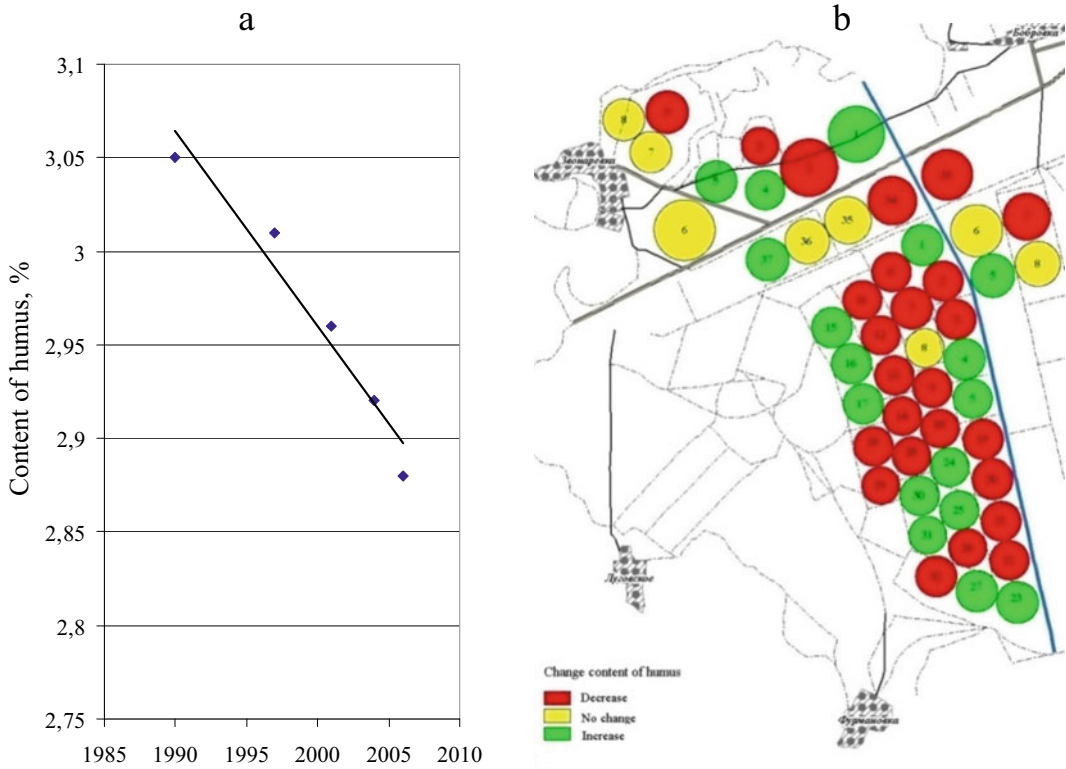


Fig. 28.6 Changes in the humus content of the Dark Chestnut soil irrigated for 35 years (Agrocompany “Volga”, Site No. 2) (1990–2007) (**a**—average for irrigated area; **b**—for individual fields of the farm)

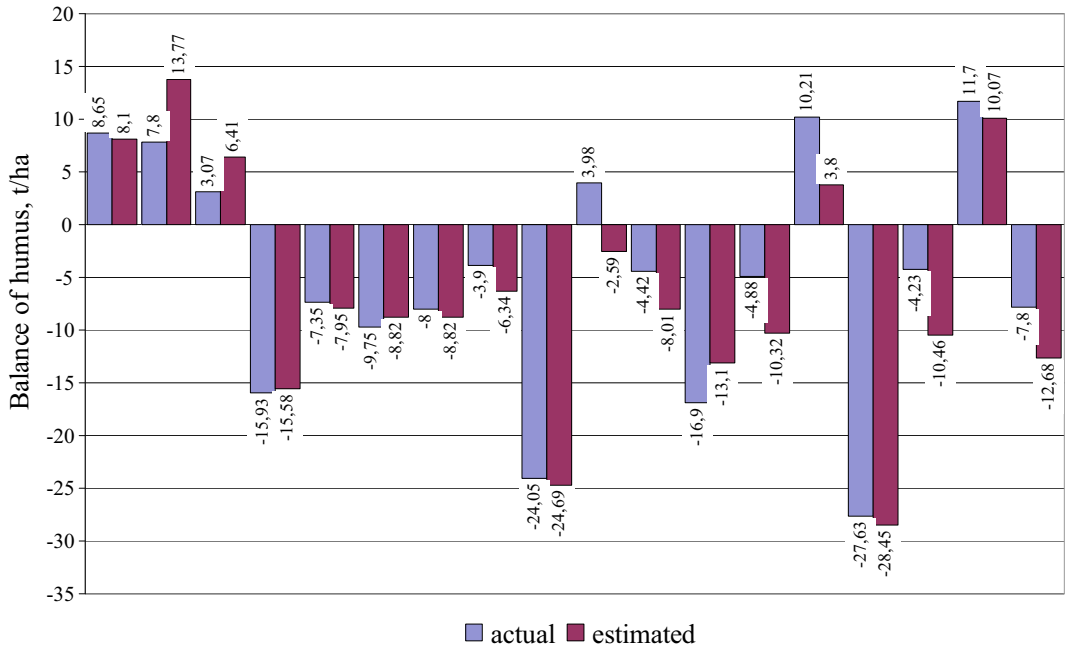


Fig. 28.7 Estimated and actual humus balance in the fields of Site No. 2 (“Agrofirma Volga”) from 1990 to 2007

calculated and actual values is within the range of analytical accuracy (correlation coefficient is 0.95).

Soil organic matter consists of many different forms and compounds that undergo the process of decomposition in a cascading fashion, with a different turnover time depending on various factors (Kononova 1961). Jenkinson and Ladd (1981) established that the first phase of decomposition lasts about 1–2 years in a temperate climate and a loss of about 1/4–2/3 of the initial organic carbon, usually called labile SOM. Then, a slowed phase of decomposition takes place, with a total loss of about 90% OM and lasting about 10–100 years; this is called an intermediate OM pool. Last, the most recalcitrant phase undergoes decomposition, with a turnover time of about 100 to >1000 years; this is called recalcitrant OM. This third phase is responsible for the long-term stabilisation of carbon in soil (Falloon and Smith 2000). The mechanisms of stabilisation of SOM are not clear yet (Lützow et al. 2006), but the stability of recalcitrant OM is evidently explained by its origin and composition and most probably associated with the highly aromatic structure of humic acids (Oades, 1988; Kögel-Knabner et al. 1992a, 1992b; Eusterhues et al. 2003; Semenov et al. 2013). Other researchers found that organo-mineral complexes also play a great role in stabilising SOM (Baldock and Skjemstad, 2000; Kaiser et al. 2002; Ludwig et al. 2011; Kleber et al. 2004). Soil organic matter stability is influenced by the surface area of clay particles, which physically protects organic substances inside the aggregates against microbial attack and decomposition (Quesada et al. 2020). Pronko et al. (2018) suggest that the stabilisation in humus content in the soils they studied was mainly due to the high content of physical clay. In addition, the Dark Chestnut soil studied is inherently well supplied with humus, which formed over millennia under rich steppe vegetation, the biomass of which was returned to the soil, replenishing it with fresh organic substrates and, consequently, various fractions of SOM, including the synthesis of

high-molecular-weight-persistent aromatic organic structures (Lützow et al. 2006). However, during 35 years of intensive irrigated land use, the resistant compounds of SOM were subject to decomposition due to the better air and moisture conditions under irrigated land tillage, where the mineralised nutrients were harvested with crop biomass. Yefremov et al. (2016) suggest that to obtain high, stable crop yields, the consumption of nitrogen and potassium should be compensated for 100%, and the phosphorus input should be 1.5–2 times higher than the output. They found that under excessive moistening, losses of nitrogen in fertilised soils may reach 25–30 kg/ha. Pavlova et al. (2018) found that positive changes in the fractional composition of soil humus were a consequence of the high level of agricultural technology compared with poor land management technologies.

Long-term irrigation in the Trans-Volga dry steppes resulted in the degradation of Kastanozems through losses of soil organic matter, a shift in the ratio of humic to fulvic acids, the downward leaching of active fractions of SOM and losses of soil stable aggregates through clay disintegration and redistribution. The dehumification of the irrigated Dark Chestnut soils was associated with pronounced humus mineralisation compared to non-irrigated soil. The decrease in the content and reserves of humus during irrigation was accompanied by negative changes in its composition.

In addition, in the soils which were studied, irrigation caused an increase in the soil density, block structure and clay content, as well as an increase in the dispersion (higher specific surface area), and a decrease in total porosity. Changes in differential porosity were most pronounced in the irrigated soils during the formation of hydro-morphic conditions. The formation of hydro-morphic conditions was manifested in an increase in the number of micropores with water that was inaccessible or poorly accessible for plants, along with a decrease in the number of capillary and aeration pores that provide a favourable air regime.

28.4 Conclusions

The results of the study showed that the once fertile soils of the dry steppes of the Trans-Volga region have significantly lost their original fertility and stability with a long, varied history of intensive irrigation. Summarising our own studies on long-term irrigated agriculture and the literature, we suggest that it is possible to adjust the existing irrigation technology in the region to prevent further losses of SOM and the deterioration of its physical and productive parameters. Controlling the rate of SOM mineralisation and humus growth by adding organic fertilisers, and managing crop residues and the rates and frequency of irrigation can help regulate a zero or positive balance of soil organic matter and stabilise the physical properties of the soil. Therefore, further research should be aimed at revising existing approaches to cultivation and irrigation, as well as developing and adopting an environmentally friendly approach to growing crops in the area studied.

References

- Agneessens L, De Waele J, De Neve S (2014) Review of alternative management options of vegetable crop residues to reduce nitrate leaching in intensive vegetable rotations. *Agronomy* 4:529–555. <https://doi.org/10.3390/agronomy4040529>. <https://www.mdpi.com/2073-4395/4/4/529>
- Alexandrova LN (1980) Soil organic matter and processes of its transformation. Leningrad, Nauka, p 287. (Александрова Л.Н. Органическое вещество почвы и процессы его трансформации. Ленинград, Наука, стр. 287)
- Andreeva OV, Kust GS (2020) Assessment of the state of land in Russia based on the latest concept of the neutral balance of land degradation. *Izvestiya RAN. Geogr Ser* 5:737–749 (О. В. Андреева, Г. С. Куст, Оценка состояния земель в России на основе концепции нейтрального баланса их деградации. Известия Российской академии наук. Серия географическая). <https://doi.org/10.31857/S2587556620050052>
- Ayuso SV, Onatibia GR, Maestre FT, Yahdjian L (2019) Grazing pressure interacts with aridity to determine the development and diversity of biological soil crusts in Patagonian rangelands. *Land Degrad Develop* 31(4):488–499. <https://doi.org/10.1002/ldr.3465>
- Baldock JA, Skjemstad JO (2000) Role of the soil matrix and minerals in protecting natural organic materials against biological attack. *Org Geochem* 31:697–710. [https://doi.org/10.1016/S0146-6380\(00\)00049-8](https://doi.org/10.1016/S0146-6380(00)00049-8)
- Basga SD, Tsozué D, Jean Pierre T, Jules B, Jean Pierre N (2018) Land use impact on clay dispersion/flocculation in irrigated and flooded vertisols from Northern Cameroon. *International Soil and Water Conservation Research* 6(3):237–244. <https://doi.org/10.1016/j.iswcr.2018.03.004>
- Blum WEH (2011) Physical degradation of soils, risks and threats. In: Gliński J, Horabik J, Lipiec J (eds) *Encyclopedia of agrophysics*. Encyclopedia of earth sciences series. Springer, Dordrecht. https://doi.org/10.1007/978-90-481-3585-1_111
- Bondi G, O’Sullivan L, Fenton O, Creamer R, Marongiu I, Wall DP (2020) Trafficking intensity index for soil compaction management in grasslands. *Soil Use Manag.* <https://doi.org/10.1111/sum.12586>
- Borelli P, Robinson D, Fleischer L et al (2017) An assessment of the global impact of 21st century land use change on soil erosion. *Nat Commun* 8(1):2013. <https://doi.org/10.1038/s41467-017-02142-7>
- Bünemann EK, Bongiorno G, Bai Zh et al (2018) Soil quality—a critical review. *Soil Biol Biochem* 120:105–125. <https://doi.org/10.1016/j.soilbio.2018.01.030>. <https://edepot.wur.nl/441556>
- Chenu C, Bissonnais YL, Arrouays D (2000) Organic matter influence on clay wettability and soil aggregate stability. *Soil Sci Soc Am J* 64(4):1479–1486. <https://doi.org/10.2136/sssaj2000.6441479x>
- Chenu C, Guéris J (1991) Mechanical strength of clay minerals as influenced by an adsorbed polysaccharide. *Soil Sci Soc Am J* 55:1076–1080. <https://doi.org/10.2136/sssaj1991.03615995005500040030x>
- Chukov SN (1998) Study of humus acids in anthropogenically disturbed soils using ¹³C NMR spectroscopy. *Eur Soil Sci* 31(9):979–986
- Cook RL, Langford CH (1998) Structural characterization of a fulvic acid and a humic acid using solid-state Ramp-CP-MAS ¹³C nuclear magnetic resonance. *Environ Sci Technol* 32:719–725. <https://doi.org/10.1021/es970488c>
- Correa J, Postma JA, Watt M, Wojciechowski T (2019) Soil compaction and the architectural plasticity of root systems. *J Exper Botany* 70(21):6019–6034. <https://doi.org/10.1093/jxb/erz383>
- Currie DR (2006) Soil physical degradation due to drip irrigation in vineyards: evidence and implications. PhD thesis, University of Adelaide, p 108. <https://digital.library.adelaide.edu.au/dspace/bitstream/2440/58642/8/02whole.pdf>. Accessed 7 Mar 2021
- Czyż EA, Tomaszewska J, Dexter AR (2001) Response of the spring to changes of compaction and aeration of sandy soil under model condition. *Int Agrophys* 15:9–12. <http://www.international-agrophysics.org/Response-of-spring-barley-to-changes-of-compaction-and-aeration-of-sandy-soil-under-model-condition.106816.0.2.html>. Accessed 7 Mar 2021

- Delfiner P, Chilès JP (2000) Geostatistics: modeling spatial uncertainty. *J Am Stat Assoc* 95(449):695. <https://doi.org/10.2307/2669569>. Wiley
- Dospkheov BA (1985) Methods of field experience (with the basics of statistical processing of research results), 5th edn. Agropromizdat, Moscow, p 351 (Методы полевого опыта (с основами статистической обработки результатов исследования). 5-е изд., Москва, Агропромиздат)
- Edelgeriev RSKh (2019) National report “Global climate and soil cover of Russia: desertification and land degradation, institutional, infrastructural, technological adaptation measures (agriculture and forestry), vol 2. Moscow, p 476. <https://cc.voeikovmgo.ru/images/sobytiya/2020/03/docclipoch.pdf>. Accessed 7 Mar 2021
- Egorov VV, Ivanova EN, Fridland VM (1977) Classification and soil diagnostics of the USSR. *Kolos*, p 225. <http://www.geokniga.org/books/3460>
- Eusterhues K, Rumpel C, Kleber M, Kögel-Knabner I (2003) Stabilisation of soil organic matter by interactions with minerals as revealed by mineral dissolution and oxidative degradation. *Org Geochem* 34(12):1591–1600. <https://doi.org/10.1016/j.orggeochem.2003.08.007>
- Falkovich AS, Pronko NA, Korsak VV (2017) Promising methods of land reclamation in counteraction against the degradation of irrigated land (using the example of the Saratov region). *Sci J Russ Res Inst Land Reclam* 1(25) (Перспективные приемы мелиорации в борьбе с деградацией орошаемых земель (на примере Саратовской области) <http://www.rosniipm-sm.ru/archive?n=458&id=467>. Accessed 7 Mar 2021
- Falloon PD, Smith P (2000) Modelling refractory soil organic matter. *Biol Fertil Soils* 30:388–398. <https://doi.org/10.1007/s003740050019>
- Franco U, Witing F (2020) Dynamics of soil organic matter in agricultural landscapes. In: Mirschel W, Terleev V, Wenkel KO (eds) *Landscape modelling and decision support*. Innovations in landscape research. Springer, Cham, pp 283–298. https://doi.org/10.1007/978-3-030-37421-1_14
- Franzluebbers A (2002) Soil organic matter stratification ratio as an indicator of soil quality. *Soil Till Res* 66(2):95–106. <http://www.dzumervis.nic.in/MicrobesandMetalsInteraction/pdf/Soilorganicmatterstratification.pdf>. Accessed 7 Mar 2021
- Gajić B, Kresović B, Pejić B, Tapanarova A, Dugalić G, Životić Lj, Sredojević Z, Tolimir M (2020) Some physical properties of long-term irrigated fluvisols of valley the river Beli Drim in Klina (Serbia). *Zemljište I Biljka* 69(1):21–35. <https://doi.org/10.5937/ZemBilj2001021G>, http://www.sdpz.rs/images/casopis/2020/zin_69_1_64.pdf. Accessed 7 Mar 2021
- Ganzhara NF, Borisov BA, Baybekov RF (2002) Workshop on soil science. Agroconsult, Moscow, p 280 (Ганжара НФ, Борисов БА, Байбеков РФ. Практикум по почвоведению. Агроконсалт)
- Ghabbour EA, Davies G, Wang K, Dickinson LC, Xing B (2001) Investigation of molecular motion of humic acids with 1-D and 2-D solution NMR. In: Ghabbour EA, Davies G (eds) *Humic substances: structures, models and functions*. Royal Society of Chemistry: Cambridge, UK, pp 73–82. <https://doi.org/10.1039/9781847551085-00073>
- GOST 26424-85 (1986) Soils. Methods for determination of carbonate and bicarbonate ions in water extract (Почвы. Методы определения ионов карбоната и бикарбоната в водной вытяжке) http://snipov.net/c_4702_snip_104831.html
- Gregorich EG, Carter MR, Angers DA, Monreal CM, Ellert BH (1994) Towards a minimum data set to assess soil organic matter quality in agricultural soils. *Can J Soil Sci* 74(4):367–385. <https://doi.org/10.4141/cjss94-05>
- Guerra CA, Rosa IMD, Valentini E et al (2020) Global vulnerability of soil ecosystems to erosion. *Landscape Ecol*. <https://doi.org/10.1007/s10980-020-00984-z>
- Guggenberger G, Bischoff N, Shibistova O, Muller C, Rolinski S, Puzanov A, Prishchepov AV, Schierhorn F, Mikutta R (2020) Interactive effects of land use and climate on soil organic carbon storage in Western Siberian steppe soils. In: Frühauf M, Guggenberger G, Meinel T, Theesfeld I, Lentz S (eds) *KULUNDA: climate smart agriculture*. Müller L (Series ed) *Innovations in landscape research*. Springer, Nature, pp 183–199. <https://www.springer.com/gp/book/9783030159269>
- Guidelines for the integrated monitoring of soil fertility of agricultural land (approved by the Ministry of Agriculture of Russia on September 24, 2003, by the Agricultural Academy on September 17, 2003) (Методические указания по проведению комплексного мониторинга плодородия почв земель сельскохозяйственного назначения)
- Gupta R, Rabi NS, Abrol IP (2019) Does soil testing for fertiliser recommendation fall short of a soil health card? *J Agron Res* 1(3):15–26. <https://doi.org/10.14302/issn.2639-3166.jar-18-2496>
- Hoffland E, Kuypers TW, Comans RNJ et al (2020) Eco-functionality of organic matter in soils. *Plant Soil* 455:1–22. <https://doi.org/10.1007/s11104-020-04651-9>
- Isweiri H, Qian Y (2017) Long-term effects of effluent water irrigation on soil chemical properties of sand-based putting greens. In: Arman H, Yuksel I (eds) *Arid environments and sustainability*. IntechOpen. <https://doi.org/10.5772/intechopen.72227>. <https://www.intechopen.com/books/arid-environments-and-sustainability/long-term-effects-of-effluent-water-irrigation-on-soil-chemical-properties-of-sand-based-putting-gre>. Accessed 7 Mar 2021
- Jenkinson DS, Ladd JN (1981) Microbial biomass in soil: measurement and turnover. In: Paul EA, Ladd JN (eds) *Soil biochemistry*, vol 5. Marcel Dekker, Inc., New York, pp 415–471
- Jensen JL, Schjøning P, Watts CW, Christensen BT, Obour PB, Munkholm LJ (2020) Soil degradation and

- recovery—changes in organic matter fractions and structural stability. *Geoderma* 364:114181. <https://doi.org/10.1016/j.geoderma.2020.114181>
- Kaiser K, Eusterhues K, Rumpel C, Guggenberger G, Kögel-Knabner I (2002) Stabilisation of organic matter by soil minerals—investigations of density and particle-size fractions from two acid forest soils. *J Plant Nutr Soil Sci* 165:451–459. [https://doi.org/10.1002/1522-2624\(200208\)165:4%3c451::AID-JPLN451%3e3.0.CO;2-B](https://doi.org/10.1002/1522-2624(200208)165:4%3c451::AID-JPLN451%3e3.0.CO;2-B). Accessed 7 Mar 2021
- Kalinichenko VP, Bezuglova OS, Solntseva NG, Skovpen AN, Chernenko VV, Il'ina LP, Boldyrev AA, Shevchenko DV, Skvortsov DA (2012) Unfavorable effect on soil of existing ways of watering and opportunities for use of intrasoil pulse continually-discrete irrigation paradigm. *Sci J Russ Res Inst Land Reclam Probl Novocherkassk* 2(06):12 (Неблагоприятное влияние орошения на почву, возможности и перспективы использования парадигмы внутрипочвенного импульсного континуума-дискретного орошения). <https://cyberleninka.ru/article/n/neblagopriyatnoe-vliyanie-orosheniya-na-pochvu-i-vozmozhnosti-i-perspektivy-primeneniya-vnutripochvennoy-impulsnoy-kontinualno/viewer>. Accessed 7 Mar 2021
- Keller T, Sandin M, Colombi T, Horn R, Or D (2019) Historical increase in agricultural machinery weights enhanced soil stress levels and adversely affected soil functioning. *Soil Till Res* 194:104293. <https://doi.org/10.1016/j.still.2019.104293>
- Khalaf M, Kohl SD, Klumpp E, Rice JA, Tombácz E (2003) Comparison of sorption domains in molecular weight fractions of a soil humic acid using solid-state ¹⁹F NMR. *Environ Sci Technol* 37:2855–2860. <https://doi.org/10.1021/es0206386>
- Kleber M, Mertz C, Zikeli S, Knicker H, Jahn R (2004) Changes in surface reactivity and organic matter composition of clay subfractions with duration of fertilizer deprivation. *Eur J Soil Sci* 55:381–391. <https://doi.org/10.1111/j.1365-2389.2004.00610.x>
- Kleber M, Lehmann J (2019) Humic substances extracted by alkali are invalid proxies for the dynamics and functions of organic matter in terrestrial and aquatic ecosystems. *J Environ Qual* 48:207–216. <https://doi.org/10.2134/jeq2019.01.0036>
- Kögel-Knabner I, de Leeuw JW, Hatcher PG (1992a) Nature and distribution of alkyl carbon in forest soil profiles: implications for the origin and humification of aliphatic biomacromolecules. *Sci Total Environ* 118:175–185. [https://doi.org/10.1016/0048-9697\(92\)90085-7](https://doi.org/10.1016/0048-9697(92)90085-7)
- Kögel-Knabner I, Hatcher PG, Tegelaar EW, deLeeuw JW (1992b) Aliphatic components of forest soil organic matter as determined by solid state ¹³C NMR and analytical pyrolysis. *Sci Total Environ* 113:89–106. [https://doi.org/10.1016/0048-9697\(92\)90018-N](https://doi.org/10.1016/0048-9697(92)90018-N)
- Kögel-Knabner I, Rumpel C (2018) Advances in molecular approaches for understanding soil organic matter composition, origin, and turnover: a historical overview. *Adv Agron* 149:1–48. <https://doi.org/10.1016/bs.agron.2018.01.003>
- Kononova MM (1961) Soil organic matter. Pergamon, New York
- Kononova MM (1963) Soil organic matter. Its nature, properties and methods of study. Publishing house of the Academy of Sciences of the USSR, Moscow, p 314 (Кононова М.М. Органическое вещество почвы. Его сущность, свойства и методы исследования. Москва, Издательство АН СССР, с. 314)
- Kuvaeva YuV (2012) Group composition of humus and fractions of the fine-dispersed phase of sod-podzolic medium-loamy soil in a long-term experiment Dokuchaev Soil Bulletin 70: 18–42 (Куваева Ю.В. Групповой состав гумуса и фракций тонкодисперсной фазы дерновоподзолистой среднесуглинистой почвы в длительном опыте. Бюллетень Почвенного института им. В.В. Докучаева. 70: 18–42)
- Laird DA, Chappell MA, Martens DA, Wershaw RL, Thompson M (2008) Distinguishing black carbon from biogenic humic substances in soil clay fractions. *Geoderma* 143:115–122. <https://doi.org/10.1016/j.geoderma.2007.10.025>
- Lal R (2004) Soil carbon sequestration impacts on global climate change and food security. *Science* 304:1623–1627. <https://doi.org/10.1126/science.1097396>
- Lal R (2020) Soil erosion and gaseous emissions. *Appl Sci* 10(8):2784. <https://doi.org/10.3390/app10082784>
- Li Y, Li J, Gao L, Tian Y (2018) Irrigation has more influence than fertilisation on leaching water quality and the potential environmental risk in excessively fertilized vegetable soils. *PLoS One* 13(9):e0204570. <https://doi.org/10.1371/journal.pone.0204570>
- Lorenz K, Lal R, Ehlers K (2019) Soil organic carbon stock as an indicator for monitoring land and soil degradation in relation to United Nations' sustainable development goals. *Land Degrad Develop* 30(7):824–838. https://catalogue.unccd.int/394_Article_Lorenz_et_al-2019-Land_Degradation_&_Development.pdf. Accessed 7 Mar 2021
- Ludwig B, Geisseler D, Michel K, Joergensen RG, Schulz E, Merbach I, Raupp J, Rauber R, Hu K, Niu L, Liu X (2011) Effects of fertilisation and soil management on crop yields and carbon stabilisation in soils. *A Rev Agron Sustain Dev* 31:361–372. <https://doi.org/10.1051/agro/2010030PhysicalPropertiesofSoilsAffectedbytheUseofAgriculturalWaste>:10.5772/intechopen.7799325
- Lützw MV, Kögel-Knabner I, Ekschmitt K, Matzner E, Guggenberger G, Marschner B, Flessa H (2006) Stabilisation of organic matter in temperate soils: mechanisms and their relevance under different soil conditions—a review. *Eur J Soil Sci* 57(4):426–445. <https://doi.org/10.1111/j.1365-2389.2006.00809.x>
- Mineev VG (2001) Workshop on agrochemistry. Moscow State University Publishing House, p 689 (Минеев В.Г. Практикум по агрохимии, МГУ)

- Montgomery D (2007) Soil erosion and agricultural sustainability. *Proc Natl Acad Sci USA* 104:13268–13272. <https://doi.org/10.1073/pnas.0611508104>, <https://www.ncbi.nlm.nih.gov/pmc/articles/PMC1948917/>
- Murray RS, Grant RS (2007) The impact of irrigation on soil structure. *Land Water Aust* 31. <https://library.dbca.wa.gov.au/static/FullTextFiles/070521.pdf>
- Ndzelu BS, Dou S, Zhang ZW (2020) Changes in soil humus composition and humic acid structural characteristics under different corn straw returning modes. *Soil Res* 58(5):452–460. <https://doi.org/10.1071/SR20025>
- Negev I, Shechter T, Shtrasler L, Rozenbach H, Livne A (2020) The effect of soil tillage equipment on the recharge capacity of infiltration ponds. *Water* 12:541. <https://doi.org/10.3390/w12020541>. <https://www.mdpi.com/2073-4441/12/2/541>
- Nikolskii YuN, Aidarov IP, Landeros-Sanchez C, Pchyolkina VV (2019) Impact of long-term freshwater irrigation on soil fertility. *Irrig Drain* 68(5):993–1001. <https://doi.org/10.1002/ird.2381>
- Nikolskii-Gavrilov I, Aidarov IP, Landeros-Sanchez C, Herrera-Gomez S, Bakhlaeva-Egorova O (2014) Evaluation of soil fertility indices of freshwater irrigated soils in Mexico across different climatic regions. *J Agric Sci* 6(6):98–107
- Nunes MR, Karlen DL, Moorman TB (2020) Tillage intensity effects on soil structure indicators—A US meta-analysis. *Sustainability* 12(5):2071. <https://doi.org/10.3390/su12052071>. <https://www.mdpi.com/2071-1050/12/5/2071/>
- O’Sullivan MF, Simota C (1995) Modelling the environmental impacts of soil compaction: a review. *Soil Tillage Res* 35:69–84. <https://doi.org/10.1007/s13593-011-0071-8>
- Oades JM (1988) The retention of organic matter in soils. *Biogeochemistry* 5:35–70. <https://doi.org/10.1007/BF02180317>
- Obalum SE, Chibuike GU, Peth S, Ouyang Y (2017) Soil organic matter as sole indicator of soil degradation. *Environ Monit Assess* 189(4). <https://doi.org/10.1007/s10661-017-5881-y>
- Olk DC, Brunetti G, Senesi N (2000) Decrease in humification of organic matter with intensified lowland rice cropping: a wet chemical and spectroscopic investigation. *Soil Sci Soc Am J* 64:1337–1347. <https://doi.org/10.2136/sssaj2000.6441337x>
- Olsson L, Barbosa H, Bhadwal S et al (2019) Land degradation. In: Climate change and land: an IPCC special report on climate change, desertification, land degradation, sustainable land management, food security, and greenhouse gas fluxes in terrestrial ecosystems. In: Shukla PR, Skea J, Calvo Buendia E, Masson-Delmotte V, Pörtner H-O, Roberts DC, Zhai P, Slade R, Connors S, van Diemen R, Ferrat M, Haughey E, Luz S, Neogi S, Pathak M, Petzold J, Portugal Pereira J, Vyas P, Huntley E, Kissick K, Belkacemi M, Malley J (eds). <https://www.ipcc.ch/srccl/chapter/chapter-4/>, accessed on May 23, 2020
- Orlov DS (1998) Organic substances of Russian soils. *Eurasian Soil Sci* 31:946–953. <http://pascal-francis.inist.fr/vibad/index.php?action=getRecordDetail&idt=2383645>. Accessed 7 Mar 2021
- Parkhomenko GG, Voinash SA, Sokolova VA, Krivonogova AS, Rzhavtsev AA (2019) Reducing the negative impact of undercarriage systems and agricultural machinery parts on soils. *IOP Conf Ser Earth Environ Sci* 316:012049. <https://doi.org/10.1088/1755-1315/316/1/012049>
- Pavlova O, Litvinovich A, Lavrishchev A, Saljnikov E (2018) Effect of different anthropogenic impacts on pH and humus composition of soddy-podzolic soil. *Zemljiste i Biljka* 67(1):46–63. http://www.sdpz.rs/images/casopis/2018/ZIB_vol67_no1_2018_pp46-63.pdf
- Platonova TK, Shmyglya LN (1986) Differential porosity and fractional composition of pore solutions of Dark-Chestnut soils of the Low Syrt plain. *Pochvovedenie* 6:98–102 (Платонова Т.К., Шмыглия Л.Н. Дифференциальная пористость и фракционный состав поровых растворов темно-каштановых почв Низко-Сыртской равнины. Почвоведение)
- Plotnikova TA, Orlova NE (1984) Determination of the content of acid functional groups in preparations of humic acids. Modern methods of physical and chemical research and chemical analytical control in agriculture. In: Proceedings of the all-union conference, Tuumen, p 124 (Плотникова Т.А., Орлова Н.Е. Определение содержания кислотных функциональных групп в препаратах гуминовых кислот. Современные методы физико-химических исследований и химико-аналитического контроля в сельском хозяйстве. Материалы Всесоюзной конференции, Тюмень с.124.), http://www.bio.vsu.ru/soil/Современные%20методы%20физико-химического%20анализа%20почвы%20методичка_.pdf. Accessed 7 Mar 2021
- Poeplau C, Sigurdsson P, Sigurdsson BD (2020) Depletion of soil carbon and aggregation after strong warming of a subarctic Andosol under forest and grassland cover. *Soil* 6:115–129. <https://doi.org/10.5194/soil-6-115-2020>
- Popov AI (2004) Humic substances: properties, structure, formation. In: Ermakov EI (eds) Faculty of Biology, St. Petersburg State University, p 248 (Попов А.И. Гуминовые вещества: свойства, структура, образование. Э. Ермаков (ред.), Санкт-Петербургский Государственный Университет, Биологический факультет). <http://почвовед.рф/wp-content/uploads/2017/04/0476-Попов-А.И.-2004.pdf>. Accessed 7 Mar 2021
- Pronko NA, Korsak VV (2001) Method of calculating of doses of organic and mineral fertilizers for crops on irrigated crop rotations according to the predicted rotary balance of nutrient elements. *Agrokhimia* 7:66–71 (Пронько Н.А., Корсак В.В. Методика расчета доз органических и минеральных удобрений для сельскохозяйственных культур при орошаемых

- севооборотах по прогнозируемому круговому балансу элементов питания. *Агробиология*, 7: 66–71)
- Pronko NA, Korsak VV, Falkovich AS (2014) Irrigation in the Volga region: do not repeat mistakes. *Melioratsiya i Vodnoe Khozaystvo* 4:16–19 (Пронько Н.А., Корсак В.В., Фалькович А.С. Орошение в Поволжье: не повторять ошибок. Мелиорация и Водное хозяйство). http://www.iwep.ru/ru/struct/LLVEP/lich/sp_publ/Melioratsiyavodnoehozaystvo2014_4.pdf. Accessed 7 Mar 2021
- Pronko NA, Korsak VV, Romanova LG, Kravchuk AV, Afonin VV (2018) The effect of prolonged irrigation on the Volga Region. *Int J Eng Technol Special Issue* 38:1210–1213. <https://www.sciencepubco.com/index.php/ijet/article/view/27764/14434>
- Pronko NA, Romanova LG, Falkovich AS (2005) Change in fertility of irrigated chestnut soils of the Volga region in the process of long-term use and the scientific basis of its regulation. Publishing house of Saratov State Agrarian University, Saratov, p 220 (Пронько Н. А., Романова Л. Г., Фалькович А. С. Изменение плодородия орошаемых каштановых почв Поволжья в процессе длительного использования и научные основы его регулирования Саратов: Изд-во Саратовского государственного аграрного университета, с. 220)
- Quesada CA, Paz C, Mendoza EO, Philips OL, Saiz G, Lloyd J (2020) Variations in soil chemical and physical properties explain basin-wide Amazon forest soil carbon concentrations. *Soil* 6(1):53–88. <https://doi.org/10.5194/soil-6-53-2020>
- Rengasamy P (2019) Irrigation water quality and soil structural stability: a perspective with some new insights. In: *Prime archives in agronomy*. Vide Leaf, Hyderabad, India. <https://videleaf.com/wp-content/uploads/2020/02/Irrigation-Water-Quality-and-Soil-Structural-Stability-A-Perspective-with-Some-New-Insights.pdf>. Accessed 7 Mar 2021
- Savvinov NI (1931) The structure and stability of soil on virgin, fallow and old-arable soils. In: Williams VR (ed) *SelchozGiz*, Moscow, p 46 (Саввинов Н.И. Структура и прочность почвы на целине, перелог и старопашотных участках. СельхозГиз)
- Seiler MN (1999) Modeling our world: the ESRI guide to geodatabase design. Environmental Systems Research Institute, Inc., 380 New York Street, Redlands, California 92373-8100 USA, p 202. http://downloads2.esri.com/support/documentation/ao_/Modeling_our_World.pdf. Accessed 18 Mar 2021
- Semenov VM, Semenov NA, Ivannikova LA (2013) Humification and nonhumification pathways of the organic matter stabilisation in soil: a review. *Eur Soil Sci* 46(4):355–368
- Shein YV (2005) Soil physics course. MGU Publisher, p 432 (Шейн Ю.В. (2005) Курс физики почв. Издательство МГУ стр. 432)
- Slade PG, Quirk JP, Norrish K (1991) Crystalline swelling of smectite samples in concentrated NaCl solutions in relation to layer charge. *Clays Clay Miner* 39:234–238. <https://doi.org/10.1346/CCMN.1991.0390302>
- Sposito G, Skipper NT, Sutton R, Park S, Soper AK, Greathouse JA (1999) Surface geochemistry of the clay minerals. *Proc Natl Acad Sci USA* 96:3358–3364. <https://doi.org/10.1073/pnas.96.7.3358>
- Susic M (2016) Replenishing humic acids in agricultural soils. *Agronomy* 6(4):45. <https://doi.org/10.3390/agronomy6040045>
- Sutton R, Sposito G (2006) Molecular structure in soil humic substances: the new view. *Environ Sci Technol* 39(23):9009–9015. <https://doi.org/10.1021/es050778q>
- Tebebu TY, Bayabil HK, Steenhuis TS (2020) Can degraded soils be improved by ripping through the hardpan and liming? A field experiment in the Ethiopian Highlands. *Land Degrad Develop*. <https://doi.org/10.1002/ldr.3588>
- Tisdall JM, Oades JM (1982) Organic matter and water-stable aggregates. *J Soil Sci* 33:141–163. <https://doi.org/10.1111/j.1365-2389.1982.tb01755.x>
- Titova NA, Travnikova LS, Kuvaeva YuV, Volodarskaya IV (1989) Composition of organic and mineral components of fine particles of arable sod-podzolic soil. *Pochvovedenie* 6:89–97 (Титова Н.А., Травникова Л.С., Куваева Ю.В., Володарская И.В. Состав органических и минеральных компонентов мелких частиц пахотной дерново-подзолистой почвы. *Почвоведение* 6: 89–97)
- Totsche KU, Amelung W, Gerzabek MH et al (2018) Microaggregates in soils. *J Plant Nut Soil Sci* 181(1):104–136. <https://doi.org/10.1002/jpln.201600451>
- Travnikova LS, Titova NA, Shaimukhametov MSH (1992) The role of products of interaction of organic and mineral components in the genesis and fertility of soils. *Pochvovedenie*, 10:81–96 (Травникова Л.С., Титова Н.А., Шаймухаметов М.С. Роль продуктов взаимодействия органических и минеральных компонентов в генезисе и плодородии почв. *Почвоведение*, 10: 81–96)
- Tuninetti M, Tamea S, Dalin C (2019) Water debt indicator reveals where agricultural water use exceeds sustainable levels. *Water Resour Res* 55(3):2464–2477. <https://doi.org/10.1029/2018WR023146>
- Tuyev NA (1989) Microbiological processes of humus formation. Agropromizdat Publisher, Moscow, p 239 (Туев Н.А. Микробиологические процессы гумусообразования. Москва, Агропромиздат, с. 239)
- UN (2015) Agenda 2030: sustainable development goals. 17 goals to transform our world. <https://www.un.org/sustainabledevelopment/>. Accessed 7 Mar 2021
- UNDP (2019) Combatting land degradation. Securing a sustainable future. https://www.undp.org/content/dam/undp/library/planet/environment/Combatting_Land_Degradation%20E2%80%93Securing_A_Sustainable_Future.pdf. Accessed 7 Mar 2021
- Unger PW, Kaspar TC (1994) Soil compaction and root growth: a review. *Agron J* 86:759–766
- Vadyunina AF, Korchagina ZA (1986) Methods for the study of soil physical properties. Agropromizdat,

- Moscow, p 416 (Вадюнина А.Ф., Корчагина З.А. Методы исследования физических свойств почв. Москва, Агропромиздат, с. 416.)
- Warrington DN, Goldstein D, Levy GJ (2007) Clay translocation within the soil profile as affected by intensive irrigation with treated wastewater. *Soil Sci* 172(9):692-700
- Whittig LD (1965) X-ray diffraction techniques for mineral identification and mineralogical composition. *Methods of soil analysis, part I. Agronomy* 9. American Society of Agronomy Inc., Madison, pp 671–698. <https://doi.org/10.2134/agronmonogr9.1.c49>
- Wiesmeier M, Urbanski L, Hobbey E Lang B, von Lützw M, Marin-Spiotta E, van Wesemael B, Rabot E, Ließ M, Garcia-Franco N, Wollschläger U, Vogel HJ, Kögel-Knabner I (2019) Soil organic carbon storage as a key function of soils—a review of drivers and indicators at various scales. *Geoderma* 333:149–162. <https://doi.org/10.1016/j.geoderma.2018.07.026>
- WRB (2014) World reference base for soil resources. Food and Agriculture Organisation of the United Nations Rome 2015. <http://www.fao.org/3/i3794en/I3794en.pdf>. Accessed 7 Mar 2021
- Xu L, Wang M, Xie X et al (2020) Assessment of soil aggregation properties after conversion from rice to greenhouse organic cultivation on SOC controlling mechanism. *J Soils Sediments* 20:1920–1930. <https://doi.org/10.1007/s11368-020-02589-0>
- Yefremov EN, Sychev VG, Romanenkov VA (2016) Balance of nutrients and the optimisation of their use in agroecosystems of the Russian Federation. In: Mueller L et al (eds) *Novel methods for monitoring and managing land and water resources in Siberia*. Springer Water. Springer International Publishing Switzerland. https://doi.org/10.1007/978-3-319-24409-9_28
- Zhang X, Davidson EA, Zou T, Lassaletta L, Quan Z, Li T, Zhang W (2020) Quantifying nutrient budgets for sustainable nutrient management. *Glob Biogeochem Cycles* 34(3):e2018GB006060. <https://doi.org/10.1029/2018GB006060>
- Zhao N, Yang Xi, Huang G, Lü Yi, Zhang Ji, Fan Yu, Drury CF, Yang X (2021) Chemical and spectroscopic characteristics of humic acid from a clay loam soil in Ontario after 52 years of consistent fertilisation and crop rotation. *Pedosphere* 31(1):204–213. [https://doi.org/10.1016/S1002-0160\(20\)60019-4](https://doi.org/10.1016/S1002-0160(20)60019-4)
- Zhou M, Liu C, Wang J et al (2020) Soil aggregates stability and storage of soil organic carbon respond to cropping systems on black soils of Northeast China. *Sci Rep* 10:265. <https://doi.org/10.1038/s41598-019-57193-1>



Fertility Decline in Arable Chernozem and Chestnut Soils in Volga Steppes Versus Their Virgin Analogues

Victor V. Pronko, Dmitry Yu. Zhuravlev,
Tatyana M. Yaroshenko, and Nadezhda
F. Klimova

Abstract

Soil types on cropland in the Volga dry steppe area were studied for changes in agrochemical properties due to long-term crop production compared to their virgin analogues (long-term non-fertilised grassland and rangeland). In cropped soils, a decline in soil fertility parameters was observed. The most intensive losses were found for Southern Chernozem, the least intensive in Typical Chernozem soils. These changes were found in the fractional composition of organic matter. In all the Chernozem soils studied (typical, ordinary, and southern), the share of humic acids decreased and the share of mobile fulvic acids increased with a negative consequence. The relative accumulation of fulvic acids was also noted due to the systematic application of mineral fertilisers. Chernozem soils also lost some of their nitrogen reserves due to cultivation. The biggest losses were observed for typical Chernozems. At the same time, a sharp decrease in the fraction of easily hydrolysable

N was observed on all subtypes of Chernozem. The prolonged use of fertilisers partially compensated for the loss of phosphorus in all Chernozems studied. Changes in the agrochemical properties depended on the subtype of Chernozem. Cropping on typical Chernozems led to a decrease in the amount of exchangeable cations and a certain increase in potential acidity. At the same time, an increase in the amount of bases and a decrease in the potential acidity were noted in the arable ordinary Chernozems. The cultivation of virgin Chestnut (Kastanozem) soils (in the 1950s) decreased the content of organic matter, indicating a high intensity of mineralisation of soil organic matter in the dry steppe, since the share of humic acids decreased and that of fulvic acid increased. The most intensive losses of humic compounds occurred in a meadow Chestnut soil, and the least intensive in dark Chestnut terraced soils. We conclude by commenting on the need for progress in research aimed at developing approaches and tools for productive and sustainable cropping systems, and for scientific-based monitoring and management practices on cropland to control soil carbon and stop nutrient mining.

V. V. Pronko (✉)

“Power of Life” Scientific Production Association,
st. Bolshaya Sadovaya, 239, Saratov, Russia
e-mail: victor-pronko@mail.ru

D. Yu. Zhuravlev · T. M. Yaroshenko · N. F.
Klimova

Research Institute of Agriculture of the South-East,
St. Tulaykova, 7, Saratov, Russia

Keywords

Volga steppe soils · Chernozem · Chestnut soil · Soil carbon · Soil N · Soil P · Exchangeable cations · Virgin land · Arable land

29.1 Introduction

Long-term agricultural activities may cause changes in soil fertility and plant quality indices (e.g. see Zhao et al. (2021a, 2021b)). The Volga region is the main provider of agricultural products in the Russian Federation. Agriculture is characterised by the production of grain, fodder and industrial crops (Pronko et al. 2021). In the steppes of the Volga Basin, agriculture development began relatively recently. The conversion of Chernozemic soils into cropland of the right bank of the Volga River was initiated 250–300 years ago. In the beginning, the farmlands were located near fortified military settlements and church monasteries. However, large-scale ploughing of soil in the dry steppes of the Volga region began in 1954. In a relatively short period (5–7 years), millions of hectares of virgin land were brought to cultivation. Such large-scale transformations of soil cover triggered changes in the vegetation, water and temperature regimes. The latter changes, in turn, influenced the soil-forming processes.

In the second half of the twentieth century, soils' long-term agricultural use led to a decrease in their fertility (Ivanov and Denikin 1996). Even highly fertile and well-buffering soils, such as Chernozem (Classification and soil diagnostics of the Soviet Union 1977), were subject to degradation (Mineev and Rempe 1990; Chub 1998, 2013; Sychev et al. 2014).

From previously published sources, it follows that the rate of degradation of Chernozem depends on many environmental factors that vary considerably even within the same soil-climatic zone (Mineev and Rempe 1990; Pronko et al. 2018). In the 1950s, the intensive use of Chestnut soils (Classification and soil diagnostics of the Soviet Union (1977) corresponding to

Kastanozem in the WRB classification system) on dry steppes in the Volga region led to a deterioration in their agrochemical, agrophysical, and physicochemical properties in a relatively short period (Gamzikov and Kulagina 1992; Orlov et al. 1996; Chizhikova et al. 2011; Mamontov 2013). This was due to the predominance of soil mineralisation processes over humification, a small input of organic residues into the soil, and a sharp continental climate (Tuyev 1989; Grishina et al. 1990; Anisimova 2005; Lai et al. 2013).

Different subtypes of Chestnut soil were formed under the influence of different climatic conditions and on different parent rocks (Pronko and Grishin 2005). These were key reasons for the level of soil degradation. To date, however, a comparative assessment of the transformation of the fertility parameters of different subtypes of Chestnut soil has not been carried out in the region. Soil degradation processes include physical, chemical and biological deterioration (Lal 2009). In this study, we have compared arable soils (Chernozem and Kastanozem) with their virgin analogues in terms of changes in nutritional capacity due to long-term cultivation.

The goal of this research was to study the magnitude of decline in organic matter and other soil fertility parameters due to cropping on the main subtypes of Chernozem and Chestnuts soils in the Volga dry steppes by comparing soils under cropland with their virgin analogues under grassland and rangeland.

29.2 Materials and Methods

To achieve this goal, samples of a soil subtype were simultaneously taken from plots of virgin soil and arable land located in close proximity to one another. The agrochemical indices in the virgin land were assumed to correspond to the initial parameters of the corresponding soil subtype in the arable area before ploughing. Surveys monitoring the state of soil cover were carried out starting in 2007. In total, for Chernozem soil (Fig. 29.1), 42 soil profiles (7 for virgin and 7 for arable soils) were studied on 3 subtypes of



Fig. 29.1 Chernozems are soils best cropped with winter wheat, sugar beet (left-hand side) and other valuable crops; the right-hand side shows largely natural grassland, which covers only a few areas



Fig. 29.2 Kastanozems bear different cereals (left side) and fodder crops, semi-natural grassland (right side) and rangeland

Chernozem soils. On Chestnut soil (Fig. 29.2), 50 profiles were studied (5 on virgin and 5 on arable soils), examining five subtypes of Chestnut soil.

The Chernozem soils studied were typical, ordinary and southern (Classification and Diagnostics of Soils of the Soviet Union 1977). They were sampled from the experimental stations in Lopukhovka, the village of Elizavetino and the Research Institute of the South-East Region (Saratov Trans-Volga region).

The Chestnut soils studied were dark Chestnut terrace, dark Chestnut syrt, Light Chestnut and meadow Chestnut in the plains of Saratov Trans-Volga (Classification and Diagnostics of Soils of the Soviet Union 1977). The arable analogues of all the selected soils were studied to reveal any changes in soil properties as a result of long-term cultivation. The site studied was located in the Saratov region near the villages of Zvonarevka, Lipovka, Bobrovka, Vodopiyanovka and the Krasnokutsk Agricultural Experimental Station.

In the places where the research was carried out, grain-oriented farms prevailed. The cultivated crops included winter and spring wheat, barley, oats, millet, corn for grain and sunflower. In the study area, crop rotations such as grain-fallow, grain-grass and grain-tilled crop rotations are dominant. The areas of meadows and pastures are represented by natural cereal and cereal-forb perennial vegetation.

It was important that groups of soil types and subtypes of virgin soils did not significantly differ from groups of cropped soils in terms of their horizon sequence, landscape position and texture. The content of humus was determined using the Tyurin method as modified by CINAQ, where organic matter was digested in a 0.4 N potassium chromate $K_2Cr_2O_7$. Analysis of the fractional composition of organic carbon was performed using Kononova and Belchikova's accelerated method, by extracting humic acids with 0.1 M $Na_4P_2O_7 \times 10H_2O$ and 0.1 n NaOH (Mineev 2001). To determine the various forms

of nitrogenous compounds, the Shkonde-Koroleva method was applied using 0.5 and 5.0 N H₂SO₄ (Mineev 2001). The conversion factor from organic carbon to organic matter (humus) is 1.724 (Mineev 2001). For soil phosphorus fractionation, the Chang-Jackson method was used, where Group I (P I, loosely bound phosphates) was released with 1 N NH₄Cl, Group II (P II, aluminium and calcium phosphates)—0.5 N NH₄F, Group III (P III iron phosphates)—0.1 N NaOH, IV group (P IV, highly basic calcium phosphates)—0.5 N H₂SO₄ (Mineev 2001). The total nitrogen and total potassium were determined together in a single sample after wet combustion with concentrated H₂SO₄ as described by Kjeldahl (Mineev 2001). Absorbed bases were determined using the Kappen–Gilkovitz method and a 0.1 N HCl solution. The soil acidity was analysed in an aqueous solution using an Ionomer-500 instrument. The exchange acidity was determined using a 1.0 N KCl solution. Soil hydrolytic acidity was determined in a 1.N CH₃COONa (Mineev 2001).

29.3 Results and Discussion

29.3.1 Soil Humus

The content of humus in the arable Chernozem under long-term use decreased markedly compared with its virgin analogue. Its highest absolute losses in organic carbon were observed in the southern subtype and amounted to 33% (Fig. 29.3). This decrease was mainly due to the removal of nutrients from the soil as a result of long-term crop production with and/or without additional nutrition with mineral and organic fertilisers (Tan et al. 2005; Funakawa et al. 2007; Saljnikov et al. 2005; Koković et al. 2018).

In the ordinary Chernozem, the reserves of humus have decreased quite substantially; by 25% compared to the virgin analogue. In the typical Chernozem, the loss compared to virgin soil did not exceed 7%. The application of mineral fertilisers did not have a considerable effect on the humus content at a depth of 0–20 cm in

any of the studied subtypes of Chernozem soils. Losses of total nitrogen reserves occurred most actively in dark Chestnut terrace soils. In the study by Eremin (2016), the total humus reserves in 1 m of ploughed Chernozem decreased by 8.5% over 38 years of cultivation. Thus, the losses of total humus content vary between different Chernozem soils, determined by their chemical and physical characteristics, which in turn are determined by their origin, parent rocks and climate.

29.3.2 Fractional Composition of Soil Organic Matter

The results showed that the narrowest ratio of humic acids (HA) to fulvic acids (FA) was observed in the ordinary and southern Chernozems at depths of 0–20 and 20–40 cm. In the arable southern Chernozem, the share of FAs increased from 10.5 to 14.4% of the total organic carbon content compared with the virgin soil at a depth of 0–20 cm. A considerable increase in the share of FAs was also noted in the unfertilised area of ordinary Chernozem where, at a depth of 0–20 cm, the share of FAs increased from 11.6 to 13.9% of the total organic carbon content. The use of mineral fertilisers also contributed to an increase in the share of FAs in ordinary Chernozem from 11.6 to 14.8% and from 10.5 to 14.8% on southern black soil at a depth of 0–20 cm, compared to virgin soil. In the typical Chernozem, cultivation led to a decrease compared to the virgin soil in the share of FAs in the unfertilised plot of 13.2 to 10.3% at a depth of 20–40 cm. The opposite situation was found on the southern Chernozem, where a considerable growth of FAs was observed in the arable soil compared to the virgin soil at a depth of 20–40 cm. The most intensive losses of humic compounds among the subtypes of Chestnut soils studied compared to their virgin analogues occurred in meadow Chestnut soil, and the least intensive in dark Chestnut terrace soils on the left bank of the Volga River. This indicates a high intensity of organic matter mineralisation processes in the cultivated land (Fig. 29.4). Dark

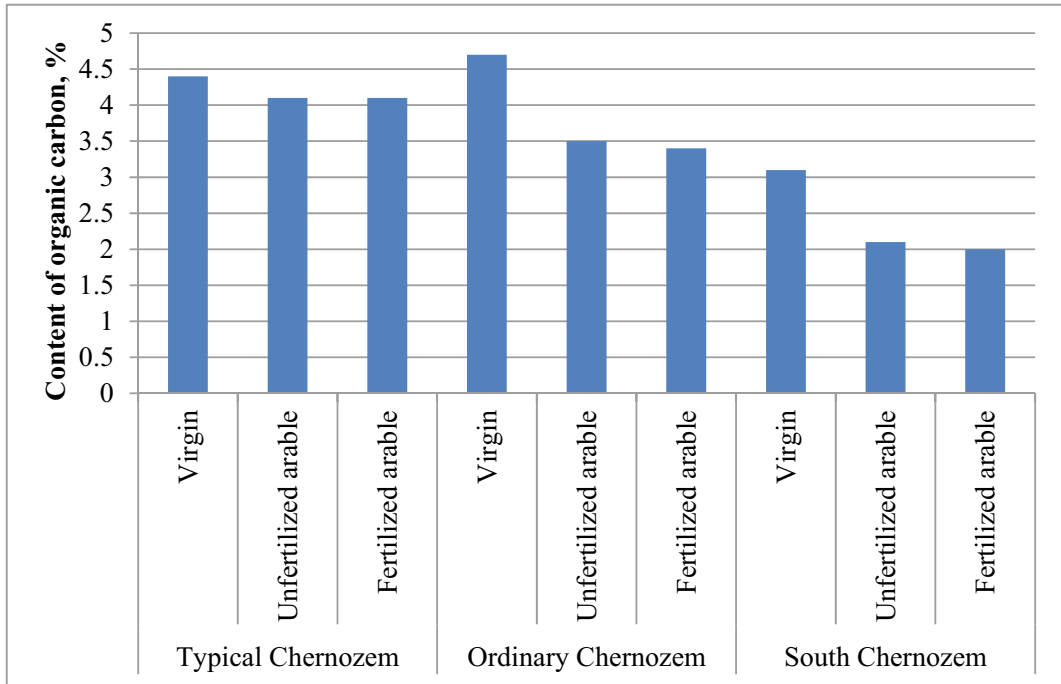


Fig. 29.3 Organic carbon content¹¹ (C, %) in the Chernozem soils of the Volga steppe (at 0–20 cm), read commas as points

Chestnut terraced soils located on the left bank of the Volga River had a medium loamy texture. The organic carbon content on virgin soil averaged 1.68% at 0–30 cm. In the composition of humus, the fraction of HAs was almost twice as high as FAs (38.2% and 17.2%, respectively). The humus content on cultivated dark Chestnut terraced soils decreased by 0.17% (in absolute values) compared to virgin soil. The cultivation of dark Chestnut soil led to a decrease in the share of HAs by 35% at 0–30 cm. The content of FAs changed slightly. Dark Chestnut syrt soils had a heavier texture than the soil on the second terrace of Volga River, above the floodplain. The organic carbon content of the virgin soil was 2.16%.

The cultivation of dark Chestnut syrt soils led to a sharp decrease in organic carbon content (from 2.16 to 1.55%). The content of HAs decreased by 6% compared to virgin analogues, while the content of FAs, conversely, increased (by 9%). As a result, their ratio changed. The differences in the content of organic carbon in the

Chestnut syrt (formed in drier conditions) and its virgin analogue were less than in the dark Chestnut soil (1.58%). The content of HAs decreased (compared to dark Chestnut syrt), and the content of FAs increased at a depth of 0–30 cm. This indicates an increase in the mobility of humus in Chestnut syrt soils. The cultivation of Chestnut syrt soils led to the loss of organic carbon (up to 1.24%) and a decrease in the share of HAs. The content of organic carbon in virgin light Chestnut syrt soils averaged 1.36%. As for the fractions of humic and FAs, the above tendency was observed, i.e. an increase in FA and a decrease in HA. Cultivation of this soil led to a decrease in the content of total organic carbon by 0.97%. The meadow Chestnut had more favourable moisture conditions, with a greater accumulation of plant biomass and as a consequence a higher input of organic matter. This ensured that the humus content of virgin soil at a depth of 0–30 cm was at a level of 5.18%. The cultivation of meadow Chestnut soil led to a decrease in the content of organic carbon by

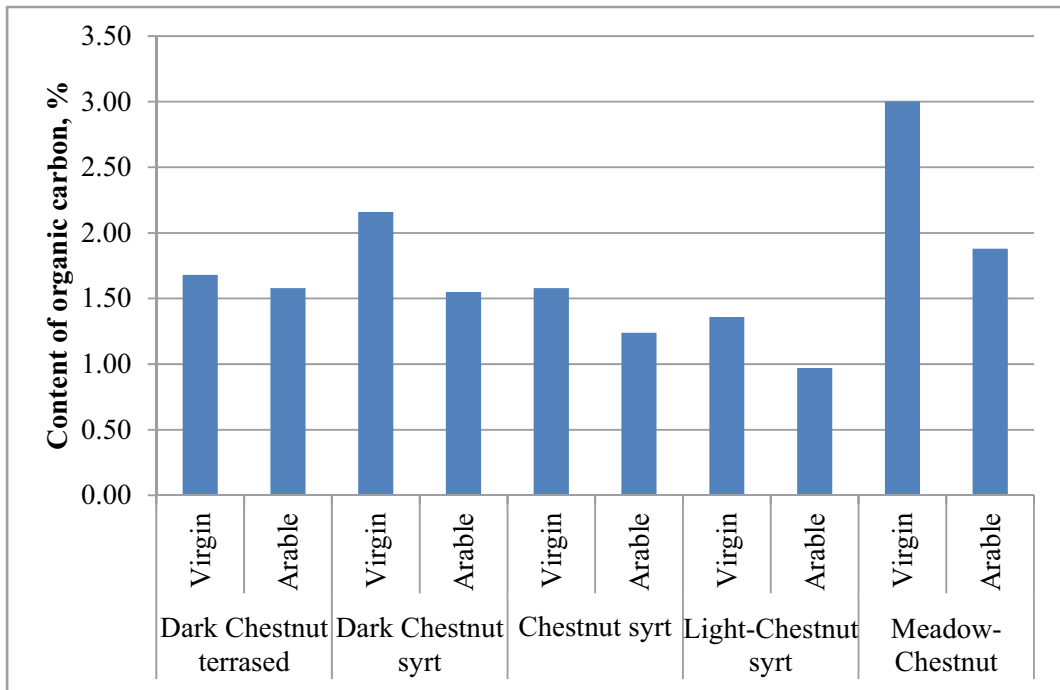


Fig. 29.4 Organic carbon content (C, %) in subtypes of Chestnut soil of the Volga steppe (at 0–20 cm), read commas as points

37%. At the same time, the share of HAs was 29.9% at a depth of 0–30 cm. The ratio of HAs to FAs at a depth of 0–30 cm changed slightly.

29.3.3 Soil Nitrogen

Of the three subtypes studied, the highest content of total nitrogen was observed in the virgin typical Chernozem, and the lowest in the southern Chernozem. The highest losses of N due to cultivation were found for a typical Chernozem (20% and 14% of N in the virgin and southern subtypes, respectively). The application of mineral fertilisers did not lead to the accumulation of total nitrogen reserves. The long-term cultivation of Chernozem soils not only led to a certain decrease in the content of total nitrogen, but also changed its fractional composition (Fig. 29.5).

The results showed that, first of all, the content of easily hydrolysable nitrogen decreased by 1.5 or more times (Fig. 29.5) compared to the virgin soil. Moreover, this form of nitrogen is known as the most available for plant nutrition. At the same time, in the typical and southern Chernozems, the reserves of poorly hydrolysable and non-hydrolysable forms of N decreased. By contrast, this trend was not observed for the ordinary Chernozem. These changes are explained by the fact that, under more favourable climatic conditions, the supply of plant residues to virgin Chernozem is much higher than on arable land. This, in turn, promotes the activation of the protease enzyme, which is involved in the decomposition of proteins to amino acids, thus enriching the soil with an easily hydrolysable form of nitrogen. Mineral fertilisers applied on all subtypes of Chernozem, in comparison with the unfertilised areas, increased the content of mineral and hydrolysable N and slightly reduced the content of non-hydrolysable forms.

¹ The ratio between organic carbon and humus is 1 g (C): 1,724 g (humus).

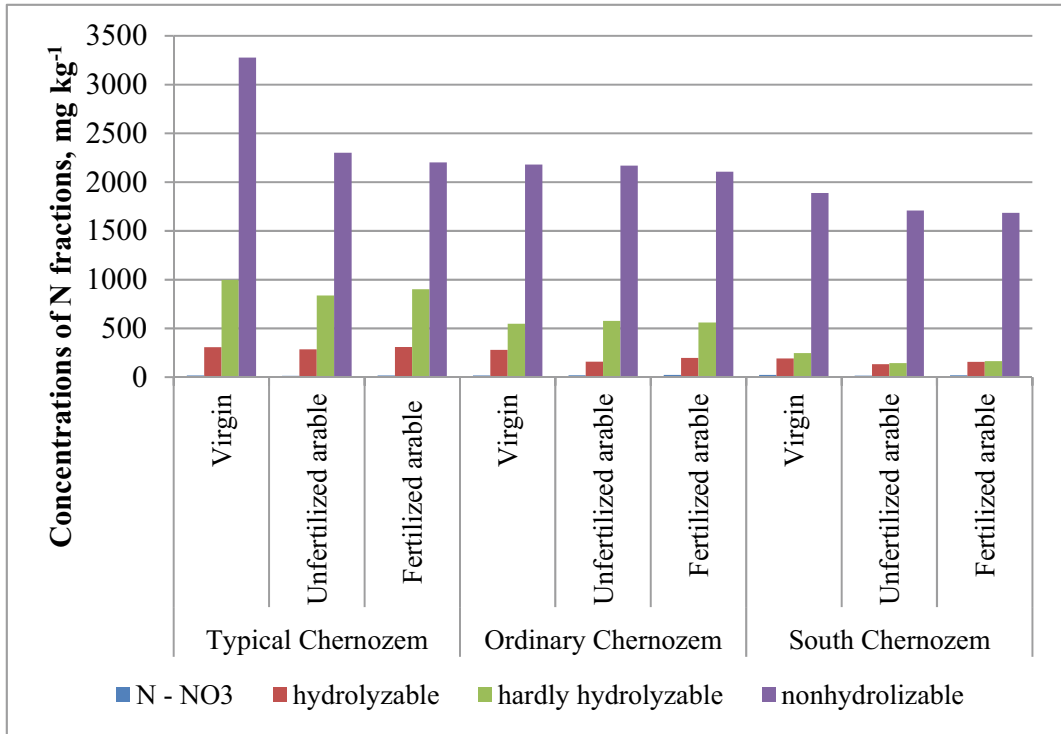


Fig. 29.5 Fractional composition of organic N in Chernozems of the Volga steppe, mg kg⁻¹ (0–20 cm)

In our studies, marked changes in the content of different N forms were also observed in Chestnut soils in the Saratov Trans-Volga region (Fig. 29.6). The cultivation of dark Chestnut terraced soils led to a sharp decline in the reserves of mineral nitrogen (by 702 mg kg⁻¹). At the same time, the amount of both easily and poorly hydrolysable N also decreased. The share of non-hydrolysable N, which is the main nitrogen source in these soils, decreased quite sharply (35.5% compared with virgin soils at a depth of 0–30 cm). A similar pattern was observed on the heavy loam dark Chestnut syrt soils. Cultivation of this soil reduced the content of both total N and all its fractions. The highest loss, 49%, was found for poorly hydrolysable N. The losses of non-hydrolysable and easily hydrolysable fractions were 30 and 37%, respectively. On virgin Chestnut syrt soil, the losses of N were slightly lower than on the virgin analogues of dark Chestnut terraced and syrt soils. The cultivation

of Chestnut syrt soils also led to a decrease in N content by 32% at a depth of 0–30 cm. The content of easily hydrolysable N decreased on average more than 1.5 times. The content of poorly hydrolysable N decreased by 58.86 mg kg⁻¹, and that of non-hydrolysable nitrogen by 389.81 mg kg⁻¹ (Fig. 29.6).

The transition from dark Chestnut to light Chestnut soil exhibited a tendency towards a decrease in the content of mineral N. In light Chestnut soil, the amount of readily hydrolysable N decreased, and the reserves of poorly hydrolysable N amounted to 263.01 mg kg⁻¹ in the 0–30 cm, which is 12% less than in the virgin Chestnut syrt soils. The agricultural use of light Chestnut syrt soils led to a decrease in the content of mineral N content by 325 mg kg⁻¹. It was noted that a decrease in the content of mineral N occurred in all fractions. Similar to the previous subtypes, the content of the poorly hydrolysable N decreased most.

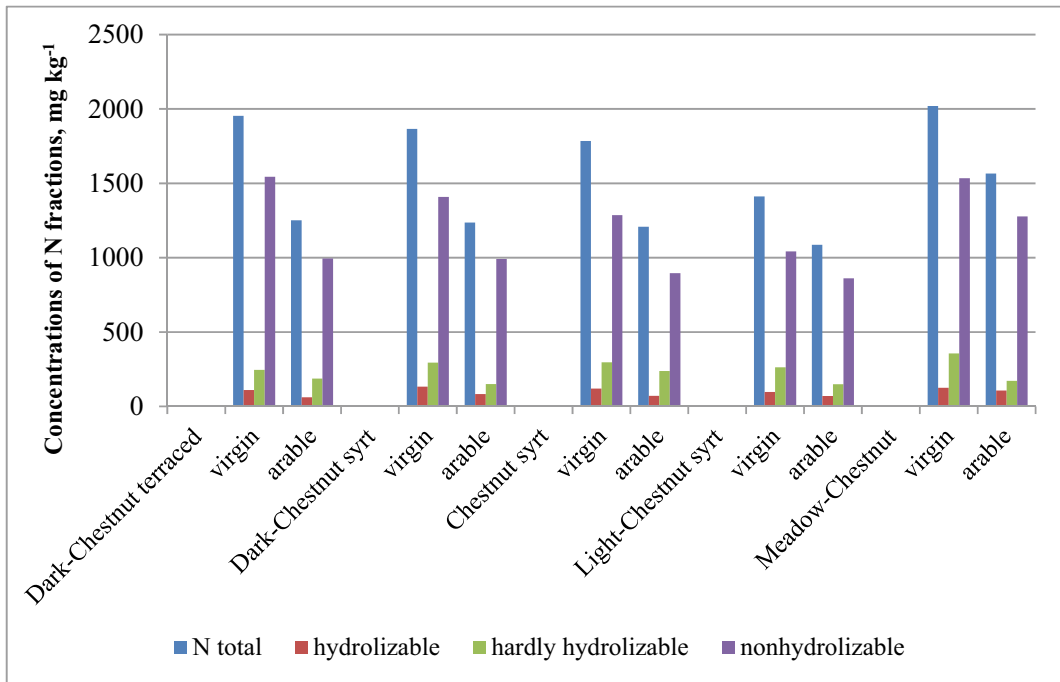


Fig. 29.6 Fractional composition of N in Chestnut soil of the Volga steppes, mg kg⁻¹ (0–30 cm)

In addition, the meadow Chestnut soils formed under the best humidity conditions. The favourable humidity promoted the activation of various chemical and biochemical processes and provided a higher input of organic biomass into the soil. Therefore, of the soil subtypes studied, the highest content of mineral N was observed in these soils. The cultivation of meadow Chestnut soils also led to an average decrease in the content of total N by 22% at a depth of 0–30 cm, compared to the virgin analogues. The sum of easily and poorly hydrolysable N decreased by 52%, and that of non-hydrolysable N by 17%.

29.3.4 Soil Phosphorus

Phosphorus in the soil is usually at low concentrations and solubility (<0.01 mg P kg⁻¹). Therefore, it is commonly a critical nutrient limiting plant growth. In natural environments, the main source of inorganic phosphorus in neutral and weakly alkaline soils is rocks of calcium phosphates (Saljnikov and Cakmak

2011). The total reserves of phosphorus in the arable Chernozem without fertilisation decreased slightly compared to the virgin soil. This is explained by the greater mineralisation of soil organic phosphorus under long-term cultivation: crops cultivated over a longer time period utilised soil mineral P that was released from the soil biochemically from organic compounds and chemically from mineral compounds. Bünemann (2015) found that gross net mineralisation rates of soil organic P under grassland and forest were higher than under arable soils.

Long-term fertilisation showed a trend towards partial compensation for the loss of the total phosphorus on all the Chernozem subtypes studied, although the differences were not significant (Fig. 29.5). On Chernozem soils, in addition to the total reserves on unfertilised arable land, the fractional composition of mineral phosphorus also changed (Fig. 29.7). The Chang–Jackson fractionation method was used to determine this value. The results showed that due to repeated cultivation and the use of fertilisers on the typical and southern Chernozem, the share

of the most mobile phosphorus in groups I and II increased (P I and P II). This may indicate an increase in the mineralisation processes of organic phosphorus. The simultaneous accumulation of mobile and poorly soluble mineral phosphorus in groups III and IV occurred on arable ordinary Chernozem. This was largely due to the changes in pH of this soil subtype. At the same time, on the typical Chernozem, the P III and P IV fractions remained almost at the same level both on the virgin and arable soil. In general, the content of loosely bound phosphorus and the phosphorus associated with calcium and aluminium increased by more than 1.5 times in unfertilised arable land compared to virgin land, and the systematic application of mineral fertilisers intensified this process.

Our studies also revealed considerable changes in the phosphorus pool of various subtypes of Chestnut soils (Fig. 29.8). On virgin dark Chestnut terraced soils (at 0–20 cm), the total P content was 0.177%, with P IV the largest and P I the smallest (393.3 and 16.4 mg kg⁻¹,

respectively). The cultivation of dark Chestnut terraced soils led to a slight decrease in the amount of total phosphorus (by 7%). However, the content of P I decreased by almost 3 times, and the P II by a third. At the same time, the content of P III, which is the closest reserve to replenish mobile phosphorus, decreased by 17% compared to the virgin analogue. The total decrease in the amount of phosphorus was 17%. On virgin dark Chestnut syrt soils, the amount of mineral P was almost at the same level as on the virgin dark Chestnut terraced soils. Agricultural use of these soils led to the greatest decrease in the share of the P II (40%) in the 0–20 cm layer compared with virgin soil. In Chestnut syrt soil, the amount of phosphorus decreased by 11%. The share of P I remained almost unchanged at a depth of 0–20 cm compared to dark Chestnut syrt soils. The cultivation of these soils led to a decrease in the amount of total phosphorus by 4% at a depth of 0–20 cm. The content of P I and P IV fractions decreased by 10%, and that of P II by 25%, compared to virgin soil. The amount of

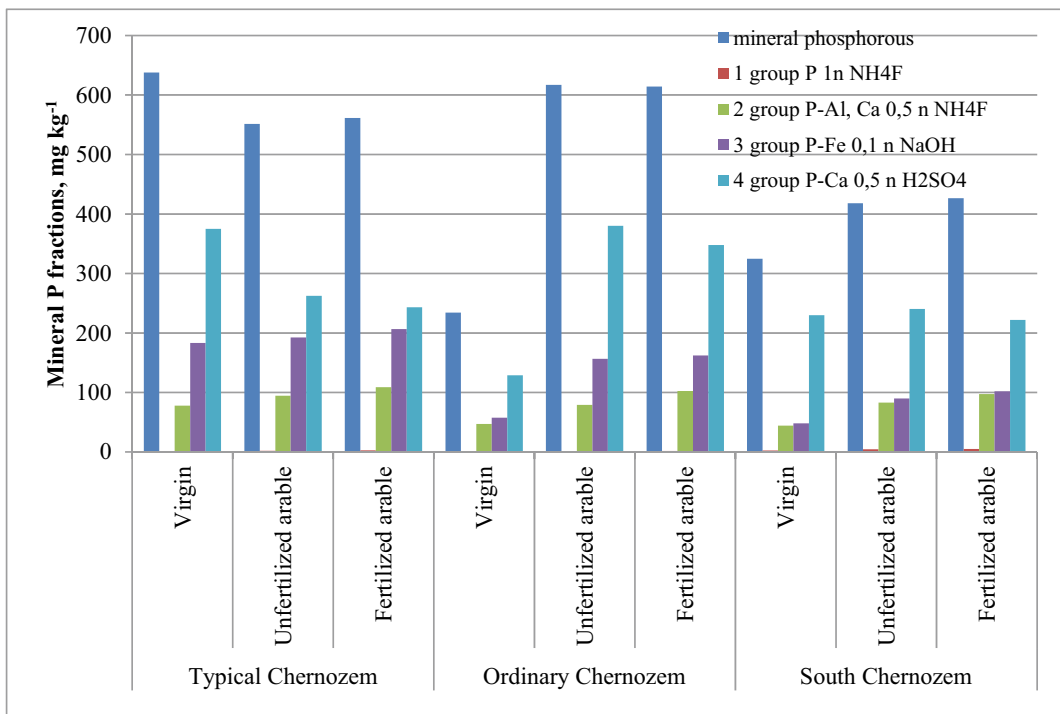


Fig. 29.7 Fractional composition of mineral P in Chernozem of the Volga steppe, mg kg⁻¹ (0–20 cm)

mineral phosphorus on the virgin light Chestnut syrt soils (at 0–20 cm) was lower than on the other subtypes of Chestnut soil. The content of P I fraction in this soil was 1.12 mg kg⁻¹, which is 72% less than on Chestnut syrt and 93% less than on terraced soils at a depth of 0–20 cm. The cultivation of light Chestnut syrt soils decreased the content of P by 38% compared with virgin soil (at a depth of 0–20 cm). However, the amount of P I fraction in this soil increased by more than two times, P II increased by 13% and the P III increased by 3.5 times. By contrast, the most stable P IV fraction was 2 times lower.

On the meadow Chestnut soil, the amount of P in total was 56.10 mg 100 g⁻¹, which is 10% less than on the virgin dark Chestnut terraced soils, and 34% less than on the virgin light Chestnut syrt soil. The cultivation of meadow Chestnut soil led to an increase in the amount of loosely bound P I fraction by 22% compared to virgin soil and to a decrease in the content of P II, P III and P IV fractions by 58%, 44% and 7%, respectively. In total, the content of P fractions

decreased by 17% compared to virgin (at a depth of 0–20 cm). Because soil organic P originates in microorganisms, plant and animal residues, it is closely associated with soil organic matter (Rita et al. 2013). Therefore, the discussed pattern of distribution of the phosphorus forms is largely explained by the high organic matter content in the soils studied.

29.3.5 Further Chemical Properties of Chernozem and Chestnut Soils

In Chernozems, Ca ions prevailed in the absorbed bases, their content being 3–10 times higher than that of Mg, depending on land use. At the same time, the amount of Ca and Mg greatly differed in different subtypes of Chernozem. The virgin typical Chernozem had considerably lower exchangeable and hydrolytic acidity but with a similar content of exchangeable bases, compared to arable land. Moreover, at a depth of 0–40 cm,

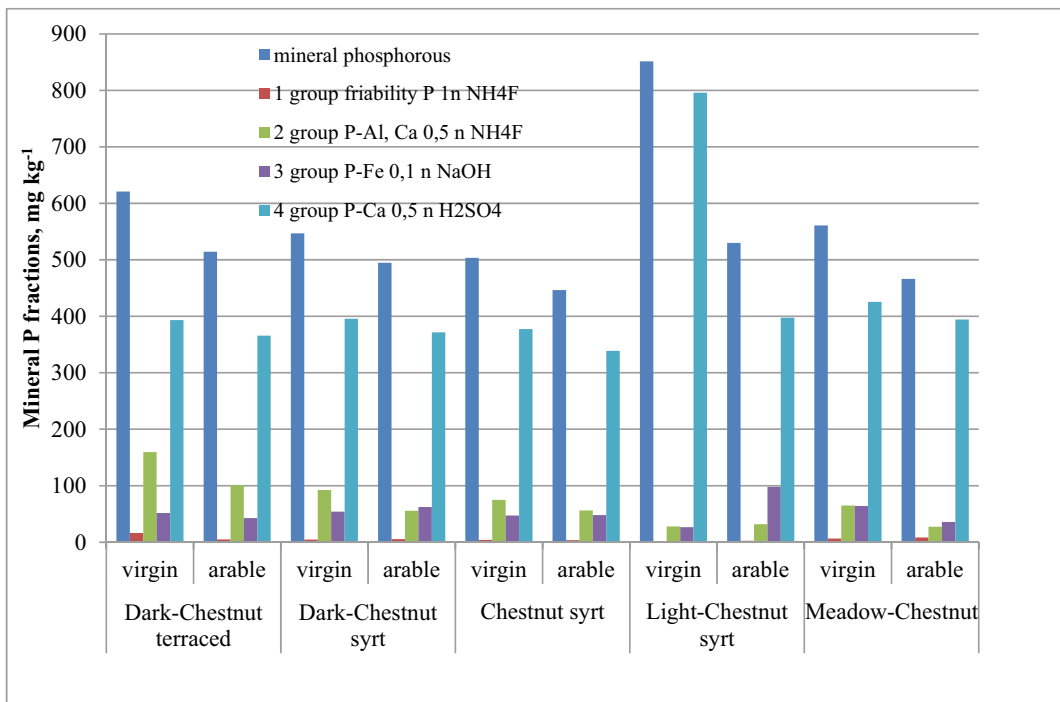


Fig. 29.8 Fractional composition of mineral P in Chestnut soil of the Volga steppe, mg kg⁻¹ (0–20 cm)

the amount of exchangeable bases on unfertilised arable land decreased by 3 mEq 100⁻¹ g compared to virgin soil due to a decrease in Ca²⁺ and Mg²⁺. The opposite situation was observed on ordinary Chernozems: their content in the unfertilised soil increased by 10 mEq 100⁻¹ g compared to virgin soil, at 0–20 cm (Fig. 29.9). On the southern Chernozem, the amount of Ca and Mg remained almost unchanged, but a change in the ratio of Ca²⁺ and Mg²⁺ was observed both on fertilised and unfertilised soils: the share of Mg slightly increased. The potential acidity in the studied subtypes of Chernozem showed an increase in hydrolytic acidity in fertilised and unfertilised soils, especially at a depth of 20–40 cm: from 4.55 to 7.87 mEq 100⁻¹ g, compared to their virgin analogues (3.93–1.75 mEq 100⁻¹ g) (Fig. 29.9). This value was the highest of all of our data on hydrolytic acidity in Chernozem soils. The observed increase in the potential acidity of arable soils is explained by increased microbiological activity, mainly associated with the mineralisation of soil organic matter. On ordinary Chernozem under long-term cultivation and fertilisation, a slight decrease in actual acidity was observed at depths of both 0–20 and 20–40 cm, compared to virgin soil, while the exchangeable and hydrolytic acidities increased slightly.

The unfertilised southern Chernozem and its virgin analogue had similar acidity values; nearly neutral with a slight potential acidity. The use of mineral fertilisers on southern Chernozem did not substantially affect its acidity. The amount of absorbed bases on virgin dark Chestnut terraced soils was 25% higher than in the arable soil (at a depth of 0–20 cm). At the same time, Ca²⁺ made up 54.3% of absorbed bases, and Mg²⁺ 45%. Based on the degree of alkalinity, this subtype of Chestnut soil was not alkaline, since the share of Na⁺ did not exceed 1–3% (Fig. 29.10). The cultivation of dark Chestnut terraced soils led to a decrease in the amount of absorbed bases (by 20%) at a depth of 0–20 cm, compared to virgin soil. The loss of Ca²⁺ was 1.7% (in absolute values). The amount of Mg²⁺ and Na⁺ ions

increased by 1.3 and 0.4%, respectively. An increase in the amount of absorbed bases (by 1.56 mEq 100 g⁻¹) was observed on the virgin dark Chestnut syrt soils compared to the terraced soils. The content of Mg²⁺ decreased by 12%, while Ca²⁺ and Na⁺ increased by 9 and 12.5%, respectively. The cultivation of dark Chestnut syrt soils led to a decrease in the amount of absorbed bases by 6.3% compared to the virgin analogues. Although the amount of Ca decreased due to cultivation (by 12.4%), it was still the predominant cation. Also, on the terraces, the content of Mg and Na increased by 15 and 53%, respectively.

The sum of the absorbed bases on Chestnut syrt soils was 10% less than on the dark Chestnut terrace soil and 14% less than on dark Chestnut syrt soils. The relative amount of Ca increased considerably (by 25%) compared to the dark Chestnut syrt soils. The content of Mg in the upper layer decreased by more than 2.5 times compared to the dark Chestnut syrt soils and 3 times compared to the terraced soils. The amount of Na increased by more than 6 times compared to the dark Chestnut soil. The cultivation of Chestnut syrt soils increased the amount of absorbed bases by 7% compared to the virgin soil. At the same time, the share of Ca due to cultivation decreased by 11%, while the amount of Mg increased by 37%. The content of Na remained almost unchanged. The amount of absorbed bases on the virgin light Chestnut syrt soil decreased by 10% compared to Chestnut soil and by 22% compared to dark Chestnut. The Ca decreased by 36%, while Mg and Na increased by 64 and 35%, respectively, compared to the Chestnut syrt soils). The long-term agricultural use of light Chestnut syrt soils led to a decrease in the amount of absorbed bases by 7% compared to the virgin land. The Ca content increased by 8%, while the amount of Mg decreased by 10%. On the virgin meadow Chestnut, the amount of absorbed bases was 9%, 18% and 29% less than on the virgin light Chestnut syrt, the Chestnut syrt and dark Chestnut soil, respectively. The Ca content

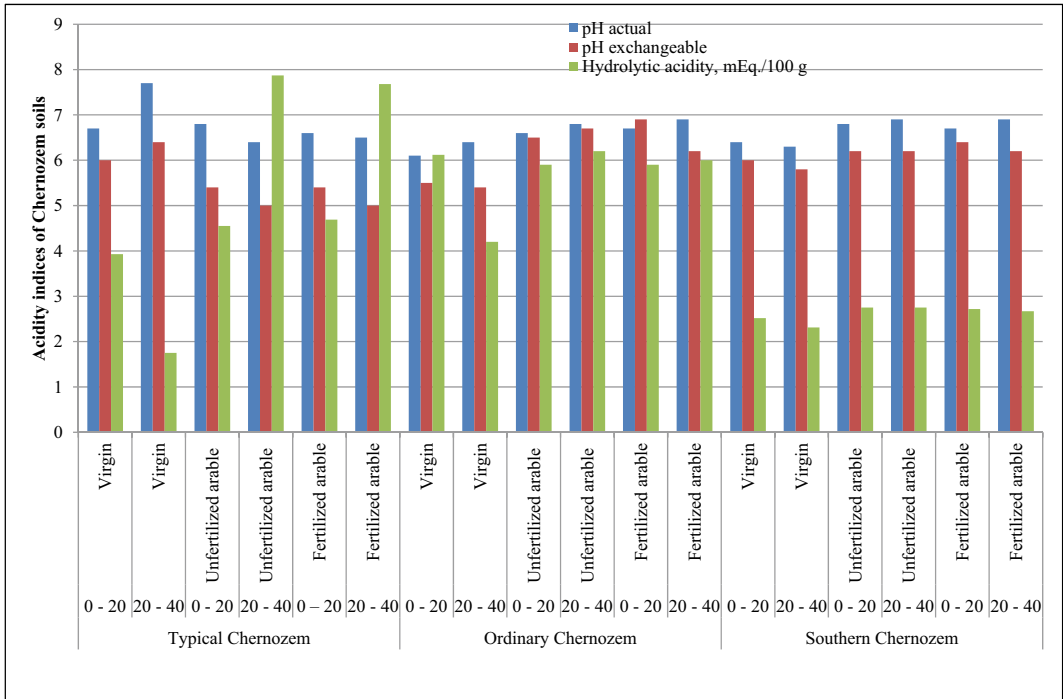


Fig. 29.9 Acidity of Chernozem soils of the Volga steppe (0–20 and 20–40 cm)

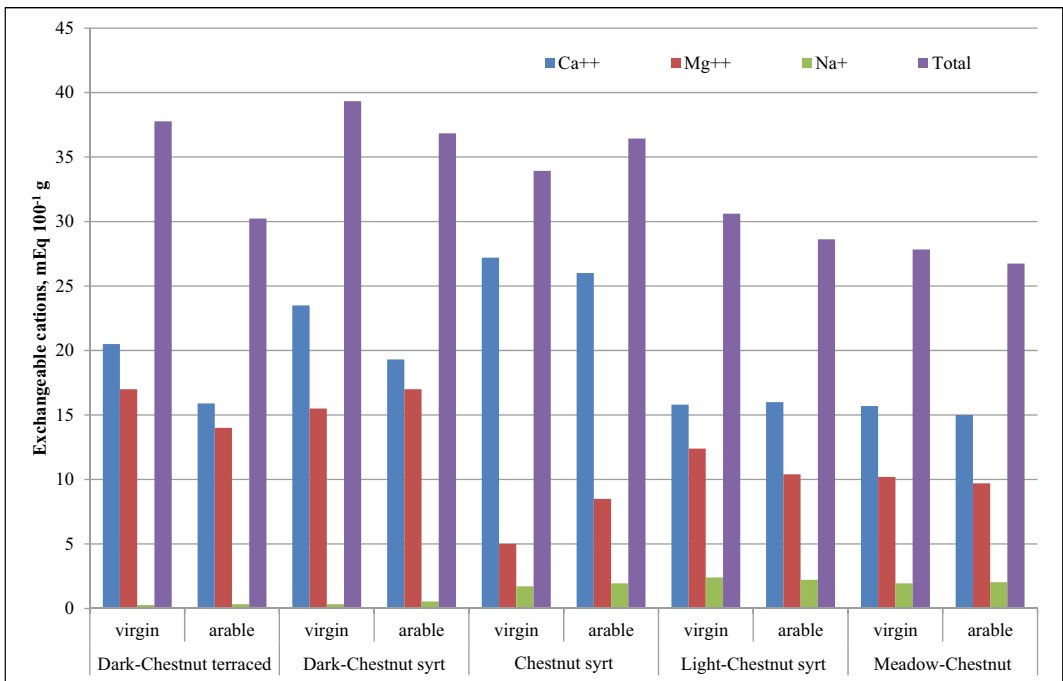


Fig. 29.10 Exchangeable cations of Chestnut soils of the Volga steppe, mEq/100 g (0–20 cm)

considerably exceeded the virgin analogues of Chestnut syrt soils (by 30%). The amount of Mg increased by 60% compared to the Chestnut syrt and decreased by 10% compared to the light Chestnut syrt soils. The amount of Na greatly increased compared to the dark Chestnut terraced soils (by 10 times) and less considerably compared to the Chestnut soil (27%). The cultivation of meadow Chestnut resulted in a slight decrease in the amount of absorbed bases as compared with virgin soil.

Thus, a comparison of the data showed that the highest losses of absorbed bases (about 20%) compared to the virgin analogues were on the arable dark Chestnut terrace soils and the lowest (4%) on the meadow Chestnut (Mg ranged from 14.7 to 46.3%; Ca from 51.6 to 80.2%; Na from 0.7 to 7.9%).

29.4 Outlook

Our data provide a rough indication of the magnitudes of changes in soil chemical properties relevant to plant growth that occurred in the past when steppe grassland was converted into cropland. They also give an indication of soil carbon levels and other parameters that could be achieved by re-converting cropland to largely natural grassland.

If soils of natural ecosystems such as steppes or forest are converted into managed ecosystem types, or are subjected to a drier climate, a significant loss of soil carbon and nitrogen is a process that is observed generally (Murty et al. 2002; Melillo et al. 2011; Sanderman et al. 2017; Mikhailova et al. 2020; Guggenberger et al. 2020). New states of quasi-equilibrium develop in the course of long-term cropping (Körschens 2021). These states must be recognised based on long-term experiments and modelling approaches (Guggenberger et al. 2020; Poulton and Johnston 2021; Körschens 2021; Romanenkov et al. 2021). On this basis, site-specific management strategies can be developed for the reproduction

of organic matter on cropland, which will always be significantly lower than on grassland (Kundler 1989; Romanenkov et al. 2021; Körschens 2021).

The loss of plant nutrients, however, is not inevitable when converting grassland to cropland. If it occurs in steppe soils, where leaching losses are low or negligible, it is a result of nutrient mining cropping practices and/or erosion. Plant nutrition via nutrients in soils can be properly controlled by suitable organo-mineral fertilisation strategies (Ivanov et al. 2021; Pronko et al. 2021; Tauchnitz et al. 2021) based on research experiments, soil and plant analyses, balancing approaches and agro-ecosystem modelling (Kundler 1989; Franko and Witing 2020; Romanenkov et al. 2021). In contrast to the organic matter control, theoretically, the same soil nutrient levels could be maintained on cropland as on virgin grassland. However, it makes no sense and is costly to provide excessively high nutrient levels in cropland soils, which are not needed for high yields. Thus, fertilisation strategies are based on thresholds of plant-available nutrients that should not be undercut, and on the amount required by crops (Kundler 1989; Chernenok and Barkusky 2014; Pronko et al. 2021).

Our data also indicate that the term “soil degradation” can mean different things at different scales. Referring to a broader landscape or national scale, where land can be converted from grassland to cropland and vice versa—a process associated with significant changes in ecosystem properties and services—this conversion can be seen as soil and land degradation or rehabilitation. At the scale of an ecosystem, such as grassland or cropland, or even in a smaller agrolandscape, designed to provide specific functions and services, soil degradation must be defined specifically within the boundaries of that landscape or ecosystem.

Soil fertility is a property that is largely related to cropland or agrolandscapes designed for cropping. Thus, our data do not yet provide

information about the status of possible degradation of cropland soils in terms of limitations of soil productivity and other functions and ecosystem services offered by soils. This requires further studies based on advanced research methods.

Chernozems and Chestnut soils (Kastanozems) are some of the most fertile soils in the world (Mueller et al. 2010) and are the backbone of agricultural production in the Russian Federation. Our data and experience indicate the need for research on maintaining and enhancing the fertility, quality and health of the soils in our study. This includes defining criteria and thresholds for chemical, physical and biological soil degradation, and for cropping practices that are productive in the long term. Modern monitoring systems also need to be developed and set into operation. This is required to achieve the sustainable intensification of cropland soils (Schiefer et al. 2021), e.g. enhancing both the productivity and sustainability of soil management in agrolandscapes.

29.5 Conclusions

In Chernozems of the Volga steppe, a decrease in the humus content and an increase in the share of fulvic acids were caused by insufficient fertilisation and nutrient removal by crops. Losses of N were most pronounced in typical and southern Chernozems, where the use of mineral fertilisers did not contribute to the accumulation of mineral N. The content of total P decreased slightly in cultivated Chernozems due to the mineralisation of organic P compounds. The content of K was not affected by cultivation.

Changes in the physicochemical properties depended on the subtype of Chernozem. In typical Chernozem, the amount of exchangeable bases decreased due to cultivation, while acidity increased. Ordinary Chernozem exhibited an increase in the amount of exchangeable bases, and a decrease in hydrolytic acidity. Southern Chernozem did not show any considerable changes.

Chestnut arable soils of the Saratov Trans-Volga region had the highest content of organic C (about 37%) compared with the virgin analogue. The most intensive losses of N were found on dark Chestnut terraced soils. The highest losses of mineral phosphorus compared to the virgin analogues (about 7%) were observed on the arable dark Chestnut terraced and syrt soils and the lowest (2%) on meadow Chestnut syrt soils. Cultivation decreased the amount of absorbed bases and the content of Ca and caused a slight increase in the amount of Mg in Chestnut and dark Chestnut soils.

Our data indicate a need to stop the decline in fertility in the soils in our study. Modern approaches and technologies for researching into, monitoring and managing soils need to be developed and set into operation.

Acknowledgements The authors would like to thank the editors and anonymous reviewers for their helpful comments and suggestions.

References

- Anisimova TYu (2005) Humus loss in arable soils under the influence of intensive farming and erosion (Потери гумуса на пахотных почвах под влиянием интенсивного земледелия и эрозии. Плодородие). *Plodородie* 1:18–19
- Bünemann (2015) Assessment of gross and net mineralization rates of soil organic phosphorus—a review. *Soil Biol Biochem* 89:82–98. <https://doi.org/10.1016/j.soilbio.2015.06.026>
- Chernenok V, Barkusky D (2014) Diagnosis and optimization of phosphorus nutrition conditions of grain crops in Northern Kazakhstan. In: Mueller L, Saparov A, Lischeid G (eds) *Novel measurement and assessment tools for monitoring and management of land and water resources in agricultural landscapes of Central Asia*. Environmental science and engineering. Springer, Cham. https://doi.org/10.1007/978-3-319-01017-5_43
- Chizhikova NP, Baranovskaya VA, Khitrov NB (2011) The effect of long-term irrigation on the state of aggregation and mineralogical composition of the silt fraction of Kastanozems in the trans-Volga region (Влияние длительного орошения на степень агрегированности и минералогический состав илистой

- фракции темно-каштановых почв Заволжья). *Soil Science (почвоведение)* 8:978–994
- Chub MP (1998) Chernozem soils of the Volga region, their distribution, composition and use (taking the example of the Saratov region). In Chub MP, Medvedev IF, Gyurova ES (eds) *Fertility of Russian Chernozem soils*. Agrokonsalt, Moscow, pp 509–552 (Чуб М.П. Черноземы Поволжья, их распространение, состав и использование (на примере Саратовской области). Под ред. Чуб М.П., Медведев И.Ф., Гюрова Е.С. Плодородие черноземов России. Москва, Агроконсалт, с. 509 – 552)
- Chub MP (2013) The effect of long-term use of fertilizers on the agrochemical properties of southern black soils and the productivity of crops of grain-pair crop rotation. In: Chub MP, Pronko VV, Yaroshenko TM, Klimova NF, Nikonov NI (eds) *Problems of agrochemistry and ecology, vol 1*, pp 3–8 (Чуб М.П. Влияние длительного применения удобрений на агрохимические свойства южных черноземов и урожайность посевов зернопарного севооборота. В М.П. Чуб, В.В. Пронько, Т. Ярошенко, Н.Ф. Климова, Н. Никоноров (ред.), *Проблемы агрохимии и экологии 1: 3–8*)
- Classification and Diagnostics of Soils of the Soviet Union (Kolos, Moscow, 1977), 223 pp (Классификация и диагностика почв Советского Союза)
- Eremin DI (2016) Changes in the content and quality of humus during agricultural use of Leached Chernozem in the forest-steppe zone of the Trans-Urals. *Pochvovedenie* 5:584–592 (Еремин Д.И. Изменение содержания и качества гумуса при сельскохозяйственном использовании чернозема выщелоченного лесостепной зоны Зауралья. *Почвоведение* 5: 584–592)
- Franko U, Witing F (2020) Dynamics of soil organic matter in agricultural landscapes. In: Mirschel W, Terleev V, Wenkel KO (eds) *Landscape modelling and decision support*. Innovations in landscape research. Springer, Cham. https://doi.org/10.1007/978-3-030-37421-1_14
- Funakawa S, Yanai J, Takata Y, Karbozova-Salnikov E, Akshalov K, Kosaki K (2007) Dynamics of water and soil organic matter under grain farming in Northern Kazakhstan—toward sustainable land use both from the agronomic and environmental viewpoints. In: Lal R, Suleimenov M, Stewart BA, Hanson DO, Doraiswamy P (eds) *Climate change and terrestrial carbon sequestration in Central Asia*. Taylor & Francis, Leiden, Netherlands, pp 279–331
- Gamzikov GP, Kulagina MN (1992) The change in the content of humus in the soil as a result of agricultural use (Review). Moscow p. 48 (Гамзиков Г.П., Кулагина М.Н. Изменение содержания гумуса в почве в результате сельскохозяйственного использования (Обзор), Москва с 48)
- Grishina LA, Kotsik GN, Makarov MI (1990) Transformation of soil organic matter. Moscow State University, Moscow, p 195 (Гришина Л.А., Кондик Г.Н., Макаров М.И. Трансформация органического вещества почвы. Москва, МГУ – п.195)
- Guggenberger G, Bischoff N, Shibistova O, Müller C, Rolinski S, Puzanov A, Prishchepov AV, Schierhorn F, Mikutta R (2020) Interactive effects of land use and climate on soil organic carbon storage in Western Siberian Steppe soils. In: Frühauf M, Guggenberger G, Meinel T, Theesfeld I, Lentz S (eds) *KULUNDA: climate smart agriculture. Innovations in landscape research*. Springer, Cham. https://doi.org/10.1007/978-3-030-15927-6_13
- Ivanov AI, Ivanova ZhA, Konashenkov AA (2021) Chapter 15: Environmental landscape conditions of the Russian Northwest, the fertility of sod-podzolic soils, and the efficiency of precise fertilizer systems. In: Mueller L, Sychev VG, Dronin NM, Eulenstein F (2021) (eds) *Exploring and optimizing agricultural landscapes*. Innovations in landscape research. Springer, Cham. In print
- Ivanov IV, Denikin VA (1996) Problems of the genesis and evolution of steppe soils: history and current state. *Soil Sci* 3:324–334 (Иванов И.В., Деникин В.А. Проблемы генезиса и эволюции степных почв: история и современное состояние. *Почвоведение* 3: 324 – 334)
- Körschens M (2021) Chapter 8: Long-term field experiments (LTEs)—importance, overview, soil organic matter. In: Mueller L, Sychev VG, Dronin NM, Eulenstein F (2021) (eds) *Exploring and optimizing agricultural landscapes*. Innovations in landscape research. Springer, Cham. In print
- Koković N, Dinić Z, Sikirić B, Mrvić V, Nerandić B (2018) Hemijske osobine zemljišta posle 50 godišnjeg đubrenja zemljišta mineralnim đubrivima. *Zemljište i Biljka* 67(2):1–9. <https://scindeks.ceon.rs/article.aspx?query=ISSID%26and%2614568&page=0&sort=8&stype=0&backurl=%26issue.aspx%36issue%3d14568>. Accessed 13 Dec 2020
- Kundler P (1989) *Erhöhung der Bodenfruchtbarkeit*. VEB Deutscher Landwirtschaftsverlag Berlin, 1st edn, 452 pp
- Lai L, Li Y, Tian Y, Jiang L, Zhao X, Zhu L et al (2013) Effects of added organic matter and water on soil carbon sequestration in an arid region. *PLoS ONE* 8 (7):e70224. <https://doi.org/10.1371/journal.pone.0070224>
- Lal R (2009) Soil degradation as a reason for inadequate human nutrition. *Food Sec* 1:45–57. <https://doi.org/10.1007/s12571-009-0009-z>
- Mamontov VG (2013) Irrigated chernozem and chestnut soils: composition, properties, transformation processes (Орошаемые черноземы и каштановые почвы: состав, свойства, процессы трансформации).

- ISBN 978-5-9675-0872-1. Timiryazev State Agrarian Academy RGAU-MTAA, Moscow, p 290
- Melillo JM, Butler S, Johnson J, Mohan J, Steudler P, Lux H, Burrows E, Bowles F, Smith R, Scott L, Vario C, Hill T, Burton A, Zhou Yu-M, Tang J (2011) Soil warming, carbon–nitrogen interactions, and forest carbon budgets. *PNAS* 108(23):9508–9512. <https://doi.org/10.1073/pnas.1018189108>
- Mikhailova EA et al (2020) Cultivation effects on soil carbon and nitrogen contents at depth in the Russian Chernozem. *Soil Sci Soc Am J* 64(2). <https://doi.org/10.2136/sssaj2000.642738x>
- Mineev VG (ed) (2001) Workshop on agrochemistry. Moscow State University Publishing House, 689 pp
- Mineev VG, Rempe EK (1990) Agrochemistry, biology and soil ecology. Rosagropromizdat, Moscow, p 287 (Агрохимия, биология и экология почв. Москва, Росагропромиздат п. 287)
- Mueller L, Schindler U, Mirschel W, Shepherd TG, Ball B, Helming K, Rogasik J, Eulenstein F, Wiggering H (2010) Assessing the productivity function of soils: a review. *Agron Sustain Dev* 30(3):601–614. <https://doi.org/10.1051/agro/2009057>
- Murty D, Kirschbaum MUF, Mcmurtrie RE, MCGilvray H (2002) Does conversion of forest to agricultural land change soil carbon and nitrogen? A review of the literature. *Glob Change Biol* 8(2):105–123. <https://doi.org/10.1046/j.1354-1013.2001.00459.x>
- Orlov DS, Biryukova ON, Rozanova MS (1996) Real and apparent loss of organic matter in the soils of the Russian Federation. *Soil Sci* 2:197–207 (Реальная и кажущаяся потеря органического вещества в почвах Российской Федерации. Почвоведение 2: 197–207)
- Poulton PR, Johnston AE (2021) Chapter 9: Can long-term experiments help us understand, and manage, the wider landscape—examples from Rothamsted, England. In: Mueller L, Sychev VG, Dronin NM, Eulenstein F (eds) Exploring and optimizing agricultural landscapes. Innovations in landscape research. Springer, Cham. In print
- Pronko VV, Grishin PN (2005) State and ways of regulating the fertility of black earth and chestnut soils of the Saratov region. *Agrar Sci J* 3:28–31 (Состояние и пути регулирования плодородия черноземных и каштановых почв Саратовской области. Аграрный научный журнал 3: 28–31)
- Pronko NA, Korsak VV, Romanova LG, Kravchuk AV, Afonin VV (2018) The effect of prolonged irrigation on the Volga region (Влияние длительного полива на Поволжье). *Int J Eng Technol Special Issue* 38:1210–1213. <https://www.sciencepubco.com/index.php/ijet/article/view/27764/14434>. Accessed 13 Dec 2020
- Pronko VV, Yaroshenko TM, Zhuravlev DY, Klimova NF (2021) Chapter 31: The role of mineral fertilizers for the optimization of agrolandscapes in the Volga Steppe region. In: Mueller L, Sychev VG, Dronin NM, Eulenstein F (2021) (eds) Exploring and optimizing agricultural landscapes. Innovations in landscape research. Springer, Cham. In print
- Rita JCO, Gama-Rodrigues AC, Gama-Rodrigues EF, Zaia FC, Nunes DAD (2013) Mineralization of organic phosphorus in soil size fractions under different vegetation covers in the north of Rio de Janeiro. *Rev Bras Ciênc Solo* 37(5):1207–1215. <https://doi.org/10.1590/S0100-06832013000500010>
- Romanenkov VA, Rukhovich OV, Belichenko MV (2021) Chapter 21: Geographical network of long-term experiments with fertilizers in the agroecological monitoring system of Russia. In: Mueller L, Sychev VG, Dronin NM, Eulenstein F (2021) (eds) Exploring and optimizing agricultural landscapes. Innovations in landscape research. Springer, Cham. In print
- Saljnikov E, Cakmak D (2011) Phosphorus: chemism and interactions, pp 1–28. Chapter 1. In: Gungor BO (ed) Principles, application and assessment in soil science. INTECH Open Access Publisher, p 406. <https://doi.org/10.5772/1860>. ISBN 978-953-307-740-6
- Saljnikov E, Hospodarenko H, Funakawa Sh, Kosaki T (2005) Effect of fertilization and manure application on nitrogen mineralization potentials in Ukraine. *Zemljiste i biljka* 54(3):221–230
- Sanderman J, Hengl T, Fiske GJ (2017) Soil carbon debt of 12,000 years of human land use. *PNAS* 114(36):9575–9580. <https://doi.org/10.1073/pnas.1706103114>
- Schiefer J, Lair GJ, Mueller L, Blum WEH (2021) Chapter 12: Evaluation of framework conditions and soil potential for the sustainable intensification of agriculture. In: Mueller L, Sychev VG, Dronin NM, Eulenstein F (2021) (eds) Exploring and optimizing agricultural landscapes. Innovations in landscape research. Springer, Cham. In print
- Sychev VG, Romanenkov VA, Shevtsova LK, Rukhovich OV (2014) Modern directions of research and the results of long-term field experiments of the geo-network (Современные направления исследований и результаты многолетних полевых экспериментов геосети. Плодородие 5:2–5). *Plodородie* 5:2–5
- Tan ZX, Lal R, Wiebe KD (2005) Global soil nutrient depletion and yield reduction. *J Sustain Agric* 26(1). <http://www.haworthpress.com/web/JSA>. Accessed 13 Dec 2020

- Tauchnitz N, Bischoff J, Schrödter M, Ebert S, Meissner R (2021) Chapter 32: Strip-till combined with slurry band injection below maize seeds—a new approach to enhance the nitrogen efficiency of organic fertilizers. In: Mueller L, Sychev VG, Dronin NM, Eulenstein F (2021) (eds) Exploring and optimizing agricultural landscapes. Innovations in landscape research. Springer, Cham. In print
- Tuyev NA (1989) Microbiological processes of humus formation (Микробиологические процессы гумусообразования). Agropromizdat Publisher, Moscow, 239 pp
- Zhao N, Yang Xi, Huang G, Lü Yi, Zhang Ji, Fan Yu, Drury CF, Yang X (2021a) Chemical and spectroscopic characteristics of humic acid from a clay loam soil in Ontario after 52 years of consistent fertilization and crop rotation. *Pedosphere* 31(1):204–213. [https://doi.org/10.1016/S1002-0160\(20\)60019-4](https://doi.org/10.1016/S1002-0160(20)60019-4)
- Zhao Yu, Liang Ch, Shao Sh, Xie H, Zhang W, Chen F, He H, Zhang X (2021b) Interactive effects of elevated CO₂ and nitrogen fertilization levels on photosynthesized carbon allocation in a temperate spring wheat and soil system. *Pedosphere* 31(1):191–203. [https://doi.org/10.1016/S1002-0160\(20\)60056-X](https://doi.org/10.1016/S1002-0160(20)60056-X)



Labile Soil Carbon as an Indicator of Soil Organic Matter Quality in the Province of Vojvodina, Serbia

30

Srdan Šeremešić and Vladimir Ćirić

Abstract

Labile carbon fractions such as particulate organic carbon (POC) and hot-water-extractable organic carbon (HWOC) are pools of soil carbon that undergo significant transformation and could therefore serve as an indicator of changes in the quality and quantity of soil organic carbon (SOC). They represent 1–5% of the total organic matter and comprise a heterogeneous mixture of materials. The aim of this study was to assess the labile carbon pool change in relation to soil type and management. The procedure involves labile carbon extraction by separation in water or liquids with adjusted density following the aspiration of organic matter from the surface of an aqueous suspension. Our data demonstrated that the land use systems had a predominant effect on the organic matter stabilisation. This study showed that non-arable land use systems were higher in labile carbon, mostly due to lower microbiological activity. In arable soils, management practices have a significant influence on both labile fractions. Preserving the soil organic carbon would require the retention of crop residue in combination with judicious fertilisa-

tion. Our result could contribute to a better understanding of SOC fractions' relevance in the Province of Vojvodina related to the cropping management, and could help select cropping practices for better SOC preservation.

Keywords

Soil organic carbon · Labile carbon · Land use · Soil degradation

30.1 Introduction

The content of soil organic matter (SOM) in arable soils is considered one of the main factors that improve soil resources and increase soil fertility. When SOM is analysed in terms of crop productivity and long-term yield stability, it is one of the most important indicators of agroecosystems' production potential (Reeves 1997). Given the immense importance of SOM, the inherited fertility of Chernozem soil and changes in SOM have not been adequately elaborated. During the twentieth century, a relatively small number of research studies reviewed the causes and consequences of reduced SOM levels in the soil. Over the past decade, the number of projects and studies in this field has increased markedly, which indicates the higher relevance of this subject and the increased number of influencing factors affecting the dynamics of SOM. Currently,

S. Šeremešić (✉) · V. Ćirić
Faculty of Agriculture Novi Sad, University of Novi Sad, Sq. D. Obradovića 8, 21000 Novi Sad, Serbia
e-mail: srdjan.seremesic@polj.uns.ac.rs

data on the properties of arable soils in Serbia indicate that there is an overall trend of SOM loss, regardless of the land use and type of soil (Vidojević 2018). Moreover, the maintenance of SOM has been strongly associated with an impact on environmental quality and the provision of ecosystem services (Schmidt et al. 2011). Determining historical losses in soil organic carbon (SOC) can thus provide useful information on potential soil degradation and carbon sequestration potential, and can be used as a guideline for soil protection (Ćirić et al. 2013a).

The Province of Vojvodina covers the northernmost part of Serbia, north of the Sava and the Danube rivers within the Pannonian Basin, and occupies an area between 45° 38' and 46° 10' northern latitude and 18° 0' to 21° 15' eastern longitude. Cropland in the province totals 1,509,800 ha, of which 933,900 ha is Chernozem soil, while Chernozem and Chernozem-like meadow soils cover approximately 1,300,000 ha. Vertisols are found less frequently; they are affected by groundwater, mainly occupy depressions at river terraces and can be characterised with the supplementary qualifier Gleyic. Fluvisols and Gleysols are affected by both ground and surface water and tend to occur near rivers. The Solonetz soil type is characterised by unfavourable chemical and physical properties caused by the high clay content and the presence of adsorbed Na in the B_t horizon (Živković et al. 1972). Sodium causes the peptisation of colloids and a highly alkaline reaction. In most of the areas in Vojvodina, however, pedogenesis has produced highly fertile soils which, when combined with appropriate agricultural practices, can produce high crop yields of good quality. The prevailing climate in the Province of Vojvodina is continental, with an average annual precipitation of 611 mm, while the annual temperature is 11.1 °C. Therefore, the average annual climatic conditions can be considered favourable for agricultural production.

An analysis of the available literature suggests that the problem of SOM decline in Vojvodina was not addressed properly in the twentieth century as it is today. Nejšebauer (1951) was among the first to report that Chernozems in

Vojvodina had lost about 50% of its humus since their formation, i.e., from an initial 7–8% to 3–5% recorded in the 1940s. Bogdanović (1954), examining the characteristics of humus, recognised the interdependence of changes in the properties of soil organic matter and the type of land use. Later, a study conducted by Vučić (1987) estimated that the annual loss of humus in the soils of Vojvodina is about 1000 kg ha⁻¹ per year; he thus proposed measures for its preservation. A similar trend in SOM changes was observed by other authors who studied Chernozem soils. For example, analysing Chernozems in Moldova, Kupernikov et al. (2011) found a significant loss of SOM from the initial 5–6% (1897) to 3–3.5% with a tendency towards further decline. A century of cultivation of native Chernozems under the prairies in Canada has reduced soil organic carbon by approximately 15–30% (Monreal and Janzen 1993). According to the “Thematic Strategy for Land Protection”, it is estimated that 45% of European soils have a low level of SOM, which poses a threat to the functioning of the land within its capacity (Blum 2008).

Contemporary knowledge based on the incubation studies has shown that 1–2% of the total amount of humus is lost in mineralisation processes annually. To a large extent, it is also a consequence of unfavourable crop rotation, the burning of crop residues, inappropriate management of crop residues, lack of use of manure, etc. According to Bogdanović et al. (1993), a steady trend of decrease in SOM was found in the last decades of the twentieth century, from 0.2 to 0.81%, on average by 0.38%. Sekulić et al. (1998) reported a decrease in the SOM content of Chernozems for the 1970–1990 period from 0.27 to 0.41% as compared with the values obtained during earlier soil surveys. For the investigated area in Srem (Vojvodina, Serbia), Nešić et al. (2008) found a decrease in SOM content by 0.68% in 250 soil samples. Based on the analysis of 77,388 samples from the Province of Vojvodina, Sekulić et al. (2010) reported that as much as 39% of the high-quality soil in Vojvodina belongs to the class of low humic soils, with a SOM content from 1 to 3%. Of the arable soil

samples analysed, 59% had a good supply of humus (3–5%). The same authors found that in the class of soils with a low humus supply, the samples with a SOM content from 2 to 3% prevail, while in the class with a favourable humus content (3–5%), soils with a SOM content from 3 to 4% prevailed. Analyses of the basic soil chemical properties revealed significant differences in fertility both between plots and in the same plot, which is attributed to the fertiliser quantity applied to preceding crops, differences in recommendations for fertiliser use, and land use type (Sekulić et al. 2006, 2007, 2011; Vasin and Sekulić 2005). The analysis of SOM in 25,125 samples in the area of Central Serbia in 2008 shows that most of the tested soil samples belong to the classes of soils with a lower (49.9% of samples) and a medium humus supply (41.7% of samples) (Vidojević and Manojlović 2010).

The literature examined indicates that the problem of SOM loss is profound and the classification does not reflect the SOM disturbance and its relationship with soil properties. In addition, a relatively small number of scientific papers published in Serbia over the past century have investigated the causes and consequences of reduced SOM levels in the soil. Consequently, the problem has escalated and contributed to a poor understanding of SOM content, since in most studies it is difficult to establish a direct link between soil organic carbon changes and yield (Lal 2006). Yield change has been attributed to the climatic extremes and unfavourable weather conditions rather than to the changes in soil properties. Therefore, the trend towards a declining SOM content reflects the establishment of a crop management system, and this will require SOM preservation to be incorporated into soil legislation and the national sustainable development agenda.

30.2 Soil Management and Carbon Pools

In managed agro-ecosystems, changes in soil organic carbon (SOC) are influenced by cropping practices, soil biota and environmental

conditions (Manojlović et al. 2008; Šeremešić et al. 2011, 2020). According to Frank et al. (2015), soil management can be considered a tool for capturing and preserving the SOC. However, knowledge on how much carbon the soil can capture as a carbon sink varies (Gomiero 2003), and depends on many factors. For this reason, management practices must be selected based on the environmental conditions and crop requirements, and occasionally harmonised if conditions change. Different qualitative fractions of SOC derived from the formation pathways could be evaluated to better understand carbon cycling in the specific cropping systems. Accordingly, we need an approach that emphasises SOC turnover and allocation into three different reservoirs: (i) a labile (active) fraction recovered within 1–5 years, (ii) a medium fraction that is physically protected or chemically stabilised with a recovery time of 20–40 years; and (iii) a passive fraction (humus) that is extremely stable with a regeneration time of 200–1500 years (Parton et al. 1987). Consequently, to protect the SOC, we need to focus on three main mechanisms used to stabilise it (Six et al. 2002): (i) chemical stabilisation (Hassink 1997), (ii) physical protection and (iii) biochemical stabilisation (Christensen and Johnson 1997; Stevenson 1994).

Soil organic carbon fractions were identified according to their role in the carbon turnover and relationship with the chemical, physical and microbiological soil properties. These fractions can be determined based on the position, composition and stability of complexes established between SOC and other soil components (clay, Ca^{2+} , Al^{3+} , and Fe^{3+}). The complexity of the SOC distribution in soil calls for a multilevel assessment of its significance for soil properties. In recent decades, an increasing number of fractionation approaches have been proposed for separating and identifying the different labile and stable fractions as proxies for the SOC pool and their role in soil quality (Baldock and Nelson 2000). Each of the fractions contains specific information relevant to estimate the effects of land use on the SOC pool turnover and stabilisation.

Changes in cropping systems and tillage practices over time can cause problems with the quantification of the SOC pool due to a large number of existing backgrounds and spatial variations (Haynes 2000). Therefore, the prospects of interpreting the SOC based on the total carbon pool do not provide a clear, accurate means of explaining the dynamics and relationship between the SOC content and related soil properties. The turnover of the labile SOC fraction is relatively fast, and since this fraction quickly responds to changes in land use and soil management, it can be explained as an early and sensitive indicator of the changes in total SOC (Plaza-Bonilla et al. 2014). Thus, the use of various soil C fractions with the shortest response to changes in agricultural management compared to the total SOM has been identified as an effective tool for optimising the agricultural practices which increase the stock and quality of SOC. It has been suggested that labile SOC fractions play an essential role in the short-term turnover of nutrients in the soil and are a greater sink for nitrogen compared to the total SOC (Compton et al. 2002). The concentration and fluxes of SOC fractions obtained with fractionation approaches lead to a similar conceptual SOC pool, but offer a different perception of the

factors causing their occurrence and renewal in the soil.

30.2.1 The Effects of Land Use on Soil Organic Carbon Changes

30.2.1.1 Total Organic Carbon

The determination of the total organic carbon usually precedes a labile carbon assessment because it can give a rough estimate of soil quality and productivity. Commonly, soil organic matter has been used to report the humus content (%) whereas soil organic carbon is used as an indicator of organic carbon (C) in the soil (g kg^{-1}). In our study, different land use systems were assessed on Chernozem soil—maize monoculture, unfertilised 2-year rotation (maize-winter wheat), fertilised 2-year rotation (maize-winter wheat), fertilised 3-year rotation (maize-soybean-winter wheat) with manure, untilled grassland (UG) and oak forest (OF)—to obtain the relationship between the total and labile SOC (Fig. 30.1).

A comparison of different land use systems reveals that the highest content of SOC was found in the untilled grassland (25.4 g kg^{-1}), and the lowest in the unfertilised 2-year rotation (9.7 g kg^{-1}). The lowest SOC values obtained in

Fig. 30.1 Land use system on Chernozem in Vojvodina (orig.)



the arable soils are associated with intensive mineralisation, which is faster on arable soils, whereas non-agricultural soils facilitate the accumulation of soil organic carbon (Fig. 30.2). The higher SOC value obtained on the untilled grassland indicates soil structure stabilisation, which enables SOC sequestration. Under agricultural crops, mould-board ploughing in the autumn followed by soil preparation (disking) led to regular soil tilth disturbance and aeration that promotes microbial activity and mineralisation. Carrying out the same experiment, Molnar (2003) presented data from 1991 where 12.12 g kg⁻¹ of SOC was found in the unfertilised 2-year rotation, while SOC averaged 15.14 g kg⁻¹ on the fertilised rotation. Comparing this study with current results, continuous SOC decline was found regardless of crop rotation and fertilisation. Many studies confirmed that the amount of crop residues and farmyard manure are responsible for SOC content maintenance (van Wesemael et al. 2010). However, some suggest that retaining residue can be a sustainable solution for SOC preservation when there is a lack of manure. In our study, the application of manure contributed to SOC preservation by altering the soil's physical and microbial properties. The higher SOC with the maize monoculture could be explained by the higher amount of residue carbon added to soil compared to other arable cropping systems, even for grassland and oak forest.

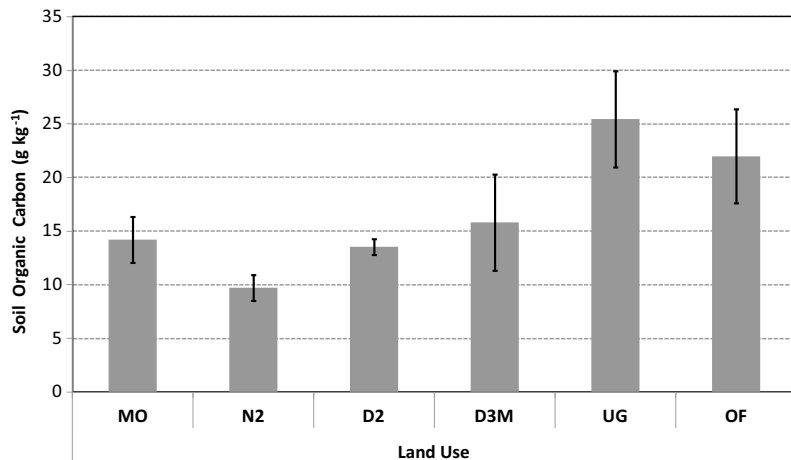
30.2.1.2 Labile Fraction of Soil Organic Matter

In the soils, the input of organic matter comes in the form of crop residues or litter that is returned to the soil surface, from root turnover during crop growth and from root material left in the soil. As this plant material decomposes, particulate organic carbon (POC) is formed. This partially decomposed material can be extracted by density fractionation or as the MOC (<20 mm fraction) by dispersion and sieving (Haynes 2005). Particulate organic carbon is readily available for microorganisms and a short-term reservoir of nutrients for plants. The nature of the fraction can vary; a microscopic evaluation of the POC revealed that it contains fungal hyphae, spores, seeds, faunal skeletons and charcoal, while the hot-water-extracted organic matter was largely composed of carbohydrates and N-containing compounds, amino-N species and amides (Leinweber et al. 1995).

30.2.1.3 Hot-Water-Extractable Soil Organic Carbon

Hot-water-extractable organic carbon (HWOC) fractions are the most active SOM compounds (Kalbitz and Kaiser 2008). They can contribute to SOC concentration changes and can strongly affect soil processes, as well as soil biogenicity. The changes in this "light fraction" of SOC can be a reliable indicator of the intensity of its assimilation by microorganisms. The fractions

Fig. 30.2 Total soil organic carbon content of different land use systems (0–30 cm) (MO—maize monoculture, N2—unfertilised 2-year rotation, D2—fertilised 2-year rotation, D3M—fertilised 3-year rotation with manure, UG—grassland, OF—forest)



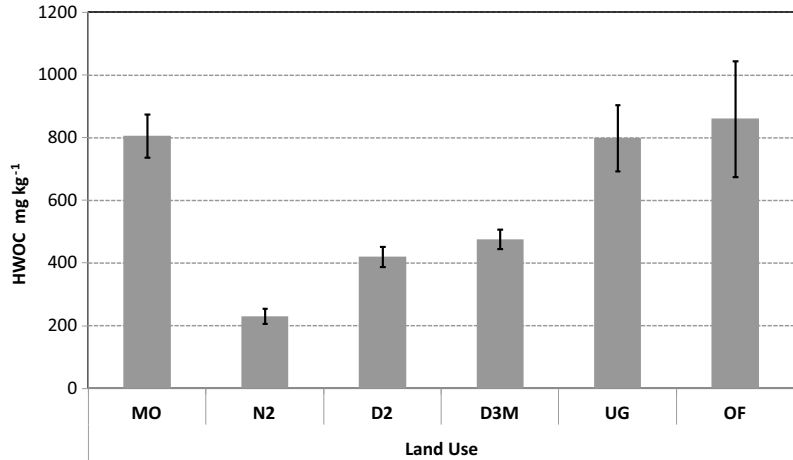
characterised as HWOC are uncomplexed, readily mineralisable, pass through a 0.45 μm filter mesh and consist mainly of carbohydrates derived from plant roots, microorganisms, amino acids, humic substances and, rarely, phenol and lignin monomers, proteins and chitin. Although HWOC comprises only a few percent of the SOM, it plays an important role in the stabilisation and preservation of SOM (Seremešić et al. 2013). The high degree of biodegradability of HWOC fractions affects the soil CO_2 efflux (Kim et al. 2012) and can thus contribute to the global carbon cycle and global climate change. Dalal and Mayer (1986) determined that the changes in the light fraction are 11 times the size of the stable fraction of the SOM. Decomposition studies by Gregorich et al. (2003) provided evidence that the HWOC fraction of soil C is highly labile; the authors estimated that they accounted for about 70% of the total water-soluble matter. Fischer (1993) showed that the HWOC content in soils was strongly correlated with CO_2 evolution, which indicated that a proportion of C must be easily available for microbial utilisation. Ghani et al. (2003) found that HWOC reflected the changes in SOC caused by different soil management practices compared with the stable SOC pool.

The highest content of HWOC in our study was found in the samples taken from forest soil (860.3 mg kg^{-1}), while the lowest content was measured in N2 (230.3 mg kg^{-1}) (Fig. 30.3). We assumed that after maize growth on the unfertilised 2-year rotation, with the lowest SOC, a small quantity of labile organic SOC is produced and simultaneously stabilised with clay and CaCO_3 , which prevent any further decline in SOC. Bouajila and Gallali (2008) also found a lower HWOC content in the soils with the highest content of CaCO_3 . Leinweber et al. (1995) reported that higher amounts of HWOC were measured at the end of the growing season due to easily decomposable mucilage created by microorganisms living in the rhizospheres. Generally, processes of microbial activity and concentrations of free carbohydrate in the arable soils lead to significant changes in HWOC at different times of the year. Some studies found

that manure application could influence the HWOC content. Liang et al. (2012) interpreted the increase in HWOC as being due to manure affecting microbial activity. Manure's positive effects on HWOC compared with the control and mineral fertilisation were confirmed by Böhme and Böhme (2006). According to Šimon (2008), single organic manuring did not increase the HWOC significantly as compared to the single NPK variant, but increased the HWOC content significantly in comparison with the control. These findings also support the proposition that manure is more valuable with the addition of NPK fertilisers (Blair et al. 2006). The values of HWOC obtained in our study make up an average of 0.84–2.27% of the total SOC. The highest distribution of HWOC in SOC was measured in the maize monoculture (805.6 mg kg^{-1}) and is attributed to the long-term production of a higher quantity of crop residues, the very high soil moisture level at the time of sampling and the presence of a large number of weeds (e.g. *Sorghum halepense*). Janzen et al. (1992) also found a high content of labile SOC in continuous monoculture on Chernozems in Canada. Leinweber et al. (1995) found 430–650 mg kg^{-1} HWOC in Bad Lauchstädt, while Sparling et al. (1998) determined a HWOC content that is comparative with our results. Accordingly, an increase or decrease in total biomass and net primary production of the specific cropping systems could contribute to soil carbon allocation through the soil profile.

To assess the labile carbon after winter wheat, a study was conducted on arable and non-arable soils on Haplic Chernozems (Šeremešić et al. 2013). Based on the results of the one-way analysis of the variance, it has been determined that the selected treatments affected the HWOC content, which led to the differences among them (Fig. 30.4). The results obtained are derived from the differences in the management technology, fertilisation pattern and a historic loss of the initial organic matter content in the agricultural soil over >60 years of experimental duration. The average content of labile fraction on arable soils, represented by the HWOC, ranged from 125 to 226 mg kg^{-1} . On the plots under native

Fig. 30.3 Hot-water-extractable carbon in soil samples after maize (0–30 cm) (MO—maize monoculture, N2—unfertilised 2-year rotation, D2—fertilised 2-year rotation, D3M—fertilised 3-year rotation with manure, UG—grassland, OF—forest)



vegetation, significantly higher values were determined (from 354 to 388 mg kg⁻¹) compared to the arable plots. Assessment of the same plots and land uses revealed that a higher HWOC was found in the spring and autumn as compared to samples taken in July (summer) after the winter wheat harvest. Our findings are similar to those presented in Chen et al. (2009) in the plough layer and the deeper soil layer of Cambisol in Southwest Germany, where average HWOC values in the arable soil ranged from 375 to 273 mg kg⁻¹. The values obtained can be related to the microbiological activity, which was more intensive with increased humidity. Apart from that, root activity, fresh organic matter production (root exudates) and management with plant residue are also believed to affect the labile fraction of SOM. According to Ghani et al. (2003), the soils used as grassland have HWOC reservoir values which vary from 3 to 6%, while Šimon (2008) reported HWOC values comparable to our results. According to the results gained by Soon et al. (2007) on a Luvisol in the north-western Alberta (Canada), the HWOC makes up 3.5 to 4.8% of the total OM.

Since the HWOC is considered as an indicator that largely reflects microbiological activity, the differences between the treatments may be related to soil biogenesis (Sparling et al. 1998). The assumption is made that the number and activity of microorganisms are not a limiting factor, but that the availability of the substrate for the

microbiological degradation can play a significant role in the turnover of the labile fraction. The total HWOC content may be an indicator of general soil fertility as the soil has more HWOC with a higher SOM content due to the processes of intensive transformation of fresh organic matter. As far as the fertilised treatments are concerned, the application of the mineral nitrogen can increase the microbiological activity and therefore the assimilation of a significant part of the labile organic matter. Higher SOC and HWOC values are associated with the aggregation of soil particles (Tobiašova et al. 2013). Natural forest, meadow and ruderal habitats can generally improve soil aggregation, which protects the SOM in the soil. Water-extractable organic carbon fractions are positively correlated with microbial biomass (Balaria et al. 2009), mineralisable N and aggregate stability; therefore, they can be used as an indicator of soil quality (Ghani et al. 2003).

Comparing the SOC and the HWOC contents, a positive correlation ($r^2 = 0.756$) was determined (Fig. 30.5). With an increase in the unit content of soil organic matter, the HWOC is also increased by 21.54 mg kg⁻¹. The result obtained is in accordance with values in the literature (Sparling et al. 1998). A higher amount of total soil OM is assumed to promote more intense mineralisation processes and a higher HWOC content. Therefore, an increase in total SOM when manure and crop residue are incorporated leads to a higher SOM and preserves soil fertility.

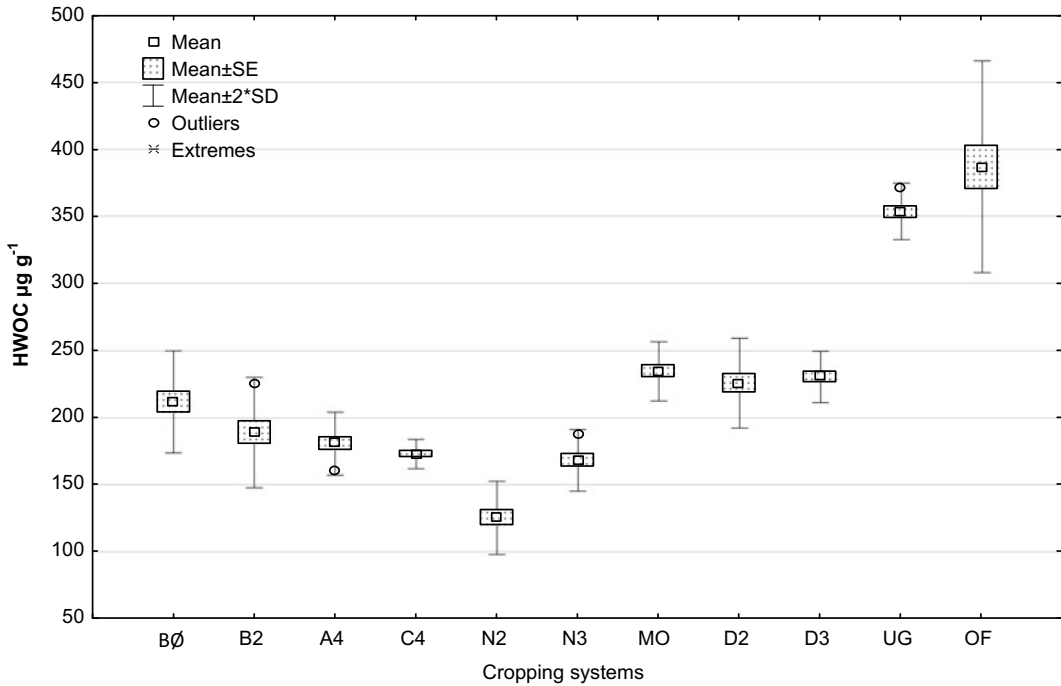


Fig. 30.4 Hot-water-extractable carbon (HWOC) in soil samples after winter wheat. Legend: BØ—4-year rotation with manure, B2—4-year rotation with manure and nitrogen, A4—4-year rotation with NPK and residue incorporation, C4—4-year rotation with NPK residue

removed, MO—winter wheat monoculture, N2—unfertilised 2-year rotation, N3—unfertilised 3-year rotation, D2—fertilised 2-year rotation, D3—fertilised 3-year rotation, UG—grassland, OF—oak fores

Likewise, Šeremešić (2017) noted that maintaining an average of 3% of SOM in the topsoil would require the incorporation of 750 C g ha⁻¹ m² with crop residues each year.

Ćirić et al. (2016) investigated the sensitivity of hot-water-extractable organic carbon (HWOC) and cold-water-extractable organic carbon (CWOC) fractions to land use in three soil types (Chernozems, Vertisols and Solonchaks) (WRB 2006) using an extraction procedure proposed by Ghani (2002). Field research was conducted in the Province of Vojvodina, Serbia, with three different land uses (cropland, meadow and forest).

The soil samples in the 0–20 cm layer of Chernozems from the natural habitat (meadow and forest) showed an HWOC concentration of 316–388 mg kg⁻¹, whereas, under continuous tillage, the values were significantly lower (125–226 mg kg⁻¹) compared to natural soils. The

surface horizon of forest soils contained 533–987 mg kg⁻¹ of HWOC, whereas the subsurface horizons had lower concentrations (100–400 mg kg⁻¹) (Table 30.1). The concentration of HWOC in arable soils ranged from 290 to 350 mg kg⁻¹ in the surface horizon and decreased with depth. In the surface layer of all observed soil types, the concentrations of easily decomposable SOC fractions, CWOC and HWOC were significantly lower on arable land compared to forest land.

Changes in CWOC and HWOC induced by land use and management for other pedo-climatic conditions have been reported previously (Ghani et al. 2003; Chantigny 2003; Ćirić 2014). This indicates higher proportions of bioavailable carbon and a higher degree of labile SOC in soils under forest compared to arable land. A higher concentration of SOC and its labile fractions is more common in forest ecosystems compared to

Fig. 30.5 Correlation between HWOC and SOC for different cropping systems on Chernozems

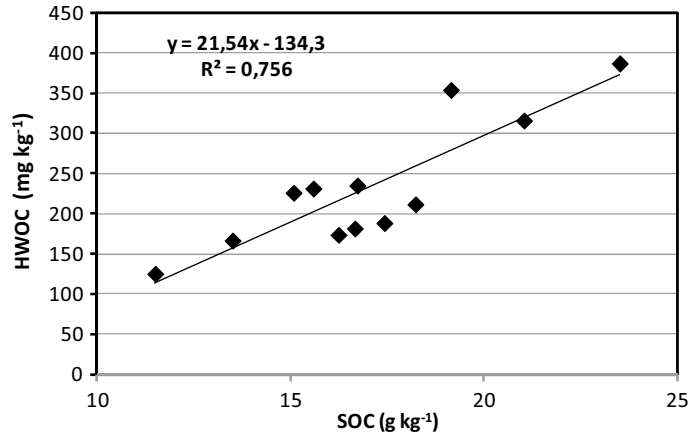


Table 30.1 The concentration of HWOC fractions and their relative contribution in SOC

Soil type	Land use	Depth	CWOC ± SE (mg kg ⁻¹)	HWOC ± SE (mg kg ⁻¹)	SOC ± SE (g kg ⁻¹)	CWOC in SOC (%)	HWOC in SOC (%)
Chernozem	Arable land	0–30	98 ± 16.0	297 ± 27.0	13.59 ± 1.25	0.72	2.19
		30–60	60 ± 6.0	190 ± 53.0	7.61 ± 0.46	0.79	2.49
		60–90	14 ± 2.0	86 ± 9.0	2.80 ± 0.32	0.50	3.09
	Forest land	0–30	138 ± 13.0	533 ± 30.0	18.63 ± 0.38	0.74	2.86
		30–60	27 ± 4.0	116 ± 3.0	10.63 ± 1.37	0.26	1.09
		60–90	26 ± 5.0	101 ± 21.0	4.07 ± 0.14	0.64	2.47
Vertisol	Arable land	0–30	170 ± 24.0	321 ± 17.0	14.17 ± 0.85	1.20	2.26
		30–60	83 ± 35	158 ± 34.0	5.47 ± 0.40	1.52	2.89
		60–90	7 ± 3.0	59 ± 7.0	2.51 ± 0.15	0.28	2.36
	Forest land	0–30	462 ± 23.0	987 ± 65.0	22.14 ± 1.04	2.09	4.46
		30–60	131 ± 15.0	272 ± 16.0	9.16 ± 0.43	1.44	2.97
		60–90	46 ± 12.0	151 ± 14.0	3.46 ± 0.44	1.32	4.38
Solonetz	Arable land	0–30	129 ± 3.0	355 ± 21.0	11.27 ± 0.18	1.15	3.15
		30–60	135 ± 23.0	240 ± 11.0	5.28 ± 0.15	2.56	4.54
		60–90	22 ± 5.0	111 ± 13.0	4.10 ± 0.20	0.54	2.71
	Forest land	0–30	290 ± 10.0	845 ± 25.0	17.34 ± 0.40	1.67	4.87
		30–60	110 ± 11.0	398 ± 10.0	7.42 ± 0.70	1.48	5.37
		60–90	53 ± 4.0	125 ± 21.0	5.03 ± 0.37	1.05	2.49

Legend: SOC—soil organic carbon, HWOC—hot-water-extractable organic carbon, CWOC—cold-water-extractable organic carbon

agro-ecosystems (Tobiašova et al. 2013). Land use systems are an important factor regulating SOC decomposition by altering natural soil characteristics under the same climatic/ecological conditions (Manojlović et al. 2011). Similarly,

CWOC and HWOC act as valuable indicators of anthropogenic impacts on soil, keeping in mind the differences obtained in soils under native vegetation compared to the intensively used arable soil. In particular, the concentration of

CWOC in the surface layer of Chernozem, Vertisol and Solonetz was lower, from 28 to 63% in arable compared to forest soils, but 44–68% lower for HWOC concentration. This indicates greater differences in HWOC than in CWOC between two land uses emphasising HWOC as a more sensitive (informative) indicator of SOC quality than CWOC. Hamkalo and Bedernichek (2014) proposed the same approach. This is probably because HWOC exhibits higher biodegradability rates than CWOC (Gregorich et al. 2003).

The concentration of CWOC in the upper horizon was highest in Vertisols (170–462 mg kg⁻¹), compared to Solonetz (129–290 mg kg⁻¹) and Chernozem (98–138 mg kg⁻¹), whereas in the subsurface horizons (30–60 and 60–90 cm), it varied from 7 to 131 mg kg⁻¹ in the Vertisol, from 22 to 135 mg kg⁻¹ in the Solonetz and from 14 to 60 mg kg⁻¹ in the Chernozem soil. Similarly, in the surface horizon, the HWOC concentration was highest in Vertisol, followed by Solonetz and Chernozem soils, whereas in the subsurface horizons, HWOC was highest in Solonetzes, followed by Vertisols, while the differences between arable and forest land within the soil types were less pronounced with depth. The differences in CWOC and HWOC between land use systems were less pronounced in Chernozem and Solonetz but not in Vertisol soil. This could be explained by a higher absorption capacity and clay content in Vertisol, which prevents SOC fractions from leaching into deeper horizons. Furthermore, Vertisol is characterised by pedoturbation, a process that leads to the mixing of surface and subsurface horizons, minimising horizon differentiation (Belić et al. 2011). The function and dynamics of dissolved organic carbon fractions in soils are defined by their quality and quantity and depending on their origin (Kalbitz et al. 2000).

30.2.1.4 Mineral-Associated and Particulate Organic Carbon

Particulate organic carbon (POC) is considered to be an intermediate pool of organic matter between fresh plant residues and humified

organic matter (Gregorich and Janzen 1996) that is sensitive to management practices and soil structure formation (Cambardella and Elliott 1993). Therefore, POC acts as a soil binding agent responsible for stabilising macro-aggregates and intra-aggregate structures (Six et al. 2002). Particulate organic matter is a major food and energy source for endogeic (soil-dwelling) soil fauna, including many earthworms (Curry et al. 1998). Bayer et al. (2004) explained that organic matter in POC is more sensitive to management practices than C obtained in the total SOC pool. Martinez–Mena et al. (2012) indicated that the interaction between POC and mineral-associated carbon (MOC) improved our understanding of the role of labile C in SOC dynamics.

The inter-aggregate fraction consists of plant residues and biotic soil biomass and exhibits preferential absorptions of OH, NH and aliphatic CH bonds in mid-IR spectra, whereas the intra-aggregate and silt fractions have a much larger presence of carboxylic and aromatic groups that correspond to lignin and humic substances (Paul et al. 2015). It is generally accepted that sequestered C is mainly composed of a mineral-associated fraction with a greater C-stabilising capacity (Bajgai et al. 2012). Thus, the labile POC fraction is considered to be a C pool associated with the activity and abundance of microorganisms (Schimel and Schaeffer 2015; Cookson et al. 2008) as a microbial community controls SOC turnover. Mineral-associated organic carbon (MOC) is considered to be an organic material that is difficult for microbial decomposition, and it is part of the SOC which is usually associated with the particle size distribution. Because of this, the highest SOC in the soil resulted in the highest MOC. MOC contains a more stable C fraction which positively correlates with the clay content. This indicates that clay minerals have a certain ability to form complexes with SOC (Mikutta et al. 2006).

To assess the POC and MOC, soil samples were taken from the long-term Plodoredi field experiment at the Institute of Field and Vegetable Crops in Novi Sad. The selected plots differ in terms of fertilisation and crop rotation, but

receive the same management practices for selected crop varieties. Of the soil properties, the pH and soil texture changed the least compared to initial values. The highest content of MOC in our study was found in the oak forest and untilled grassland (Table 30.2). The content of MOC did not exhibit a clear pattern of change with increasing soil depth. The differences are related to the soil bulk density and the relationship between the total SOC and MOC. Comparing different land use systems, non-agricultural soil samples had significantly higher MOC contents compared with the arable land. The manured treatment (S3) had a significantly higher MOC content than the 2-year crop rotation, but not higher than MO, which indicates that C from the manure was transformed by microorganisms and probably diluted in the soil over time. The sampling time affected the MOC content, since higher values were observed in October. This increase was obtained from non-agricultural samples and may be due to the chemical composition of soil organic matter and the strength of the connection with clay (Leifeld and Kögel-Knabner 2005).

By performing Principal Component Analyses (PCAs), the relationship between soil properties can be closely analysed. On the PCA score plot, several groups of factors were clearly separated: MOC and HWOC were closely distributed; the soil organic matter and POC were linked, while the activity of microorganisms was dispersed over the plot (Fig. 30.6). Fractions of soil organic carbon were inversely represented by *Azotobacter* and fungi, indicating a weaker correlation among them. This suggests that the activity of *Azotobacter* in soil and an increased number of fungi could decrease the soil organic matter. Our results are in agreement with a study by Stamenov et al. (2016) in which microbiological activity was assessed in the same experiment, and analysis showed that fertilisation did not exert a significant influence on the number of free-living nitrogen-fixing *Azotobacter* sp. bacteria. Marinković et al. (2018) found the highest number of microorganisms in non-agricultural soil and unfertilised soil under 2-year and 3-year rotation, while the highest dehydrogenase

activity was measured in non-agricultural and the wheat monoculture soil. Accordingly, this indicates that the soil organic carbon can stabilise during the fallow phase or between the vegetation seasons. The first principal component, PC1, accounts for 47% of the total data variance, and the second for 17%. The separation is largely based on the first principal component.

30.3 Particulate and Mineral-Associated Organic Carbon with Different Soil Types and Land Uses

The depletion of SOC is of major concern; it will accelerate a chain reaction of the deterioration of interconnected soil properties (Čirić et al. 2017).

As particulate and mineral-associated organic carbon are dependent on land use strategies and soil types, a field study was conducted in the Province of Vojvodina, Serbia, on five soil types (Arenosols, Chernozems, Fluvisols, Vertisols and Solonchets) (WRB 2006 soil resources, 2006), as presented in Fig. 30.7. Each soil type was observed in three locations and within each location under three different land uses (cropland, meadow and forest) (Fig. 30.8). Soil samples were taken from a depth of 0–30 cm with 3 replications approximately 10 m apart. Particulate organic carbon was determined using adapted procedures based on those by Cambardella and Elliott (1993). One common procedure involves labile carbon extraction by density separation with sodium polytungstate adjusted to a density of 1.85 g cm⁻³ and the aspiration of organic matter floating on the surface of an aqueous suspension.

The concentration of POC fraction in Vertisols was higher than in other soil types (Fig. 30.9). A higher concentration of POC was found in the forests and meadows compared to the arable soil. These results showed a 42–44% reduction in POC due to changes in land use. The measured POC values ranged from 3.8 to 7.9 g kg⁻¹.

A higher concentration of MOC was found in the Vertisols compared to other soil types

Table 30.2 Content of mineral-associated organic carbon (MOC) and particulate organic carbon (POC) in the soil of different land use systems at the Rimki Šančević experimental station (Novi Sad) (g kg^{-1})

C fractions	Sampling time	Depth (cm) De	Land use systems (Lu)								Average De	Average St
			MO	N2	D2	S3	UG	OF				
MOC	May	0–10	16.70 ± 0.3	15.81 ± 0.3	13.71 ± 0.1	20.21 ± 0.8	24.31 ± 0.1	25.41 ± 0.2	19.36	18.69B		
		10–20	18.48 ± 0.2	16.54 ± 0.3	15.83 ± 0.3	17.88 ± 0.3	22.37 ± 0.1	14.99 ± 0.1	17.68			
		20–30	19.00 ± 0.3	16.67 ± 0.2	14.47 ± 0.2	21.62 ± 0.4	20.87 ± 0.7	21.56 ± 0.5	19.03			
	St/De	18.06	16.34	14.67	19.91	22.51	20.65					
	October	0–10	23.32 ± 0.4	12.65 ± 0.1	17.30 ± 0.2	18.32 ± 0.5	29.48 ± 0.2	35.87 ± 0.1	22.82	21.49A		
		10–20	17.46 ± 0.3	15.45 ± 0.2	16.46 ± 0.2	19.74 ± 0.2	33.48 ± 0.1	26.91 ± 0.3	21.58			
		20–30	19.26 ± 0.2	14.67 ± 0.2	15.21 ± 0.4	18.33 ± 0.3	27.94 ± 0.1	24.89 ± 0.3	20.05			
	St/De	20.01	14.26	16.32	18.80	30.30	29.22					
	MOC (Average) Lu		19.03b	15.30c	15.49c	19.35b	26.40a	24.93a				
POC	May	0–10	2.55 ± 0.7	1.29 ± 0.1	2.37 ± 0.2	2.47 ± 0.5	9.82 ± 1.4	8.91 ± 0.7	4.57	3.77A		
		10–20	2.58 ± 0.2	1.17 ± 0.3	2.20 ± 0.3	3.37 ± 0.6	5.82 ± 2.8	7.27 ± 2.5	3.74			
		20–30	3.16 ± 0.6	1.17 ± 0.2	1.95 ± 0.3	3.13 ± 0.7	5.93 ± 3.7	2.62 ± 0.3	2.99			
	St/De	2.76	1.21	2.17	2.99	7.19	6.27					
	October	0–10	3.39 ± 0.8	1.21 ± 0.2	2.40 ± 0.8	3.32 ± 1.0	9.44 ± 1.2	11.84 ± 0.0	5.27	3.93A		
		10–20	2.40 ± 0.6	1.23 ± 0.1	2.49 ± 0.6	2.54 ± 0.1	6.73 ± 0.8	7.76 ± 1.1	3.86			
		20–30	2.36 ± 0.1	1.31 ± 0.2	2.37 ± 0.3	2.83 ± 0.2	3.50 ± 0.1	3.51 ± 0.3	2.65			
	St/De	2.72	1.25	2.42	2.89	2.90	6.56					
	POC (Average) Lu		2.74b	2.23c	2.29b	2.94b	5.04a	6.41a				

^{ABC/abc} Data followed by the same letter within a row or a column do not differ significantly at the $P \leq 0$ (MO—maize monoculture, N2—unfertilised 2-year rotation, D2—fertilised 2-year rotation, D3M—fertilised 3-year rotation with manure, UG—grassland, OF—forest)

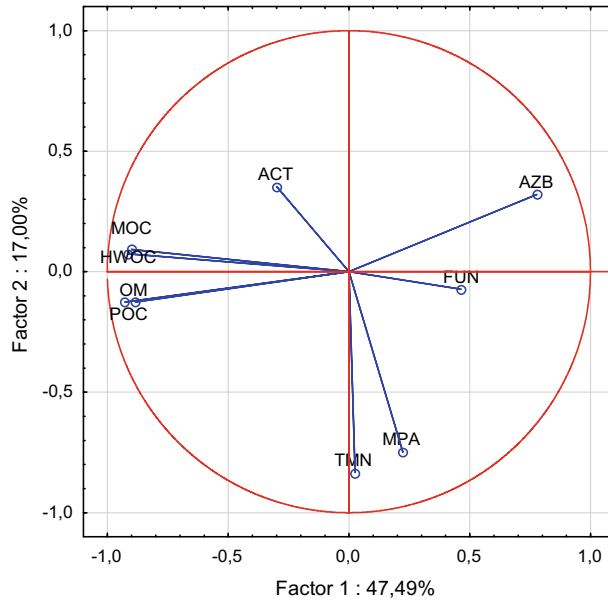


Fig. 30.6 PCA ordination of soil organic carbon fraction and microorganisms based on component correlations (SOC—Soil organic carbon; OM—total organic matter; POC—particulate organic carbon; MOC—mineral-associated carbon; ACT—*Actinomycetes*; TMN—Total microbial number; AZB—*Azotobacter*; MPA—*Ammonifiers*; FUN—*Fungi*)

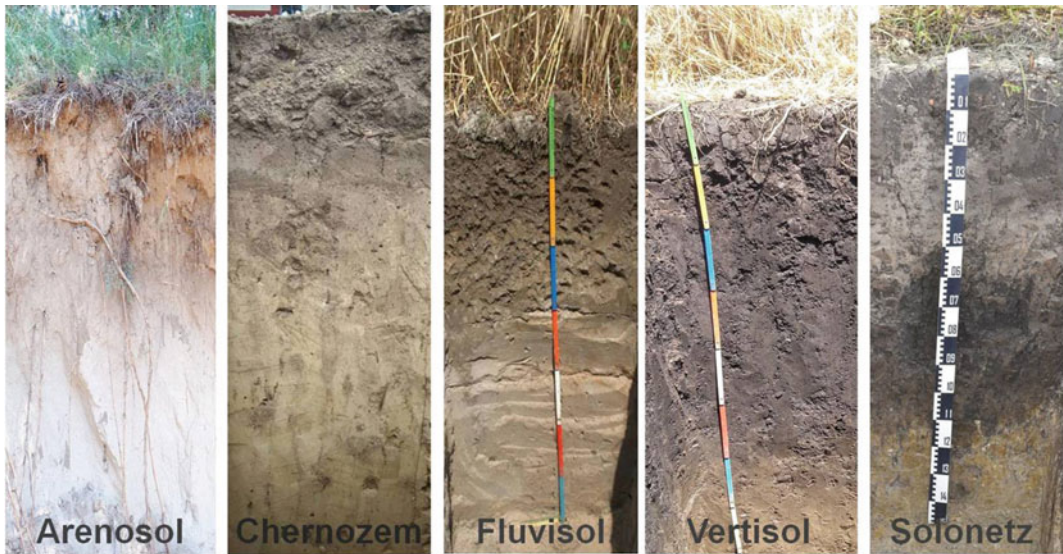


Fig. 30.7 Different soil types included in the study (Orig.)

(Fig. 30.10). In terms of order, Chernozems and Solonetz had a lower concentration than Vertisols, Fluvisols had a lower MOC concentration than Chernozems and Solonetz, and Arenosols exhibited an even lower concentration than Fluvisols. Mineral-associated organic carbon did not differ between different land uses. MOC values ranged from 6.7 to 20.1 g kg⁻¹.



Fig. 30.8 Different land uses included in the study (Orig.)

Fig. 30.9 Concentration of POC (g kg^{-1}) with soil types and land uses (0–30 cm). Columns labelled with different capital letters are significantly different in terms of land use ($p \leq 0.05$). Columns labelled with different letters are significantly different in terms of the soil type ($p \leq 0.05$)

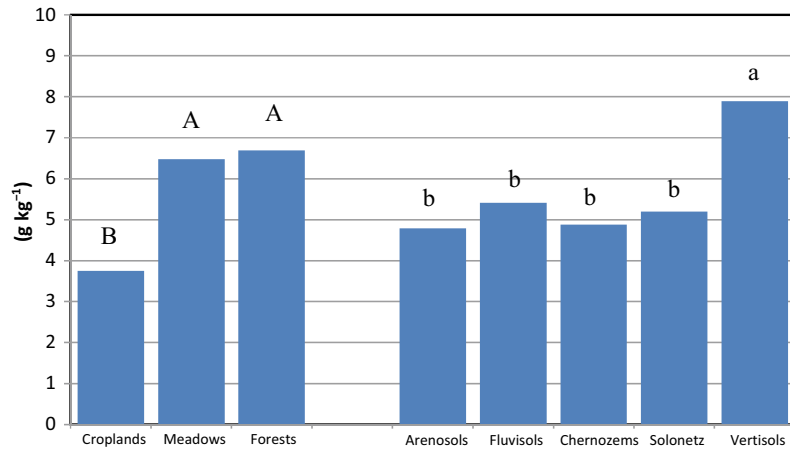
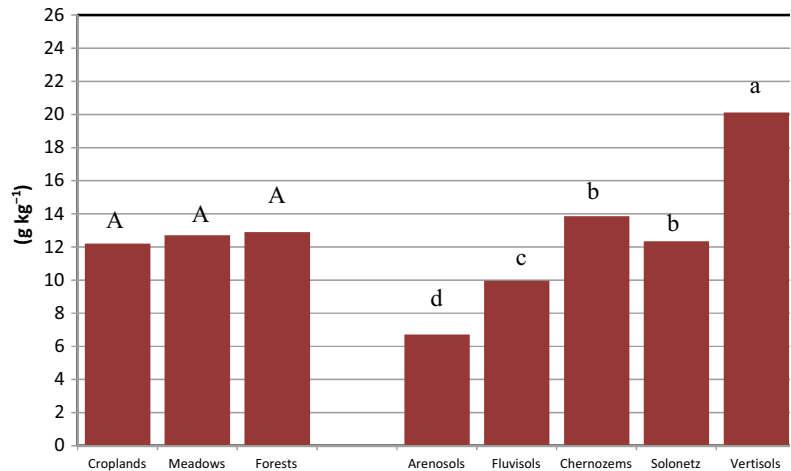


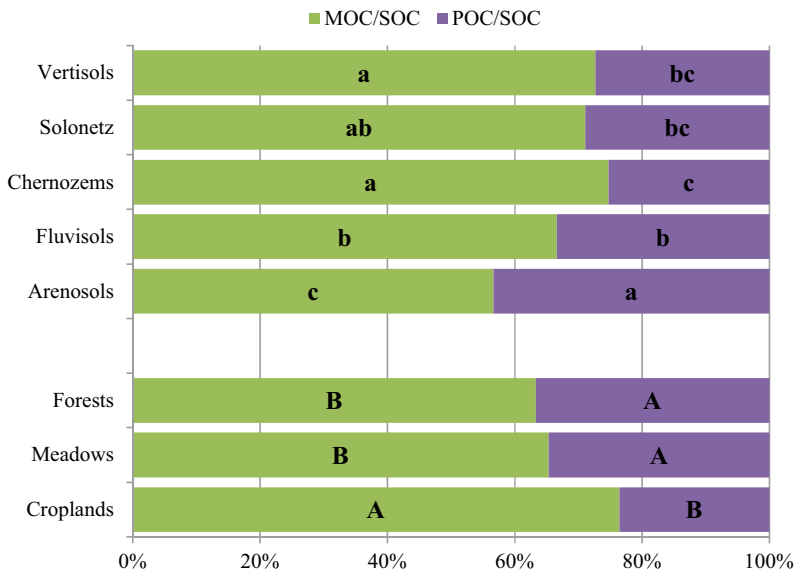
Fig. 30.10 Concentration of MOC (g kg^{-1}) with soil types and land uses (0–30 cm). Columns labelled with different capital letters are significantly different in terms of land use ($p \leq 0.05$). Columns labelled with different letters are significantly different in terms of the soil type ($p \leq 0.05$)



The relative contribution of the MOC fraction is higher in all observed soil types and land uses than in the POC fraction (Fig. 30.11). It is clearly seen that Chernozems and Vertisols had the highest share of MOC fraction and, logically, the

lowest share of the POC fraction. Solonetz had a slightly lower share of MOC than the two soils mentioned, but still more than 70%. Fluvisols had a low amount of MOC, while Arenosols had the lowest.

Fig. 30.11 Share of POC and MOC in SOC (%) by soil types and land uses (0–30 cm). Columns labelled with different capital letters are significantly different in terms of land use ($p \leq 0.05$). Columns labelled with different letters are significantly different in terms of the soil type ($p \leq 0.05$)



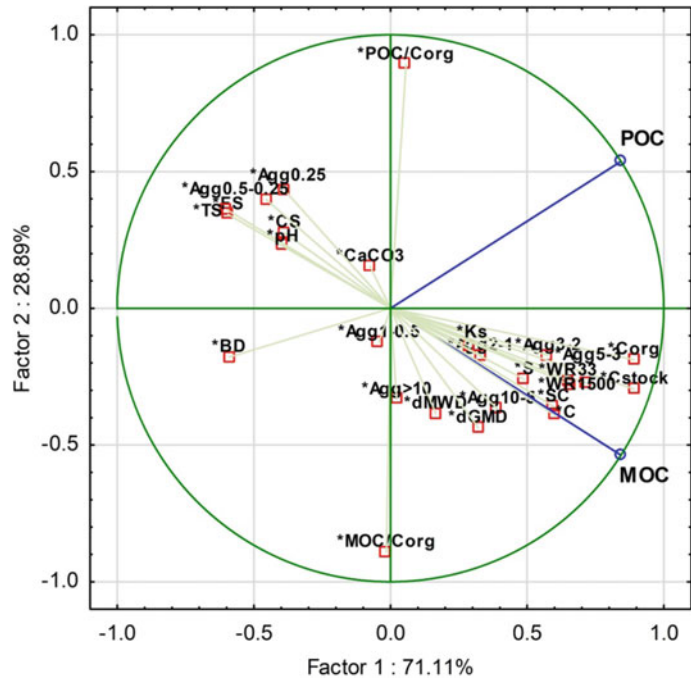
Cropland had a higher MOC share (>75%), and therefore a lower share of POC compared to the meadows and forests. The values for the POC/SOC varied in a wide range from 56.7 to 76.4%, and those for MOC/SOC varied from 23.6 to 43.3%.

The highest concentration of POC measured in Vertisols was the result of the highest SOC concentration found in these soils compared to others. In terms of MOC concentration, the soil types were more clearly differentiated due to their inherent properties. The fact that the highest MOC concentration was observed in Vertisols, followed by Chernozems and Solonetz, indicates that there is a relationship between the concentration of MOC and clay content in soils. On the other hand, the formation of mollic humus and a higher SOC concentration in these soils compared with Fluvisols and Arenosols also contributes to an increase in MOC concentration. Chernozems, Vertisols and Solonetz had the highest share of MOC fraction in SOC (>75%). Fluvisols exhibited a lower MOC concentration due to periodically interrupted pedogenesis and the formation of organo-mineral complexes caused by fluvial deposits. The lowest MOC concentration in Arenosols was due to wind erosion and coarse texture, which is characterised by a low adsorption capacity and the ability to bind organic molecules. The established content of the

MOC fraction was higher in all soil types and land uses than the content of the POC fraction. The share of POC/SOC ranged from 56.7 to 76.4%, and that for MOC/SOC from 23.6 to 43.3%. A higher concentration of MOC compared to POC was also found in the studies by de Figueiredo et al. (2010) and Martínez-Mena et al. (2012).

Particulate organic carbon has proven to be a sensitive indicator of land use changes. The concentration of POC decreased by 42–44% due to the conversion of forests and meadows into arable land, in contrast to the share of the MOC, which did not respond to these changes. These facts indicate that the SOC decrease caused by land use changes occurred only in the POC fraction, while the MOC fraction remained stable. Changes in the concentration of SOC with a change in land use occurred mainly in the POC fraction >53 mm (de Figueiredo et al. 2010). This is a much more sensitive indicator of changes caused by land use and tillage than the SOC concentration (Franzluibbers and Arshad 1997; Bayer et al. 2004). The close relationships between the MOC and soil mineral part protect it from the oxidation process, which leads to the loss of MOC fraction. This fraction is fully humified and has a high degree of stability. The silt and clay fractions (<53 μm) are the best protectors of SOC (Ćirić et al., 2013b). In

Fig. 30.12 PCA analysis of POC and MOC fractions (active variables) and selected soil properties (supplementary variables). CS, Coarse sand; FS, Fine sand; TS, Total sand; S, Silt; C, Clay; SC, Silt + Clay; WR33, Water retention at—33 kPa; WR1500, Water retention at v1500 kPa; BD, Bulk density; Agg, Different classes of aggregates; dMWD, Dry mean weight diameter; dGMD, Geometric mean diameter; Ks, Structural coefficient; C_{org} , Soil organic carbon concentration; C_{stock} , Soil organic carbon stock



contrast, POC, which linked microaggregates to macroaggregates, is a labile fraction that is very sensitive to changes in land use (He et al. 2008).

The results of PCA analysis for the POC and MOC fractions (as active variables) and selected soil properties (as supplementary variables) are summarised in Fig. 30.12. The first component (PC1), explaining about 71% of the data variance, showed high loads for C_{org} (0.89) and C_{stock} (0.89). High loads were also seen for the PC1 count WR33 and WR1500 (0.65 and 0.71, respectively), Agg5-3 (0.65) and C (0.60). The second component (PC2), accounting for nearly 29% of the total variation, is heavily loaded on POC/C_{org} (0.89), MOC/C_{org} (-0.89), dGMD (-0.44) and Agg < 0.25 (0.43). The obtained PCA results indicate a clear relationship between certain soil properties (C_{org} concentration and stock, structural aggregates and clay particles) and an influence on the distribution and dynamics of POC and MOC in soil.

30.4 Conclusions

The labile carbon pools play an important role in understanding the changes in SOC. Hot-water-extractable carbon exhibited higher variability and sensitivity in cropping systems and land uses compared to the POC fraction. The concentration of MOC differed between land uses only in a relative proportion. In non-agricultural soils, the total and labile SOC differed significantly as a function of pedogenesis, while they played an important role in the management of agricultural land. Therefore, the threshold level varies significantly and depends upon the crop and production systems. In general, the labile SOC reflects a central role in soil processes and fertility preservation. Consequently, the adoption of management practices that sustain the process of labile SOC transformation will ensure the maintenance of total SOC as a key soil resource.

References

- Balaria A, Johnson CE, Xu Z (2009) Molecular-scale characterization of hot-water-extractable organic matter in organic horizons of a forest soil. *Soil Sci Soc Am J* 73(3):812–821
- Bajgai Y, Kristiansen P, Hulugalle N, McHenry M (2012) Particulate and mineral-associated organic carbon fractions as influenced by corn residue incorporation and simulated tillage. In: Proceedings of 16th Australian agronomy conference. (http://regional.org.au/asa/2012/climatechange/8063_bajgai.htm). Accessed 25 June 2019
- Baldock JA, Nelson PN (2000) Soil organic matter. In: Sumner ME (ed) *Handbook of soil science*. CRC Press, Boca Raton, pp B25–B240
- Bayer C, Matin-Neto L, Mielniczuk J, Pavinato A (2004) Armazenamento de carbono em frações lábeis da matéria orgânica de um Latossolo Vermelho sob plantio direto. *Pesq Agropec Bras* 39:677–683. <https://doi.org/10.1590/S0100-204X2004000700009>
- Belić M, Nešić Lj, Čirić V, Vasin J, Milošev D, Šeremešić S (2011) Characteristics and classification of gleyic soils of Banat. *Field Veg Crop Res* 48:375–382
- Blair N, Faulkner RD, Till AR, Körschens M, Schulz E (2006) Long-term management impacts on soil C, N and physical fertility. Part II. Bad Lauchstadt static and extreme FYM experiments. *Soil till Res* 91:39–47. <https://doi.org/10.1016/j.still.2005.11.001>
- Blum WEH (2008) Characterization of soil degradation risk: an overview. In: Tóth G, Montanarella L, Rusco E (eds) *Threats to soil quality in Europe*. JRC, Office for Official Publications of the European Communities, Luxembourg
- Bogdanović D, Ubavić M, Dozet D (1993) Hemijska svojstva i obezbeđenost zemljišta Vojvodine neophodnim mikroelementima. In „Teški metali i pesticidi u zemljištima Vojvodine“ Kastori R (eds) *Poljoprivredni fakultet, Institut za ratarstvo i povrarsstvo, Novi sad*, pp 197–215
- Bogdanović M (1954) *Odlike humusa u glavnim tipovima zemljišta NR Srbije*. Faculty of Agriculture, Zemun, Belgrade. Doctoral dissertation
- Böhme L, Böhme F (2006) Soil microbiological and biochemical properties affected by plant growth and different long-term fertilization. *Eur J Soil Biol* 42:1–12. <https://doi.org/10.1016/j.ejsobi.2005.08.001>
- Bouajila A, Gallali T (2008) Soil organic carbon fractions and aggregate stability in carbonated and no carbonated soil in Tunisia. *J Agron* 7:127–137. <https://doi.org/10.3923/ja.2008.127.137>
- Cambardella CA, Elliott ET (1993) Methods for physical separation and characterization of soil organic matter fractions. *Geoderma* 56:449–457. <https://doi.org/10.1016/B978-0-444-81490-6.50036-4>
- Chantigny MH (2003) Dissolved and water-extractable organic matter in soils: a review on the influence of land use and management practices. *Geoderma* 113:357–380. [https://doi.org/10.1016/S0016-7061\(02\)00370-1](https://doi.org/10.1016/S0016-7061(02)00370-1)
- Chen HQ, Marhan S, Billen N, Stahr K (2009) Soil organic carbon and total nitrogen stocks as affected by different land uses in Baden-Württemberg, Southwest Germany. *J Plant Nutr Soil Sci* 172:32–42. <https://doi.org/10.1002/jpln.200700116>
- Christensen BT, Johnson AE (1997) Soil organic matter and soil quality—lessons learn from the long-term experiments at Askov and Rothamsted. In: Gregorich EG, Carter MR (eds) *Soil quality in crop production and ecosystem health*. Elsevier, Amsterdam, pp 399–430
- Čirić V (2014) *Qualitative and quantitative characteristics of organic matter in different soil types [dissertation]*. University of Novi Sad, Novi Sad
- Čirić V, Belić M, Nešić Lj, Šeremešić S, Pejić B, Bezdán A, Manojlović M (2016) The sensitivity of water extractable soil organic carbon fractions to land use in three soil types. *Arch Agron Soil Sci* 62 (12):1654–1664. <https://doi.org/10.1080/03650340.2016.1165345>
- Čirić V, Manojlović M, Nešić Lj, Belić M (2013a) Soil organic carbon loss following land use change in a semiarid environment. *Bulg J Agri Sci* 19:461–466
- Čirić V, Manojlović M, Belić M, Nešić Lj, Šeremešić S (2013b) Effects of land use conversion on soil aggregate stability and organic carbon in different soils. *Agrociencia* 47(6):539–552
- Čirić V, Drešković N, Mihailović DT, Mimić G, Arsenić I, Đurđević V (2017) Which is the response of soils in the Vojvodina Region (Serbia) to climate change using regional climate simulations under the SRES-A1B? *CATENA* 158:171–183. <https://doi.org/10.1016/j.catena.2017.06.024>
- Compton JE, Boone RD (2002) Soil nitrogen transformation and the role of light fraction organic matter in forest soil. *Soil Biol Biochem* 34:933–943
- Cookson WR, Murphy DV, Roper MM (2008) Characterizing the relationships between soil organic matter components and microbial function and composition along a tillage disturbance gradient. *Soil Biol Biochem* 40:763–777. <https://doi.org/10.1016/j.soilbio.2007.10.011>
- Curry JP (1998) Factors affecting earthworm abundance in Soils. In: Edwards CA (ed) *Earthworm ecology*. St. Lucie Press, Boca Raton, FL, pp 37–64
- Dalal RC, Mayer RJ (1986) Long-term trends in fertility of soils under continuous cultivation and cereal cropping in southern Queensland: III Distribution and kinetics of soil organic carbon in particle-size fractions. *Aust J Soil Res* 24:281–292. <https://doi.org/10.1071/SR9860301>
- de Figueiredo CC, Resck DVS, Carneiro MAC (2010) Labile and stable fractions of soil organic matter under management systems and native cerrado. *Rev Bras Ciênc Sol* 34:907–916. <https://doi.org/10.1590/S0100-06832010000300032>
- Fischer T (1993) Einfluß von Winterweizen und Winterroggen in Fruchtfolgen mit unterschiedlichem Getreideanteil auf die mikrobielle Biomasse und jahreszeitliche Kohlenstoffdynamik des Bodens. *Arch Acker Pflanzenbau Bodenkd* 37:181–189

- Frank S, Schmid E, Havlík P, Schneider UA, Böttcher H, Balkovič J, Obersteiner M (2015) The dynamic soil organic carbon mitigation potential of European cropland. *Global Environ Chan* 35:269–278. <https://doi.org/10.1016/j.gloenvcha.2015.08.004>
- Franzluebbers AJ, Arshad MA (1997) Particulate organic carbon content and potential mineralization as affected by tillage and texture. *Soil Sci Soc Am J* 61:1382–1386. <https://doi.org/10.2136/sssaj1997.03615995006100050014x>
- Ghani A, Dexter M, Perrott KW (2003) Hot-water extractable carbon in soils: a sensitive measurement for determining impacts of fertilization, grazing and cultivation. *Soil Biol Biochem* 35:1231–1243. [https://doi.org/10.1016/S0038-0717\(03\)00186-X](https://doi.org/10.1016/S0038-0717(03)00186-X)
- Ghani A (2002) Hot-water carbon is an integrated indicator of soil quality. Paper presented at: confronting new realities in the 21st century. 17th world conference of soil science, Bangkok, Thailand
- Gomiero T (2003) Alternative land management strategies and their impact on soil conservation. *Agriculture* 3(3):464–483. <https://doi.org/10.3390/agriculture3030464>
- Gregorich EG, Janzen HH (1996) Storage of soil carbon in the light fraction and macro-organic matter. In: Carter MR, Steward BA (eds) *Structure and soil organic matter storage in agricultural soils*. CRC Press, Boca Raton, FL, pp 167–190
- Gregorich EG, Bear M, Stoklas U, St-Georges P (2003) Biodegradability of soluble organic matter in maize cropped soils. *Geoderma* 113:237–252. [https://doi.org/10.1016/S0016-7061\(02\)00363-4](https://doi.org/10.1016/S0016-7061(02)00363-4)
- Hamkalo Z, Bedernichek T (2014) Total, cold and hot water extractable organic carbon in soil profile: impact of land-use change. *Žemdirbystė* 101:125–132. <https://doi.org/10.13080/z-a.2014.101.016>
- Hassink J (1997) The capacity of soils to preserve organic C and N by their association with clay and silt particles. *Plant Soil* 191:77–87. <https://doi.org/10.1023/A:1004213929699>
- Haynes RJ (2000) Interactions between soil organic matter status, cropping history, method of quantification and sample pretreatment and their effects on measured aggregate stability. *Biol Fert Soil* 30:270–275. <https://doi.org/10.1007/s003740050002>
- Haynes RJ (2005) Labile organic matter fractions as central components of the quality of agricultural soils: an overview. *Adv Agron* 85:221–268. [https://doi.org/10.1016/S0065-2113\(04\)85005-3](https://doi.org/10.1016/S0065-2113(04)85005-3)
- He Y, Xu Z, Chen C, Burton J, Ma Q, Ge Y, Xu J (2008) Using light fraction and macroaggregate associated organic matters as early indicators for management-induced changes in soil chemical and biological properties in adjacent native and plantation forests of subtropical Australia. *Geoderma* 147(3–4):116–125. <https://doi.org/10.1016/j.geoderma.2008.08.002>
- Janzen HH, Campbell CA, Brandt SA, Lafond GP, Townley-Smith L (1992) Light-fraction organic matter in soils from long-term crop rotation. *Soil Sci Soc Am J* 56:1799–1806. <https://doi.org/10.2136/sssaj1992.03615995005600060025x>
- Kalbitz K, Solinger S, Park JH, Michalzik B, Matzner E (2000) Controls on the dynamics of dissolved organic matter in soils: a review. *Soil Sci* 165:277–304
- Kalbitz K, Kaiser K (2008) Contribution of dissolved organic matter to carbon storage in forest mineral soils. *J Plant Nutr Soil Sci* 171:52–60. <https://doi.org/10.1002/jpln.200700043>
- Kim YS, Yi MJ, Lee YY, Son Y, Koike T (2012) Characteristics of soil CO₂ efflux in even-aged alder compared to Korean pine plantations in Central Korea. *J Forest Sci* 28:232–241. <https://doi.org/10.7747/JFS.2012.28.4.232>
- Kupernikov IA, Boincean BP, Dent D (2011) *Ecological principles for sustainable agriculture on chernozem soils*. Springer, pp 1–143
- Lal R (2006) Enhancing crop yields in the developing countries through restoration of the soil organic carbon pool in agricultural lands. *Land Degrad Dev* 17(2):197–209. <https://doi.org/10.1002/ldr.696>
- Leifeld J, Kögel-Knabner I (2005) Soil organic matter fractions as early indicators for carbon stock changes under different land-use? *Geoderma* 124:143–155. <https://doi.org/10.1016/j.geoderma.2004.04.009>
- Leinweber P, Schulten HR, Körschens M (1995) Hot water extracted organic matter: chemical composition and temporal variations in a long-term field experiment. *Biol Fert Soil* 20:17–23. <https://doi.org/10.1007/BF00307836>
- Liang Q, Chen H, Gong Y, Fan M, Lal R, Kuzyakov Y (2012) Effects of 15 years of manure and inorganic fertilizers on soil organic carbon fractions in wheat–maize system in the North China Plain. *Nut Cycl Agroecosys* 92:21–33. <https://doi.org/10.1007/s10705-011-9469-6>
- Manojlović M, Aćin V, Seremesic S (2008) Long-term effects of agronomic practices on the soil organic carbon sequestration in Chernozem. *Arch Agr Soil Sci* 54:353–367. <https://doi.org/10.1080/03650340802022845>
- Manojlović M, Čibilovski R, Sitaula B (2011) Soil organic carbon in Golija mountain (Serbia) soils: effects of land use and altitude. *Pol J Environ Stud* 20:977–986
- Marinković J, Bjelić D, Šeremešić S, Tintor B, Ninkov J, Živanov M, Vasin J (2018) Microbial abundance and activity in chernozem under different cropping systems. *Field Veg Crop* 55(1):6–11
- Martinez-Mena M, Lopez J, Almagro M, Albaladejo J, Castillo V, Ortiz R, Fayos B (2012) Organic carbon enrichment in sediments: effect of rainfall characteristics under different land uses in a Mediterranean area. *CATENA* 94:36–42. <https://doi.org/10.1016/j.catena.2011.02.005>
- Mikutta R, Kleber M, Torn MS, Jahn R (2006) Stabilization of soil organic matter: association with minerals or chemical recalcitrance? *Biogeochemistry* 77(1):25–56. <https://doi.org/10.1007/s10533-005-0712-6>

- Molnar I (2003) Cropping systems in Eastern Europe: past, present and future. *J Crop Prod* 9:623–647. https://doi.org/10.1300/J144v09n01_11
- Monreal CM, Janzen HH (1993) Soil organic carbon dynamics after 80 years of cropping a Dark Brown Chernozem. *Can J Soil Sci* 73:133–146. <https://doi.org/10.4141/cjss93-014>
- Nejgebauer V (1951) Vojvođanski černozeem njegova veza sa černozeemom istočne i jugoistočne Evrope i pravac njegove degradacije. *Matica srpska J Nat Sci I*
- Nešić, Lj., Pucarević, M., Sekulić, P., Belić, M., Vasin, J., Ćirić, V. (2008): Osnovna hemijska svojstva u zemljištima Srema. *Zbornik radova Instituta za ratarstvo i povrtarstvo. Novi Sad* 45:247–255
- Parton WJ, Schimel DS, Cole CV, Ojima DS (1987) Analysis of factors controlling soil organic levels of grasslands in the Great Plains. *Soil Sci Soc Am J* 51:1173–1179
- Paul EA, Kravchenko A, Grandy AS, Morris S (2015) The ecology of agricultural landscapes: long-term research on the path to sustainability. *Soil organic matter dynamics: Controls and management for sustainable ecosystem functioning. Oxford University Press, New York*, pp 104–134
- Plaza-Bonilla D, Álvaro-Fuentes J, Cantero-Martínez C (2014) Identifying soil organic carbon fractions sensitive to agricultural management practices. *Soil till Res* 139:19–22. <https://doi.org/10.1016/j.still.2014.01.006>
- Reeves DW (1997) The role of soil organic matter in maintaining soil quality in continuous cropping systems. *Soil till Res* 43:131–167. [https://doi.org/10.1016/S0167-1987\(97\)00038-X](https://doi.org/10.1016/S0167-1987(97)00038-X)
- Schimel JP, Schaeffer SM (2015) Microbial control over carbon cycling in soil. In: Nemergut DR, Shade A, Violle C (eds) *The causes and consequences of microbial community structure. Frontiers in microbiology*, pp 155–166
- Schmidt MW, Torn MS, Abiven S, Dittmar T, Guggenberger G, Janssens IA, Nannipieri P (2011) Persistence of soil organic matter as an ecosystem property. *Nature* 478:367–49. <http://doi.org/https://doi.org/10.1038/nature10386>
- Sekulić P, Ubavić M, Dozet D (1998) Effects of fertilizer application on chemical soil properties. In: *Proceedings of 2nd Balkan symposium on field crops, Novi Sad*, pp 303–309
- Sekulić P, Gavrić M, Hansman Š (2000) *Informacioni Sistem o Zemljištu. Ratar Povrt* 33:5–12
- Sekulić P, Hadžić V, Ubavić M, Maksimović L, Nešić L (2006) Karakterizacija i uređenje zemljišta za proizvodnju visoko vredne hrane od pšenice, kukuruza, soje, suncokreta, povrća i krompira. *Ratar Povrt* 42(2):133–148
- Sekulić P, Kurjački I, Vasin J, Šeremešić S (2007) Plodnost poljoprivrednih površina na privatnom sektoru u Vojvodini. *Ekon Poljop* 54(1):73–84
- Sekulić P, Ninkov J, Hristov N, Vasin J, Šeremešić S, Zeremski-Škorić T (2010) Sadržaj organske materije u zemljištima AP Vojvodine i mogućnost korišćenja žetvenih ostataka kao obnovljivog izvora energije. *Ratar Povrt* 47:591–598
- Sekulić P, Ninkov J, Zeremski-Škorić T, Vasin J, Milić S (2011) Monitoring kvaliteta zemljišta AP Vojvodine. In: *Proceedings of 1st symposium “Zemljište korišćenje i zaštita”, Novi Sad*, pp 70–76
- Šeremešić S, Milosev D, Djalovic I, Zeremski T, Ninkov J (2011) Management of soil organic carbon in maintaining soil productivity and yield stability of winter wheat. *Plant Soil Environ* 57:216–221
- Seremesic S, Milosev D, Sekulic P, Nestic L, Ciric V (2013) Total and hot-water extractable carbon relationship in Chernozem soil under different cropping systems and land use. *J Cent Europ Agri* 14(4):1479–1487. <https://doi.org/10.5513/jcea.v14i4.2346>
- Šeremešić S, Ćirić V, Milošev D, Vasin J, Djalovic I (2017) Changes in soil carbon stock under the wheat-based cropping systems at Vojvodina province of Serbia. *Arch Agron Soil Sci* 63:388–402. <https://doi.org/10.1080/03650340.2016.1218475>
- Šeremešić S, Ćirić V, Djalović I, Vasin J, Zeremski T, Siddique KHM, Farooq M (2020) Long-term winter wheat cropping influenced soil organic carbon pools in different aggregate fractions of Chernozem soil. *Arch Agron Soil Sci* 66(14):2055–2066. <https://doi.org/10.1080/03650340.2019.1711065>
- Šimon T (2008) The influence of long-term organic and mineral fertilization on soil organic matter. *Soil Water Res* 3:41–51
- Six J, Conant RT, Paul EA, Paustian K (2002) Stabilization mechanisms of soil organic matter: Implications for C-saturation of soils. *Plant Soil* 241(2):155–176. <https://doi.org/10.1023/A:1016125726789>
- Soon YK, Arshad MA, Haq A, Lupway N (2007) The influence of 12 years of tillage and crop rotation on total and labile organic carbon in a sandy loam soil. *Soil till Res* 85:38–46. <https://doi.org/10.1016/j.still.2006.10.009>
- Sparling G, Vojvodić-Vuković M, Schipper LA (1998) Hot-water-soluble C as a simple measure of labile soil organic matter: the relationship with microbial biomass C. *Soil Biol Biochem* 30:1469–1472
- Stamenov D, Đurić S, Hajnal JT, Šeremešić S (2016) Fertilization and crop rotation effects on the number of different groups of microorganisms. *Ratar Povrt* 53(3):96–100
- Stevenson FJ (1994) *Humus chemistry: genesis, composition, reactions*, 2nd edn. Wiley
- Tobiašova E, Debska B, Banach-Szott M (2013) Stability of organic matter of Haplic Chernozem and Haplic Luvisol of different ecosystems. *J Cent Eur Agric* 14:1558–1566. <https://doi.org/10.5513/JCEA01/14.4.1393>
- Van Wesemael B, Paustian K, Meersmans J, Goidts E, Barancikova G, Easter M (2010) Agricultural management explains historic changes in regional soil carbon stocks. *PNAS* 107:14926–14930. <https://doi.org/10.1073/pnas.1002592107>
- Vasin J, Sekulić P (2005) Plodnost Zemljišta u Vojvodini. *Ekon Poljopr* 52(4):495–502

- Vidojević D (ed) (2018) Report on soil state in the Republic of Serbia 2016–2017. Environmental Protection Agency, Ministry of Environmental Protection, pp 1–51
- Vidojević D, Manojlović M (2010) Procena sadržaja organske materije u zemljištima Srbije. Zbornik Naučnih Radova Instituta PKB Agroekonomik 16(1–2):231–244
- Vučić N (1987) Vodni, vazdušni i toplotni režim zemljišta. Vojvođanska akademija nauka i umetnosti, Novi Sad, pp 1–324
- Živković B, Nejgebauer V, Tanasijević Đ, Miljković N, Stojković L, Drezgić P (1972) Soils of Vojvodina. Institute for Field and Vegetable Crops Novi Sad, Novi Sad.
- WRB – IUSS Working Group (2006) World reference base for soil resources (2006) World soil resources reports 103. FAO, Rome



Changes in Key Physical Soil Properties of Post-pyrogenic Forest Ecosystems: a Case Study of Catastrophic Fires in Russian Sub-boreal Forest

Ekaterina Chebykina and Evgeny Abakumov

Abstract

In this chapter, the physical properties of soils were determined after forest fires in pine forests near the city of Togliatti (Russia) in 2010. The aim of the study was to assess (1) what part organic matter of pyrogenic origin played in the formation of the fire-affected clay fraction and (2) the degree of hydrophobicity of the soil under the influence of pyrogenic exposure. The soil parameters studied were the particle size distribution, solid-phase density, specific surface area, contact angle of soil wetting, soil organic matter content and air-dry moisture. Two methods of particle size distribution were compared: laser diffraction and classical sedimentation methods. The sedimentation method revealed a higher clay content due to underestimation of the density and an increase in black carbon components, rather than an actual increase in very fine earth particles. This method enabled the effect of the pseudo-fraction to be observed, when particles of organic matter, including components of black carbon, partially form a clay fraction that was not there previously. While the set of methods proposed has proven suitable to assess

changes in post-fire soils, there is a need to harmonise the methods of particle size distribution. The electrophysical profiling effectively identified the vertical heterogeneity of the soil layers. The contact angle of wetting showed an increase in hydrophobicity in the upper horizons of the soil after fires, especially crown fires. These expose soil to surface runoff and thus a higher risk of erosion. Further, deeper interdisciplinary research is needed to determine soil quality and degradation risks in fire-prone forest ecosystems.

Keywords

Biogenic-abiogenic interactions · Specific surface area of solid phase · Forest fires · Pyrogenic changes · Contact angle of wetting

31.1 Introduction

Fires are one of the main factors that destabilise natural forests, changing the structure and dynamics of forest communities (Certini 2005; Bogdanov et al. 2009; Licht and Smith 2020). Forest fire strongly alters the physicochemical and biological parameters of the soil; the degree of this alteration depends on the temperature developing at the soil surface (Garcia-Corona et al. 2004). As the temperature rises, heating increases, causing a decrease in the clay and silt content (Ketterings et al. 2000). In addition, if the

E. Chebykina (✉) · E. Abakumov
Department of Applied Ecology, Saint-Petersburg
State University, 16th line of Vasilievsky Island, 29,
Saint-Petersburg 199178, Russian Federation

temperature reaches a high enough level, the clay denatures and loses its charge, making it less dispersible (Reynard-Callanan et al. 2010). The impact of fires on forest vegetation and grassland differs significantly, as grassland is capable of rapid self-healing (Neary and Leonard 2020). In addition, ash from forest fires is a potential pollutant that can affect crops and vegetation hundreds of kilometres from the affected area, significantly decreasing plant productivity (Yue and Unger 2018) and resulting in a loss of plant biodiversity as the fire's high temperatures destroy most of the seed stocks stored in the forest floor (Neary and Leonard 2020). Another side effect of forest fires is the accumulation of polycyclic aromatic hydrocarbons (PAHs) in post-pyrogenic soils, the amount of which depends significantly on the intensity and frequency of forest fires (Piskareva 2019). One of the most significant externalities of forest fires is the huge contribution to greenhouse gas emissions (Ribeiro-Kumara et al. 2020; Neary and Leonard 2020). In addition, a wide range of wildlife, especially forest dwellers, have been severely affected by large-scale fires as they have lost the niches enabling them to live and eat (UN 2020). Today, natural fires (from lightning) make up about 7–8% of forest fires; that is, the occurrence of other fires is associated with human activity (Balch et al. 2017). Areas affected by fires are highly vulnerable to erosion due to the loss of protective vegetation cover, especially in areas affected by forest fires (Basso et al. 2019), where a small proportion of fires are responsible for much of the burned area (Roye et al. 2019). There is little information on how forest fires affect the physical characteristics of the soil.

Forest fires have both a direct impact (pyrolysis) and a huge indirect impact, as they lead to the degradation of natural ecosystems and a decrease in biological diversity. Changes to newly formed natural communities inevitably lead to a simplification of the floristic

composition and homogenisation of the vegetation cover, as well as to a decrease in the ecological capacity of landscapes, and the number of biotopes and plant biomass (Kogan and Panina 2010). Fires can affect soils through:

- the direct impact of high temperatures on the solid phase of the soil;
- the input of a large amount of ash from mineralised litter and other materials;
- changes in the structure and quality of soil organic matter;
- the replacement of indigenous plant communities.

All these factors greatly change the soil's physical and chemical properties, particle size distribution, edaphic conditions, air, water and hydrothermal regimes, and microbiological, biochemical and biological properties (Bogdanov et al. 2009; Kogan and Panina 2010; Zaidelman and Rydkin 2003; Zaidelman and Shvarov 2002).

Many researchers have studied the effect of post-pyrogenic changes on soil properties, regimes and functions in the boreal zone. Various studies are devoted to the pyrogenic transformation of the water regime, vegetation and forest landscapes in general (Bogdanov et al. 2009; Graber and Hadas 2009; Maksimova and Abakumov 2017; Zaidelman and Rydkin 2003; Zaidelman and Shvarov 2002). However, there are few studies on post-pyrogenic changes in soils in sub-boreal landscapes (in particular, island pine forests). The physical properties of the soil are one of the most important characteristics that affect many properties and regimes: water and heat regimes, absorbing capacity, nutrient transformation and soil fertility. Any quantitative soil characteristic usually begins with an assessment and characterisation of the particle size distribution (PSD) (Shein 2009). The main way in which fire negatively affects the soil's physical properties is due to the

combustion of organic matter (Garcia-Corona et al. 2004), which is controlled by the intensity and duration of the fire, as well as the type of soil and climatic conditions.

Post-fire ash characteristics significantly affect runoff and erosion, but the direction of fire-induced changes and transformations such as increases or decreases in potential runoff and erosion (e.g. Onda et al. 2008; Cerdà and Doerr 2008; Woods and Balfour 2010) need further investigation. Particular attention should be paid to changes in post-fire soil parameters in relation to the transformation of soil organic matter and changes in water regimes (Hou and Orth 2020). The role of pyrogenic organic matter from the point of view of its role in stabilising soil physical properties is largely unknown (Schiedung et al. 2020). This study was devoted to assessing (1) what part organic matter of pyrogenic origin played in the formation of the clay fraction affected by fires and (2) the degree of hydrophobicity of the soil under the influence of pyrogenic exposure. Studying the physical properties of pyrogenically altered soils will expand our understanding of the mechanisms of pyrogenic transformation in forest-steppe landscapes.

31.2 Materials and Methods

31.2.1 Site Description

A long period of abnormally hot weather occurred in Russia in June–August 2010 (Russian forests in the twenty-first century 2009). The forest fires were extremely fast and continuous due to very dry air and forest litter as well as windy weather. The fires completely burned all tiers of vegetation and occasionally (at night or with weak wind) turned into intense surface fires (Vorobiev et al. 2004).

Studies were conducted during 2010–2015 on the permanent monitoring sites in the Stavropol pine forest (Institute of Ecology of the Volga Basin, Togliatti, Samara Region). The site was located on the dune hills of the Kuibyshev Reservoir basin (53°29′43.80″ N; 49°20′56.44″) (Fig. 31.1). The object of the study was the post-pyrogenic and background soils of island pine forests that suffered from catastrophic forest fires in 2010. Three soil profiles were studied to compare the effect of different types of fires on the soils: (1) the site affected by a surface forest fire (end of July 2010), (2) crown forest fire (end

Fig. 31.1 Location of the site



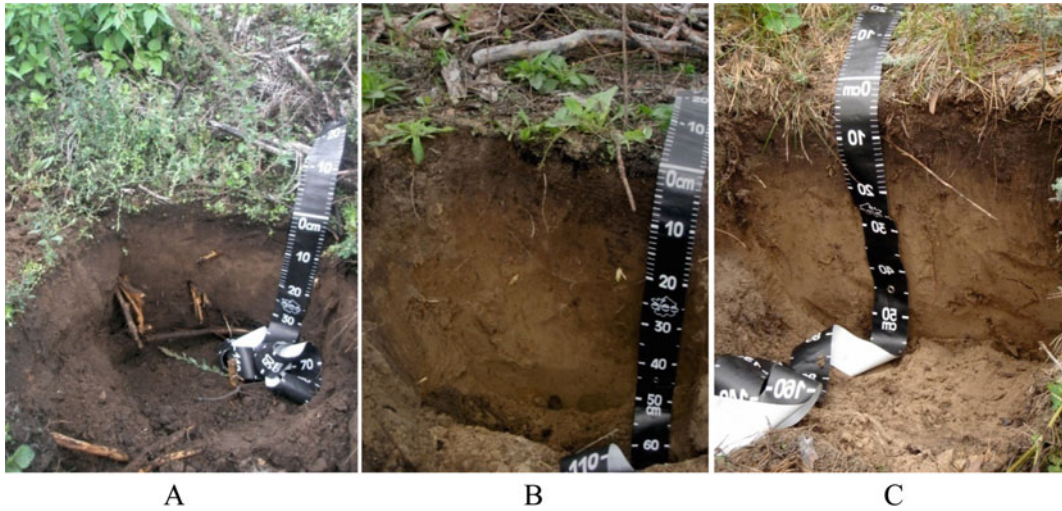


Fig. 31.2 Soils studied: surface fire-affected soil (a), crown fire-affected soil (b), control soil (c)

of July 2010) and (3) unaffected control site (mature forest) (Fig. 31.2). In total, 54 soil samples were selected horizontally at each soil profile, including the control site.

31.2.2 Field and Laboratory Analyses

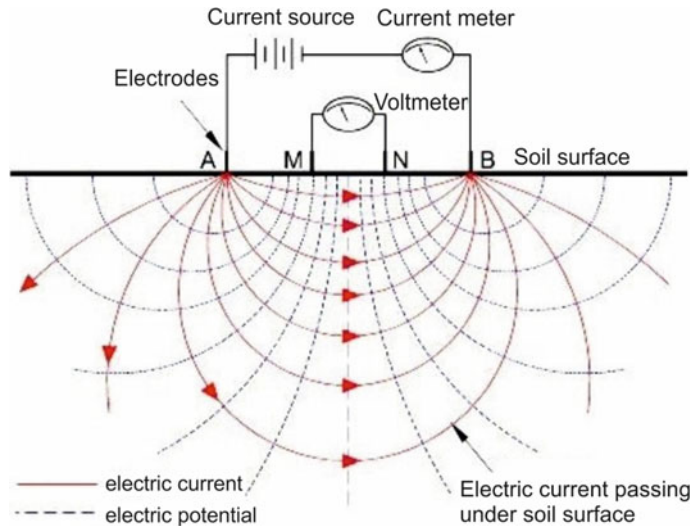
The characteristics which were determined were the particle size distribution (PSD), the density of the solid phase, the specific surface area, the contact angle of the soil wetting, the soil organic matter content and air-dry moisture. General soil characteristics included the determination of chemical and physical soils, especially soil moisture, parameters by standard techniques (Rastvorova et al. 1995; Vorobyeva 2006). The specific surface area (S) was calculated after determining the hygroscopic humidity (hh) using the equation: $S \text{ (m}^2 \text{ g}^{-1}\text{)} = 19.5 * \text{hh (\%)}$ (Rastvorova 1983). The density of the solid phase (ρ) was determined using a pycnometer and calculated as the ratio of the soil mass (m) to the volume of its compact non-porous skeleton V (Rastvorova 1983): $\rho_u = m/V$.

Fine soil particles, especially the silt fraction, are a very important characteristic of hydrophysical soil properties (Kulizhsky et al. 2010). The laser diffraction method is rapid and enables any output ranges to be selected. The

main idea of the laser diffraction method is based on the fact that particles of a certain size diffuse light with a countable angle. The diffraction angle is inversely proportional to the size of the particle, and the intensity of the diffracted beam for a certain angle is a measure of the number of particles in the path of an optical beam with a certain cross-sectional area. Many authors emphasise the benefits of using laser diffraction to estimate soil PSD, due to the speed and reproducibility of the analysis, the exceptionally wide range of size distributions, the small amount of samples required, the large number of possible categories and the digital results (e.g. Blochin and Kulizhsky 2009; Kulizhsky et al. 2010).

Classical pipette sedimentation and laser diffraction analysis often show large differences in output results (Fedotov et al. 2007; Kulizhsky et al. 2010; Shein 2009). In this chapter, the soil PSD was examined to identify the degree of polydispersity using two approaches: (1) a preliminary pyrophosphate peptisation of microaggregates (sedimentation) (Rastvorova 1983) and (2) a laser diffraction method. The second approach involved an SALD-2201 universal laser diffraction particle size analyser (Shimadzu, Japan) with a volumetric cuvette. The measuring range was $0.03 \mu\text{m}$ to 1 mm . A particle fraction of $1\text{--}0.25 \text{ mm}$ was collected mechanically, using an

Fig. 31.3 Conceptual scheme of vertical electrical sounding. M and N—receiver electrodes; A and B—transmitter electrodes



0.25 mm sieve followed by drying and weighing. The laser diffraction results were adjusted in accordance with the Kachinsky classification (Rastvorova 1983). The sedimentation method was carried out in several steps: from soil treatment with chemical reagents to eliminate soil adhesion (with sodium pyrophosphate), up to direct pipette sampling. The size and number of the elementary soil particles were defined depending on their sedimentation rate and calculated using the Stokes equation.

Soil moisture was determined by measuring the weight loss of moisture during soil air-drying.

The hydrophilic or hydrophobic properties are also characterised based on the contact angle of soil wetting. The contact angle of the soil wetting was determined using the DSA100 Drop Shape Analysis System (KRUSS, Germany) at the Department of Soil Physics and Reclamation (Lomonosov Moscow State University). The samples were prepared using the Bykova (2014b) method. The test liquid used was water, which was dropped onto the surface of the prepared samples in drops of 0.003 ml. The process from the moment the droplet attached to the surface and was absorbed was recorded on video. After that, an image that fixes the moment of full contact of the droplet with the soil surface was selected, followed by the baseline drawn at the boundary of the solid and liquid phases using the

software. Finally, the contact angle of the soil wetting was calculated.

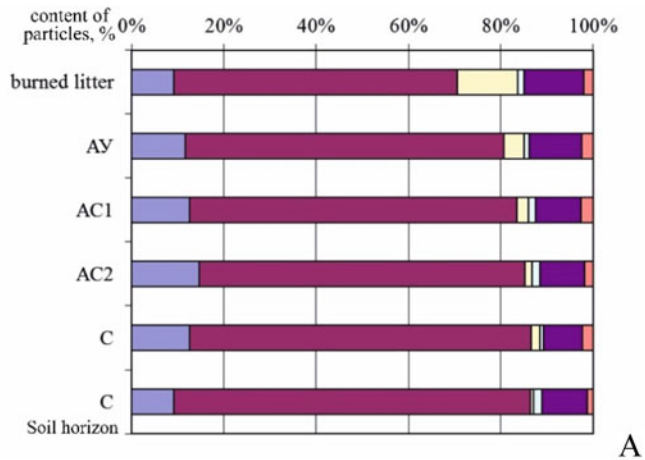
The apparent resistance of the soil was measured using a portable landmapper device, at a spacing of MN 10 (receiver electrodes M and N) and $AB/2$ (transmitter electrodes A and B): 10, 20, 30, 40, 50, 60, 70, 80, 90, 100, 150, 200 and 300 cm. This made it possible to establish the values of the soil's apparent electrical resistance at the corresponding depths (Fig. 31.3). The results of the field measurements were recalculated using the method proposed by Pozdnyakov (Pozdnyakov and Fedotov, 2006) in accordance with geometric constants for different depths and spacings of AB and MN electrodes (Abakumov and Tomashunas 2016). The results were further processed as a one-dimensional model (axes: resistance/depth) as well as ANOVA statistics.

31.3 Results and Discussion

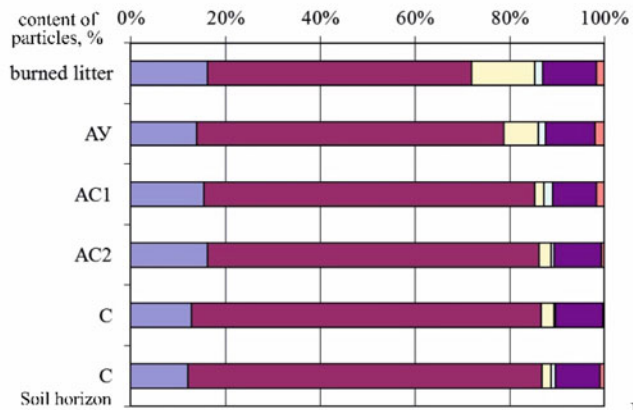
31.3.1 Particle Size Distribution

The post-pyrogenic soils which were studied were characterised by the domination of fine earth due to the sandy parent material (Fig. 31.4). Fine sand was the predominant fraction in all three sites (50–75% using the sedimentation method; 56–87% using the laser diffraction method). The amount of

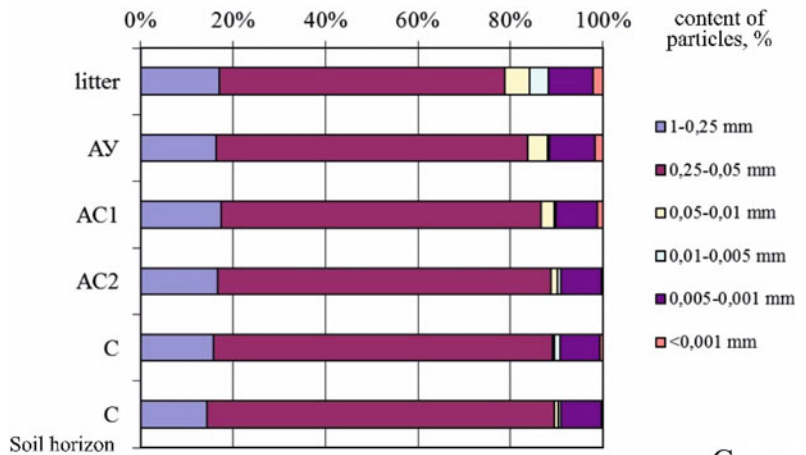
Fig. 31.4 Particle size distribution of the soils after a surface forest fire (a), after a crown fire (b) and in control soil (c)



A



B



C

particles <0.01 mm was 9–16% and 1.5–8% in the sedimentation and laser diffraction analyses, respectively. An increase in the number of fine particles was observed along the profile of all soils. This was due to the nature of the parent material—the alluvial Volga sands. A smaller content of coarse silt fraction (about 5% in the upper horizon) was observed at the control site compared to the post-fire soils. An analysis of the PSD showed that forest fires do not significantly affect the initial content of particles. The content of the silt + clay fraction in the soils affected by fires was slightly higher than in the control. Laser diffraction showed that surface fires change the distribution of particles in soils to a certain extent. A decrease in the sand fraction and an increase in the silt + clay fraction occurred under surface fire compared to crown fire and the control. However, crown fire does not have any effect. Small differences in the content of individual fractions were apparently due to the spatial variation of the sites studied. The PSD did not change for five years but, due to the linear soil erosion, a decrease in the content of coarse fractions in the upper horizons was observed. The PSD for different landscapes and geochemical positions showed that the clay fraction tends to accumulate, and is smallest in the slopes.

The differences in the content of fractions obtained with the sedimentation and laser diffraction methods were significant (Fig. 31.5). In the laser diffraction method, the content of coarse silt (0.005–0.001 mm) was 1.3–12.3 times higher (along the profile) compared to the sedimentation method and the medium silt fraction (0.05–0.01 mm) was 1.2–7.2 times higher. At the same time, the amount of fine dust was underestimated by 1.4–6.3 times. The fraction of coarse and medium sand (1–0.25 mm) was 1.04–1.5 times lower. The observed irregular discrepancy in the content of the fine sand fraction (0.25–0.05 mm) measured using the two methods was most likely due to the technical limitations of the measuring device.

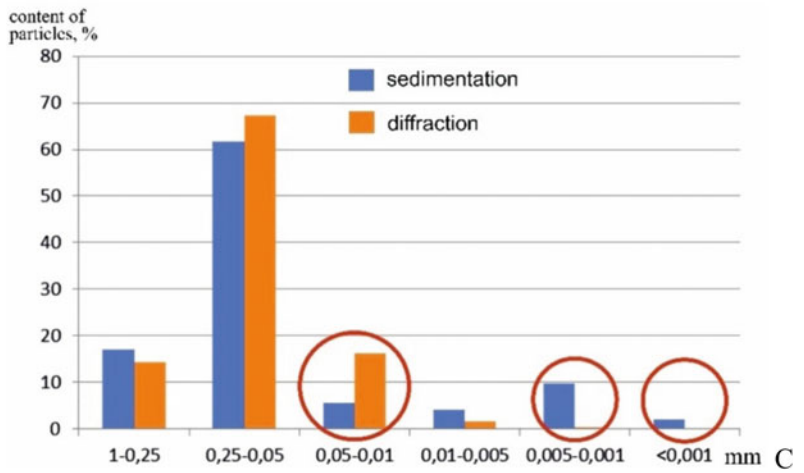
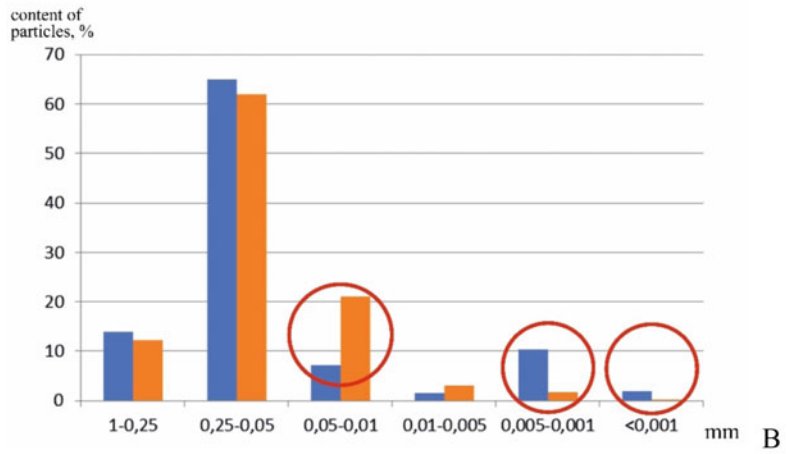
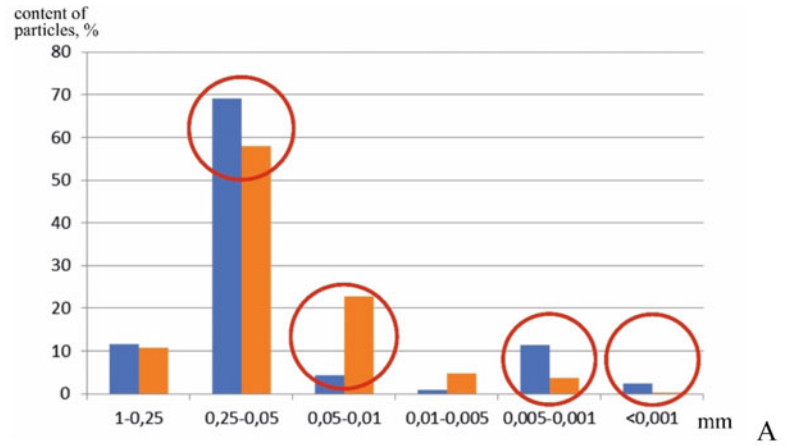
The clay fraction (<0.001 mm) had the greatest variation. The clay content was underestimated by 1.2–26 times, and the silt + clay (<0.01 mm) by 1.27–8 times in the laser diffraction compared to the sedimentation.

Despite significant differences in the content of the clay, coarse and medium silt fractions, the silt + clay fraction did not show significant differences between the results obtained by sedimentation and diffraction. The sedimentation of clay from the surface fire site was significantly different from the control and crown fire sites ($F = 4.46$; $p = 0.03$); laser diffraction of the silt + clay showed a statistically significant trend of differences ($F = 3.07$; $p = 0.07$) between the control and post-fire soils. Post-hoc testing showed that the sedimentation of clay in the control soil differed significantly from the surface ($p = 0.01$) and crown ($p = 0.02$) fire sites. The sedimentation of the silt + clay fraction of the control soil only differed significantly from the surface fire site ($p = 0.05$). Similar regularities were obtained for the laser diffraction method ($p = 0.02$). The soils which were studied were classified as sandy-loam soils using the sedimentation method and as cohesive and loose sands using laser diffraction methods. The differences between the two methods can be attributed to the differences in particle densities, the shapes of the particle surfaces and the nature of their heterogeneity.

When analysing particle sizes using the sedimentation method and the Stokes equation, the following parameters are usually taken into account: the shape of spherical particles, the absence of turbulent processes in water, interaction between particles and similar densities (Blochin and Kulizhsky 2009; Fedotov et al. 2007; Kulizhsky et al. 2010). However, these assumptions cause systematic errors. Therefore, the sedimentation method can be used in PSD analysis only if the difference in the density of precipitating particles is constant or slightly differs from a constant value. In fact, this can be applied to reference soils. The studied soils contain a significant amount of black carbon of various sizes. Due to the low sedimentation rate, they make up smaller fractions according to the sedimentation analysis. Therefore, the underestimation of particle density during sedimentation is the reason for these differences.

An increase in the density of the solid phase along the soil profile (from 2.46 to 2.70 g cm^{-3}) is

Fig. 31.5 Differences in soil fractions after the surface fire (a), after the crown fire (b), in control (c)



a common case for all soils studied. Burnout of the upper layer of the litter leads to a decrease in its density and denudation of the soil surface. This is probably due to a change in the vegetation cover of the soil. During forest fires, it is mainly the upper and most unconsolidated layers of the litter which burn out (Atkin and Atkina 1985), while denser components such as coal and ash particles enter the soil (Bezkorovaynaya et al. 2005; Tarasov et al. 2008). This is supported by a significant increase (from 20 to 45%) in ash content in the soil upper layer. Due to the destruction of forest litter and decrease in the total projective cover (GPC) of the forest after fire, favourable conditions for grass vegetation emerge. The root mass of various grasses contributed to the consolidation of the upper soil layer.

In laser diffraction analysis, it is also assumed that all particles have a spherical shape. This leads to averaging of the particle diameter when the laser processes different angles. As a result, soil particles with a flat shape will be assumed to be larger than spherical particles of the same volume. Since clay particles are often flat, the laser perceives them as larger.

Though each of the two methods has certain methodological disadvantages, it seems that the content of clay, fine and medium silt determined by laser diffraction is more reliable and closer to the true state of PSD in the soil (Kulizhsky et al. 2010). However, the results were seen to agree well when coarse and medium sand were examined using the two methods, although slightly higher values were obtained with the sedimentation method. Similar results have been reported previously (Stefano et al. 2010).

The low content of clay and silt + clay fractions obtained by laser diffraction can be associated with fine organic matter. Soil particles are covered with a firm membrane of organo-mineral colloidal structures. They can cause the elementary soil particles to adhere and form larger aggregates, which leads to a decrease in density and an increase in size. Consequently, the sedimentation rate decreases and determining the true sizes of elementary particles become complicated (Kulizhsky et al. 2010).

The interval of sedimentation of the OM particles with a low specific weight is comparable to the sedimentation of particles of fine soil minerals. Therefore, small OM particles are referred to as “pseudo-fractions” of PSD (Muhametova et al. 2013). There was a negative correlation between the light fraction of SOM and clay and silt + clay fraction content (correlation index = -0.84) in laser diffraction. The discussion above suggests that the determination of the size and number of elementary soil particles is complicated due to the limitations in both methods and due to the interference of OM particles.

31.3.2 Soil Moisture

After forest fires, the content of air-dry soil moisture in the upper horizons of the post-pyrogenic soils decreased from $5.92 \pm 2.27\%$ (litter) to 2%. The differences were statistically significant (after a surface fire $2.85 \pm 0.79\%$, and after a crown fire $2.37 \pm 0.36\%$). This can be explained by the higher speed and combustion temperature in the case of the crown fire (900–1200 °C, compared with up to 900 °C for the surface fire) (Melekhov 1980). This leads water to evaporate from the exposed surface of the soil in large quantities. However, the litter, as an additional buffer, protects the soil from high temperatures, so not all moisture evaporates from the upper horizons. In addition, the forest litter with a high moisture content does not burn completely, reducing the thermal effect on the soil.

In 2014, after a surface fire, a twofold increase in dry air moisture was observed, approaching the humidity in the control site over the entire soil profile. In the case of the crown fire, an increase in this parameter was observed only in the upper part of the profile, but it was not as significant as in the case of the surface fire. This increase in air-dry moisture content under the surface fire was due to the formation of new litter containing moisture. Thus, the overall litter becomes more hydrophilic, making it able to absorb a greater amount of moisture.

The moisture content in air-dry soil was closely related to the physical clay in all three sites studied, but it was completely unrelated to the content of clay fraction. This indicates that the fraction <0.001 mm was less involved in soil formation than the fractions of medium and fine dust.

Forest fires are known to alter the hydrological and basic physical properties of soils. As a rule, they depend on the surface properties of the solid phase of the soil, and in particular hydrophilic or hydrophobic properties.

31.3.3 Contact Angle of Soil Wetting and Specific Surface Area of Solid Phase

The contact angle of soil wetting is the angle between the solid surface and the tangent drawn from the contact point of the three contact phases (solid, liquid and gaseous) (Bykova 2014a). The contact angle of soil wetting depends on the free surface energy of the solid phase and the surface tension of the soil solution. It varies from 0° to

90° for hydrophilic soil, and is larger for hydrophobic soil. Water forms spherical droplets on the surfaces of the minerals in hydrophobic soil. Soils where the particles are completely covered with a hydrophobic membrane repel water (Bykova 2014a). All natural soils tend to be moistened to a level of strong adhesion between the water and soil particles. However, in some cases, the soil has a wetting from 0° to 140° (Bachmann et al. 2003). The contact angle of soil wetting was determined in 2010 and 2013 (in 12 replications) (Table 31.1). It ranged from 65° to 112°. A tendency to increase in hydrophobicity along the soil profile was observed for all sites. Hydrophilic properties were typical of the underlying layer of the control site due to the presence of hydrophobic litter consisting of organic residues. Due to fires, a part of the organic matter burned out, and the contact angle of soil wetting decreased in the ash. This may also be due to the composition of the pyrogenic organic matter (black carbon), primarily due to its amphiphilic properties. The above discussion implies that if the contact angle of soil wetting is not taken into consideration, this may lead to the

Table 31.1 Contact angle of soil wetting (°) and specific surface area of solid phase

Sample, depth	Specific surface area of solid phase (m ² g ⁻¹)	Contact angle of soil wetting (°)
2010		
Surface fire Burned litter, 0–5 cm	113.8	95.6
Surface fire AY 5–14 cm	61.9	98.7
Crown fire Burned litter, 0–5 cm	104.2	101.9
Crown fire AY, 5–10 cm	86.5	104.0
Control Litter, 0–5 cm	351.8	112.0
Control AY, 5–8 cm	72.6	76.2
2013		
Surface fire Burned litter, 0–3 cm	111.6	68.3
Surface fire AY, 3–12 cm	82.3	81.9
Crown fire Burned litter, 0–3 cm	119.5	72.6
Crown fire AY, 3–10 cm	94.2	89.9

incorrect conclusion that fires cause hydrophobisation of the solid phase of the soil.

The surface of the soil solid phase ranged from 62 to 352 m²g⁻¹ (Table 31.1). A tendency toward a decrease in the specific surface of the solid phase was observed in the post-fire soils, which showed increased hydrophobicity. The specific surface area of the upper horizons of post-pyrogenic soils was 104/113 m²g⁻¹, and for the control soil it was 352 m²g⁻¹ (Table 31.1). In a laboratory-controlled heat experiment, Garcia-Corona et al. (2004) found that hydraulic conductivity decreased with increasing temperature up to 220 °C and then remained at very low levels at higher temperatures. In their study, the lowest hydraulic conductivity was correlated with increased water repellence in the 170–220 °C range. They suggest that because the hydrophobicity disappears at higher temperatures, the low hydraulic conductivity can be ascribed to the strong disaggregation of the soils above 220 °C due to the loss of organic matter through burning.

Soils affected by the crown fires were more hydrophobic than those affected by surface fires. This was due to the higher intensity of crown fire. In the control soils, an increase in hydrophilic properties was observed after 4 years. Garcia-Corona et al. (2004) found that heating the soil to 170 and 220 °C did not lead to significant changes in the distribution of aggregates by size or total porosity, but increased the stability of water aggregates and pore volume 0.2–30 µm.

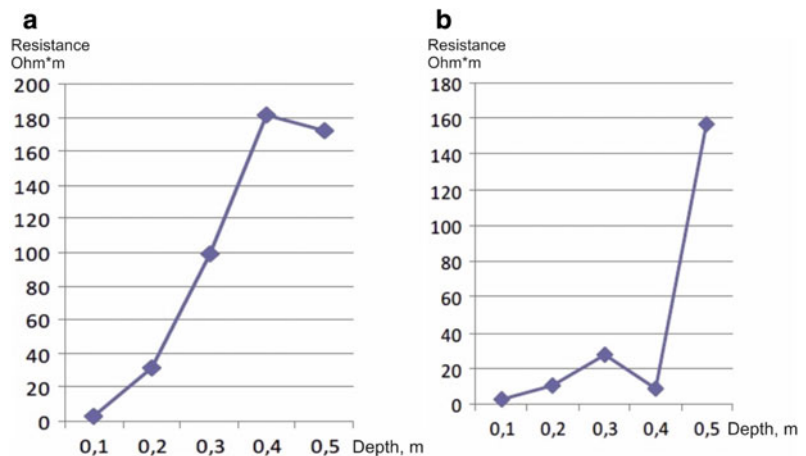
However, at temperatures of 380 and 460 °C, all the parameters studied underwent more dramatic changes. In their study, although hydrophobicity disappeared at higher temperatures, the very low hydraulic conductivity remained due to the decreased infiltration capacity, which could trigger soil erosion problems in the post-pyrogenic soils. Reduced infiltration capacity may cause the destruction of soil aggregates and compaction (Keller et al. 2019; Negev et al. 2020). In addition, compacted soil restricts root growth and development (Tebebu et al. 2020).

The contact angle of soil wetting was inversely proportional to the specific surface area of the solid phase. Therefore, the smaller the particles, the more hydrophilic they are. The correlation of the specific surface area with the contact angle of wetting showed a clear negative dependence.

31.3.4 Electro-Physical Profiling

The apparent resistance of soil layers studied using the electro-physical profiling method determined the degree of vertical heterogeneity of post-pyrogenic soils (Fig. 31.6). There was a decrease in the apparent soil resistance for the post-pyrogenic scenario compared to the control. This was due to the accumulation of black carbon. In addition, during the surface fire, a uniform increase in Ra with depth was observed, in

Fig. 31.6 Apparent soil resistance after the surface fire (a) and crown fire (b)



contrast to the crown fire. Vertical changes in the values of apparent soil resistance showed an increase in Ra content with depth, the highest content being in the parent rock layer. The application of the method of electro-physical profiling, first applied to post-pyrogenic soils, allowed us to identify the vertical heterogeneity of the layers for selected soil horizons more efficiently and with much less effort.

31.4 Conclusion

1. A comparative analysis of the two methods showed that, firstly, the soil PSD changes slightly due to fires, and secondly, there are differences in the results of the two methods of PSD analysis. The laser diffraction method slightly overestimated the size of flat-shaped particles as their diameter was averaged, while the sedimentation method underestimated some of the sizes due to an underestimation of the density and influence of soil organic matter. The differences between the two methods can be attributed to fine soil particles, which are covered with a firm membrane of organo-mineral colloids. These particles are “pseudo-fractions” of PSD or light fractions of SOM. In addition, the contact angle of soil wetting first showed hydrophobisation of the solid soil phase, then, after a few years, an increase in hydrophilic properties. Studying post-fire effects is essential to understand the quality and performance of soils in forest ecosystems
2. The physical pyrogenic effects measured revealed significant, irreversible changes in the water and physical properties of the surface soil horizons, a decrease in their water capacity, and an increase in hydrophobicity. The soil becomes more prone to surface runoff. This means a higher risk of erosion.
3. Methodologically, the set of measurement methods that were developed and applied were suitable. The harmonisation of particle size distribution measurement methods requires more attention in further studies.

4. Overall, further interdisciplinary studies are required to better understand the complex interactions of the factors determining soil quality and the risks of degradation in forest ecosystems prone to fires.

Acknowledgements This work was supported by the grant of the Russian Scientific Foundation, project 17-16-01030. The authors would like to express their gratitude to the following people for organising and implementing the research: Prof. Rosenberg G.S., Prof. Saksonov S.V., Dr. Senator S.A. and Prof. Shein E.V.

References

- Abakumov E, Tomashunas V (2016) Electric resistivity of soils and upper permafrost layer of the Gydan peninsula. *Polarforschung* 86 (1):27–34. https://epic.awi.de/id/eprint/42692/1/Polarforschung_86-1_27-34.pdf
- Atkin AS, Atkina LI (1985) Stocks of soil vegetation combustible materials in pine forests. Forest fires and their consequences: collection of works. ILID, Krasnoyarsk, pp 92–101 (Аткин А.С., Аткина Л.И. Запасы напочвенных горючих материалов в сосняках. Лесные пожары и их последствия. Красноярск, ИЛИД СО АН СССР)
- Bachmann J, Woche SK, Goebel WO, Kirkcham MB, Horton R (2003) Extended methodology for determining wetting properties of porous media. *Water Resour Res* 39(12). <https://doi.org/10.1029/2003WR002143>
- Balch JK, Bradley BA, Abatzoglou JT, Nagy RC, Fusco EJ, Mahood AL (2017) Human-started wildfires expand the fire niche across the United States. *Proc Natl Acad Sci USA* 114(11):2946–2951. <https://doi.org/10.1073/pnas.1617394114>
- Basso M, Vieira DCS, Ramos TB, Mateus M (2019) Assessing the adequacy of SWAT model to simulate postfire effects on the watershed hydrological regime and water quality. *Land Degrad Develop* 31(5):619–631. <https://doi.org/10.1002/ldr.3476>
- Bezkorovaynaya IN, Ivanova GA, Tarasov PA, Bogorodskaya AV (2005) Pyrogenic soil transformation in pine forests of the middle taiga in Krasnoyarsk Region. *Sib Ecol J* 1:143–152 (Безкоровойная ИН, Иванова ГА, Тарасов ПА и др. Пирогенная трансформация почв сосняков средней тайги Красноярского края. Сибирский экологический журнал)
- Bloch AN, Kulizhsky SP (2009) Assessment of laser diffractometry method application in particle size distribution determination. Tomsk State University. *Biology* 1:37–43 (Блохин А.Н., Кулижский С.П.)

- Оценка применения метода лазерной дифрактометрии в определении гранулометрического состава почв. Вестник Томского государственного университета. Биология № 1. С. 37–43)
- Bogdanov VV, Prokushkin AS, Prokushkin SG (2009) Surface fires' influence on the soil organic matter mobility in larch forests of a cryolithic zone of Middle Siberia. *KrasGAU* 2:88–93 (Богданов В.В., Прокушкин А.С., Прокушкин С.Г. Влияние поверхностных пожаров на подвижность органического вещества почвы в лиственничниках криолитозоны Средней Сибири. *КрасГАУ* 2: 88–93)
- Vykova GS (2014a) Contact angle of solid phase surface wetting of typical chernozems. *Mater Rus Soil Stud* 8 (35):125–130 (Быкова Г.С. Краевой угол смачивания поверхности твердой фазой черноземов типичных. *Материалы по изучению русских почв* 8 (35): 125–130)
- Vykova GS (2014b) Contact angle of soil wetting of main morphones and morphemes of the texturally differentiated sod podzolic soil. *Proc Int Sci Conf XVII Docuchaev's conference for youth scientists "New milestones in soil science development: modern technologies as a cognition means"*, 3–6 March 2014, St. Petersburg, pp 31–32 (Быкова Г.С. Краевой угол смачивания основных морфонов и морфем текстурно-дифференцированной дерново-подзолистой почвы. XVII Докучаевская конференция для молодых ученых «Новые вехи в развитии почвоведения: современные технологии как средство познания», 3–6 марта 2014 г., Санкт-Петербург, 31–32). <http://www.dokuchaevskie.ru/wp-content/uploads/2018/04/MDH2014-11.pdf>. Accessed 7 Mar 2021
- Cerdà A, Doerr SH (2008) The effect of ash and needle cover on surface runoff and erosion in the immediate post-fire period. *CATENA* 74:256–263. <https://doi.org/10.1016/j.catena.2008.03.010>
- Certini G (2005) Effects of fire on properties of forest soils: a review. *Oecologia* 143:1–10. <https://doi.org/10.1007/s00442-004-1788-8>
- Fedotov GN, Shein EV, Putlyayev VI, Arkhangel'skaya TA, Eliseev AV, MilanovskyEYu (2007) Physical and chemical bases of differences between sedimentometry and laser diffractometry methods of particle size distribution determination. *Eurasian Soil Sci* 3:310–317. eLIBRARY ID: 13550727. <https://doi.org/10.1134/S1064229307030064>
- Garcia-Corona R, Benito E, de Blas E, Varela ME (2004) Effect of heating on some soil physical properties related to its hydrological behaviour in two north-western Spanish soils. *Int J Wildland Fire* 13:195–199
- Graber ER, Hadas E (2009) Potential energy generation and carbon savings from waste biomass pyrolysis in Israel. *Annu Environ Sci* 3:207–216
- Hou X, Orth R (2020) Observational evidence of wildfire-promoting soil moisture anomalies. *Sci Rep* 10:11008. <https://doi.org/10.1038/s41598-020-67530-4>
- Keller T, Sandin M, Colombi T, Horn R, Or D (2019) Historical increase in agricultural machinery weights enhanced soil stress levels and adversely affected soil functioning. *Soil Tillage Res* 194:104293. <https://doi.org/10.1016/j.still.2019.104293>
- Ketterings QM, Bigham JM, Laperche V (2000) Changes in soil mineralogy and texture caused by slash-and-burn fires in Sumatra, Indonesia. *SSSAJ* 64:1108–1117. <https://doi.org/10.2136/sssaj2000.6431108x>
- Kogan RM, Panina OYu (2010) Influence of surface forest fires on soils of deciduous forests (on the example of the Jewish Autonomous Region). *Reg Probl* 13(1):67–70 (Коган Р.М., Панина О.Ю. Исследование влияния поверхностных лесных пожаров на почвы широколиственных лесов (на примере Еврейской автономной области). *Региональные проблемы* 13 (1): 67–70). http://икарп.рф/reg_problems/rp-13-1-2010/Коган,%20Панина.pdf. Accessed 7 Mar 2021
- Kulizhsky SP, Koronatova NG, ArtyumukSYu, Sokolov DA, Novokreshchennykh TA (2010) Comparison of sedimentometry and laser diffractometry methods when soils particle size distribution determination of natural and technogenic landscapes. *Tomsk State University. Biology* 4(12):21–31 (Кулижский С.П., Коронатова Н.Г., и др. Сравнение методов седиментометрии и лазерной дифрактометрии при определении гранулометрического состава почв естественных и техногенных ландшафтов. *Томский государственный университет, Биология* 4 (12): 21–31). <https://www.elibrary.ru/item.asp?id=16031565>. Accessed 7 Mar 2021
- Licht J, Smith NG (2020) Pyrogenic carbon increases pitch pine seedling growth, soil moisture retention, and photosynthetic intrinsic water use efficiency in the field. *Front for Glob Chang* 3:31. <https://doi.org/10.3389/fgc.2020.00031>
- Maksimova E, Abakumov E (2017) Micromorphological characteristics of sandy forest soils recently impacted by wildfires in Russia. *Solid Earth* 8:553–560. <https://doi.org/10.5194/se-8-553-2017>
- Melekhov IS (1980) *Forest science. Forest industry, Moscow, 406 pp* (Мелехов И.С. *Лесоведение. Москва: Лесная промышленность, 406 с.*)
- Muhametova NV, Abakumov EV, Rumin AG (2013) Particle size distribution of Antarctic soils according to laser diffraction and sedimentation methods. *Agrophys* 3 (11):1–6 (Мухаметова Н.В., Абакумов Е.В., Рюмин А.Г. Гранулометрический состав почв Антарктики по данным лазерной дифракции и седиментации. *Агрофизика* 3 (11): 1–6). http://www.agrophys.ru/Media/Default/Page/Agrophys_magazine/11%202013/Muhametova_13.pdf. Accessed 7 Mar 2021
- Nearly DG, Leonard JM (2020) Effects of fire on grassland soils and water: a review, grasses and grassland aspects. *Valentin Missiakô Kindomihou. IntechOpen*. <https://doi.org/10.5772/intechopen.90747>. <https://www.intechopen.com/books/grasses-and-grassland-aspects/effects-of-fire-on-grassland-soils-and-water-a-review>. Accessed 7 Mar 2021
- Negev I, Shechter T, Shtrasler L, Rozenbach H, Livne A (2020) The effect of soil tillage equipment on the

- recharge capacity of infiltration ponds. *Water* 12:541. <https://doi.org/10.3390/w12020541>
- Onda Y, Dietrich WE, Booker F (2008) Evolution of overland flow after a severe forest fire, Point Reyes, California. *CATENA* 72:13–20. <https://doi.org/10.1016/j.catena.2007.02.003>
- Piskareva VM (2019) Postpyrogenic soils of the national park “Land of the Leopard” and the Reserve “Cedar fall” In: Proceedings of XXII Dokuchaev Youth Readings “Soil as a System Functional Communications in Nature”, St. Petersburg, 25 February–2 March, Russia (Пискарева В. М. Постпирогенные почвы национального парка «Земля леопарда» и заповедника «Кедровая опад») В: Материалы XXII Докучаевских молодежных чтений «Почва как система функциональных коммуникаций в природе», Санкт-Петербург, 25 февраля–2 марта, Россия)
- Pozdnyakov AI, Fedotov GN (2006) Electrophysical methods of soil field studies. *Melior Water Manag* 4:50–52 (Поздняков А.И., Федотов Г.Н. Электрофизические методы полевых исследований почв. Мелиорация и водное хозяйство 4: 50–52)
- Rastvorova OG (1983) Soil physics. Practical guidance. Publishing House of the Leningrad University, Leningrad, p 196 (Растворова О.Г. Физика почвы. Практическое руководство. Ленинград: Изд-во Ленинградского университета, 196.)
- Rastvorova OG, Andreev DP, Gagarina EI (1995) Chemical analysis of soils. Education guidance. Publishing house of St. Petersburg State University, St. Petersburg, 263 pp (Растворова О.Г., Андреев Д.П., Гагарина Е.И. Химический анализ почв. Руководство по образованию. Санкт-Петербург: Изд-во СПбГУ, 263 с.). <http://почвовед.рф/wp-content/uploads/2017/04/0784-Растворова-О.Г.-и-др.-1995.pdf>. Accessed 7 Mar 2021
- Reynard-Callanan JR, Pope G, Gorring ML, Feng H (2010) Effects of high-intensity forest fires on soil clay mineralogy. *Phys Geogr* 31(5):407–422. <https://doi.org/10.2747/0272-3646.31.5.407>
- Ribeiro-Kumara C, Pumpanen J, Heinonsalo J et al (2020) Long-term effects of forest fires on soil greenhouse gas emissions and extracellular enzyme activities in hemiboreal forest. *Sci Total Environ* 718:135291. <https://doi.org/10.1016/j.scitotenv.2019.135291>
- Roye D, Tedim F, Martin-Vide J et al (2019) Wildfire burnt area patterns and trends in Western Mediterranean Europe via the application of a concentration index. *Land Degrad Develop* 31(3):311–324. <https://doi.org/10.1002/ldr.3450>
- Russian forests in the XXI century: materials of the second international scientific and practical Internet conference, Nov 2009, St. Petersburg State Forestry Academy of S.M. Kirov, St. Petersburg. 249 pp
- Schiedung M, Belle S-L, Sigmund G, Kalbitz K, Abiven S (2020) Vertical mobility of pyrogenic organic matter in soil: a column experiment. *Biogeosciences EGU*. <https://doi.org/10.5194/bg-2020-276>
- Shein EV (2009) Particle size distribution of soils: problems of research methods, results interpretation and classifications. *Eurasian Soil Sci* 3:309–317. <https://doi.org/10.1134/S1064229309030053>
- Stefano CDi, Ferro V, Mirabile S (2010) Comparison between grain-size analyses using laser diffraction and sedimentation methods. *BiosystEng* 106:205–215. <https://doi.org/10.1016/j.biosystemseng.2010.03.013>
- Tarasov PA, Ivanov VA, Ivanova GA (2008) Features of the temperature soil regime in pine forests of the middle taiga after surface fires. *Conifers of the boreal area XXV(3–4):300–304* (Тарасов П.А., Иванов В. А., Иванова Г.А. Особенности температурного режима почвы в сосняках средней тайги после наземных пожаров. Хвойные породы бореальной зоны XXV (3–4), С. 300–304.)
- Tebebu TY, Bayabil HK, Steenhuis TS (2020) Can degraded soils be improved by ripping through the hardpan and liming? A field experiment in the Ethiopian Highlands. *Land Degrad Develop*. <https://doi.org/10.1002/ldr.3588>
- UN Environment Programme (2020) <https://www.unenvironment.org/news-and-stories/story/ten-impacts-australian-bushfires>. Accessed 7 Mar 2021
- Vorobiev YuL, Akimov VA, Sokolov YuI (2004) Forest fires in Russia: status and problems, Ministry of Emergency Situations of Russia. DEKS-PRESS, Moscow, 312 pp (Воробьев Ю.Л., Акимов В.А., Соколов Ю.И. Лесные пожары в России: состояние и проблемы, МЧС России. Москва: ДЭКСПРЕСС, 312 с.)
- Vorobyeva LA (2006) Theory and practice of chemical soil analysis. GEOS, Moscow, 400 pp (Воробьева Л. А. Теория и практика химического анализа почв. Москва: ГЕОС, 400 с.)
- Woods SW, Balfour VN (2010) The effects of soil texture and ash thickness on the post-fire hydrological response from ash-covered soils. *J Hydrol* 393:274–286. <https://doi.org/10.1016/j.jhydrol.2010.08.025>
- Yue X, Unger N (2018) Fire air pollution reduces global terrestrial productivity. *Nat Commun* 9(1). <https://doi.org/10.1038/s41467-018-07921-4>
- Zaidelman FR, RydkiYuI (2003) Soil of high plains in forest zone—genesis, hydrology, land reclamation and use. *Pochvovedenie* 3:261–274 (Зайдельман Ф.Р., Рыдкин Ю.И. Почвы ополей лесной зоны генезис, гидрология, мелиорация и использование. Почвоведение, 2003. № 3. С. 261–274.)
- Zaidelman FR, Shvarov AP (2002) Pyrogenic and hydrothermal degradation of peat soils, their agroecology, sand cultures of farming, reclamation. Publishing House of Moscow State University, Moscow, 168 pp (Зайдельман Ф.Р., Шваров А.П. Пирогенная и гидротермальная деградация торфяных почв, их агроэкология, песчаные культуры земледелия, мелиорация. Москва: МГУ, 168 с.)



Remote Sensing Sensors and Recent Techniques in Desertification and Land Degradation Mapping—A Review

32

Subramanian Dharumarajan, S. Veeramani,
Amar Suputhra, Manish Parmar,
B. Kalaiselvi, Manickam Lalitha, R. Vasundhara,
Rajendra Hegde, and A. S. Rajawat

Abstract

Land degradation is a serious environmental stress, which is identified and analysed through advanced remote sensing technique at a global level. Vegetal degradation, soil erosion, salinity and alkalinity, deforestation, changes in land cover are a few factors, which raise the severity of desertification and land degradation. The changes caused by these factors lower the land and food production and eventually leads to environmental and socio-economic sustainability. Periodical monitoring and observation of the factors, which are the root causes for desertification/land degradation can be evaluated through remote sensing and modelling techniques. The present chapter aims to review the various remote sensing sensors and the recent techniques in mapping desertification and land degradation processes. Remote sensing and GIS techniques serve as an aid to assess and monitor various land degradation processes, and to compare trends across spatial and temporal scales. In the

future, the convergence of high-resolution data products with modern classification and modelling techniques could be explored more broadly to assess and obtain more detailed information on monitoring and modelling desertification and land degradation.

Keywords

Desertification · Land degradation · Sensors · Remote sensing · Recent techniques

32.1 Introduction

Land degradation is the process of deterioration of land quality, vegetation, and water resources, due to excessive or inappropriate exploitation (Environmental Management Agency 2015; UNCCD and FAO 2020; Borrelli et al. 2020). A large part of the drylands is increasingly losing their soil health and productivity that eventually leads to desertification. According to the United Nations Convention to Combat Desertification (UNCCD), desertification is the loss of land in arid, semi-arid, and dry sub-humid environments caused mostly by human activities and environmental fluctuations. Desertification and land degradation have been identified as important risks to the global environment, with significant consequences for human health and community development. Rapid economic development and

S. Dharumarajan (✉) · S. Veeramani · A. Suputhra ·
B. Kalaiselvi · M. Lalitha · R. Vasundhara · R.
Hegde
ICAR-National Bureau of Soil Survey and Land Use
Planning, Hebbal, Bangalore 560024, India

M. Parmar · A. S. Rajawat
Space Application Centre, ISRO, Ahmadabad, India

growing population are the potential accelerators of land degradation in developing countries due to ever-increasing pressure on land use systems (Runnström 2000; UNCCD 2019; Lyu et al. 2020). The UNCCD anticipates that desertification will displace around 50 million people over the next 10 years. Desertification has also important implications in climate change (Dharumarajan et al. 2019) as it may lead to increased CO₂ emissions to the atmosphere. Mapping the features of desertification and land degradation over large areas can effectively be assessed using Earth Observation (EO) data's and techniques (Symeonakis and Higginbottom 2014; Hurtt et al. 2020). Monitoring and assessing the land degradation by interpretation of remotely sensed data in conjunction with field investigation provides valid datasets for proper planning (Dharumarajan et al. 2016). The first global assessment of the extent of desertification was performed in 1984 in order to verify the measures outlined in the Plan of Action to Combat Desertification. The initial observation showed that the desertification process had not been prevented or stopped but it had been exacerbated at the global level, having expanded its boundaries to part of the sub-humid regions (Zonn et al. 2017). The United Nations has periodically focused on desertification notably by adopting the Convention to Combat Desertification (CCD) in 1992 (UNCCD 1994) and designated 2006, as the International Year of the Desert and Desertification (Reynolds et al. 2007). UNCCD reported that one-third of the earth's land surface and 250 million people were directly affected due to desertification. In particular, dryland ecosystems, which are the areas having an aridity index of less than 0.65 (UNEP 1997), are more prone to desertification. Altogether, a quarter of the world population is threatened by the effects of degradation, which affects nearly 84% of agricultural lands (FAO 2008). The major cause of increasing land degradation in India is the over-exploitation of natural resources. Proper land-use management, conservation of important agricultural lands, and frequent monitoring of desertification-sensitive regions

are just a few of the strategies that might help to mitigate the severity.

Since desertification/land degradation is a dynamic process, remote sensing technologies may help to assess and monitor the visual features of this dynamism using a variety of methodologies. The different type of land degradation in South India is given in Fig. 32.1.

Several remote sensors have become available during the past 30 years, with the potential to provide useful information for assessing land degradation. The land degradation and desertification studies were conducted by the researchers majorly using sensors like LANDSAT Thematic Mapper (TM), LANDSAT Enhanced Thematic Mapper (ETM), MODIS, AVHRR, IKONOS, SPOT, IRS AWiFS and LISS (Tables 32.1). The overview of applications of different sensors in mapping desertification and land degradation processes is described below (Table 32.1, Figs. 32.2 and 32.3).

32.1.1 Landsat Sensors

Landsat satellite is the first earth-observing satellite launched in 1972 and the mission program continued as Landsat 1, 2, 3, 4, 5, 7 and 8. Almost 40 years of Landsat data provided by USGS is more helpful in analysing the change detection over the period. The most commonly used sensors such as Multi-Spectral Scanner (MSS), Thematic Mapper (TM), and Enhanced Thematic Mapper (ETM) were used for desertification studies and for identifying the kind of desertification processes such as forest degradation (Symeonakis and Higginbottom 2014), vegetative degradation (Shalaby and Tateishi 2007), Karst rock desertification (Huang and Cai 2007), soil erosion (Collado et al. 2000) and salinity (Dwivedi and Sreenivas 1998). The advanced Landsat 8 Operational Land Imager (OLI) and Thermal Infrared Sensor (TIRS) images have nine spectral bands with a spatial resolution of 30 m for Bands 1–7, and the sensor provides signal-to-noise radiometric (SNR) performance, leading to a better characterization of



Severe water eroded areas in Chamarajnar district, Karnataka

Land degradation due to severe salinity in Bellary district, Karnataka



Vegetal degradation in Anantapur district, Andhra Pradesh

Land degradation due to Brick mining in Bidar district, Karnataka

Fig. 32.1 Examples of land degradation in South India

land cover state and condition. The most utilized Landsat imagery showed greater accuracy rate of more than 90% in spatial monitoring of desertification with an overall kappa rating of 0.87. Landsat image was considered good for supervised classification and identification of different land degradation and desertification processes.

32.1.2 MODIS

NASA's Terra and Aqua satellites launched MODIS in 2002 to observe Earth's surface even in cloudy regions. The availability of moderate spatial resolution (250 m), high temporal resolution (2 images per day) and time series since 2000 make it suitable for monitoring vegetation variability and land degradation at the national/regional scale. MODIS NDVI time

series data interpret negative trends in agriculture/vegetation cover in relation to land degradation (Dubovyk et al. 2013b). The high resolution of MODIS data provides information on degradation to the extent possible of agricultural landscape level. MODIS sensor was used in several studies related to forest degradation (Asner et al. 2009), vegetation degradation (Dubovyk et al. 2013a), and soil erosion (Vrieling et al. 2008).

32.1.3 AVHRR

The National Environmental Satellite Data and Information Service (NESDIS) of the National Oceanic and Atmospheric Administration (NOAA) have been operating the Advanced Very High-Resolution Radiometer (AVHRR)

Table 32.1 Details of satellites used in land degradation assessment

Satellite	Sensor	Resolution (M)	Data type
Landsat 5	THEMATIC MAPPER	30	Optical
Landsat 7	ETM+	30	Optical
Landsat 8	OLI	30	Optical
Sentinel-1	C-SAR (C-band Synthetic Aperture Radar)	Interferometry Wide Swath: 250 km Swath, 5 × 20 m spatial resolution	Radar
Sentinel-2	MSI	20	Optical
ASTER	DEM (RADIOMETER)	30	DEM (radar)
SRTM	DEM (RADIOMETER)	30	DEM radar
Cartosat DEM	DEM (OPT STEREO PAIR)	2.5	DEM optical
MODIS	SPECTROMETER	250	Optical
IRS-P6	LISS-III	23.5	Optical
Cartosat	LISS-IV	5.8 m	Optical
ALOS PALSAR	L-band synthetic aperture radar	25 m	Radar
HYPERION–EO	HSI-220 CHANNELS	30 m	Hyperspectral
RISAT-1	SAR-C	1 m	Radar
MODIS	TERRA, AQUA	250–1000	Hyperspectral
QUICK BIRD	PAN, MS	0.6–2.44	Optical
IKONOS	PAN, MS	1–4	Optical
AVHRR	RADIOMETER	1100	Radar
GEOEYE	PAN, VISIBLE, IR	0.46–1.84	Optical
SPOT-4	HRVIR	20	Optical

since 1978 as part of its Polar-orbiting Operational Environmental Satellites (POES). Later the Initial Joint Polar-orbiting Operational Satellite System (IJPS) operated the AVHRR for environment monitoring (Davis 2007). Its temporal ability of 14 times per day is a major advantage for analysing changes in the land surface. The Advanced Very High-Resolution Radiometer's Normalized Difference Vegetation Index (NDVI) is used in the majority of land degradation investigations (AVHRR). The daily NDVI series with worldwide coverage obtained from AVHRR data has been widely utilized in land cover change studies, notably in forest degradation (Olander et al. 2008) and vegetation degradation (Prince 1991). In particular, the AVHRR data

set allows access to spatial scales and time resolutions and produces more quantitative results.

32.1.4 IKONOS

Digital Globe operates IKONOS high-resolution satellite sensor, which has 3.2 m multispectral and 0.82 m panchromatic resolution at nadir. The launch of IKONOS in the year 1999 by Space Imaging provides high-resolution satellite imagery and promotes the mapping applications of satellite imagery. The high-resolution images are also used as ground truth to validate land cover maps in the remotest area where no measurements are possible. The utility of the

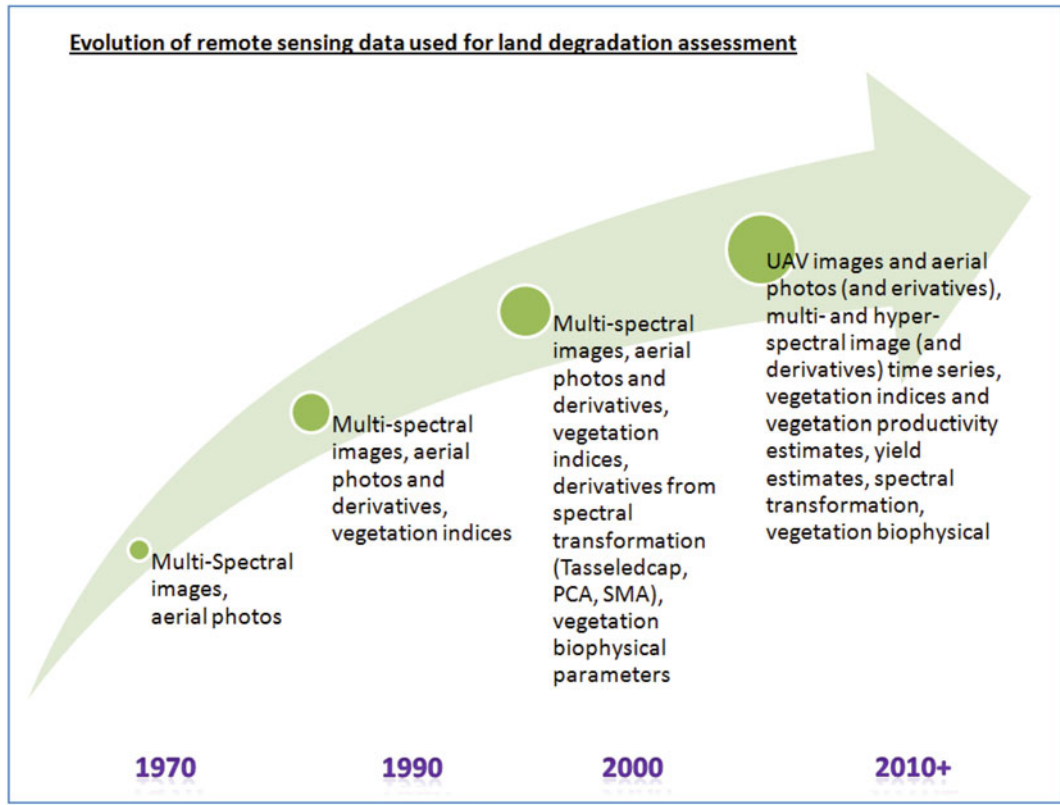


Fig. 32.2 Evolution of remote sensing data used for land degradation assessment

IKONOS image is again yet extended for the identification and verification of tree samples in the study area (Wang et al. 2005). Hence, the pan-sharpened IKONOS images are popularly being used in ground forest-cover mapping (Wang et al. 2005) and forest degradation (Clark et al. 2004) by the researchers.

32.1.5 SPOT

Satellite Pour l'Observation de la Terre (SPOT) satellites were launched by French Centre National d'Etudes Spatiales in cooperation with Belgium and Sweden in 1986. It provides High-Resolution Visible sensor with a moderate spatial resolution of 20 and 10 m. The SPOT-4 and 5 satellites each have sensors that collect data in the visible, near-infrared and shortwave infrared wavelengths, which are commonly utilized in

vegetation research. Desertification monitoring by SPOT image produces high-quality maps especially for vegetation degradation (Huang and Siegert 2006) and soil erosion (Pradhan et al. 2011) classes.

32.1.6 Resourcesat (AWIFS, IRS LISS IV, LISS III)

Resourcesat-1, an Indian Remote Sensing (IRS) satellite launched in 2003, has a sun-synchronous polar orbit of 817 km and contains three sensors. The Advanced Wide Field Sensor (AWIFS) has a resolution of 56 m and a swath width of 740 km with four VNIR-SWIR bands. IRS-P6 (Resourcesat) AWiFS geo-coded False Colour Composite (FCC) data were analysed using visual interpretation techniques to generate desertification/land degradation status map

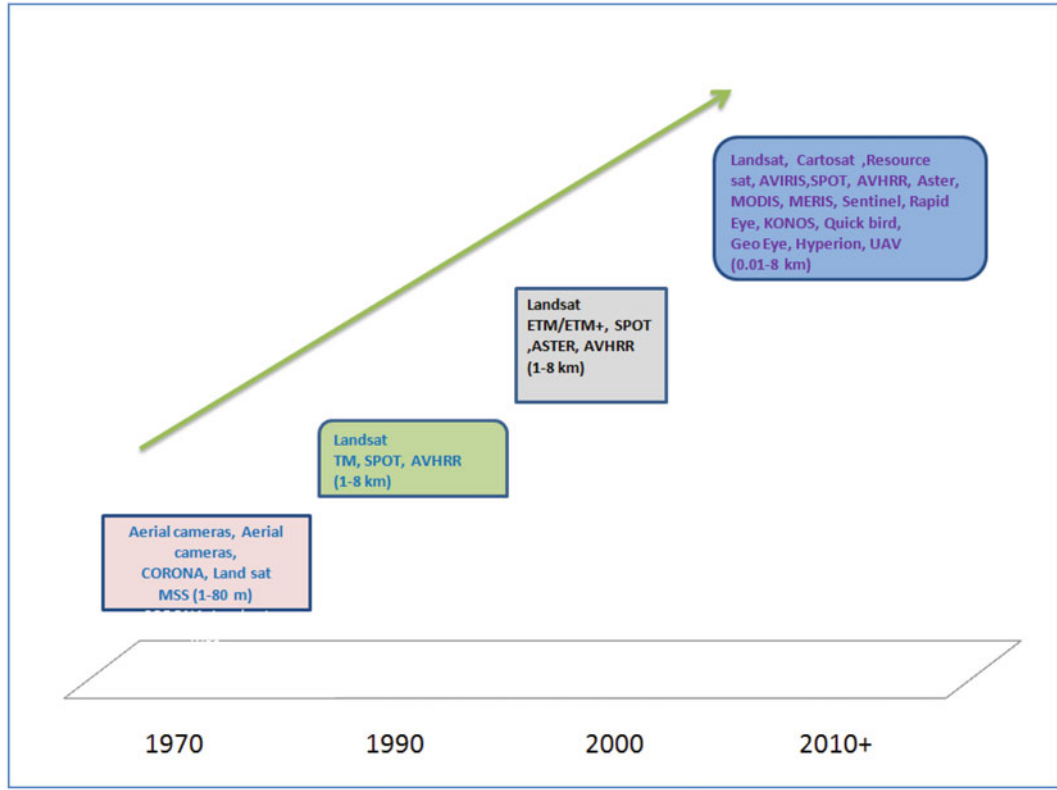


Fig. 32.3 Sensors in land degradation and desertification assessment

(DSM) of India on a 1:500,000 scale (Ajai et al. 2009; SAC 2016; Dharumarajan et al. 2018a). The Medium Resolution Linear Imaging Self-Scanner (LISS-III) characterizes four bands with a 23.5 m resolution and 141 km swath width. The erosion categories such as sheet erosion, gullied and stony waste were identified using LISS III along with ancillary data to classify different land use/land covers categories (Tagore et al. 2012). LISS III data was also helpful in determining soil salinity and alkalinity problems (Dwivedi 2002). The High-Resolution Linear Imaging Self-Scanner (LISS-IV) has three VIS–NIR bands and a spatial resolution of 5.8 m. Overall, Resourcesat datasets are helpful in achieving high mapping accuracy in the delineation of wasteland classes (Nathawat et al. 2010) soil salinity (Zolekar and Bhagat 2014) and soil erosion (Abdel Rahman et al. 2016).

32.1.7 Image Pre-processing

The crucial development of satellite image provision always takes careful pre-processing, correction, and analysis techniques. Large-scale, multi-frame, satellite-based land cover picture data presents pre-processing challenges such as consistent geometric correction, reducing noise due to atmospheric effects, correcting for changing lighting geometry, and reducing instrument intrinsic errors. Such errors can hinder the ability to derive land surface information reliably and consistently. This part of the raw image contains distortions that cannot be used directly with map base products in a geographic information system (GIS). To avoid such distortions in land degradation and desertification studies, typical image pre-processing will be carried out which includes radiometric

correction, geometric correction, atmospheric corrections, ortho-rectification, and contrast enhancements.

32.1.8 Image Classification

Remote sensing classification is a complex process that demands the involvement of multiple factors, including the selection of a suitable classification system, each selection of training samples, a selection of suitable classification approaches, post-classification processing, and accuracy assessment. In a broad sense, image classification is described as the process of deriving distinctive classes or themes from raw remotely sensed satellite data, such as land use classifications and plant species. The overall goal of the image classification technique is to assign land cover classes or themes to all pixels in an image.

32.1.9 Traditional Methods

The traditional methods of classification procedures are visual interpretation, supervised classification, and unsupervised classification (Fig. 32.4). Visually interpreting digitally enhanced imagery needs to balance the complementing capacities of the human mind and the computer (Shalaby and Tateishi 2007). The mind is quite excellent at deciphering spatial information of an image and may discover obscure or subtle characteristics. Based on land use, land degradation, vegetation cover and erosion, desertification severity map can be visually interpreted (Tripathy et al. 1996). Del Valle et al. (1998) observed that, 71.4% success rate of desertified regions were identified through visual interpretation. A signature of any feature can be developed by traditional per-pixel classifiers by combining pixel training sets. Similarly, in pixel-based techniques, land cover classes can be prepared by supervised or unsupervised classifiers. For any image classification, the number of training samples and their representativeness are crucial.

The Unsupervised classification determines the spectral classes in the image from which the image analyst determines the related information to the spectral classes. This approach is based on the natural groupings of spectral properties of the pixels by the Remote Sensing software without any user influence. Unsupervised classification is used in NDVI images for calculation of desert area, cultivated land and bare soil classes (Ahmad 2013). This classification frequently represents more than one status class in desertification studies (Del Valle et al. 1998).

In **Supervised** classification, the user/image analyst specifies the various pixels values or spectral signatures for each class in the classification process. It is a fundamental tool for obtaining quantitative data from remotely sensed image data. Maximum likelihood classifier under supervised classification has been deemed the most accurate classifier for monitoring land cover change because it evaluates both the variance and covariance of the spectral response patterns when classifying an unknown pixel. It was also determined that integrating visual interpretation with supervised classification led to an increase in the overall accuracy by about 10 percent (Shalaby and Tateishi 2007). The integration method used in the determination of land cover mapping produced approximately 96% accuracy, which proves it is an effective method for the identification of changes in land cover (Abd El-Kawy et al. 2011).

32.2 Recent Techniques

Many modern classification algorithms, such as Artificial Neural Networks (ANN), object-oriented classification, fuzzy sets, and expert systems, have been widely used for picture classification in recent years. **Artificial Neural Network (ANN)** is developed with a simple processing unit to evaluate the complex phenomena, which is used for classifying land degradation and desertification processes. It has the benefits of self-learning, self-organization and self-adaptation, as well as the capacity to imitate the expert's thought process in land

Evolution of remote sensing methods used for land degradation assessment

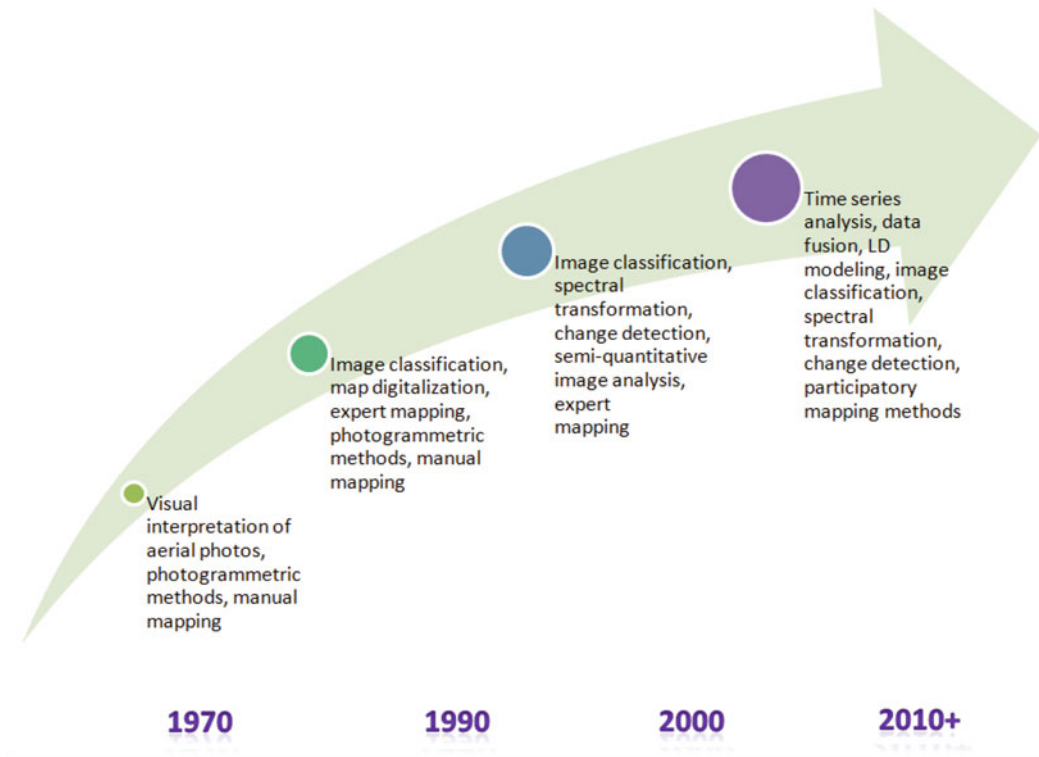


Fig. 32.4 Evolution of remote sensing methods used for land degradation assessment

degradation assessment (Fig. 32.5). The acceptable results of relatively high accuracy of more than 90% of land degradation detection are achieved through ANN (Yue et al. 2016).

Object-Oriented Classification is a type of advanced classification, which considers a set of pixels instead of single pixel as visual phenomena and through this method, the process of segmentation can be achieved (Fig. 32.6). In the next stage, classification is performed based on training samples and fuzzy logic (Mohamadi et al. 2016). The Object-Oriented Classification system resulted in a classification accuracy of 80–96%, which was a high precision compared to maximum likelihood classifier, support vector machines classifier, and neural network method in land degradation studies (Mohamadi et al. 2016).

Fuzzy Logic Modelling addresses the unpredictability of global data sets as well as the

fuzzy character inherent in land categorization using a variety of criteria (Cai et al. 2011). The systems employ a fuzzy semantic import technique, which allows for the incorporation of multi-disciplinary information into basic sets of fuzzy rules (Fig. 32.7). The changes in likelihood, nature and magnitude were the outputs of the fuzzy logic knowledge based system. The output maps are then combined with the landscape information and represented in the form of GIS layers to derive the hazard prediction model (Metternicht 2001). This model helps in locating the vulnerable areas and identifying the severity to mitigate the effects of desertification (Dasgupta et al. 2013).

The Random Forest Model (RFM) is based on the assemblage of many Classification and Regression Trees using two levels of randomization for each tree in the forest (Breiman 2001). Random Forest technique was applied to predict

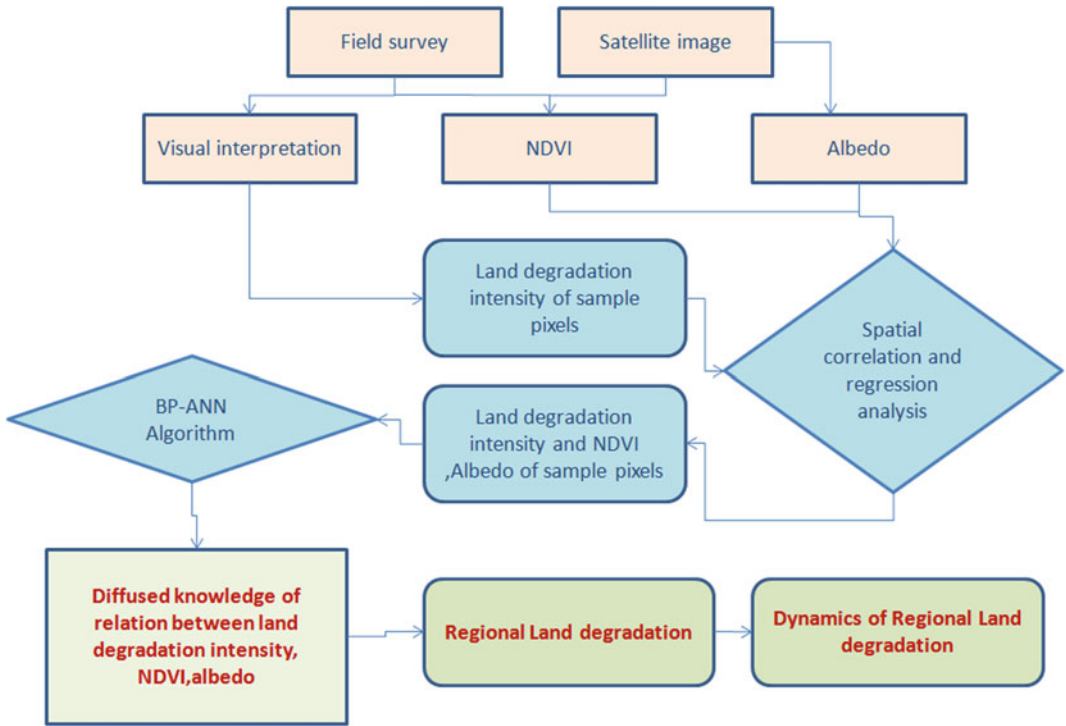


Fig. 32.5 Artificial neural network approach for land degradation mapping

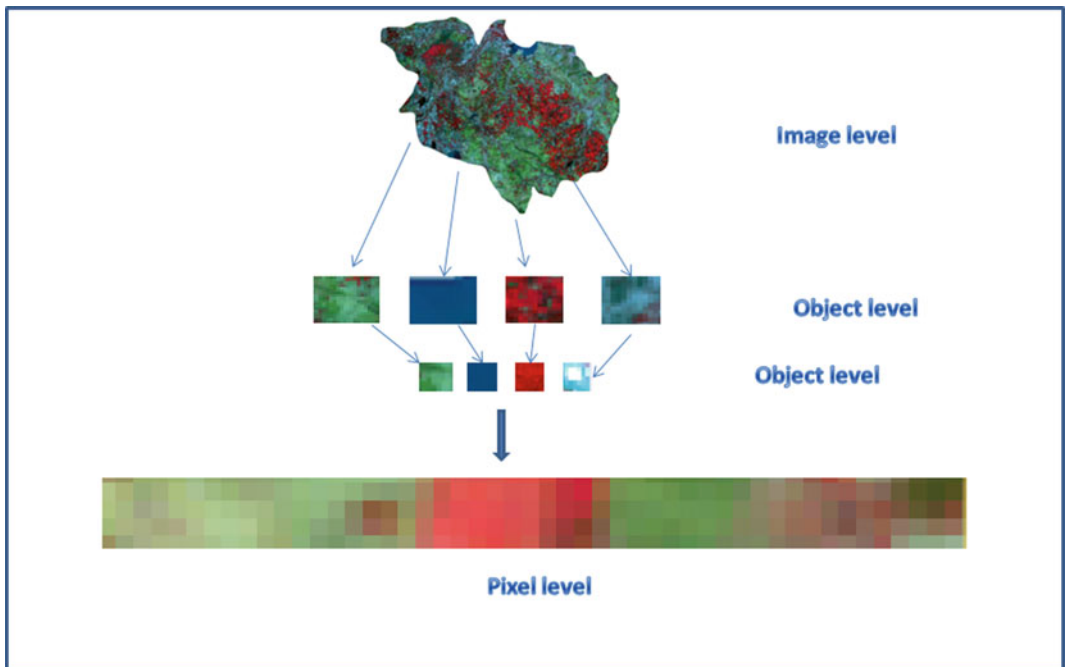


Fig. 32.6 Object-oriented classification workflow

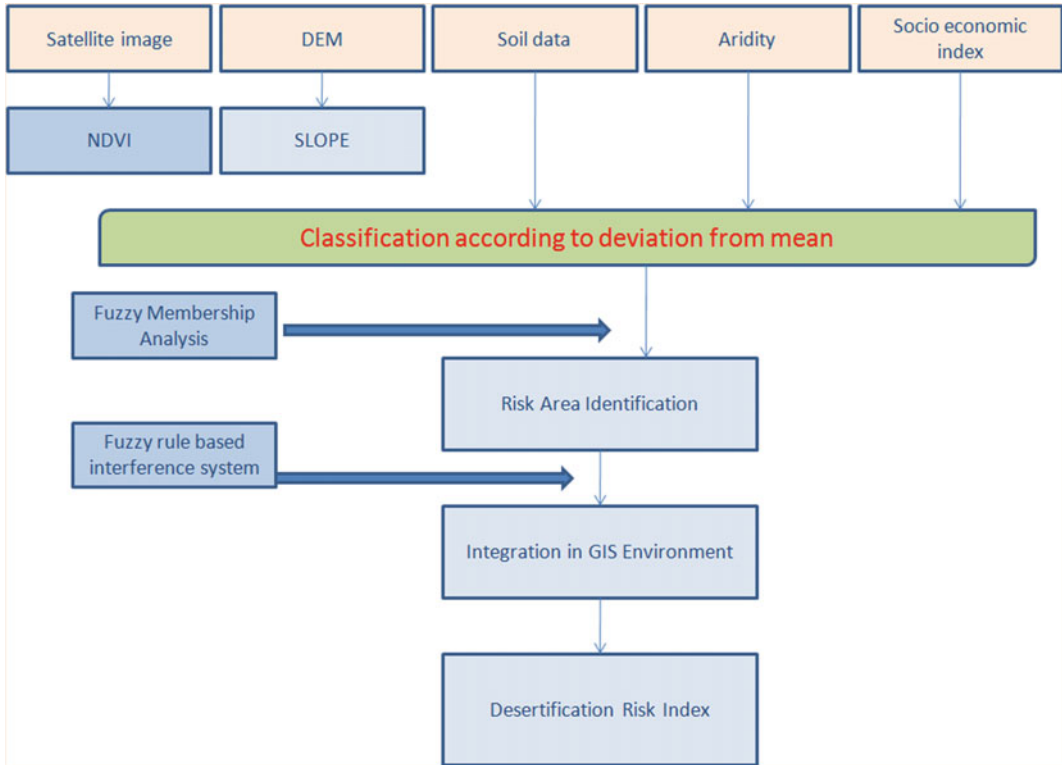


Fig. 32.7 Fuzzy model approach for land degradation and desertification assessment

the different desertification processes in the Anantapur district, which yielded the overall accuracy and Kappa rate of 85.5 and 75.8%, respectively (Dharumarajan et al. 2018b). This method can also be useful in regions where sample information and the amount of data are limited (Wiesmeier et al. 2011).

32.2.1 Hyperspectral Imaging

HYMAP, Hyperion and AVIRIS are the different hyperspectral sensors used in land degradation and desertification mapping. Shrestha et al. (2005) classified the HYMAP hyperspectral data to identify the soil surface features and assessing desertification and land degradation units by Spectral Angle Mapper (SAM) using linear unmixing classification techniques. Hyperion scene classification using the Support Vector Machines (SVM) classifier versus object-

oriented approach suggested relatively higher overall accuracy and Kappa accuracy for the object-oriented approach (81.30% and 0.779) than the SVM classifier (76.30% and 0.719) (Petropoulos et al. 2012). Several other researchers also indicated that the potentiality of hyperspectral imaging in land degradation studies in the different parts of the world (Chabrilat et al. 2003; Ustin et al. 2004; Gao and Liu 2008).

32.3 Desertification/land Degradation Vulnerability Analysis—Case Studies

Identification of vulnerable areas helps the policymakers and planners to prepare an action plan to reverse or combat desertification and land degradation. Desertification is caused by a combination of biophysical and socio-economic variables such as topography, climate, land use,

soil and human influences (Dharumarajan et al. 2018b). To identify desertification-vulnerable locations, a multidisciplinary approach based on biophysical and socioeconomic aspects is necessary (Fig. 32.8). Several mathematical and geostatistical models have been developed by the different researchers to delineate the areas vulnerable to desertification and land degradation processes (Salvati and Zitti 2009; Dharumarajan et al. 2018b).

Soil Quality Index, Vegetation Quality Index, Climate Quality Index and Management Quality Index were used in MEDALUS methodology to develop Environmental Sensitivity Index (ESI) by (Kosmas et al. 1999). Though the model has a weakness of assigning equal weightage for different indices, this index was useful, particularly in the Mediterranean region. Salvati and Zitti (2009) developed an index based on biophysical and socio-economical factors. Some of the recent studies on desertification/land degradation vulnerability mapping are described below in detail.

Dharumarajan et al. (2018b) developed Desertification Vulnerability Index in Anantapur District, Andhra Pradesh, India using a multivariate index model. The total geographical area (TGA) of the study area was 19,130 km² and falls under hot arid bioclimatic conditions. IRS-

LISS III data was utilized for visual interpretation to classify desertification and land degradation. The developed desertification units were confirmed and finalized after intensive ground-truthing. The desertification vulnerability index was calculated using a multivariate index model. Unlike the traditional method of identifying land degradation, a modified weighted index was employed to categorize the various criteria of land degradation. The biophysical index (BPI) was developed by integrating climate, soil and land use indices in a GIS environment to delineate the vulnerable areas of desertification. Human intervention has a significant impact on the environment and land degradation. Hence, the Socio-Economic Index (SEI) was also considered to determine the desertification vulnerability areas. As a result, the final Desertification Vulnerability Index (DVI) was computed using expert knowledge inference techniques to integrate the socio-economic index with the biophysical index. The DVI maps showed that 10.2% of lands were classified as very high vulnerability index and about 18.7% and 34.4% of lands were having highly and moderately vulnerability, respectively.

Dave and Sur (2018) conducted research on the “Fuzzy Integrated Desertification Risk

Fig. 32.8 Components of desertification/land degradation vulnerability index



Model” in order to estimate regional desertification vulnerability in the Bhavnagar district of Gujarat, India. Fuzzy logic blends the complicated classical analytic hierarchy process with the grey clustering approach for coefficient estimation. The study focused on a fuzzy membership analysis model that was incorporated into a geospatial environment. Aridity, slope, soil and NDVI were employed as natural parameters for climate, topography, soil and vegetation analysis, and numerous socio-economic aspects were employed to assess economic pressures in the research region. The parameters were USGS Landsat-7 (30 m), DEM (Carto DEM), Soil Data from NBSSLUP (Slope, pH, Texture, Erosion, and Drainage, etc.), Climatic Data from CGIAR CSI (Global Aridity Index) and Census-2011 for socio-economic factor (Population, Education, Income, etc.). The application of remote sensing methods, GIS and fuzzy logic to evaluate risk would aid an expert in effective resource allocation and decision-making. Individual classes of individual parameters’ normal density functions were spatially represented in a GIS context to determine the areas at risk of desertification and their severity. The study revealed that Bhavnagar district was under moderate desertification vulnerability and high alarming areas were in patches around the main urban zones.

Tssemelis et al. (2019) used the Standardized Drought Susceptibility Index (SDVI) and the Environmentally Sensitive Areas Index (ESAI) to assess desertification vulnerability in Greece. The objective was to find out the common drivers for the drought and desertification process. The indices were computed using data from October 1983 to September 1996, when the study region was frequently subjected to severe droughts. The SDVI is a composite indicator that attempts to combine the numerous symptoms of drought (meteorological, hydrological, agricultural, social and economic) into a single value. The strategy provided a composite measure composed of four environmental and anthropogenic factors: Soil Quality Quality Index (SQI), Vegetation Quality Index (VQI), Climate Quality Index (CQI) and

Management Quality Index (MQI). The ESAI classified desertification vulnerability into eight types. ESAI assessed an area's susceptibility to drought and desertification by examining variables such as soil, geology, vegetation, climate and human behaviours. Both indices were reclassified and prepared as new maps and compared the vulnerability on a common scale. The study found that both indices might give helpful information to policymakers and may be used to compel local adaptation steps to these threats.

In Khorasan-Razavi, Iran, Pashaei et al. (2017) created an Integrated Desertification Vulnerability Index. To construct an integrated desertification index, remote-sensor indices such as Enhanced Vegetation Index (EVI), precipitation index, soil salinity (SI), evapo-transpiration index, soil moisture index and Land Surface Temperature (LST) index were developed (IDI). The degree of desertification vulnerability was assessed for Razavi Khorasan, an Iranian province with an area of approximately 128,430 km², over a 14-year period from 2000 to 2014. Images from the MODIS satellite, a combination of Terra and Aqua satellites (MCD12Q1) from 2000 and 2013, were used to map land cover work units. During the years 2000–2014, the Biophysical Index fluctuated owing to changes in factors. The map of sensitive areas prone to desertification will be evaluated using standard accuracy estimate factors such as overall accuracy, manufacturing precision, user accuracy, and the kappa index. The derived IDI classes were very low with a range of 0–0.15 (Not subjected areas), low with a range of 0.15–0.30 (Potential areas), medium with a range of 0.30–0.50 (Fragile areas), high with a range of 0.50–0.70 (Critical areas) and very high with a range of 0.70–1.0 (Degraded areas). The Kappa index of the DVI map was obtained to be 0.75. The high Kappa index for the validity of the model showed the reliability of the map. Among the vulnerability zones identified, high vulnerability zones were found in major areas (56,099.3 km²) followed by medium vulnerable zones (25,916.6 km²). As a result, the IDI approach demonstrated

that it is a successful tool for analysing the degree of vulnerability index of desertification and the changes in this phenomenon over time.

32.4 Research Gaps and Future Prospects

Many remote sensing techniques, methods and instruments are in trail mode to monitor land degradation and desertification processes. One among is microwave remote sensing that provides Synthetic Aperture Radar (SAR) data, which can be explored to get clear information and algorithms related to land degradation processes. Though it has the advantage of monitoring at night times and penetrates through clouds, its availability is very limited. Another improved remote sensing data is hyperspectral image from which soil resources and vegetation data can be extracted to monitor the land degradation processes. AVIRIS (Airborne Visible Infrared Imaging Spectrometer) is one of the very high spatial resolution sensors that has a large number of spectral bands which provides a huge amount of spatial observation on land degradation and dryland ecosystem. But AVIRIS data is very expensive and limited to a small area. These satellite data can be utilized in recent and advanced multivariate models (artificial neural networks, random forest, partial least square regression, object-oriented classification) to determine the better classification and attain higher accuracy. In future, the convergence of high-resolution data products with recent classification and modelling techniques could be explored in a broader way to assess and obtain more detailed information about monitoring and modelling of desertification and land degradation.

32.5 Conclusion

Desertification/land degradation is the major challenge in natural resource, ecological and economic management and its sustainability. Remote sensing and GIS technique serves as an

aid for assessing and monitoring the different land degradation processes as well as to compare the trend on a spatial and temporal scale. The convergence of remote sensing and advanced modelling techniques has given the opportunity to identify the degraded areas accurately and timely.

References

- Abd El-Kawy OR, Rød JK, Ismail HA, Suliman AS (2011) Land use and land cover change detection in the western Nile delta of Egypt using remote sensing data. *Appl Geogr* 31:483–494. <https://doi.org/10.1016/j.apgeog.2010.10.012>
- Abdel Rahman MAE, Natarajan A, Srinivasamurthy CA, Hegde R (2016) Estimating soil fertility status in physically degraded land using GIS and remote sensing techniques in Chamarajanagar district, Karnataka, India. *Egypt J Remote Sens Space Sci* 19:95–108. <https://doi.org/10.1016/j.ejrs.2015.12.002>
- Ahmad F (2013) Land degradation pattern using geo-information technology for KotAddu, Punjab Province, Pakistan. *Glob J Hum Soc Sci Geogr Geo-Sci Environ* 13(1). Online ISSN: 2249-460x and Print ISSN: 0975-587X. https://globaljournals.org/GJHSS_Volume13/1-Land-Degradation-Pattern-Using.pdf
- Ajai AS, Arya Dhinwa PS, Pathan SK, Ganesh Raj K (2009) Desertification/land degradation status mapping of India. *Curr Sci* 97(10):1478–1483. http://www.indiaenvironmentportal.org.in/files/Desertification_0.pdf
- Asner GP, Knapp DE, Balaji A, Páez-Acosta G (2009) Automated mapping of tropical deforestation and forest degradation: CLASlite. *J Appl Remote Sens* 3:033543. <https://doi.org/10.1117/1.3223675>
- Borrelli P, Robinson DA, Panagos P, Lugato E, Yang JE, Alewell C, Wuepper D, Montanarella L, Ballabio C (2020) Land use and climate change impacts on global soil erosion by water (2015–2070). *PNAS* 117(36):21994–22001. <https://doi.org/10.1073/pnas.2001403117>
- Breiman L (2001) Random forests. *Mach Learn* 45:5–32. <https://doi.org/10.1023/A:1010933404324>
- Cai X, Zhang X, Wang D (2011) Land availability for biofuel production. *Environ Sci Technol* 45(1):334–339. <https://doi.org/10.1021/es103338e>
- Chabrilat S, Kaufmann HJ, Hill J, Mueller AA, Merz B, Ehtler H (2003) Research opportunities for studying land degradation with spectroscopic techniques. In: *Proceedings of SPIE 4886, remote sensing for environmental monitoring, GIS applications, and geology II*, 14 Mar 2003. <https://doi.org/10.1117/12.462362>
- Clark DB, Read JM, Clark ML, Cruz AM, Dotti MF, Clark DA (2004) Application of 1-m and 4-m resolution satellite data to ecological studies of

- tropical rain forests. *Ecol Appl* 14(1):61–74. <https://doi.org/10.1890/02-5120>
- Collado AD, Chuvieco E, Camarasa A (2000) Satellite remote sensing analysis to monitor desertification processes in the crop-rangeland boundary of Argentina. *J Arid Environ* 52:121–133. <https://doi.org/10.1006/jare.2001.0980>
- Dasgupta A, Sastry KLN, Dhinwa PS, Rathore VS, Nathawat MS (2013) Identifying desertification risk areas using fuzzy membership and geospatial technique—a case study, Kota District, Rajasthan. *J Earth Syst Sci* 122(4):1107–1124. <https://doi.org/10.1007/s12040-013-0331-x>
- Dave VA, Sur K (2018) Fuzzy integrated desertification vulnerability model. *ISPRS Int Arch Photogramm Remote Sens Spat Inf Sci XLII-5:395–401*. <https://doi.org/10.5194/isprs-archives-XLII-5-395-2018>
- Davis G (2007) History of the NOAA satellite program. *J Appl Remote Sens* 1:1–18. <https://doi.org/10.1117/1.2642347>
- Del Valle HF, Elissalde NO, Gagliardini DA, Milovich J (1998) Status of desertification in the Patagonian region: assessment and mapping from satellite imagery. *Arid Land Res Manag* 12(2):95–121. <https://doi.org/10.1080/15324989809381502>
- Dharumarajan S, Lalitha M, Rajendra Hegde, Janani N, Rajavat AS, Sastry KLN, Singh SK (2018a) Status of desertification in South India—assessment, mapping and change detection analysis. *Curr Sci* 115(2):331–338. <https://doi.org/10.18520/cs%2Fv115%2F2%2F331-338>
- Dharumarajan S, Bishop TFA, Hegde R, Singh SK (2018b) Desertification vulnerability index—an effective approach to assess desertification processes: a case study in Anantapur District, Andhra Pradesh, India. *Land Degrad Dev* 29(1):1–12. <https://doi.org/10.1002/ldr.2850>
- Dharumarajan S, Lalitha M, Vasundhara R, Hegde R (2016) The major biophysical indicators of desertification in arid and semiarid regions of India. *Agropedology* 26:189–197. <http://isslup.in/wp-content/uploads/2018/09/Agropadiology-Dec-2016-8.pdf>
- Dharumarajan S, Veeramani S, Kalaiselvi B, Lalitha M, Janani, Srinivasan R, Rajendra Hegde (2019) Potential impacts of climate change on land degradation and desertification: land degradation and climate change. Climate change and its impact on ecosystem services and biodiversity in arid and semi-arid zones. In: Singh V (eds) *Impacts of climate change on biodiversity and ecosystem services: current trends*. IGI Global, pp 183–195. <https://doi.org/10.4018/978-1-5225-7387-6.ch010>. Accessed 20 May 2019
- Dubovyk O, Menz G, Conrad C, Kan E, Machwitz M, Khamzina A (2013a) Spatio-temporal analyses of cropland degradation in the irrigated lowlands of Uzbekistan using remote-sensing and logistic regression modelling. *Environ Monit Assess* 185:4775–4790 (2013). <https://doi.org/10.1007/s10661-012-2904-6>
- Dubovyk O, Menz G, Conrad C, Lamers JPA, Lee A, Khamzina A (2013b) Spatial targeting of land rehabilitation: a relational analysis of cropland productivity decline in arid Uzbekistan. *Erekunde* 67(2):167–181. <https://doi.org/10.3112/erdkunde.2013.02.05>. <https://pdfs.semanticscholar.org/57c2/dc158ddec4b53be22987b9881fed69c8320f.pdf>
- Dwivedi RS (2002) Spatio-temporal characterization of soil degradation. *Tropical Ecology* 43(1):75–90. http://tropecol.com/pdf/open/PDF_43_1/43107.pdf
- Dwivedi RS, Sreenivas K (1998) Image transforms as a tool for the study of soil salinity and alkalinity dynamics. *Int J Remote Sens* 19(4):605–619. <https://doi.org/10.1080/014311698215883>
- Environmental Management Agency (2015) EMA annual report. https://www.ema.co.zw/agency/downloads/file/2015_EMA%20annual%20report.pdf
- FAO (2008) Land degradation on the rise—one fourth of the world’s population affected says new study. <http://www.fao.org/newsroom/en/news/2008/1000874/index.html>
- Gao J, Liu Y (2008) Mapping of land degradation from space: a comparative study of Landsat ETM+ and ASTER data. *Int’l J Remote Sens* 29(14):4029–4043. <https://doi.org/10.1080/01431160801891887>
- Huang Q-H, Cai Y (2007) Spatial pattern of Karst rock desertification in the Middle of Guizhou Province, Southwestern China. *Environ Geol* 52:1325–1330. <https://doi.org/10.1007/s00254-006-0572-y>
- Huang S, Siebert F (2006) Land cover classification optimized to detect areas at risk of desertification in North China based on SPOT VEGETATION imagery. *J Arid Environ* 67(2):308–327. <https://doi.org/10.1016/j.jaridenv.2006.02.016>
- Hurtt GC, Chini L, Sahajpal R et al (2020) Harmonization of global land use change and management for the period 850–2100 (LUH2) for CMIP6. *Geosci Model Dev* 13:5425–5464. <https://doi.org/10.5194/gmd-13-5425-2020>
- Kosmas C, Ferrara A, Briasouli H, Imeson A (1999) Methodology for mapping Environmentally Sensitive Areas (ESAs) to desertification. In: *The Medalus project: Mediterranean desertification and land use Manual on key indicators of desertification and mapping environmentally sensitive areas to desertification*. In: Kosmas C, Kirkby M, Geeson N (eds) *European Union 18882*. ISBN 92-828-6349-2, pp 31–47
- Lyu Y, Shi P, Han G, Liu L, Guo L, Hu X, Zhang G (2020) Desertification control practices in China. *Sustainability* 12:3258. <https://doi.org/10.3390/su12083258>
- Metternicht G (2001) Assessing temporal and spatial changes of salinity using fuzzy logic, remote sensing and GIS. *Foundations of an expert system. Ecol Model* 144(2–3):163–179. [https://doi.org/10.1016/S0304-3800\(01\)00371-4](https://doi.org/10.1016/S0304-3800(01)00371-4)
- Mohamadi A, Heidarzadi Z, Nourollahi H (2016) Assessing the desertification trend using neural network classification and object-oriented techniques

- (Case study: Changouleh watershed—Ilam Province of Iran). *J Fac for Istamb Univer* 66(2):683–690. <https://doi.org/10.17099/jffiu.75819>
- Nathawat MS, Rathore VS, Pandey AC, Singh SK, Shankar GR (2010) Monitoring and analysis of wastelands and its dynamics using multiresolution and temporal satellite data in part of Indian state of Bihar. *Int'l J Geomatics Geosci* 1(3):297–307. <http://ipublishing.co.in/jggsvol1no12010/EIJGGS2003.pdf>
- Olander LP, Gibbs HK, Steining M, Swenson JJ, Murray BC (2008) Reference scenarios for deforestation and forest degradation in support of REDD: a review of data and methods. *Environ Res Lett* 3:025011. <https://doi.org/10.1088/1748-9326/3/2/025011>
- Pashaei M, Rashki A, Sepehr A (2017) An integrated desertification vulnerability index for Khorasan-Razavi. *Iran* 5(3):44–55. <https://doi.org/10.13189/nrc.2017.050302>
- Petropoulos GP, Arvanitis K, Sigrimis N (2012) Hyperion hyperspectral imagery analysis combined with machine learning classifiers for land use/cover mapping. <https://doi.org/10.1016/j.eswa.2011.09.083>. https://www.academia.edu/3296197/Hyperion_hyperspectral_imagery_analysis_combined_with_machine_learning_classifiers_for_land_use_cover_mapping
- Pradhan B, Chaudhari A, Adinarayana J, Buchroithner MF (2011) Soil erosion assessment and its correlation with landslide events using remote sensing data and GIS: a case study at Penang Island, Malaysia. *Environ Monit Assess* 184:715–727. <https://doi.org/10.1007/s10661-011-1996-8>
- Prince SD (1991) Satellite remote sensing of primary production: comparison of results for Sahelian grasslands 1981–1988. *Int'l J Remote Sens* 12:1301–1311. <https://doi.org/10.1080/01431169108929727>
- Reynolds JF, Smith DMS, Lambin EF (2007) Global desertification: building a science for dryland development. *Science* 316:847–851. <https://doi.org/10.1126/science.1131634>
- Runnström MC (2000) Is Northern China winning the battle against desertification? *A J Hum Environ* 29(8):468–476. <https://doi.org/10.1579/0044-7447-29.8.468>
- SAC (2016) Desertification and land degradation Atlas of India (Based on IRS AWiFS data of 2011–13 and 2003–05). Space Applications Centre, ISRO, Ahmedabad, India, p 219. ISBN 978-93-82760-207
- Salvati L, Zitti M (2009) Convergence or divergence in desertification risk? Scale-based assessment and policy implications in a Mediterranean country. *J Environ Planning Manag* 52:957–970. <https://doi.org/10.1080/09640560903181220>
- Shalaby A, Tateishi R (2007) Remote sensing and GIS for mapping and monitoring land cover and land-use changes in the North-western coastal zone of Egypt. *Appl Geogr* 27:28–41. <https://doi.org/10.1016/j.apgeog.2006.09.004>
- Shrestha DP, Margate DE, Meer FVD, Anh HV (2005) Analysis and classification of hyperspectral data for mapping land degradation: an application in southern Spain. *Int'l J Appl Earth Obs Geoinform* 7(2):85–96. <https://doi.org/10.1016/j.jag.2005.01.001>
- Symeonakis E, Higginbottom T (2014) Bush encroachment monitoring using multi-temporal LANDSAT data and random forests. *Int Arch Photogramm Remote Sens Spat Inf Sci XL-2*. ISPRS Technical Commission II symposium, 6–8 Oct 2014, Toronto, Canada. <https://doi.org/10.5194/isprsarchives-XL-2-29-2014>
- Tagore GS, Bairagi GD, Sharma NK, Sharma R, Bhelawe S, Verma PK (2012) Mapping of degraded lands using remote sensing and GIS techniques. *J Agric Phys* 12(1):29–36. https://www.researchgate.net/publication/263487317_Mapping_of_Degraded_Lands_Using_Remote_Sensing_and_GIS_Techniques
- Tripathy GK, Ghosh TK, Shah SD (1996) Monitoring of desertification process in Karnataka state of India using multi-temporal remote sensing and ancillary information using GIS. *Int'l J Remote Sens* 17(12):2243–2257. <https://doi.org/10.1080/01431169608948771>
- Tsesmelis DE, Karavitis CA, Oikonomou PD, Alexandris S, Kosmas C (2019) Assessment of the vulnerability to drought and desertification characteristics using the standardized drought vulnerability index (SDVI) and the environmentally sensitive areas index (ESAI). *Resources* 8(1):6. <https://doi.org/10.3390/resources8010006>
- UNCCD (1994) United Nations convention to combat desertification, elaboration of an international convention to combat desertification in countries experiencing serious drought and/or desertification, particularly in Africa (U.N. Doc. A/AC.241/27, 33 I.L.M. 1328 UN)
- UNCCD and FAO (2020) Land degradation neutrality for water security and combatting drought. Bonn, Germany. <http://www.fao.org/publications/card/en/c/CA7468EN/>
- UNCCD (2019) Land degradation, poverty and inequality. <https://www.unccd.int/publications/land-degradation-poverty-and-inequality>
- UNEP, United Nations Environmental Programme (1997) In: Middleton N, Thomas D (eds) *The World Atlas of desertification*. London New York, Sydney, Auckland. ISBN 0340691662. <https://digitallibrary.un.org/record/245955>
- Ustin SL, Roberts DA, Gamon JA, Asner GP, Green RO (2004) Using imaging spectroscopy to study ecosystem processes and properties. *Bioscience* 54(6):523–534. <https://doi.org/10.1641/0006-3568>
- Vrieling A, Jong SM, Sterk G, Rodrigues SC (2008) Timing of erosion and satellite data: a multi-resolution approach to soil erosion risk mapping. *Int'l J Appl Earth Obs Geoinform* 10(3):267–281. <https://doi.org/10.1016/j.jag.2007.10.009>

- Wang C, Qi J, Cochrane M (2005) Assessment of tropical forest degradation with canopy fractional cover from Landsat ETM+ and IKONOS imagery. *Earth Interact* 9. <https://doi.org/10.1175/EI1133.1>
- Wiesmeier M, Barthold F, Blank B, Kögel-Knabner I (2011) Digital mapping of soil organic matter stocks using random forest modeling in a semi-arid steppe ecosystem. *Plant Soil* 340:7–24. <https://doi.org/10.1007/s11104-010-0425-z>
- Yue Y, Li M, Zhu A, Ye X, Mao R, Wan J, Dong J (2016) Land degradation monitoring in the Ordos Plateau of China using an expert knowledge and BP-ANN-based approach. *Sustainability* 8:1174. <https://doi.org/10.3390/su8111174>
- Zolekar RB, Bhagat VS (2014) Use of IRS P6 LISS-IV data for land suitability analysis for cashew plantation in hilly zone. *Asian J Geoinformatics* 14(3):23–35. <https://www.semanticscholar.org/paper/Use-of-IRS-P6-LISS-IV-data-for-Land-Suitability-for-Bhagat/5ffb8aeb49501acae4e8a30e76347188822566ba>
- Zonn IS, Kust GS, Andreeva OV (2017) Desertification paradigm: 40 years of development and global efforts. *Arid Ecosyst* 7(3):131–214. <https://doi.org/10.1134/S2079096117030118>



Mapping the Caspian Sea's North Coast Soils: Transformation and Degradation

33

Konstantin Pachikin, Olga Erohina,
Gabit Adamin, Azamat Yershbulov, and
Yersultan Songulov

Abstract

The purpose of the studies conducted under the 2015–2017 project of the Ministry of Science and Education of the Republic of Kazakhstan (“Assessment of the environmental state of the Caspian Sea northern coast soil cover”), consisted in a comprehensive assessment of the current state of the soil cover of the northern coastal zone of the Caspian Sea. The research focused on soils and soil cover on part of the northern coast of the Caspian Sea, adjacent to the modern delta of the Ural River. Soil transformation in the territory was caused both by an increased anthropogenic impact and changes in soil formation factors, associated with the decline of the Caspian Sea's level in recent years. Materials from previous soil studies were selected and analysed to evaluate the existing knowledge in this area. Based on the obtained results, 26 soil taxonomic units, including varieties, were identified on the site. The degree of soil

degradation was assessed. On the basis of the available materials, a soil map and a map of soil degradation (1:100,000 scale) were composed for the northern coast of the Caspian Sea. Until now, no similar studies had previously been implemented in the area. The study showed that, due to the fluctuation in the Caspian Sea's level and due to climate changes such as frequent droughts and rising temperatures, soil formation processes are undergoing modification (decrease in humus and nitrogen content, increase in the content of water-soluble salts) on the northern coast of the Caspian Sea.

Keywords

Caspian north coast · Soil map · Soil degradation map

K. Pachikin (✉) · O. Erohina · G. Adamin ·
A. Yershbulov · Y. Songulov
U. Uspanov Research Institute of Soil Science and
Agrochemistry, Al-Farabi 75B, 050060 Almaty,
Republic of Kazakhstan

K. Pachikin
Science Research Center for Ecology and
Environment of Central Asia, Al-Farabi 75B,
050060 Almaty, Republic of Kazakhstan

33.1 Introduction

Anthropogenic impacts on soil are the most diverse, leading to a variety of changes in soil formation processes and soil properties. Extreme impacts lead to the destruction of soils, which sometimes causes irreparable damage, especially to agricultural production. The development of industries for the economic growth of the country leads to excessive deforestation and land being used in such a way that it has lost its natural

quality. An increasing population and demand for more residential and commercial areas also contribute to land loss and soil degradation. In addition, agricultural practices such as irrigation, the excessive use of fertilisers and pesticides, or over-tillage also adversely affect the natural quality and fertility of cultivation land (Williams et al. 2020). Bouma and Bajtes (2000) concluded that of all the world's anthropogenically degraded soils, about 38% were slightly degraded, about 46% soils were moderately degraded; about 15% were strongly degraded and about 0.46% were extremely degraded.

Globally, pollution with crude oil and its products has become a major environmental concern. At least 0.08 to 0.4% of the oil produced internationally has been estimated to spill into the marine ecosystem as pollutants (National Research Council 1989). The operation of oil fields has been estimated to potentially impact the health and environment of over 600 million people worldwide (O'Callaghan-Gordo et al. 2016). Bearing in mind the growing global population, the need for higher fuel production keeps rising, implying that the problems associated with soil contamination with oil products and by-products will continue, along with the resulting environment pollution. Waste from the oil and gas industry, which may contain petroleum hydrocarbons, metals, naturally occurring radioactive materials, salts and toxic chemicals, can contaminate the soil and prevent vegetation growth. In addition, the contaminated water produced in pits or evaporation ponds often spills, thus jeopardising the vegetation and soil biota. Contaminants that enter the soil often migrate down the soil and pollute the groundwater, or migrate up through the soil and are released into the air. A typical oil well has been in operation for 20–30 years, while related activities, such as construction, production, processing and transportation have been going on in the region for several decades. Since crude oil contains carcinogenic hydrocarbons, such as naphthalene, acenaphthene, fluorene, pyrene and benzene (Wang and Xu 2017; Johnston et al. 2019): If these seep into the soil and groundwater, they can affect public health (Johnston

et al. 2019), as oil contaminants in soil can enter the food chain (Tarakbay et al. 2019).

The Caspian Sea is the world's largest endorheic lake. Located in western Asia, it is possibly the world's third-largest reservoir of oil and natural gas after the Persian Gulf and Russia (Nadim et al. 2006). Kazakhstan has the largest recoverable crude oil reserves in Central Asia, with current oil production of *approximately* 1.8 million barrels a day. According to the 2017 EITI Report, Kazakhstan produced a record volume of 86.2 million tonnes of oil since 1991 (<https://eiti.org/kazakhstan>). Particularly, the northern coast of the Caspian Sea is an area of intensive oil production, with a high population density, which predetermines a high anthropogenic pressure on the soil cover (Fig. 33.1). The growing economic potential of the coastal zone of the Caspian Sea also inevitably resulted in an increase in degraded pastures, disturbed lands, secondary salinisation and soil pollution. All these negative changes were exacerbated by the general aridification of the climate, with an acute shortage of water resources.

The Caspian Sea's water level has shown cyclic fluctuations but an overall lowering has been reported since the end of the Little Ice Age ($\sim 2 \text{ cm yr}^{-1}$) (Beni et al. 2013). Hu et al. (2020) reported that approximately 76.1% of Kazakhstan land is considered desertification-sensitive areas, of moderate and higher sensitivity. The Kazakhstan Caspian coastal regions include West Kazakhstan and the Atyrau and Aktau regions. West Kazakhstan accounts for the highest percentage of all the degraded lands in the entire country in terms of the areas affected by desertification (26.8%), while all three coastal regions account for 41.6% of desertified areas in Kazakhstan (Hu et al. 2020).

In the legislation of the Republic of Kazakhstan, the phenomenon of land degradation is considered to be a complex of processes that affect the functions of lands as elements of the natural environment, the quantitative and qualitative deterioration of soil and natural and economic devaluation (RND 03.7.0.06-96 1996; RND 2005). The latter document identifies the following types of soil degradation: agrofusio-



Fig. 33.1 Area studied in a coastal zone of the Caspian Sea

pollution (chemical and biological), radioactive contamination and technological (operational) degradation. In the period from the 1950s to the 1970s, systematic soil research was carried out in the Northern Caspian Sea by the staff of the Institute of Soil Science, Alma-Ata, Kazakhstan (Pachikina 1962; Ivanova 1966; Faizov 1970; Ivanova et al. 1977; Sadykov et al. 1978; Volga-Ural project 1982). A comparison of previous and recent studies (2009–2011) revealed significant changes in the structure of the soil cover and properties that occurred between those periods (Erokhina and Pachikin 2009, 2010; Erokhina et al. 2011). This happened due to both natural phenomena (fluctuations in the level of the Caspian Sea, extinction of the delta channels) and anthropogenic factors. The level of the Caspian Sea is subject to significant fluctuations. Until the 1930s, it was relatively stable (–25 to –26 m below sea level) and later in the 1970s it began to decline (to –29 m). This sharp drop was followed by an equally rapid rise in the sea level (in 1994 it reached –26.6 m) (Golitsyn 1995). Currently, the shoreline has been

retreating. At the beginning of 2019, according to the “RGP KazGidroMet” metrological service, the average sea level (including the fluctuations of tides) was –28.1 m (RGP KazGidroMet 2019). The modern retreat of the shoreline of the Caspian Sea is accompanied by the drying up of the coastal zone, a decrease in the groundwater level and the desertification of ecosystems, including transformations of the soil cover.

In the literature, there are a wide range of studies on the deterioration of soil properties due to anthropogenic or/and naturally caused destabilisation in general (AbdelRahman et al. 2019; Bonfante et al. 2019; Gu et al. 2019; Lorenz et al. 2019; IPCC 2019; Borelli et al. 2020; Lal 2020; Chang et al. 2020; Jensen et al. 2020; Oliveira et al. 2020) and in coastal landscapes particularly (IUCN 2003; Buzmakov and Kulakova 2010; FAO/UN 2011; Mukasheva 2012; Tacij 2012; Zubkova et al. 2014; Marjani and Jamali 2014; Romo-Leon et al. 2014; Sjøgaard et al. 2017; Issanova and Abuduwaili 2017; Salehin et al. 2018; Olsson et al. 2019; Hu et al. 2020). However, in the coastal zone of the Caspian Sea,

detailed studies of the soil cover have not been carried out, including soil classification, digital mapping and soil categorisation by the degree of degradation. In particular, focusing on the anthropogenic impact on soil properties (oil mining), there is a lack of data on soil degradation levels in this region. The surveyed coastal zone of the Caspian Sea adjacent to the modern delta of the Ural River and part of the ancient delta is a combination of natural and inhabited lands. There are areas of oil production, various industrial, technical facilities and related infrastructure. In addition, there are residential areas, agricultural land and natural landscapes that experience a certain technological impact.

In order to reveal the problems associated with soil degradation due to oil mining and agricultural land use in the Caspian region of Kazakhstan, it is necessary to have information both on the characteristics of soil properties and on their spatial distribution, i.e. thematic soil maps. The compilation of any soil map is usually preceded by a classification design, as the basis for the legend. However, to date, there is no generally accepted classification of anthropogenic soils and methods for their mapping. Moreover, in the territory studied, no detailed soil survey was conducted, and neither was a detailed soil map compiled to determine the degree of soil and land degradation. In this regard, it is relevant to study the morphogenetic and chemical properties for the development of soil classification, digital mapping and the compilation of a soil degradation map, including the load of natural and anthropogenic factors, on the Caspian Sea coast.

33.2 Mapping Region and Soil Survey

The objects of study were the soils of the northern coast of the Caspian Sea and the modern delta of the river Ural. The site studied covered 3250 km² and was located between 46°48' and 47°15' N and 51°00'–52°00' E. The availability of materials from previous studies for a reliable assessment of the degree of soil transformation

was a decisive factor in the selection of the survey area. The soil cover of the northern Caspian zone belongs to an extremely complex desert subzone, often with an absolute predominance of intrazonal soils over zonal soils. This is due to the geological youth of the country, which emerged from under the sea only in the late Quaternary era. After that, rivers appeared and disappeared in this territory, flowing from the Obshchy Syrt and the Trans-Ural plateau into the retreating sea (Ibadullaeva et al. 2015).

The basic principle of the classification of anthropogenically disturbed soil was a morphogenetic approach based on a quantitative and qualitative assessment of changes in the genetic soil profile as compared to its natural analogue (Isachenko 1980; Sokolov 2004). The preliminary soil contours were selected using GIS technologies and remote sensing techniques (Yashin et al. 2000; Korsunov et al. 2002). The main method for processing spatial information was indirect indication decryption (Smirnov 2005; Kravtsova 2005). This method is based on establishing a connection between the soil and landscape components that are best displayed on satellite images, primarily with vegetation and topography. For decryption, large-scale spectrozonal satellite images were used.

Field soil studies were carried out using the transect-key method based on a visual analysis of the decrypted information (Yashin et al. 2000), as well as the methods of classical mapping (Soil Survey 1959). The morphological methods used (Rozaev 2004) ensured the reliability and validity of the field soil diagnostics, mapping and results of the basic morphological properties. The locations of the soil profiles and semi-profiles were chosen so as to cover as many areas as possible that have not been previously studied. At the same time, the locations were selected as close as possible to the retrospective profiles, for the subsequent comparison of changes in soil properties.

Analytical work was implemented in the laboratory at the U. Usmanov Research Institute of Soil Science in Almaty (Kazakhstan). There, the soil humus was determined with the Tyurin wet-combustion method by oxidising a small portion

of the soil with potassium dichromate, then titrating the excess potassium dichromate with Mohr's salt (Mineev 2001). The total nitrogen was determined using the Kjeldahl distillation method; the concentration of exchangeable Ca^{++} , Mg^{++} was determined with an atomic absorption analyser, and K and Na were determined with a flame photometer (Arinushkina 1962; Aleksandrova and Najdenova 1986; Mineev 2001).

To determine the degree of soil transformation, paired or triple sections were opened for virgin and disturbed soils. These soils formed in the same bioclimatic, hydrological and geological-geomorphological conditions. According to the analytical results, the degree of soil degradation was determined. A newly developed soil map was used as a background for compiling the map of soil degradation. The cartographic materials and satellite images were scaled, satellite images were decrypted and soil mapping was performed in the MapInfo Professional software.

33.3 Effect of Soil Drying on Soil Organic Matter and Salt Distribution

In the territory studied, instable and irregular soil-forming conditions are associated with anthropogenic impacts and natural factors. The main natural factor is the decrease in groundwater levels and the drying (desertification) of the alluvial-delta and coastal soils. Studying the desertification of agrolandscapes in Kazakhstan, Hu et al. (2020) reported that in the Aktobe, Mangystau and Atyrau and Western Kazakhstan regions, the desertification process was mainly driven by climate changes such as rising temperature and decreasing precipitation. The situation was aggravated by the construction of the Irekly reservoir in the Orenburg region of the Russian Federation, which significantly reduced the flow of the Ural River, especially during floods. These natural and anthropogenic factors resulted in the originally marshland soils drying out. However, our analytical results showed that the degree of soil transformation, in addition to

the reduction in the groundwater level, was significantly affected by the soil type and genetic properties. The drying marshy coastal soils (Fig. 33.2) greatly affected the depth of the humic horizon and reduced the content of organic matter by 56% due to accelerated mineralisation (Table 33.1). Soil moisture is one of the primary physical factors that control microbial activity (Manzoni et al. 2020; Herbst et al. 2020) and thus the rate of soil organic matter (SOM) decomposition. Many studies showed that drained wetland soils are hotspots of carbon dioxide emissions. Säurich et al. (2019) studied the mineralisation rate of drained wetland soils by measuring respiration rates (basal and specific basal respirations) in laboratory aerobic incubation experiments. They found that CO_2 emissions from both slightly and heavily disturbed organic soils were high. The microorganisms of aqueous media are sensitive to changes in osmotic potential. In conditions of increasing osmotic stress, they accumulate electrolytes and small organic solutes across their membranes (Wood 2011), resulting in a high intracellular osmotic potential which suppresses the production and activity of enzymes in soil microorganisms (Kredics et al. 2000). Because of its sensitivity, the microbial pool is the first thing to be exposed to any climatic stress (e.g. see Delgado-Baquerizo et al. 2019). Enzymatic activity, the community composition and the total activity of bacteria and fungi inhabiting unsaturated soils significantly depend on the concentration of dissolved substances (osmotic potential) and reduced water content (matrix potential) (Manzoni and Katul 2014; Tecon and Or 2017). It is important to note that during soil drying, dissolved substances are concentrated in pore water, which further reduces the osmotic potential (changes towards large negative values) (Ghezzehei et al. 2019).

In our study, the transition from percolation to exudation water regimes led to a fourfold increase in the content of water-soluble salts in the surface horizons. This promoted the active penetration of sodium into the soil absorption complex (575%) (Table 33.1). The coastal meadow drying soils (Fig. 33.3) were characterised



Fig. 33.2 Drying marsh soil under desiccated reed (species of genus *Phragmites*)

by a noticeable loss of humus due to the extinction of mesophytic vegetation and a sharp decrease in the inputs of organic matter (by 72%) (Table 33.1). The coastal meadow soils which were studied have a light textured upper horizon (sandy loam, light loamy) that promoted the rapid mineralisation of organic matter under desert conditions. On the other hand, the light texture of soil prevented the accumulation of salts when the capillary rim separated from the surface (by 98%) of the total salts compared to the virgin analogue, thus preventing the salinisation processes. The content of exchangeable sodium in the drying coastal meadow soils decreased by 72% (Table 33.1). Similarly, studying the effect of different soil texture on salt accumulation and leaching, Berezniak et al. (2018) showed that salt accumulation was observed predominantly beyond the coarse part of the manipulated soil, while in a homogeneously textured soil a significant salt accumulation was observed. Gelaye et al. (2019), studying saline soils, reported that sandy loam soils significantly and strongly reduced salinity through leaching compared to clay loam soil.

An observable decrease in the humus content (by 33% in the upper horizons) was expected in cultivated drying estuary meadow soils, because

this is also associated with an imbalance between the input and decomposition of organic matter (Fig. 33.4) (Table 33.1). Loke et al. (2019) reported that in a more sensitive climatic soil ecosystem the loss of soil carbon in a cultivated agrosystem was 27–90% compared to natural grassland. Many researches showed that the loss of soil organic matter is heavily influenced by both anthropogenic loads such as tillage and cropping intensity, crop residue management and nutrient mining (Rumpel and Kögel-Knabner 2011; Baveye et al. 2020; Wiesmeier et al. 2020; Saljnikov et al. 2018) and by climate change factors (Lal 2020; Morán-Ordóñez et al. 2020; Moinet et al. 2020). Changes in the redox conditions in wetland soils are responsible for changes in the structure of organic substances in soil, which is reflected in the fact that the properties of high molecular weight substances change from hydrophilic to hydrophobic (Szajdak and Szatyłowicz 2010). The changes in soil volume due to shrinkage result in soil vertical movement and bulk density changes (Brandyk et al. 2001). All these factors lead to the depletion of organic matter in wetland soils when they are drained (Inisheva and Dementieva 2000).

Similarly to our findings, Szajdak et al. (2020) reported that reducing the water level in

Table 33.1 Changes in the basic properties of hydromorphic drying soils compared to their virgin analogues

Soil types	Depth of sample, cm	Humus content, %	Total nitrogen, %	CO ₂ , %	Exchangeable cations, mg-equiv/100 g					pH	Sum of salts, %
					Ca	Mg	Na	K	Sum		
<i>Coastal marsh salty soils</i>											
Virgin	0–7	5.61	0.322	20.24	11.8	9.5	1.85	1.11	24.26	8.06	0.232
	13–23	0.41	0.070	14.53	5.8	4.2	1.30	0.38	11.68	8.44	0.192
	55–65			24.36						8.29	0.130
Drying	0–6	2.50	0.140	4.56	16.5	4.5	0.42	0.34	21.76	7.58	1.269
	7–17	0.47	0.070	2.89	4.0	3.5	23.12	0.23	30.85	8.49	0.489
	18–28	0.24	0.042	3.95	6.5	4.5	0.88	0.20	12.08	8.13	0.901
	30–40			7.59						7.98	0.723
<i>Coastal meadow solonchak-like soils</i>											
Virgin	0–8	1.55	0.084	6.65	12.0	3.5	0.80	1.15	17.45	8.66	1.438
	9–19	0.28	0.028	8.13	4.2	2.5	1.47	1.42	9.59	8.09	0.073
	20–30	0.42	0.028	5.67	10.5	3.0	0.38	0.36	14.24	7.91	0.203
	30–40			2.08						8.09	0.368
	55–65			5.71						8.12	1.345
Drying	0–4	0.44	0.098	7.70	4.0	3.5	0.36	0.28	28.5	8.80	0.034
	4–10	0.17	0.042	9.17	1.8	3.3	0.33	0.18	14.2	9.09	0.038
	10–15			6.62						9.20	0.104
	40–50			6.19						8.60	1.039
<i>Cultivated drying estuary meadow soils</i>											
Virgin	0–10	1.90	–	5.00	19.5	5.5	0.71	–	–	–	0.106
	20–30	1.80	–	5.00	20.0	7.0	1.08	–	–	–	0.235
	30–40	1.60	–	6.00	18.7	6.3	0.62	–	–	–	0.306
Drying	0–7	1.27	0.140	4.8	20.5	6.5	1.85	0.55	29.40	8.90	0.101
	8–18	1.12	0.126	5.22	20.0	7.5	2.15	0.24	29.90	9.09	0.095
	19–29	1.05	0.098	5.01	16.5	11.2	2.98	0.17	30.85	8.98	0.106
	32–42	1.02	0.098	5.05	15.2	12.5	4.49	0.25	32.45	8.77	0.182
	65–75			4.38						8.57	0.368

peatlands activates oxidative processes and accelerates the mineralisation of SOM. At the start of wetland drainage, an increase in nutrient availability, especially nitrogen and phosphorus, is typically observed due to accelerated mineralisation (Koeselman and Verhoeven 1995). However, this higher level of nutrients is quickly depleted (Kajak and Okruszko 1990) due to the depletion of the labile part of the SOM.

Moreover, in drained soils, organic carbon accumulates at a slower rate than in non-drained analogue (Benavides 2014), which is probably associated with faster decomposition rate than the deposition of organic substrate. In addition, Szajdak et al. (2020) found that soil drying lowers the water storage capacity of peat soils, making them more susceptible to water-table fluctuations and droughts.

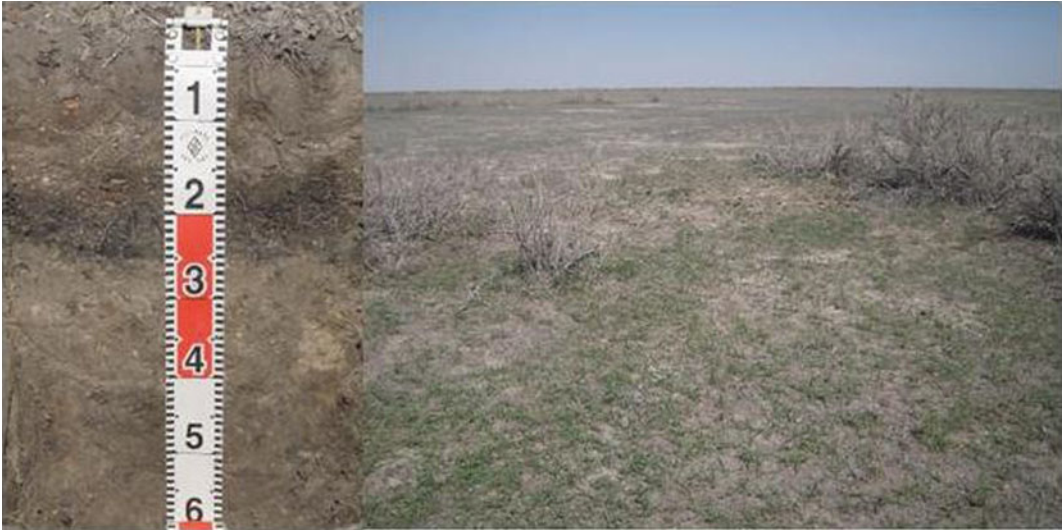


Fig. 33.3 Coastal meadow drying soil under cereal vegetation with dead tamarix (species of *Tamarix* genus)



Fig. 33.4 Estuary-meadow drying soil under quinoa (*Chenopodium quinoa*)

33.4 Soil Cover on the Northern Coast of the Caspian Sea

33.4.1 Formation of Soil Cover and Systematic Soil Classes Identified

The soils studied differed in terms of the soil formation environment, age and genesis: the modern Ural River Delta, part of the ancient Novobogatinsky Delta and the Novokaspiysky coastal plain. The soils of the modern Ural delta were characterised by heterogeneity and contrasting properties, which is mainly due to the influence of hydrological factors in soil formation. The hydrology of the region affected the relief-forming processes very dynamically. The soils of the delta are constantly rejuvenated by solids deposition from the river runoff, and from the coastal zone, as well as by marine sediments with alternating erosion and re-deposition processes. Parent rocks were represented by the layered deposits of mixed genesis (marine and alluvial-delta), predominantly by light-textured highly saline and calcareous rocks. In the modern delta, the processes of marsh, meadow and salty marsh formation prevailed in soil formation. The overlapping and combination of these processes

resulted in a high degree of variability in the morphological and chemical properties of the soils. The prevailing soils on the lowland floodplain terraces were meadow-marsh and marsh soils (Fig. 33.5).

Higher altitudes of the floodplain terraces, and the bottoms of drying channels, were occupied by alluvial-meadow soils. At some places, they can be found in combination with meadow solonchak. The elevated areas of the delta plain that separates the active and drying channels were occupied by drying alluvial-meadow saline soils (Fig. 33.6).

The formation of meadow coastal drying soils is obviously associated with the retreat of the Caspian Sea and a decrease in the level of groundwater (Erokhina et al. 2016). Arpe et al. (2014) reported that the Caspian Sea's water level has changed 100 times faster in comparison to global sea level changes over the last century. Cretaux et al. (2011) found that the SWL of Caspian decreased by more than 2 m from 1995. Pekel et al. (2016) reported that most of the northeastern coast of Caspian has already changed from a permanent to a seasonal water body.

Analysing the historical data and our soil survey data, we suggest that the modern surface of the Novobogati delta was influenced by



Fig. 33.5 Marsh soils under reed vegetation (*Phragmites australis*)



Fig. 33.6 Alluvial-meadow drying soils under saltwort (species of *Salsoloideae* sub-family) and tamarisk (species of genus *Tamarix*)

accumulative and erosion processes due to many channels. These channels created a specific hollow-plain relief, dissected by meandering flat depressions and smooth elevations. Soil-formation rocks were represented by delta-alluvial layered sediments, predominantly clayey from the surface. The regressive retreat of the coastline of the Caspian Sea and the related extinction of channels initiated the desertification of the region. Currently, the soils within the Novobogati delta are represented by drying-up meadow estuaries with varying degrees of salinity and alkalinity, and by the ordinary and takyric meadow solonchak soils. Floodplain meadow soils and partly meadow-marshy saline soils were also found, confined to a few waterlogged channels. On extensive flattened elevations, solonetz and salty solonetz soils were formed.

The modern Caspian Sea's coastal plain is slightly dissected by small depressions of uncertain shape and blind channels. In some places, it is interrupted by elongated elevations, i.e. remnants of the coastal ramparts separating the sea terraces. The relief and soil of the coastal strip are greatly influenced by the runoff processes and continually experience desiccation

and inundation: they are the battleground of terrestrial and marine ecosystems (Soldatov 1956). Our studies showed that the modern Caspian Plain is composed of layered saline marine sediments, overlaid by light and medium loam which is not very thick (20–30 cm and less). Soils on the coastline were formed under a high level of very saline groundwater (1–1.5 m). However, the recent decline in sea level has changed the direction of soil formation towards desertification.

The coastal plain solonchak soil (Fig. 33.7) formed extensive homogeneous contours and complexes with coastal-meadow solonchak soils, including drying ones. Drying coastal marsh and meadow-marsh soils were also widespread, while salty marshes were found in the area flooded during tides.

The following soil types were identified in the study area: meadow, irrigated meadow, drying aged meadow, alluvial-meadow, drying alluvial-meadow, drying meadow estuaries, coastal meadow, drying coastal meadow, forest-meadow, meadow-marsh, drying meadow-marsh, alluvial meadow-marsh, marsh, drying marsh, coastal marsh, drying coastal marsh, flooded marsh, automorphic solonetz, semi-



Fig. 33.7 Coastal solonchak under *Halocnemum strobilaceum*

hydromorphic solonetz, meadow solonchak, ordinary solonchak, takyric solonchak, coastal solonchak, coastal takyric solonchak, marsh solonchak and secondary solonchak. The main properties of the soils studied are presented in the paper by Erokhina and Pachikin (2010).

Many arid and semiarid regions are inherently endorheic: the surface flow is unable to break topographic barriers, and is retained in land-locked storage that equilibrates through evaporation (Hammer 1986). Because surface flow is scarce on the endorheic Caspian Sea's northern coast, water storage takes on vital ecological and social importance (Wang et al. 2018). However, due to climate change, warming and drying in many arid/semiarid regions (Dai 2013) have caused severe water imbalances, exacerbated by water withdrawals to sustain life and agriculture, dams and water intakes (Reager et al. 2016). Wang et al. (2018) reported that approximately two-thirds of the global endorheic water loss ($-73.64 \text{ Gt yr}^{-1}$) stems from Central Eurasia, with over half of the total zonal loss concentrated on the Caspian Sea Basin alone. Investigating the fluctuations in the Caspian Sea's level using satellite imaging models, Ataei et al. (2018) concluded that the decrease in the SWL could be

attributed to the rise of evaporation rather than precipitation and inlet river discharges. Since climatic factors (humidity and temperature) are the main driving forces of soil formation (Dokuchaev 1883) and determine its genetic characteristics, all of the above factors and changes have ultimately led to the modification of soil formation processes in the coastal zone of the northern Caspian Sea.

33.4.2 The Soil Cover Map

A soil field survey was conducted using traditional methods, such as remote sensing and GIS technologies, which permitted the development of a digital soil map at a scale of 1:100,000. The legend of the map was composed in accordance with the soil system featuring 26 soil formations and 2 non-soil formations. The created soil map contains 290 contours. Each contour contains information on the corresponding soil structure (complexes, combinations, spots, etc.), the taxonomic attribution of soil components (up to three per contour), their ratio (%), and the mechanical composition of a main soil component (Fig. 33.8).

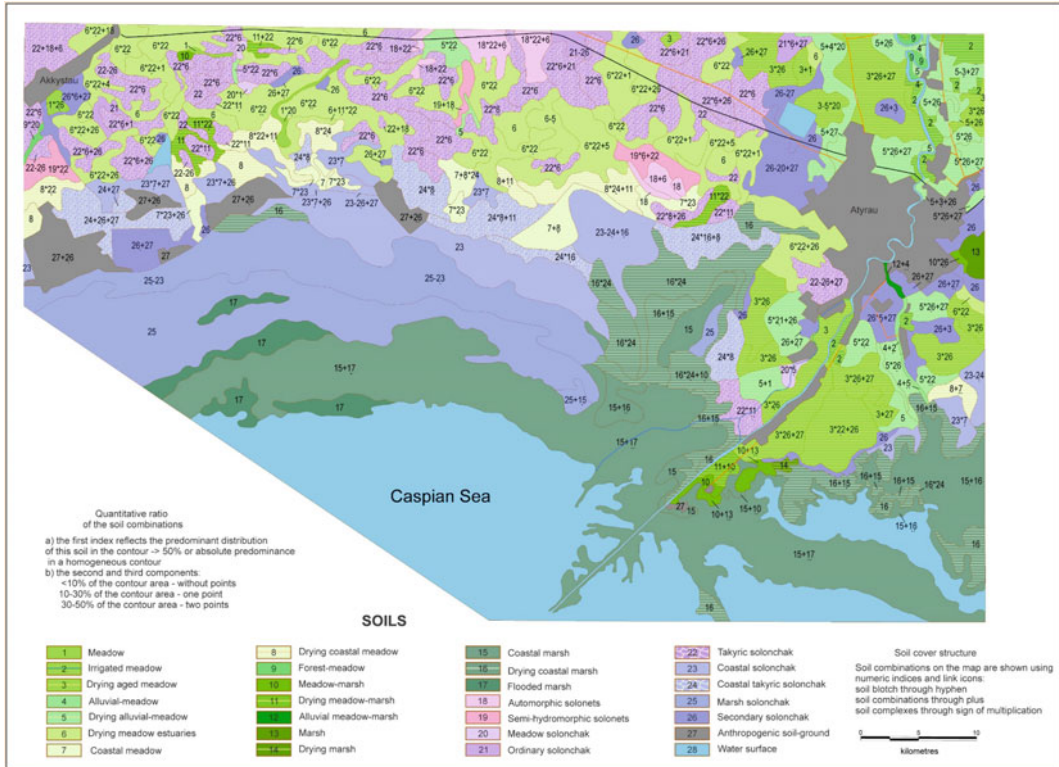


Fig. 33.8 Soil map of the northern coast of the Caspian Sea

33.5 Soil Degradation Mapping

33.5.1 Anthropogenic Transformation

A national regulatory document composed with the participation of leading experts in soil science (RND 03.7.0.06-96 1996; RND 2005) was adopted as the basis for determining the degree of soil degradation in this area. Given the regional characteristics in the coastal zone of the Northern Caspian, the main diagnostic indicators of anthropogenic soil transformation at the stage of field research were the depth of the humus horizon (A + B) and the depth of visually determined water-soluble salts.

In previously irrigated and presently abandoned fallow soils (Fig. 33.9), the salt layer was generally deeper. This was expected due to the dominance of irrigated soils with a percolation

moisture regime. However, in the absence of irrigation, under conditions of exudation, backward migration of water-soluble salts occurred (Funakawa et al. 2000). By contrast, a stable occurrence of the salt layer, at the lower boundary of the humus horizon, was found in the young deposits. When irrigation was discontinued, capillary uplift caused the accumulation of salt from shallow groundwater, which usually occurs in irrigated areas (Brammer 2014). Once the water table reached a critical depth below the ground surface, this water evaporated by capillary rise, transporting soluble salts upward to the active root zone and topsoil (Beltrán 1999; Salehin et al. 2018). Gupta and Khosla (1996) reported that the critical depth can range from 1 m in coarse-textured soil to a few metres in fine-textured soils.

Typically, the hydrochemical regime of groundwater in wetlands is characterised by the presence of an intra-annual circulation that is

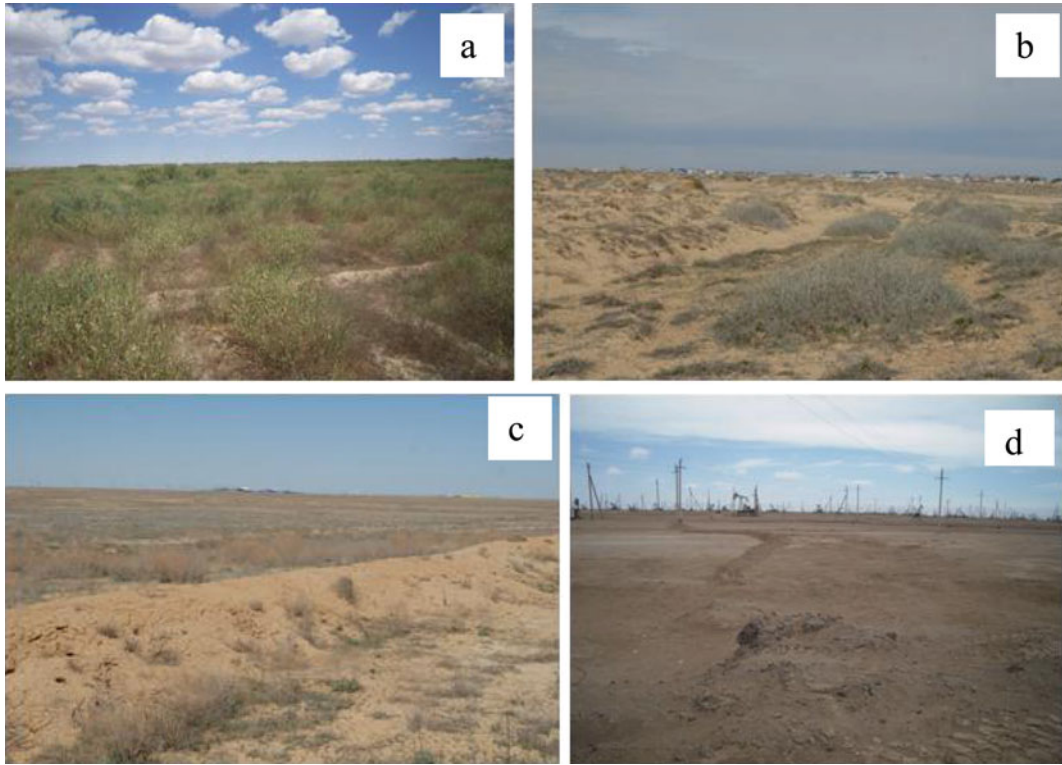


Fig. 33.9 Landscapes with technogenic soil disturbances: **a** formerly irrigated abandoned land, **b** sand deflation near settlement, **c** linear degradation (oil and gas pipelines, roads), **d** area degradation (oil and gas fields, industrial sites)

controlled by the infiltration dynamics. Draining these soils changes their chemical composition, leading to an increase in the concentration of the main ions. In an extensive study examining how draining and cultivating marshy soils affects their chemical composition, Okulik (1984) thus found a 1.1–3.2-fold increase in salt ions. Generally, landscapes that are subject to periodical flooding and drying (such as the coastal strip of the Caspian lowland) are distinguished by a specific regime of soil formation and radical changes in environmental conditions due to the level regime of the Caspian Sea (Asgerova et al. 2016). Changes in the profile and spatial aspects of semi-desert soil are formed in short intervals in the absence of human intervention (Asgerova et al. 2016). However, anthropogenic disturbance such as oil mining, waste disposal, drainage and cultivation substantially have altered the natural dynamics of these soils' changes and formation. In our study, the territories in the vicinity of the

settlements were characterised by numerous disturbances of the soil cover, such as the retreat of pastures, anthropogenic disturbances and the unauthorised storage of household waste and other types of waste. This inevitably led to a deterioration in the depth of the humus horizon (or its complete destruction), while salinisation and deflation of the light-textured soils sharply increased. The most critical changes in the morphological structure occur in the soils located in areas adjacent to oil fields. In fact, these soils are already devoid of vegetation and a humus horizon, and have a high degree of salinisation.

The parameters of anthropogenically disturbed soils of the coastal zone of the Northern Caspian Sea are presented in Table 33.2. The results confirm that the condition of the soils adjacent to oil fields is catastrophically poor compared to fallow soils. This is because, in contrast to the soils affected by oil mining activities, abandoned fallow soil can be returned

to agricultural production after appropriate land reclamation (Rakhimgalieva et al. 2018).

† negative sign is % decrease; positive sign is % increase.

33.5.2 The Soil Degradation Map

The key indicators for defining the soil surfaces which are vulnerable to desertification can be divided into four broad categories defining the qualities of soil, climate, vegetation and management (stressor indicators) based on remotely

sensed images, topographic data (maps or DEMs) data on the climate, soils and geology, at scales of 1:250,000 to 1,000,000) (Kosmas et al. 1999). Based on the soil map which was created and the analytical results obtained, a digital map of the degree of soil degradation was compiled (Fig. 33.10). The map also provides information on the factors behind the soil disturbance and the degree of their impact (alphanumeric indexes inside the contours). The areas not subject to degradation occupied less than 30% of the total area of 2726 km². Areas with slightly degraded soils occupied 19.3%, moderately degraded soils

Table 33.2 Degree of degradation of anthropogenically disturbed soils

Soil type	Increase/decrease in values of soil parameters (%)						Degree of degradation
	Depth (A + B) horizon	Humus	Sum of ex. cations	Ex. Na	Water-soluble salts	Projective vegetation cover	
Alluvial-meadow drying fallow land, formerly irrigated, saline clay soil	+20	-52	-60	+46	-88	-20	Average
Alluvial-meadow drying fallow land formerly irrigated, saline clay soil	+56	-52	-13	+56	+291	0	Very strong
Alluvial-meadow drying anthropogenically disturbed saline clay soil (near settlement)	0	-32	-27	+30	+64	0	Very strong
Alluvial-meadow drying fallow land, formerly irrigated, slightly saline, light-loamy soil	0	-28	-25	-63	-84	0	Weak
Estuary meadow drying fallow land formerly irrigated, saline clay soil	+33	+57	-7	+214	+42	-60	Strong
Alluvial-meadow drying, anthropogenically disturbed, saline clay soil (near settlement)	-14	-19	-60	+11	+7	-10	Average
Alluvial-meadow drying, anthropogenically disturbed, slightly saline, light-loamy soil (near settlement)	-14	-36	-33	-50	-30	-70	Weak
Secondary solonchak clay (oil field) (near settlement)	-40	-5	+87	+584	+676	-90	Very strong
Secondary solonchak, clay (near settlement)	-37	+49	+83	+25	+117	-20	Very strong
Secondary solonchak, clay (near settlement)	0	-35	-33	+225	+719	-90	Extreme
Secondary solonchak, clay (oil field)	-100	+113	+252	+480	+1735	-100	Extreme
Secondary solonchak, clay (oil field)	-100	+127	+196	+291	+1843	-100	Extreme
Secondary solonchak, clay (oil field)	-100	+208	+246	+261	+3743	-100	Extreme
Secondary solonchak, clay (oil field)	-100	+148	+99	+376	+2995	-100	Extreme

14.0%, strongly degraded soils 21.4%, very strongly degraded soils 8.8% and extremely degraded soils occupied 7.0% of the total area.

The processes contributing to desertification are regulated by systems of causes and driving forces, where the determining factors are very heterogeneous, and the cause–effect relationships and interactions between these factors are not always obvious and tend to manifest themselves to varying degrees depending on the different scales of spatial and temporal observation. In addition, these systems of causes are often connected to specific regional or local conditions (Venkatraman and Shah 2019). We agree with the suggestion by Säurich et al. (2019) that it is difficult to separate the interrelated effects of climate, hydrology, agricultural management and soil properties in the field. In the Caspian coastal landscapes of Kazakhstan in particular, no detailed studies have been carried out on the soil quality parameters until now. Our findings,

which are supported by Leiber-Sauheitl et al. (2014), Tiemeyer et al. (2016), Säurich et al. (2017) and others, showed that drained wetland soils are highly vulnerable to the imposed anthropogenic impacts and to climatic changes in the area studied. The soil cover and soil degradation maps which were created made it possible to identify the spatial distribution of soils and assess their current state of degradation with the appropriate classification. Further recommendations imply the rehabilitation of the disturbed lands. This issue is of particular importance given the fragility of the soils which were studied, which are under a high technogenic load. More than 60% of the Caspian coast is characterised by an arid climate (Akbari et al. 2020). Therefore, water consumption for human activities and the needs of agriculture—in the light of the constantly evolving industrial and oil-producing sector—can contribute to changes in the Caspian sea water level and groundwater

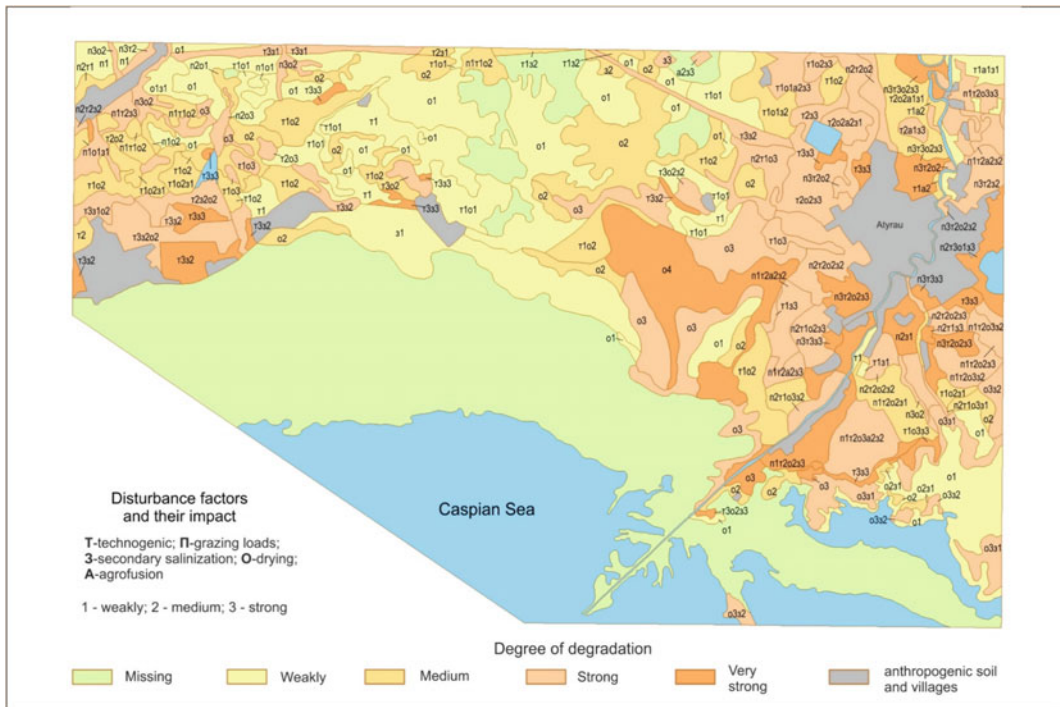


Fig. 33.10 Soil degradation map of the northern coast of the Caspian Sea

level, which is mainly controlled by the climate (Beni et al. 2014; Wang et al. 2018) and intensified by human activities (Reager et al. 2016).

33.6 Conclusions

1. On the northern coast of the Caspian Sea, the technogenic impact on soils was aggravated by natural transformations of the soil cover due to the retreat of the coastline.
2. These transformations resulted in the drying-out (desertification) of alluvial-delta and coastal soils.
3. This in turn caused negative changes in the soil properties (decrease in humus and nitrogen content, increase in the content of water-soluble salts, etc.).
4. Further, deeper and systematic studies of all soil quality parameters are necessary to mitigate the degradation processes and to elaborate and test effective measures for preventing their further degradation.

References

- AbdelRahman MAE, Natarajan A, Hegde R, Prakash SS (2019) Assessment of land degradation using comprehensive geostatistical approach and remote sensing data in GIS model builder. *Egypt J Remote Sens Space Sci* 22(3):323–334. <https://doi.org/10.1016/j.ejrs.2018.03.002>
- Akbari M, Baubekova A, Roozbahani A, Gafurov A, Shiklomanov A, Rasouli K, Ivkina N, Kløve B, Haghghi AT (2020) *Environ Res Lett* 15(11):115002. <https://doi.org/10.1088/1748-9326/abaad8>
- Aleksandrova LN, Najdenova OA (1986) Soil science laboratory and practical training (Лабораторно-практические занятия по почвоведению). *Agropromizdat, Leningrad*, p 295
- Arinushkina EV (1962) Guidance to the chemical analysis of soils (Руководство по химическому анализу почв). MSU, Moscow, p 491
- Arpe K, Leroy SAG, Wetterhall F, Khan V, Hagemann S, Lahijani H (2014) Prediction of the Caspian sea level using ECMWF seasonal forecasts and reanalysis. *Theor Appl Climatol* 117:41–60. <https://doi.org/10.1007/s00704-013-0937-6.pdf>
- Asgerova DB, Byibolatova ZD, Batyrmurzaeva PA, Zhelnovakova VA (2016) Changes in flooded soils of Caspian coastal line during their drying and aridisation. *Arid Ecosyst* 22, 2(67):56–62. <https://cyberleninka.ru/article/n/izmenenie-zatoplennyh-pochv-pribrezhnoy-polosy-kaspiya-v-periody-ih-issusheniya-i-aridizatsii/viewer>. Accessed 7 Mar 2021
- Ataei HS, Jabari AKh, Khakpour AM, Adjami M, Neshaei SA (2018) Investigation of Caspian sea level fluctuations based on ECMWF satellite imaging models and rivers discharge. *Intn'l J Coastal Offshore Eng* 2(2):21–30. http://ijcoe.org/browse.php?a_code=A-10-198-1&sid=1&slc_lang=en
- Baveye PC, Schnee LS, Boivin P, Laba M, Radulovich R (2020) Soil organic matter research and climate change: merely re-storing carbon versus restoring soil functions. *Front Environ Sci* 8:579904. <https://doi.org/10.3389/fenvs.2020.579904>
- Beltrán JM (1999) Irrigation with saline water: Benefits and environmental impact. *Agric Water Manag* 40(2–3):183–194. [https://doi.org/10.1016/s0378-3774\(98\)00120-6](https://doi.org/10.1016/s0378-3774(98)00120-6)
- Benavides JC (2014) The effect of drainage on organic matter accumulation and plant communities of high-altitude peatlands in the Colombian tropical Andes. *Mires Peat* 15:1–15. <http://www.mires-and-peat.net/>. ISSN 1819-754X
- Beni AN, Lahijani H, Mousavi Harami R, Arpe K, Leroy SAG, Marriner N, Berberian M, Andrieu-Ponel V, Djamali M, Mahboubi A, Reimer PJ (2013) Caspian sea-level changes during the last millennium: historical and geological evidence from the south Caspian Sea. *Clim past* 9:1645–1665. <https://doi.org/10.5194/cp-9-1645-2013>
- Beni AN, Lahijani H, Pourkerman M, Jokar R, Hosseindoust M, Marriner N, Djamali M, Andrieu-Ponel V, Kamkar A (2014) Caspian Sea-level changes at the end of Little Ice Age and its impacts on the avulsion of the Gorgan River: a multidisciplinary case study from the southeastern flank of the Caspian Sea. *Mediterranean* 122:145–155. <https://doi.org/10.4000/mediterranee.7226>
- Berezniak A, Ben-Gal A, Mishael Y, Nachshon U (2018) Manipulation of soil texture to remove salts from a drip-irrigated root zone. *Vadoze Zone J* 17(1):1–11. <https://doi.org/10.2136/vzj2017.01.0019>
- Bonfante A, Terribile F, Bouma J (2019) Refining physical aspects of soil quality and soil health when exploring the effects of soil degradation and climate change on biomass production: an Italian case study. *Soil* 5(1):1–14. <https://doi.org/10.5194/soil-5-1-2019>
- Borelli P, Robinson DA, Panagos P, Lugato E, Yang JE, Alewell C, Wuepper D, Montanarella L, Ballabio C (2020) Land use and climate change impacts on global soil erosion by water (2015–2070). *PNAS* 117(36):21994–22001. <https://doi.org/10.1073/pnas.2001403117>
- Bouma J, Bajtes NH (2000) Trends of world-wide soil degradation. “Bodenschutz” Verlag Gunter Heimbach, 27–29 January 2000

- Brammer H (2014) Bangladesh's dynamic coastal regions and sea-level rise. *Clim Risk Manag* 1:51–62. <https://doi.org/10.1016/j.crm.2013.10.001>
- Brandyk T, Oleszczuk T, Szatylowicz J (2001) Investigation of soil water dynamics in a fen peat-moorsh soil profile. *Int Peat J* 11:15–24
- Buzmakov SA, Kulakova SA (2010) Assessment of the soil cover state in the oil field areas (Оценка состояния почвенного покрова на территории нефтяных месторождений) <https://cyberleninka.ru/article/n/otsenka-sostoyaniya-pochvennogo-pokrova-na-territorii-neftnyanh-mestorozhdeniy>. Accessed 7 Mar 2021
- Chang C, Lin F, Zhou X, Zhao G (2020) Hyper-spectral response and estimation model of soil degradation in Kenli County, the Yellow River Delta. *PLOS ONE* 15(1):e0227594. <https://doi.org/10.1371/journal.pone.0227594>
- Cretaux J, Jelinski W, Calmant S (2011) SOLS: a lake database to monitor in the Near Real Time water 418 level and storage variations from remote sensing data. *Adv Sp Res* 47:1497–1507. Online 419. http://hydroweb.theia-land.fr/hydroweb/view/L_caspian?lang=en
- Dai AG (2013) Increasing drought under global warming in observations and models. *Nat Clim Change* 3:52–58. <https://www.cgd.ucar.edu/cas/adai/papers/Dai-NatureClimChange-final.pdf>. Accessed 7 Mar 2021
- Delgado-Baquerizo M, Doulier G, Eldridge DJ et al (2019) Increases in aridity lead to drastic shifts in the assembly of dryland complex microbial networks. *Land Degrad Develop* 31(3):346–355. <https://doi.org/10.1002/ldr.3453>
- Dokuchaev VV (1883) Russian Chernozem: report to the free economic society. St Petersburg, Decleron and Evdokimov Publ, House, III, IV, p 376
- Erokhina OG, Pachikin KM (2009) Main regularities of formation and soil cover structure of the Northern Caspian Sea. *Pochvovedenie i Agrochimia* 4:5–12. (Основные закономерности формирования и структура почвенного покрова Северного Прикаспия. *Почвоведение и агрохимия* 4:5–12)
- Erokhina OG, Pachikin KM (2010) Features of formation and structure of the soil cover of the North-Eastern Caspian Sea. *Pochvovedenie i Agrochimia* 4:5–14. (Особенности формирования и структура почвенного покрова Северо-Восточного Прикаспия. *Почвоведение и агрохимия* 4:5–14)
- Erokhina OG, Pachikin KM, Nasyrov RM, Adamin GK (2016) Soils and soil cover of northern coast of Caspian Sea. *Agrochimia* 27–40 (Почвы и почвенный покров северного побережья Каспийского моря. *Агрохимия*)
- Erokhina OG, Pachikin KM, Nasyrov RM, Kasymov MA, Lukbanova RS (2011) Anthropogenic transformation of the soil cover of the North-Eastern Caspian Sea. *Pochvovedenie i Agrochimia* 4:5–12. (Антропогенная трансформация почвенного покрова Северо-Восточного Прикаспия. *Почвоведение и агрохимия* 3:5–14).
- Eswaran H, Lal R, Reich PF (2001) Land degradation: an overview. In: Bridges EM, Han-nam ID, Oldeman LR, DeVries WTP, Scherr SJ, Sombatpanit S (eds) *Response to land degradation*. Science Publishers Inc, Enfield, pp 20–35
- Faizov KSh (1970) Soils of the Kazakh SSR. *Pochvy Kazahskoi SSR*. Issue 13. The Guriev region (Почвы Казахской ССР. Вып. 13. Гурьевская область). Alma-Ata Nauka, p 352.
- FAO/UN (2011) Land degradation assessment in drylands —LADA. Methodology and results. Final draft, Rome
- Funakawa Sh, Suzuki R, Karbozova E, Kosaki T, Ishida N (2000) Salt-affected soils under rice-based irrigation agriculture in southern Kazakhstan. *Geoderma* 97:61–85. [https://doi.org/10.1016/S0016-7061\(00\)00026-4](https://doi.org/10.1016/S0016-7061(00)00026-4)
- Gelaye KK, Zehetner F, Loiskandl W, Klik A (2019) Effects of soil texture and groundwater level on leaching of salt from saline fields in kesem irrigation scheme, Ethiopia. *Soil Water Res* 14(4):221–228. <https://doi.org/10.17221/137/2018-sw>
- Ghezzehei TA, Sulman B, Arnold CL, Bogie NA, Berhe AA (2019) On the role of soil water retention characteristics on aerobic microbial respiration. *Biogeosciences* 16:1187–1209. <https://doi.org/10.5194/bg-16-1187-2019>
- Golitsyn GS (1995) The Caspian Sea rises (Каспий поднимается. *Новый Мир*). *Novyj Mir* 7:87–103
- Gu X, Zhang Q, Li, J, Singh VP, Liu J, Sun P, Cheng Ch (2019) Attribution of global soil moisture drying to human activities: a quantitative viewpoint. *Geophys Res Lett* 46(5):2573–2582. <https://doi.org/10.1029/2018GL080768>
- Gupta SK, Khosla BK (1996) Salinity control in the root zone of irrigated agriculture. In: *Proceedings of the workshop on waterlogging and soil salinity in irrigated agriculture*, 12–15 Mar, New Delhi
- Hammer UT (1986) *Saline lake ecosystems of the world*. Dr W. Junk Publishers, Dordrecht, The Netherlands
- Herbst M, Tappe W, Kummer S, Vereecken H (2020) The influence of soil structure on heterotrophic respiration response to soil water content. *EGU General Assembly 2020*. Online 4–8 May 2020. EGU2020-3365. <https://doi.org/10.5194/egusphere-egu2020-3365>
- Hu Y, Han Y, Zhang Y (2020) Land desertification and its influencing factors in Kazakhstan. *J Arid Environ* 180:104203. <https://doi.org/10.1016/j.jaridenv.2020.104203>
- Ibadullaeva SZh, Usen K, Sauytbaeva GZ, Nurgaliyeva AA, Ospanova GK (2015) Regularities of vegetation distribution in the coastal part of the northeastern Caspian. *Adv Modern Nat Sci* 9(3):492–495 (Закономерности распространения растительности в прибрежной части северо-восточного Каспия. *Успехи современного естествознания* 9(3): 492–495)
- Inisheva LI, Dementieva TV (2000) Mineralisation rate of organic matter in peats. *Pochvovedenie* 2:196–203 (Скорость минерализации органического вещества торфа. *Почвоведение*, № 2, стр. 196–203)

- IPCC (2019) Index. In: Climate change and land: an IPCC special report on climate change, desertification, land degradation, sustainable land management, food security, and greenhouse gas fluxes in terrestrial ecosystems. Shukla PR, Skea J, Calvo Buendia E, Masson-Delmotte V, Pörtner H-O, Roberts DC, Zhai P, Slade R, Connors S, van Diemen R, Ferrat M, Haughey E, Luz S, Neogi S, Pathak M, Petzold J, Portugal Pereira J, Vyas P, Huntley E, Kissick K, Belkacemi M, Malley J (eds). In press
- Isachenko AG (1980) Methods of applied landscape research. Leningrad Nauka, p 222 (Методы прикладных ландшафтных исследований. Наука с.222).
- Issanova G, Abuduwaili J (2017) Aeolian processes as dust storms in the deserts of Central Asia and Kazakhstan. Springer Nature Singapore Pte Ltd. <https://doi.org/10.1007/978-981-10-3190-8>
- IUCN (2003) Environmental Degradation and impacts on livelihood: sea intrusion—a case study. International Union for Conservation of Nature, Sindh Programme Office, Pakistan. IUCN, Gland, Switzerland, p 77
- Ivanova EN (ed) (1966) Genesis and classification of semi-desert soils. Nauka, Moscow, p 236 (Генезис и классификация полупустынных почв. Наука, с. 236)
- Ivanova EN, Fridland VM, Budina LP (eds) (1977) Soil zoning of the Caspian lowland and prospects of its agricultural use. Scientific reports of the Dokuchaev Soil Institute, Moscow, Russia, p 187 (Почвенное районирование Прикаспийской низменности и перспективы ее сельскохозяйственного использования. Научные доклады Почвенного Института Докучаева, Москва, с.187)
- Jensen JL, Schjøning P, Watts CW, Christensen BT, Obour PB, Munkholm LJ (2020) Soil degradation and recovery—changes in organic matter fractions and structural stability. *Geoderma* 364:114181. <https://doi.org/10.1016/j.geoderma.2020.114181>
- Johnston JE, Lim E, Roh H (2019) Impact of upstream oil extraction and environmental public health: a review of the evidence. *Sci Total Environ* 657:187–199. <https://doi.org/10.1016/j.scitotenv.2018.11.483>
- Kajak A, Okruszko H (1990) Grasslands on drained peats in Poland. In: Breymer AI (ed) *Ecosystems of the world 17A: managed grasslands*. Elsevier Sc. Publ., Amsterdam, The Netherlands, pp 213–253
- Koeselman W, Verhoeven JTA (1995) Eutrophication of fen ecosystems: external and internal nutrient sources and restoration strategies. In: Wheeler BD, Show SC, Fojt WJ, Robertson RA (eds) *Restoration of temperate wetlands*. Willey, Chichester, UK, pp 91–112
- Korsunov VM, Krasekha EN, Ral'din BB (2002) Methodology of soil ecogeographical research and cartography of soils. Ulan-Ude BNC SO RAN, p 232. (Методология почвенных эколого-географических исследований и картографии почв. Улан-Уде, с. 232)
- Kosmas C, Kirkby M, Geeson N (1999) Manual on: key indicators of desertification and mapping environmentally sensitive areas to desertification. EC, Energy, Environment and Sustainable Development, EUR 18882, 87 pp
- Kravtsova VI (2005) Space methods of soil investigation. Aspect-Press, Moscow, p 180 (Космические методы исследования почв. Аспект пресс, с. 180)
- Kredics L, Antal Z, Manczinger L (2000) Influence of water potential on growth, enzyme secretion and in vitro enzyme activities of *trichoderma harzianum* at different temperatures. *Curr Microbiol* 40:310–314. <https://doi.org/10.1007/s002849910062>
- Lal R (2020) Managing soils for resolving the conflict between agriculture and nature: the hard talk. *Eur J Soil Sci* 71:1–9
- Leiber-Sauheitl K, Fuß R, Voigt C, Freibauer A (2014) High CO₂ fluxes from grassland on histic Gleysol along soil carbon and drainage gradients. *Biogeosciences* 11:749–761. <https://doi.org/10.5194/bg-11-749-2014>
- Loke PF, Kotze E, du Preez CC, Twigge L (2019) Dynamics of soil carbon concentrations and quality induced by agricultural land use in Central South Africa. *SSSAJ Soil Chem* 83(2):366–379. <https://doi.org/10.2136/sssaj2018.11.0423>
- Lorenz K, Lal R, Ehlers K (2019) Soil organic carbon stock as an indicator for monitoring land and soil degradation in relation to United Nations' Sustainable Development Goals. *Land Degrad Develop* 30(7):824–838
- Manzoni S, Chakrawal A, Fischer T, Schimel JP, Porporato A, Vico G (2020) Rainfall intensification increases the contribution of rewetting pulses to soil heterotrophic respiration. *Biogeosciences* 17:4007–4023. <https://doi.org/10.5194/bg-17-4007-2020>
- Manzoni S, Katul G (2014) Invariant soil water potential at zero microbial respiration explained by hydrological discontinuity in dry soils. *Geophys Res Lett* 41:7151–7158. <https://doi.org/10.1002/2014GL061467>
- Mineev VG (2001) Workshop on agricultural chemistry: textbook. State University Publ., Moscow, p 689 (Практикум по агрохимии: Учеб. Пособие, с. 689)
- Marjani A, Jamali M (2014) Role of exchange flow in salt water balance of Urmia Lake. *Dyn Atmos Ocean* 65:1–16. <https://doi.org/10.1016/j.dynatmoce.2013.10.001>
- Moinet GYK, Moinet M, Hunt JE, Rumpel C, Chabbi A, Millard P (2020). Temperature sensitivity of decomposition decreases with increasing soil organic matter stability. *Sci Total Environ* 704:135460. <https://doi.org/10.1016/j.scitotenv.2019.135460>
- Morán-Ordóñez A, Duane A, Gil-Tena A, De Cáceres M, Aquilué N, Guerra CA et al. (2020). Future impact of climate extremes in the mediterranean: soil erosion projections when fire and extreme rainfall meet. *Land Degrad Dev*. <https://doi.org/10.1002/ldr.3694>

- Mukasheva MA (2012) The current state of the soil cover in Karaganda (Современное состояние почвенного покрова города Караганды). http://www.rusnauka.com/11_NPE_2012/Ecologia/6_107686.doc.htm. Accessed 7 Mar 2021
- Nadim F, Bagtzoglou AS, Iranmahboob J (2006) Management of coastal areas in the Caspian Sea region: environmental issues and political challenges. *Coast Manag* 34(2):153–165. <https://doi.org/10.1080/08920750600567226>
- National Research Council (NRC) (1989) Using oil spill dispersants on the sea National. Academy Press, Washington DC. <https://doi.org/10.17226/736>
- O'Callaghan-Gordo C, Orta-Martínez M, Kogevinas M (2016) Health effects of non-occupational exposure to oil extraction. *Environ Health* 15:56. <https://doi.org/10.1186/s12940-016-0140-1>
- Okulik VA (1984) Impact of drainage and agricultural use of land on the quality of natural waters (on the example of the Belarusian Polesye). Doctoral thesis, Moscow
- Oliveira FCC, Ferreira G WD, Souza JLS, Vieira MEO, Pedrotti A (2020) Soil physical properties and soil organic carbon content in northeast Brazil: long-term tillage systems effects. *Scientia Agricola* 77(4): e20180166. Epub 04 Nov 2019. <https://doi.org/10.1590/1678-992x-2018-0166>
- Olsson L, Barbosa H, Bhadwal S et al (2019) Land degradation. In: Shukla PR, Skea J, Calvo Buendia E et al (eds) Climate change and land: an IPCC special report on climate change, desertification, land degradation, sustainable land management, food security, and greenhouse gas fluxes in terrestrial ecosystems. In press
- Pachikina LI (1962) Coastal soils of the Northern Caspian Sea. In *Soil-geographical and reclamation studies in Kazakhstan Alma-Ata Izd. AN Kaz SSR*, p. 190. (Приморские почвы Северного Прикаспия. Академия Наук Казахской ССР, с. 190)
- Pekel JF, Cottam A, Gorelick N, Belward AS (2016) High-resolution mapping of global surface water and its long-term changes. *Nature* 540:418–22. <https://doi.org/10.1038/nature20584>
- Rakhimgaliyeva S, Sukhanberdina L, Yesbulatova A, Alzhanova B (2018) Fertility state of fallow soils of dry steppe zone. *Zemljiste I Biljka* 67(2):48–56. http://www.sdpz.rs/images/casopis/2018/ZIB_vol67_no2_2018_pp48-56.pdf. Accessed 7 Mar 2021
- Reager JT, Gardner AS, Famiglietti JS, Wiese DN, Eicker A, Lo M-H (2016) A decade of sea level rise slowed by climate-driven hydrology. *Science* 351:699–703. <https://doi.org/10.1126/science.aad8386>
- RGP KazGidroMet. <http://kazhydromet.kz/ru/p/obzorosostoaia-vodnoj-poverhnosti-kaspijskogo-mora>. Accessed 7 Mar 2021
- RND (2005) Environmental requirements in the field of protection and use of land resources (including agricultural lands) (Экологические требования в области охраны и использования земельных ресурсов (в том числе земель сельскохозяйственного назначения)). Astana the RK Ministry of Agriculture RND 03.7.0.06-96 Instructions on implementation of the state control over protection and use of land resources (1996) (Инструкция по осуществлению государственного контроля за охраной и использованием земельных ресурсов). Almaty Ministry of Ecology and bioresources of the Republic of Kazakhstan, 25
- Romo-Leon JR, van Leeuwen WJD, Castellanos-Villegas A (2014) Using remote sensing tools to assess land use transitions in unsustainable arid agro-ecosystems. *J Arid Environ* 106:27–35. <https://doi.org/10.1016/j.jaridenv.2014.03.002>
- Rozanov BG (2004) The soil morphology. *Akademicheskij proekt, Moscow*, p 432. (Морфология почв, с. 432)
- Rumpel C, Kögel-Knabner I (2011) Deep soil organic matter—a key but poorly understood component of terrestrial C cycle. *Plant Soil* 338:143–158. <https://doi.org/10.1007/s11104-010-0391-5>
- Sadykov ZhS, Bochkareva VA, Dzhangirants DA (eds) (1978) Soil reclamation conditions in the Volga-Ural interfluves (1979). Alma-Ata Nauka, p 256 (Почвенно-мелиоративные условия Междуречья Урал – Волга. Алма-Ата, Наука, с. 256)
- Salehin M et al. (2018) Mechanisms and drivers of soil salinity in coastal Bangladesh. In: Nicholls R., Hutton C., Adger W., Hanson S, Rahman M, Salehin M (eds) *Ecosystem Services for Well-Being in Deltas*. Palgrave Macmillan, Cham. https://doi.org/10.1007/978-3-319-71093-8_18
- Saljnikov E, Rakhimgaliyeva S, Raymbek A, Tomic S, Mrvic V, Sikiric B, Pachikin K (2018) Effect of fallowing on soil organic matter characteristics on wheat monoculture in arid steppes of northern Kazakhstan. *Zemljiste i Biljka* 64(2):17–26. http://www.sdpz.rs/images/casopis/2015/ZIB_vol64_no2_2015_pp17-26.pdf. Accessed 7 Mar 2021
- Säurich A, Tiemeyer B, Don A, Bechtold M, Amelung W, Freibauer A (2017) Vulnerability of soil organic matter of anthropogenically disturbed organic soils. *Biogeosciences Discuss* <https://doi.org/10.5194/bg-2017-127>. <https://bg.copernicus.org/preprints/bg-2017-127/bg-2017-127.pdf>
- Säurich A, Tiemeyer B, Don A, Fiedler S, Bechtold M, Amelung W, Freibauer A (2019) Drained organic soils under agriculture—the more degraded the soil the higher the specific basal respiration. *Geoderma* 355 (1):113911. <https://doi.org/10.1016/j.geoderma.2019.113911>
- Sjøgaard KS, Treusch AH, Valdemarsen TB (2017) Carbon degradation in agricultural soils flooded with seawater after managed coastal realignment. *Biogeosciences* 14:4375–4389. <https://doi.org/10.5194/bg-14-4375-2017>

- Smirnov LE (2005) Aerospace methods of geographical research. St. Petersburg University, p 348. (Аэрокосмические методы географических исследований, с. 348)
- Soil survey (1959) Moscow AN SSSR, p 346 (Почвенная съемка, Академия наук СССР, с. 346)
- Sokolov IA (2004) Theoretical problems of genetic soil science. Novosibirsk Gumanitarnye tekhnologii, p 288. (Теоретические проблемы генетического почвоведения. Гуманитарные технологии, с. 288)
- Soldatov AS (1956) Soil research in Dagestan. Materials of the Department of Soil Science of Dagestan Branch of the USSR Academy of Sciences 3:5–62
- Szajdak L, Szatyłowicz J (2010) Impact of drainage on hydrophobicity of fen peat-peat-morsh soils. In: Kļavinš M (ed) Mires and Peat. University of Latvia Press, Riga, Latvia, pp 158–174
- Szajdak LW, Jezierski A, Wegner K, Meysner T, Szczepański M (2020) Influence of drainage on peat organic matter: implications for development, stability, and transformation. *Molecules* 25(11):2587. <https://doi.org/10.3390/molecules25112587>
- Tacij YuG (2012) Assessment of soil cover condition in the zone of the Karabash copper smelting plant operation after its modernization. In: Landscape geochemistry and soil geography (to the 100th anniversary of Glazovskaya MA). Reports of the All-Russian scientific conference, 4–6 April MSU, Moscow, pp 317–318
- Tarabay A, Serik A, Baitemirova A, Zhaksylyk T (2019) Contamination of soil by oil spills in Kazakhstan. Project Rep Nazarbayev Univ. <https://doi.org/10.13140/RG.2.2.31233.40802>
- Tecon R, Or D (2017) Biophysical processes supporting the diversity of microbial life in soil. *FEMS Microbiol Rev* 41:599–623. <https://doi.org/10.1093/femsre/flux039>
- Tiemeyer B, Albiac Borraz E, Augustin J et al (2016) High emissions of greenhouse gases from grasslands on peat and other organic soils. *Glob Chang Biol* 22 (2016):4134–4149. <https://doi.org/10.1111/gcb.13303>
- Venkatramanan V, Shah S (2019) Climate smart agriculture technologies for environmental management: the intersection of sustainability, resilience, wellbeing and development. In: Shah S, Venkatramanan V, Prasad R (eds) Sustainable green technologies for environmental management. Springer, Singapore
- Volga-Ural project (1982) Volga-Ural interfluvium as an irrigation object. Nauka, Alma-Ata, p 240. (Междуречье Волга–Урал как объект орошения. Алма-Ата, Наука, с. 240)
- Wang J, Song C, Reager JT, Yao F, Famiglietti JS, Sheng Y, MacDonald GM, Brun F, Schmied HM, Marston RA, Wada Y (2018) Recent global decline in endorheic basin water storages. *Nat Geosci* 11:926–932. <https://doi.org/10.1038/s41561-018-0265-7>
- Wang S, Xu Y (2017) The harm of petroleum-polluted soil and its remediation research. <https://doi.org/10.1063/1.4993039>
- Wiesmeier M, Mayer S, Burmeister F, Hübner R, Kögel-Knabner I (2020). Feasibility of the 4 per 1000 initiative in Bavaria: a reality check of agricultural soil management and carbon sequestration scenarios. *Geoderma* 369:114333. <https://doi.org/10.1016/j.geoderma.2020.114333>
- Williams H, Colombi T, Keller T (2020) The influence of soil management on soil health: an on-farm study in southern Sweden. *Geoderma* 360:114010. <https://doi.org/10.1016/j.geoderma.2019.114010>
- Wood JM (2011) Bacterial osmoregulation: a paradigm for the study of cellular homeostasis. *Annu Rev Microbiol* 65:215–238. <https://doi.org/10.1146/annurev-micro-090110-102815>
- Yashin IM, Shishov LL, Raskatov VA (2000) Soil-environmental research in landscapes. Timiryazev State Agrarian Academy, MSKha, p 558 (Почвенно-экологические исследования в ландшафтах. Государственный Тимирязевский Аграрный Университет, с. 558)
- Zubkova TA, Tashninova LN, Kotenko ME, Tashninova AA (2014) The western pre-caspian plains soils and problem of their using. Electronic Scientific Edition Almanac Space and Time. The Space and Time of The Caspian Dialogue 5.1(2) Web.2227–9490e-aprov_r_e-ast5–1–2.2014.33> (In Russian)



Soil Acidification Patterns Due to Long-Term Sulphur and Nitrogen Deposition and How They Affect Changes in Vegetation Composition in Eastern Serbia

Jelena Beloica, Snežana Belanović Simić,
Dragana Čavlović, Ratko Kadović,
Milan Knežević, Dragica Obratov-Petković,
Predrag Miljković, and Nenad Marić

Abstract

A rapid change in soil chemistry caused by long-term acidic deposition directly and indirectly disturbs natural habitats and ecosystem functions. The aim of this paper was to analyse long-term depositions of sulphur and nitrogen, their relationship with the soil's chemical properties, and areas currently/potentially at risk of ecosystem degradation. Models recommended by the Convention on Long-Range Transboundary Air Pollution (CLRTAP) were applied. Critical Loads calculations were derived for acidification, eutrophication and biodiversity using the VSD model. Changes in plant diversity and soil properties of beech forests and highland grasslands were simulated using the VSD + PROPS model based on future air pollution and RCP 4.0 climate scenarios. The results showed areas and biological receptors with varying degrees of vulnerability and susceptibility to air pollutants, as well as identifying areas that are adversely affected by

the long-term deposition of sulphur and nitrogen. Mountain forests and high mountain grasslands developed on shallow soils exhibit the highest levels of sensitivity to acidic pollutants and climate change in Eastern Serbia. To provide a background for interpreting the results of the comparative analysis on air pollution and climate change effects at regional level, process-based and spatial distribution modelling were used. Estimated critical loads on both a regional and local level indicate ecosystems' sensitivity and potential risk of degradation, providing a good basis for planning emission reduction on a regional level and evolving adaptive management measures in situ.

Keywords

Soil acidification · Air pollution · Critical loads · Climate change · Biodiversity

J. Beloica (✉) · S. Belanović Simić · D. Čavlović ·
R. Kadović · M. Knežević · D. Obratov-Petković ·
P. Miljković · N. Marić
Faculty of Forestry, University of Belgrade, Kneza
Višeslava 1, 11030 Belgrade, Serbia
e-mail: jelena.beloica@sfb.bg.ac.rs

34.1 Introduction

Acidification is a process of decreasing soil pH value over time as a result of numerous biogeochemical processes (Boruvka et al. 2007). Anthropogenic factors, excessive emissions of sulphur and nitrogen, inadequate ecosystem

management, land use changes and global climate change cause a significantly accelerated and intensified acidification process which can be seen as a form of soil degradation (Johanston et al. 1986; Sverdrup and Vries 1994). Soil acidification induced by the deposition of sulphur and nitrogen is considered as a global environmental problem due to the negative effects it has had on natural ecosystems and biodiversity loss in the past 70 years.

The negative effect of air pollution emitted from burning processes in densely populated cities and its negative effects for human health and vegetation have already been described since the mid-seventeenth century in England (Evelyn 1661; Graunt 1665). In the industrial age, smoke, acid rain and their impacts on ecosystems in Europe rapidly increased (Ducros 1845; Smith 1852) due to the rising use of coal. The acidification of terrestrial ecosystems has been studied more intensively since the 1970s (Odén 1968; Gorham 1976; Ulrich et al. 1980), when the negative consequences of air pollutants were evident on a large scale (deforestation, acidification of lakes and loss of fish in Northern Europe). Thus, in 1977, under the Convention on Long-Range Transboundary Air Pollution (CLRTAP), a programme for monitoring and evaluation of air pollutants was developed, named the European Monitoring and Evaluation Programme (EMEP), and the issue became a subject of international political concern.

Under the LRTAP convention, the “Critical Loads” methodology was developed to quantify the environmental impact of pollution and to provide exact guidelines for reducing air pollutant emissions. This concept can be considered as a tool for the integrated monitoring of air pollution effects on ecosystems and a great contribution to international environmental law and national clean air policies. Critical Loads (CLs) have been defined as “the highest load of pollutants that will not cause chemical changes leading to long-term harmful effects in the most sensitive ecological systems” (Nilsson and Grennfelt 1988) and provide a useful approach for dealing with the problem of acid (S and N) and heavy metal (Pb, Hg, Cd) deposition.

To reduce acidification and other negative effects of air pollutants under the UNECE (The United Nations Economic Commission for Europe) programme and the LRTAP Convention, to predict how terrestrial ecosystems would respond to global changes and establish mitigation policies, a long-term observation database was required. Thus, ICP Forests (a monitoring programme) was launched. The ICP Forest monitoring is based on around 6000 observation plots (16×16 km grids) across Europe and around 500 plots in selected forest ecosystems to determine cause–effect relationships. At present, 42 countries participate in ICP Forests.

This paper used the methodology proposed by the ICP Modelling and Mapping programme (CLRTAP 2015, 2017) in the framework of CLRTAP to define how sensitive forest ecosystems and highland grasslands are to acidification and eutrophication processes caused by S and N depositions. The objectives of the ICP Modelling and Mapping are to determine and map receptor-specific critical loads and excess concentrations of various air pollutants, as well as establishing appropriate methods for assessing potential damage, e.g. via dynamic modelling (UNECE).

The effects of interactions between air pollution and climate change on biodiversity are currently being enhanced and improved using the *Critical Loads for Biodiversity* indicator (Hetteling et al. 2014). These assessments could help support the multi-effect policies that are jointly formulated under the UN Conventions and EU strategies on air pollution, the climate and biodiversity. Several studies have been carried out taking into account how interactions between air pollution and climate change affect soil dynamics and vegetation structure change (Rizzetto et al. 2016; Dirnböck et al. 2017, 2018; Holmberg et al. 2018). These studies confirmed that when climate change is included in the scenario analysis, the variability of the results increases (Holmberg et al. 2018; Dirnböck et al. 2018).

The aim of this study was to assess forest and highland grassland sensitivity to acidification and nitrogen-caused eutrophication in Eastern Serbia. The VSD + PROPS (Bonten et al. 2016) model

was used to assess critical loads for biodiversity and to simulate the combined effects of atmospheric acid deposition and climate change on soil chemistry and habitat suitability change for beech forest and highland grasslands. Spatial distribution modelling was also performed for long-term shifts in forest-grassland habitats in the Balkan Mountains (Stara Planina).

34.2 Study Area

Eastern Serbia covers 20,005 km² or 22.63% of the territory of the Republic of Serbia. The research area contains 43 protected natural areas (about 10% of the total area), characterised by significant values of flora and fauna diversity. This includes relict and endemic species and their communities in particular. They therefore require a special regime of monitoring and protection.

The Stara Planina nature park (the protected area with the largest spatial coverage in Eastern Serbia) was selected for the assessment of *Critical Loads for biodiversity*, and of the combined effects of atmospheric acid deposition and climate change on habitat suitability change in beech forest and highland grasslands. The forest

line and treeline ecotones were selected because they are widely considered to be habitats that are sensitive to changes in the climate and other abiotic and biotic factors (Fig. 34.1). The vegetation of Stara Planina is characterised by a diversity of forest shrub, grassland and pasture communities, including peat bogs, making it one of the centres of floristic diversity in the Balkan Peninsula. A total of 147 endangered and endemic species have been recorded in this area.

34.2.1 Parent Material Weathering—lithological Composition

Mineral weathering is a main source of long-term buffering capacity in soils (Sverdup and Warfvinge 1988). Base cation weathering is important for soil fertility and long-term sustainable forest management, and is important to mitigate the soil acidification process in the case of high acid deposition or intensive harvesting (Koseva et al. 2010).

The geological structure of the study area is very complex, resulting from a long and varied geological history. According to Filipović et al. (2005), the study area features three geotectonic

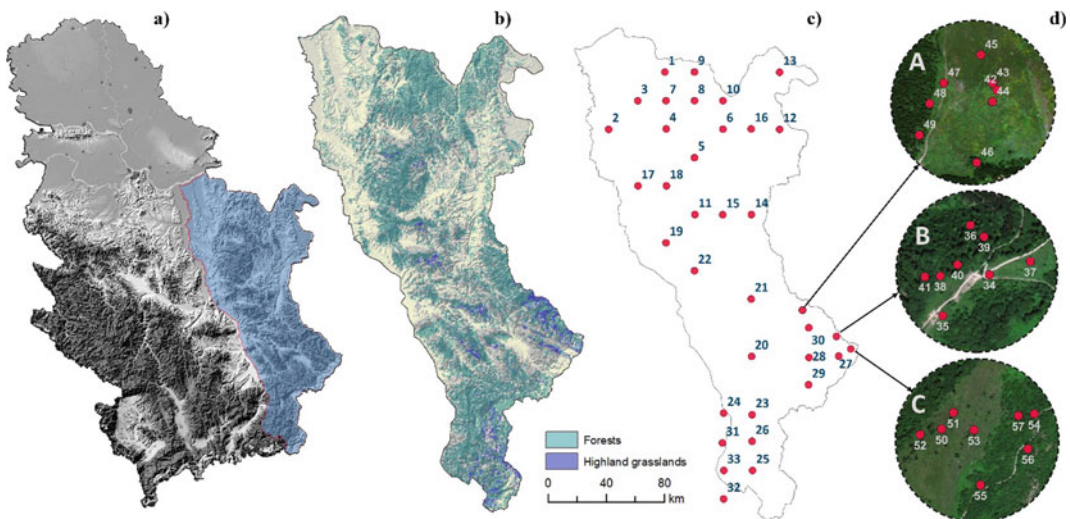


Fig. 34.1 Study area: **a** Eastern Serbia; **b** forest and highland grasslands; **c** soil sampling plots; **d** soil and vegetation sampling plots A, B, C treeline ecotone sites (from left to right) (Beloica et al. 2015)

Table 34.1 Classification and distribution of soil parent material in the study area, according to FAO (2006) methodology

Rock type/consolidation degree	Geochemical character/rock genesis	Dominant rock type	Proportion (%)
Igneous rock	Igneous—acid	granite, rhyolite	6.62
	Igneous—intermediary	andesite, dacite	1.24
	Igneous—basic	gabbro, diabase	1.86
	Total		9.72
Sedimentary rock	Sedimentary—clastic consolidated	sandstone, claystone	25.81
	Sedimentary—clastic unconsolidated	gravel, sand, clay	13.07
	Sedimentary—calcareous and organic	limestone, dolomite	20.70
	Total		59.58
Metamorphic rock	Metamorphic—foliated	schist, phyllite	30.49
	Metamorphic—non-foliated	marble, serpentinite	0.19
	Total		30.68
Anthropogenic material	Heterogeneous technogenic material	/	0.02
	Total		0.02

units of differing genesis: The Dacian Basin, the Carpatho-Balkanides and the Serbian Crystalline Core Region. The lithological constituents were analysed using the Basic Geological Map of Yugoslavia on a scale of 1:100.000, compiling data from sheets depicting the study area. The percentage of the different rock types' distribution and their classification according to the FAO (2006) methodology for soil parent material are given in Table 34.1.

Most of the study area consists of sedimentary rocks (59.58%). The proportion of metamorphic and igneous rocks is much lower (30.68% and 9.72%, respectively). Anthropogenic material (mine dumps and landfills) covers about 0.20% of the study area. In sedimentary rocks, consolidated clastics are dominant (25.81%), followed by calcareous and organic sediments (20.7%) and unconsolidated clastic sediments (13.07%). Foliated metamorphic rocks (30.49%) outnumber non-foliated rocks (0.19%). Within igneous formations, acid rocks dominate (6.62%), followed by basic magmatic rocks (1.86%) and intermediate magmatic rocks (1.24%).

34.2.2 Soil Types

Eastern Serbia was allocated for the analysis due to the acid soils (Dystric Cambisol, Dystric Rankers, Regosols) with a very low buffer capacity which occupies 43% of the area. An extremely low soil pH was measured in the Bor District (Košanin and Knežević 2005). In this area, significant negative effects of acid deposition have been recorded in the past 30 years due to the copper mine operation in Bor.

Table 34.2 shows the most common soil types under forest and highland grasslands in eastern Serbia, according to the Pedological Map of Serbia (R 1: 50,000) based on FAO classification (1974):

34.2.3 Vegetation

In this study, vegetation structure change was simulated for beech forest and highland grasslands. Beech forest is the most widespread forest type both in Serbia as a whole and in Eastern

Table 34.2 The main soil types of eastern Serbia under forests and highland grasslands

Soil type_FAO74	Proportion (%)
Cambisol	34.98
Rendzina	17.96
Ranker	15.00
Lithosol	7.77
Regosol	7.76
Luvisol	7.40
Vertisol	5.40
Other soil types	4.10

Serbia. At sites A and C, a community of mountain beech forests is recorded (*Fagetum moesiacaе montanum* B. Jov. 1953), EUNIS (The European Nature Information System 2020; Srbije 2005) type G1.69. The *typicum sub-association* is present with two facies, *nudum* and *asperulosum*, both at altitudes of 1280–1290 m. The *nudum* facies was recorded on a western exposure and 15–20° slopes. It is characterised by poor plant species of ground flora. The *asperulosum* facies was recorded on a north-western exposure and slopes of 25–30°. At site B, the association *Fagetum moesiacaе subalpinum* Greb. 1950 was recorded (EUNIS G1.69).

Highland grasslands: Association *Agrostietum vulgaris (capillarıs)* Pavlović 1955. (EUNIS E1.7) in Stara Planina is the dominant type of grasslands and thus is widespread. The community *Agrostietum vulgaris* is characterised by considerable floristic richness. The number of species in the study sites in this community is similar (89 species at site A, 88 species at site B and 93 species at site C, Fig. 34.1). This community has a secondary anthropogenic origin as a result of two factors: a reduction in forest area on the one hand and cutting on the other.

34.3 Methods

The system of models and data sets used is shown in Fig. 34.2. Critical loads and excesses of air pollutants are one of the main indicators of a forest and terrestrial ecosystem's sensitivity to acidification, eutrophication and biodiversity

change. In this paper, Critical Loads were assessed according to the ICP M&M methodology (CLRTAP 2015, 2017) using **VSD + PROPS** dynamic models (Version 5.6.3, Bonten et al. 2016) developed by the Working Group on Effects (WGE) and the Coordination Center for Effects (CCE) under the LRTAP convention. The methodology is based on the soil microbial biomass (SMB) concept, calculating fluxes of base cations (deposition, weathering from parent material, plant uptake), H⁺ and Al³⁺ ions in soil solution.

Process-based single-site modelling

The **VSD + Studio** model (Version 5.5.1; Bonten et al. 2016) is a dynamic single-layer biochemical soil model specifically made to calculate how the deposition of nitrogen (N) and sulphur (S) affects soil acidification and eutrophication on a regional/national scale (Reinds et al. 2014). In conjunction with the VSD + model, two pre-processing models were used: MetHyd and GrowUp. MetHyd (v1.5.1; Alterra, CCE), a meteo-hydrological model, was used to calculate the daily evapotranspiration, soil moisture and percolation (runoff) and parameters related to (de)nitrification and mineralisation. The GrowUp model (v1.3.2, Alterra, CCE) was used to compute N and base cation uptake from specific data on tree growth and forest management.

Chemical criteria for the assessment of Critical Loads for acidification were selected on the basis of a combination of laboratory studies (Sverdrup and Warfinge 1993) on terrestrial ecosystems and individual plant species. For

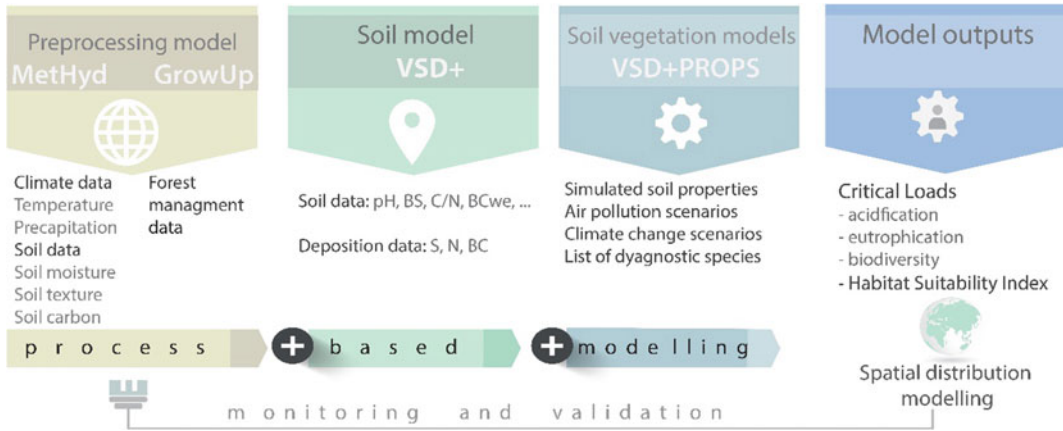


Fig. 34.2 Graphic scheme of models and data sets used (orig.)

beech forest soils, the threshold selected is the molar ratio of the concentration of base cations (Ca, Mg and K) and aluminium (Al) of $BC/Al = 0.6$, and $BC/Al = 2$ for the grasslands.

A **PROPS** module (v.5.5.1.; Alterra, CCE) was used to analyse changes in ground vegetation cover. This model was developed as a means of assessing changes in plant species diversity caused by changes in air pollution and climate, and computing critical loads of sulphur and nitrogen for biodiversity (Reinds et al. 2015). The PROPS model estimates the probability of plant species occurrence as a function of abiotic conditions such as the soil pH and C:N ratio, and climatic variables such as temperature and precipitation. The model uses an aggregate indicator for species occurrence in a habitat known as the Habitat Suitability Index (HSI) (Rowe et al. 2016). The HS index is defined as the arithmetic mean of the “normalised” probabilities (possibilities) of the species of “interest” occurring (Posch et al. 2014). The selection of suitable species is crucial, as proposed within the model (Reinds et al. 2014). The selected species should be “typical”, “desired”, or “diagnostically important species” for the respective habitat for computing HS indices (Reinds et al. 2014). The vegetation change was simulated and Critical Loads for biodiversity were calculated for beech forest and grasslands of the forest line and

treeline ecotone on the Stara Planina area: areas sensitive to acid deposition.

Spatial distribution modelling

The **Maximum Entropy model—MaxEnt** Version 3.4.1 (Phillips et al. 2020) was used to model the species distribution. Besides the bioclimatic variables listed above, the altitude and soil pH were used as environmental variables. The dominant species for beech forest *Fagus moesiaca*, and for *Agrostis capillaris* grasslands were selected for the modelling, and 24 presence points were included in this analysis in total.

34.4 Materials

34.4.1 Air Pollution Data

Nitrogen (N) and sulphur (S) deposition data (1980–2015) were obtained from the database of the European Monitoring and Evaluation Programme (EMEP) model results, using data from the grid cell corresponding to the analysed location (https://www.emep.int/mscw/mscw_moddata.html). Data on base cation deposition were also obtained from the EMEP database (throughfall data). Scenario analyses of N and S deposition effects were run with the presumption that deposition would maintain its current trend (the average value for the last 10 years), in

conjunction with the A1B climate scenario (Nakićenović et al. 2000).

34.4.2 Climate Data

The Coupled Regional Climate Model, EBU-POM (Djurdjevic and Rajkovic 2008; Kržič et al. 2011) was used for the climate simulations for the 2001–2100 period. The EBU (Eta Belgrade University) model and the POM (Princeton Ocean Model) were calibrated with the E-OBS data set for the exact location (Stara Planina). For analysing climate changes, the Special Report on Emissions Scenarios (SRES) was used. The IPCC (Intergovernmental Panel on Climate Change) emissions scenario A1B (Nakićenović et al. 2000) was selected mainly because of its moderation in climate change predictions; it relies on the balanced use of all energy sources.

Climate change simulation—EBU-POM model—A1B scenario

Comparing the reference data from the 2nd half of the 20th century and projected data for the middle of the 21st century, there is a considerable decrease in annual precipitation (−115.95 mm), and an even more serious increase in annual temperature (4.64 °C). Even more important is the change in the temperature and the distribution of precipitation during the year, especially in the vegetation period. The dry period (June–October) with high average temperatures (July–September) is likely to seriously disturb mountain vegetation after 2071. The simulation of future precipitation gives ambiguous results. The projected values indicate that precipitation will be inconsistent and unpredictable. By contrast, in 2001–2100, the temperature increment is very clearly noticeable (Table 34.3).

Bioclimatic variables

To model the species distribution, ten bioclimatic variables (BIO1, BIO5, BIO6, BIO10, BIO11, BIO12, BIO13, BIO14, BIO16 and BIO17) from WORLDCLIM database (WORLDCLIM 2020) (<https://worldclim.org/data/index.html>) were used, taking into consideration climate scenario RCP 4.0 (corresponding to SRES A1B). Those particular variables were selected after the model fitting.

Changes in climate were analysed by comparing the variables from normal periods in 1961–1990 from the Republic Hydrometeorological Service of Serbia database (RHMSS 2020) with their projected values in 2071–2100 (EBU-POM) (Table 34.3). A time series of the variables for the 1980–2100 period was used as an addition to MetHyd model, for the VSD + Studio model run.

34.4.3 Soil and Vegetation Data

The assessment of forest and highland grasslands' sensitivity to air pollution was based on soil sampling plots of the ICPF (International Co-operative Programme on Assessment and Monitoring of Air Pollution Effects on Forests), examining Level I monitoring data (long-term forest monitoring sites), additional sampling on Stara Planina, and geospatial data on soil and other characteristics of forest and highland grassland ecosystems in Eastern Serbia (Fig. 34.1). For the Republic of Serbia, soils were sampled by the Faculty of Forestry University of Belgrade and the Institute of Forestry of Serbia (ICPF_RS 2020) in 2003 and 2013 on 33 ICPF bioindication plots in Eastern Serbia. An additional 24 samples were taken from the grassland (12 plots in beech forests and 12 on grassland areas) in 2003 (A, B and C site Fig. 34.1) (Belanović 2007; Beloica 2015). The soil samples were taken from depths of 0–10 cm and 10–20 cm. Figure 34.4 shows the main soil properties: the pH, base saturation soil C/N ratio and correlation between pH and Al concentrations.

The vegetation was analysed at three sites (A, B, C) on the Stara Planina using the Braun–Blanquet (1964) phytocoenological method (Belanović 2007; Beloica 2015). When defining diagnostically important species for the model simulations, two criteria were used: (1) site-dominant species (2) species that are defined as diagnostically important for certain habitats according to the EUNIS habitat classification (<https://www.eea.europa.eu/data-and-maps/data/eunis-habitat-classification>).

Table 34.3 Temperatures and precipitation in reference 30-year period (1961–1990) and model predictions for A1B scenario, 2001–2100 and 2041–2060 and 2071–2100

STARA PL	Jan	Feb	Mar	Apr	May	Jun	Jul	Aug	Sep	Oct	Nov	Dec	Annual	
Temperature °C	MODEL (2001–2100)	-1.89	0.92	4.10	9.07	13.55	17.67	20.21	19.41	15.21	9.54	3.6	-0.1	9.27
	MODEL (2041–2060)	-0.14	2.14	6.75	11.5	15.19	19.68	21.45	21.08	17.82	12.38	7.72	2.21	11.48
	MODEL (2071–2100)	0.24	2.36	5.03	10.26	14.88	19.09	22.55	20.96	16.6	10.85	5.09	1.61	10.79
	RHMS (1961–1990)	-3.83	-1.93	1.94	6.42	11.49	15.04	16.91	16.64	12.66	7.55	1.29	-2.05	6.84
Precipitation mm	Δ	3.69	4.07	4.81	5.08	3.70	4.64	4.54	5.16	4.83	6.43	4.26	4.64	
	MODEL (2001–2100)	35.73	25.83	40.45	52.03	60.20	64.59	55.50	40.26	33.12	42.59	48.93	40.40	539.64
	MODEL (2041–2060)	33.58	28.34	27.43	53.53	61.75	53.55	48.32	29.07	21.06	40.57	44.32	48.15	489.66
	MODEL (2071–2100)	30.69	28.7	46.49	55.07	58.54	57.7	42.12	38.34	28.22	42.52	53.09	38.33	519.83
	RHMS (1961–1990)	33.95	28.78	40.89	57.72	80.98	75.50	64.27	40.53	46.83	44.10	51.72	40.36	605.61
Δ	-0.37	-0.44	-13.47	-4.19	-19.23	-21.95	-15.95	-11.46	-25.77	-3.53	-7.40	7.79	-115.95	

Δ—difference between 2041–2060 period and 1961–1990 period

34.5 Results

34.5.1 Parent Material Weathering Rates

Parent material weathering rates were calculated according to the ICP M&M Manual (CLRTAP 2017). The highest values for BC-we (base cation weathering) corresponded to the terrains on the sedimentary rocks, primary calcareous and organic sediments (limestone and dolomite). The lower BC-we values corresponded to the magmatic (andesite, dacite, gabbro), with the lowest values observed in terrains made of acid rocks (granite) (Fig. 34.3).

34.5.2 Soil Properties

The main soil properties affected by acid deposition (pH, base saturation soil C/N ratio, Al concentration) are shown in Fig. 34.4. The Group 1 box plot shows all measured values for forests and grasslands. Group 2 and Group 3 present forest data taken in two-time Sections (2003 and 2013) for the same location plots. For these two groups, it can be seen that that pH and BS values are lower in 2013 than in 2003. Group 4 represents separated grassland plots. In comparison with forest sites, those soils have a narrower pH range and significantly lower base saturation. Figure 34.4d represents pH trigger values (pH 4.2–4.3) taking into account the increase in the Al concentration and potential plant toxicity.

34.5.3 Acid Deposition Trend and Critical Loads Assessment

34.5.3.1 Sulphur, Nitrogen and Base Cation Deposition Trends

Acid deposition (1980–2015): According to the EMEP MSC-W database (the EMEP's Meteorological Synthesizing Centre–West), sulphur and nitrogen deposition data for eastern Serbia

indicate that different amounts of deposition occurred on an annual and cumulative basis (Fig. 34.5).

For the 1980–2015 period, areas with the greatest amount of sulphur deposition were recorded in the Bor basin (384–496.4 kg ha⁻¹) and the Stara Planina (384–432 kg ha⁻¹). The highest annual deposition of sulphur in the study area was 30.4–33.6 kg ha⁻¹, measured in the 1980–1985 period. From 1990, the amount of sulphur deposition decreased. For the 1980–2015 period, the deposition of sulphur decreased by about 53–57%, and in the 2000–2015 period, the deposition decreased by 22–30%.

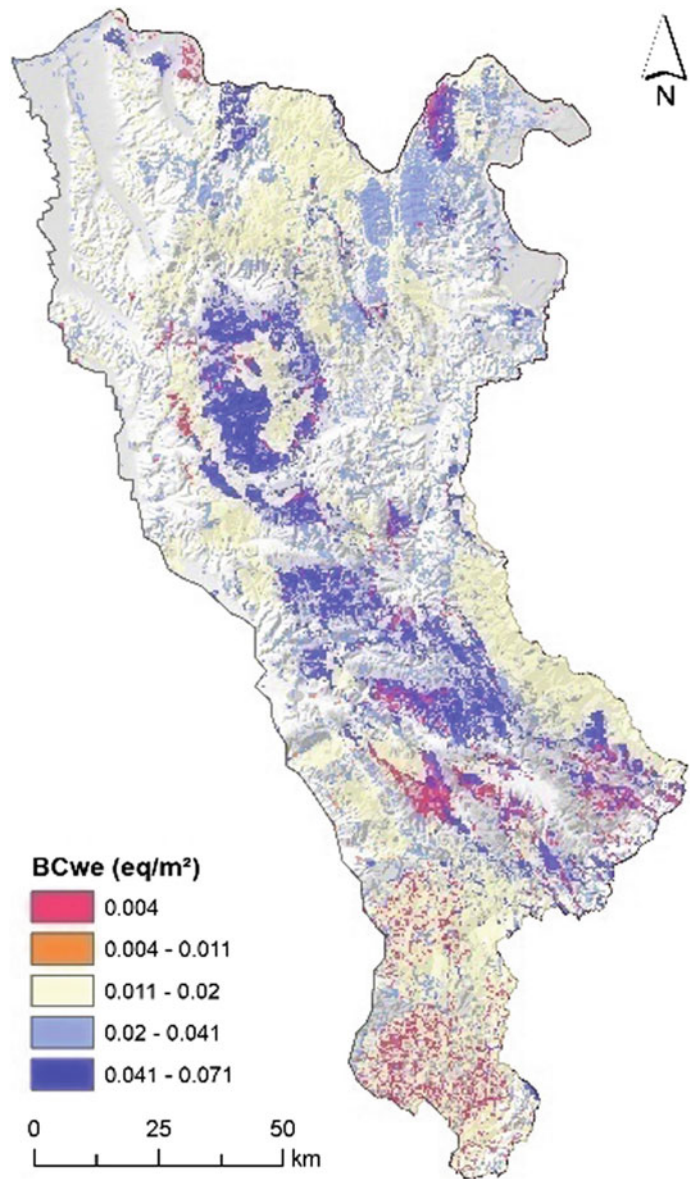
For the 1980–2015 period, the areas with the highest cumulative values for the deposition of the reduced and oxidised forms of nitrogen were characteristic for the wider area of Majdanpek and Bor and amount to 228.9–248.9 kg ha⁻¹. The high values for oxidised nitrogen occurred in the Niš region, and those for the reduced form of nitrogen in the Stara Planina area. In the 1980–2015 period, the nitrogen distribution mainly decreased. However, eastern Serbia is characterised by an increase in nitrogen deposition (ammonium form) by 22–30%.

Base cation deposition (1984–2015): According to the EMEP database for the 1980–2015 period, the highest deposition of base cations (Ca, Mg, K) was recorded in 1991 (0.24 eq m⁻²) and the deposition of base cations has decreased since 1993 (Fig. 34.6).

34.5.3.2 Critical Loads for Sulphur and Nitrogen Deposition: Forests and Highland Grasslands

The terrestrial ecosystems most sensitive to air pollution with sulphur and nitrogen were found to be the high mountain grasslands of Stara Planina and the highland grasslands in the south of the study area. The most sensitive soils (the lowest Critical Load values) were recorded in grassland sites on Dystric Rankers and Dystric Cambisols. The lowest Critical Load values (S) for the specified area range from 459.44–658.6 eq ha⁻¹ (7.36–10.54 kg ha⁻¹) (Fig. 34.7).

Fig. 34.3 Base cation weathering (BCwe) rates



The maximum excess of sulphur relates to the alpine grassland zone in the east and southeast of Serbia and amounts to approximately 1200 eq ha⁻¹ (19.2 kg ha⁻¹) in the 1980–1985 period. From 1985, the indicators declined until 2003–2004, and have risen to 400 eq ha⁻¹ (6.4 kg ha⁻¹) since 2004.

The excess nitrogen in relation to soil acidification which occurred during the 1980–1995 period was about 9 kg ha⁻¹, while an excess of nutrient nitrogen was present throughout the entire observed period from 1980–2015 (Fig. 34.8).

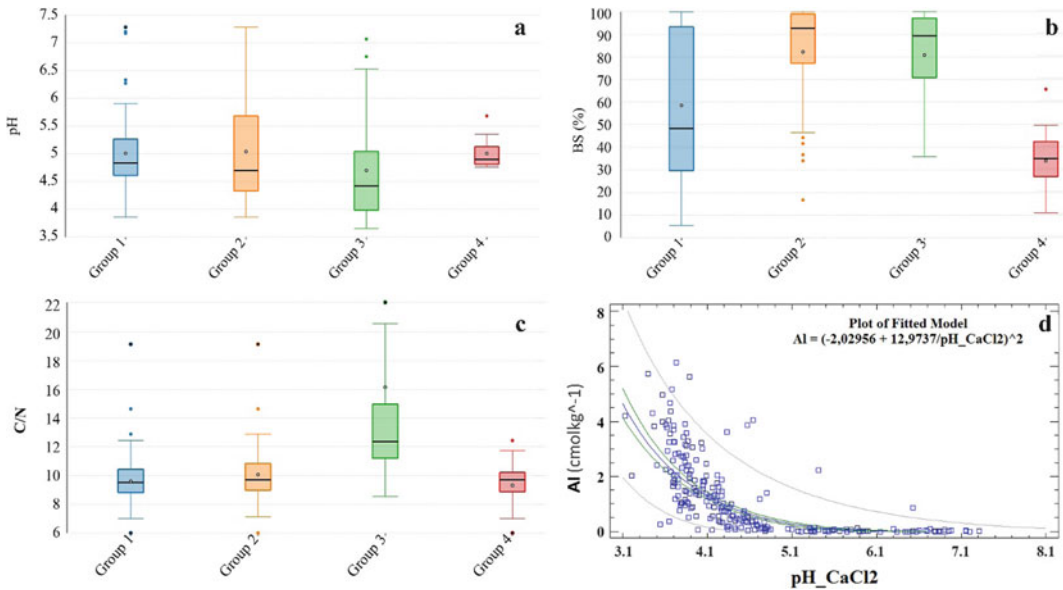


Fig. 34.4 Main soil properties a) pH (measured in CaCl_2), b) BS% (base saturation), c) C/N ratio, d) Al cmol kg^{-1} in relation with pH; Group 1—forest and grassland soil data for a depth of 0–20 cm; Group 2—

ICPF data for eastern Serbia, 2003; Group 3—ICPF data eastern Serbia, 2013; Group 4—soil grassland data for a depth of 0–20 cm (cmol kg^{-1})

The excess of nitrogen was calculated based on CL_{nut} N derived from the soil solution criterion (SMB approach). The largest excess of nutritive nitrogen relates to the highland grasslands areas in the 1980–1985 period, with 650 eq ha^{-1} (9.1 kg ha^{-1}). The 1985–2008 period was characterised by a decrease in excess nutritive nitrogen, while from 2008–2014 the excess was up to 400 eq ha^{-1} (5.74 kg ha^{-1}).

34.5.3.3 Critical Loads for Biodiversity and Habitat Suitability Change

In order to compare empirical critical loads of nitrogen (Table 34.4; Bobbink and Hettelingh 2011) and critical loads for biodiversity (Table 34.5), the PROPS-CLF model (CCE; Posch 2016) was applied. Using the species response functions, PROPS, the CLs for beech forest habitat types were higher than the empirical CLs and mass balance CLs for N. For grasslands, the values are slightly below or above the given empirical range.

34.5.3.4 Combined Effect of Acid Deposition and Climate Change on Habitat Suitability of Beech Forest and Highland Grassland

Dynamic model using HSI single site analyses:

The HSI was used as a measure of the influence of future climate changes (A1B scenario) and nitrogen input on the quality of habitat that might affect species occurrence. Habitat suitability simulations were performed for two sets of variables. The first simulations were run for the pH and N_{dep} (nitrogen deposition) and the second for the pH, N_{dep} and soil C:N ratio (Fig. 34.10). The beech forest sites in this treeline ecotone exhibited a different trend when different sets of variables applied. The HSI decreased when the species occurrence probability was added as a function of pH and N_{dep} , and there was a strong increment in the case of site “C” (Figs. 34.1 and 34.9).

The HSI for highland (dry) grasslands increases until the end of the simulation period

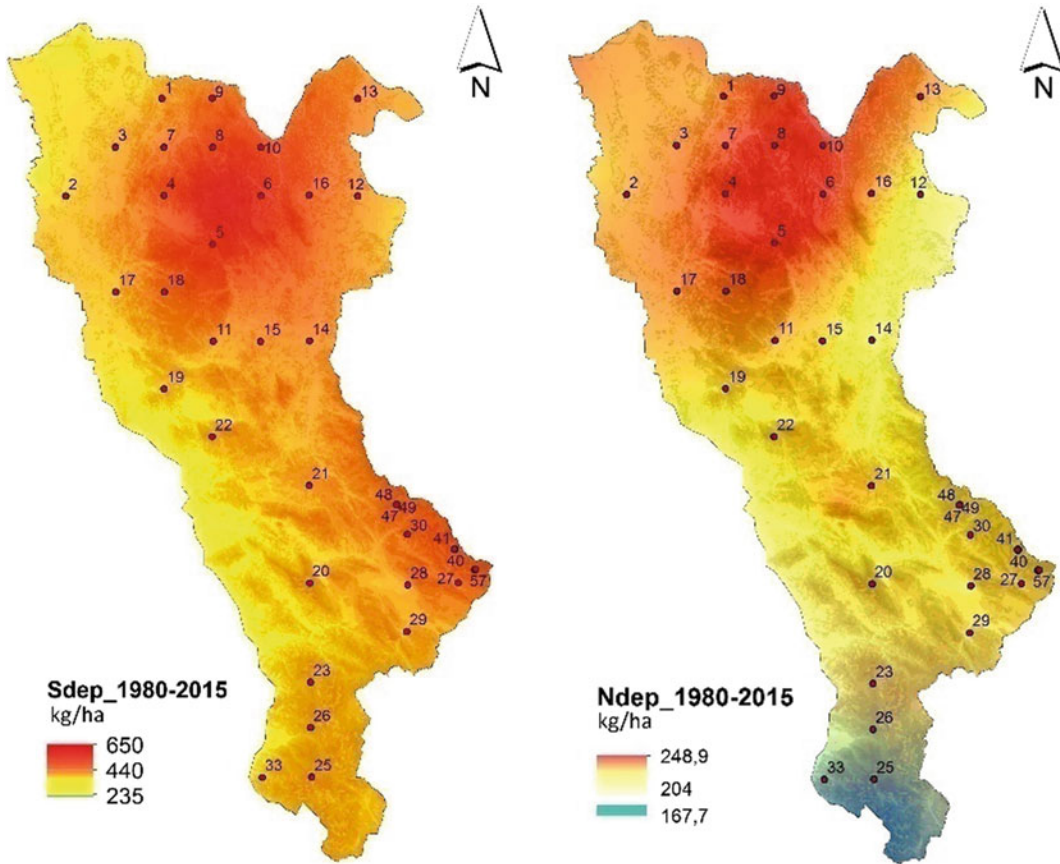
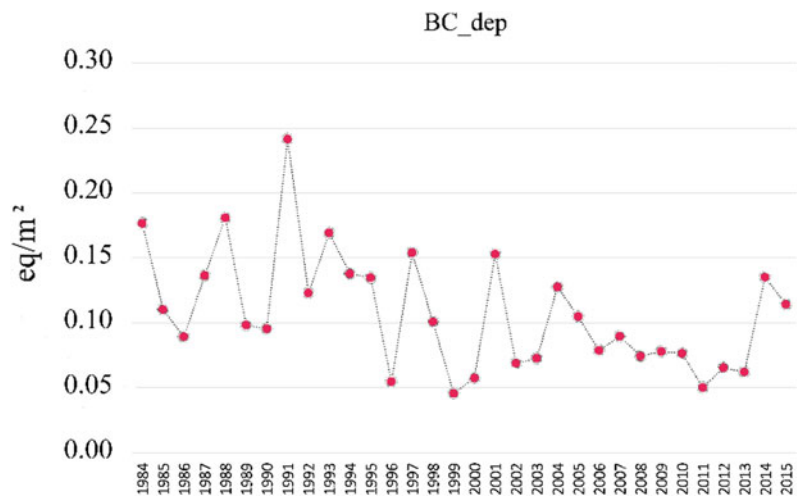


Fig. 34.5 Cumulative depositions of sulphur (S_{dep} , left) with highest amounts in the Bor district (ICPF plots 4, 5, 6, 7, 8, 9, 10) and Stara Planina (plots 30, 40, 41, 48, 49, 57) and total nitrogen deposition (N_{dep} , right) with the highest amounts in the Bor district (ICPF plots 4, 5, 6, 7, 8, 9, 10) for the 1980–2015 period based on EMEP data

Fig. 34.6 Base cation deposition for 1984–2015 period. *Source* EMEP



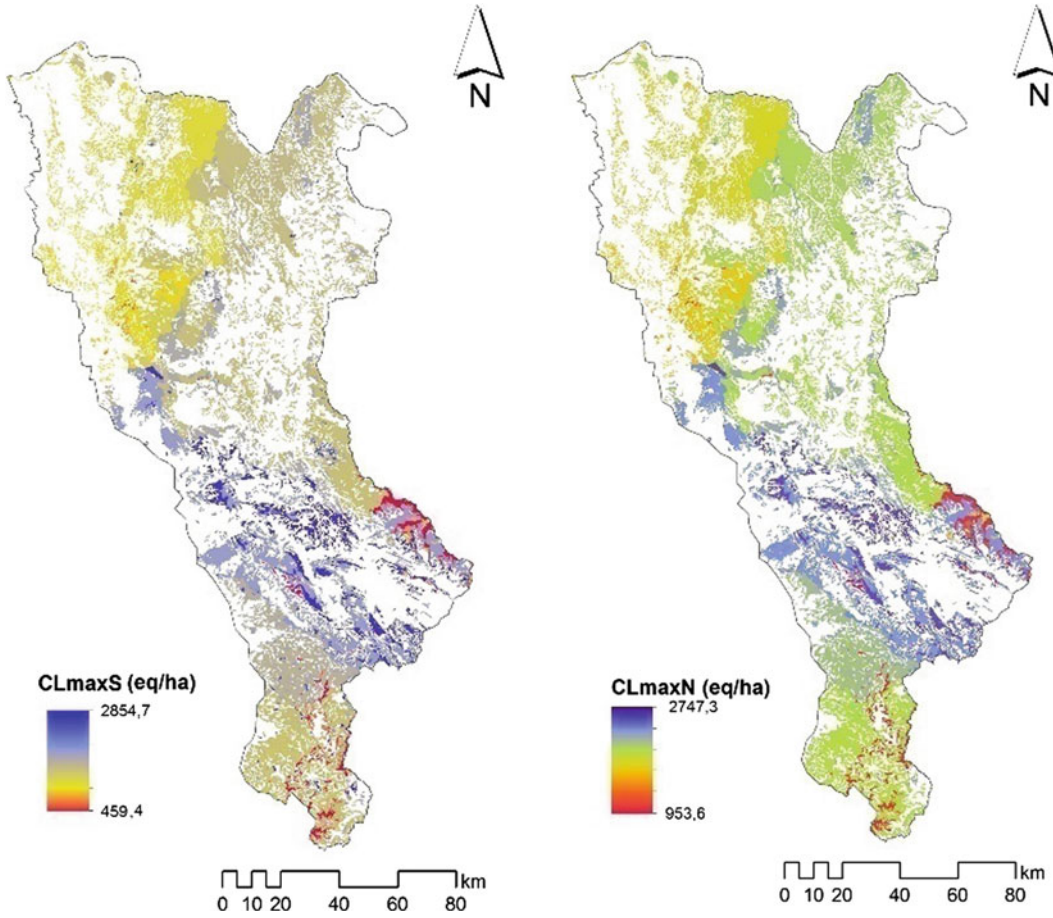


Fig. 34.7 Critical Loads for acidification of sulphur (left) and nitrogen (right) (Beloica 2015)

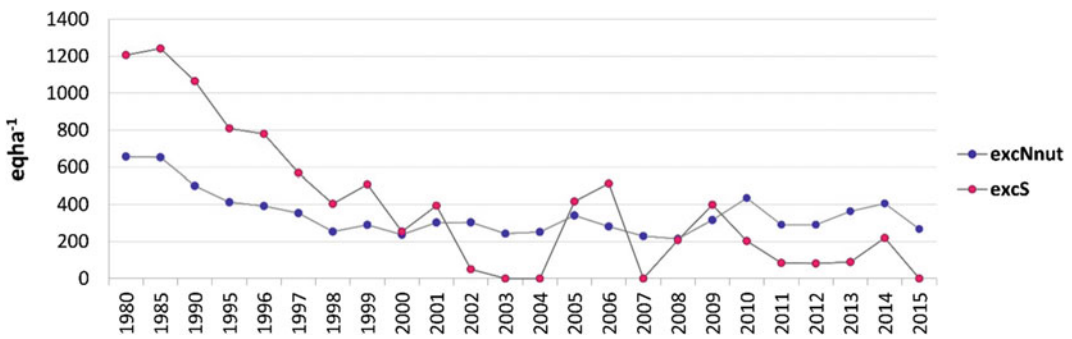


Fig. 34.8 The trend of maximum excess per year of sulphur and nitrogen for forest and highland grasslands in Eastern Serbia

(2100) when both sets of variables are run (Fig. 11). For the first set of variables, the HSI increased from 0.18–0.44, and for second set the

HIS exhibited a larger increment from 0.3–0.87. This result is due to the fact that the pH values and N deposition are at the lower limit for beech

Table 34.4 Overview of the empirical critical loads of nitrogen deposition ($\text{kg N ha}^{-1} \text{ yr}^{-1}$) for forest and grassland ecosystems (column 1), classified according to EUNIS (column 2), as originally established in 2003 (column 3), and as revised in 2010 (column 4). The reliability is qualitatively indicated by ##—reliable; #—quite reliable and (#)—expert judgement (column 5). Column 6 provides a selection of effects that can occur when critical loads are exceeded (Bobbink and Hetteling 2011)

Ecosystem type	EUNIS code	2003 $\text{kg N ha}^{-1} \text{ yr}^{-1}$	2010 $\text{kg N ha}^{-1} \text{ yr}^{-1}$	Indication of excess
Fagus woodland	G1.6	–	10–20 (#)	Changes in ground vegetation and mycorrhiza, nutrient imbalance, changes in soil fauna
Non-Mediterranean dry acid and neutral closed grassland	E1.7a #	10–20 #	10–15 ##	Increase in graminoids, decline in typical species, decrease in total species richness

Table 34.5 Overview of environmental habitat suitability drivers (pH, C:N ratio) and critical loads for biodiversity of sulphur and nitrogen deposition [kg ha^{-1}], based on the PROPS-CLF model for forest and grassland ecosystems, using two different lists of plant species: EU habitat proposed diagnostic-constant list of species and the list of the most frequent species recorded on site

PROPS model HSI drivers	Forests G1.692		Grasslands E1.742	
	EU habitat species	Recorded species	EU habitat species	Recorded species
pH	4.7–5.9	4.7–6.4	3.8–4.8	5.6–7.2
C:N	16.2–18	16.2–17.5	17.5–22	8–11
N	11–29 [kg ha^{-1}]	11–24 [kg ha^{-1}]	5–12 [kg ha^{-1}]	7–17 [kg ha^{-1}]
S	– [kg ha^{-1}]	17–24 [kg ha^{-1}]	4–8 [kg ha^{-1}]	4–8 [kg ha^{-1}]

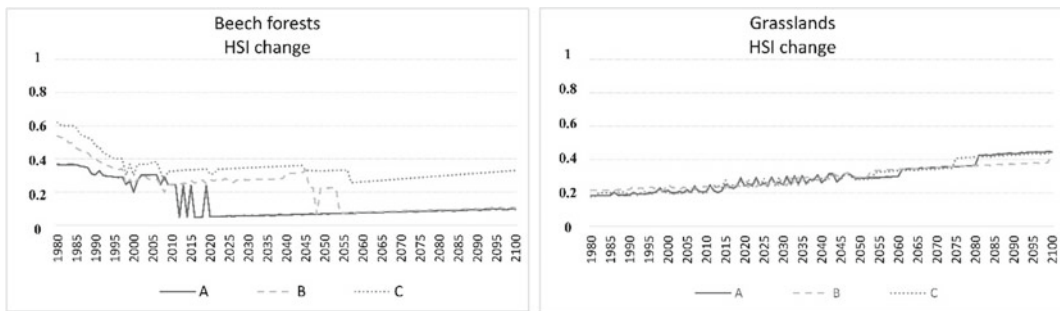


Fig. 34.9 Habitat suitability change simulation using acid deposition and climate RCP4.0 scenario for beech forest (left) and dry highland grasslands (right) regarding the 1980–2100 period for treeline ecotones and sites A, B and C

forest but might be more suitable for highland dry grassland habitats. As for the critical loads, this result means that current and future deposition does not exceed a biodiversity threshold; instead, future changes are caused by increasing

temperatures and fluctuating precipitation, and their effects on the C/N ratio (Figs. 34.1 and 34.9).

Habitat suitability based on climate scenarios and geospatial distribution analyses:

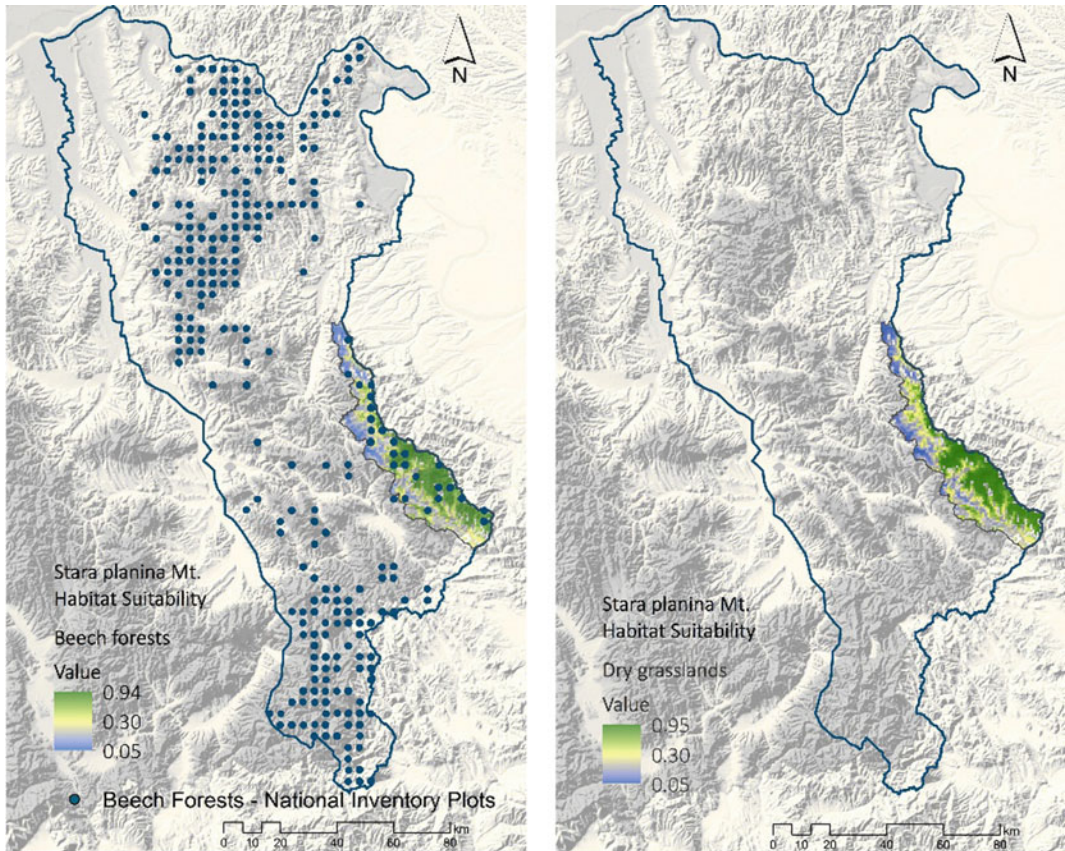


Fig. 34.10 Treeline ecotones of beech forests (left) and dry grasslands (right): future habitat suitability and shifting towards higher altitudes, regarding climate

change scenario RCP 4.0 for the 2041–2060 period—MaxEnt model simulation results (orig.)

The focus of this analysis was to explore the future eco-climatic potentials of Stara Planina for beech forests and dry grassland habitats. The model has a very high predictive power for beech forests (AUC = 0.987) and grasslands (AUC 0.997). The AUC (Area Under the ROC Curve) index provides a single measure of overall accuracy that is not dependent upon a particular threshold (Deleo 1993). So, the results can be analysed with greater certainty.

The future distribution of *Fagus moesica* forests shows that habitats on Stara Planina will be more suitable for the development of beech forests in the 2041–2060 period (Fig. 34.10). It should be noted that the habitat suitability increase is assessed in the area of potential natural vegetation labelled *mountain and subalpine*

Norway spruce forest. The analysis performed for grasslands also reveals high habitat suitability indices for *Agrostis capilaris* grasslands (Fig. 34.10). Habitat suitability for beech forest and dry highland grasslands is shifting towards higher altitudes.

34.6 Conclusions

- Regarding soil acidification, weathering rates are central to critical load assessments. In this study, we used an ICP M&M methodology to calculate the weathering rates depending on the soil type and parent material, and this can be a source of uncertainty. A further improvement will be to measure and to

calibrate weathering rates for different soil types under forest and grassland habitats.

- Regarding CLs for biodiversity, there is a difference when a different number of typical species is used. Since results have to be comparable on regional level, this calls for more precise instructions regarding the most relevant list and number of plant species for certain habitats. Now, this is still based on expert judgement.
- It is not possible to assess the CLs for biodiversity on a national level because of a lack of data. Following the current CLRTAP concept, the sensitivity of forest ecosystems to air pollution was based on ICPF monitoring data (Level I) plots as long-term forest monitoring sites. These sites usually represent the dominant forest habitats on a national level, but they do not include rare habitats under conservation protection. Since newly developed critical loads are based on biodiversity preservation and focus on that issue, priority must be given to including most threatened/protected habitats of endangered, rare and relict species in calculations and assessments of critical loads. This requires a database on the long-term monitoring of these ecosystems.
- Further research and improvements to the models are needed in order to include synecological processes as a variable of ecosystem changes.

Acknowledgements This research was part of the project “Studying climate change and its influence on the environment: impacts, adaptation and mitigation” (43007) financed by the Ministry of Education and Science of the Republic of Serbia within the framework of integrated and interdisciplinary research for the 2011–2019 period; reference no. 451-03-9/2021-14/200169

References

Beloica J, Čavlović D, Đurđević V, Simić SB, Obratov-Petković D, Kadović R, Bjedov I (2015) Ground vegetation composition change in beech forest and highland grasslands of Eastern Serbia (in relation to atmospheric depositions, soil properties, temperatures

and precipitation amounts). International cooperative programme on modelling and mapping of critical levels and loads and air pollution effects. Risks and Trends (ICP M&M) 25TH CCE WORKSHOP AND 31ST TASK FORCE MEETING on assessments of impacts of air pollution, and interactions with climate change, biodiversity and ecosystem services, Zagreb. https://www.researchgate.net/publication/277138795_Ground_vegetation_composition_change_in_beech_forest_and_highland_grasslands_of_Eastern_Serbia_in_relation_to_atmospheric_depositions_soil_properties_temperatures_and_precipitation_amounts. Accessed 20 Nov 2020

Beloica J (2015) Acidification process as a factor of soil degradation in Eastern Serbia. Ph.D thesis, University of Belgrade Faculty of Forestry, 279. <http://eteze.bg.ac.rs/application/showtheses?thesesId=2647>. Accessed 20 Nov 2020

Bobbink R, Hettelingh JP (2011) Review and revision of empirical critical loads and dose-response relationships. In: Proceedings of an expert workshop, Noordwijkerhout, RIVM, Bilthoven, NL, 23–24 June 2010

Bonten LTC, Reinds GJ, Posch M (2016) A model to calculate effects of atmospheric deposition on soil acidification, eutrophication and carbon sequestration. *Environ Model Softw* 79:75–84. <https://doi.org/10.1016/j.envsoft.2016.01.009>. Accessed 20 Nov 2020

Boruvka L, Mladkova L, Penížek V, Drabek O, Vašat R (2007) Forest soil acidification assessment using principal component analysis and geostatistics. *Geoderma* 140(4):374–382

Braun-Blanquet J (1964) *Pflanzensoziologie. Grundzüge der vegetationskunde*. 3rd ed. Springer, Vienna

CLRTAP (2015) Dynamic modelling, chapter VI of manual on methodologies and criteria for modelling and mapping critical loads and levels and air pollution effects, risks and trends. UNECE convention on long-range transboundary air pollution. www.icpmapping.org. Accessed 20 Nov 2020

CLRTAP (2017) Mapping critical loads for ecosystems, chapter V of manual on methodologies and criteria for modelling and mapping critical loads and levels and air pollution effects, risks and trends. UNECE convention on long-range transboundary air pollution. www.icpmapping.org. Accessed 20 Nov 2020

Deleo JM (1993) Receiver operating characteristic laboratory (ROCLAB): software for developing decision strategies that account for uncertainty. In: Proceedings of the second international symposium on uncertainty modelling and analysis, College Park, MD: IEEE Computer Society Press, pp 318–325

Dirnböck T, Djukic I, Kitzler B, Kobler J, Mol-Dijkstra JP, Posch M, Reinds GJ, Schlutow A, Starlinger F, Wamelink WG (2017) Climate and air pollution impacts on habitat suitability of Austrian forest ecosystems. *PLoS ONE* 12(9):184–194

Dirnböck T, Pröll G, Austnes K, Beloica J, Beudert B, Canullo R, Marco AD et al (2018) Currently legislated decreases in nitrogen deposition will yield only limited plant species recovery in European forests.

- Environ Res Lett 13(2018). <https://doi.org/10.1088/1748-9326/aaf26b>. Accessed 20 Nov 2020
- Djordjević V, Rajković B (2008) Verification of a coupled atmosphere-ocean model using satellite observations over the Adriatic Sea. *Ann Geophys* 26(7):1935–1954
- Ducros M (1845) Observation d'une pluie acide. *J Pharmacie Chimie* 3(7):273–277
- EMEP (2020) https://www.emep.int/mscw/mscw_moddata.html. Accessed 20 Nov 2020
- EUNIS (2020) <https://www.eea.europa.eu/data-and-maps/data/eunis-habitat-classification>. Accessed 20 Nov 2020
- Evelyn J (1661) *Fumifugium, or, the inconveniencie of the aer and smook of London dissipated together with some remedies humbly proposed/by J.E. esq. to his sacred majestie, and to the parliament now assembled. Fumifugium Bedel and Colins, London*
- FAO (2006) Guidelines for soil description. Food and Agriculture Organization of the United Nations, Rome, Italy, p 109. <http://www.fao.org/3/a-a0541e.pdf>. Accessed 20 Nov 2020
- FAO-Unesco (1974) Soil map of the world, 1:5 000 000. vol 1—legend. United Nations Educational, Scientific, and Cultural Organization, Paris. <http://www.fao.org/3/as360e/as360e.pdf>. Accessed 11 Nov 2020
- Filipović B, Krnić O, Lazić M (2005) Regionalna hidrogeologija Srbije. Rudarsko geološki fakultet Beograd
- Gorham E (1976) Acid precipitation and its influence upon aquatic ecosystems an overview. *Water Air Soil Pollut* 6(2):457–481
- Graunt J (1665) Natural and political observations mentioned in a following index and made upon the bills of mortality. Royal Society, London
- Hammer Ø, Harper DAT, Ryan PD (2001) PAST: Paleontological statistics software package for education and data analysis. *Palaeontol Electron* 4(1):9. http://palaeo-electronica.org/2001_1/past/issue1_01.htm. Accessed 20 Nov 2020
- Hettelingh JP, de Vries W, Posch M, Reinds GJ, Slootweg J, Hicks WK (2014) Development of the critical loads concept and current and potential applications to different regions of the world. In: Hicks WK, Haeuber R, Sutton MA (eds) Nitrogen deposition, critical loads and biodiversity. Springer, Dordrecht, pp 281–293
- Holmberg M, Aherne J, Austnes K, Beloica J, Marco AD, Dirnböck T, Fornasier F et al (2018) Modelling study of soil C, N and pH response to air pollution and climate change using European LTER site observations. *Sci Total Environ* 640–641:387–399
- ICPF_RS (2020) <https://www.forest.org.rs/?icp-forests-srbija>. Accessed 11 Nov 2020
- Johnston AE, Goulding KWT, Poulton PR (1986) Soil acidification during more than 100 years under permanent grassland and woodland at Rothamsted. *Soil Use Manag* 2(1):3–10
- Košanin O, Knežević M (2005) Zemljišta N.P. Đerdap, Tipovi šuma Đerdapa. Univerzitet u Beogradu Šumarski fakultet i Ministarstvo za nauku i zaštitu životne sredine Republike Srbije, Beograd
- Koseva IS, Watmough SA, Aherne J (2010) Estimating base cation weathering rates in Canadian forest soils using a simple texture-based model. *Biogeochemistry* 101:183–196
- Kržić A, Tošić I, Djurdjević V, Veljović K, Rajković B (2011) Changes in some indices over Serbia according to the SRES A1B and A2 scenarios. *Climate Res* 49:73–86
- Nakićenović N, Davidson, Davis G, Grübler A, Kram T, Rovere LLE, Bert M, Tsuneyuki M, Peper W, Hugh P, Sankovski A, Priyadarshi S, Swart R, Watson R, Zhou D (2000) Special report on emissions scenarios. A special report of working group III of the intergovernmental panel on climate change. Cambridge University Press, Cambridge, United Kingdom and New York, NY, USA. <http://ipcc.ch/pdf/special-reports/spm/sres-en.pdf>. Accessed 20 Nov 2000
- Nilsson J, Grennfelt P (eds) (1988) Critical loads for sulphur and nitrogen. Report from a workshop held at Skokloster
- Oden S (1968) The acidification of air precipitation and its consequences in the natural environment. *Bulletin of Ecological Research Communications NFR, Arlington*
- Phillips SJ, Dudík M, Schapire RE [Internet] (2020) Maxent software for modeling species niches and distributions (Version 3.4.1). http://biodiversityinformatics.amnh.org/open_source/maxent/. Accessed 20 Nov 2020
- Posch M, Hettelingh J-P, Slootweg J, Reinds GJ (2014) Deriving critical loads based on plant diversity targets. In: Slootweg J, Posch M, Hettelingh J-P, Mathijssen L (eds) Modelling and mapping the impacts of atmospheric deposition on plant species diversity in Europe, CCE status report 2014, Report 2014–0075, RIVM, Bilthoven, the Netherlands, pp 41–46. <http://hdl.handle.net/10029/557117>. Accessed 20 Nov 2020
- Posch M (2016) PROPS-CLF—a program to compute biodiversity critical loads based on the PROPS model. Version 1.3—November 2016, Coordination Centre for Effects (CCE), RIVM, Bilthoven, NL
- Reinds GJ, Mol-Dijkstra J, Bonten L, Wamelink W, Vries WD, Posch M (2014) VSD+PROPS: Recent developments. In: Slootweg J, Posch M, Hettelingh J-P, Mathijssen L (eds) Modelling and mapping the impacts of atmospheric deposition on plant species diversity in Europe. CCE status report 2014, RIVM, Bilthoven, the Netherlands, pp 47–53. <http://hdl.handle.net/10029/557117>. Accessed 20 Nov 2020
- Reinds GJ, Mol-Dijkstra J, Bonten L, Wamelink W, Hennekens S, Goedhart P, Posch M (2015) Probability of plant species (PROPS) model: Latest developments. In: Slootweg J, Posch M, Hettelingh JP (eds) Modelling and mapping the impacts of atmospheric deposition of nitrogen and sulphur. CCE status report 2015, National Institute for Public Health and the Environment, RIVM Report 2015–0193, Bilthoven, Netherlands, pp 55–62. <http://wge-cce.org/>

- Publications/CCE_Status_Reports. Accessed 20 Nov 2020
- RHMSS (2020) <http://www.hidmet.gov.rs/eng/meteorologija/klimatologija.php> Accessed 20 Nov 2020
- Rizzetto S, Belyazid S, Gégout JC, Nicolas M, Alard D, Corket E, Gaudio N, Sverdrup H, Probst A (2016) Modelling the impact of climate change and atmospheric N deposition on French forests biodiversity. *Environ Pollut* 213:1016–1027. <https://doi.org/10.1016/j.envpol.2015.12.048>. Accessed 20 Nov 2020
- Rowe EC, Ford AES, Smart SM, Henrys PA, Ashmore MR (2016) Using qualitative and quantitative methods to choose a habitat quality metric for air pollution policy evaluation. *PLoS-ONE* 11(8): e0161085. <https://journals.plos.org/plosone/article?id=10.1371/journal.pone.0161085> Accessed 20 Nov 2020. <https://doi.org/10.1371/journal.pone.0161085>
- Smith A (1852) On the air and rain of Manchester. *Mem Lit Phil Soc Manchester* 2(10):207–217
- Srbije S (2005) <https://www.habitat.bio.bg.ac.rs>. Accessed 20 Nov 2020
- Sverdrup H, Warfvinge P (1988) Chemical weathering of minerals in the Gardsjon catchment in relation to a model based on laboratory rate coefficients. In: Nilsson J, Grennfelt P (eds) Critical loads for sulphur and nitrogen. Nordic Council of Ministers and the United Nations Economic Commission for Europe, Stockholm, pp 81–130
- Sverdrup H, Vries WD (1994) Calculating critical loads for acidity with the simple mass balance method. *Water Air Soil Pollut* 72(1):143–162
- Sverdrup H, Warfvinge P (1993) The effect of soil acidification on the growth of trees, grass and herbs as expressed by the (Ca+Mg+K)/Al ratio. Reports in ecology and environmental engineering 2, Lund University, Lund Sweden, 19–24 March 1988. *Miljörapport* 15:1–418
- Ulrich B, Mayer R, Khanna PK (1980) Chemical changes due to acid precipitation in a loess-derived soil in Central Europe. *Soil Sci* 130:193–199. Currently legislated decreases in nitrogen deposition will yield only
- WORLDCLIM (2020) <https://worldclim.org/data/index.html>. Accessed 20 Nov 2020



Urban Soils in the Historic Centre of Saint Petersburg (Russia)

35

Natalia N. Matinian, Ksenia A. Bakhmatova,
and Anastasia A. Sheshukova

Abstract

The aim of the study was to characterise urban soils in central Saint Petersburg. The research was carried out in two urban parks: the Sheremetev Gardens and the Polish Gardens, both situated on the Fontanka River embankment. The soils were classified according to the Russian Soil Classification System (2001) and the WRB (2014). The chemical properties of the soils were determined using conventional techniques. The soil cover in central Saint Petersburg consists of Urbostratozems (*Urbic Technosols*). Profile of Urbostratozem formed from a series of filled-in organic and mineral layers that have a significant (over 10%) content of construction waste and household waste. The thickness of the anthropogenic (cultural) layer in the Sheremetev Gardens is 94–175 cm, and that in the Polish Gardens is 81–177 cm. The Urbostratozems are characterised by an alkaline reaction and a higher content of organic matter and phosphorus. The negative properties of the urban soils which were studied are increased density, significant amount of artefacts (construction debris) and local technogenic pollution by

heavy metals. The concentration of Pb, Cu and Zn in anthropogenic layers exceeds the approximate permissible concentration by 1.5–10 times. The specific feature of the parks in central Saint Petersburg is the frequent presence of buried natural soils (Umbric Gleysols and Podzols) under anthropogenic strata. These soils were the main components of the natural soil cover before urbanisation. The properties of modern urban soils significantly differ from the properties of original natural soils and their modern analogues. As urban soils are polluted by heavy metals and are prone to eutrophication, the assessment and monitoring of their degradation state will be of importance.

Keywords

Urban soils · Saint Petersburg · Urbostratozems · Urbic Technosols · Soil pollution · Heavy metals

35.1 Introduction

The world population is expected to reach 9 billion in 2050 (United Nations 2015). At the same time, about 54% of the world's population lives in urban areas (Seto et al. 2014). Therefore, the quality of the urban environment is of great importance to the growing urban population. Urbanisation significantly affects the

N. N. Matinian (✉) · K. A. Bakhmatova · A. A. Sheshukova
Saint Petersburg State University, 7–9
Universitetskaya Emb., St Petersburg 199034,
Russia

environment and results in marked changes in terrain features, hydrological conditions and vegetation cover, to name a few. Since the 1970s, urban soils have been the subject of numerous studies (e.g. Blume 1975; Fanning et al. 1978; Bullock and Gregory 1991; Effland and Pouyat 1997; Hiller 2000; Charzyński et al. 2013; Burghardt et al. 2015; Krupski et al. 2017). In an urban environment, the natural vegetation is subjected to extensive loss and simplification (Alberti et al. 2017), and is replaced by ornamental plant species cultivated in the parks and gardens of cities. These changes inevitably cause native ecosystems to be replaced by new urban ecosystems, and lead to the formation of urban soils (Pavao-Zuckerman and Byrne 2009). The sealing of soil is one of the most threatening degradation processes globally (EU 2012; Manna et al. 2017; Pristeri et al. 2020; Xiao et al. 2020). Scalenghe and Franco (2009) reported that, in Europe, the area of the soil covered with an impermeable material (i.e. sealed soil) is around 9%. Moreover, the increase in soil sealing in recent decades has occurred due to extensive urbanisation (suburbanisation) and not due to the increase in population. Criado et al. (2020) reported that in 71% of cases, urbanisation caused the sealing of productive agricultural soils, almost 20% of which were of the highest quality.

When the natural ecosystem is replaced with constructions and paved roads, which bring traffic loads, this greatly affects soil biota in the green urban areas (Scalenghe and Franco 2009; Bach et al. 2020), in terms of both its diversity and distribution (Savard et al. 2000). One of the negative aspects of green urban areas is the elevated concentration of pathogenic microorganisms in public parks (Ramirez et al. 2014) due to large number of visitors and anthropogenic loads (Abawi and Widmer 2000). Biochemical processes in soil are primarily controlled by the soil biota, while sealing soils alters the dynamics of the food substrate for soil microorganisms. This subsequently results in the alteration of the organic carbon cycle, carbon dioxide emissions and carbon sequestration (Vodyanitskii 2015). Pavao-Zuckerman (2008) recognised that

understanding the ecology of urban soils would help restore the urban ecology. A more detailed review of the literature on biodiversity in urban soils is given in Guill and et al. (2018).

Another very negative impact of soil sealing is the deterioration of the soil's physical properties, such as water permeability, bulk density, loss of structure, etc.) (Ungaro et al. 2014), as well as the direct effect on the urban climate (Yuan and Bauer 2007). Obstructing water infiltration prevents groundwater recharge, which in turn leads the groundwater to dry up (Dougherty et al. 2004; Lanen and Peters 2000). On sealed surfaces, water runoff in intensified and increased (Ungaro et al. 2014), which results in the transport and distribution of pollutants from locally polluted places to green urban areas.

Heavy metals are the most common contaminants of urban soils and have been studied by many researchers (e.g. Cannon and Horton 2009; Ajmone-Marsan and Biasioli 2010; Luo et al. 2012; Mitchell et al. 2014; Delbecque and Verdoodt 2016; Cakmak et al. 2018; Pavlovic et al. 2018; Kumar and Hundal 2016). The pollution of urban soils with so-called "urban metals"—Pb, Cu and Zn—is mainly related to human activities (Miguel et al. 1997; Lee et al. 2006). These metals are of particular interest as they pose a high risk to human health, especially the most sensitive group, children, who have direct and close contact with the ground (Brown et al. 2016; Cakmak et al. 2018).

Because urban soils exhibit different physical, chemical and biological characteristics in comparison to altered non-urbanised soils, they can serve as indicators of the ecosystem status. Monitoring and controlling the ecological state of urban soils can provide a better understanding and restoration of urban ecology. According to Blanchart et al. (2018), the role of urban soils in ecosystem services is underestimated, and the organisation of the green areas in cities is not well managed.

In 2006, urban soils were included in the WRB classification system (WRB 2006, 2014; Lehmann and Stahr 2007; Rossiter 2007; Montgomery et al. 2016). The various negative impacts of the urban environment on the soil led

to the vast majority of urban soils being included in the Technosols group (WRB 2006, 2014), with different qualifiers, indicating urban soil diversity (Lehmann 2006; Charzyński et al. 2013). Russian soil scientists developed the “Moscow soil classification” (Stroganova and Prokofieva 2001; Prokofyeva et al. 2011) and some aspects of that classification have been introduced into the Russian Soil Classification System (2001) (Prokofieva et al. 2014; Prokofieva and Gerasimova 2018).

Urban soils have some specific characteristics, such as the presence of a large number of artefacts, an alkaline pH, a high content of organic carbon and nutrients and a high content of contaminants (Lehmann and Stahr 2007). Generally, published sources on urban soils are related to pollution with heavy metals, the impacts of soil biodiversity and vegetation changes (e.g. Guillard et al. 2018). However, there are few studies on pedogenesis of the soils in an urban environment. The direction of pedogenesis in an urban environment strongly depends on the properties of the soil-forming substrate (e.g. cultural layer) and climate (Aleksandrovskaya and Aleksandrovskiy 2000; Aleksandrovskiy et al. 2012). The spatial and vertical heterogeneity of urban soils depends on the current and previous type of land use (e.g. park, residential area, roadside area, etc.) (Mao et al. 2014; Greinert 2015). The parent material for urban soils is human-altered and human-transported material (Huot et al. 2017). The term “fill” has been proposed “for material used to infill a void or cavity in the earth’s surface or sub-surface”; “constructional fill (man-made ground) is material placed above the natural earth surface” (Rosenbaum et al. 2003).

The urban soils of Saint Petersburg, Russia’s second largest city and one of the largest cities in Northern Europe, have been studied since the 1980s (Dolotov and Ponomareva 1982). There are several publications devoted to the genesis and properties of urban soils in Saint Petersburg (Rusakov and Novikov 2003; Aparin and Sukhacheva 2014; Matinyan et al. 2017; Aparin et al. 2018). This study focuses on urban soils in the centre of the city. The aim of the study was to

study the characteristics of urban soils in the Sheremetev and Polish gardens in St. Petersburg and to demonstrate the relationship between the history of the city and the soil properties.

35.2 Area Studied

Saint Petersburg was founded in 1703 in the northwestern part of Russia (59°57′N, 30°19′E) on the banks of the Neva River and the eastern coast of the Gulf of Finland. The climate is continental humid; the average annual temperature is 5.8 °C, and the average annual precipitation is about 660 mm (Fig. 35.1). The historical central part of Saint Petersburg which was studied is located on the low coastal terrace (absolute height of 0–3 m, which is due to anthropogenic stratification reaching up to 4.5 m in some places). There are more than 80 watercourses (rivers and canals) and about 100 waterbodies on the city’s territory (Encyclopedic Handbook 1992). Additionally, 20–33% of the central city area is currently occupied by an underground hydrological network. The shallow water table has a significant influence on the soil formation. The groundwater level at the moment of the soil survey was 1.0–1.8 m from the soil surface. Until the construction of the dam separating the Gulf of Finland from Neva Bay in 2011, these soils were periodically submerged due to occasional rises in groundwater levels and the flooding of the Neva River (Fig. 35.1). The natural soil parent materials are marine sand and loamy-sand sediments, formed several thousand years ago by the Littorina Sea (the last stage of the Baltic Sea’s evolutionary development). The urban soils were formed on human-altered and human-transported materials. The measured thickness of the soils in the locations studied was between 0.8–2.0 m.

The research location was chosen in the green urban areas located on the left bank of the Fontanka River: in the gardens and the main courtyard of the former Sheremetev Palace, as well as in the gardens of the former estate of G.R. Derzhavin—the Polish Garden. Since their foundation, these parks have evolved from being

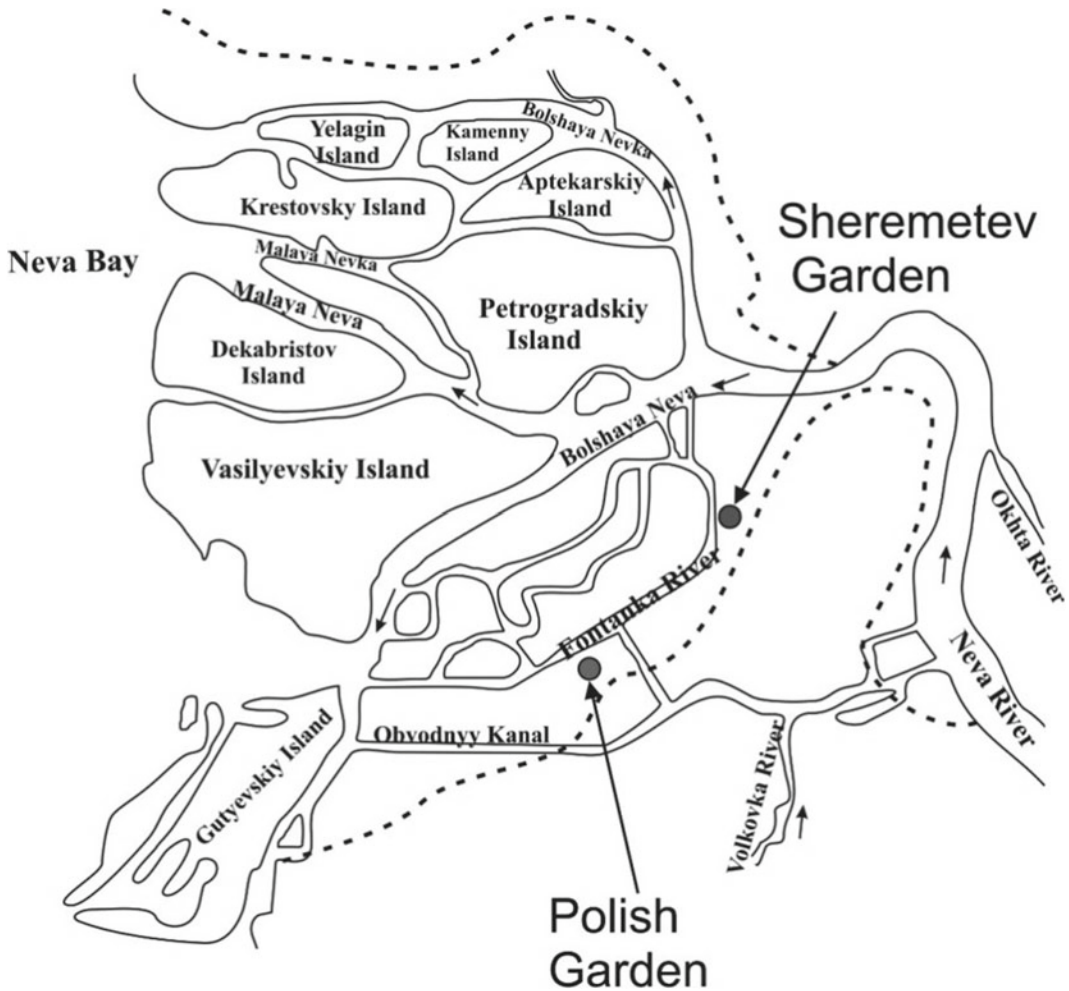


Fig. 35.1 Neva delta scheme: the boundary of flooding when the water level rises to a height of 4.1 m

suburban manor gardens to parks in the major urban centre. The opportunity to explore the soils in the parks of the city centre arose during their reconstruction before the celebration of the 300th anniversary of St. Petersburg. Therefore, in this chapter the composition of vegetation is given as it was at that time.

35.3 Soil Diagnostics

Soil names and indexes of natural soil horizons are given according to the Russian Soil Classification System (2001). This system (Prokofieva et al. 2014) and the WRB (2014) classification

system were used for diagnostics of urban soils. Soils typical of an urban environment were defined as “Urbostratozems” The urbic horizon (*UR*) is the diagnostic horizon of Urbostratozems that gradually formed due to the accumulation of different substrates added to the surface in urban and rural settlements. The horizon contains more than 10% artefacts (mainly construction waste and household waste), often with a large amount of sand or stone. Usually, it has a neutral to alkaline pH and a high content of phosphorus. The humus content may vary significantly. For the urbic horizon, as the humus-accumulative surface horizon, additional qualifiers such as: *ay* (grey humus) and *au* (dark humus) can be used.

The qualifier *ur* indicates the presence of an urbic horizon with a thickness of less than 40 cm overlying the remains of the natural soil, or a stratified organomineral material containing urbo-industrial inclusions. This qualifier is applied to transitional urbo-natural soils (“urbo-soils”). *TCH* is a technogenic horizon consisting of man-made or man-transported materials and characterised by higher hardness and density, with anthropogenic inclusions (Prokofieva et al. 2014). *R* is a mineral bulk horizon without (or with <5%) anthropogenic inclusions.

35.4 Analytical Methods

A set of traditional analytical methods was used to obtain the physical and chemical characteristics of the soils (Vorobieva 2006). The organic carbon content was determined by titration with dichromate oxidation, pH was measured electrometrically in an aqueous suspension at a soil-to-water ratio of 1 to 2.5; the carbonate content was determined using the alkalimetric method, and the exchangeable bases content was determined using complexometric titration after extraction using 1 N NaCl solution (Vorobieva 2006). The content of plant-available potassium (K) and phosphorus (P) compounds was determined using a 1% solution of $(\text{NH}_4)_2\text{CO}_3$ in a soil-to-solution ratio of 1:20 and a pH of 9. Phosphorus was measured photometrically (FEK-3) in an extract tinged with ammonium-heptamolybdate and ascorbic acid reagent. Potassium was determined by photoelectric flame photometry. The content of the mobile forms of phosphorus and potassium was estimated using the scales designed for agricultural plants with the highest nutrient demands. The exchangeable bases content was determined in the samples that lacked free carbonates (i.e. samples that did not exhibit a “fizz” reaction when a drop of 10% hydrochloric acid was applied).

Pre-urban vegetation was reconstructed by analysing phytoliths and spore pollen in buried soils, as described previously (Golyeva 2001; Piperno 2006). The total concentrations of heavy metals (HMs), namely Cu, Pb, Zn, Sn, V, Co, Ni

and Cd, were determined by atomic emission spectroscopy (AES), with the digestion of samples carried out by evaporation from the carbon electrode channel (OST 41–08–265–04 2004; Vorobieva 2006). The analysis was carried out at the central laboratory of the A.P. Karpinsky Russian Geological research institute (Saint Petersburg) (a member of the International Association of Geoanalysts—IAG). To evaluate the heavy metal concentration, the approximate permissible concentrations (APCs) were considered (Hygienic Standard 2.1.7.2042.06). The results were statistically processed with the PAST statistical software (Hammer et al. 2001).

35.5 Soils of the Sheremetev Gardens

35.5.1 Anthropogenic Soil Formation Factors

The gardens and the main courtyard of the former Sheremetev Palace (Fontanka River embankment, house no 34) cover about 0.95 hectares. The main courtyard (*cour d'honneur*) is in the front of the main facade of the palace, facing the Fontanka River. The gardens were founded at the beginning of the eighteenth century. At that time, there was a formal garden with straight alleys, a parterre lawn and a large fountain. From the beginning of the 19th century, the gardens began to acquire landscaped features: an oval meadow lawn replaced the parterre lawn and the fountain, and some of the longitudinal straight alleys were filled in. Later, the garden was repeatedly re-planned; new plots, flowerbeds and lawns were created, and previously filled paths were restored. The Sheremetev Palace was turned into a museum after the revolution in 1917; folk festivals took place in the garden, and an orchestra stage was built. From 1930, the Institute of the Arctic and Antarctic was located in the Palace, and warehouses were located in the gardens. Wooden sheds were used to store lime materials, resin, lumber, construction waste and laboratory dumps and waste, and a parking lot was built in the gardens. Vehicles broke up the

paths; several trees were damaged by rusty iron and bricks. The restoration of the gardens began in 1981 and was completed in 2003.

There are about 80 trees of 10 species in the gardens (*Ulmus laevis*, *Quercus robur*, *Aesculus hippocastaneum*, *Acer negundo*, *Acer platanoides*, *Larix sibirica*, *Fraxinus excelsior*, *Tilia cordata*, *Malus sibirica*, *Padus avium*). The dominant species is the Norway maple (*Acer platanoides*), several varieties of which are found in the gardens. The trees are 80–100 years old and more. The vital status for most of the trees is 55% (mediocre). They have inclined, damaged trunks, one-sided and poorly developed crowns and dry branches. There are many shrubs in the gardens: *Crataegus sanguinea*, *Lonicera tatarica*, *Syringa vulgaris*, *Syringa josikaea*, *Cornus stolonifera*, *Spiraea chamaedryfolia*, *Spiraea salicifolia*, *Spiraea media*, *Philadelphus coronaries*, *Cotoneaster lucida*, *Symphoricarpos albus*, *Padus avium*, *Rosa canina*, *Rosa rugosa*. The basic species presented on the lawns are grasses: *Poa pratensis*, *Festuca pratensis*, *Festuca rubra*.

35.5.2 Soil Description and Properties

Eleven soil profiles have been studied in the Sheremetev gardens, and two more profiles have been studied in the courtyard (on the west and east lawns) (Fig. 35.2). The soil cover of the gardens is homogeneous and consists of Urbostratozems and Urbostratozems on buried soils. Urbostratozems were divided into three groups depending on the thickness of the anthropogenic layer: low (40–70 cm), medium (70–100 cm) and high (more than 100 cm).

Gleyed Urbostratozems (*Urbic Technosols*, *Gleyic*) with a medium-thick anthropogenic layer on buried grey-humus gley soils (*Umbric Gleysols*) were found in the northern part of the gardens. Urbostratozems (*Urbic Technosols*) with a medium-thick anthropogenic layer on buried soddy podzols (*Albic Umbric Podzols*) were common in the eastern part of the gardens. Urbostratozems (*Urbic Technosols*) and gleyed

Urbostratozems (*Urbic Technosol*, *Gleyic*) with a very thick anthropogenic layer on marine loamy-sand sediments were found in the rest of the gardens. The soil cover of the main courtyard consisted of Urbostratozems (*Urbic Technosols*) with a thick anthropogenic layer on buried grey-humus gley soils (*Umbric Gleysols*) and Urbostratozems (*Urbic Technosols*) with a shallow anthropogenic layer on marine loamy-sand sediments.

The humus horizon of the buried native soil (Profile 1-k, 175–206 cm) in the main courtyard contains a significant amount of plant litter including tree detritus, such as microparticles of coniferous wood. Plenty of fungal hyphae were found, along with pollen grains, some of which were deformed. There were few phytoliths of mosses and grasses. Our data indicate that in the past there was a coniferous forest in the area studied.

All the garden soils exhibited considerable heterogeneity of the anthropogenic (cultural) layer. There were a number of anthropogenic horizons that differ in terms of their humus content, as well as in their type and colour uniformity. Inclusions of construction debris, metal, ceramics and glass were observed throughout the layers. The anthropogenic layer in the main courtyard was more uniform compared to the gardens. These differences can be explained by numerous redevelopments in the layout of the gardens (Fig. 35.3). The thickness of the anthropogenic layers also varied in different parts of the main yard, reaching 175 cm on the western lawn, and only 84 cm on the eastern lawn. The difference in the thickness of these layers could potentially indicate the heterogeneous nature of the primary relief (before the construction of Sheremetev Palace). It can be assumed that in the western part the yard was about 1 m lower than in the eastern part.

The cultural layer of urban soils was characterised by an appreciable content of coarse particles (>1 mm), which showed that their relative amounts were widely distributed across the layers (from 0.5–64%, Fig. 35.4). These particles are predominantly of technogenic origin: pieces of brick, fragments of granite, lime, charcoal and

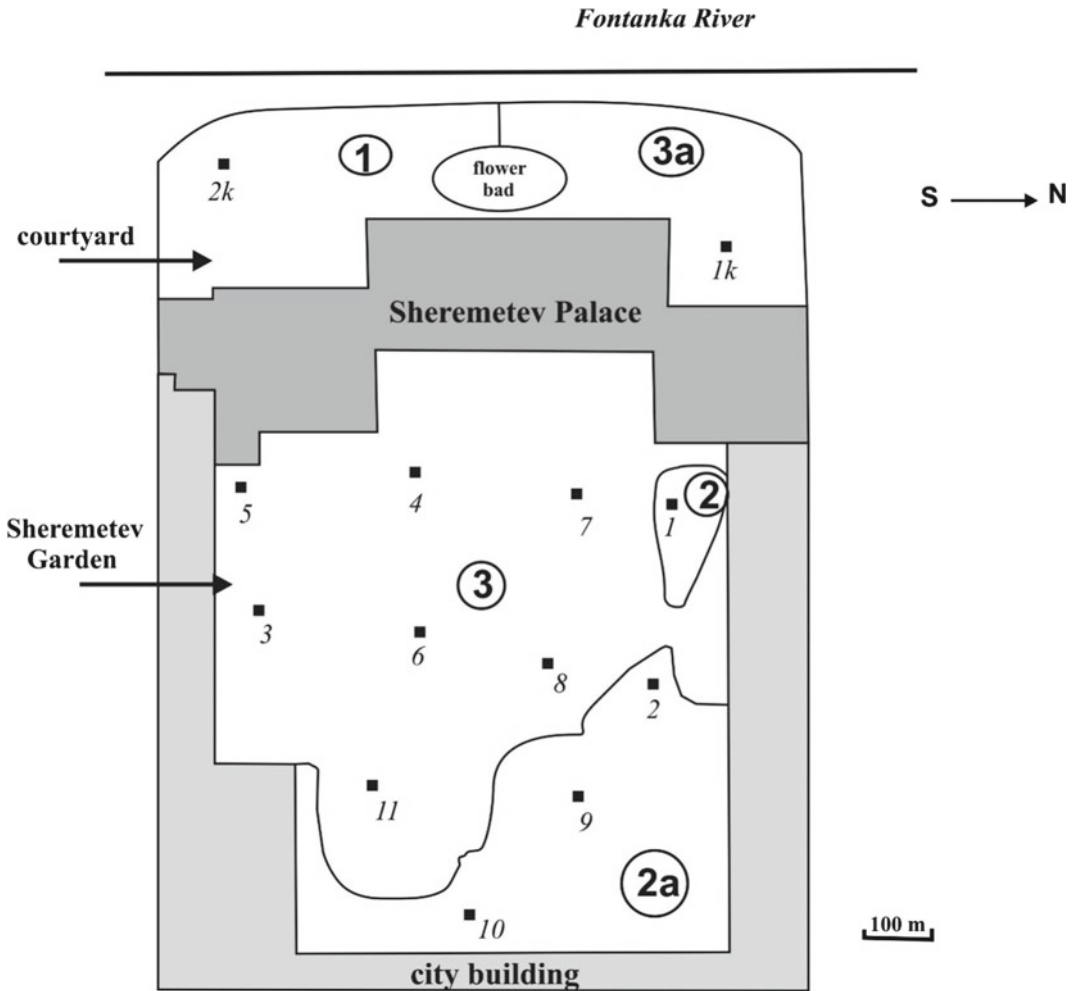


Fig. 35.2 Schematic soil map of Sheremetev Palace. Soil contours (numbers in circles): **1**—Urbostratozems with shallow anthropogenic layer on marine loamy-sand sediments; **2**—gleyed Urbostratozems with medium-thick anthropogenic layer on buried grey-humus gley soils; **2a**—Urbostratozems with medium-thick anthropogenic

layer on buried soddy podzols; **3**—Urbostratozems and gleyed Urbostratozems with very thick anthropogenic layer on marine loamy-sand sediments; **3a**—Urbostratozems with very thick anthropogenic layer on buried grey-humus gley soils; Black squares with numbers indicate locations of the soil profiles

coal, fragments of rusty metal, glass and ceramics. The artefacts were relatively similar in all the profiles studied. A large amount of construction debris in the soil, as a rule, disrupts the development of trees' root systems, delaying their growth.

The pH values of the surface soil horizons were alkaline due to the presence of lime, cement dust, bricks, etc. The content of carbonate in the anthropogenic horizons varied in the profile from 0.1–39% (Table 35.1). The natural soil and

parent materials in the Saint Petersburg area do not contain carbonates. Light textures facilitate water penetration to a significant soil depth, and as a result, an alkaline reaction is often observed even in the native horizons. Phosphorus and potassium were distributed unevenly along the profiles. The surface part of the anthropogenic layer contained higher amounts of the nutrients compared to the humus horizons of natural soils of the North-West region of Russia.

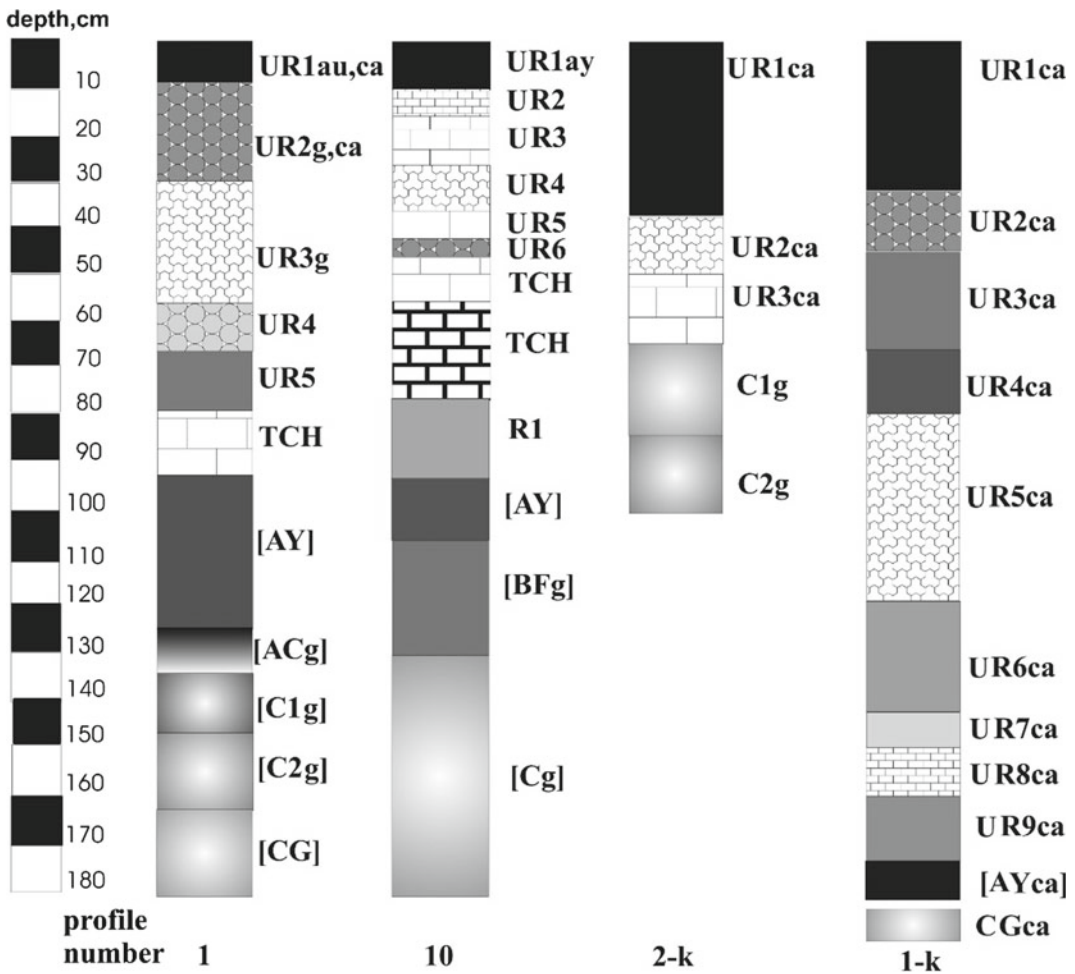


Fig. 35.3 The structure of the soil profiles 1—Gleyed Urbostratozem (Urbic Technosol, Gleyic) on buried grey-humus gley soil (Umbric Gleysol); 10—Urbostratozem (Urbic Technosol) on buried gleyed soddy podzol (Umbric Gleyic Podzol); 2-k—Urbostratozem (Urbic Technosol) on marine loamy-sand sediments; 1-k—Urbostratozem (Urbic Technosol) on buried grey-humus gley soil (Umbric Gleysol)

The soils of central St. Petersburg, including the Sheremetev Gardens, are contaminated with heavy metals from various sources. Analysis of the content of heavy metals in 15 surface samples (0–15 cm) showed elevated concentrations of copper, zinc and lead throughout the garden. High concentrations of heavy metals were found in the middle parts of the soil profiles, coinciding

with the accumulation of anthropogenic debris (Fig. 35.5).

Profile 11 was located at the dump for technogenic waste generated while the Institute of the Arctic and Antarctic was located in Sheremetev Palace. There was a particularly high concentration of Zn, Pb, Cu, Sn and Cd in this place (Fig. 35.6).

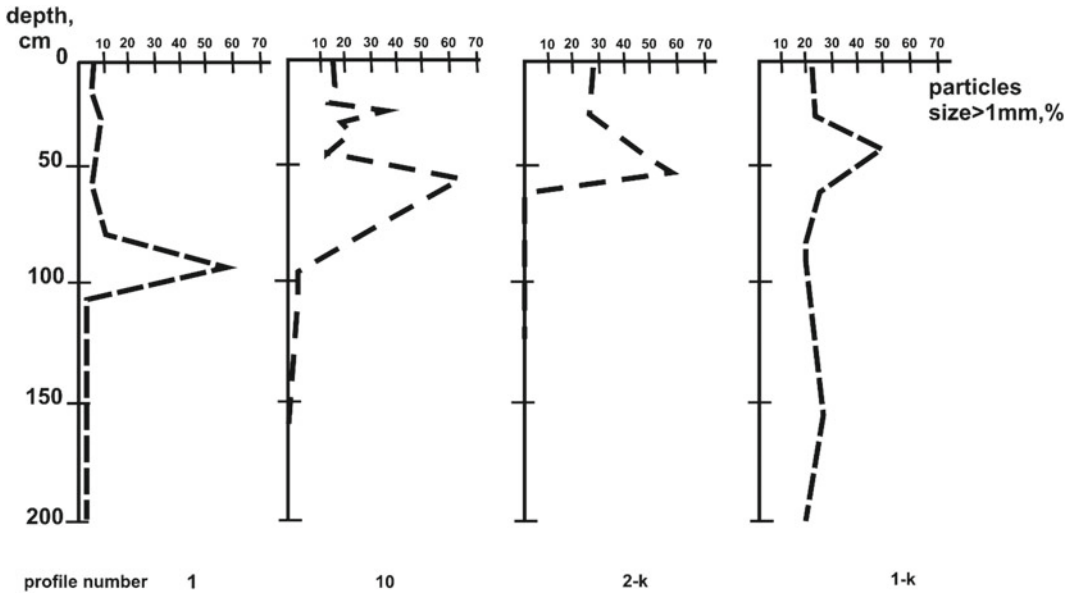


Fig. 35.4 Distribution of coarse particles in soil profile (> 1 mm). Note: 1—Gleyed Urbostratozem (*Urbic Technosol (Gleyic)*) on buried grey-humus gley soil (*Umbric Gleysol*); 10—Urbostratozem (*Urbic Technosol*) on buried gleyed soddy podzol (*Umbric Gleyic Podzol*); 2-k—Urbostratozem (*Urbic Technosol*) on marine loamy-sand sediments; 1-k—Urbostratozem (*Urbic Technosol*) on buried grey-humus gley soil (*Umbric Gleysol*)

Table 35.1 Selected properties of Urbostratozems of the Sheremetev Gardens

Horizon	Depth, cm	pH H ₂ O	Total organic C, %	CaCO ₃ , %	Mobile forms, mg kg ⁻¹	
					K ₂ O	P ₂ O ₅
Profile 1 Gleyed Urbostratozem (<i>Urbic Technosol, Gleyic</i>) on buried grey-humus gley soil (<i>Umbric Gleysol</i>)						
UR1au, ca	0–8	7.2	2.8	6.2	180	156
UR2g, ca	8–20	6.1	2.2	1.9	120	260
UR2g, ca	20–30	6.5	1.6	1.8	120	130
UR3g	30–55	6.7	2.9	6.2	140	182
UR4	55–63	7.3	2.1	3.3	140	234
UR5	63–79	7.6	3.0	2.7	-	-
TCH	79–92	7.9	1.0	6.6	-	-
[AY]	92–123	8.0	1.6	6.1	-	-
[ACg]	123–131	8.0	0.9	7.5	40	182
[C1g]	131–143	7.8	0.4	0.9	20	104
[C2g]	143–162	7.8	0.5	2.8	-	-
[CG]	162–180	7.6	0.4	0.6	-	-

(continued)

Table 35.1 (continued)

Horizon	Depth, cm	pH H ₂ O	Total organic C, %	CaCO ₃ , %	Mobile forms, mg kg ⁻¹	
					K ₂ O	P ₂ O ₅
Profile 10. Urbostratozem (<i>Urbic Technosol</i>) on buried gleyed soddy podzol (<i>Umbric Gleyic Podzol</i>)						
UR1ay	0–10	7.7	3.8	15.3	250	338
UR2	10–17	7.8	3.2	4.7	180	156
UR3	17–28	8.0	0.9	1.3	140	130
UR4	28–37	7.8	1.2	2.5	160	260
UR5	37–42	8.0	0.7	3.7	120	182
UR6	42–47	8.1	0.9	2.8	120	156
TCH	47–57	8.1	1.0	31.7	-	-
TCH	57–78	8.1	0.3	39.4	180	104
R1	78–94	8.2	2.1	6.1	-	-
[AY]	94–107	8.0	4.0	0.2	180	104
[BFg]	107–130	8.0	0.8	1.1	-	-
[Cg]	130–170	7.9	0.2	1.6	-	-
p.1-k. Urbostratozem (<i>Urbic Technosol</i>) on buried grey-humus gley soil (<i>Umbric Gleysol</i>)						
UR1ca	0–31	7.4	3.3	0.6	178	170
UR2ca	31–44	7.9	1.8	4.1	92	840
UR3ca	44–64	7.9	1.5	0.9	70	280
UR4ca	64–76	7.8	1.4	1.0	40	420
UR5ca	76–116	8.0	0.7	1.3	40	260
UR6ca	116–140	8.2	0.7	2.0	36	280
UR7ca	140–150	8.0	0.7	1.7	42	230
UR8ca	150–160	8.1	1.0	1.1	57	180
UR9ca	160–175	8.0	1.0	2.3	60	180
[AY]ca	175–206	7.9	1.4	0.4	75	104
CGca	206–216	7.8	0.2	0.1	58	100
p.2-k. Urbostratozem (<i>Urbic Technosol</i>) on marine loamy-sand sediments						
UR1ca	0–39	7.5	4.2	6.1	198	340
UR2ca	39–50	7.7	7.3	1.5	184	420
UR3ca	50–60	8.0	0.8	8.1	-	-
C1g	65–84	8.1	0.5	1.4	-	-
C2g	84–135	7.9	0.1	2.1	-	-

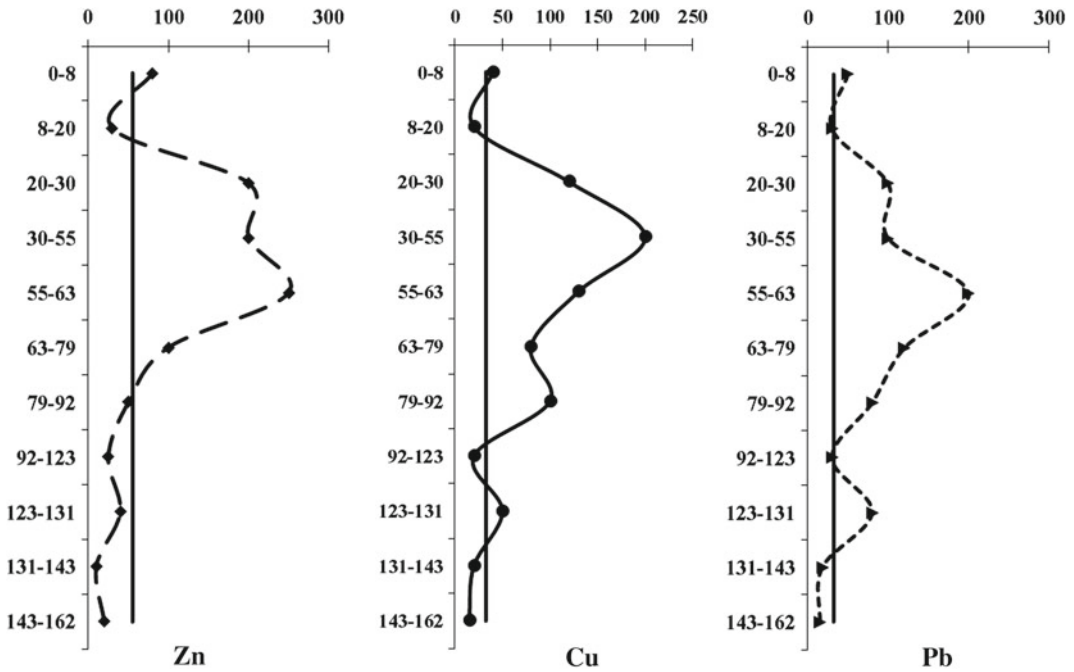


Fig. 35.5 Distribution of heavy metals (mg kg⁻¹) in Profile 1: Gleyed Urbostratozem (*Urbic Technosol* (Gleyic)) on buried grey-humus gley soil (*Umbric*

Gleysol). The straight line indicates the approximate permissible concentrations (APCs) for sandy soils (Hygienic standard 2.1.7.2042-06 (2006))

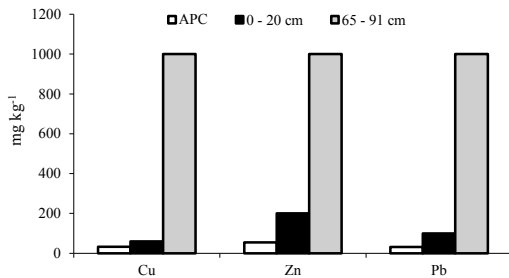


Fig. 35.6 Concentrations of Cu, Zn and Pb in Profile 11 (*Urbostratozem* (*Urbic Technosol*) on marine loamy-sand sediments). Note: APC—approximate permissible concentration

35.6 Soils of the Polish Gardens

35.6.1 Anthropogenic Soil Formation Factors

The area of the modern garden is 2.63 ha. The garden was founded in the last decade of the eighteenth century as part of a small estate. The

famous Russian poet and statesman G.R. Derzhavin acquired the estate in 1791. The main gardening work was carried out at that time. The recreation part of the garden occupied about 1/3 of the territory, and the rest was under vegetables. The wide lawn was the centre of the landscape composition, and the water system on the periphery of the gardens consisted of three small ponds connected with a narrow brook. Trees and shrubs were planted along the brook. In 1846, the estate, along with the land tenure, was sold to the Roman Catholic Church. In 1847, the area of the recreational part of the garden was expanded due to the vegetable zone and its composition was renewed. Since then, the gardens have been called the Polish Gardens. Vegetables were grown in the southern part until the beginning of the twentieth century. In 1917, the Polish Gardens became a place for public recreation. The gardens had been abandoned for some time before their reconstruction in 2007–2011. The most abundant tree species in the gardens are *Fraxinus excelsior*, *Ulmus glabra* and *Tilia*

cordata. There are also *Quercus robur*, *Betula pendula*, *Acer negundo*, *Acer platanoides*, *Acer tataricum*, *Larix sibirica*, *Malus sibirica*, *Populus canadensis*. The shrub layer consists of *Padus avium*, *Crataegus sanguinea*, *Syringa vulgaris*, *Syringa josikaea*.

35.6.2 Soil Description and Properties

Eleven soil profiles were studied in the Polish Gardens. Natural soils in the Polish Gardens had been destroyed or buried under the cultural layer. The soil cover of the park is homogeneous in composition and consists of Urbostratozems on natural parent materials, Urbostratozems on technogenic materials, gleyed Urbostratozems and Urbostratozems on buried natural soils (Fig. 35.7). Urbostratozems with a medium-thick anthropogenic layer were found in the northern part of the area, next to the house where there used to be an arboretum. Urbostratozems with a very thick anthropogenic layer prevailed in the rest of the gardens, where vegetables were previously grown. The soil profiles are characterised by a number of filled layers of different colours, thicknesses and compositions. The surface horizons are 16–17 cm thick and dark grey. Anthropogenic material consisting mainly of construction waste and household waste (fragments of bricks, ceramics, pieces of asphalt, broken glass, coal, bones, pieces of tin, wire, nails, wood, etc.) was mixed with sandy or loamy-sandy fine earth material.

Some anthropogenic layers contain organic matter, which indicates that the relief was repeatedly filled with humus material and aligned. There are also layers consisting entirely of construction debris. A continuous layer of brick fragments (TCH), was found in Profile 5 at a depth of 60–97 cm, in Profile 7 at a depth of 19–41 cm (the bricks had imprinted dates: 1834, 1838, 1854, 1878), and in Profile 8 at a depth of 35–47 cm. The presence of compacted layers of construction debris significantly limits the

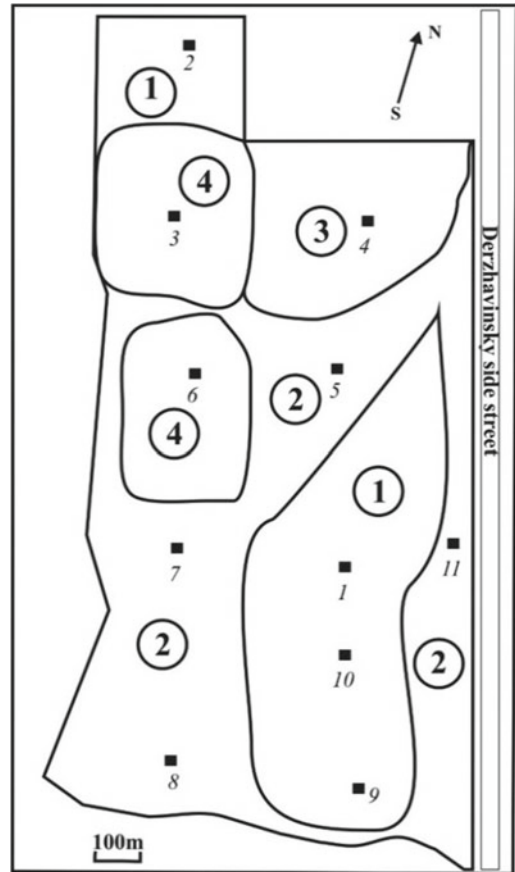


Fig. 35.7 Schematic soil map of the Polish Gardens. Soil contours (numbers in circles): 1—Urbostratozems with very thick anthropogenic layer on buried grey-humus gley soils; 2—Urbostratozems with very thick anthropogenic layer; 3—Urbostratozems with medium-thick anthropogenic layer; 4—gleyed Urbostratozems with medium-thick anthropogenic layer; black squares with numbers indicate location of the soil profiles

development of root systems, which leads to a decrease in plant productivity.

Urbostratozems on buried soils were located in the northern and eastern part of the gardens. The buried soils were grey-humus gley soils (*Umbric Gleysols*). A biomorphic analysis of the buried humus horizon revealed the typical pattern of boreal forest soil. Plant and tree detritus were found along with the roots of trees and grasses, fungal hyphae and amorphous humic substances. Phytoliths are characteristic of

coniferous forests with moss cover; therefore, the phytoliths of mosses dominated. The area of gleyed Urbostratozem (*Urbic Technosol*, Gleyic) was located near the main house where the pond used to be. The groundwater level was at 105 cm during the soil survey.

Most soils in the Polish Gardens have a loam-sandy texture. The content of coarse particles (1–7 mm) of technogenic origin (construction debris) reaches 72% in some horizons of Urbostratozems (Fig. 35.8). The stoniness gives the soil a high thermal conductivity and a low moisture capacity. The upper horizons of the garden soils were over-compacted due to excessive recreational load. Root zone compaction inhibits tree growth, causes trees to die and leads to the poor condition of grasses on the lawns.

The surface horizons (0–30 cm) of the garden soils have a neutral or slightly alkaline reaction, which increases with depth to pH = 8.3–8.9 (Table 35.2). Soil alkalinity is associated with the use of de-icing reagents on the soil surface (calcium and sodium salts). Another reason for soil alkalinisation is the release of calcium due to water penetrating through construction debris

(cement, bricks, etc.). Many of the garden soils contain a significant amount of building lime. A continuous layer of lime is located at a depth of 112–134 cm in Profile 1, and at a depth of 58–81 cm in Profile 4. The organic matter content in the garden soils varied significantly depending on the content of organic carbon in the substrate applied to the soil as organic fertiliser. The average content of organic carbon in the soils of the Polish Gardens was 2.3–3.5%, the maximum 5.2%. The distribution of organic matter along the profile was cumulative; in the lower horizons the content of organic matter was 0.6–1.2%. The content of calcium carbonate in the soils of the gardens was 1–5%, while the maximum content was in the upper part of the profile. Plant nutrients (phosphorus, potassium) were unevenly distributed along the soil profile in garden soils. Anthropogenic layers were rich in nutrients compared to the horizons of natural soils; this is associated with the presence of household waste and construction debris in the soils. The nutrient supply in the garden soils is rated as high and very high. The content of heavy metals was determined in Urbostratozems on buried soils in

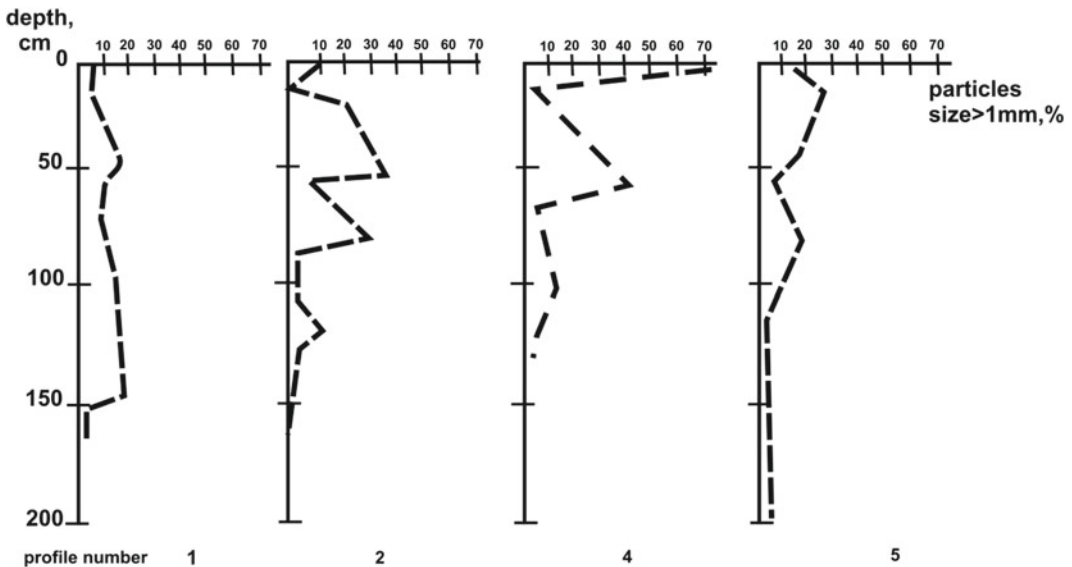


Fig. 35.8 Distribution of coarse particles (>1 mm) in soil profile. 1—Urbostratozem (*Urbic Technosol*) on buried grey-humus gley soil (*Umbric Gleysol*); 2—Urbostratozem (*Urbic Technosol*) on buried grey-humus

gley soil (*Umbric Gleysol*); 4—Gleyed Urbostratozem (*Urbic Technosol*, Gleyic) on marine loamy-sand sediments; 5—Urbostratozem (*Urbic Technosol*) on buried grey-humus gley soil (*Umbric Gleysol*)

the north (Profile 2) and south (Profile 1) of the garden. The distribution of Pb, Cu and Zn in the profiles revealed higher concentrations of the metals in the anthropogenic layers (0–120 cm) (Fig. 35.9).

35.7 Discussion

The soil cover of central St. Petersburg is homogeneous and is represented by Urbostratozems. A similar situation was observed in central Moscow (Prokofieva and Martynenko 2017). Like other urban soils, Urbostratozems of the historical centre of St. Petersburg formed on the cultural stratum with numerous artefacts. The relatively narrow anthropogenic layer (<2 m) allowed the soils of the pre-urban period to be identified. The complex nature of urban soil profiles—due to the supply of anthropogenic materials and the burial of native soil profiles—was also observed by Prokofieva and Poputnikov (2010) in the outskirts of Moscow and by Chupina (2020) in St. Petersburg.

An acidic reaction, a low humus content and plant nutrients are typical of the natural soils of the northwest region of Russia, where St. Petersburg is located (Dobrovolsky and Uru-sevskaya 2004). Thus, the impact of urbanisation can be traced in the soil alkalisation. A high soil pH, as a typical feature of urban soils, has been noted by many researchers (Gerasimova et al. 2003; Lehmann and Stahr 2007; Puskás and Farsang 2009; Musielok et al. 2018). These properties of urban soils correspond to the composition of urban plant communities, where there are many ornamental plants introduced from more southern regions with neutral soils. However, the alkaline reaction of urban soils (pH >8) which was observed in the soils of the Polish Gardens (Table 35.2) can adversely affect plants, e.g. due to the lower availability of micronutrients (Messenger 1986; Harrell et al. 1988).

The increased bulk density of the upper horizons and the large number of artefacts (construction debris) throughout the profile were found in the soils of both gardens. They affect the

development of roots and reduce the water-holding capacity of soils (Mao et al. 2014).

The high content of organic matter observed in the soils of urban gardens in St. Petersburg is considered a typical characteristic of garden and park soils (Lehmann and Stahr 2007; Burghardt et al. 2015; Rozanova et al. 2016; Musielok et al. 2018; Lindén et al. 2020). An increase in the plant nutrient content, especially phosphorus, has also been widely reported (Lehmann and Stahr 2007; Hulisz et al. 2018; Mazurek et al. 2016). Some authors (Burt et al. 2014) have attributed the high level of P to the frequent application of fertiliser in urban soils for landscaping.

The geochemical signature of urban soil is determined by the local history (Cannon and Horton 2009; Burt et al. 2014). The extent of heavy metal contamination depends on how such pollution occurs. One of the options is a continuous release of pollutants over time (e.g. due to exhaust gases or ongoing industrial discharges). This type of process leads to the surface layers exhibiting the highest concentrations of heavy metals; concentrations gradually decrease with increased depth. Another possible explanation is the introduction of pollutants over time, such as the discharge of contaminated material into the soil profile. In this case, the concentration of pollutants is likely to be higher in deeper horizons than in the upper ones.

The results obtained are in agreement with a geochemical study of the topsoil of Planty Park in Kraków (Çaşıorek et al. 2017). Data from a geochemical survey of the surface horizons of St. Petersburg soils with a light texture showed a median concentration of Pb—60, Zn—200 and Cu—50 mg kg⁻¹ (Golubev and Sorokin 2004), which are lower than in the gardens studied. The background concentrations of heavy metals for light-textured soils were calculated based on data from the geochemical atlas (Reimann et al. 2003). The median values were as follows: Pb—16, Cu—15 and Zn—51 mgkg⁻¹ (Matinian et al. 2007). Comparison of data on the content of these elements in the garden soils studied showed an excess of background concentrations by up to 25 times. The approximate permissible

Table 35.2 Selected properties of Urbostratozems of the Polish Gardens

Horizon	Depth, cm	pH H ₂ O	Total organic C, %	CaCO ₃ , %	Mobile forms, mg kg ⁻¹	
					K ₂ O	P ₂ O ₅
Profile 1—Urbostratozem (<i>Urbic Technosol</i>) on buried grey-humus gley soil (<i>Umbric Gleysol</i>)						
UR1ay	0–15	7.2	5.4	2.9	198	466
UR2	15–47	7.8	3.2	2.7	159	289
UR3rt	47–60	7.9	6.9	4.6	275	385
UR4	60–99	8.2	2.7	2.9	386	358
UR5rt	99–112	8.3	5.2	4.3	482	348
UR6	124–140	8.4	4.5	3.3	988	303
UR7	140–155	8.1	2.9	2.2	–	–
[AY]	155–170	7.7	1.9	1.3	838	241
CG	171–176	8.2	0.5	1.5	–	–
Profile 2—Urbostratozem (<i>Urbic Technosol</i>) on buried grey-humus gley soil (<i>Umbric Gleysol</i>)						
UR1ay	0–7	7.1	4.3	2.9	84	94
UR2	7–17	7.7	2.5	3.2	84	122
UR3	17–35	8.0	1.7	5.1	84	105
UR4	35–56	8.2	0.8	3.4	96	100
UR5	56–64	7.9	1.1	4.9	–	–
UR6	64–81	8.0	1.8	4.2	–	–
UR7g	81–88	7.9	1.0	3.2	–	–
UR8g	88–103	8.0	0.6	3.8	–	–
UR9	103–122	8.1	0.9	5.4	–	–
[AYg, ur]	122–150	6.2	2.4	1.5	196	70
CG	150–170	7.6	0.1	2.5	–	–
Profile 4—Gleyed Urbostratozem (<i>Urbic Technosol</i> , <i>Gleyic</i>) on marine loamy-sand sediments						
UR1ay	0–5	7.5	3.6	3.5	608	175
UR2ay	5–17	7.8	1.5	2.3	326	92
UR3	17–33	8.1	1.9	4.3	360	73
UR4	33–59	8.5	1.2	2.0	340	84
UR5	59–81	8.4	1.2	2.3	–	–
UR6G	81–100	8.5	1.5	2.2	–	–
CG	100–125	8.9	0.4	1.5	–	–
Profile 5—Urbostratozem (<i>Urbic Technosol</i>) on buried grey-humus gley soil (<i>Umbric Gleysol</i>)						
UR1ay	0–6	7.5	4.6	3.0	280	168
UR2	6–16	7.8	3.2	2.8	280	109
UR3	16–40	7.8	3.1	1.1	320	84

(continued)

Table 35.2 (continued)

Horizon	Depth, cm	pH H ₂ O	Total organic C, %	CaCO ₃ , %	Mobile forms, mg kg ⁻¹	
					K ₂ O	P ₂ O ₅
UR4rt	40–56	7.8	3.7	2.5	–	–
UR5	56–60	8.1	1.2	4.1	–	–
UR6	97–130	8.2	0.9	4.0	–	–
[AYg]	177–200	7.7	5.3	3.4	–	–
CG	200–215	7.8	0.4	2.5	–	–

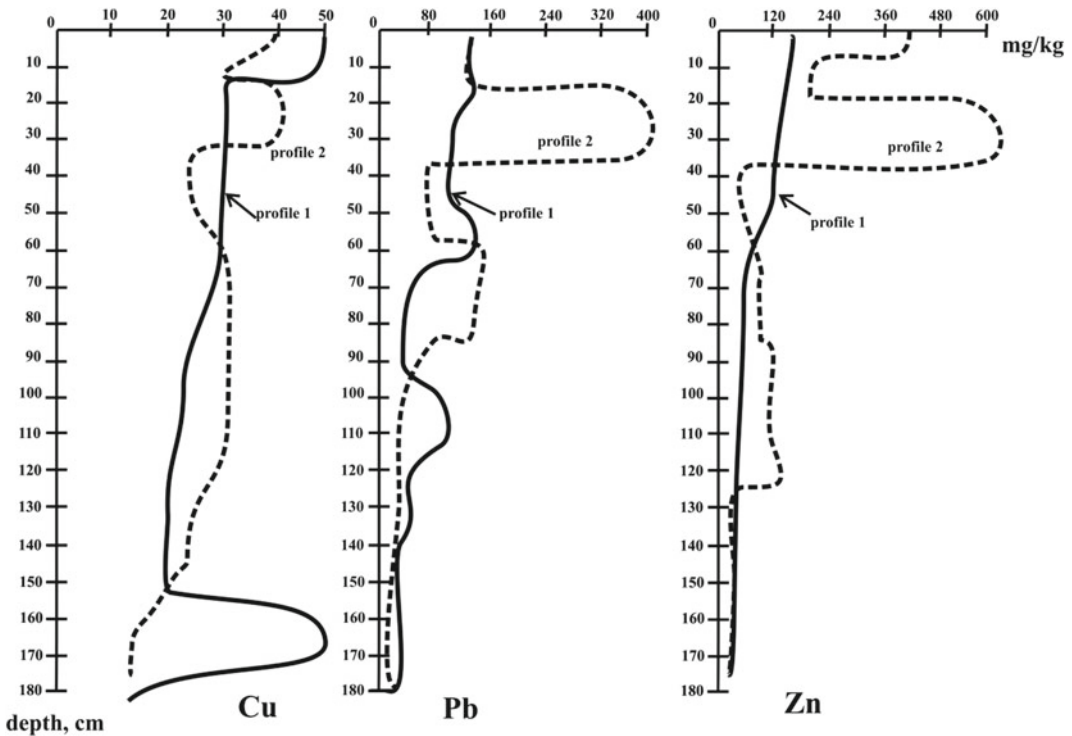


Fig. 35.9 Distribution of heavy metals (mg kg⁻¹) in soil profiles of the Polish Gardens: 1—Urbostratozem (*Urbic Technosol*) on buried grey-humus gley soil (*Umbric Gleysol*); 2—Urbostratozem (*Urbic Technosol*) on buried grey-humus gley soil (*Umbric Gleysol*)

concentrations are also exceeded by several times in both gardens, which is potentially dangerous for human health.

35.8 Conclusion

1. The soils of St. Petersburg experienced fundamental anthropogenic overprinting and

replacement. Native *Umbric Gleysols* and *Podzols* under coniferous forests have been replaced by *Urbostratozems* (*Urbic Technosols*) under garden plantations.

2. Soils are characterised by an alkaline pH, a high content of organic matter and plant-available phosphorous. The concentration of “urban metals” (Pb, Cu and Zn) in

anthropogenic layers exceeds their background content in natural unpolluted soils by 4–25 times. Soils are thus polluted and prone to eutrophication.

3. Assessing and monitoring the soils' ecosystem services and their state of degradation is a task for future research. Our study provided some initial analytical data for this purpose.

Acknowledgements The authors thank Dr. Alexandra Golyeva for the phytolith analysis and Dr. Michael Tarasev for his useful comments and assistance in preparing the manuscript.

References

- Abawi GS, Widmer TL (2000) Impact of soil health management practices on soilborne pathogens, nematodes and root diseases of vegetable crops. *Appl Soil Ecol* 15:37–47. [https://doi.org/10.1016/S0929-1393\(00\)00070-6](https://doi.org/10.1016/S0929-1393(00)00070-6)
- Ajmone-Marsan F, Biasioli M (2010) Trace elements in soils of urban areas. *Water Air Soil Pollut* 213:121–143. <https://doi.org/10.1007/s11270-010-0372-6>
- Alberti M, Marzluff J, Hunt VM (2017) Urban driven phenotypic changes: empirical observations and theoretical implications for eco-evolutionary feedback. *Philos Trans Royal Soc B* 372:1712. <https://doi.org/10.1098/rstb.2016.0029>
- Aleksandrovskaia EI, Aleksandrovskiy AL (2000) History of the cultural layer in Moscow and accumulation of anthropogenic substances in it. *Catena* 41:249–259. [https://doi.org/10.1016/S0341-8162\(00\)00107-7](https://doi.org/10.1016/S0341-8162(00)00107-7)
- Aleksandrovskiy AL, Dolgikh AV, Aleksandrovskaia EI (2012) Pedogenetic features of habitation deposits in ancient towns of European Russia and their alteration under different natural conditions. *Boletín de la Soc Geol Mex* 64(1):71–77. <https://doi.org/10.18268/BSGM2012v64n1a6>
- Aparin BF, Sukhacheva EY (2014) Principles of soil mapping of a megalopolis with Saint Petersburg as an example. *Eurasian Soil Sci* 7:650–661. <https://doi.org/10.1134/S106422931407003>
- Aparin BF, Sukhacheva EY, Bulysheva AM, Lazareva MA (2018) Humus horizons of soils in urban ecosystems. *Eurasian Soil Sci* 51(9):1008–1020. <https://doi.org/10.1134/S1064229318090016>
- Bach E, Ramirez KS, Fraser TD, Wall DH (2020) Soil biodiversity integrates solutions for a sustainable future. *Sustainability* 12:2662. <https://doi.org/10.3390/su12072662>
- Blanchart A, Séré G, Cherel J, Warot G, Stas M et al (2018) Towards an operational methodology to optimize ecosystem services provided by urban soils. *Landsc Urban Plan* 176:1–9. <https://doi.org/10.1016/j.landurbplan.2018.03.019>. Hal-02008732
- Blume HP (1975) Zur gliederung anthropogener böden. *Mitteilungen Der Deutschen Bodenkundlichen Gesellschaft* 22:597–602
- Brown SL, Chaney RL, Hettiarachchi GM (2016) Lead in urban soils: a real or perceived concern for urban agriculture? *J Environ Qual* 45:26–36. <https://doi.org/10.2134/jeq2015.07.0376>
- Bullock P, Gregory P (eds) (1991) Soils in the urban environment. Blackwell Great Britain, p 184
- Burghardt W, Morel L, Zhang GL (2015) Development of soil research about urban, industrial, traffic, mining and military area (SUITMA). *Soil Sci Plant Nutr* 61(1):3–21. <https://doi.org/10.1080/00380768.2015.1046136>
- Burt R, Hernandez L, Shaw R, Tunstead R, Ferguson R, Peaslee S (2014) Trace element concentration and speciation in selected urban soils in New York City. *Environ Monit Assess* 186:195–215. <https://doi.org/10.1007/s10661-013-3366-1>
- Cakmak D, Perovic V, Kresovic M, Jaramaz D, Mrvic V, Simic SB, Saljnikov E, Trivan G (2018) Spatial distribution of soil pollutants in green urban areas (a case study in Belgrade). *J Geochem Explor* 188:308–317. <https://doi.org/10.1016/j.gexplo.2018.02.001>
- Cannon WF, Horton JD (2009) Soil geochemical signature of urbanization and industrialization—Chicago, Illinois, USA. *Appl Geochem* 24:1590–1601. <https://doi.org/10.1016/j.apgeochem.2009.04.023>
- Caşiorek M, Kowalska J, Mazurek R, Pająk M (2017) Comprehensive assessment of heavy metal pollution in topsoil of historical urban park on an example of the Planty Park in Krakow (Poland). *Chemosphere* 179:148–158. <https://doi.org/10.1016/j.chemosphere.2017.03.106>
- Charzyński P, Markiewicz M, Świtoniak M (eds) (2013) Technogenic soil atlas. Polish Society of Soil Science, Torun, p 167. [http://www.suitma7.umk.pl/pliki/Technogenic_soils_atlas_P.Charzynski_M.Markiewicz_M.Switoniak_\[Eds.\]_2013.pdf](http://www.suitma7.umk.pl/pliki/Technogenic_soils_atlas_P.Charzynski_M.Markiewicz_M.Switoniak_[Eds.]_2013.pdf). Accessed 7 Mar 2021
- Chupina VI (2020) Anthropogenic soils of botanical gardens: a review. *Eurasian Soil Sci* 53:523–533. <https://doi.org/10.1134/S1064229320040043>
- Criado M, Santos-Francés F, Martínez-Graña A, Sánchez Y, Merchán L (2020) Multitemporal analysis of soil sealing and land use changes linked to urban expansion of Salamanca (Spain) using Landsat images and soil carbon management as a mitigating tool for climate change. *Remote Sens* 12(7):1131. <https://doi.org/10.3390/rs12071131>
- De Miguel E, Llamas JF, Chacón E, Berg T, Larssen S, Røyset O, Vadset M (1997) Origin and patterns of distribution of trace elements in street dust: unleaded petrol and urban lead. *Atmospheric Environ* 31:2733–2740. [https://doi.org/10.1016/S1352-2310\(97\)00101-5](https://doi.org/10.1016/S1352-2310(97)00101-5)
- Delbecque N, Verdoodt A (2016) Spatial patterns of heavy metals contamination by Urbanisation.

- J Environ Qual 45(1):9–17. <https://doi.org/10.2134/jeq2014.11.0508>
- Dobrovolsky GV, Urusevskaya IS (2004) Soil geography. State University Press, Moscow, p 720 (География почв. Московский Государственный Университет)
- Dolotov VA, Ponomareva VV (1982) To the characterisation of the soils of Leningrad summer garden. Pochvovedenie 9:134–138 (К характеристике почв Летнего сада Ленинграда)
- Dougherty M, Dymond RL, Goetz SJ, Jantz CA, Goulet N (2004) Evaluation of impervious surface estimates in a rapidly urbanizing watershed. Photogramm Remote Sens 70(11):1275–1284, Edmonton, Canada, p 283. <https://www.woodwellclimate.org/wp-content/uploads/2015/09/DoughertyetalPhoEngRS.04.pdf>. Accessed 7 Mar 2021
- Effland WR, Pouyat RV (1997) The genesis, classification, and mapping of soils in urban areas. Urban Ecosyst 1:217–228. <https://doi.org/10.1023/A:1018535813797>
- Encyclopedic Handbook (1992) Saint Petersburg, Petrograd, Leningrad. Moscow, scientific publishing house big Russian encyclopedia, p 687 (Энциклопедический справочник (1992) Санкт-Петербург. Петроград. Ленинград. Москва, “Большая Российская Энциклопедия”)
- EU (2012) Guidelines on best practice to limit, mitigate or compensate soil sealing. Luxembourg: European union. http://ec.europa.eu/environment/soil/pdf/guidelines/pub/soil_en.pdf. Accessed 7 Mar 2021
- Fanning DS, Stein SE, Paterson JC (1978) Theories of genesis and classification of highly man-influenced soils. In: Abstract of commission papers, vol 1. 11th congress of the international society soil science, Edmonton, Canada, p 283
- Gerasimova MI, Stroganova MN, Mozharova NV, Prokofeva TV (2003) Anthropogenic soils: genesis, classification, rehabilitation and use. Smolensk, Oykumena, p 268 (Антропогенные почвы: генезис, классификация, реабилитация и использование. Смоленск, Ойкумена)
- Golubev AD, Sorokin ND (eds) (2004) The environmental situation in Saint Petersburg: analytical review of environmental situation in Saint Petersburg for 25 years. Saint Petersburg. Format (Голубев А.Д., Сорокин Н.Д. (ред.) Экологическая ситуация в Санкт-Петербурге: аналитический обзор экологической ситуации в Санкт-Петербурге за 25 лет Санкт-Петербург, Формат)
- Golyeva AA (2001) Biomorphological analysis as a part of soil morphological investigations. Catena 43(3):217–230
- Greinert A (2015) The heterogeneity of urban soils in the light of their properties. J Soils Sediments 15(8):1725–1737. <https://doi.org/10.1007/s11368-014-1054-6>
- Guillard C, Maron PA, Damas O, Ranjard L (2018) Biodiversity of urban soils for sustainable cities. Environ Chem Lett 16(4):1267–1282
- Hammer Ø, Harper DAT, Ryan PD (2001) PAST: paleontological statistics software package for education and data analysis. Palaeontol Electron 4(1):9. http://palaeo-electronica.org/2001_1/past/issue1_01.htm
- Harrell MO, Pierce P, Mootr D (1988) Pin oak and silver maple chlorosis treatment with ferric ammonium citrate solution. J Arboric 14:156–158. <http://pascal-francis.inist.fr/vibad/index.php?action=getRecordDetail&idt=7757953>. Accessed 7 Mar 2021
- Hiller DA (2000) Properties of Urbic anthrosols from an abandoned shunting yard in the Ruhr area, Germany. Catena 39:245–266. [https://doi.org/10.1016/S0341-8162\(00\)00081-3](https://doi.org/10.1016/S0341-8162(00)00081-3)
- Hulisz P, Charzyński P, Greinert A (2018) Urban soil resources of medium-sized cities in Poland: a comparative study of Toruń and Zielona Góra. J Soils Sediments 18:358–372. <https://doi.org/10.1007/s11368-016-1596-x>
- Huot H, Joyner J, Córdoba A, Shaw RK, Wilson MA, Walker R, Muth TR, Cheng Z (2017) Characterizing urban soils in New York City: profile properties and bacterial communities. J Soils Sediments 17:393–407. <https://doi.org/10.1007/s11368-016-1552-9>
- Krupski M, Kabala C, Sady A, Gliński R, Wojcieszak J (2017) Double- and triple-depth digging and Anthrosol formation in medieval and modern-era city (Wrocław, SW Poland). Geoarchaeological research on past horticultural practices. Catena 153:9–20. <https://doi.org/10.1016/j.catena.2017.01.028>. <https://www.cabdirect.org/cabdirect/abstract/20173161517>
- Kumar K, Hundal LS (2016) Soil in the City: sustainably improving urban soils. J Environ Qual 45:2–8. <https://doi.org/10.2134/jeq2015.11.0589>
- Lanen HAJV, Peters E (2000) Definition, effects and assessment of groundwater droughts. In Vogt JV, Somma F (eds) Drought and drought mitigation in Europe. Kluwer Academic Publishers, pp 49–61
- Lee CS, Li X, Shi W, Cheung SC, Thornton I (2006) Metal contamination in urban, suburban, and country park soils of Hong Kong: a study based on GIS and multivariate statistics. Sci Total Environ 356:45–61. <https://doi.org/10.1016/j.scitotenv.2005.03.024>. <https://pubmed.ncbi.nlm.nih.gov/15913711/>
- Lehmann A (2006) Technosols and other proposals on urban soils for the WRB (world reference base for soil resources). Int Agrophys 20(2):129–134
- Lehmann A, Stahr K (2007) Nature and significance of anthropogenic urban soils. J Soils Sediments 7(4):247–260. <https://doi.org/10.1065/jss2007.06.235>
- Lindén L, Riikonen A, Setälä H, Yli-Pelkonen V (2020) Quantifying carbon stock in urban parks under cold climate conditions. Urban For Urban Green 49:126633. <https://doi.org/10.1016/j.ufug.2020.126633>
- Luo XS, Yu S, Zhu YG, Li XD (2012) Trace metal contamination in urban soils of China. Sci Total Environ 421–422:17–30. [10.1016/j.scitotenv.2011.04.020](https://doi.org/10.1016/j.scitotenv.2011.04.020)
- Manna P, Basile A, Bonfante A, D’Antonio A, De Michel CM, Iamarino M, Langella G, Mileti AF, Pileri P, Vingiani S, Terribile F (2017) Soil sealing: quantifying impacts on soil functions by a geospatial decision support system. Land Degrad Develop 28(8):2513–2526. <https://doi.org/10.1002/ldr.2802>
- Mao Q, Huang G, Buyantuev A, Wu J, Luo S, Ma K (2014) Spatial heterogeneity of urban soils: the case of

- the Beijing metropolitan region. *China Ecol Processes* 3:23. <https://doi.org/10.1186/s13717-014-0023-8>
- Matinian NN, Reimann C, Bakhmatova KA, Rusakov AV (2007) The background concentration of heavy metals and as in arable soils of North-West of Russia (based on the materials of international geochemical atlas). *Vestnik of Saint Petersburg State University* 3(3):123–134 (Фоновое содержание тяжелых металлов и As в пахотных почвах Северо-Запада России (по материалам международного геохимического атласа). *Вестник СПбГУ*)
- Matinyan NN, Bakhmatova KA, Korentsvit VA (2017) Soils of the Summer Garden (Saint Petersburg). *Eurasian Soil Sci* 50(6):637–645. <https://doi.org/10.1134/S1064229317060060>
- Mazurek R, Kowalska J, Čašiorek M, Setlak M (2016) Micromorphological and physico-chemical analyses of cultural layers in the urban soil of medieval city—a case study from Krakow, Poland. *Catena* 141:73–84. <https://doi.org/10.1016/j.catena.2016.02.026>
- Messenger S (1986) Alkaline runoff, soil pH and white oak manganese deficiency. *Tree Physiol* 2:317–325. <https://doi.org/10.1093/treephys/2.1-2-3.317>. <https://pubmed.ncbi.nlm.nih.gov/14975865/>
- Mitchell RG, Spliethoff HM, Ribaud LN, Lopp DM, Shayler HA, Marquez-Bravo LG, Lambert VT, Ferenz GS, Russell-Anelli JM, Stone EB, McBride MB (2014) Lead (Pb) and other metals in New York City community garden soils: factors influencing contaminant distributions. *Environ Pollut* 187:162–169. <https://doi.org/10.1016/j.envpol.2014.01.007>. <https://pubmed.ncbi.nlm.nih.gov/24502997/>
- Montgomery JA, Klimas CA, Arcus J, DeKnock C, Rico K, Rodriguez Y, Vollrath K, Webb E, Williams A (2016) Soil quality assessment is a necessary first step for designing urban green infrastructure. *J Environ Qual* 45:18–25. <https://doi.org/10.2134/jeq2015.04.0192>
- Musieliok L, Drewnik M, Stolarczyk M, Gus M, Bartkowiak S, Kozyczkowsky K, Lasota J, Motak A, Szczechowska K, Wąty M (2018) Rates of anthropogenic transformation of soils in the Botanical Garden of Jagiellonian University in Kraków (Poland). *Catena* 170:272–282. <https://doi.org/10.1016/j.catena.2018.06.023>
- OST 41–08–265–04 (2004) The industry standard. Quality control of analytical work M., VIMS publishing (ОСТ 41–08–265–04 (2004) (Стандарт отрасли. Контроль качества аналитической работы М., Издательство ВИМС). <https://files.stroyinf.ru/Data2/1/4293741/4293741855.pdf>
- Pavao-Zuckerman MA (2008) The nature of urban soils and their role in ecological restoration in cities. *Restor Ecol* 16(4):642–649. <https://doi.org/10.1111/j.1526-100X.2008.00486.x>
- Pavao-Zuckerman MA, Byrne LB (2009) Scratching the surface and digging deeper: exploring ecological theories in urban soils. *Urban Ecosyst* 12:9–20. <https://doi.org/10.1007/s11252-008-0078-3>
- Pavlović D, Pavlović M, Čakmak D, Kostić O, Jarić S, Sakan S, Đorđević D, Mitrović M, Gržetić I, Pavlović P (2018) Fractionation, mobility, and contamination assessment of potentially toxic metals ion urban soils in four industrial Serbian cities. *Arch Environ Contam Toxicol* 75(3):335–350. <https://doi.org/10.1007/s00244-018-0518-x>
- Piperno DR (2006) *Phytoliths: a comprehensive guide for archaeologists and paleoecologists*. Lanham, New York, Toronto, Oxford: AltaMira Press (Rowman & Littlefield), p 238. 0–7591–0385–2. <https://doi.org/10.1017/S0016756807003159>
- Pristeri G, Peroni F, Pappalardo SE et al (2020) Mapping and assessing soil sealing in Padua municipality through biotope area factor index. *Sustainability* 12 (12):5167. <https://doi.org/10.3390/su12125167>
- Prokofieva TV, Gerasimova MI (2018) Urban soils: diagnostics and taxonomic position according to materials of scientific excursion in Moscow at the Suitma-9 workshop. *Eurasian Soil Sci* 51(9):995–1007. <https://doi.org/10.1134/S1064229318090090>
- Prokofieva TV, Poputnikov VO (2010) Anthropogenic transformation of soils in the Pokrovskoe-Streshnevo Park (Moscow) and adjacent residential areas. *Eurasian Soil Sci* 43(6):701–711. <https://doi.org/10.1134/S1064229310060116>
- Prokofieva TV, Gerasimova MI, Bezuglova OS, Gorbov SN, Bakhmatova KA, Matinyan NN, Goleva AA, Zharikova EA, Nakvasina EN, Sivtseva NE (2014) Inclusion of soils and soil-like bodies of urban territories into the Russian soil classification system. *Eurasian Soil Sci* 47(10):959–967. <https://doi.org/10.7868/S0032180X14100104>
- Prokofieva TV, Martynenko IA (2017) Urban soil surveys. The case study of Moscow, Russia. In: Levin MJ, Kim KJ, Morel JL, Burghardt W, Charzynski P, Shaw RK (eds) *Soils within cities. Global approaches to their sustainable management—composition, properties, and functions of soils in the urban environment*, IUSS Working Group SUITMA, pp 129–138
- Prokofyeva TV, Martynenko IA, Ivannikov FA (2011) Classification of Moscow soils and parent materials and its possible inclusion in the classification system of Russian soils. *Eurasian Soil Sci* 44(5):561–571
- Puskás I, Farsang A (2009) Diagnostic indicators for characterizing urban soils of Szeged, Hungary. *Geoderma* 148:267–281. <https://doi.org/10.1134/S1064229311050127>
- Ramirez KS, Lef JW, Barberán A, Bates ST, Betley J, Crowther TW, Kelly EF, Oldfield EE, Shaw EA, Steenbock C, Bradford MA, Wall DH, Fierer N (2014) Biogeographic patterns in belowground diversity in New York City’s central park are similar to those observed globally. *Proc Biol Sci* <https://doi.org/10.1098/rspb.2014.1988>
- Reimann C, Siewers U, Tarvainen T, Bitjukova L, Eriksson J, Gilucis A, Gregorauskiene V, Lukashchev VK, Matinian NN, Pasieczna A (2003)

- Agricultural soils in northern Europe: geochemical atlas. Geologisches Jahrbuch, E. Schweizerbart'sche Verlagsbuchhandlung, Stuttgart, Germany, p 279
- Rosenbaum MS, McMillan AA, Powell JH, Cooper AH, Culshaw MG, Northmore KJ (2003) Classification of artificial (man-made) ground. *Eng Geol* 69:399–409. [https://doi.org/10.1016/S0013-7952\(02\)00282-X](https://doi.org/10.1016/S0013-7952(02)00282-X)
- Rossiter DG (2007) Classification of urban and industrial soils in the world reference base for soil resources. *J Soils Sediments* 7(2):96–100. <https://doi.org/10.1065/jss2007.02.208>
- Rozanova MS, Prokofeva TV, Lysak LV, Rakhleeva AA (2016) Soil organic matter in the Moscow State University botanical garden on the Vorobevy Hills. *Eurasian Soil Sci* 49(9):1013–1025. <https://doi.org/10.1134/S106422931609012X>
- Rusakov AV, Novikov VV (2003) Biological activity in modern and buried soils of the historical centre of Saint Petersburg. *Microbiology* 72(1):117–25. <https://doi.org/10.1023/A:1022242509992> (Русаков В, Новиков ВВ. Биологическая активность современных и погребенных почв исторического центра Санкт-Петербурга. *Микробиология* 72(1):117–25)
- Russian Soil Classification System (2001) Arnold RW (ed), V.V. Dokuchaev Soil Science Institute, p 220
- Savard JPL, Clergeau P, Mennechez G (2000) Biodiversity concepts and urban ecosystems. *Landsc Urban Plan* 48:131–142
- Scalenghe R, Franco AM (2009) The anthropogenic sealing of soils in urban areas. *Landsc Urban Plan* 90 (1–2):1–10. <https://doi.org/10.1016/j.landurbplan.2008.10.011>
- Seto KC, Dhakal S, Bigio A, Blanco H, Delgado GC, Dewar D, Huang L, Inaba L, Kansal A, Lwasa S, McMahon JE, Müller DB, Murakami J, Nagendra H, Ramaswami V, (2014) Human settlements, infrastructure and spatial planning. In: Edenhofer O, Pichs-Madruga R, Sokona Y, Farahani E, Kadner S, Seyboth K, Adler A, Baum I, Brunner S, Eickemeier P, Kriemann B, Savolainen J, Schlömer S, Stechow CV, Zwickel T, Minx JC (eds) *Climate change 2014: mitigation of climate change. Contribution of working group III to the 50th assessment report of the intergovernmental panel on climate change*. Cambridge University Press, Cambridge, United Kingdom and New York, NY, USA. https://www.ipcc.ch/site/assets/uploads/2018/02/ipcc_wg3_ar5_chapter12.pdf. Accessed 7 Mar 2021
- Hygienic Standard 2.1.7.2042–06 (2006) Approximate permissible concentrations of chemical substances in soil (Гигиенический норматив 2.1.7.2042–06, Ориентировочно допустимые концентрации химических веществ в почве)
- Stroganova M, Prokofieva T (2001) Urban soils classification for Russian cities of the taiga zone. European soil bureau—research report no. 7:153–156. <https://citeseerx.ist.psu.edu/viewdoc/download?doi=10.1.1.156.4056&rep=rep1&type=pdf>. Accessed 7 March 2021
- Ungaro F, Calzolari C, Pistocchi A, Malucelli F (2014) Modelling the impact of increasing soil sealing on runoff coefficients at regional scale: a hydro-pedological approach. *J Hydrol Hydromech* 62(1):33–42
- United Nations (2015) World urbanisation prospects: the 2014 revision (ST/ESA/SER.A/366). Department of Economic and Social Affairs, Population Division 2015. <https://www.un.org/en/development/desa/publications/2014-revision-world-urbanization-prospects.html>. Accessed 7 Mar 2021
- Vodyanitskii YuN (2015) organic matter of urban soils: a review. *Eurasian Soil Sci* 48(8):802–811. <https://doi.org/10.1134/S1064229315080116>
- Vorobieva LA (ed) (2006) Theory and practice of chemical analysis of soils. Moscow, MGU (Теория и практика химического анализа почв. Москва, МГУ)
- WRB (2006) World reference base for soil resources. World soil resources reports no. 103. FAO, Rome
- WRB (2014) World reference base for soil resources 2014. International soil classification system for naming soils and creating legends for soil maps. World soil resources reports no. 106. FAO, Rome, p 181
- Xiao R, Tian Y, Xu G (2020) Spatial gradient of urban green field influenced by soil sealing. *Sci Tot Environ* 735:139490. <https://doi.org/10.1016/j.scitotenv.2020.139490>
- Yuan F, Bauer ME (2007) Comparison of impervious surface area and normalized difference vegetation index as indicators of surface urban heat island effects in Landsat imagery. *Remote Sens Environ* 106 (3):375–386



Agrosoils in the City of St. Petersburg: Anthropogenic Evolution and Current State

36

Vyacheslav Polyakov, Evgeny Abakumov,
George Shamilishvily, Ekaterina Chebykina,
and Anton Lavrishchev

Abstract

Over the past 30 years, agricultural land in the Russian Federation has decreased by a significant area; 97 million hectares. This withdrawn arable land has become part of the fallow land that is no longer used for cropping. This land has undergone significant physical and chemical changes due to the degradation of the upper fertile horizons and the partial afforestation of the landscape. This chapter presents data on the current state and evolution of fallow land in urban St. Petersburg. The morphological and mesomorphological characteristics of soils were studied using vertical electrical resistivity sounding (VERS). An assessment was also made of changes in soil agrochemical parameters and the level of soil pollution with Zn, Cu and hydrocarbons. The negative changes in fallow

urban soils were found to be due to the reduction and cessation of agrochemical and agrotechnical measures designed to maintain soil fertility and quality, which in turn resulted in a reduction in the arable area, a decline in agricultural production and an increase in the area of the degraded soils. Finally, technological measures were proposed for reclaiming fallow land of different levels of degradation. The creation of a regional centre for the restoration of fallow soils was proposed.

Keywords

Soil degradation · Fallow land ·
Agrolandscapes · Agrosoils · Suburban soils

V. Polyakov · E. Abakumov (✉) · G. Shamilishvily
· E. Chebykina

Department of Applied Ecology, Faculty of Biology,
St. Petersburg State University, 16th Liniya V.O.,
29, St. Petersburg, St. Petersburg 199178, Russian
Federation

e-mail: e_abakumov@mail.ru

V. Polyakov · A. Lavrishchev
Department of Soil Science and Agrochemistry,
Faculty of Agricultural Technology, Soil Science
and Ecology, Saint Petersburg State Agrarian
University, Petersburg Highway 2, Pushkin, St.
Petersburg 196601, Russian Federation

36.1 Introduction

The current stage of development and implementation of agriculture in Russia is characterised by a significant reduction in the area of cropland. Nevertheless, some stabilisation in the reduction of abandoned fallow land has been observed in the last 5–7 years. Currently, the total area of agricultural land in Russia is 167.6–194.4 million hectares (depending on the published source). This includes arable land that occupies an area of about 115–120 million hectares, while the area of former arable land that is presently withdrawn fallow land is more than 30 million hectares. This

fallow land is overgrown with shrubs and weeds (Dobrovolsky 2004). From 1990–2016, the area of fallow land decreased by 97.2 million hectares (44% of the country's total agricultural land). The economic downturn in the 1990s and early 2000s coincided with land misuse, which led to a reduction in arable land by 11 million hectares and a reduction in the sown area by 40 million hectares. This happened spontaneously due to economic failure and improper land use policies. Along with marginal land, a lot of productive fertile land was withdrawn from active use and transformed into abandoned fallow land of different ages. The cost of economic losses from the withdrawal of arable land is estimated at about 500 billion roubles (Zakharenko 2008; Dmitrakova and Abakumov 2018). Large areas of the arable land, pastures and grassland that were out of control and out of active agricultural use have become a real economic and environmental disaster. In those years, the lack of grain, industrial crops, fodder and other products deprived the country of food independence (Kashtanov and Sizov 2008; Lal 2002, 2004). Significant areas of intensively cultivated and reclaimed land supplying North-West Russia with crops ceased to be cultivated (Liuri et al. 2010). Throughout the entire period of St. Petersburg's existence, suburban land has been used as highly productive agricultural land. However, a soil survey in the 1920s showed that restoring the boundaries of natural soil types was difficult due to the long-term cultivation and application of urban waste and peat as a fertiliser. According to official sources, at present, between 30–40 million hectares of arable land in Russia have been left to lie fallow and are not used. This is due to the natural and anthropogenic processes of soil formation, soil self-development, forest overgrowing, sodding, flooding, waterlogging, etc. (Ivanov et al. 2008; Liuri et al. 2010). In the North-West Federal District (NWFD) of the Russian Federation, according to the Federal Register Service, as of 01.01.2017, the area of agricultural land was 31,418,400 ha, which is 18.6% of the total district and 8.2% of the agricultural land in Russia. By 1985, about 6,00,000 hectares of arable land and 2.4 million hectares of agricultural land had been

withdrawn from use in the North-West Federal District. Half of these losses occurred in the Pskov, Leningrad and Novgorod regions. The area of grain decreased from 1,150,000–250,000 ha (4.6 times), flax from 125,000–9,000 ha (13.8 times), potatoes from 228,000–101,000 ha (2.2 times) and vegetables from 25,000–20,000 ha (1.3 times), while the share of unproductive perennial herbs increased.

The global anthropogenic evolution of the Earth's surface in the twentieth century replaced local anthropogenic impact within a separate natural-urban complex. Whereas in the last century, technogenesis was in a sense opposed to anthropogenesis, emphasising the technogenic impact on nature, now, the anthropogenesis of nature is rarely carried out without powerful technical means. Thus, these concepts are gradually converging due to the increased anthropogenic impact on the environment (Kodiwo et al. 2014). Urban soils transformed from previously cultivated land are one of the most important components of the urban environment, and an integral part of the habitat of plants and living organisms, as well as being an environment for urban activities (business and recreation). When assessing the ecological state of agricultural land, soil is important as the initial link in the food chain, a secondary source of air and water pollution, and the only indicator of the ecological state of the environment. City territories often extend to adjacent agricultural land, where the agrogenic horizon is developed on various agro-natural soils and Anthrosols. Similarly to other metropolitan cities, St. Petersburg also sees negative trends in land use, some of which are inevitable. The constant construction of urban structures and infrastructure often requires new land, including that in agricultural use. A considerable technogenic pressure is the cause of significant environmental tensions in the city (Shamilishvily et al. 2018).

In agricultural landscapes, human activities lead to changes in the chemical composition, physical properties and soil regimes. When an agrogenic impact comes to an end, processes of post-agrogenic transformation begin in the landscape, leading to the restoration of the natural

soil profile. The duration of the post-agrogenic transformation is measured in decades and centuries and depends on the regenerative capacity of the soil (Simakova and Topkopogova 2006; Lal 2002). After arable soils are withdrawn from use, the natural vegetation cover is restored in several stages (grassland, forest) (Jenkinson and Coleman 2008). Succession changes continue until a combination of species is established that most closely matches the regional climate (Lal 2004).

In addition, agricultural soils located in and near urban zones are at high risk of contamination with potentially toxic and hazardous elements. Polycyclic aromatic hydrocarbons (PAHs) are ubiquitous organic contaminants, with soil being the most important sink. The increasing contamination of urban soil by persistent organic pollutants is a major environmental issue (Zhang et al. 2019), exposing living organisms to health risks (Zhang et al. 2020; Ehigbor et al. 2020). PAHs are hardly degraded by microorganisms due to their stable aromatic ring structures, and some PAHs are known to be carcinogenic and mutagenic (IARC 2010). A large quantity of PAHs released into the atmosphere are deposited in soil via dry and wet deposition (Kwon and Choi 2014; Schuster et al. 2015). PAHs are persistent and hydrophobic, so can be found in the soil matrix long after being adsorbed by the soil and sediment organic matter (Wang et al. 2013; Bergamasco et al. 2014). Agricultural soils located near urban zones with PAHs are widely reported to be contaminated (e.g. Kim et al. 2019; Stogiannidis and Laane 2015). Soil pollution with heavy metals is a growing environmental pollution problem due to various human activities including untreated municipal and industrial waste water, vehicle emissions etc., particularly in the urban environment (Shamilishvili et al. 2015; Kasimov and Vlasov 2018; Čakmak et al. 2018; Seleznev et al. 2019; Dytłow and Górka-Kostrubiec 2020; Trujillo-González et al. 2016). Agricultural landscapes are the prime link in the environment, acting as a reservoir or sink for pollutants including heavy metals in the food chain (Kelly et al. 1996; Mielke et al. 1999; Aiman et al.

2016; Ninkov et al. 2018; Antić-Mladenović et al. 2018; Saljnikov et al. 2019; Mahmood et al. 2020).

Active and fallow agroecosystems are unique objects represented by models of development, degradation, progradation and, in general, the evolution of the components of biogeocenoses over time and space. During the twentieth century, this happened on the territory of the Russian Federation due to positive and negative dynamics of an agrogenic impact. From this perspective, the North-West region is of particular interest, since there was both large-scale land development and an uncontrolled transformation of arable land to and from the fallow state. There were also processes of drainage, irrigation and intensive amelioration. All this led to the formation of soil and vegetation succession with varying degrees of exposure to agrogenic factors (Karavaev and Denisenko 2008; Lyubimova et al. 2008).

Agricultural development in the Russian northwest began with the most heavily drained territories. Periodic deforestation and shifting agriculture turned powerful forest soils into Podzols. There is an assumption that the boundary of Podzols was artificially shifted to the north due to the anthropogenic transformation of Podzols (Kechaykina et al. 2011). Agricultural development of the Northwest was especially intense in the twentieth century (Giani et al. 2003). These soils are characterised by thick humus horizons (as a result of intensive cultivation). It is formed directly on the clay parent material and is represented in the southern suburbs of St. Petersburg, in the Prinevskaya lowland (Malakhovskiy et al. 1993). Now, this agricultural land is part of the suburban farms and is still considered one of the most fertile soils of the North-West. The plaggen-agrozem formed in the eighteenth century is a local example and a result of the intensive farming. Most of the land was primitively cultivated in the Northwest with simple agricultural means. The last foci of “slash-and-burn cultivation” only disappeared in the Leningrad region in the middle of the twentieth century. Soils were mainly ploughed on the southern slopes, while the northern slopes were

used as hayfields and pastures. In the currently forested soils of the farms that disappeared at the beginning of twentieth century, agrogenic signs have been found (Veenstra and Burras 2015).

The conservation of soil and land resources and the possibility of their agricultural use should be a national and regional strategy aimed at ensuring food independence. Studying the properties of fallow land helps determine the origin and causes of changes in the soils over time. This will subsequently make it possible to scientifically substantiate the forecasting of positive and negative agricultural processes in the soils left without any anthropogenic pressure. Further, studying these processes will enable an optimal solution to be found for the use of this land—it may be returned to or withdrawn from agricultural use—and help develop recommendations for land use (haymaking, pasture or forestry). Therefore, the aim of this work was to study the current state of former arable and currently fallow land in St. Petersburg, as well as to propose measures for returning the fallow land to agricultural use. The following goals were set:

- study the morphological and mesomorphological characteristics of fallow land
- conduct vertical electrical resistivity sounding (VERS) on the fallow soils
- assess agrochemical parameters of fallow soils
- assess contamination of fallow soils with heavy metals and hydrocarbons
- introduce a methodology for the reclamation of fallow land.

36.2 Site Description

The study area belongs to the Prinevskaya lowland, located in the city of St. Petersburg. It is the main area of suburban farming, providing the city with potatoes and vegetables as well as a livestock feed production area. In the past, this land was actively cultivated using drainage, liming and the application of high doses of organic and mineral fertilisers (Chukov 2001). The withdrawal of arable land from use and its

subsequent natural overgrowing is common; not only in the last 15–20 years. Historically, most of the southern taiga subzone has been subject to anthropogenic impact to some extent. Many modern Podzol soils were thus formed as a result of the evolution of former arable land into forest land (Kechaykina et al. 2011; Dmitrakova et al. 2018).

St. Petersburg has a moderate type of climate, with an average annual rainfall of 662 mm, and an average number of 75 sunny days. The average air temperature of the coldest month (February) is -5.8 °C, the warmest month (July) is $+18.8$ °C, and the average annual air temperature is $+5.8$ °C. The area studied and the sampling sites are presented in Fig. 36.1.

The following land use types were selected to study the ecological state and post-agrogenic transformation: fallow (abandoned) soils in the former state farms (Detskoselsky (1.1 Anthrosol; 1.3 Umbrisol), in Kuzmino (1.2 Anthrosol; 1.5 Anthrosol) and at St. Petersburg State Agrarian University, SPBSAU (1.4 Umbrisol); garden soils derived from soils in agricultural use and abandoned soils (4.1, 4.2, 4.3 and 4.4 soils); old arable soil in new residential zones (2.1, 2.2, 2.3, 3.1 and 3.2 soils) (fertile arable soil sealing).

The soils studied represented the following types (WRB 2015) according to their number:

- 1.1 Anthrosol of fallow (abandoned) soils
- 1.2 Anthrosol of fallow (abandoned) soils
- 1.3 Umbrisol of fallow (abandoned) soils
- 1.4 Umbrisol of fallow (abandoned) soils
- 1.5 Anthrosol of old arable soil in new residential zone
- 2.1 Anthrosol of old arable soil in new residential zone
- 2.2 Anthrosol of old arable soil in new residential zone
- 2.3 Anthrosol of old arable soil in new residential zone
- 3.1 Podzols of old arable soil in new residential zone
- 3.2 Anthrosol of old arable soil in new residential zone
- 4.1 Podzol of garden soils derived from soils in agricultural use and abandoned soils

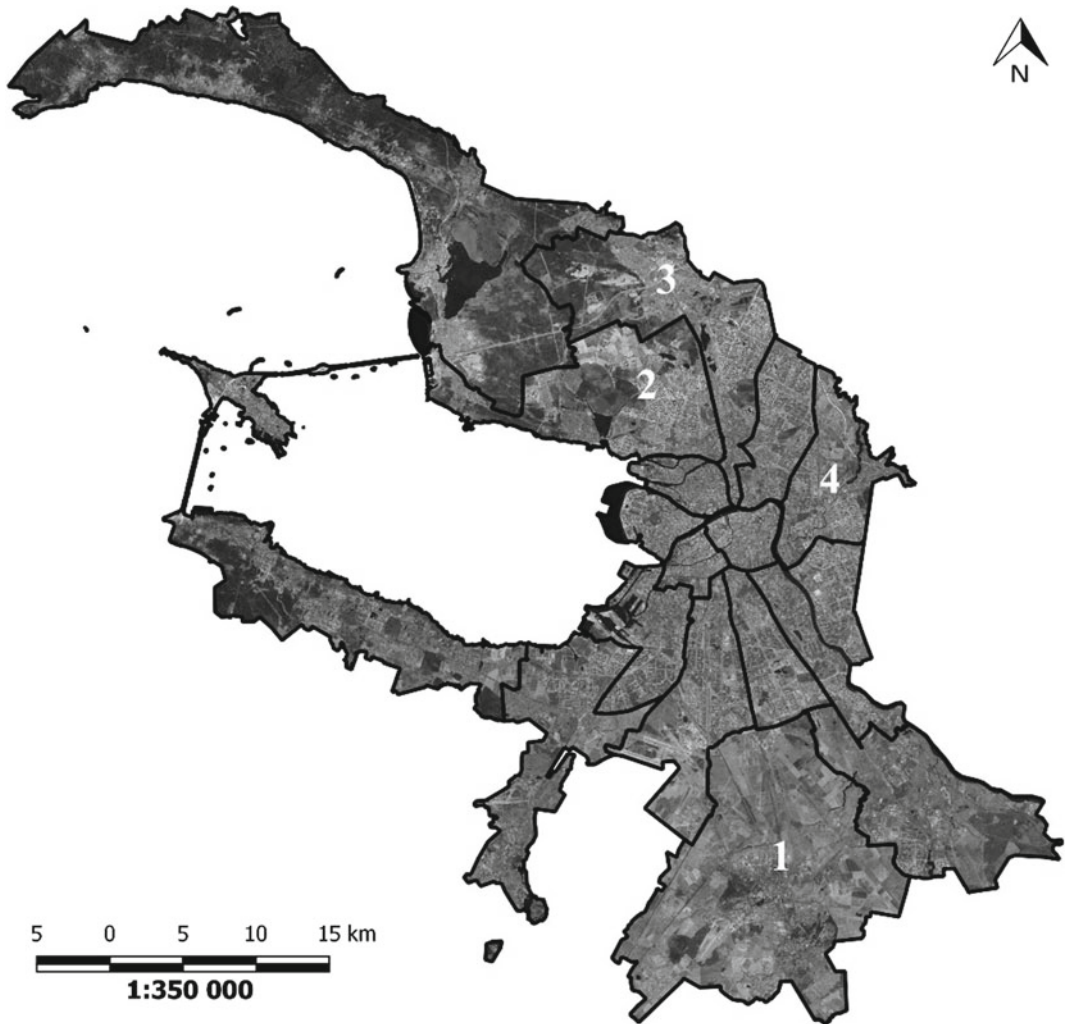


Fig. 36.1 Study districts in Saint Petersburg: 1—Pushkin; 2—Primorsky; 3—Vyborgskiy; 4—Krasnogvardeisky

4.2 Technosol of garden soils derived from soils in agricultural use and abandoned soils

4.3 Anthrosol of garden soils derived from soils in agricultural use and abandoned soils

4.4 Anthrosol of garden soils derived from soils in agricultural use and abandoned soils.

diagnostics were made according to the “Soil Classification and Diagnostics” (Shishov et al. 2004) and the World Base of Soil Resources (WRB 2015). For further processing, the soils were packed and delivered to the Department of Applied Ecology, Saint Petersburg State University.

36.3 Field Analyses

Soil samples were taken in October and November 2018. The following districts of St. Petersburg were chosen for the study: Pushkin, Primorsky, Vyborgskiy and Krasnogvardeisky (Fig. 36.1). Soil

36.3.1 Soil Morphological Characteristics

A morphological view of selected studied soil profiles is shown in Fig. 36.2 and their description is presented in Table 36.1. The main factor



Fig. 36.2 Representative soils of study sites: 1.1—Anthrosol; 1.2—Anthrosol; 2.1—Podzol; 2.2—Anthrosol; 3.1—Podzol; 4.1—Podzol (WRB 2015)

distinguishing the soil cover in the study area was the moisture regime. All soils at the site were subject to waterlogging, either periodically or in the long term.

The soils in the areas studied were characterised by different genesis and varying degrees of disturbance—from the man-made soil formations of the residential zone to the natural relatively intact soils of the recreational zone. The soils in the areas with increased anthropogenic pressure had modified profiles (thicker compared to natural soils), with a large number of

inclusions of anthropogenic artifacts in the form of construction debris and utility remains, as well as a medium to high degree of surface disorder, soil thinness and chemical pollution.

36.3.2 Mesomorphological Analysis of the Soils Studied

A mesomorphological study of soils was carried out in the Pushkin, Vyborg and Primorsky regions. The results are presented in Fig. 36.3. It

Table 36.1 Morphological description of studied soils

Horizon	Depth, cm	Description	Texture class*	Soil type
Pushkin district (1)				
P	0–37	Humus horizon,, roots, uneven border, 7.5 YR 2.5/1	Sandy loam	Anthrosol (1.1)
BCtur	37–60	Clay inclusions, grey spots (gley), red spots, 7.5 YR 5/1	Sandy loam	
P	0–29	Humus horizon, wet, 7.5 YR 2.5/1	Loam	Anthrosol (1.2)
Gox	29–40	Wet, rusty spots, 7.5 YR 6/6	Loam	
AY	0–38	Roots, wet, humic horizon, 7.5 YR 2.5/1	Sandy loam	Umbrisol (1.3)
BC	38–65	Wet, coarse sand, 7.5 YR 6/6	Sand	
AY	0–23	Anthropogenic inclusions (glass, brick), clay and sand lenses 7.5 YR 2.5/1	Loam	Umbrisol (1.4)
P	0–29	Humus horizon, roots, 7.5 YR 2.5/1	Loam	Anthrosol (1.5)
Gox	29–40	Wet, rusty spots, roots, 7.5 YR 6/6	Loam	
Primorsky district (2)				
AY	0–20	Humus horizon, loose, abundance of roots, structure along the roots, 7.5 YR 3/1	Sandy loam	Anthrosol (2.1)
AYe	20–30	Presence of light powder, loose, abundance of roots, 7.5 YR 8/2	Loam	
C	30–40	Cemented sand with separate inclusions of clay, humified gray inclusions over the roots, 7.5 YR 7/3	Loam	
[AY]	40–47	Dry, loose, unstructured, single roots, 7.5 YR 5/2	Sandy loam	
P	0–20	Roots, wet, solid, 7.5 YR 3/1	Loam	Anthrosol (2.2)
PC	20–40	Roots, wet, solid, rusty spots, 7.5 YR 6/6	Clay loam	
Gox	40–50	Roots, wet, solid, rusty and grayish spots, 7.5 YR 6/6	Clay	
AY	0–25	Humus horizon, solid, 7.5 YR 3/1	Loam	Anthrosol (2.3)
AY2	25–30	Humus horizon, solid, rusty spots, 7.5 YR 6/6	Loam	
C	30–35	Solid, roots, 7.5 YR 3/1	Sandy loam	
AYg	35–40	Solid, rusty spots, 7.5 YR 6/6	Sand	
Cg	40–50	Solid, rusty spots, 7.5 YR 5/6	Sand	
Vyborg district (3)				
P	0–20	Abundant roots, moist, 7.5 YR 6/1	Sandy loam	Podzol (3.1)
PC	20–40	Presence of roots, wet, red spots, 7.5 YR 7/4	Sandy loam	
Gox	40–50	Wet, rusty spots, gley, 7.5 YR 5/6	Loam	
AY	0–17	Humus horizon, presence of roots, 7.5 YR 5/2	Sandy loam	Anthrosol (3.2)
BEL	17–19	Roots, 7.5 YR 5/1	Loam	
BC	19–42	Roots, 7.5 YR 7/3		

(continued)

Table 36.1 (continued)

Horizon	Depth, cm	Description	Texture class*	Soil type
			Sandy loam	
Krasnogvardeisky (4)				
AY	0–23	Wet, roots, 7.5 YR 7/1	Loam	Podzol (4.1)
EL	23–30	whitish spots, 7.5 YR 7/3	Sandy loam	
BI	30–54	7.5 YR 7/6	Loam	
C	54–80	Dusty, 7.5 YR 6/3	Loam	
U	0–10	Wet, roots, 7.5 YR 7/1	Loam	Technosol (4.2)
U2	10–20	Anthropogenic inclusions, 7.5 YR 7/3	Sandy loam	
P	0–20	Solid, roots, humus horizon, 7.5 YR 6/1	Sandy loam	Anthrosol (4.3)
BF	20–50	Dense, rusty spots, roots, 7.5 YR 5/1	Sandy loam	
BF2	50–60	Dense, rusty spots, 7.5 YR 5/1	Loam	
Gox	60–80	Dense, rusty spots, gley, 7.5 YR 5/6	Loam	
P	0–10	Wet, roots, humus horizon, 7.5 YR 5/3	Sandy loam	
P2	10–20	Wet, roots, humus horizon, 7.5 YR 4/4	Sandy loam	Anthrosol (4.4)
R	20–40	Wet, whitish spots, 7.5 YR 6/4	Loam	
[PU]	40–60	Wet, humus horizon, 7.5 YR 6/6	Sandy loam	
[Gox]	60–83	Wet, rusty spots, gley, 7.5 YR 5/6	Loam	
[Cg]	83–93	Solid, rusty spots, 7.5 YR 5/6	Loam	

*according to WRB (2015)

has been established that soil aggregates differ in terms of water strength and structural organisation in different soil horizons of the studied soils on fallow land. An increase in the cuboid structure and a decrease in plant residues and humus content with depth were also noted.

36.3.3 Vertical Electrical Resistivity Sounding (VERS) of the Studied Soils

Electrophysical methods enable the necessary information about soil characteristics to be obtained with no mechanical impact on the soil

or changes in its current state. The data obtained using vertical electrical resistivity sounding (VERS) revealed the features of each layer (horizon) of fallow soils (Table 36.2). The study area was located on the border between marine sediments (sands and silts) and moraine sediments (loams, clays and gravel material). The data show a gradual increase in electrical resistance values with depth. That distribution was because the topsoil layer underwent significant changes during the anthropogenic activities (cultivation, ploughing), leading to its compaction. The parent materials were represented by deposits of sea sand and were looser, which is reflected in the obtained data.

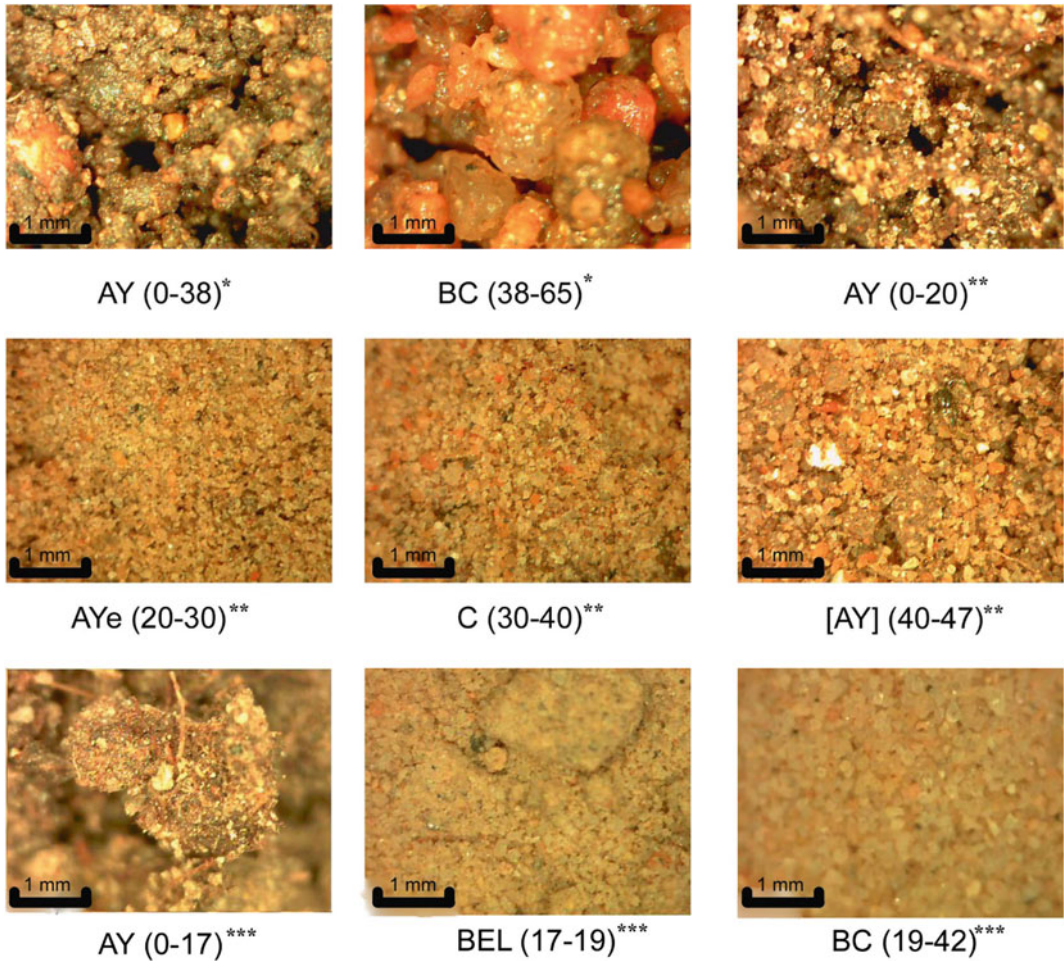


Fig. 36.3 The mesomorphological structure of the soil horizons of the studied soil type: *Umbrisol in Pushkin district AY (0–38), BC (38–65); **Anthrosol in

Primorsky district AY (0–20), Aye (20–30), C (30–40), [AY] (40–47); ***Anthrosol in Vyborg district AY (0–17), BEL (17–19), BC (19–42)

The vertical heterogeneity of the soil profile was determined by the vertical electrical resistivity sounding (VERS) method, which measures soil resistivity by passing an electrical current into the ground and measuring the resulting potentials created in the soil stratum. The method involves injecting a direct current or low-frequency alternating current into the ground through a pair of current electrodes and measuring the resulting potential across another pair of electrodes, called potential electrodes. The apparent electrical resistance of the soil and soil strata was measured using a portable Landmapper instrument with spacing of electrode MN of 10 cm and with

spacing of electrode AB of 2 10, 20, 30, 40, 50, 60, 70, 80, 90, 100, 150, 200, 300, 400 and 500 cm. This allowed the magnitudes of the apparent electrical resistance of the soil to be established at the corresponding depths. The results of the field measurements were recalculated in accordance with the geometrical coefficients for different depths and spacing of the AB and MN electrodes (Pozdnyakov et al. 2012). Zond IP software was used to model apparent resistivity data.

The ecological risk of urban soil pollution by a complex of heavy metals was carried out using the total chemical contamination index (Zc) (SanPiN 4266–87, 1987).

Table 36.2 Electrical resistance of the soil studied

Depth, cm	Electrical resistance of former state farms, Ohm × m				
	Lensovetovsky (soil 1.1)	Lensovetovsky (soil 1.3)	SPSAU (horticulture) (soil 1.4)	Kuzmino (soil 1.2)	Kuzmino (soil 1.5)
10	1288	2280	569.7	961.2	953.2
20	1298	2293	580.8	956.7	943.4
30	1329	2279	586.8	975.2	968.4
40	1284	2265	576.5	1509	1499
50	1277	2273	563.3	975	956.1
60	1290	2221	553.5	967.4	938.7
70	1277	2234	546.4	1046	1113
80	1268	2219	533	1497	1503
90	1279	2224	527.2	1575	1566
100	1273	2157	510.6	971.5	982.1
150	1265	3028	500.6	941.1	947.2
200	1260	2978	487.6	945.6	950.3
250	1236	2969	470.1	943.9	947.8
300	1259	2932	476.6	952.1	967.7

$$Z_c = \sum_{i=1}^n Kc - (n - 1) \quad (36.1)$$

Here, Kc is the concentration coefficient of the chemical element (i) and n is the number of elements entering the geochemical association.

$$Kc = \frac{C_i}{C_{back}} \quad (36.2)$$

Here, C_i is the actual content of the element and C_{back} is the geochemical background.

36.4 Laboratory Analyses

36.4.1 Agrochemical Characteristics of Studied Soils

The studies were carried out using standard techniques for describing the soil, such as soil profiling and morphological description. The laboratory analyses included measurements of the main soil agrochemical properties (pH, available phosphorus P_2O_5 and potassium K_2O ,

mineral nitrogen ($N-NH_4$ and $N-NO_3$), the content of heavy metals (Cu and Zn) and petroleum hydrocarbons (PAHs), and the degree of soil pollution. The main soil characteristics were determined using standard analysis procedures. The soil textural class was determined based on the particle size density using Kachinsky's pipette method (Rozhkov et al. 2002). The content of carbon and nitrogen was analysed with a CHN analyser (EA3028-HT EuroVector, Pravia PV, Italy). The content of heavy metals was extracted using an *aqua regia* solution according to the standard ISO 11047–1998 (1998) and determined on an atomic absorption spectrophotometer (Kvant 2 M model, Moscow, Russia). The content of polycyclic aromatic hydrocarbons (PAHs) was determined with a Fluorat-02 liquid chromatograph. The content of petroleum product in the soil was measured with a Fluorat 02-3 M fluorometric detector. The content of nitrate and ammonium nitrogen was determined according to the method outlined in 14,256–1-2003 (2003) using potassium chloride solution. The content of mobile potassium and phosphorus was determined with the Kirsanov method (ISO

54650–2011, 2011). The soil pH was determined in aqueous and salt suspensions (1:2.5). The soil mesomorphological characteristics were determined using the Webbers 2Fn digital microscope (Moscow, Russia). The content of basic soil fertility parameters is presented in Table 36.3 for the Pushkin and Primorsky districts.

Generally speaking, almost all soils in Russia are poorly supplied with phosphorus compared to nitrogen and potassium (Mineev 2006). After the large phosphorus mining site in Kingisepp, Leningrad region, was closed in 2006, the region lost the sources to replenish the region with phosphorus (Mineev 1984; Adhami et al. 2012;

Table 36.3 Agrochemical properties of the soils studied

Horizon/district	Depth, cm	P ₂ O ₅ , mg kg ⁻¹	K ₂ O, mg kg ⁻¹	N-NH ₄ , mg kg ⁻¹	N-NO ₃ , mg kg ⁻¹	C, %	N, %	C/N
Pushkin district								
Anthrosol (1.1)								
P	0–37	694	378	7.05	5.77	2.99	0.15	19
BCtur	37–60	422	306	0.94	0.44	0.16	–	–
Umbrisol (1.3)								
AY	0–38	262	241	0.54	0.48	3.89	0.33	12
BC	38–65	115	97	0.87	0.07	0.31	0.02	15
Umbrisol (1.4)								
AY	0–23	345	386	2.15	1	2.31	0.3	8
Anthrosol (1.2)								
P	0–29	124	164	2.01	0.15	1.51	0.19	8
Gox	29–40	70	138	1.41	1.33	0.15	0.01	15
Anthrosol (1.5)								
P	0–29	147	235	5.7	0.11	1.65	0.22	7
Gox	29–40	74	94	1.88	1.15	0.17	0.01	17
Primorsky district								
Podzol (2.1)								
AY	0–20	641	497	23.4	0.59	3.01	0.23	13
AYe	20–30	180	92	3.15	0.41	2.67	0.18	15
C	30–40	246	96	2.01	0.22	0.48	0.02	24
[AY]	40–47	67	61	2.35	0.16	1.95	0.09	22
Anthrosol (2.2)								
P	0–20	178	233	8.52	1.81	2.1	0.28	7.5
PC	20–40	137	202	5.1	0.55	1.47	0.21	7
Gox	40–50	5	160	2.35	0.07	0.2	0.01	20
Anthrosol (2.3)								
AY	0–25	210	187	8.86	0.04	2.97	0.19	16
AY2	25–30	49	50	4.03	0.11	2.63	0.17	15
C	30–35	51	46	3.69	0.41	1.01	0.08	13
AYg	35–40	41	36	3.42	0.52	1.86	0.11	17
Cg	40–50	66	19	2.72	0.37	0.23	0.03	8

Kovyazin 2008). An imbalance in man-made habitats can significantly slow down the processes of overgrowing on fallow land (Aleksandrova 1980; Lorenz and Lal 2009; Lykov et al. 2004; Kovyazin et al. 2017). These results showed that the highest content of phosphorus and potassium was found in the upper horizons of soil profiles (from 210 mg kg⁻¹ for P₂O₅ in the Anthrosols of Primorsky to 694 mg kg⁻¹ in the Anthrosols of Pushkin, and from 187 mg kg⁻¹ for K₂O in the Anthrosols of Primorsky to 497 mg kg⁻¹ in the Podzols of Primorsky). The soils characterised by a sandy texture had a small concentration of potassium, unlike the clayey soils, where potassium is included in the mineral composition (Mineev 2006; Wilson and Kleb 1996; Kovyazin et al. 2010).

Concentrations of N-NH₄ varied from 0.54–7.05 mg kg⁻¹ in the upper horizons and from 0.87–1.88 mg kg⁻¹ in the lower horizons. This distribution did not allow a trend in the vertical distribution of ammonium nitrogen to be identified. The concentrations of nitrate nitrogen (N-NO₃) indicate the availability of mineral N in the soil. The values of this indicator are significantly lower than N-NH₄ and vary in a wide range from

0.07–5.77 mg kg⁻¹, while the average value does not exceed 1 mg kg⁻¹. Comparing our data with other sources (Kabata-Pendias and Pendias 1989; Rebristaya and Khitun 1997), we found that nutrient elements (N, P, K) can persist in soil for a long time, and when agricultural activities are resumed, abandoned soils can return to their previous forms.

36.4.2 Concentrations of Petroleum Products (PPs) and Polyaromatic Hydrocarbons (PAHs) in Soil Studied

The study of the content of hydrocarbons in the soil was performed in the Pushkin district at the former state farms (Kuzmino, SPSAU, Lensovetsky) (Table 36.4).

A high degree of soil contamination with benzo[a]pyrene (BP) was found, which exceeded the maximum allowed concentration (MAC) in the majority of agricultural soils studied. The highest BP content was observed in the Anthro-sol (1.2) of the former Kuzmino farm (Pushkin

Table 36.4 Content of benzo [a] pyrene (BP) petroleum product (PP) in the soils studied at the Pushkin site

Horizon	Depth, cm	pH in H ₂ O	BP, ng g ⁻¹	PP, mg kg ⁻¹
Anthrosol (1.1)				
P	0–10	7.3	125	209
BCtur	10–30	7.9	7	150
Gox	30–40	5.1	61	153
Anthrosol (1.2)				
P	0–10	7.5	151	217
BCtur	10–30	7.5	697	538
Gox	30–40	5.2	33	235
Umbrisol (1.4)				
AY	0–20	6.7	< 5	57
Anthrosol (1.5)				
P	0–20	5.9	21	216
BCtur	20–40	5.3	18	11
Gox	40–60	5.3	21	6
Umbrisol (1.3)				
AY	0–30	6.3	6	10

District) (697 ng g^{-1}) at 10–30 cm depth; this exceeded the MAC value for PAHs by 34 times. The lowest concentrations of PAHs (below the MAC) were found in the Umbrisol (1.3) at the former Lensovetsky farm and the former gardens of St. Petersburg State Agrarian University. This was mainly due to the remote location of these farms from major transport interchanges, and also due to the wind direction, which prevents the deposition of dust and exhaust gases from traffic. In most of the studied soils, the concentration of BP decreased with depth.

In terms of the composition of polycyclic aromatic hydrocarbons, large part is made up of high-molecular polyarenes (Minkina et al. 2020). In our study, an additional source of PAHs was probably fresh organic material (peat) applied to the soil, since the heavy polyarenes can lead to secondary soil pollution. The highest BP concentrations found in the soils of large transport interchanges are due to incomplete fuel combustion, since PAHs are a by-product (Lodygin et al. 2008; Chukov et al. 2006; Dymov et al. 2013). In the city, BP mainly spreads through the air (Cheng et al. 2018; Zgłobicki et al. 2018; Soltani et al. 2015), so the upper mineral horizons are most often contaminated. Minkina et al. (2020) found that in urban soils of the city of Tyumen, the total amount of PAHs exceeded the background level by up to three times ($341.0 \mu\text{g kg}^{-1}$), while the total PAH in the residential area content was twice as high as in the industrial areas. In their study, the maximum accumulation was found for phenanthrene, pyrene and fluoranthene.

36.4.3 Heavy Metal (HM) Concentration in the Studied Soils and Total Contamination Index of Soil Pollution (Zc)

This study was conducted in the Krasnogvardeisky district of St. Petersburg. Functional zoning sites were selected as objects of study in accordance with the General Plan of St. Petersburg dated December 21, 2005: (a) industrial area; (b) recreational area; (c) residential zone; (d) agricultural area (Table 36.5).

Using the soil pollution index normalised to the background values is a reliable approach to assess the level of soil environmental pollution with heavy metals and PAHs (Chen et al. 2019; Gope et al. 2018). The total soil contamination index (Zc) with mobile forms of Zn and Cu was calculated for each horizon to estimate the migration of these elements down the profile. The Zc index was also calculated for the combined samples selected using the point method. On average, for all the soils studied, the total pollution index in the arable layer was characterised by low values ($Z_c < 16$) (including combined sampling), which classifies the studied soils according to the permissible pollution category as follows:

- $Z_c = 3.09$ —for recreational zone (“Okhta Forest”)
- $Z_c = 4.60$ —for sanitary protection zone of a chemical plant (“Krasnoznamenets”)
- $Z_c = 2.38$ (3.16 in the buried horizon)—for the garden site (“Garden”).

Table 36.5 Study area in Krasnogvardeisky district

Functional zone	Object
Recreational	Territory of the Rzhevsky Forest Park (“Okhta Forest”) (4.1)
Residential	Territory of residential development (“Great Okhta”) (4.2)
Industrial	Sanitary protection zone of a chemical plant (“Krasnoznamenets”) (4.3)
Agricultural	Territory of garden plots (“Garden”). (4.4)

These results are confirmed by the soil ecology research previously conducted in this area (Aparin and Rusakov 2003). An exception to the general rule was the technogenic soil-like bodies of the residential area on the territory of “Great Okhta”, where the average Zc index in 0–30 cm layer was 56.90, which is a dangerous category of soil pollution (Fig. 36.4).

For the soils studied, the actual concentrations of mobile forms of HMs in the samples were compared with their background content, i.e. the content of mobile elements in the arable layer of the natural Podzol of North-West Russia. Figure 36.4 shows that the actual concentration of mobile Cu in the metamorphic soil of the “Okhta Forest” recreation area was below the background value (2.7 mg kg⁻¹ of soil), averaging 1.93 mg kg⁻¹. The average content of Zn exceeded the background level (1.2 mg kg⁻¹) by 3.5 times, reaching 4.04 mg kg⁻¹.

In the Anthrosol (4.2 soil) of the industrial zone, despite its proximity to the potential sources of chemical pollution, no significant concentrations of mobile Zn and Cu were found. The average Cu content was about 2.2 mg kg⁻¹, which is less than the background value. The concentration of Zn showed that the background value was four times too high, with an average content of 4.9 mg kg⁻¹. This can be explained by a slightly acidic/neutral soil and high humus content, the combined effect of which reduced

the mobility of heavy metals (Qu et al. 2019; Palansooriya et al. 2020) and led to the results of the analysis being underestimated. In Anthrosols of the agricultural area (4.4.), a slight excess of the background Zn level (about 2.5 times) was observed, with an average of 3.03 mg kg⁻¹ in the surface arable horizon. In the buried horizon [PU] (4.4 soil) the average Zn concentration also exceeded the background, reaching 3.16 mg kg⁻¹. For Cu, no excess was observed for the background level in the Anthrosols (4.3 and 4.4): 2.22 mg kg⁻¹ (Table 36.6).

One of the convenient indicators of technogenic impact and a reliable source of data on the possible long-term pollution of atmospheric air and other landscape components is the quality of soil. The very high concentration of Zn and the pollution index (Zc) in the residential zone suggests that the main cause of soil contamination in the residential zone soils is most probably the emissions of these elements from motorised vehicles. Ufimtseva and Terekhina (2014) reported similar findings when conducting an ecological and geochemical assessment of the central district of St. Petersburg. In their study, factor analysis identified that Cu, Zn, Pb, Cd and Ba made up 48.85% of soil pollution from anthropogenic sources. Dust from the urban streets contains large amounts of pollutants from vehicle emissions (Pan et al. 2017; Cheng et al. 2018; Dytłow and Górka-Kostrubiec 2020).

Fig. 36.4 Content of mobile forms of Zn and Cu in studied soils, mg kg⁻¹; Zc—soil pollution index; MPC—maximum permissible concentration

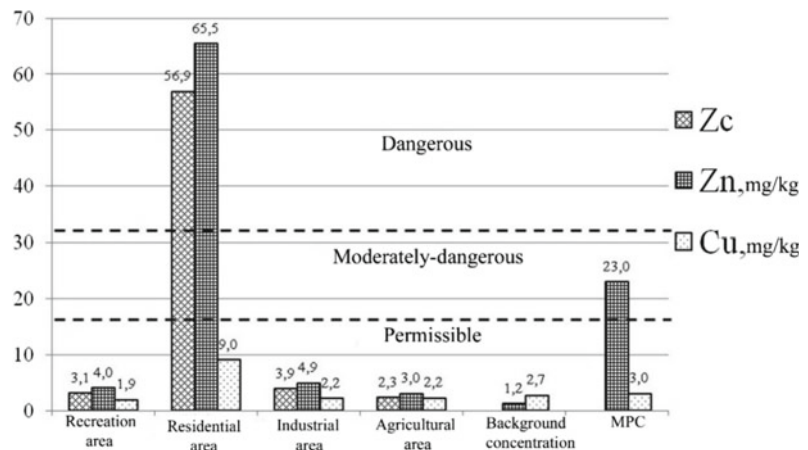


Table 36.6 Content of mobile form of zinc (Zn) and copper (Cu) (mg kg^{-1})

No. of soil	Horizon	Depth, cm	Zn	Cu	K_c (Zn)	K_c (Cu)	Z_c
4.1	AY	0–23	5.35 ± 0.02	2.13 ± 0.04	4.46	0.79	4.25
	EL	23–30	0.88 ± 0.03	1.60 ± 0.02	0.73	0.59	0.33
	BI	30–54	0.24 ± 0.02	2.15 ± 0.04	0.2	0.8	0
	C	54–80	0.07 ± 0.01	2.51 ± 0.04	0.06	0.93	–
4.2	U	0–10	66.51 ± 0.62	7.81 ± 0.02	55.43	2.89	57.32
	U2	10–20	69.31 ± 0.43	11.74 ± 0.04	57.76	4.35	61.11
4.3	P	0–20	3.44 ± 0.06	1.91 ± 0.02	2.87	0.71	2.57
	BF	20–50	0.18 ± 0.01	1.71 ± 0.04	0.15	0.63	–
	BF2	50–60	0.25 ± 0.01	1.31 ± 0.01	0.21	0.49	–
	Gox	60–80	0.84 ± 0.01	2.33 ± 0.04	0.7	0.86	0.56
4.4	P	0–10	3.30 ± 0.01	2.20 ± 0.05	2.75	0.81	2.56
	P2	10–20	2.83 ± 0.02	1.78 ± 0.04	2.36	0.66	2.02
	R	20–40	1.36 ± 0.01	1.86 ± 0.03	1.13	0.69	0.82
	[PU]	40–60	4.08 ± 0.08	2.04 ± 0.04	3.4	0.76	3.16
	[Gox]	60–83	0.30 ± 0.01	2.27 ± 0.05	0.25	0.84	0.09
	[Cg]	83–93	0.99 ± 0.03	2.41 ± 0.01	0.83	0.89	0.72

Note K_c is the concentration coefficient; Z_c is the pollution index

Soil horizons were identified according to the Russian Soil Classification (Soil field guide 2008)

In our study, urban street dust and vehicle emissions greatly contributed to the accumulation of Zn in the studied urban soils. However, in agricultural soils, concentrations of the mobile forms of Cu and Zn were found to be non-specific, with few manifestations.

Xie et al. (2019) found that the age of the residential community, the distance to the city centre, the population density and the distance from the sampling point to the nearest residential building were significantly correlated with the contents of Cu, Cd, Pb and Zn in residential soils. They also found that green spaces lowered the heavy metal concentration in residential soils. Moreover, different vegetative types were found to have a significant influence on heavy metal accumulation. They suggested that the accumulations of Cu, Pb and Zn in urban residential soils depended on atmospheric deposition. Studying pollution in the urban soils of St. Petersburg, Russia, Gyekye and Movchan (2009) found that concentrations of copper, lead, zinc and manganese in soils were significantly high—5–10 times above the regional background level—and

distributed as follows: $\text{Cu} > \text{Zn} > \text{Mg} > \text{Pb} > \text{Cd}$. Matinyan et al. (2017), studying the soils of the Summer Garden in St. Petersburg, Russia, found that the total content of Cu and Zn exceeded the tentative permissible concentrations for coarse-textured soils by 2–6 and 4–20 times, respectively. In most cases, the main sources of soil contamination with the heavy metals were nearby highways and local urban waste from nearby households.

The adsorption and desorption of heavy metals in soils is controlled by processes such as mineral precipitation (dissolution, ion exchange and adsorption), desorption, complexation, pH and redox conditions, biological (im) mobilisation and transformation, and plant uptake and leaching (El-Naggar et al. 2019, 2018; Palansooriya et al. 2020). Soil physico-chemical properties such as pH, Eh, CEC, EC and OM content, in particular, directly correlate with the mobility and availability of heavy metals (Palansooriya et al. 2020). The behaviour of HMs in various environmental conditions should be considered, taking into account effective

measures to eliminate them. The degree of manifestation and direction of the processes affecting the mobility of heavy metals can be controlled by the degree and nature of the anthropogenic pressure and activity. A recent study by Polyakov et al. (2020) on alluvial urban soils showed that pollution with HMs and PAHs exceeded the maximum permissible concentration (MAC).

36.5 Perspectives for the Restoration and Use of Fallow Land

The results of the study showed that over the past 10 years, there have been negative changes in the quality of soil of agricultural land in the northwest part of Russia. These changes are associated with a significant reduction in the use of fertilisers and lime and the cessation of necessary measures to maintain and restore soil productivity. These factors resulted in an increase in the area of soils that are in poor condition and have thus been abandoned (fallow land). Many of these former and active agricultural soils showed signs of irreversible degradation. Therefore, there is a need to develop reliable technological support for the restoration, improvement and efficient use of fallow land. At present, farmers' economic situation is improving and the production of domestic agricultural machinery is being restored. This can greatly facilitate not just the restoration of fallow land, but also the region's agriculture as a whole. Therefore, we recommend that, prior to beginning any fieldwork on fallow land, a thorough agroecological and agroeconomic assessment should be carried out to determine whether it is suitable and productive to return it to active agricultural use. Based on previous experience and the research discussed in this chapter, we have developed different technological recommendations to improve the quality and productivity of these fallow urban soils, depending on the degree of their degradation. The priority for restoration should be given to the soils with high potential for agricultural production to restore livestock, such as pastures and hayfields.

36.5.1 Sample Technologies Proposed for Restoration of Fallow Land in Northwestern Russia

36.5.1.1 *Option I (Bare Fallow Fields for Spring Crops)*

First, an early bare field is prepared for sowing spring crops (grain, industrial crops, fodder, etc.) on more abandoned, weed-infested land. Grain, industrial crops and fodder crops have a strong root system that helps to improve the physical condition of the soil. Then, in April–May, it is necessary to plough and mix the weeds with the soil by loosening to a depth of 10–14 cm, in order to prevent their development. In late spring (May–June), deep ploughing or loosening at a depth of 20–30 cm is necessary. This mixes the soil, aerates it and encourages the ingress of organic residues from the upper horizons to the lower ones at the depth of ploughing for cultivated crops. In summer, cultivation and loosening to a depth of 6–12 cm should be performed. This increases the moisture for the root systems. The following year, in the spring, the field is cultivated for spring crops and fertilised. After that, the spring crops are planted with an initial dose of mineral fertilisers. The seeding rate, planting depth and fertiliser doses are set depending on the crop and zone.

36.5.1.2 *Option II (Clover Fallow Fields for Winter Crops)*

This option is designed for clover fallow fields that are less weed-infested, e.g. for winter crops (wheat, rye, barley, etc.). According to this scheme, it is necessary to plough and mix the weeds with the soil in spring by loosening to a 10–14 cm depth. Depending on the crops, the depth of ploughing is different. In the spring, plant residues are buried in the topsoil so that the mineral elements are within the arable horizon. In the spring and early summer, loosening should be carried out to a depth of 22–45 cm. This increases the moisture and aeration of the root systems. In the autumn, winter crops are planted

with an initial dose of mineral fertilisers. The seeding rate, planting depth and fertiliser doses are set depending on the crop and zone.

36.5.1.3 Option III (For Spring Crops)

This option implies minimum operations (direct seeding). The seeding rate, planting depth and fertiliser doses are set depending on the crop and zone. It is necessary to take into account the degree of soil cultivation (content of nutrients in the soil and the texture class).

36.5.1.4 Option IV (For Spring Crops)

Other technologies can also be used depending on local climatic and soil conditions and the capabilities of each particular farm. The final decision should be made directly in the field, taking into account soil and weather conditions. When developing and choosing the technology used to restore fallow land, it is necessary to carefully consider all the parameters of the soils, including their degree of degradation, crop selection, the crop rotation scheme, tillage techniques, plant protection, etc. In addition, the technology should be strictly differentiated and adapted to local soil climate conditions, economic and other conditions, such as liming, and de-contamination of HM-polluted soils by biological and electrical means of reclamation (Savich et al. 2013). In addition, the designed technology should be energy-saving, ecologically safe and adapted to the landscape conditions and local agriculture traditions (Webster et al. 2000).

36.6 Conclusions

Over the past 10 years, negative changes have been observed in the quality of soil cover on agricultural land in the urban zone of northwest Russia. This was caused by a general decline in agricultural production, which led to a reduction

in or complete cessation of the measures for maintaining and restoring soil productivity. This included a significant reduction in the use of all types of fertilisers, liming, a reduction in arable area and an increase in the area of the soils that are in poor condition. Many agricultural soils showed signs of irreversible degradation.

Studying the soil ecology and geochemical state of the agricultural land is important both for understanding the soil geochemistry processes occurring in anthropogenic ecosystems and for solving practical problems related to environmental protection and human health. To ensure the quality of technological measures for rehabilitating and restoring arable land, the restoration of the soil and vegetation in the fallow land of St. Petersburg and the Leningrad Region must be monitored. To achieve this goal, a regional interdepartmental centre must be created for the restoration of fallow soils in the urban zone. This centre could be engaged in soil environmental monitoring on fallow abandoned land and ensure the practical implementation of the recommendations.

Acknowledgements This work was supported by the Government of Saint Petersburg (Committee for Science and Higher Education), the project “Soils of abandoned fallow lands of the Saint Petersburg and Leningrad region: diversity, state and perspectives of use” and the Grant of Saint Petersburg State University “Urbanized ecosystems of the Russian Arctic: dynamics, state and sustainable development”. Special thanks to Ivan Alekseev for this assistance in conducting the fieldwork.

References

- Adhami E, Ranaghi A, Karimian N, Molavi R (2012) Transformation of phosphorus in highly calcareous soils under field capacity and waterlogged conditions. *Soil Research*, 50:249–255. https://www.researchgate.net/publication/233864688_Transformation_of_phosphorus_in_highly_calcareous_soils_under_field_capacity_and_waterlogged_conditions

- Aiman U, Mahmood A, Waheed S, Malik RN (2016) Enrichment, geo-accumulation and risk surveillance of toxic metals for different environmental compartments from Mehmood Booti dumping site. Lahore city, Pakistan. *Chemosphere*, 144:2229–2237. <https://pubmed.ncbi.nlm.nih.gov/26598991/>
- Aleksandrova LN (1980) Organic matter of soils and transformation processes. *L science* p 286 (Александрова Л.Н. (1980) Органическое вещество почвы и процессы трансформации, Ленинград, Наука с 286)
- Antić-Mladenović S, Kresović M, Čakmak D, Perović V, Saljnikov E, Ličina V, Rinklebe J (2018) Impact of a severe flood on large-scale contamination of arable soils by potentially toxic elements (Serbia). *Environ Geochem Health* 41(1):249–266. <https://doi.org/10.1007/s10653-018-0138-4> <https://pubmed.ncbi.nlm.nih.gov/29909443/>
- Aparin BF, Rusakov AV (2003) Soils and soil cover of the eastern half-ring of the ring road (Ring Road) around St. Petersburg. *Bull St Petersburg Univ* 2 (11):103–116 (Апарин Б.Ф., Русаков А.В. Почвы и почвенный покров восточного полукольца КАД Санкт-Петербурга. Вестник Санкт-Петербургского университета)
- Bergamasco A, Culotta L, De Stefano C, Orecchio S, Sammartano S, Barreca S (2014) Composition, distribution, and sources of polycyclic aromatic hydrocarbons in sediments of the gulf of Milazzo (Mediterranean Sea, Italy). *Polycycl Aromat Compd* 34:397–424. <https://doi.org/10.1080/10406638.2014.900642>
- Čakmak D, Perovic V, Kresovic M, Jaramaz D, Mrvic V, Belanovic-Simic S, Saljnikov E, Trivan G (2018) Spatial distribution of soil pollutants in urban green areas (a case study in Belgrade). *J Geochem Explor* 188:308–317. <https://doi.org/10.1016/j.gexplo.2018.02.0011>
- Chen X, Guo M, Feng J, Liang S, Han D (2019) Characterization and risk assessment of heavy metals in road dust from a developing city with good air quality and from Shanghai, China. *Environ Sci Pollut Res* 26:11387–11398. <https://doi.org/10.1007/s11356-019-04550-2>
- Cheng Z, Chen L, Li H, Lin J, Yang Z, Yang Y et al (2018) Characteristics and health risk assessment of heavy metals exposure via household dust from urban area in Chengdu, China. *Sci Total Environ* 619–620:621–629
- Chukov SN, Lodygin ED, Gabov DN, Beznosikov VA (2006) Polycyclic aromatic hydrocarbons in the soils of St. Petersburg. *Bull St Petersburg Univ* 3:119–129 (Чуков С.Н., Лодыгин Е.Д., Габов Д.Н., Безносиков В.А. (2006) Полициклические ароматические углеводороды в почвах Санкт-Петербурга. Вестник Санкт-Петербургского университета)
- Chukov SN (2001) Structural and functional parameters of soil organic matter under anthropogenic impact. *Publ St. Petesburg Univ* 216 (Чуков С.Н. Структурно-функциональные параметры почвенного органического вещества при антропогенном воздействии. Вестник Санкт-Петербургского университета)
- Dmitrakova Y, Rodina O, Alekseev I, Polyakov V, Petrova A, Pershina E, Ivanova E, Abakumov E, Kostecki J (2018) Restoration of soil-vegetation cover and soil microbial community at the Pechurki limestone quarry (Leningrad region, Russia). *Soil Sci Annu* 69(4):272–286
- Dmitrakova J, Abakumov E (2018) Dynamics of soil organic carbon of reclaimed lands and the related ecological risks to the additional CO₂ emission. *SUITMA 2017: urbanization: challenge and opportunity for soil functions and ecosystem services*, pp 97–105. https://doi.org/10.1007/978-3-319-89602-1_13
- Dobrovolsky GV (2004) Problems of soil science in solving modern environmental problems. Let's save the planet Earth. IP MSU-RAS, 2004. (Добровольский Г.В. (2004) Проблемы почвоведения в решении современных экологических проблем. Спасем планету Земля ИП МГУ-РАН, 2004 г.)
- Dymov AA, Kaverin DA, Gabov DN (2013) Properties of soil and soil-like bodies, Vorkuta. *Eurasian Soil Sci* 2:240–248. <https://doi.org/10.1134/S1064229313020038>
- Dytłow S, Górka-Kostrubiec B (2020) Concentration of heavy metals in street dust: an implication of using different geochemical background data in estimating the level of heavy metal pollution. *Environ Geochem Health*. <https://doi.org/10.1007/s10653-020-00726-9>
- Ehigbor MJ, Iwegbue CMA, Eguavoen OI et al (2020) Occurrence, sources and ecological and human health risks of polycyclic aromatic hydrocarbons in soils from some functional areas of the Nigerian megacity, Lagos. *Environ Geochem Health* 42:2895–2923. <https://doi.org/10.1007/s10653-020-00528-z>
- El-Naggar A, Shaheen SM, Ok YS, Rinklebe J (2018) Biochar affects the dissolved and colloidal concentrations of Cd, Cu, Ni, and Zn and their phytoavailability and potential mobility in a mining soil under dynamic redox-conditions. *Sci Total Environ* 624:1059–1071. <https://europepmc.org/article/med/29929223>
- El-Naggar A, Shaheen SM, Hseu Z-Y, Wang S-L, Ok YS, Rinklebe J (2019) Release dynamics of As, Co, and Mo in a biochar treated soil under pre-definite redox conditions. *Sci Total Environ* 657:686–695. <https://europepmc.org/article/med/30677934>
- Giani L, Chertov O, Gebhardt C, Kalinina O, Nadporozhskaya M, Tolkdorf-Lienemann E (2003) Plagganthrepts in northwest Russia? Genesis, properties and classification. *Geoderma* 121:113–122. <https://doi.org/10.1016/j.geoderma.2003.10.007>
- Gope M, Mastro RE, George J, Balachandran S (2018) Tracing source, distribution and health risk of potentially harmful elements (PHEs) in street dust of Durgapur, India. *Ecotoxic Environ Safety* 154:280–293. <https://doi.org/10.1016/j.ecoenv.2018.02.042>
- Gyekye KA, Movchan VM (2009) Patterns of heavy metals contents in urban soils of Vasileostrovsky and

- Elagin ostrov of Saint Petersburg, Russia. *Ghana J Geogr* 1:67–78. <https://www.ajol.info/index.php/gjg/article/view/1107211>
- IARC (2010) Some non-heterocyclic polycyclic aromatic hydrocarbons and some related exposures. *IARC Monogr Eval Carcinog Risks Hum* 92:765–772. 978–92–832–1292–8
- ISO 11047–1998 (1998) Soil Quality—Determination of Cadmium, Cobalt, Copper, Lead, Manganese, Nickel and Zinc in Aqua Regia extracts of soil—flame and electrothermal atomic absorption spectrometric methods. p 18. <https://www.iso.org/obp/ui/#iso:std:iso:11047:ed-1:v1:en>
- ISO 14256–1–2003 (2003) Soil quality—Determination of nitrate, nitrite and ammonium in field moist soils by extraction with potassium chloride solution—part 1: Manual method (ISO/TS 14256–1–2003:2003). p 14. <https://www.iso.org/obp/ui/#iso:std:iso:ts:14256:-1:ed-1:v1:en>
- ISO 54650–2011 (2011) Determination of mobile phosphorus and potassium compounds by Kirsanov method modified by CINAO. p 9. <http://docs.cntd.ru/document/gost-r-54650-2011>
- Ivanov AL, Zavalin AA, Kuznetsov MS et al (2008) Agroecological state and prospects for the use of Russian lands that have been removed from active agricultural use. *Rosinformagrotech*, Moscow, p 64 (Иванов А.Л., Завалин А.А., Кузнецов М.С. и др. Агроэкологическое состояние и перспективы использования земель России, выведенных из активного сельскохозяйственного использования. Москва: Росинформагротех, 64 с.)
- Jenkinson DS, Coleman K (2008) The turnover of organic carbon in subsoils, part 2. Modelling carbon turnover. *Eur J Soil Sci*. <https://doi.org/10.1111/j.1365-2389.2008.01026.x>
- Kabata-Pendias A, Pendias H (1989) *Microelements in soils and plants*. Mir, Moscow, p 16
- Karavaev NA, Denisenko EA (2008) Postagrogenic restoration of the properties of chernozem and vegetation on dated deposits of central Chernozem region proceedings of the All-Russian scientific conference Agroecological status and prospects for the use of land in Russia, alienated from active agricultural use, Dokuchaev Soil Institute, Moscow Russian Academy of Agricultural Sciences, pp 303–306 (Кароваев Н.А., Денисенко Е.А. Постагрогенное восстановление свойств чернозема и растительности на датированных отложениях Центрального Черноземья Материалы Всероссийской научной конференции «Агроэкологическое состояние и перспективы использования земель в России, отчужденных от активного сельскохозяйственного использования». Докучаева, Москва, Российская академия сельскохозяйственных наук, 303–306 стр.)
- Kashtanov NI, Sizov OA (2008) Problems of restoration of land retired from agricultural use. *Agric Econ Russia* 11:174–183. (Каштанов Н.И., Сизов О.А. (2008) Проблемы восстановления земель, выбывших из сельскохозяйственного использования. Экономика сельского хозяйства России, 11: 174–183)
- Kasimov NS, Vlasov DV (2018) Heavy metals and metalloids in urban soils of Russian cities (according to the annual reports of Rosgidromet). *Vestnik Moskovskogo universiteta, Seriya V, Geografiya* 3:14–22. https://vestnik5.geogr.msu.ru/jour/article/view/413?locale=en_US
- Kechaykina IO, Rumin AG, Chukov SN (2011) The post-agrogenic transformation of the organic matter of sod-podzolic soils. *Pochvovedenie* 10:1178–1193. <https://doi.org/10.1134/S0032180X11100030>
- Kelly J, Thornton I, Simpson PR (1996) Urban geochemistry: a study of the influence of anthropogenic activity on the heavy metal content of soils in traditionally industrial and non-industrial areas of Britain. *Appl Geochem* 11(1–2):363–370. [https://doi.org/10.1016/0883-2927\(95\)00084-4](https://doi.org/10.1016/0883-2927(95)00084-4)
- Kim L, Jeon H, Kim Y et al (2019) Monitoring polycyclic aromatic hydrocarbon concentrations and distributions in rice paddy soils from Gyeonggi-do, Ulsan, and Pohang. *Appl Biol Chem* 62:18. <https://doi.org/10.1186/s13765-019-0423-7>
- Kodiwo M, Oindo B, Ang'awa F (2014) Intensity of farmland cultivated and soil bulk density in different physiographic units in Nyakach district. *IOSR J Humanit Soc Sci (IOSR-JHSS)* 19(1):86–91. <http://iosrjournals.org/iosr-jhss/papers/Vol19-issue1/Version-1/L019118691.pdf>
- Kovyazin VF, Uskov IB, Derzhavin LM (2010) St. Petersburg park ecosystems of different degree of urbanization and agrochemical properties of their soils. *Agrochimiya* 3:58–66. (Ковязин В.Ф., Усков И.Б., Державин Л.М. (2010) Парковые экосистемы Санкт-Петербурга разной степени урбанизации и агрохимических свойств почв. Агрохимия 3: 58–66) <http://naukarus.com/parkovye-ekosistemy-sankt-peterburga-razlichnoy-stepeni-urbanizatsii-i-agrohimicheskie-svoystva-ih-pochv>
- Kovyazin VF, Martynov AN, Kan KK, Fam TK (2017) Features of soils in Pavlovo park of St. Petersburg. *Bull Perm Agrarian* 2(18):111–115 (Ковязин В.Ф., Мартынов А.Н., Кан К.К., Фам Т.К. (2017) Особенности почв Павловского парка Санкт-Петербурга. Вестник Пермского Аграрного сектора)
- Kovyazin VF (2008) Dynamics of agrochemical properties of soils of St. Petersburg. *Fertility* 3(42):34–36 (Ковязин В.Ф. Динамика агрохимических свойств почв Санкт-Петербурга. Плодородие, 3(42):34–36)
- Kwon HO, Choi SD (2014) Polycyclic aromatic hydrocarbons (PAHs) in soils from a multi-industrial city, South Korea. *Sci Total Environ* 470–471:1494–1501. <https://doi.org/10.1016/j.scitotenv.2013.08.031>
- Lal R (2002) Soil carbon dynamics in cropland and rangeland. *Environ Pollut* 116(3):353–362. [https://doi.org/10.1016/S0269-7491\(01\)00211-1](https://doi.org/10.1016/S0269-7491(01)00211-1)
- Lal R (2004) Soil carbon sequestration impacts on global climate change and food security. *Science* 304(5677):1623–1627. <https://doi.org/10.1126/science.1097396>

- Liuri DI, Goriachkin SV, Karavaeva NA (2010) Dynamics of agricultural lands in Russia in the 20th century and the post-growth restoration of vegetation and soils. Moscow: GEOS, p 426. 9785891185005 (Люри Д.И., Горячкин С.В., Каравеева Н.А., Денисенко Е. А. и др. Динамика сельскохозяйственных земель России в XX веке и постарогенное восстановление растительности и почв)
- Lodygin ED, Chukov SN, Beznosikov VA, Gabov DN (2008) Polycyclic aromatic hydrocarbons in the soils of Vasilyevsky Island (St. Petersburg). *Eurasian Soil Sci* 12:1494–1500 (Е. Д. Лодыгин, С. Н. Чуков, В. А. Безносиков, and Д. Н. Габов. Полициклические ароматические углеводороды в почвах Васильевского острова (Санкт-Петербург). *Почвоведение*, (12):1494–1500, 2008)
- Lorenz K, Lal R (2009) Biogeochemical C and N cycles in urban soils. *Environ Int* 35:1–8. <https://doi.org/10.1016/j.envint.2008.05.006>
- Lykov AM, Yeskov AI, Novikov MN (2004) Organic matter of arable Nonchernozem soil. VNIPTIOU, p 631 (Лыков А.М., Еськов А.И., Новиков М.Н. (2004) Органическое вещество пашни Нечерноземья. ВНИПТОО, с 631)
- Lyubimova IN, Motuzov VY, Bondarev AG (2008) Agroecological status and prospects for the use of abandoned lands of the dry-steppe zone with complex soil cover. In: Proceedings of the All-Russian scientific conference Agroecological status and prospects for the use of land in Russia withdrawn from active agricultural use, Dokuchaev Soil Institute, Moscow Russian Academy of Agricultural Sciences, pp 227–236 (Любимова И.Н., Мотузов В.Ю., Бондарев А.Г. Агроэкологическое состояние и перспективы использования заброшенных земель засушливой степной зоны со сложным почвенным покровом. Материалы Всероссийской научной конференции «Агроэкологическое состояние и перспективы использования земель в России, отчужденных от активного сельскохозяйственного использования», Докучаевский почвенный институт МКАД РАСХН, стр. 227–236)
- Mahmood A, Mahmoud AH, El-Abedein AIZ, Ashraf A, Almunqedhi BMA (2020) A comparison study of metals concentration in agricultural soil and vegetables irrigated by wastewater and tube well water. *J King Saud Univ Sci* 32(3):1861–1864. <https://doi.org/10.1016/j.jksus.2020.01.031>
- Malakhovskiy DB, Arslanov KA, Gay NA, Dzhi-noridze RN (1993) New data on the history of the Neva river. Russian Geographical Society. The evolution of natural environments and the current state of the Lake Ladoga geosystem, pp 74–84 (Малаховский Д.Б., Арсланов К.А., Гай Н.А., Джиноридзе Р.Н. Новые данные по истории реки Невы. Русское географическое общество. Эволюция природных сред и современное состояние геосистемы Ладожского озера, с 74–84)
- Matinyan NN, Bakhmatova KA, Korentsvit VA (2017) Soils of the Summer Garden (Saint Petersburg). *Eurasian Soil Sc* 50:637–645. <https://doi.org/10.1134/S1064229317060060>
- Mielke HW, Gonzales CR, Smith MK, Mielke PW (1999) The urban environment and children's health: soils as an integrator of lead, zinc, and cadmium in New Orleans, Louisiana, USA. *Environ Res* 81(2):117–129. <https://doi.org/10.1006/enrs.1999.3966>
- Mineev VG (1984) Agrochemistry and biosphere. MSU publishing house, p 245 (Минеев В.Г. Агрохимия и биосфера. Издательство МГУ, с 245)
- Mineev VG (2006) Agrochemistry. MSU publishing house, p 719 (Минеев В.Г. Агрохимия. Издательство МГУ, с 719)
- Minkina T, Sushkova S, Konstantinova E, Yadav BK, Mandzhieva S, Konstantinov A, Khoroshavin V, Nazarenko O, Antonenko E (2020) Polycyclic aromatic hydrocarbons in urban soils within the different land use: a case study of Tyumen, Russia. *Polycyclic Aromatic Compounds* 40(4):1251–1265. <https://doi.org/10.1080/10406638.2018.1540997>
- Ninkov J, Milić S, Banjac B, Vasin J, Jakšić S, Marinković J, Živanov M (2018) Influence of soil particle size on content and availability of trace elements in soils under vineyards. *Zemljiste i Biljka* 76(1):88–100. http://www.sdpz.rs/images/casopis/2018/ZIB_vol67_no1_2018_pp88-100.pdf
- Palansooriya K, Shaheen SM, Chen SS, et al. (2020) Soil amendments for immobilization of potentially toxic elements in contaminated soils: a critical review. *Environ Int* 134:105046. <https://doi.org/10.1016/j.envint.2019.105046>
- Pan H, Lu X, Lei K (2017) A comprehensive analysis of heavy metals in urban road dust of Xi'an, China: contamination, source apportionment and spatial distribution. *Sci Tot Environ* 609:1361–1369. <https://doi.org/10.1016/j.scitotenv.2017.08.004>
- Polyakov V, Reznichenko O, Abakumov E, Kostecki (2020) Ecotoxicological state and pollution status of alluvial soils of St. Petersburg, Russian Federation. *Soil Sci Ann* 71(3):221–235. <https://doi.org/10.37501/soilsa/127089>
- Pozdnyakov AI, Eliseev PI, Rusakov AV (2012) Electric resistance as a possible indicator of the domestication of arable sandy soils of the humid zone. *Bull Moscow Univ* 17(2):54–60 (Поздняков А.И., Елисеев П.И., Русаков А.В. Электрическое сопротивление как возможный показатель приручения пахотных песчаных почв гумидной зоны. Вестник Московского университета)
- Qu C, Chen W, Hu X, Cai P, Chen Ch, Yu X-Y, Huang Q (2019) Heavy metal behavior at mineral-organism interfaces: Mechanisms, modelling and influence factors. *Environ Int* 131:104995. <https://doi.org/10.1016/j.envint.2019.104995>
- Rebristaya O, Khitun O (1997) Restoration potential of the Yamal flora. In: Development of the north and problems of reclamation. Ecology of taiga soils of the North, Syktyvkar, pp 100–107 (Ребристая О, Хитун О. Восстановительный потенциал флоры Ямала.

- Освоение Севера и проблемы мелиорации. Экология таежных почв Севера, Сыктывкар, 100–107 с.)
- Rozhkov VA, Bondarev AG, Kuznetsova IV, Rakhmatulloev KR (2002) Physical and hydrophysical properties of soils. Manual. Moscow: MGUL, p 75 (Рожков В.А., Бондарев А.Г., Кузнецова И.В., Рахматуллоев К.Р. Физические и гидрофизические свойства почв. Руководство. Москва: МГУЛ)
- Saljnikov E, Mrvic V, Cakmak D, Jaramaz D, Perovic V, Antic-Mladenovic S, Pavlovic P (2019) Pollution indices and sources apportionment of heavy metal pollution of agricultural soils near the thermal power plant. *Environ Geochem Health* 41:2265–2279. Online ISSN 1573-2983 pp 5-15 <https://doi.org/10.1007/s10653-019-00281-y>
- SanPiN 4266–87 Methodological guidelines for assessing the degree of danger of soil contamination with chemicals. p 10 (САНПИН 4266–87 Методические указания по оценке степени опасности загрязнения почв химическими веществами). <https://files.stroyinf.ru/Data2/1/4293852/4293852444.htm>
- Savich VI, Belopukhov SL, Nikitochkin DN, Filipova AV (2013) New methods of treatment soils polluted with heavy metals. *J Orenburg State Agrarian Univ* 4(42):216–218 (Савич В.И., Белопухов С.Л., Никиточкин Д.Н., Филиппова А.В. Новые методы обработки почв, загрязненных тяжелыми металлами. Вестник Оренбургского государственного аграрного университета)
- Schuster JK, Harner T, Su K, Mihele C, Eng A (2015) First results from the oil sands passive air monitoring network for polycyclic aromatic compounds. *Environ Sci Technol* 49:2991–2998. <https://doi.org/10.1021/es505684e>
- Seleznev AA, Yarmoshenko IV, Malinovsky GP (2019) Assessment of total amount of surface sediment in urban environment using data on solid matter content in snow-dirt sludge. *Environ Process* 6:581–595 (Селезнев А.А., Ярмошенко И.В., Малиновский Г.П. Оценка общего количества поверхностных наносов в городской среде по данным о содержании твердого вещества в снежно-грязевых илах. Процессы окружающей среды)
- Shamilshvili GA, Abakumov EV, Ryumin AG (2015) Assessment of the mobile forms of zinc and copper content in soil samples from areas of different land use on example of the Krasnogvardeisky District of the St. Petersburg. *Environ Earth Sci* 74:3417–3431. <https://doi.org/10.1007/s12665-015-4379-6>
- Shamilshvily G, Abakumov E, Gabov D (2018) Polycyclic aromatic hydrocarbon in urban soils of an Eastern European megalopolis: distribution, source identification and cancer risk evaluation. *Solid Earth* 9(3):669–682. <https://doi.org/10.5194/se-9-669-2018>
- Shishov LL, Durmanov DN, Karmanov II, Efremov VV (2004) Theoretical foundations and ways to control soil fertility. *Agropromizdat*, p 305 (Шишов Л.Л., Дурманов Д.Н., Карманов И.И., Ефремов В.В. Теоретические основы и способы регулирования плодородия почв. Агропромиздат)
- Simakova MS, Topkopogova VD (2006) Soil formation processes. *Soil institute of V.V. Dokuchaev*, p 510 (Симакова М.С., Топкопогова В.Д. Почвообразовательные процессы. Почвенный институт им. В.В. Докучаева). <http://почвовед.рф/wp-content/uploads/2017/04/1216-Ананко-Т.В.-и-др.-2006.pdf>
- Soil field guide (2008) *Soil institute of V.V. Dokuchaev*, p 182 (Почвенный полевой справочник. Почвенный институт им. В.В. Докучаева, 182 с.). http://soils.narod.ru/download/field_guide_int.pdf
- Soltani N, Keshavarzi B, Moore F, Tavakol T, Lahijan-zadeh AR, Jaafarzadeh N et al (2015) Ecological and human health hazards of heavy metals and polycyclic aromatic hydrocarbons (PAHs) in road dust of Isfahan metropolis. *Iran Sci Tot Environ* 505:712–723. <https://doi.org/10.1016/j.scitotenv.2014.09.097>
- Stogiannidis E, Laane R (2015) Source characterization of polycyclic aromatic hydrocarbons by using their molecular indices: an overview of possibilities. In: Whitacre DM (ed) *Reviews of environmental contamination and toxicology*. Springer, Cham, pp 49–133. https://doi.org/10.1007/978-3-319-10638-0_2
- Trujillo-González JM, Torres-Mora MA, Keesstra S, Brevik EC, Jiménez-Ballesta R (2016) Heavy metal accumulation related to population density in road dust samples taken from urban sites under different land uses. *Sci Tot Environ* 553:636–642. <https://doi.org/10.1016/j.scitotenv.2016.02.101>
- Ufimtseva MD, Terekhina NV (2014) Ecological and geochemical assessment of soil state in the historical center of St. Petersburg. *Bull St Petersburg Univ* 7(2):122–136
- Veenstra JJ, Burras CL (2015) Soil profile transformation after 50 years of agricultural land use. *Soil Sci Soc Am J* 79:1154–1162. <https://doi.org/10.2136/sssaj2015.01.0027>
- Wang XT, Miao Y, Zhang Y, Li YC, Wu MH, Yu G (2013) Polycyclic aromatic hydrocarbons (PAHs) in urban soils of the megacity Shanghai: occurrence, source apportionment and potential human health risk. *Sci Total Environ* 447:80–89. <http://www.sciencedirect.com/science/article/pii/S0048969712016439>
- Webster EA, Chudek JA, Hopkins DW (2000) Carbon transformations during decomposition of different components of plant leaves in soil. *Soil Biol Biochem* 32:301–314. [https://doi.org/10.1016/S0038-0717\(99\)001530-4](https://doi.org/10.1016/S0038-0717(99)001530-4)
- Wilson SD, Kleb HR (1996) The influence of prairie and forest vegetation on soil moisture and available nitrogen. *Am Midl Nat* 136(2): 222–231. Published by: The University of Notre Dame. <https://doi.org/10.2307/2426727>
- WRB (2015) International soil classification system for naming soils and creating legends for soil maps. IUSS WORKING GROUP WRB 2015, World reference base for soil resources 2014, p 213. <http://www.fao.org/3/i3794en/I3794en.pdf>

- Xie T, Wang M, Chen W et al (2019) Impacts of urbanization and landscape patterns on the accumulation of heavy metals in soils in residential areas in Beijing. *J Soils Sediments* 19:148–158. <https://doi.org/10.1007/s11368-018-2011-6>
- Zakharenko VA (2008) Pesticides in the agrarian sector of Russia at the end of the XX—beginning of the XXI century. *Agrochemistry* 11:86–96 (Захаренко В.А. Пестициды в аграрном секторе России в конце XX - начале XXI века. *Агрохимия*). <http://naukarus.com/pestitsidy-v-agrarnom-sektore-rossii-kontsa-xx-nachala-xxi-veka>
- Zgłobicki W, Telecka M, Skupiński S, Pasierbińska A, Koziel M (2018) Assessment of heavy metal contamination levels of street dust in the city of Lublin, Poland. *Environ Earth Sci* 77:1–11. <https://doi.org/10.1007/s11356-019-06496-x>
- Zhang H, Wang J, Bao H, Li J (2020) Wu F (2020) Polycyclic aromatic hydrocarbons in urban soils of Zhengzhou city, China: occurrence, sources and human health evaluation. *Bull Environ Contam Toxicol* 105:446–452. <https://doi.org/10.1007/s00128-020-02982-y>
- Zhang Y, Peng C, Zh G, Xiao X, Xiao R (2019) Polycyclic aromatic hydrocarbons in urban soils of China: distribution, influencing factors, health risk and regression prediction. *Environ Pollut A* 254:112930. <https://doi.org/10.1016/j.envpol.2019.07.098>